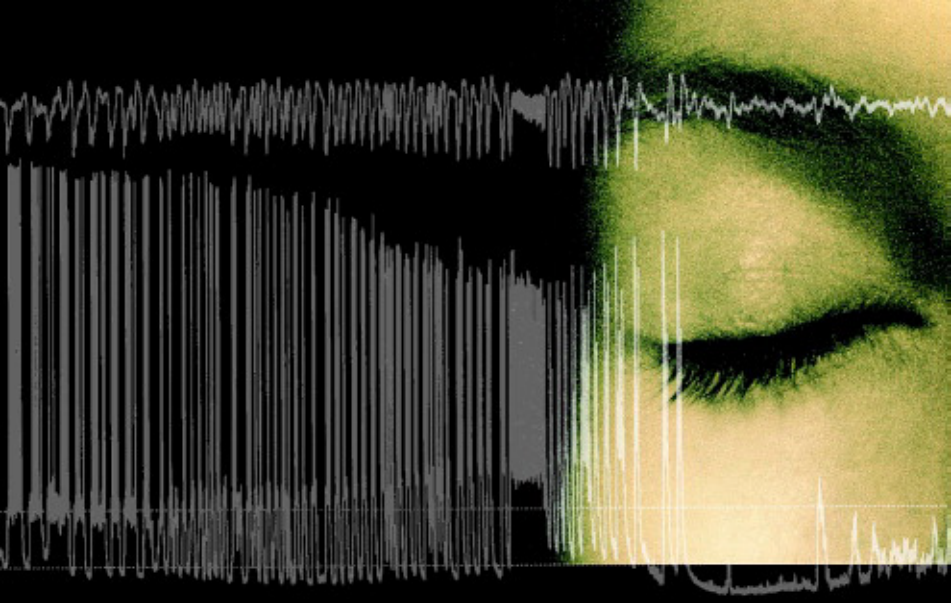

Neuronal Substrates of Sleep and Epilepsy

MIRCEA STERIADE

CAMBRIDGE

This page intentionally left blank

Neuronal Substrates of Sleep and Epilepsy

Contrary to the conventional wisdom that sleep is a resting state of the brain, with negligible activity of cortical neurons, the author brings evidence favoring the idea that, during this behavioral state, memory traces acquired during waking are consolidated. Many physiological correlates of waking and sleep states as well as diverse types of epileptic seizures are discussed. The author focuses on the coalescence of different sleep rhythms in interacting corticothalamic networks and on three types of paroxysmal disorders; namely spike-wave seizures as in absence epilepsy, Lennox–Gastaut seizures, and temporal lobe epilepsy. Profusely illustrated with figures from *in vivo, in vitro* and "*in computo*" studies, the majority coming from the author's own laboratory, *Neuronal Substrates of Sleep and Epilepsy* is essential reading for neuroscientists and clinical researchers.

MIRCEA STERIADE has held the position of Professor and Head of the Laboratory of Neurophysiology at Laval University, Quebec since 1968 and is a Fellow of the Royal Society of Canada (Academy of Sciences). His main areas of interest have focused on states of vigilance, epilepsy, the cerebral cortex, the thalamus, and brainstem, and has employed intracellular studies of all of these. He has published over 300 scientific articles. He is co-author of *Thalamic Oscillations and Signaling* (1990), *Brainstem Control of Wakefulness and Sleep* (1990), *The Visual Thalamocortical System and its Modulation by the Brainstem Core*, *Thalamus* (Vol. 1, 1997), and co-editor of *Brain Cholinergic Systems* (1990) and *Thalamus* (Vol. 2, 1997). His most recent book is *The Intact and Sliced Brain* (2001).

Neuronal Substrates of Sleep and Epilepsy

MIRCEA STERIADE

CAMBRIDGE
UNIVERSITY PRESS

PUBLISHED BY THE PRESS SYNDICATE OF THE UNIVERSITY OF CAMBRIDGE
The Pitt Building, Trumpington Street, Cambridge, United Kingdom

CAMBRIDGE UNIVERSITY PRESS
The Edinburgh Building, Cambridge CB2 2RU, UK
40 West 20th Street, New York, NY 10011-4211, USA
477 Williamstown Road, Port Melbourne, VIC 3207, Australia
Ruiz de Alarcón 13, 28014 Madrid, Spain
Dock House, The Waterfront, Cape Town 8001, South Africa

http://www.cambridge.org

First published in printed format 2003

ISBN 0-521-81707-2 hardback

This book is dedicated to my daughters, Donca and Claude, and to Jacqueline.

Contents

Preface

This monograph is a synthesis of the ongoing efforts toward the understanding of neuronal mechanisms underlying sleep stages and different forms of paroxysmal (epileptiform) activities that preferentially occur during the states of drowsiness and slow-wave sleep. I have been interested in the neurophysiological basis of electrographic seizures since the 1960s, and this interest intensified during the early 1970s when I investigated spike-wave seizures during light sleep in behaving monkeys. This work inspired my idea that such seizures originate within the neocortex and set the scene for our recent intracellular work *in vivo*, throughout the 1990s. The journey continues this century, along the same conceptual lines, with new collaborators who have joined my team.

The two major topics of my laboratory are the neocortical and thalamic neuronal bases of sleep and of paroxysmal activities that mimic different forms of epilepsy in humans, more particularly absence seizures and Lennox–Gastaut syndrome. This is why sleep and these two forms of paroxysmal activities found a place of choice in the present monograph. Nonetheless, I have also attempted to relate these topics with a series of other forms of epilepsy. There are some edited volumes in which many authors express their views, sometimes discrepant, on sleep and/or epilepsy, but I decided to write a monograph because this may allow an expression of coherence, even if the views in this book might be, of necessity, biased by my ideas and personal experimental data. Let the reader judge the soundness of data and whether they support my concepts in this field. I have also included related clinical data but, of course, the reader may find more complete clinical phenomenology in handbooks of epilepsies. This monograph is for those basic neuroscientists and clinicians that want to spend some time over the text and figures to decipher the neuronal basis of normal and pathological phenomena.

The reader will find, as in my previous monograph on *The Intact and Sliced Brain* (The MIT Press, 2001), significant dissimilarities between the results from *in vivo* and some *in vitro* experiments, especially when the latter arise from work on isolated thalamic

slices. Although I consider that the work *in vitro* led to important discoveries of the ionic nature of different voltage-gated currents and the identification of receptors implicated in synaptic transmission, and that every laboratory should have electrophysiological setups for both *in vivo* and *in vitro* experiments, I remain allergic to extrapolations from single cells and simple networks recorded in a 0.4-mm tissue to global notions such as "sleep" and "absence epilepsy", when even our animals with intact brain connectivity are quite absent during experimental procedures. This is why I refrain from using the clinical term of epilepsy when describing the neuronal basis of electrographic seizures. I hope, however, that the stereotyped events we are exploring in animal models may be similar to what future investigators will be able to detect by using intracellular recordings from different forms of epileptic diseases in humans.

Acknowledgments

The memory of my mentor Frédéric Bremer continues to be an inspiration for me.

The personal work described in this monograph would not have been possible without the skillful and creative collaboration of my young colleagues. Among the many Ph.D. students and postdoctoral fellows that have worked in my laboratory at Laval University since 1968, I mention here (in order of appearance in my laboratory) the most prominent, with whom work on sleep and/or epilepsy was performed: V. Apostol, P. Wyzinski, G. Yossif, M. Deschênes, N. Ropert, L.L. Glenn, L. Domich, B. Hu, D. Paré, R. Curró Dossi, A. Nuñez, F. Amzica, D. Contreras, I. Timofeev, D. Neckelmann, and F. Grenier. Collaboration with T.J. Sejnowski, A. Destexhe, M. Bazhenov, and W.W. Lytton was instrumental in the computational studies of cortical and thalamic networks implicated in sleep and epilepsy.

Since 1968, my work has been continuously supported by grants from the Medical Research Council of Canada (now Canadian Institutes for Health Research), Natural Science and Engineering Research Council of Canada, Human Frontier Science Program, National Institute of Health (U.S.A.), Savoy Foundation for Epilepsy Research, and the Research Fund of Laval University.

Finally I thank some people from Cambridge University Press: Gavin Swanson, who encouraged me to start writing this monograph; Sarah Price, for careful reading and helpful suggestions; Zoe Naylor, for the design of the book; and Carol Miller, production editor.

Chapter 1 Pioneering steps in studies on sleep and epilepsy

This book is essentially devoted to analyses of neuronal substrates underlying sleep with low-frequency oscillations, so-called sleep with synchronized electroencephalogram (EEG) or resting sleep [1], and a series of seizures that preferentially develop during this state of sleep. The reader will find data on intrinsic neuronal properties and network operations in corticothalamic, hippocampal-entorhinal and neuromodulatory systems that control forebrain normal and paroxysmal activities. This brief introductory chapter is not intended to discuss in detail the history of ideas on two bedfellows, sleep and epilepsy, but only to resurrect some of the most important figures and concepts that are directly related to what is discussed at length, essentially at the neuronal level, in the following chapters.

1.1. Brain, neurons and sleep across centuries

Different states of vigilance, such as waking and sleep states with or without dreams, have been recognized in ancient cultures [2]. The deafferentation theory of falling asleep dates back to Lucretius, in the first century B.C. [3], was revitalized in the early 19th century by Macnish [4] and Purkinje [5], and was finally developed during the past century by three major figures of sleep research: Bremer, Moruzzi and Kleitman. As discussed in Chapter 3, the concept of passive or active sleep is a false dilemma as both brain deafferentation from external signals and actively sleep-inducing (humoral and neuronal) factors may lead to sleep, since the presumed actively hypnogenic neurons exert their inhibitory effects on activating neurons in the brainstem and posterior hypothalamus, thus disconnecting the forebrain, as postulated in the passive theory.

Two of the above-mentioned modern scientists, Bremer and Moruzzi [6] (Fig. 1.1), initiated their research on states of vigilance within the framework of the passive sleep concept, but finally turned their attention to structures that were hypothesized to play an active role in the process of falling asleep.

[1] None of the terms is fully deserved. Although the term "EEG-synchronized" is usually taken in contrast with the conventional term of "desynchronized" activity in wakefulness and REM sleep, fast rhythms in the beta and gamma range (~20–60 Hz) occur during the depolarizing phase of the slow oscillation in natural non-REM sleep and are synchronized over restricted cortical territories and thalamocortical systems, as is also the case in waking and REM sleep (Steriade et al., 1996a-b). As to the term "resting", it was designed to underline that virtually nothing mentally important happens in the brain during this state of sleep, in line with a series of older concepts that regarded sleep similar to cerebral death (Hypnos brother of Thanatos, as in Homer's *Iliad*) or, closer to us, an "abject annihilation of consciousness" (see note [224] in Chapter 3). This obsolete view can be refuted on the basis of high firing rates of neocortical neurons, short-term plasticity, and mental processes during this state (see section *3.2.4.2* in Chapter 3 and section ***4.3.3*** in Chapter 4). Therefore, I shall use, throughout this book, the descriptive term slow-wave (or non-REM) sleep. It is justified by the fact that the slow oscillation (generally 0.5–1 Hz), which was initially discovered in intracellular recordings from neocortical neurons in animals and found with the same characteristics in natural sleep of both animals and humans, appears from the very onset of non-REM sleep and groups other sleep rhythms, spindles, and delta oscillation (see section ***3.2.3*** and Fig. 3.6 in Chapter 3).

[2] The Indian textbook of philosophy, *Upanishad* (~1,000 B.C.), described different states of consciousness, among them wakefulness, dreamless sleep (*susupta*) and dreaming sleep (see Wolpert, 1982; and Chapter 1 in Borbély, 1984).

[3] See the 1988 translation of Lucretius' book *On the Nature of the Universe* (55 B.C.).

[4] Macnish (1830).

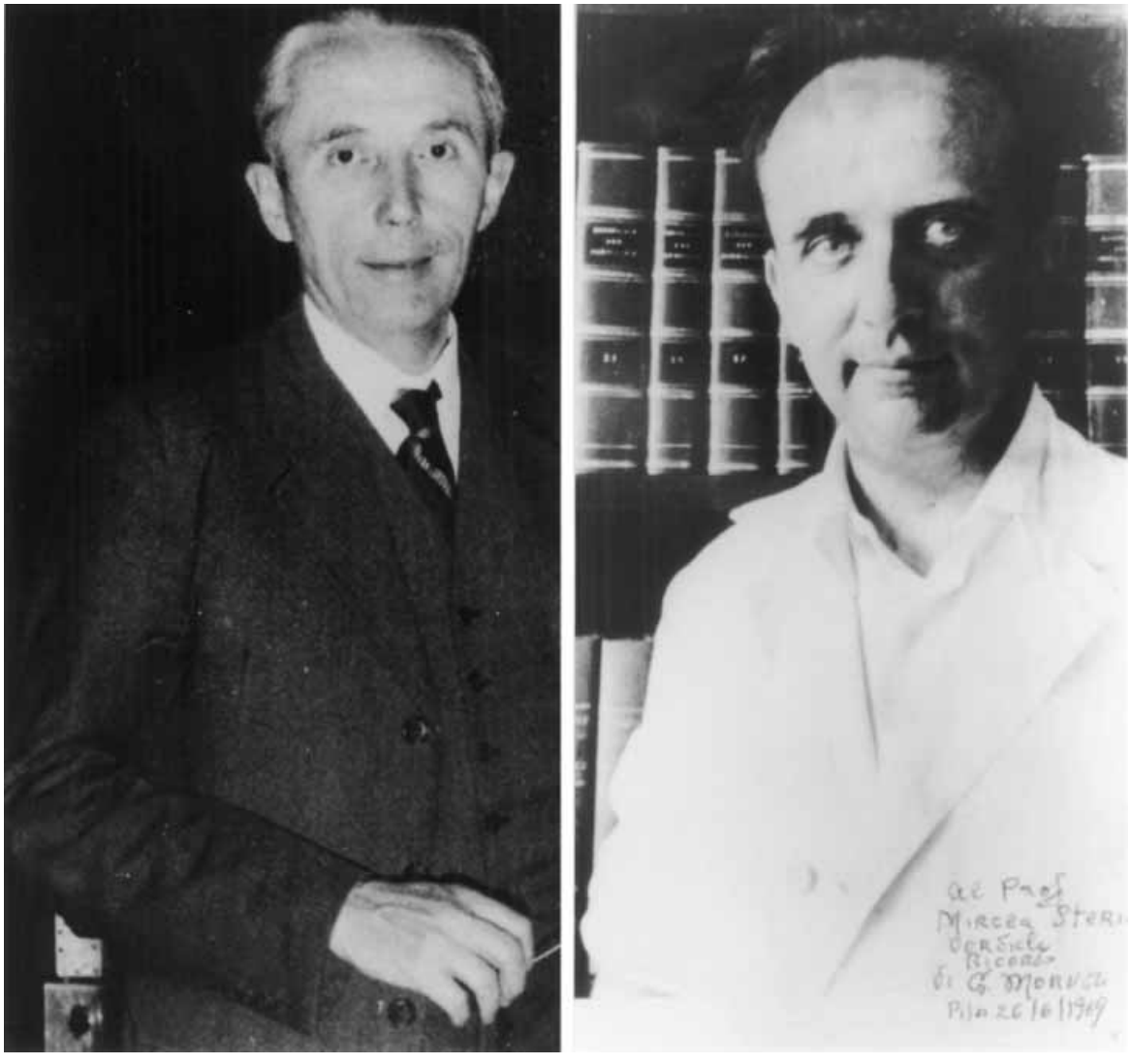

Fig. 1.1 Two pioneers in the research on slow-wave sleep and brain activation: Frédéric Bremer (1892–1982, left) and Giuseppe Moruzzi (1910–1986, right).

[5] Cited in Moruzzi's (1964) historical essay.

[6] Short biographical notes of these two great neurophysiologists can be found in a recent monograph (Steriade, 2001b; see notes [14] and [16] in Chapter 1 of that book). For Moruzzi, see also the interview by Marshall (1987).

[7] Bremer (1935). In his 1937 paper (see Fig. 1.2), Bremer clearly stated his concept that, after disconnection from brainstem influences, the effect at the EEG level is the "*expression d'une diminution de ce que l'on pourrait appeler le tonus cortical et diencéphalique*" (p. 78–79). The concept of a diminished cerebral tone after brainstem disconnection by intercollicular transection announced Moruzzi and Magoun's experiments, a decade later (see below, [11]). As to the apparent contradiction concerning the role played by *specific* (Bremer) versus *nonspecific* (Moruzzi) structures in the maintenance of brain arousal, see the main text and section ***3.1.2*** in Chapter 3. Besides his seminal contributions in the field of states of vigilance, Bremer was among the first scientists to emphasize the "fundamental autorhythmicity" of neurons ("*l'automatisme rythmique des cellules nerveuses*", 1949, p. 177 and 191), a notion that led to modern investigations on intrinsic neuronal properties (reviewed in Llinás, 1988). In that visionary 1949 paper, Bremer emphasized the "cortico-diencephalic interactions", an idea supported by recent dual intracellular recordings from cortical and thalamic neurons demonstrating the coalescence of different sleep rhythms within corticothalamocortical loops (see Steriade, 2001a-b).

[8] Bremer (1975, p. 268; and p. 271).

[9] The often made distinction that Bremer specified the role of ascending *specific* projections in maintaining the state of waking whereas Moruzzi discovered the role of *nonspecific* brainstem reticular pathways is tenuous (but possibly efficient in lectures to undergraduate students) because forebrain activation is maintained by both these systems. Sleep EEG patterns are not only produced by interruption of ascending reticular activating systems but also appear, confined to the visual cortical areas, after bilateral transection of optic nerves (Claes, 1939) and bilateral interruption of trigeminal nerves similarly produces a state of brain electrical synchronization (Roger et al., 1956).

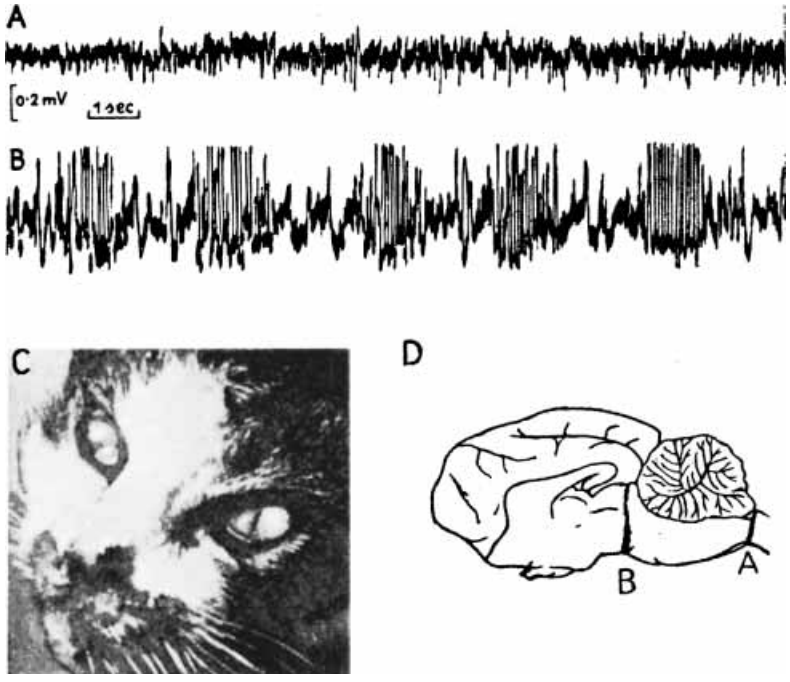

Fig. 1.2 EEG and ocular behavior in the acute *encéphale isolé* (isolated encephalon; EEG trace in *A* and bulbo-spinal section in *D*) and *cerveau isolé* cat (isolated forebrain; EEG trace in *B* and transection at the collicular level in *D*). *A*, activity typical for the waking state. *B*, spindling activity interrupted by inter-spindle lulls, as in the sleeping brain (see also fissurated myosis in *C*). From Bremer (1937).

Bremer left the isolated forebrain of the decerebrate cat *in situ*, instead of destroying it, and discovered that brain electrical activity contains spindles, associated with another sleep sign, extreme myosis (Fig. 1.2) [7]. He had "the shock one experiences in the face of a novel natural phenomenon" [8] and, indeed, we now know that sleep spindles occur by disconnecting thalamic neurons from the depolarizing influence of brainstem reticular cells. Although Bremer continuously emphasized that afferent signals maintain the *tonus cérébral* and that the EEG/ocular sleep syndrome he described in 1935 was due to interruption of sensory pathways [9], as in the passive theory of sleep, he turned in the early 1970s to the idea that the preoptic area in the anterior hypothalamus may play a hypnogenic role by inhibiting the rostral mesencephalic reticular core [10] that was known to exert activating effects on the thalamus and cortex. In one of his later contributions, Bremer, while well aware of the role played by the ascending reticular ("nonspecific") formation in arousal (and acknowledging that if he would have

"been more anatomically minded", he would have concluded that an activating structure lies between the medulla and midbrain), remained firmly within the concept of passivesleep maintained by specific sensory projections [8]. In his words, "there is little doubt that sensory lemniscal impulses impinging *without a reticular participation* on cat's somatosensory area contribute efficiently to the maintenance of its local tone" (see also experiments mentioned in note [9]). Anyway, Bremer was the first neuroscientist to place emphasis on "brain sleep", when all were turned on "body sleep".

Moruzzi, a pupil of Bremer in the late 1930s, also interpreted the results of his 1949 experiments with Magoun as indicating wakefulness maintained by the ascending brainstem reticular system,"while reduction in its activity . . . may . . . precipitate normal sleep" [11]. The reticular formation activation concept became so famous in the 1950s and 1960s that "wherever any really interesting fun was going on in brain research, that part was immediately claimed as part of the reticular system" [12]. However, that discovery fell into desuetude during the 1970s because of lack of knowledge on connectivity and neurotransmitters used by brainstem reticular cells. More recently, with the disclosure of pathways and chemical codes of these neurons, the concept of brainstem-thalamic activation has repeatedly been supported by single-cell recordings of midbrain reticular neurons during natural waking-sleep states. Also, the facilitatory action from the mesencephalic reticular core upon thalamocortical neurons was demonstrated at the intracellular level showing depolarization and increase in the apparent input resistance, and activation of thalamic intralaminar neurons, major targets of the upper brainstem reticular formation, was detected during complex tasks in humans [13].

While Bremer focused on the presumed hypnogenic properties of the preoptic area, Moruzzi and his younger colleagues (among them Berlucchi, Pompeiano, Batini, Rossi, and Zanchetti) proposed another candidate for an actively sleep-promoting area, which they located in and around the nucleus of the solitary tract in the medulla. This view was based on experiments using low-frequency stimulation of that nucleus and other experimental manipulations, including transections at the midpontine level that created a virtually permanent state of brain arousal due to the removal of a hypothesized inhibitory role of hypnogenic medullary structures [14]. However, at variance with the destiny of preoptic neurons, which became more and more fashionable in sleep research, no cellular data have as yet confirmed the presence of sleep-promoting neurons in the medulla. By contrast, Moruzzi and Magoun's 1949 findings and conclusions were, and still remain,

[10] Bremer's (1973) study, using electrical stimulation and field potential recordings, followed a series of lesions and stimulation experiments initiated by Nauta (1946) and inspired by earlier clinico-anatomical data of von Economo (1918, 1929). These studies are continued and, nowadays, neurons in the ventrolateral part of the preoptic area are considered as best candidates for playing an inhibitory, GABAergic role in promoting sleep (see section *3.1.2.3* in Chapter 3).

[11] Moruzzi and Magoun (1949). Before his stage with Magoun in U.S.A., Moruzzi worked with Adrian in Cambridge and, during 1937–1938, with Bremer in his laboratory at the Université de Bruxelles, where he published some papers as sole author. At the 1980 Pisa symposium in honor of Moruzzi, he recalled Bremer in terms of "vivid imagination and clear scientific thinking". My recollection of that 1980 symposium was the pleasure I experienced presenting experimental data with unit recordings relating the upper brainstem reticular core neurons with thalamic intralaminar neurons, which fully supported Moruzzi and Magoun's seminal data and major theoretical issues (Steriade, 1981).

[12] Jefferson (1958, p. 729).

[13] Reviewed in previous monographs by Steriade and McCarley (1990); and Steriade (2001b); for human studies, see Kinomura et al. (1996).

[14] Reviewed in Moruzzi (1972); see also section *3.1.2.1* in Chapter 3.

[15] Kleitman (1963). He was born at the end of the 19th century in Kishinev (then Russia), came to America in 1915, earned a Ph.D. at the University of Chicago where he did research until he retired as a full professor in 1960 (but remained productive; see his 1993 chapter), and died in 1999, at the age of 104. At the 1995 celebration for his 100th birthday, only 20–25 people were present at the *Sleep and Aging* session in Nashville meeting, but Kleitman was among them. William Dement was his student; he recorded Kleitman's EEG during full nights in 1954 and finished the revision of Kleitman's 1963 book on *Sleep and Wakefulness*, first published in 1939 (see Dement, 2001).

[16] Aserinsky and Kleitman (1953, 1955). Aserinsky was Kleitman's graduate student in physiology.

[17] Dement and Kleitman (1957) scored recordings over 126 nights in 33 subjects and found a cyclic variation in EEG and eye movements, with waking developing to different stages of slow-wave sleep and, after termination of stage 4, entering REM sleep. This cyclic variation repeated throughout the night at intervals of 90 to 100 min from the end of one REM period to the end of the next.

[18] Jouvet and Michel (1959); Jouvet et al. (1959). The neuronal mechanisms underlying muscular atonia have been worked out by Pompeiano and colleagues (reviewed in Pompeiano, 1967a-b). Later on, intracellular recordings of spinal cord neurons in naturally sleeping cats have further revealed the mechanisms of tonic inhibition of motoneurons during REM sleep (Morales and Chase, 1978; Glenn and Dement, 1981; Chase and Morales, 1983).

[19] Jouvet (1962, 1972). Jouvet, his colleagues in Lyon, as well as some other fellows call REM sleep "*sommeil paradoxal*", to emphasize that during this sleep state the brain is aroused, but paralyzed because of motoneuronal inhibition.

[20] Jouvet (1986). In his recent "monologue which traces the life of a handful of neurobiologists", Jouvet (1999) is aware that the scientific intelligentsia may not appreciate the idea of psychological inheritance, but states that this has nothing to do with his hypothesis (see p. 15–16 and Chapter 7 in that book). Those who are familiar with French may want to read his novel *Le Château des Songes* (1992), with fabulous dreams and commentaries on them by a character of the 18th century.

Fig. 1.3 Nathaniel Kleitman, a prominent figure for the concept of passive sleep (1895–1999).

among the most influential discoveries in sleep research and continue to be supported by modern experiments conducted at the single-cell level [13].

Kleitman (Fig. 1.3) is another leading proponent of the passive theory of sleep, as he emphasized that what needs to be explained is not sleep, but wakefulness, because there was not a single fact in those times supporting the theory of active sleep, and all data could be interpreted as a let down of the waking activity [15]. Since the 1920s, Kleitman conducted experiments on prolonged sleep deprivation and argued that his observations were incompatible with Piéron's notion of a continual buildup of hypnotoxin (see section ***3.1.1*** in Chapter 3). Probably, the major discovery of Kleitman pertains to the sleep stage with rapid eye movements (REMs) that he reported in three seminal papers, first with Aserinsky [16] and then with Dement [17].

The man who further described all major signs of REM sleep, including muscular atonia that typically characterizes this sleep stage and differentiates it from other states of vigilance [18], and performed the first animal experiments to localize the brainstem and forebrain structures responsible for the physiological correlates of this sleep state [19], is Jouvet. Some of the seminal contributions of Jouvet in the monoaminergic control of waking and sleep states are dealt with in Chapter 3 (section *3.1.2.2*). Jouvet hypothesized that REM sleep is a guardian of psychological personality, a repeated reprogramming of individuality during dreaming [20].

[21] Hobson et al. (1975); McCarley and Hobson (1975).

[22] See mathematical model of McCarley and Massequoi (1986), Steriade and McCarley (1990), and a more recent paper (Hobson et al., 2000) in which the original and revised models of reciprocal interactions between cholinergic and monoamine-containing neurons are discussed.

[23] Sakai et al. (2001).

[24] Chandler et al. (1980); Chase et al. (1980); Ito and McCarley (1984); Ito et al. (2002).

[25] Hirsch et al. (1983).

[26] Steriade et al. (2001a); Timofeev et al. (2001b).

[27] Among the numerous *in vitro* studies on brainstem, thalamic and cortical neurons devoted to analysis of phenomena observed during states of vigilance, here are some of them: Greene et al. (1986); Kita and Kitai (1990); Leonard and Llinás (1990, 1994); Von Krosigk et al. (1993); Huguenard and Prince (1992, 1994a-b); Bal et al. (1995a-b); Sanchez-Vives and McCormick (2000).

[28] Computational studies related to sleep states and their physiological correlates, performed by Sejnowski and his colleagues Destexhe and Bazhenov in collaboration with *in vivo* experimenters using intracellular recordings, may be found in Destexhe et al. (1994a-b, 1996, 1998, 1999b) and Bazhenov et al. (1998a-b, 1999, 2000).

[29] John Hughlings Jackson (1835–1911).

[30] Penfield and Jasper (1954, p. 20). However, see also note [33] with Jasper's opinion on seizures with prevalent inhibitory processes.

[31] Jackson (1864, 1931) isolated a form of epilepsy with localized paroxysms, now called Jacksonian seizures (also called Bravais-Jacksonian seizures, because of a 1827 doctorial thesis presented at the Université de Paris by a young physician, Bravais, who described focal seizures). Jackson also surmised that several symptoms, now known to define temporal lobe epilepsy, constitute "a particular variety of epilepsy". He remarked that not all epileptic seizures are associated with

Tentative models of the waking-sleep cycle and REM generation varied according to the evolution of knowledge on connections and transmitters released by brainstem cholinergic, glutamatergic and monoaminergic systems. The attention focused on the brainstem because of Jouvet's demonstration that cardinal signs of REM sleep occur in brainstem-transected animals [19]. During the mid-1970s, it was proposed that the executive elements of REM sleep are gigantocellular cholinergic neurons located in the medial pontine reticular formation, which were thought to be self-excitatory and inhibited by serotoninergic dorsal raphe and noradrenergic locus coeruleus neurons [21]. As immunohistochemical studies could not reveal cholinergic neurons in the medial pontine reticular formation, emphasis was more recently placed on neurons in the mesopontine cholinergic nuclei that project to thalamocortical systems, produce tonic activation of the forebrain, and generate ponto-geniculo-occipital waves (see section **3.3** and Fig. 3.55 in Chapter 3). The postulated inhibitory actions of monoaminergic, especially serotoninergic, neurons on mesopontine cholinergic cells have been confirmed. Cholinergic neurons become increasingly active toward the end of slow-wave sleep and, further on, during REM sleep, because of their disinhibition, as monoaminergic neurons are virtually silent in REM sleep. This sequence of events [22] was further elaborated by adding the actions of medullary adrenergic, ponto-medullary noradrenergic and, to a lesser extent, hypothalamic dopaminergic neurons to the inhibitory (or permissive) mechanisms exerted on executive, REM-on brainstem cholinergic and glutamatergic neurons [23].

The evolution of research into neuronal and molecular substrates of sleep states during the 1980s and 1990s led to significant advances in the field of connectivity among chemically coded neurons in various brain areas that proved in earlier studies to be critical for waking and sleep by using stimulation and electrolytic or excitotoxic lesions. Intracellular recordings of brainstem, thalamic and cortical neurons, whose input-organization has to be identified by standard electrophysiological criteria, revealed their behavior during contrasting EEG patterns under different types of anesthesia and, importantly, during shifts in natural states of vigilance. The intracellular recordings during long periods of natural waking and sleep states in chronically implanted animals, which seemed science fiction not long ago because of stability problems, have been performed in the spinal cord [18], brainstem reticular and trigeminal motoneurons [24], thalamocortical neurons [25], and neocortical pyramidal and local-circuit inhibitory neurons [26]. *In vitro* studies of brainstem, thalamic and cortical

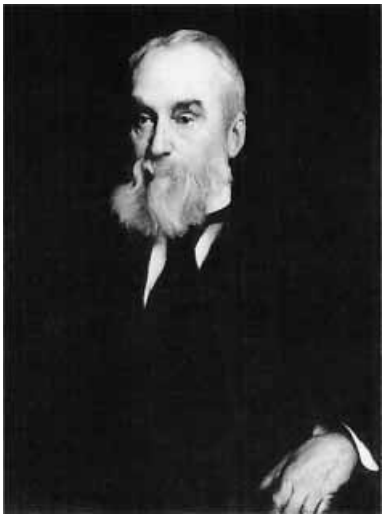

Fig. 1.4 John Hughlings Jackson (1835–1911) was a pioneer of clinical neurology in the United Kingdom.

motor components and that there are also sensory discharges that take the form of "reminders of common sensations". The publication of Jackson's observations on localized motor seizures preceded by a few years the experimental work by Fritsch and Hitzig (1870) and by Ferrier (1876), using motor cortex stimulation (it seems that Jackson discussed his data with these colleagues). Two decades later, Beevor and Horsley (1890) mapped the orang-outan's precentral cortex with extreme precision. Another contribution of Jackson is his concept on non-abrupt delineations of various neocortical areas, which was developed in experiments conducted by the Italian physiologist Luciani (1840–1919) showing that each sensory modality in dog's cerebral cortex "possesses a territory of its own, (but) in addition has a common territory, the parietal lobe, . . . *where partial fusion of the sensation occurs*" (Luciani, 1911, p. 159; italics mine). This concept of associational areas in the parietal lobe eventually led to the disclosure of neocortical areas 5 and 7 in the suprasylvian gyrus of dogs and cats, and of homologous areas in a primate's brain.

[32] Wilson et al. (1955); Jasper et al. (1969).

slices have worked out the biophysical properties and different receptor types of neurons implicated by *in vivo* experiments in the generation of different physiological correlates of waking and sleep states [27]. And studies *in computo* have predicted a series of mechanisms underlying behavioral states and their electrographic correlates, which led to new experiments [28].

This avalanche of analytical investigations brought sleep to the scene of modern science, performed with methods that are dealt with in the next section (**1.2**), together with those employed in analyses of epileptic seizures. All in all, it is my opinion that the most significant advance in sleep research is not the identification of various ionic channels or the expression of different neuronal types during shifts in natural states of vigilance, but the recent disclosure that, far from being a neuronal desert, as postulated since ancient times until quite recent days [1], the cerebral cortex is highly active during slow-wave sleep, capable of developing synaptic plasticity, and displaying during this state noble properties, such as consolidating memory traces acquired during the state of wakefulness. These properties have recently been investigated at the neuronal level (see Chapter 4) and human studies have demonstrated the overnight improvement of discrimination tasks, some steps depending on the early stages of slow-wave sleep (see section *3.2.4.2* in Chapter 3).

1.2. Evolution of concepts and methods used in studies on epileptic seizures

Classical definitions of epileptic seizures, such as that proposed by Jackson [29] (Fig. 1.4) and re-formulated by Penfield and Jasper as "state(s) produced by an abnormal excessive neuronal discharge within the central nervous system" [30] may apply to many, but not all, paroxysms. This is why, along with the term used by Jackson [31] and others [32], "*the epilepsies*" indicate that these neurological diseases are produced by a variety of factors. The "abnormal excessive neuronal discharge" characterizes grand-mal, tonico-clonic epilepsy and other paroxysms, but certainly not thalamocortical neurons during spike-wave seizures of the absence or petit-mal type, when the majority of those neurons are silent, being tonically and phasically inhibited by thalamic GABAergic reticular cells [33]. Also, some seizures resembling the pattern of the Lennox–Gastaut syndrome may display sustained hyperpolarization of neocortical cells, associated with largely decreased input resistance and no spike discharges [34].

Epileptic fits have been described since ~1700–1600 B.C. in China and Egypt [35], and both Hippocrates and Aristotle mentioned that epileptic seizures, "the sacred disease", may occur during sleep [36]. The appearance of grand-mal seizures during sleep was also reported in the 19th century by Gowers [37]. The role played by lesions in the Ammon's horn in what is now known as temporal lobe epilepsy was mentioned more than a century ago [38].

Major advances in studies on sleep and epilepsy have been due to the discovery that the brain of animals and humans displays electrical activity, which varies with the behavioral state and becomes paroxysmal during epileptic seizures. Caton [39] is credited for having first observed, in rabbits, cats and monkeys under anesthesia, that "feeble currents of varying directions" are "markedly influenced by stimulation of light", and that "a variation of the current intensity occurred when the rabbit awoke from sleep". These observations (between 1870 and 1880) have been followed by similar findings reported by Eastern European physiologists, such as Beck and Cybulski in Poland, Danilevski and Prawdicz-Neminsky in Ukraine, and Kaufman in Russia [40]. They led, four decades later, to Berger's [41] fundamental observations (between 1929 and 1938) of alpha and beta waves recorded from the human scalp, and of alpha blockade by visual stimulation [42]. In 1931, Berger also reported that interictal EEG "spikes" are common in epileptic patients and recorded spike-wave activity in some patients [43]. In North America, the Gibbs couple, Lennox, and Jasper used the EEG in clinical investigations on different forms of epilepsy, starting in the mid-1930s [44]. In the 1937 article by Gibbs, Gibbs and Lennox, the term *cerebral dysrhythmia* can first be found, used to describe the state of epilepsy, during which "the harmony of the orchestra becomes a single note" [45]. The cellular basis of EEG activity related to sleep and seizures began to be studied three decades later, from the early 1960s, with intracellular recordings from cortical and thalamic neurons performed by Purpura, Creutzfeldt and Andersen [46], continuing since the early 1980s with single, dual and triple intracellular recordings from identified excitatory and inhibitory neurons, both *in vivo* and *in vitro* [47].

Experimental and clinical studies on epileptic seizures rely on various methods and models, conceived to mimic different types of epileptic fits in humans. The main methods used are as follows: recordings of EEG, local field potentials, extracellular and intracellular activities (which will not be discussed here because they are exposed at length in all following chapters), electrical

[33] Steriade and Contreras (1995). Long ago, Jasper (1975) emphasized that, although some seizures are characterized by excessive discharges of cortical neurons, "there may be excessive inhibition" (p. 586) in other types of seizures. This is the case of thalamocortical neurons during spike-wave (sw) seizures, as shown in our 1995 study, using dual intracellular recordings from neocortical and thalamocortical neurons (see details in section *5.5.3.2* and Figs. 5.39–5.41 in Chapter 5). For a discussion of the hypothesized origin of SW seizures in the "centrencephalic system" and some arguments against that concept, see section **5.1** in Chapter 5.

[34] See Fig. 5.63 in section *5.6.2.6* of Chapter 5.

[35] Temkin (1971); Scott (1993).

[36] Cited by Passouant (1984).

[37] Gowers (1885). He is also known for having warned of the side effects of potassium bromide, an anticonvulsive drug that had been introduced in the second half of the 19th century.

[38] Sommer (1880); Bratz (1899).

[39] Caton (1842–1926) was a British physician and physiologist. The two citations in the main text are from his 1875 and 1887 papers.

[40] See books and book chapters on the history of brain electrical activity by Brazier (1961), Niedermeyer (1993), and Marshall and Magoun (1998).

[41] Berger (1873–1941) studied medicine in Berlin and, later, in Jena where he worked at the Psychiatric Clinic.

[42] Berger (1929, 1937). The alpha blockade by visual input was confirmed by Adrian and Matthews (1934) using the beetle's electrical activity and Adrian's own brain activity. All Berger's papers on human EEG have been translated into English by Gloor (1969).

[43] Reproduced in O'Leary and Goldring (1976).

[44] The studies by Gibbs and Gibbs, Lennox, and Jasper are reported in Chapter 5.

stimulation and lesions, production of seizure foci in various animal species by topical convulsants and freezing, repetitive sensory (auditory and photic) stimulation [48], local or intraventricular perfusion with high K^+, different genetic epileptic-like states (convulsive or non-convulsive), and magnetic resonance imaging and positron emission tomography for the detection and localization of different epileptic disorders. Several criteria have been proposed to judge the validity of a given experimental model for human epilepsy, the cardinal one being the similarities between the electrical (as well as, possibly, behavioral) manifestations of the model and those known to characterize that form of human epilepsy [49].

To begin with, electrolytic or excitotoxic lesions and electrical or chemical stimulation have been performed in various animal species and humans to demonstrate the locus of seizure initiation, to challenge the role that has been conventionally ascribed to some structures in the generation of seizures, and to provide diagnostic and/or therapeutic tools in human epilepsy. For example, the preferential sensitivity and vulnerability of hippocampus and related systems to intraventricular injection of kainic acid have been used in attempts to replicate in rodents the pathology found in temporal lobe epilepsy [50]; electrical stimuli applied to central structures mimic fast oscillations (ripples, ~100 Hz) that are thought to initiate electrical seizures in neocortex and hippocampus of rats, cats and humans [51]; and decortication or thalamectomy have been used to demonstrate the role of neocortex in the generation of electrical and behavioral seizures with spike-wave complexes at ~3 Hz in monkeys and cats [52]. Electrical stimulation has also been used during neurosurgery procedures in epileptic patients, with pulse-trains applied to neocortex to elicit focal afterdischarges [53] or to amygdala in a patient with temporal lobe epilepsy, who displayed dysphasia and some degree of unresponsiveness [54]. In the latter case, stimulation of the left amygdala, applied to reproduce typical aspects of pure amnestic seizures, evoked an electrical seizure that spread to also involve the right amygdala and hippocampus; however, the patient's behavior remained entirely normal during the time the seizure involved only the left temporal lobe, as she was vivacious and in full contact with the physician, "named pictures correctly and repeated a test phrase correctly . . . Yet, after the seizure she had not the slightest recollection of any of these items . . ." [54] (Fig. 1.5). During the 1990s, deep brain stimulation (DBS) in thalamic nuclei, especially the centromedian-parafascicular (CM-Pf) complex, has been used in intractable seizure patterns [55]. The mechanism(s) underlying DBS' effects are still unresolved. It has

[45] Gibbs et al. (1937, 1938). The term *dysrhythmia*, introduced by Gibbs and his colleagues for epilepsy, was reproduced more than 60 years later, to characterize abnormalities in electrical activity of thalamocortical systems in a series of neurological and psychiatric disorders, such as Parkinson's disease, neurogenic pain, tinnitus, depression and obsessive-compulsive syndrome (Llinás et al., 1999, 2001; Jeanmonod et al., 2001).

[46] Purpura and Cohen (1962); Purpura and Shofer (1963); Purpura et al. (1966); Creutzfeldt et al. (1966); Andersen and Andersson (1968).

[47] The results of these modern intracellular studies on intrinsic neuronal properties and network operations related to sleep and epilepsy are fully discussed in Chapters 2 to 5.

[48] Collins (1975); Naquet and Meldrum (1975); Naquet and Valin (1990). See also sections **5.1** and **5.3** in Chapter 5.

[49] Jasper (1975) gave as example the focal cortical afterdischarge produced by cobalt powder applied on the precruciate gyrus of a chronically implanted cat, associated with clonic movements during waking, less often during slow-wave sleep, and completely lacking the convulsive movements in REM sleep (because of motoneuronal inhibition in the latter sleep state). He concluded that, under these conditions, cortical electrical activity becomes the most reliable index of a seizure (p. 588). The same is valid in modern studies using intracellular recordings in acute experiments carried out in paralyzed animals, for stability purposes.

[50] Nadler et al. (1978); Ben-Ari (1985).

[51] Ylinen et al. (1995); Kandel and Buzsáki (1997); Traub et al. (2001); Grenier et al. (2002).

[52] Marcus et al. (1968a-b); Steriade and Contreras (1998).

[53] See Figs. 1–2 in Ajmone-Marsan (1975).

[54] Gloor (1997, p. 713).

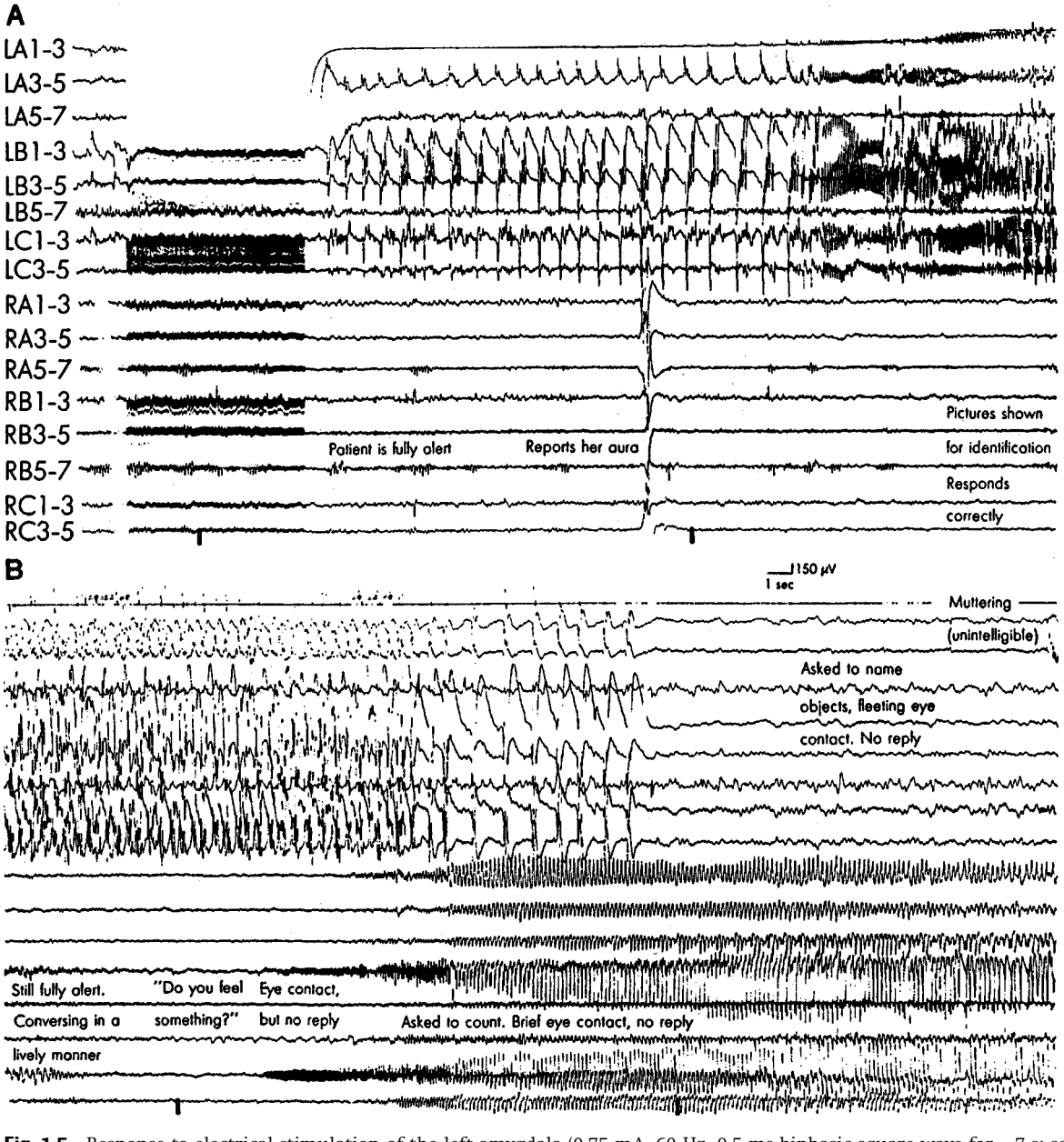

Fig. 1.5 Response to electrical stimulation of the left amygdala (0.75 mA, 60 Hz, 0.5 ms biphasic square wave for ~7 s; see stimulation artifact in panel *A*). Patient (36-year-old woman) with pure amnestic seizures in temporal lobe epilepsy. *A*, electrical afterdischarge involving the left mesial temporal (MT) structures (LA1-3, LA3-5, LB1-3, LB3-5, LC1-3, LC3-5), with no spread to the superficial isocortical contacts (LA5-7, LB5-7), during which the patient behaved and responded entirely normally. *B*, spread of afterdischarge (which starts after a gap of 58 s) to the contralateral temporal lobe, first to the hippocampus (RB1-3, RC1-3), then to the amygdala (RA1-3) and shortly thereafter to the more superficial right temporal isocortex (LA5-7, RB5-7). The patient became verbally unresponsive and was probably aphasic. Modified from Gloor (1997).

been suggested that, since the effects of small electrolytic lesions in thalamus or basal ganglia for different syndromes are similar to those produced by DBS, the high-frequency stimulation (100–250 Hz) used in the latter method may block local cell activity [56]. However, in light of the ability of some rostral intralaminar thalamic neurons to fire spike-bursts with intra-burst frequencies as high as 1,000 Hz, with no evidence of depolarization block [57], and the fact that many other thalamic and basal ganglia neurons fire spike-bursts or spike-trains at frequencies up to 300 Hz, it was suggested that the DBS' effect is not due to depolarization block, but to failure of synaptic transmission by transmitter depletion [58, 59].

Different epileptogenic substances have been topically applied on neocortex or hippocampus, among them acetylcholine, pentylenetetrazol, picrotoxin, strychnine and, especially, penicillin [60]. Intracellular studies of foci produced by topical application of different drugs started in the 1960s and the results of those investigations led to the description of paroxysmal depolarizing shifts (PDSs) as giant postsynaptic potentials [61]. Isolated PDSs, induced by topical application of penicillin on neocortex and leading to electrical seizures, may be used to investigate the differential effect of arousing brainstem reticular formation or midline thalamic stimulation on single PDSs occurring immediately after drug application, which are suppressed by brainstem core or thalamic stimuli, and on full-blown seizures, which are potentiated by the same type of stimulation [62]. The suggestion in earlier studies [63] that inhibitory postsynaptic potentials (IPSPs) are prominent in the penicillin focus is supported by recent investigations showing prominent Cl^--dependent IPSPs during the PDSs of cortically generated spike-wave seizures and increased firing rates of fast-spiking (GABAergic local-circuit neocortex) neurons during these paroxysmal depolarizations [64].

Topical application of convulsants metals, such as alumina cream or cobalt [65], and focal freezing of neocortex [66] have been employed to produce seizures in acutely prepared and chronically implanted animals.

Following the classic findings of Lennox and Lennox [67] on the heritability of seizures in a relatively high proportion of relatives of children with absence (petit-mal) epilepsy, different types of animal models have been bred to display absence epilepsy in rats, absence and myoclonic seizures in tottering, lethargic and stargazer mice, and tonico-clonic seizures in mongolian gerbils [68]. Cellular data recorded from some of these models, especially related to typical

[55] The first use of deep brain stimulation (DBS) dates back to the 1950s, and has been employed in patients suffering from depression, anorexia, schizophrenia and other psychic disorders (Heath, 1954; Pool, 1954). For a review of DBS and its future prospects, see Mogilner et al. (2001). DBS in the region of thalamic centromedian-parafascicular (CM-Pf) complex has been used in intractable seizures by Velasco et al. (1995, 2001).

[56] Benazzouz and Hallett (2000); Beurrier et al. (2001).

[57] Steriade et al. (1993c).

[58] Urbano et al. (2001). The hypothesis of synaptic transmission failure in deep brain stimulation was confirmed by these authors in studies performed in thalamocortical slices, using voltage-sensitive dye imaging.

[59] Bishop et al. (1959); Curtis and Eccles (1960). See also Grill and McIntyre (2001) for other hypotheses and computational models for the effects of deep brain stimulation.

[60] See Table 1, drug concentration, and different experimental methods in Prince (1975).

[61] Dichter and Spencer (1969a-b); Matsumoto et al. (1969); Johnston and Brown (1981, 1984). See also section **5.4** in Chapter 5.

[62] Steriade (1960). As this paper was published in Romanian, see Fig. 68 reproduced in Kreindler (1965).

[63] Prince (1968).

[64] Steriade et al. (1998c); Timofeev et al. (2002c). See details in sections **5.4**, **5.5** and Fig. 5.65 in Chapter 5.

[65] Reviewed in Ward (1975).

[66] Morrell (1960) recorded discharges in "mirror foci" contralateral to the induced freezing area. Independent "mirror foci" could also be recorded in the unanesthetized frog forebrain (Wilder and Morrell, 1967). Smith and Purpura (1960) used a metal rod attached to a refrigerant chamber. Intracellular recordings from neocortex revealed a variety of patterns (depolarizations and hyperpolarizations) in different neurons during the depth-positive focal EEG waves induced by freezing (Goldensohn and Purpura, 1963).

[67] Lennox and Lennox (1960).

[68] Reviewed in Buchhalter (1993), Danober et al. (1998), Noebels (1999) and Seyfried and Todorova (1999). For a discussion of clinical aspects in different types of genetic generalized epilepsies, see Treitman and Treitman (1999).

spike-wave complexes at ~3 Hz and to electrographic patterns of the Lennox–Gastaut syndrome, are discussed and illustrated in sections **5.5** and **5.6** of Chapter 5.

In the following chapters, I shall discuss at length the neuronal substrates of sleep and epilepsy states, which constitute the aim of this monograph.

Chapter 2 Neuronal types and circuits in sleep and epilepsy

[1] Albe-Fessard and Buser (1955).

[2] Li and McIlwain (1957); Yamamoto and McIlwain (1966).

[3] Connors et al. (1982).

[4] Schwartzkroin (1975); Wong et al. (1979).

[5] Jahnsen and Llinás (1984a-b).

[6] Kita and Kitai (1990); Leonard and Llinás (1990, 1994).

The understanding of neuronal mechanisms underlying different states of sleep and epilepsy requires a detailed exposé of various neuronal types and networks in the major brain structures that generate these behavioral conditions; that is, neocortex, archicortex and related systems (rhinal cortices and amygdala), thalamus, and generalized systems that modulate the excitability of forebrain structures. Despite the innumerable neurons located in these structures and their diverse temporal patterns of repetitive firing, unifying principles can group individual neurons into a limited number of classes. This chapter deals with neuronal types and with local and distant connections among neurons, placing emphasis on peculiar neuronal features that may play a role in certain aspects of sleep and seizures.

One of the conclusions resulting from data presented in this chapter is that synaptic activities within complex neuronal networks modulate, and often overwhelm, intrinsic neuronal properties. In the absence of rich synaptic activity, as is the case in brain slices and isolated cortical slabs *in vivo*, neuronal properties mainly result from a host of voltage-dependent and transmitter-gated conductances. Analyses of the same neuronal types in the intact brain, under anesthesia and especially in naturally alert preparations, demonstrate that intrinsic neuronal properties display dramatic alterations with changes in membrane potential and increased synaptic activity during behavioral states.

The intrinsic properties of cortical and thalamic neurons were first revealed in brain slices. Following *in vivo* intracellular recordings of neocortical neurons in the early 1950s [1], extra- and intracellular recordings from isolated neocortical tissue and slices from allocortex maintained *in vitro* were initiated during the late 1950s and 1960s [2], and intensive researches on intrinsic neuronal properties in neocortex [3], archicortex [4], thalamus [5] and brainstem cholinergic nuclei [6] were conducted between the 1970s and the early 1990s. The advantages of studies in slices are the control of the extracellular ionic environment, the possibility of investigating the actions of neurotransmitters on various neuronal types after

blockage of synaptic transmission, and the simultaneous exploration of different neuronal compartments. However, investigators *in vitro* have recommended that the enthusiasm for work in slices must be tempered with caution [7] because the biological and physical reactions occurring in the traumatized tissue may change the physiological properties of neurons described *in vitro*, compared to those seen in the intact brain. Besides, the majority of studies are still conducted on isolated slices, leaving related systems aside [8]. Despite these disadvantages, work in slices has provided new insights into the functions of different brain structures and changed our thinking on the electrical properties of central neurons by replacing the purely reflexologic view of input-output operations with concepts based on intrinsic properties of neurons [9].

2.1. Neocortical neuronal types

Neocortical neurons are characterized electrophysiologically by their responses to depolarizing current pulses, and intracellular staining reveals their morphology. The classification of neuronal types by their intracellularly recorded responses to direct depolarization results from work in slices maintained *in vitro* [3, 10], in acutely prepared animals under deep anesthesia [11, 12, 13] and, recently, in chronic experiments on naturally awake cats [14, 15].

2.1.1. Four major types of neocortical neurons and their subclasses

Four cellular types are commonly described in neocortex (Fig. 2.1). *(a)* Regular-spiking (RS) neurons constitute the majority of cortical neurons. They display trains of single spikes that adapt quickly or slowly to maintained stimulation. *(b)* Fast-rhythmic-bursting (FRB) neurons give rise to high-frequency (300–600 Hz) spike-bursts recurring at fast rates (30–50 Hz). *(c)* Intrinsically bursting (IB) neurons generate clusters of action potentials, with spike inactivation, followed by hyperpolarization and neuronal silence. *(d)* Fast-spiking (FS) neurons fire thin action potentials and sustain tonically very high firing rates without frequency adaptation. The duration of intracellularly recorded action potentials at half amplitude, measured during the state of natural waking in chronically implanted cats, shows modes between 0.6 and 1 ms in RS neurons. Slightly longer spikes are fired by IB neurons. In contrast, both FRB and FS neurons demonstrate much shorter action potentials, with modes at about 0.3 ms (Fig. 2.1) [14].

[7] Connors and Gutnick (1990).

[8] More recently, investigations have been performed in slices containing some of the reciprocal connections between thalamus and cortex (Agmon and Connors, 1991; Kao and Coulter, 1997; Tancredi et al., 2000; Urbano et al., 2001).

[9] See Llinás (1988).

[10] McCormick et al. (1985).

[11] Nuñez et al. (1993).

[12] Gray and McCormick (1996). These authors recorded *in vivo* neurons termed "chattering", which, in our nomenclature, are called fast-rhythmic-bursting (FRB; see [13]). *In vitro*, FRB neurons are not seen in visual cortex of ferrets that are less than 4 months of age (Brumberg et al. 2000). The factor that complicates the recording of this neuronal type in cortical slices is the composition of the ionic medium that requires 1.2 mM $[Ca^{2+}]_o$, while most *in vitro* studies use $[Ca^{2+}]_o$ of 2 mM or more. An increased excitability by decreasing $[Ca^{2+}]_o$ (Hille, 1992) may lead to the transformation of neuronal firing patterns, from an RS into an FRB type (see main text). With an ionic composition *in vitro* closer to that in the intact brain, FRB neurons could be recorded from slices (Brumberg et al., 2000).

[13] Steriade et al. (1998b).

[14] Steriade et al. (2001a). One of the ideas expressed in this paper, namely, that intrinsic properties of neocortical cells are not invariant, as they are seen in slices maintained *in vitro*, but are much more flexible, depending on synaptic activity and/or shifts in the state of vigilance (see below, Figs. 2.12 and 2.13, section ***2.1.3***), was recently supported by an *in vivo* intracellular study of prefrontal cortical neurons (Dégenètais et al., 2002). These authors demonstrated that intrinsically bursting and fast-adapting regular-spiking cells display different firing patterns depending on the intensity of depolarizing current. They also demonstrated that non-inactivating bursting cells displayed variations in their discharge patterns, ascribable to the impact of synaptic activity.

[15] Timofeev et al. (2001b).

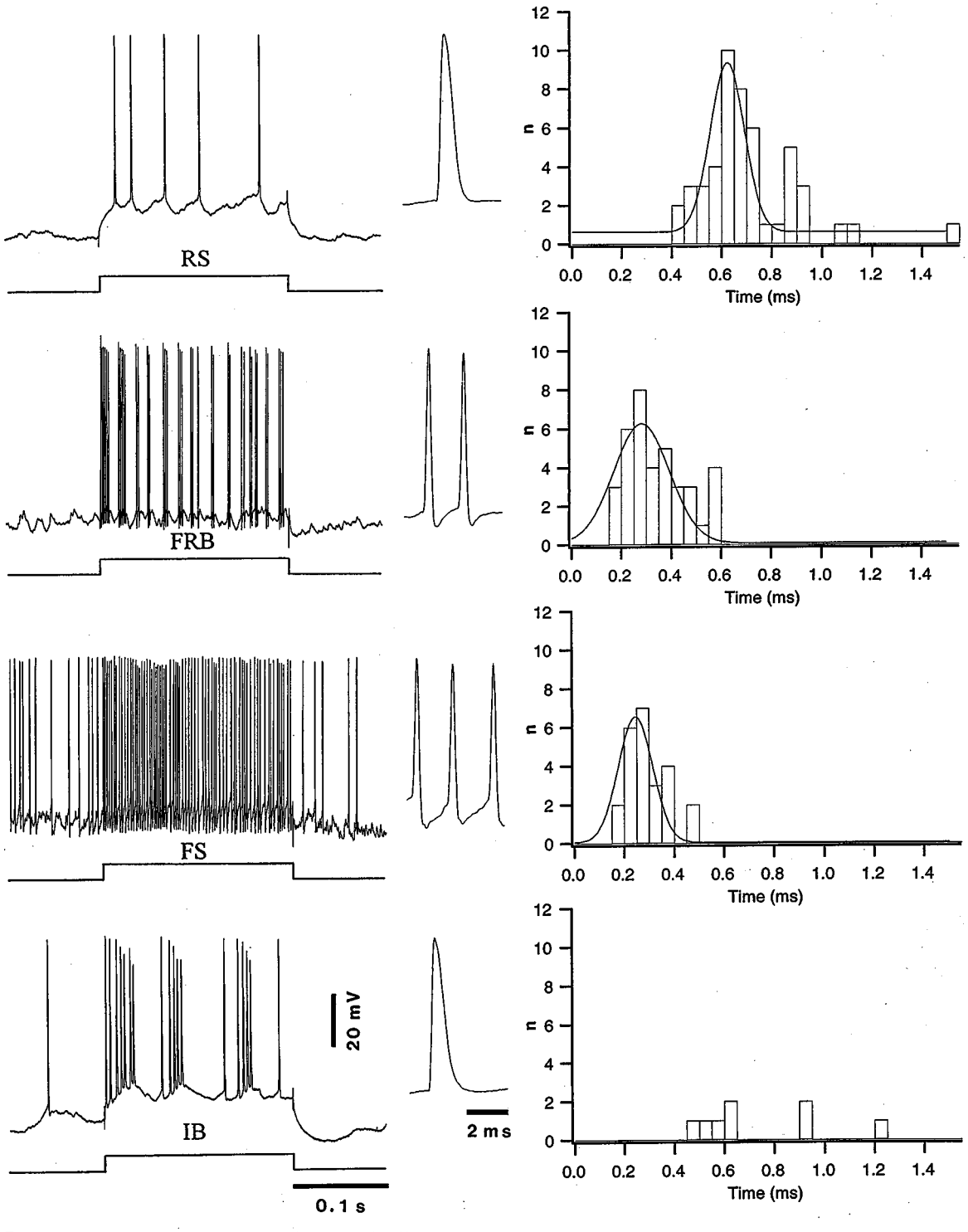

Fig. 2.1 Electrophysiological identification of different cell classes in neocortex. Chronically implanted, awake cat. Left column depicts responses of regular-spiking (RS), fast-rhythmic-bursting (FRB), fast-spiking (FS) and intrinsically bursting (IB) neurons from area 4 to depolarizing current pulses (0.2 s, 0.8 nA). At the right of each depolarizing current pulse, action potentials of each cell class are shown; note thin spikes of FRB and FS neurons, compared to those of RS and IB neurons. Right column illustrates the width of action potentials (at half amplitude) in a sample of 117 neurons (48 RS, 37 FRB, 24 FS and 8 IB, corresponding to patterns depicted on the left). See description of neuronal responses in text. From Steriade et al. (2001a).

The rhythmic bursting of IB neurons is different from that of FRB neurons because of at least two features: the interspike intervals are distributed regularly within the spike-bursts of FRB neurons (Fig. 2.2), thus lacking the first long interspike intervals that are typical for IB neurons (Fig. 2.1); and action potentials are not inactivated during the bursts of FRB neurons (Fig. 2.2). The spike-bursts in IB neurons develop from a depolarizing afterpotential (DAP), as is also the case for FRB neurons (see arrows in Fig. 2.2). The DAPs of IB neurons are enhanced by Ca^{2+} channel blockade and are sensitive to substances such as tetrodotoxin (TTX) and QX314, which suggests that DAPs are due to the activation of the persistent Na^+ current, $I_{Na(p)}$ [16]. As to the high-frequency repetitive firing of FRB neurons, it is probably related to the presence of voltage-gated K^+ currents of the Kv3 subfamily, which are characterized by very fast deactivation rates, a property that underlies fast repolarization of action potentials without compromising spike initiation or height [17]. The very brief duration of spikes fired by FRB neurons, ~0.3 ms at half amplitude (see Fig. 2.1), may be ascribed, at least partially, to these K^+ currents [18].

Generally, RS, FRB and IB neurons are pyramidal-shaped neurons, while FS firing patterns are conventionally regarded as defining local GABAergic cells (GABA is γ-aminobutyric acid). However, in addition to pyramidal-shaped FRB neurons, other neurons, with the same FRB firing patterns, are local-circuit, sparsely spiny or aspiny interneurons [13] (Fig. 2.2*B*). And, some local inhibitory interneurons discharge like RS or bursting cells [19]. These are variations around a theme, in contrast with the invariable responses obtained in extremely simplified preparations, thus indicating that each of the aforementioned four firing patterns does not necessarily apply to a single class of neurons. Below, I will take a few examples to show that the location of various neuronal types is far from being exclusively confined to distinct cortical layers, as suggested in earlier slice studies, and that the electrophysiological characteristics of different cortical cell types are much more flexible than conventionally thought.

Initially, IB neurons recorded from sensorimotor cortical slices were found at a narrow range of depths, comprising layer IV and the more superficial parts of layer V [3]. This precise localization ascribed a unique physiological signature to pyramidal neurons in layer V [20]. Subsequent studies, both *in vivo* [21] and *in vitro* [16, 22], found that IB neurons are also located in superficial layers. The majority (~70%) of IB neurons located in layer III displayed an initial burst followed by single action potentials, while the remaining neurons exhibited repetitive bursting (Fig. 2.3).

[16] Nishimura et al. (2001). An earlier paper by the same authors (1996) revealed the presence of IB neurons in layer III of cat sensorimotor cortex. The more recent (2001) study investigated the ionic mechanisms generating bursting in layer III IB cells, in particular the $I_{Na(p)}$ (see main text). The same current, $I_{Na(p)}$, found in hippocampal pyramidal neurons (MacVicar, 1985; French et al., 1990), seems to be responsible for intrinsically generated bursts in hippocampal neurons. Other currents of cortical pyramidal neurons are a hyperpolarization-activated, inwardly rectifying cation current, I_H (Solomon et al., 1993); a low-threshold Ca^{2+} current de-inactivated by hyperpolarization (Kawaguchi, 1993; de la Peña and Geijo-Barrientos, 1996); high-threshold Ca^{2+} currents (Brown et al., 1993); and a series of K^+ currents (Schwindt et al., 1988a-b, 1989) (see also [17]).

[17] Rudy and McBain (2001).

[18] FRB (or "chattering") neurons have been described in cats [12–13] and have not yet been described in rats and mice, species in which Kv3 proteins have not been detected in cortical pyramidal neurons (see Chow et al., 1999).

[19] Thomson et al. (1996).

[20] Connors and Amitai (1995).

[21] Steriade et al. (1993e).

[22] Chen et al. (1996). This *in vitro* work on cat motor cortex investigated the electrophysiology and morphology of regular-spiking (RS) and intrinsically bursting (IB) neurons in another species than rodents that are usually employed in slice studies. The authors found bursting neurons "in all layers below layer I", with apical dendrites densely coated with dendritic spines.

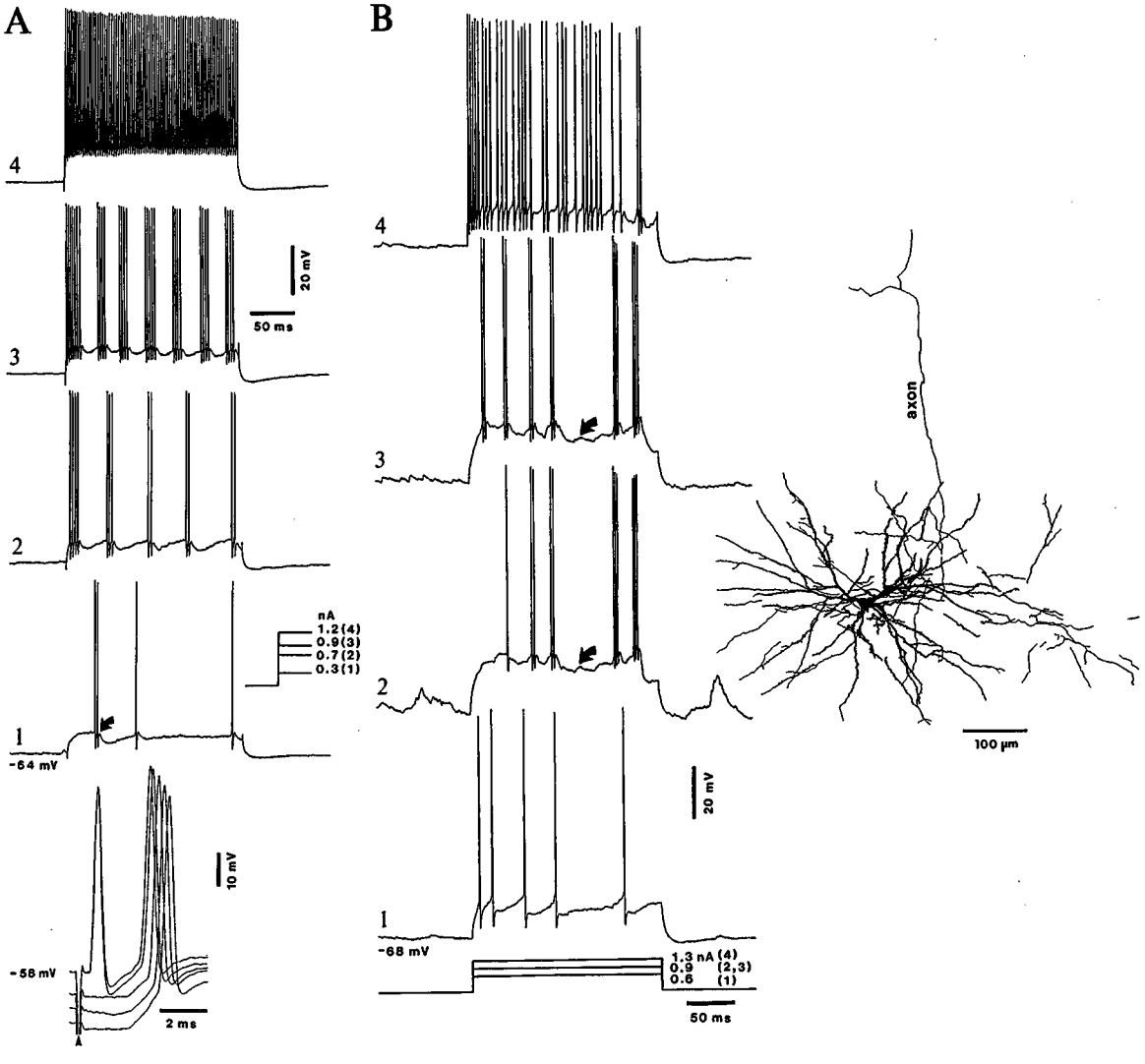

Fig. 2.2 Corticothalamic neurons and local-circuit (basket-type) neurons display fast-rhythmic-bursting (FRB) firing patterns that develop into fast-spiking (FS) patterns. Intracellular recordings in cats under ketamine-xylazine anesthesia. *A*, corticothalamic neuron from area 7, projecting to the lateroposterior (LP) nucleus. Depolarizing current pulses at different intensities (shown) elicited changing patterns, from single spikes (*1*) to spike-bursts at 25–35 Hz (*2–3*) and, eventually, FS patterns (*4*). A depolarizing afterpotential (DAP) is indicated by an arrow in *1*. Below, antidromic identification of a corticothalamic neuron, displaying the same changes in firing patterns. Stimulus (arrowhead) was applied to the thalamic LP nucleus. Note failure of antidromic response at membrane potentials more negative than −58 mV and appearance of excitatory postsynaptic potentials (EPSPs). This is a typical example of a neuron interposed in a corticothalamocortical loop. *B*, morphologically identified local-circuit (basket-type) cell located in layer III of area 7. Spontaneous action potentials showed their very brief duration (0.3 ms at half amplitude; not depicted). Changes in firing patterns, from regular-spiking (RS in *1*) to FRB (*2–3*) and finally to FS patterns (*4*), similarly to those shown in panel *A* for a corticothalamic neuron. DAPs are marked by arrows in *2–3*. At right, camera-lucida reconstruction of this neuron (see photomicrograph in Steriade et al., 1998b). Modified from Steriade et al. (1998b).

[23] In their *in vitro* study of layer VI pyramidal neurons from cat motor cortex (area 4γ), Kang and Kayano (1994) made the incidental observation ("to our surprise") that, after prolonged and strong direct depolarization, the firing of an RS neuron developed into that of an FRB neuron, with spike-bursts at ~20 Hz (see their Fig. 3). This change is similar to that depicted in Fig. 2.2 for both corticothalamic and local-circuit inhibitory neurons recorded *in vivo*, which develop their discharges into FRB patterns by increasing the strength of direct depolarization.

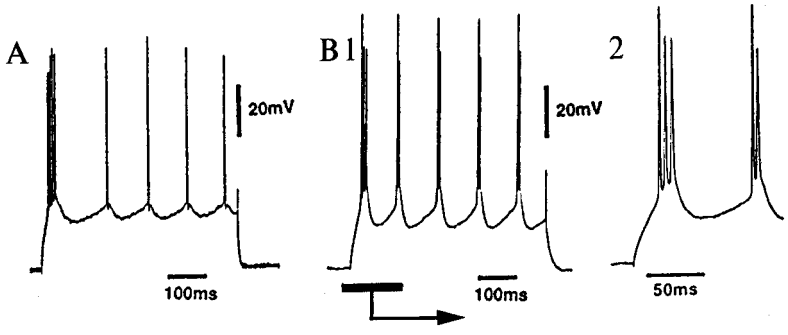

Fig. 2.3 Burst-and-regular firing and repetitive spike-bursts of intrinsically bursting (IB) cells in layer III from *in vitro* slices of cat motor cortex. *A*, burst followed by single action potentials (0.35 nA depolarizing current pulse). *B*, repetitive spike-bursts of IB neuron (0.25 nA depolarizing current pulse). The initial bursts are expanded on the right. Modified from Nishimura et al. (2001).

Similarly to the case of IB neurons, which were initially found only in layers IV–V, but subsequently recorded from all layers below layer I, FRB (also termed "chattering") neurons were only found in superficial layers of the visual cortex [12], but subsequently recorded at all investigated depths, from 0.25 to 1.5 mm, in motor and association cortical areas [13]. The deep location of FRB neurons was demonstrated by antidromic invasion from appropriate thalamic nuclei (Fig. 2.2*A*) and intracellular staining [13], both procedures demonstrating their location in layer VI [23].

One of the difficulties in maintaining a strict classification in four distinctly separate cortical cell classes (RS, FRB, IB, and FS) stems from the fact that neurons with brief (0.3–0.4 ms) action potentials and tonic firing without frequency adaptation (like FS-firing cells), conventionally regarded as local-circuit GABAergic neurons, were actually identified as long-axoned, corticothalamic cells (Fig. 2.2*A*). An adding factor against this strict classification is the transformation of firing patterns in the same cortical neuron. Thus, the same intracellularly recorded and stained corticothalamic neuron, or local-circuit sparsely spiny basket (presumably inhibitory) interneuron, may pass from an RS to an FRB and eventually an FS firing pattern by increasing the strength of the depolarizing current pulse (Fig. 2.2*A*–*B*). This transformation in discharge patterns, by increasing the intensity of direct depolarization, also occurs in chronically implanted, naturally awake animals (Fig. 2.4).

Network activity during various functional states modifies the firing patterns generated by intrinsic neuronal properties. Typical FRB patterns, evoked during the silent background activity of

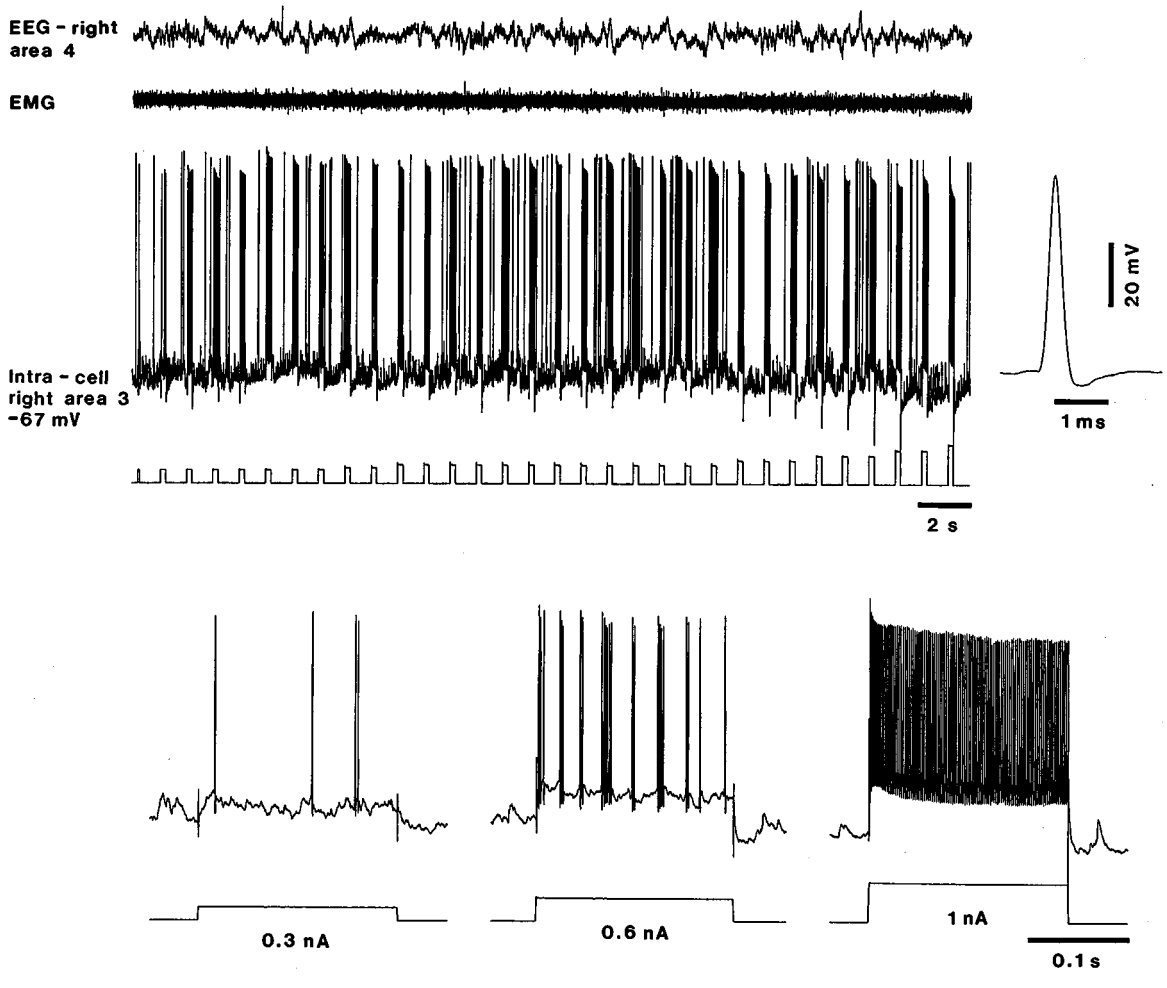

Fig. 2.4 Changing firing patterns in the same cortical neuron by increasing the strength of direct depolarization. Chronically implanted, awake cat. Intracellular recording from area 3 (somatosensory) neuron, together with EEG from area 4 and electromyogram (EMG). Depolarizing current pulses (0.2 s in duration) with different intensities evoked different firing patterns: RS (0.3 nA), FRB (0.6 nA) and FS (1 nA). Compare with similar data in anesthetized cats, depicted in Fig. 2.2. Unpublished data by M. Steriade, I. Timofeev and F. Grenier.

inter-spindle lulls (similar to the absence of, or poor, background activity seen in slices), develop into patterns resembling FS-type firing during epochs with spindle sequences, with rich synaptic activity produced by thalamocortical volleys (Fig. 2.5). The importance of synaptic activity in a living animal, compared to slices, is underlined by striking differences in connectivity and incidences of synaptic potentials between slightly different sizes of slices. *In vitro* studies on sensorimotor neocortex showed that, out of 595 dual recordings in which an interneuron was recorded simultaneously with a pyramidal neuron in slices 400 μm thick, 39 yielded

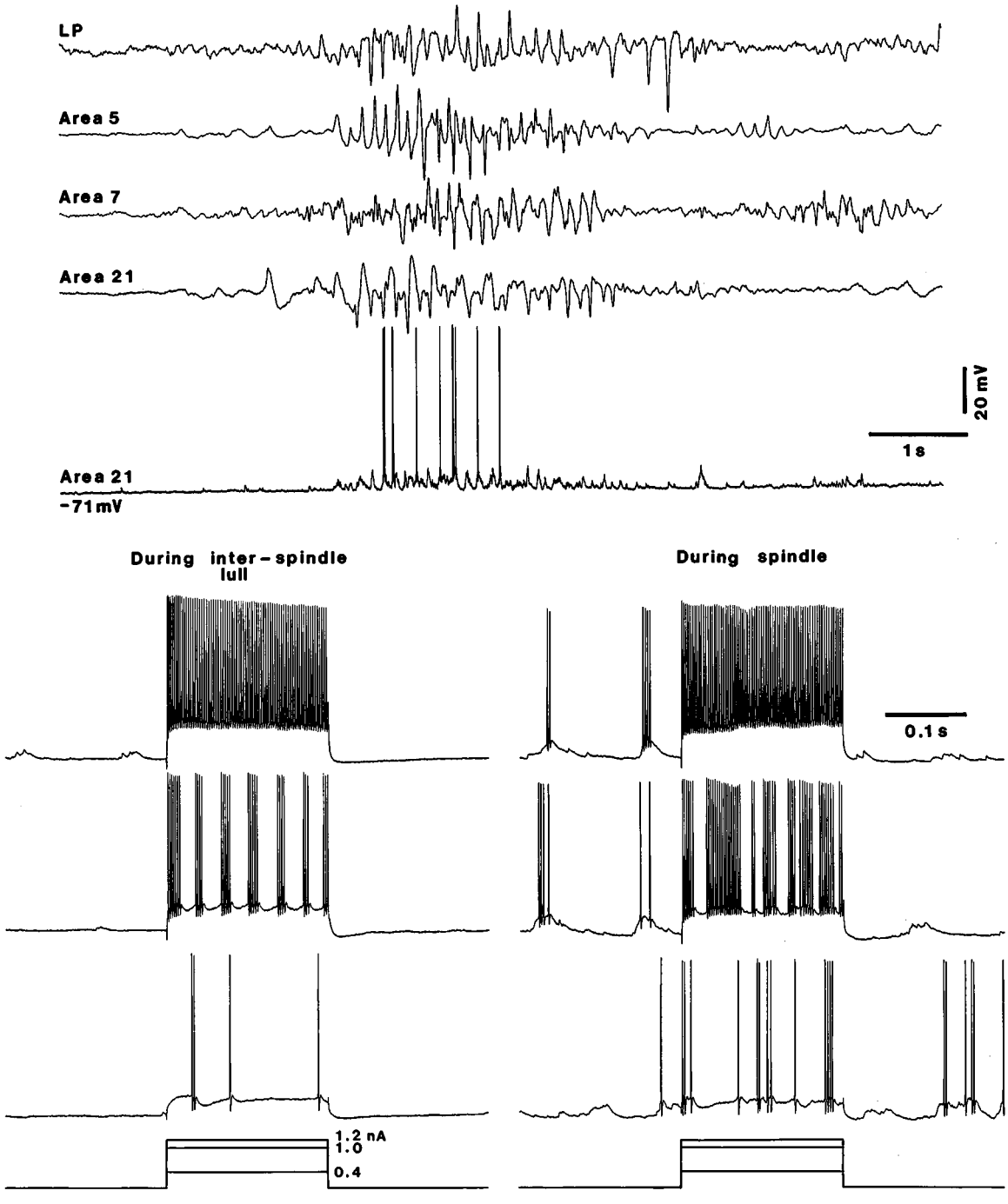

Fig. 2.5 Changes in responses of a corticothalamic neuron from area 21 (antidromically identified from the lateroposterior, LP, nucleus) to depolarizing current pulses with different intensities during periods poor and rich in synaptic activity. Cat under barbiturate anesthesia. Field potentials were simultaneously recorded from the related thalamic LP nucleus and from the depth of cortical areas 5, 7 and 21 (the latter in the immediate vicinity of the impaled neuron). Depolarizing current pulses (duration 200 ms) with three intensities (0.4, 1, and 1.2 nA) were applied during inter-spindle lulls, with negligible or absence of synaptic activity (as in slices), and during spindle sequences, rich in synaptic activity generated by thalamocortical volleys. Note, at 1.0 nA (middle trace), the transformation from rhythmic (35 Hz) spike-bursts (FRB pattern) during inter-spindle lull into high-frequency tonic firing (450 Hz) with short interruptions in activity (similar to the FS-like pattern) during network synaptic activity produced by spindles. Modified from Steriade et al. (1998b).

monosynaptic, single axon IPSPs, i.e. an average probability of 1:15 of each recorded inhibitory interneuron contacting a neighboring pyramidal cell; however, with slices 500 μm thick, the probability of connections rose about three times and spontaneous activity increased significantly [19, 24]. The increase in connectivity and background activity on increasing the slice thickness by just 0.1 mm may explain the differences between some results from slices and those from the intact brain.

The above data show that changes in membrane potential and a high degree of synaptic activity in the intact brain decisively modulate, and even transform, the firing patterns due to intrinsic neuronal properties and expressed by responses to direct depolarization.

The local-circuit inhibitory cortical neurons express a high diversity that arises not only from the fact that, morphologically, cortical interneurons are of at least five to seven classes [25], but also from their different electrophysiological features. Then, in the light of recent studies, the earlier classification of cortical neurons, with one category of local interneurons displaying FS firing patterns [10], cannot encompass the diversity of synaptic contacts from interneurons on different compartments of pyramidal neurons as well as interneuronal responses to synaptic volleys of different origins. Before the immunohistochemical identification of the GABAergic nature of local-circuit cortical neurons, Ramón y Cajal [26], Lorente de Nŏ [27] and Szentágothai [28] described the axonal arborizations of local interneurons in cortex. Among different types of local-circuit GABAergic neurons (Fig. 2.6), *(a)* basket cells are located in all layers, mainly III and V/VI, their axons contact the soma and proximal dendrites of pyramidal neurons, and they innervate themselves through autapses; *(b)* chandelier neurons are mainly located in layers II/III and their main target is the initial segment of pyramidal cell axons, thus having a strategic location for preventing the latter to communicate with other neurons; *(c)* double bouquet dendritic neurons are concentrated in layers II/III and their vertical axons contact pyramidal and local interneurons; *(d)* neurogliaform cells, the smallest interneurons (soma diameter, 10–12 μm), are found in superficial layers, mainly layer I, and have a very dense axonal arbor; and *(e)* Martinotti cells are found in deep layers, mainly layer VI [29]. In addition to GABA, some local cortical interneurons are immunoreactive to somatostatin, vasointestinal peptide, calcium-binding proteins and nitric oxide synthase [30]. Three distinct families of GABAergic neurons could be identified in the visual cortex by the expression of parvalbumin (PV), calretinin

[24] Thomson (1997).

[25] Jones (1975) and his comprehensive reviews (1995, 1998). See also Colonnier (1966, 1968) who described the large variety of local interneurons and the fact that somata of pyramidal neurons, on which basket cells terminate, are covered by type II synapses (Gray 1959), presumably inhibitory.

[26] Ramón y Cajal (1911).

[27] Lorento de Nó (1933).

[28] Szentágothai (1978).

[29] Jones (1975); Somogyi (1977, 1989); Somogyi and Soltesz (1986); Somogyi et al. (1985); DeFelipe (1993); Hestrin and Armstrong (1996)

[30] Kawaguchi and Kubota (1993, 1996, 1997). Another study combined whole-cell recordings with simultaneous detection of three calcium-binding proteins in slices from frontal cortex of rats and described three groups of non-pyramidal neurons according to their patterns of discharges (Cauli et al., 1997).

[31] Gonchar and Burkhalter (1997).

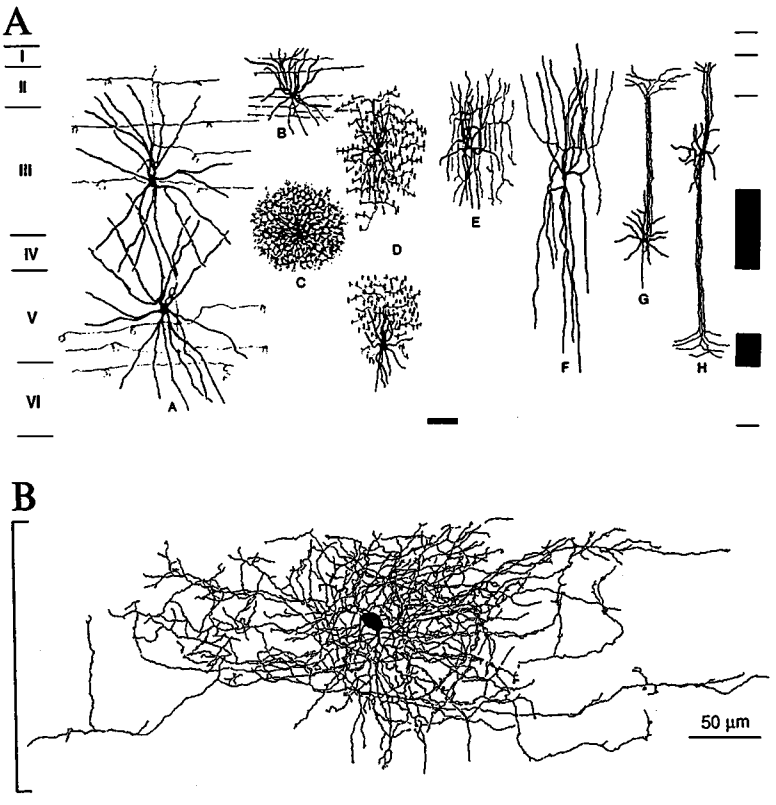

Fig. 2.6 Morphology of local neocortical interneurons. *A*, the principal types of local interneurons in the sensory and motor areas of monkeys, drawn from Golgi stains. **(A)**, large basket cells. **(B-C)**, small basket cells. **(D)**, chandelier cells. **(E)**, peptide cells. **(F)**, bipolar cell. **(G)**, small spiny cell. **(H)**, double bouquet cell. The dark rectangles to the right locate the zones of termination of specific thalamocortical axons and layers of highest density of immunocytochemical staining for glutamic acid decarboxylase. Bar: 0.1 mm. *B*, a biocytin-stained neurogliaform in layer I of rat visual cortex. Borders of layer I are indicated at the left of the drawing. The extensive axonal arbor extends close to the border of layer I but does not enter layer II. The central location of the soma is typical of these cells. Modified from Jones (1975; *A*) and from Hestrin and Armstrong (1996; *B*).

(CR) and somatostatin (SOM); the majority of PV, CR and SOM are GABA positive (Fig. 2.7) [31].

The complex connections between GABAergic interneurons and glutamatergic pyramidal neurons, as well as the connections among GABAergic neurons themselves, are depicted in Fig. 2.8. In essence, distinct classes of GABAergic cells innervate pyramidal cells and other GABAergic cells in a domain-specific manner, co-aligning their termination zone with glutamatergic pathways; the output of pyramidal neurons is controlled by chandelier (axo-axonic) neurons; and axons arising from generalized modulatory

[32] Somogyi et al. (1998).

[33] Somogyi and Cowey (1981); Tamás et al. (1997).

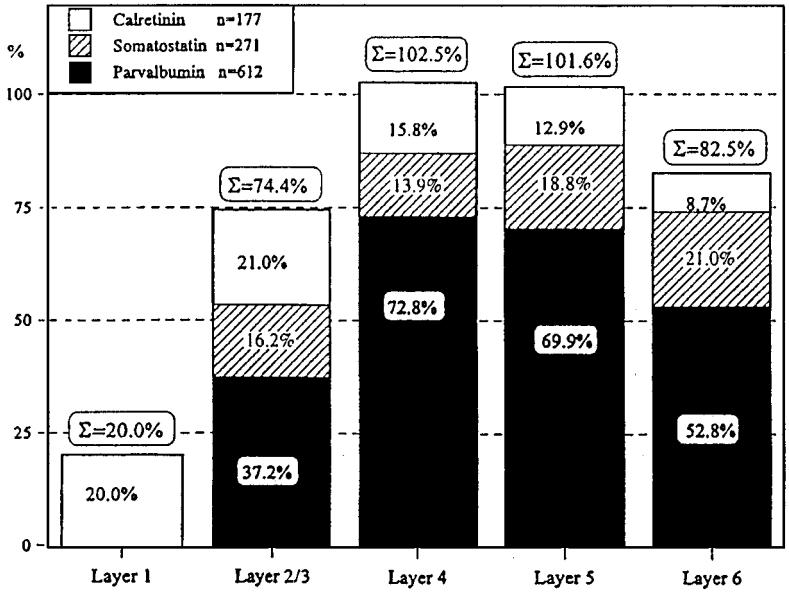

Fig. 2.7 Summed proportions of parvalbumin (PV), calretinin (CR), and somatostatin (SOM) immunoreactive neurons in different layers of rat visual cortex (area 17). Values >100% in layers IV and V indicate that the number of GABAergic neurons in the overall population was slightly underestimated. From Gonchar and Burkhalter (1997).

(monoaminergic and cholinergic) systems innervate specific local-circuit neuronal classes. The basic circuit is repeated in each layer, and both tangential and columnar connections are established through additional specific links, involving local-circuit GABAergic and pyramidal glutamatergic neurons [32]. In addition to the usual terminations of interneuronal axons at the perisomatic domain of pyramidal neurons, some GABAergic cells (such as double bouquet, neurogliaform and bitufted cells) terminate on distal dendrites and spines of pyramidal neurons [33].

The responses of pyramidal and local-circuit neurons to stimulation of GABAergic interneurons have been studied in slices, using dual, triple and quadruple intracellular recordings. With dual intracellular recordings from presynaptic interneurons and postsynaptic pyramidal cells, three classes of interneurons (classical FS, RS, and burst firing) activated $GABA_A$ receptors in the perisomatic domain of pyramidal cells [19]. Simultaneous recordings from inhibitory cells and multiple postsynaptic targets led to several classifications according to the firing patterns of interneurons that determine the functional impact of various interneuronal classes, the spatial distribution of their axonal trees, and the efficacy of

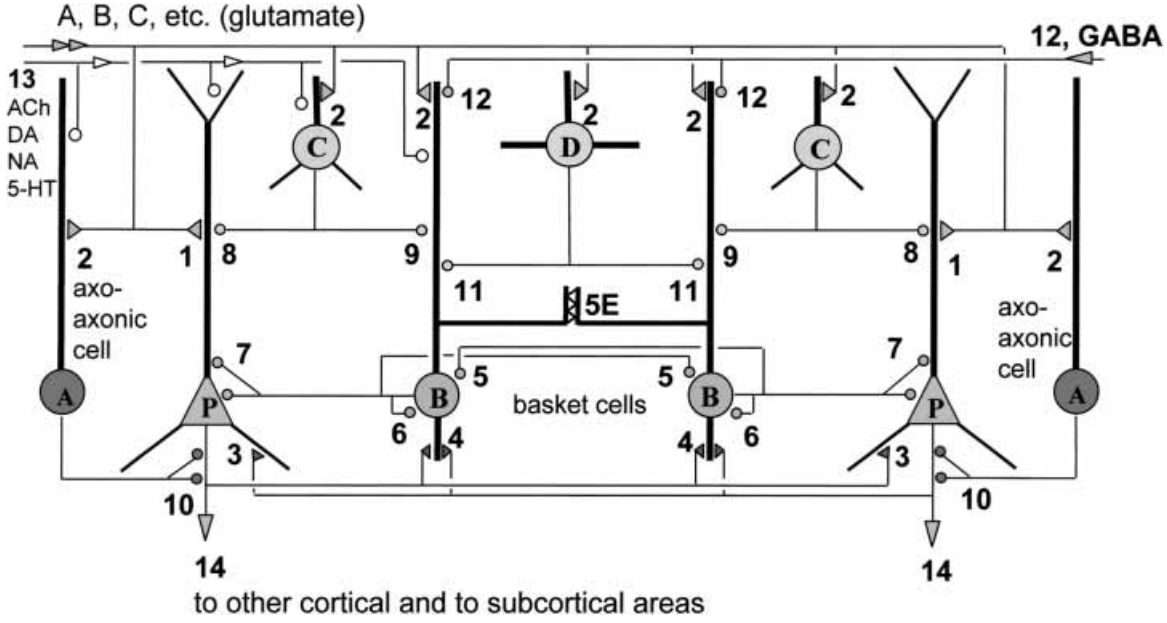

Fig. 2.8 Simplified summary of the major classes of synaptic connections in the basic cortical circuit of the cerebral cortex. Only one type of pyramidal cell (P) and a set of local-circuit GABAergic cells (filled circles) are shown. They are innervated by sets of extrinsic glutamatergic pathways (A, B, C, etc.; only one shown for clarity) making synapses with both the principal cells (1), and GABAergic interneurons (2). Ensembles of pyramidal cells are extensively interconnected (3), and also innervate some classes of GABAergic cell (4). The perisomatically terminating (7) basket cells (B) are also extensively interconnected through both chemical (5) and electrical synapses (5E), and innervate themselves through autapses (6). Several distinct classes of GABAergic cells (C, one class shown for clarity) innervate the pyramidal cells (8), and other GABAergic cells (9) in a domain-specific manner, co-aligning their termination zone with glutamatergic pathways (1, 2). The output of pyramidal cells is influenced by the GABAergic axo-axonic cells (A), which are unique to the cortex and selectively innervate (10) the axon initial segments. Some GABAergic cells (D) specialize in the innervation of other GABAergic cells (11). Extrinsic GABAergic (12) and monoaminergic (13, including acetylcholine (ACh)) afferents innervate specific interneuron classes as well as principal cells. The output of the circuit is predominantly via the pyramidal axons (14). In the isocortex, this circuit is repeated in each layer of a column, sometimes several times as multiple sets of output neurones evolved, and both tangential and columnar connections are established between the basic circuits through additional specific links, involving both the GABAergic and the glutamatergic neurons. (Modified by P. Somogyi after Somogyi et al., 1998.) Courtesy of Dr. P. Somogyi. See Plate section for color version of this figure.

[34] Gupta et al. (2000).

[35] Thomson et al. (1993a); Markram (1997); Markram et al. (1997a, 1998); Thomson and Deuchars (1997).

[36] Galarreta and Hestrin (1999).

synapses made with pyramidal neurons [34]. Studies using paired recordings from pyramidal and local interneurons also demonstrated that synaptic transmission is differentially exerted by the same axon of a pyramidal neuron innervating another pyramidal cell and a local inhibitory interneuron, with synaptic depression in the former case and facilitation in the latter [35]. These effects are important for understanding the rules underlying frequency-dependent plasticity.

Paired-cell recordings also revealed networks of electrically and chemically coupled inhibitory interneurons. Some FS neurons are connected by both electrical and chemical synapses [36]. When

recording from two types of local-circuit GABAergic neurons, FS-type and low-threshold-spiking (LTS-) type, electrical synapses are only found among the same type [37]. However, chemical inhibitory synapses are found between both types (FS and LTS) of interneurons (Fig. 2.9*A*). Excitatory inputs from thalamocortical pathways are much stronger in FS than in LTS interneurons (Fig. 2.9*C*) and fast repetitive stimuli of thalamic axons produce depression in FS interneurons, quite opposite to the facilitation produced by axons from cortical RS neurons at the same fast frequency (Fig. 2.9*D*). These connections are important for the oscillatory properties in normal (Chapter 3) and paroxysmal (Chapter 5) states [38].

2.1.2. Different incidences of neuronal types under various experimental conditions

The incidences of different neuronal types in neocortex are generally taken from studies performed on slices maintained *in vitro* [3, 10] or from *in vivo* studies conducted on deeply anesthetized cats [11]. The conditions of an alert behavioral condition may change these incidences by the presence of intense synaptic activity.

To determine the proportions of different discharge patterns of various neuronal classes under different experimental conditions, a sample of 120 neurons, which were selected because depolarizing current pulses could be applied in chronically implanted animals during the steady state of quiet waking without phasic motor events [14], was compared with more than 1000 intracellularly recorded neurons recorded from intact cortex under anesthesia [11, 21, 39, 40] and with 160 intracellularly recorded neurons from small isolated cortical slabs *in vivo* [41]. Neurons displaying the firing patterns of conventional FS (presumably local GABAergic) neurons, defined by thin action potentials, high-rate discharges without frequency adaptation and a linear relationship between firing rate and strength of current injection, are much more numerous in experiments on naturally alert animals (24%) than in previous experiments on the intact cortex of anesthetized animals (10%) or in small isolated cortical slabs *in vivo* (4%) (Fig. 2.10). On the contrary, neurons displaying IB firing patterns are found in only 4% of neurons of awake animals, whereas they represent 15% of neurons in anesthetized animals and reach 40% of neurons in isolated cortical slabs (Fig. 2.10) [42]. The difference between the proportions of these firing patterns in any pair of these experimental conditions (namely, awake vs. anesthetized animals; awake animals vs. isolated cortical slabs; and anesthetized animals with intact cortex vs. isolated cortical slabs) is highly significant ($p < 0.0001$, chi-square test).

[37] Gibson et al. (1999). Electrical synapses between LTS-type interneurons contain the gap junction protein connexin36, since electrical coupling is absent in knockout mice and the synchrony of rhythms is weaker (Deans et al., 2001).

[38] Chandelier (axo-axonic) interneurons, which are found in both neocortex and circuits implicating entorhinal cortex and hippocampus, are probably the most efficient inhibitory elements. They were first described in neocortex (Szentágothai and Arbib, 1974; and Somogyi, 1977, who called them axo-axonic cells to specify their functional role) and thereafter also found in the hippocampus (Somogyi et al., 1983, 1985; see section ***2.2.1***). These inhibitory cells are reduced or lost in epileptic foci, in experimental animals and epileptic patients. For example, a selective loss of chandelier cells' axons was found in rat hippocampal transplants that show paroxysmal discharges (Freund and Buzsáki, 1988). In epileptic patients too, there is a decreased incidence of chandelier neurons in entorhinal cortex and subiculum of patients who exhibit a severe neuronal loss in the CA1 field (DeFelipe, 1999). Similar changes were reported in neocortex from patients with temporal lobe epilepsy (Marco and DeFelipe, 1997). The hypothesis was then advanced that the loss of chandelier neurons may be a factor toward the development of epilepsy (DeFelipe, 1999).

[39] Contreras and Steriade (1995).

[40] Amzica and Steriade (1995a-b).

[41] Timofeev et al. (2000a).

[42] The dramatic increase in the incidence of IB neurons in simplified preparations can also be exemplified by the results of a slice study on pyramidal neurons from layers V/VI of rat prefrontal cortex showing that IB neurons represented 64% of recorded neurons, compared to only 19% RS neurons (Yang et al., 1996).

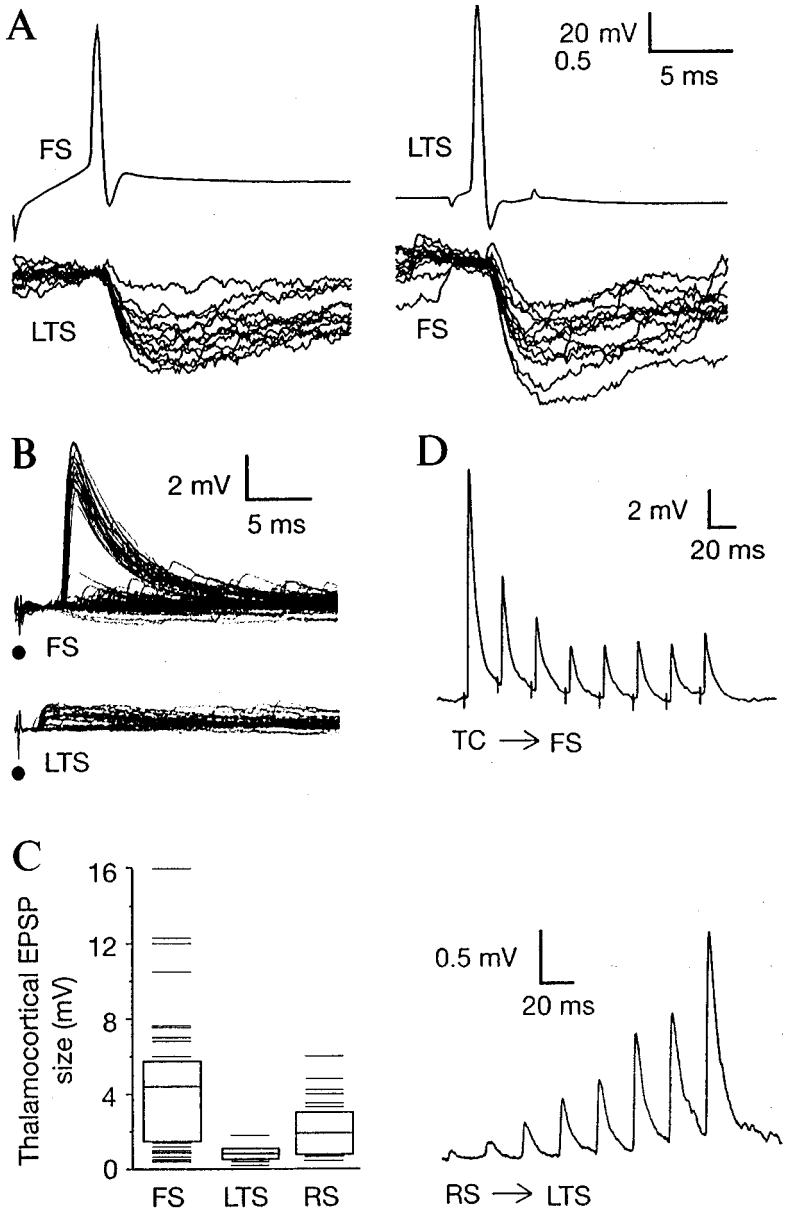

Fig. 2.9 Chemical synaptic connections of cortical inhibitory interneurons. Intracellular recordings from two types of interneurons (FS, fast spiking; LTS, low-threshold spiking) in barrel (somatosensory) cortex of rat thalamocortical slices. *A*, inhibitory synapses interconnecting FS and LTS neurons. During paired recordings, spikes in an FS cell evoked IPSPs in a neighboring LTS cell (left); in a different pair, spikes in an LTS cell evoked IPSPs in an FS cell (right). In each case, 12 trials are illustrated from the postsynaptic cell, each aligned on the presynaptic spike that evoked it, and a single presynaptic spike is shown for each pair. *B*, thalamocortical (TC) EPSPs evoked in an FS and an LTS cell with threshold stimuli. Multiple trials are overlaid. *C*, summary of mean single-axon TC-evoked EPSPs amplitudes, showing that FS cells responded more strongly than both LTS and regular-spiking (RS) cells. Boxes delineate the 25th and 75th percentiles, the line within the box is the sample mean, and lines outside the boxes plot the rest of the range ($n = 38$ FS, 8 LTS, 26 RS cells). *D*, upper trace shows that TC inputs to FS cells strongly depress (average of 20 trials of suprathreshold stimuli applied at 40 Hz). Lower trace, intracortical excitatory inputs to LTS cells strongly facilitate (LTS response from presynaptic RS cell spikes evoked at 40 Hz; average of 20 trials). From Gibson et al. (1999).

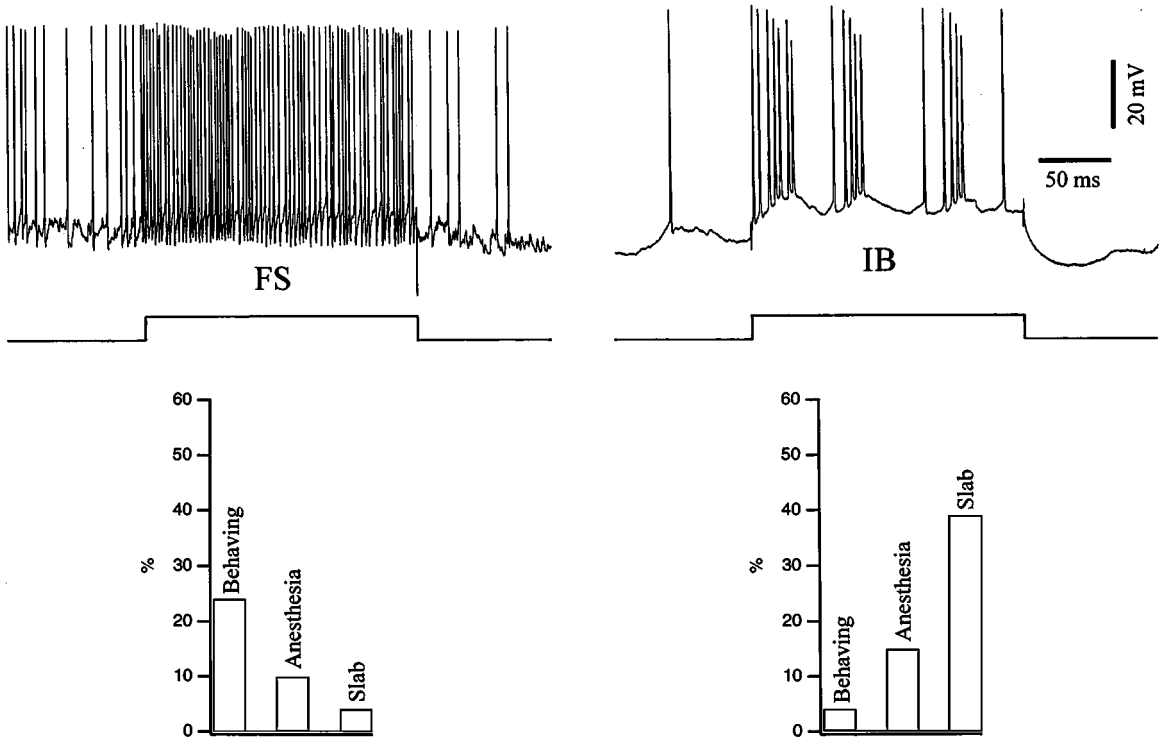

Fig. 2.10 Different proportions of fast-spiking (FS) and intrinsically bursting (IB) cortical neurons under different experimental conditions. The two neurons in the top panel are the same as in Fig. 2.1. Below, histograms of percentage distribution in samples from two neuronal types (FS and IB) in behaviorally awake cats with intact brain, intact cortex of cats under deep anesthesia (ketamine-xylazine and urethane), and small isolated cortical slabs *in vivo* under ketamine-xylazine anesthesia. Data from Steriade et al. (2001a).

[43] Buzsáki and Chrobak (1995); Llinás et al. (1991); Lytton and Sejnowski (1991); Traub et al. (1999a).

[44] Steriade et al. (1993a); Wang and McCormick (1993).

How can these differences be explained? The increased proportion of FS (presumably inhibitory) neurons may be due to the transformation of other firing patterns into that of FS cells. Such a transformation, from FRB-type to FS-type firing pattern, by increasing the level of depolarization, is depicted in Figs. 2.2 and 2.4. This is conceivable because FS neurons have been implicated in the generation of fast (20–40 Hz) rhythms [43], which characterize the spontaneous activity in the waking state and during high alertness, states of network activity that are accompanied by depolarized levels of membrane potential. On the other hand, the strikingly diminished proportion of IB firing patterns in the alert condition is likely due to the relatively depolarized membrane potential, enhanced synaptic activity, and increased release of some modulatory neurotransmitters, all conditions that may transform IB into RS firing patterns [44]. Such transformations suggest that a high degree of synaptic activity in the intact brain,

which is lacking in brain slices or in isolated cortical slabs *in vivo*, decisively modulates and may even overwhelm the intrinsic neuronal properties expressed by responses to direct depolarization. The impact of network activity on intrinsic neuronal properties is further discussed in the next section.

2.1.3. Transformations of firing patterns during shifts in behavioral states

In contrast to stable responses obtained in preparations with negligible or no spontaneous activity, the firing patterns that define a certain neuronal class may be drastically transformed during states with intense synaptic activity. This is due, in part, to differences in membrane potential and apparent input resistance between neurons recorded under different experimental conditions. A study of differences between *in vivo* and *in vitro* recordings of the same type of pyramidal neurons showed the strikingly dissimilar aspects of their spontaneous activity in these two conditions (Fig. 2.11). The standard deviation of the intracellular signal was 10–17 times lower *in vitro* than *in vivo*; and, the input resistance measured *in vivo* during relatively quiescent periods was reduced by up to 70% during epochs associated with intense synaptic activity, and increased by up to 70%, approaching the *in vitro* values, after tetrodotoxin (TTX) application *in vivo* [45]. In the same line, the mean membrane potential is −70 mV and the apparent input resistance is 49 MΩ in small isolated cortical slabs *in vivo*, whereas in intact (adjacent) cortical areas of the same animal the values are −62 mV and 22 MΩ, respectively [41]. These data would predict that the input resistance would be diminished during the state of natural wakefulness, when so many conductances are open because of the increased synaptic activity due to inputs from thalamocortical, intracortical, and generalized activating systems. Surprisingly, this was not found with intracellular recordings in naturally awake animals. Indeed, during the tonically depolarized state of wakefulness, the input resistance is twice as high as during the depolarizing phase of the slow oscillation in slow-wave sleep [14] (see Fig. 3.33 in Chapter 3). The explanation of the increased input resistance during wakefulness is probably the higher release of acetylcholine (ACh) in cortex during brain-active states [46] and the ACh-induced increase in input resistance of neocortical neurons [47]. The increased input resistance during wakefulness may be related to data showing an enhanced antidromic and synaptic responsiveness of monkey's neocortical neurons during this behavioral state, compared to slow-wave sleep [48].

[45] Paré et al. (1998). A model based on experimental data (Destexhe and Paré, 1999) showed that, in the presence of voltage-dependent dendritic currents, the convergence of hundreds of synaptic inputs is required to evoke action potentials reliably. These dendritic currents minimize the response variability, with distal apical dendrites being as effective as basal dendrites. This computational study made several predictions, one of them being that neurons recorded intracellularly during the natural state of wakefulness (an experimental condition that was not present at the time of that study) should have markedly reduced input resistance, by a 5-fold factor. Intracellular recordings performed later showed, however, that the input resistance is increased and more stable during natural wakefulness [14] (see Fig. 3.33 in Chapter 3 and also the main text in this chapter for possible factors accounting for this unexpected result).

[46] Jasper and Tessier (1971).

[47] Krnjević et al. (1971); McCormick (1992).

[48] Steriade et al. (1974a).

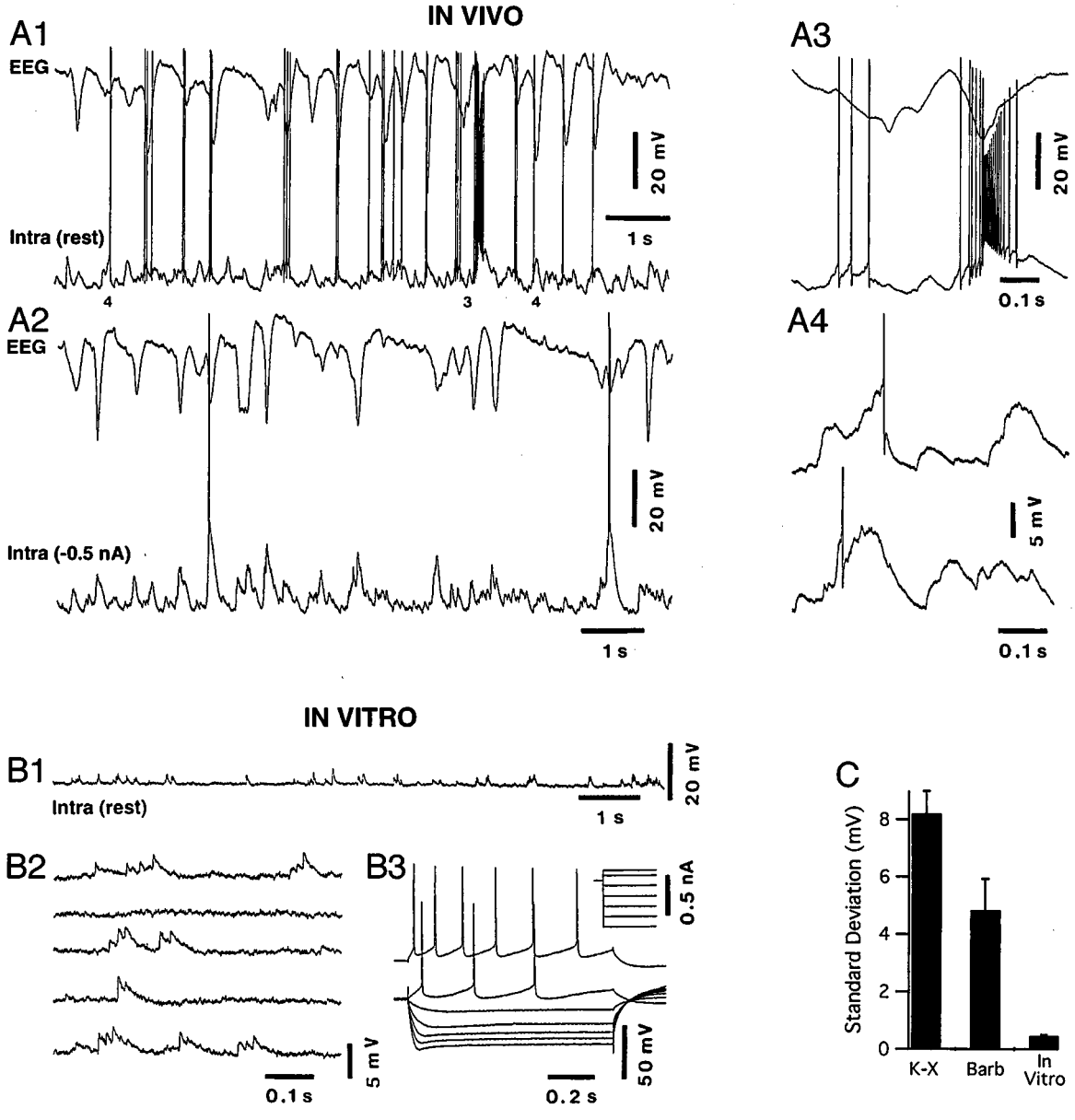

Fig. 2.11 Comparison of spontaneous synaptic activity displayed by cat neocortical neurons *in vivo* (*A*) and *in vitro* (*B*). *A*, intracellular recording of an infragranular regular-spiking (RS) cortical neuron at rest (−64 mV; *A1*) and at −82 mV (*A2*) and simultaneously recorded EEG under barbiturate anesthesia. Note large amplitude PSPs coinciding with depth-negative EEG potentials. Intracellular events marked by numbers in *A1* are expanded in *A3* and *A4*. *B1*, intracellular recording of an infragranular RS neuron cortical neuron at rest (−76 mV) recorded in a cat slice at 34°C. Same gain and time base as in *A1*. *B2*, spontaneous synaptic potentials at a higher gain (same as in *A4*). *B3*, responses of the same neuron to current pulses of various amplitudes. *C*, histogram comparing the standard deviation of the intracellular signal *in vivo* under ketamine-xylazine (K-X; $n = 10$) or barbiturate (Barb; $n = 10$) anesthesia as well as *in vitro* ($n = 10$). From Paré et al. (1998).

[49] Mason and Larkman (1990).

[50] Steriade and McCarley (1990).

The above data, showing differences in passive properties and responsiveness of neocortical neurons investigated in simplified preparations and during natural behavioral states, are behind the transformations observed in firing patterns of neocortical neurons when passing from a state of vigilance to another. Below, I take a few examples of such transformations using intracellular recordings in acute experiments and during natural states of vigilance.

The transformation, under certain physiological conditions, of a firing pattern that conventionally characterizes one neuronal type into another type of discharge was shown both for IB and FRB neurons. Such conditions are, for example, the transition from deafferented to brain-active behavioral states. The maintained depolarization of IB neurons results in burst inactivation [41, 49]. Figure 2.12 shows the transformation of a burst response of an IB cell into a regular-spiking (RS) response by a steady depolarizing current (*A*) and the development from bursting oscillatory activity, in another IB cell, into tonic activity during brain arousal elicited by stimulation of brainstem cholinergic nuclei (*B*). It was proposed that thick layer V neurons could operate in two modes, switching between bursts and tonic discharges, as a function of modulatory neurotransmitters [49]. The enhanced synaptic activity during brain activation by setting into action the ascending brainstem reticular system and *in vitro* application of some neurotransmitters [44] released in the intact brain by generalized activating systems [50] are both conditions that may transform IB into RS firing patterns. This idea, from earlier studies in acutely prepared animals, is now substantiated by a similar transformation during shifts from the natural state of slow-wave sleep to either wakefulness or rapid-eye-movement (REM) sleep when the membrane potential of cortical neurons is slightly depolarized [14]. Figure 2.13 shows different (IB and RS) firing patterns of the same neuron, evoked by depolarizing current pulses applied during slow-wave sleep and REM sleep, respectively. The mode of interspike intervals during the spontaneous activity in slow-wave sleep was at 3–3.5 ms, reflecting the presence of spike-bursts, while this mode was absent in REM sleep, and there were many more long intervals (20–100 ms) during REM sleep, reflecting the single action potentials in this brain-active state.

Generally, then, the transition from slow-wave sleep, a state with a more negative membrane potential, to either waking and REM sleep is associated with the replacement of spike-bursts, which characterize IB neurons, by tonic discharges and single spikes. Usually very slight (<3 mV) differences are seen between the membrane potential in slow-wave sleep and waking or REM sleep [14]; however, the opposite was observed in a few neurons which exhibited

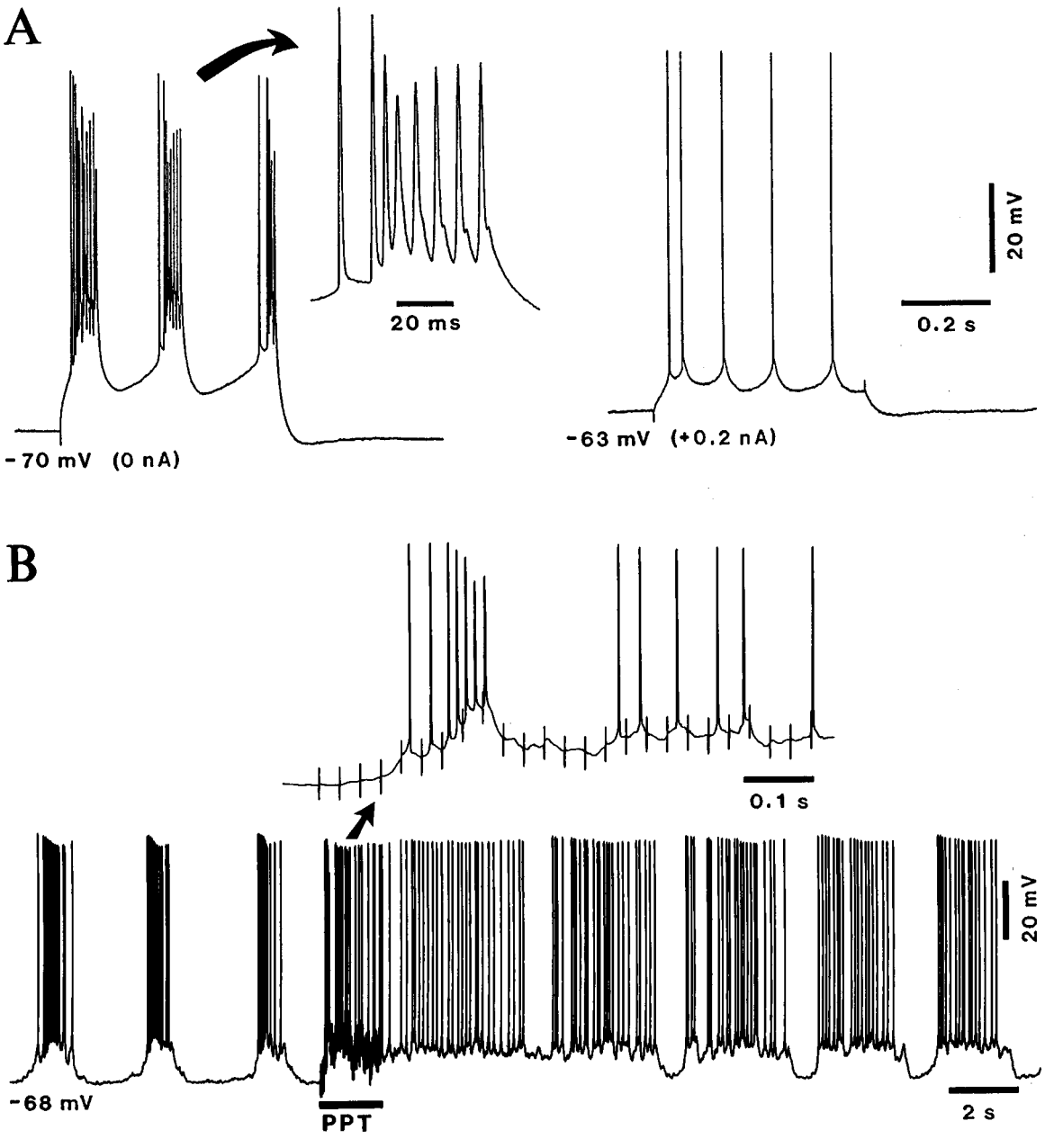

Fig. 2.12 Transformation of bursting to tonic firing patterns in neocortical neurons by changing the membrane potential (V_m) and synaptic activity. *A*, responses of an intrinsically bursting (IB) neuron in isolated cortical slab from suprasylvian gyrus (cat under ketamine-xylazine anesthesia) to the same intensity of depolarizing current pulse (0.5 nA) at the resting V_m (−70 mV) and under slight depolarization (+0.2 nA, −63 mV). A typical burst is expanded at right (arrow). *B*, area 7 neuron in cat under urethane anesthesia. An IB cell, identified by depolarizing current pulses, fired spike-bursts during the slow sleep oscillation and transformed this burst firing into tonic, single action potentials following brain activation produced by stimulation (horizontal bar, 1.8 s, 30 Hz) of the pedunculopontine tegmental (PPT) nucleus. Arrow points to an expanded detail showing a spike-burst followed by single spikes. Modified from Steriade et al. (1993a) and Timofeev et al. (2000a).

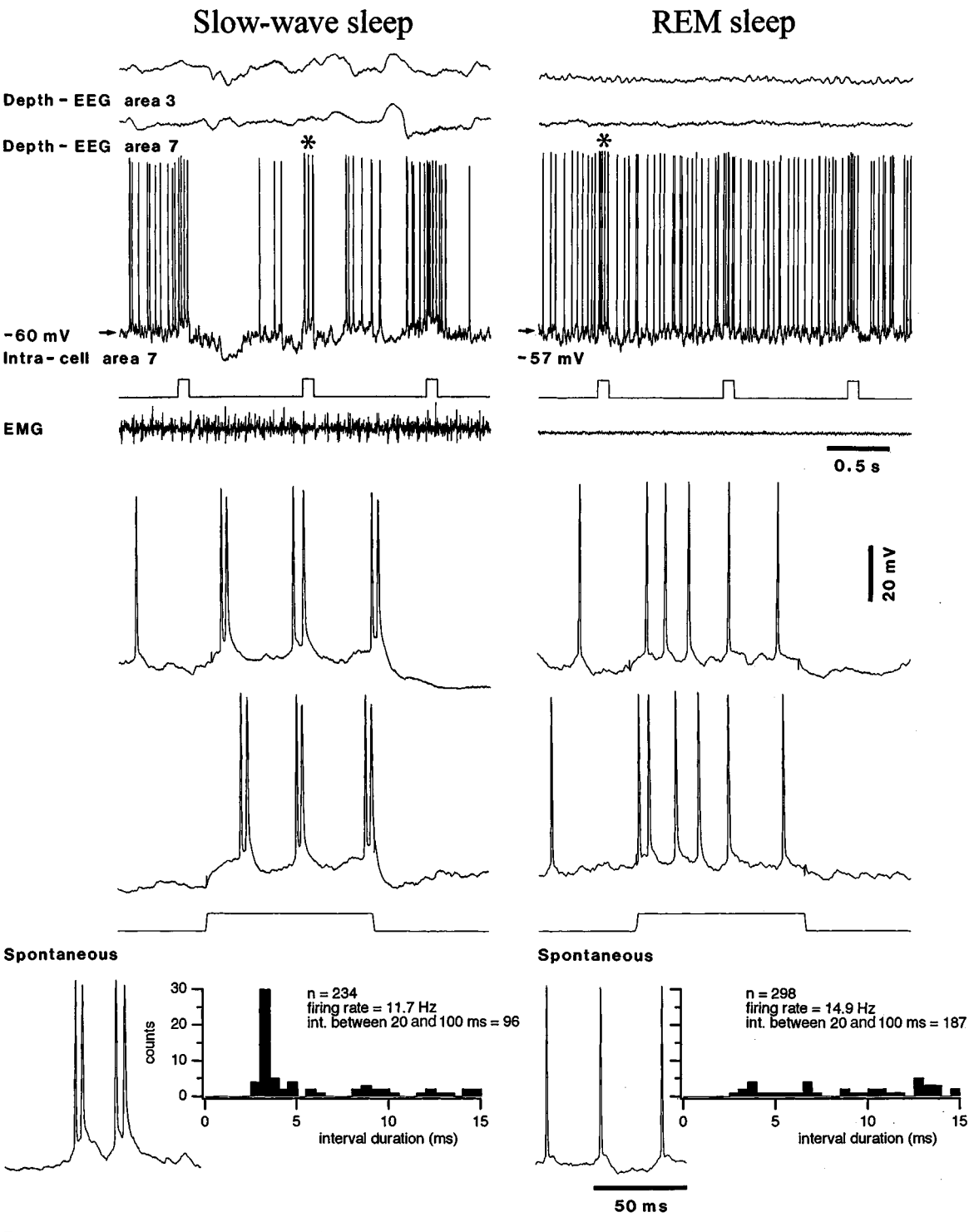

Fig. 2.13 Changes in firing patterns of an intrinsically bursting (IB) cortical neuron from area 7 during slow-wave sleep (SWS) and REM sleep in a chronically implanted cat. Top panels show EEG and EMG patterns characterizing the two states, as well as an intracellular recording of this neuron together with three depolarizing current pulses (indicated by current monitor). Below, responses to depolarizing current pulses (the first response is indicated by asterisk in the top panel). Note spike doublets in SWS and single spiking in REM sleep. At the bottom, examples of spontaneous firing of this neuron during SWS and REM sleep. The interspike interval histograms in each state show a mode at 3–3.5 ms in SWS (reflecting bursting activity), the absence of this mode in REM sleep, and many more long intervals (20–100 ms) in REM sleep, reflecting single spike firing. From Steriade et al. (2001a).

large depolarizations (5–10 mV) in the two brain-active states compared to slow-wave sleep. One of those few cases is illustrated in Fig. 2.14, showing an RS-type firing pattern during slow-wave sleep and increased discharges with IB-type spike-bursts in wakefulness. In such cases, the marked depolarization during the waking may have activated a Na^+-dependent current that generates DAPs, which promote spike-bursts in IB [16] and other bursting cells.

Neurons identified by their FRB responses to depolarizing current steps may also episodically display such trains of high-frequency, fast spike-bursts in a spontaneous manner during wakefulness (Fig. 2.15). As shown above (section ***2.1.1***), corticothalamic neurons recorded *in vivo* may fire like FRB neurons in response to depolarizing current pulses, but below that level they fire like RS neurons and, at more depolarized levels, like FS neurons (see Figs. 2.2, 2.4, 2.5). The transformation of output pattern, from RS single-spike firing to FRB burst discharges may render unreliable cortical synapses reliable [51].

2.1.4. Neuron-glia networks

Accumulating data challenge the traditional view that non-spiking glial cells do not influence neuronal operations. These data mainly arose from studies of slices and cultures, but investigations *in vivo* also provided results indicating that although the glia is not normally implicated in wakeful brain operations, it may have a pacing role in neuronal operations during brain-disconnected states, such as slow-wave sleep and paroxysmal oscillations [52].

A role for glial cells in the dialogue with neurons is suggested, among much other evidence [53], by the fact that different neurotransmitters (among them glutamate) and neuromodulators (such as acetylcholine and norepinephrine) activate glia [54] and that, in turn, some glial cells release glutamate [55]. There is also evidence of opening Cl^- channels in glia by $GABA_A$ action [56]. Astrocyte stimulation increases the probability of release at excitatory and inhibitory synapses [57]. Besides, electrotonic coupling via gap junctions between neurons and astrocytes was revealed in some brain structures [58]. All these data indicate that glial cells receive information, transfer it to neurons, and modulate synaptic operations. While most of these studies have been conducted in structures other than neocortex, recent *in vivo* studies in neocortex [52] suggest that pure neuronal networks cannot account alone for sleep oscillations and seizures, and provide evidence for the involvement of glial cells in these global activities (see Chapters 3 and 5).

[51] Lisman (1997). The switch from RS to FRB pattern, and further from FRB pattern to rapid tonic discharges as in FS pattern, demonstrated in intracellular recordings from cat neocortical neurons [13] (see Figs. 2.2 and 2.4), was also found in recent experimental data from rat temporal cortex slices and multi-compartmental models (Traub et al., 2002). These authors showed that axonal excitability plays a critical role in generating fast, rhythmic spike-bursts. They also suggested that the most important membrane properties contributing to FRB patterns are the kinetics of fast Na^+ and fast K^+ channels that allow spike afterdepolarization (DAP) to occur and promote a ready tendency to produce spike multiplets. In Traub's model, reduction in somadendritic $g_{K(Ca)}$ could induce FRB firing patterns in response to depolarizing stimuli, even in the absence of $g_{Na(p)}$.

[52] Amzica and Steriade (1998b, 2000); Amzica and Neckelmann (1999); Amzica et al. (2002).

[53] Bezzi and Volterra (2001).

[54] Sontheimer et al. (1988); Steinhäuser and Gallo (1996); Kang et al. (1998); Dzubay and Jahr (1999).

[55] Parpura et al. (1994); Araque et al. (1999); Innocenti et al. (2000).

[56] Kettenmann and Schachner (1985).

[57] Araque et al. (1998).

[58] Alvarez-Maubecin et al. (2000). This study was conducted in locus coeruleus. At this time, there are no consistent data on electrotonic coupling between glia and neurons in other central structures.

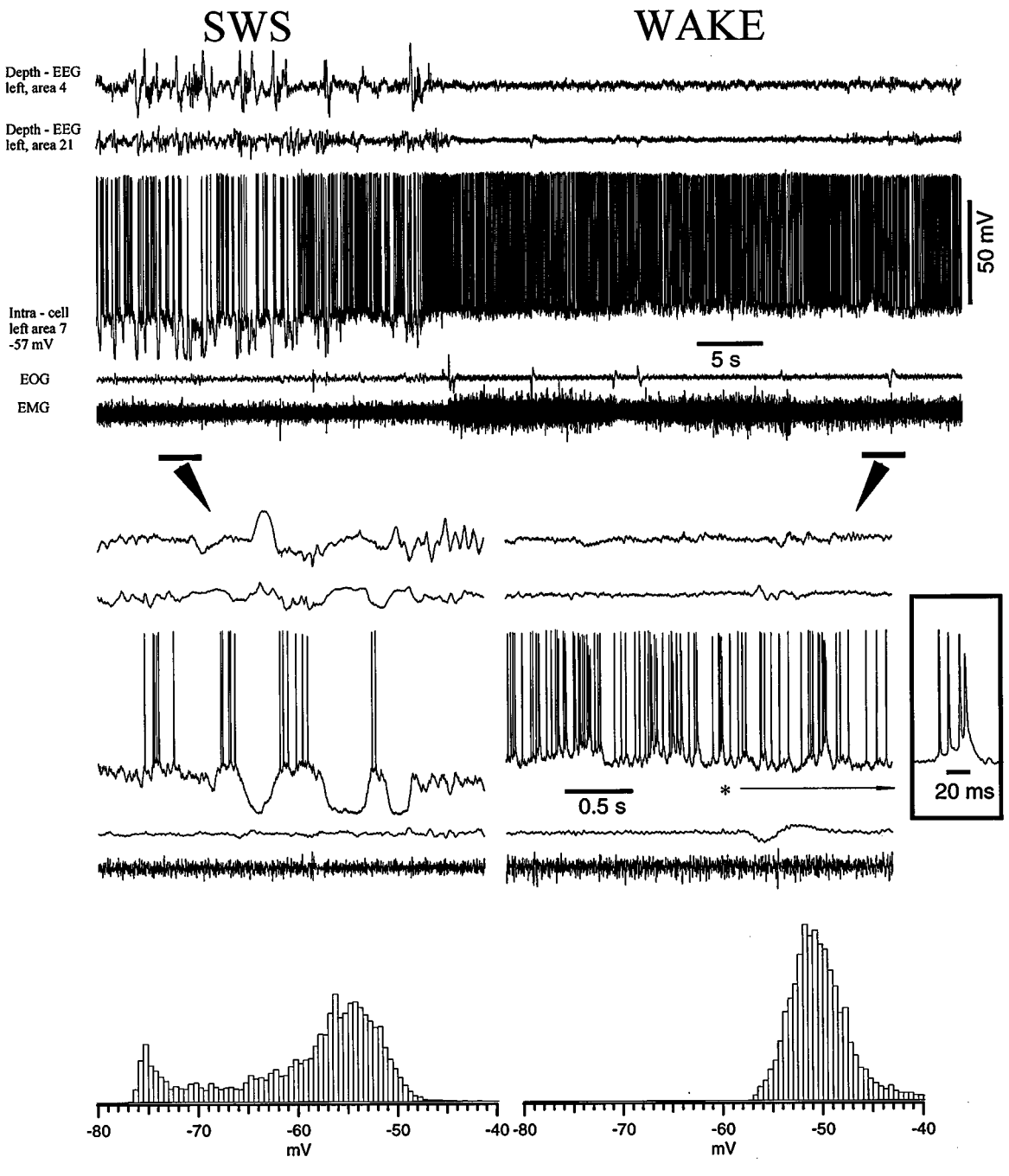

Fig. 2.14 Unusual transformation from RS-type firing to IB-type firing in a cortical neuron, during the shift from natural slow-wave sleep to wakefulness. Intracellular recording from cat area 7, together with depth-EEG from ipsilateral areas 4 and 21, electroculogram (EOG) and EMG. Upper panel shows transition from slow-wave sleep (SWS) to waking state. Note increased muscular tone and EEG activation. Two episodes, marked by horizontal bars in SWS and waking, are expanded below (arrows). One spike-burst, marked by an asterisk in waking, is expanded on the right. Bottom panel depicts histograms of membrane potential during SWS and wake state; note hyperpolarizing tail (to −75 mV) and major mode around −55 mV in SWS, and the Gaussian-like histogram with a peak around −50 mV in waking. Unpublished data by M. Steriade, I. Timofeev and F. Grenier.

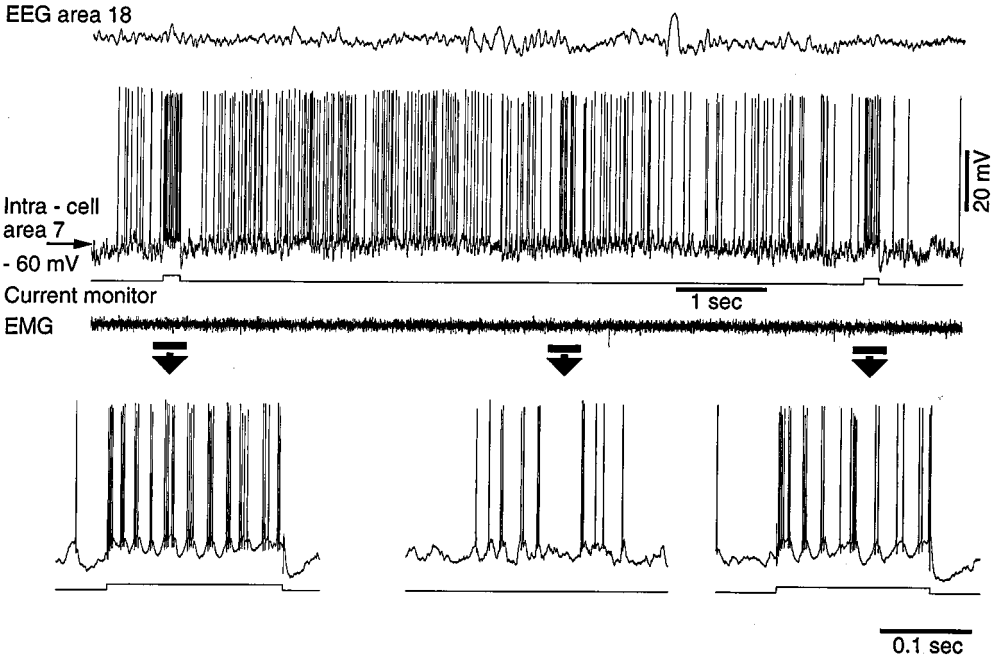

Fig. 2.15 Neuron displaying FRB responses to direct depolarization also exibits, episodically, trains of high-frequency, fast (40–50 Hz) spike-bursts during natural wakefulness. Intracortical recording of area 7 neuron in chronically implanted cat, together with EMG. Current monitor below the intracellular trace. Responses to two depolarizing current pulses (left and right) are expanded below (arrows). In the middle part of the trace, a spontaneously occurring episode with repetitive spike-bursts is also expanded below. Unpublished data by M. Steriade, I. Timofeev and F. Grenier.

2.2. Neuronal types in archicortex and related systems

The functional properties of neuronal types in the hippocampus, entorhinal cortex and amygdala nuclei have been the topic of numerous investigations because of the relatively simpler synaptic organization of these structures, compared to neocortex, their accessibility to studies *in vitro*, the key role played in certain aspects of learning and memory, the wide interest in a form of plasticity (long-term potentiation) that some consider relevant for the mnemonic function, the presence of a neuronal type ("place cells") tuned to spatial co-ordinates of the environment, the generation of an oscillation (theta rhythm) that was intensively investigated because it characterizes certain types of behavior in rodents, and their high propensity to epileptic activity.

2.2.1. Hippocampus

The hippocampal formation consists of three fields, CA1–CA3 [59], which constitute Ammon's horn proper and the dentate gyrus (fascia dentata and hilus) [60]. The dentate gyrus is the target of

[59] CA2 field is less defined in some species and is often ignored.

[60] Reviewed in Amaral and Witter (1989), Lopes da Silva et al. (1990) and Gloor (1997).

[61] There is a back-projection from pyramidal neurons located in the ventral part of the hippocampal CA3 field to the molecular layer of the dentate gyrus (Li et al., 1994).

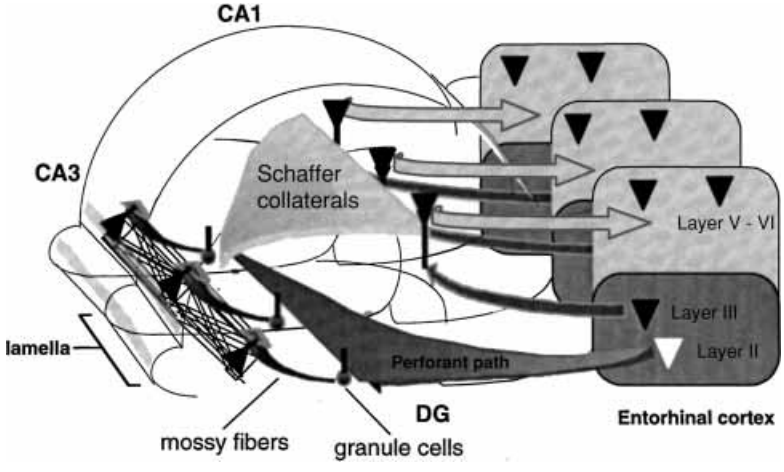

Fig. 2.16 Main excitatory connections in the hippocampal formation. Layer II of the entorhinal cortex forms a longitudinally widespread projection to granule cells of fascia dentata and CA3 pyramidal neurons via the perforant pathway. The next stage is the mossy fiber projection, organized in a lamellar fashion, from the granule cells to the CA3 pyramidal cells. The CA3-CA1 associational system (Schaffer collaterals) is longitudinally widespread. In contrast with the divergent multisynaptic system, layer III pyramidal cells of the entorhinal cortex provide a direct and spatially restricted innervation (in the transverse dimension) of CA1 pyramidal cells, which in turn project back to deep layers of entorhinal cortex. DG, dentate gyrus. Modified from Freund and Buzsáki (1996).

the perforant path, formed by axons originating in layers II–III of the entorhinal cortex, and is the first stage of the intrahippocampal trisynaptic loop (Fig. 2.16). The next stage is the mossy fiber projection from the granule neurons, which are principal cells of the dentate gyrus, to the CA3 field where they form synapses on the proximal dendrites of pyramidal cells that are interconnected by a recurrent associational system [61]. The apical dendrites of CA3 pyramidal neurons are radially oriented in the strata radiatum and lacunosum moleculare, while the basal dendrites run in stratum oriens toward the alveus. A direct projection from the entorhinal cortex reaches the distal dendritic domain in the stratum lacunosum moleculare. The third stage of the loop is represented by axons of pyramidal neurons in field CA3, which form the Schaffer collaterals that project to field CA1. Pyramidal cells in this final stage of the trisynaptic loop form the stratum pyramidale; their apical dendrites terminate in the stratum lacunosum moleculare, while their basal dendrites are within the stratum oriens. The interactions between pyramidal cells in field CA1 are less rich than in field CA3. The targets of pyramidal cells in field CA1, which is the major hippocampal output, are subiculum and entorhinal cortex,

where they terminate in layers V–VI (see Fig. 2.16), and other limbic cortices and subcortical structures. In essence, the entorhinal cortex is mapped onto field CA1 and the trisynaptic, intrahippocampal "diffuse" system is superimposed on this organized topography [62].

Since the 1960s, the excitatory connections in this trisynaptic loop have been analyzed using intracellular recordings from granule cells in the fascia dentata, and from principal (pyramidal) cells in fields CA1 and CA3, *in vivo* [63] and *in vitro* [64]. Briefly, the perforant path axons produce EPSPs on the distal third of the granule cells' dendrites; the large pyramidal cells in field CA3 receive the excitatory input from mossy fibers on their proximal dendrites; and the smaller pyramidal cells in field CA1 receive excitatory inputs from Schaffer fibers (collaterals of CA3 pyramidal cells' axons) as well as from axons originating in the entorhinal cortex that terminate on more distal parts of their apical dendrites. Although the contacts made by axons from entorhinal cortex on CA1 pyramidal cells are on distal dendrites, the EPSPs are quite effective because of the compact electrotonic structure of CA1 cells [65]. A modeling study of CA1 pyramidal cells [66] predicted some aspects of their dendrites' properties. Among them, the fast prepotentials [67] were predicted to arise from Na^+-dependent dendritic hot spots. This model suggested that alterations in Ca^{2+} electroresponsiveness of CA1 neurons may lead to bursting behavior, as seen in epileptic neuronal activity. Besides chemical synapses, electrotonic coupling exists between the granule cells of fascia dentata and among hippocampal pyramidal cells [68], which may facilitate or disrupt the synchronous firing evoked through chemical synapses [69].

The initial EPSP produced by antidromic or orthodromic volleys in the pyramids of fields CA1–CA3 is followed by a large IPSP, which may lead to a post-inhibitory rebound [70]. While antidromically evoked IPSPs are relatively simpler, orthodromic IPSPs are multiphasic and involve both a GABA-mediated dendritic component and a non-GABA-mediated component [71]. IPSPs have also been elicited in hippocampal pyramids by direct activation of local interneurons [72].

The IPSPs are produced by different types of interneurons contacting pyramids at symmetrical synapses. Despite the relatively small number of inhibitory interneurons (<10% of the total neuronal population), they effectively control the excitability of hippocampal pyramidal cells by divergent inhibitory connections and strategically wired axonal projections. Following the description of different hippocampal cell types by Ramón y Cajal [26] and subsequent investigators using Golgi impregnation methods, the

[62] Freund and Buzsáki (1996).

[63] Kandel and Spencer (1961); Kandel et al. (1961); Andersen et al. (1966).

[64] Schwartzkroin (1975, 1977); McNaughton et al. (1981); reviewed in Schwartzkroin and Mueller (1987).

[65] Andersen et al. (1980b).

[66] Traub and Llinás (1979).

[67] Spencer and Kandel (1961).

[68] MacVicar and Dudek (1981, 1982).

[69] Traub and Wong (1981).

[70] Andersen et al. (1964, 1969); Ben-Ari et al. (1981).

[71] Alger and Nicoll (1982). Depolarizing IPSPs can be evoked in pyramids of CA1 field by orthodromic stimulation in strata oriens and radiatum, and they are localized to the dendrites in the stimulated field.

[72] Knowles and Schwartzkroin (1981).

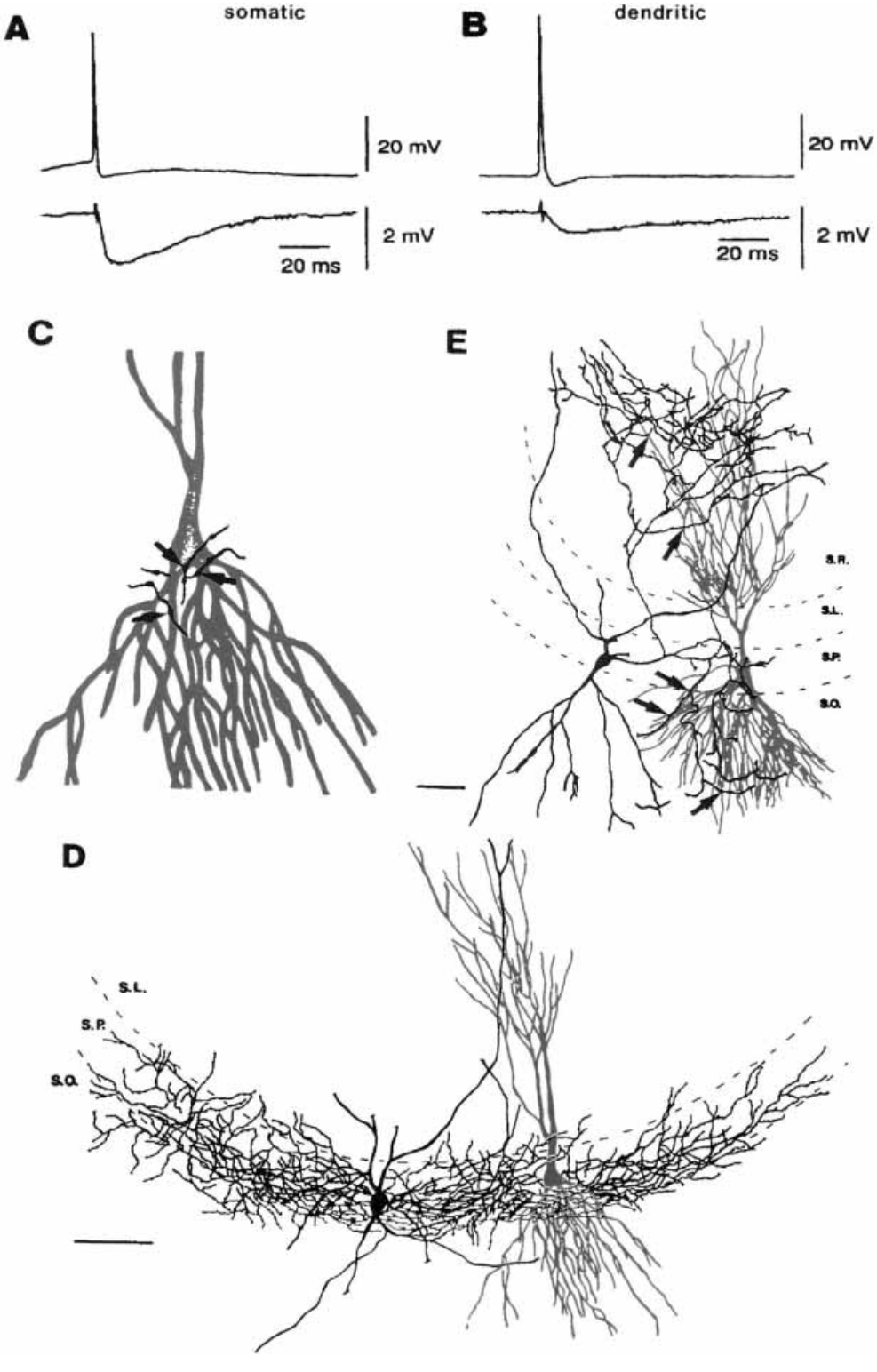
A
somatic
20 mV
2 mV
20 ms
B
dendritic
20 mV
2 mV
20 ms
C
E
S.R.
S.L.
S.P.
S.O.
D
S.L.
S.P.
S.O.

[73] Reviewed in Somogyi and Freund (1989) and Freund (1993).

[74] Han et al. (1993).

[75] Lacaille and Schwartzkroin (1988a-b); Sik et al. (1995).

[76] Martina et al. (2000).

input-output organization of hippocampal interneurons was investigated by combining tracing methods with immunocytochemistry and by intracellular recording/staining techniques [73]. A more recent classification [62] integrates the morphological, neurochemical and electrophysiological features of various hippocampal interneurons. The main types follow.

(a) Chandelier (or axo-axonic) cells [38] are found in both dentate gyrus, where they are contacted by axons of the perforant path as well as by recurrent axonal collaterals of granule cells [74], and hippocampus proper. As in neocortex, the axons of these cells terminate selectively on the initial segment of pyramids' axons.

(b) Basket cells are similar in the dentate gyrus and CA1-CA3 hippocampal fields. Although they are termed as in the cerebellum, where they were originally described, these interneurons do not form typical baskets around the somata of pyramidal cells, but terminate both perisomatically and on the dendritic tree of pyramidal cells. IPSPs at the somatic location have a larger amplitude and faster time to peak than do dendritic IPSPs (Fig. 2.17).

(c) Dendritic inhibitory cells are distinguished from chandelier and basket cells by their prevalent innervation of the dendritic trees of granule and pyramidal cells. The alveus/oriens interneurons in the CA1 field, with lacunosum-moleculare axonal arborization (O-LM), are similar to dentate gyrus interneurons with hilar dendrites and ascending axons. The firing patterns of O-LM neurons, with high-frequency discharge, brief action potentials, and responses to direct depolarization without adaptation [75], are similar to those of other cortical inhibitory interneurons. O-LM interneurons of the CA1 field, some of them immunopositive for somatostatin, demonstrate multiple action potential initiation sites, as shown by simultaneous intracellular recordings from soma and dendrites [76]. This study, conducted in hippocampal slices, reported that,

Fig. 2.17 (opposite) Postsynaptic potentials evoked by inhibitory basket cells that terminate in the somatic (*A*) or in the dendritic region (*B*) of rat hippocampal pyramidal cells, as revealed by paired intracellular recordings. An action potential (upper trace) triggered by intracellular current pulse in the interneuron evoked IPSPs in the postsynaptic pyramidal cells (lower trace). The number and location of synaptic contacts were identified by light and electron microscopy, following intracellular biocytin filling. *C–E*, reconstructions of the cell pairs (pyramids drawn in red, interneurons in black). The basket cell in *D* that produced the IPSPs shown in *A* formed three synaptic contacts on the postsynaptic pyramidal cell, as shown by the arrows at higher magnification in *C*. The bistratified interneuron in *E*, responsible for the IPSP shown in *B*, arborized in strata oriens and radiatum. It formed two synapses on the apical, and three synapses on the basal, dendrites of the pyramidal cell (arrows). All contacts identified at the light microscopic level were confirmed by correlated electron microscopy. Scale bars in *D–E* = 50 μm. From Gulyas et al. (1993). See Plate section for color version of this figure.

after initiation of action potentials in the axon, they reliably propagate over the dendritic domain. *In vivo*, the dendritic invasion of successive action potentials is substantially attenuated, decreasing as a function of distance from the soma [77].

(d) Local-circuit GABAergic cells specialized in innervating other interneurons, termed interneuron-selective (IS) cells, are present in the dentate gyrus and fields CA1–CA3, and their different subclasses are also immunoreactive to some calcium-binding proteins and peptides.

2.2.2. Entorhinal cortex

Neocortical connections with the hippocampus are relayed via mesocortical structures, the entorhinal cortex being the cortical area with direct access to the hippocampus via the perforant path (see ***2.2.1***). The entorhinal cortex, located in the medial wall of the rhinal sulcus, receives direct inputs from multimodal association isocortical areas of the frontal, parietal, and temporal lobes. The role of perirhinal cortical areas in normal recognition and associative memory was demonstrated in animals experiments [78] and human studies showing that the entorhinal cortex is the earliest and most severely damaged in Alzheimer's disease [79].

As neurons in superficial layers of the entorhinal cortex have a key role in gating afferent information from neocortex to hippocampus (layer II mainly to granule cells in fascia dentata, layer III directly to field CA1), they were regarded as "relay" cells and, until recently, little consideration was given to their own processing capabilities and implication in different oscillatory types, including paroxysmal states [80]. However, studies *in vitro* and *in vivo* have analyzed the properties of neurons of entorhinal cortex, their involvement in long-term processes of increased synaptic efficacy, and their relation to hippocampal "place cells" [81].

Neurons from superficial layers in entorhinal cortex were investigated in most detail, using brain slices from rats. The most common neurons in layer II are stellate cells that give rise to the perforant path; non-stellate, generally pyramidal cells, also contribute to this projection. The main difference between these two cellular types is that stellate cells generate depolarization-dependent rhythmic subthreshold oscillations in the theta frequency range, ~8.5 Hz (Fig. 2.18), that depends on the activation of $I_{Na(p)}$, whereas pyramidal-like cells do not oscillate [82]. The theta rhythm generated primarily by layer II entorhinal cells was also shown *in vivo* [83]. The rhythmic properties of stellate cells, revealed *in vitro* [82], qualify them among the elements that generate theta activity. The neuronal synchronization underlying population activity in the

[77] Buzsáki et al. (1996); Kamondi et al. (1998).

[78] Reviewed in Zola-Morgan and Squire (1993); Suzuki (1996).

[79] Van Hoesen et al. (1991).

[80] This view of entorhinal cortical neurons as "relay" cells, with few or no integrative capacity, may be compared to that regarding thalamocortical cells as merely serving as an anteroom for relaying signals from the external world to cortex, without considering local and long-range inhibitory processes underlying complex integrative functions within the thalamus (see Chapter 1 in Steriade et al., 1997).

[81] Jones and Heinemann (1988); Alonso et al. (1990); Quirk et al. (1992).

[82] Alonso and Klink (1993). In addition to theta-like oscillation, stellate cells in layer II of the entorhinal cortex display, upon direct depolarization, trains of spikes interspersed with subthreshold oscillations in the beta frequency range (~22 Hz). The property of generating subthreshold oscillations in the beta-gamma frequency range has also been described in thalamocortical (Steriade et al., 1991b), thalamic reticular (Pinault and Deschênes, 1992a), and neocortical (Llinás et al., 1991) neurons.

[83] Mitchell and Ranck (1980); Dickson et al. (1995).

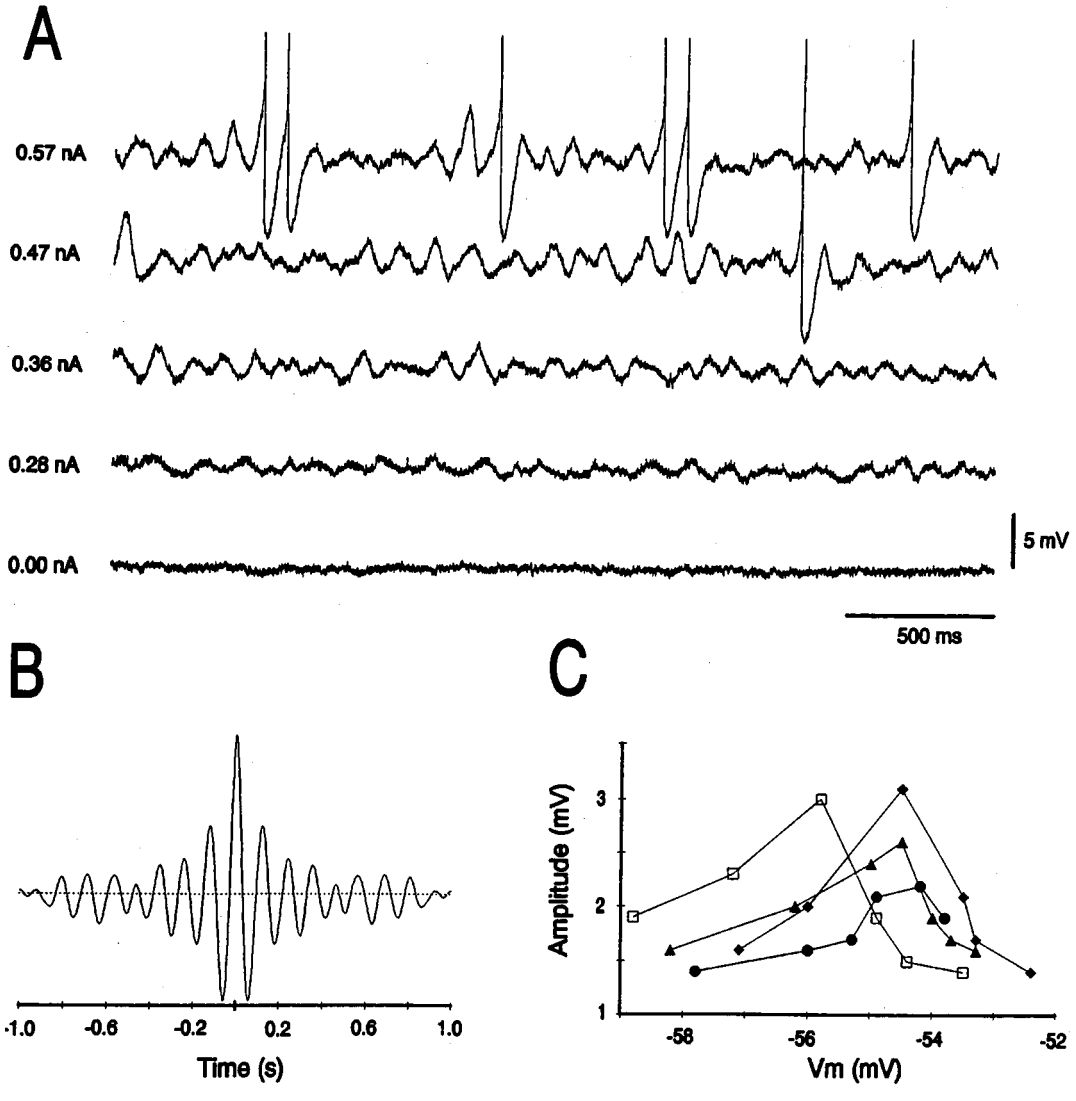

Fig. 2.18 Subthreshold rhythmic oscillation of stellate cells in rat entorhinal cortex, *in vitro*. *A*, development of oscillations with increasing levels of depolarization. At rest (0 nA, $V_m = -64$ mV), no membrane potential oscillations were present, but they clearly developed with current injection of 0.28 nA ($V_m = -58$ mV). *B*, autocorrelogram for the 0.36 nA current injection level ($V_m = -55$ mV), demonstrating clear rhythmicity at a dominant frequency of 8.3 Hz. Dotted line on the autocorrelogram: 0 level. *C*, graphic representation of the average amplitude of the subthreshold oscillations plotted against V_m from four different neurons. From Alonso and Klink (1993).

intact brain is probably due to the network of recurrent axonal collaterals of stellate cells [84] but also requires inputs from some neuromodulatory systems. Indeed, layer II neurons in rat entorhinal cortex receive cholinergic innervation from the septum [85] and a muscarinic agonist, carbachol, produces membrane depolarization of stellate cells associated with oscillations in the theta frequency range by induction of a Ca^{2+}-activated cationic conductance, possibly mediated by the m1 receptor subtype [86]. The muscarinic activation also promotes paroxysmal activity in principal (pyramidal) cells in layer II, even after their surgical isolation of this layer *in vitro* [87]. The cholinergic-induced depolarization of principal cells has a multiphasic reversal potential, which suggests a concurrent glutamatergic and GABAergic input, but field "spikes" survive the blockage of excitatory neurotransmission, thus indicating the involvement of pools of entorhinal inhibitory interneurons in this epileptic-like activity [87]. That pyramidal neurons fire in phase with local inhibitory interneurons during paroxysmal depolarizing shifts (PDSs) was also demonstrated in neocortex by measurements of membrane conductance in pyramidal cells and direct recordings from interneurons [88] (see also Chapter 5).

Pyramidal neurons in layer III of entorhinal cortex contribute to the monosynaptic component of the perforant pathway that terminates in field CA1. These neurons do not display subthreshold oscillations, as stellate cells in layer II do, but fire tonically at relatively low frequencies, like regular-spiking cells in neocortex, and are probably implicated in the high-fidelity transfer of incoming signals en route to CA1 [89].

2.2.3. Amygdala

The importance of the amygdala in physiology and pathology resides in its role in fear and anxiety as well as in its low threshold for epileptic seizures. Stimulation of the amygdala in humans elicits anxiety in epileptic subjects [90], patients with bilateral amygdala lesions are unable to recognize facial expressions of fear [91], wild monkeys are transformed into docile animals if the amygdala is lesioned [92], and the amygdaloid complex is necessary for the formation of Pavlovian fear-conditioned responses [93].

The amygdala consists of about ten or twelve nuclei, according to different classifications, grouped into two major divisions [94]. The input stations mainly consist of basolateral (BL) and basomedial (BM) nuclei, while the output arises from the central nucleus (CE) that has a lateral (CE_L) and a medial (CE_M) sector (Fig. 2.19). The BL complex receives inputs from some thalamic nuclei and from association neocortical areas, while CE_M is the major output

[84] Alonso and Llinás (1989).

[85] Alonso and Köhler (1984).

[86] Klink and Alonso (1997a-b). The evoked theta activity produced by carbachol has a lower frequency (~6 Hz) than in the absence of this muscarinic agent, when it varies between 8 and 9 Hz.

[87] Dickson and Alonso (1997). The role played by entorhinal cortical neurons in epilepsy is also known from clinical data, which show that sclerotic lesions that include entorhinal cortex promote temporal epilepsy in humans (Gloor, 1991). Removal of entorhinal cortex controls intractable temporal seizures (Goldring et al., 1992).

[88] Steriade et al. (1998c); Neckelmann et al. (2000); Timofeev et al. (2002c).

[89] Dickson et al. (1997).

[90] Gloor et al. (1982).

[91] Adolphs et al. (1994).

[92] Klüver and Bucy (1937).

[93] LeDoux et al. (1990); Romanski and LeDoux (1992); LeDoux (1996).

[94] For organization and projections of amygdala nuclei in non-human primates, see Amaral and Price (1984) and Amaral et al. (1992).

[95] Paré et al. (1995).

[96] The local interneurons in the BL and BM nuclei represent a population of 10–15% of the total neuronal population. In addition to their immunoreactivity to GABA (McDonald and Augustine, 1993; Paré and Smith, 1993), they also express immunoreactivity for different peptides and calcium-binding proteins (McDonald, 1994).

[97] Besides intrinsic operations within the amygdala complex, the intercalated cell masses (ICMs) have distant projections to the basal forebrain (Paré and Smith, 1994). It is not yet known whether, at that level, ICM neurons contact cholinergic or GABAergic cells.

[98] Sugita et al. (1993).

[99] Lang and Paré (1997).

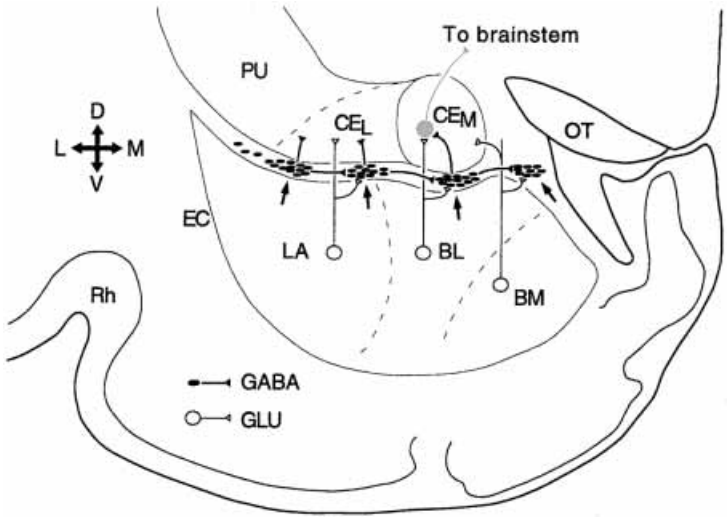

Fig. 2.19 Schematization of different nuclei in the amygdaloid complex of guinea-pig and the intercalated cell masses as an inhibitory interface between the inputs and outputs of the amygdala. Coronal section. Abbreviations of nuclei: LA, lateral; BL, basolateral; BM, basomedial; CE_L and CE_M, lateral and medial sectors of the central nucleus. The intercalated cell masses are interconnected by lateromedial connections; they receive glutamatergic inputs from components of the basolateral complex (LA, BL, BM) and contribute a GABAergic projection to CE_L and CE_M. Other abbreviations: EC, external capsule; OT, optic tract. PU, putamen; Rh, rhinal sulcus. Arrows indicate dorsal, ventral, medial and lateral. From Royer et al. (2000b).

structure for fear-conditioned responses and projects to hypothalamic and brainstem core structures implicated in the elaboration of autonomic reactions that are part of emotional responses. Anterograde tracing and electron microscope analyses in cat's amygdala concluded that BL and BM nuclei project to CE_M, and form asymmetric synaptic contacts with spines in this sector of the CE nucleus [95].

In addition to excitatory projections from BL-BM nuclei to output CE nucleus, there are local inhibitory interneurons within BL, BM, and CE_L nuclei [96], and a group of GABAergic neurons, called intercalated cell masses (ICMs), which is intercalated between BA/BL nuclei and CE nucleus (Fig. 2.19), thus representing an inhibitory interface that gates the transmission of signals from input to output amygdaloid nuclei [97].

The electrophysiological features of different neuronal types in the amygdala complex have been investigated using intracellular recordings *in vivo* and *in vitro*. In BA-BL projection neurons, stimulation of major input structures induces, after the early EPSP, a prolonged hyperpolarization that consists of $GABA_{A\text{-}B}$ IPSPs [98, 99],

whose time-course and dependency of Cl^- and K^+ conductances, respectively, are similar to such biphasic IPSPs in hippocampus and thalamus (see ***2.3.1***), and glycinergic IPSPs [100]. GABAergic IPSPs result from activation of local interneurons. The major component of these IPSPs is a Cl^--dependent, $GABA_A$ IPSP, while the later phase of the long hyperpolarization is a synaptically activated $I_{K(Ca)}$ [99].

As projection neurons in BL amygdala display little or no spontaneous activity under most conditions [101], their powerful inhibition exerted by local interneurons [96] is plausible. In fact, weak inputs excite projection amygdala neurons, whereas intense stimuli activate local GABAergic neurons and, thus, silence projection cells [102]. This is illustrated in Fig. 2.20 that compares synaptic responses evoked by stimulation of perirhinal cortex in a projection and a local-circuit inhibitory cell of the lateral amygdala. Stimuli with increasing intensity produced a shift from depolarizing to hyperpolarizing responses in the projection neuron, whereas they evoked increasing excitation in the local interneuron. The evoked IPSP in amygdala local interneurons is mediated by a Cl^- conductance.

Most of projection cells in the CE_M nucleus (95%) that play a key role in output amygdala operations implicated in fear conditioning are termed late-firing neurons, because they display a delay between the onset of a depolarizing current step and the first action potential, due to a voltage- and time-dependency outward rectification in the depolarizing direction [103]. Only few ($\sim$5%) CE_M neurons produce a low-threshold spike, similar to that of thalamic neurons (see **2.3**). And, similar electrophysiological properties are exhibited by different neuronal populations in $CM_{L\text{-}M}$ in spite of their morphologically different features [104].

The GABAergic neurons of ICMs, interposed between BL and CE nuclei, show a lateromedial topography. As the position of the recording micropipette in the ICMs is shifted medially, the BL-evoked bisynaptic inhibitory response is seen in more medial sectors of the CE nucleus [105]. Thus, the BL inputs to CE have a dual effect: a direct glutamatergic excitation and a GABAergic inhibition mediated by ICMs cells. The gain of the BL-to-CE inhibition can be changed by inputs arising in other amygdala nuclei and by the connectivity among GABAergic neurons within the ICMs. These inhibitory interactions were studied by whole-cell recordings in coronal slices of guinea pig amygdala showing that the connections between ICM cell clusters tend to run in a lateromedial direction [106]. The circuit depicted in Fig. 2.21 shows that BL stimulation excites both CE_M cells and ICM cells located below the CE_M. As a

[100] Danober and Pape (1998).

[101] Ben-Ari et al. (1974); Paré and Gaudreau (1996).

[102] Lang and Paré (1998).

[103] Martina et al. (1999).

[104] This absence of correspondence between conventional definitions of electroresponsive properties and neuronal morphology was also noted in neocortex. Some local GABAergic neurons, generally defined by their fast-spiking (FS) characteristics, fire like regular-spiking or bursting neurons [19] and FS firing patterns are produced by long-axoned (corticothalamic) neurons at increasing levels of membrane depolarization [13].

[105] Royer et al. (1999).

[106] Royer et al. (2000a).

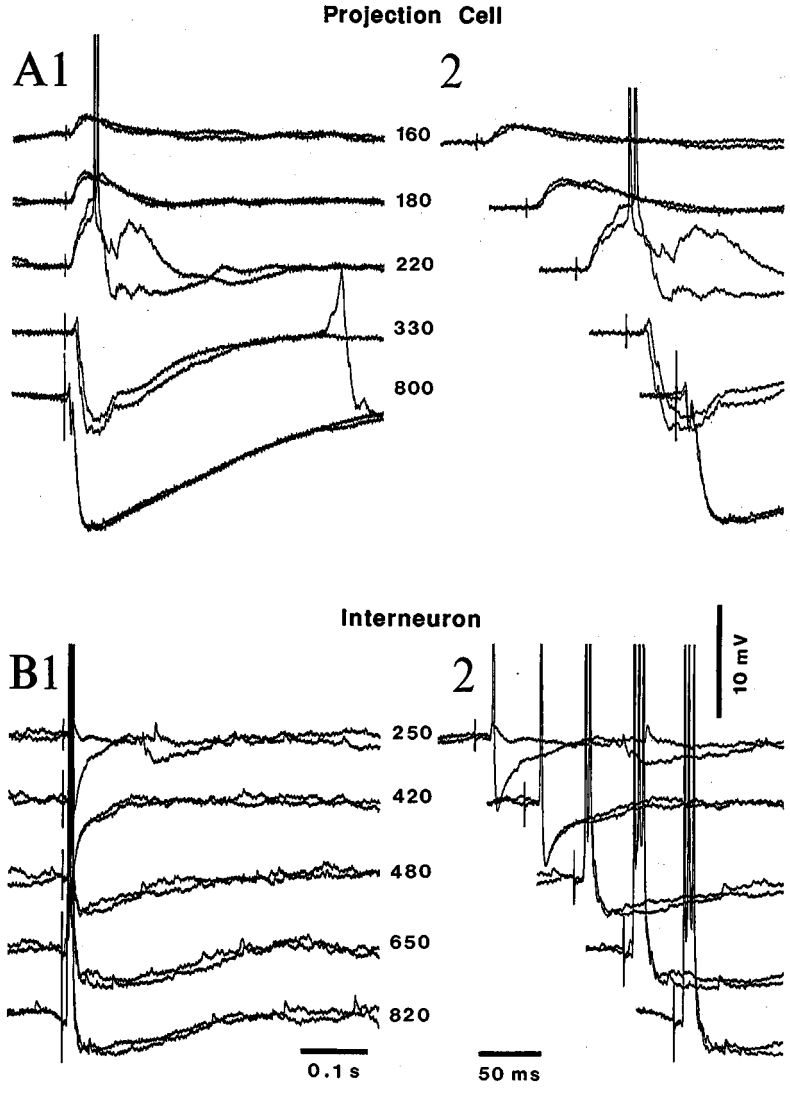

Fig. 2.20 Differing synaptic response profiles for a projection cell (*A*) and an interneuron (*B*) in lateral amygdala, as a function of stimulation intensity. Cat under barbiturate anesthesia. *A*, responses of a projection cell to perirhinal stimuli shown at low (1) and fast (2) sweep speeds. All responses elicited from $V_m = -62$ mV. Note the shift from depolarizing to hyperpolarizing responses with increasing stimulation intensity (indicated in μA). *B*, responses of interneuron, with similar low and fast sweep speed as in *A*. All responses are from $V_m = -62$ mV. Note the increasing excitation with increasing strength of stimuli (intensity indicated in μA). Stimulus duration in both *A* and *B* was 0.1 ms. For interneuron, only stimulation intensities of 250 μA and higher are depicted because this cell did not respond to lower intensities. Action potentials are truncated in *A* and *B*. From Lang and Paré (1998).

[107] Royer et al. (2000b).

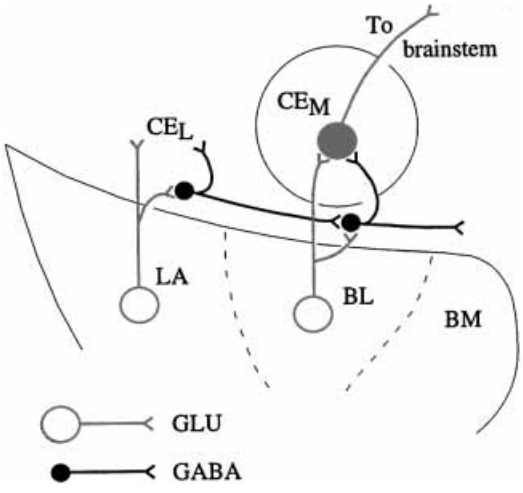

Fig. 2.21 Circuit involved in the gating of inputs from basolateral (BL) complex to the medial sector of central nucleus (CE_M) cells in guinea pig amygdala. See main text for explanation. From Royer et al. (2000a).

result, the excitatory response of CE_M cells is attenuated. Stimulation of lateral amygdala (LA) nucleus increases the impact of BL inputs to CE_M by inhibiting the progenitors of the feed-forward inhibition via the excitation of ITC neurons located more laterally.

An interesting property of ICM cells is a voltage-dependent K^+ current, termed I_{SD} for slowly de-inactivating, which activates in the subthreshold regime, inactivates in response to suprathreshold depolarizations and slowly de-inactivates upon the return to rest [107]. This current, resulting from the closure of a K^+ conductance, provides ICM cells with a state of increased excitability, associated with increased input resistance and membrane depolarization. Thus, these neurons may express a higher probability of responses to excitatory inputs. Together with the lateromedial inhibitory interactions in ICMs, this property may be operational in altering the neuronal properties of target CE_M neurons, with obvious effects on emotional reactivity, particularly during expression of fear (see above).

2.3. Thalamic neurons

There are three classes of thalamic cells: thalamocortical (TC), which are glutamatergic, thus excitatory; local-circuit GABAergic neurons, whose axons remain within the limits of the dorsal thalamic nucleus where their somata are located; and thalamic reticular (RE), which send their axons to the dorsal thalamus and are all GABAergic.

2.3.1. Thalamocortical neurons

TC neurons are bushy and their variations are linked mainly to soma size, large neurons projecting to deep and middle cortical layers, whereas small neurons project preferentially to superficial layers [108, 109]. The intrinsic electrophysiological properties of TC neurons [110] are important for the generation and synchronization of normal and pathologic thalamic oscillations (see Chapters 3 to 5).

(a) The transient Ca^{2+} current is probably the best example of a similarity between results obtained *in vitro* and *in vivo*. It is inactive at rest or depolarized levels, is de-inactivated by hyperpolarization, and generates low-threshold spikes (LTSs) crowned by rebound spike-bursts. The ability of thalamic neurons to display a paradoxical form of excitation resulting from their hyperpolarization has been known since the late 1960s [111], but systematic studies on the postinhibitory rebound and the discovery of the Ca^{2+}-dependent transient current, I_T, underlying this intrinsic neuronal property were only made possible by the advent of slice studies [5, 112]. Tonic firing at depolarized levels, at which I_T is inactivated, and burst firing at hyperpolarized levels, at which I_T is de-inactivated, were also described *in vivo* [113]. In intact-brain preparations, the LTSs crowned by Na^+-mediated spike-bursts are indispensable for the transfer of thalamically generated oscillations to cortex.

The time-dependence of the LT conductance de-inactivation is shown in Fig. 2.22. Graded de-inactivation is produced by temporal pairing of two short-lasting hyperpolarizing current pulses (panel *A*) and by trains of short, subthreshold hyperpolarizing steps (panel *B*). Moreover, when periodic hyperpolarizing current ramps were injected at a frequency of 12.5 Hz, rhythmic burst discharges were elicited at a frequency of ~2.5 Hz. This frequency transformation indicates that temporal integration of hyperpolarization could lead to periodic production of LTSs in TC neurons [114]. The time-to-peak, amplitudes, and latencies of LTSs are also graded (Fig. 2.23; see also Fig. 3.14 in Chapter 3).

In TC neurons located in the large-cell part of rostral intralaminar nuclei and antidromically activated from cortex at latencies indicating very fast conduction velocities (40–50 m/s), the LTS has a shorter refractory phase (60–70 ms) than in other TC neurons (150–200 ms), which allows the latter to fire rebound spike-bursts following each IPSP during sleep spindles at ~10 Hz [115].

(b) The hyperpolarization-activated cation current (I_H) produces a depolarizing sag [116] and is implicated, together with I_T, in the generation of a clock-like oscillation in the frequency range of sleep delta waves [117] (see Chapter 3, ***3.2.2***).

[108] Jones (1985).

[109] Steriade et al. (1997).

[110] Reviewed in previous monographs on thalamic neurons (Steriade et al., 1990b, 1997). See also the monograph focused on computational studies by Destexhe and Sejnowski (2001).

[111] Andersen and Andersson (1968).

[112] Reviewed in Llinás (1988); Huguenard (1996). The LTS of TC neurons also contains a component mediated by a persistent Na^+ current ($I_{Na(p)}$) (Parri and Crunelli, 1998).

[113] Deschênes et al. (1984); Steriade and Deschênes (1984). See recent intracellular recordings in conscious cats (Woody et al., 2003).

[114] Steriade et al. (1985).

[115] Steriade et al. (1993c). The thalamic rostral (centrolateral, CL) intralaminar neurons investigated in our study on cats generated unusually high-frequency (900–1000 Hz), fast and rhythmic (20–60 Hz) spike-bursts at relatively depolarized levels, quite an uncommon feature in the thalamus. Although some authors failed to record such thalamic intralaminar cells in slices from black mice (Pedroarena and Llinás, 2001), Seidenbecher and Pape (2001) succeeded to record very high-frequency spike-bursts in CL thalamic neurons in rats, and those rostral intralaminar neurons displayed a differential behavior, compared to other TC neurons, during spike-wave seizures in a genetic model of absence epilepsy.

[116] Leresche et al. (1990, 1991); McCormick and Pape (1990a); Soltesz et al. (1991).

[117] Steriade et al. (1991a); Curró Dossi et al. (1992a); Nuñez et al. (1992a-b). Low-frequency oscillations recorded *in vitro* and depending on interactions between thalamic reticular and relay cells are reduced or blocked by a peptide termed nociceptin/orphanin FQ (see Figs. 7–8 in Meis et al., 2002).

[118] Hernández-Cruz and Pape (1989); Kammermeier and Jones (1997).

[119] McCormick (1991); Budde et al. (1992).

[120] Timofeev et al. (2001a).

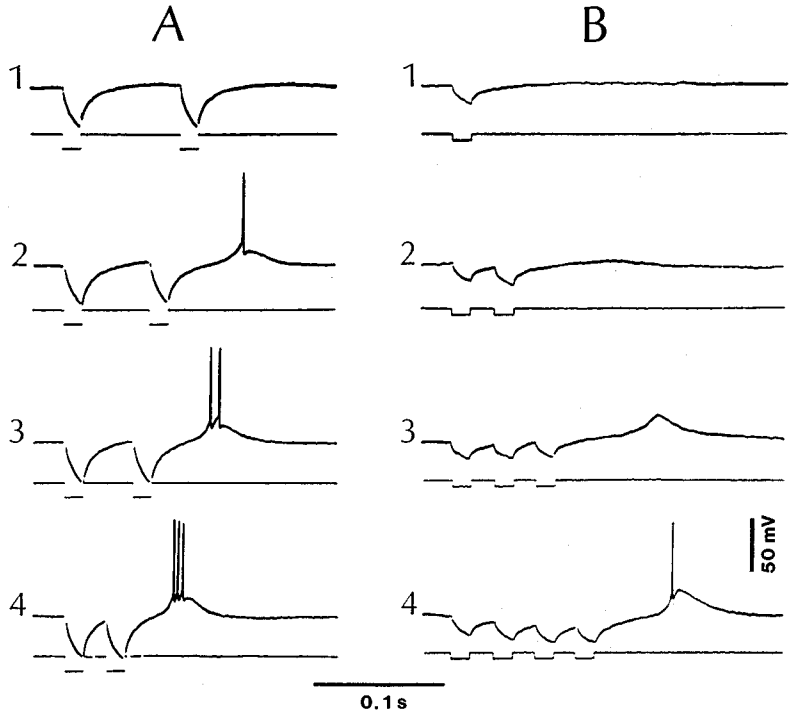

Fig. 2.22 Time-dependency of low-threshold conductance in thalamocortical (TC) neuron from ventrolateral nucleus. Intracellular recording in a cat under barbiturate anesthesia. Pairing of two (*A*) or one-to-four (*B*) hyperpolarizing current pulses with 2 nA (*A*) and 1 nA (*B*). Further explanations in text. Modified from Steriade et al. (1985).

(c) There are a variety of high-voltage-activated Ca^{2+} currents. Some are activated at −40 to −30 mV, others display a medium range for activation, −50 mV [118].

(d) The persistent Na^+ current ($I_{Na(p)}$) is activated by depolarization, near action potential threshold in TC neurons (around −55 mV) [5] and contributes to the responsiveness of TC cells in the single-spike mode.

Finally, *(e)* there are different types of K^+ currents in TC cells [119].

The intrinsic properties of TC cells are influenced by the degree of synaptic activity. This makes the occurrence of LTSs variable (see Fig. 2.23), which is a major factor in the desynchronization of oscillatory neurons and, consequently, the termination of spindle sequences [120] (see Fig. 3.14 in Chapter 3). That synaptic activity greatly modifies the LTSs is also demonstrated by reduction or abolition of LTSs and the crowning spike-bursts under the influence of fast oscillations (up to 100 Hz), which consist of EPSPs

[121] Timofeev and Steriade (1997).

[122] Bazhenov et al. (2000).

[123] Crunelli and Leresche (1991); Uhlrich and Huguenard (1997).

[124] Steriade (2001a-b).

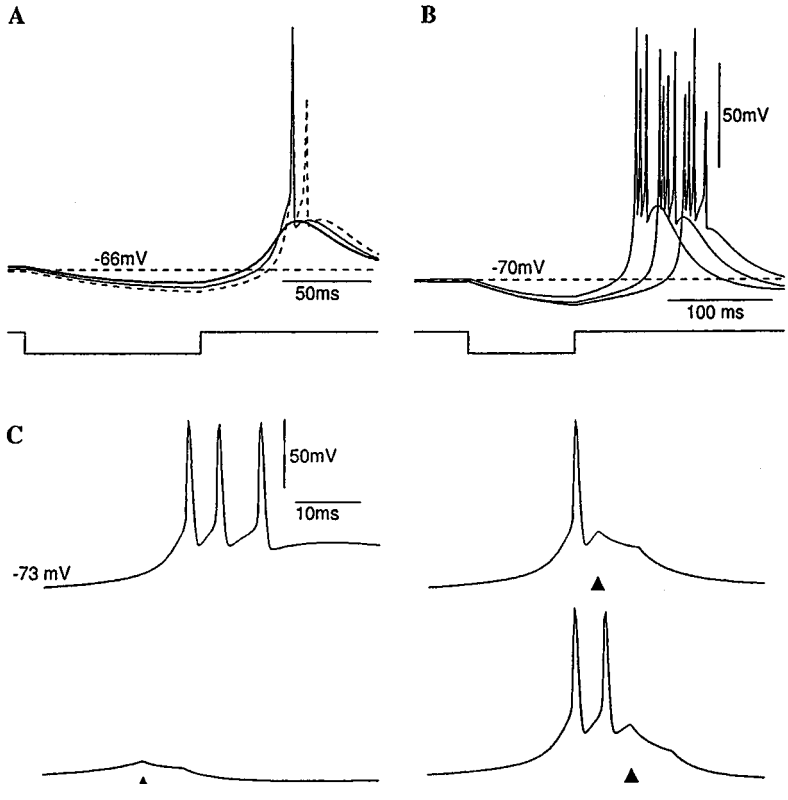

Fig. 2.23 Properties of LTSs in modeled thalamic neurons. Negative d.c. current (100 ms duration) was applied to an isolated TC cell (*A-B*) or to the TC cell from an isolated RE-TC pair (*C*). *A*, small variations of the resting membrane potential (±2 mV) elicited an LTS in isolation, or an LTS associated with a single spike or with a spike-doublet. *B*, variations of the maximal conductance for I_T (between 1.5 and 2 mS/cm^2) and I_H (between 0.005 and 0.02 mS/cm^2) significantly altered LTS' delay time. *C*, shunting effect of RE-evoked IPSP on LTS in TC neurons. Upper left panel shows an intact LTS in a TC neuron. Spikes in an RE neuron (marked by triangles) evoked IPSPs leading to earlier LTS termination. From Timofeev et al. (2001a).

arising in cerebellothalamic neurons [121]. Barrages of EPSPs tonically depolarize TC neurons, prevent the appearance of spindles in intracellularly recorded TC neurons, and disrupt the long-range synchronization of this sleep oscillation [122]. $GABA_{A\text{-}B}$-mediated IPSPs, associated with increased membrane conductance [123], have a shunting influence on LTSs by significantly delaying them, thus also contributing to the desynchronization of rhythmic thalamic activity. The interaction of IPSPs with LTSs, resulting in a delay in generation of rebound LTSs, is illustrated in Fig. 2.24. Other effects of network activities on intrinsic properties of TC neurons are discussed elsewhere [124].

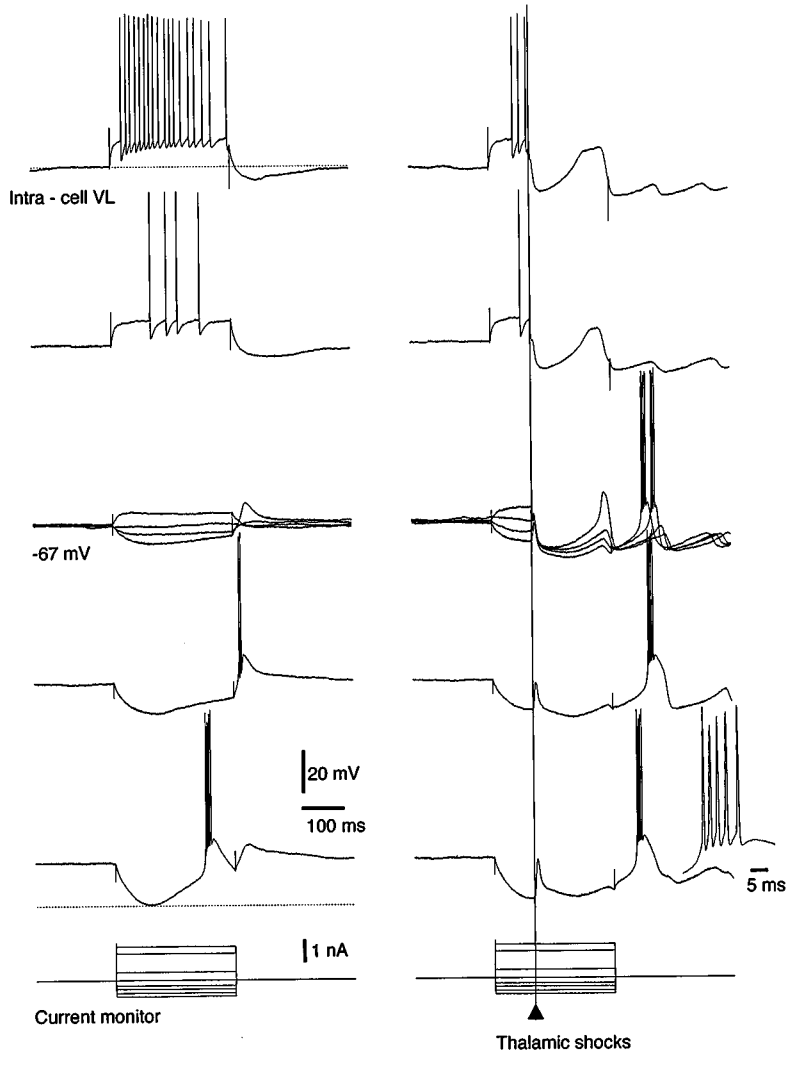

Fig. 2.24 The low-threshold spike (LTS) and its interaction with synaptic responses in TC neurons. Intracellular recordings from ventrolateral nucleus in cat under barbiturate anesthesia. Left column shows responses to intracellularly applied current pulses (depolarizing and hyperpolarizing) during periods largely free of synaptic events (inter-spindle lulls). In the right column, local thalamic stimuli (marked by the triangle) were applied during the current pulses. Note the delays in generation of rebound LTSs. From Timofeev et al. (2001a).

2.3.2. Local inhibitory interneurons

The presence and numbers of local GABAergic neurons vary in different species and dorsal thalamic nuclei. For example, these neurons are negligible in dorsal nuclei of rodents, most notably in the ventroposterior complex, but are present in the dorsal lateral geniculate nucleus, which contains as many of these cells (20–30%) as there are in cats and primates [125].

In early extracellular studies, presumed local interneurons were recorded in different dorsal thalamic nuclei and tentatively recognized by high-frequency spike-bursts in response to afferent volleys and the absence of antidromic invasion from all stimulated sites. In some of those studies, the oscillatory property of bursting interneurons was related to the spindle oscillation in TC and RE neurons [126]. Recent intracellular studies of local inhibitory interneurons, all performed on slices from lateral geniculate nucleus of cats [127] and rats [128, 129], have investigated the propensity to burst firing of these cells, with emphasis on the functional balance between two opposing currents (I_T and I_A) in promoting spike-bursts and on the oscillatory properties of local-circuit cells. Thus, it was shown that A-type K^+ current opposes the burst [128].

The burst firing of morphologically identified interneurons upon a depolarizing step at a hyperpolarized membrane potential and burst oscillation (5–15 Hz) in these cells are illustrated in Fig. 2.25 (see panel *C*). The burst oscillation could be initiated by stimulation of optic tract fibers [129], suggesting that it may occur in natural conditions. These oscillations are similar to those previously reported to occur in presumed interneurons recorded *in vivo* at the level of other thalamic nuclei [126].

Local GABAergic neurons in dorsal thalamic nuclei of cat produce biphasic, $GABA_{A\text{-}B}$ IPSPs in TC neurons [130]. As most dorsal thalamic nuclei receive inputs from GABAergic RE neurons, the only nuclei in which the action of local-circuit neurons can be safely studied in isolation from other inhibitory inputs are cat anterior nuclei, which are devoid of connections from the RE nucleus [131]. $GABA_{A\text{-}B}$ IPSPs are evoked in anterior thalamic neurons by afferent inputs (Fig. 2.26). An earlier, smaller amplitude IPSP is also recorded from these neurons and is ascribed to intraglomerular processes [132].

2.3.3. Thalamic reticular neurons

The RE nuclear complex, a thin sheet of neurons that surrounds the rostral and lateral surfaces of the thalamus, is unique because all neurons are GABAergic [133]. The term *reticular* was coined because the continuity of this neuronal sheet is interrupted by bundles of

[125] Spreafico et al. (1993). At variance with other mammalian species (including non-human primates), GABAergic neurons in dorsal association thalamic nuclei of humans migrate from the telencephalon to the diencephalon (Letinic and Rakic, 2001). This may contribute to the increased population of local GABAergic neurons in mediodorsal and pulvinar nuclei, and to the expansion of these nuclei in humans.

[126] Steriade et al. (1972).

[127] McCormick and Pape (1988); Pape and McCormick (1995).

[128] Pape et al. (1994).

[129] Zhu and Lo (1999); Zhu et al. (1999a-b).

[130] Hirsch and Burnod (1987); Crunelli et al. (1988).

[131] Steriade et al. (1984); Velayos et al. (1989).

[132] Paré et al. (1991). For the development and significance of presynaptic dendrites, see Perreault et al. (2003) and Steriade (2003).

[133] Houser et al. (1980); Benson et al. (1991).

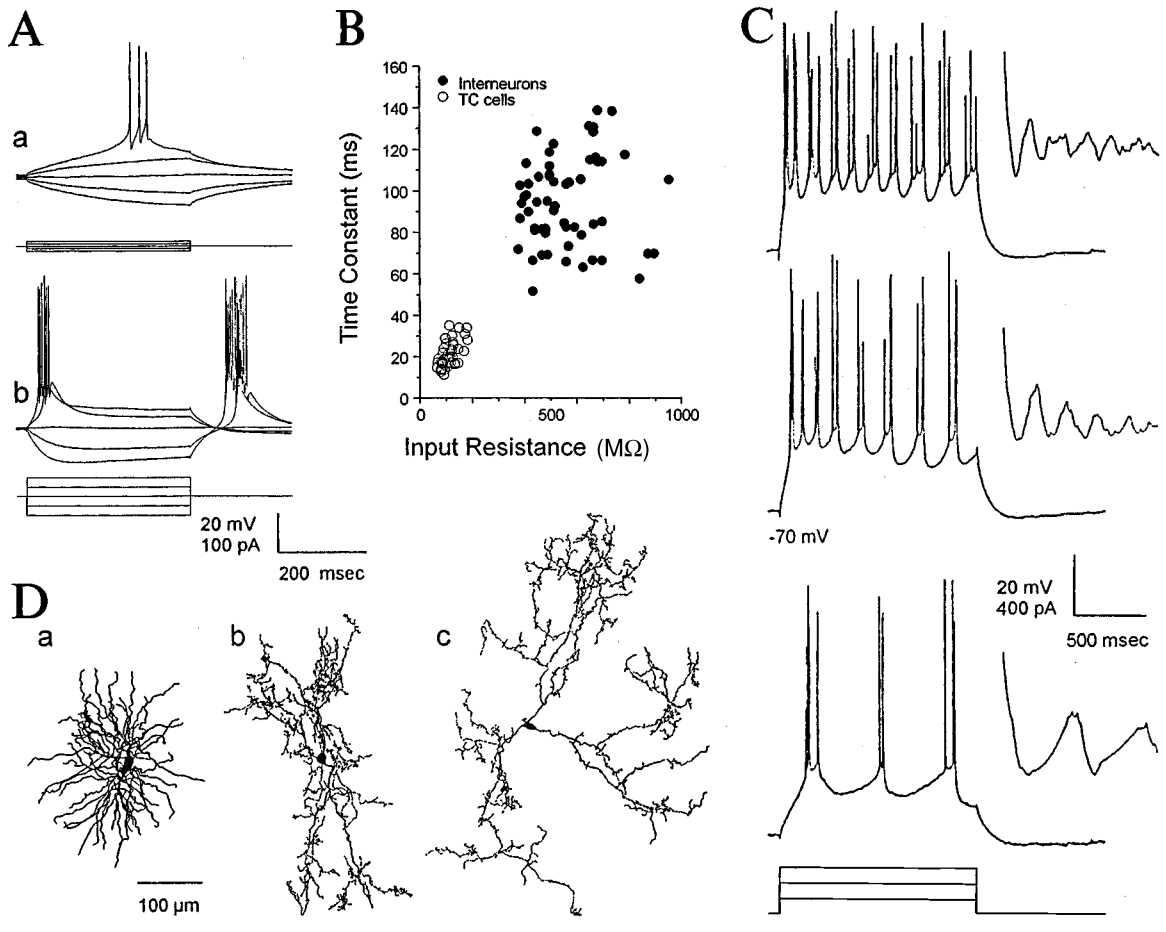

Fig. 2.25 Physiological and morphological characteristics of bursting and oscillatory behavior of rat lateral geniculate (LG) local interneurons *in vitro*. Whole-cell patch recordings. *A*, responses to a series of current pulses of an interneuron (*Aa*) and a thalamocortical neuron (*Ab*). The resting membrane potentials were −66 mV (*Aa*) and −71 mV (*Ab*). Spike height was truncated artificially due to digital sampling. *B*, the interneuron has a higher input resistance and longer membrane time constant than the thalamocortical neuron. *C*, varying burst oscillation with increasing current injection in the LG interneuron. Right, autocorrelation function for each trace. *D*, camera lucida reconstructions of a physiologically identified thalamocortical neuron (*a*) and two interneurons (*b-c*). Modified from Zhu et al. (1999a).

axons that provide excitatory inputs from cortical and TC neurons. RE neurons project back to TC neurons, thus forming a feedback inhibitory loop that is crucially implicated in the synchronization of sleep spindles and the inhibition of TC neurons during cortically generated spike-wave seizures (see ***2.4.1*** and Chapter 5).

RE neurons have long dendrites, whose secondary and tertiary branches possess vesicle-containing appendages that form synapses on the dendrites of neurons in the same nucleus. These dendrodendritic synapses are common in cats [134] and rats [135] as well as in primates, but seemingly less frequent in this species [135] in which intra-RE communication may operate via axo-dendritic contacts or

[134] Deschênes et al. (1985); Yen et al. (1985).

[135] Originally, Ohara and Lieberman (1985) were unable to find dendrodendritic synapses in the posterior sector of rat RE nucleus. However, Pinault et al. (1997), working on ultrathin horizontal sections of RE nucleus in the adult rat, reported the presence of numerous dendrodendritic contacts. Williamson et al. (1993) worked on non-human primates.

[136] Steriade et al. (1986).

[137] Domich et al. (1986).

[138] Mulle et al. (1986); Huguenard and Prince (1992).

[139] Contreras et al. (1993).

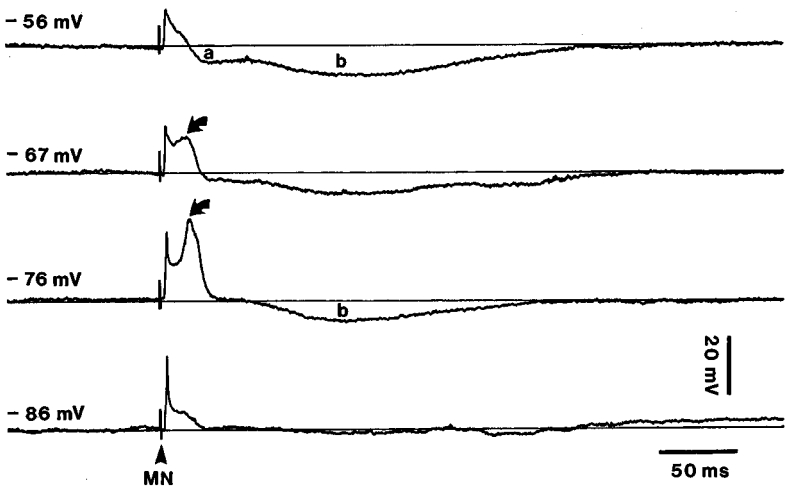

Fig. 2.26 $GABA_{A–B}$ IPSPs mediated by local inhibitory interneurons in cat anteroventral (AV) thalamic nucleus. Urethane anesthesia. In the cat, anterior nuclei are devoid of connections from the other type of thalamic inhibitory neurons, reticular cells. Stimulation (arrowhead) applied to mammillary nucleus (MN). At resting V_m(−56 mV), MN evoked a primary EPSP (stimulus adjusted below the threshold of the action potential) and a biphasic IPSP, consisting of two (*a*–*b*) components. Under steady hyperpolarization (−76 mV), the EPSP increased in amplitude, a low-threshold spike (LTS) was triggered (arrows), and the early Cl^--dependent IPSP (*a*) was reversed. The reversal of the late (*b*), probably K^+-mediated, component was at −86 mV. Unpublished data by D. Paré and M. Steriade.

other mechanisms. Thus, contrary to TC neurons, which do not communicate from one dorsal thalamic nucleus to another, but only through intermediary RE and/or neocortical neurons, RE neurons form an interconnected network that accounts for the initiation of spindles even when disconnected from thalamus and cortex (see Chapter 3).

Like TC neurons, RE neurons operate in two functional modes: tonic discharges during brain-active states and rhythmic spike-bursts during natural slow-wave sleep [136]. The spike-bursts are much longer (30–80 ms, but up to 1 s when followed by a tonic tail) than in TC neurons (5–15 ms), and RE-cells' bursts display an *accelerando-decelerando* pattern, different from the progressively increasing interspike intervals in TC neurons [137]. These studies on naturally awake and sleeping cats were followed by intracellular recordings in acute experiments, both *in vivo* and *in vitro*, which showed that the LTSs of RE neurons are located in dendrites [138]. The presence of spike-bursts in presumed dendritic recordings from RE neurons and the graded nature of dendritic LTSs (Fig. 2.27) were revealed in intracellular recordings *in vivo* [139]. The prolonged burst response of RE neurons is modulated by both

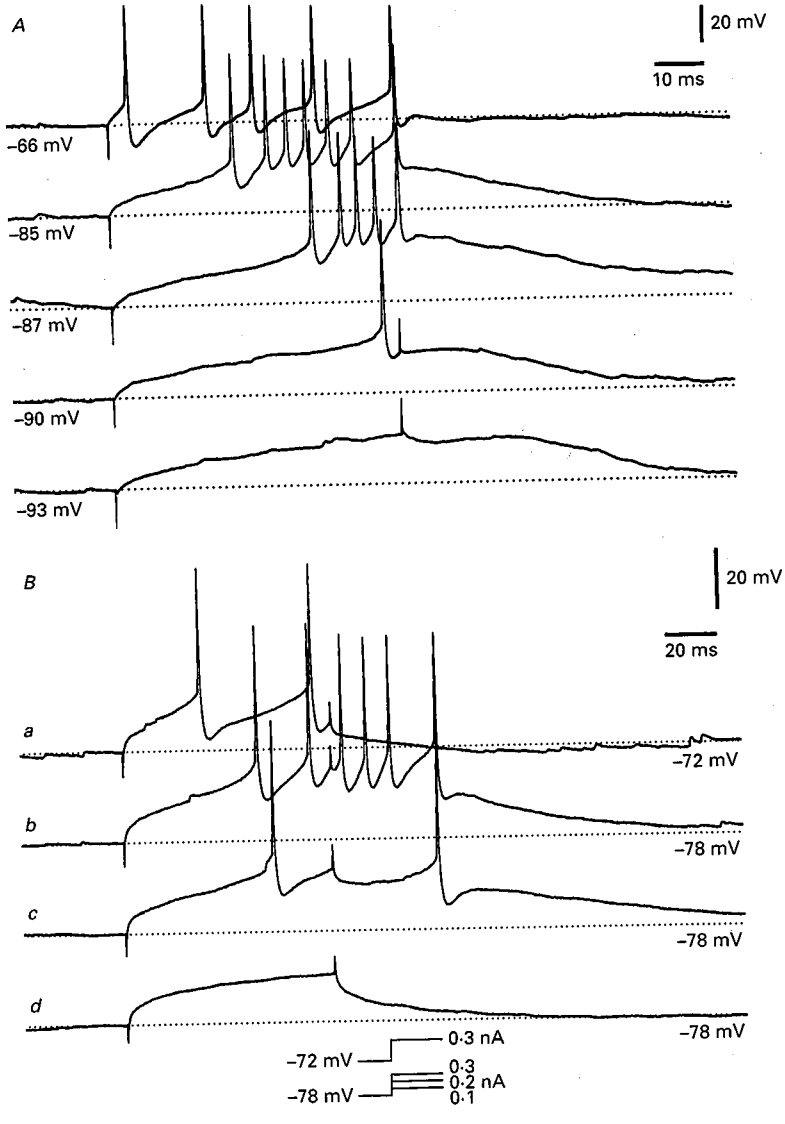

Fig. 2.27 Gradual nature of the burst response in cat RE neurons, recorded from the rostrolateral sector of the nucleus. Urethane anesthesia. *A*, a depolarizing pulse of constant amplitude was applied while the cell was progressively hyperpolarized by direct current. *B*, a depolarizing pulse of 0.3 nA was applied at rest (trace *a*) and at a hyperpolarized V_m (trace *b*). The V_m was then kept constant and the pulse was reduced in amplitude. The burst response diminished in parallel. From Contreras et al. (1993).

[140] Contreras and Steriade (1996).

[141] Contreras et al. (1992).

[142] Crunelli et al. (1987).

[143] Bal and McCormick (1993).

the level of membrane hyperpolarization and the intensity of depolarizing inputs, indicating that RE neurons exhibit a bursting behavior with a broad range of integrative properties.

Figure 2.28 illustrates the electrophysiological identification of an RE neuron, consisting of an antidromic response evoked by stimulation in the dorsal thalamus (ventrolateral, VL, nucleus), followed by a burst and a sequence of oscillatory spike-bursts in the frequency range of spindles. Barrages of EPSPs in the postinhibitory rebound excitation of the RE neuron depicted in Fig. 2.28 developed concomitantly with the negative field potential recorded from the VL nucleus, and thus could be due to the high-frequency spike-bursts of TC cells, whereas the field potential recorded focally from area 4 developed later. However, cortical neurons outside the site of focal recording might have also been at the origin of these EPSPs. Indeed, the best way to trigger spindle oscillations by acting directly on their pacemaker, the RE nucleus, is to stimulate the cerebral cortex [126, 140].

While the majority of RE neurons display spike-bursts at hyperpolarized levels of membrane potential, ∼20% of this GABAergic population does not fire spike-bursts to large depolarizing current pulses at all levels of hyperpolarization, even when the membrane potential reaches −100 mV [141]. These cells fire at 8–10 Hz at the resting membrane potential and at higher frequencies (40 Hz) under slight depolarization that mimics the setting into action of ascending activating systems using glutamate as neurotransmitter. The absence of spike-bursts in this neuronal class from the RE nucleus might be related to the facts that (a) the overwhelming majority of ventral lateral geniculate neurons, which share a common embryological origin with RE neurons [108], do not express I_T [142], and (b) there is a peculiar balance of currents in these neurons, which prevents them from firing burst discharges.

The ionic basis of rhythmic spike-bursts and tonic discharges in RE neurons was investigated in slices from the perigeniculate sector of this nuclear complex, maintained *in vitro* [143], and is illustrated in Fig. 2.29. Briefly, the high-frequency burst of Na^+-K^+ fast action potentials, crowning the Ca^{2+}-dependent LTS produced by a hyperpolarizing current pulse, likely activates high-threshold Ca^{2+} currents that result in the activation of $I_{K(Ca)}$, and therefore an after-hyperpolarization whose depth and duration determine the amplitude of the subsequent LTS. The authors [143] also postulated that the entry of Ca^{2+} into RE cells activates a non-selective cation current, I_{CAN}, which results in a slow after-depolarization and the generation of tonic discharges at the end of the oscillatory firing (panel *A* in Fig. 2.29). Activation of systems with depolarizing

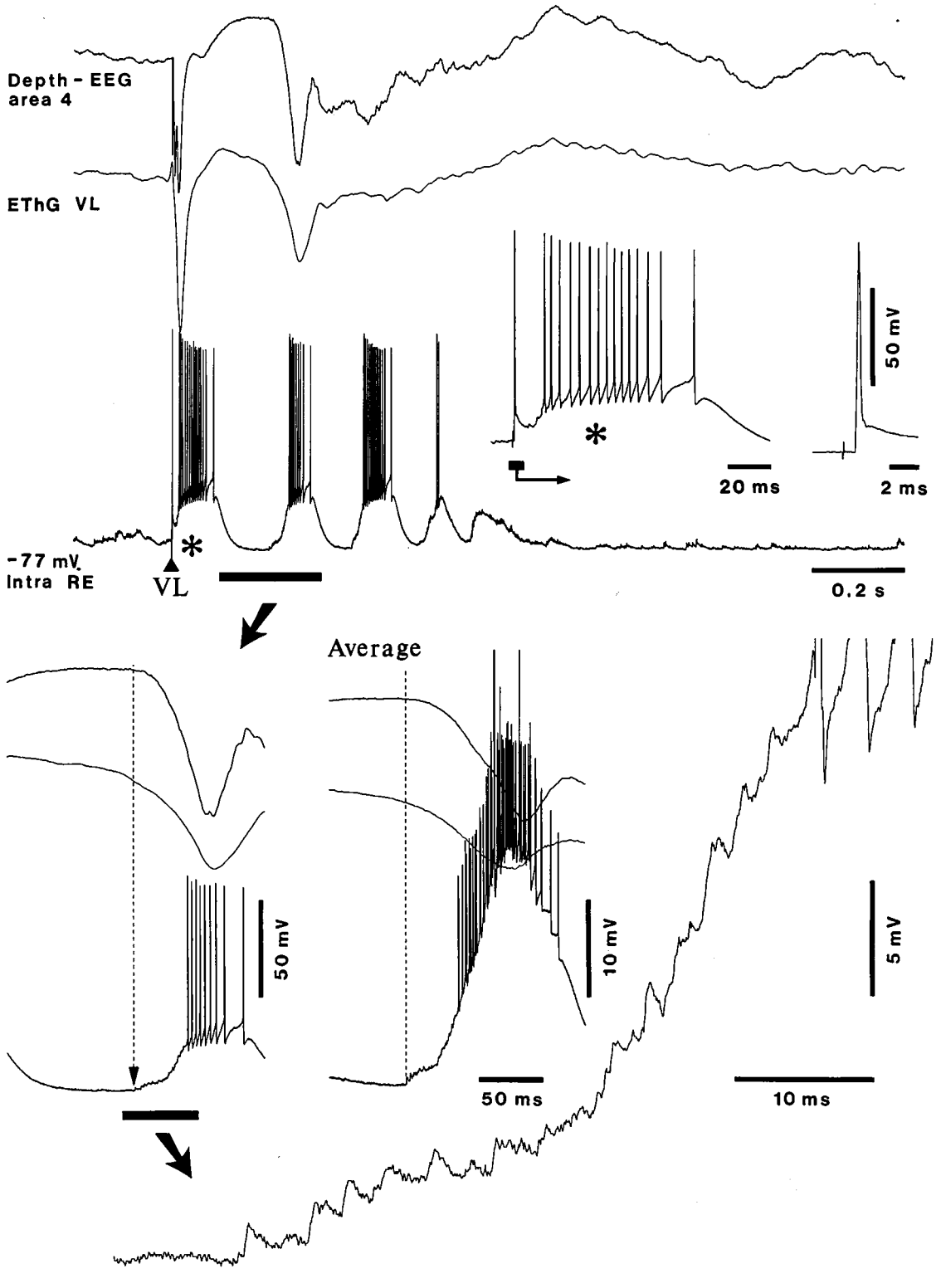
Depth - EEG
area 4
EThG VL
50 mV
20 ms
2 ms
-77 mV
Intra RE
VL
0.2 s
Average
50 mV
10 mV
5 mV
50 ms
10 ms

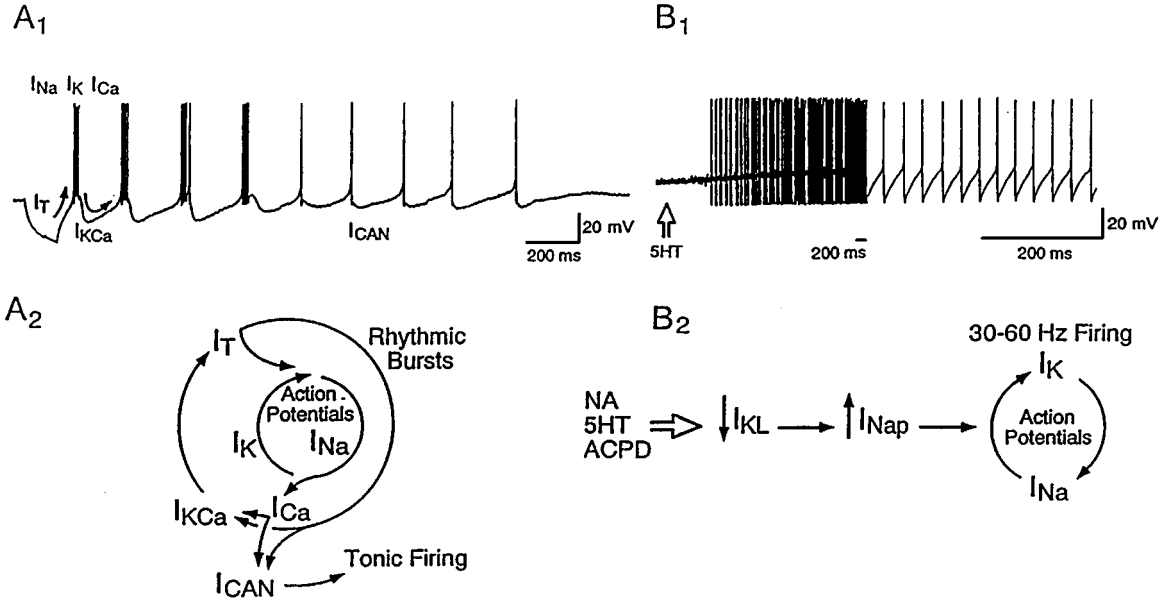

Fig. 2.29 Scheme of the ionic basis of rhythmic burst and tonic firing in RE neurons from *in vitro* studies of perigeniculate neurons. Full explanations in the main text. From Bal and McCormick (1993).

[144] Kim and McCormick (1998). The depolarizing plateau giving rise to tonic firing is probably mediated by $I_{Na(p)}$ as it was blocked by tetrodotoxin.

actions on RE neurons, mediated by glutamate metabotropic, noradrenergic and serotoninergic receptors [44], results in a tonic depolarization through the reduction in a "leak" K^+ current (panel *B* in Fig. 2.29), and leads to firing at high rates, 30–40 Hz, as seen during natural waking [136]. The long spike-bursts of RE neurons are also followed by a tonic tail of single action potentials. This was reported, first, using extracellular recordings (that preclude a compromised integrity of membrane properties) in naturally sleeping animals [136], and was also found with intracellular recordings *in vivo* [39] and *in vitro* [144], at membrane potentials closer to those observed *in vivo*.

Fig. 2.28 (opposite) Electrophysiological identification of an RE neuron from the rostrolateral sector of the nucleus. Cat under ketamine-xylazine anesthesia. Intracellular recording of an RE neuron together with field potentials from the thalamic ventrolateral (VL) nucleus and depth of cortical area 4. Top panel depicts a VL-evoked early response as well as spindle oscillation. The early response of the RE neuron is expanded on the right to show the initial antidromic discharge, followed by a high-frequency burst (asterisk). Bottom panels show: (*a*) on the left, first postinhibitory rebound excitation (expanded from the part marked by the horizontal bar and arrow in the above trace); dotted line and arrow indicate the beginning of EPSPs in the RE neuron, slightly in advance of the onset of field negativity in area 4 but simultaneously with the developing rebound excitation in the field potential from the VL nucleus; RE-cell EPSPs are further expanded below (horizontal bar and arrow); these EPSPs are triggered by rebound spike-bursts in TC cells; and (*b*) EPSP-triggered (dotted line) average ($n = 5$) of the field potential in cortex and VL nucleus. From Grenier et al. (1998).

[145] Thomson (1988a-b).

2.4. Intrathalamic, intracortical, and corticothalamic neuronal circuits

Synaptic articulations between thalamic and neocortical neurons are decisive in synchronizing different oscillatory types in states of vigilance and during paroxysmal states, and to make them similar to what is observed in natural life. Some rhythms, within the frequency range of waking or SWS oscillations, may arise from single TC or neocortical neurons through their intrinsic properties. This is the case, for example, of the clock-like delta oscillation that is produced by the interplay between two intrinsic currents of TC neurons or of fast (gamma) oscillations triggered by direct depolarization of TC and cortical neurons (see Chapter 3, ***3.2.2*** and ***3.3.2***). However, such oscillations at the single-cell level cannot reproduce the synchronization features seen in the intact-brain because of the absence of long-range connectivity in extremely simplified preparations. *In vivo*, corticothalamic projections acting on GABAergic RE neurons synchronize the intrinsically generated delta oscillation in TC neurons so that the rhythm can be observed in field potential recordings from the dorsal thalamus, and this activity of TC neuronal pools can be transferred to cortex where it is coalesced with that of cortically generated slow oscillation [117]. In this section, I discuss the synaptic networks that are implicated in normal and epileptic oscillations.

2.4.1. Relations between thalamic relay and thalamic inhibitory neurons

With the exception of cat anterior thalamic and some midline thalamic neurons [131], virtually all TC neurons project to, and are targets of, GABAergic RE neurons in all investigated species. The RE-induced powerful inhibition of TC neurons was demonstrated by loss of prolonged hyperpolarizations, consisting of $GABA_{A\text{-}B}$ IPSPs, in TC neurons following transections separating the RE nucleus from the dorsal thalamus or excitotoxic lesions of RE neurons *in vivo* [114] and by the effects of stimulating RE neurons in thalamic slices [145]. In the latter, *in vitro* study, trains of RE-triggered GABA-mediated IPSPs in TC cells, at similar frequencies as those displayed by sleep spindles, evoked LTSs crowned by spike-bursts, irrespective of other synaptic inputs. This corroborated the idea of the role played by RE neurons in initiating spindle sequences in dorsal thalamus [114]. The IPSPs evoked by RE stimulation resembled the biphasic nature of responses elicited by electrophoretically applied GABA [145]. Simultaneous intracellular recordings from RE and TC neurons during spindle oscillations *in vivo* reveal

[146] Bal et al. (1995a-b).

[147] Graybiel and Elde (1983); Oertel et al. (1983).

[148] Uhl et al. (1985); Señaris et al. (1994).

[149] Leresche et al. (2000).

[150] Beranek et al. (1997).

[151] Delphs and Dichter (1983).

the time-relation between depolarizing waves associated with spike-bursts in RE neurons and consequent hyperpolarizing IPSPs in TC neurons (Fig. 2.30).

The interactions between RE and TC neurons in spindle generation have also been investigated in slices from the perigeniculate nucleus, the visual sector of the RE nucleus [146]. These studies identified the synaptic-activated conductances and time-relations between activities of RE and TC neurons. Thus, the spike-burst of RE neurons lasted for ∼30 ms and was followed by EPSPs at a latency of ∼130 ms, while the IPSP generated in TC neurons by burst discharges in RE neurons was ∼130 ms in duration if it was followed by a rebound LTS and ∼150 ms in duration if it was not. The spike-burst in TC cells was ∼10 ms in duration. These differences between spike-bursts crowning LTSs in RE and TC cells, displaying much longer duration in RE cells, corroborate data from *in vivo* recordings during natural sleep [137].

The majority of GABAergic RE neurons also express immunoreactivity for somatostatin [147]. Although somatostatin was not initially identified in axon terminals of RE neurons in the dorsal thalamus and this peptide could have been regarded as a "silent passenger", somatostatin receptors are found in both sensory nuclei of the dorsal thalamus and the RE nucleus itself [148]. In thalamic slices from cat and rat, somatostatin has no effect on passive properties of TC ventroposterior and lateral geniculate neurons (Fig. 2.31*A*) but reduces the amplitudes of $GABA_{A\text{-}B}$ IPSPs (Fig. 2.31*B*) via a presynaptic mechanism, and the action is stronger on bursts of inhibitory postsynaptic currents (IPSCs) than on single IPSCs in TC cells [149]. Since peptides are released preferentially during bursts of action potentials, as is the case of RE-cells' discharges during spindles, this study suggests that the release of somatostatin is increased in the dorsal thalamus, thus reducing the inhibitory-rebound sequences in TC during this sleep rhythm. It is known that exogenous administration of somatostatin or its analogues reduces slow-wave sleep (SWS) [150]. In an earlier work [136], we called upon the possible effects of somatostatin in the thalamus to explain different relations between RE and TC cells during natural states of SWS and wakefulness (reciprocal images and similar aspects, respectively), by referring to studies showing that somatostatin decreases the amplitudes of IPSPs and induces depolarization in cortical neurons [151]. The recent study showing a somatostatin-induced decrease in amplitudes of inhibitory postsynaptic potentials (IPSPs)/IPSCs in TC cells [149] indicates that the relation between RE and TC neurons, usually considered as only inhibitory via GABA release, is probably more complex. Additionally, in that

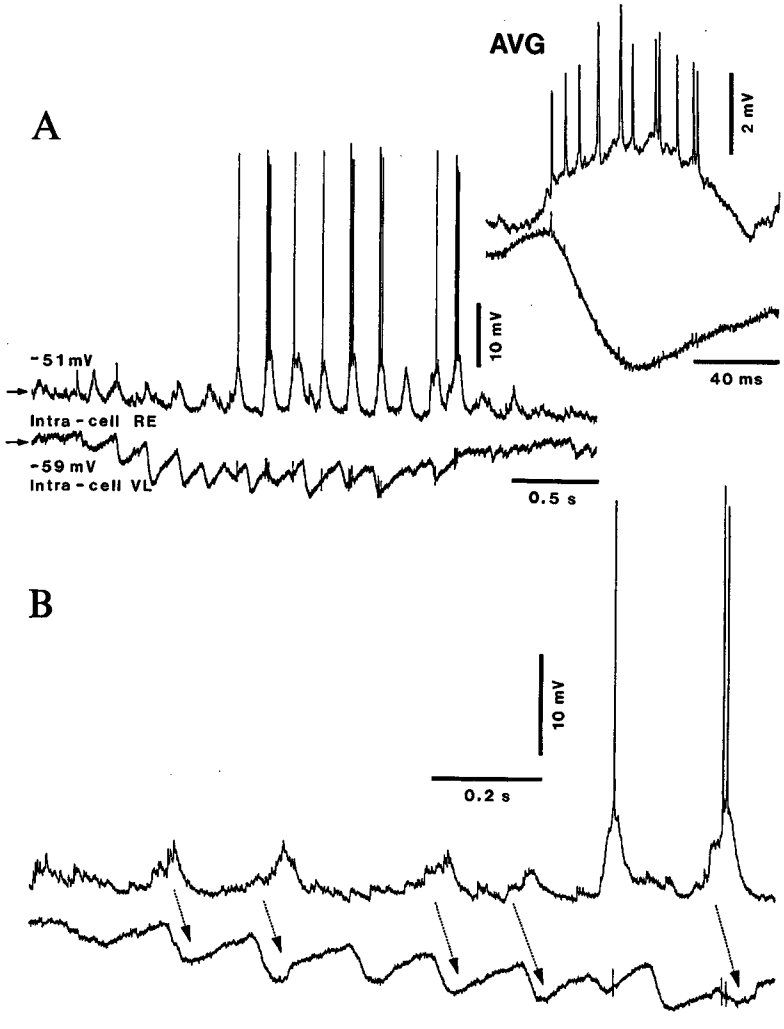

Fig. 2.30 Relations between simultaneously recorded depolarizing spindle waves in a rostrolateral RE cell and hyperpolarizing IPSPs in a TC cell from the ventrolateral (VL) nucleus. Decorticated cat under ketamine-xylazine anesthesia. *A*, spindle sequence. Inset: averaged (AVG. $n = 15$) activity triggered by the onset of IPSPs in a VL neuron. *B*, another spindle sequence showing the close time relation between the depolarizing waves in an RE cell and IPSPs in a VL cell. Small deflections in the trace from the VL cell are capacitive coupling artifacts from RE cell's action potentials. From Timofeev and Steriade (1996).

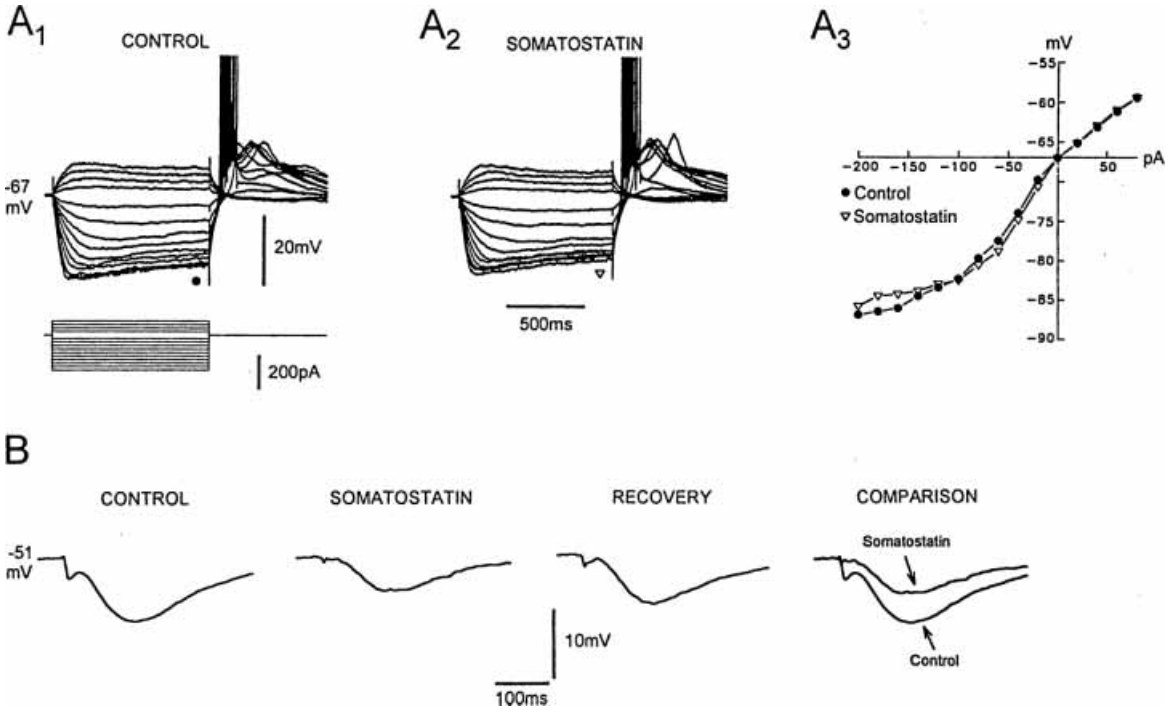

Fig. 2.31 Somatostatin decreases the amplitude of $GABA_{A\text{-}B}$ IPSPs but has no effect on passive membrane properties of cat TC neurons. Intracellular recordings under current clamp in thalamic slices from dorsal lateral geniculate (dLG) nucleus. *A1-A2*, family of voltage responses to current steps shows the lack of action of 10 μM somatostatin on the membrane properties of a TC cell from dLG nucleus. Data from this neuron were used to construct the voltage-current plot depicted in *A3*. Action potentials in *A1-A2* have been truncated for clarity. *B*, bath application of 10 μM somatostatin reduced the amplitude of $GABA_{A\text{-}B}$ IPSPs elicited in the TC cell from dLG nucleus. Each trace is the average of five consecutive events. From Leresche et al. (2000).

earlier article [136], we also considered the possibility that RE neurons also contact local-circuit GABAergic neurons in various dorsal thalamic nuclei, which may lead to disinhibition of TC neurons. This hypothesis is based on anatomical and physiological data, discussed below.

Synaptic profiles of RE-cells' origin contact not only the somadendritic domain of TC cells, but also presynaptic dendrites of local inhibitory cells [152]. About 8–10% of RE neurons project to local thalamic interneurons [153] and, although apparently minor, this GABAergic-to-GABAergic projection may produce significant effects on the ultimate targets, TC neurons, the more as, in other brain structures, GABAergic neurons are much more sensitive to GABA than other neuronal types [154]. Indeed, a greatly increased incidence of IPSPs in TC neurons was observed after destruction of RE neurons, reflecting the release from the inhibition of local interneurons after the excitotoxic lesion of RE perikarya [114]. The

[152] Montero and Singer (1985).

[153] Liu et al. (1995).

[154] Grace and Bunney (1979, 1985).

[155] See Box 1 in Steriade (1999b).

[156] DeFelipe and Farinas (1992); Mountcastle (1997, 1998); Somogyi et al. (1998).

[157] Thomson and West (1993).

[158] Markram et al. (1997a).

[159] Thomson et al. (1988).

[160] Stafstrom et al. (1985); Markram and Sakmann (1994); Stuart and Sakmann (1995); Fleidervish and Gutnick (1996).

[161] Galarreta and Hestrin (1998).

[162] Timofeev et al. (2000b).

[163] Kawaguchi (1995).

connection between the two types of thalamic GABAergic cells, RE and local-circuit interneurons, may also be important for focusing attention to relevant signals. In this hypothesis [155], RE neurons, which are directly connected to TC neurons that receive signals from ascending pathways, may contribute to enhancement of relevant activity by inhibiting the appropriate pool of local-circuit GABAergic elements. Simultaneously, the activity in adjacent RE areas would be suppressed by RE-to-RE GABAergic contacts within the nucleus. The consequence would be the disinhibition of related local interneurons and the inhibition of weakly excited TC neurons in areas adjacent to the active focus.

2.4.2. Intracortical neuronal networks

The local excitatory-inhibitory circuitry in neocortex has been studied by paired and multiple intracellular recordings *in vitro*, while long-range connections have been explored using multi-site extracellular and dual intracellular recordings *in vivo*.

Pyramidal neurons constitute 70–75% of neocortical neurons and each of them receives 5000 to 60 000 synapses [156]. Single-axon EPSPs, reflecting connections among pyramidal cells, have been investigated in slices from rat somatosensory and motor cortices [35, 157, 158] and in isolated slabs from cat association cortex *in vivo* [41]. The amplitude of single-axon EPSPs *in vitro* varies from 0.1 to 9 mV, with means around 1–1.5 mV. Similar values are found *in vivo*, using paired intracellular recordings from presynaptic intrinsically bursting (IB) and postsynaptic regular-spiking (RS) neurons, which show larger-amplitude, compound EPSPs in postsynaptic RS neurons after spike-bursts in IS neurons, compared to postsynaptic responses elicited by single action potentials (Fig. 2.32). The increased amplitude and duration of single-axon EPSPs under depolarization within physiological limits [35, 157, 158, 159] can be explained by activation of voltage-dependent currents, such as low-voltage-activated Ca^{2+} and slowly inactivating or persistent Na^{+} current, $I_{Na(p)}$ [160]. While *in vitro* experiments show that presynaptic stimulation at fast (20 Hz) frequency produces a synaptic depression to about 4% of the control value [161], pulse trains applied *in vivo* at even higher frequencies (40 Hz) induce, first, a facilitation, and only later depression [162].

Local inhibitory cortical interneurons (20–30% of the total neuronal population) exhibit different morphology and immunoreactivity to GABA, calcium-binding proteins and peptides (see Figs. 2.6–2.7), and different electroresponsive properties [30, 34, 163]. Some differences between the results of *in vitro* and *in vivo* studies concern the IPSPs elicited in pyramidal cells by local-circuit GABAergic cells;

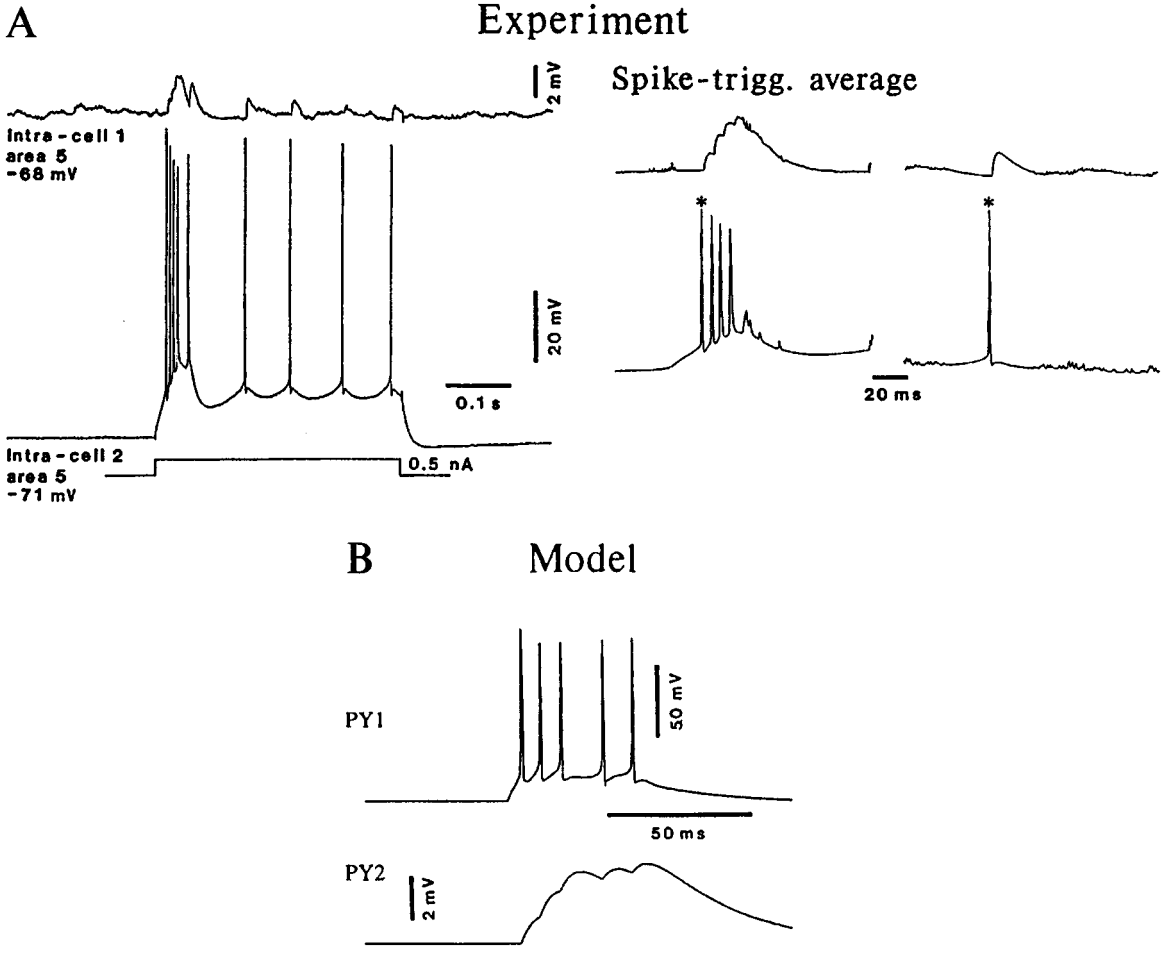

Fig. 2.32 Burst firing induced by a depolarizing current pulse in a presynaptic intrinsically bursting (IB) neuron results in a larger-amplitude postsynaptic response in a regular-spiking (RS) neuron, compared to that elicited by single action potentials. Paired recordings from an isolated cortical slab from cat suprasylvian gyrus, under ketamine-xylazine anesthesia. *A*, direct depolarization (0.5 nA) applied to the IB cell elicited a high-frequency burst, followed by a tail of tonic firing. Spike-triggered (asterisk in IB cell) averaged postsynaptic responses to bursts (left) and single spikes (right). *B*, model of paired pyramidal (PY) neurons; burst in PY1 resulted in a train of EPSPs in PY2, similar to experimental data shown in *A*. Modified from Timofeev et al. (2000a).

[164] Van Brederode and Spain (1995).

[165] Douglas and Martin (1991).

[166] Contreras et al. (1997d).

[167] Connors et al. (1988).

namely, the laminar location of IPSPs in different areas and the different components of these inhibitory potentials. Strong $GABA_{A\text{-}B}$ IPSPs in slices from motor cortex are present in layers II/III but weakly in layer V [164], whereas IPSPs are more pronounced in deep layers of cat visual cortex *in vivo* [165]. Another *in vivo* study on cat association cortex could not find any prevalent depth for the location of IPSPs [166]. The biphasic, $GABA_{A\text{-}B}$, IPSPs found *in vitro* [164, 167] are different from the monophasic, $GABA_A$, Cl^--dependent IPSPs recorded *in vivo* [166]. In the latter experimental condition, in which an important background synaptic

activity is present, the $GABA_A$ IPSP shuts off cellular activity in a large proportion of cells, thus leading to a generalized phenomenon of disfacilitation that accounts for the tail of hyperpolarization after the IPSP [166]. Long-lasting, monophasic IPSPs in neocortical neurons have also been described in earlier *in vivo* studies [168].

Reciprocal responses of pyramidal and local inhibitory neurons have been investigated with paired intracellular recordings. Single-axon EPSPs and IPSPs between identified neurons revealed the mechanisms for coupling the inputs reaching various cortical layers and showed that synaptic transmission is differentially exerted by the same axon of a pyramidal neuron innervating another pyramidal cell and a local inhibitory interneuron, with synaptic depression in the former case and facilitation in the latter [34, 35]. Pyramidal neurons are best recruited by tonic presynaptic firing in other pyramidal cells, while local inhibitory neurons are preferentially recruited by spike-bursts in presynaptic pyramidal neurons [169]. The responses of spiny inhibitory interneurons to paired-pulse stimulation of presynaptic pyramidal cells show facilitation at intervals shorter than 50 ms [170]. All these effects may apply to the mechanisms underlying frequency-dependent plasticity (see Chapter 4).

Other data on intrinsic properties of neocortical cells and interconnections of pyramidal neurons, local inhibitory neurons, as well as between pyramidal and local GABAergic neurons are dealt with in section ***2.1.1*** (see also Figs. 2.8–2.9).

Intracortical connections are due to horizontal projections of pyramidal neurons, spanning from 2 mm up to 8 mm in the visual cortex and allowing communication between neurons having widely separated receptive fields [171]. Other (somatosensory, auditory, and motor) cortical areas display similar features of connectivity [172]. The longest-range intracortical connections generally link association neocortical areas in cats [173] and primates [174]. Figure 2.33 illustrates the results of a double labeling study in macaques showing the projections of cortical areas 46 and 7a over a dozen targets (only some are depicted). Among the richest intracortical connections, the cat suprasylvian gyrus, which integrates polymodal signals from heterogeneous sources, contains several association areas that are related to somatosensory and visual systems and are reciprocally linked [175]. Dual intracellular recordings from anterior and posterior parts of the suprasylvian gyrus (areas 7 and 5), approximately 10 mm apart, revealed reciprocal connections between these fields, with prevalent projections from caudal to rostral sites [40] (Fig. 2.34). That these connections were

[168] Pollen and Lux (1966); Renaud et al. (1974).

[169] Thomson et al. (1993b).

[170] Thomson et al. (1995).

[171] Gilbert and Wiesel (1983); Gilbert (1992); Albowitz and Kuhnt (1993).

[172] Jones et al. (1978); Imig and Reale (1981); Cauller and Connors (1994); Keller (1993).

[173] Bignall et al. (1966).

[174] Reviewed in Goldman-Rakic (1987, 1988).

[175] Grüner et al. (1974); Avendaño et al. (1988). Cortical areas 5 and 7 of the suprasylvian gyrus also receive inputs from the thalamic rostral intralaminar nuclei and lateroposterior-pulvinar complex (Avendaño et al., 1985; Jones, 1985). TC neurons from these nuclei send monosynaptic, high-security projections to areas 5–7 and receive in turn inputs from these cortical areas (Steriade et al., 1977a, 1998d; see also the corticothalamic neuron in Fig. 2.38). The widespread cortical projections of intralaminar nuclei contribute to the large-scale synchronization of low-frequency sleep rhythms.

[176] Lidocaine is used for functional inactivation of relatively long-range connections. The maximal radius of intracortical spread of lidocaine, assessed autoradiographically (Martin, 1991), is about 1.7 mm. With a higher concentration and volume of lidocaine (10–20%, 1–10 μl), as used in our study (Amzica and Steriade, 1995a), to obtain immediate local effects and avoid changes in the global state of brain electrical activity, the recovery after lidocaine inactivation occurred after 4–6 h (see Fig. 2.37), while it takes 15–45 min in studies on motor systems (Martin and Ghez, 1988).

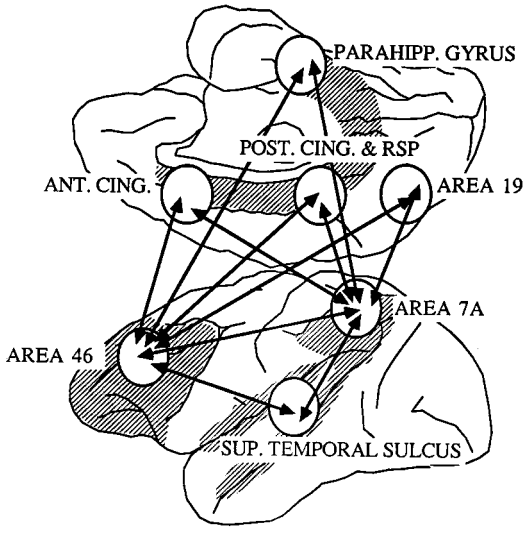

Fig. 2.33 The results of a double labeling study in macaques in which WGA-HRP (or 3-H leucine and proline) was placed in area 7a and tritiated amino acids (or WGA-HRP) were placed in area 46 in the same hemisphere of the same animal. Paired sections were superimposed and analyzed. Cross hatched regions represent areas that have been reported to receive afferents from the thalamic medial pulvinar nucleus. RSP, retrosplenial gyrus. See also main text. From Goldman-Rakic (1988).

within the gyrus was shown by abolition of responses in the caudo-rostral direction by infusion of lidocaine in the middle of the suprasylvian gyrus (Fig. 2.35) [176].

These intra-gyral connections and even more distant ones are implicated in the synchronization of long-range sleep oscillations. Multi-site, extra- and intracellular recordings from areas 5 & 7, visual association (Fig. 2.36), and motor cortical areas demonstrate neuronal synchrony during the slow oscillation, with the shortest time lag of ~12 ms to ~30 ms, depending on the analyzed areas, but also long time lags (~120 ms) due to inhibition-rebound sequences in interposed neurons [40]. The intracortical synchrony of the slow oscillation is disrupted by disconnecting cortical neuronal networks, using coronal transection in the middle of the suprasylvian gyrus (Fig. 2.37). In this figure, the disorganized sequences of slow oscillation between the rostral and caudal sites in the gyrus stood in contrast with the absence of effects on each side of the transection (see also Fig. 3.44 in Chapter 3). After disconnection, by transection or functional inactivation using lidocaine, the full or partial recovery of synchrony is due to intra- or inter-gyral paths [40].

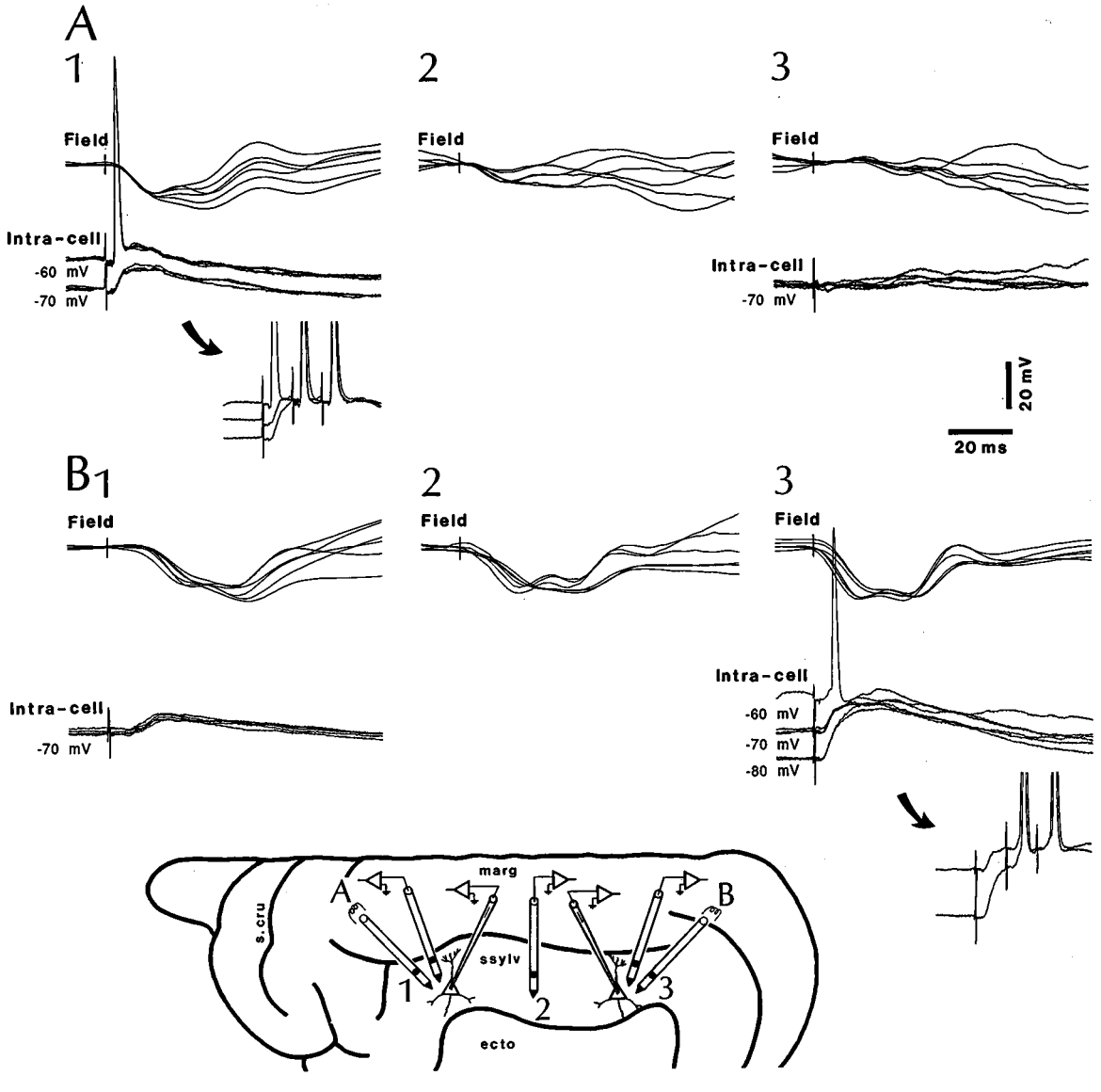

Fig. 2.34 Electrophysiological identification of intracortical pathways in suprasylvian gyrus of cat. Ketamine-xylazine anesthesia. Two simultaneous intracellular recordings at sites 1 and 3 in the rostral and caudal suprasylvian gyrus (see bottom scheme). Close (1 mm) to each intracellular micropipette there were two coaxial electrodes, one for bipolar recording of field potentials (FPs), the other for stimulation. An additional FP was recorded in the middle suprasylvian gyrus (site 2). Stimulation through the anterior electrode (*A*) elicited an antidromic action potential with a latency of 3 ms at the resting membrane potential (−60 mV) in a nearby cell (*A1*). An EPSP was revealed by hyperpolarizing the membrane at −70 mV. The same stimulation evoked a biphasic depth-negative FP. The inset in *A1* shows three responses of this neuron, at different membrane potentials, to a three-shock train at 100 Hz. The anterior stimulation was less effective towards the caudal recording sites, as shown by the progressively reduced amplitude of FPs and absence of overt EPSPs in the posterior intracellular recording (*A2–A3*). By contrast, stimuli delivered at the posterior site (*B*) induced EPSPs in both (posterior and anterior) cells, with shorter latencies in the posterior neuron. The inset in *B3* displays the temporal summation of EPSPs to 100 Hz stimulation. From Amzica and Steriade (1995a).

[177] Cunningham and LeVay (1986).

[178] The corticothalamic neuron from area 7, depicted in Fig. 2.38, was antidromically activated from the intralaminar centrolateral nucleus at a latency of <0.5 ms (see inset in Fig. 3 in Steriade et al., 1998d).

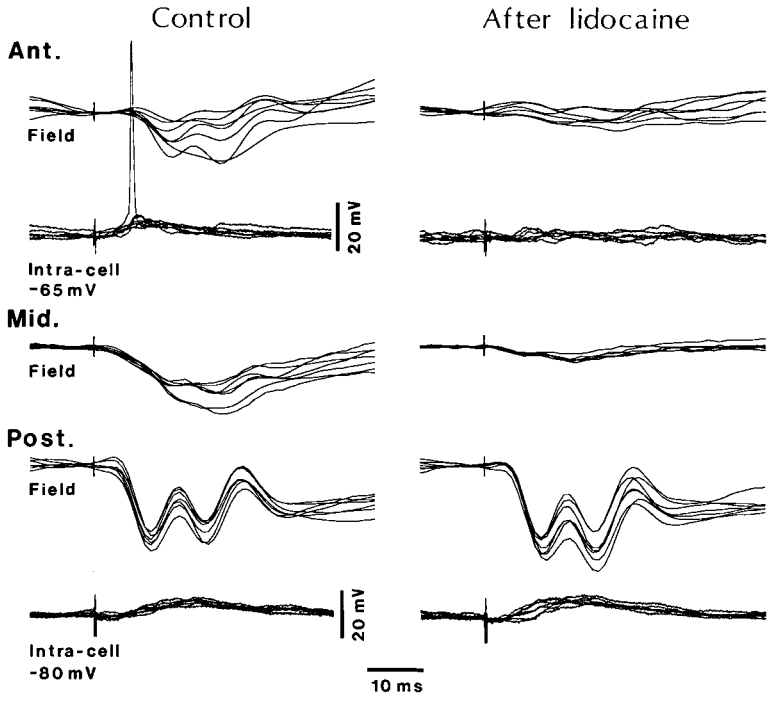

Fig. 2.35 Effect of lidocaine inactivation on intracortical responsiveness. Cat under ketamine-xylazine anesthesia. Superimposed sweeps from dual intracellular recordings in anterior and posterior parts of the suprasylvian gyrus; same arrangement of electrodes as in Fig. 2.34. Stimulation was applied close to the posteriorly located neuron. During the control period (left), both cells were orthodromically driven and the respective field potential (FP) recording displayed depth-negative components. After lidocaine infusion in the middle suprasylvian gyrus (Mid.), half way between the anterior (Ant.) and posterior (Post.) recording electrodes, the responses in the anterior neuron and FP, as well as in the FP close to the injection site, were abolished, while the responses in the posterior site preserved the same pattern (right). From Amzica and Steriade (1995a).

2.4.3. Corticothalamic loops

Every neocortical area returns axons to the thalamus, originating in layers VI or V [109]. The exception to this rule may be the projection from thalamic rostral intralaminar nuclei to primary visual cortex, which does not send back fibers to these thalamic nuclei [177]. The corticothalamic projection outnumbers the thalamocortical one by almost one order of magnitude. Corticothalamic axons are thin, <1 μm, and generally slowly conducting, but short latencies of antidromic invasion from the thalamus may also be obtained, especially in the case of cortical projections to the lateroposterior/pulvinar (LP-PUL) complex and to the intralaminar centrolateral (CL) nucleus, which originate in layer V of some association cortical areas [178]. Generally, thin corticothalamic axons

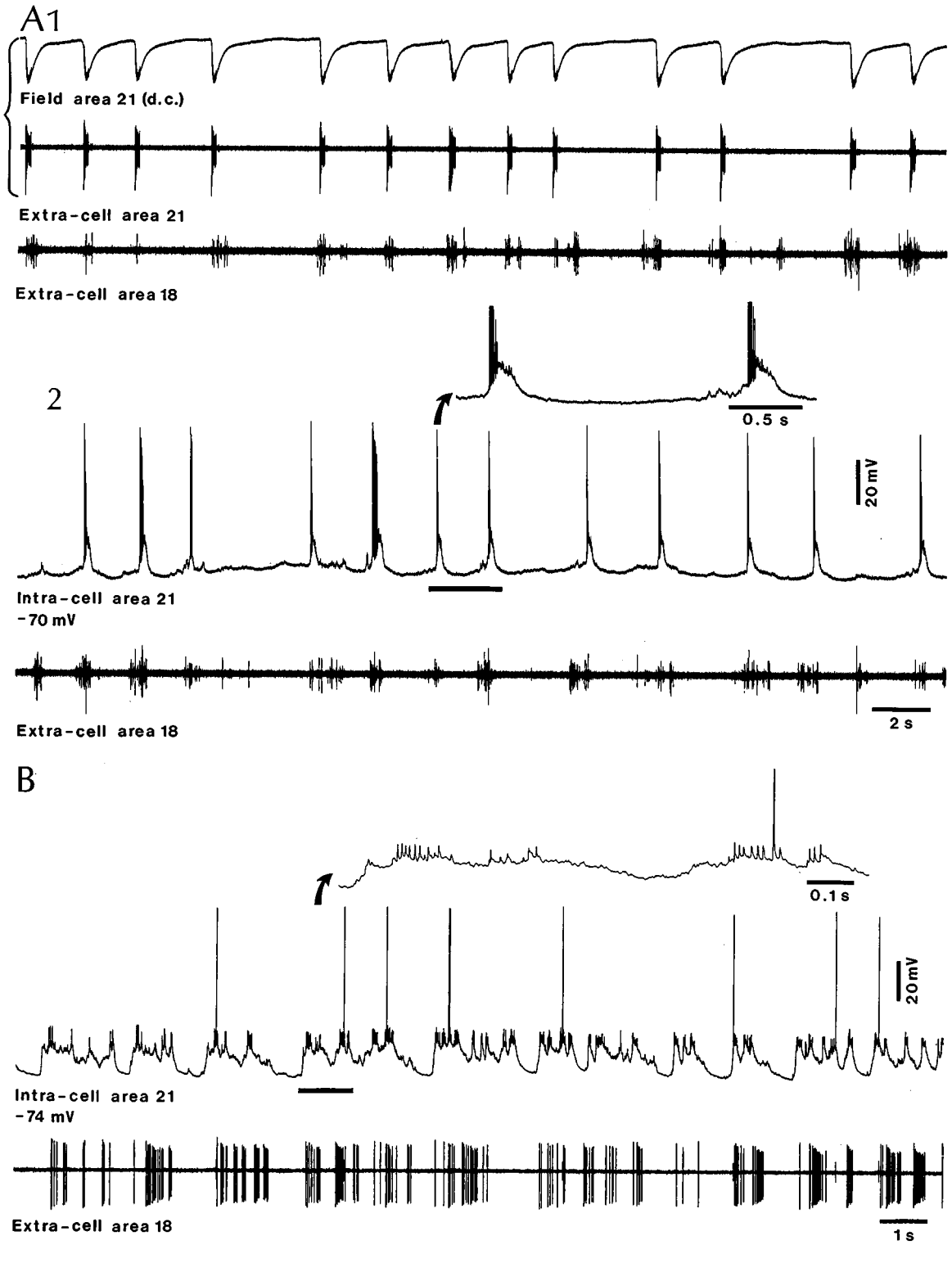
A1
Field area 21 (d.c.)
Extra-cell area 21
Extra-cell area 18
2
0.5 s
20 mV
Intra-cell area 21
-70 mV
Extra-cell area 18
2 s
B
0.1 s
20 mV
Intra-cell area 21
-74 mV
Extra-cell area 18
1 s

originate in layer VI, whereas thick fibers arise from layer V; some of these large axons are collaterals of long-range corticofugal projections ending in the striatum, brainstem, and spinal cord [179]. In addition to ipsilateral corticothalamic projections, contralateral projections arise in frontal cortex and terminate in medial (mainly anterior and mediodorsal) thalamic nuclei of non-human primates, after crossing the midline in the interthalamic adhesion [180].

The functional role of corticothalamic pathways remained unknown until recently and a series of studies, using reversible cooling or stimulation of cortical areas, reported a variety of effects, from depressed to enhanced activity in the thalamus, or simply lack of any consistent result. The first advances in the field of corticothalamic operations stemmed from the identification of different targets among the three major neuronal types in the thalamus (see **2.3**), with the consequence that the excitatory or inhibitory sign of cortical actions actually depends on a delicate balance between a prevalent effect exerted on one or the other of these thalamic neuronal classes. In thalamic relay cells, corticothalamic axons account for more than 50% of the total synapses. Axons from layer V cortical neurons form synapses with more proximal dendrites of TC cells than axons from layer VI that usually end on distal dendrites [181]. Axons of cortical origin terminate over the whole somadendritic domain of perigeniculate (RE) neurons [182]. In local thalamic GABAergic interneurons, axons of cortical origin end as small terminals with round vesicles on the parent dendrites, outside glomeruli [183].

Although the corticothalamic projection to all three major types of thalamic neurons is glutamatergic, therefore excitatory, synchronous volleys occurring naturally during cortical sleep oscillations, during paroxysmal activity, or induced artificially using electrical stimuli produce powerful depolarizing actions on both types of thalamic GABAergic (RE and local-circuit) neurons and hyperpolarizing actions on TC neurons. The short-latency excitation of RE neurons by cortical volleys and the ensuing cyclic spike-bursts within the frequency range of sleep spindles are illustrated in Fig. 2.38 [184]. Local inhibitory interneurons are also powerfully

[179] Abramson and Chalupa (1985); Ojima (1994); Bourassa et al. (1995); Lévesque et al. (1996). Another study (Paré and Smith, 1996) described thick cortical axons ending in lateroposterior-pulvinar complex of cat, contributing clusters of large-sized varicosities.

[180] Preuss and Goldman-Rakic (1987).

[181] Jones and Powell (1969); Harding and Powell (1972); Hoogland et al. (1991); Montero (1991).

[182] Montero (1987).

[183] Somogyi et al. (1978); Rainey and Jones (1983); Weber et al. (1989).

[184] That volleys of cortical origin are most efficient in triggering spindle oscillations by acting directly on thalamic RE neurons is known from earlier extracellular recordings (Steriade and Wyzinski, 1972; also [126]) and has been repeatedly shown intracellularly [e.g., 140].

Fig. 2.36 (opposite) Simultaneous recordings from visual association areas 21 and 18. Cat under ketamine-xylazine anesthesia. *A1*, extracellular recordings from area 21 (field potential and unit discharges, before impaling this neuron; see *A2*) and area 18. *A2*, same couple after impaling area 21 neuron. Epoch marked by the horizontal bar is expanded above (arrow; spikes truncated) to show the bursting feature of this neuron. *B*, another neuronal couple from areas 21 and 18, displaying a composite pattern of slow (0.4–0.5 Hz) and delta (~4 Hz) oscillations. Epoch marked by the horizontal bar is expanded above (arrow; spike truncated). Note synchrony between discharges in area 18 and intracellular membrane fluctuations. From Amzica and Steriade (1995b).

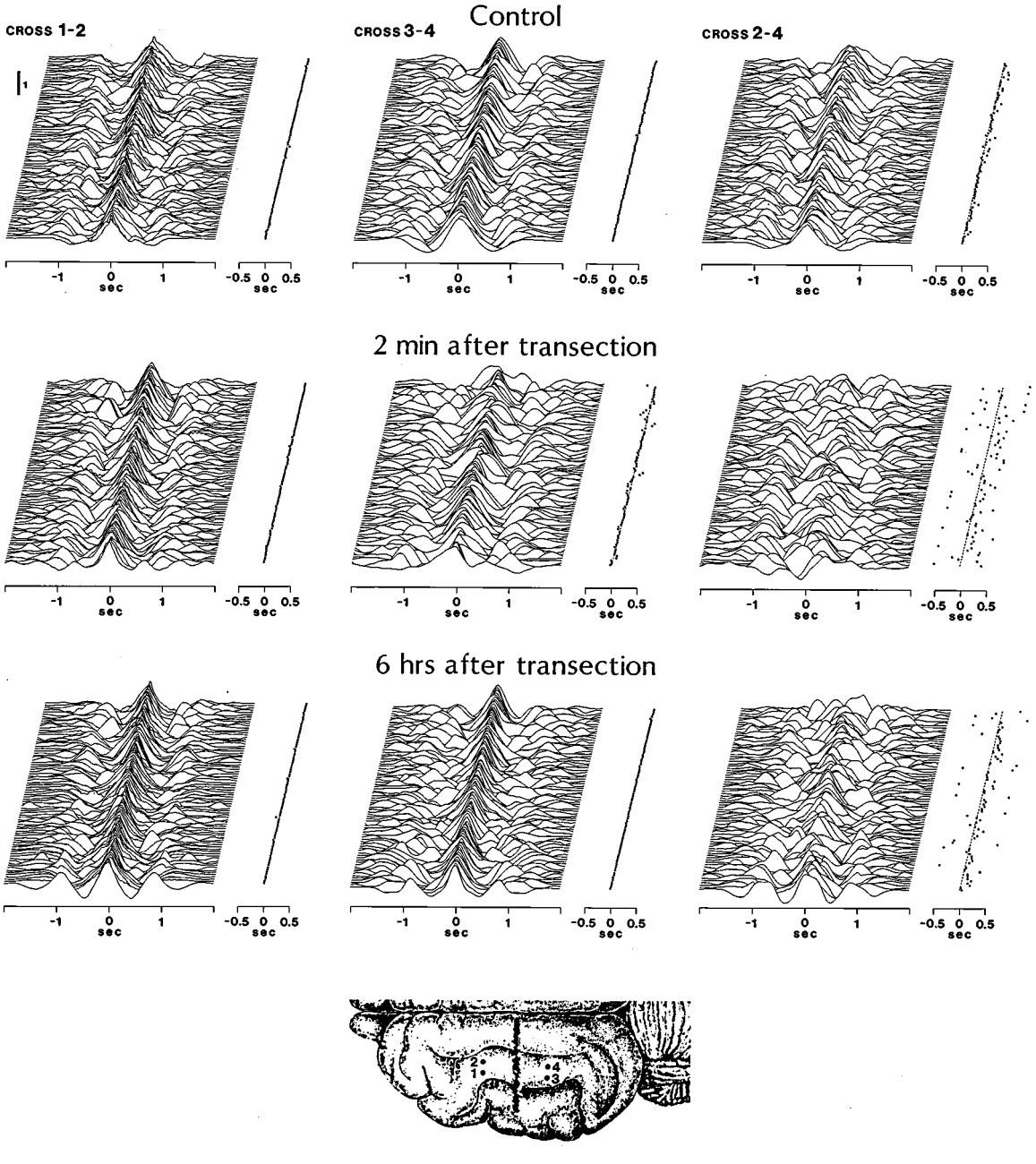

Fig. 2.37 Disrupting effect of a coronal transection, from marginal to ectosylvian gyri, upon intracortical synchrony of slow oscillation. Cat under ketamine-xylazine anesthesia. Two couples of electrodes recorded field potentials (FPs) in the suprasylvian gyrus, rostrally (1–2) and caudally (3–4) from the transection plane (see extension of transection at bottom). Each panel depicts sequential cross-correlations (CROSS) between FPs and, on the right, sequential time-lags seen from the same view angle as the CROSS (see methodological details in that paper). The dispersion of correlation peaks was increased after transecting the cortex between rostral and caudal recorded sites (CROSS 2–4), while it did not significantly change in recordings on the same side of the cut (CROSS 1–2 and CROSS 3–4). From Amzica and Steriade (1995a).

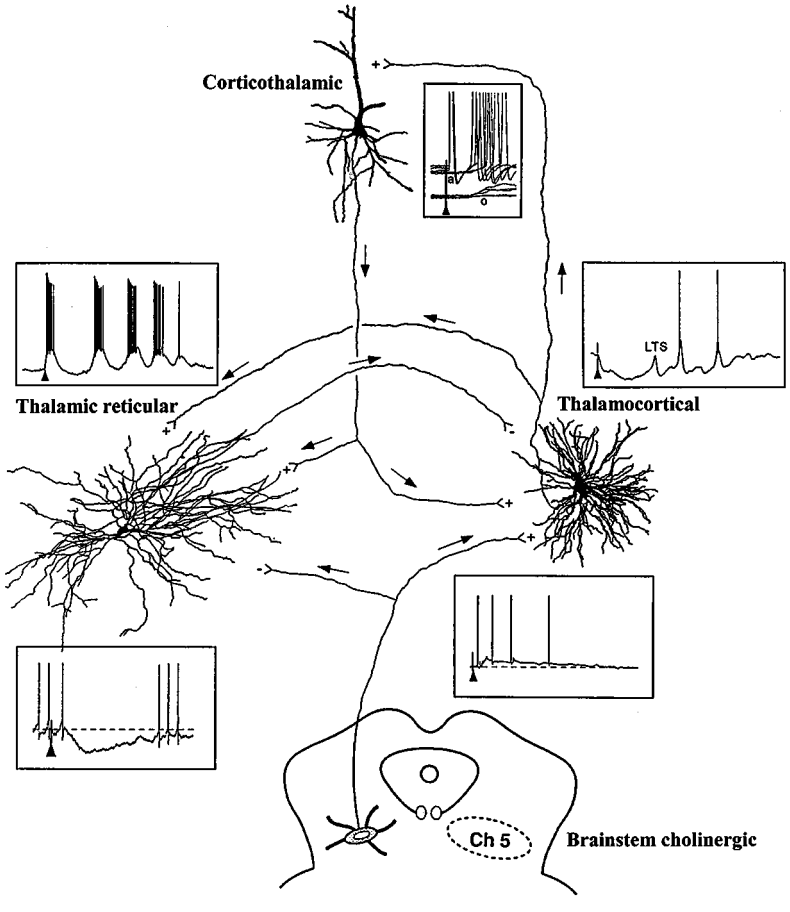

Fig. 2.38 Neuronal loops in corticothalamic networks implicated in coherent oscillations and their control by brainstem cholinergic neurons. The top three neurons have been recorded and stained intracellularly in anesthetized cats. The direction of their axons is indicated by arrows. Insets represent their responses to thalamic and cortical stimulation (arrowheads point to stimulus artifacts). The corticothalamic neuron (spikes truncated) from area 7 responded to thalamic stimulation of the centrolateral intralaminar nucleus with antidromic (*a*) and orthodromic (*o*) action potentials (top superimposition, at a membrane potential of −55 mV). At more hyperpolarized levels (bottom superimposition, at −64 mV), the antidromic response failed but the orthodromic response survived as subthreshold EPSPs. In addition to such closed loops, in which the cortical neuron is excited from a given thalamic nucleus and projects back to the same nucleus, cortical neurons may project to thalamic nuclei that are different from those representing the input source for the cortex. Such cases provide the substrate for distribution of activities beyond the site of their generation in the cerebral cortex. The thalamic reticular (RE) GABAergic neuron (recorded from the rostrolateral district of the nucleus) responded to motor cortical stimulation with a high-frequency spike-burst, followed by a sequence of spindle waves on a depolarizing envelope (membrane potential, −68 mV). Spindle waves occur spontaneously, with a frequency of 7–14 Hz in animals (12–14 Hz in humans) during light sleep. In this case, spindles are elicited by cortical stimulation. The thalamocortical (TC) neuron, recorded from the ventrolateral nucleus, responded to motor cortex stimulation with a biphasic IPSP, leading to a low-threshold spike (LTS) and a sequence of hyperpolarizing spindle waves (membrane potential, −70 mV). For the sake of simplicity, local-circuit inhibitory neurons in cortex and thalamus are not illustrated. Shown below, the dual effects of brainstem cholinergic neurons, namely hyperpolarization of the RE neuron and depolarization of the TC neuron. Recordings are modified from Hu et al. (1989a), Curró Dossi et al. (1991), Contreras et al. (1996b), Steriade et al. (1998d) and Steriade (1999b).

[185] Pedroarena and Llinás (1997).

[186] Steriade and Deschênes (1987); Deschênes and Hu (1990).

excited by corticofugal axons. This is also seen in cat anterior thalamic (AT) nuclei that are devoid of connections from GABAergic RE neurons [131] and, therefore, this corticothalamic action is not complicated by projections from RE neurons to local-circuit cells [153]. In AT local interneurons, cortical inputs exert direct depolarization and also elicit a profound facilitatory action on PSPs evoked by prethalamic stimuli, outlasting the duration of the cortical pulse-train [132].

In contrast to these direct excitatory effects on both types of thalamic inhibitory neurons, the cortical action on TC neurons is a long-lasting hyperpolarization, consisting of a biphasic ($GABA_{A\text{-}B}$) IPSP (Fig. 2.38). This is a bisynaptic IPSP, mediated by GABAergic RE neurons, and is followed by rebound excitations in the frequency range of spindles. The involvement of RE neurons in these IPSP-rebound sequences is demonstrated by experiments showing that, following excitotoxic lesions of RE neurons or transections separating them from the remaining thalamus, the prolonged IPSPs and postinhibitory rebound spike-bursts, characteristic of spindles in TC neurons, disappear; instead, TC neurons receive numerous, short-lasting IPSPs from local interneurons [114]. Besides these prevalent inhibitory projections from cortex to TC neurons, which are mediated through RE neurons during highly synchronized activities, excitatory cortical actions on TC neurons can also be revealed when RE neurons fire in the single-spike mode, as in wakefulness [136], and their impact on TC neurons is less pronounced than when they fire long spike-bursts. During alert states, corticothalamic neurons that display powerful spike-bursts recurring at 30–40 Hz [13] may activate high-threshold Ca^{2+} conductances, which are preferentially located in the dendrites of TC neurons, and thus generate fast oscillations in corticothalamocortical loops [185]. The direct excitatory actions exerted by the cortex on TC neurons can be observed in isolation using excitotoxic lesions of RE neurons or transections separating them from TC cells. Under these experimental conditions, creating artificial cortico-TC projections in the absence of RE cells, the cortically evoked depolarization in TC cells is much longer, as it is not shunted by the IPSP produced by RE neurons in normal conditions, and the cyclic inhibitory-rebound sequences are absent [186].

Then, in the intact brain, the prevalent corticothalamic actions are inhibitory on TC cells and are mediated by RE neurons. This is particularly obvious in species, such as rodents, that lack local inhibitory cells in most dorsal thalamic nuclei. Recent studies provided evidence supporting the above electrophysiological data. Indeed, the numbers of glutamate receptor subunits GluR4 are

3.7 times higher at corticothalamic synapses in RE neurons, compared to TC neurons, and the mean peak amplitude of corticothalamic excitatory postsynaptic currents (EPSCs) is about 2.5 higher in RE, than in TC, neurons (Fig. 2.39) [187]. During slow-wave sleep (SWS), and even more so during some types of electrical seizures that develop from SWS patterns, the spike-bursts fired by RE neurons induce greater postsynaptic inhibitory responses in TC neurons than those elicited by single spikes. The synchronous discharges of corticothalamic neurons during the slow sleep oscillation impinge upon, and excite, RE neurons, eventually inducing prolonged hyperpolarizations and rebound spike-bursts in target TC neurons (see Chapter 3, ***3.2.3***). This sequence of events underlies the coalescence of different SWS rhythms, slow and spindle oscillations. Similar phenomena occur during cortically generated spike-wave seizures, when the majority of TC neurons are steadily hyperpolarized and display phasic IPSPs [188]. These inhibitory potentials are mediated by RE neurons that faithfully follow each paroxysmal depolarizing shift in cortical neurons (see details in Chapter 5).

2.5. Control of thalamocortical systems by generalized modulatory systems

Neuromodulatory systems exert global activating actions by shifting the brain from one state of vigilance to another and also improve neuronal responses to behaviorally relevant stimuli in specific sensory systems. Activation is defined as a state of readiness in cerebral networks, a state of membrane polarization which brings neurons closer to firing threshold, thus ensuring safe synaptic transmission and quick responses to either external stimuli during waking or internal drives during REM sleep [189]. The similarities between waking and REM sleep, and their electrophysiological characteristics that are opposite to those of SWS, result from data showing virtually identical patterns of background neuronal activity in thalamus and neocortex, increased rates of spontaneous discharges as well as enhanced excitability to antidromic or orthodromic volleys in TC and corticofugal neurons during these two brain-active states [190], as well as similar aspects of sensory-evoked field potentials in humans [191]. Only a few neuronal types, particularly the serotoninergic and noradrenergic neurons in the upper brainstem and histaminergic neurons in the posterior hypothalamus, are active in waking and silent during REM sleep [192].

Activation processes in thalamic and cortical neurons include sculpturing inhibition that ensures discriminative responses.

[187] Golshani et al. (2001). In those experiments, care was taken to distinguish between the direct cortico-RE EPSCs (latencies exceeding 6 ms) from those that could result from antidromic stimulation of TC axons, with axon reflex stimulation of RE neurons. Similar data, namely, three times more GluR4 units at corticothalamic synapses onto RE neurons compared to ventral posterior neurons, were obtained by Mineff and Weinberger (2000). The higher number of glutamate receptors and higher amplitude of cortically-evoked EPSCs in RE neurons, compared to thalamocortical neurons, accounts for the fact that highly synchronous cortical volleys inhibit thalamocortical neurons during both sleep and paroxysmal oscillations, an inhibition mediated by RE neurons (Steriade, 2001c).

[188] Steriade and Contreras (1995); Pinault et al. (1998); Steriade and Timofeev (2001).

[189] Steriade (1991).

[190] Reviewed in previous monographs [109–110]; see also Steriade and Llinás (1988) and Llinás and Paré (1991).

[191] Yamada et al. (1988).

[192] Hobson et al. (1975); McCarley and Hobson (1975); McGinty and Harper (1976); Vanni-Mercier et al. (1984); Aston-Jones and Bloom (1991).

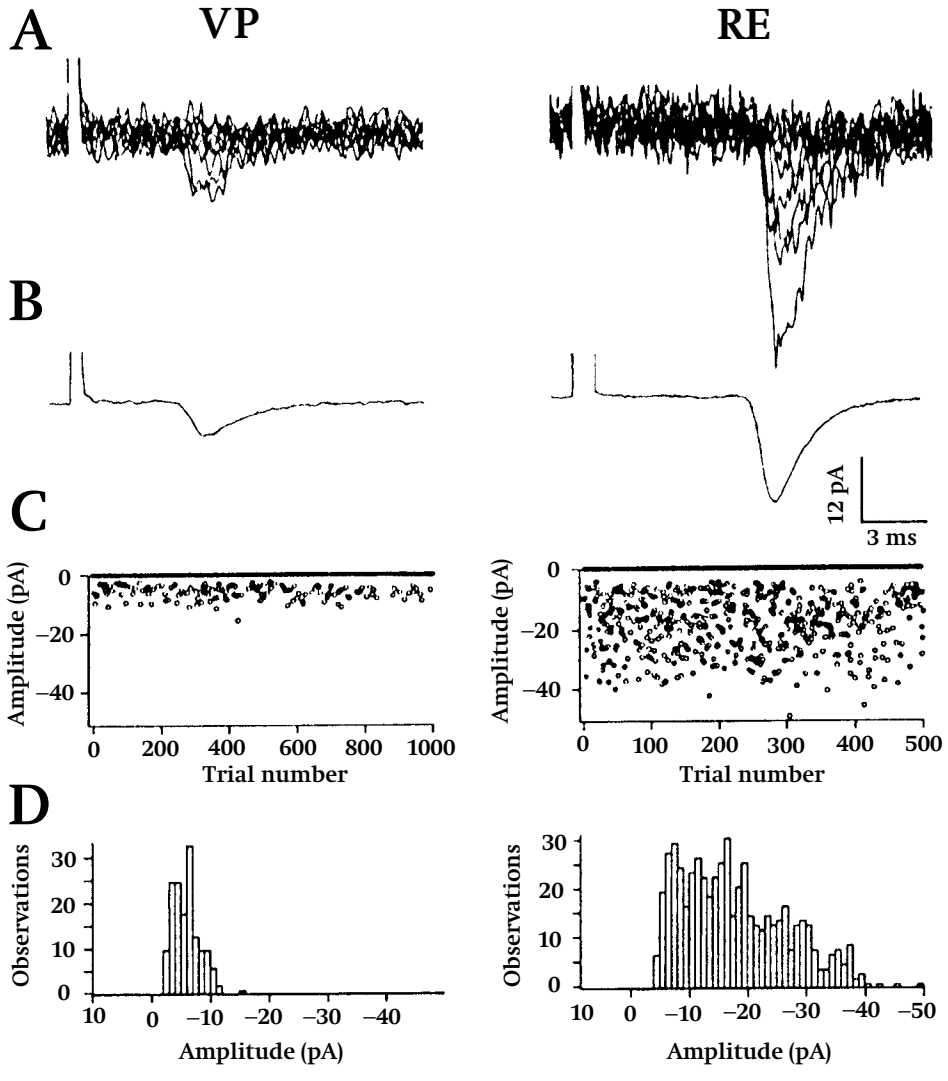

Fig. 2.39 Amplitude of excitatory postsynaptic currents (EPSCs) evoked in RE neurons by minimal stimulation of corticothalamic axons is ~2.5 times larger than in TC neurons. Whole-cell recordings from thalamic slices of mice. *A*, overlay of 10 voltage-clamp traces from a thalamic ventroposterior (VP) neuron (left) and an RE neuron (right), following minimal stimulation of corticothalamic fibers, showing EPSC successes and failures. Minimal EPSC amplitudes are larger in RE neurons than in VP neurons. *B* (left), average of EPSC successes recorded from the VP neuron (500 stimuli). *B* (right), average of EPSC successes recorded from the RE neuron (1000 stimuli). *C*, graph illustrating the trial-to-trial variability in EPSC peak amplitudes recorded in the VP (left) and RE (right) neurons showing the large number of failures and small size of EPSCs. *D*, distribution of EPSC amplitudes recorded in the VP (left) and RE (right) neurons showing comparatively narrow amplitude distribution of EPSC successes in the VP neuron and range of amplitudes of EPSC successes in the RE neuron. Modified from Golshani et al. (2001).

Although activation was initially viewed as associated with global disinhibition in the thalamus [193], more recent studies at extracellular [194] and intracellular [195] levels demonstrated that, during natural awakening or arousal elicited by brainstem reticular formation, long-lasting and cyclic thalamic inhibitory processes are blocked, but the early inhibitory phase, during which spontaneous firing ceases and neurons are unresponsive to antidromic or orthodromic volleys, is preserved. This is valid for both thalamic [194, 195] and cortical [196] neurons. In the thalamus, the earliest phase of the IPSP, which is generated within glomeruli, may be implicated in the high-fidelity transfer of information [132, 195].

Because of the similar changes in excitability of thalamic and neocortical neurons during waking and REM sleep, and because brainstem and basal forebrain cholinergic neurons, together with glutamatergic neurons in the upper brainstem core and thalamic nuclei with widespread cortical projections, are highly activated during both these states of vigilance, the focus in this section will be on modulatory systems releasing acetylcholine (ACh) and glutamate (Glu). The actions exerted by monoaminergic systems with generalized projections, releasing serotonin (5-HT), norepinephrine (NA) and histamine (HA), will also be reported but, at the present time, these effects on identified neuronal types in the thalamus and cerebral cortex are less well understood.

2.5.1. Cholinergic and glutamatergic systems

The cholinergic and glutamatergic neurons that give to ascending projections toward thalamic and cortical neurons are discussed together because *(a)* these neurons are similarly active during wakefulness and REM sleep, much less active in SWS, and both these neuronal types similarly display precursor changes in firing rates in advance of the most precocious electrographic signs during shifts in states of vigilance, thus suggesting their crucial role in determining changes from the deafferented state of SWS to brain-activated states (see Figs. 3.16–3.17 and 3.56 in Chapter 3) [197]; *(b)* some effects on thalamic relay and cortical neurons, i.e., reduction in some K^+ currents, are similarly exerted by ACh and Glu (see below); and *(c)* cholinergic neurons in the mesopontine nuclei display co-localization with Glu [198].

Originally it was thought that the brainstem reticular core was a homogenous structure, but research in the early 1980s found that it contained chemically specific pathways, of which cholinergic neurons were among the first to be identified. However, now it is clear that the majority of neurons in the whole reticular formation are not cholinergic (or norepinephrinergic or serotoninergic) and

[193] Purpura et al. (1966); Purpura (1970); Singer (1977).

[194] Steriade et al. (1977b).

[195] Steriade (1984); Curró Dossi et al. (1992b).

[196] Steriade and Deschênes (1974).

[197] That extracellularly recorded neurons from the mesopontine pedunculopontine and laterodorsal tegmental (PPT/LDT) neurons with enhanced firing rates in wakefulness and REM sleep (Steriade et al., 1990a) are indeed cholinergic was supported by *in vivo* microdialysis studies in the thalamus (Williams et al., 1994). The average increase in acetylcholine (ACh) concentration in the dorsal thalamus during wakefulness and REM sleep proved to be basically the same, more than twice higher that during SWS, similarly to the increase in firing rates of PPT/LDT neurons in waking and REM sleep (median 20–30 Hz) compared to SWS (median 10–15 Hz) (Steriade et al., 1990a).

[198] Clements and Grant (1990); Lai et al. (1993); Lavoie and Parent (1994).

are probably glutamatergic, especially the large ones [199]. Glu is also released by thalamic neurons with widespread cortical projections that play an important role in activation processes [200]. Glu acts on different types of postsynaptic ionotropic (kainate, AMPA, and NMDA) and metabotropic receptors; some of these excitatory actions consist not only of depolarizing target cells but also increasing their input resistance [201]. The role of glutamatergic neurons is also important in maintaining brainstem cholinergic neurons in a depolarized state, especially during waking when monoaminergic neurons are active and exert an inhibitory tone upon them [202]. Numerous neurons in the pontine and midbrain reticular formation, which are immunoreactive to Glu, project to pedunculopontine and laterodorsal tegmental (PPT/LDT) cholinergic nuclei [203]. Brainstem and basal forebrain cholinergic neurons also contain high levels of nitric oxide synthase (NOS), which is biochemically and immunochemically identical to neuronal NADPH-diaphorase, a reliable marker of cholinergic neurons [204]. Similarly to ACh, nitric oxide (NO) produces depolarization of TC neurons and inactivates the hyperpolarization-dependent currents that generate the clock-like, pacemaker oscillation (1–4 Hz) in these neurons [205], thus shifting the electrical activity from delta sleep to activated patterns. NO, a gaseous messenger implicated in diffuse activation processes, is also involved in more specific increases of neuronal responses to sensory inputs [206]. This may be related to the fact that ACh actions are mediated by both non-junctional specializations (volume or paracrine transmission) and less numerous conventional synaptic profiles [207].

In essence, the actions of brainstem cholinergic neurons on thalamic relay (TC) neurons are powerfully excitatory, resulting from a direct depolarization of TC cells associated with increased input resistance [208] due to a suppression of a "leak" K^+ current, I_{KL}, and their disinhibition following the hyperpolarization with activation of a K^+ conductance in thalamic GABAergic RE neurons [209] (see these brainstem cholinergic actions on TC and RE neurons in Fig. 2.38). The next step in the bisynaptic (brainstem–thalamic–cortical) activating pathway, from TC cells to cortex, is glutamatergic. The parallel activating bisynaptic (brainstem–nucleus basalis–cortical) pathway is different, in the sense that the first step is glutamatergic and the second one, from nucleus basalis to cortex, is cholinergic. Indeed, the projection from cholinergic PPT/LDT neurons to nucleus basalis neurons cannot be regarded as excitatory because ACh hyperpolarizes basalis neurons [210], much the same as the action of ACh on brainstem cholinergic neurons [211]. This is why we proposed that the excitatory actions from the brainstem

[199] B.E. Jones (2000).

[200] Rostral intralaminar nuclei are activated during states of alertness (Glenn and Steriade, 1982) and during complex cognitive tasks in humans (Kinomura et al., 1996), and their lesions lead to prolonged hypersomnolence in humans (Façon et al., 1958; Castaigne et al., 1962). See also Minamimoto and Kimura (2002).

[201] McCormick and von Krosigk (1992). The actions of various neurotransmitters and modulators are reviewed in Chapter 8 of Steriade et al. (1997a).

[202] Both non-NMDA and especially NMDA receptors contribute to excitatory transmission in mesopontine cholinergic neurons (Leonard et al., 1995; Sanchez and Leonard, 1996). Inhibitory actions on cholinergic cells are exerted by projections from monoamine-containing neurons (Lübke et al., 1992; Williams and Reiner, 1993; Leonard and Llinás, 1994).

[203] Semba and Fibiger (1992); Steininger et al. (1992).

[204] Dawson et al. (1991); Snyder and Bredt (1991). NADPH-diaphorase-positive neurons in the brainstem core display co-localization of three subunits of Glu receptors and an NMDA receptor subunit (Inglis and Semba, 1996). Local electrical stimulation in brainstem slices from laterodorsal tegmental cholinergic nucleus produces increased extracellular nitric oxide (Leonard et al., 2001).

[205] Pape and Mager (1992); Pape (1995).

[206] Do et al. (1994).

[207] Umbriaco et al. (1994); Descarries et al. (1997); Turrini et al. (2001).

[208] Curró Dossi et al. (1991). The muscarinic depolarization of TC neurons has two components: *(a)* the early one is mediated by an m3 receptor and is associated with little change in input resistance; and *(b)* the late component is mediated by m1 receptor and is associated with a decrease in a "leak" K^+ current, I_{KL}, and a large increase in input resistance (Zhu and Uhlrich, 1998). The suppression of I_{KL} by ACh as well as by metabotropic Glu receptors (McCormick and von Krosigk, 1992; reviewed in Steriade et al., 1997) explains the similar actions of brainstem-thalamic cholinergic and corticothalamic glutamatergic actions on

TC neurons. The corticothalamic system acts, therefore, as a descending activating system, having rather similar effects on TC neurons as the ascending reticular cholinergic system.

[209] *In vitro* (McCormick and Prince, 1986) and *in vivo* (Hu et al., 1989a) studies.

[210] Khateb et al. (1991).

[211] Leonard and Llinás (1994).

[212] Steriade et al. (1993a).

[213] Rasmusson et al. (1994, 1996).

[214] Metherate et al. (1992).

[215] Kosaka et al. (1987); Honda and Semba (1995); Jones (1995). In the human brain too, cholinergic PPT/LDT neurons (∼20,000) are intermixed with non-cholinergic neurons, especially in the pars dissipata of the PPT nucleus that contains few cholinergic cells (Manaye et al., 1999).

[216] Kang and Kitai (1990); Leonard and Llinás (1990). In the latter study, the thalamic projections of LDT cholinergic cells (as identified by NADPH-diaphorase staining) were determined by rhodamine-labeled microspheres retrogradely transported from two dorsal thalamic nuclei to LDT neurons. Both the above-mentioned studies, reporting that only very few PPT/LDT neurons possess a Ca^{2+}-dependent low-threshold current (I_T), were conducted on slices from adult animals. At variance, *in vitro* studies from young rats (9 to 15 days old) showed that the majority of LTS-bursting brainstem LDT neurons are cholinergic (Kamondi et al., 1992; Lübke et al., 1992).

[217] Steriade et al. (1990a).

reticular neurons to nucleus basalis are glutamatergic [212], which proved to be valid [213]. The cholinergic projection from nucleus basalis to cortex depolarizes cortical neurons and changes their slow oscillatory potentials to fast rhythms [214]. The presence of these two parallel activating pathways (from brainstem to cortex, via synaptic relays within the thalamus or nucleus basalis) is supported by *in vivo* experiments showing that brainstem-induced depolarization of cortical neurons, their enhanced excitability, and replacement of slow oscillations by fast rhythms can be achieved after extensive lesions of either thalamus or nucleus basalis [212]. Stimulation of the PPT nucleus leads to the blockage of slow cortical oscillation and the induction of tonic activity, an effect that is antagonized by scopolamine (Fig. 2.40). Muscarinic, but not nicotinic, blockers antagonize the PPT effects on the same slowly oscillating corticothalamic neuron (Fig. 2.41).

When I mention PPT/LDT "cholinergic" nuclei, I simplify a more complex reality as these nuclei contain catecholaminergic and GABAergic neurons, besides an important contingent of neurons immunoreactive to choline acetyltransferase [215]. A similar heterogeneity of different neuronal types was reported for all, so-called chemically coded, brainstem nuclei, in particular monoaminergic cell aggregates. In the case of mesopontine cholinergic nuclei, data reporting significantly increased firing rates of thalamically projecting PPT/LDT neurons during waking and REM sleep, compared to SWS, fit well with the results from experiments using microdialysis of ACh release in the thalamus during these states of vigilance [197].

The intrinsic cellular properties of cholinergic PPT/LDT neurons were investigated *in vitro* [216]. In slices from adult animals, the majority of these neurons are characterized by a transient outward K^+ current (I_A). Other neurons display high-threshold Ca^{2+} spikes, while a minority of mesopontine cholinergic possesses a low-threshold Ca^{2+} current (I_T). The fact that very few PPT/LDT cholinergic neurons display spike-bursts in slices [216] is corroborated by *in vivo* studies of PPT/LDT neurons during natural states of vigilance showing that very short (<5 ms) interspike intervals, reflecting high-frequency spike-bursts, represent only 2–4% of intervals during wakefulness and slow-wave sleep, and less than 7% of intervals during REM sleep [217], related to the generation of ponto-geniculo-occipital (PGO) waves in one type of PPT/LDT neurons. Concerning the high-threshold Ca^{2+}-mediated spike-bursts described *in vitro* [216], these are the slice equivalent of high-frequency (>500 Hz) spike-bursts, occurring 20–40 ms before the thalamic PGO waves during REM sleep *in vivo* that are preceded by a period

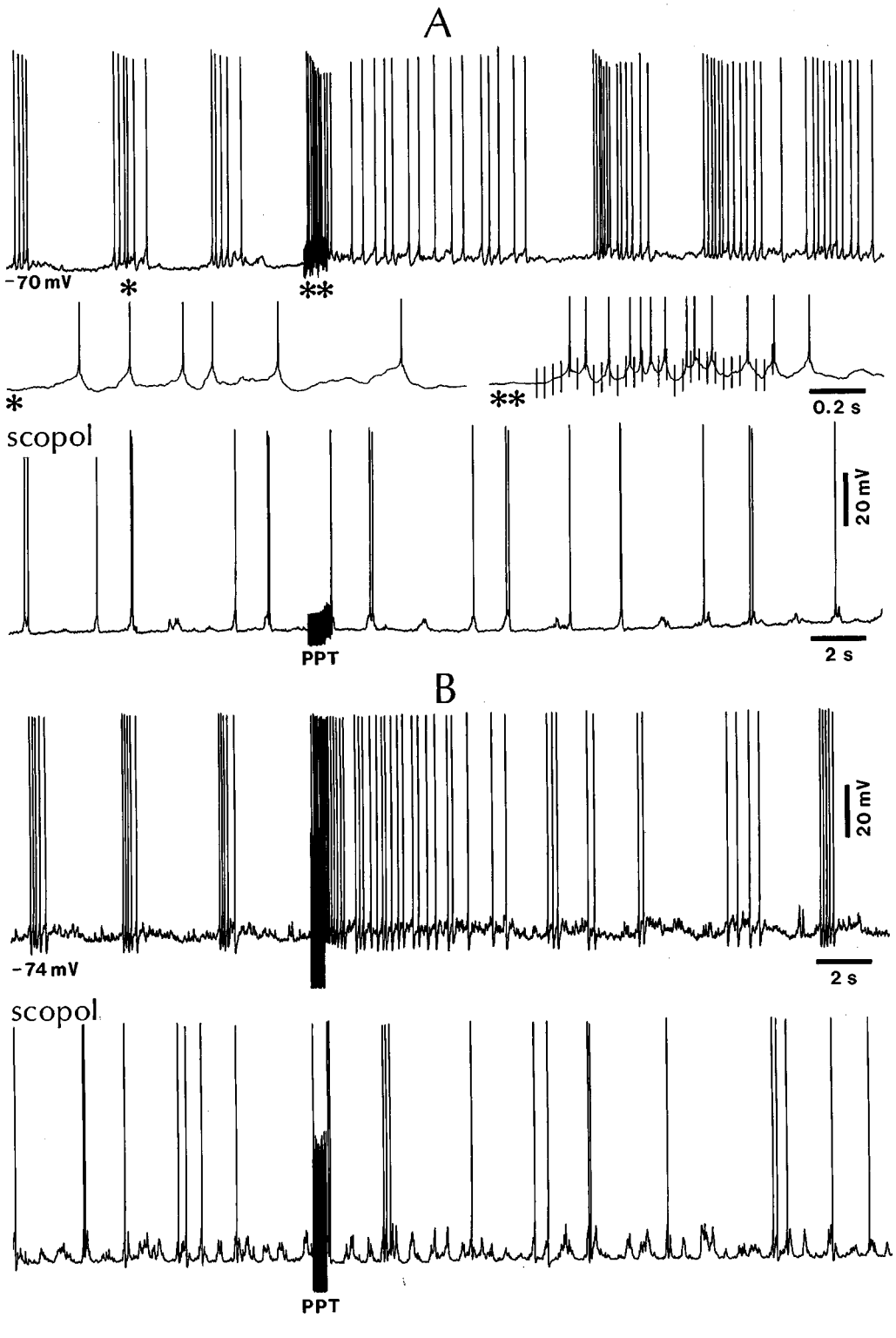
A
−70 mV
*
**
*
**
0.2 s
scopol
20 mV
PPT
2 s
B
20 mV
−74 mV
2 s
scopol
PPT

[218] Steriade et al. (1990c).

[219] Steriade and Amzica (1996).

[220] Steriade et al. (1996a)

[221] Castro-Alamancos and Calcagnotto (2001).

[222] Contreras and Llinás (2001).

of discharge acceleration suggesting their progressive depolarization [218].

The modulation of thalamic and cortical neurons by cholinergic systems results in the production of fast (generally 20–60 Hz) activities, so-called gamma rhythms, an effect that is sensitive to muscarinic blockers [219]. This effect can be evoked by pulse-trains at ~30 Hz, close to the firing rates of PPT/LDT during wakefulness and REM sleep, states in which fast rhythms are prevalent, but two short-delayed stimuli applied to the PPT nucleus are enough to induce coherent oscillations at 35–45 Hz at the surface and depth of neocortical areas (Fig. 2.42). Simultaneous recordings from cortex and thalamus revealed that the intracortical synchronization of spontaneously occurring fast oscillations, intracolumnar as well as extending horizontally to adjacent cortical foci [220], is accompanied by coherent activity in corticothalamic systems. Such synchronization, more obvious during activated epochs than during deafferented periods of activity (Fig. 2.43), was found in those instances in which the sites of recordings were identified to be reciprocally connected by using monosynaptic corticothalamic and thalamocortical responses (see bottom panel in Fig. 2.43), thus emphasizing that coherence of fast rhythms is mainly observed within cortical territories linked with appropriate thalamic nuclei [219]. These data are related to the activation, by brainstem reticular formation stimulation *in vivo* and ACh application *in vitro*, of high-frequency corticothalamic inputs, whereas the same experimental manipulations led to suppression of low-frequency responses [221]. Thus, during arousal, the flow of gamma oscillation from cortex to thalamus is facilitated. *In vitro* studies combining voltage-sensitive dye imaging with intracellular recordings from neocortical neurons showed that repetitive stimulation of white matter at a frequency of ~40 Hz restrained the area of excitation to a small columnar site above the stimulating electrode, whereas activation patterns elicited by low-frequency stimulation extended laterally over a large portion of the slice [222]. These data corroborate the notion that corticocortical and especially thalamocortical responses in the frequency range of ~10 Hz, i.e., incremental

Fig. 2.40 (opposite) Scopolamine antagonizes the suppression of slow cortical oscillation induced by the pedunculopontine tegmental (PPT) nucleus. Cat under urethane anesthesia. *A*, regular-spiking (RS) area 5 neuron. Slow oscillation (~0.3 Hz) was suppressed for 10 s after a PPT pulse-train (30 Hz, 1 s). A depolarizing phase (*) and the immediate effect of PPT stimulation (**) are expanded below (spikes truncated). Scopolamine (scopol) administration (0.5 mg/kg, i.v.) reduced the discharges during the rhythmic depolarizations as well as the duration of the silent periods (thereby increasing the frequency of the slow rhythm to 0.6 Hz) and blocked the PPT effect. *B*, similar effect of PPT stimulation on slow oscillation and scopolamine sensitivity in another RS area 5 neuron. From Steriade et al. (1993a).

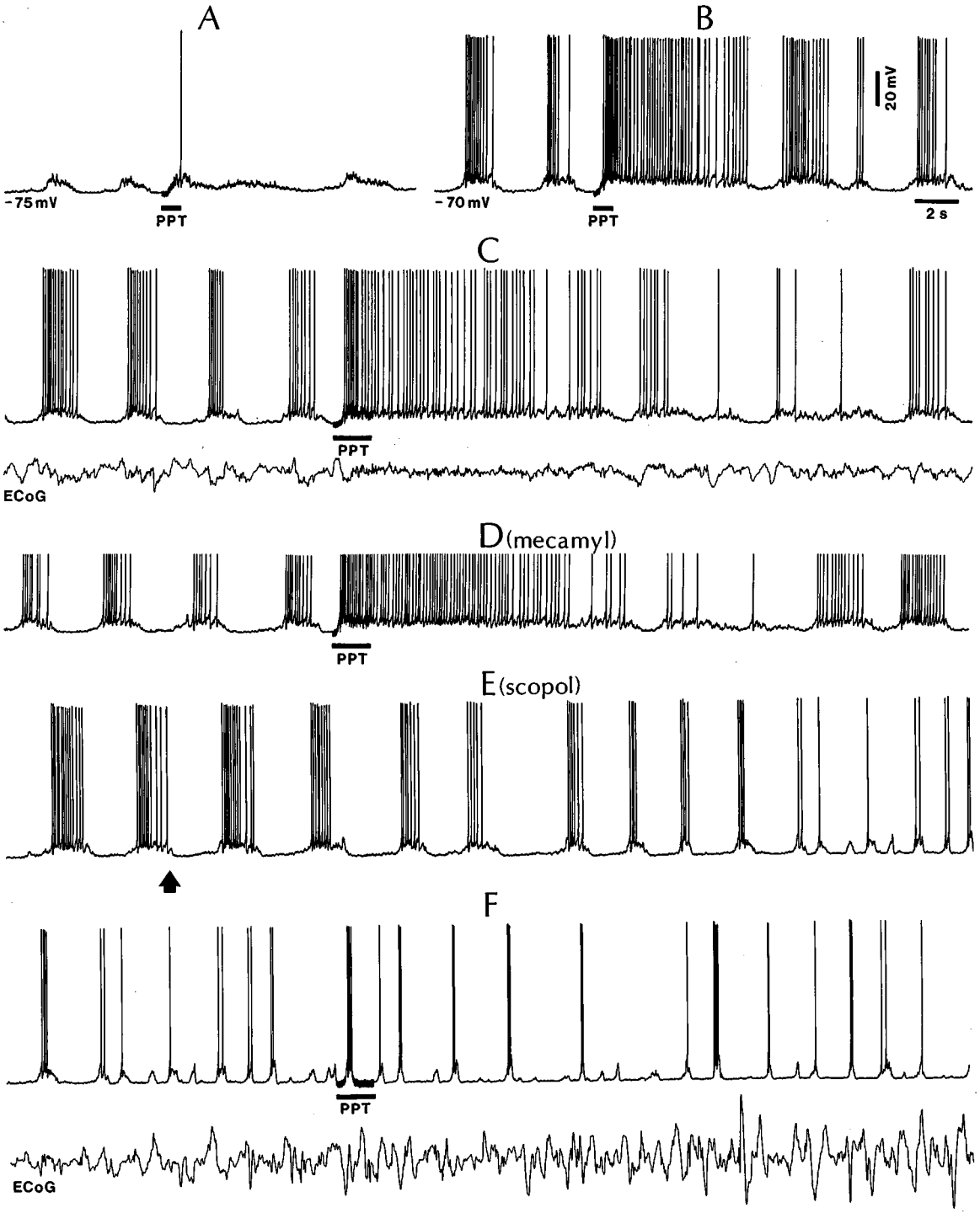
A
B
20 mV
-75 mV
PPT
-70 mV
PPT
2 s
C
PPT
ECoG
D (mecamyl)
PPT
E (scopol)
F
PPT
ECoG

potentials, are relatively diffuse and mimic the widespread occurrence of sleep spindles (see Chapter 4), compared to fast (gamma) oscillations that are confined within restricted cortical territories and specific corticothalamic systems (see Fig. 2.43 and [219–220]).

2.5.2. Monoaminergic systems

Some monoaminergic systems exert excitatory actions on given thalamic neuronal types and inhibitory on others, as well as differential effects on various types of cortical neurons located in various layers. To anticipate, in contrast with rather consistent facilitatory effects exerted by cholinergic systems on thalamocortical systems, the search for coherent effects of monoamine-containing neurons is still at its beginnings.

Serotonin (5-HT), released by neurons in the dorsal raphe nucleus, depolarizes thalamic RE neurons but hyperpolarizes TC neurons in all investigated dorsal thalamic nuclei. Application of 5-HT in thalamic slices results in prolonged depolarization associated with a decrease in a K^+ current, I_{KL}, in thalamic RE (and perigeniculate) neurons, an action mediated by 5-HT_2 and possibly 5-HT_{IC} receptors [223] (see Fig. 3.2 in Chapter 3). In contrast, 5-HT hyperpolarizes and suppresses the tonic firing mode in neurons recorded from relay nuclei, such as thalamic association (pulvinar and lateroposterior), intralaminar (center median and centrolateral), mediodorsal, ventrobasal, and medial geniculate nuclei [224]. This action occurs through an increase in K^+ conductance, mediated by 5-HT_{1A} receptors. Besides this direct mechanism obtained in the presence of tetrodotoxin that blocks synaptic transmission, 5-HT activates local-circuit GABAergic neurons, which results in an increased frequency of IPSPs in TC neurons [224]. In neocortex, 5-HT may increase the excitability of pyramidal neurons through a reduction of various K^+ currents, I_{AHP}, I_{KL}, and I_M [109, 225].

[223] McCormick and Wang (1991).

[224] Monckton and McCormick (2002). In a previous study, 5-HT was found to produce a small depolarization of dorsal lateral geniculate (dLG) neurons (Lee and McCormick, 1996), thus contrary to the 5-HT-evoked hyperpolarization found in this recent study within widespread dorsal thalamic nuclei (see main text). Monckton and McCormick (2002) explained these opposite actions exerted by 5-HT on dLG versus many other dorsal thalamic nuclei by invoking the site of release, concentration, and postsynaptic receptor-effector mechanisms.

[225] Reviewed in McCormick (1992).

Fig. 2.41 (opposite) Muscarinic, but not nicotinic, blockers antagonize PPT effects on slow (~0.3 Hz) cortical oscillation. Cat under urethane anesthesia. Regular-spiking (RS) area 5 neuron, antidromically activated by stimulating the thalamic rostral intralaminar centrolateral (CL) nucleus and synaptically driven from the thalamic lateroposterior (LP) nucleus. *A*, rhythmic depolarizing phases at the resting membrane potential (V_m) and their reduction by a pulse-train (30 Hz, 0.85 s) to the PPT nucleus. *B*, suppressing effect of PPT stimulation on slow oscillation under DC depolarizing current (+0.2 nA). *C–F*, same depolarizing current as in *B*. *C*, PPT pulse-train (30 Hz, 1.7 s, double duration as in *B*) led to suppression of the slow oscillation, which was twice as long as in *B* (note electrocorticogram (ECoG) activation). *D*, administration of the nicotinic blocker mecamylamine (mecamyl) (30 μg/kg, i.v.) had no effect on PPT action (spikes truncated). *E*, 20 s after scopolamine (scopol) administration (at arrow, 0.5 mg/kg, i.v.), the number of action potentials of each oscillatory sequence diminished and the frequency of the slow oscillation increased (as in Fig. 2.40). *F* (without interruption after *E*), lack of any effect of PPT stimulation on slow cellular and ECoG oscillation (same parameters of stimulation as in *C–D*). From Steriade et al. (1993a).

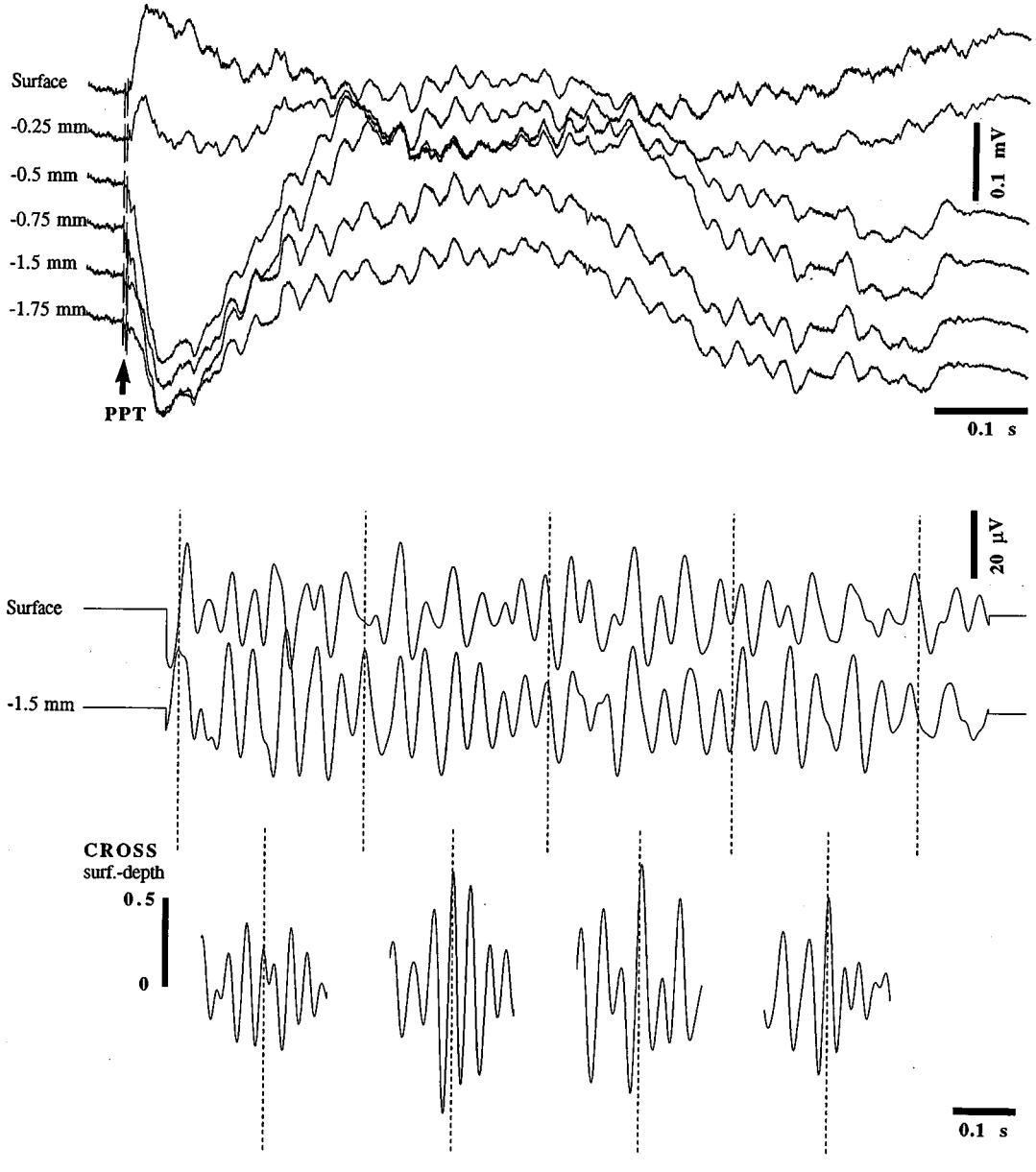

Fig. 2.42 Fast oscillations induced at the surface and depth of cortical area 5 by stimulation of cholinergic pedunculopontine tegmental (PPT) nucleus. Cat under ketamine-xylazine anesthesia. Top, averaged responses ($n = 15$) to two short-delayed (3 ms) PPT stimuli. The response started with a surface-positive (depth-negative) wave lasting for ~60 ms, followed by fast waves that were in-phase at the surface and depth leads. Bottom, the surface-evoked and depth-evoked (1.5 mm) potentials were filtered (15–80 Hz) and cross-correlated (CROSS) within four windows. Note in-phase relations in windows 2 to 4. From Steriade et al. (1996a).

[226] Kayama et al. (1982).

[227] Pinault and Deschênes (1992b).

[228] McCormick and Pape (1990b).

[229] Buzsáki et al. (1991).

[230] Foehring et al. (1989). This *in vitro* study also showed that NE application in cortical slices produces a voltage- and time-dependent increase in the persistent Na^+ current, $I_{Na(p)}$.

[231] Svensson et al. (1975).

[232] Egan and North (1985).

[233] McCormick and Williamson (1991).

[234] Uhlrich et al. (2002); see also Parmentier et al. (2002).

[235] Haas and Greene (1986).

Norepinephrine (NE), released in the thalamus and cerebral cortex by locus coeruleus (LC) neurons, depolarizes thalamic RE neurons recorded *in vitro*, like the 5-HT action [223]. *In vivo* too, LC stimulation excites RE neurons [226] and lesion of LC cells or local application of the α_1-antagonist prazosin decreases the firing frequency of RE neurons [227]. In the very few dorsal thalamic nuclei that have been investigated, NE depolarizes TC cells and enhances a hyperpolarization-activated cation current, I_H, through β-adrenoceptors [228]. The effects of α-adrenergic drugs administered *in vivo* are dual, blocking and promoting high-voltage spindle oscillations through α_1 and α_2 receptors, respectively [229]. In the cerebral cortex, NE excites large pyramidal neurons by selectively reducing slow Ca^{2+}- and Na^+-mediated currents via β_1-adrenergic receptors [230]. *In vivo*, a comparison between the effects induced by brief pulse-trains to LC and those induced by stimulating the PPT cholinergic nucleus with the same parameters showed that, although both stimulated structures blocked the slow sleep oscillation, the threshold of this effect was lower, and the duration was longer, with PPT than with LC stimulation (Fig. 2.44). The LC effect was antagonized by systemic administration of clonidine (Fig. 2.45), an α_2-agonist that inhibits LC-cells' discharges and NE release [231]. As to the more powerful effect exerted by PPT, compared to LC, stimulation on the cortical slow oscillation (see Fig. 2.44*B*), it may be explained by reciprocal interactions between these two (PPT and LC) structures. Indeed, LC neurons extend their long dendrites (0.4–0.5 mm) to adjacent areas, up to the PPT nucleus, where NE hyperpolarizes cholinergic neurons via α_2 receptors [202], whereas ACh excites LC neurons via m_2 receptors [232]. Then, when PPT is stimulated, LC neurons may be simultaneously activated, whereas LC stimulation may inhibit PPT neurons. In other words, although in brain slices ACh and NE act on different cell types via pharmacologically distinct receptors, during natural arousal both PPT and LC nuclei are implicated with rather complex interactions.

Histamine (HA) is released by neurons in the tuberomammillary nucleus of the posterior hypothalamus. It produces slow depolarizing responses in TC neurons recorded from dorsal lateral geniculate (dLG) slices, associated with an increase in the apparent input resistance, due to a decrease in a leak K^+ current [233]. In the intact brain, HA switches the burst firing of dLG X- and Y-cells into tonic firing and promotes sensory input, apparently with no clear-cut effect on inhibitory neurons [234]. In the neocortex and hippocampus, HA activates pyramidal neurons through inhibition of a K^+ current, I_{AHP} [225, 235].

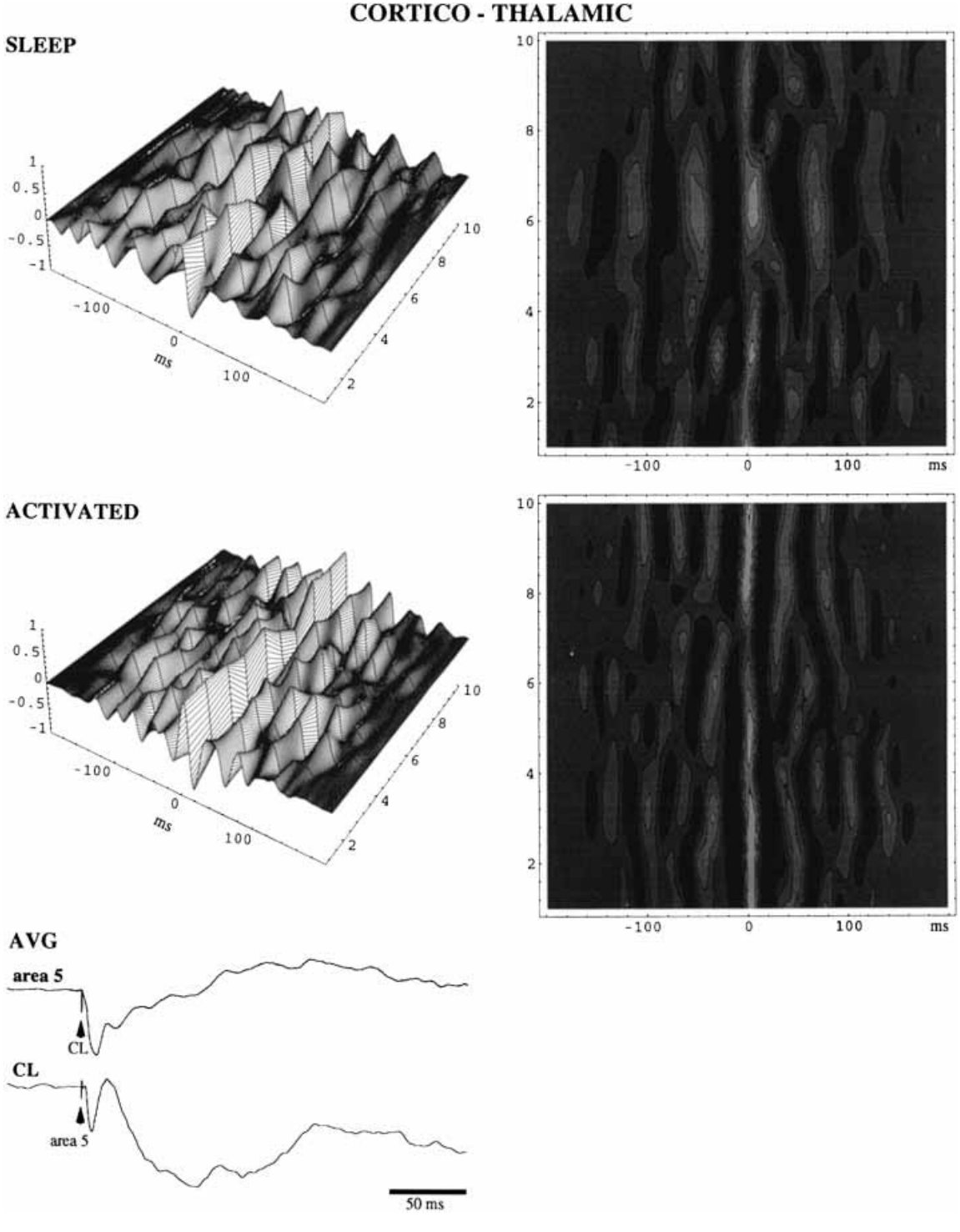
CORTICO - THALAMIC
SLEEP
ACTIVATED
AVG
area 5
CL
CL
area 5
50 ms
ms
-100
0
100
2
4
6
8
10
1
0.5
0
-0.5
-1

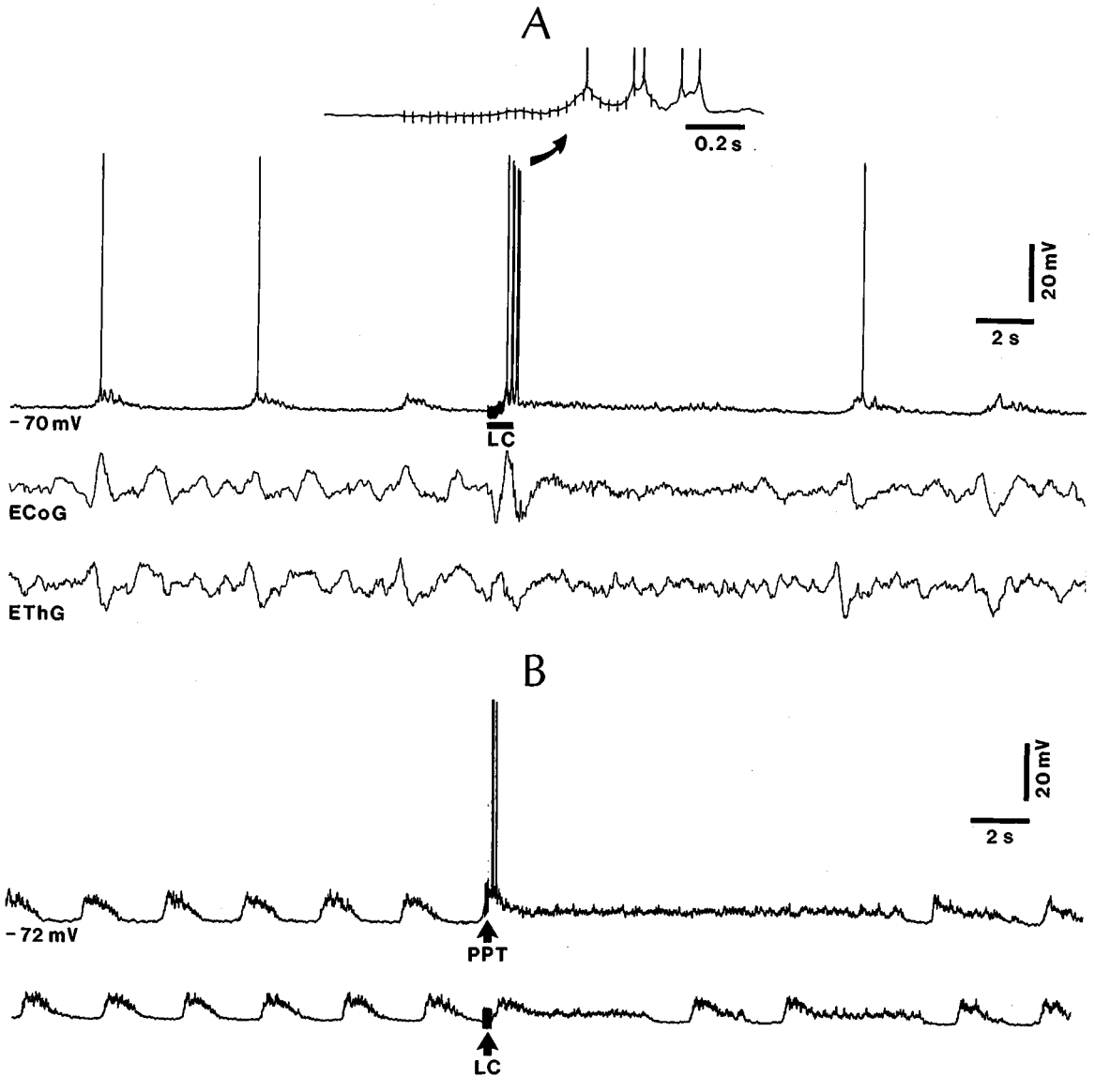

Fig. 2.44 Effects of locus coeruleus (LC) stimulation on slow cortical oscillation. Cat under urethane anesthesia. *A*, regular-spiking (RS) area 5 neuron. LC pulse-train (1 s, 30 Hz; marked by horizontal bar) blocked the slow oscillation, simultaneously with an activated electrocorticogram (ECoG) and electrothalamogram (EThG) response lasting for ~8 s. *B*, another area 5 neuron antidromically activated from thalamic centrolateral and lateroposterior nuclei at latencies of 5 and 4 ms, respectively. PPT stimulation (10 stimuli at 100 Hz) blocked the slow oscillation for 15 s. The same parameters of stimulation applied to LC had no effect (not shown); by increasing the duration of the LC pulse-train (30 stimuli at 100 Hz), a blocking efect appeared and lasted for 6 s. From Steriade et al. (1993a).

Fig. 2.43 (opposite) Corticothalamic synchronization of fast (gamma) rhythms. Cat under ketamine-xylazine anesthesia. Sequential cross-correlations (three-dimensional surfaces on the left, topogram on the right; see techniques in Amzica and Steriade, 1995a) from periods with slowly oscillating patterns characteristic of sleep (top) and from an activated epoch following PPT stimulation (middle). Cross-correlations were computed between filtered (15–80 Hz) EEG waves recorded from the depth of cortical area 5 and the thalamic intralaminar centrolateral (CL) nucleus, and derive from sequential windows of 0.2 s each. Note the increased corticothalamic synchrony during the PPT-activated epoch and the coherence of the 25-Hz oscillation (see four symmetrical secondary peaks). Bottom, averaged ($n = 30$) monosynaptic responses (latencies, 2–3 ms) evoked in area 5 by CL stimulation and evoked in CL nucleus by area 5 stimulation, recorded through the same cortical and thalamic electrodes that provided data in the above panels. From Steriade and Amzica (1996).

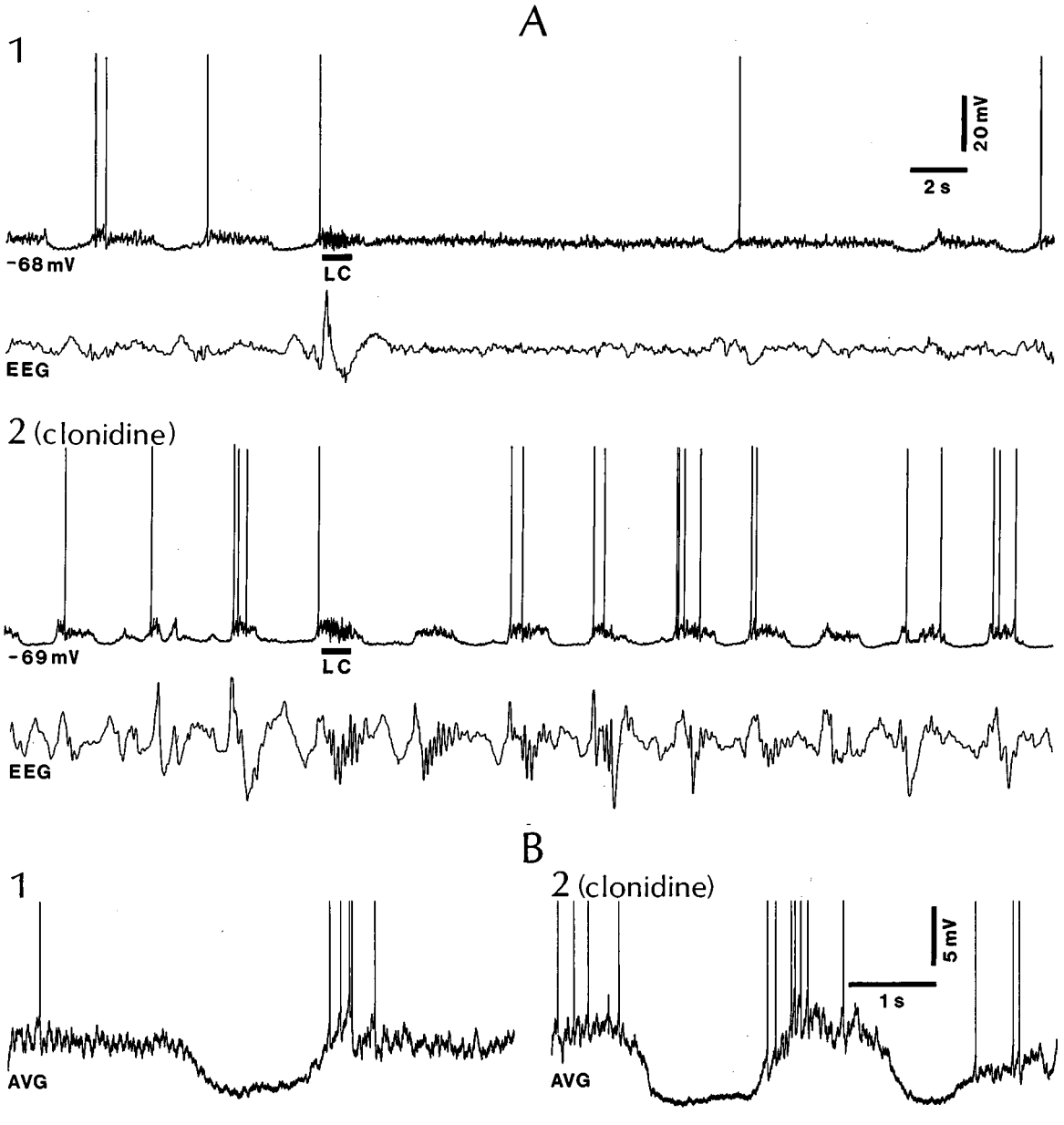

Fig. 2.45 Clonidine antagonizes the LC-induced suppressive effect on slow cortical oscillation. Cat under urethane anesthesia. RS neuron from area 5. *A1*, LC pulse-train (1 s, 30 Hz) blocked the cellular and EEG slow oscillation for ~14 s. *A2*, clonidine (50 μg/kg, i.v.) increased EEG synchronization and virtually blocked the LC suppressive effect on the slow oscillation (compare to *A1*). Note EEG spindle sequences recurring periodically, in close time relation with the slow cortical oscillation, after LC stimulation. *B*, averaged (AVG, $n = 10$) oscillatory traces before (*B1*) and after (*B2*) clonidine administration (spikes truncated). From Steriade et al. (1993a).

2.6. Concluding remarks

(a) The high degree of synaptic activity in the intact brain, which is lacking in brain slices or in isolated cortical slabs *in vivo*, decisively modulates and may even overwhelm the intrinsic neuronal properties expressed by responses to direct depolarization in several neocortical cell classes. Thus, intracellular recordings in behaving animals demonstrate that changes in natural states of vigilance may transform the response pattern of an intrinsically bursting neuron to that of a regular-spiking neuron. And, under certain physiological conditions, the firing pattern of fast-rhythmic-bursting ("chattering") neurons is transformed into that of fast-spiking neurons. Reciprocal responses of pyramidal and local inhibitory neocortical neurons have been investigated with paired intracellular recordings. Single-axon EPSPs and IPSPs between identified neurons revealed the mechanisms for coupling the inputs reaching various cortical layers. Intracortical connections, due to horizontal projections of pyramidal neurons, are implicated in the long-range synchronization of the slow sleep oscillation.

(b) The excitatory synaptic responses in the trisynaptic loop between neurons in the dentate gyrus (targets of layers II–III of the entorhinal cortex) and fields CA3-CA1 of the hippocampus are followed by inhibitory responses produced by a series of GABAergic interneurons targeting the initial axonal segment, soma, and dendrites of pyramidal neurons.

(c) A group of inhibitory neurons in the amygdala, called intercalated cell masses, constitutes the interface between input (basolateral) and output (central) nuclei of this nuclear complex that is implicated in various aspects of emotional reactivity.

(d) As in neocortex, the intrinsic properties of thalamocortical and thalamic reticular neurons are influenced by the degree of synaptic activity. This makes the low-threshold spike highly variable, which is a major factor in the desynchronization of oscillatory neurons and, consequently, determines the termination of thalamically generated spindles. Contrary to thalamocortical neurons that do not communicate from one dorsal thalamic nucleus to another, but only through the intermediary of thalamic reticular or neocortical neurons, thalamic reticular neurons form an interconnected network that accounts for the initiation of spindles even when disconnected from thalamus and cortex. Thalamic reticular neurons also project to local thalamic interneurons in various dorsal thalamic nuclei. This GABAergic-to-GABAergic projection produces

significant effects on the ultimate targets, thalamocortical neurons. Indeed, a greatly increased incidence of IPSPs in thalamocortical neurons was observed after destruction of thalamic reticular neurons. The connection between the two types of thalamic GABAergic cells may be important for focusing attention to relevant signals.

(e) With few exceptions, the corticothalamic reciprocal loops connect neocortical areas with dorsal thalamic nuclei and the corticothalamic projection outnumbers the thalamocortical one by almost one order of magnitude. Although the corticothalamic projection to all three major types of thalamic neurons is glutamatergic, therefore excitatory, synchronous volleys occurring naturally during cortical sleep oscillations, during paroxysmal activity, or induced artificially using electrical stimuli, produce powerful depolarizing actions on thalamic GABAergic reticular neurons and hyperpolarizing actions on thalamocortical neurons because the numbers of some glutamate receptor subunits is much higher in thalamic reticular, compared to relay, neurons.

(f) Neuromodulatory systems with generalized effects on forebrain neurons originate in the upper brainstem reticular core, posterior hypothalamus, and basal forebrain. The cholinergic and glutamatergic neurons that give rise to ascending projections toward thalamus and cortex are similarly active during wakefulness and REM sleep, much less active in slow-wave sleep, and display changes in firing rates suggesting their crucial role in determining the shift from the deafferented state of slow-wave sleep to brain-activated states. Some effects on thalamic relay and cortical neurons are similarly exerted by acetylcholine and glutamate. The actions of brainstem cholinergic neurons on thalamocortical neurons are excitatory, resulting from a direct depolarization associated with increased input resistance due to suppression of a "leak" K^+ current, and disinhibition following the hyperpolarization of thalamic GABAergic reticular neurons. Among the less often investigated monoaminergic actions, serotonergic neurons hyperpolarize thalamocortical neurons, while noradrenergic neurons depolarize thalamic reticular neurons and excite some pyramidal cortical neurons.

Chapter 3 Neuronal properties, network operations and behavioral signs during sleep states and wakefulness

The popular view that behavioral quiescence is the predominant sign of sleep may be valid for the full-blown state of resting sleep, but not for the preparatory period during which many animal species display complex motor behaviors directed at finding a home for sleep. However, this aspect of behavioral immobility alone cannot differentiate sleep from wakefulness since humans and other mammals are motionless at increasing levels of vigilance, especially during expectancy and hunting conditions associated with characteristic bioelectrical rhythms. The defining signs of the period when one falls asleep are peculiar changes in brain electrical activity (electroencephalogram, EEG) produced by network operations in the thalamus and cerebral cortex. These changes are the cause, rather than the reflection, of a quiescent behavioral condition. Indeed, the brain oscillations that define the transition from wakefulness to sleep are associated with long periods of inhibition in thalamocortical cells, with the consequence that the incoming messages are blocked and the cerebral cortex is deprived of information from the outside world. Following the appearance of these initial signs, other oscillatory types mark the late stage of resting sleep and they further deepen the unresponsiveness of thalamic and cortical neurons, disconnecting the brain from the external world.

In this chapter, I discuss the neuronal properties and network mechanisms underlying the behavioral and bioelectrical signs of waking and two major sleep stages: sleep with high-amplitude, synchronized slow waves (SWS), and sleep with rapid eye movements (REM sleep). First I will deal with SWS and then with two brain-active states of waking and REM sleep.

3.1. Falling asleep

Before discussing the neuronal substrates of SWS, it is necessary to mention the state of our knowledge on humoral factors that are often invoked as promoters of sleep. At the time of writing, most scientists investigating the mechanism of sleep onset at the

neuronal level either regard humoral theories of sleep as based on data derived from experiments that lack stringent methodological criteria, or they simply ignore the theories. However, one should remember that the genesis and maintenance of the enduring state of sleep are not attributable entirely to neuronal mechanisms operating at relatively short time scales. Indeed, the mechanisms of falling asleep will only be fully elucidated when we have data showing how sleep humoral factors modulate the actions of neurons in critical areas of the brain; only then will we be able to fully interpret our single-neuron recordings. As shown in the first section of this chapter, we know very little about the effects of sleep-promoting chemical substances upon neurons of cerebral structures that are hypothesized to promote sleep.

3.1.1. Humoral factors

Piéron [1] introduced almost a century ago the notion of a humoral sleep factor, under the term hypnotoxin, which was nondialyzable and thermolabile. He kept dogs awake day and night, removed a sample of their cerebrospinal fluid (CSF), injected it into animals allowed to rest normally, and observed that the CSF-injected animals fell asleep. The conclusion was that the need for sleep is due to a hypothetical substance accumulated when wakefulness is maintained over long periods of time. Although the technique of removing CSF was primitive at that time, other authors basically confirmed Piéron's results. In those experiments [2], goats were used as CSF donors because of the large amount of CSF that could be extracted from their brain, and rats as recipient animals because they needed to be injected with small quantities of CSF. Later on, recipient animals were rabbits because they displayed less variability of EEG-synchronized sleep. The technique was progressively improved by comparing the effects of an infused chemical substance under investigation with those of an infused inactive control solution.

The terms sleep factor (SF) or sleep-promoting substance (SPS) are commonly used for substances hypothesized to promote sleep. The list of putative SFs is quite long and many researchers have claimed that the active substance promoting sleep was finally discovered before control experiments slowed down the initial enthusiasm. There are about 40 to 60 SFs and some models have proposed interactions between various substances having the capacity to modify sleep for quite long periods. A few SFs are discussed below. This choice was dictated by the possibility of connecting some SFs with presumed target neurons in brain areas that are implicated in sleep regulation by lesion and stimulation experiments. However, the possibility of interaction between SFs and glial

[1] Piéron (1913).

[2] Pappenheimer et al. (1967); Fencl et al. (1971).

elements, with direct influences on sleep onset, is also open. Below, there is a brief account of SFs; full details may be found in previous reviews on this topic [3].

The delta-sleep-inducing peptide (DSIP), termed so because initial reports claimed that it is released by brain electrical stimulation and promotes sleep with delta EEG waves, may act through the modulation of endocrine systems and/or by direct action on lower brainstem or anterior hypothalamic neurons. Indeed, DSIP stimulates growth hormone release [4], which has also been implicated in sleep induction. In slices of lower brainstem, DSIP induces a calcium-dependent release of met-enkephalin [5]. This is a possible mechanism of the antinociceptive action of DSIP when injected in the giganto- and paragigantocellular fields of the medullary reticular formation, which are highly sensitive sites in the production of opioid analgesia [5]. Thus, DSIP may be a factor in reducing alertness to noxious stimuli and in favoring sleep onset. DSIP was immunohistochemically localized in the anterior hypothalamic region comprising, among other structures, the preoptic area [6], one of the cerebral candidates for sleep induction. The literature data on DSIP-induced sleep are, however, contradictory and more information is needed on DSIP actions at brain sites hypothesized to control sleep onset.

Growth hormone releasing factor (GRF) belongs to the family of secretin-glucagon peptides. Its intraventricular administration produces EEG synchronization associated with reduction of motor activity, and inhibition of GRF suppresses sleep [7]. The GRF-containing hypothalamic neurons around the ventromedial nucleus project to the basal forebrain [8]. Thus, they might exert their presumed sleep-promoting action through an effect upon the hypothesized hypnogenic basal forebrain area, but the precise neuronal actions of GRF remain to be investigated.

The vaso-intestinal peptide (VIP) increases both quiet and REM sleep in rats [9]. However, REM sleep appears with a very long latency and the possibility was raised that, rather than a direct VIP action on the mesopontine cholinergic generator of REM sleep, VIP modulates the release of prolactin that, in turn, may promote REM sleep.

Prostaglandins (PGs) D_2 and E_2 are endogenous substances that are hypothesized to induce sleep and wakefulness, respectively [10]. PGD_2 and PGE_2 are actively synthesized and metabolized in the mammalian brain. The putative receptor of PGs was studied by autoradiography and the binding protein was found in the posterior hypothalamus and preoptic area [11], which are postulated to be critical zones for regulating waking and sleep, respectively.

[3] Borbély and Tobler (1989); Kapas et al. (1993); Krueger and Toth (1994); Krueger et al. (1999); Pabst et al. (1999).

[4] Iyer and McCann (1987).

[5] Nakamura et al. (1988, 1989).

[6] Charnay et al. (1989).

[7] Obál et al. (1988, 1991).

[8] Daikoku et al. (1986).

[9] Riou et al. (1982).

[10] Hayaishi (1988).

[11] Yamashita et al. (1983).

[12] Ueno et al. (1983).

[13] Krueger et al. (1982, 1984).

[14] Jouvet (1972).

[15] Shoham et al. (1987); Shoham and Krueger (1988).

[16] Shibata et al. (1989).

[17] Eisenman (1982).

[18] Adenosine receptors are blocked by theophylline and caffeine, two substances known for their arousing properties (Dunwiddie, 1985).

[19] Feldberg and Sherwood (1954); Haulica et al. (1973); Radulovacki (1985).

[20] Porkka-Heiskanen et al. (1997).

[21] Borbély (1982).

[22] Portas et al. (1997). Microdialysis perfusion of adenosine into cholinergic areas of the mesopontine tegmentum and nucleus basalis produced a reduction in wakefulness, to 50% of the basal level.

[23] Rainnie et al. (1994). Whole-cell and extracellular recordings from brainstem slices of rats showed that the adenosine inhibition of cholinergic neurons in the laterodorsal tegmental nucleus is mediated postsynaptically by an inwardly rectifying K^+ current.

[24] Steriade et al. (1990a).

The sleep-promoting effect of PGD_2 was demonstrated by microinjections into preoptic area that increased the duration of EEG-synchronized sleep about 6-fold [12]. It was claimed that two SFs, muramyl dipeptide and interleukin-1, stimulate astrocytes to produce PGD_2, and that the hypnogenic effects of those two substances may be due to their stimulating actions on PGD_2 production [10].

Other studies were mainly related to the increased sleepiness during infectious diseases. Quantitative measurements in rabbits inoculated with *Staphylococcus* (*S.*) *aureus* determined a biphasic action on sleep duration, with an enhancement of EEG-synchronized sleep beginning 4–6 h after inoculation. *S. aureus* contains muramyl peptides (MPs) in its cell wall. MPs were proposed as an SF whose hypnogenic activity can be dissociated from its pyrogenic action [13]. The MP structure is similar to that of serotonin (5-HT), a neurotransmitter that was initially proposed to promote sleep [14] but, subsequently, it was shown that 5-HT neurons are more active in waking than in sleep states. The MPs action on astrocytes and microglia may result in the production of interleukin-1 (IL1), a cytokine that was also found to increase EEG-synchronized sleep [15]. In the light of the demonstrated linkage between sleep and temperature regulation, it is possible that the somnogenic properties of IL1 are due to its action upon thermosensitive hypothalamic neurons. Thus, IL1 alters the neuronal firing of warm- and cold-sensitive hypothalamic cells [16] and may even change the intrinsic properties of some neurons. Indeed, elements initially insensitive to changes in temperature become sensitive if exposed to IL1 [17].

Probably, the candidate most likely to exert hypnogenic effects is adenosine, a purine nucleoside whose production is linked to high neuronal metabolic activity during wakefulness [18], which eventually may shift the behavioral state toward sleep by inhibitory actions exerted on generalized activating systems. It has been known since the 1950s that adenosine is a sleep-inducing substance [19]. More recently, adenosine was shown to mediate the sleep-inducing effects of prolonged wakefulness [20] (Fig. 3.1), in line with the idea that the propensity for sleep is proportional to the duration of the prior state of waking [21]. Adenosine inhibits basal forebrain neurons [22] as well as mesopontine cholinergic neurons [23] that fire at high rates during wakefulness, compared to SWS [24].

Clearly, a single neurochemical regulatory substance could not account for the genesis of the complex behavioral state of sleep. The neuronal actions of SFs substances, which facilitate or promote sleep when injected into given brain areas, should now be submitted to electrophysiological studies to shed light on chemically modulated ionic currents of neurons located in brain areas implicated

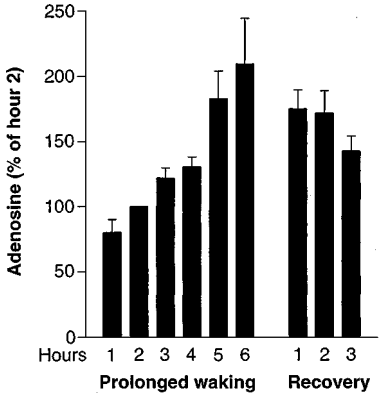

Fig. 3.1 Prolonged wakefulness and recovery sleep. Microdialysis measurements of adenosine in freely moving cats. Mean extracellular adenosine values increased in the basal forebrain during 6 h of prolonged wakefulness. The adenosine values decreased in the subsequent 3 h of spontaneous recovery sleep. See more details in Fig. 2 of the paper by Porkka-Heiskanen et al. (1997).

in sleep regulation by experiments using single-cell recordings and excitotoxic lesions. As it stands now, the field of sleep research seems dissociated into two distinct "wet" and "dry" camps, glaring at one another, but displaying little effort to combine their interests.

3.1.2. Neuronal mechanisms

The concepts postulating that sleep is a passive phenomenon due to closure of cerebral gates (brain deafferentation) or, alternatively, an active phenomenon promoted by inhibitory mechanisms arising in some cerebral areas have long been considered as opposing views. However, during brain disconnection from the outside world, the absence of a steady excitatory bombardment may produce disfacilitation in some brain structures, eventually followed by rebound cellular excitation that would set in motion a series of structures which may promote sleep through active inhibitory processes. Also, firing of some neuronal groups in the preoptic area, hypothesized to actively promote sleep, may inhibit posterior hypothalamic histaminergic neurons that have activating properties, thus leading to sleep through deafferentation, as postulated in the passive theory of sleep. Therefore, the two (passive and active) mechanisms of sleep onset are probably successive steps within a chain of events, and they are complementary rather than opposed. This view is elaborated in a recent monograph [25].

One of the major arguments supporting the notion that sleep is promoted by active cerebral processes is derived from ethology. Looking actively for a safe place to fall asleep is what prompted Konorski [26] to refute the idea "that somnolence is a less active state than any other drive" and to postulate that "somnolence and sleep are easily conditionable and are subject to the same rules as hunger drive and feeding". He concluded with a short ethological survey leading to the statement that "a sleepy animal looks actively for some place to fall asleep, just as the hungry animal looks for food". This idea followed an earlier suggestion [27] and observations of ethologists that sleep is an instinctive behavior as animals seek for a place of maximum security to fall asleep. In one of his last theoretical contributions, Moruzzi [28] concluded that animals' "behavior before the onset of sleep strikingly recalls the appetitive phase of the instincts" while "sleep may be regarded as a chain of consummatory acts, represented by the alternation of (EEG) synchronized and desynchronized episodes".

I will present the evolution of pioneering concepts for an actively generated sleep state by inhibitory mechanisms. The experimental data supporting this idea are still at an embryonic stage.

[25] Steriade (2001b). For a discussion of concepts on passive and active sleep, with emphasis on sleep by deafferentation, see section 1.1.4 in that 2001 monograph.

[26] Konorski (1967), pp. 300–301.

[27] Claparède (1905).

[28] Moruzzi (1969), pp. 211–212.

[29] Pavlov (1923).

[30] Jasper (1981).

[31] Steriade et al. (2001a).

[32] Hess (1944).

3.1.2.1. Sensory and brain stimulation leading to sleep

The first experimental argument for sleep as an active inhibitory process derived from the effects of monotonous stimulation of sensory receptors leading to habituation (that is, loss of interest) and eventually to sleep. These studies were initially carried out in Pavlov's laboratories and led him to propose that inhibition of conditioned reflexes and sleep are two aspects of the same process [29]. The "inhibition" was inferred from the extinction of the orienting reaction. Later on, habituation was recorded as a progressive diminution of EEG desynchronization and decreased amplitude of field potentials evoked by repeated sensory stimulation [30]. In his theory of the "inhibitory perceptive recurrent reflex", Konorski [26] assumed that a new stimulus-object activates (in addition to the corresponding sensory pathway) the arousal system that increases the excitability of the gnostic field. By contrast, a known or habituated stimulus-object reaches inhibitory systems that, by suppressing the arousal system, lead to diminution and abolition of stimulus-object perception. Obviously, the reader is aware of the mystery surrounding these presumed inhibitory systems. As to Pavlov's view [29] that sleep derives from a mass inhibition irradiating over the whole cerebral cortex, it was refuted by all single-unit recordings, including intracellular ones, which showed that virtually no cortical cell is silent during sleep and that some cortical cell types discharge at higher rates during some SWS epochs than during waking [31].

Sleep was also induced by electrical stimulation of the brain. Some regard these effects as strong evidence for the active nature of sleep. The first attempt to produce sleep by brain stimulation was reported by Hess [32] who claimed that sleep was induced in the cat after low-rate (8–10 Hz) stimulation of a midline thalamic area near the massa intermedia or nucleus reuniens. The difficulty in interpreting Hess' studies comes from the long latencies of the observed effects and the fact that the cat is a good sleeper and, without a careful assessment of the behavioral and EEG state of the animal preceding the stimulation, these effects may well have been due to the cat's natural propensity toward sleep; this issue is discussed elsewhere [25].

Other central sites whose low-frequency stimulation (around 10 Hz) elicited EEG synchronization in the long search for hypnogenic structures are not enumerated here, since many cerebral areas that are stimulated with such frequencies may induce synchronized EEG waves that do not outlast the stimulation period and do not induce behavioral manifestations of sleep. The only brainstem structure worthy of mentioning is the nucleus of the solitary tract (NST) in the medulla. The lower brainstem was thought to

inhibit the upper activating brainstem reticular formation and/or to counteract its influence at the diencephalic level [33]. Experiments initiated by Dell and continued by his colleagues [34] have shown that a complete sleep sequence is triggered by stimulation of rapidly conducting vagal afferents to the NTS. While this "vago-aortic sleep" seemed to persist after surgical destruction or pharmacological inactivation of the raphe system [35], more recent experiments indicated the dependence of NST-induced sleep upon serotonergic afferents.

3.1.2.2. Serotonin and sleep

Jouvet [14] propounded the sleep theory implicating raphe nuclei and their major transmitter, serotonin (5-hydroxytryptamine, 5-HT). Most experimental data supporting this theory were accumulated during the 1960s and are as follows: (*a*) sleeplessness after subtotal destruction of medullary and mesopontine raphe nuclei or after a split brainstem with a mid-sagittal section that lesioned raphe nuclei; (*b*) EEG synchronization accompanied by sedation or true resting sleep after ventricular infusions of 5-HT (which does not cross the blood-brain barrier in adult animals) and local application of 5-HT at the level of the preoptic area in the anterior hypothalamus or the area postrema in the medulla; (*c*) insomnia after administration of *p*-chlorophenylalanine (PCPA), an inhibitor of 5-HT biosynthesis; and (*d*) sleep recovery after a small dose of 5-hydroxytryptophan (5-HTP), the direct precursor of 5-HT, which crosses the blood-brain barrier. In one spectacular case of Morvan's syndrome in man (extreme insomnia associated with choreiform movements), 5-HTP administration restored natural EEG-synchronized sleep [36].

This monument had apparently collapsed during the 1970s when the basic results of raphe lesions and PCPA administration could not be confirmed, and the advent of cellular recordings in naturally sleeping animals refuted the possible role of raphe neurons in the genesis of quiet sleep. Here are those data: (*a*) 90% depletion of forebrain 5-HT by PCPA induces only transient insomnia and has no significant effect on EEG-synchronized sleep [37]; (*b*) the cryogenic blockade of linearis and dorsal raphe nuclei (which provide the serotonergic innervation of the forebrain) induces EEG-synchronized sleep followed by REM sleep, which is the opposite of what was expected [38]; (*c*) 5-HT release from the neocortex is lower during quiet sleep than during wakefulness [39]; (*d*) when the serotonergic blockade is added to the cholinergic blockade, all signs of EEG desynchronization and cerebral activation are eliminated [40], which suggests a role for 5-HT in processes underlying

[33] See Moruzzi's (1972) review.

[34] Dell and Padel (1965); Puizillout et al. (1984).

[35] Puizillout and Ternaux (1974).

[36] Fischer-Perroudon et al. (1974).

[37] Dement et al. (1973); Rechtschaffen et al. (1973).

[38] Cespuglio et al. (1979). Also, lesions of raphe nuclei had no significant effect on sleep (Mouret and Coindet, 1980).

[39] Disclosed by radioenzymatic assays and voltammetric measures (Puizillout et al. 1979; Cespuglio et al., 1984).

[40] Vanderwolf (1988).

[41] McGinty and Harper (1976); Trulson and Jacobs (1979); Shima et al. (1986); Lydic et al., (1987).

[42] Gaudin-Chazal et al. (1982).

[43] Puizillout et al. (1979).

[44] Nosjean et al. (1987).

[45] Stevens et al. (1992).

[46] Khateb et al. (1989).

[47] Consolazione et al. (1984).

[48] Steriade et al. (1988).

[49] Paré et al. (1988).

EEG activation, rather than in EEG-synchronized sleep; and (*e*) neurons recorded from the dorsal raphe and other nuclei of the raphe system decrease the rates of their regular discharges when the animal passes from wakefulness to EEG-synchronized sleep [41].

The above results provide evidence against a role for raphe nuclei and 5-HT in the regulation of resting sleep and its physiological correlates. While Jouvet's original claims seem unfounded in the light of subsequent experiments conducted in other laboratories and by his own group, more recent results may bring the raphe (as well as other serotonergic) projections and 5-HT neuromodulatory actions back on the scene as good candidates for inducing neuronal events related to EEG-synchronized sleep. Two series of data are mentioned below: the serotonergic control of the NST in the medulla (see above), and the inhibition exerted by 5-HT on diencephalic and telencephalic neurons through an increased K^+ conductance that can induce electrophysiological events promoting resting sleep.

The serotonergic innervation of the NST is provided, in addition to raphe projections, by the nodose vagal nerve ganglia [42]. The 5-HT-containing cells of nodose ganglia projecting to NST have been implicated in the induction of "vago-aortic sleep" [43]. Selective lesions of 5-HT fibers reaching the commissural region of the rat's NST induce a decrease in EEG-synchronized sleep over the long term [44]. This result was interpreted as the consequence of the removal of a facilitatory action of 5-HT upon the NST neuronal mechanisms contributing to the induction of EEG-synchronized sleep. The 5-HT actions on various NST cell populations and the serotonergic involvement in the NST-induced "vago-aortic sleep" are an open field of investigation. With the advent of *in vitro* studies, the complexity of 5-HT effects on different brainstem neurons has begun to be deciphered. In pontine reticular slices, one population of neurons responded with membrane hyperpolarization and decreased input resistance, a response mediated by 5-HT_1 receptors, and another population showed depolarization and increased input resistance, probably a non-5-HT_1 response [45]. In midbrain reticular neurons, the effects of 5-HT are mainly inhibitory [46].

The serotonergic projections of raphe nuclei to the thalamus have been identified by combining the retrograde transport technique with immunohistochemistry [47]. Discrete injections of retrograde tracers in all types of thalamic nuclei revealed that the dorsal raphe nucleus projects to relay, associational [48], intralaminar and reticular [49] thalamic nuclei of the cat. While some thalamic nuclei display good correspondence between the distribution of 5-HT terminals and 5-HT_{1-2} receptors, there is a mismatch in

the intralaminar nuclei between dense 5-HT inputs and low 5-HT receptor density [50].

The 5-HT projection to the thalamic reticular (RE) nucleus may be of importance in view of the generation of oscillatory events within the RE nucleus, sleep spindles, associated with rhythmic inhibitory processes in thalamocortical neurons, with the consequence of blocking the transfer of information from the outside world, thus predisposing to cortical deafferentation and sleep (see below, **3.2**). Dense patches of 5-HT immunoreactive fibers coincide with clusters of RE neurons in the monkey [51]; in other species the RE nucleus appears to be relatively weakly labeled with most ligands for 5-HT receptors [52]. In the 1980s, the dorsal raphe serotonergic effect on RE neurons was viewed as inhibitory, but more recent results *in vitro* showed depolarizing actions. Thus, in earlier experiments [53], the inhibitory actions of dorsal raphe stimulation and 5-HT application upon RE thalamic neurons might have been viewed as a factor behind the appearance of RE-generated spindle oscillations, marking the transition from waking to sleep onset, immediately after a drop in the discharge rate of raphe serotonergic neurons during the transition from waking to sleep [54]. However, application of 5-HT to RE neurons in thalamic slices results in a prolonged depolarization associated with a decrease in potassium currents [55] (Fig. 3.2). Instead of 5-HT, acetylcholine (ACh)

[50] Herkenham (1987). The apparent low density of 5-HT_{1A} receptors in the thalamus of rats, cats and primates (Kia et al., 1996; Ito et al., 1999) stands in contrast with data from experiments on thalamic slices from ferrets showing a hyperpolarization of thalamocortical neurons recorded from a series of nuclei (especially pulvinar, but also some intralaminar and sensory relay nuclei) associated with increased membrane conductance and mediated through the 5-HT_{1A} receptor (Monckton and McCormick, 2002). These authors explained this discrepancy between their results and the relatively low level of 5-HT_{1A} receptors by species differences (in the pulvinar of cats and monkeys, 5-HT leads to an enhancement of the depolarization sag of the cation current I_H) and/or age, as the hyperpolarizing response to 5-HT in the pulvinar of ferrets is age-dependent, decreasing with age.

[51] Morrison and Foote (1986).

[52] Reviewed in Asanuma (1997).

[53] Yoshida et al. (1984).

[54] Trulson et al. (1984).

[55] McCormick and Wang (1991).

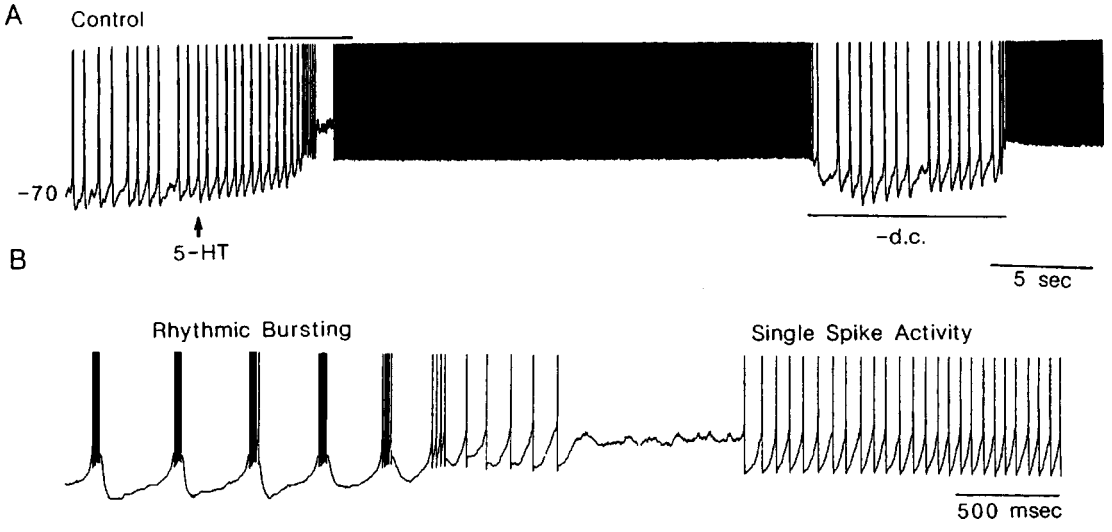

Fig. 3.2 Serotonin (5-HT) modulates firing mode in guinea pig thalamic reticular (RE) neurons *in vitro*. *A*, application of 5-HT to a rhythmically bursting RE neuron results in a depolarization of the membrane potential which is associated initially with an increase in the rate of burst generation followed by a complete inhibition of bursts and the appearance of single-spike activity (transition expanded in *B* for detail). Repolarization of the membrane with intracellular injection of current (−d.c.) reinstated the rhythmic burst firing. From McCormick and Wang (1991).

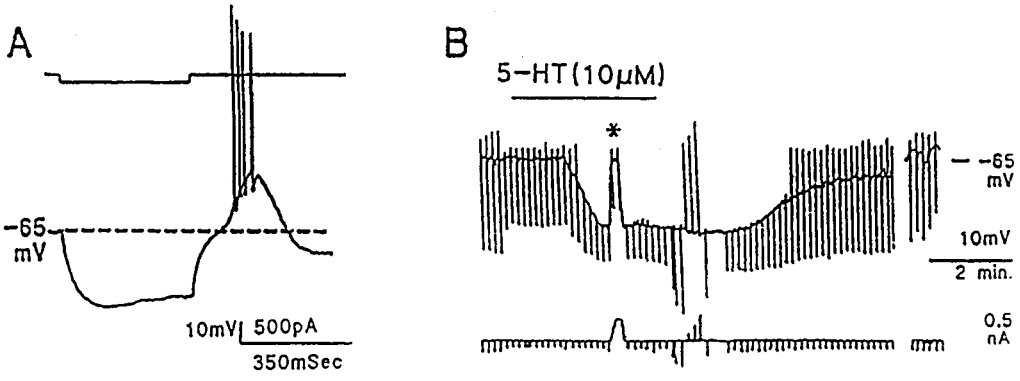

Fig. 3.3 Serotonin (5-HT) inhibits cholinergic neurons in the mesopontine laterodorsal tegmental nucleus. Intracellular recording from rat *in vitro* preparation. *A*, with the membrane potential held at –65 mV, a hyperpolarizing current step resulted in a low-threshold rebound spike-burst. *B*, application of 10 μM 5-HT to a bursting neuron resulted in a hyperpolarization of the membrane potential, a response that other experiments showed to persist in the presence of tetrodotoxin, indicating that inhibition was a direct serotoninergic effect. The voltage deflections in the top trace are responses to constant current pulses used to measure input resistance; repolarization of the membrane to the resting level (asterisk) demonstrates a decrease in input resistance that was independent of the change in membrane potential. Modified from Lübke et al. (1992).

should be considered as a permissive factor for the generation of sleep spindles [56]. In contrast with changing views on the effects exerted by 5-HT on GABAergic thalamic RE neurons (see above), other data consistently show that 5-HT neurons inhibit cholinergic neurons located at the mesopontine junction [57] (Fig. 3.3) and as well as neurons recorded from the cholinergic area of the basal forebrain [58]. Given the known effects exerted by brainstem [59] and basal forebrain [60] cholinergic neurons on thalamic and neocortical neurons during activation processes associated with the state of wakefulness, it is reasonable to suggest that dorsal raphe 5-HT neurons inhibit the progenitors of activation processes and, thus, assist in promoting sleep. Moreover, the general conclusion that dorsal raphe neurons diminish their firing rates during sleep [41] was recently challenged by recordings of atypical neurons, distributed unevenly in the cat dorsal raphe nucleus, which displayed the highest discharge frequencies during SWS, with suppression of firing in both waking and REM sleep [61]. Of course, the chemical code of these atypical neurons remains to be demonstrated, which is not a small task when the animal is awake and unrestrained.

It is fair to state that no firm conclusions can yet be drawn from the investigations of 5-HT's action on brainstem, diencephalic, and forebrain structures implicated in sleep-related processes.

[56] The permissive role of cholinergic projections arising in the mesopontine reticular formation was shown by experiments demonstrating that brainstem-thalamic neurons cease firing in advance of the first spindle sequence during transition from waking to resting sleep (Steriade, 1984; Steriade et al., 1990a). The sudden withdrawal of activity in brainstem-thalamic cholinergic neurons is one of the major factors for spindle genesis, knowing that acetylcholine (ACh) inhibits GABAergic RE thalamic neurons (McCormick and Prince, 1986) and that stimulation of the brainstem cholinergic peribrachial area prevents spindling by interrupting the depolarizing envelope of spindle oscillations in pacemaker RE neurons (Hu et al., 1989a). As to locus coeruleus neurons, they also diminish their firing rates before spindles (Aston-Jones and Bloom, 1981). However, the action of norepinephrine upon RE thalamic neurons is not yet clearly understood as both inhibitory and excitatory effects have been reported in different studies on thalamic neurons (Pape and Eysel, 1987; McCormick and Prince, 1988; Pape and McCormick, 1989; McCormick and Pape, 1990b).

[57] Lübke et al. (1992).

3.1.2.3. Sleep-active neurons in and around the preoptic area

There are now some grounds to believe that the search for the neuronal processes leading to drowsiness and EEG-synchronized sleep should be directed to within the interconnected networks of the diencephalon, basal forebrain, and upper brainstem reticular core.

The role of posterior hypothalamic areas in waking maintenance has been postulated since von Economo's anatomo-clinical observations, during the 1920s [62], on lethargic encephalitis (sleep-sickness) with lesions in the posterior hypothalamus and rostral midbrain tegmentum. During the 1940s, Nauta's experiments supported the notion of a waking "center" [63] in the posterior hypothalamus and, in addition, suggested that the anterior hypothalamus (corresponding to the region of the preoptic area and suprachiasmatic nucleus) promotes sleep because a transection in the rostral half of the hypothalamus leads to striking insomnia, eventually ending in death [64].

In early studies, the thalamus and cerebral cortex were not considered to play an essential role in sleep regulation since after chronic decortication or total thalamectomy the succession of waking and sleep stages seemed to be similar to that seen in the normal animal. Jouvet [65] is probably the first to report the absence of SWS (non-REM) sleep in decorticate animals. Quantitative studies on the duration of different sleep stages after ablation of the entire neocortex, striatum and most of the rhinencephalon (diencephalic cats) or after total thalamectomy (athalamic cats) concluded that, compared to about 53% of the time spent by brain-intact cats in a drowsy state and non-REM sleep, there was an impressive reduction in these EEG-synchronized sleep stages, down to 19–20%, for both diencephalic and athalamic preparations followed up to the 180th post-operative day [66].

The major argument for postulating the diencephalic and telencephalic neuronal networks as generators of the sleep-waking cycle was provided by experiments using chronic preparations after precollicular or low collicular transections in the cat. The conclusion of those experiments was that, after an initial comatose state, cycles of EEG synchronization and desynchronization reappeared from 7 to 10 days after the brainstem transection. These results led Moruzzi (see note [63]) to conclude that "structures lying within the isolated cerebrum (i.e., in front of the mesencephalon) may account for the reappearance of the sleep-waking cycle" (p. 46).

The experiments using electrical stimulation, transections, and electrolytic lesions constituted the main body of evidence for the cerebral sites involved in sleep regulation until the late 1970s. Some

[58] Khateb et al. (1993). In keeping with these *in vitro* data showing hyperpolarization of neurons recorded from the cholinergic area in the basal forebrain, injection of 5-HT into the region of nucleus basalis of naturally sleeping-waking rats produces a dose-dependent decrease in fast cortical EEG waves in the gamma frequency band (Cape and Jones, 1998) that betrays a state of cortical activation (see note [60]). For the hyperpolarizing effect exerted by 5-HT on thalamocortical neurons, see also note [50].

[59] Steriade et al. (1990a).

[60] Buzsáki et al. (1988b); Cape and Jones (2000).

[61] Sakai and Crochet (2001a).

[62] von Economo (1929).

[63] For a discussion on hypothetical brain "centers", see my previous monograph (2001b, Chapter 1). The notion of "center" implies initiation at the top of a command chain, without parallel processing and reciprocal information transfer between chain elements. The major reason for abandoning the idea of brain "centers" is that none of the presumed structures has proved to be necessary and sufficient for the induction and maintenance of complex behaviors. In the case of the waking "center", the criterion *necessary and sufficient* does not apply to the upper brainstem reticular core, regarded since the late 1940s as the arousal center. Indeed, in chronic stages, more than 300 days after midbrain transection, the animal displays clear-cut EEG patterns of wakefulness (see details in Moruzzi, 1972). This unexpected evolution is due to the presence of other (not necessarily redundant) activating systems, in front of the mesencephalic transection.

[64] Nauta (1946). For a recent review on the role of anterior and posterior hypothalamic areas in promoting sleep and arousal, respectively, see Saper et al. (2001).

[65] Jouvet (1962).

[66] Villablanca (1974).

conclusions of those studies are plagued by the common drawback of such methods, the co-activation or lesions of passing fibers. The imbalanced function of the brainstem after large thalamectomy may result from a thalamic descending influence, as the RE nucleus projects to the rostral brainstem reticular core [67], but may also be ascribed to the undesirable lesion of axons issuing from the basal forebrain and cerebral cortex.

The stimulation and lesion experiments postulating a sleep-promoting role of the preoptic area began in the 1940s. Electrical stimulation of the medial preoptic area in patients under local anesthesia induced a state of drowsiness and then unresponsiveness [68]. Thereafter, systematic studies used stimulation and lesion experiments in the cat preoptic region to demonstrate the hypnogenic property of this brain area [69]. These studies were criticized because of long delays in appearance of insomnia after electrolytic lesions of the preoptic area and the lack of a dynamic picture of the development of insomnia since the animals were not permanently recorded. As with other stimulation experiments, the induction of sleep after electrical stimulation of the preoptic area was not related to the previous behavioral state of the cat, and the induced effect might have instead been the natural propensity of the animal to fall asleep. Stimulation with both low and fast frequencies of the preoptic area and comparison between stimulation and control trials (counterbalanced blocks during an 8-h experimental period) led to refutation of the sleep-promoting role played by the preoptic area [70]. The possible involvement of 5-HT terminals in the stimulated preoptic area [71] was also emphasized, an idea in keeping with data showing that the pretreatment of cats with p-chlorophenylalanine (which depletes 5-HT terminals) prevents the hypnogenic effect induced by stimulation of the preoptic area [72]. These controversial results, pointing to or denying the sleep-promoting role of the preoptic area in the anterior hypothalamus, are probably due to the complexity of this region, a crossroad of ascending and descending axons, consisting of neurons using a great variety of transmitters.

The effects of posterior and anterior hypothalamic lesions by means of excitotoxic agents that leave intact passing fibers, and data resulting from single-cell recordings related to the process of falling asleep, are discussed below.

Recently the long-standing concept that the posterior hypothalamus is one among several awakening systems and that the anterior hypothalamus promotes sleep was validated. The results were based on the effects produced by injections of ibotenic acid, which destroys perikarya while leaving passing fibers intact, and by local

[67] Parent and Steriade (1984). The descending inhibitory pathway from GABAergic thalamic reticular neurons to the midbrain reticular formation may inhibit arousing systems that originate in the upper brainstem core. Thalamic reticular cells discharge single spikes during waking but give rise to high-frequency (around 200 Hz) spike-bursts during the transitional period from waking to sleep, as well as throughout slow-wave sleep (Steriade et al., 1986). These sleep-related spike-bursts can exert powerful and prolonged inhibitory effects on midbrain reticular neurons, with the consequence of de-activating (disfacilitating) thalamocortical systems, a prerequisite for falling asleep.

[68] White (1940). It is worth noting that stimulation was performed at a frequency of 60 Hz. Such fast stimuli are required to ascertain a real hypnogenic effect since EEG hypersynchrony (sometimes associated with drowsiness and somnolence) may be obtained from many brain structures, even those that are implicated in activation processes, when stimulated at low frequency rates (10–15 Hz or below).

[69] Sterman and Clemente (1962a-b); McGinty and Sterman (1968).

[70] LoPiccolo (1977).

[71] Jouvet (1988). That serotonergic inputs impact on the ventrolateral preoptic nucleus, together with other monoamine-containing neurons, was also recently demonstrated using retrograde tracer techniques and immunohistochemistry for monoaminergic markers (Chou et al., 2002). The connections from histaminergic and other monoamine-containing cell groups to the preoptic area are reciprocal (Steininger et al., 2001).

[72] Wada and Terao (1970).

[73] Sallanon et al. (1986).

[74] Lin et al. (1989).

[75] Sallanon et al. (1989).

[76] Gritti et al. (1994).

[77] Lin et al. (1988).

injections of muscimol, a GABA agonist that reversibly inactivates neurons. During the period corresponding to the ibotenic-induced neuronal loss in the ventrolateral part of the posterior hypothalamus, there was a 60% increase in EEG-synchronized sleep, but the effects lasted for only 2–3 days [73]. Muscimol injections in the ventrolateral part of the posterior hypothalamus led to the persistence of sleep with cortical slow waves (stage 2 of EEG-synchronized sleep in the cat) for 3 to 12 h, depending upon the amount of injected muscimol [74].

Opposite effects were obtained by lesioning or reversibly inactivating anterior hypothalamic neurons. Long-lasting insomnia, lasting for 2–3 weeks in animals with large lesions and characterized by a dramatic decrease of sleep with cortical slow waves as well as REM sleep, was produced by ibotenic lesions of the anterior hypothalamus, especially the medial preoptic area [75]. The animal with the major sleep impairment in that study also had a bilateral lesion of the vertical and horizontal limbs of diagonal band nuclei. Similar, but rapidly reversible, effects were induced by muscimol injections in the same anterior hypothalamic areas [74]. These results led to the hypothesis that the insomnia after the anterior hypothalamic lesion was due to an exalted excitability of the waking posterior hypothalamic system, which would be normally dampened by the anterior hypothalamic GABAergic and/or some peptidergic neurons projecting to the posterior hypothalamus [76]. In support of this idea, muscimol injection into the posterior hypothalamus of insomniac cats with preoptic lesions produced a transient sleep recovery [77].

Thus, the integrity of preoptic areas in the anterior hypothalamus is not a necessary condition for sleep onset, as sleep can be restored by inhibition of posterior hypothalamic neurons. The general conclusion of these studies is that the sleep-promoting role of the anterior hypothalamus results from the inhibition of the posterior hypothalamic waking system, and particularly from the inhibition of histaminergic cells located in the ventral part of the posterior hypothalamus. Evidence thought to support this hypothesis was that systemic injection of mepyramine, a histamine H_1-receptor antagonist, produced an increased duration of stage 2 of SWS, without modifying the thalamic-generated spindle oscillations. However, only lesioning or reversible inactivating *homogenous* structures can lead to conclusive evidence. This is not the case for any of the hypothalamic areas. There is a significant population of GABAergic neurons in the same tuberomammillary magnocellular area where histaminergic cells are located. When muscimol is injected in the posterior hypothalamus, GABAergic neurons are likely to be most

[78] Grace and Bunney (1985).

[79] Szymusiak and McGinty (1986).

[80] Szymusiak and McGinty (1989). In this study, the authors identified antidromically some of "sleep-active" neurons by responses to brainstem or cortex stimulation.

[81] Semba et al. (1989).

[82] Détári et al. (1984); Parmeggiani et al. (1986); Détári and Vanderwolf (1987); Détári et al. (1997).

[83] Buszáki et al. (1988b).

severely inhibited as, in other structures, GABAergic cells are many times more sensitive than non-GABAergic cells to GABA [78]. The inhibition of short-axoned GABAergic cells within the posterior hypothalamus would lead to local effects that would be more complex than a simple inhibition of histaminergic cells. Such effects may even include the disinhibition of histaminergic neurons that are targets of GABAergic cells. With the advent of chemical tools that selectively destroy GABAergic neurons, the effects of muscimol will be easier to interpret.

I will now focus on studies dealing with the state-dependent activities of anterior hypothalamic neurons, related to the results of lesion and inactivation experiments described in the previous text. Some neurons that increase their firing rates during EEG-synchronized sleep were not originally found in the medial preoptic area of the anterior hypothalamus (whose lesion produced insomnia; see above), but at more rostral and lateral sites, in the horizontal limb of the diagonal band nuclei and substantia innominata of the basal forebrain [79]. Those sleep-active cells (more active during SWS than in waking and REM sleep) comprised 24% of sampled neurons and were hypothesized to be cholinergic. The great majority of neurons were waking-active or state-indifferent. Changes in the firing rates of sleep-active neurons preceded the appearance of high-amplitude spindle oscillations. In a subsequent article [80], the authors reported data on a sample of sleep-active neurons located in substantia innominata, ventral to the globus pallidus and medial to the central nucleus of amygdala. Whereas this study in cat mentioned that there was no anatomical segregation between basal forebrain cells with antidromically identified ascending or descending projections, another investigation in rat found a clear segregation of cortical-projecting and brainstem-projecting neurons of the basal forebrain [81]. The former were located quite ventrally, in or near clusters of immunohistochemically identified cholinergic neurons, whereas the latter were located more dorsally and were not cholinergic. In contrast to studies pointing to sleep-active neurons as characterizing the basal forebrain and preoptic areas, other research groups reported that the overwhelming majority of basal forebrain (substantia innominata) neurons of cats and rats (or from the preoptic area, some identified as cortical-projecting neurons) increase their firing rates during active waking and REM sleep or during EEG-activation in anesthetized animals [82, 83].

Therefore, until quite recently there were no data supporting the idea that preoptic neurons, with formally identified chemical code, increase their activity prior to or during SWS. The initial

assumption (sleep-active neurons are cholinergic) does not fit with the established actions of ACh at two major targets of the basal forebrain: the cerebral cortex and reticular RE thalamic nucleus. In the cortex ACh is an excitatory agent on long-axoned pyramidal cells, whereas the same neurotransmitter hyperpolarizes RE thalamic neurons [84]. Cortical excitation (with direct depolarization of long-axoned elements and blockage of their long-lasting hyperpolarizations) is not what would be expected when sleep is promoted. As well, the inhibition of RE thalamic neurons by cholinergic basal forebrain neurons may account for the blockade of spindle oscillations [85], but this is contrary to what was found, namely, an increased discharge of those sleep-active neurons just before the occurrence of spindle oscillations [79, 80]. One possibility is that recordings from sleep-active neurons were performed from cortical-projecting GABAergic neurons [86] that are intermingled with cholinergic cells. The increased activity of GABAergic neurons at sleep onset would make more sense. The difficulties in systematically identifying GABAergic cells by recordings performed in behaving preparations seem insurmountable at this time.

Recent studies tested the hypothesis of a hypnogenic role played by preoptic neurons through their inhibitory (GABAergic) projection to the posterolateral hypothalamus. This descending inhibitory pathway from the preoptic region to the tuberomammillary nucleus [76] was confirmed and immunohistochemical studies identified the fos protein, an immediate early gene product, which was accumulated in a group of preoptic neurons that were specifically activated during the state of SWS in rats [87]. *In vitro* experiments showed the GABAergic nature of neurons recorded from the ventrolateral preoptic area; those neurons are inhibited by norepinephrine or acetylcholine [88]. Unit recordings from the ventrolateral preoptic area revealed a group of cells that fired at higher rates during SWS than during wakefulness (Fig. 3.4) and whose discharge patterns in waking-sleep cycles were reciprocally correlated with those of putative histaminergic neurons recorded from the tuberomammillary nucleus (Fig. 3.5) [89].

It should be mentioned that, before these recent results [87, 89], the postulate of active inhibitory processes underlying the onset and maintenance of sleep was tested by using the (2-^{14}C)deoxyglucose method for measuring local cerebral glucose utilization. The expectation was that enhanced neuronal activity in discrete regions of the brain would be accompanied by increased local metabolic rate. Of the 75 structures measured in monkey, including many of those hypothesized as hypnogenic (such as the preoptic area in the anterior hypothalamus or raphe nuclei), none exhibited a higher

[84] Reviewed in McCormick (1992).

[85] Steriade and Buzsáki (1990).

[86] Fisher et al. (1988).

[87] Sherin et al. (1996). The number of fos-immunoreactive neurons in the preoptic area was found to be positively correlated with the time spent asleep. See also the review by Saper et al. (2001).

[88] Gallopin et al. (2000). Whether those neurons recorded *in vitro* from preoptic slices were "sleep-promoting", as indicated in the puzzling title of that paper, remains a naïve belief in the ability of a brain slice to fall asleep! Nowadays, such jumps, from a neuron recorded *in vitro* to a global behavior, are quite often found in the literature.

[89] Szymusiak et al. (2001).

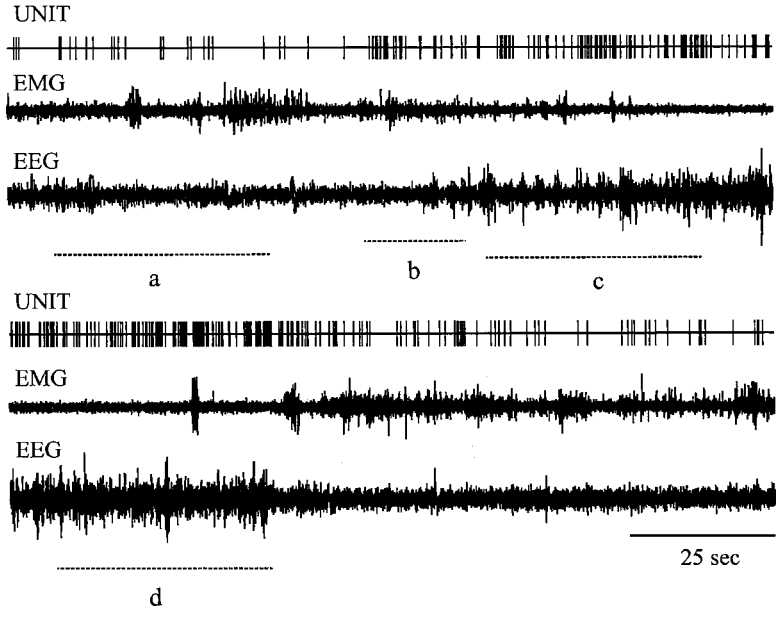

Fig. 3.4 "Sleep-active" neurons in the ventrolateral part of the rat preoptic area. Example of such a neuron during consolidated waking (dotted line *a*), the wake to non-REM transition period (dotted line *b*), early non-REM sleep (the initial one-third of the non-REM sleep episode; dotted line *c*), and late non-REM sleep (dotted line *d*). From Szymusiak et al. (2001).

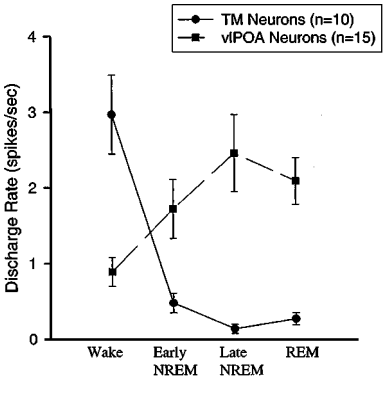

Fig. 3.5 Comparison of sleep/wake state-dependent discharge of neurons with sleep-related discharge in the ventrolateral part of the preoptic area and of putative histaminergic neurons exhibiting REM-off discharge patterns recorded in the tuberomammillary nucleus (TM). Discharge rates were calculated during waking, early non-REM sleep, late non-REM sleep, and REM sleep. Note the reciprocal relationship of discharge patterns across the sleep-wake cycle between these two cell types. From Szymusiak et al. (2001).

metabolic rate in SWS than in wakefulness [90]. Surprisingly, when considering all the assumptions as to the hypnogenic nature of the preoptic area, the studies by Sokoloff and his colleagues [90] showed a statistically significant *decrease* of the metabolic rate in the preoptic area during slow-wave sleep compared to waking, in keeping with the results of studies using single-cell recording [82, 83]. These results cannot justify a firm denial of increased activity in presumed inhibitory neurons at sleep onset because the technique of 2-deoxyglucose autoradiography cannot distinguish between intermingled groups of neurons with different chemical codes and properties in the explored areas. The question is open: are isolated pools of neurons in a given structure capable of inducing a state such as sleep, with global repercussions on the whole brain?

In conclusion, data show that, among all neuronal candidates that are implicated in promoting sleep, GABAergic neurons in the ventrolateral part of the preoptic area play a role by inhibiting activating neurons in the posterior hypothalamus. The postulated inhibitory action of preoptic neurons on posterior hypothalamus takes place within the conceptual framework of sleep as a product of brain disconnection from ascending activating generalized

systems. The permissive factors of sleep are some environmental conditions, such as a rise in ambient temperature, and especially the absence of proprioceptive and teleceptive stimuli that have access to generalized activating systems. Moruzzi [33], who stressed during his last writings the active nature of sleep, added however that this state "requires a level of (brainstem) reticular activation too low to be compatible with conscious behavior" (p. 141). Disconnection from sensory bombardment is an obvious factor that promotes sleep, and disengagement from any sort of activity proved to induce a significant enhancement in total sleep time. Experimental and clinical evidence point to a series of structures, mainly the upper brainstem core and the thalamic/hypothalamic continuation of the brainstem reticular formation, whose lesions produce states of decreased vigilance, from neglect to drowsiness, lethargy and full-blown sleep [91].

There is no need to conclude that sleep results from either brain deafferentation or the initiation of inhibitory processes that act upon activating systems ultimately leading to the disfacilitation of their targets. Passive or active sleep is a false dilemma since all mechanisms discussed in this section (humoral factors, disconnection from external and internal signals, and inhibitory neurons acting on activating ones) should be considered in concert.

3.2. Brain oscillations during slow-wave sleep

The defining signs of the period when one falls asleep are peculiar changes in brain electrical activity (EEG), which are the cause, rather than the reflection, of a quiescent behavioral condition. The EEG oscillations defining the transition from wakefulness to sleep, mainly spindles, are associated with long periods of inhibition in thalamocortical (TC) cells, with the consequence that the incoming messages are blocked and the cerebral cortex is deprived of external signals. Following the appearance of these initial signs, other oscillatory types (slow and delta) mark the late stage of resting sleep and they further deepen the inhibition of thalamic and cortical cells.

In humans, the common electrographic definition of sleep onset is the change from EEG alpha waves during relaxed wakefulness to a mixed-frequency pattern of low-voltage waves (termed stage 1 sleep). However, in contrast to spindles the major aspects of whose neuronal mechanisms have been elucidated (see ***3.2.1***), the basic cellular electrophysiology of human stage 1 sleep has not been explored for obvious reasons. Since stage 1 sleep may or may not coincide with perceived sleep onset in humans, many investigators

[90] Kennedy et al. (1982). In rat, similarly disappointing results for the active sleep theory were reported by Ramm and Frost (1983). More recently, Sokoloff's team measured local rates of cerebral glucose utilization ($ICMR_{glc}$) and reported that $ICMR_{glc}$ was unchanged in any of the 60 brain structures examined (including medial and lateral preoptic areas) in sleep-deprived rats (Everson et al., 1994).

[91] The syndrome of neglect is induced experimentally by lesions of thalamic intralaminar nuclei in monkeys and in humans (Heilman et al., 1985; Bougousslavsky et al., 1986). Bilateral lesions of thalamic intralaminar nuclei in humans may also lead to gross disturbances of vigilance, such as long-lasting somnolence and even hypersomnia (Façon et al., 1958; Castaigne et al., 1962). We ascribed the prolonged hypersomnia to bilateral lesions of the ascending activating (midbrain-thalamic) system due to a stenosis at the bifurcation of the basilar artery (Façon et al., 1958). More recently, the role of medial-intralaminar thalamic nuclei in sustaining the state of wakefulness was also documented by Bassetti et al. (1996) who reported cases of hypersomnia following thalamic paramedian stroke; their Figs. 1 and 2*B*, with brain magnetic resonance from two patients, depict "butterfly-shaped" lesions affecting bilaterally the ventral part of the dorsomedial nucleus and especially intralaminar nuclei, quite similar to the lesion illustrated originally in the late 1950s (Façon et al., 1958; Castaigne et al., 1962; see those lesions in Fig. 16.2 of Steriade, 1997b). The neuronal substrate of the role played by thalamic intralaminar nuclei in ascending activation processes in the cerebral cortex is the monosynaptic excitation from the upper midbrain reticular core of antidromically identified thalamocortical neurons recorded from intralaminar nuclei (Steriade and Glenn, 1982). Plum (1991) has analyzed his and other data in the literature concerning disturbances of arousal mechanisms in humans after rostral midbrain and paramedian thalamic lesions. He reached the conclusion that prolonged lethargy and coma do not usually result from unilateral lesions of the midbrain reticular core and its rostral continuation, the thalamic nuclei with diffuse cortical projections. In humans, lesions of the midbrain-thalamic activating system interfere not only with the state of waking, but also destroy the cerebrum's capacity to energize its motor functions (Plum, 1991).

recognize the clear-cut onset of sleep by the EEG correlates of stage 2 sleep [92]. Among these correlates, a major sign is the appearance of spindle oscillations and K-complexes associated with the slow oscillation (see ***3.2.3***). The possibility that neural processes associated with the genesis of thalamic spindles operate from the very onset of human sleep (as is the case with spindles in cats) cannot be ruled out since the EEG is usually recorded from the human scalp, while spindle oscillations primarily appear in discrete thalamic foci [93]. The absence of global thalamic synchronization during stage 1 sleep in humans may also explain why cortical spindling is not visible at the usual inspection of the EEG.

Although spindles and K-complexes are conventionally taken as electrographic landmarks of early sleep stages, at least in cats (the species of choice for investigating neuronal substrates of sleep rhythms), spindles and the slow oscillation occur conjointly from the very onset of sleep. Thus, the slow oscillation (***3.2.3***) dominates brain electrical activity throughout SWS, whereas spindles appear during early SWS stages, are overwhelmed by delta waves (***3.2.2***) during late SWS stages, and reappear towards the end of SWS (Fig. 3.6). These changes that occur throughout SWS, from prevalent spindles to prevalent delta and back to spindles, are attributable to changes in the membrane potential of TC neurons (see ***3.2.2***). Our view that basic cellular electrophysiology can explain and simplify all low-frequency sleep rhythms, through the pervasive influence of the newly described slow oscillation that groups other cortical and thalamic sleep oscillations (see below, *3.2.3.2*), is supported by recent quantitative measures of human EEG sleep activity that show a uniformly increasing trend across low-frequency bands starting with stage 2 sleep [94].

The mechanisms of generation and synchronization of the three major oscillatory types that characterize SWS are described in what follows.

3.2.1. Spindles, a thalamic rhythm under neocortical influence

This sleep rhythm is termed so because of the spindle shape of the oscillation envelope. It has a frequency of 7 to 14 Hz in cats, and 12 to 15 Hz in humans. Spindle sequences recur rhythmically, every 2 to 5 s (see below, Fig. 3.11). Since the old days of clinical EEG, it has been observed that "low-frequency" and "fast-frequency" spindles (~12 Hz and ~14 Hz, respectively) show a different topographic localization, with the former localized more anteriorly [95]. The same view was expressed during the 1990s [95]. A more unified way to see different spindles' frequencies is based on results

[92] Carskadon and Dement (2000). Quantitative measures of microstructural EEG changes in humans also point to the start of stage 2 as a reliable and discriminative boundary between wakefulness and sleep (De Gennaro et al., 2001).

[93] That spindles' occurrence should be searched in the thalamus is obvious by examining the results of developmental studies. It was initially postulated that *cortical* EEG slow waves appear earlier in mammals' ontogenesis than do EEG spindles (Jouvet-Mounier et al., 1970). This observation was correct. However, when both thalamic and neocortical recordings were performed in kittens, spindles were disclosed in the thalamus from the first day of postnatal life, whereas at this age cortical spindling was lacking and could only be detected after the 8th postnatal day (Domich et al., 1987), probably because of the late development of synapses made in cortex by thalamofugal axons. In fact, while prethalamic and corticothalamic axons reach thalamic nuclei before birth both in cats (Shatz, 1983) and monkeys (Shatz and Rakic, 1981), thalamocortical axons develop much later and the process of synaptogenesis continues for weeks after thalamocortical axons have entered the cortex (Cragg, 1975; Wise et al., 1979). The fact that spindles occur in the thalamus much earlier (Domich et al., 1987) than previously assumed is not surprising because some of the earliest arising thalamic neurons in ontogeny are those of the spindle pacemaker, the RE nucleus, which develops well before birth (Altman and Bayer, 1979). However, to my knowledge there are no ultrastructural data about the development of dendro-dendritic synaptic contacts in the cat's RE nucleus; these contacts operate to produce spindling within the RE nucleus (see ***3.2.1***).

[94] De Gennaro et al. (2001).

[95] Gibbs and Gibbs (1952). Borbély's group (Werth et al., 1997) also found two modes of human spindle frequencies, at 11.5 and 13 Hz, with a trough at 12.25 Hz. In rats, anterior frontal spindles occur at a frequency of ~12 Hz, while posterior parietal spindles are slightly faster, at ~14 Hz (Zygierewicz et al., 1999).

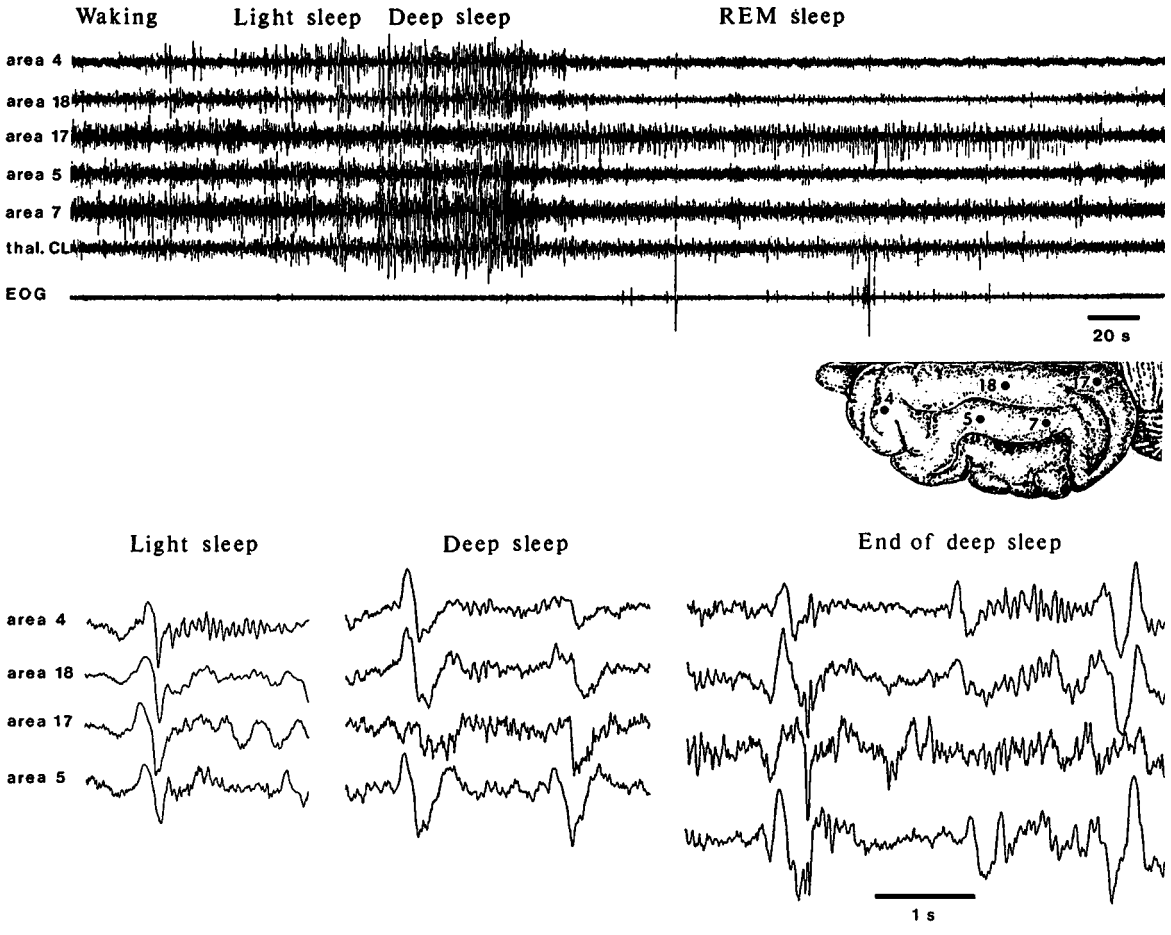

Fig. 3.6 Chronology of SWS rhythms in a naturally sleeping cat. Multi-site recordings of field potentials from the cortical depth (about 1 mm in areas 4, 18, 17, 5, and 7; see brain figurine) and thalamic centrolateral (CL) rostral intralaminar nucleus. Below the long-term recording of a full wake-sleep cycle (440 s), three panels illustrate expanded recordings during light sleep, deep sleep, and the end of SWS, before entering REM sleep. During light sleep, one cycle of the slow oscillation followed by a spindle sequence is depicted. Two cycles of slow oscillation (about 0.7 Hz) are depicted during deep SWS. Note, at the end of SWS, more pronounced spindles than during deep SWS. Modified from Steriade and Amzica (1998).

using intracellular recordings of TC neurons: low-frequency spindles are due to long-lasting hyperpolarizations (lasting 100–150 ms) followed by rebound spike-bursts, whereas relatively shorter hyperpolarization-rebound sequences (70–100 ms) account for faster spindles. It is possible that TC neurons projecting to anterior cortical fields in humans display longer hyperpolarizations during spindles, thus accounting for lower-frequency of spindles.

Spindles have been investigated at the neuronal level since the 1960s. Most aspects were first elucidated by intracellular studies

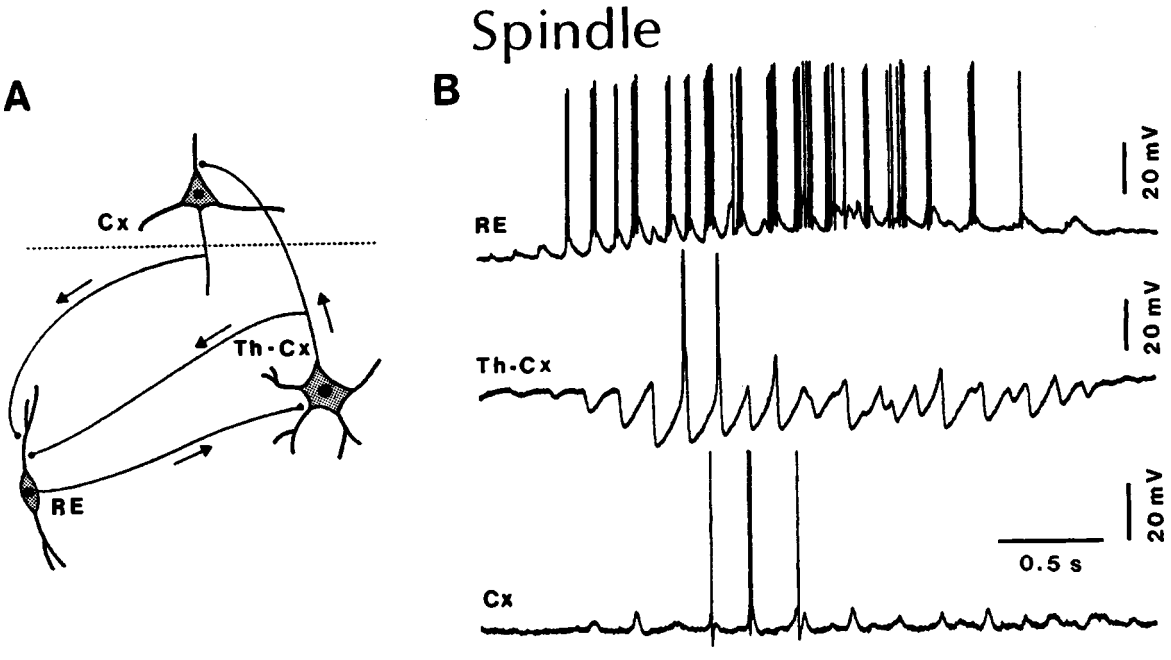

Fig. 3.7 Spindle oscillations in reticular thalamic (RE), thalamocortical (Th-Cx, ventrolateral nucleus), and cortical (Cx, motor area) neurons. *A*, circuit of three neuronal types. *B*, intracellular recordings from cats under barbiturate anesthesia. Note rhythmic spike-bursts of RE neuron during a spindle sequence and concomitant IPSPs leading to postinhibitory rebound bursts in Th-Cx neuron. See also text. Modified from Steriade and Deschênes (1988).

conducted on virtually all types of thalamic nuclei *in vivo*, mainly in cats, and thereafter *in vitro*, mainly on slices from the ferret visual thalamus. Since there is general agreement among contemporary researchers on most issues related to this activity and because this oscillation has repeatedly been discussed in reviews, handbook chapters, and monographs [96], I shall present here only the basics and emphasize some issues arising from recent developments in this field. In essence, spindles arise in GABAergic thalamic RE neurons whose rhythmic spike-bursts induce inhibitory postsynaptic potentials (IPSPs) in target TC neurons; the IPSPs de-inactivate a transient low-threshold Ca^{2+} current that promotes burst firing, which is transferred to cortical neurons where it induces rhythmic excitatory postsynaptic potentials (EPSPs) and occasional action potentials (Fig. 3.7).

3.2.1.1. Thalamic reticular nucleus, pacemaker of spindles

It has been known since the 1980s that GABAergic thalamic RE neurons are pacemakers of spindles: spindles disappear in

[96] Steriade and Llinás (1988); Steriade et al. (1990b, 1997); Steriade (1999a).

[97] Steriade et al. (1985).

[98] Steriade et al. (1987a).

[99] Thomson (1988a) reported that, in thalamic slices maintained *in vitro*, rhythmic oscillations of the membrane potential within the frequency range of spindles outlasted the pulse-train applied to the RE nucleus. This synaptic effect contrasted with the absence of self-maintained oscillations after current pulses injected into dorsal thalamic cells. The optimal frequency of RE stimulation was around 160 Hz, that is, the same as that displayed by RE spike-bursts during spindles in natural sleep (Steriade et al., 1986). The effects of chemical excitation of RE neurons were studied *in vivo* (Marini et al., 1992).

[100] Wang and Rinzel (1993); Destexhe et al. (1994a); Golomb et al. (1994).

[101] Von Krosigk et al. (1993).

thalamocortical systems after disconnection from RE neurons [97] and they are preserved within the RE nucleus disconnected from the remaining thalamus and cerebral cortex [98]. In addition, electrical stimulation of RE neurons *in vitro* produces IPSPs followed by rebound excitation in dorsal thalamic nuclei and chemical stimulation of RE perikarya *in vivo* produces a dramatic increase in spindle density at the level of target thalamocortical systems [99].

These experimental data were corroborated in different types of computational models of isolated RE neurons, shown to be capable of displaying oscillations within the frequency range of spindles [100].

The failure to detect spindles in the visual sector of the RE nuclear complex investigated in slices maintained *in vitro* [101] was attributed to an incomplete collection of intact RE neurons [102] due to the slice procedure that cuts the very long dendrites of RE neurons, which are essential for the generation of spindles [103]. Also, slices lack inputs from brainstem monoaminergic systems that depolarize RE neurons [55], thus allowing the expression of spindles [104].

The inhibitory interactions between RE neurons have been studied *in vitro*, leading to the conclusion that IPSPs among RE neurons are mediated by $GABA_A$ receptors [105]. In contrast with the assumption that these IPSPs would prevent burst firing and, thus, desynchronize intra-RE neuronal activity, intracellular recordings *in vivo* found that reversed IPSPs between RE neurons (at hyperpolarized membrane potentials, close to values seen during natural sleep) can directly trigger low-threshold spikes (LTSs) followed by rebound spike-bursts [106] (Fig. 3.8). This intra-RE activity propagates inside the RE network and, in two-dimensional models, $GABA_A$-mediated oscillations initiate spindle sequences [107]. IPSPs-based waves of excitation (reversed IPSPs that generate spike-bursts) propagate with a constant velocity of 25–150 neurons per second; increasing the $GABA_A$ receptor conductance between RE neurons reduces the time delay between IPSPs' onset and between the occurrences of Na^+ action potentials (Fig. 3.9). Another way of synchronization could be realized by electrotonic coupling [108]. Preliminary results suggested the presence of a gap junction protein (GJP) in a series of brain structures, including the RE nucleus [109]. Whether the presence of GJP immunoreactivity in the rostrolateral district of the RE nuclear complex is related to glia or to both glia and neuronal structures remains to be determined. Although electrical and dye coupling have already been demonstrated for some central structures, these features have been only recently reported

[102] Steriade et al. (1993d).

[103] Initially, it was hypothesized [98] that dendro-dendritic inhibitory synapses among GABAergic RE cells generate spindles by an avalanche process within the deafferented RE nucleus; namely, hyperpolarization of the postsynaptic dendrites would de-inactivate a low-threshold Ca^{2+} conductance (see Chapter 2) that triggers a spike-burst, followed by hyperpolarization in synaptically coupled dendrites, until a critical mass of RE neurons is entrained in the oscillation. The demonstration that low-threshold spikes (LTSs) of RE neurons are located in the dendrites (Mulle et al., 1985; Huguenard and Prince, 1992), the graded bursting behavior of RE neurons, and the presence of spike-bursts in presumed dendritic recordings from RE neurons (Contreras et al., 1993) support the above hypothesis. That the dendrites of RE neurons are implicated in the bursting properties that lead to synchronized spindle oscillations was also demonstrated in a combined experimental (*in vivo* and *in vitro*) and modeling study (Destexhe et al., 1996). Dendro-dendritic synaptic contacts exist in both cats and primates. As to species in which dendro-dendritic synapses are rare, the intra-RE synchronization may operate through axonal collaterals of RE neurons. However, after an initial failure to find such synapses in rats, there is now evidence of numerous dendro-dendritic synapses in this species (see note [135] in Chapter 2). Intracellular staining of neurons located in the somatosensory part of the rat's RE nucleus revealed two main types of RE neurons: one of them possesses axonal branches distributed within the RE nucleus, a large fusiform soma, and dendrites arborizing mainly in the horizontal plane (Spreafico et al., 1988).

[104] Destexhe et al. (1994b).

[105] Sanchez-Vives and McCormick (1997a); Sanchez-Vives et al. (1997); Uhlrich and Huguenard (1997).

[106] Bazhenov et al. (1999).

[107] Bazhenov et al. (2000).

[108] Gap junctions and corroborative electrophysiological data have been reported for some of the mammalian central neurons (see Llinás, 1985).

[109] Nagy et al. (1988).

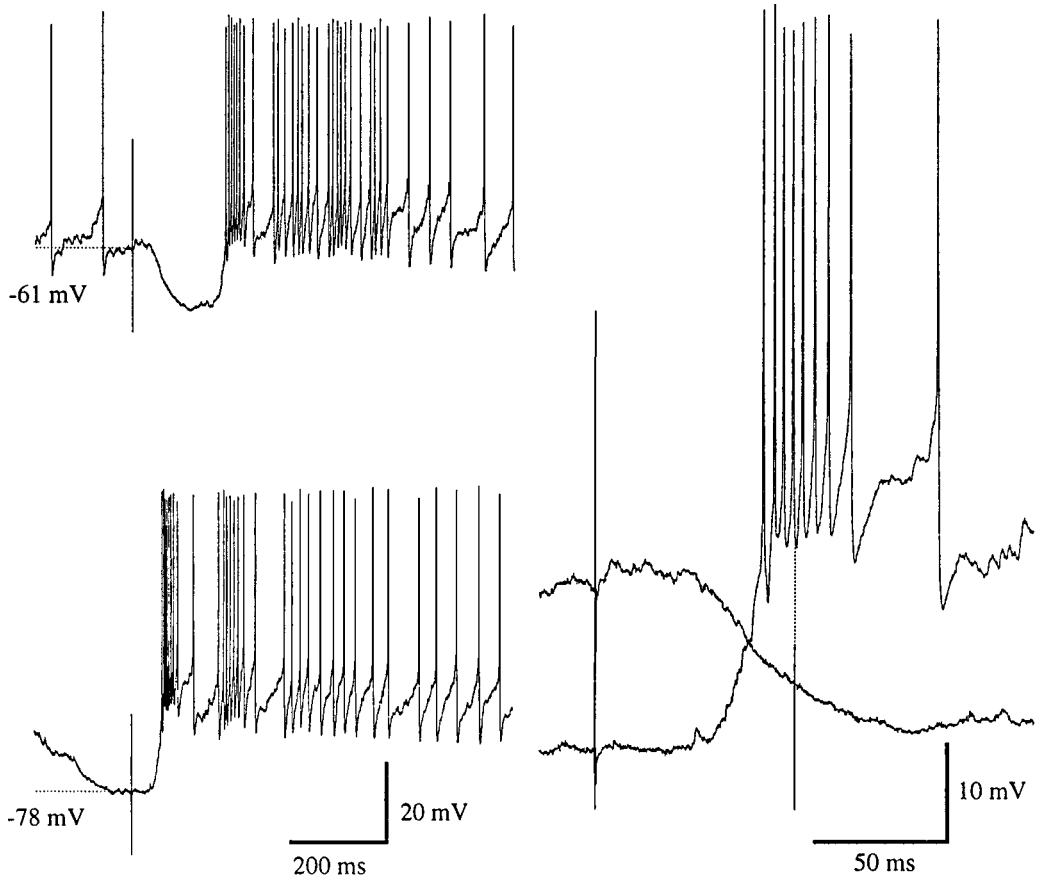
-61 mV
-78 mV
20 mV
200 ms
10 mV
50 ms

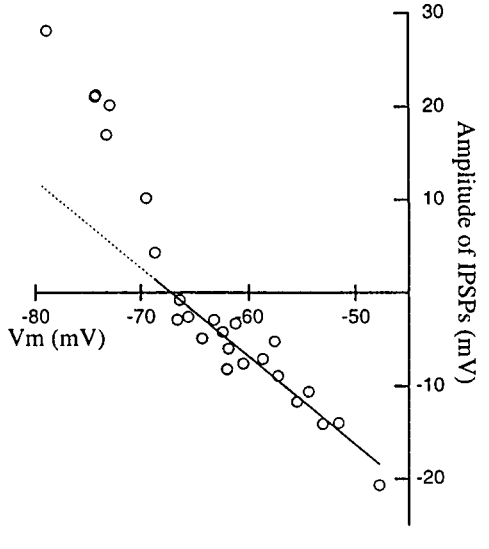
30
20
10
-10
-20
-80
-70
-60
-50
Vm (mV)
Amplitude of IPSPs (mV)

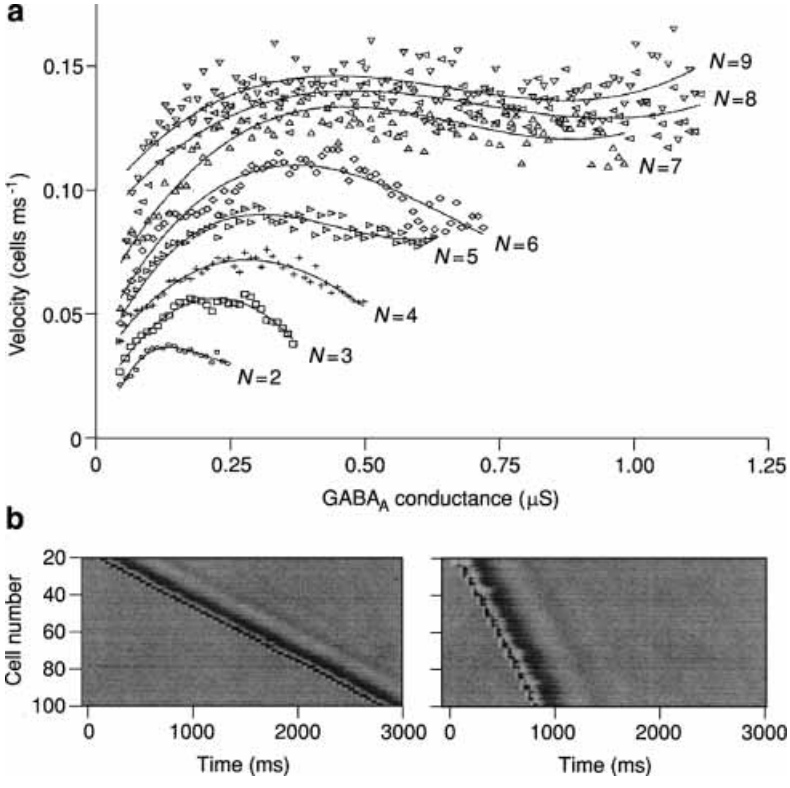

Fig. 3.9 Velocity of the traveling wave as a function of $GABA_A$ receptor coupling strength and radius of RE-RE connections in a one-dimensional RE network model. (**a**), velocity of propagation as a function of $GABA_A$ conductance. N is the radius of connections. For $N > 6$ and $g_{GABAA} > 0.2$ μS, the speed of propagation showed only a weak dependence on $GABA_A$ receptor coupling and radius of RE-RE connections. The solid curves are the non-linear fits of the calculated data (indicated by different symbols). (**b**) Localized activity propagating with different speed: $g_{GABAA} = 0.1$ μS, $N = 2$ (left) and $g_{GABAA} = 0.4$ μS, $N = 7$ (right). From Bazhenov et al. (1999).

Fig. 3.8 (opposite) Reversed IPSPs in a thalamic reticular (RE) neuron *in vivo* directly triggers a low-threshold spike (LTS). Cat under ketamine-xylazine anesthesia, with intact thalamocortical connections. *Top*, responses of an RE neuron to stimuli applied to the thalamic ventrolateral (VL) nucleus. At a relatively depolarized membrane potential (V_m) (−61 mV), low-intensity thalamic stimuli evoked an IPSP-rebound sequence. When the stimulus (same parameters) occurred during the hyperpolarizing phase of the slow oscillation, the IPSP reversed and (at −78 mV) directly triggered an LTS crowned by a spike-burst. The latency of the LTS was in the range of 40–50 ms. The early parts of two responses (at −61 mV and at −78 mV) are enlarged on the right. *Bottom*, the amplitude of the postsynaptic response, measured 75 ms after the stimulus, is plotted against V_m. The IPSP depended linearly on V_m from depolarized levels to the reversal potential (−68 mV); thereafter, the depolarizing IPSPs directly activated the LTS, which added a depolarizing deflection to the linear function (solid and dotted lines). From Bazhenov et al. (1999).

in a subset of RE cells (see note [110]). In rats, plasma membranes of dendritic bundles and of contiguous somata are commonly observed in direct contact, but gap junctions have not yet been detected [110].

The effect of RE-cells' spike-bursts on TC neurons is illustrated above (Fig. 3.7). It consists of IPSPs that de-inactivate LTSs followed by spike-bursts transferred to cortex. Although virtually all thalamic neurons possess the intrinsic neuronal property of firing spike-bursts after prolonged and/or deep enough hyperpolarizations, both *in vitro* and *in vivo* (see Chapter 2), not all thalamic nuclei display spindles. The LTS-generated spike-bursts have the same characteristics in anterior thalamic neurons as found in other thalamic neurons [111]. However, as cat anterior thalamic neurons do not receive synaptic inputs from the RE nucleus [112] (Fig. 3.10) and the RE nucleus is the spindle pacemaker (see above), spindles are absent from anterior thalamic nuclei (Fig. 3.10) as well as from limbic cortical areas where these nuclei project [111]. A similar case is that of lateral habenular neurons that have intrinsic properties similar to those of TC neurons [113] but the absence of inputs from the RE nucleus explains the absence of spindles in those neurons that, instead, display fluctuations within the frequency range of the theta rhythm, generated in the hippocampus.

These data show the importance of connections with the pacemaker RE nucleus for the induction of spindle oscillations and the fact that activities in long-range synaptic networks, rather than intrinsic properties, may generate different types of brain rhythms.

3.2.1.2. Neocortex governs spindle synchronization

The generation of spindles does not depend on the cerebral cortex, as this oscillation was recorded in thalamus of decorticated animals [114] and in thalamic slices [101, 115], but cortical volleys act as the most powerful trigger for spindle induction in the thalamus [116] and, importantly, the presence of neocortex is necessary for the long-range synchronization of spindles [117]. Indeed, while spindles sequences propagate in slices from visual thalamus [118], spindling is nearly simultaneous throughout the thalamus and the cortex in intact-brain animals and humans (Fig. 3.11) [117]. Following decortication, spindle sequences are no longer simultaneous in the thalamus (Fig. 3.11) [117] without, however, displaying propagation as in slices.

These contrasting results between *in vivo* and *in vitro* experiments are, of course, due to the absence of cortex in thalamic slices (Fig. 3.12). The role of the cortex in the long-range synchronization of spindles was also demonstrated by showing a diminished

[110] Ohara and Lieberman (1985). Recent studies, using current-clamp recordings from pairs of neurons in rats and mice, revealed that electrical synapses play a role in mediating neuron-to-neuron communication in slices from thalamic RE nucleus (Landisman et al., 2002). Electrical synapses were absent in mice with a null mutation for the connexin36 gene. Puzzlingly, however, inhibitory chemical synapses, as revealed in virtually all *in vivo* and *in vitro* studies on RE neurons, were not at all detected in this recent study. The authors (Landisman et al., 2002) recognized that their "limited testing protocol may have missed synaptic events of low probability", that "it seems very likely that inhibitory synaptic connections within the (RE nucleus) exist", and that their results are valid for "at least a subset of (RE) cells" (p. 1007).

[111] Mulle et al. (1985); Paré et al. (1987).

[112] Steriade et al. (1984); Velayos et al. (1989).

[113] Wilcox et al. (1988).

[114] Morison and Bassett (1945).

[115] Bal et al. (1995a-b); Jacobsen et al. (2001).

[116] That synchronous cortical stimuli produce spindles in the thalamus, which are fed back to cortex, was observed with both artificial (electrical) and natural (sleep-related) volleys. To avoid antidromic activation of thalamocortical axons and axon-reflex excitation of thalamic RE neurons, thalamic spindles were elicited from the contralateral cortex (Steriade et al., 1972). This involved the callosal and corticothalamic pathways. (Steriade et al., 1974b; Cissé et al., 2003). On the other hand, the synchronous firing of cortical neurons during the slow sleep oscillation sets into action the thalamic neuronal equipment and, thus, a brief sequence of spindles is seen after each cycle of the slow oscillation (Contreras and Steriade, 1995; Timofeev and Steriade, 1996; see ***3.2.3***).

[117] Contreras et al. (1996a, 1997a). The quasi-simultaneity of spindle sequences over widespread cortical areas in humans was also reported using a new method of low-resolution brain electromagnetic tomography (Anderer et al., 2001; see Fig. 2 in that paper).

[118] Kim et al. (1995).

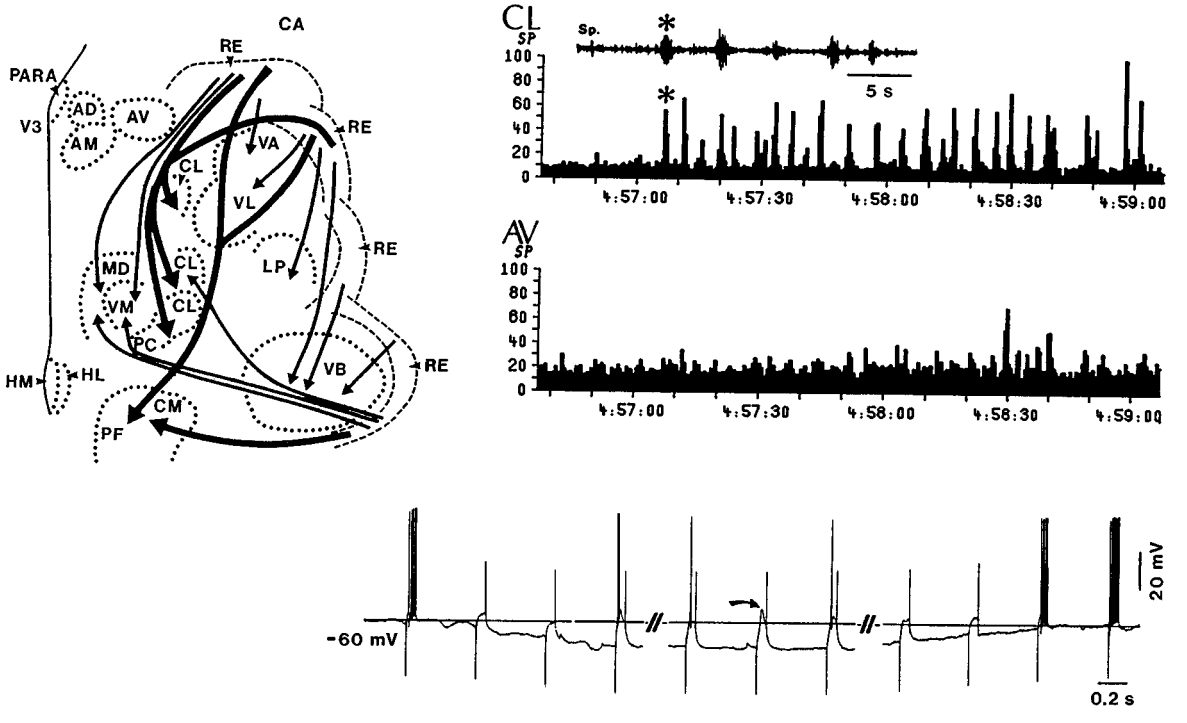

Fig. 3.10 Anterior thalamic (AT) nuclei of cat are devoid of afferent from the RE nucleus and, despite the fact that the intrinsic property of LTS is present in AT neurons, they do not display spindles because there are no synaptic connections from the pacemaking RE nucleus. *Left diagram* summarizes the RE projections to various dorsal thalamic nuclei, as resulting from retrograde tracing experiments in cats. Heavy lines indicate prominent projections to intralaminar nuclei. Note absence of projections to AT nuclei. Abbreviations are as follows: AD, AM and AV, anterodorsal, anteromedial and anteroventral nuclei; CA, caudate nucleus; CL-PC, central lateral and paracentral (rostral intralaminar) nuclei; CM-PF, centre median-parafascicular (caudal intralaminar) nuclei; HM, HL, medial and lateral habendula; LP, lateral posterior nucleus; MD, mediodorsal nucleus; PARA, paraventricular nucleus; VA, ventroanterior nucleus; VL, ventrolateral nucleus; VM, ventromedial nucleus; VB, ventrobasal complex; RE, reticular nucleus; V3, third ventricle. *Right part* depicts simultaneous recordings of field potentials (filtered for spindles, *SP*, between 7 and 14 Hz) from CL and AV nuclei in cat. Unanesthetized *cerveau isolé* (collicular-transected) preparation. Abscissae indicate real time (h, min, s). Data were obtained by applying each filtered EEG signal (see above CL trace, filtered EEG spindles, the first sequence corresponding to the one depicted below) to a full-wave rectifier, a voltage-controlled oscillator, and to a laboratory computer (see technical details in that paper). Note regularly recurring spindle sequences in CL nucleus and absence of spindles in the AV nucleus. *Below*, intracellular recording of an AT neuron, showing tonic firing at a relatively depolarized V_m (−60 mV), LTSs crowned by spike-bursts under steady hyperpolarization when the V_m reached −72 mV, and recovery of tonic firing at −60 mV. Modified from Steriade et al. (1984) and Paré et al. (1987).

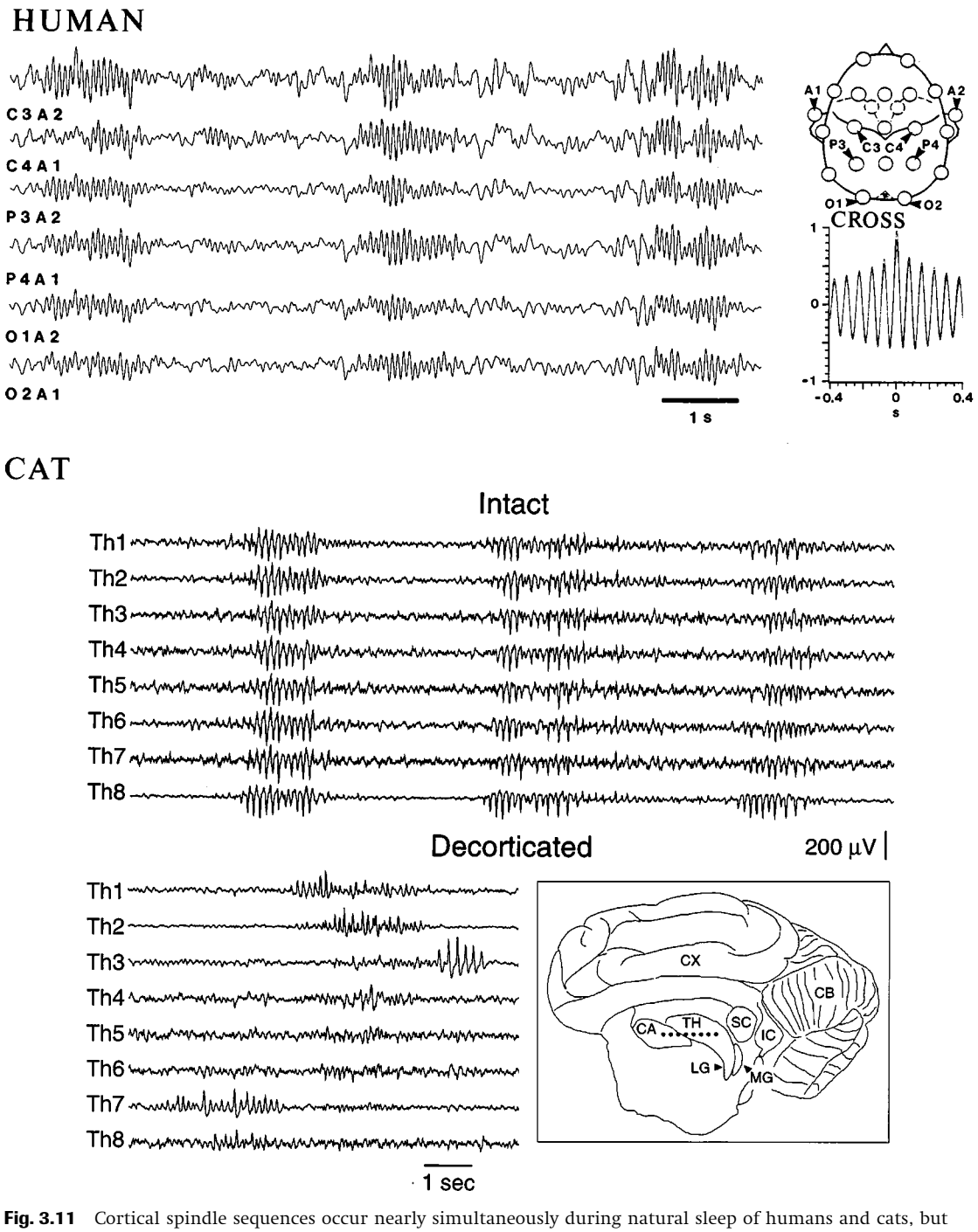

Fig. 3.11 Cortical spindle sequences occur nearly simultaneously during natural sleep of humans and cats, but decortication disorganizes the widespread coherence of thalamic spindles. In the *top panel* illustrating natural sleep in *HUMAN*, spindles were recorded from six standard EEG derivations (indicated in the schematic on the right, arrowheads) in a normal subject, during stage 2 sleep. Cross-correlations of individual spindle sequences ($n = 15$) were calculated between C3A2 and each one of the other channels. Averaged correlations (*CROSS*) showed rhythmicity at 14 Hz and central peak values between 0.7 and 0.9. *Below*, spindles were simultaneously recorded from seven leads in the thalamus of intact-cortex cat under barbiturate anesthesia. Note the virtual simultaneity of spindle sequences. After decortication (see scheme), recordings from the same thalamic sites showed disorganization of spindle simultaneity. Abbreviations are as follows: CA, caudate nucleus, CB, cerebellum; CX, cortex; IC, inferior colliculus; LG, lateral geniculate; MG, medial geniculate; SC, superior colliculus; TH, thalamus. Modified from Contreras et al. (1996a, 1997a).

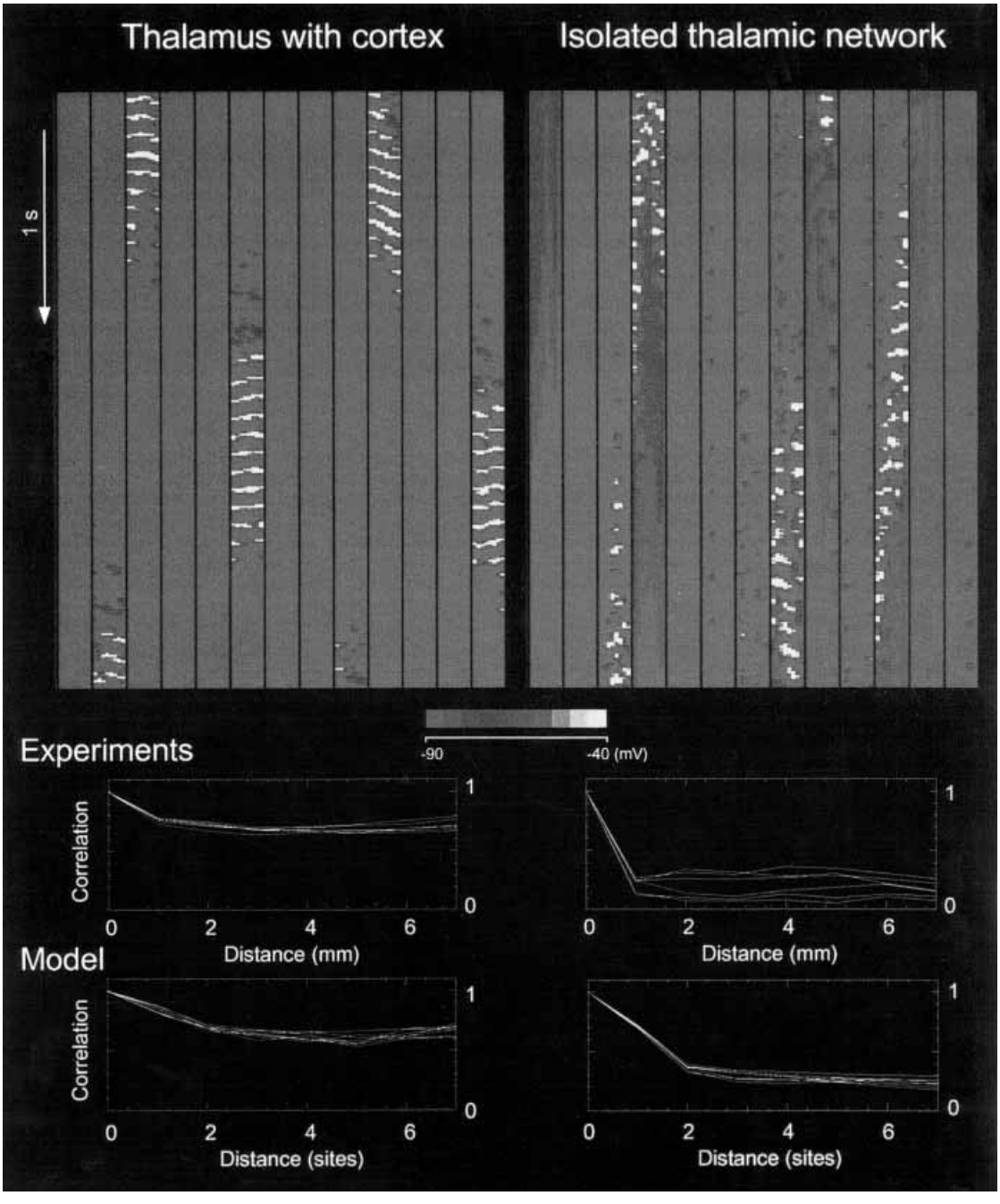

Fig. 3.12 Presence of cortical feedback determines spatiotemporal coherence of spindle oscillation in experiments and models of thalamocortical networks. *Top*, spatiotemporal maps were constructed from local thalamic averages of spontaneous spindles in the presence of cortex (left) and in an isolated thalamic network, with the same parameters (right). Each frame consisted of a horizontal stripe of 8 color spots representing the membrane potential of thalamic averages (see Fig. 5 in that paper). Frames were arranged from top to bottom in 13 columns (a total of 40 s of activity is shown). Colors ranged in 10 steps from –90 mV or below (blue) to –40 mV or above (yellow; see color scale). *Bottom*: decay of correlations with distance. Cross-correlations were computed for all possible pairs of sites and value at time zero from each correlation was represented as a function of intersite distance. Experiments: decay of correlations of thalamic local field potentials in intact (left) and decorticate (right) cats under barbiturate anesthesia. Model: decay of correlation calculated for local averaged potentials in the presence of cortex (left) and in isolated thalamic network (right). Modified from Destexhe et al. (1998). See Plate section for color version of this figure.

[119] Contreras et al. (1997b).

[120] Destexhe et al. (1998, 1999a).

[121] Steriade (2001c).

[122] Golshani et al. (2001); Liu et al. (2001).

[123] Gottselig et al. (2001). Brain-damaged patients with thalamic lesions were excluded.

[124] Bal and McCormick (1996); Lüthi and McCormick (1998).

[125] The hypothesis of spindle disruption by network desynchronization was first formulated by Andersen and Andersson (1968): "After the system has been brought into a rhythmic behavior, it will continue to operate rhythmically for a certain time because of the similarity of the participating neurons and the simultaneity of the powerful inhibition in many neurons. However, the stable rhythmicity cannot be maintained indefinitely. . . . The main reason for the disruption of the rhythm is the slightly different duration of the IPSPs of the participating cells . . . One of the neurons is firing prematurely . . . (and) this neuron recruits a number of cells to its rhythm. Consequently, a small number of cells surrounding the partisan cell is in an inhibited stage when the main group of cells fires as a rebound effect . . ." (p. 132–134; and Fig. 10.5 in that monograph, from a previous paper by Andersen and Sears, 1964). In this hypothesis, the inhibitory elements were thought to be local-circuit interneurons driven by recurrent collaterals of thalamocortical axons. Such intra-nuclear phasing does not exist in dorsal thalamic nuclei, as (with the possible exception of the lateral geniculate nucleus) intracellular staining of thalamocortical cells showed that their axons do not deliver collaterals in the nucleus where the neuron is located (Steriade and Deschênes, 1984; Jones, 1985) but in the thalamic RE nucleus. Instead of intrinsic interneurons, the progenitors of inhibition and pacemakers of spindling are RE neurons [97, 98]. Moreover, the participation of local-circuit inhibitory neurons in spindling is ancillary.

spatiotemporal coherence of spindle oscillations during barbiturate anesthesia, when corticothalamic neurons display poor spontaneous activity, as well as during cortical depression produced by applying a highly concentrated potassium acetate solution [119]. Experiments and modeling studies showed that the simultaneity of oscillations is increased and the phase shift is reduced by increasing the activity of corticothalamic neurons that lead to inhibition of TC neurons via RE neurons [120] (Fig. 3.13). This indicates that corticothalamic feedback produces a large-scale coherent activity by recruiting thalamic circuitry through prevalent projections to RE nucleus [121]. Studies combining electron microscopy and analysis of EPSCs quantified the much greater efficacy of corticothalamic projections acting on GABAergic RE neurons, compared to the cortical projection to TC neurons [122], thus eventually leading to inhibition of the latter. This action is not only effective for the widespread synchronization of sleep spindles, but it also explains the inhibition of most TC neurons throughout cortically generated spike-wave seizures (see Chapter 5).

The role of corticothalamic projections in the long-range synchronization of thalamically generated spindles was recently analyzed in humans by comparing control subjects and patients with damaged cortex during different phases following hemispheral stroke [123]. These findings provided evidence showing that patients with damaged cortex display significantly reduced spindle coherence spectra from derivations ipsilateral to the lesion, thus supporting the results of experimental studies with intact and decorticate cats [117].

In addition to their role in the widespread synchronization and near-simultaneity of spindle sequences, corticothalamic neurons are operational in the process of terminating spindle sequences. *In vitro* studies have investigated the role of the hyperpolarization-activated depolarizing (cation) current (I_H) and have shown that spindles are terminated by Ca^{2+}-induced up-regulation of I_H in TC neurons [124]. Another factor that may account for the termination of individual spindle sequences is the different duration of IPSPs in TC neurons that participate in spindles, with the consequence of different times at which postinhibitory rebound spike-bursts are fired, so that the synchrony in the whole thalamic circuit is disrupted and spindles are terminated. This earlier hypothesis [125] did not consider the role of neocortex in the induction and synchronization process of spindles. Recently, we investigated *in vivo* the extreme variability of LTSs generated in the same neuron, by using threshold hyperpolarizing current pulses (Fig. 3.14*A*). The same intrinsic variability of LTSs can be seen during spindles

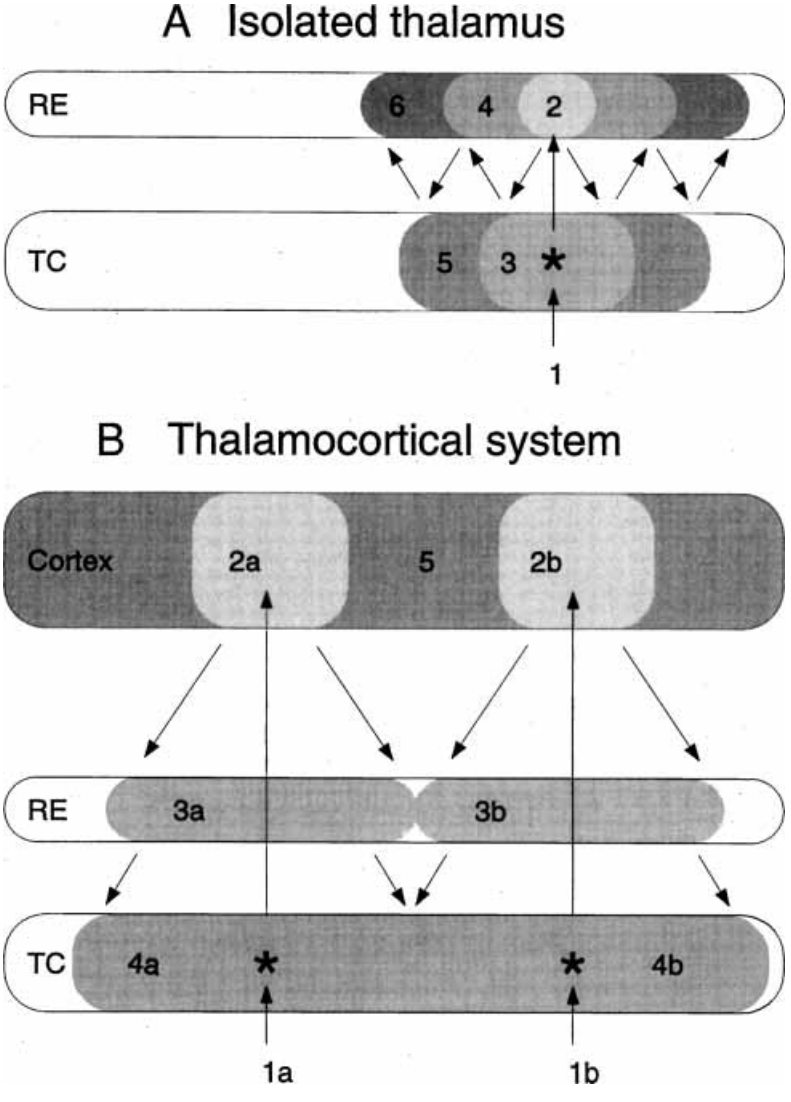

Fig. 3.13 Mechanisms of large-scale synchrony in thalamocortical systems. *A*, synchronization mechanisms in isolated thalamus following a mutual recruitment of thalamocortical (TC) relay cells and thalamic reticular (RE) cells. From an initial discharge of a TC cell (1; *), a localized area is recruited (2), which in turn recruits a larger area of TC cells (3), etc. Progressively larger areas of the thalamus are recruited at each successive cycle (4, 5, 6, . . .) through topographic structure of connectivity. An array of electrodes in a thalamic slice, deprived of cortex, would record the propagation of spindles (Kim et al., 1995). *B*, postulated recruitment mechanism in the presence of cortex. Two approximately simultaneous initiation sites in the thalamus (1a, 1b) recruit localized cortical areas (2a, 2b), which in turn recruit connected sectors of RE nuclear complex (3a, 3b), which in turn recruit larger territories of thalamocortical neurons (4a, 4b), and so forth. At the next cycle, the entire cortical area is recruited (5). In this case, corticothalamic connections supersede "private" thalamic recruitment mechanisms shown in *A* and oscillations reach a state of large-scale synchrony within a few cycles, consistent with the simultaneous spindling over widespread cortical and thalamic territories seen *in vivo* (Contreras et al., 1996a, 1997a). Modified from Destexhe et al. (1998).

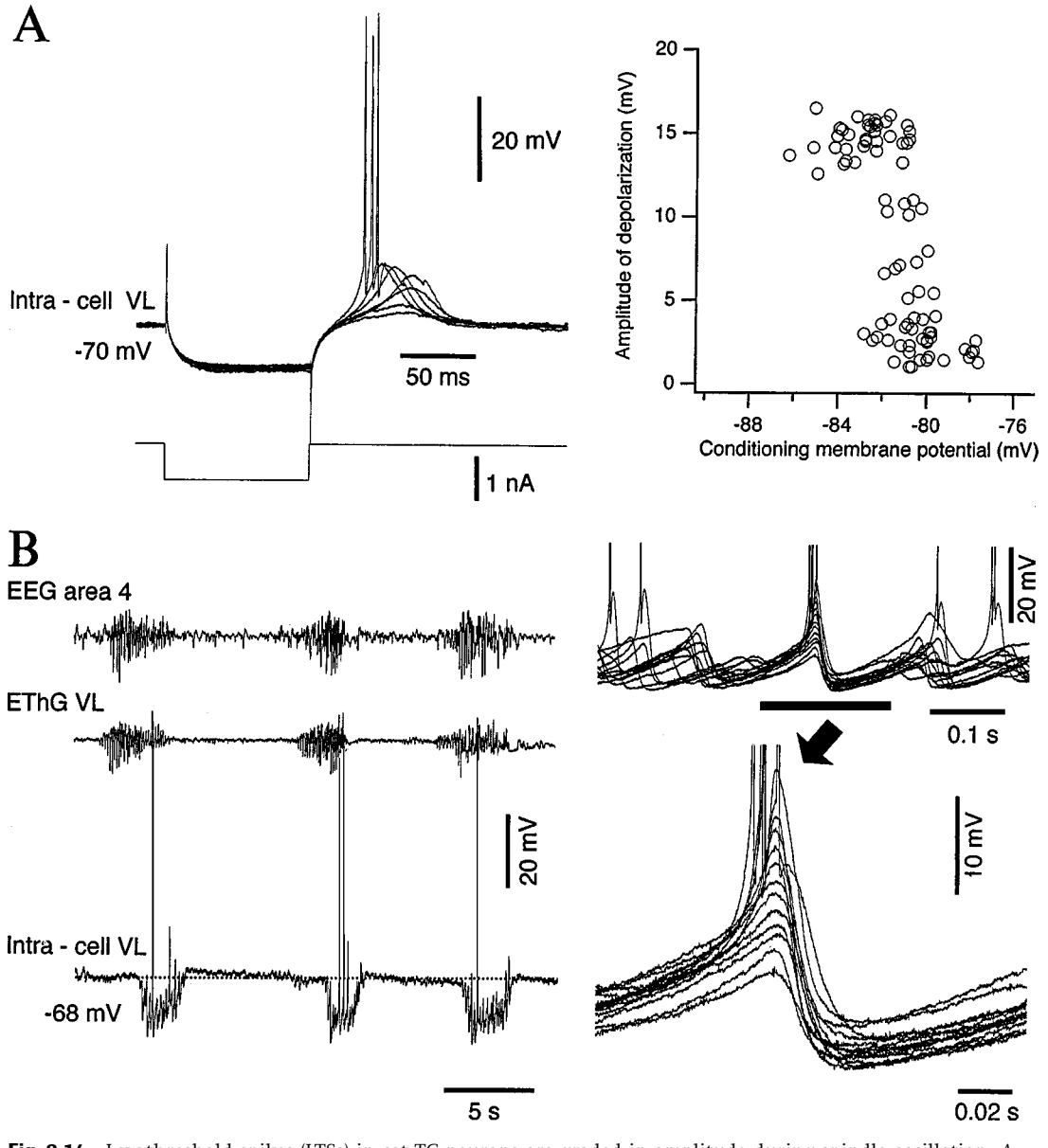

Fig. 3.14 Low-threshold spikes (LTSs) in cat TC neurons are graded in amplitude during spindle oscillation. *A*, ketamine-xylazine anesthesia. Intracellular recording from the thalamic ventrolateral (VL) nucleus. Fluctuations in time-to-peak and amplitude of LTS at the break of the threshold hyperpolarizing current pulse (−0.8 nA, 0.1 s). Plot on the right: conditioning V_m is the V_m just before the end of the current pulse; amplitude of maximal depolarization was calculated from baseline V_m. *B*, barbiturate anesthesia. Simultaneous field potential from cortical area 4 and VL nucleus, together with intracellular recording from VL nucleus. *Right*, an expanded spindle sequence, further expanded below (arrow). Modified from Timofeev et al. (2001a).

[126] Steriade et al. (1998b).

[127] Timofeev et al. (2001a).

[128] Contreras and Steriade (1996); Timofeev and Steriade (1996).

(Fig. 3.14*B*). As a consequence of the asynchronous burst firing of TC neurons, the membrane potential of their targets, RE neurons, would be kept at a relatively depolarized level, thus preventing the de-inactivation of the low-threshold Ca^{2+} current and diminishing firing probability in RE neurons. Probably, the most important source of spindle desynchronization is corticothalamic input, for the following reasons. *(a)* Slightly depolarized fast-rhythmic-bursting (FRB) neurons (see Chapter 2, ***2.1.1***), whose projections to thalamus were identified by antidromic invasion, discharge non-accommodating spike-trains throughout a spindle sequence [126]. Such bursting neurons may also recruit other cortical neurons into a state that may be out-of-phase with thalamic neurons. *(b)* During the late phase of spindles, neocortical neurons become tonically depolarized, eventually leading to firing (Fig. 3.15*A*), and spike-triggered averages by cortical neurons do not reveal a phase relationship between cortical and TC neurons. Thus, this depolarization of cortical neurons toward the end of spindle sequences is maintained by intrinsic currents and synaptic activities in intracortical networks.

The idea that the corticothalamic input, which is predominant during the late part of a spindle sequence, is effective in desynchronizing thalamic networks and terminate spindles [127] was tested in a model that included four layers of neurons: RE, TC, cortical pyramidal (PY), and cortical local interneurons (IN). The RE-TC isolated network oscillated infinitely and up-regulation of I_{H} alone was not sufficiently strong to terminate spindling. With the addition of the corticothalamic feedback, the spindles in the RE-TC network were short (Fig. 3.15*B*), resembling the exclusively waning spindle sequence (lacking the initial waxing component) that is observed after a highly synchronous cortical volley during the slow sleep oscillation because, in this case, most of thalamic neurons are set into action from the onset of the spindle [128].

To sum up:

(a) The first part of a spindle sequence is generated in the pacemaker RE nucleus [98].

(b) During the first two to four IPSPs composing the spindles, TC neurons do not display rebound spike-bursts (see Figs. 3.7 and 3.15*C*), thus they do not return signals to RE neurons and do not contribute to this phase of a spindle sequence.

(c) The middle part of a spindle sequence is due to the activity in the RE-TC-RE loop [101, 102].

(d) The termination of spindles is due to the depolarizing action of I_H and/or the depolarizing action of corticothalamic neurons [124, 127].

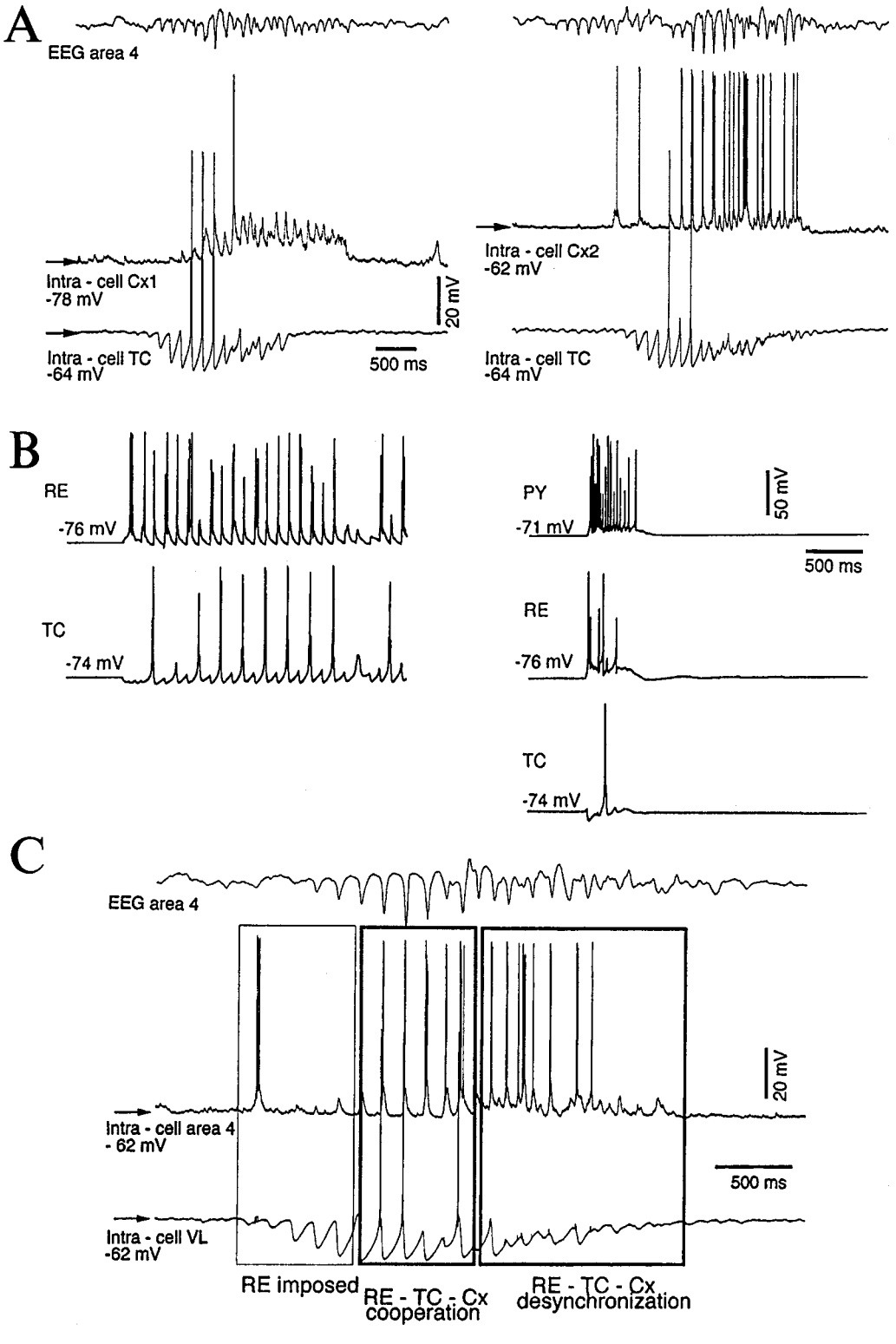
A
EEG area 4
Intra - cell Cx1
-78 mV
20 mV
Intra - cell TC
-64 mV
500 ms
Intra - cell Cx2
-62 mV
Intra - cell TC
-64 mV
B
RE
-76 mV
TC
-74 mV
PY
-71 mV
50 mV
500 ms
RE
-76 mV
TC
-74 mV
C
EEG area 4
20 mV
Intra - cell area 4
- 62 mV
500 ms
Intra - cell VL
-62 mV
RE imposed
RE - TC - Cx
cooperation
RE - TC - Cx
desynchronization

[129] Hallanger et al. (1987); Paré et al. (1988); Smith et al. (1988); Raczkowski and Fitzpatrick (1989).

[130] Steriade et al. (1987b); Parent et al. (1988).

[131] Hallanger and Wainer (1988).

[132] Asanuma (1989).

[133] Asanuma and Porter (1990); Asanuma (1997).

3.2.1.3. Permissive factors for development of spindles at sleep onset

Spindles appear as a consequence of diminished firing rates, at sleep onset, of activating neurons, some of them cholinergic, located in the upper brainstem (Fig. 3.16) and basal forebrain (Fig. 3.17) [85]. This effect is mainly due to the removal of cholinergic inhibition exerted on pacemaking RE neurons.

Brainstem cholinergic neurons project to the rostrolateral part and perigeniculate sector of the thalamic RE nucleus [129]. Cholinergic as well as noncholinergic afferents arising in basal forebrain aggregates also project to the rostral sector of RE nucleus [130]. The afferent cholinergic fibers (which could be of brainstem and/or basal forebrain origin) are very small (<0.25 μm), with spherical vesicles and asymmetrical synaptic contacts onto distal dendritic profiles of RE neurons, and form no axo-axonic contacts, thus precluding a presynaptic cholinergic effect upon thalamo-RE or cortico-RE terminals [131]. The terminals of brainstem cholinergic axons on distal dendrites of rostrolateral RE neurons contrast with the more often perisomatic location of axons originating in the basal forebrain [132]. Because less than 25% of basal forebrain neurons projecting to the cat's RE nucleus are cholinergic and because of the numerous GABAergic elements in substantia innominata and diagonal band nuclei [130], we hypothesized that the majority of basal forebrain projections to the rostral pole of the RE nucleus arise in GABAergic cells. This was demonstrated by combining the retrograde labeling of nucleus basalis neurons with their immunoreactivity to GABA [133].

Both ACh and GABA are powerful inhibitors of RE neurons [56]. This explains the permissive role of both brainstem and basal forebrain systems in spindle genesis (Figs. 3.16 and 3.17) and the powerful inhibition of spindles, with hyperpolarization of RE neurons, by stimulating cholinergic neurons at the mesopontine junction

Fig. 3.15 (opposite) Role of corticothalamic input in terminating thalamic spindle sequences. Cats under barbiturate anesthesia and computational model. *A*, two cortical neurons (left and right), impaled successively, were recorded intracellularly simultaneously with the same thalamocortical (TC) neuron. Note depolarizing plateau in the cortical neuron during the late part of the spindle; this depolarization as well as the cortical EEG spindle outlast the termination of spindles in the TC neuron. *B*, model of thalamic network. *Left*, thalamic network disconnected from the cortex. Weak I_H up-regulation was not strong enough to terminate the spindle, which continued infinitely. *Right*, intact thalamocortical system. Activity patterns in the pyramidal-interneuronal (PY-IN) network were maintained by PY-PY excitation and persistent Na^+ current. Corticothalamic input depolarized RE and TC neurons and terminated spindle oscillation after a few cycles. *C*,three phases of a spindle sequence. Dual intracellular recording of cortical and TC neurons. The initial phase is imposed by a pacemaking RE network. During the middle phase of the spindle, the activity of cortical, RE and TC neurons is phase-locked. At the end of spindles, cortical firing induces depolarization of both RE and TC neurons, which creates conditions for spindle termination. Modified from Timofeev et al. (2001a).

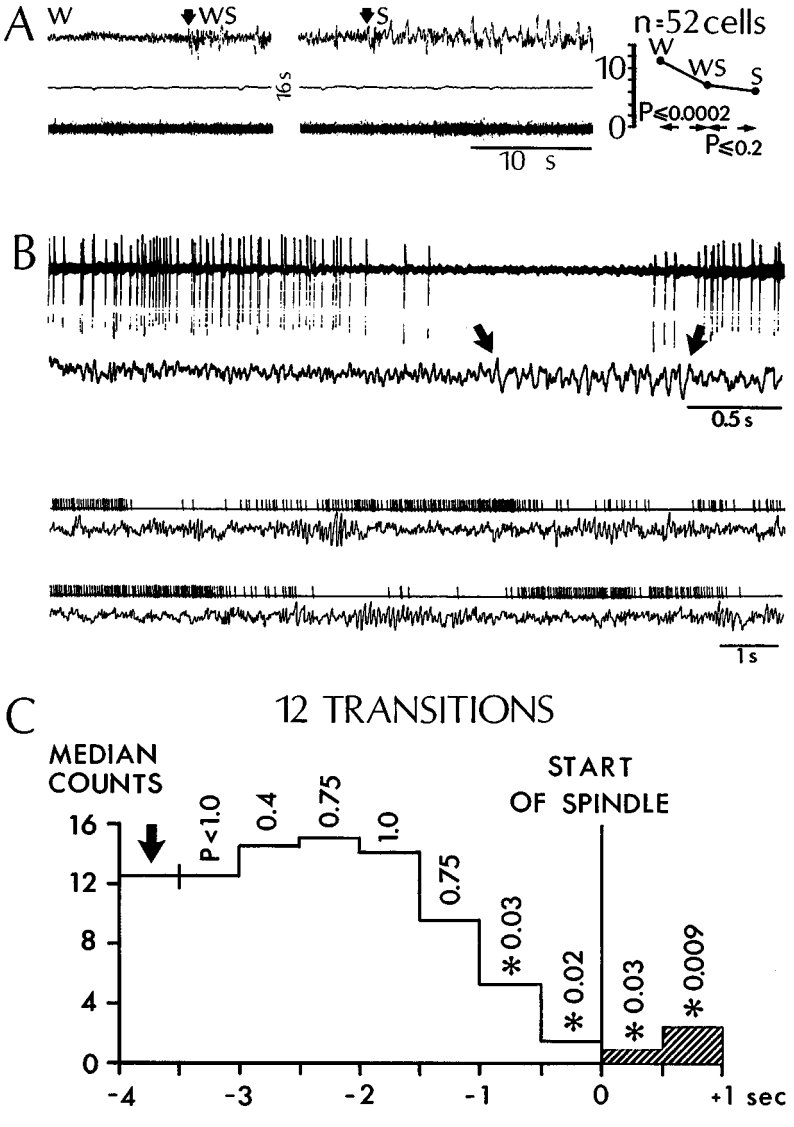

Fig. 3.16 Firing rates of midbrain reticular formation (MRF) neurons decrease in advance of the first electrographic signs during transition from waking (W) to slow-wave sleep (S), and decreased firing rates in these neurons precede the appearance of spindles. *A*, electrographic criteria of the transitional state from W to S (WS). Graph shows median firing rates in a sample of 52 MRF neurons during the W, WS, and S states; note that the major and significant decrease in firing rate occurs from W to WS. *B*, neuron antidromically identified from the intralaminar thalamus. Top two traces: original spikes and EEG waves simultaneously displayed on the oscilloscope. Note the decreased firing rate, leading to neuronal silence, before the first EEG spindle sequence (between arrows) during the transition from W to S. Bottom: same activities during repeated EEG activation-synchronization transitions. *C*, 12 such transitions of unit firing with respect to the start of EEG spindle (time 0). A significantly decreased firing rate occurred 1 s before spindle onset. Modified from Steriade (1984).

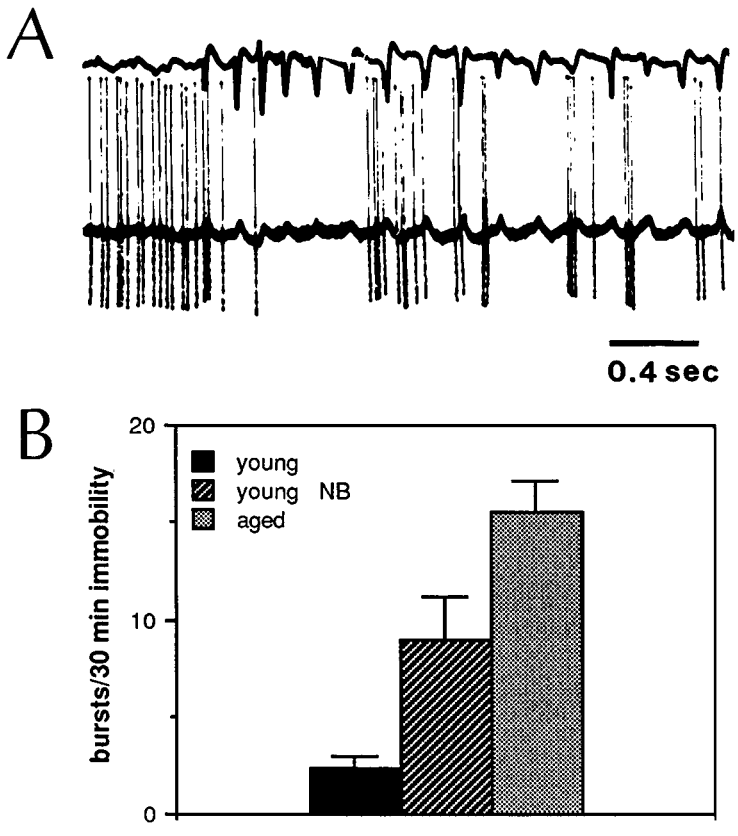

Fig. 3.17 Nucleus basalis (NB) control of thalamocortical rhythmicity in chronically implanted rats. *A*, epidural recording of neocortical EEG during immobility and extracellular recording from NB neuron. Note sudden drop in discharge frequency coinciding with the onset of neocortical spindle. *B*, number of spindles in 30-min immobility epochs in young (4–8 months) control rats, in young rats with bilateral damage to the NB, and in intact aged rats with shrunken cholinergic NB neurons. Modified from Buzsáki et al. (1988b).

(Fig. 3.18). The role of ACh in blocking spindles at their very site of genesis, the RE nucleus, is corroborated by microdialysis studies showing that the decrease of ACh in the brainstem during halothane anesthesia is associated with the increase in spindle activity, by releasing the RE neurons from cholinergic inhibition [134].

[134] Keifer et al. (1994). It is interesting to note that, whereas halothane increases spindles, it reliably stops seizures with spike-wave (SW) complexes. This is another argument against the idea that SW seizures evolve from mechanisms similar to those generating spindling (see Chapter 5).

[135] Hirsch et al. (1983).

3.2.1.4. Disconnecting effects of spindles on incoming signals

The transfer of information from the outside world to the cerebral cortex is prevented throughout the state of SWS because TC cells are hyperpolarized by 7–10 mV during this sleep state [135] and afferent stimuli can hardly produce an EPSP to reach firing threshold.

[136] Deschênes et al. (1984).

[137] Steriade (1991). These data, emphasizing that the decreased transfer of information during resting sleep is not detected within relay stations prior to the thalamus (see also Steriade et al., 1969), are consistent with the effects of brainstem reticular stimulation or natural awakening upon responses of various sensory and motor thalamic nuclei. Indeed, the enhancing effects of mesencephalic reticular stimulation on photically evoked potentials in the lateral geniculate nucleus are not accompanied by potentiating influences upon the responses recorded simultaneously from the optic tract (Steriade and Demetrescu, 1960). In support of these data, lateral geniculate neurons follow the changes in sine-wave photic stimulation very closely during waking, such relation is lost during EEG-synchronized sleep, and no fluctuations are seen in retinal ganglion cells during shifts in the state of vigilance (Maffei et al., 1965). Similarly, the evoked activity of neurons in prethalamic somatosensory relays is unchanged with transition from waking to EEG-synchronized sleep (Carli et al., 1967). Recent data showed differential processing of information through the thalamus between low-frequency and fast signals (Castro-Alamancos, 2002a-b).

[138] Hubel (1960).

[139] Steriade (1970).

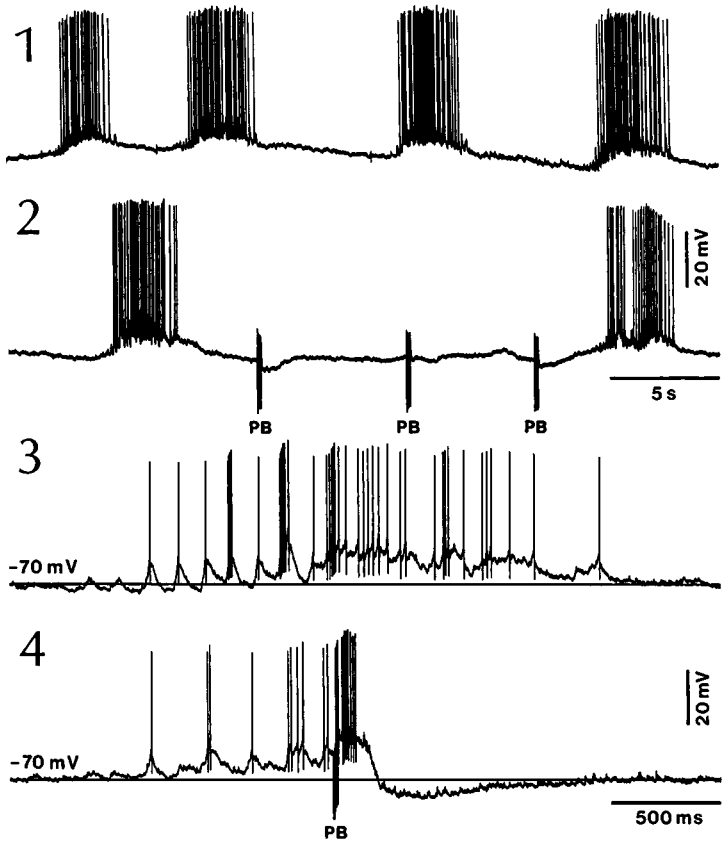

Fig. 3.18 Blockage of spindle oscillations in the thalamic reticular (perigeniculate) neuron by stimulation of the peribrachial (PB) cholinergic area at the mesopontine junction. Unanesthetized, deafferented (brainstem-transected) cat. *1–2*, rhythmic sequences of spontaneously occurring spindles were prevented by stimulation of PB area. Traces in *1–2* are continuous. A spindle sequence is expanded in *3*, and in *4* another sequence was aborted by PB stimulation. Modified from Hu et al. (1989a).

The fact that evoked potentials can be recorded in cortex during SWS is due to the fact that, at given levels of hyperpolarization (−70 to −75 mV), the LTS of TC neurons is de-inactivated and promotes burst firing [96]; however, these responses are stereotyped, they do not reflect the frequency code of stimuli with various intensities, do not follow rapid repetition of stimuli (because of the long, 150–270 ms, refractory period of the LTS), and thus are quite different from those recorded during the adaptive state of wakefulness.

Although thalamic responsiveness is globally decreased throughout SWS, due to the hyperpolarization of TC cells, gating of incoming signals is most effective during epochs in which spindles are present because this oscillation is built-up by prolonged IPSPs,

[140] Steriade et al. (1971); Glenn and Steriade (1982).

[141] Timofeev and Steriade (1997).

[142] Elton et al. (1997).

[143] Event-related-potentials (ERPs) are used to monitor information processing in awake and sleeping subjects. They consist mainly of a long-latency "vertex" complex, with three major waves, P1-N1-P1 at peak latencies of 0.05, 0.1, and 0.2 s.

[144] Hansen and Hillyard (1980).

[145] Winter et al. (1995).

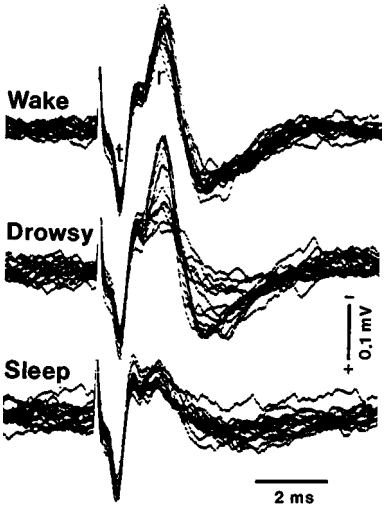

Fig. 3.19 Blockade of synaptic transmission in the thalamus at sleep onset in the behaving cat. Field potentials evoked in the thalamic ventrolateral (VL) nucleus by stimulation of cerebello-thalamic axons. Note progressively diminished amplitude of the monosynaptically relayed (*r*) wave during drowsiness, up to its complete disappearance during full-blown sleep, in spite of the lack of changes in the afferent volley monitored by the presynaptic (tract, *t*) component. Modified from Steriade (1991).

with increased membrane conductance, in TC neurons. The spindle-related hyperpolarizations of TC neurons can be reversed in sign by current and Cl^- injections [136], thus indicating that they mainly consist of IPSPs imposed by GABAergic RE cells. The thalamus is the first relay structure where blockage of afferent signals occurs from the very onset of sleep, during drowsiness, despite the fact that the magnitude of the presynaptic volley is unchanged, thus showing that no significant changes are seen prior to the thalamus [137] (Fig. 3.19). The presence of high-frequency bursts in thalamic neurons during sleep, contrasting with absence of changes in discharge patterns in prethalamic axons with passage from waking to sleep [138], further indicates that the inhibitory processes responsible for the high-frequency bursts and associated with spindling are intrathalamic. The generalized inhibition of responsiveness in all tested thalamic nuclei [139] suggests that it mostly depends on GABAergic RE thalamic neurons with widespread thalamic projections. The lower excitability of soma during SWS is shown by the decreased probability of antidromic responses in relay and intralaminar thalamocortical neurons, and the failure of antidromic invasion predictably announces the occurrence of spindle sequences [140] (Fig. 3.20). That the first, declining phase of the hyperpolarization in each spindle wave is most effective in reducing the amplitude and duration of incoming signals was demonstrated by recording cerebellar-induced EPSPs in TC neurons, and by comparing this phase of spindles with other periods of sleep patterns [141]. The result (Fig. 3.21) shows that the amplitude of cerebellar-evoked EPSPs diminishes by about 40%, and the duration by 50%, during the hyperpolarizing phase of spindle-related IPSPs, which is associated with a markedly increased membrane conductance.

The above data, from studies on experimental animals, are corroborated in humans by investigating the role of spindles in gating information processing to protect the sleeper from disturbing sounds [142]. The authors tested event-related potentials (ERPs) during spindle activity and epochs in which spindles were absent. ERPs consist of several components [143], of which the negative wave at a latency of 0.1 s (N1) is known to increase when the subject is actively attending the stimulus [144] and to decrease at sleep onset [145]. The N1 component significantly decreased during epochs with spindle activity [142]. This result indicates that, besides the steady hyperpolarization of TC neurons during SWS, spindles represent an additional, significant factor to prevent incoming information from reaching the cortex during this sleep state.

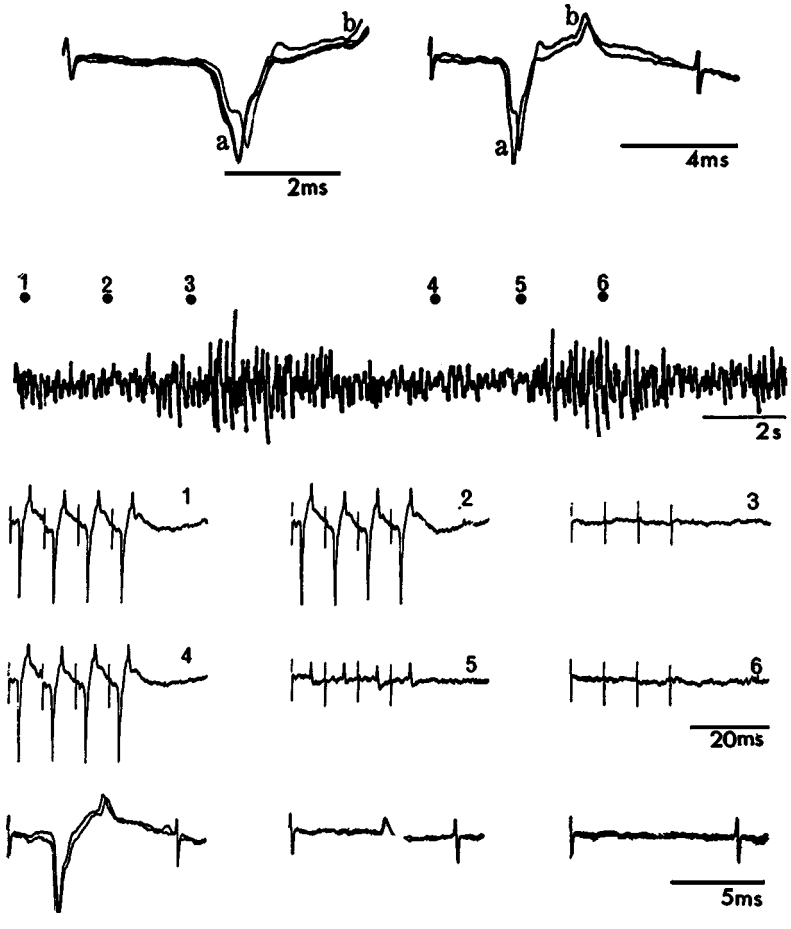

Fig. 3.20 Inhibition of antidromic responses in TC neurons during, and preceding, spindles. Cat maintained under repeated doses of short-acting barbiturate. *Top*, two neurons (positive action potential *a* and negative action potential *b*) were simultaneously recorded from the thalamic ventrolateral (VL) nucleus and could be activated antidromically by stimulating the motor cortex. Note the break between the initial segment (IS) and somadendritic (SD) spikes in neuron *a*, more marked after the last (fourth) stimulus in the pulse-train. Below these oscilloscopic records, the ink-written trace shows the EEG from the ipsilateral motor cortex. Figures on the EEG record indicate the application of the testing pulse-train corresponding to those depicting the evoked discharges on the oscilloscopic (see below). During inter-spindle lulls (1, 2, 4) both *a* and *b* antidromically activated neurons responded without failure at 100 Hz stimuli. During EEG spindles (3, 6), evoked discharges were abolished. Note that the larger *a* evoked spike disappeared 0.5 s prior to the appearance of the EEG spindle, when neuron *b* was still responding (5). Traces 4–6 are also depicted at faster speed on the bottom line. From Steriade et al. (1971).

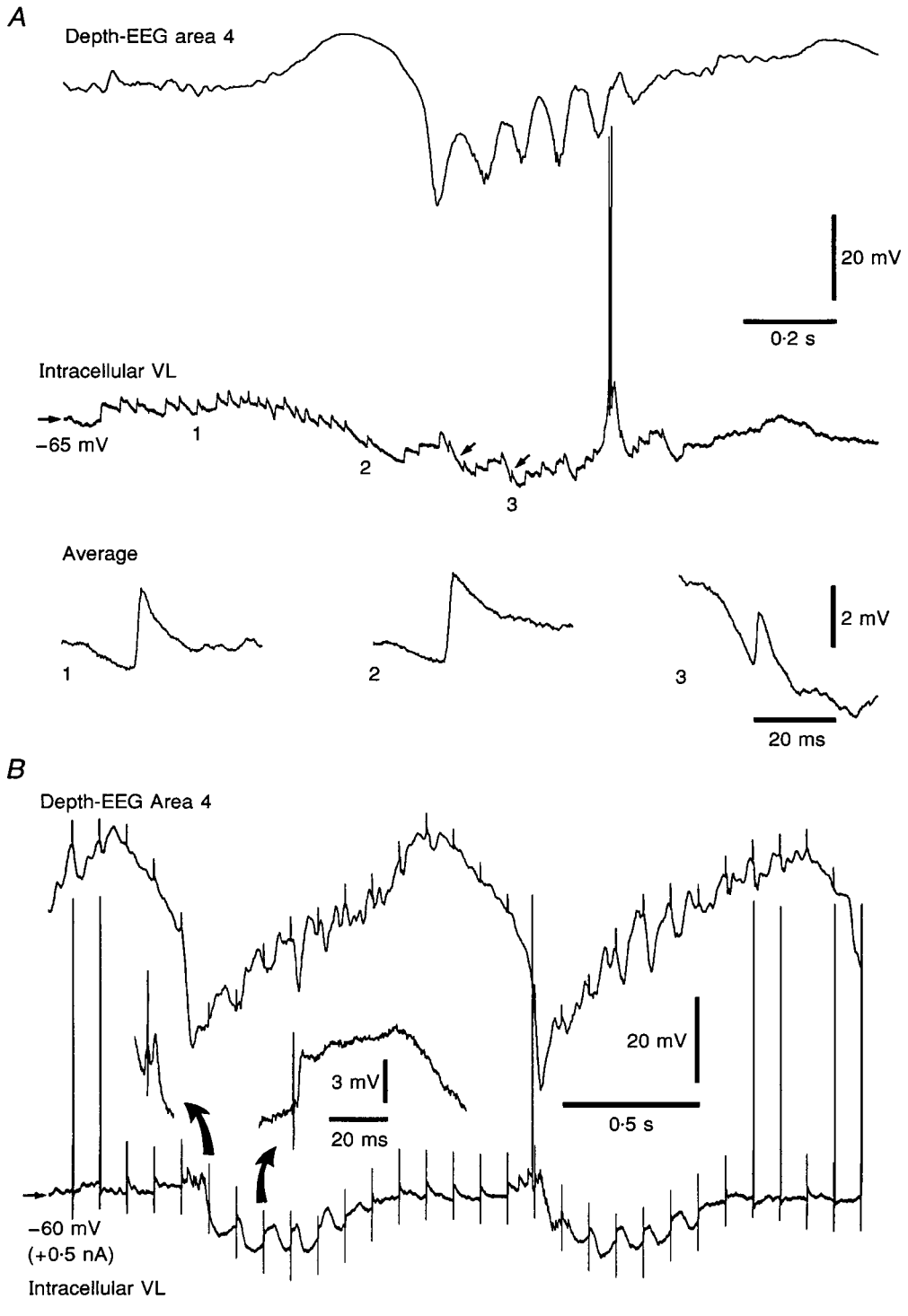

Fig. 3.21 Alterations in amplitude and duration of thalamic responses to fast stimuli of cerebellar origin during different phases of sleep oscillations, with the emphasis on spindles. Cat under ketamine-xylazine anesthesia. Intracellular recordings from two neurons in the ventrolateral (VL) nucleus. *A*, one cycle of the slow oscillation, showing the epochs (1, 2, and 3) from which averages ($n = 40$, shown below with corresponding numbers) of fast EPSPs were computed. Compare 1–2 with 3, that is the descending phase of the hyperpolarization of spindle-related IPSPs (small arrows in the top trace) that follow the slow oscillation (see EEG trace). *B*, responses to brachium conjunctivum (BC) stimulation in another TC neuron (under 0.5 nA depolarizing current; V_m without current was −68 mV). BC stimuli were applied at a fast rate (10 Hz) to detect differences between BC-evoked fast events during the descending and ascending phases of spindle-related IPSPs (see enlarged trace insets indicated by curved arrows). From Timofeev and Steriade (1997).

[146] Oscillations in the range of 0.025–0.01 Hz were described in the thalamic lateral geniculate nucleus in anesthetized and awake rats (Albrecht et al., 1998). The underlying mechanisms of these activities have not yet been revealed intracellularly.

[147] Parri et al. (2001) have shown that astrocytes recorded from *in vitro* slices of thalamic ventrobasal nucleus (5- to 17-day-old rats) display an intrinsic $[Ca^{2+}]_i$ oscillation that was not driven by neuronal activity as the number of active astrocytes was similar in the presence or absence of tetrodotoxin (TTX). The frequencies of this extremely slow oscillation ranged in different types of astrocytes between 0.01 Hz and 0.003 Hz. The oscillation propagated to neighboring astrocytes and eventually triggered NMDA receptor-mediated inward currents in adjacent neurons. It is known that astrocytes release neurotransmitters, such as glutamate (Parpura et al., 1994; Innocenti et al., 2000). The oscillation described by Parri and his colleagues (2001), generated by glial cells, is distinctly different from the slow oscillation (0.5–1 Hz) that is generated by neocortical neurons and reflected in glial cells (Amzica and Steriade, 2000; see *3.2.3.1* and Fig. 3.34).

[148] Gloor et al. (1977); Steriade et al. (1990d).

[149] Field potential and extracellular recordings have indicated that thalamic neurons display waves and unit discharges within delta (1–4 Hz) frequencies during EEG-synchronized sleep (McCarley et al., 1983), which are suppressed during EEG-activation patterns induced by midbrain reticular stimulation (Steriade et al., 1971). Some of these so-called "delta"-related spike-bursts may, however, be interpreted as spindle-related spike-bursts, knowing that TC neurons do not fire after each hyperpolarizing wave within a spindle sequence (see Figs. 3.7 and 3.15) and, thus, the overall frequency of extracellularly recorded spike-bursts and/or associated field potentials can be at 4 Hz or even lower. Still, delta waves occur in RE nucleus after disconnection from the cerebral cortex [98] and RE neurons fire spike-bursts at 7–14 Hz throughout the spindle sequence (Fig. 3.7).

3.2.2. Delta: intrinsically generated thalamic rhythm and cortical waves

Before the relatively recent discovery of the slow oscillation (<1 Hz) in animals and humans (see ***3.2.3***), waves within the frequency range between 0.5 and 4 Hz were interchangeably termed slow or delta waves. In view of different frequencies, mechanisms, and dynamics during night sleep in humans, the delta (1–4 Hz) and slow (0.5–1 Hz) oscillations are now demonstrated to be distinct types of oscillatory activities. Oscillations at much lower frequencies, below 0.1 Hz [146] or even slower, do not belong to the category of delta and slow oscillation, and some of them arise from non-neuronal processes [147]. Here, only delta waves occurring during sleep and anesthesia or in slices maintained *in vitro* are discussed. For pathological (polymorphic) delta activities, resulting from metabolic disturbances or different types of brain lesions, see previous reviews [148].

There are two sources of delta activities: the thalamus and the neocortex. TC neurons give rise to a delta rhythm generated by the interplay among their intrinsic properties; this rhythm is transferred to the cortex and can be episodically seen at the EEG level, often in conjunction with the cortical slow oscillation. Cortical neurons generate, through their intrinsic properties and network activities, another type of delta wave activity. This dichotomy and the complex neuronal processes that underlie the generation and synchronization of delta oscillations, and especially the dissociation between delta and slow oscillatory activities, are not yet fully understood by those who examine macroscopically brain electrical activity, although recent human studies using EEG and magnetoencephalography (MEG) have pointed to the distinctness of these oscillations and different models predicted a series of mechanisms.

3.2.2.1. Thalamic delta rhythm: cortical synchronization and brainstem suppression

The pure clock-like pattern, with fixed frequency, of this stereotyped oscillation (Fig. 3.22) is unlikely to characterize long periods of electrical activity recorded in brain-intact animals and humans, as the EEG consists of a variety of rhythms that are coalesced, especially during SWS. The prerequisite for the appearance of thalamic delta oscillation is the hyperpolarization of TC neurons, generally more negative than −65 or −70 mV, but delta rhythm may occur at more positive membrane potentials (see Fig. 3.22). Although the presence of delta oscillation in the thalamus in different thalamic nuclei was detected using *in vivo* recordings during the 1970s and early 1980s [149], the mechanisms of generation

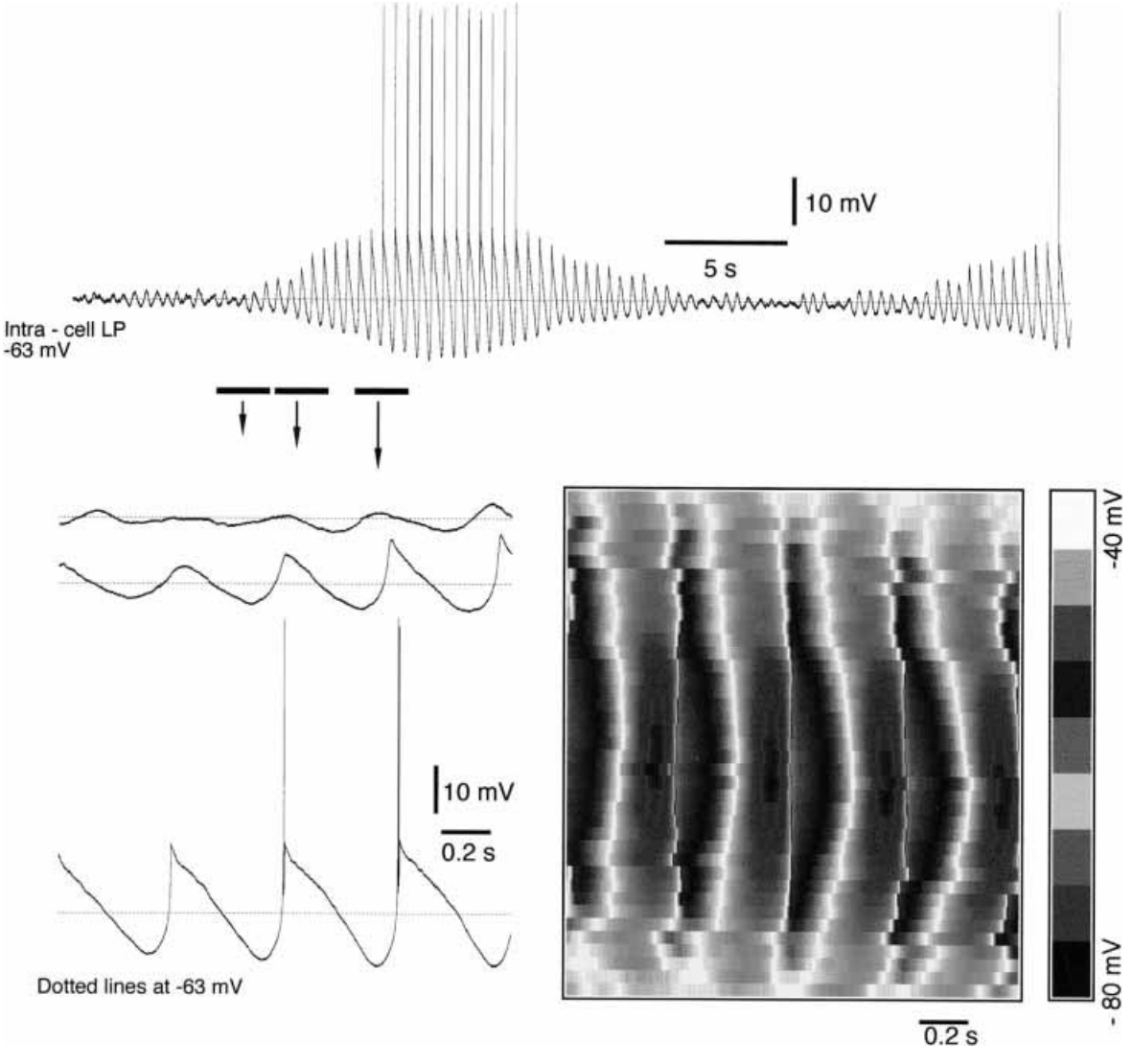

Fig. 3.22 Clock-like thalamic delta activity in decorticated cat. Ketamine-xylazine anesthesia. Intracellular recording from thalamic lateroposterior (LP) neuron. Note waxing and waning potentials. Periods of delta oscillations start from subtle fluctuations of the membrane potential. The amplitude of this activity starts and declines without changes in frequency (2.2 Hz). Periods indicated by horizontal bars are expanded below. A topographical plot of delta activity emphasizes the stable frequency of delta activity regardless of the amplitude of LTSs (right). Successive sweeps are aligned by the maximal depolarization during LTS (bottom to top); time is left to right; colors code the voltage. From Timofeev et al. (2001a). See Plate section for color version of this figure.

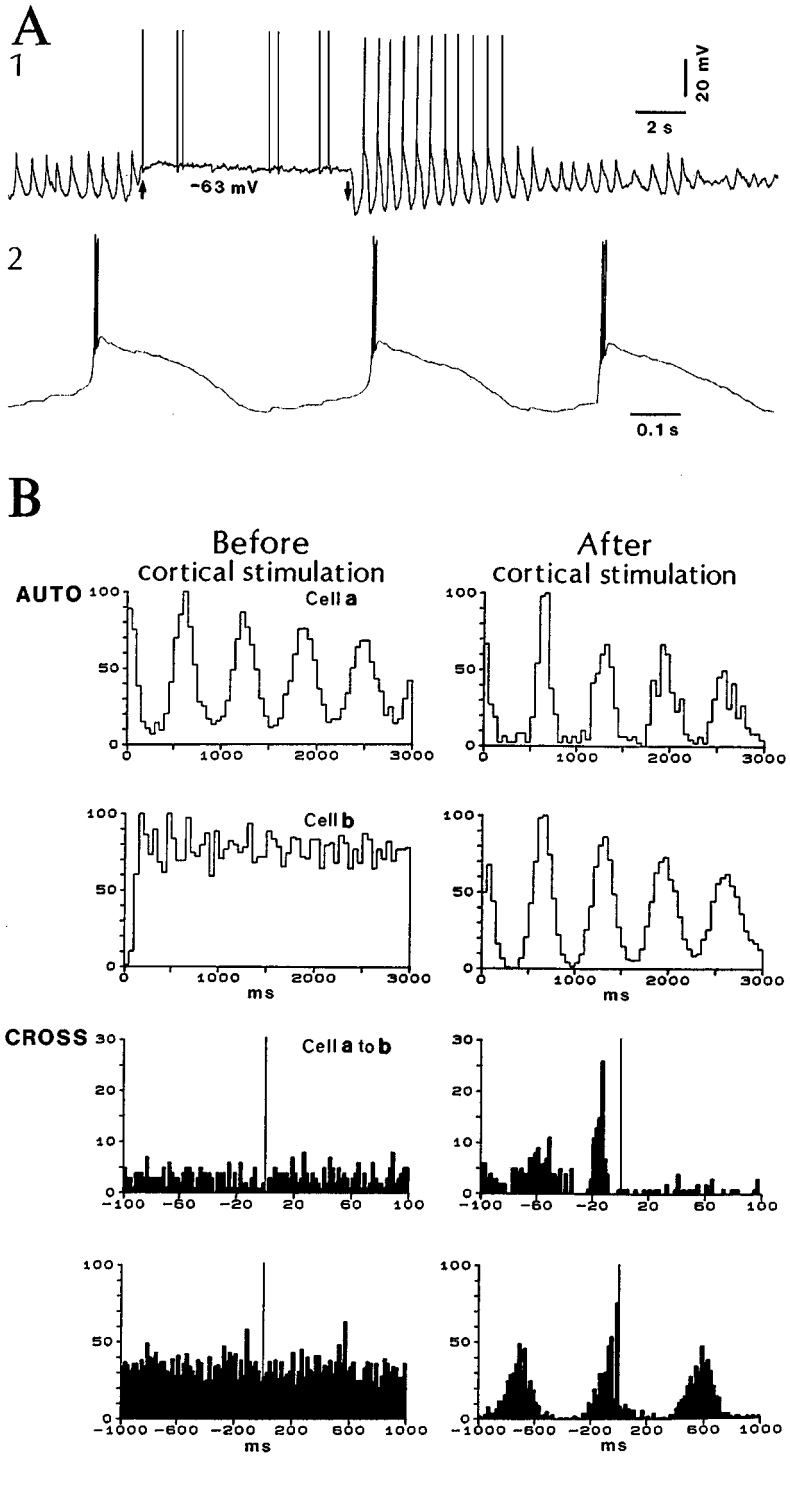
A
1
20 mV
2 s
-63 mV
2
0.1 s
B
Before
cortical stimulation
After
cortical stimulation
AUTO
Cell a
Cell b
ms
CROSS
Cell a to b
ms

and synchronization were only revealed in the 1990s, with intracellular studies *in vitro* [150, 151] and *in vivo* [152]. These studies revealed that, in contrast to the spindle oscillation that is generated by synaptic interactions in thalamic networks that necessarily include RE nucleus, the delta oscillation is an intrinsic oscillation depending on two inward currents of TC neurons.

In vitro studies [150] identified two currents whose interplay generates delta oscillation: (*a*) I_H, a hyperpolarization-activated, inward rectifier carried by Na^+ and K^+, which is expressed as a depolarizing sag of membrane potential toward rest; and (*b*) I_T, a transient Ca^{2+} current underlying the LTS. The model for the genesis of 1–4 Hz oscillation proposes that, at hyperpolarized levels of the membrane potential (more negative than −65 or −70 mV), I_H is activated. This depolarization activates I_T (that was de-inactivated because of the membrane hyperpolarization), thus underlying an LTS which gives rise to a burst of high-frequency fast Na^+ action potentials. The latter depolarization de-activates I_H. Repolarization of the membrane is followed by a hyperpolarizing overshoot that, in turn, activates I_H, which depolarizes the membrane toward another Ca^{2+}-dependent LTS. The cycle is then repeatable. The delta oscillation is modulated by substances that act on purinergic and adrenergic receptors and up- or down-regulate the I_H [151].

Studies *in vivo* [152] have shown that antidromically identified TC cells recorded from a variety of sensory, motor, associational, and intralaminar thalamic nuclei display a delta rhythm induced by imposed hyperpolarization to values characteristic of late stages of EEG-synchronized sleep. Removal of the hyperpolarization current leads to the disappearance of the oscillation (Fig. 3.23*A*). Moreover, spontaneously occurring delta oscillation (without injecting current pulses) could be obtained by ablating the cortical areas projecting to the recorded thalamic nucleus. This deafferentation procedure removes the powerful depolarizing impingement from

[150] McCormick and Pape (1990a-b); Leresche et al. (1990, 1991); Soltesz et al. (1991). A postnatal development study of slices from rat lateral geniculate nucleus concluded that no intrinsic delta oscillation is observed until P17 and that the frequency of this rhythm is lower (∼0.35 Hz) than in adult animals (1.5 to 2 Hz) (Pirchio et al., 1997).

[151] Pape and McCormick (1989); Pape and Mager (1992); Pape (1996); Yue and Huguenard (2001).

[152] Steriade et al. (1991a); Curró Dossi et al. (1992a); Nuñez et al. (1992a). These studies were carried out on thalamic relay nuclei. A study in the perigeniculate (PG) sector of the RE nuclear complex recorded delta activity (Amzica et al., 1992), but we were unable to conclude whether these clock-like spike-bursts were intrinsically generated in RE neurons or reflected the rhythmic delta activity of lateral geniculate neurons.

Fig. 3.23 (opposite) Clock-like delta oscillation in TC neurons, and synchronization of this intrinsic oscillation in different TC neurons by corticothalamic synaptic volleys. Cats under urethane anesthesia. *A*, neuron from the thalamic lateroposterior nucleus. At "rest", the neuron oscillated spontaneously at 1.7 Hz. A 0.5 nA depolarizing current (between arrows) prevented the oscillation and its removal set the cell back in the oscillatory mode. Three cycles after removal of depolarizing current in *1* are expanded in *2* to show high-frequency spike-bursts crowning LTSs. *B*, auto- and cross-correlograms of two cells (*a* and *b*), recorded simultaneously in the thalamic ventrolateral nucleus. Four correlograms (before and after cortical stimulation) depict, from top to bottom, the autocorrelogram of cells *a* and *b*, and cross-correlograms of both cells (cell *b* is the reference cell) with different bins (2 and 20 ms). Note, before cortical stimulation, delta rhythm (1.6 Hz) of cell *a*, flat contour (absence of rhythmicity in cell *b*), and absence of coupling between these neurons. After corticothalamic synaptic volleys, the background noise in cell *a* was reduced, cell *b* became rhythmic at the same frequency as cell *a* (1.6 Hz), and cross-correlograms show that cell *a* firing preceded cell *b* firing by about 10–20 ms. Modified from Steriade et al. (1991a).

corticothalamic neurons and sets thalamic cells at a more hyperpolarized membrane potential where delta oscillation is generated. The fact that rhythmic LTSs occurred in isolation (see Fig. 3.23*A*1), without superimposed fast action potentials that could have synaptically engaged other elements in the thalamic and cortical networks, supports the idea that this oscillation is intrinsic. Delta oscillation is sensitive to barbiturates and even very low doses of short-acting barbiturates are effective in blocking it. This effect is due to an increased conductance of TC cells produced by barbiturates, which prevents the interplay between the two inward currents responsible for the delta genesis.

Delta oscillation is blocked by spindle sequences, even those that occur in *cerveau isolé* preparations (with transection at the midcollicular level), i.e., in the absence of barbiturates [153]. We proposed that the mechanism of delta occlusion by spindles is the increased membrane conductance that is seen during and a few seconds after a spindle sequence [152]. The hyperpolarization of TC neurons outlasting the spindle sequence is ascribed to the long-lasting, tonic spike barrage of RE neurons that follows the spindle-related spike-bursts in this GABAergic cell type [154]. The increased membrane conductance of TC cells during this prolonged hyperpolarization unbalances the interplay between I_H and I_T. This incompatibility between spindles and delta waves, which only occurs at the level of single neurons, is also seen by the fact that these two oscillatory types appear at different membrane potentials of TC neurons. Around −60 mV or at more positive values, TC neurons display spindles, whereas at membrane potentials more negative than −65 or −70 mV spindles progressively decrease in amplitude and the oscillations are within the delta frequency range [152, 153]. We have thus postulated a progressive hyperpolarization of TC cells with the deepening of SWS, which is attributable to the progressive decrease in firing rates, during SWS, of corticothalamic, midbrain reticular core, and mesopontine cholinergic neurons with thalamic projections, and some monoaminergic nuclei [155]. Conversely, at the end of SWS, approaching REM sleep, when TC neurons become less hyperpolarized because of increased firing rates of mesopontine cholinergic neurons, which precede the onset of REM sleep and excite TC neurons (see **3.3**), spindles are more obvious than during preceding epochs of deep SWS (see Fig. 3.6).

It is known from human and animal studies that spindles and delta waves prevail during different sleep stages and that these two rhythms reciprocally oscillate within EEG-synchronized sleep [156]. The intracellular data reported above [152, 153] revealed the

[153] Nuñez et al. (1992b).

[154] Steriade et al. (1986).

[155] The state-related firing rates of different neuronal types are discussed in the monograph by Steriade and McCarley (1990). Their transmitters produce a depolarization of TC neurons [84, 96].

[156] Uchida et al. (1991); Lancel et al. (1992). Dijk and Czeisler (1995) remarked that our cellular data showing a progressive hyperpolarization of TC neurons during SWS [152–153], which is responsible for the transition from spindles to delta activity, is indeed related to the progression of sleep rather than to the endogenous circadian phase. Significant differences between the dynamics of spindles and delta waves in night sleep have also been observed after sleep deprivation in humans (Dijk et al. 1993).

[157] Merica et al. (1997); Terman et al. (1996).

[158] Hofle et al. (1997). See also Maquet et al. (1992).

[159] Steriade (1978).

[160] McCormick and von Krosigk (1992).

mechanisms accounting for this relative incompatibility between spindle and delta sleep rhythms, mainly due to their differential voltage dependency. Hypotheses and computational models based their assumptions on the biphasic origin (thalamic and cortical) of delta oscillations and proposed that the transition from spindles to clock-like delta rhythm, generated in the thalamus, occurs with changes in the inhibitory impact of RE neurons upon TC neurons [157]. Human studies of natural sleep, using EEG recordings in conjunction with regional cerebral blood flow (rCBF) studied with positron emission tomography (PET), concluded that delta activity (1.5–4 Hz) covaried negatively with rCBF in the thalamus and brainstem reticular core, and that after the effect of delta activity was removed, an additional negative covariation (∼35%) between spindles and the residual rCBF was still visible in the medial thalamus [158]. Again, these data suggest that spindles have a significant role in protecting the stability of sleep by disconnecting the subject from the outside world and may be a prerequisite for falling asleep more deeply (see also above; and Figs. 3.19 to 3.21).

Cortical volleys potentiate delta oscillation in TC cells [152]. This synaptic action indicates that delta oscillation, resulting from the intrinsic properties of thalamic cells, is powerfully modulated by network operations (Fig. 3.23*B*). The facilitatory process is expressed by the transformation, as an effect of cortical stimulation, of subthreshold delta oscillation into rhythmic LTSs crowned by fast sodium action potentials. The LTSs may persist for 10–20 s as a self-sustained activity, after cessation of cortical volleys.

How are corticothalamic inputs able to either depolarize TC neurons (directly) or hyperpolarize them (via GABAergic RE neurons) and, in the latter case, to potentiate delta oscillation? The answer should take in consideration the different firing patterns of corticothalamic neurons during waking and SWS. Tonic, high-discharge firing rates of corticothalamic cells during waking [159] exert a depolarizing impingement on thalamic cells through the release of excitatory amino acids acting on non-NMDA, NMDA, as well as metabotropic glutamate receptors. The prolonged excitation of thalamic relay cells resulting from the reduction of a "leak" I_K through the activation of glutamatergic metabotropic receptors is capable of maintaining the activation patterns of TC neurons, acting as a descending activation system [160]. The action of repetitive action potentials with depolarizing effects in the corticothalamic pathway prevents, during the alert state, the delta genesis since the interplay between I_H and I_T is dependent upon membrane

[161] Amzica and Steriade (1998b).

[162] Calvet et al. (1964); Petsche et al. (1984).

[163] Schwindt et al. (1988a-b).

hyperpolarization. Distinctly from the discharge patterns of corticothalamic cells during wakefulness, the same neurons have lower rates and fire high-frequency bursts in SWS [159], which are more effective in driving RE and local-circuit inhibitory thalamic cells, thus creating the conditions for the appearance of the delta oscillation.

Although the thalamic delta rhythm is generated through intrinsic properties of TC neurons and is then expected to be seen in single neurons, corticothalamic volleys are also capable of synchronizing delta-oscillating thalamic cells that were uncoupled prior to cortical stimuli (Fig. 3.23*B*). This synchronizing effect, visible in thalamic field potentials within the frequency range of delta, is produced by network operations involving corticothalamic projections, with an intermediate link in the RE nucleus. To be expressed at the macro-level of field potential, single cells should be united into neuronal ensembles by synchronizing devices that must have access to many dorsal thalamic nuclei. The only candidate for such a synchronization process is the RE thalamic nucleus that projects to widespread dorsal thalamic territories [112].

3.2.2.2. Cortical delta waves

That another delta component is generated in cortex is demonstrated by the presence of this activity after thalamectomy [66]. The mechanisms of cortical delta waves are much less well understood than those underlying the clock-like thalamic delta rhythm. Upon depolarizing current pulses, intrinsically bursting cortical neurons fire repetitively, within delta frequency [161], but, in view of the highly synchronous neuronal activity in the delta frequency range, the major role is probably played by many other neuronal types and their interconnections within cortical networks. Cortical delta waves result from vertically arranged dipoles between layers II–III and layer V [162]. There is a relationship between the firing probability and surface-positive (depth-negative) delta waves, whereas the depth-positive waves are associated with a diminished discharge rate or even firing suppression [85]. These relations might suggest that the depth-positive component of delta waves reflects the inhibition of pyramidal-shaped neurons and is associated with maximal firing of local-circuit cells. However, this has not been found. Instead, it was suggested [85] that cortical delta waves are generated by summation of long-lasting afterhyperpolarizations (AHPs) produced by a variety of potassium currents in deeply lying pyramidal neurons. AHPs are mainly due to a Ca^{2+}-activated K^+ current, $I_{K(Ca)}$. Three types of AHPs were described: fast-decaying (fAHP), medium-duration (mAHP), and slow (sAHP) [163]. Because of the duration

of EEG delta waves (>250 ms), only sAHP can be taken into consideration because the duration of mAHP at its maximum amplitude (reached following 20 spikes at 100 Hz) averages 112 ms. The duration of the early part of the sAHP (several hundred milliseconds) fits in with the duration of EEG slow waves. It is conceivable that the high-frequency spike-bursts of various types of pyramidal neurons during EEG-synchronized sleep [159] lead to sAHP, since this outward current was elicited in slice preparations by stimuli at 100 Hz [163]. Moreover, the decreased excitability that accompanies the sAHP is consistent with the decreased synaptic and antidromic responsiveness of pyramidal tract and other corticofugal neurons during EEG epochs with delta waves [164]. Another feature of this K^+ conductance that makes it a likely candidate for generating EEG delta waves is its reduction or abolition by muscarinic agonists that, by contrast, are unable to affect the mAHP [163]. It is known that the suppression of delta waves upon arousal results from the action of cortical-projecting basal forebrain cholinergic neurons [60] and that ACh increases the excitability of cortical neurons by reducing a voltage-dependent current (I_M) and a $I_{K(Ca)}$ [84, 165].

Data exposed in the next section will show that delta and slow oscillations are distinct types of sleep activities, that both thalamically and cortically generated delta activities may be coalesced with slow oscillatory cycles in complex wave-sequences, and that the shape of the sleep K-complex (the excitatory component of the slow oscillation) contributes to the spectrum of the 1–4 Hz delta frequency band.

3.2.3. The cortical slow oscillation

The slow oscillation (<1 Hz, generally 0.5–1 Hz) was first described using intracellular recordings from different neuronal types in anesthetized cats and, in the same initial article, was also detected in EEG recordings during natural SWS in humans [166]. The surprisingly recent (1993) disclosure of this EEG rhythm is possibly due to usual filtering of slow activities, which have long been disregarded [167], or more probably an inadequate choice of windows for fast-Fourier transform (FFT) analyses (see below, *3.2.3.2*). Nonetheless, though the slow rhythm was not explicitly described and analyzed, cyclic groups of delta waves at 3–4 Hz, recurring with a slow periodicity (0.3–0.4 Hz), can be seen in some figures of previous publications [168]. The grouping of these two oscillatory types, within frequency bands of 1–4 Hz and 0.3–1 Hz, is one of the arguments supporting the distinctness between delta and slow sleep oscillations [169].

[164] Steriade et al. (1974a).

[165] Krnjević et al. (1971).

[166] Steriade et al. (1993e). The frequency of the slow oscillation depends on the anesthetic used and behavioral state: it is mainly 0.3–0.6 Hz under urethane, 0.6–0.9 Hz under ketamine-xylazine, and between 0.7 and 1 Hz or sometimes slightly higher during natural sleep. The anesthetic that best mimics the slow oscillation in natural sleep and that is used to investigate intracellularly the mechanisms of this oscillation is ketamine combined with xylazine. Ketamine, a blocker of NMDA receptors, effectively induces SWS patterns on a background of waking (Feinberg and Campbell, 1993), and xylazine, an α_2-receptor agonist, increases a K^+ conductance in a variety of brain structures (Nicoll et al., 1990). The similarity between the slow oscillation occurring during natural sleep and that occurring under ketamine-xylazine anesthesia was demonstrated in the same chronically implanted animal (Amzica and Steriade, 1997). See a recent model in Bazhenov et al. (2002).

[167] For example, spindles (7–14 Hz) are grouped in sequences that recur rhythmically, every 2 to 5 seconds (faster in natural sleep than under barbiturate anesthesia), but this slow rhythm of spindles was described much later [136] than the intraspindle frequency.

[168] See, for example, Fig. 3*A* in Petsche et al. (1984).

[169] Achermann and Borbély (1997) investigated the slow oscillation in human sleep and supported the clear-cut distinction between delta activity (1–4 Hz) and slow oscillation (range 0.55–0.95 Hz) since the typical decline in delta activity from the first to the second SWS episode was not present at frequencies characteristic of the slow oscillation. See slow oscillation in electromyographic activity in humans (Westgaard et al., 2002). Another type of brain electrical activity, the "cyclic alternating pattern" (CAP), which recurs at 20-s or longer intervals and associated with enhancement of muscle tone and heart rate (Terzano et al., 1988), is also quite distinct from the slow sleep oscillation, as CAP was described under the term "arousal-related phasic events", whereas the slow oscillation typically occurs during SWS and is blocked during arousal in acute experiments as well as during awakening in behaving animals (see main text).

The cortical nature of the slow oscillation was demonstrated by (*a*) its survival in the cerebral cortex after thalamectomy [170]; (*b*) its absence in the thalamus of decorticated animals [171]; and (*c*) the disruption of its long-range synchronization after disconnection of intracortical synaptic linkages [172].

The slow oscillation was recorded in all four major types of neocortical neurons (regular-spiking, RS; fast-spiking, FS; fast-rhythmic-bursting, FRB; and intrinsically bursting, IB; see Chapter 2, *2.1.1*), as identified electrophysiologically and by intracellular staining (Fig. 3.24). Identical oscillations were detected in all explored cortical fields: motor (areas 4-6), somatosensory (areas 3-1-2), association (areas 5-7-21) and visual (17-18). Despite the presence of a clear-cut slow oscillation recorded from the primary visual cortex, in neurons driven monosynaptically from the thalamic lateral geniculate nucleus (Fig. 3.25), the incidence of slow oscillation in this area is lower than in other cortical fields, particularly during light sleep epochs, possibly because of a powerful bombardment from retinogeniculate afferents.

3.2.3.1. Depolarizing and hyperpolarizing phases in neurons and glia cells

The slow oscillation consists of a prolonged depolarizing phase, followed by a long-lasting hyperpolarization (Figs. 3.24–3.25). In intracellular recordings from cortical neurons in chronically implanted, naturally sleeping animals, the slow oscillation with clear-cut hyperpolarizing phases appears from the very onset of SWS (Fig. 3.26), as also shown with EEG recordings in Fig. 3.6. The SWS-related cyclic hyperpolarizations depicted in Fig. 3.26, which illustrate that these long periods of neuronal silence constitute the distinguishing feature between waking and SWS, are episodic at sleep onset, but they become regular with deepening of sleep [31].

Depending on the anesthetic used, the depolarizing phase (also called "up-state") may last as long as 0.8–1.5 s under urethane, but it is much shorter (0.3–0.5 s) under ketamine-xylazine, and its duration is further shorter during natural slow-wave sleep when the frequency of the oscillation rises to 1 Hz or even slightly beyond it. Under a background of urethane anesthesia, administration of ketamine (an NMDA blocker) drastically diminishes the duration of the depolarizing phase and increases the oscillation frequency [166]. In addition to NMDA-mediated events, the depolarizing phase consists of non-NMDA-mediated EPSPs, fast prepotentials (FPPs), a voltage-dependent persistent Na^+ current ($I_{Na(p)}$), and fast IPSPs reflecting the action of synaptically coupled GABAergic local-circuit cortical cells. Data on the depolarizing phase are summarized below.

[170] Steriade et al. (1993f). The results of these experiments showing the presence of the slow oscillation after thalamectomy as well as in the *cerveau isolé* preparation are supported by recording this sleep rhythm in the isolated forebrain after midbrain transections in early postnatal stages of kittens (Villablanca et al., 2001). The fact that the cortex alone, in the absence of thalamus, can generate rhythmic activity in the frequency range of the slow oscillation (Steriade et al., 1993f) was recently confirmed by Sanchez-Vives and McCormick (2000) using cortical slices maintained *in vitro*. The possibilities accounting for the presence of this rhythmic activity in a 0.4-mm-thick slice, as opposed to the absence of this oscillation in a larger isolated neocortical slab (10 mm × 6 mm) *in vivo* (Timofeev et al., 2000a), are discussed below [199]). Spontaneous activity recorded from mice visual cortex slices, with some rhythmicity, was also reported by Mao et al. (2001; see Fig. 2*D* in that paper). A slow oscillation (<1 Hz) recorded from hippocampal slices perfused with CsCl (Zhang et al., 1998) is basically different from the neocortical slow oscillation as the rhythmicity of this hippocampal oscillation is regulated by $GABA_A$-receptor-mediated events, arising from a GABAergic interneuronal network. By contrast, the hyperpolarizations that sculpt the neocortical slow oscillation are not due to GABAergic processes as they are not affected by recordings with KCl-filled pipettes and are associated with an increase in the apparent input resistance (see main text and Figs. 3.32 and 3.33).

[171] Timofeev and Steriade (1996).

[172] Amzica and Steriade (1995a).

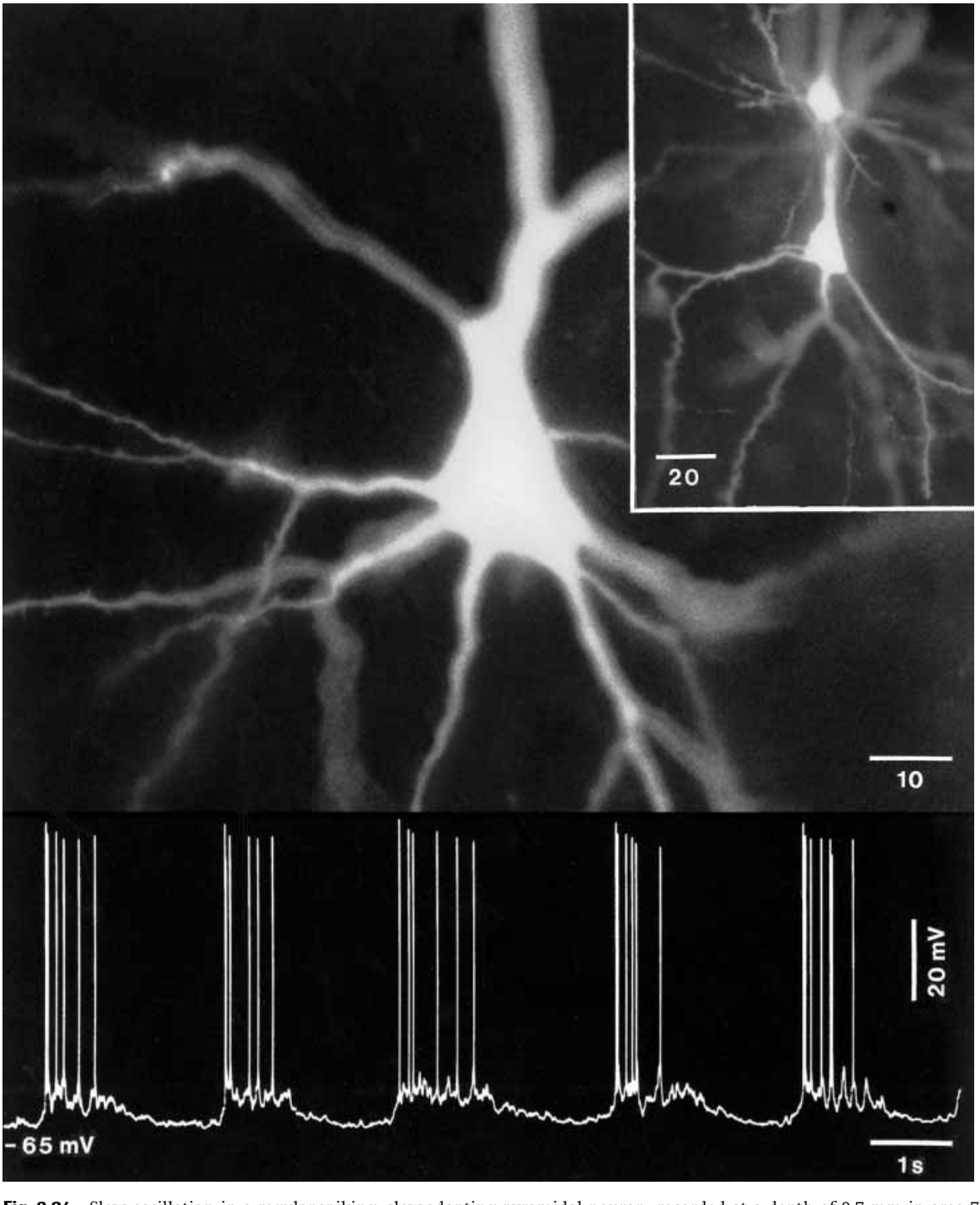

Fig. 3.24 Slow oscillation in a regular-spiking, slow-adapting pyramidal neuron, recorded at a depth of 0.7 mm in area 7. Cat under urethane anesthesia. Intracellular staining with Lucifer yellow (LY). The neuron responded with EPSPs to thalamic lateroposterior (LP) and intralaminar centrolateral (CL) nuclei. *Inset*: dye coupling following LY injection in a single cell; radially arranged neurons, at a depth of ~0.5 mm in area 5 (bars in μm). The neuron that was injected was slowly oscillating spontaneously; it displayed intrinsic bursts by depolarizing current pulses and was driven synaptically from both LP and CL thalamic nuclei. *Bottom*: intracellular recording showing the slow oscillation. Modified from Steriade et al. (1993e). See Plate section for color version of this figure.

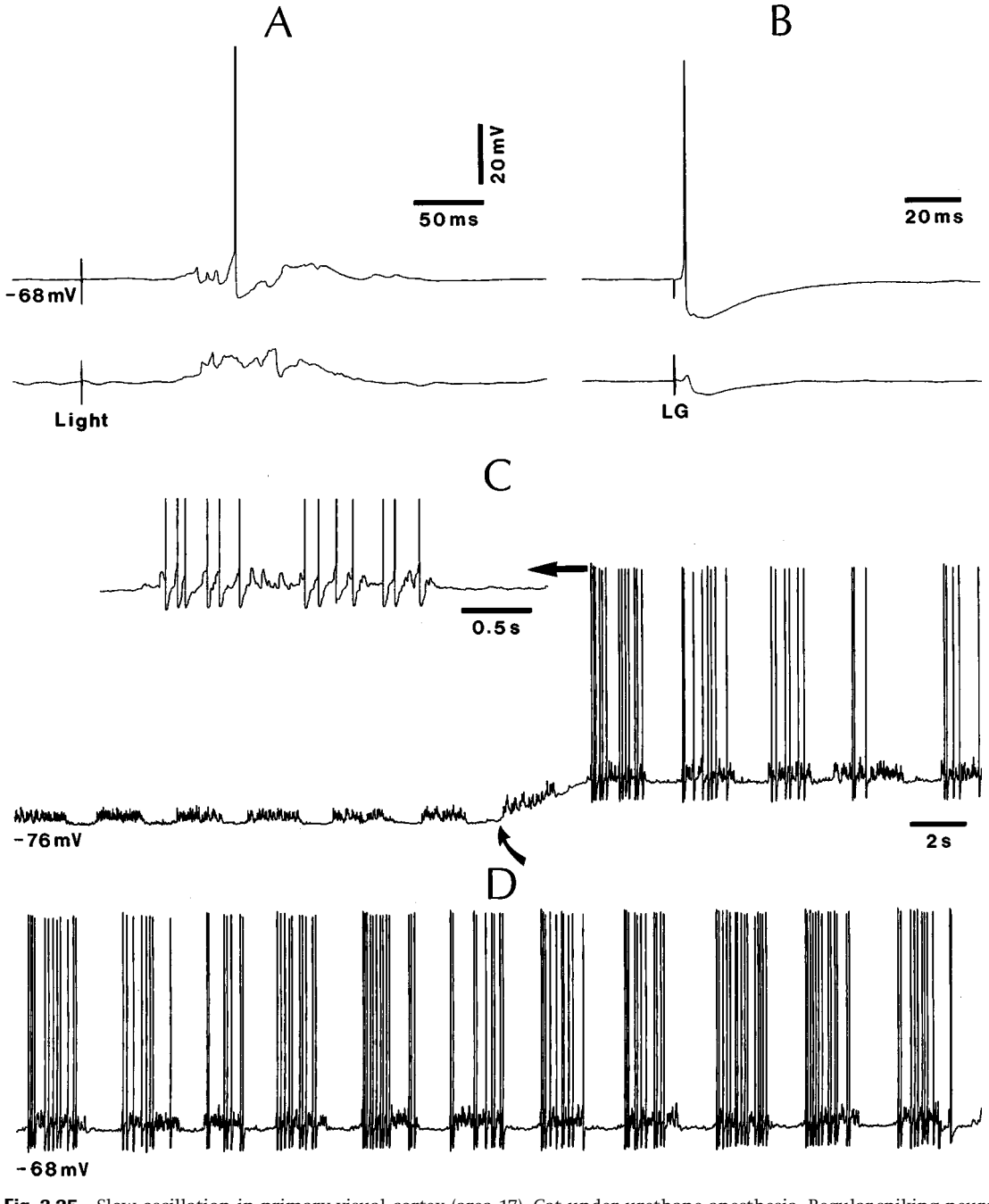

Fig. 3.25 Slow oscillation in primary visual cortex (area 17). Cat under urethane anesthesia. Regular-spiking neuron recorded at a depth of 0.8 mm. *A*, two depolarizing responses to light flashes (1 ms in duration). *B*, responses to lateral geniculate (LG) stimulation through two different stimulating electrodes; action potential generated in the upper trace, pure EPSP-IPSP sequence in the bottom trace. *C–D*, spontaneous activity under −0.2 nA DC current and, at oblique arrow, back to resting V_m (−68 mV). The first spike-train is expanded on the left (see arrow; spikes truncated). Modified from Steriade et al. (1993e).

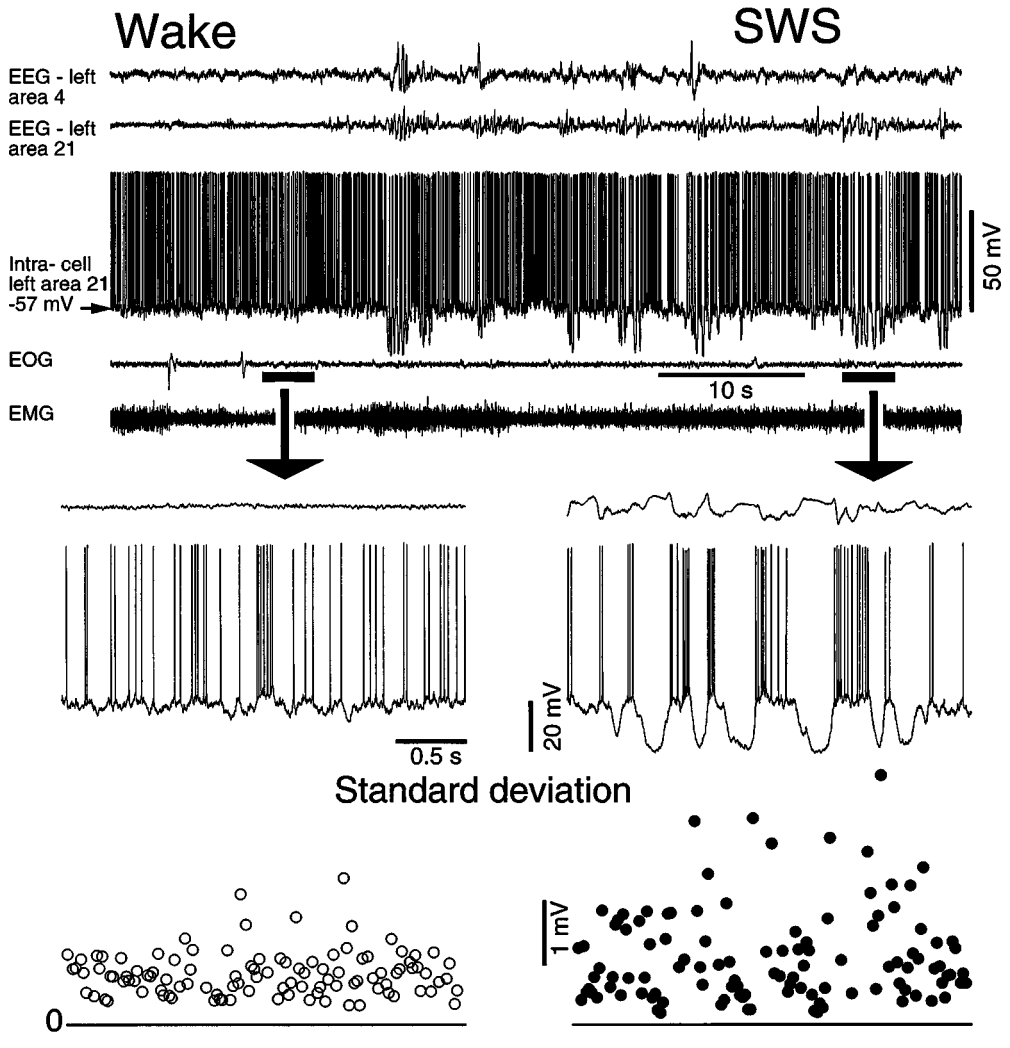

Fig. 3.26 Membrane potential fluctuations are higher during natural SWS than in wakefulness. Intracellular recording of regular-spiking neuron from left cortical area 21 of a chronically implanted cat, together with depth-EEG from left areas 4 and 21, electro-oculogram (EOG) and electromyogram (EMG). Transition from waking to SWS. Two epochs, one in waking and the other in SWS, are marked by horizontal traces (below EOG) and expanded below (arrows). Note occurrence of episodic cyclic hyperpolarizations of the slow oscillation from the very onset of SWS, as indicated by EEG. The standard deviation (SD) of the membrane potential was calculated for every 20 consecutive milliseconds and is shown below for waking (left) and SWS (right). Sampling rate 125 μs. An increase in SD associated with action potentials was omitted. Note an increase in SD during SWS compared to waking. From Steriade et al. (2001a).

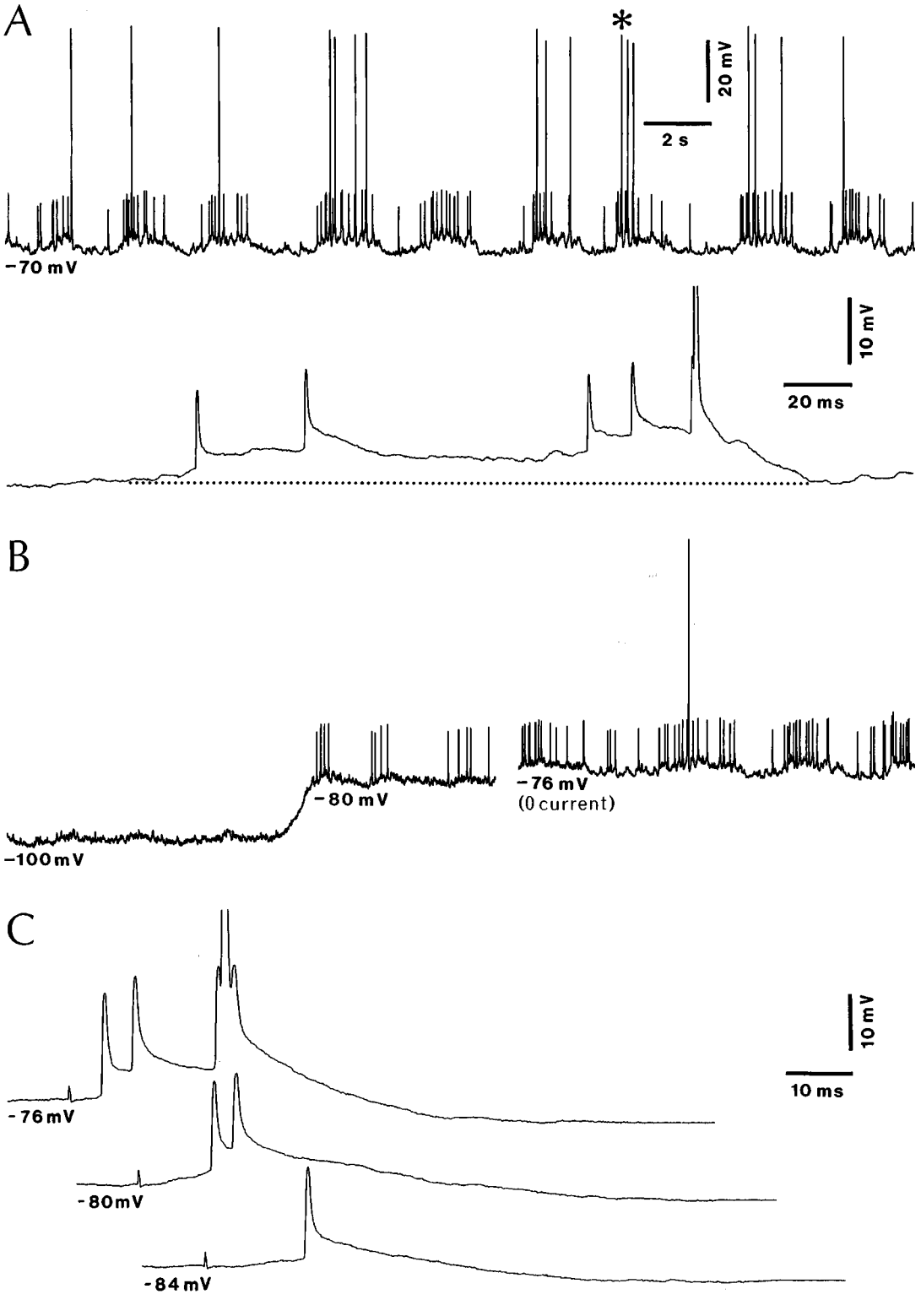
A
*
20 mV
2 s
−70 mV
10 mV
20 ms
B
−80 mV
−76 mV
(0 current)
−100 mV
C
10 mV
10 ms
-76 mV
-80 mV
-84 mV

[173] Connors and Prince (1982).

[174] Andreasen and Hablitz (1993); Perkins and Wong (1995).

[175] Nathan et al. (1990).

About 30% of recorded neurons displayed relatively small (3–10 mV), rapid, all-or-none events after obliteration of full action potentials by hyperpolarization (Fig. 3.27). These FPPs are probably dendritic spikes as their time-to-peak and rising slope were much faster and more abrupt than those of EPSPs; they were also elicited by depolarizing current pulses, and were blocked in an all-or-none fashion by DC hyperpolarization (Fig. 3.27). Recording with QX-314-filled pipettes basically showed a depolarization of neurons, as this substance blocks not only Na^+ currents [173] but also some K^+ outward currents [174] and $GABA_B$-mediated IPSPs [175]; a few minutes after impalement with the QX-314-filled pipette (4' in Fig. 3.28), dendritic spikes occurred with the same incidence as the EPSPs in the preceding epoch (2') when full action potentials were already blocked, but the ample depolarizing plateau seen at 2' was no longer present at 4' after QX-314 infusion. This suggests a role for the $I_{Na(p)}$ in the generation of the slow depolarizing plateau.

In addition to excitatory events, the depolarizing phase includes repetitive IPSPs, grouped in periodic sequences and clearly visible at depolarized levels (Fig. 3.29). These IPSPs did *not* reflect synaptic engagement of local GABAergic interneurons by spindle oscillations arising in the thalamus because spindles were not apparent in cortical and thalamic EEG recordings (Fig. 3.29*B*) and the slow cortical oscillation is preserved after thalamectomy [170]. The presence of IPSPs with increased membrane conductance on the depolarizing envelope of the slow oscillation explains, at least partially, the strikingly reduced responsiveness of cortical neurons during this phase, compared to the hyperpolarizing phase of the same oscillation (Fig. 3.30).

At a first sight, the hyperpolarizing phase of the slow oscillation ("down-state") might be ascribed to the action of local inhibitory neurons. However, as is also the case with the depth-positive phase of field potentials within the frequency range of delta waves, which reflect neuronal hyperpolarization but could not be related to increased activity of GABAergic local-circuit cells

Fig. 3.27 (opposite) Blockage of presumed dendritic spikes and reduction of rhythmic (~0.3 Hz) depolarizing envelopes of the slow oscillation under DC hyperpolarization. Cat under urethane anesthesia. Intracellular recording of regular-spiking, slowly adapting neuron recorded at 1.4 mm in area 5 (antidromically activated from thalamic LP nucleus and orthodromically activated from thalamic CL nucleus). Resting V_m was −76 mV (see right part in *B*). *A*, under DC depolarization (+0.3 nA). Episode marked by asterisk is expanded below to show the buildup of the depolarizing envelope (dotted line indicates the baseline). *B*, unitary events and depolarizing envelopes were virtually blocked at −100 mV. On the right, recovery of slow rhythm by removing the DC hyperpolarizing current. *C*, presumed dendritic spikes evoked by thalamic CL stimulation at different V_ms. An underlying slow EPSP was seen at −90 mV (not shown). From Steriade et al. (1993e).

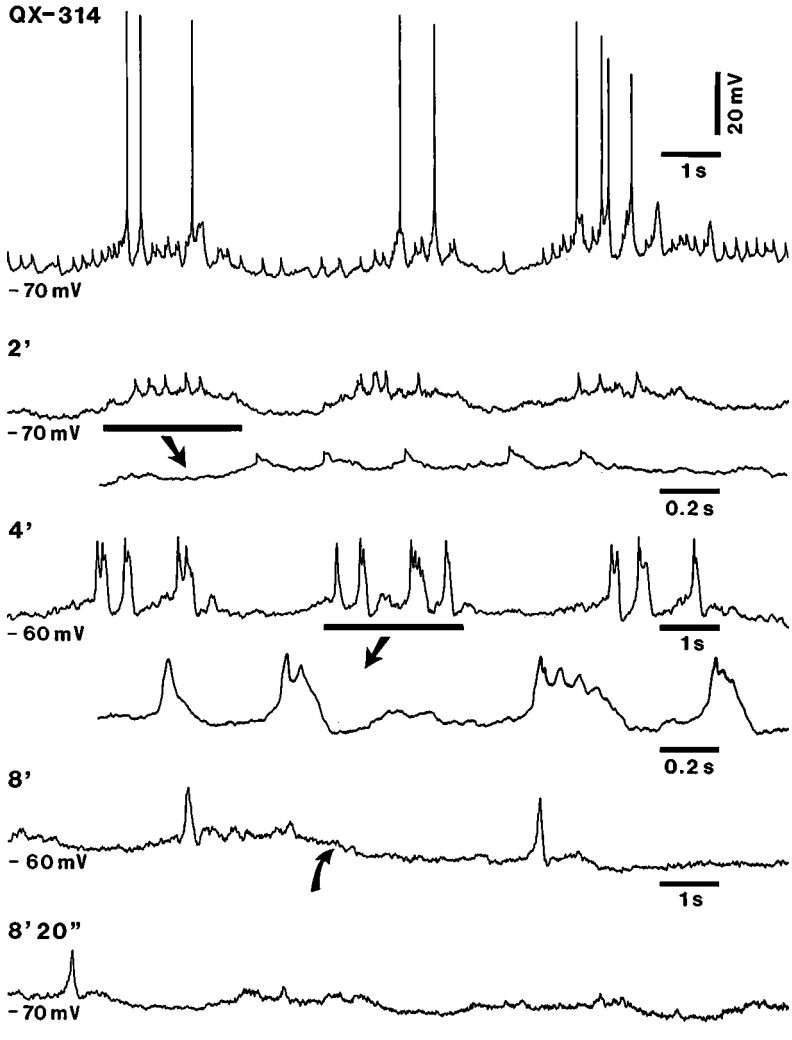

Fig. 3.28 Effect of QX-314 on the depolarizing events of the slow oscillation. Cat under urethane anesthesia. Intracellular recording with a QX-314-filled micropipette from neuron in area 7. Traces show, from the top: *(a)* immediately after impalement; *(b)* 2', disappearance of Na^+-mediated full action potentials and persistence of the rhythmic depolarization with EPSPs; part marked by horizontal bar is expanded below (arrow); *(c)* 4', neuron became more depolarized (see text); ample, phasic depolarizing events (presumably dendritic spikes) were grouped cyclically, with the frequency of the slow oscillation (comparable with the frequency seen in the top trace and at 2'), but the depolarizing envelope of the slow oscillation was diminished (compare to 2'); part marked by horizontal bar is expanded below (arrow); *(d)* 8' and 8'20", reduced oscillation and decreased incidence of dendritic spikes; at arrow, slight DC hyperpolarization brought the V_m to −70 mV. Unpublished data by M. Steriade, A. Nuñez, and F. Amzica.

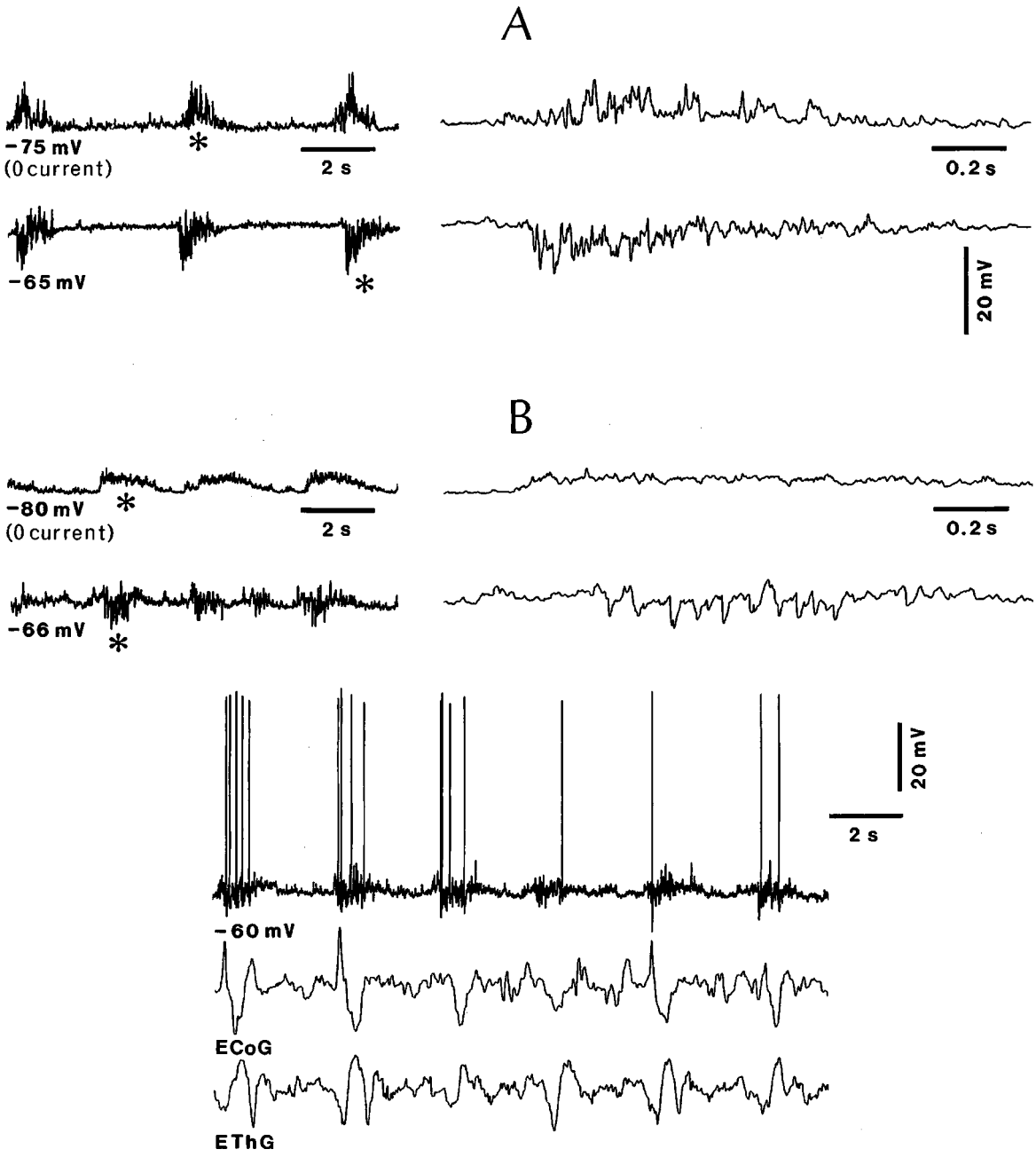

Fig. 3.29 Sequences of repetitive IPSPs are included in the depolarizing phase of the slow oscillation. Cat under urethane anesthesia. *A*, intracellular recording from neuron recorded at 0.6 mm in area 5. At rest (−75 mV) the oscillation consisted of rhythmic depolarizations. IPSPs were revealed by DC depolarization (+0.6 nA) bringing the V_m to −65 mV. Episodes marked by asterisks are expanded on the right. *B*, cell recorded at 0.9 mm in area 7. Rhythmic depolarizations at rest (−80 mV) and sequences of IPSPs revealed by DC depolarization (+1.6 nA), bringing the V_m to −66 mV. Episodes marked by asterisks are expanded on the right. *Bottom*, under further DC depolarization (V_m −60 mV), slow oscillation with occasional action potentials; simultaneous recordings of the ipsilateral electrocorticogram (ECoG) and electrothalamogram (EThG). From Steriade et al. (1993e).

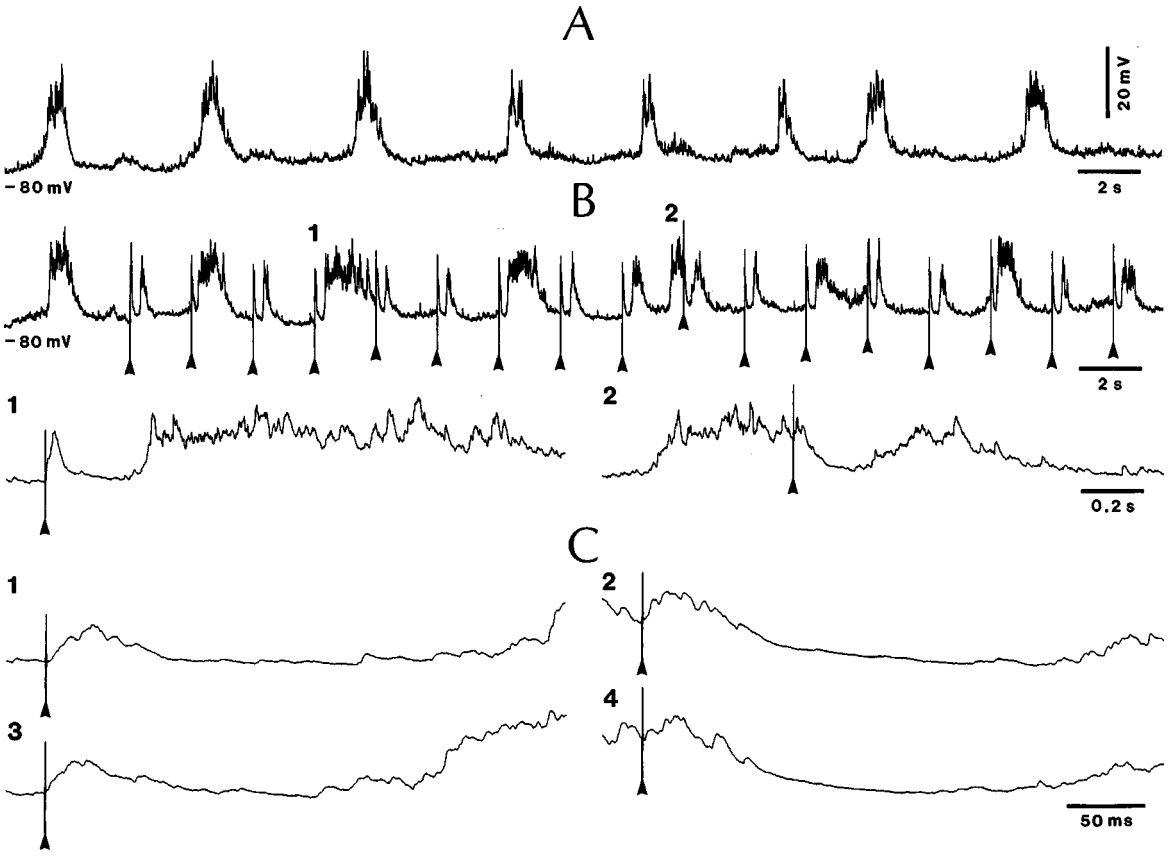

Fig. 3.30 Testing the responsiveness of cortical neurons during the depolarizing and hyperpolarizing phases of the slow oscillation. Cat under urethane anesthesia. Intracellular recording from area 5 neuron. *A*, slow oscillation at hyperpolarized V_m (−80 mV, without current). *B*, cortical stimuli were applied every 2 s, and they fell during the hyperpolarizing (1) or depolarizing (2) phase of the slow oscillation. Below, expanded responses. *C*, further expanded responses to stimuli during the hyperpolarizing phase (1, 3) and depolarizing phase (2, 4) of the slow oscillation. Unpublished data by M. Steriade, A. Nuñez, and F. Amzica.

[176] Contreras and Steriade (1995). See Fig. 1*C* in that paper, with a morphologically identified basket cell oscillating, during the slow rhythm, in phase with other types of cortical (pyramidal) neurons.

(see *3.2.2.2*), the "down-state" of the slow oscillation in neocortical neurons was demonstrated to be due to disfacilitation (removal of synaptic, mainly excitatory, inputs) in intracortical and thalamocortical networks, and to some K^+ currents, but not to active inhibitory processes. Data leading to this conclusion are discussed below.

Contrary to the expectation that inhibitory neurons would fire during the hyperpolarizing phase of the slow oscillation, neurons identified electrophysiologically as conventional fast-spiking cells [31] as well as morphologically as basket, aspiny cells [176], during either natural sleep (Fig. 3.31) or ketamine-xylazine anesthesia,

behave in phase with regular-spiking (pyramidal) neurons; namely, they fire during the depolarizing phase and are silent during the hyperpolarizing phase. Of more than 2000 cortical neurons recorded to date, we have only observed one neuron fire during the hyperpolarizing phase, and we could not identify the nature of that neuron [177].

In keeping with the above, intracellular recordings with Cl^--filled pipettes from naturally sleeping animals did not affect the prolonged hyperpolarizations of the slow oscillation in SWS [31, 178]. One example is illustrated in Fig. 3.31 and another one in Fig. 3.32, the latter also showing that recordings with Cs^+-filled pipettes reduced and often abolished the hyperpolarizing phase of the slow oscillation. Knowing that Cs^+ blocks non-specifically K^+ currents, a partial conclusion is that the hyperpolarizations during the slow oscillation are produced by a series of K^+ currents, most probably $I_{K(Ca)}$, as stimulation of cholinergic afferents blocks selectively the prolonged hyperpolarizations, even without changes in membrane potential [179] and ACh increases the excitability of cortical neurons by reducing some voltage- and Ca^{2+}-dependent K^+ currents [84, 165]. It should be noted, however, that a very short part in the initial phase of the long-lasting hyperpolarization was reduced when recording with Cl^--filled pipettes in anesthetized animals (see Fig. 8 in [166]), suggesting that, under anesthesia, the prolonged hyperpolarizations may be initiated by (but not entirely ascribed to) $GABA_A$-mediated IPSPs.

The other factor accounting for the prolonged hyperpolarizations is the disfacilitation of cortical networks. Indeed, in a sample of cortical neurons tested during natural sleep, the apparent input resistance (R_{in}) was almost double during the hyperpolarizing phase of the slow oscillation in SWS (30.8 $\pm$ 4.3 MΩ), compared to the depolarizing phase of this oscillation (16.8 $\pm$ 2.3 MΩ) (Fig. 3.33) [31]. This further indicates that GABAergic interneurons do *not* mediate the prolonged hyperpolarizations, as GABAergic hyperpolarizations are associated with increased membrane conductance. The increased R_{in} during the hyperpolarizing phase, compared to the depolarizing one, was also demonstrated under anesthesia [180], thus indicating that disfacilitation is the major mechanism underlying the prolonged hyperpolarizations. The disfacilitation might be explained by a progressive depletion of $[Ca^{2+}]_o$ during the depolarizing phase of the slow oscillation [181], which would produce a decrease in synaptic efficacy and an avalanche reaction that would eventually lead to the functional disconnection of cortical networks.

[177] Steriade et al. (1994b). At that time, we reported that in more than a thousand neurons tested, only one cell's discharges closely corresponded to the hyperpolarizing phases of other neurons. Since then we have investigated a further 1000 neurons, and we haven't observed any neocortical firing during the hyperpolarizing phase of the slow oscillation (see also below, note [199]).

[178] Timofeev et al. (2001b). This study was conducted on naturally sleeping cats. That the hyperpolarizations of the slow oscillations are reduced in amplitude a few minutes after impalement with Cs^+-filled pipettes was also reported in anesthetized animals [166].

[179] Steriade et al. (1993a).

[180] Contreras et al. (1996b).

[181] Massimini and Amzica (2001). Previous data have shown that a drop in $[Ca^{2+}]_{out}$ occurs during activation processes (Nicholson, 1980). This decrease is mainly due to Ca^{2+} inflow at the postsynaptic level (Heinemann and Pumain, 1981; Borst and Sakmann, 1999).

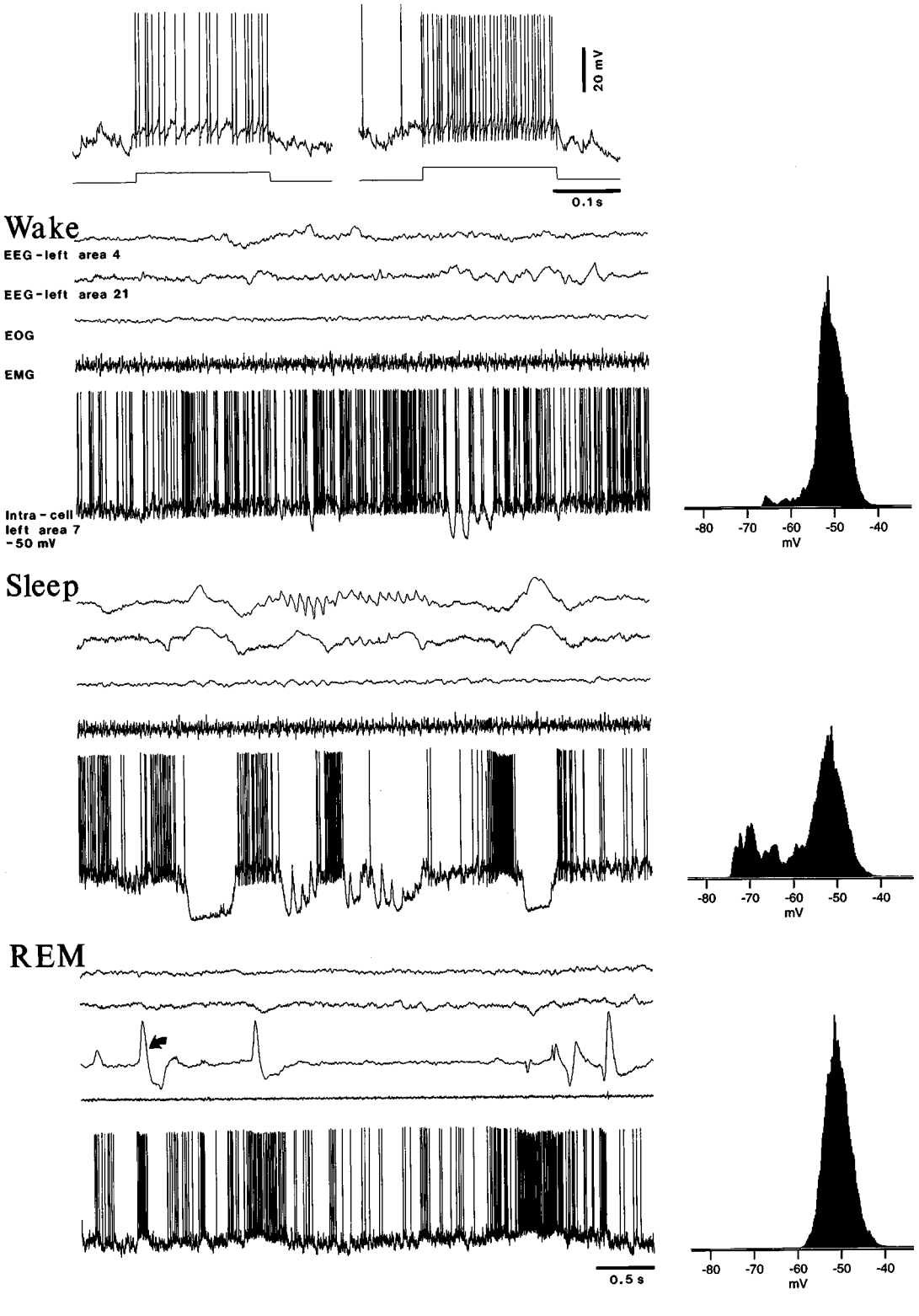
20 mV
0.1 s
Wake
EEG - left area 4
EEG - left area 21
EOG
EMG
Intra - cell
left area 7
- 50 mV
-80 -70 -60 -50 -40
mV
Sleep
-80 -70 -60 -50 -40
mV
REM
0.5 s
-80 -70 -60 -50 -40
mV

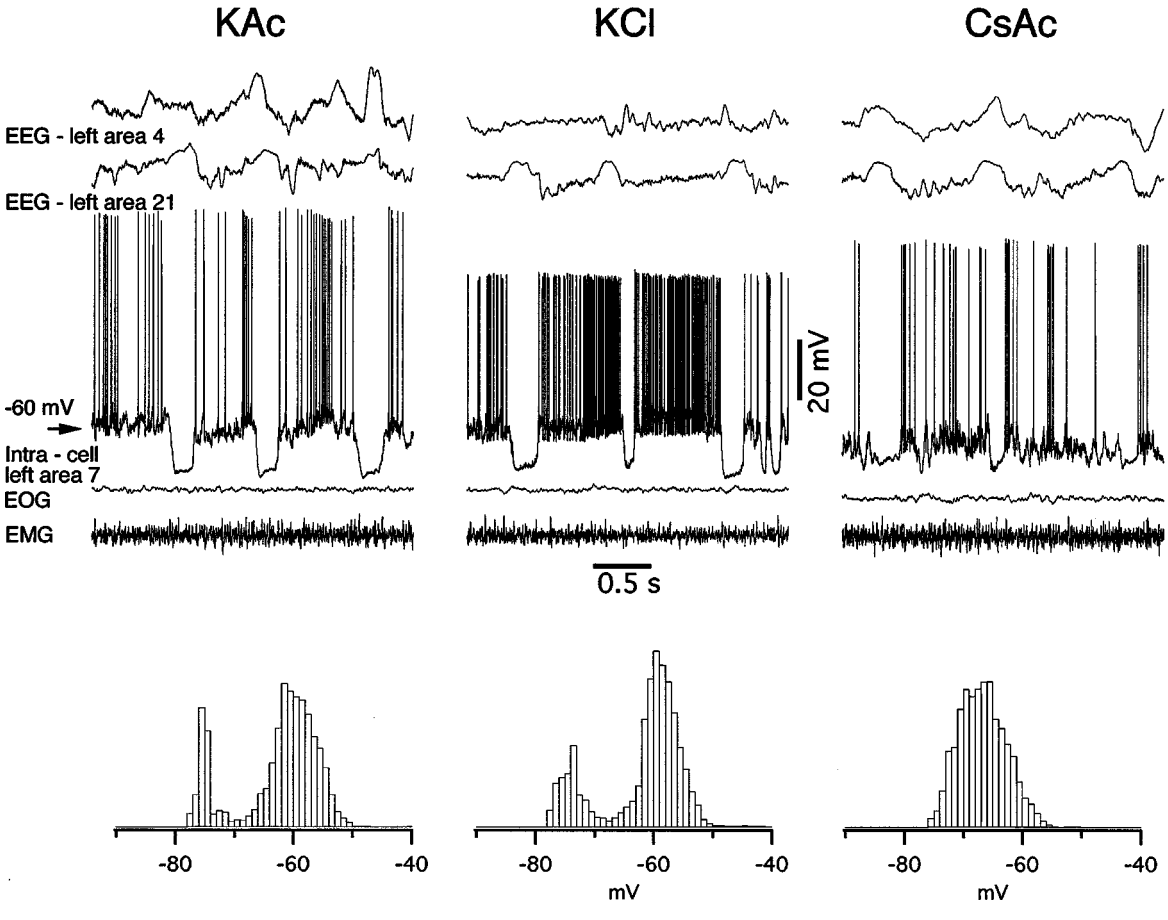

Fig. 3.32 Ionic nature of long-lasting hyperpolarizations during natural SWS. Chronically implanted cats. Periods of field potential and intracellular activities in three different cortical neurons from area 7 are shown during SWS. EEG from areas 4 and 21, EOG and EMG are also shown. *Left*, control recording with KAc-filled pipette. *Center*, pipette filled with KCl. *Right*, pipette filled with CsAc. Note that long-lasting hyperpolarizations are reduced or abolished by Cs^+, a non-specific blocker of K^+ currents, but not affected by Cl^-. Histograms represent membrane potential distribution. Note bimodal histogram in recordings with KAc and KCl, and unimodal histogram in recording with CsAc. Modified from Timofeev et al. (2001b).

Fig. 3.31 (opposite) Changes in membrane potential and firing patterns of conventional fast-spiking neuron during natural wake and sleep states. Intracellular recording in chronically implanted cat. Recording with KCl-filled pipette. *Top*, responses to two depolarizing current pulses (different intensities) showing fast and tonic firing without frequency adaptation (spike duration was <0.4 ms at half amplitude). *Below*, neuronal firing patterns during waking, SWS and REM sleep, as characterized by EEG, EOG and EMG activities. Tonic firing during waking and REM sleep was interrupted during SWS by long periods of hyperpolarizations and spindles, corresponding to EEG depth-positive waves and spindles. Note prolonged hyperpolarizations and silenced firing during SWS, similar to that of the regular-spiking neuron depicted in Fig. 3.26, despite the fact that this neuron was recorded with KCl-filled pipette (see also text). Also note increased firing rate during ocular saccade in REM sleep (arrow; this aspect is discussed in section ***3.3.1***). On the right, histograms of membrane potential during the three states of vigilance, showing Gaussian-like distribution, with a mode around −50 mV, during both waking and REM sleep, and a hyperpolarizing tail up to −75 mV during SWS. Modified from Steriade et al. (2001a).

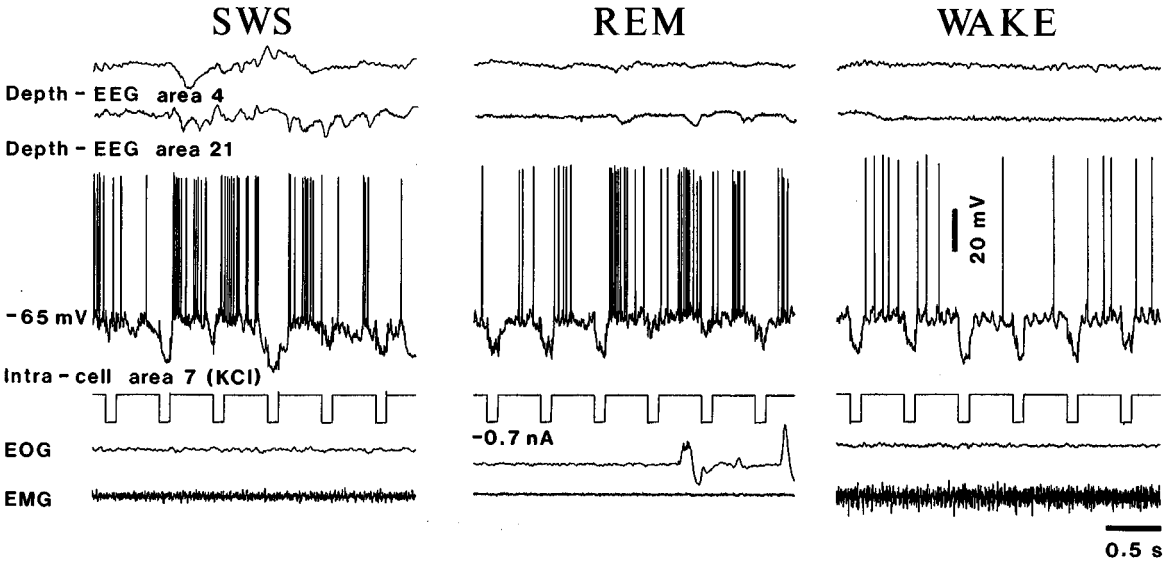
SWS
REM
WAKE
Depth - EEG area 4
Depth - EEG area 21
-65 mV
Intra - cell area 7 (KCl)
EOG
EMG
-0.7 nA
20 mV
0.5 s

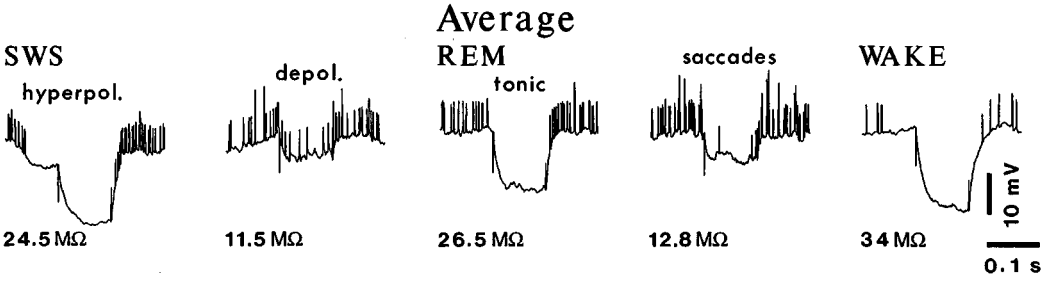
Average
SWS
hyperpol.
depol.
REM
tonic
saccades
WAKE
24.5 MΩ
11.5 MΩ
26.5 MΩ
12.8 MΩ
34 MΩ
10 mV
0.1 s

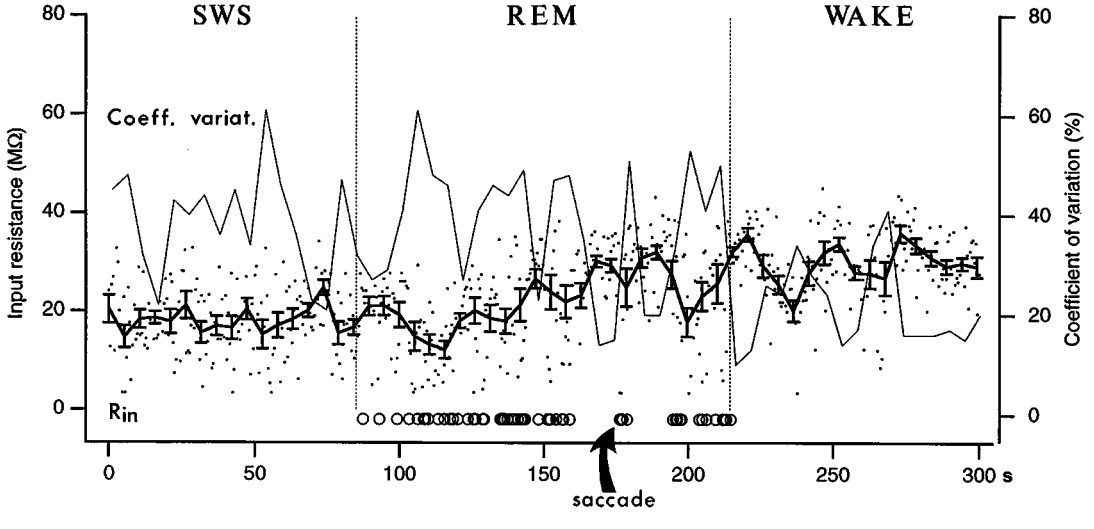
SWS
REM
WAKE
Coeff. variat.
Input resistance (MΩ)
Coefficient of variation (%)
Rin
saccade
0
20
40
60
80
0
50
100
150
200
250
300 s

[182] Amzica and Steriade (1998b, 2000).

[183] Amzica and Neckelmann (1999).

[184] Amzica et al. (2002); Amzica and Massimini (2002).

[185] Kang et al. (1998); Dzubay and Jahr (1999); Bezzi and Volterra (2001).

[186] Kettenmann and Schachner (1985). This study was done in cultured astrocytes.

The depolarizing and hyperpolarizing envelopes of the slow oscillation were also observed, with a different time-course, in cortical glial cells. Dual simultaneous intracellular recordings from neurons and adjacent glial cells were performed during sleep-like patterns produced by ketamine-xylazine anesthesia [182–184] to explore the possibility that glia may not only passively reflect, but also influence, the state of neuronal networks. A dialogue between neurons and glial cells is conceivable because different transmitters and modulators, such as glutamate, GABA, ACh, and norepinephrine, have been found to activate glia [185] and astrocytes release glutamate [147]. A typical response by simultaneous intracellular recordings of a neuron and a glial cell is illustrated in Fig. 3.34*C*–*D*. The neuronal response to a cortical stimulus consisted of an initial depolarization crowned by action potentials, an inhibitory potential, and a rebound excitation. The corresponding responses in the glia were a sluggish depolarizing slope, a further depolarization, and a negative wave, respectively. The fact that the neuronal IPSP is reflected in the glia by a depolarizing potential (Fig. 3.34*C*–*D*) may be explained by the opening of Cl^- channels in glia by $GABA_A$ action [186]. During spontaneously occurring slow oscillation in anesthetized animals, the onset of the depolarizing phase in neurons is followed, after a lag of ~90 ms, by the depolarization of simultaneously recorded, adjacent (1–2 mm) glial cells (Fig. 3.34*E*) [182–183]. Measurements of $[K^+]_{out}$ during the depolarizing phase of the slow oscillation indicate that glial cells phasically uptake part of the $[K^+]_{out}$ extruded by neurons [184]. Toward the end of the depolarizing phase, the glial membrane begins to repolarize before neurons. In view of the fact that the maximal glial depolarization is reached much later than the end of neuronal depolarization and that the glial membrane potential returns to the control value at the end of the slowly recurring oscillatory cycles, glial cells might control the pace of the oscillation through changes in $[K^+]_{out}$, which is known to modulate neuronal excitability.

Fig. 3.33 (opposite) Apparent input resistance (R_{in}) of neocortical neurons during natural states of vigilance. Chronically implanted cat. Upper panel shows three periods of intracellular recording from the same regular-spiking neuron during SWS, REM sleep, and waking (recording was done in this order). R_{in} was measured by applying 0.1-s hyperpolarizing current pulses, every 0.5 s. Below, averages of responses of this neuron during different epochs in the three states of vigilance (note differences between the hyperpolarizing and depolarizing phases of the slow oscillation in SWS; and between epochs with and without ocular saccades in REM). The plot at bottom shows the dynamic changes of R_{in} during the three states of vigilance, obtained from continuous recording throughout the sleep-waking cycle. Dots represent individual measurements of R_{in}; thick line and SD bars are the means of R_{in} from every 10 consecutive measurements; thin line is the coefficient of variation from corresponding periods; circles indicate ocular saccades in REM sleep. Note that, during quiet wakefulness, R_{in} increased and this increase was associated with a decrease in the coefficient of variation. From Steriade et al. (2001a).

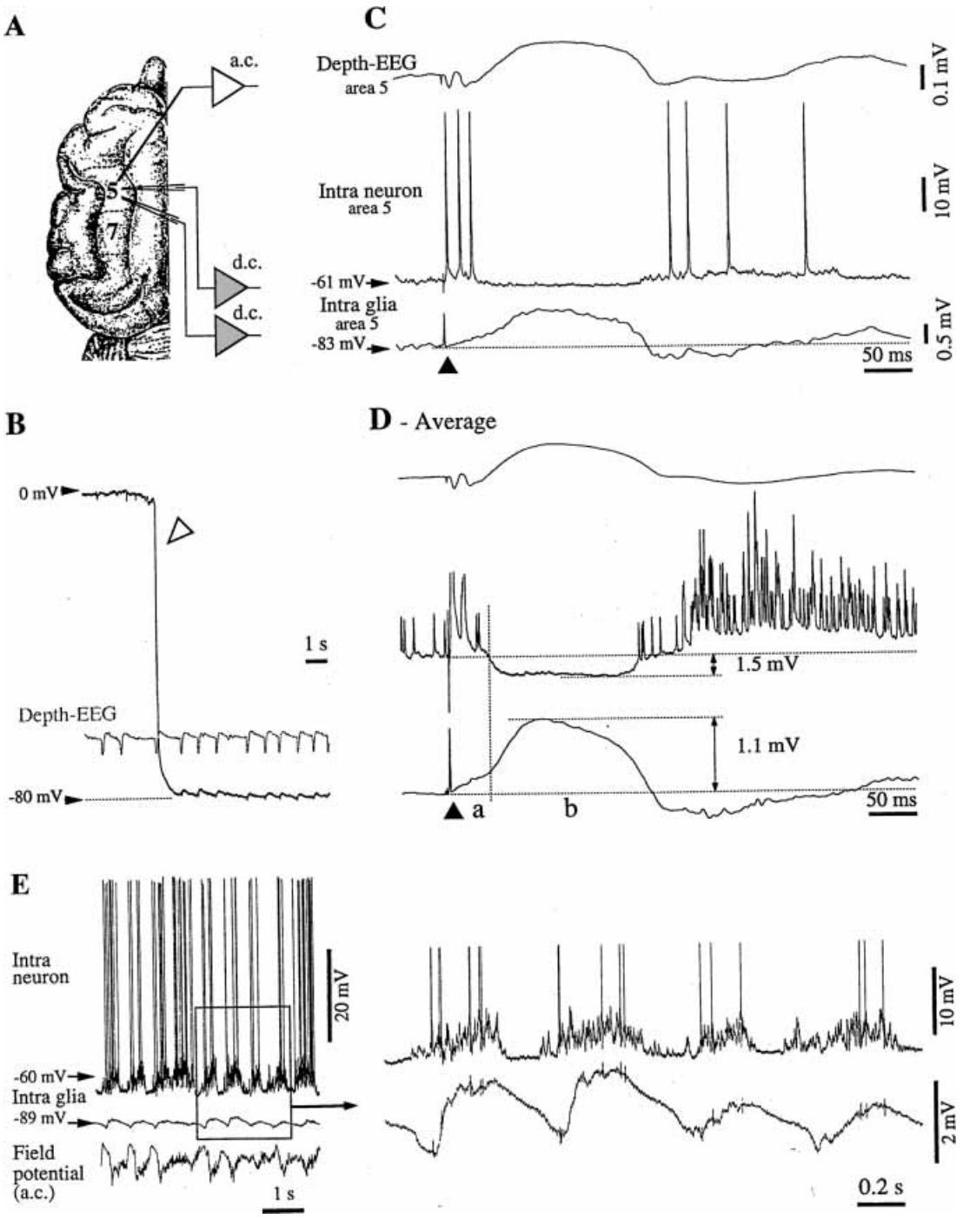

Fig. 3.34 Responsiveness to cortical stimulus and spontaneously occurring slow oscillation in cortical neuron and glial cell. Dual simultaneous recordings in cat under ketamine-xylazine anesthesia. *A*, top view of cat's brain with the localization of association areas 5 and 7 in the suprasylvian gyrus. *B*, impalement of a glia cell is marked (open arrowhead) by a sudden voltage deflection from extracellular potential values (~0 mV) to −80 mV. Intraglial potentials (slow depolarizations) are reversed with respect to the extracellular ones. *C*, dual intracellular (neuron and glia) and field potential recording in cortical area 5. Response to a single cortical stimulus (black triangle) delivered close to the field electrode. The recordings sites correspond to those indicated in *A*. See text for description of responses. *D*, average of 25 responses evoked by cortical stimulation. The initial glial depolarization (*a*) is clearly separated from the following positive wave (*b*) by a change in the depolarizing slope. *E*, slow oscillation in simultaneously recorded neuron and glial cell. Modified from Amzica and Steriade (2000, *A–D*) and Amzica and Neckelmann (1999, *E*).

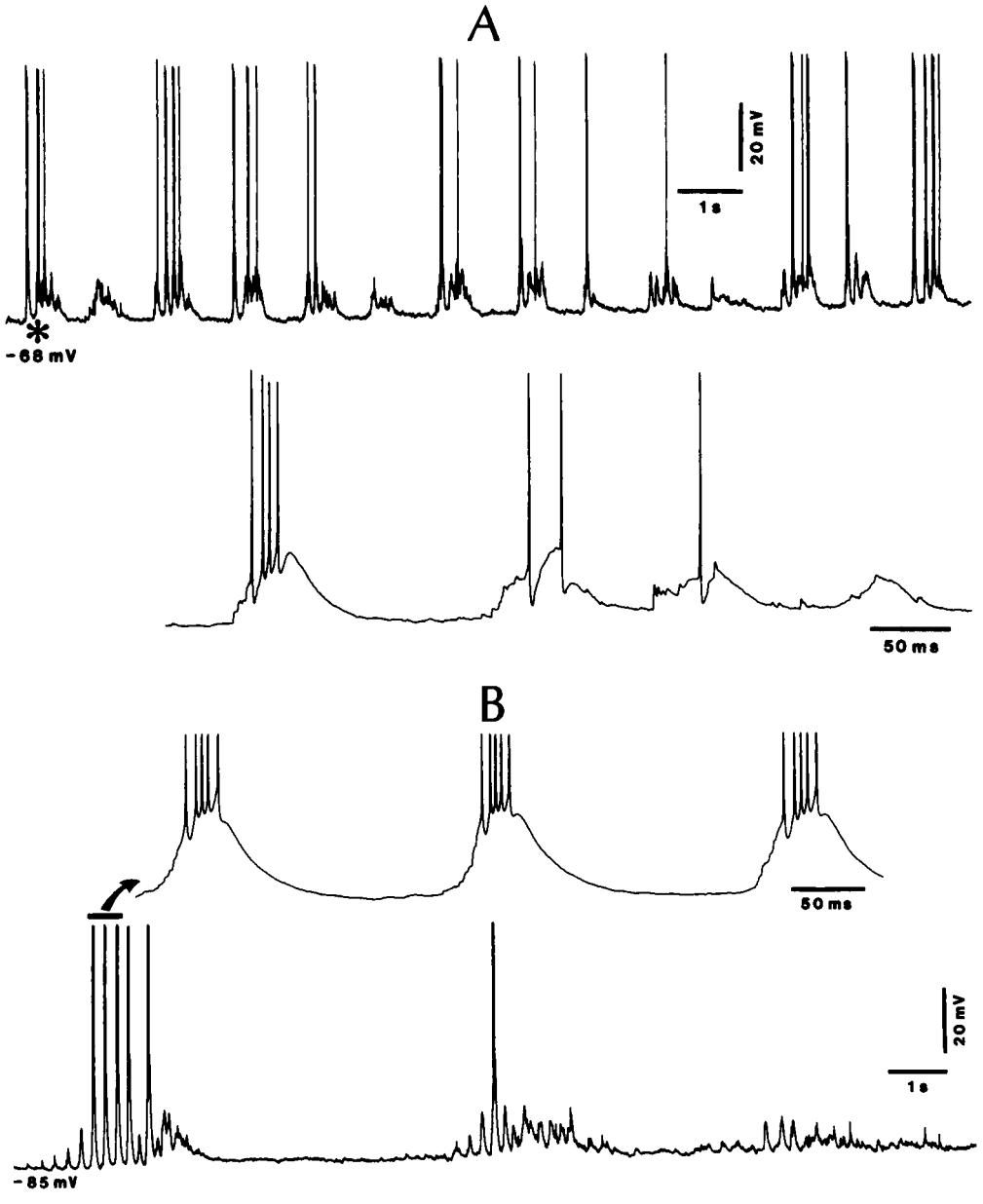

Fig. 3.35 Slow oscillation associated with spindle oscillations in thalamic RE neurons. Cat under ketamine-xylazine (*A*) and urethane (*B*) anesthesia. *A*, neuron displaying slowly recurring (0.9 Hz) depolarizations consisting of oscillations at 8 Hz (spindle frequency range). Depolarizing phase marked by asterisk is expanded below. *B*, another RE neuron, oscillating at 0.2 Hz, with waxing and waning depolarizing events at ~5 Hz. Part marked by horizontal bar is expanded above (spikes truncated). From Steriade et al. (1993b).

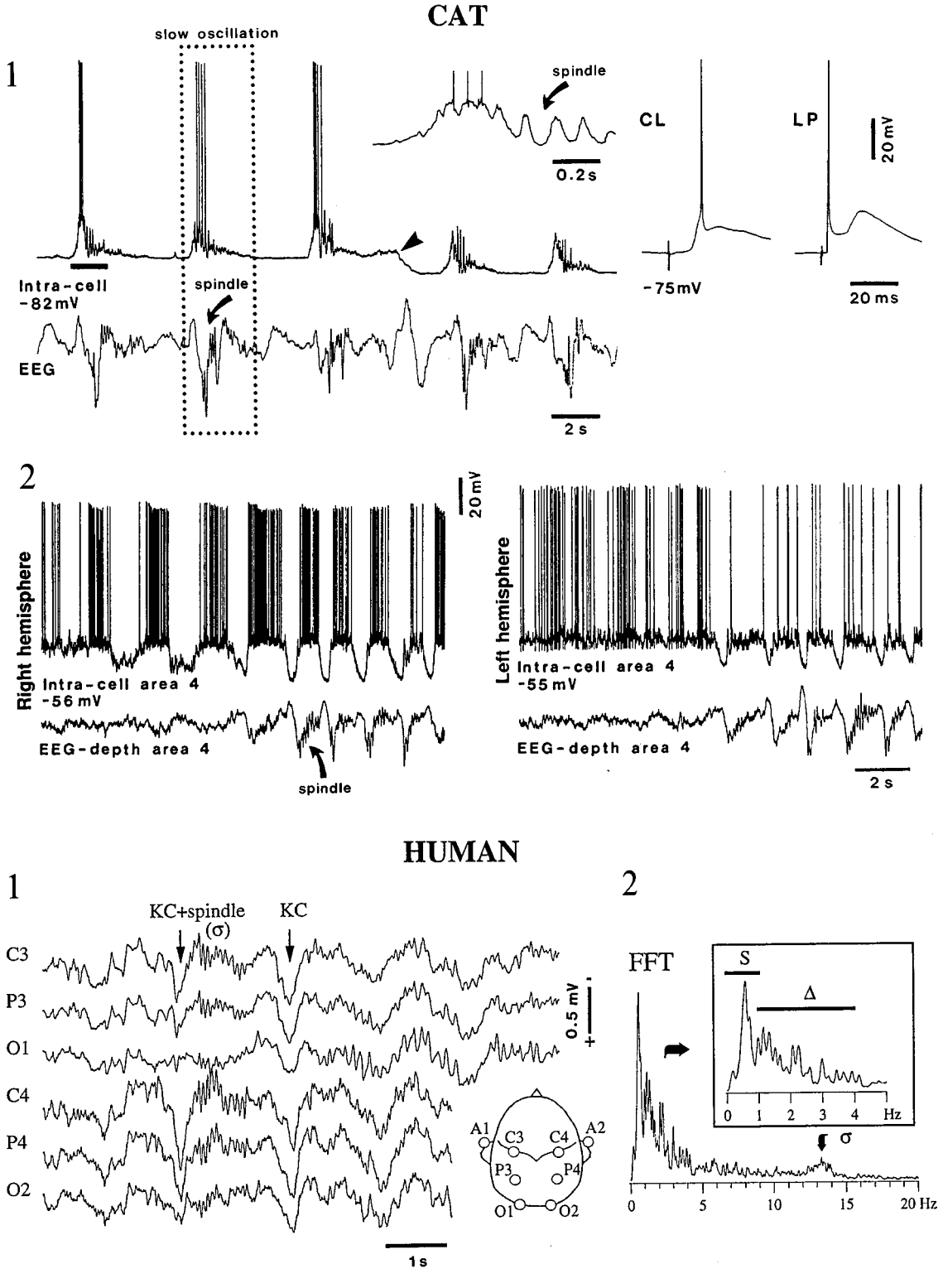
CAT
1
slow oscillation
spindle
0.2s
CL
LP
20 mV
Intra-cell
-82mV
spindle
-75mV
20 ms
EEG
2 s
2
20 mV
Right hemisphere
Intra-cell area 4
-56 mV
EEG-depth area 4
spindle
Left hemisphere
Intra-cell area 4
-55 mV
EEG-depth area 4
2 s
HUMAN
1
KC+spindle
(σ)
KC
C3
P3
O1
C4
P4
O2
0.5 mV
A1
C3
C4
A2
P3
P4
O1
O2
1s
2
FFT
S
Δ
0 1 2 3 4 Hz
σ
0 5 10 15 20 Hz

[187] Futamachi et al. (1974).

[188] Steriade et al. (1993b).

During the slow sleep oscillation, the $[K^+]_{out}$ amplitude reaches 1–2 mM, which, when added to the physiological values of resting concentration (~3 mM) [187], may assist cortical neurons in oscillating between hyper- and hypoexcitability. The possible role of glia in pacing normal oscillatory activities and in the development from sleep rhythms to seizure episodes is discussed in Chapter 5 (section **5.10**).

3.2.3.2. The slow oscillation groups spindles, delta, fast, and ultra-fast rhythms

Unlike "pure" rhythms within distinct frequency bands, generated in restricted circuits of extremely simplified preparations, such as slices maintained *in vitro*, the living brain does not generally display separate oscillations during SWS, but a real coalescence of slow oscillation with other sleep rhythms as well as with fast rhythms that are conventionally thought to define activated states.

The fact that the cortical slow oscillation is also observed in thalamic RE neurons, with the same characteristics of depolarizing-hyperpolarizing sequences [188], suggests that the synchronous firing of cortical neurons during the depolarizing envelope would impinge upon RE neurons, create conditions for the formation of spindles (Fig. 3.35), and transfer the latter to thalamocortical systems. The efficacy of corticothalamic projections acting on GABAergic RE neurons [121] is known from studies combining electron microscopy and analysis of EPSCs [122]. These connectivity and functional features explain why a cycle of the slow oscillation is followed by a brief sequence of spindles in TC neurons as well as in the cortical EEG [176] (Fig. 3.36, *CAT*).

The sequence of grapho-elements consisting of an ample surface-positive transient, corresponding to the excitation in deeply

Fig. 3.36 (opposite) The cortical slow oscillation groups thalamically generated spindles. *CAT 1*, intracellular recording in cat under urethane anesthesia from area 7 (1.5 mm depth). Electrophysiological identification (on the right) shows an orthodromic response to stimulation of the thalamic centrolateral (CL) intralaminar nucleus and an antidromic response to stimulation of the lateroposterior (LP) nucleus. Note the slow oscillation of neuron and related EEG waves. One cycle of the slow oscillation is framed in dots. Part marked by horizontal bar below the intracellular trace (on the left) is expanded above (on the right) to show spindles following the depolarizing envelope of the slow oscillation. *CAT 2*, dual simultaneous intracellular recordings from right and left cortical area 4. Note spindle during the depolarizing envelope of the slow oscillation and synchronization of EEG when both neurons synchronously display prolonged hyperpolarizations. *HUMAN*, the K-complex (KC) in human natural sleep. Scalp monopolar recordings with respect to the contralateral ear are shown (see figurine). Traces show a short episode from a stage 3 non-REM sleep. The two arrows point to two K-complexes, consisting of a surface-positive wave, followed (or not) by a sequence of spindle (sigma) waves. Note the synchrony of K-complexes in all recorded sites. On the right, frequency decomposition of the electrical activity from C3 lead into three frequency bands: slow oscillation (S, 0 to 1 Hz), delta waves (Δ, 1 to 4 Hz) and spindles (σ, 12 to 15 Hz). Modified from Steriade et al. (1993f and 1994b, *CAT*) and from Amzica and Steriade (1997, *HUMAN*).

[189] Loomis et al. (1938); Roth et al. (1956); Niedermeyer (1993).

[190] Amzica and Steriade (1997, 1998a).

[191] Grey Walter (Walter, 1936) first used the term delta waves and assigned it to pathological potentials due to cerebral tumors. IFSECN (1974) considers delta waves as waves with a duration of more than 250 ms, thus implying a frequency band between 0 and 4 Hz. In reality, there are several oscillatory types within this frequency band, and delta (1–4 Hz) and slow (0.5–1 Hz) oscillations are quite distinct phenomena, with different underlying sites of genesis and electrophysiological mechanisms, both in animals and humans.

lying cortical neurons, followed by a slower, surface-negative component and eventually a few spindle waves represents this combination between the slow and spindle oscillation, and is usually termed the K-complex (Fig. 3.36, *HUMAN*). This is a reliable sign for stage 2 of human sleep, but it is apparent in all stages of quiet sleep [189]. We analyzed this landmark of EEG sleep in humans and investigated its cellular substrates in cats [190]. Spectral analysis in humans (Fig. 3.36) demonstrated the periodic recurrence of human K-complexes, with main peaks at 0.5–0.7 Hz, reflecting the slow oscillation (S); the other frequency band (1–4 Hz) represents delta activity (Δ); and 12–15 Hz reflects the presence of spindles (σ). The laminar profile and intracellular substrates of the K-complex during sleep or anesthesia of cats revealed that the surface-recorded, positive K-complexes reverse at a cortical depth of about 0.3 mm, and that the sharp depth-negative (surface-positive) wave of the K-complex is associated with cells' depolarizations, eventually leading to a spindle sequence.

These investigations indicate that the K-complexes are the expression of the *spontaneously* occurring, cortically generated slow oscillation. Of course, K-complexes may also be triggered by sensory stimuli [189], though such evoked events are the exception considering that sleep usually occurs in environments free of auditory or other stimuli. Through their shape, K-complexes contain spectral components belonging to the delta band. There is uncertainty in the literature as to whether delta activity should be considered as *waves* or *rhythm*. Generally, delta is used to designate waves that last more than 250 ms [191]. As to the rhythmicity of K-complexes, whose shape contribute to the delta band, they are less frequent and less rhythmic during early sleep stages, and become more numerous and rhythmic (<1 Hz) during the full expression of the slow oscillation in deeper sleep stages [190]. This may explain why some investigators consider deep SWS as equivalent to delta sleep.

The slow oscillation is related to both (thalamic and cortical) types of delta activities in several ways.

(1) Firstly, each synchronous corticothalamic volley that originates in the synchronous firing of cortical neurons during the slow oscillation excites directly and inhibits indirectly (via GABAergic thalamic RE neurons) TC neurons, which were set at the required hyperpolarized membrane potential to generate the clock-like delta oscillation (see *3.2.2.1*). Depending on the strength and frequency of this corticothalamic input, the effect may be synchronization of simultaneously delta-oscillating TC

neurons (see Fig. 3.23*B*) or the grouping of clock-like potentials in TC neurons within the frequency range of the slow oscillation. The grouping of clock-like delta rhythm in TC cells is due to PSPs of cortical origin. This corticofugal grouping effect can be observed with spontaneously occurring delta oscillation in TC neurons (Fig. 3.37) and with delta oscillation resulting from hyperpolarizing current pulses in TC neurons (Fig. 3.38).

(2) Secondly, when pools of delta-oscillating single TC neurons are synchronized, their clock-like activity is reflected at the cortical level and seen in conjunction with the slow oscillation (Fig. 3.39*A*).

(3) The depolarizing phase of the slow oscillation is composed of activity in the delta frequency range [182, 192]. The combined slow and delta oscillations in a bursting cell and in two, simultaneously recorded, cortical neurons are illustrated in Fig. 3.39*B-C*.

Besides the coalescence between the slow cortical oscillations and other low-frequency sleep rhythms, fast (20–60 Hz) or ultra-fast (80–200 Hz) rhythms develop over the depolarizing phase of the slow oscillation under deep anesthesia as well as during natural SWS [193, 194].

The presence of fast waves within the beta and gamma frequency bands (generally 20–60 Hz) over the depolarizing phase of the slow sleep oscillation may be surprising for those who relate unequivocally these fast rhythms with states of cognition and consciousness. In reality, fast rhythms occur as a function of membrane depolarization in thalamic and cortical neurons. The depolarization phase associated with fast rhythms characterizes the slow oscillation during natural SWS or deep anesthesia (see details in section 3.3).

As to ultra-fast rhythms (80–200 Hz but even higher frequencies), also termed *ripples*, they occur during the depolarizing phase of the slow oscillation in neocortical neurons [194]. Similar rhythms were found in the hippocampus and perirhinal cortex, associated with bursts of sharp potentials during anesthesia, behavioral immobility and natural sleep [195]. The independence of neocortical ripples from hippocampal ones was demonstrated by the presence of this oscillation in isolated neocortical slabs [194]. The association of ripples with different forms of paroxysmal activities in animals and humans is discussed in Chapter 5.

Ripples appear at about the same time in different neocortical foci and cross-correlations between field potentials show time-lags varying from ~0.7–1.2 ms down to virtually zero time difference

[192] Steriade (1997a). The fact that the slow oscillation has the virtue of grouping other sleep rhythms is supported by recent results of selective deprivation of slow-wave sleep in humans (Ferrara et al., 2002). These authors found generalized increases in EEG power after sleep deprivation, indicating the coalescence of different frequency bands, which are usually described in isolation by clinical electroencephalographers but have recently been demonstrated to represent the coherency of various oscillatory types in corticothalamic neuronal loops (see main text). See also Mölle et al. (2002).

[193] Steriade et al. (1996a-b). In addition to this work performed in various neocortical areas, the association of slow oscillation and fast rhythms in the gamma band (~30 Hz) was also found in the perirhinal cortex and lateral amygdala (Collins et al., 2001).

[194] Grenier et al. (2001).

[195] Chrobak and Buzsáki (1996); Collins et al. (1999); Csicsvari et al. (1998, 1999). Ripples or even higher-frequency (>200 Hz) potentials were also found associated with neocortical high-voltage spindles or spike-and-wave patterns in rat (Kandel and Buszáki, 1997) and in sensory-evoked potentials in barrel cortex (Jones and Barth, 1999). The relation between hippocampal ripples and cortical spindles was demonstrated in rats (Siapas and Wilson, 1998). This coactivation of hippocampal and neocortical pathways was implicated in the process of consolidation from short-term memory in hippocampus to longer-term memory in neocortical areas.

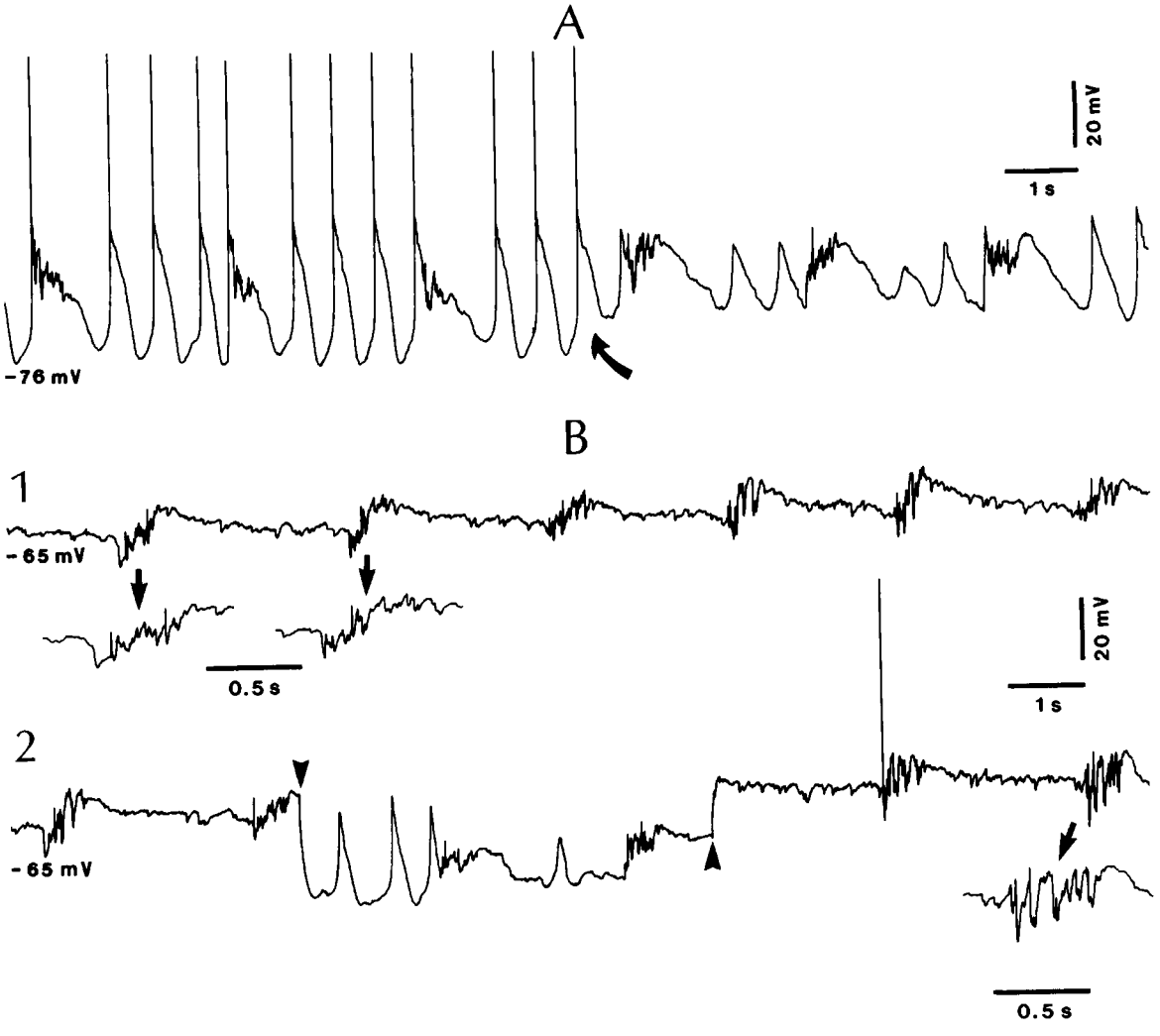

Fig. 3.37 Effect of slow cortical oscillation (0.4 Hz) on clock-like delta oscillation in TC neurons. Intracellular recordings in cats under urethane anesthesia. *A*, delta oscillation (1.5–2 Hz) occurred when the V_m was more negative than −75 mV (cell held under DC hyperpolarization of −0.4 nA) and was suppressed by bringing the neuron at its resting V_m (oblique arrow). The same neuron also displayed a slow oscillation (0.35 Hz) consisting of PSPs sequences of cortical origin. *B*, another neuron showing the slow rhythm of PSPs at the resting V_m (*1*). In *2*, a hyperpolarizing current pulse (−0.3 nA, between arrowheads) induced three cycles of delta oscillation, quickly prevented by the appearance of fast PSPs of cortical origin. At the extreme right in *2*, slight depolarization (+0.1 nA) revealed that the majority of fast PSPs of slowly recurring sequences were IPSPs. Three downward arrows point to expanded sequences of fast PSPs at the resting V_m (in *1*) and at a slightly depolarized level (right part in *2*). From Steriade et al. (1993b).

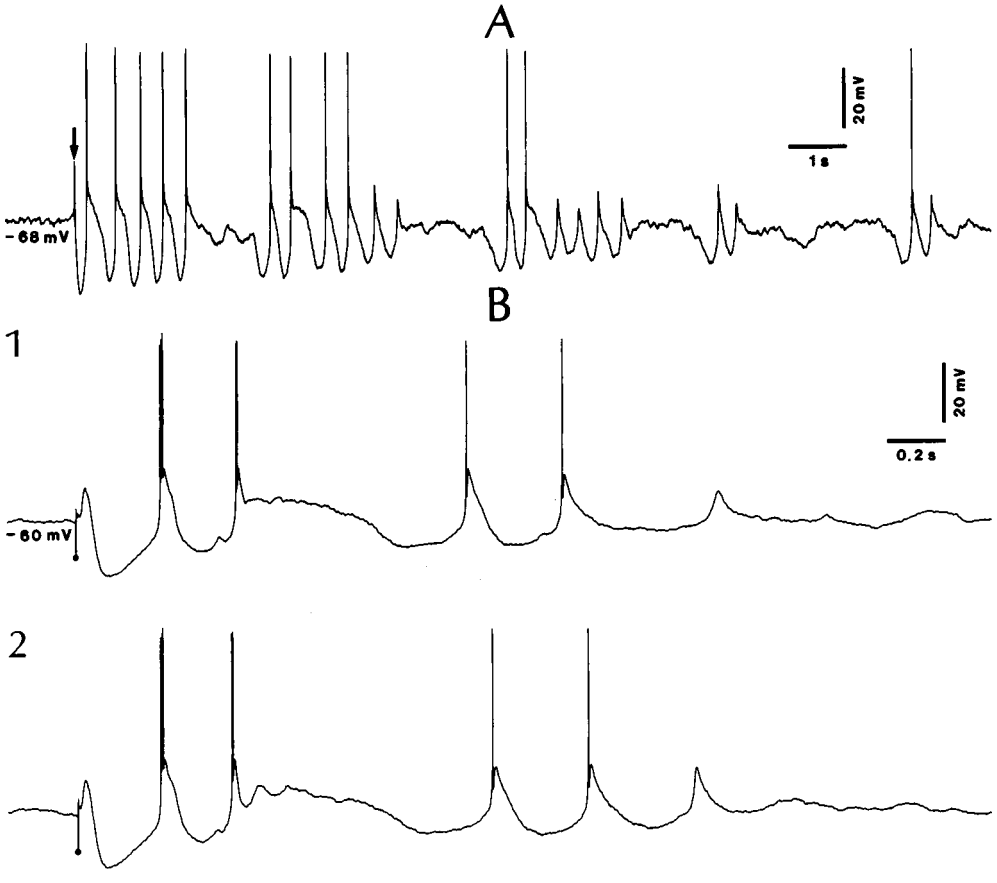

Fig. 3.38 Grouping of clock-like delta potentials in TC neurons within the frequency of cortical slow oscillation. Intracellular recording of thalamic ventrolateral (VL) neuron in cat under urethane anesthesia. *A*, hyperpolarizing current pulse (−0.6 nA, arrow) from resting V_m induced clock-like delta oscillation (2.5 Hz) that tended to dampen and periodically revived within the frequency of the slow rhythm (~0.3 Hz). *B*, same neuron. Stimulation of postcruciate cortical area 4 induced delta oscillation (3–4 Hz), dampening and reappearing periodically. From Steriade et al. (1993b).

that can be ascribed to averaging (Fig. 3.40). The synchronous occurrence of ripples is explained by their strict relation with the depolarizing phase of the slow oscillation, corresponding to the depth-negative field potentials, and the fact that the slow oscillation was found to be coherent in different, adjacent but also distant, cortical areas [196]. The dependence of ripples on neuronal depolarization was demonstrated using intracellular recordings of different neuronal types [194]. A strong relation was found between ripples in filtered field potentials (80–200 Hz) and neuronal depolarization leading to firing and, among all cellular types, fast-rhythmic-bursting (FRB) and fast-spiking (FS) neurons fired at higher

[196] Amzica and Steriade (1995b). The intrinsic circuitry of cat suprasylvian gyrus, in which these experiments were conducted, accounts for more than 70% of the synapses (Grüner et al., 1974; Avendaño et al., 1988). Within this gyrus, monosynaptic responses between rostral and caudal sites have been demonstrated by means of dual intracellular recordings from areas 5 and 7 [172] (see also Chapter 2, ***2.4.2***). Other neocortical areas are also linked by means of reciprocal connections. The horizontal projections of pyramidal and local-circuit neurons allow communication between neurons in various sensory and motor fields (Jones et al., 1978; Gilbert, 1992).

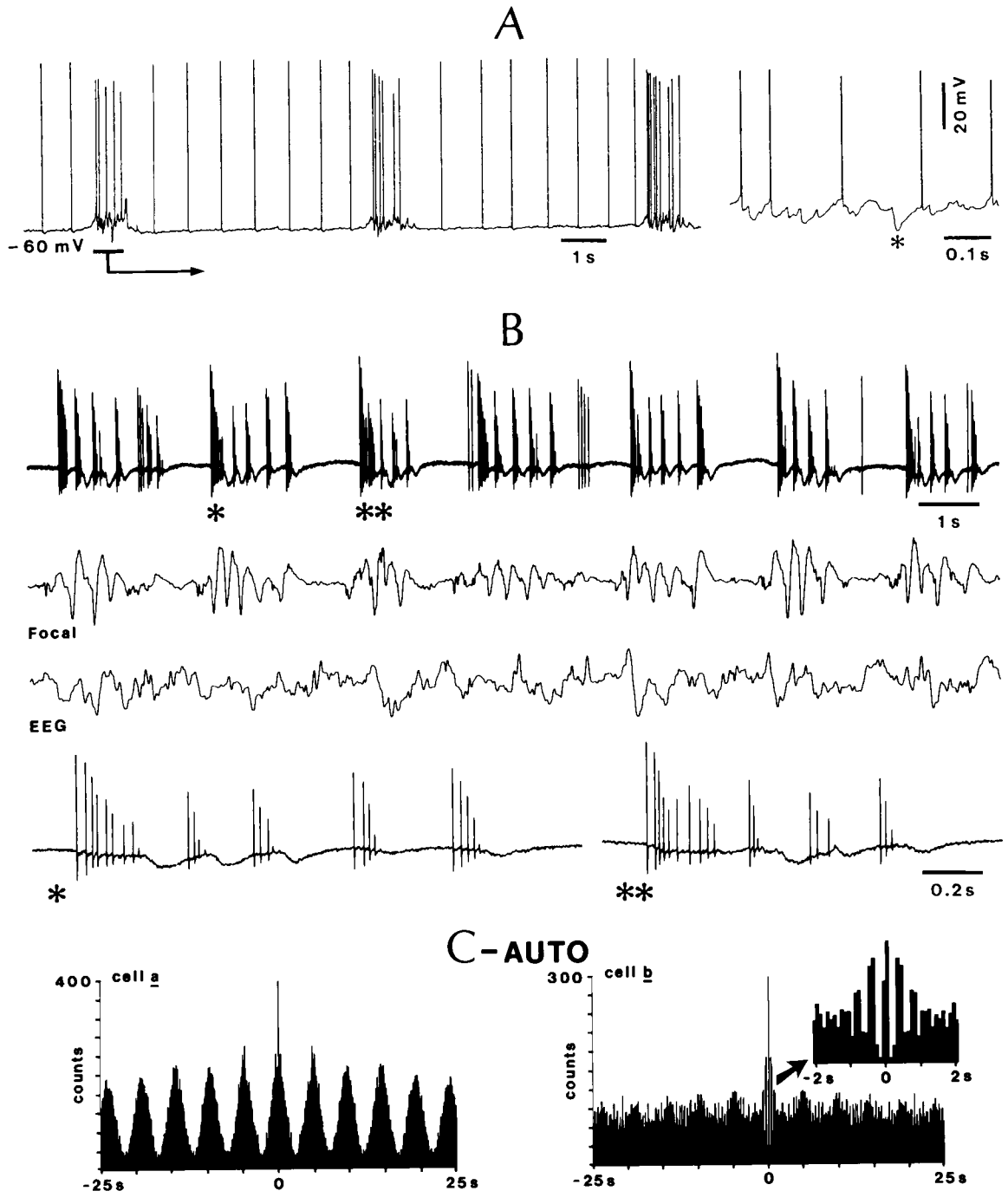

Fig. 3.39 Combined slow (<1 Hz) and delta (1–4 Hz) oscillations in neocortex. Cats under urethane anesthesia. *A*, clock-like delta activity, generated in the thalamus (see text), occurs between depolarizing cycles of slow oscillation in a neuron from area 5. Period marked by horizontal bar is expanded on the right to show an IPSP (asterisk) during the depolarizing phase of the slow oscillation. *B*, extracellular recording of a bursting neuron at 0.6 mm in suprasylvian area 7, convergently excited by stimulation of lateroposterior (LP) and centrolateral (CL) thalamic nuclei. Below the cellular traces, focal waves (field potentials) recorded through the same micropipette and EEG waves recorded from the cortical surface are depicted. The sequences of spike-bursts marked by one or two asterisks are expanded below. Note delta waves grouped by the slow rhythm. *C*, autocorrelogram (AUTO) of two (*a* and *b*) neurons recorded simultaneously by the same extracellular microelectrode at a depth of 1.3 mm in motor area 4. Autocorrelograms (0.1 s bin width) show the slow rhythm in both cells. The delta rhythm (2.5 Hz) within the slowly (0.2 Hz) recurring discharge sequences in cell *b* is depicted in the expanded inset (arrow). Modified from Steriade et al. (1993f).

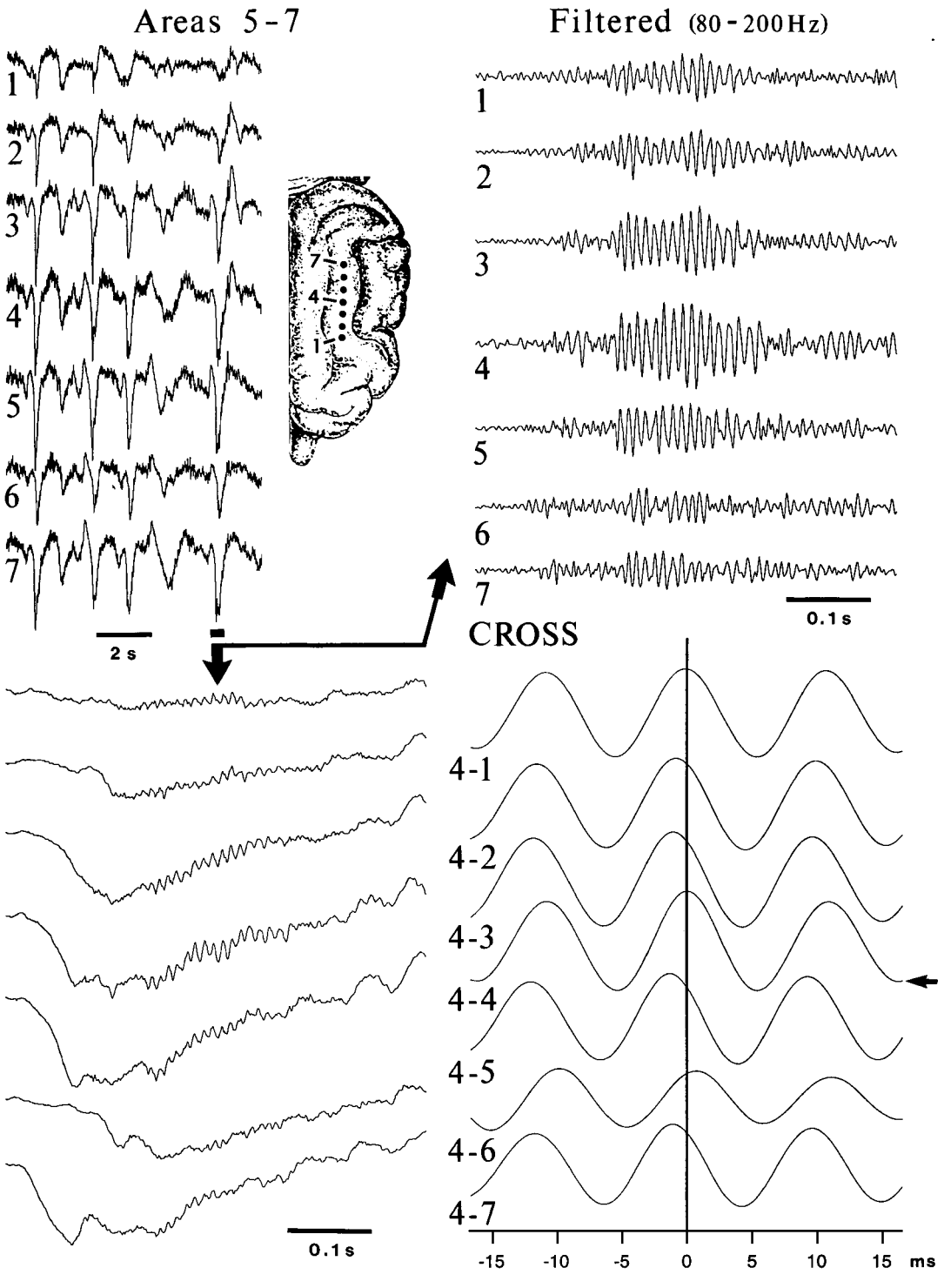

Fig. 3.40 Synchronization of ripples (80–200 Hz) during the slow sleep oscillation. Cat under ketamine-xylazine anesthesia. Field potential recordings from the depth (~1 mm) of areas 5 and 7. Seven electrodes, separated by 1.5 mm, were aligned along the antero-posterior axis (see brain figurine). *Top left* panel displays the slow sleep oscillation (0.8–0.9 Hz), synchronous in the seven different leads. One cycle of the slow oscillation is expanded at *bottom left*; ripples are superimposed on the late part of the depth-negativity. The trace of the same epoch was filtered between 80 and 200 Hz to illustrate only ripples (*top right*). Cross-correlations between point 4 and other recorded foci, as well as autocorrelation (4-4), are displayed at *bottom right*. Note that activity from various recorded foci is correlated, with time-lags varying from ~0.7–1.2 ms down to virtually zero time difference (4-1). From Grenier et al. (2001).

[197] It was also reported that, in the hippocampus, the phase relation between intracellular recordings of pyramidal cells and field ripples was modified when recordings were made with KCl-filled pipettes (Ylinen et al., 1995; see Fig. 3.42 for the same phenomenon in neocortex). The generation of fast rhythms has also been ascribed to axo-axonal gap junctions between principal cells in hippocampal slices (Draguhn et al., 1998; Traub et al., 1999b). Sensory-evoked very fast oscillations (400–600 Hz) in the rat barrel cortex were reported to be due to synchronous firing of fast-spiking neurons (Jones et al., 2000).

frequencies than regular-spiking (RS) and intrinsically bursting (IB) neurons (see characteristics of these neuronal classes in Chapter 2). Figure 3.41 shows progressively increased amplitude of ripples in field potentials with increased depolarization of an FRB neuron during the slow oscillation. This phenomenon was observed in a great majority of recordings, for all neuronal classes, and the relation between the membrane potential and the normalized amplitude of ripple oscillation showed that, when a period was associated with high amplitude of ripples, the membrane potential had a stronger tendency towards depolarized levels than when the ripple amplitude was closer to zero. Even though gamma oscillations (generally 30–60 Hz, but up to 80 Hz) are usually associated with tonic activation of cortical networks, the tendency to depolarization during gamma oscillations was never as strong as with the faster (80–200 Hz) ripples [194].

The presence of inhibition during ripples, even though they are associated with neuronal depolarization and firing, was revealed with dual intracellular recordings from pairs of very close neurons (<0.5 mm), in which one recording pipette was filled with potassium-acetate (KAc, to control the state of the network) and the other one with potassium-chloride (KCl, to reverse Cl^--mediated $GABA_A$ IPSPs) (Fig. 3.42). Firing probability increased with increasing ripple amplitude for both cells, but more so for the cell recorded with a KCl-filled pipette. Spike-triggered averages of filtered EEG traces (80–200 Hz) revealed that action potentials in the RS cell recorded with KAc occurred around 1 ms before the peak negativity of the field potential but, in contrast, the relation between the firing of cell 2 (KCl-filled pipette) and the ripple cycle was shifted by about 4 ms. This suggests that $GABA_A$ inhibition is involved in the precise timing of firing during ripple oscillations. The possible involvement of inhibition in the phase-locking of neurons during ripples was corroborated by the increased activity of FS neurons in relation to ripples [197].

In summary, the depolarizing phase of the cortical slow sleep oscillation is reflected as a depth-negative (surface-positive) field potential, termed K-complex. This excitatory component is associated with the presence of fast and ultra-fast rhythms, which are voltage (depolarization) dependent. The synchronous firing of neocortical neurons (among them corticothalamic neurons that have access to both RE and TC neurons) during the excitatory phase of the slow oscillation is effective in grouping cortically generated delta waves, thalamically generated clock-like delta potentials, and in producing a widespread synchronization of spindles in thalamocortical

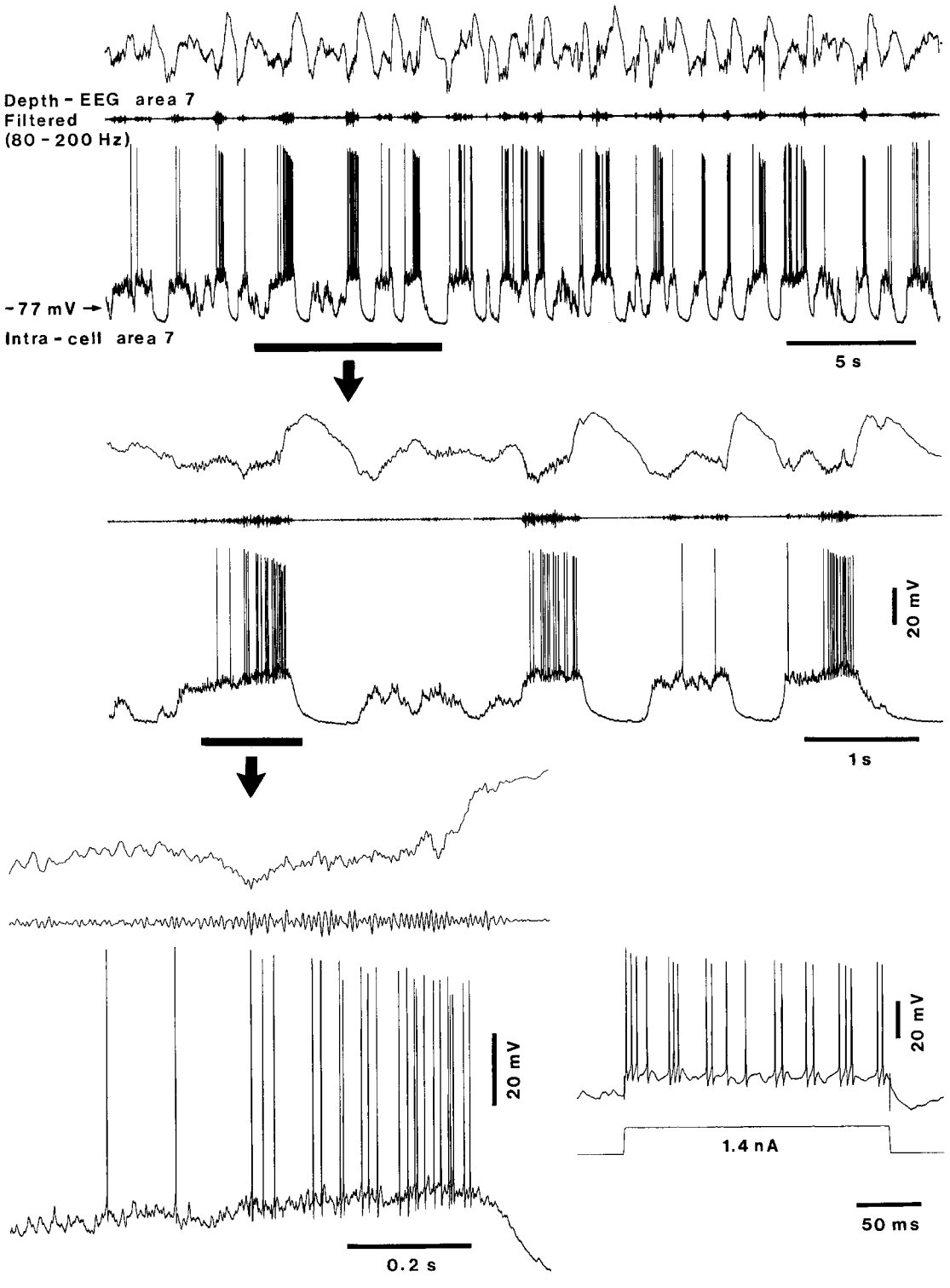

Fig. 3.41 Progressively increased amplitude of ripples with increased depolarization of cortical neurons during the slow oscillation under ketamine-xylazine anesthesia. Intracellular and depth-EEG recordings from cat area 7. *Top panel* illustrates an epoch with the slow oscillation (0.6–0.7 Hz). Fast-rhythmic-bursting (FRB) neuron; see electrophysiological identification of this neuronal type at *bottom right* (see also Chapter 2). Below the EEG trace, a filtered trace (80–200 Hz) is also shown. Part indicated by *horizontal bar* and *arrow* is expanded below and the cycle on the left is further expanded at the bottom. Note, in the *bottom trace*, the progressively increased amplitude of ripples in EEG field potentials, in parallel with neuronal depolarization and increased frequency of action potentials. From Grenier et al. (2001).

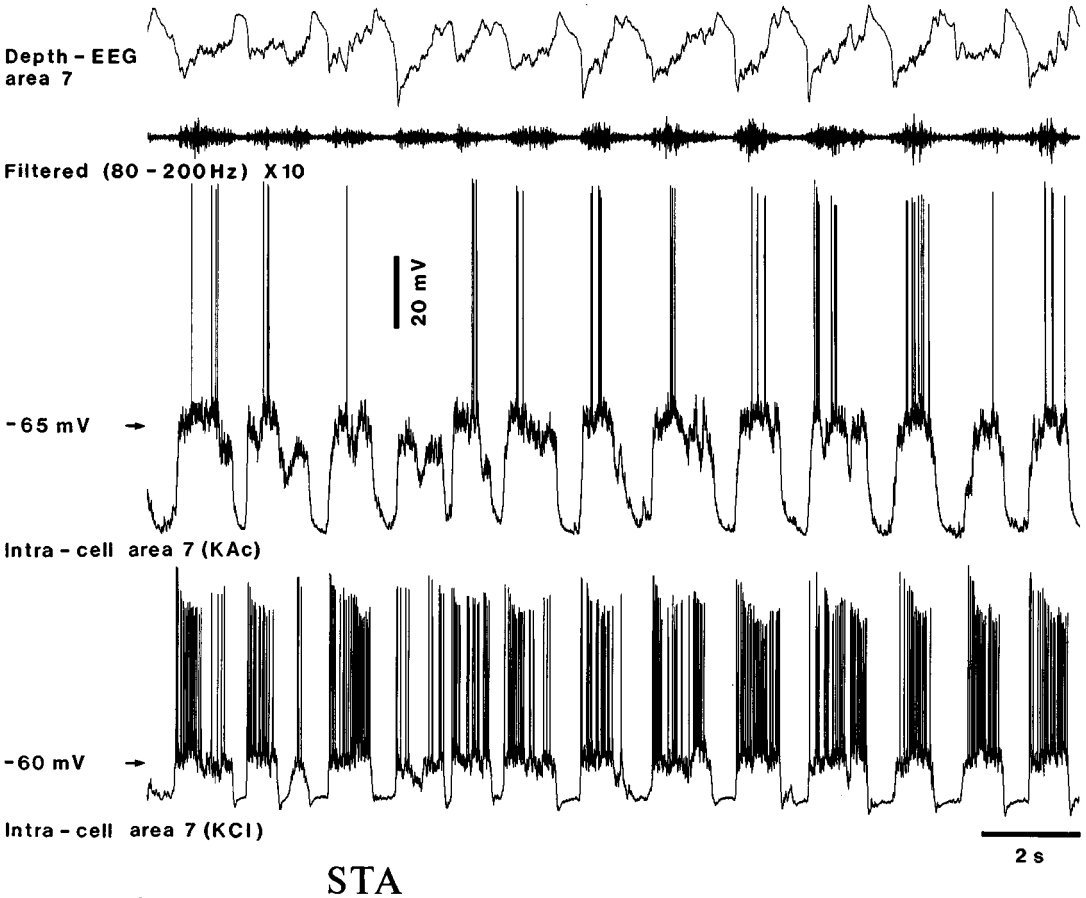
Depth - EEG
area 7
Filtered (80 - 200Hz) X10
20 mV
-65 mV
Intra - cell area 7 (KAc)
-60 mV
Intra - cell area 7 (KCl)
2 s

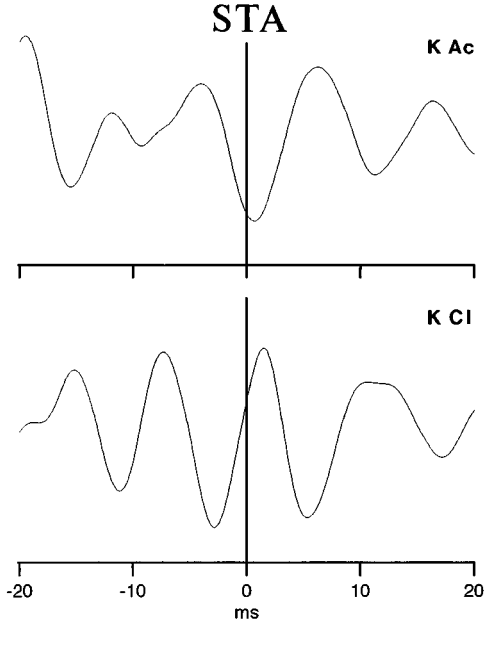
STA
K Ac
K Cl
-20
-10
0
10
20
ms

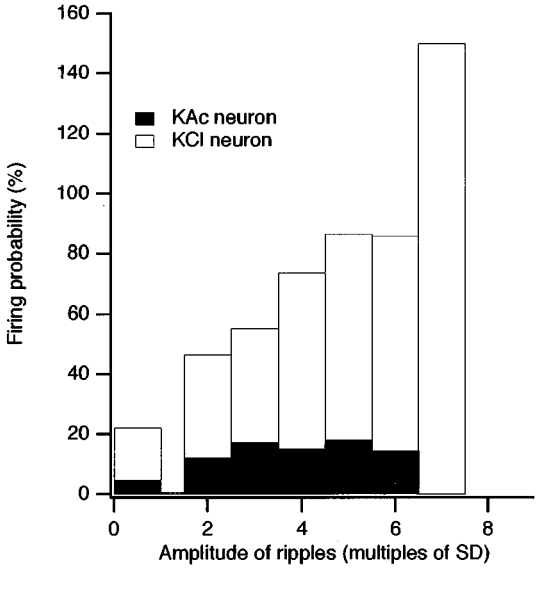
KAc neuron
KCl neuron
Firing probability (%)
160
140
120
100
80
60
40
20
0
0
2
4
6
8
Amplitude of ripples (multiples of SD)

systems. Figure 3.43 shows: the K-complex driving thalamic RE neurons, which produce spindles that are fed back to cortex via TC neurons (*A*); the cortical induction of hyperpolarization-dependent clock-like activity in TC neurons through prior excitation of GABAergic RE neurons (*B*); and the induction of cortical delta waves through the intrinsic property of bursting cortical neurons themselves (*C*).

3.2.3.3. Synchronization of slow oscillation and effects on distant structures

The intracortical synchronization of the slow oscillation was demonstrated by dual intracellular and field potential recordings from distant cortical foci, and by the disruption of synchronization after lidocaine injection between the two foci (Fig. 3.44). Multisite recordings from visual, association and motor cortical areas showed that closer located, slowly oscillating neurons are also "closer" in time. The shortest time-lags between the slow oscillation within adjacent fields were about 11–12 ms, while the longest time-lags found in distant recordings (from visual and motor cortices) were about 100–120 ms [196]. Such long latencies do not necessarily imply numerous synaptic linkages but rather inhibition-rebound sequences in interposed cortical neurons and/or in corticothalamocortical loops.

The long-range coherence of the slow oscillation was also demonstrated in naturally sleeping animals [198]. SWS displayed cycles of slow oscillation of a remarkable spatiotemporal coherence, as indicated by the high values of spatial correlation for large distances, in contrast with the steeper decline, with distance, of spatial correlations among neuronal activities during wakefulness and REM sleep (Fig. 3.45).

The intracortical synchronization of the slow oscillation was investigated in *in vitro* slices from visual cortex [199]. Extracellular

[198] Destexhe et al. (1999b).

[199] Sanchez-Vives and McCormick (2000). The higher excitability of neurons in layer V, which were reported in that *in vitro* study to initiate the slow oscillation, might be ascribed to a peculiar sensitivity of layers V/VI neurons to the concentration of K^+ in the bathing milieu used in slices (3.5 mM K^+), slightly higher than is the case *in vivo* (around 3 mM K^+, ranging between 2.7 and 3.2 mM K^+; Lux and Neher, 1973; Futamachi et al., 1974; Gutnick et al., 1979). This rather small difference (~3 mM *in vivo* vs 3.5 mM in the *in vitro* study) may also explain why the slow oscillation was present in 0.4-mm-thick slices, whereas the same oscillation was not present in isolated neocortical slabs of 10 mm × 6 mm (Timofeev et al., 2000a). Alternatively, despite the fact that the microscopic aspect of *in vivo* slabs showed perfectly normal cellular populations and triple intracellular recordings demonstrated propagated activity induced by stimuli, the absence of a spontaneously occurring slow oscillation in *in vivo* cortical slabs might have been due to uncontrolled changes (reduction?) in the $[K^+]_{out}$ after the surgical preparation. Anyway, the abnormally high excitability of layers V/VI neurons (without reaching, however, paroxysmal states) in that work on visual cortex slices can be seen in Fig. 3.46 (Fig. 2 in the paper by Sanchez-Vives and McCormick, 2000) showing that *layers V/VI neurons discharged heavily during the silent phases of neurons from other layers*. Intracellularly, the silent phases represent hyperpolarizing potentials. During the hyperpolarizing ("down-state") phases of the slow oscillation, there is virtually no action potential in any type of neurons investigated *in vivo*, during either anesthesia or natural SWS (see Figs. 3.25 to 3.33 in the present section and note [177]).

Fig. 3.42 (opposite) Chloride-mediated inhibition plays a role in the generation of ripples. Cat under ketamine-xylazine anesthesia. Dual intracellular recordings of regular-spiking (RS) neurons from area 7 (one pipette filled with KAc, the other filled with KCl), together with depth-EEG from the same suprasylvian area. Neurons were close to each other (<0.5 mm) and to the EEG electrode (<1 mm). *Top panel* depicts an epoch with depth-EEG recording and, below, filtered EEG trace (80–200 Hz, multiplied by 10), together with simultaneous intracellular recordings from two neurons. *Bottom left* panels depict spike-triggered average (STA) of filtered EEG activities (*upper*, neuron recorded with KAc-filled pipette; *bottom*, KCl-filled pipette). The action potentials (time 0) were selected when they occurred within ±5 ms of a ripple cycle whose negative peak had an amplitude of at least 4 times the standard deviation of the filtered trace. Note that the phase relation between the action potentials and the ripples in the field potential was shifted when the neuron was recorded with a KCl-filled pipette. *Bottom right* panel shows the firing probability of neurons around ripple cycles of increasing amplitudes. The increased firing rate of the RS neuron recorded with the KCl-filled pipette is much more dramatic than that of the RS neuron recorded with a KAc-filled pipette. A firing probability of 150% means that the neuron fired on average 1.5 action potentials per ripple cycle. From Grenier et al. (2001).

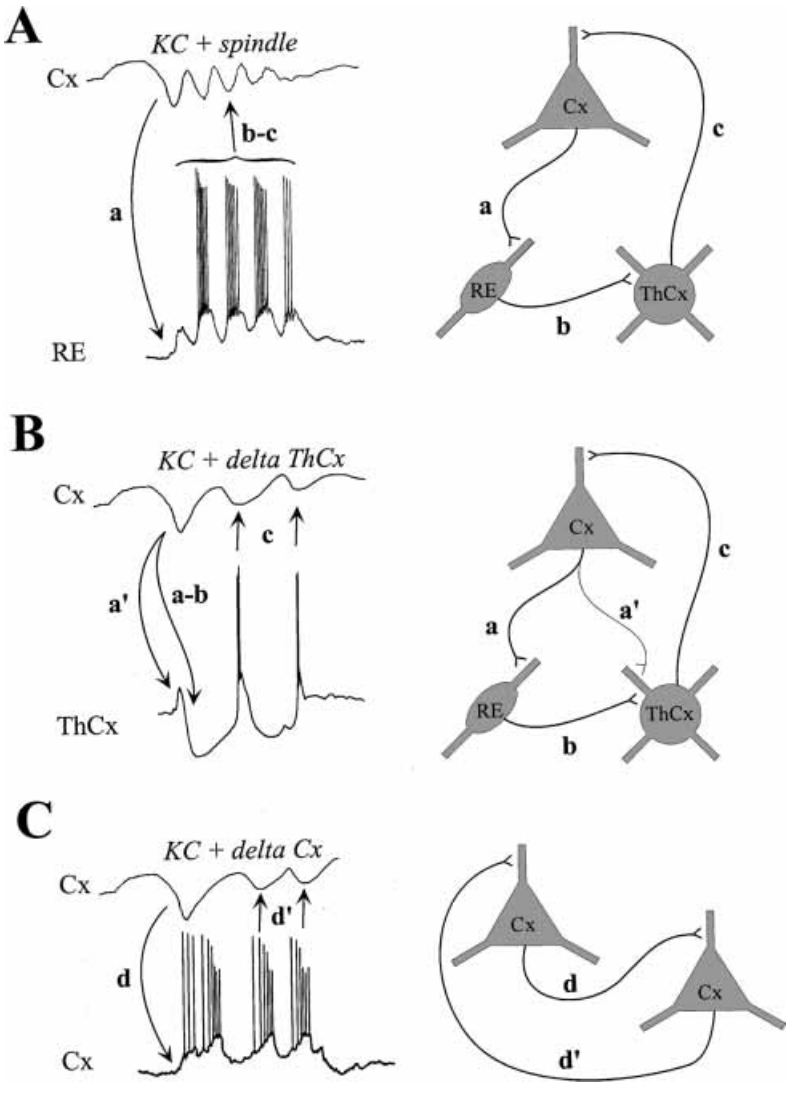

Fig. 3.43 Coalescence of the depolarizing phase of the slow oscillation (K-complex, KC) with other sleep rhythms. In the left column, field potential and intracellular recording. In the right column, scheme of the circuit involved in the generation of the respective EEG pattern. The synaptic projections are indicated with small letters, corresponding to the arrows on the left, which indicate the time sequence of the events. *A*, combination of a KC with a spindle sequence. A KC in the cortex (*Cx*) travels through the corticothalamic pathway (*a*) and triggers in the thalamic RE nucleus (*RE*) a spindle sequence that is transferred to thalamocortical cells (*ThCx*) of the dorsal thalamus (*b*) and thereafter back to the cortex (*c*) where it shapes the tail of the KC. *B*, modulation of a KC by a sequence of clock-like delta waves originating in the thalamus. The KC travels along the corticothalamic pathway (*a′*) eliciting an EPSP curtailed by an IPSP produced along the cortico-RE (*a*) and RE-ThCx (*b*) projections. The hyperpolarization of the thalamocortical cell generates a sequence of low-threshold potentials crowned by high-frequency spike-bursts at delta frequency that may reach the cortex through the thalamocortical link (*c*). *C*, modulation of a KC by a sequence of delta waves originating in the cortex. When the KC impinges upon bursting cells (*d*) it triggers a series of rhythmic bursts of spikes at delta frequency that may have a greater impact on target cells (*d′*) than single action potentials, thus synchronizing several neurons whose membrane potentials will be reflected in local field potentials as delta waves. From Amzica and Steriade (2002).

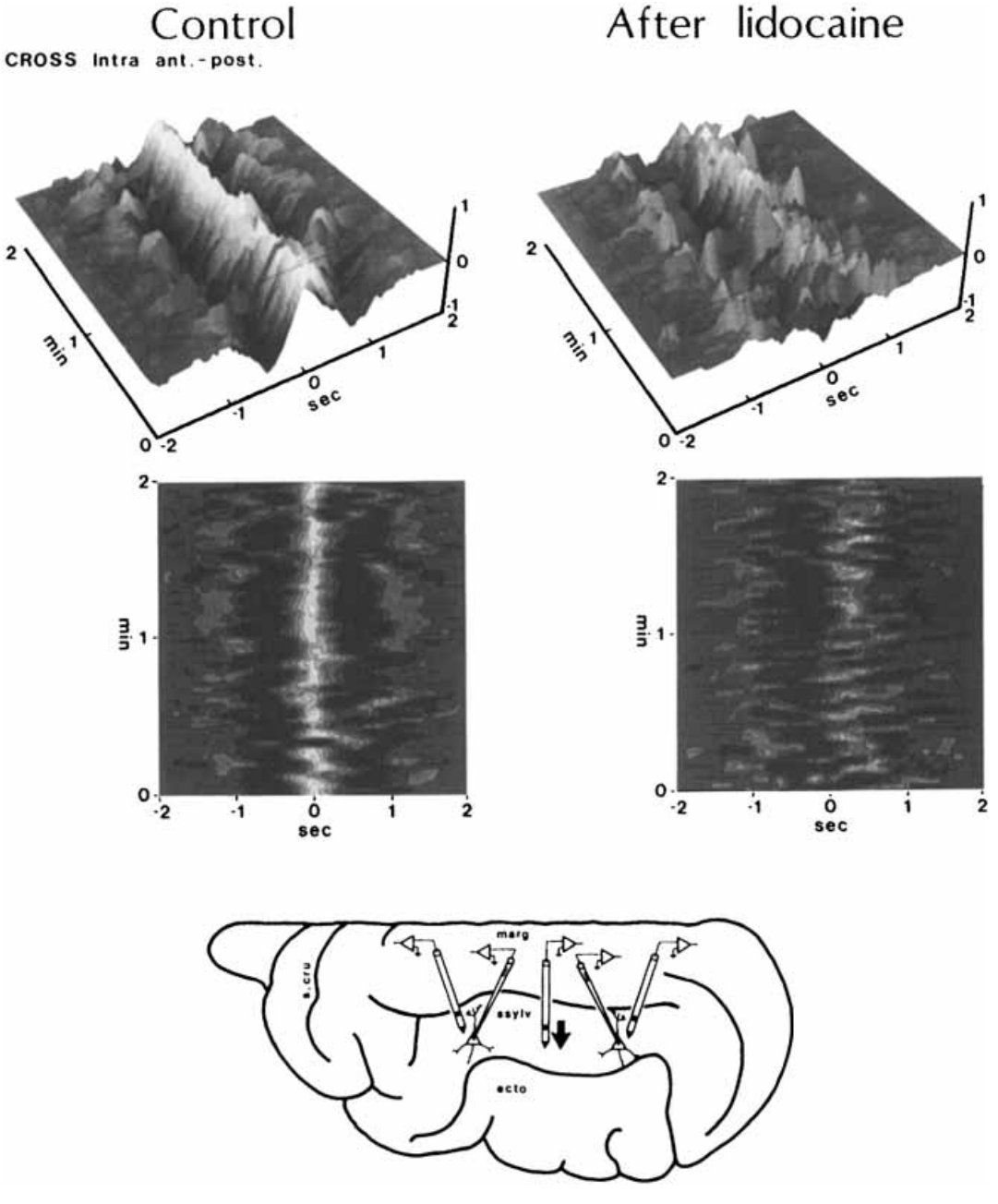

Fig. 3.44 Disruption of synchronization of slow oscillation by intracortical disconnection of synaptic linkages. Cat under ketamine-xylazine anesthesia. Dual intracellular recordings from the anterior and posterior parts of the suprasylvian gyrus; lidocaine injection (40 μl, 20%) between the two micropipettes (see brain figurine). The synchrony and its disruption after lidocaine injections are represented by sequential field analyses. The control synchrony was characterized by well-aligned, high central peaks. After lidocaine injection, the previous pattern was replaced by a blurred sequence of lower peaks and lower valleys deviating from the central plane. Modified from Amzica and Steriade (1995a).

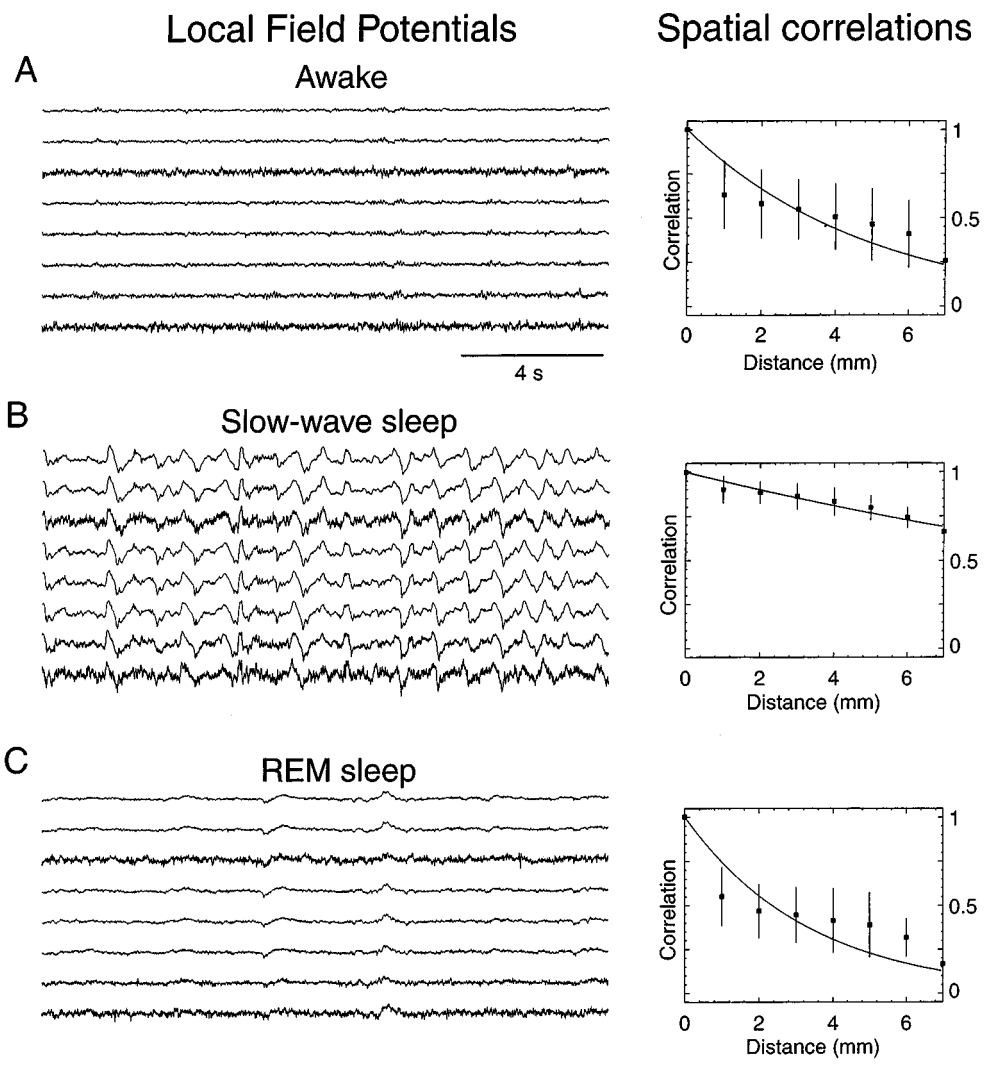

Fig. 3.45 Multi-site local field potentials in cerebral cortex during natural waking and sleep states. Chronically implanted cat. Eight bipolar electrodes (inter-electrode distance of 1 mm) were inserted into the depth (1 mm) of areas 5–7 of cat suprasylvian gyrus. Local field potentials (LFPs) are shown (left panels) together with correlations as a function of distance (right panel). *A*, when the animal was awake, LFPs were characterized by low-amplitude fast activities in the beta/gamma frequency range (15–75 Hz). Correlations decayed steeply with distance. *B*, during SWS, the LFPs were dominated by large-amplitude slow-waves complexes recurring at a slow frequency (<1 Hz, but slightly higher frequency on the extreme right in the left panel). Correlations stayed high for larger distances than in waking and REM sleep. *C*, during episodes of REM sleep, LFPs and correlations had similar characteristics as during waking periods. Modified from Destexhe et al. (1999b).

multi-unit recordings revealed that the slow oscillation was most robust and occurred first in layer V, followed after a short delay by activity in layer VI, and, finally, after an additional delay by activity in layers II/III (Fig. 3.46). In those slices, the slow oscillation displayed a clear-cut horizontal propagation (eight recording electrodes), and the conclusion was drawn that the slow oscillation propagates horizontally as a column of activity that appears earliest in or near layer V [199]. By contrast, eight simultaneous field potentials plus dual intracellular recordings *in vivo* showed that the slow oscillation and the associated ultra-fast activity (see *3.2.3.2*) are nearly simultaneous over relatively large distances (Fig. 3.47), compared to the more reduced slice tissue [200]. A similar simultaneity of slow oscillation during natural SWS is illustrated in Fig. 3.45.

In all the above studies conducted *in vivo*, the intracellularly recorded slow oscillation was very well correlated not only with local EEG field potentials, but also with EEG activity recorded from foci that were distant from the site of intracellular recordings (see Figs. 3.26, 3.31–3.32, etc), during either anesthesia or natural SWS. This strong correlation between intracellular and extracellular recordings was also reported for the slow oscillation recorded *in vitro* [199]. Surprisingly, a study of cortical neurons reported that the coherent activity between the slowly recurring intracellular activity of neurons and EEG was weak [201]; this failure to detect the strong relation between intracellular and macroscopic activities was probably due to the fact that the EEG was recorded from "cranial screws" and not using electrodes inserted within the cortex.

The cortical slow oscillation is also synchronized in homotopic foci of both hemispheres. Dual intracellular recordings, conjointly with local field potentials from areas linked by callosal projections, display coherent slow oscillations (see Fig. 3.36, *CAT2*). Because of direct cortical projections to thalamic RE neurons, the depth-negative (excitatory) field component of the slow oscillation is closely related to repetitive spike-bursts in RE neurons (Fig. 3.48) that, in turn, produce rhythmic IPSPs and postinhibitory rebound bursts in thalamocortical neurons, the basis of sleep spindles. This is the mechanism of combined cycles of slow oscillation with brief sequences of spindle waves, i.e. the K-complex.

Besides the thalamus, the slow oscillation is also expressed in the caudate nucleus where it is driven from neocortex [202]. Strong correlation was found between the slow oscillation recorded intracellularly from striatal neurons and by electrocorticogram

[200] This difference is reminiscent of a similar difference between the simultaneous appearance of spindle oscillations in both animals and humans [117] and the systematic propagation of spindle sequences in slices from the visual thalamus of ferrets [118].

[201] Lampl et al. (1999).

[202] Wilson (1993); Wilson and Kawaguchi (1996).

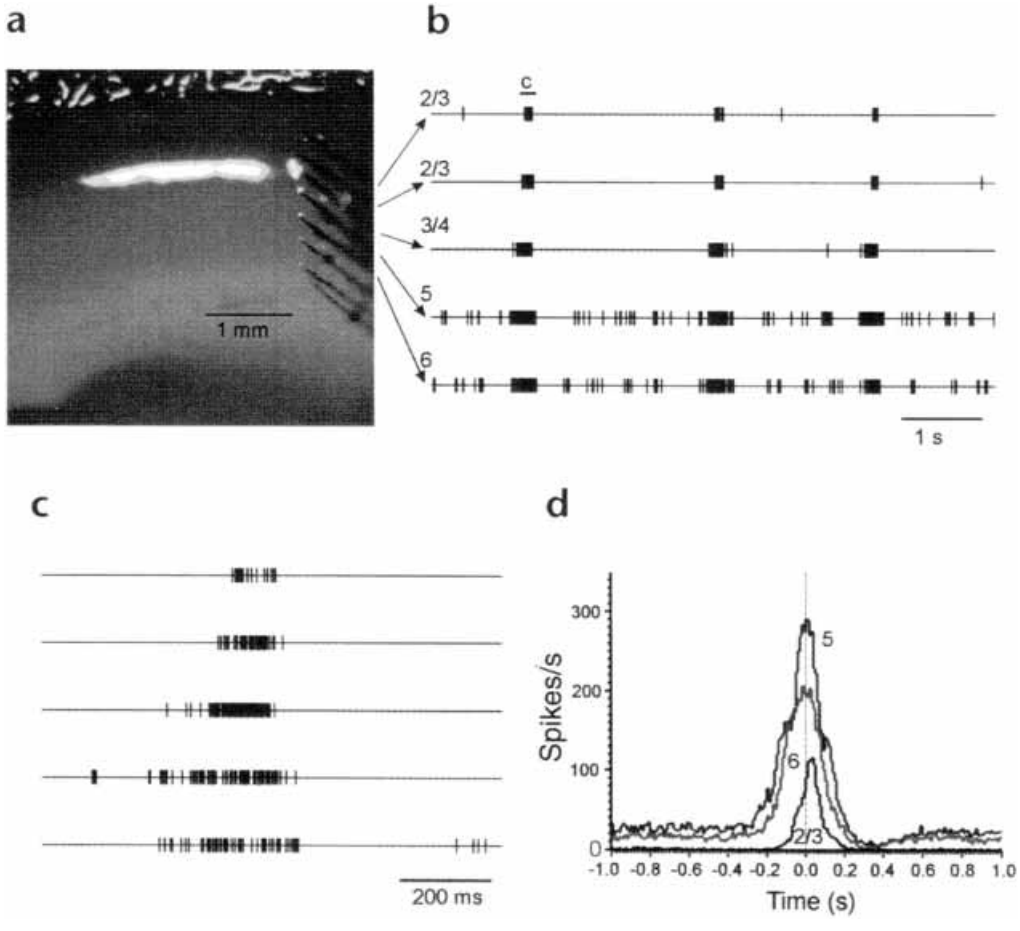

Fig. 3.46 In *in vitro* slices from ferret visual cortex, the slow oscillation is generated first around layer V and propagates vertically. (***a***), the extracellular recording microelectrode array (0.25 mm inter-electrode spacing) placed vertically in the cortical slice. (***b***), simultaneous extracellular multi-unit recording from layers II/III to VI reveal the slow oscillation to initiate around layer V, followed, on average, by activity in layers VI and II/III. The burst of activity indicated is expanded in (***c***). The third electrode was at the border between layers III and IV, whereas the fourth electrode was at the top of layer V. Each tic mark represents a detected action potential in the multi-unit recording. (***d***), unit histogram aligned to the peak of activity in layer V for each of the up-states of the slow oscillation reveals that layers V and VI generate spontaneous activity before the onset of the up-state, but that this activity decreases following the up-state. The up-state begins slightly earlier in layer V than layer VI and is more intense. See comments in note [199]. From Sanchez-Vives and McCormick (2000). See Plate section for color version of this figure.

Fig. 3.47 (following) Temporal relations between slow oscillation recorded over a distance of ~10–11 mm across the suprasylvian cortex. The eight electrodes were aligned along the antero-posterior axis and separated by 1.5 mm (see brain figurine). In addition, dual intracellular recording was performed: cell 1 was recorded less than 1 mm from the second most anterior EEG electrode, while cell 2 had the same relation with the fifth most anterior EEG electrode. *Note near-simultaneity of the slow oscillation over the suprasylvian gyrus (~10–11 mm).* Neuronal firing was related to local ripple amplitude. Two epochs are expanded on the right with the filtered EEGs (between 80 and 200 Hz). Neuronal firing was related to ripple amplitude in the closest EEG recordings. The number of action potentials occurring within ±5 ms of a ripple of given amplitude was computed for the two cells in relation to each of the EEG electrodes. The closer the cell was to the site of EEG recording, the more chance a ripple of a given level had of being linked to an action potential in the cell. Ripples were strongly phase-locked between the different sites, but their amplitudes might vary between different leads. From Grenier et al. (2001).

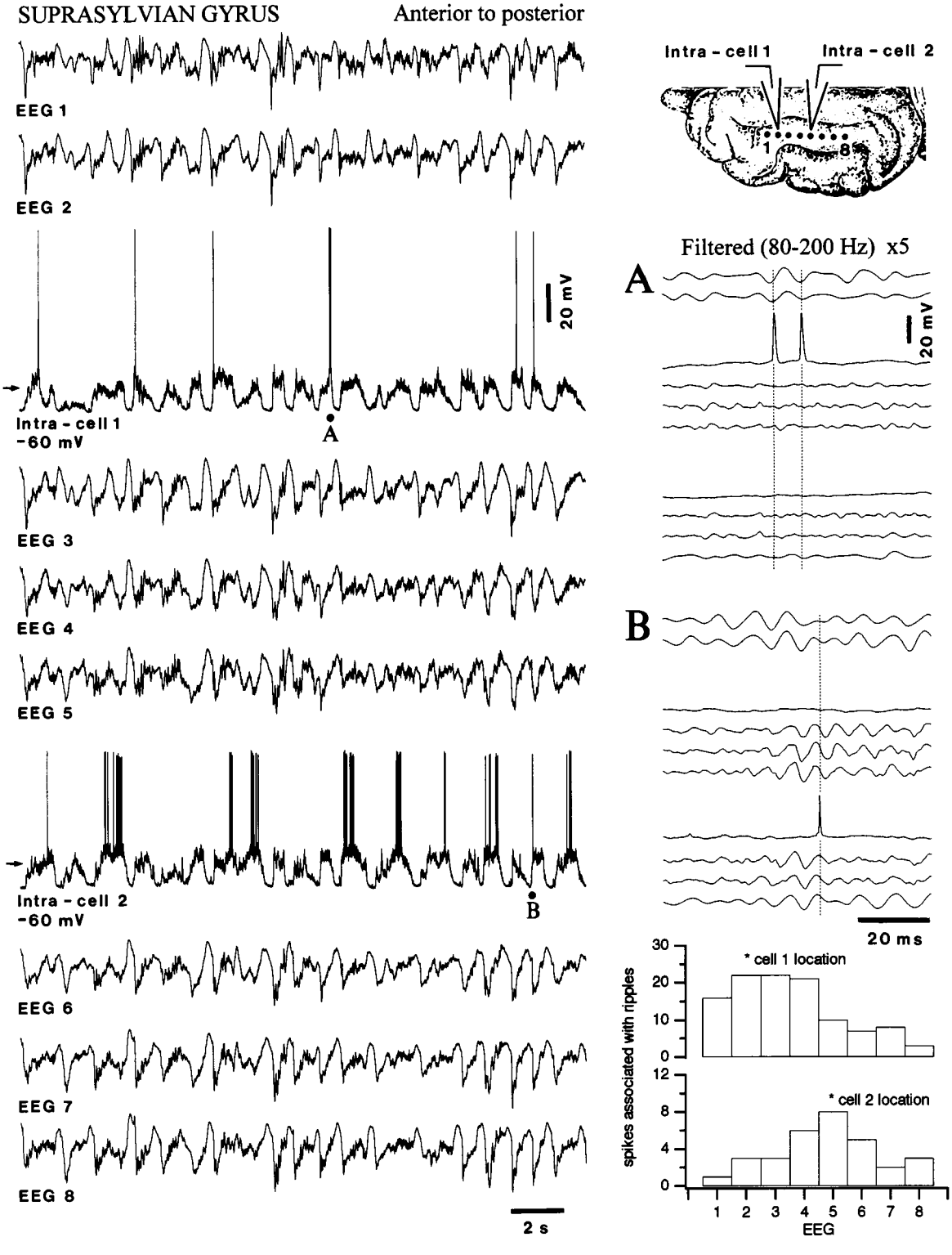
SUPRASYLVIAN GYRUS
Anterior to posterior
EEG 1
EEG 2
20 mV
Intra - cell 1
-60 mV
A
EEG 3
EEG 4
EEG 5
Intra - cell 2
-60 mV
B
EEG 6
EEG 7
EEG 8
2 s
Intra - cell 1
Intra - cell 2
1
8
Filtered (80-200 Hz) x5
A
20 mV
B
20 ms
spikes associated with ripples
* cell 1 location
* cell 2 location
EEG

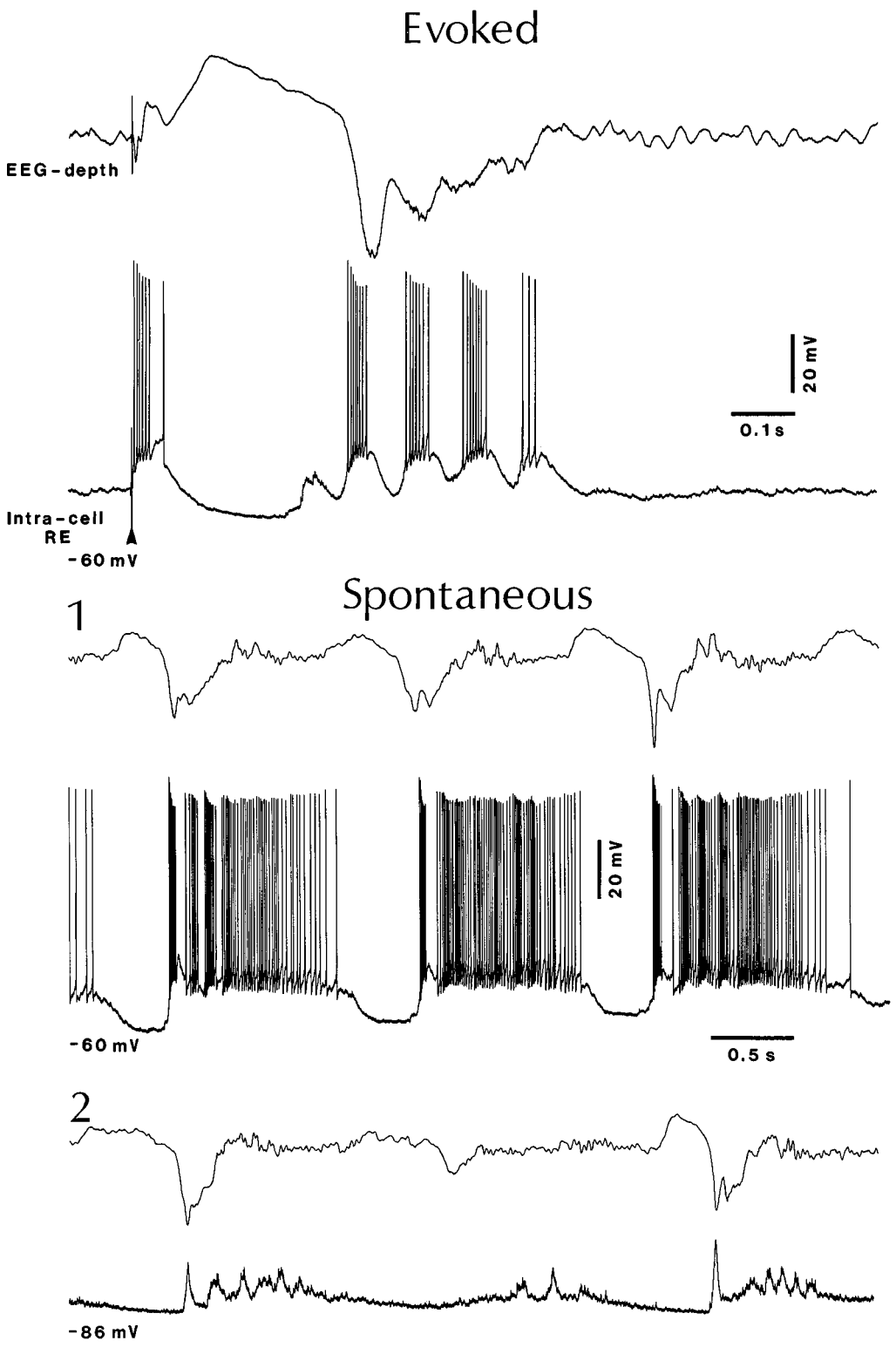
Evoked
EEG-depth
20 mV
0.1 s
Intra-cell
RE
-60 mV
Spontaneous
1
20 mV
-60 mV
0.5 s
2
-86 mV

(Fig. 3.49) [203]. Similar cortico-striatal correlations were found for various forms of rhythmic activities, depending on various substances used for anesthesia, and particularly during the slow oscillation under ketamine-xylazine anesthesia (Fig. 3.50) [204]. In epochs of robust cortical synchronization during sleep-like oscillations, the timing of action potentials in striatal output neurons suggested a high reliability of the information flow from the cortex to the basal ganglia [204].

The slow oscillation was also recorded from the subthalamic-pallidus network [205], basal forebrain [206], brainstem nuclei at the mesopontine junction [207], and cuneate neurons in the medulla [208]. In some of the above-mentioned subcortical structures, the slow oscillation disappeared after cortical ablation or functional inactivation, thus showing its cortical origin.

3.2.3.4. Slow oscillation and other sleep rhythms in humans

After the initial description, during human sleep, of delta waves grouped in sequences recurring within the frequency range of the slow oscillation [166], the slow oscillation was studied by other investigators [169, 209] who illustrated, during human sleep, EEG and magnetoencephalographic (MEG) patterns similar to those seen in animals. The MEG recording in Fig. 3.51, from human sleep, displays the bilateral prevalence of the slow oscillation on frontal, temporal and parietal fields, and smaller amplitudes of this sleep rhythm over other leads, with frequencies (~0.8–1 Hz) similar to those reported in naturally sleeping or anesthetized cats (see above). Visual areas are largely devoid of slow oscillation in this recording, in line with the much less obvious slow oscillation in the visual cortex of animals. The coherence analysis of EEG sleep rhythms in humans also led to the conclusion that there was little evidence for inter-hemispheric coherent activity, at any frequency, in the posterior (occipital) part of the brain (Fig. 3.52). By contrast, for anterior leads, the coherence in the "low-Δ" range (which includes the upper range of the slow oscillation; see Fig. 3.52) was

[203] Tseng et al. (2001). Intracellular recordings showed that striatal projection neurons from rats with a chronic nigrostriatal lesion had a more depolarized membrane potential during both up (depolarizing) and down (hyperpolarizing) states of the slow oscillation, and an increased firing probability during the up phases.

[204] Mahon et al. (2001). These authors found similar slowly recurring activities in intracellularly recorded corticostriatal and striatal output neurons, both types being coherent with the slow oscillation in the electrocorticogram.

[205] Magill et al. (2000). It was also found that activity in subthalamic neurons is correlated with cortical slow-wave activity in both control and 6-hydroxydopamine-lesioned animals, and that the removal of the ipsilateral cortex abolished the slow oscillation in subthalamic neurons (Magill et al., 2001). For the impact of the slow sleep oscillation on amygdala, see Paré et al. (2002).

[206] Nuñez (1996).

[207] Steriade et al. (1994a).

[208] Mariño et al. (2000).

[209] Simon et al. (1999, 2000).

Fig. 3.48 (opposite) Thalamic RE GABAergic neurons oscillate in phase with the cortical slow oscillation. Cat under ketamine-xylazine anesthesia. Upon internal capsule stimulation (*Evoked*, arrowhead), the RE neuron responded with an initial high-frequency spike-burst followed by a hyperpolarization of 0.2 s duration and a spindle sequence riding on a depolarizing envelope. The first wave of the spindle sequence occurred about 70 ms before the beginning of the cortical depth-negativity. *Spontaneous*, both the depth cortical EEG (motor cortex) and the RE neuron oscillated spontaneously at 0.6 Hz. At a membrane potential of −60 mV (in *1*), the depolarizing phases of RE neuron were characterized by an initial spike-burst followed by tonic firing modulated at the spindle frequency. When the RE neuron was hyperpolarized (−86 mV, in *2*), EPSPs were revealed at the same frequency. Note in *2* the correlation between the cortical EEG and RE cell's depolarization. Modified from Contreras and Steriade (1995).

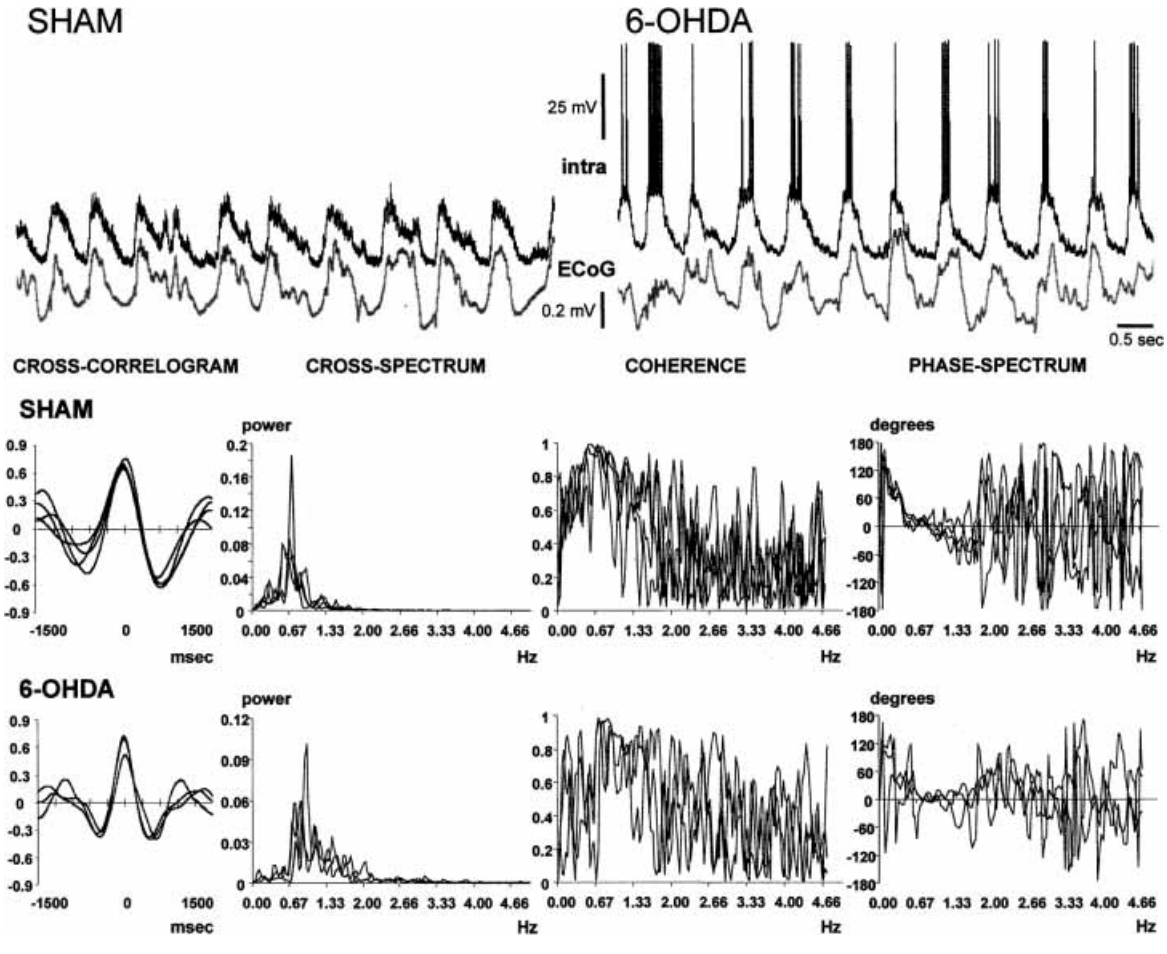

Fig. 3.49 Close temporal relation between the slow oscillation (~0.7–0.9 Hz) in frontal electrocorticogram and intracellular activity of striatal neurons. Sprague Dawley rats under urethane anesthesia. The signals are displayed as they were recorded, but note that they were down-sampled, smoothed, and standardized before analysis. The synchronization between cortical and striatal signals is substantiated through the analysis of cross-correlograms and by means of coherence analysis. Each row of graphics shows the cross-correlograms, cross-spectrum, coherence-spectrum, and phase-spectrum corresponding to the signal pairs displayed in the upper part of the figure (top row of graphics, sham-lesioned rat; bottom row of graphics, rat with nigrostriatal lesion). In each graphic, the results of the analysis of several 30-s epochs from the same signal pair were superimposed. The four disjoined 30-s epochs depicted for the sham-lesioned rat were chosen from a recording session lasting 15 min. A 12-min recording session from a 6-OHDA-lesioned (where 6-OHDA is 6-hydroxydopamine) rat provided the three 30-s epochs that were chosen for the bottom row of graphics. Both signal pairs showed strong correlations. The cross-spectra revealed a powerful common frequency of ~0.7 Hz (*SHAM*) or ~0.9 Hz (*6-OHDA*), and the signals displayed a very high coherence and linear phase relationship at the dominant frequency. From Tseng et al. (2001).

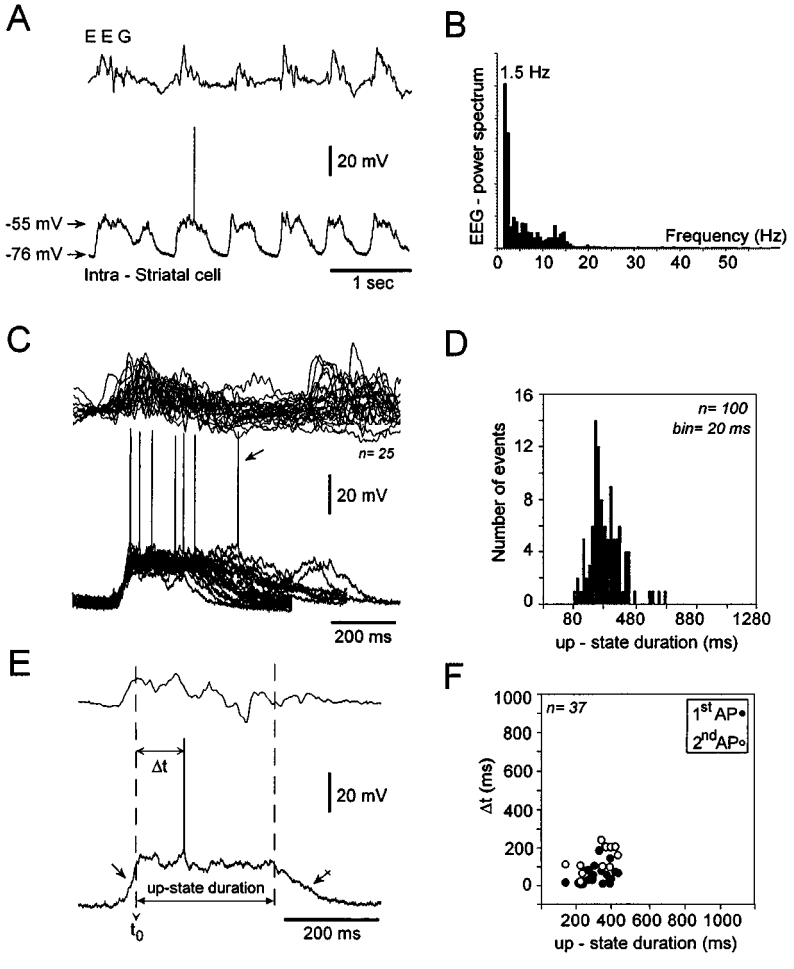

Fig. 3.50 Coherent slow oscillation in striatal activity and EEG waves under ketamine-xylazine anesthesia in rat. *A*, intracellular activity of a striatal output neuron (lower trace) simultaneously recorded with the corresponding surface EEG (upper trace). The rhythmic fluctuations of membrane potential consisted of depolarizing plateaus (−55 mV, up-state) interrupted by hyperpolarizing periods (−76 mV, down-state). The striatal cell oscillated with depolarizing phases associated with slow surface-positive field potentials that began with an initial sharp deflection of EEG waves. *B*, spectral analysis of the EEG record shown in *A*. *C*, superimposition of 25 successive striatal up-states and of the corresponding cortical potentials. The onset of the rise time to the up-state was used for alignment of the traces. The supra-threshold up states ($n = 5$ of 25) led to one or two action potentials and exceptionally to a third spike (arrow). *D*, histogram distribution of up-state durations. The mean value was 290 ± 104.7 ms. *E*, example of a striatal spontaneous depolarization (lower trace) and the associated EEG wave (upper trace). Dashed lines indicate the duration of the depolarizing phase. The slope of transition to the depolarized state was sharper (arrow) than the return to the hyperpolarized state (crossed arrow). Spike timing was assessed by measuring spike latency (Δt) from onset (t_0) of the stable period of the depolarizing state. *F*, relationship between spike timing (Δt) of the first and second action potentials and up-state duration. The mean value of Δt was 79.8 ± 69.4 ms. From Mahon et al. (2001).

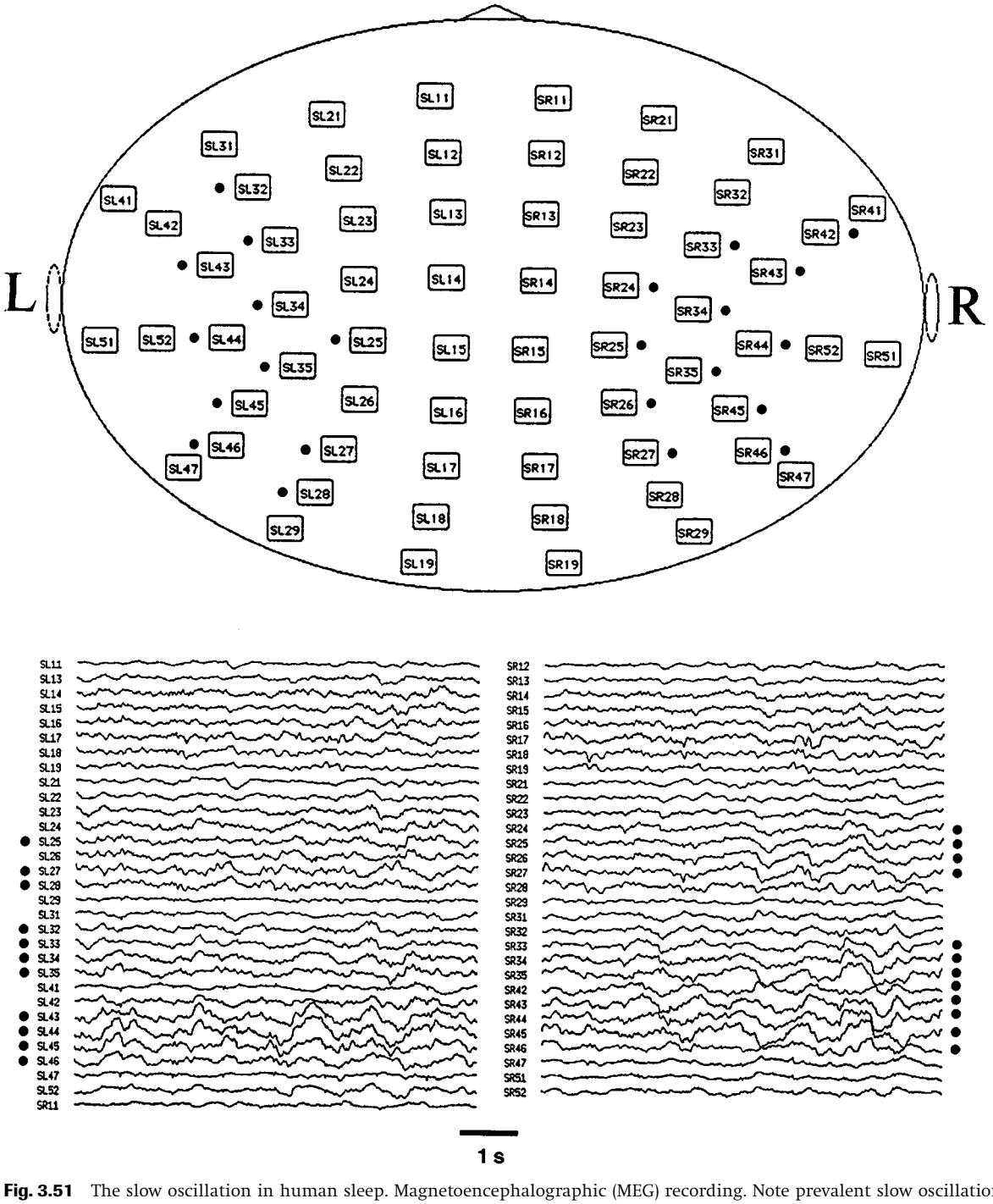

Fig. 3.51 The slow oscillation in human sleep. Magnetoencephalographic (MEG) recording. Note prevalent slow oscillation on leads marked by filled circles and much less visible slow oscillation over occipital leads. L, left; R, right. See also text. Modified from Simon et al. (1999).

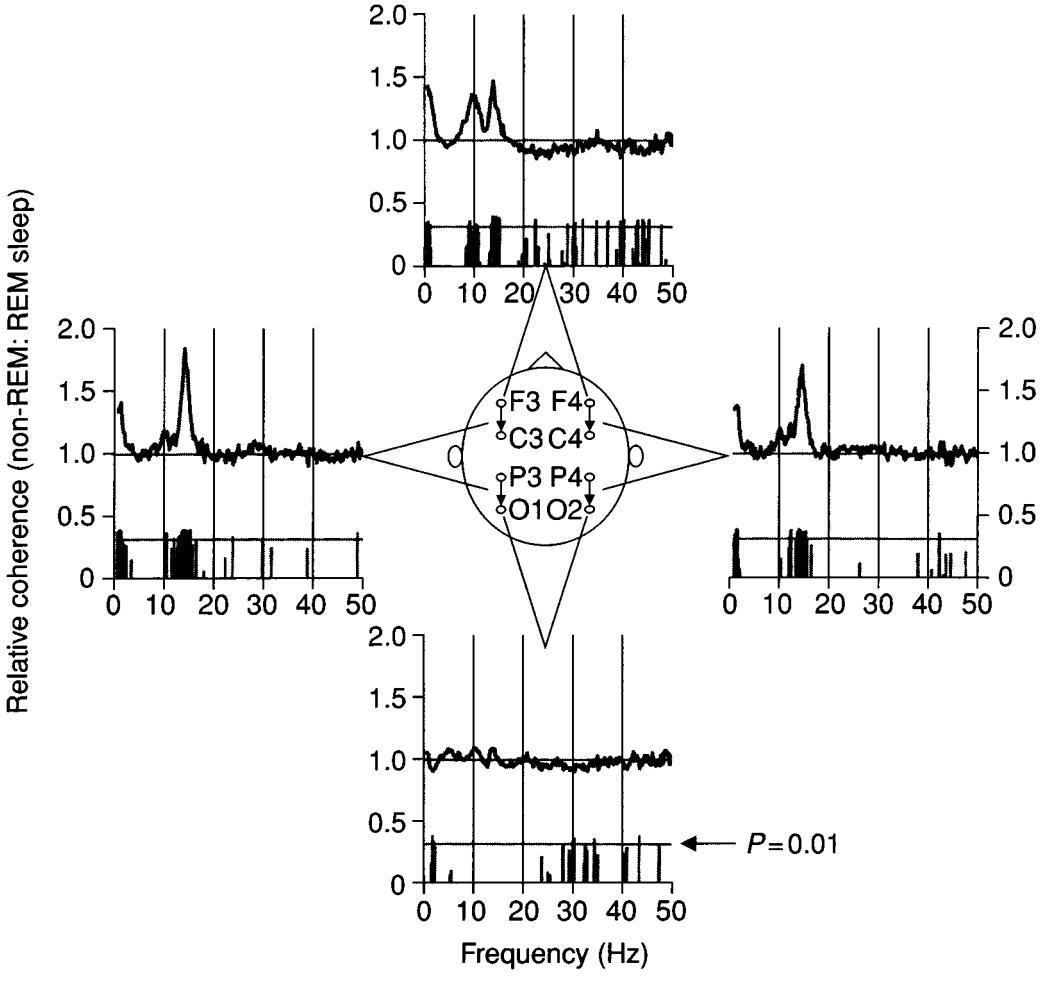

Fig. 3.52 Coherence analysis of the EEG reveals coherent activity during non-REM sleep between areas in one cerebral hemisphere (left and right graphs) and between right and left frontal regions (top) but not between right and left posterior regions (bottom). The coherence spectra are plotted as the ratio of non-REM:REM sleep in each frequency bin; vertical bars indicate that the significant differences ($p < 0.05$) between non-REM and REM sleep are mainly in the low-Δ, α and spindle frequency ranges. ("Low-Δ" includes the upper range of the slow oscillation; my note.) Center, the pairs of bipolar derivations used to calculate the spectra. Mean of eight male subjects. Modified from Achermann and Borbély (1998b).

elevated both within one hemisphere and between the two hemispheres [210], in keeping with experimental data using unit and field potential recordings from multiple cortical sites [196]. Direct current (DC) potentials were recorded from the human scalp and a dynamic regulation of their level in association with sleep cycles revealed a negative shift during the initial 10–15 min of SWS and a more subtle positive slope during the subsequent SWS period [211]. Such changes were ascribed to increasing and decreasing changes in neuronal excitability observed during the slow (0.5–1 Hz) sleep oscillation [166] and/or in infra-slow (~0.01 Hz) potential oscillations [212].

Functional brain imaging of human sleep mainly uses positron emission tomography (PET), to compare the regional cerebral blood flow (rCBF) between two or more brain areas and functional states [213], and functional magnetic resonance imaging (fMRI). These methods were employed in studies on the two main structures that generate sleep oscillations, thalamus and cerebral cortex. During sleep oscillations or unconsciousness produced by anesthetic drugs, the most marked decrease of rCBF was found, besides the brainstem reticular formation, in the medial thalamus [214, 215, 216], with a significant covariation between the midbrain and the thalamus [217] whose direct connections are known from experimental studies (see Chapter 2). In the cerebral cortex, most marked decrease in rCBF during SWS was found in the orbitofrontal, anterior cingulate, and precuneus fields [214, 216]. These results emphasized that the distribution of rCBF is not homogenous within the cortex and that the most marked changes in SWS are seen in some of those cortical areas that are most active during adaptive behavior in wakefulness.

3.2.4. Significance of sleep oscillations: why do we sleep?

Several questions concerning the neuronal mechanisms underlying SWS oscillations were discussed in the preceding sections of this chapter, but the available answers provide only very little insight on the *why* of sleep. In fact, neurophysiologists, like myself, look at the brain from inside and even within the neurons whose properties and input-output organization they identify, but often they only use sleep as a reproducible behavioral condition to reveal cellular mechanisms underlying changes in brain excitability. Probably, electrophysiologists are so overwhelmed by technical difficulties and by putting together cellular data to make sense of operations in complex networks that they do not succeed in testing hypotheses about the function(s) of sleep. At best, they spare a few embellishing ideas on the functional significance of sleep at the end of their

[210] Achermann and Borbély (1998a-b).

[211] Marshall et al. (1998).

[212] Aladjalova (1964).

[213] See a historical perspective of methods used to assess changes in brain circulation and temperature in Raichle (1998). For reviews on functional neuroimaging methods in normal human sleep, see Maquet and Phillips (1998) and Maquet (2000).

[214] Braun et al. (1997).

[215] Hofle et al. (1997).

[216] Maquet et al. (1997). See also Ferrara et al. (2002).

[217] Fiset et al. (1999).

articles or chapters. On the other hand, psychologists, interested in the states of the mind, and general physiologists, interested in the functions of different vital systems during the wake-sleep cycle, do not manipulate the necessary tools that would allow them to reveal the neuronal processes that control, or are associated with, the states of vigilance. Instead, they evaluate sleep functions in ontogeny and phylogeny by recording a series of macro-physiological variables (body temperature, energy expenditure, weight) and by comparing normal with sleep-deprived subjects. As yet, neither neuroscientists nor psychologists have provided a clear picture as to the *why* of SWS. Even the conventional wisdom that SWS has a restorative function (in view of the fact that SWS is enhanced by extending the prior waking period) should be regarded with caution because SWS is exclusively defined on the basis of the EEG and there is yet little evidence to correlate sleep quality with physiological processes (growth hormone secretion and body temperature) other than the EEG.

In what follows, I shall briefly expose two different views on sleep function, from those who investigate metabolic parameters and record scalp EEG, but do not enter the brain, and from those who record neuronal activities during sleep and related brain functions.

3.2.4.1. Views from studies on metabolic parameters and scalp EEG

In one type of experiment, the role of SWS was studied by depriving animals or humans of this stage of sleep and by recording a series of physiological parameters, other than brain processes. This recalls the old paradigm that consists of destroying the cerebellum, the cerebral cortex or other brain structures, and observing what goes wrong with the behavior of the lesioned animal. Such methods have provided valuable information in sleep research; some of them have been used to weight the role played by various forebrain structures in triggering and/or maintaining resting sleep. However, the role played by the ablated structures in the intact brain always remained to be assessed by analyzing the excitability of their constituent neurons in relation to various signs of sleep states. Such is the case with the sleep-deprived brain.

The effects of sleep deprivation can be dramatic. To reveal whether or not sleep subserves vital functions, deprivation should be enforced for very long periods of time. This procedure leaves open the question of whether the impairments following sleep deprivation result from sleep loss or from the frequent and stressing stimuli used to prevent sleep. It is obvious that such studies, with prolonged deprivation under rigid experimental controls, leading

to severe physiological disturbances and eventually to death, were only conducted on animals. A method was designed to allow deprivation of an experimental animal from a given stage of sleep, while only slightly affecting the sleep of a simultaneously housed, control animal [218]. The apparatus was used to deprive rats from a fraction of SWS associated with EEG slow waves of the highest amplitudes. This deprivation can be regarded as mostly affecting the late stage of SWS, comparable to humans' stage 4 sleep. It was not clear, however, to what extent other parts of SWS were also disrupted, nor was it possible to deprive the animals from the late stage of quiet sleep without also producing some loss of REM sleep [219]. After this type of sleep deprivation, animals died within 23 to 66 days. The sleep-deprived animals developed a debilitated appearance, skin lesions, showed weight loss despite a significant increase in food intake, acute rises in temperature but an overall temperature decline during the last half of survival, and the increase in energy expenditure was significant but lower than in animals deprived of REM sleep. These studies cautiously concluded that the role of SWS could not be precisely determined because no stage deprivation was completely selective. The idea that SWS sleep is a primer for REM sleep was also questioned because, after total sleep deprivation, animals displayed virtually no SWS prior to the rebound compensation of REM sleep [220]. Assuming that at least a part of the above effects of sleep deprivation were due to the loss of SWS (and that the concomitant loss of some REM sleep did not account for the whole range of phenomena leading to death), what brain processes might have mediated those fatal signs? Considering the impaired thermal and metabolic control, the attention should be focused on different hypothalamic areas. The difficulty of depriving the animals of SWS without interfering with REM sleep will probably hinder any experimental attempt to find the cerebral bases of metabolic disturbances due to the selective loss of SWS.

The suggestion was made that SWS is essential for replenishment of cerebral glycogen stores that are depleted during waking [221]. The function of SWS to conserve energy may be controversial because of the rather small reduction in metabolic savings (25%) during sleep, compared to wakefulness. Nonetheless, sleep is part of different energy conservation strategies. This was not only determined by means of recording a drop in body temperature during sleep, but also by recording a decreased responsiveness of temperature sensor neurons in the preoptic area of the anterior hypothalamus during SWS, compared to wakefulness, eventually reaching the lowest values during REM sleep [221].

[218] See the remarkable series of papers (I to X) devoted to sleep deprivation in rat, published by Rechtschaffen's team (first paper: Rechtschaffen et al., 1989a), and his more recent review on the function of sleep (Rechtschaffen, 1998).

[219] Gilliland et al. (1989).

[220] Rechtschaffen et al. (1989b).

[221] Heller et al. (1988); Parmeggiani (1988); Benington and Heller (1995).

[222] Horne (1988).

[223] Moruzzi (1966, p. 376).

Based on the fact that, after sleep deprivation, only about 30% of the total sleep lost seems to be reclaimed (mostly stage 4 with slow waves and REM sleep), some have concluded that stage 2 sleep with spindle oscillations is a very dispensable stage, as most of it is not reclaimed afterwards [222]. This led to a hypothesis about "core" sleep (including stage 4 and REM sleep) and "optional" sleep (represented by stage 2 sleep). It would be surprising that stage 2, which occupies about 45–55% of the total sleep time, would represent "optional" sleep, unless one believes that all sleepers could reduce by a half their sleep time. The reality is probably very different, and the reason behind this hypothesis is that it emerged from human recordings, a view from the scalp. If SWS subserves rest, this is true for both the thalamus (which generates spindling) and the cerebral cortex (which generates the slow oscillation and one component of delta waves). I am sure that stage 2 sleep with spindling oscillations, which provide a generalized inhibition of TC neurons and, consequently, a well-deserved cortical deafferentation, cannot be regarded as merely "optional" sleep. These two cerebral (thalamic and cortical) levels of brain rest, but also a special type of activity, during SWS are discussed below in the light of neuronal recordings.

3.2.4.2. Views from studies on neuronal activities

The defining bioelectrical features of SWS are spindles and slow waves that are characterized by long-lasting inhibitory processes in thalamic and cortical neurons, respectively. I proposed in the introduction to this chapter that the peculiar changes in EEG patterns during wake-to-sleep transition, namely the appearance of spindle oscillations, are the cause rather than the reflection of the quiescent behavioral condition. Indeed, the underlying cellular events of spindles are potent hyperpolarizations associated with increased conductance in TC neurons, preventing them from relaying incoming messages and, thus, setting the scene for the closed, sleepy brain. The even longer hyperpolarizations in cortical neurons that sculpt neuronal discharges during the slow oscillation are additional events and they complete the picture of cerebral deafferentation. All available data are congruent with the idea that, during SWS, the thalamus and neocortex are impermeable to, or at least cannot reflect faithfully, the signals from the outside world.

Do we spend a great part of our lives in a useless state of unconsciousness or could the loss of consciousness serve "as a period of recuperation for ... synapses where plastic (macromolecular) changes occur during wakefulness" [223]?. Moruzzi's hypothesis did not concern the fast recovery processes in routine synapses

underlying stereotyped activities. Instead, he referred to slow recovery during sleep, not "for the entire cerebrum", but predominantly in those structures in which plastic activities are "associated with the higher nerve functions, and above all with consciousness". This idea that pioneered many recent efforts in this direction is often forgotten.

Despite the fact that sleep functions are not yet elucidated, the study of spontaneous brain oscillations and changes in neuronal excitability during sleep states is fundamental because it reveals the reorganization of thalamic and cortical networks during fluctuations in global behavioral states and raises intriguing questions that may eventually lead to the disclosure of sleep functions. In contrast to the obsolete ideas that, during SWS, there is a global inhibition in cortex and subcortical structures, that the brain lies in total darkness and is associated with annihilation of consciousness [224], neurons in neocortical areas display unexpectedly high levels of spontaneous activity [31, 225] and, although the thalamic gates are closed for signals from the outside world (see Fig. 3.19) [137, 226], the intracortical dialogue is maintained during SWS [227]. These experimental results suggest that SWS, which is commonly regarded only under its attribute of complete brain rest, may subserve important cerebral functions.

During SWS episodes with spindle oscillations, rhythmic and synchronized spike-bursts of TC neurons strongly depolarize the dendrites of cortical neurons, which is probably associated with massive Ca^{2+} entry [228]. However, Ca^{2+} entry is not accompanied by excessive neuronal firing in pyramidal-type neurons. This may be due to strong inhibition of pyramidal neurons during spindles, as shown by recording cortical neurons with chloride-filled micropipettes (Fig. 3.53*A3*). Combination of these experimental data with computational models (Fig. 3.53*B*) suggested that the spindle-related thalamic inputs to cortical pyramidal neurons evoke powerful glutamatergic conductances in parallel with strong inhibitory (GABAergic) conductances [229]. Depolarizing pulses of Ca^{2+} trigger enzyme cascades and have long-lasting effects on gene regulation. It was also hypothesized [230] that Ca^{2+} entry during sleep spindles may provide an effective signal to efficiently activate calcium calmodulin-dependent protein kinase II (CaMKII), which is implicated in the synaptic plasticity of excitatory synapses in the cortex and other sites in the nervous system [231].

Similar phenomena, with Ca^{2+} entry in dendrites and somata of cortical neurons, may occur in SWS during the rhythmic spike-trains associated with the lower-frequency oscillations in the slow (0.5–1 Hz) or delta (1–4 Hz) bands, and could provide the long-time

[224] Pavlov (1923); Sherrington (1955); Eccles (1961).

[225] Evarts (1964); Steriade et al. (1974a); Steriade (1978).

[226] Changes in thalamic and cortical responses recorded from sensory and motor systems during states of brain deafferentation and during activation produced by brainstem reticular formation stimulation were reviewed long ago (Steriade, 1970). Among all sensory modalities, the auditory one is probably the most complex in its alterations of responsiveness during human sleep. Although early-latency auditory responses, generated in the acoustic nerve and brainstem, are present during SWS (Amadeo and Shagass, 1973), the results with middle-latency auditory potentials, generated in thalamic relays, and late responses, cortical in nature, are less consistent. Middle-latency responses are altered during SWS (Deiber et al., 1988) but the late cortical response, namely the P300 component, is sometimes preserved, though delayed. Interestingly, P300 is present when the subject's own name is presented, but this response does not occur for presentation of other names (Perrin et al., 1999). Portas et al. (2000), using fMRI and EEG recordings, proposed that the amygdala may play a role during SWS in mediating auditory responses with affective significance.

[227] Extracellular unit recordings in the motor cortex of monkeys showed that the spontaneous activity of callosal neurons increases from waking to SWS and their synaptic responses are also enhanced during SWS, compared to waking (Steriade et al., 1974b). This finding is corroborated by more recent intracellular data showing that, in contrast with diminished cortical responses to stimuli applied to prethalamic pathways (since the hyperpolarization of the interposed TC neurons during SWS prevents the transfer of incoming signals to cortex), cortically evoked EPSPs in cortical neurons increase linearly with hyperpolarization during the slow sleep oscillation (Timofeev et al., 1996).

[228] Yuste and Tank (1996).

[229] Contreras et al. (1997c).

[230] Sejnowski and Destexhe (2000); Destexhe and Sejnowski (2001).

[231] Soderling and Derkach (2000).

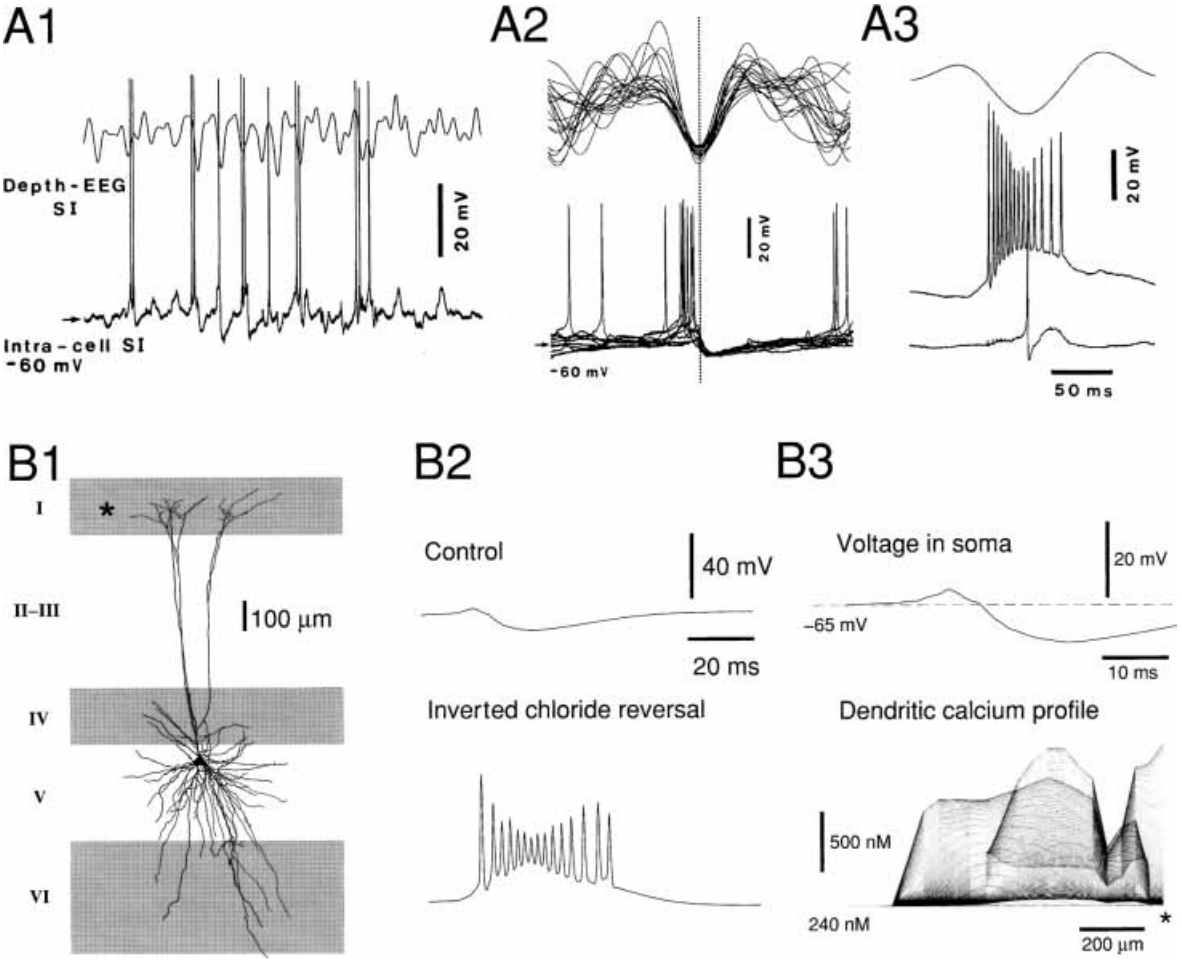

Fig. 3.53 Spindle oscillations evoke Ca^{2+} entry in cortical pyramidal neurons. Intracellular recordings in cats under barbiturate anesthesia and computational models. *A1*, simultaneous recordings of a neuron in the primary somatosensory cortex and field potential activity in the same area. *A2*, each cycle of the barbiturate-induced spindle oscillation corresponds to EPSP-IPSP sequences in a pyramidal neuron. *A3*, dual intracellular recording in which one of neurons was recorded with KCl-filled micropipette (middle trace); in this case, the EPSP-IPSP sequence was transformed into a powerful burst of action potentials. *B*, computational models of thalamic inputs to cortical pyramidal neurons. *B1*, morphology used in the simulations. A layer V pyramidal neuron recorded intracellularly in *A* was filled and its morphology was integrated into simulations. Simulations of thalamic inputs in layer I, IV and VI (gray areas) were directly compared to the experimental recordings of thalamic inputs in that neuron. *B2*, simulated EPSP-IPSP sequences and spike-bursts following inversion of the chloride reversal potential. The model could match experiments only if both excitatory and inhibitory conductances were strong. *B3*, calcium transients in the dendrites of the model following thalamic inputs. The membrane potential at the soma (top trace) consisted of an EPSP-IPSP sequence. However, representing the profile of calcium concentration (bottom trace) along a path from the soma (left) to distal apical dendrite (*) shows important calcium transients consequent to strong dendritic depolarization. From Sejnowski and Destexhe (2000), based on experimental and computational data by Contreras et al. (1997c).

scales needed to mobilize the machinery that was hypothesized as responsible for the consolidation of memory traces acquired during the state of wakefulness [188]. Ca^{2+} is regarded as a critical signal that induces the transcriptional events necessary for this consolidation [232]. The idea that low-frequency sleep oscillations may be instrumental in the consolidation of memory in corticothalamic neuronal loops [188] is supported by human studies, which demonstrate that the overnight improvement of discrimination tasks requires several steps, some of them depending on the early SWS stages [233]. The significant improvement of visual discrimination skills by early stages of sleep (associated with spindles and slow oscillation) led to the conclusion that procedural memory formation is prompted by slow-wave sleep [234].

High neuronal synchrony during SWS is observed beyond the neocortex and its consequence for memory consolidation gave rise to hypotheses and experimental data. Hippocampal sharp waves, which are predominant during SWS [235], reflect a population synchrony of up to 40 000–60 000 neurons in the CA3-CA1-subiculum-presubiculum-entorhinal cortex, which fire within the time-window of sharp potentials [236]. It was predicted that bursts of sharp potentials serve to consolidate the embedded information and transfer it to neocortical structures [237]. Dendritic recordings from CA1 pyramidal neurons revealed bursts of large-amplitude fast spikes, which occurred almost exclusively during sharp potentials, as well as wide, putative Ca^{2+} spikes that generally did not propagate to soma (Fig. 3.54) [238]. The proposal was then made that, during the time-window of sharp potentials, intracellular Ca^{2+} may be increased by several mechanisms, among them the dendritic depolarization and postsynaptic spiking may facilitate opening of *N*-methyl-D-aspartate (NMDA) channels, providing a mechanism for plasticity and suggesting that sleep patterns in the limbic system are important for the preservation of experience-induced synaptic modifications [237]. Experimental data from hippocampal recordings showed that, if a rat is confined to a place field, the firing rate of a "place cell" is increased during subsequent SWS [239] and there is an increase in the activity correlation between cell pairs whose activity was correlated during waking behavior [240]. Also, during SWS periods, after an episode of spatially extended behavior, patterns of neuronal correlation that were manifest during the behavior re-emerge in interactions between hippocampus and neocortex [241]. Thus, memory traces may be reactivated during SWS both in the hippocampus and neocortex.

All the above data show that, far from being a period of complete inactivity, SWS is implicated in mental processes related to

[232] Berridge (1998, 2000).

[233] Stickgold et al. (2000).

[234] Gais et al. (2000). See also the learning-dependent increase in sleep spindles (Gais et al., 2002).

[235] Buzsáki et al. (1983).

[236] Csicsvari et al. (1998).

[237] Buzsáki (1989, 1998).

[238] Kamondi et al. (1998).

[239] Pavlides and Winson (1989).

[240] Wilson and McNaughton (1994).

[241] Qin et al. (1997).

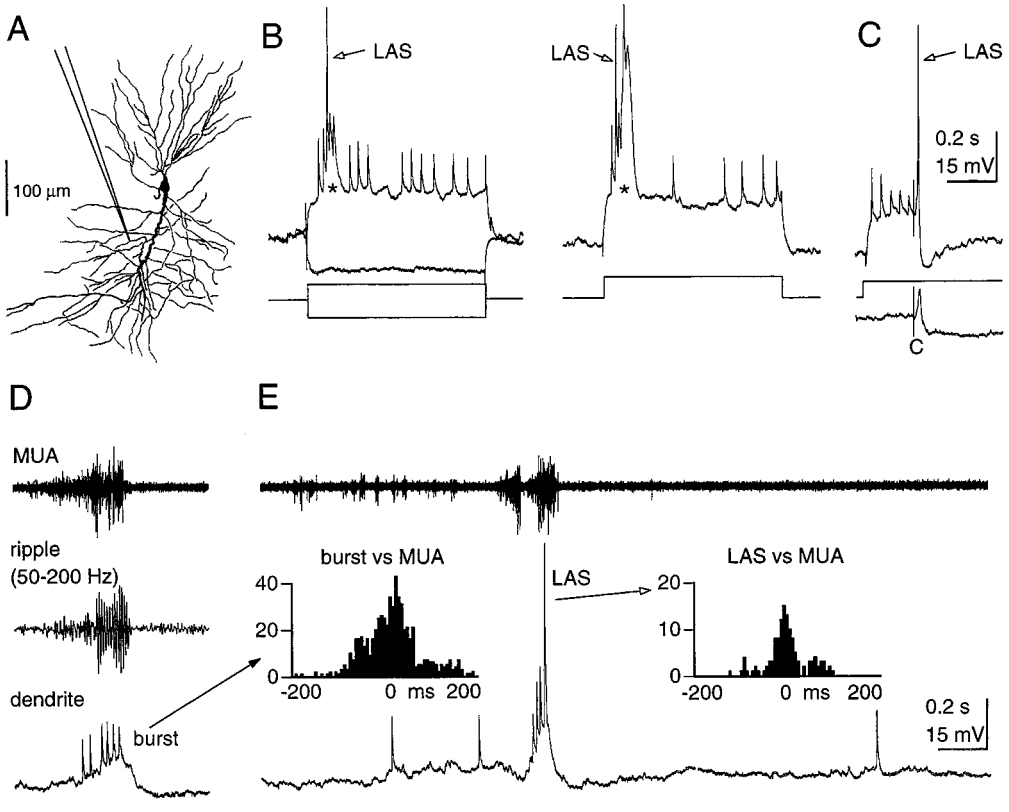

Fig. 3.54 Sharp-wave burst-induced amplitude enhancement of fast spikes. Dendritic recordings in CA1 pyramidal neurons of rat, under urethane anesthesia. *A*, reconstructed dendritic tree. The micropipette points to the anatomically verified penetrated dendrite. *B*, responses to hyperpolarizing (−0.5 nA) and depolarizing (left, +0.5 nA; right, +0.6 nA) current steps. Arrows indicate large-amplitude fast spikes (LAS); asterisks mark putative Ca^{2+} spikes. *C*, responses to commissural (*C*) stimulation. Note large-amplitude-evoked fast spike (arrow) and absence of spike (bottom trace), with and without concurrent direct depolarization of the dendrite, respectively. Same stimulus intensity was used in both cases. *D–E*, relationship between extracellularly recorded multiple unit activity (MUA) and field ripples from CA1 pyramidal layer and dendritic activity (45 s gap between *D* and *E*). Cross-correlogram (burst vs MUA) between intradendritic bursts as defined by repeating spikes at <10 ms, interspike intervals, and extracellular MUA activity illustrates that the incidence of intradendritic bursts was highest during ripple-related MUA. LASs were present exclusively during MUA bursts. From Kamondi et al. (1998).

[242] Foulkes (1967); Hobson et al. (2000); Hobson and Pace-Schott (2002).

[243] Nielsen (2000).

the consolidation of memory traces acquired during waking behavior. It is known that dreaming mentation is not confined to REM sleep, but also appears, with a different content (more logical, closer to real life events) in slow-wave sleep [242] and the recall rate of dreaming mentation in quiet sleep is quite high [243].

Evidence that neurons that fire together wire together is further discussed in Chapter 4, devoted to the analysis of plasticity processes as a consequence of repeated spike-trains of thalamic and cortical neurons during SWS oscillations.

[244] Glenn and Steriade (1982).

[245] Steriade and Deschênes (1974).

[246] Steriade et al. (2001b).

[247] Earlier extracellular recordings of cortical neurons from motor cortex of cats and monkeys [245] and from cat association cortex (Steriade et al., 1979a) showed longer and rhythmic inhibitory periods, tested by duration of suppressed firing after thalamic stimuli and probability of evoked responses, during SWS compared to wake and REM sleep states. During waking, the period of inhibition (after an initial excitation) was more marked than during REM sleep, possibly because of an overwhelmingly excitatory background activity during the latter state (Steriade et al., 1979a).

[248] Hobson et al. (1975); McCarley and Hobson (1975).

[249] McGinty and Harper (1976); Vanni-Mercier et al. (1984).

3.3. Brain-active states: waking and rapid-eye-movement sleep

In many respects, especially concerning their electrophysiological correlates in thalamic and cortical functioning, waking and REM sleep display similar features. It is indeed quite difficult to distinguish some features of the forebrain electrical activity between these two diametrically opposite behavioral states. The spontaneously occurring brain rhythms and the responsiveness of thalamic and cortical neurons are similar in the wake and REM sleep states. This is not only the case with virtually identical EEG patterns, but also with the increased probability of antidromic and synaptic responses recorded from thalamic [244] and neocortical pyramidal [164, 245], as well as with the enhanced intrinsic excitability of neocortical neurons tested by intracellular depolarizing pulses [246] during waking and REM sleep states, both compared to SWS. Probably, the only difference between the two brain-active states, exception being made for their very dissimilar psychological content, is the fact that the inhibitory processes are much better preserved in waking than in REM sleep [247] and that monoamine-containing neurons, such as norepinephrinergic locus coeruleus, serotonergic dorsal raphe and histaminergic posterior hypothalamic cells, are active in waking and virtually silent in REM sleep [248, 249]. This distinctive feature of monoaminergic neurons during REM sleep might account for the striking differences in the psychological content of this state, compared to wakefulness.

Most of these data, until 1990, and the anatomic/structural model of reciprocal interactions between cholinergic and monoaminergic neurons (Fig. 3.55), have been reviewed in a previous monograph [155]. Briefly, cholinergic neurons from pedunculopontine tegmental (PPT) and laterodorsal tegmental (LDT) nuclei, antidromically activated from thalamic nuclei (Fig. 3.56*A*), increase their firing rates in advance of the first electrographic signs of REM sleep and maintain their high discharge rates throughout this state (Fig. 3.56*B*) [24], which is just the contrary to the firing dynamics of monoaminergic neurons [248, 249]. The earlier version of the hypothesis was that norepinephrinergic and serotonergic neurons inhibit cholinergic neurons located in the medial pontine reticular formation, and the silenced firing of monoamine-containing (REM-off) neurons during REM sleep would disinhibit the executive (REM-on) medial pontine reticular neurons [248]. Later, it was found that there are virtually no cholinergic neurons in the medial pontine reticular core. After the immunohistochemical disclosure of cholinergic PPT/LDT nuclei and identification of their projections to both thalamic and some caudally located sites in

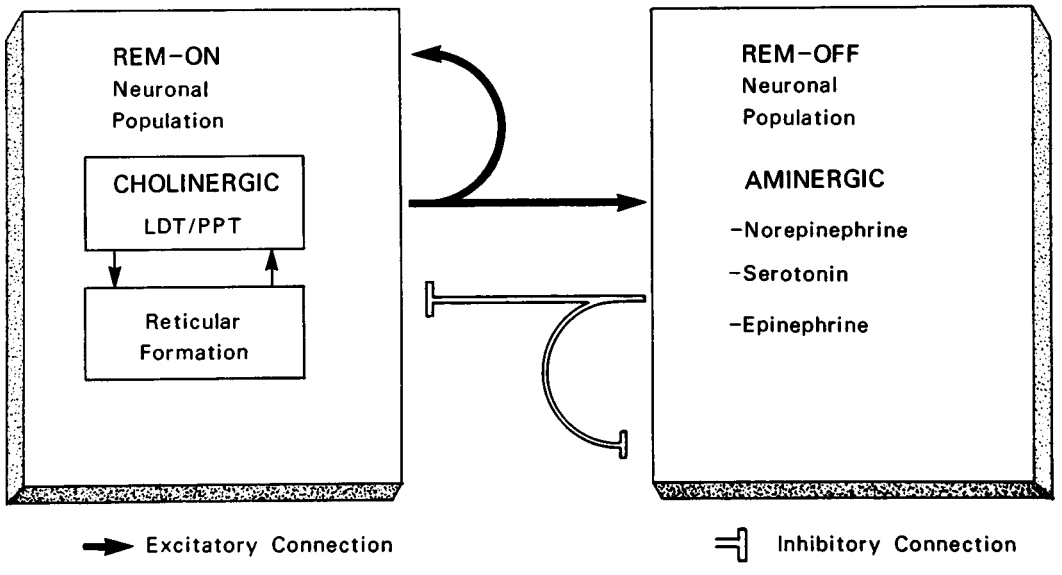

Fig. 3.55 Anatomic/structural model of REM-off and REM-on neuronal populations and their interaction. See text. From Steriade and McCarley (1990).

[250] McCarley and Massequoi (1986).

[251] GABAergic inhibition was thought to be responsible for the cessation of firing in dorsal raphe and locus coeruleus neurons (Nitz and Siegel, 1997a-b). More recently, this view was challenged by results from experiments using unit recordings and microdialysis in dorsal raphe nucleus (Sakai and Crochet, 2000). In those experiments, the virtual silence of dorsal raphe during REM sleep was not ascribed to GABAergic inhibition, but to disfacilitation, because specific antagonists of H_1 receptors and α_1-adrenoreceptors (these receptors are involved in the activation of raphe neurons) suppressed the spontaneous firing of dorsal raphe neurons.

[252] Kamondi et al. (1992).

the brainstem [155], the emphasis was mainly placed on REM-on neurons located in cholinergic PPT/LDT nuclei at the mesopontine junction (Fig. 3.55). The postulated steps in the original hypothesis of reciprocal interaction between cholinergic and monoaminergic neurons [248] and in a more recent mathematical model of the REM sleep oscillatory system [250] are as follows: (*a*) as a result of their disinhibition because of silent firing of monoaminergic neurons, REM-on neurons become increasingly active until REM sleep is produced; (*b*) REM-on neurons excite REM-off neurons and, when the REM-off population is sufficiently active, the REM episode is terminated because of the inhibition exerted by REM-off neurons on REM-on population. The diminished activity of the REM-off neuronal population was ascribed to an inhibitory feedback, but this view is controversial [251].

In the above model, it was thought that REM-on cholinergic neurons are inhibited during waking, because of the highly active monoaminergic neurons in this state. The hypothesis that brainstem cholinergic neurons are selectively active during REM sleep [252] did not take into consideration that, in addition to their inhibitory inputs from monoaminergic neurons, mesopontine cholinergic neurons are also driven by brainstem glutamatergic neurons, which are active in both waking and REM sleep, and thus able to counteract the inhibition from locus coeruleus and dorsal raphe neurons. Actually, *in vivo* experiments using microdialysis reported

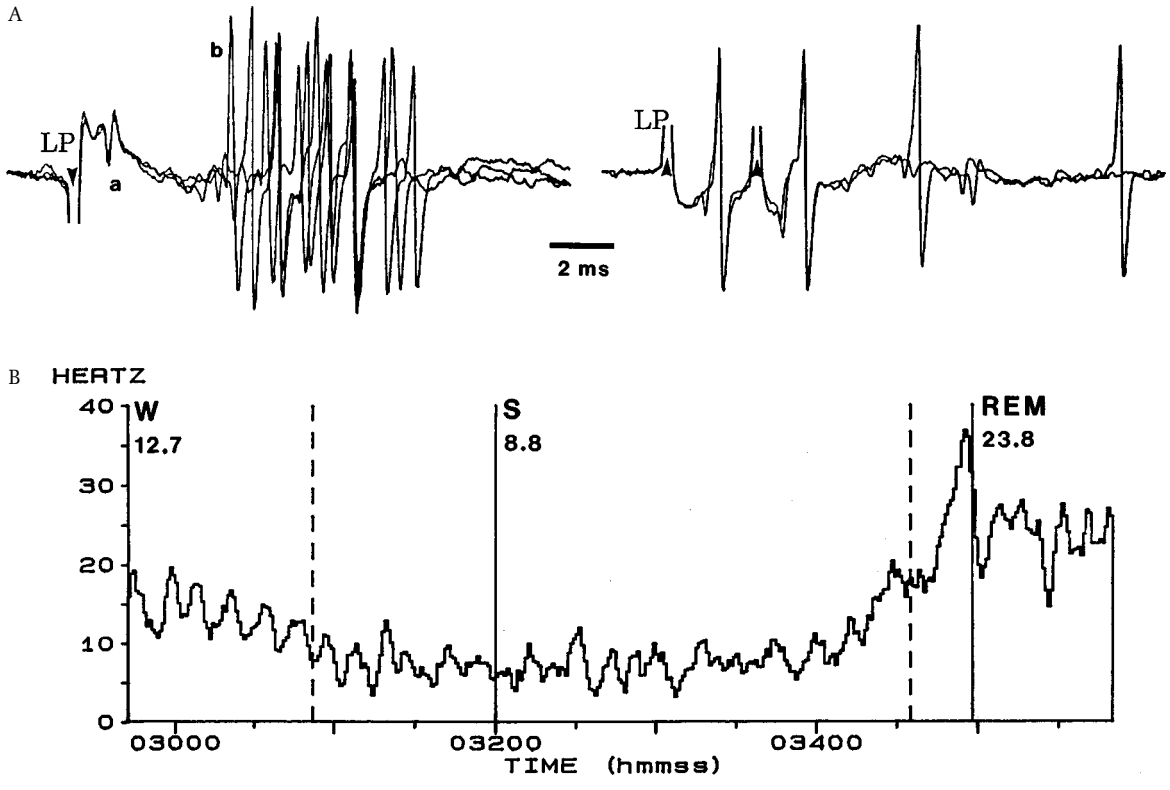

Fig. 3.56 Thalamic-projecting neurons from pedunculopontine tegmental (PPT) and laterodorsal tegmental (LDT) cholinergic nuclei decrease their firing rates from waking (W) to slow-wave sleep (S) and increase firing rates in advance of the most precocious signs of REM sleep. Extracellular recordings from chronically implanted, naturally awake and sleeping cats. *A*, stimulation of lateroposterior (LP) nucleus (arrowheads) evoked antidromic responses in two (*a* and *b*) simultaneously recorded neurons from the PPT nucleus. Neuron *a* was antidromically invaded at a fixed latency of 1.3 ms. Neuron *b* was synaptically activated, with a spike-burst at about 5 ms (probably via a complex circuit, involving thalamocortical and cortico-PPT pathways). By changing the polarity of LP stimulation (right panel), neuron *b* was antidromically activated at a latency of 1.6 ms. *B*, sequential firing rate of a PPT neuron, activated antidromically from the intralaminar thalamus, across the waking-sleep cycle. Abscissa indicates real time (hour, minutes, seconds). Mean firing rates are indicated in W (12.7 Hz), S (8.8 Hz) and REM (23.8 Hz). Transitional WS and pre-REM epochs are indicated by vertical interrupted lines (at 0:30:53 and 0:34:34, respectively). WS epoch was indicated by the first sign of EEG synchronization, while the pre-REM epoch was indicated by the first ponto-geniculo-occipital potential, over a background of fully synchronized EEG during S. Note cyclic activity toward the end of W state and increased firing rates in advance of REM sleep. Modified from Steriade et al. (1990a).

that the release of ACh in the thalamus during wakefulness and REM sleep is basically the same, more than twice higher that during SWS [253], in line with data using recordings of single brainstem-thalamic cholinergic neurons and showing similarly increased firing rates (20–30 Hz) in waking and REM sleep, compared to SWS (10–15 Hz) [24]. However, there is a minority of neurons in PPT/LDT mesopontine cholinergic nuclei that fire at very low rates in wakefulness (<2 Hz) and progressively increase their discharge rates, approaching REM sleep [24]. The possible explanation is that these neurons are prevalently driven by monoamine-containing neurons from locus coeruleus and dorsal raphe nuclei, which inhibit them.

More recently, the inhibitory role of serotonergic dorsal raphe neurons on cholinergic (REM-on) neurons was disputed, on the basis that selective 5-HT_{1A} agonists applied to the raphe dorsalis increase wakefulness and decrease SWS, but had no significant role in the generation of REM sleep [254]. These and other data revised and enlarged the sphere of neurons implicated in REM sleep generation, suggesting that medullary adrenergic, ponto-medullary norepinephrinergic and, to a lesser extent, hypothalamic dopaminergic systems exert inhibitory or permissive mechanisms in the induction of REM sleep [255].

In what follows, I analyze some neuronal properties and network operations that underlie the phasic and tonic electrical correlates of brain-active behavioral states, with emphasis on fast oscillatory activities that distinguish these states from low-frequency rhythms in SWS.

3.3.1. Phasic events

3.3.1.1. Ocular saccades and related intracellular events in cortical neurons

Neuronal circuits that are implicated in phasic events induced by external sensory stimuli during arousal and in processes triggered by brain-stored information during REM sleep include GABAergic neurons of substantia nigra pars reticulata (SNr) and their target neurons in the superior colliculus, mesopontine cholinergic nuclei, pontine reticular core, and thalamocortical systems. The complex neuronal circuits that implicate both descending and ascending projections of SNr account for different events induced by an alerting stimulus. Some of these structures are illustrated below, in Fig. 3.63, in the circuitry underlying the generation of ponto-geniculo-occipital (PGO) waves.

Novel sensory stimuli that trigger orienting reactions are accompanied by a decrease in the firing rate of SNr neurons [256],

[253] Williams et al. (1994).

[254] Sakai and Crochet (2001b). The absence of an effect on REM sleep generation occurred with concentrations of 5–500 μM of the 5-HT_{1A} agonist 8-OH-DPAT. At the highest concentrations used, REM sleep occurred directly after wakefulness, as in narcolepsy.

[255] Crochet and Sakai (1999); Sakai et al. (2001). See also Brown et al. (2002).

[256] Hikosaka and Wurtz (1983). The decrease in firing rates of GABAergic substantia nigra pars reticulata (SNr) neurons, produced by sensory stimuli, was interpreted as resulting from inhibitory inputs arising in GABAergic caudate neurons that, in turn, receive projections from the upper brainstem reticular core, medial and intralaminar thalamic nuclei, and widespread cortical areas (Graybiel and Ragsdale, 1979).

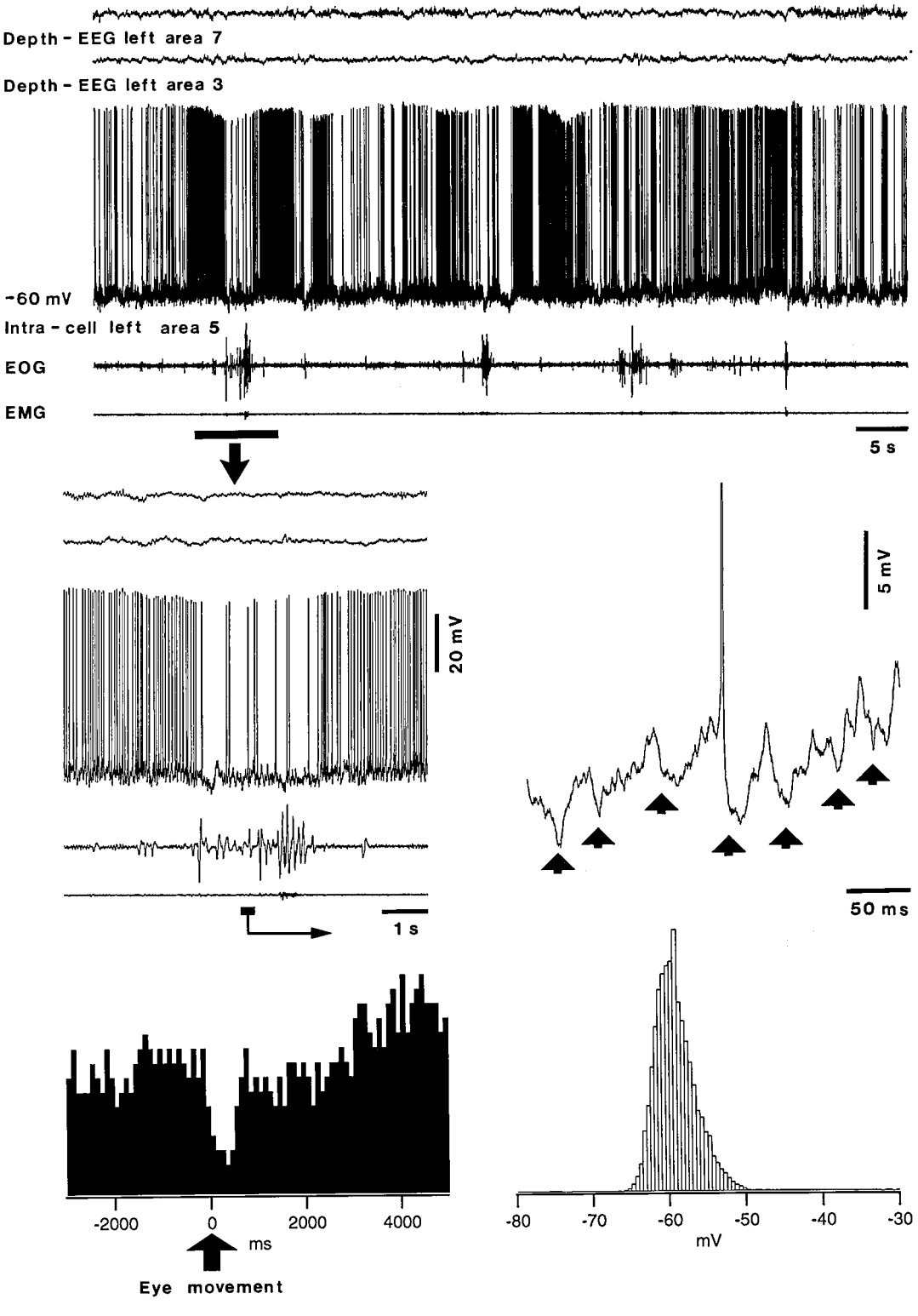
Depth - EEG left area 7
Depth - EEG left area 3
-60 mV
Intra - cell left area 5
EOG
EMG
5 s
20 mV
1 s
5 mV
50 ms
-2000
0
2000
4000
ms
Eye movement
-80
-70
-60
-50
-40
-30
mV

with the consequence of releasing from tonic inhibition, and thus producing increased firing in, superior collicular neurons, eventually leading (through collicular projections to premotor pontine neurons) to activation of oculomotor neurons. The SNr-collicular-pontine circuit is thus responsible for the phasic shift of gaze involved in the orienting behavior. The relative hyperpolarization of premotor pontine reticular neurons during the alert state [257] is a favorable condition that underlies their Ca^{2+}-dependent low-threshold spike and superimposed spike-bursts, which are operational in driving oculomotor neurons. On the other hand, brainstem cholinergic neurons and TC neurons from some dorsal thalamic nuclei, which are targets of SNr, are disinhibited during the periods of silenced firing in SNr upon sensory stimulation. The disinhibition of brainstem cholinergic neurons projecting and exciting TC neurons as well as the disinhibition of TC neurons with widespread cortical projections and depolarizing actions on the superficial cortical layer, such as the neurons in the ventromedial thalamic nucleus [258] targeted by SNr cells, are crucial in the EEG activation induced by an alerting stimulus.

During ocular saccades in REM sleep, cortical regular-spiking (RS) neurons, which are generally pyramidal-type cells and constitute more than half of all neuronal types in neocortex, decrease their firing rates and display numerous, low-amplitude (1–3 mV) and short (5–50 ms) IPSPs (Fig. 3.57), which are reversed after intracellular chloride infusion [178]. The saccade-related arrest in firing of RS neurons occur at only slightly hyperpolarized potentials or at the same membrane potentials as adjacent periods of neuronal activity (see middle left panel in Fig. 3.57), which make these hyperpolarizations very different from those of the same neurons during SWS (see above Fig. 3.26 and similar figures). To some extent, the amplitude and time-course of the short inhibitory potentials shown in Fig. 3.57 resemble the single-axon IPSPs described *in vitro* [259]. This suggests that the decreased firing during ocular saccades is due to barrages of IPSPs imposed on pyramidal neurons by inhibitory interneurons. Indeed, recordings from conventional fast-spiking (FS) neurons (presumably local inhibitory interneurons)

[257] Ito and McCarley (1984); Ito et al. (2002). The hyperpolarization of pontine reticular neurons during waking is relative to their sustained activation during REM sleep, but pedunculopontine tegmental (PPT) projections to pontine reticular neurons are activating in nature since pulse-trains applied to the PPT nucleus induce long-lasting excitatory responses in these neurons (Garcia-Rill et al., 2001). See also Immon et al. (1996) and Homma et al. (2002).

[258] Glenn et al. (1982).

[259] Thomson et al. (1996).

Fig. 3.57 (opposite) Ocular saccades during REM sleep are associated with fast IPSPs and decreased firing rates in regular-spiking (RS) neurons from association cortex. Intracellular recording from association cortex in chronically implanted, naturally sleeping cat. Five traces depict (from top to bottom): depth-EEG from left areas 7 and 3, intracellular activity of left area 5 neuron, electrooculogram (EOG) and electromyogram (EMG). Note ocular saccades and muscular atonia, characteristic of REM sleep. An ocular saccade (marked by horizontal bar) is expanded below (arrow). Further expansion of multiple IPSPs on the right (bar and arrow). *Bottom left*, peri-eye-movement histogram of neuronal firing showing decreased firing. *Bottom right*, histogram of membrane potential distribution during REM sleep. Modified from Timofeev et al. (2001b).

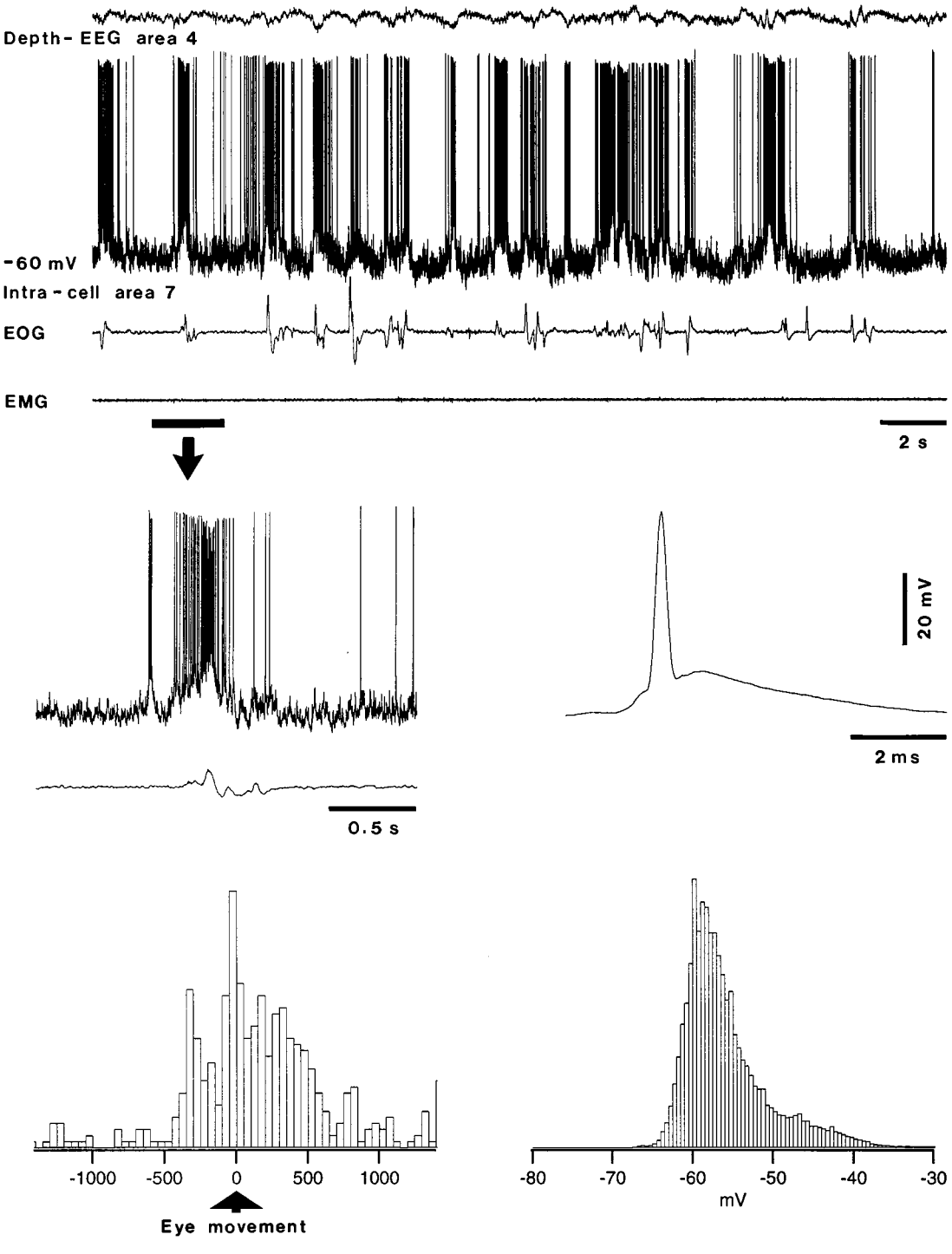

Fig. 3.58 Ocular saccades during REM sleep are associated with increased firing rate in conventional fast-spiking (FS) cortical neurons. Intracellular recording from association cortex in chronically implanted, naturally sleeping cat. Four traces depict (from top to bottom): depth-EEG from area 4, intracellular activity of area 7 neuron, EOG, and EMG. *Upper panel* shows that an FS neuron (identified by responses to depolarizing current pulses; not shown) was depolarized and increased its firing rate during ocular saccades in REM sleep. An ocular saccade is expanded below (horizontal bar and arrow). *Right middle panel*: average of spikes following synaptic potentials. *Bottom left panel*: peri-eye-movement histogram of neuronal firing. *Bottom right panel*: histogram of membrane potential distribution during REM. Modified from Timofeev et al. (2001b).

showed that they increase firing rates during ocular saccades in REM sleep (Fig. 3.58). Besides, recordings from RS neurons during REM sleep with pipettes filled with chloride showed that the firing rate of RS neurons increased almost twice during ocular saccades, thus further supporting the idea of Cl^--dependent IPSPs in RS neuron. These data from recent intracellular recordings in naturally sleeping animals support earlier results, with extracellular recordings in behaving cats, showing the selective firing of presumed interneurons in association cortex during ocular saccades in REM sleep [159, 260].

At variance with REM sleep, during wakefulness RS neurons may increase or decrease their firing rates during eye movements. In waking, the short-lasting IPSPs associated with eye movements precede the spikes and affect their timing (Fig. 3.59). These short-lasting IPSPs are chloride-dependent IPSPs as they are not observed in recordings with pipettes filled with KCl, and recordings from neurons hyperpolarized below −70 mV show tonic depolarizing potentials associated with eye movements.

3.3.1.2. Ponto-geniculo-occipital waves

PGO waves are the physiological correlate of the internal activation of the brain during REM sleep, probably "the stuff that dreams are made off". PGO field potentials appear in clusters of up to six waves, closely related to the time occurrence and the direction of eye movement saccades [261]. Although generally recorded in the thalamic lateral geniculate (LG) nucleus and visual cortex, PGO waves transcend this sensory system and are disseminated in many thalamic nuclei and in the corresponding cortical areas outside the visual cortex. Multi-site, field potential and unit recordings from sensory, motor and association neocortical areas show that PGO potentials appear synchronously over the neocortex [262]. The synchronization develops progressively from the period immediately preceding REM sleep until these potentials reach their highest degree of coherence in late stages of REM sleep (Fig. 3.60). The widespread distribution of PGO waves is explained by the generalized thalamic projections of PGO generators, the cholinergic neurons of pedunculopontine and laterodorsal tegmental (PPT/LDT) nuclei at the junction between the midbrain and pontine reticular formation. In thalamic LG nucleus, the PGO wave is associated with depolarization of TC neurons, starting at a latency of 20–40 ms and lasting for 150–300 ms when not interrupted by an IPSP [263].

One neuronal type recorded from PPT and LDT nuclei was found to discharge spike-bursts reliably preceding the PGO waves

[260] Steriade et al. (1979b).

[261] Nelson et al. (1983).

[262] Amzica and Steriade (1996).

[263] Hu et al. (1989c). That PGO-on processes in thalamic neurons are mainly cholinergic events mediated by nicotinic receptors was shown by their blockage after systemic administration (Ruch-Monachon et al., 1976) or iontophoretic application (Hu et al., 1988) of mecamylamine, a nicotinic antagosist.

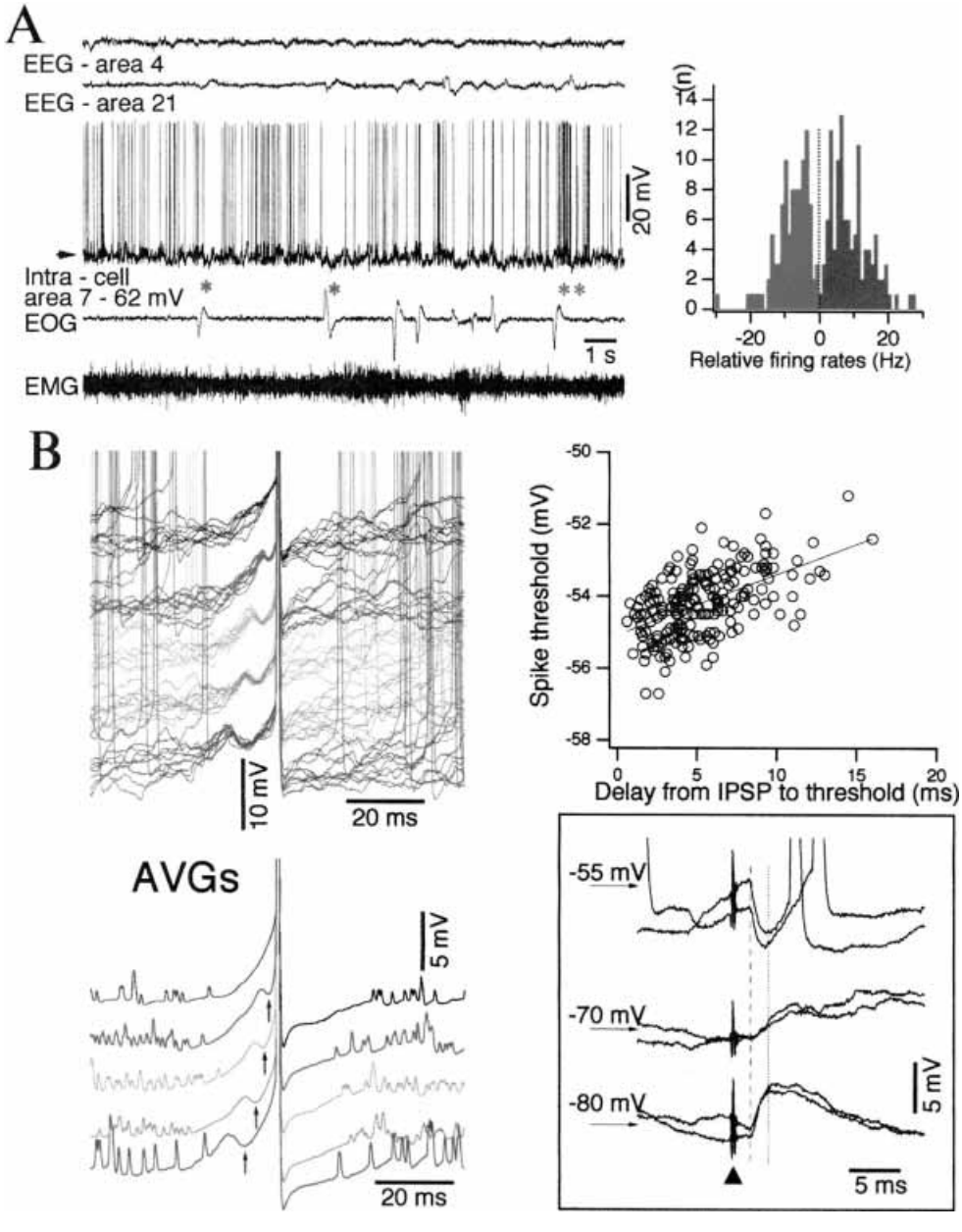

Fig. 3.59 Spontaneous IPSPs control precise firing timing of neocortical neurons in wakefulness. Intracellular recordings of cortical association neurons during natural waking in chronically implanted cats. *A*, epoch during the waking state, characterized by activated EEG, unimodal intracellular membrane potential and presence of muscular tone. Five traces depict (from top to bottom): depth-EEG from areas 4 and 21, intracellular activity of area 7 neuron, EOG, and EMG. Single asterisks (*) indicate a decrease in firing associated with eye movements, while double asterisks (**) indicate an increase in firing associated with eye movements. Histogram shows increased (blue) and decreased (red) saccade-related firing (±500 ms around saccade) for 15 neurons (>200 individual saccades), in relation to mean firing rates of the same neurons. To calculate abscissa, the firing rate during ocular saccades was subtracted from the mean firing rate. *B*, more than one-half of the spikes during waking were associated with preceding short-lasting hyperpolarizing potentials. *Inset (bottom right)*: another neuron from area 4, recorded in the waking state, in which short-lasting IPSPs were activated by stimulation of thalamic ventrolateral nucleus. Modified from Timofeev et al. (2001b). See Plate section for color version of this figure.

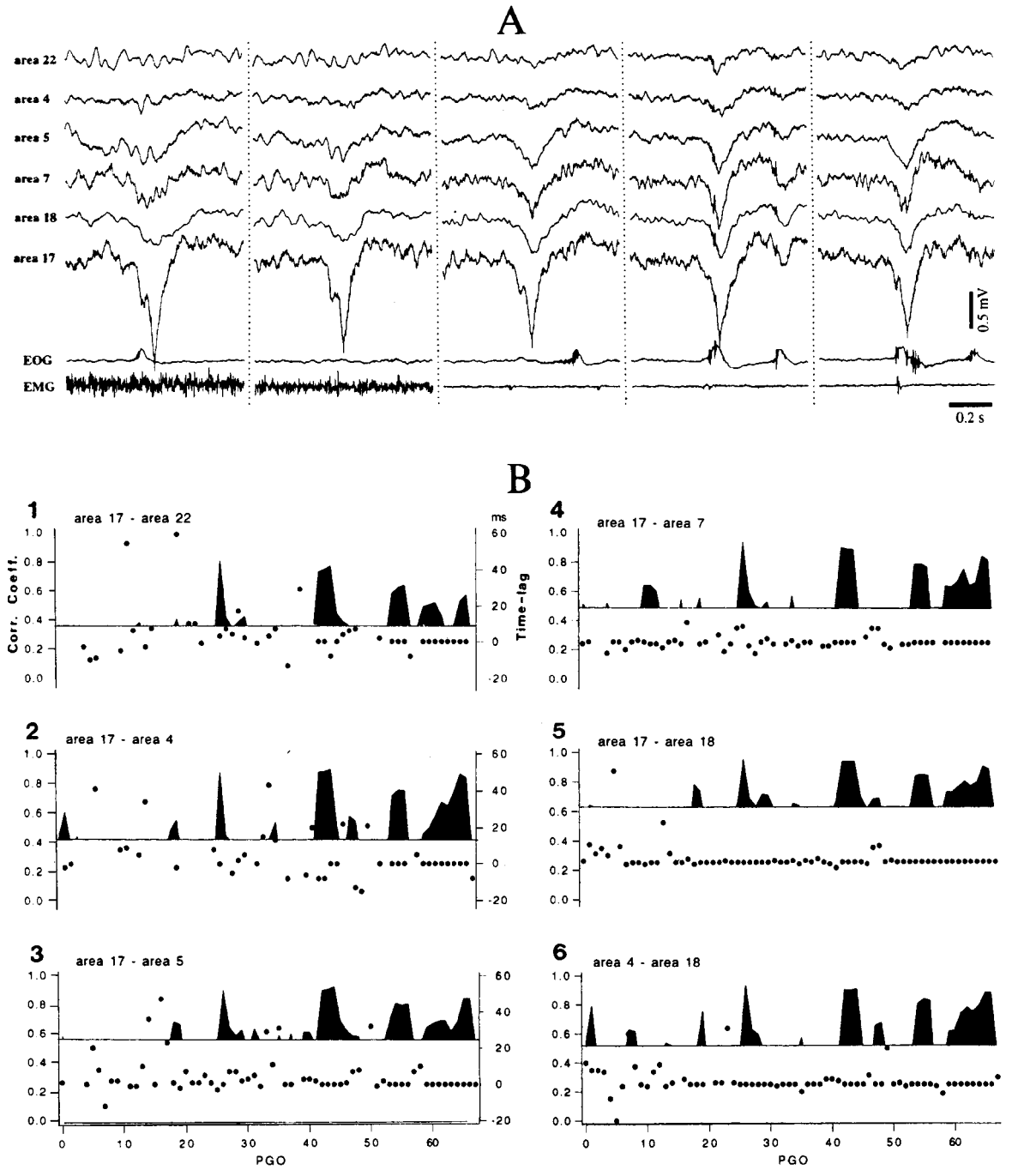

Fig. 3.60 Dynamic evolution of synchrony among PGO waves recorded from six cortical areas (ectosylvian area 22, precruciate area 4, suprasylvian areas 5 and 7, and marginal areas 17 and 18). Chronically implanted cat. *A*, the 70 PGO waves detected in area 17 during a pre-REM epoch leading to REM sleep were divided into five consecutive epochs (separated by dotted lines) with 14 PGOs in each, and averaged over each epoch. The averaged EOG and EMG traces are added below to depict the progression towards REM sleep (the first two columns correspond to the pre-REM transitional epoch), before the occurrence of muscular atonia. Note progressively increased amplitude of PGOs in areas remote from area 17 with progression of REM sleep. *B*, sequential field correlation between various cortical areas. The black-filled parts (ordinate at left) represent the progressive increase in the synchrony coefficient (height of the central correlation peak). The average correlation coefficient is indicated by the horizontal line. In each panel, dots represent the individual time-lags (ordinate at right in ms) and show shorter time-lags between the respective waves with the progression toward REM sleep. From Amzica and Steriade (1996).

[255, 261, 264]. These PGO-on neurons fire stereotyped low-frequency spike-bursts or single spikes preceding the negative peak of PGO waves in LG nucleus by 20–40 ms and otherwise display low firing rates (0.5–3.5 Hz) during all states of vigilance (Fig. 3.61*A*). They were termed sluggish-burst PGO-on neurons but were found in only a relatively small proportion (10–15%) of PPT/LDT neurons [265]. In a systematic search for all neuronal types related to PGO waves, several other firing patterns were revealed in PPT/LDT neurons [265]. The major types, besides PGO-on sluggish-burst neurons, are as follows. High-frequency spike-bursts are fired on a background of tonically increased firing rates of PPT/LDT neurons. These PGO-related bursts are triggered after a period of progressive acceleration of spontaneous discharges (Fig. 3.61*B*) and thus may be high-threshold bursts fired at a depolarized level. Other PPT/LDT neurons discharge tonically and display the longest lead-time (~150 ms) with respect to thalamic PGO waves. Unexpectedly, some neurons were found to discharge tonically during REM sleep, in a very regular manner and with high firing rates (20–30 Hz), but ceased firing 50–180 ms before the LG-PGO wave. The features of all these neuronal types are illustrated in Fig. 3.62.

How are PGO-on neurons set into action? Impulses in PGO generators can be triggered by any of the multiple input sources to the PPT/LDT nuclei; namely, the midbrain and bulbopontine reticular core (Fig. 3.63), posterior and anterior hypothalamic areas, and cerebral cortex, to name a few. While the mechanism of high-frequency bursts on a background of progressively increased firing rate is conceivably a high-threshold Ca^{2+} conductance, possibly located in dendrites of PPT/LDT neurons, the more sluggish spike-bursts, which are preceded by periods of neuronal silence, may be triggered through de-inactivation of LTSs by membrane hyperpolarization [266, 267]. The duration of LTSs in rat PPT neurons is much longer (50–150 ms) [266] than that described in thalamic neurons [268] and the intra-burst frequency of Na^{+} spikes crowning the LTSs lower than 200 Hz, which is indeed the case for PGO-on sluggish-bursts in PPT/LDT neurons. One input source that may hyperpolarize PPT neurons to produce low-threshold spike-bursts is probably GABAergic SNr neurons (Fig. 3.63) that project to PPT neurons, inhibit them [266] and display an increased activity 50–150 ms prior to the thalamic PGO waves [269]. As to PGO-off neurons (see Fig. 3.62*D*), they are probably GABAergic neurons intrinsic to PPT/LDT nuclei, as they displayed high discharge rates during all states of vigilance; like GABAergic neurons in many other structures [270], PGO-off neurons have been found in cholinergic nuclei at the mesopontine junction [271], and they could disinhibit adjacent PGO-on neurons (Fig. 3.63).

[264] Sakai and Jouvet (1980); Sakai et al. (1990).

[265] Steriade et al. (1990c).

[266] Kang and Kitai (1990).

[267] Leonard and Llinás (1990); Wilcox et al. (1989).

[268] Jahnsen and Llinás (1984a-b); Deschênes et al. (1984); Steriade et al. (1985).

[269] Datta et al. (1991).

[270] GABAergic neurons fire at higher rates, compared to other neurons, as reported for Purkinje (Eccles et al., 1967), SNr [256], thalamic RE [154], and conventional fast-spiking cortical [31] neurons. The calcium-binding protein found in GABAergic neurons would prevent the activation of $I_{K(Ca)}$ (Celio, 1986), thus reducing the afterhyperpolarizing potentials, with the consequence of increasing discharge frequency of these neurons. In all these GABAergic neurons, firing rates diminish from wakefulness to sleep (for Purkinje neurons, see Andre and Arrighi, 2001).

[271] Kosaka et al. (1987); Ford et al. (1995).

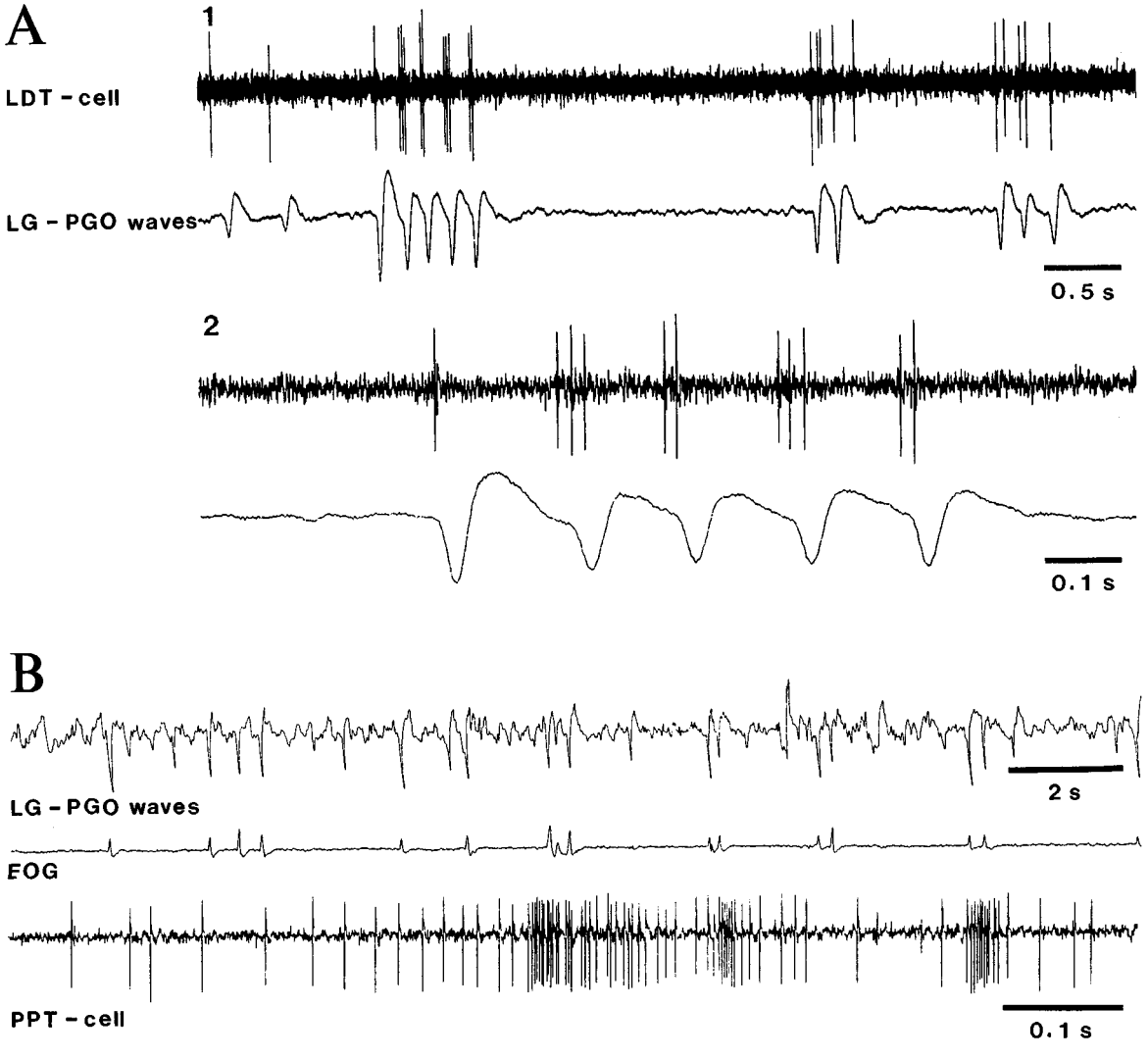

Fig. 3.61 Two types of PGO-on related neurons in cholinergic mesopontine nuclei. Chronically implanted cats. Extracellular recordings from LDT (*A*) and PPT (*B*) neurons, together with field potentials from thalamic LG nucleus. *A*, PGO-on LDT neuron discharging single spikes, doublets or triplets preceding PGO waves in LG nucleus. *B*, PGO-on PPT neuron (antidromically activated from LG nucleus) discharging high-frequency bursts preceding PGO waves and ocular saccades, following a progressive acceleration of discharges preceding the burst by ~100–150 ms. Modified from Steriade et al. (1990c).

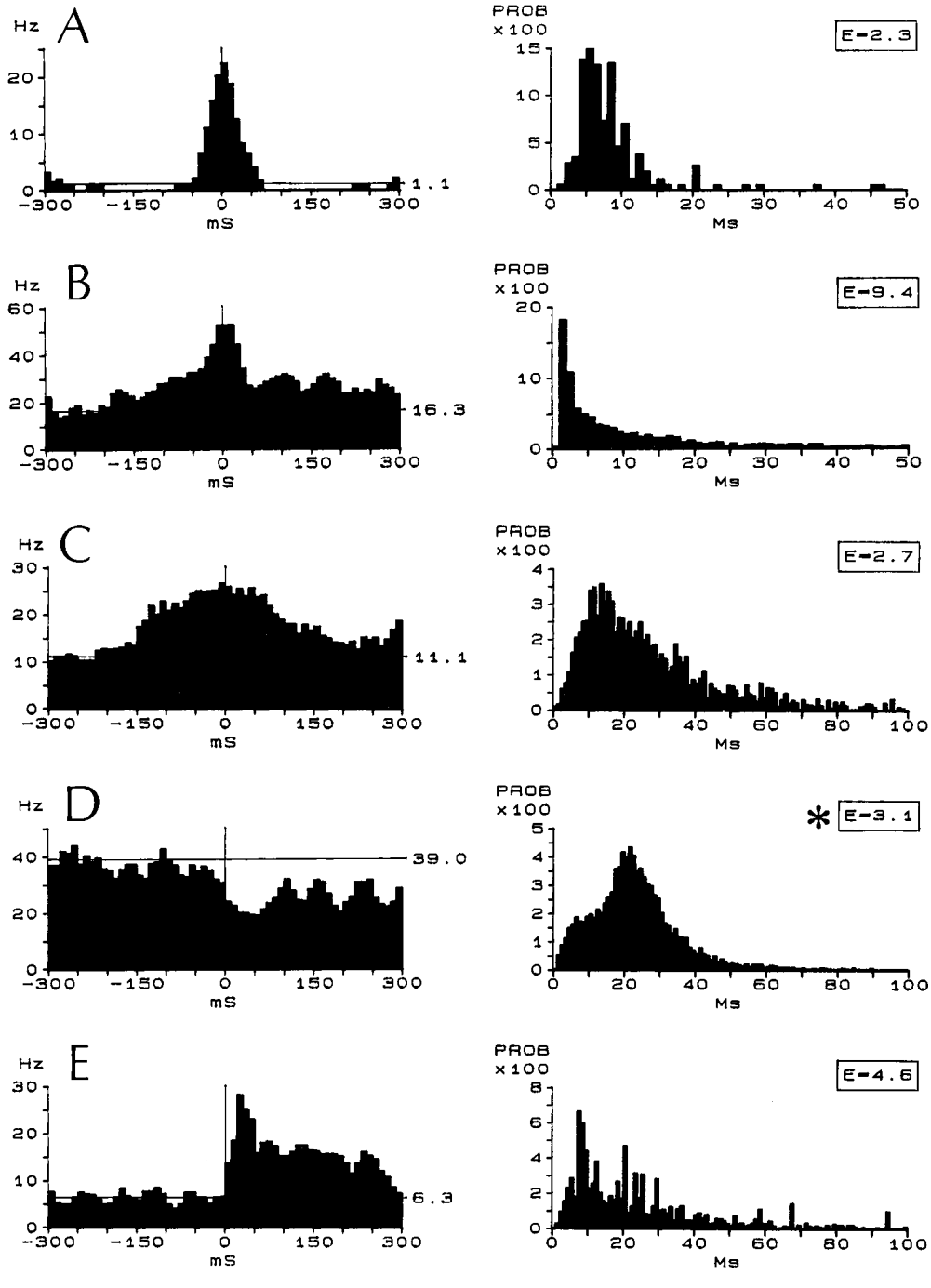

Fig. 3.62 PGO-related activities in pools of PGO-on sluggish-burst neurons in chronically implanted cats (*A*, $n = 5$); PGO-on high-frequency burst neurons with tonically increased firing rates in REM sleep (*B*, $n = 11$; as in Fig. 3.61*B*); PGO-tonic neurons (*C*, $n = 10$); REM-on but PGO-off neurons (*D*, $n = 3$); and post-PGO-on neurons (*E*, $n = 11$). Peri-PGO spike histograms (PPSHs) in left columns are depicted for all neuronal types. Peri-PGO spike histograms (PPIHs) are depicted for *A-C* and *E* neuronal types. Symbol E in PPIHs: percentage of PGO-related intervals in excess of the depicted time range. In *D*, right column (asterisk) depicts a pooled interspike interval histogram (ISIH) from REM sleep, instead of PPIH, since the peri-PGO activity consists of a drop in firing rate. From Steriade et al. (1990c).

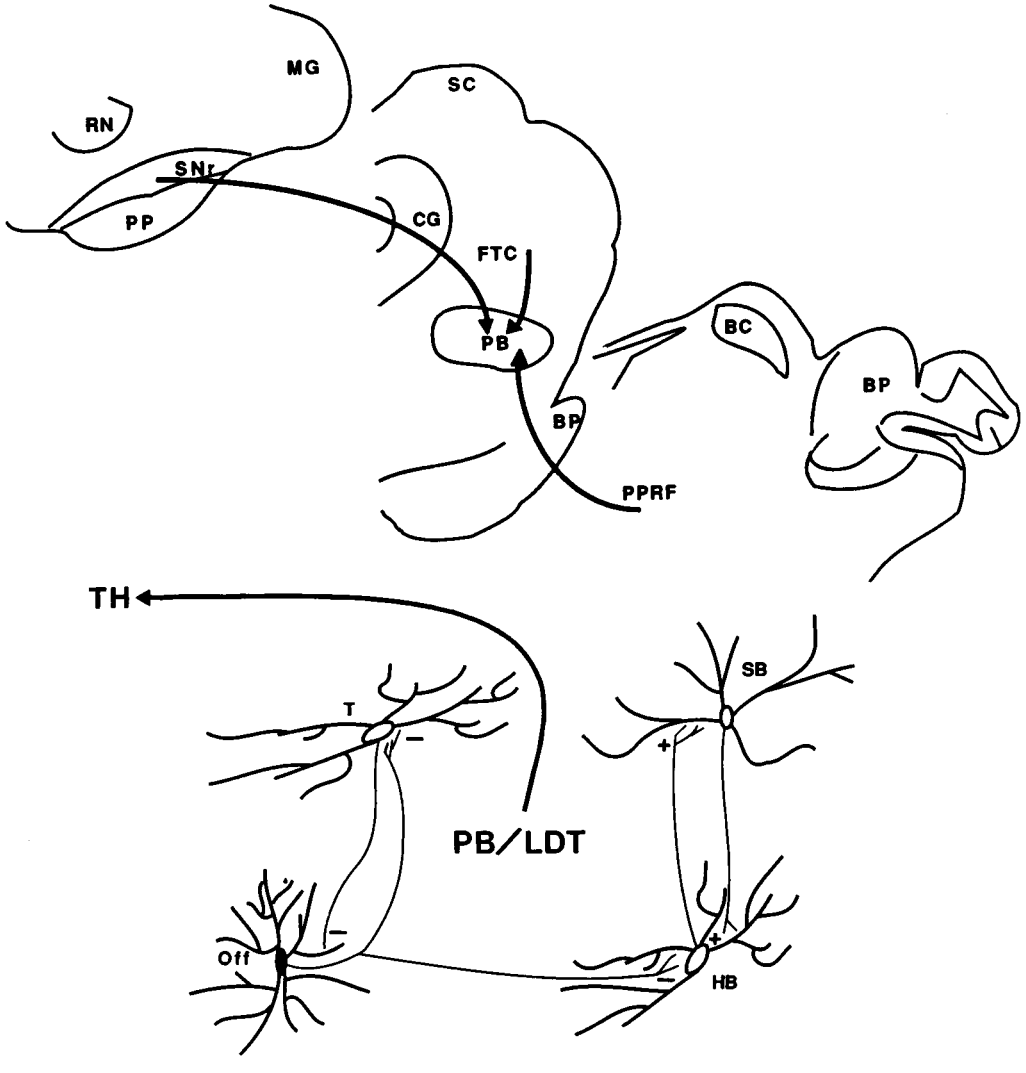

Fig. 3.63 Tentative schemes of cellular interactions underlying the genesis of PGO waves and their transfer from PPT/LDT nuclei to the thalamus (TH). *Top*, three frontal sections (from rostral to caudal) depicting the inputs to PPT area from substantia nigra, pars reticulata (SNr), central tegmental field in the midbrain (FTC), and the paramedian pontine reticular formation (PPRF). Other abbreviations: BC, brachium conjunctivum; BP, brachium pontis; CG, central gray; MG, medial geniculate nucleus; PP, pes pedunculi; RN, red nucleus; SC, superior colliculus. *Bottom*, hypothesized excitatory (+) and inhibitory (−) interactions between four cellular types (PGO-on and PGO-off) recorded from PPT/LDT nuclei. Symbols: SB, PGO-on sluggish-burst neurons; HB, PGO-on high-frequency burst neurons; Off, PGO-off neurons; T, PGO-on tonic neurons. See also text. From Steriade et al. (1990c).

Thus, cholinergic PPT/LDT neurons can be regarded as the final link in the brainstem-thalamic path that generates PGO waves. Because these phenomena occur in REM sleep when the brain is disconnected from peripheral sensory signals and because the content of oneiric behavior may relate to past experience, hypothalamic and forebrain structures, which store some of the emotionally charged information, may be most effective in driving the PGO brainstem neuronal generators. As to the functions of PGO waves, which are activating impulses during dreaming sleep, they may play a major role in the structural maturation of target structures, especially during ontogenesis when REM sleep occupies most of the sleeping time [272].

3.3.2. Fast rhythms (20–60 Hz)

Brain-active states are associated with peculiar types of oscillatory activities. One type of oscillation, theta rhythm (5–8 Hz), typical of hippocampus and subsystems in rats [273], was related to focused attention, working memory, voluntary movements, but was also observed in the absence of overt movements [274]. As I do not have first-hand experience with this rhythm, the reader is referred to extensive reviews on theta activity [275]. In this section, I will briefly focus on fast, also called beta/gamma, rhythms (usually 20–60 Hz) and on their neuronal mechanisms in thalamus and neocortex. Fast rhythms, their cellular basis and functional significance, and some controversial aspects are also discussed in my recent monograph [25].

Spontaneously occurring fast rhythms characterize the two brain-active states, wakefulness and REM sleep, during which these oscillations appear in a steady, almost uninterrupted way, in both humans [276] and animals [277]. Distinctly from the conventional term "EEG-desynchronized" that is applied to these two behavioral states, a designation used by most epigones of Moruzzi and Magoun [278] who first described the EEG patterns of an activated cerebrum, spontaneous fast rhythms are actually synchronized over neighboring cortical sites as well as across specific corticothalamic circuits [277] (Fig. 3.64*A–B*). Historically, the first demonstration that the EEG-activated response to brainstem reticular stimulation is not only the blockage of spindles and slow waves, but also includes the appearance of fast rhythms displaying a regular acceleration and synchronization ("*accélération synchronisatrice*"), belongs to Bremer and his colleagues [279]. This preceded by almost three decades the present excitement about these oscillations. Since Bremer's observation, a series of studies in various cortical areas have reported the presence of beta/gamma waves during

[272] Roffwarg et al. (1966).

[273] The cellular bases of theta waves have been intensively investigated in rats, but this limbic oscillation diminishes in amplitude and regularity from rodents to other species. In cat, the theta hippocampal activity is evident during REM sleep, but occurs only exceptionally during wakefulness (Jouvet, 1965). Theta is also poorly represented in primates (Crowne and Radcliffe, 1975; but see Stewart and Fox, 1991). The presence of theta was denied in humans, even with deep electrodes inserted in the hippocampus (Halgren et al., 1985). The normal theta activity, reflecting brain activation in rodents, should not be confused with pathological "theta" waves, due to reduction in cerebral blood flow (Ingvar et al., 1976), metabolic encephalopathies (Saunders and Westmoreland, 1979), and lesions in deeply located structures (Gloor, 1976). Nonetheless, a frontal midline theta rhythm, rather focally distributed, was found to increase in magnitude with increased memory load and improved performance in humans (Gevins et al., 1997).

[274] Adey (1967); Vanderwolf (1969); Buzsáki et al. (1979).

[275] Bland and Colom (1993); Vertes and Kocsis (1997); Buzsáki (2002).

[276] Llinás and Ribary (1993).

[277] Steriade et al. (1996a-b). These studies concerned fast oscillations in neocortical and thalamic networks. Spontaneous fast oscillations also appear in perirhinal cortex (Collins et al., 2001) and hippocampus (Buzsáki and Chrobak, 1995; Traub et al., 1996; Draguhn et al., 1998).

[278] Moruzzi and Magoun (1949).

[279] Bremer et al. (1960).

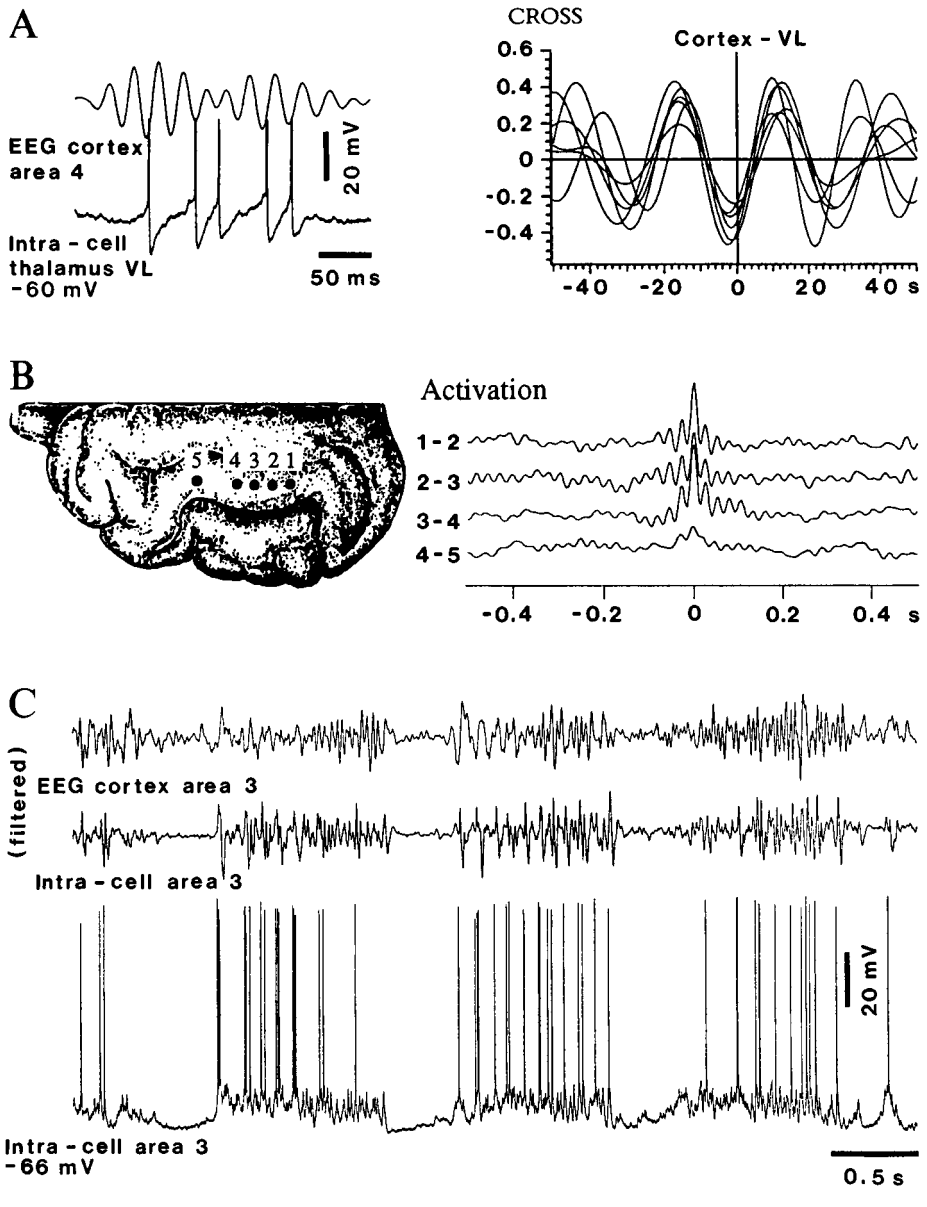

Fig. 3.64 Intracortical and corticothalamic synchronization of fast rhythms, and their relation with the depolarizing phase of the slow sleep oscillation. *A*, short episode of activation in cat cerebral cortex during ketamine-xylazine anesthesia, associated with coherent fast rhythms (about 40 Hz) in EEG from motor cortex (area 4) and intracellularly recorded thalamocortical neuron from ventrolateral (VL) nucleus. Two traces represent simultaneous recordings of depth-EEG and intracellular activity of VL neuron (spikes truncated). Note close time-relations between action potentials of VL neuron and depth-negative waves in cortical EEG (reflecting summated excitatory events in a pool of neurons) at a frequency of about 40 Hz. Cross-correlations (CROSS) between action potentials and depth-EEG shows a clear-cut relation, with opposition of phase, between the intracellularly recorded VL neuron and EEG waves. *B*, synchronization of fast rhythms (35–40 Hz) among closely spaced leads in cortical areas 5 and 7. Cross-correlations between field potentials recorded from foci *1-2*, *2-3*, *3-4*, and *4-5* (see cortex figurine at left). Note decreased correlation with a slightly increased distance (*4-5*). *C* , fast oscillations are superimposed over the depolarizing envelope of the slow cortical oscillation (0.6–0.7 Hz) and are absent during the hyperpolarizing phase of this oscillation. Cat under ketamine-xylazine anesthesia. Three traces represent (from top to bottom): depth-EEG from somatosensory cortical area 3b, intracellular activity of neuron in the same area (both these traces are filtered, 10 to 100 Hz), and unfiltered intracellular activity of the same area 3 neuron. Modified from Steriade et al. (1996a-b).

different conditions of increased alertness, such as intense attention to a visual stimulus, accurate performance of a conditioned response, tasks requiring fine finger movements and focused attention in monkey motor cortical neurons, focused arousal prior to the performance of a complex task in humans, behavioral immobility associated with an enhanced level of vigilance while a cat was watching a visible but unseizable mouse, selective attention to somatosensory and visual signals in monkeys and humans, and stimulus-dependent oscillations in the olfactory and visual cortices [280]. Figure 3.65 illustrates increased oscillations in the frequency band of 20–40 Hz during exploratory hand movements when a monkey attempted to extract raisins from the experimenter's hand [281].

The possible significance of this rhythm resides in the fact that, in addition to the spatial mapping that allows a limited number of representations, a temporal component is brought about by synchronized oscillatory (around 40 Hz) responses across spatially separate cortical columns. The conjunction of spatial and temporal factors is the basis of functionally coherent cell assemblies, distinguished by the phase and the frequency of their synchronous oscillatory activity [282]. The neuronal ensembles link spatially distributed elements and may be the bases for global and coherent properties of patterns, a prerequisite for scene segmentation and figure-ground distinction [282]. This hypothesis promoted intensive research, but is controversial and was challenged on multiple grounds. Among these aspects, let me mention the fact that the low incidence of cortical oscillatory neurons has led some to propose that such correlations contribute very little to perception [283]. Other investigators, working on the somatosensory system, found that long-range cortical synchronization may occur within narrow time periods without concomitant neuronal oscillations in the gamma frequency range [284]. Lastly, the term "40 Hz" frequency, initially reported in studies of visual cortex responses, but also used in more recent studies, should not be considered as representing a magic frequency as many subsequent studies, using both extracellular and intracellular recordings, found much lower frequencies (<20 Hz and even ~10 Hz) of oscillatory responses, in the low beta and alpha bands [285].

Besides the two major states of brain alertness (waking and REM sleep), which some experimenters and theoreticians regard as the only ones associated with spontaneous fast rhythms, the same oscillatory type is superimposed over the depolarizing (excitatory) phase of the slow oscillation during SWS, whereas it is selectively abolished during the hyperpolarizing phase of the slow sleep

[280] Lopes da Silva et al. (1970); Freeman (1975); Rougeul-Buser et al. (1983); Sheer (1984); Bouyer et al. (1987); Eckhorn et al. (1988); Freeman and Van Dijk (1988); Gray et al. (1989, 1990); Engel et al. (1991); Murthy and Fetz (1992, 1997a-b); Desmedt and Tomberg (1994); Fries et al. (2001). See Llinás and Paré (1991) who postulated reciprocal relations between thalamic intralaminar nuclei and cortex in the generation of fast rhythms in the gamma band (20–50 Hz), and the recent hypothesis of Jones (2001) who implicated the role played in this rhythm by a matrix of calbindin-immunoreactive neurons in virtually all thalamic nuclei, which project to superficial layers of cortex.

[281] Fetz et al. (2000).

[282] Singer (1990a-b).

[283] Shadlen and Movshon (1999). A very low incidence (<1%) of oscillating responses was also reported by many other authors, among them Young et al. (1992) who found fast oscillatory responses in 2 of 424 recordings. Also, experimental evidence in humans led to the conclusion that synchrony is not responsible for perception of form (Farid and Adelson, 2001).

[284] Roy et al. (2001). These authors found only 1% of neuronal pairs that displayed oscillations at the same frequency in both neurons.

[285] Bringuier et al. (1997); Farmer (1998).

[286] Llinás et al. (1991); Nuñez et al. (1992c); Gutfreund et al. (1995).

[287] Steriade et al. (1991b, 1993c). Focal stimulation of the RE nucleus induces fast oscillations in the gamma activity, which is specific to the somatosensory or auditory system, depending on the RE sector stimulated (MacDonald et al., 1998). These data fit in well with those emphasizing the presence of gamma activity in specific thalamocortical systems (Steriade et al., 1996b; see below). Pinault and Deschênes (1992a) thought that gamma oscillations in thalamic RE neurons are dependent on a pacemaker mechanism because subthreshold waves were voltage-dependent, appeared at a fixed frequency, and were not driven by synaptic inputs. However, intracellular studies of RE neurons *in vitro* (Bal and McCormick, 1993) and *in vivo* (Contreras et al., 1992) failed to confirm this hypothesis since no

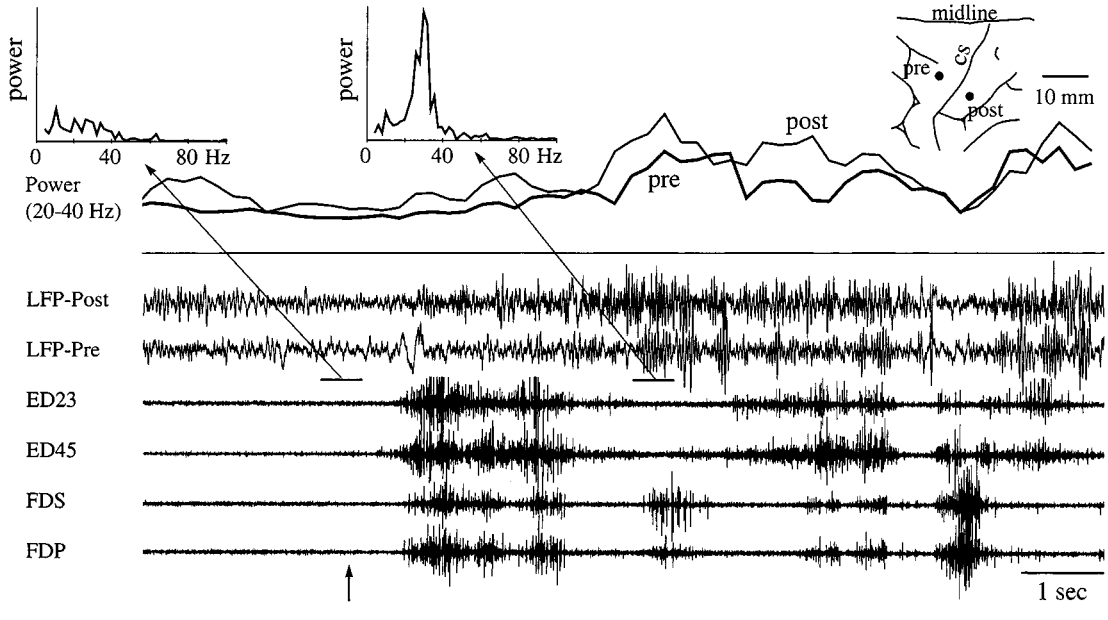

Fig. 3.65 Increases in local field potential (LFP) oscillations during exploratory hand movements in monkey. Traces from bottom up show EMG activity of forearm muscles controlling wrist and digits, LFPs recorded at pre- and postcentral sites, and LFP power in the 20–40 Hz band. Power spectra were calculated for 256-ms windows successively shifted by 100 ms. Recordings begin with monkey at rest. At the arrow, a raisin was offered to the side of the head (which was fixed in space) and the monkey extracted it from the experimenter's hand. Top insets show sample power spectra from indicated intervals during rest and movement (left), and location of cortical recording sites (right). From Fetz et al. (2000).

preferred frequency was revealed between 10 and 40 Hz and no subthreshold rhythmic activity at fixed frequency could be detected. In fact, fast oscillations (20–60 Hz) in RE neurons appear in grouped sequences that are coherent to similar rhythms in dorsal thalamic neurons and EEG (Steriade et al., 1996b) and could then be ascribed to synaptic interactions in corticothalamic networks. Fast rhythms were searched for in different sectors of the RE nuclear complex of attentive, performing animals, but their presence was denied (Canu and Rougeul, 1992; Bekisz and Wróbel, 1993).

[288] Steriade and Amzica (1996). Brainstem reticular activation facilitates synchronization of visual-evoked oscillatory responses in the gamma frequency band (Munk et al., 1996; Herculano-Houzel et al., 1999).

oscillation [277] (see above, Fig. 3.64*C*). In an extracellular position, fast cortical oscillations occur during the depth-negative field potentials, and the envelope of rhythmic activities between 15 and 80 Hz is reciprocal to slow waves between 0 and 4 Hz (Fig. 3.66*A*). Upon arousal fast waves are continuous, whereas slow waves are absent (Fig. 3.66*B*). The fact that fast oscillations appear not only during brain-aroused states, but also over the depolarizing phase of the slow oscillation during anesthesia and natural SWS (Figs. 3.64*C* and 3.66*A*), indicates that the fast oscillations are voltage (depolarization) dependent, and do not necessarily reflect a behavioral state associated with high cognitive or conscious processes. Depolarizing current pulses can trigger fast oscillations in cortical [286] and thalamic [287] neurons.

The hypothesis that 40 Hz oscillations reflect an increased level of alertness is supported by the induction of these rhythms following stimulation of PPT/LDT cholinergic nuclei at the mesopontine junction [277, 288]. Neurons recorded from these brainstem nuclei and antidromically identified as projecting to thalamus increase their firing rates during waking and REM sleep, much above the levels seen during SWS [24]. This statistically significant increase in

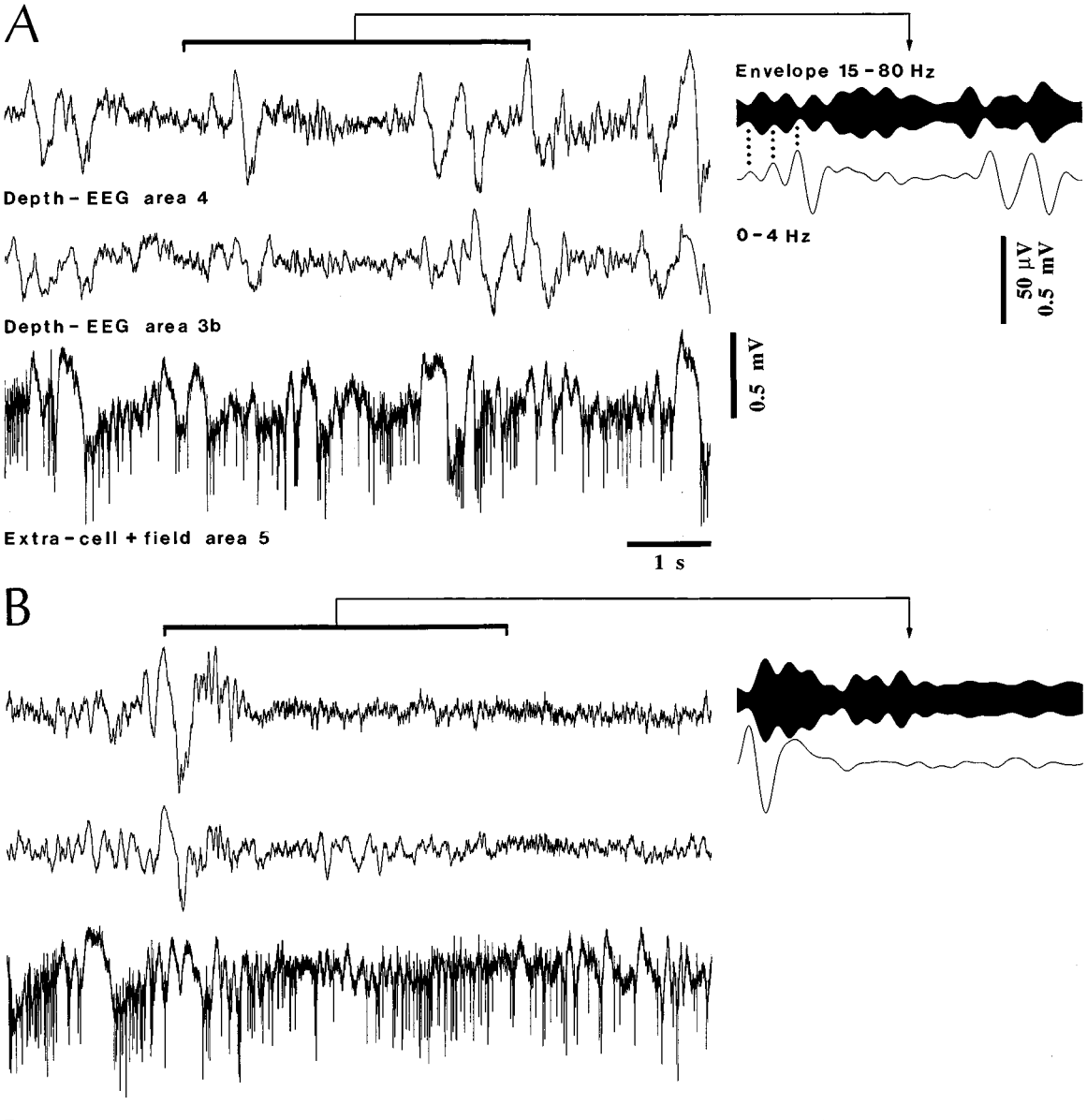

Fig. 3.66 Fast cortical oscillations occur during the depth-negative (depolarizing) phase of the slow oscillation during natural sleep, are reduced or absent during the depth-positive (hyperpolarizing) phase of the slow sleep oscillation, and are continuous during arousal. Chronically implanted cat. Three traces represent (from top to bottom): depth-EEG from areas 4 and 3b, and field potentials recorded simultaneously with action potentials from area 5. *A*, SWS epoch (part marked by horizontal line is expanded on the right, arrow). Note that fast oscillations (15–80 Hz) are reduced, up to disappearance, during depth-positive components (upward deflections) of the slow oscillation. *B*, arousal from SWS. Unpublished experiments by M. Steriade and F. Amzica.

firing rates of PPT/LDT neurons takes place 30–60 s in advance of the most precocious sign of EEG activation during the transition from SWS to either arousal or REM sleep (see Fig. 3.56*B*). Such a temporal correlation suggests that thalamically projecting cholinergic PPT/LDT neurons are causally involved in triggering and maintaining activation processes in thalamocortical systems. Mesopontine cholinergic nuclei directly and indirectly excite TC neurons. The direct excitation has two components: a short-latency, short-duration depolarization mediated by nicotinic receptors and associated with an increase in membrane conductance; and a prolonged (20–60 s) depolarization mediated by muscarinic receptors and associated with an increase in input resistance [289]. The same cholinergic nuclei indirectly excite TC neurons by inhibiting GABAergc RE cells through a hyperpolarization associated with an increase in membrane conductance [56]. Both these mechanisms are factors behind the increased firing rates and enhanced synaptic excitability of TC neurons, with consequently similar activated patterns in target neocortical neurons.

At variance with increased firing rates of mesopontine cholinergic neurons in advance of the most precocious activation signs with transition from SWS to either waking or REM sleep [24], cortical neurons are depolarized and increase their discharges several seconds *after* the first sign of EEG activation [31]. The evolution of a change in membrane potential with respect to the time 0 defining the onset of brain-activated states during transitions from SWS to either waking or REM sleep is illustrated in Fig. 3.67. The neurons showed a much higher dispersion of the membrane potential during SWS, compared to either REM sleep or waking, because of the succession of hyperpolarizing and depolarizing phases of the slow sleep oscillation. Obliteration of hyperpolarizing phases occurred at the very onset of brain-activated states (time 0) but in most cases the overt depolarization followed time 0 by about 5 to 10 s. This is distinct from the precursor changes displayed by PPT/LDT neurons and indicates that fast activities in cortical neurons follow activating impulses in brainstem-thalamic-cortical projections.

The widespread occurrence of fast oscillations during REM sleep, reflecting activation processes in brainstem cholinergic nuclei, thalamus, cortical areas, and amygdalo-hippocampal circuits, fits in well with a positive correlation of blood flow with REM sleep in all these structures [290]. It was postulated that one function of SWS is the consolidation of memory traces acquired during wakefulness [188, 233, 234]. At the neuronal level, instrumentally conditioned fast oscillations (20–50 Hz), which occurred synchronously in intracortical, intrathalamic, and corticothalamic networks, were

[289] These effects induced by stimulating brainstem cholinergic nuclei *in vivo* (Curró Dossi et al., 1991) are congruent with data from *in vitro* experiments using ACh application in some dorsal thalamic nuclei (McCormick and Prince, 1987).

[290] Maquet et al. (1996).

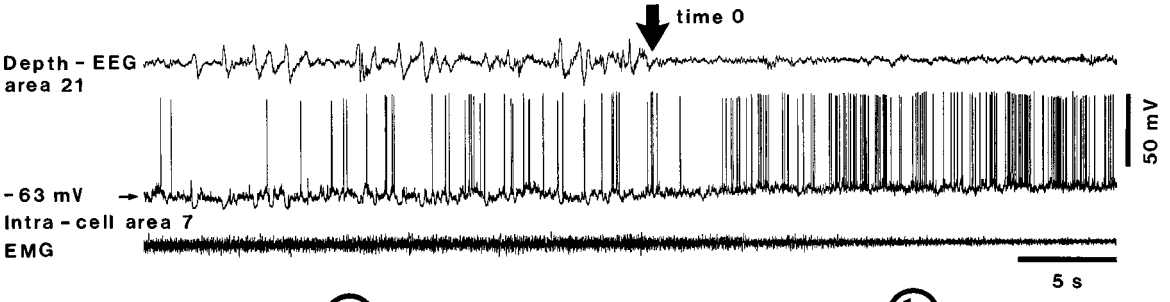
time 0
Depth - EEG
area 21
50 mV
- 63 mV
Intra - cell area 7
EMG
5 s

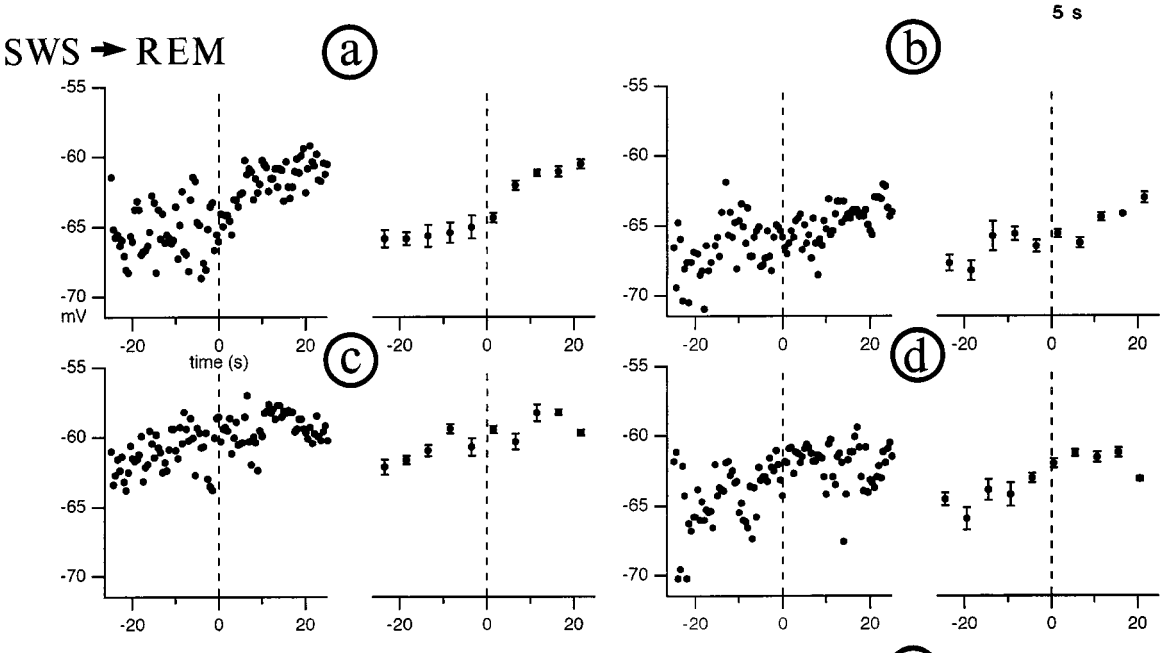
SWS → REM
a
b
c
d
-55
-60
-65
-70
mV
-20
0
20
time (s)

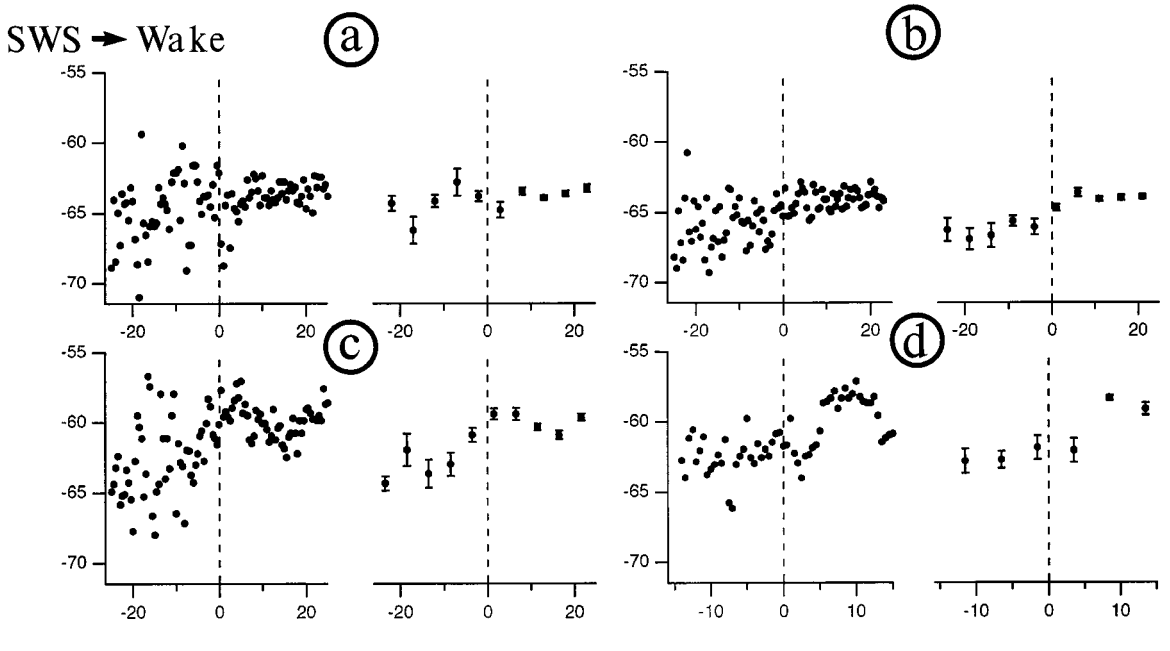
SWS → Wake
a
b
c
d
-55
-60
-65
-70
-20
0
20
-10
10

[291] Amzica et al. (1997).

[292] Hennevin et al. (1995).

[293] Maquet et al. (2000); Laureys et al. (2001).

reactivated during subsequent post-training periods of SWS and REM sleep [291]. Like SWS, REM sleep was implicated in the process of memory consolidation as periods of learning are associated with a subsequent increase in this brain-active sleep stage, whereas REM sleep deprivation impairs memory for previously learned data [292]. Positron emission tomography and regional blood flow measurements related to experience-dependent changes showed that several brain areas are significantly more active during REM sleep in human subjects previously trained on reaction time tasks than in non-trained subjects [293].

The above data suggest that a series of brain oscillations, both slow and fast frequencies, during SWS and REM sleep may favor plasticity processes and contribute to consolidation of memory traces. This aspect is elaborated in the next chapter.

3.4. Concluding remarks

(a) Since falling asleep generally requires longer time scales than those of conventional neuronal mechanisms, humoral factors should also be envisaged in this process. Although dozens of such factors have been hypothesized, very few have been investigated in relation to their effects on neurons in brain areas that have been identified as critical for the genesis and maintenance of sleep. Adenosine, a purine nucleoside, is a sleep-inducing substance that mediates its effects by inhibiting basal forebrain and mesopontine cholinergic neurons, which fire at high rates during wakefulness.

(b) There is no need to conclude unequivocally that sleep results from brain deafferentation or, alternatively, from inhibitory processes acting upon awakening systems. Passive or active sleep is a false dilemma since humoral factors, brain deafferentation from external and internal signals, and inhibitory neurons acting on activating ones should all be considered in concert. The best studied brain structure with presumed hypnogenic properties is the preoptic region in the anterior

Fig. 3.67 (opposite) Sequential alterations in the membrane potential (V_m) during transition from SWS to REM sleep and wakefulness. Chronically implanted cat. *Top panel* depicts a transition from SWS to REM sleep to indicate the time 0 taken for brain activation (arrow), as indicated by EEG changes. Three traces represent depth-EEG from area 21, intracellular recording of area 7 RS neuron, and EMG. The panel below shows the evolution of V_m in four neurons (*a* to *d*) during transition from SWS to REM sleep. In all cases, each point in the left plots represents the peak in a histogram of membrane potential distribution for 0.5-s bins, while right plots show the same epoch in 5-s bins (median and SE). Ordinate represents voltage (mV) and abscissa represents time (in seconds) before and after time 0. The same is shown below for the four neurons during transition from SWS to waking. From Steriade et al. (2001a).

hypothalamus that exerts inhibitory (GABAergic) actions onto histaminergic neurons in the posterolateral hypothalamus, which have activating effects on thalamic and neocortical neurons. Thus, the postulated hypnogenic action of preoptic neurons should be considered within the conceptual framework of sleep as a product of brain disconnection from ascending activating generalized systems.

(c) The three major oscillations during slow-wave sleep are: the slow oscillation at ~0.5–1 Hz (generated intracortically); spindles at ~7–15 Hz (whose pacemaker is the thalamic reticular nucleus, which produces hyperpolarizations leading to spike-bursts in thalamic relay neurons that transfer this oscillation to cortex); and two components of delta rhythmicity (1–4 Hz), one of them generated by an interplay between two intrinsic currents of thalamocortical cells, the other arising in the cerebral cortex. However, unlike "pure" rhythms generated in the restricted circuits of simplified preparations, such as slices maintained *in vitro*, the living brain does not display during slow-wave sleep each of these three oscillations in isolation, but exhibits a real coalescence of slow oscillation with both spindles and delta waves, as well as with fast rhythms (~20–60 Hz) that are conventionally thought to define activated states. This is due, on one hand, to the fact that synchronous discharges of neocortical neurons during the slow sleep oscillation drive thalamic neurons to generate spindle and delta oscillations. On the other hand, the depolarizing phase of the slow oscillation creates conditions for the appearance of voltage-dependent fast rhythms.

(d) Although spindles are generated within the thalamus, cortical volleys trigger spindles in the thalamus and the presence of neocortex is necessary for the long-range synchronization of spindles. Indeed, while spindles sequences propagate in thalamic slices maintained *in vitro*, spindling is nearly simultaneous throughout the thalamus and the cortex in intact-brain animals and humans. The increasing depolarization of corticothalamic neurons toward the end of spindle sequences is also operational in the process of terminating spindle sequences by producing different durations of IPSPs in thalamocortical cells and leading to asynchrony in thalamic circuits.

(e) In contrast to the obsolete ideas that, during slow-wave sleep, there is a global inhibition in cortex and subcortical structures, neurons in neocortical areas display unexpectedly high levels of spontaneous activity and the intracortical dialogue is maintained. These experimental results, partly from recent

intracellular recordings in naturally sleeping animals, suggest that slow-wave sleep subserves important cerebral functions. During slow-wave sleep oscillations, rhythmic and synchronized spike-bursts and spike-trains fired by thalamic relay and neocortical neurons depolarize the dendrites of cortical neurons, which is presumably associated with massive Ca^{2+} entry. Depolarizing pulses of Ca^{2+} trigger enzyme cascades and have long-lasting effects on gene regulation and may provide an effective signal to efficiently activate calcium calmodulin-dependent protein kinase II that is implicated in synaptic plasticity. These data show that, far from being a period of complete inactivity, slow-wave sleep is implicated in mental processes related to the consolidation of memory traces acquired during waking behavior.

(f) During REM sleep, a brain-active state, phasic events are ocular saccades and ponto-geniculo-occipital waves. Ocular saccades are generated in brainstem networks, specifically the circuits between substantia nigra reticulata, superior colliculus, and premotor pontine neurons. During ocular saccades, cortical regular-spiking neurons decrease firing rates and display numerous, low-amplitude and short, chloride-dependent IPSPs imposed on them by inhibitory interneurons. Ponto-geniculo-occipital waves, probably the "stuff that dreams are made off", are triggered by any of the multiple input sources to mesopontine cholinergic nuclei, which project to the thalamus. The cellular mechanisms underlying these waves in brainstem cholinergic nuclei are low-threshold and high-threshold spike-bursts. The functions of these waves may be the structural maturation of target structures, especially during ontogenesis when REM sleep occupies most of the sleeping time.

(g) Brain-active states are accompanied by sustained fast oscillations (20–60 Hz). It was hypothesized that, during these rhythms, synchronized cortical neuronal ensembles underlie binding of different features of an object into a global percept. This hypothesis is controversial. The fast oscillations are generated in interacting cortical and thalamic networks, under the control of ascending activating systems. In both thalamus and cortex, these rhythms are dependent on neuronal depolarization. This is why fast oscillations, which are conventionally regarded as only present during waking and REM sleep, also occur over the depolarizing phase of the slow sleep oscillation.

Chapter 4 Plastic changes in thalamocortical systems developing from low-frequency sleep oscillations

[1] Bullock (1997).

[2] Steriade (2001a).

[3] Adrian and Matthews (1934).

[4] Jasper and Shagass (1941).

[5] Steriade et al. (2001a).

[6] Steriade et al. (1993b).

[7] Maquet et al. (1997).

This chapter is a continuation of the preceding one. I shall attempt to demonstrate that, far from being epiphenomena with little or no functional significance, spontaneously occurring brain rhythms exert strong influences on neighboring neurons by changing their probability of firing and forcing them into synchrony [1] and produce plastic changes in neuronal responsiveness [2]. That spontaneous brain oscillations may be related to imagination and attention was shown by the blockade of alpha waves even in the absence of a visual stimulus when attempting to "see" in a totally darkened room [3] or when expecting a light stimulus that was omitted [4]. The hypothesized and somewhat controversial role of fast (beta/gamma) oscillations in the binding of different facets of an object into a global percept was discussed in the previous chapter (section ***3.3.2***).

Although earlier hypotheses postulated that slow-wave sleep (SWS) is associated with a global cortical inhibition that prevents any mental activity (see note [224] and related main text in Chapter 3), neocortical neurons display unexpectedly rich spontaneous activity during this sleep stage that is also associated with prolonged and cyclic hyperpolarizations [5], all of which indicates that neocortex is quite active and suggests a reorganization/specification of neuronal circuits in cortex and target structures [6]. This view is supported by studies using indicators of neuronal activities during SWS in humans, revealing more marked changes in those neocortical areas that are implicated in memory tasks and decision-making during wakefulness [7].

Here, I shall focus on the role of low-frequency ($<$15 Hz) sleep oscillations, specifically the waxing-and-waning sleep spindles and their experimental model (augmenting responses), in producing plastic changes in neuronal properties through rhythmic repetition, at an optimal frequency range of $\sim$10 Hz, of spike-bursts and spike-trains in thalamic and cortical neurons. The reasons for choosing spindles as promoters of plasticity in thalamocortical systems are, firstly, the demonstration of persistent changes in synaptic responses after prolonged or even short pulse-trains within the

frequency range of spindles as well as after naturally occurring spindles, and, secondly, the fact that augmenting responses may lead to self-sustained activity and paroxysmal discharges in neocortical neurons. Low-frequency (~5–10 Hz) activities elicited by sensory stimuli or electrical volleys applied to afferent paths, termed slow afterdischarges, characterize the electrical activity of thalamocortical reverberating loops and were long viewed as a mechanism that constitutes the "elementary physiological substratum for *the formation and the persistence* of a mental impression aroused by a sensory stimulus" [8].

The different sections of this chapter deal with:

(a) The differential responsiveness of thalamic and neocortical neurons during states of vigilance, showing that cortical neurons may be engaged in an internal dialogue during SWS despite the absence of information from the outside world.

(b) The characteristics of augmenting (or incremental) responses in thalamocortical (TC), GABAergic reticular (RE) neurons, and different types of neocortical neurons, and the dependency of these responses on behavioral states.

(c) Some notions on plasticity and consolidation of memory during SWS, with emphasis on the experimental evidence that augmenting responses and natural spindles may favor the retention of information in corticothalamic circuits.

The last section will also discuss a form of plasticity, paroxysmal states, which are the topic of the next chapter dealing with epileptic seizures.

4.1. Excitation and inhibition of thalamic and cortical neurons during states of vigilance

Overall, the responsiveness of thalamic and cortical neurons is higher during waking and REM sleep than in SWS [9]. The only electrophysiological feature that may distinguish the two brain-active states in thalamocortical systems is the diminished efficacy of inhibitory processes in REM sleep, compared to waking. The striking contrast between the mental content in waking and REM sleep, which is *not* corroborated by most electrophysiological indicators in thalamus and neocortex, might be ascribed to this difference in inhibitory processes and to the virtual silence of monoamine-containing, brainstem and posterior hypothalamic, neurons during REM sleep [10].

[8] Chang (1950, p. 255; italics mine). This remarkable neurophysiologist, who worked in the mid-1940s at Rockefeller and Yale universities, and thereafter returned to Shanghai, mentioned Ramón y Cajal's idea that corticothalamic circuits constitute the anatomical basis of sensory attention, i.e., the capacity of limiting our conscious activity to a particular region of sensory fields. However, the *reverberating* circuits in the loops between cortex and thalamus were not known at Cajal's time. Chang revived the concept of reverberating circuits between cortex and thalamus that was introduced a decade before him by Dusser de Barenne and McCulloch (1938). Although this idea was repeatedly challenged, nowadays it is supported by most experimental evidence. Chang failed to "initiate the repetitive discharges (in auditory cortex) by stimulation of the radiation fibers after destruction of the homolateral medial geniculate body" (p. 245), thus claiming for the necessary connections between thalamus and cortex. It is known, however, that the neocortex is able to sustain repetitive activity in the absence of the thalamus (see Fig. 4.33*D* in section ***4.2.3***) although thalamically evoked augmenting responses in cortex have higher amplitudes than corticocortical augmenting responses in the absence of the thalamus.

[9] The increased excitability of thalamic and neocortical neurons during both waking and REM sleep, compared to SWS, was demonstrated by testing antidromic and synaptic responses during natural states of vigilance in monkeys and cats (Steriade and Deschênes, 1974; Steriade et al., 1974a-b; Glenn and Steriade, 1982). The fact that sensory events do not give rise to conscious percepts during dreaming (REM) sleep suggested that sensory inputs are analyzed at a preconscious level in this behavioral state and that this preconscious sensory processing could be reflected in subsequent waking behavior (Paré and Llinás, 1995). In support of this hypothesis, early components of sensory-evoked potentials in humans are similar in waking and REM sleep, whereas late components, presumably dependent on attention level and task requirements (Desmedt, 1981), are depressed or absent in REM sleep (Goff et al., 1966; Velasco et al., 1980). The resetting of fast (around 40 Hz) waves by auditory stimuli is also abolished in REM sleep (Llinás and Ribary, 1993). By contrast to all these data from thalamo-neocortical systems, the excitability of the entorhino-hippocampal circuit is lower

during waking and REM sleep, both compared to SWS (Winson and Abzug, 1978).

[10] See notes [248–249] in Chapter 3.

[11] The study of fluctuations in antidromic responses during different behavioral states does not require intracellular recordings, as extracellular recordings provide enough information concerning both the probability of full antidromic spikes and the delay between the initial segment (IS) and somadendritic (SD) components of these responses. IS-SD breaks or IS abortive spikes are indicative of membrane hyperpolarization (Coombs et al., 1955; Llinás and Terzuolo, 1964). See Fig. 4.7*C* for evolution from broken IS-SD antidromic spikes in monkey's cortical neurons during SWS to unbroken action potentials with transition to wakefulness.

[12] Glenn and Steriade (1982).

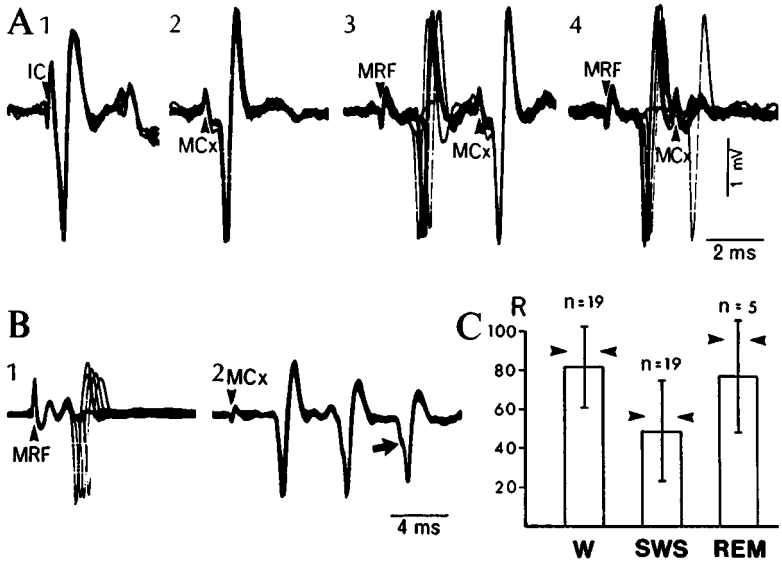

Fig. 4.1 Antidromic response probability in thalamocortical (TC) neurons from rostral intralaminar centrolateral-paracentral (CL-Pc) neurons during the waking-sleep cycle. Chronically implanted cats. *A–B*, identification of the input-output organization of thalamic rostral intralaminar centrolateral-paracentral (CL-Pc) neurons by their monosynaptic excitation from the midbrain reticular formation (MRF) and antidromic invasion from internal capsule (IC) and motor cortex (MCx). Extracellular recordings. Stimuli marked by arrowheads (in *B*, only the first of three stimuli at 250 Hz is marked). The arrow in *B* indicates fractionation of an antidromic spike to the last stimulus in the train. Collision between MRF-evoked synaptic discharges and cortically evoked antidromic spikes is shown in *A4*. *C*, median (arrowheads), mean (columns), and standard deviation (bars) for the percentage of antidromic responses in a sample of 19 CL-Pc neurons during waking (W) and slow-wave sleep (SWS). Five of these neurons were also recorded during REM sleep. *R*, percentage of stimuli that evoked an antidromic action potential. Modified from Glenn and Steriade (1982).

4.1.1. Thalamus

Antidromic responses of TC neurons have been recorded extracellularly [11] during the natural waking-sleep cycle [12]. The antidromic responsiveness increases by ~60% during waking and REM sleep, compared to SWS (Fig. 4.1), a highly significant difference. During SWS, the presence of abortive spikes and the break between initial segment and somadendritic components of antidromic responses are much more pronounced than during the two brain-active states, waking and REM sleep. In some instances, increased antidromic responsiveness can be seen 10 to 25 s in advance of the most precocious sign of EEG activation with transition from SWS to waking

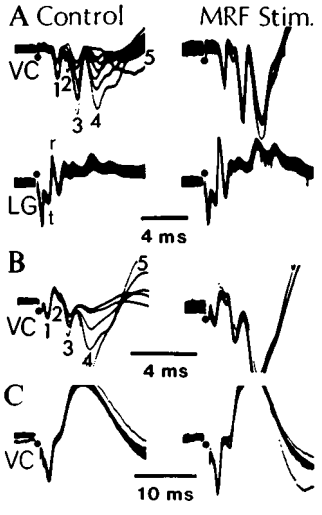

Fig. 4.2 Changes in thalamic and cortical field potentials during brainstem reticular formation stimulation. *Encéphale isolé* (bulbo-spinal transected) cats. *A*, simultaneous recordings of field potentials from thalamic lateral geniculate (LG) nucleus and at the surface of the visual cortex (VC). Positivity downwards. Superimposition of several traces. Stimuli (dots) applied to the optic tract. The LG response consisted of a presynaptic (tract, *t*) and a series of postsynaptic (relayed, *r*) components. The VC response consisted of a presynaptic (*1*) and a series of postsynaptic (*2–4*) components. Note enhancement by midbrain reticular formation (MRF) stimulation (300 Hz) of LG *r* component (without alteration in the *t* component), with a subsequent increase in the VC presynaptic (*1*) as well as all postsynaptic waves. *B*, VC response to a stimulus applied to the underlying white matter. Note enhancement of postsynaptic waves (*2–4*) without alteration in the presynaptic (*1*) component. *C*, testing stimulus applied to deep VC layers. Modified from Steriade (1970).

or REM sleep [12] and blockage of antidromic responses occurs in advance of the occurrence of sleep spindles [13].

Orthodromic responses of TC neurons were first investigated by recording field potentials, which have the advantage of monitoring the presynaptic deflection that reflects the magnitude of the incoming volley in afferent axons and, thus, can ascertain to what extent the change in the amplitude of the postsynaptic component is a function of input or depends on synaptic alterations at the recording site [14]. Generally, natural awakening from SWS or activation induced by stimulation of the brainstem reticular formation is associated with increased amplitude of the postsynaptic (relayed, *r*) wave in various thalamic nuclei, whereas the presynaptic (tract, *t*) deflection remains unchanged (Fig. 4.2*A*). In turn, the increased postsynaptic wave in thalamic nuclei gives rise to an increase in the presynaptic component of the simultaneously recorded potential in the projection cortical area, with the consequence of increased postsynaptic cortical waves (Fig. 4.2*A*). If transmission through thalamic nuclei is avoided and stimuli are applied to the white matter, just beneath the cortical area where recording is performed, brainstem reticular formation stimulation enhances postsynaptic cortical components, without changes in the presynaptic component (Fig. 4.2*B*). These changes are opposite to those undergone by thalamic field potentials with transition from waking to drowsiness and, further, to full-blown SWS, when the postsynaptic waves are progressively obliterated, without any change in the presynaptic deflection (see Fig. 3.19 in previous chapter), thus emphasizing that the first relay station where changes occur with transition from waking to SWS is the thalamus. Recording light-induced responses also led to a similar conclusion being drawn, because an increased probability of responses in the visual thalamus was observed despite no alterations in simultaneously recorded responses from the optic tract [15]. The same type of change was observed in all investigated (visual, somatosensory, auditory and motor) thalamocortical systems [14].

Similarly to TC neurons, RE neurons display an increased responsiveness during wakefulness, reflected by a higher probability and shorter latencies of discharges, compared to SWS [16]. The parallel excitation during increased alertness in the two (RE and TC) opposite neuronal classes, instead of the expected reciprocal image due to TC inhibition by RE cells, suggested that, during waking accompanied by increased responsiveness in TC neurons, directly connected RE neurons contribute to further enhancing the relevant activity by inhibiting GABAergic local-circuit neurons in dorsal thalamic nuclei [17]. This hypothesis is supported by the disclosure of

[13] Steriade et al. (1971). The abolition of antidromic responses ~0.5–1 s before the appearance of spindles on cortical EEG (see Fig. 3.20 in Chapter 3) is explained by the fact

that TC neurons display phasic IPSPs, but no rebound spike-bursts, during the period of spindle initiation in the thalamus (see Fig. 3.15*C* in Chapter 3). Then, in the absence of spike-bursts to transfer thalamically generated spindles to cortex, there is a delay between the first IPSPs in TC neurons (generated by pacemaking GABAergic RE neurons) and overt cortical EEG spindles.

[14] Steriade (1970).

[15] Steriade and Demetrescu (1960). Facilitation of thalamic LG responsiveness upon arousal was subsequently supported by a series of investigators using macro- and microelectrode recordings (Ogawa, 1963; Maffei et al., 1965; Sakakura, 1968; Coenen and Vendrik, 1972).

[16] Steriade et al. (1986).

[17] Steriade (1991). This hypothesis took also into consideration that, after excitotoxic lesions of GABAergic RE neurons, there is an increased incidence of short-lasting IPSPs in TC neurons (Steriade et al., 1985), as if local inhibitory interneurons were released from the inhibition arising in the RE nucleus.

[18] Liu et al. (1995).

[19] See note [289] and related main text in Chapter 3.

[20] See note [24] and Fig. 3.56*B* in Chapter 3.

[21] Timofeev et al. (1996).

[22] Timofeev and Steriade (1997); see Fig. 3.21 and related text in Chapter 3.

[23] Hirsch and Burnod (1987); Crunelli et al. (1988).

[24] Hirsch et al. (1983). At this time, this is the only intracellular study of TC neurons during the natural sleep cycle.

[25] Nuñez et al. (1992b).

[26] Steriade et al. (1977b).

[27] Purpura et al. (1966); Singer (1977).

GABAergic axons issuing from RE neurons and projecting to local inhibitory neurons in dorsal thalamic nuclei [18].

Intracellular recordings of TC neurons demonstrate depolarization associated with increase input resistance after stimulation of brainstem cholinergic nuclei [19], whose neurons are known to increase firing rates during, and preceding, natural states of waking and REM sleep [20]. TC responses to afferent volleys are enhanced during brain activation induced by stimulation of mesopontine cholinergic nuclei, compared to epochs of slow sleep oscillation (Fig. 4.3). Analysis of subthreshold and suprathreshold EPSPs in TC neurons evoked by afferent volleys during different epochs of the slow sleep oscillation and prior to it showed that the magnitude of subthreshold EPSPs was *not* reduced during the hyperpolarizing phase of this oscillation, compared to epochs preceding slow oscillatory cycles, but action potentials were not generated; however, low-threshold spike-bursts (see Chapter 2) were occasionally fired after the prolonged hyperpolarization of TC neurons (Fig. 4.4) [21]. Although monosynaptic EPSPs in TC neurons are not diminished during the hyperpolarizing phase of the slow sleep oscillation, spindle-related IPSPs in TC neurons diminish the amplitude and duration of these EPSPs [22] because of increased membrane conductance due to biphasic $GABA_{A-B}$ potentials [23]. This indicates that, in addition to the steady hyperpolarization of TC neurons throughout SWS [24], sequences of spindle waves are most effective at blocking, during SWS, incoming signals en route to the cortex. The decreased responsiveness of TC neurons is not confined to spindle sequences, but also appears during the early part of inter-spindle lulls, in the hyperpolarizing "tail" of spindles associated with increased membrane conductance and reduced transfer properties of TC neurons [25].

Inhibitory processes in TC neurons during activated and deactivated states were first investigated using extracellular recordings and measuring the duration of the period of suppressed firing following an afferent volley. It was concluded that, however efficiently midbrain reticular formation stimulation blocks cyclic periods of suppressed firing, it does not eliminate the early inhibitory phase during which TC neurons remain unresponsive to incoming signals [26]. This view was different from earlier assumptions postulating a complete blockage of inhibitory processes in TC neurons upon activation induced by midbrain reticular stimulation, thus resulting in disinhibition of TC neurons upon arousal [27]. The idea that the early inhibitory phase in TC neurons is preserved during brainstem reticular-induced arousal [26], which allows these neurons with feature detection properties that assist in discriminatory functions,

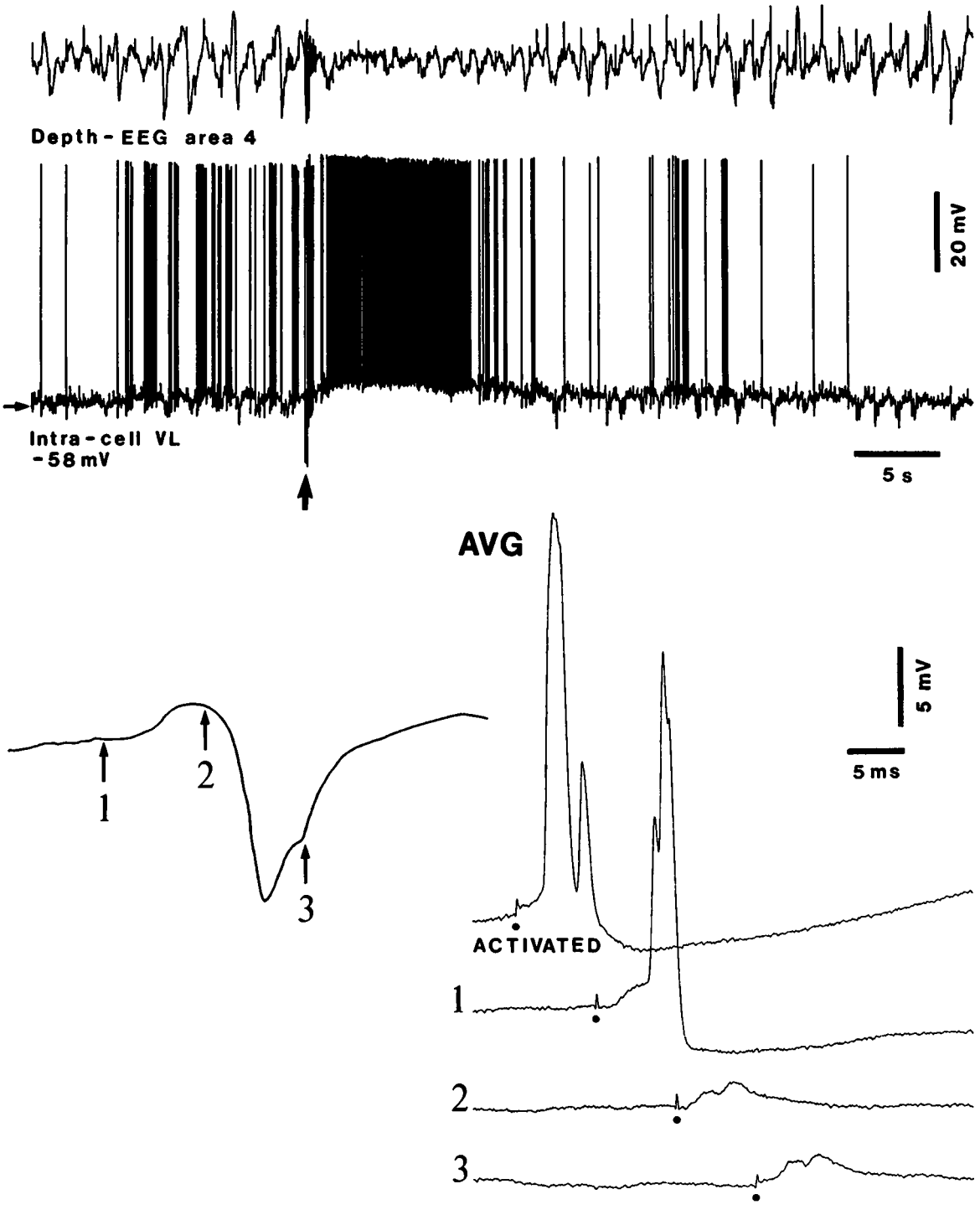

Fig. 4.3 Responsiveness of TC neuron during slow sleep-like oscillation and during activation elicited by stimulation of the mesopontine cholinergic nucleus. Intracellular recording from a TC neuron in the ventrolateral (VL) nucleus, together with depth-EEG from cortical area 4, in cat under ketamine-xylazine anesthesia. Slow oscillation at ~0.7 Hz. Stimulation of pedunculopontine tegmental (PPT) cholinergic nucleus (arrow) with a pulse-train (0.3 s) at 300 Hz. Testing stimuli applied to brachium conjunctivum (BC, cerebellothalamic pathway) every 1 s, before and after PPT stimulation. Note PPT-evoked EEG activation and VL-cell depolarization, lasting for more than 10 s. Below are illustrated averaged ($n = 6$) BC-evoked EPSPs (shortest latency 1.4 ms) as a function of their occurrence prior to the long-lasting depth-positive (inhibitory) wave of the slow oscillation (*1*), during that wave (*2*), after it (*3*), and during the activated period elicited by PPT stimulation. From Timofeev et al. (1996).

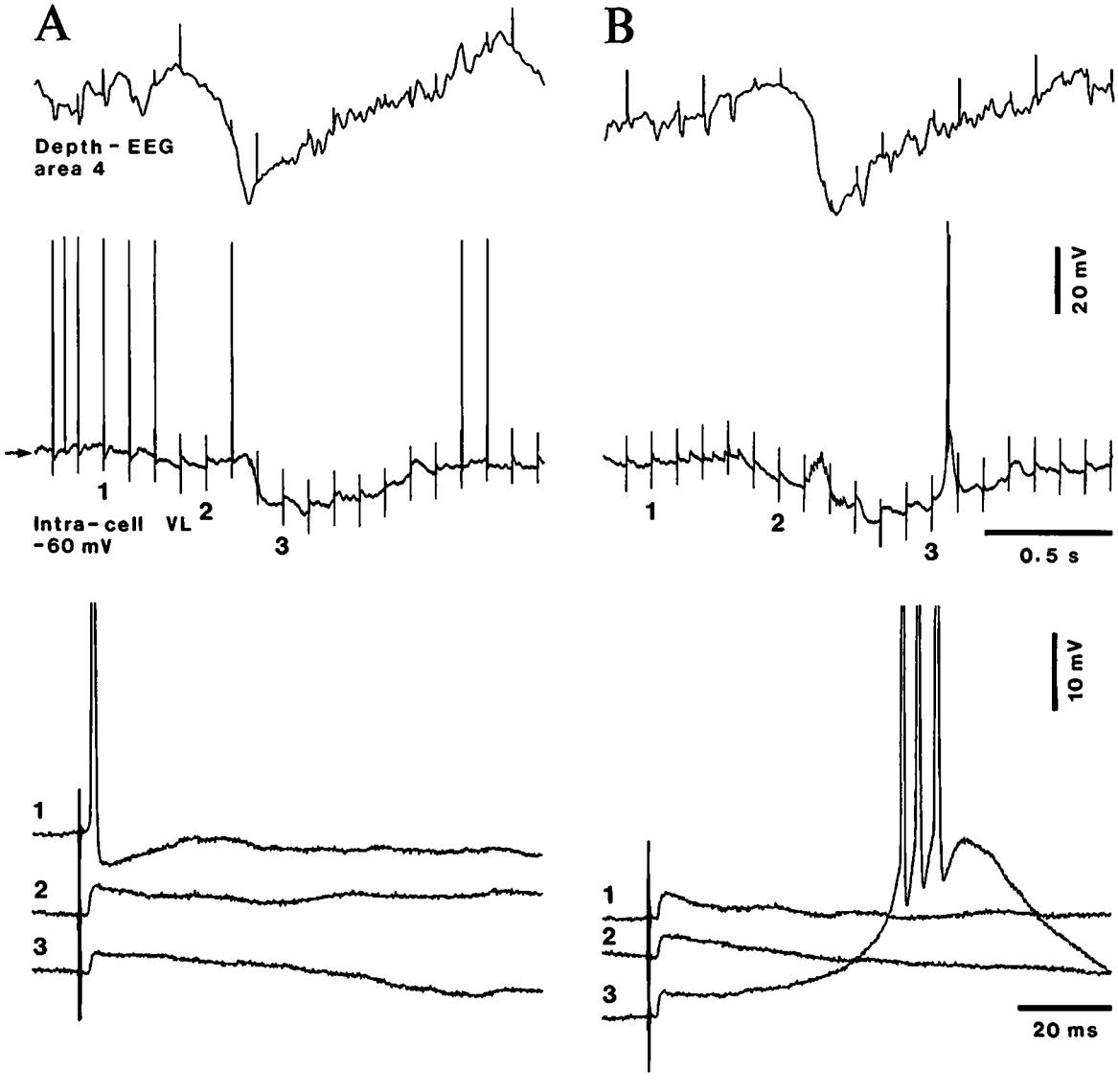

Fig. 4.4 Subthreshold and suprathreshold EPSPs evoked in TC neurons during various phases of the slow oscillation. Intracellular recording of TC neurons from VL nucleus together with depth-EEG from cortical area 4 in cat under ketamine-xylazine anesthesia. *A*, responses to brachium conjunctivum (BC) stimuli are expanded below. *B*, subthreshold EPSPs during the period preceding the slow oscillatory cycle (*1*), the prolonged depth-EEG positive wave related to hyperpolarization of TC neuron (*2*), and the return to a more depolarized level after the prolonged hyperpolarization (*3*). From Timofeev et al. (1996).

was later supported by experiments using intracellular recordings. Figure 4.5*A* depicts the effect of midbrain reticular stimulation on the long-lasting, cyclic hyperpolarizations of a TC neuron from the ventrolateral nucleus, consisting of an abolition of the prolonged tail of these hyperpolarizations and their rhythmic repetition, but the full preservation of the early, short-lasting IPSP [28]. Similar effects are exerted by setting into action mesopontine cholinergic nuclei, which abolishes the prolonged ($GABA_B$) IPSP in lateral geniculate neurons, while leaving intact the early, $GABA_A$ IPSP (Fig. 4.5*B*) [29]. The discovery of triphasic IPSPs in anterior thalamic neurons shed further light on the selective preservation of the earliest IPSP, with simultaneous abolition of later IPSPs. As cat anterior thalamic nuclei are devoid of connections from the thalamic RE nucleus [30], the earliest IPSP (called $GABA_a$, to distinguish it from the subsequent sequence of $GABA_{A\text{-}B}$ IPSPs) is presumably generated by GABA release from the intraglomerular presynaptic dendrites of local interneurons [31]. During brain activation elicited by stimulation of mesopontine cholinergic nuclei, the $GABA_a$ IPSP is preserved or even enhanced, whereas $GABA_B$ IPSP and occasionally $GABA_A$ IPSP are abolished (Fig. 4.6) [32]. The preservation of the earliest, short-lasting IPSP under conditions of brain activation may assist in the enhancement of the center-surround mechanism and lateral inhibition during attentive states.

[28] Steriade (1984).

[29] Hu et al. (1989b).

[30] Steriade et al. (1984); Velayos et al. (1989).

[31] Paré et al. (1991). The presence of triphasic IPSPs ($GABA_a$ followed by the $GABA_{A\text{-}B}$ sequence) in anterior thalamic neurons was confirmed in neurons recorded from the thalamic lateral geniculate nucleus (Soltesz and Crunelli, 1992).

[32] Curró Dossi et al. (1992b). See also the commentary (Steriade, 2003) on the paper by Perreault et al. (2003).

[33] Livingstone and Hubel (1981). The more diverse changes undergone by cortical, compared to TC neurons, is due to differential alterations of responses evoked by various types of stimuli. Thus, signals from the external world, which pass through the thalamus, are usually not transferred to cortex because of TC-cells' steady hyperpolarization and spindle-related IPSPs (see Figs. 4.3–4.4), whereas the corticocortical dialogue is maintained during SWS (see main text and Figs. 4.10–4.11).

4.1.2. Neocortex

As is the case with TC neurons, the probability of antidromic responses of corticospinal and corticothalamic neurons is enhanced, and initial segment – somadendritic broken spikes develop into unbroken action potentials, during EEG activation elicited by stimulation of the midbrain reticular formation or during natural states of waking and REM sleep, compared to EEG synchronization epochs in acute experiments or to the natural SWS state (Fig. 4.7). Since antidromic responses test somatic excitability, these results are congruous with enhancement, during wakefulness or REM sleep compared to SWS, of intrinsic somatic excitability, tested by depolarizing current pulses (Fig. 4.8).

Studies of cortical responsiveness during states of vigilance show that, in contrast with virtually all thalamic (TC and RE) neurons, which display reduced responsiveness during SWS compared to waking and REM sleep, neocortical neurons behave in more diverse ways, sometimes with opposite changes in two simultaneously recorded neurons [33]. During EEG activation, the common

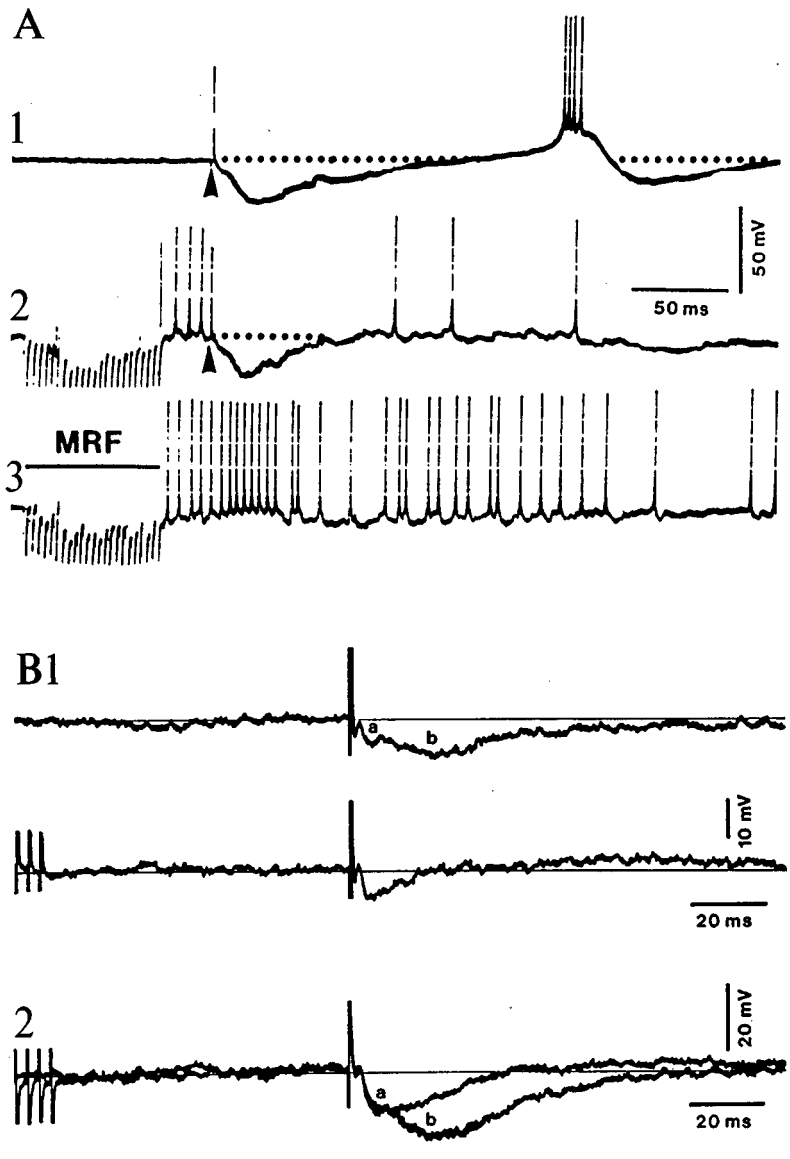

Fig. 4.5 Effects of midbrain reticular formation (MRF) stimulation on inhibitory processes in TC neurons. Intracellular recordings in cats under barbiturate anesthesia (*A*) and urethane anesthesia in a reserpine-treated animal (*B*). *A*, thalamic VL neuron. Stimulation of motor cortex (arrowheads) evokes an antidromic spike followed by rhythmic inhibitory-rebound sequences (*1*). In *2*, a conditioning pulse-train (320 Hz) to the MRF leaves intact the cortically elicited early IPSP, but abolishes the late phase of hyperpolarization and the following inhibition-rebound sequences. In *3*, the effect of the MRF stimulation alone is shown. *B*, two (*1–2*) TC neurons from the LG nucleus. Optic chiasm stimulation was adjusted to enhance the separation of the two ($GABA_A$ and $GABA_B$, marked *a* and *b* in the figure) IPSPs. When preceded by a conditioning pulse-train to the cholinergic pedunculopontine tegmental (PPT) nucleus, only the first ($GABA_A$) IPSP persisted. Note that the blockage of the second inhibitory component was obtained with PPT conditioning stimuli subthreshold for inducing an early depolarizing response in these LG neurons. Modified from Steriade (1984, *A*) and Hu et al. (1989b, *B*).

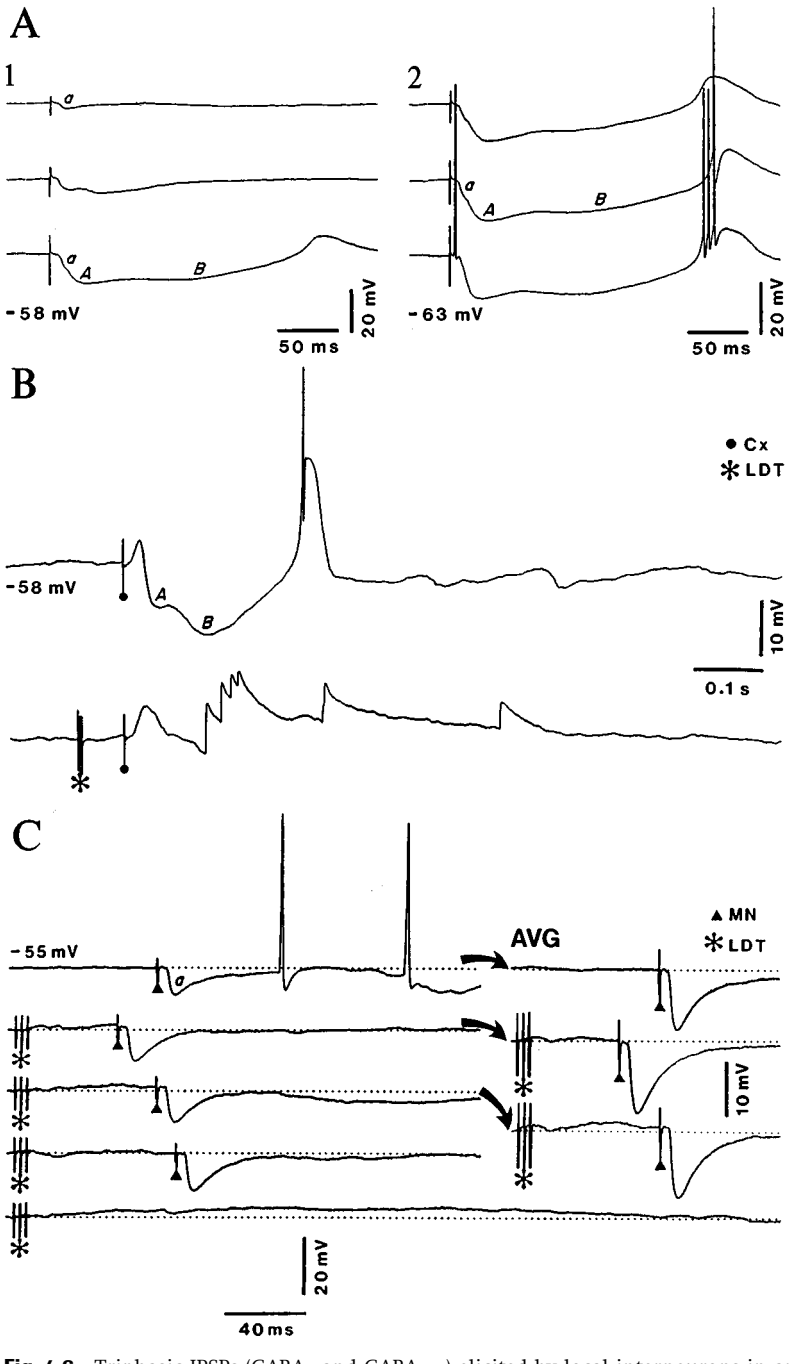

Fig. 4.6 Triphasic IPSPs ($GABA_a$ and $GABA_{A-B}$) elicited by local interneurons in anterior thalamic (AT) neurons of cat and their differential changes following stimulation of mesopontine cholinergic nuclei. Intracellular recordings under urethane anesthesia. *A*, triphasic IPSPs evoked by mammillary nucleus (MN) stimuli in two different (*1–2*) AT neurons. Increasing intensities of stimulation (from top to bottom traces). Components *a*, *A* and *B* of IPSPs are described in the text. With the higher intensities, the long-lasting IPSP leads to a low-threshold spike (LTS), sometimes crowned by a high-frequency burst of fast action potentials. *B*, cortically evoked IPSP in an AT neuron is suppressed by a preceding pulse-train to the laterodorsal tegmental (LDT) cholinergic nucleus (asterisk). Action potential crowning the LTS was truncated. *C*, MN-evoked isolated $GABA_a$ IPSP in an AT neuron, in an animal with ablation of the cingulate gyrus. *Left*, five traces depicting (from top to bottom) an MN-evoked control *a*-IPSP response; LDT + MN stimulation at three different time-intervals; and LDT stimulation alone. *Right*, averages (AVG) of five responses to stimulation of MN and LDT + MN, as indicated by curved arrows. Dotted lines tentatively indicate the baseline. Note depolarization elicited by LDT stimulation alone (left bottom trace). Modified from Curró Dossi et al. (1992b).

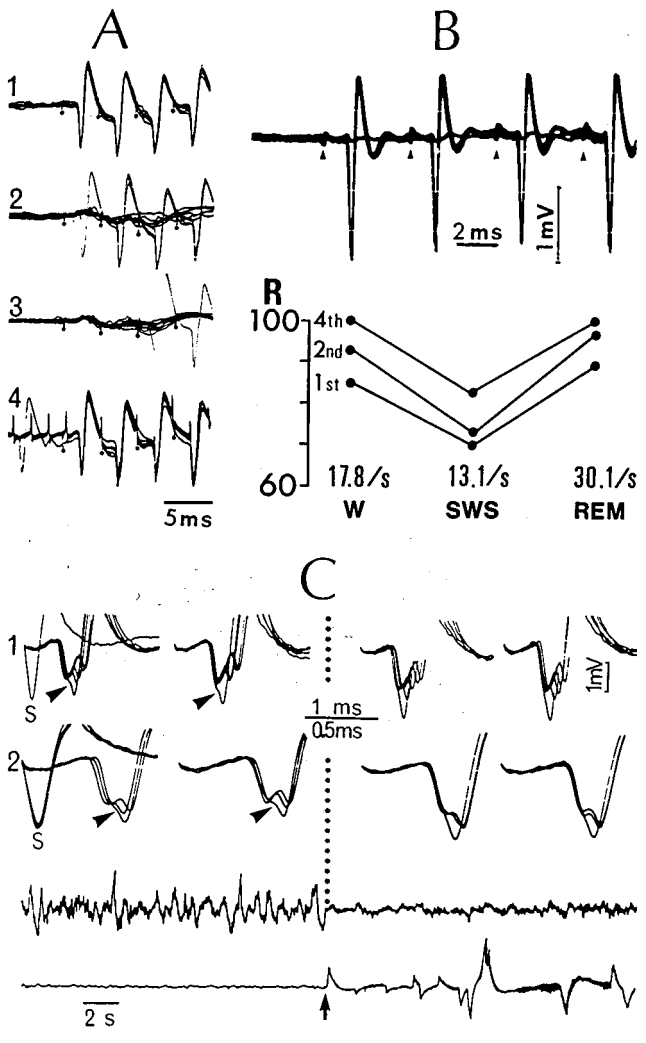

Fig. 4.7 Antidromic responses of long-axoned corticofugal neurons during waking and sleep states. *A*, facilitation of antidromic activation of a cat pyramidal tract (PT) neuron during EEG activation. Full responsiveness to a four-stimuli train during control epoch of EEG activation (*1*), depressed responsiveness during progressively developing EEG synchronization (*2-3*), and recovery of antidromic responsiveness during EEG activation elicited by a brief conditioning pulse-train (300 Hz) to the midbrain reticular formation (*4*). *B*, corticothalamic neuron from area 5, antidromically activated from the thalamic center median (CM) nucleus. Chronically implanted cat. Antidromic responsiveness was investigated with a four-stimuli train (arrowheads indicate stimuli). *Below*, percentage responsiveness (*R*) during waking, SWS, and REM sleep. Below each state is the mean firing rate (calculated during another waking-sleep cycle). *C*, patterns of antidromic invasion in precentral neuron during natural SWS (left) and awakening (right). Chronically implanted macaque monkey. Dotted line indicates arousal from SWS. Fast-conducting neuron, with 0.5 ms latency of antidromic response from pes pedunculi. *1* and *2*, responses to five-stimuli (350 Hz) and three-stimuli (110 Hz) trains, respectively, during two passages from SWS to arousal. Third and fourth traces, EEG and eye movements. Note initial segment – somadendritic fragmentation of first antidromic spike (arrowheads) during SWS and full recovery of unbroken action potentials on arousal as well as diminution of spike fragmentation of successive responses. Modified from Steriade (1976, *A*), Steriade et al. (1979a, *B*) and Steriade et al. (1974a, *C*).

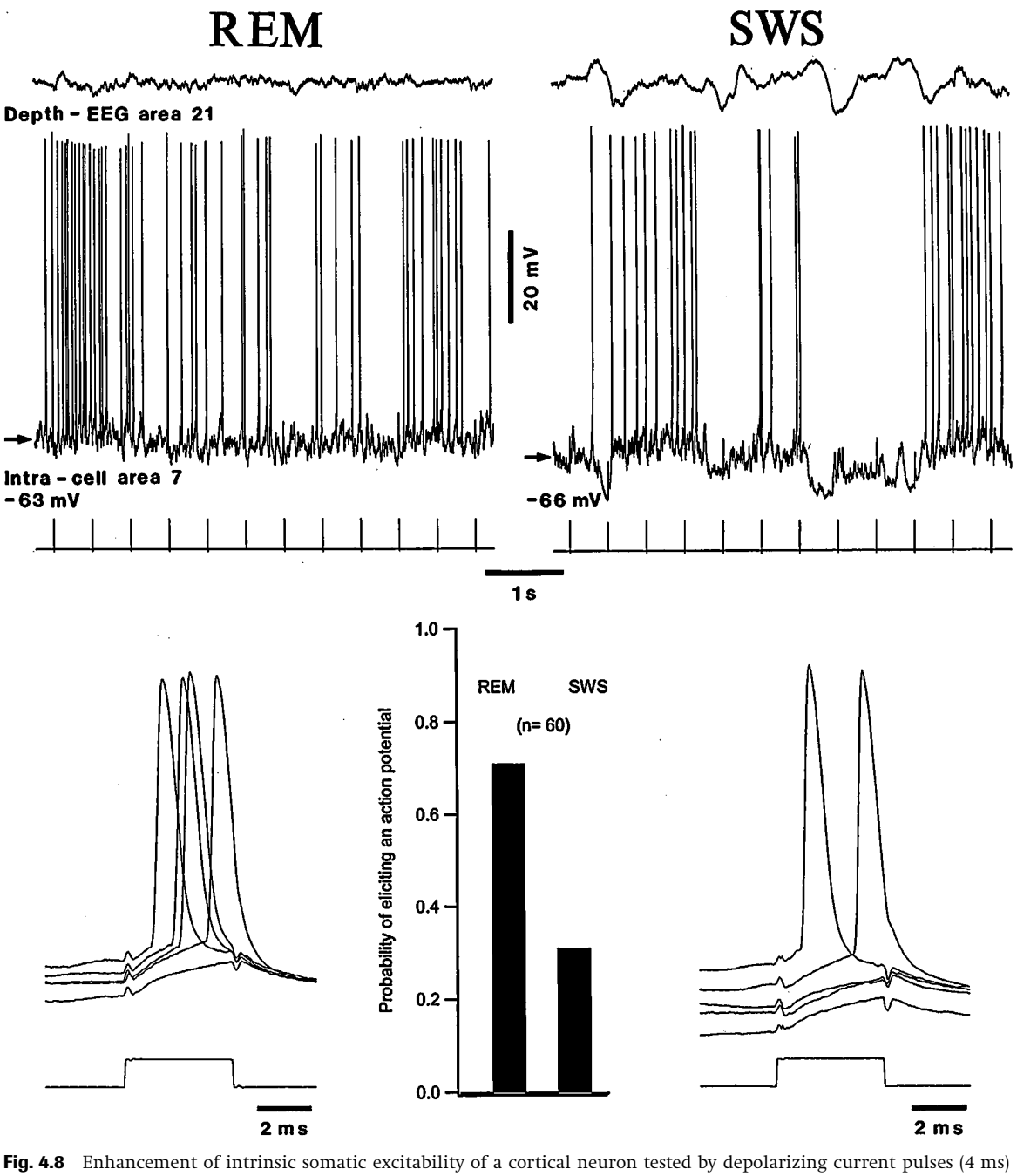

Fig. 4.8 Enhancement of intrinsic somatic excitability of a cortical neuron tested by depolarizing current pulses (4 ms) during REM sleep and SWS. Intracellular recording from area 7 (together with EEG from area 21) in chronically implanted cat. *Upper panel* shows EEG and intracellular recordings (bottom trace, short depolarizing current pulses). Below, five superimposed traces with responses to depolarizing current pulses during REM sleep (left) and SWS (right). *Middle*, histogram showing probability of action potentials evoked during REM sleep (~70%) and SWS (~30%). Unpublished experiments by F. Grenier, I. Timofeev and M. Steriade; see Steriade et al. (2001b).

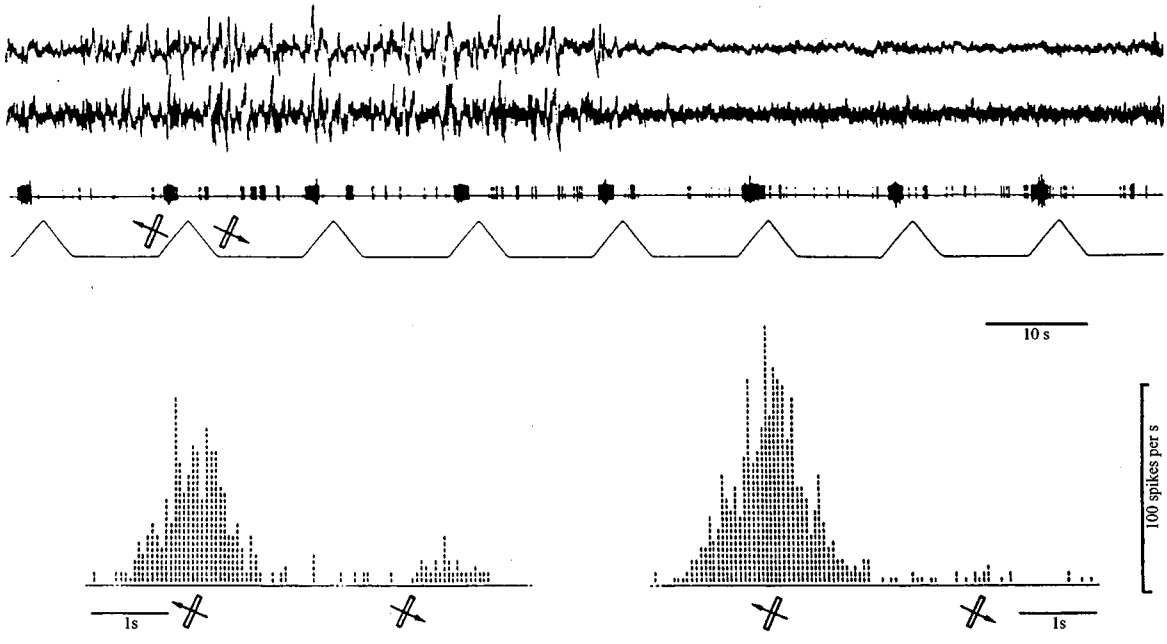

Fig. 4.9 Effect of arousal from SWS on responses and response selectivity of a neuron in layer II of cat striate cortex. About halfway through the 2-min record, the cat was aroused by a noise. An optimal slit, $1/2^\circ \times 3^\circ$, oriented 25° clockwise to vertical, evoked a response (third trace) that was much greater to movement up and to the left than down and to the right. Arousal resulted in a moderate increase in the response to leftward movement and a virtual elimination of the response to rightward movement (see histogram). Arousal also produced a reduction and smoothing of the spontaneous firing. From Livingstone and Hubel (1981).

change in the visual cortex is an enhanced response to optimally oriented moving slits of light, a response that may occur over a background of decreased background discharges (Fig. 4.9), which further increases the signal-to-noise ratio.

Contrary to the blockage of cortical responses to stimuli applied before the thalamus during SWS (because of the hyperpolarization and increased membrane conductance of TC neurons), cortical responses to ipsilateral cortical or callosal volleys are not diminished and may even be enhanced during SWS, compared to waking. This finding suggests that, during SWS, cortical neurons maintain an internal dialogue that may explain some forms of mental activities during this state in which there is a complete absence of information from external signals. Thus, monkey's precentral neurons, driven by callosal volleys, increase their spontaneous firing rates as well as their evoked discharges during SWS, compared to waking (Fig. 4.10) [34]. These extracellular data are supported by intracellular recordings of corticocortical EPSPs showing

[34] Steriade et al. (1974b). Identification of input-output organization of monkey's callosal neurons revealed a bisynaptic (cortico-cortico-thalamic) pathway, with synaptic discharges of precentral neurons elicited by stimulation of homotopic sites in the contralateral cortex and antidromic invasion of the same neurons from the thalamic VL nucleus (see Fig. 8.8*B* in that 1974 chapter). See similar data using intracellular recordings in cats (Cissé et al., 2003).

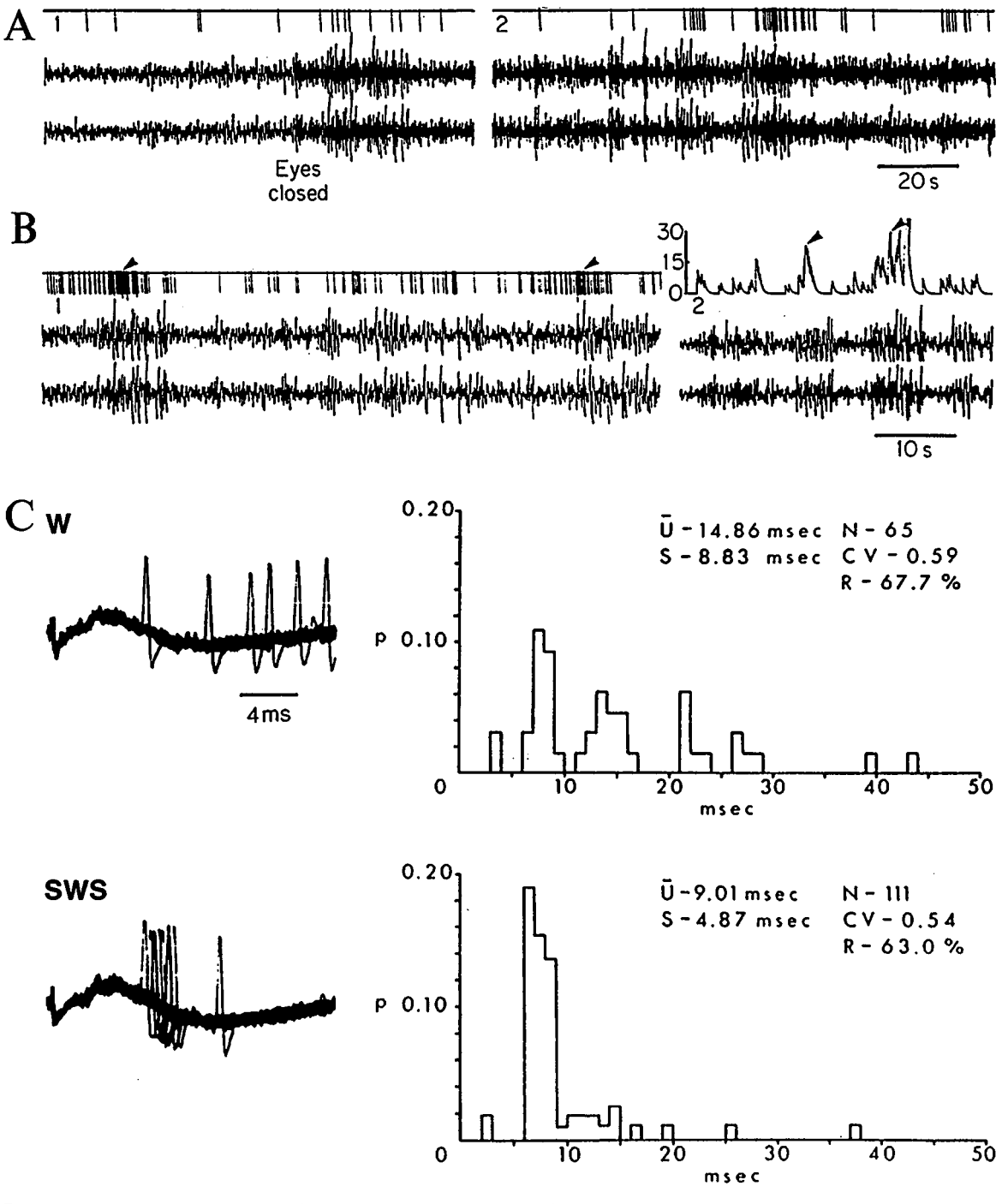

Fig. 4.10 Increase in spontaneous firing and evoked discharges of cortical neurons receiving callosal projections during SWS, compared to wakefulness. Chronically implanted *Macaca mulatta* monkey. *A-B*, two different neurons. In *A*, transitional period from waking to SWS; 30 s separates the left and right parts of the panel. In *B*, unit firing during SWS and integrated activity of the same neuron several minutes later are shown. Note increased neuronal activity (arrowheads) during sequences of high-amplitude EEG spindles and slow waves. *C*, changes in callosally evoked synaptic discharges in a precentral corticothalamic neuron during waking and SWS. Superimposition depicts several traces. Symbols in poststimulus histograms: $\bar{U}$, mean latency; S, standard deviation; CV, coefficient of variation; *N*, number of counts; *R*, percentage of evoked discharges. Note concentration of evoked discharges during SWS as opposed to dispersed activity during waking. Unpublished experiments by M. Steriade and J.Y. Hallé; see Steriade et al. (1974b).

[35] Steriade and Deschênes (1974). The method of testing recurrent inhibition in cortical pyramidal neurons consists of antidromic stimulation of axons in pes pedunculi and includes a midbrain lesion of the medial lemniscus to avoid stimulation of afferent fibers.

that they are not diminished during the hyperpolarized component of the slow sleep oscillation (Fig. 4.11).

The increased response selectivity to sensory stimuli during waking (see above, Fig. 4.9) reflects very efficient inhibitory processes upon arousal. This was indeed demonstrated using recurrent (feedback) inhibition tests by stimulating antidromically pyramidal tract neurons [35] and feedforward inhibition induced by stimulation of appropriate thalamic nuclei (Fig. 4.12). In both cases, inhibition lasts much longer during SWS than in wakefulness. Intracellular recordings in chronically implanted, naturally awake and sleeping cats essentially confirmed data on inhibitory processes obtained by means of extracellular recordings in behaving monkeys [35] and provided new information. Thus, bisynaptic IPSPs, evoked in cortical neurons by thalamic volleys, are obvious during the depolarizing phase of the slow oscillation in SWS (reversed IPSPs are observed during the hyperpolarizing phase of the slow sleep oscillation), but the total duration of the first period of hyperpolarization ($\sim$70 ms) is not different between SWS and brain-active states (Fig. 4.13). What distinguishes SWS from either REM sleep or waking is the total duration of hyperpolarization, which may reach 0.2 s in SWS and is much shorter during brain-active states (Fig. 4.14). This is in line with earlier data from experiments on monkey's cerebral cortex showing cyclic, long-lasting periods of suppressed firing followed by rebound spike-bursts during SWS, as opposed to single epochs of suppressed firing, with shorter duration [34, 35]. Deep but short-lasting inhibition in waking provides a mechanism subserving accurate discrimination and the faithful following of rapidly recurring messages.

4.2. Mechanisms of augmenting potentials in thalamocortical systems

Responses to single stimuli applied to ascending pathways that arise in the thalamus or to corticothalamic projections develop into augmenting (or incremental) responses when repetitive stimuli between 5 and 15 Hz (mainly $\sim$10 Hz) are used. With such stimuli, responses grow in size from the first to subsequent responses. Because of the waxing patterns that are similar to those displayed by initial spindles waves and because of frequencies that overlap with those of sleep spindles, augmenting responses constitute the experimental model of spindle oscillations. As will be shown in this section, augmenting responses, as well as naturally occurring spindles, lead to plastic changes in thalamic and cortical neurons, both within the process of augmentation and

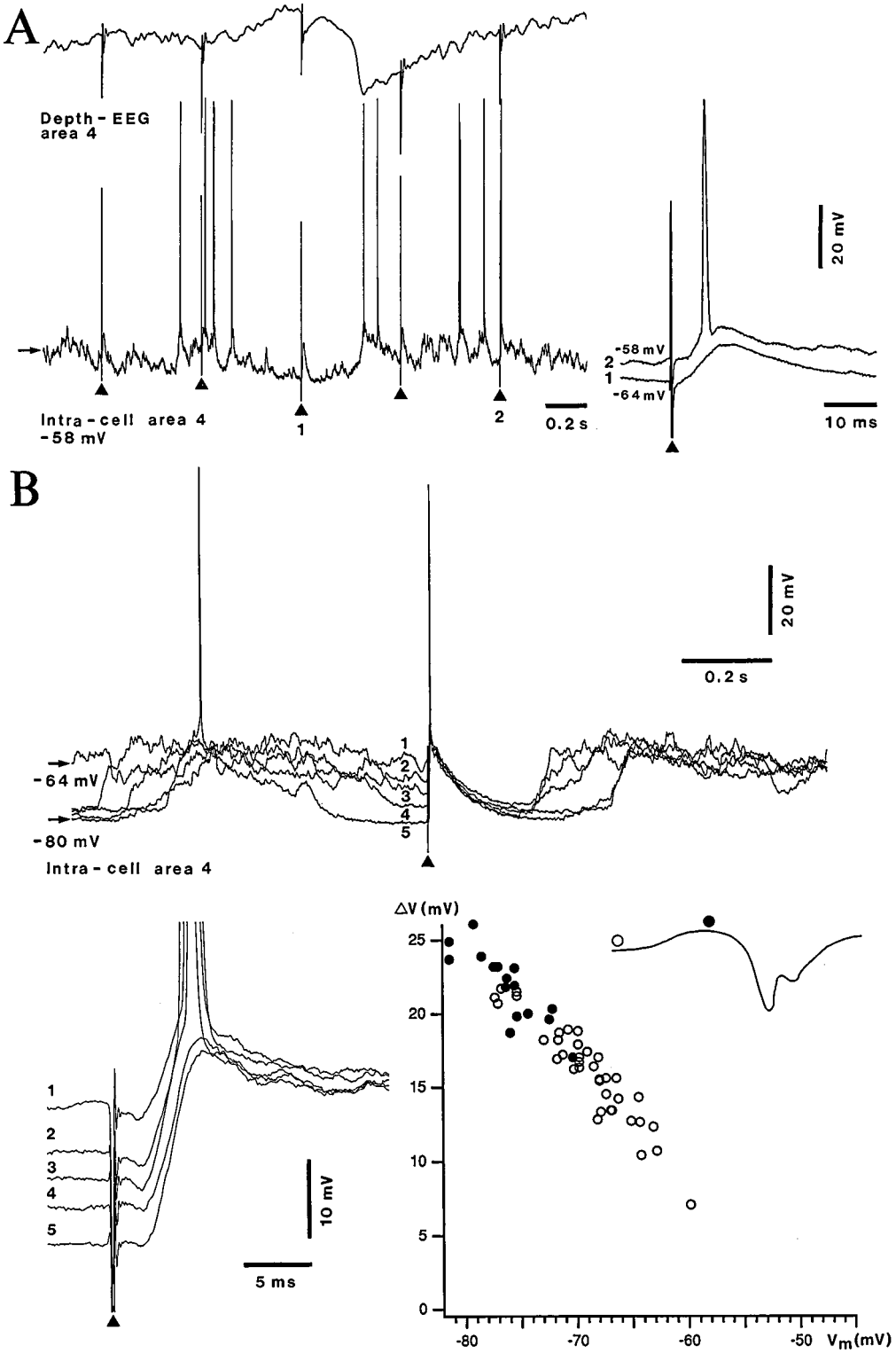
A
Depth - EEG
area 4
Intra - cell area 4
-58 mV
1
2
0.2 s
20 mV
-58 mV
-64 mV
10 ms
B
20 mV
0.2 s
-64 mV
-80 mV
Intra - cell area 4
10 mV
5 ms
ΔV (mV)
Vm (mV)

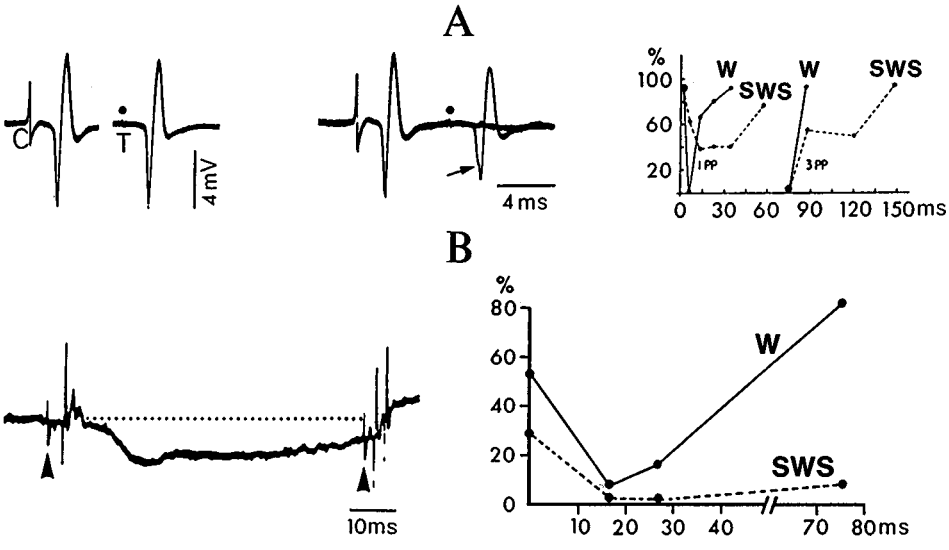

Fig. 4.12 Effects of arousal from SWS on inhibitory processes in neocortical neurons. *A*, recurrent inhibition of antidromic discharges of motor cortical neuron in cat, tested by stimulating pes pedunculi (PP) (see further explanation of method in note [35]). Conditioning volley (C) was delivered at 13 V (minimal voltage required to elicit inhibitory effects on testing response (T) induced by a stimulus at 5 V, which was the minimal voltage required to evoke 100% antidromic invasion). At paired C-T stimulation, complete inhibition of the T response or spike fragmentation (arrow) occurred. Graph depicts much longer inhibition with three PP stimuli than with single stimuli. With both conditioning procedures (one and three PP stimuli), recovery from inhibition was slower during SWS than during waking (W). *B*, feedforward inhibition of synaptic discharges elicited by stimulating the posterior part of the thalamic VL nucleus in the monkey. *Left*: field-positive wave (reflecting hyperpolarization in a neuronal pool) evoked by a first VL stimulus, and facilitation (during W) of evoked discharges by a second VL stimulus at a 75-ms interval toward the end of the inhibition. *Right*: percentage responsiveness of discharge evoked by the first stimulus (time 0) and by the second stimulus at three time intervals (15 ms, 27 ms, and 75 ms) during W and during SWS. Modified from Steriade (1976, *A*) and Steriade and Deschênes (1974, *B*).

Fig. 4.11 (opposite) Synaptic responses to corticocortical volleys are not diminished during the slow sleep oscillation and EPSPs evoked by corticocortical volleys are linearly related to the membrane potential. Cat under ketamine-xylazine anesthesia. Intracellular recording of two area 4 neurons (*A-B*), together with depth-EEG from area 4. *A*, stimuli (arrowheads) were applied at 2 Hz, in the vicinity of the recorded neuron. Responses to stimulus *1* (during the depth-positive EEG wave associated with cell hyperpolarization) and stimulus *2* (during the depth-negative EEG component and cell depolarization) are expanded on the right. Note increased amplitude of cortically evoked EPSP in *1*, during the depth-positive EEG wave. *B*, stimuli of constant intensity were applied to motor cortical area 4 while recording intracellularly in the vicinity of the stimulating electrode. Stimuli applied at five (*1–5*) membrane potential (V_m) values (from −64 to −80 mV) were selected and displayed in the top panel. Details of the initial parts of the evoked EPSPs are expanded below (left panel). The amplitudes of the EPSPs were measured and plotted against the V_m (right panel), showing a linear behavior regardless of the phase of the slow oscillation (before (○) and during (●) the depth-positive EEG wave). The hyperpolarized potentials corresponded to the depth-positive wave and the evoked EPSPs showed amplitudes that corresponded to the V_m, with no signs of attenuation. From Timofeev et al. (1996).

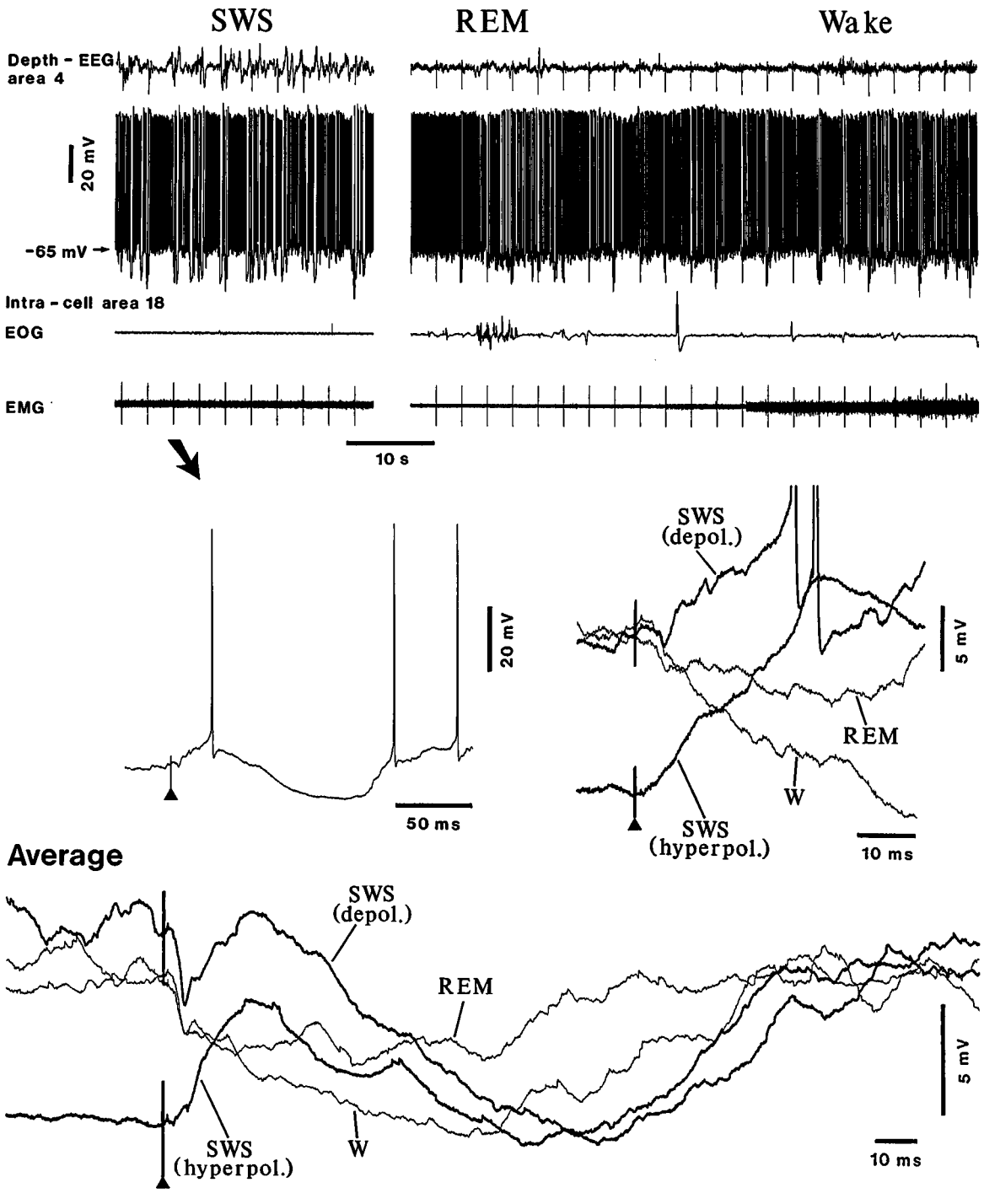

Fig. 4.13 Early inhibitory potentials in a cortical neuron during natural states of vigilance. Intracellular recording of an area 18 neuron in chronically implanted cat. Four traces in the top panel illustrate (from top to bottom): depth-EEG from area 4, intracellular recording of area 18 neuron, EOG, and EMG. Stimuli to the thalamic lateral posterior (LP) nucleus were applied every 3 s (see artifacts on EMG). A non-depicted period of 12 min separates SWS from REM sleep. One thalamically evoked response during SWS is depicted in the middle left panel (arrow). Middle right panel illustrates early responses to thalamic stimuli (arrowhead) during the depolarizing phase of the slow oscillation in SWS, during the hyperpolarizing phase of the slow oscillation in SWS, during REM sleep, and during wakefulness (W). Bottom panel depicts the averaged responses during these four epochs. Note the stimulus-evoked IPSP during the depolarizing phase of the slow oscillation in SWS and its reversal during the hyperpolarizing phase of slow sleep oscillation. Unpublished experiments by F. Grenier, I. Timofeev, and M. Steriade.

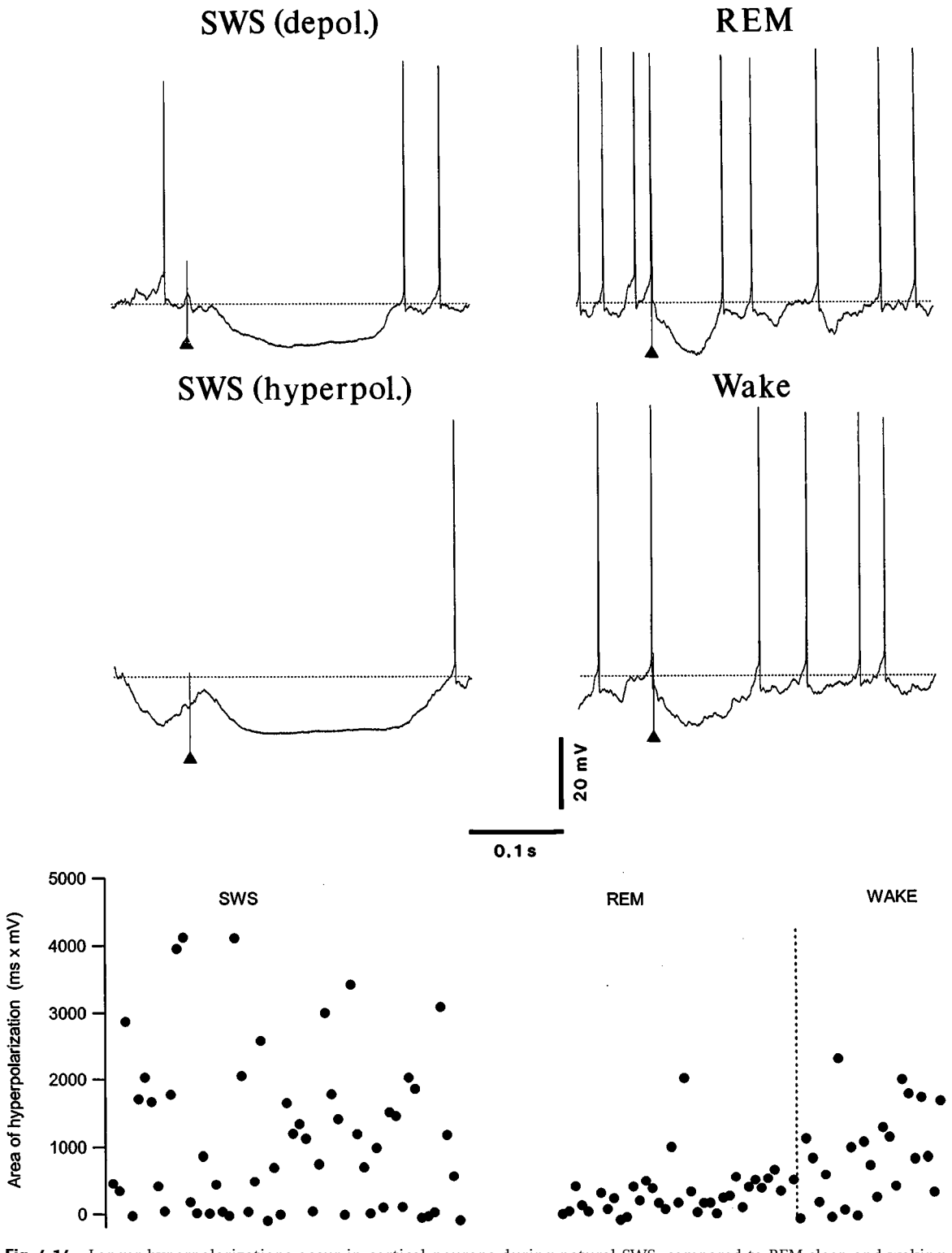

Fig. 4.14 Longer hyperpolarizations occur in cortical neurons during natural SWS, compared to REM sleep and waking. Intracellular recording of an area 18 neuron (same as depicted in Fig. 4.13). Stimulation of the thalamic LP nucleus evoked much longer hyperpolarizations during both depolarizing and hyperpolarizing phases of slow oscillation in SWS than in REM sleep and waking. Dotted line (in all cases) is at −63 mV. Bottom panel shows the area of hyperpolarization (duration in ms × mV) measured in 1-s bins. Note shortest area of hyperpolarization in REM, followed by waking, and much more dispersed and longer hyperpolarizations in SWS. Unpublished experiments by F. Grenier, I. Timofeev, and M. Steriade.

outlasting incremental responses for a given period of time. This led to the hypothesis that sleep spindles are not epiphenomena with no functional significance but electrical activities that subserve short- and medium-range plasticity, which may have a role in consolidation of memory processes (see **4.3**).

Incremental responses have been described long ago, under the term augmenting and recruiting potentials [36]. This distinction is no longer necessary [37] and just the term augmenting (or incremental) responses is sufficient. Earlier extracellular studies showed that an abnormal form of plastic changes in thalamocortical networks, spike-wave (SW) seizures, occurs after augmenting responses evoked by protracted thalamocortical [38, 39] and corticothalamic [40] volleys within the frequency range of sleep spindles. Only in the past few years have the mechanisms underlying augmenting responses been investigated intracellularly. The augmentation phenomenon occurs in thalamic TC [41] and RE neurons [42] of decorticated animals, in the intact cortex of athalamic preparations [43] and, to a lesser extent, in isolated cortical slabs *in vivo* [44] or in cortical slices maintained *in vitro* [45]. However, self-sustained activities following sequences of augmenting responses, and resembling those occurring during normal and paroxysmal events in animals and humans, require interacting thalamic and cortical networks for their best development.

In this section, I discuss the neuronal mechanisms of different types of augmenting responses, as revealed by intracellular recordings in the isolated thalamus, isolated neocortex, and intact corticothalamocortical loops.

4.2.1. Intrathalamic augmenting responses

The hemidecortication and surviving ipsilateral thalamus in which augmenting responses can be evoked by intrathalamic stimulation are illustrated in Fig. 4.15. Responses to single thalamic stimuli usually consist of an antidromic spike (latencies varying from 0.3 to 0.5 ms), an orthodromic excitation crowned by action potentials, and a long-lasting hyperpolarization leading to a postinhibitory low-threshold spike (LTS) with fast Na^+ action potentials (Fig. 4.16).

4.2.1.1. High- and low-threshold augmentation in thalamocortical cells

Rhythmic thalamic stimuli above a certain frequency produce changes in the prolonged hyperpolarization in TC neurons, which consists of two or three GABAergic IPSPs [23, 31]. Whereas at 0.5 Hz or lower frequencies there is no, or very slight, change in the

[36] Dempsey and Morison (1942); Morison and Dempsey (1942).

[37] At the time of Morison and Dempsey [36], and even more recently, it was thought that incremental thalamocortical responses are of two basically different types, *augmenting* and *recruiting*. Augmenting responses were elicited in localized cortical areas by stimulation of "specific" (relay) thalamic nuclei and their polarity was positive at the cortical surface, whereas recruiting responses elicited by stimulation of "non-specific" thalamic nuclei were negative at the cortical surface and occurred with a longer latency than that of augmenting responses. (The term non-specific reflected the lack of knowledge about their input-output organization between the 1940s and 1970s, but even some contemporary investigators use this term.) A hypothesized spread of activity from one dorsal thalamic nucleus to another, the "diffuse multineuronal system", was suggested to explain the longer latency of recruiting responses (Jasper, 1949). However, it is now known that there are no direct pathways linking dorsal thalamic nuclei. The longer latency of cortical recruiting responses is ascribable to slower conduction velocities of axons from some thalamic nuclei projecting directly to the neocortex, such as the neurons of the ventromedial nucleus (Steriade, 1995) that project preferentially to layer I and produce recruiting responses (Glenn et al., 1982). In fact, there are no pure augmenting or recruiting responses. Most are mixed responses, with augmenting preceding the recruiting or vice-versa (Spencer and Brookhart, 1961). Therefore, the distinction between augmenting and recruiting responses is no longer necessary.

[38] Steriade (1974).

[39] Steriade and Yossif (1974).

[40] Steriade et al. (1976).

[41] Steriade and Timofeev (1997).

[42] Timofeev and Steriade (1998).

[43] Steriade et al. (1993f).

[44] Timofeev et al. (2002b).

[45] Castro-Alamancos and Connors (1996b).

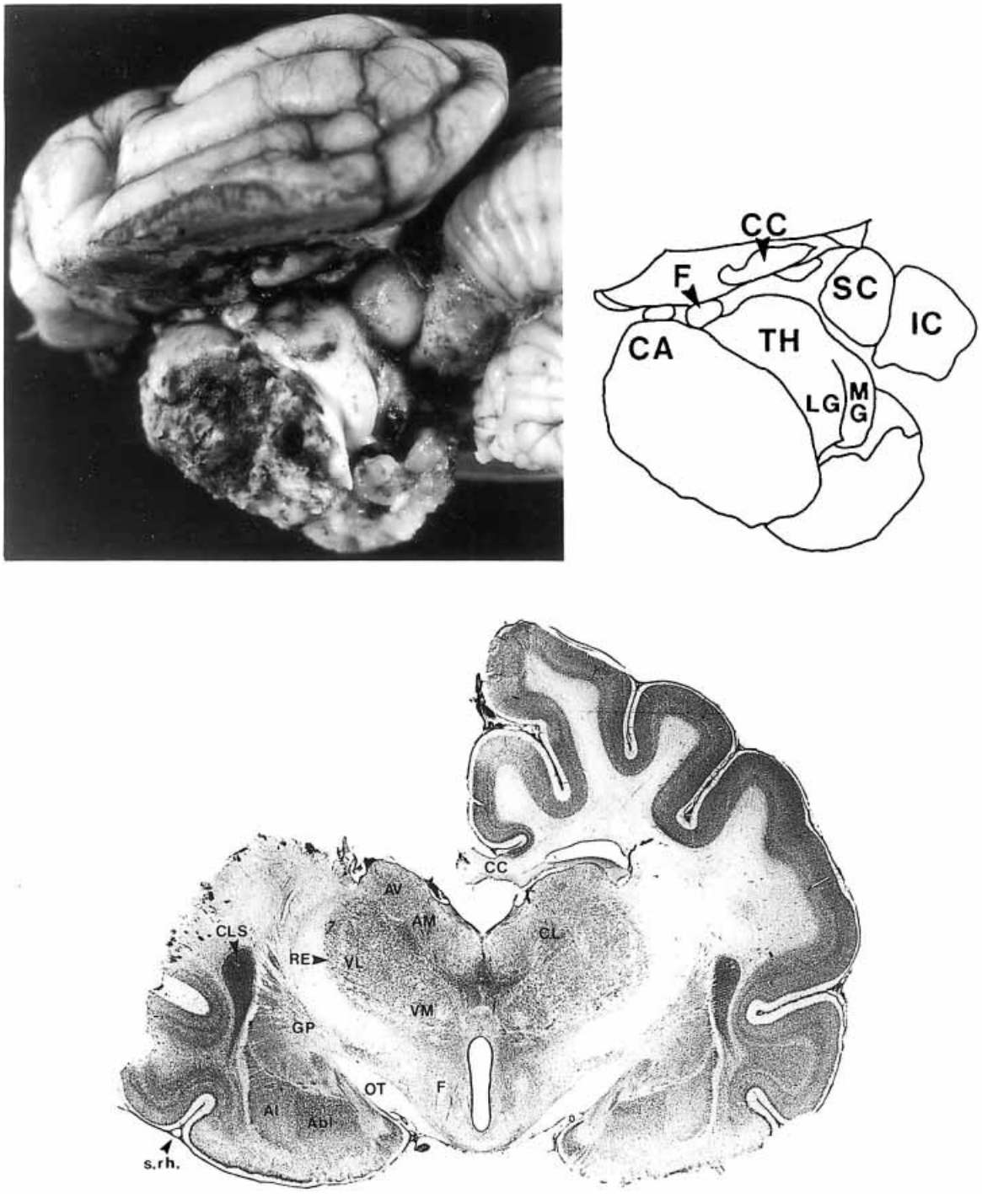

Fig. 4.15 The thalamus after ipsilateral removal of neocortex and cut of corpus callosum. Cat under ketamine-xylazine anesthesia. Top left, dorsal view of the brain showing the extent of hemidecortication. On the right, scheme with subcortical structures in the left (decorticated) hemisphere. Abbreviations: CA, caudate nucleus; CC, corpus callosum; F, fornix; IC, inferior colliculus; SC, superior colliculus; TH, thalamus; LG and MG, lateral and medial geniculate nuclei. Bottom, Nissl-stained frontal section showing the extent of hemidecortication. Note the cut of CC. Abbreviations: AV, AM, CL, RE, VL, and VM, thalamic anteroventral, anteromedial, centrolateral, reticular, ventrolateral, and ventromedial nuclei; Al and Abl, lateral and basolateral nuclei of amygdala; CLS, claustrum; GP, globus pallidus; OT, optic tract; s.rh, sulcus rhinalis (arrowhead). From Steriade and Timofeev (1997).

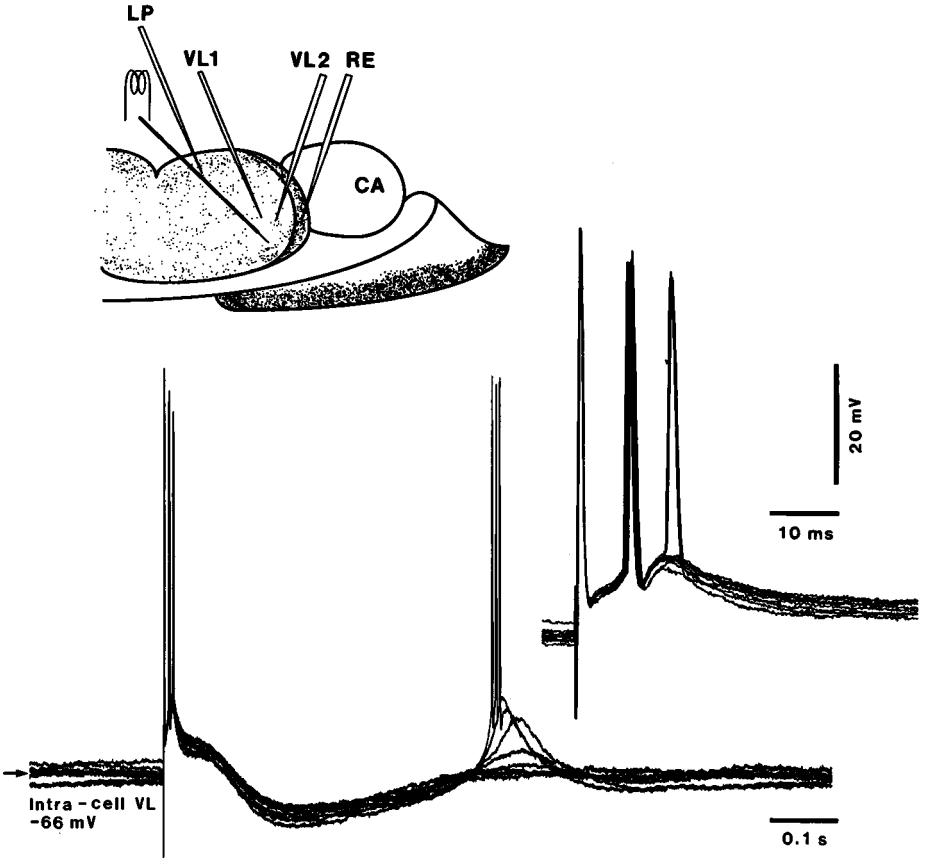

Fig. 4.16 Responses of a TC neuron from the VL nucleus to local VL stimulation. Intracellular recording in cat under ketamine-xylazine anesthesia. The diagram shows the location of two micropipettes in the VL nucleus and one stimulating electrode within the same nucleus. Two pipettes are also shown in the RE and lateroposterior (LP) nuclei. Below, VL-evoked response of a TC neuron in the VL nucleus. The early part of the response is expanded in the above inset showing an antidromic spike, followed by a synaptic response consisting of one or occasionally two action potentials. Note graded low-threshold spike following the prolonged hyperpolarization. From Steriade and Timofeev (1997).

successive IPSPs and rebound spike-bursts, with thalamic stimuli at rates equal to or higher than 1 Hz the amplitudes of IPSPs diminish by ~20–40% and postinhibitory rebound spike-bursts are reduced to an isolated low-threshold (LT) response, eventually disappearing with further stimuli (Fig. 4.17*A*). If, instead of single stimuli repeated at 1 Hz, paired stimuli (interstimuli interval, 0.1 s) are used, the same diminution of IPSP-rebound sequences is observed, but progressively augmented responses are elicited by the first and the second stimulus of the pair (Fig. 4.17*B*). This augmentation consists of a progressive increase in the number of synaptically elicited action potentials (which follow the earlier antidromic spike), associated with a progressive neuronal depolarization. The

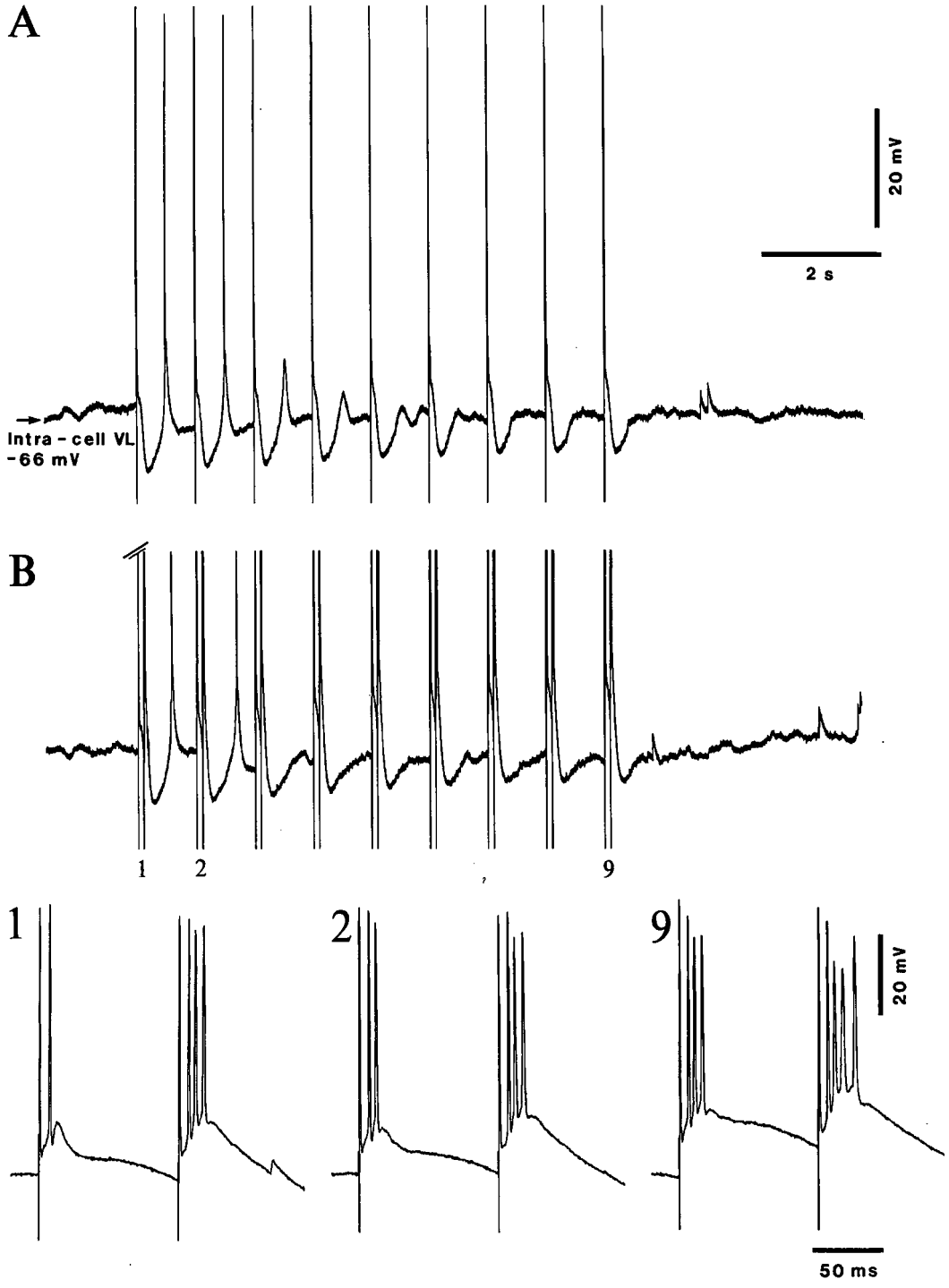

Fig. 4.17 Progressive reduction in inhibition-rebound sequences with rhythmic thalamic stimuli and augmenting responses of a TC neuron in decorticated cat. Ketamine-xylazine anesthesia. *A*, single thalamic VL stimuli were repeated at 1 Hz. The amplitudes of IPSP diminished from 8.5 mV (first two stimuli) to 7.5 mV (third stimulus) and down to 6 mV (last stimulus). These rather slight changes led to the transformation of full-blown rebound spike-bursts (first two stimuli) into a low-threshold (LT) response in isolation (third stimulus) and, thereafter, the absence of postinhibitory rebound. *B*, paired (0.1-s-delayed) VL stimuli delivered at 1 Hz. Note same phenomenon as in *A* (progressive diminution of inhibition-rebound sequences) and, in parallel, progressively augmented responses to the first and second stimuli in the three expanded paired responses (*1*, *2*, and *9*). This type of augmenting response occurred at a depolarized level and is termed high-threshold augmentation (see text). From Steriade and Timofeev (1997).

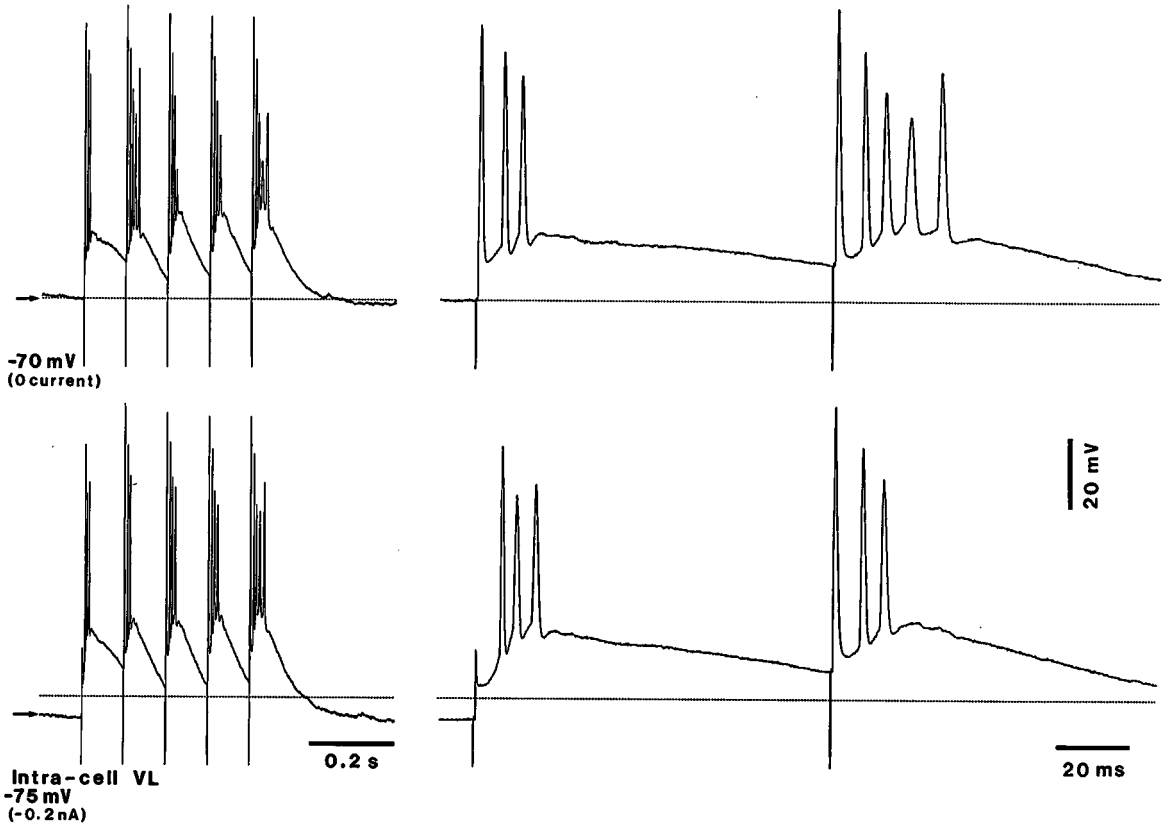

Fig. 4.18 Reduction of the number of action potentials in the second augmented (high-threshold) response of a TC neuron at hyperpolarized levels. Decorticated cat under ketamine-xylazine anesthesia. Five stimuli at 10 Hz were applied at rest (−70 mV) and under steady hyperpolarization (−0.2 nA, −75 mV). Responses to the first two stimuli in the train are expanded on the right (responses consist of an antidromic spike, followed by two to four orthodromic spikes). Note, at the hyperpolarized level, transformation of the full antidromic spike into an initial segment spike, and reduced number of synaptically elicited action potentials in the high-threshold augmented response. From Steriade and Timofeev (1997).

[46] Jahnsen and Llinás (1984a-b).

[47] Roy et al. (1984).

best frequency for eliciting this type of augmentation, based on progressive depolarization, is ~10 Hz.

The above-described type of augmentation is termed *high-threshold* (HT) [41] because it occurs at depolarized levels (Fig. 4.18). It may be ascribed a high-threshold Ca^{2+} conductance in view of *in vitro* [46] and *in vivo* [47] putative intradendritic recordings revealing such a conductance triggering all-or-none depolarizing responses followed by the activation of a $I_{K(Ca)}$. The depolarization-dependency of HT augmenting is underlined by the decrease in the number of synaptically evoked action potentials in the augmented response under slight hyperpolarization that transformed the earlier full antidromic spike into an abortive one (Fig. 4.18).

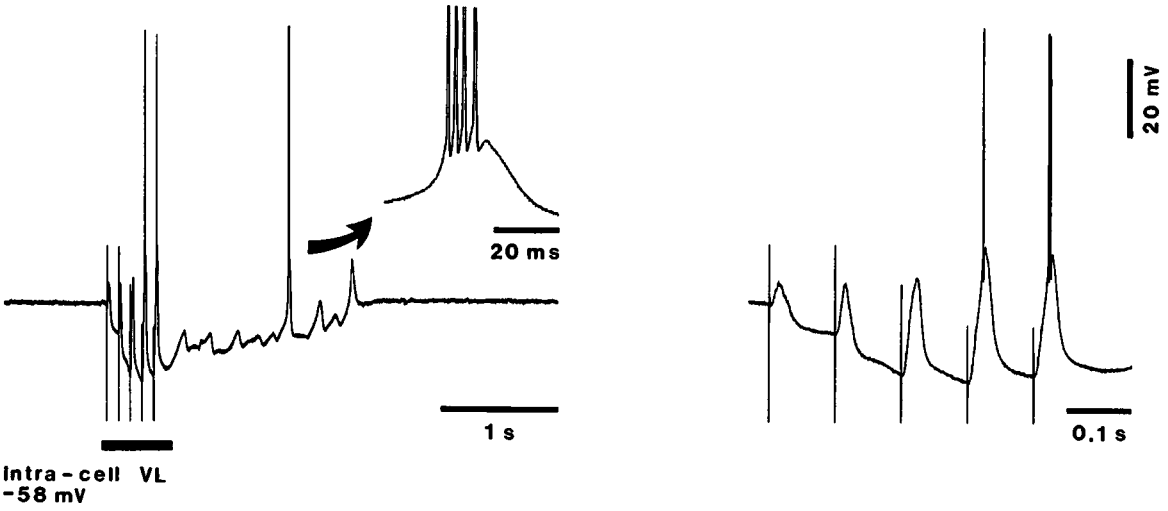

Fig. 4.19 Low-threshold augmenting responses resulting from progressive hyperpolarization of TC neurons. Decorticated cat under ketamine-xylazine anesthesia. Following VL-evoked augmenting responses in a VL neuron, showing progressive hyperpolarization and increased postinhibitory rebound spike-bursts, this neuron displayed a spindle sequence leading to rebound spike-bursts (inset shows expanded burst; spikes truncated). Part marked with the horizontal line is expanded on the right. Modified from Steriade and Timofeev (1997).

The other type of intrathalamic augmentation is termed *low-threshold* (LT) because it develops from progressively growing LT responses resulting from the increase in Cl^--dependent IPSPs during successive stimuli at ~10 Hz (Fig. 4.19) [41]. Indeed, intracellular Cl^- infusion reverses spindles and transforms LT-type augmenting responses into depolarizing responses of the HT type (Fig. 4.20). The amplitudes of intrathalamic LT responses depend on the distance between the stimulated and recorded sites. The closer the stimulation from the impaled neuron, the higher the amplitude of the depolarization area reflecting the LT-type augmented response. The depolarization area of VL neurons increased by 300–400% from the first to the fifth stimulus in a 10–Hz pulse-train when stimulating intranuclearly in the VL nucleus or in the adjacent rostral intralaminar nucleus, whereas there was only slight or no increase in the area of depolarization during rhythmic responses evoked by stimulation at more distant sites within the thalamus (Fig. 4.21).

The HT augmenting responses occurs in a limited region surrounding the stimulating site in the thalamus, whereas the LT-type augmentation can be found at sites that are distant from the stimulating electrode [41, 42].

The two (LT and HT) types of intrathalamic incremental responses can be combined, the HT response developing at a given level of depolarization produced by the LT response. The two steps

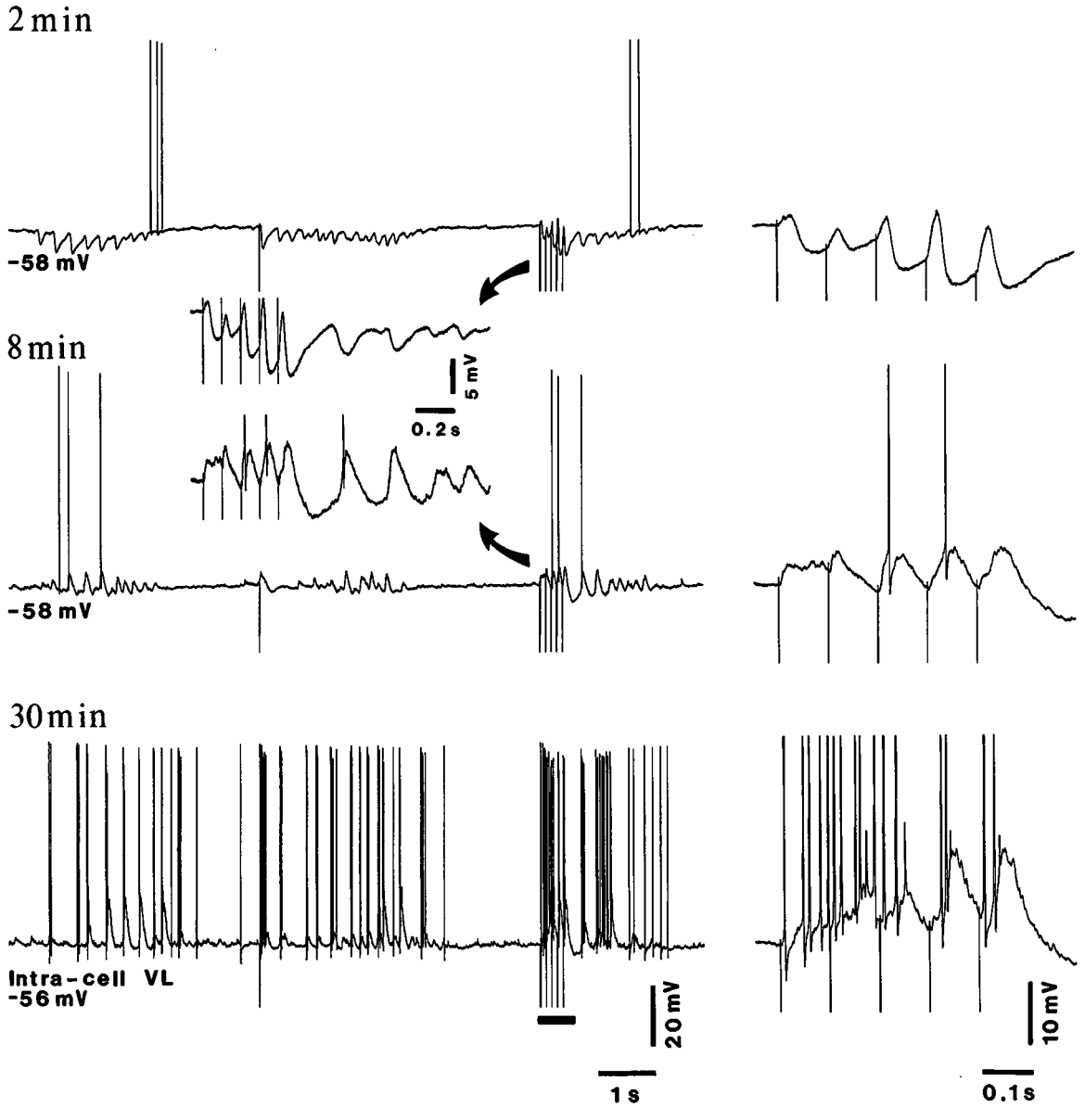

Fig. 4.20 Intracellular Cl^- infusion reverses spindle-related IPSPs and transforms low-threshold-(LT-) type augmenting into depolarizing incremental (high-threshold, HT) responses. Decorticated cat under ketamine-xylazine anesthesia. Intracellular recording of a VL neuron with a micropipette filled with K-acetate (1 M) and KCl (2 M). Shortly (2 min) after impaling, a spontaneously occurring spindle (left) and a spindle evoked by VL single-shock stimulation (middle) consisted of rhythmic IPSPs, and augmenting responses evoked by a 10-Hz pulse-train to the VL nucleus were of the LT type, over a background of hyperpolarization. After Cl^- infusion (8 min and 30 min), spindles and augmenting responses were depolarizing. Augmenting responses at 2 min and 8 min are expanded (two arrows) to show the mirror images of spindles outlasting the pulse-train at 10 Hz. On the right, expanded augmenting responses to five VL stimuli (period marked by horizontal bar at 30 min; spikes truncated at 8 min and 30 min). From Steriade and Timofeev (1997).

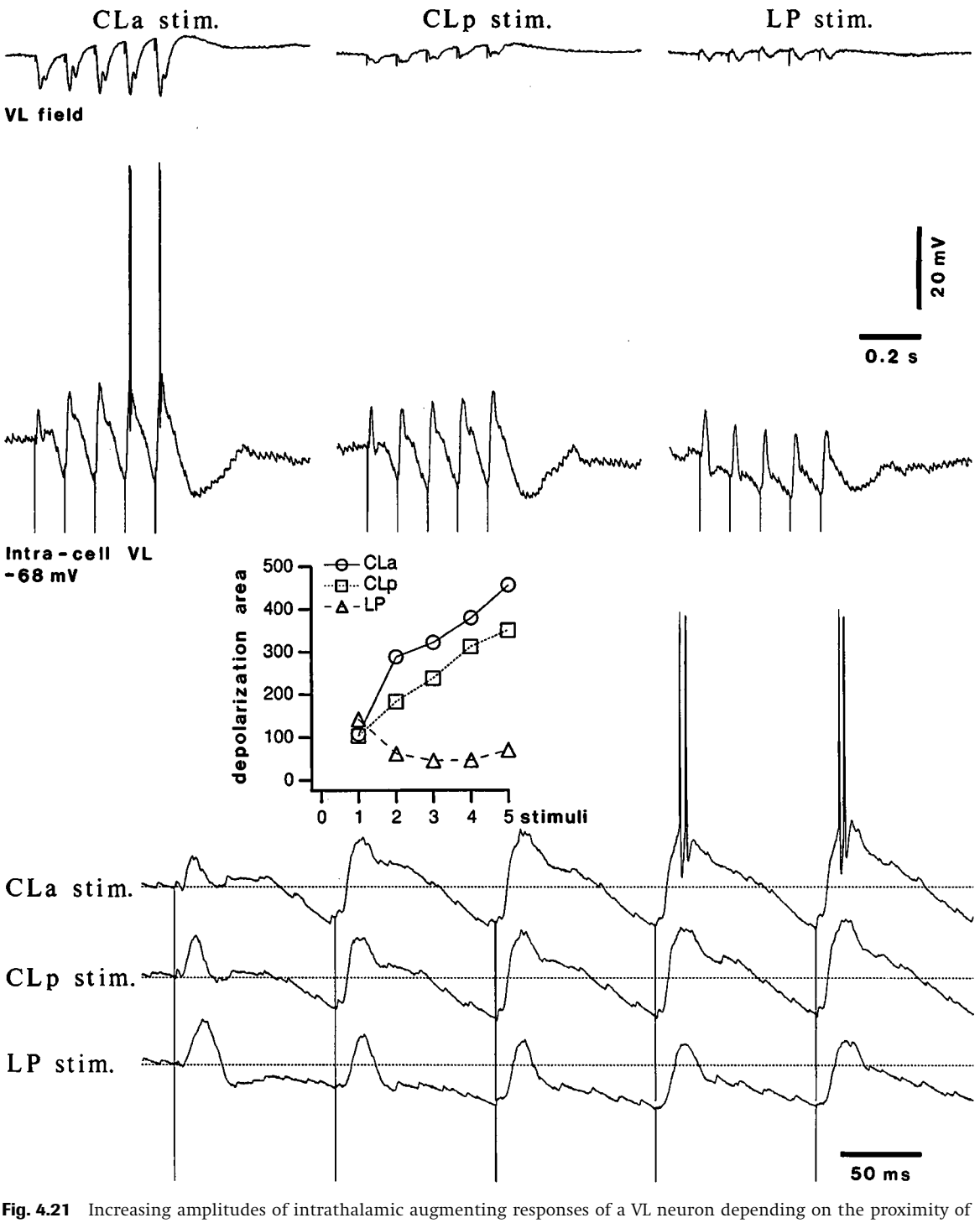

Fig. 4.21 Increasing amplitudes of intrathalamic augmenting responses of a VL neuron depending on the proximity of various stimulated thalamic sites. Decorticated cat under ketamine-xylazine anesthesia. Simultaneous intracellular recordings of a TC neuron and field potentials in the VL nucleus, while stimulating from the closest site (centrolateral anterior, CLa) to more distant sites (centrolateral posterior, CLp; and lateral posterior, LP) nuclei. The intracellular responses are expanded below. Graph depicts the depolarization area of the augmented response (ordinate) to each stimulus in the five-stimuli strain (abscissa) applied to CLa, CLp, and LP. From Timofeev and Steriade (1998).

[48] Steriade and Deschênes (1984); Jones (1985); Sawyer et al. (1994); Liu et al. (1995).

[49] See notes [97–98] in Chapter 3.

in this transformation, from LT to HT augmenting, are indicated by arrows in Fig. 4.22. A similar transformation in the same TC neuron is illustrated in Fig. 4.23*B–C*, in which the bottom arrow marks the inflection point at which the EPSP triggers an LTS, whereas the top arrow (~15 mV more positive) indicates the point at which the LT gives rise to a secondary depolarization that represents the HT augmented response. Panel *A* in this figure demonstrates that augmenting responses develop over a progressive depolarization at the expense of hyperpolarizing epochs.

These two (HT and LT) types of augmenting responses in TC neurons are due to opposite changes produced by intrathalamic stimulation in GABAergic RE neurons, which are discussed below.

4.2.1.2. Decremental and incremental responses in GABAergic reticular cells

Several lines of evidence point to RE neurons, rather than local inhibitory interneurons, as responsible for the HT and LT incremental responses in TC neurons. Synaptic activation of local-circuit GABAergic cells by intrathalamic stimuli is unlikely because of the lack of intranuclear axonal collaterals of TC neurons in VL and other dorsal thalamic nuclei [48]. Dual simultaneous intracellular recordings from thalamic ventrolateral (VL) and lateroposterior (LP) nuclei in decorticated cats show augmenting responses in both nuclei, evoked by either VL or LP repetitive stimuli, which suggests that common pools of RE neurons with divergent projections to the dorsal thalamus, rather than local-circuit inhibitory neurons, induce such responses [41]. Lastly, Cl^--dependent IPSPs are the basis of both spindles and LT-type augmenting responses (see Fig. 4.20) and, whereas RE neurons are pacemakers of spindles [49], local inhibitory interneurons are not mainly implicated in this oscillation.

Intracellular recordings in the rostrolateral part of the RE nuclear complex in decorticated cats revealed different changes in neuronal responsiveness to rhythmic (10 Hz) stimuli applied to dorsal thalamus, as a function of stimulus intensity [42]. Low-intensity stimulation (i.e., <30% of maximal intensity) produced decremental responses to successive volleys, whereas high intensity (>70% of maximal intensity, ~0.3–0.4 mA) elicited incremental responses in RE neurons (Fig. 4.24). The response of RE neurons to a single dorsal thalamic stimulus generally consists of an antidromic spike, followed by a spike-burst with the typical accelerando-decelerando pattern (see in Fig. 4.24 the response to the first stimulus in the pulse-train with an intensity of 27%), while at lowest intensities only the antidromic spike can be elicited. At up to 50% of maximal intensity, only decremental responses in the synaptically evoked

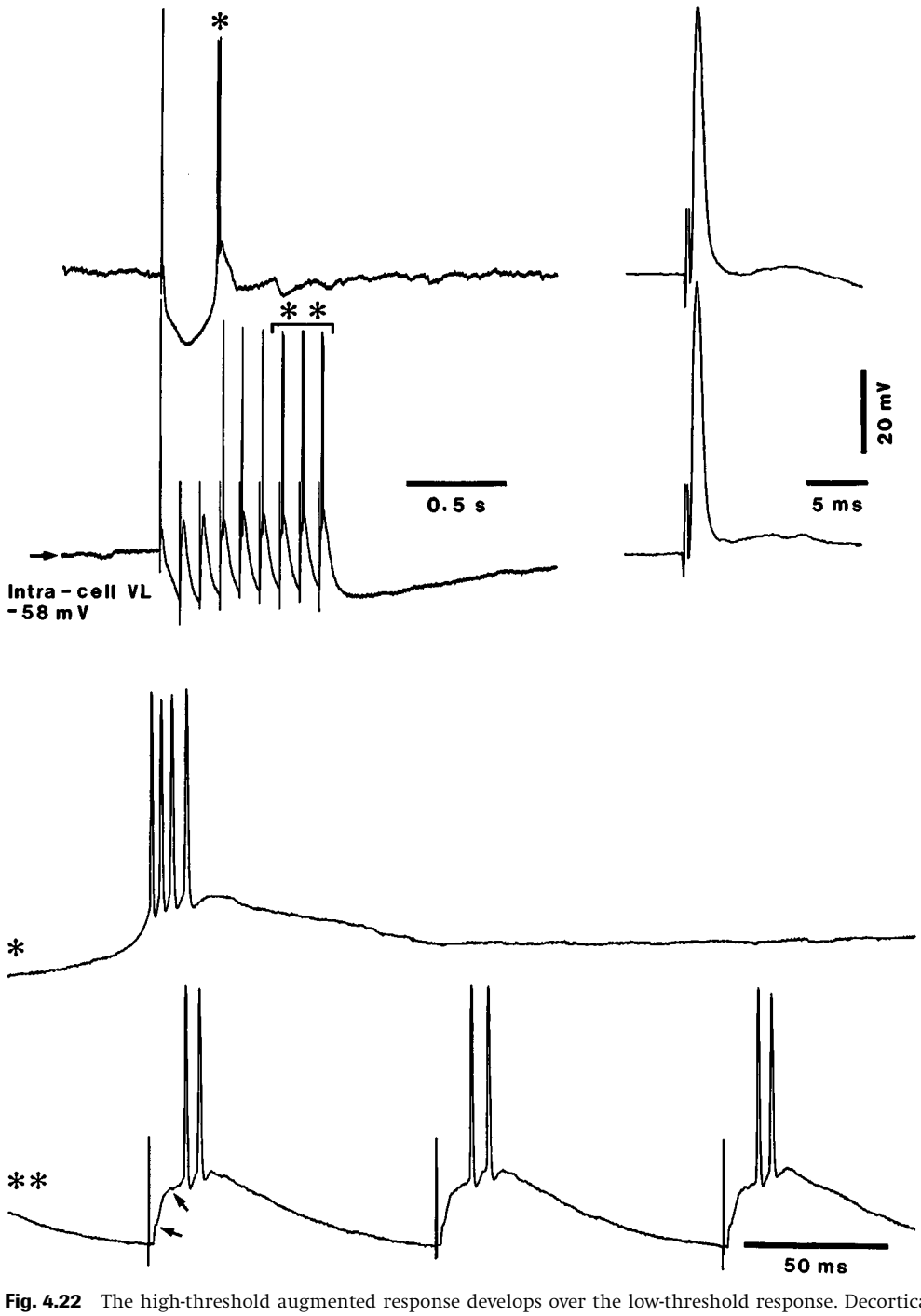

Fig. 4.22 The high-threshold augmented response develops over the low-threshold response. Decorticated cat under ketamine-xylazine anesthesia. *Top*, response of a VL neuron to a single VL stimulus (first trace) and responses to a nine-stimuli train (second trace). The early, antidromic spike is expanded on the right. Bottom, the postinhibitory rebound burst to the single stimulus (*) and the last three responses to the nine-stimuli train (**) are expanded. The first (bottom) arrow in the bottom trace indicates the level at which the EPSP gave rise to a low-threshold (LT) spike, and the second (top) arrow marks the inflection where the secondary (high-threshold) component of the augmenting response arose at a more depolarized level. Note the difference between the pattern of spike-burst crowning of the LT spike in the postinhibitory rebound to the single stimulus (*) and the doublets in the augmented response (**). From Steriade and Timofeev (1997).

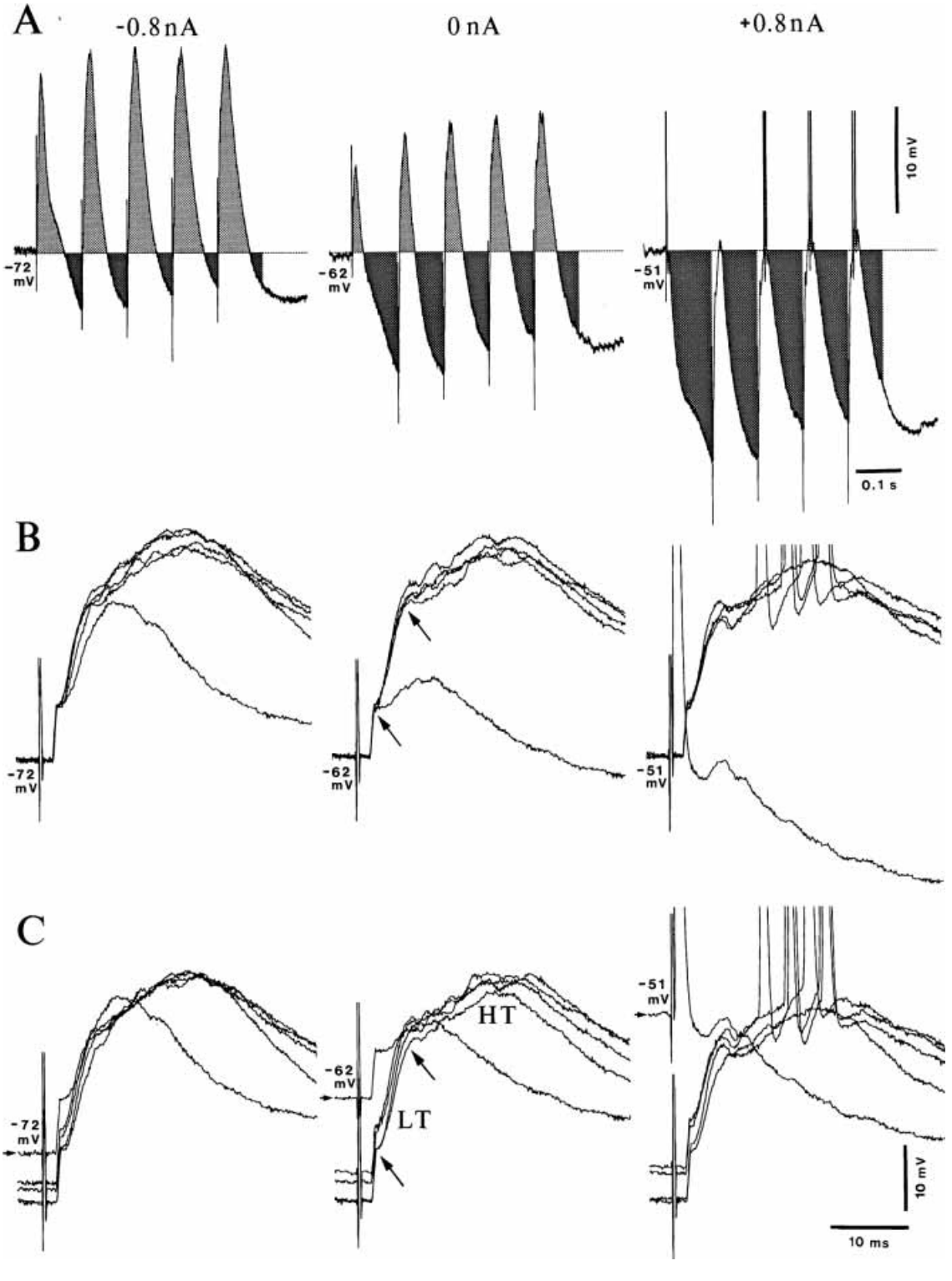
A
-0.8nA
0 nA
+0.8nA
-72 mV
-62 mV
-51 mV
10 mV
0.1 s
B
-72 mV
-62 mV
-51 mV
C
-72 mV
-62 mV
-51 mV
HT
LT
10 mV
10 ms

[50] Deschênes et al. (1985); Yen et al. (1985); Liu et al. (1995).

[51] Uhlrich and Huguenard (1996); Sanchez-Vives and McCormick (1997a-b).

[52] See notes [17–18] and related main text.

[53] Bazhenov et al. (1998a).

[54] Steriade and Contreras (1995). See also notes [39–40].

bursts were elicited, while the antidromic spike remained unaffected. At above 70%, clear-cut incremental responses occurred (Fig. 4.24). We postulated that decremental responses are due to intra-RE inhibitory processes, through dendrodendritic and recurrent collateral axonal contacts [50] that mediate $GABA_{A\text{-}B}$ IPSPs [51]. The decremental responses in RE neurons would produce a progressive release from inhibition in target TC neurons, with the consequence of developing HT augmenting responses in TC neurons. By contrast, the incremental responses in RE neurons would produce a progressive hyperpolarization in TC neurons, with the consequence of de-inactivating the Ca^{2+}-mediated LT conductance and increasing postinhibitory rebound spike-bursts. These RE-TC relations are simplified when local-circuit GABAergic interneurons are not included in this scheme [52].

Computational models of intrathalamic augmenting responses [53] showed that a network consisting of one TC and one RE neuron is the smallest circuit capable of generating augmenting responses, with properties similar to those seen in *in vivo* experiments [41]. The models also showed that the basic mechanism needed for the generation of LT-type incremental responses is $GABA_B$ inhibition leading to Ca^{2+}-mediated LT spike-bursts, as blockade of $GABA_B$ receptors in the model of the TC-RE network transformed augmenting responses of TC neurons into stereotyped responses. Another prediction of that computational study [53] was that intrathalamic activation both of RE and TC neurons may result in immediate augmentation and self-sustained activity. This prediction implies that corticothalamic volleys, which are most efficient in driving both RE and TC neurons, may produce a transition from sleep rhythms (and some forms of oscillatory activity mimicking them) into self-sustained seizures of the spike-wave (SW) type [54]. Experimental data supporting this prediction are discussed in a later section of this chapter (**4.3**).

Fig. 4.23 (opposite) Low-threshold to high-threshold augmenting responses. Decorticated cat under ketamine-xylazine anesthesia. *A*, TC neuron from the VL nucleus was tested with trains of five stimuli at 10 Hz under steady hyperpolarizing current (−0.8 nA, left), at rest (0 nA, middle), and under steady depolarizing current (+0.8 nA, right). Superimposed responses were offset at the initial V_m (see real V_m in *C*). *B*, superimposed and expanded early responses (at the same V_m as in *A*). The bottom arrow in the middle column tentatively indicates the level at which the initial EPSP gave rise to a low-threshold (LT) response, whereas the top arrow marks the inflection at which augmenting responses were initiated at a more depolarized level. Note action potentials triggered by the augmented response under +0.8 nA (right column). *C*, the early responses were superimposed and expanded, but shown at the real V_m. In all superimpositions, the response to the first stimulus in the train is at the indicated V_m (−72 mV under −0.8 nA; −62 mV without current; and −51 mV under +0.8 nA). The next two traces illustrate the responses to the fifth and fourth stimuli, and the last traces represent responses to the second and third stimuli. Note, under +0.8 nA, the antidromic spike immediately after the first stimulus in the train, but its blockage at a more hyperpolarized level. Also note transformation from LT to high-threshold (HT) augmentation. From Steriade and Timofeev (1997).

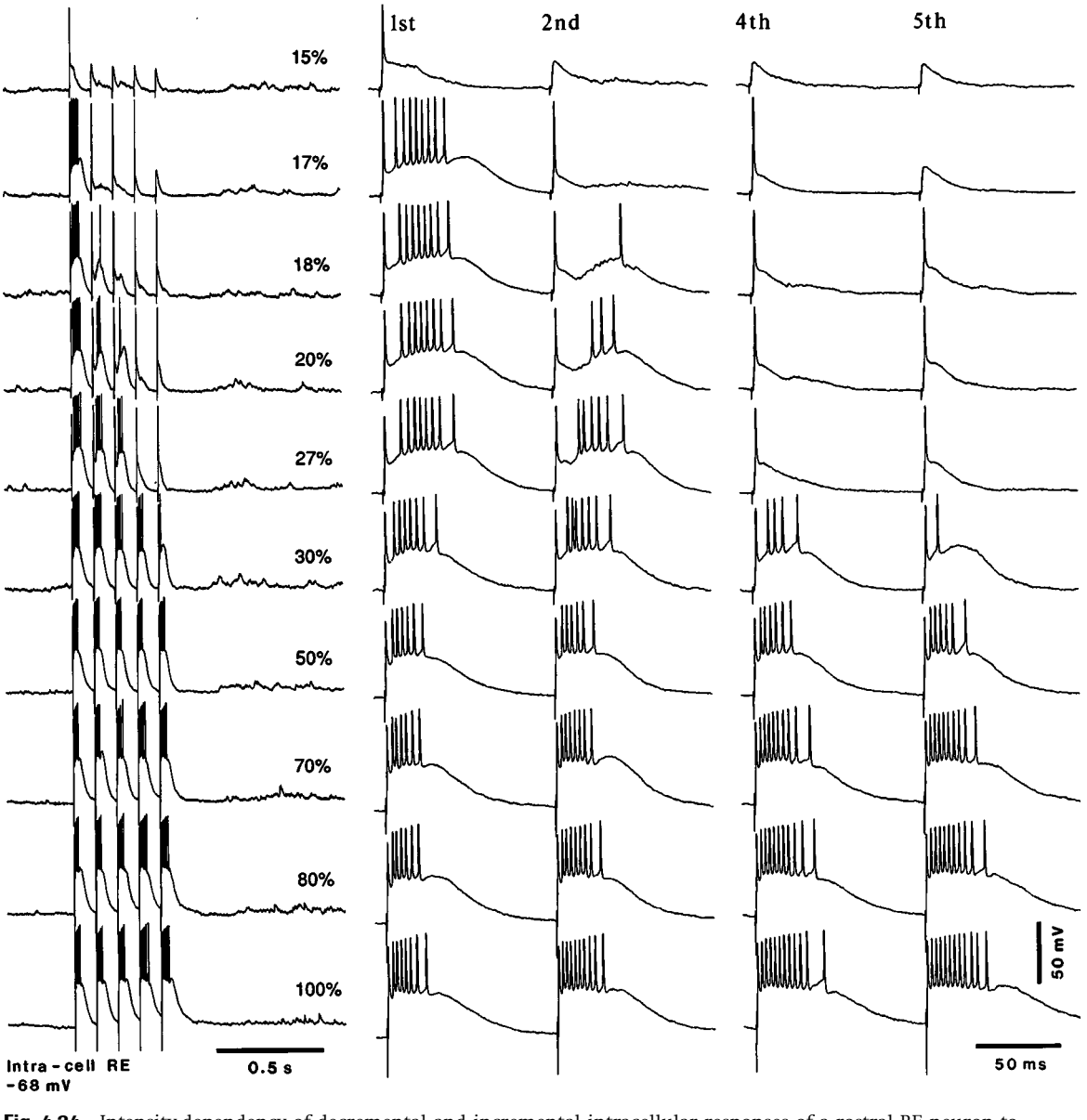

Fig. 4.24 Intensity-dependency of decremental and incremental intracellular responses of a rostral RE neuron to repetitive (10 Hz) stimulation of the VL nucleus in decorticated cat. Ketamine-xylazine anesthesia. Left column: responses to all five stimuli recorded at lower speed. Middle and right columns: responses to first and second, and fourth and fifth stimuli at 10 Hz, recorded at higher speed. Decremental responses are observed with stimuli at 15–30% of maximal intensity. Incremental responses occurred at high intensities (70–100%). At half intensity (50%) there was virtually no change in the number of spikes evoked by the five stimuli in the pulse-train. From Timofeev and Steriade (1998).

[55] Curró Dossi et al. (1991). These *in vivo* experimental data, obtained by stimulation of brainstem cholinergic nuclei, are congruent with the action of ACh applied to TC neurons recorded from thalamic slices (McCormick and Prince, 1987).

[56] Morin and Steriade (1981); Steriade and Morin (1981); Ferster and Lindström (1985).

[57] Castro-Alamancos and Connors (1996b); see Fig. 4*B* in that paper.

[58] In Fig. 4.26*A*, spike-like component *1* is presynaptic, with peak latencies from 0.4 to 0.6 ms, reflects the activity in radiation axons, and does not undergo reversal in deeper layers. Wavelet *2* occurs at a latency of 1.1–1.2 ms, is difficult to detect in many instances (because it is incorporated in the following, larger components), and is postsynaptic as it is superimposed by action potentials of cortical neurons. The major surface-positive (depth-negative) waves *3–4*, with peak latencies from 1.8 to 2.2 ms and 2.9 to 3.4 ms, respectively, undergo distinct reversal. Finally, surface-negative (depth-positive) wave 5 has a peak latency at ~6–7 ms and reverses at a greater depth than earlier components.

4.2.1.3. Alterations of thalamic augmenting responses during brain activation

If LT-type augmenting responses in TC neurons are built-up by their progressive hyperpolarization that de-inactivates the conductance giving rise to rebound spike-bursts (see Fig. 4.19), a process due to incremental responses in GABAergic RE neurons, the actions of ascending activating systems that depolarize TC neurons would block the process of augmentation. This is indeed what happens upon setting into action the thalamic projections of mesopontine cholinergic neurons (Fig. 4.25), which exert muscarinic depolarization of TC neurons [29, 55]. Similar blockage is exerted during midbrain reticular formation stimulation or natural brain arousal on cortical augmenting responses to thalamic stimulation; in that case too, the effect is mainly exerted at the level of TC neurons (see *4.2.2.1*).

4.2.2. Thalamocortical augmenting responses

Thalamically evoked augmenting responses in neocortex [36–37] have mostly been recorded in motor and association areas, but similar incremental potentials are observed in primary sensory areas [56]. The failure to elicit augmenting responses in primary somatosensory cortex of rats investigated *in vitro* [57] is probably due to species differences. The complex thalamocortical field response recorded in all primary sensory (visual, auditory, somatosensory) systems of cats, with a presynaptic and four postsynaptic deflections (Fig. 4.26*A*) resulting from successive activation of different layers [58] and thus allowing the development of augmenting responses, is lacking in rats that display a much simpler response pattern, with a single component of the thalamocortical response [57]. With field potential and superimposed extracellular unit recordings, the augmented thalamocortical response is visible from the second stimulus in a pulse-train at 10 Hz; it grows from a late (15–20 ms) depth-negative wave in conjunction with the decrement of the early, rapid components of the primary response (Fig. 4.26*A–B*). The required condition for eliciting augmentation is a given temporal relation between the evoking stimulus and the declining phase reflecting hyperpolarization in a pool of neurons or the onset of rebound (Fig. 4.26*C*). Specifically, the augmented potential cannot be elicited if the stimulus was delivered following the rebound of the preceding response. The role of connected thalamic and cortical neurons in the augmentation process is discussed below.

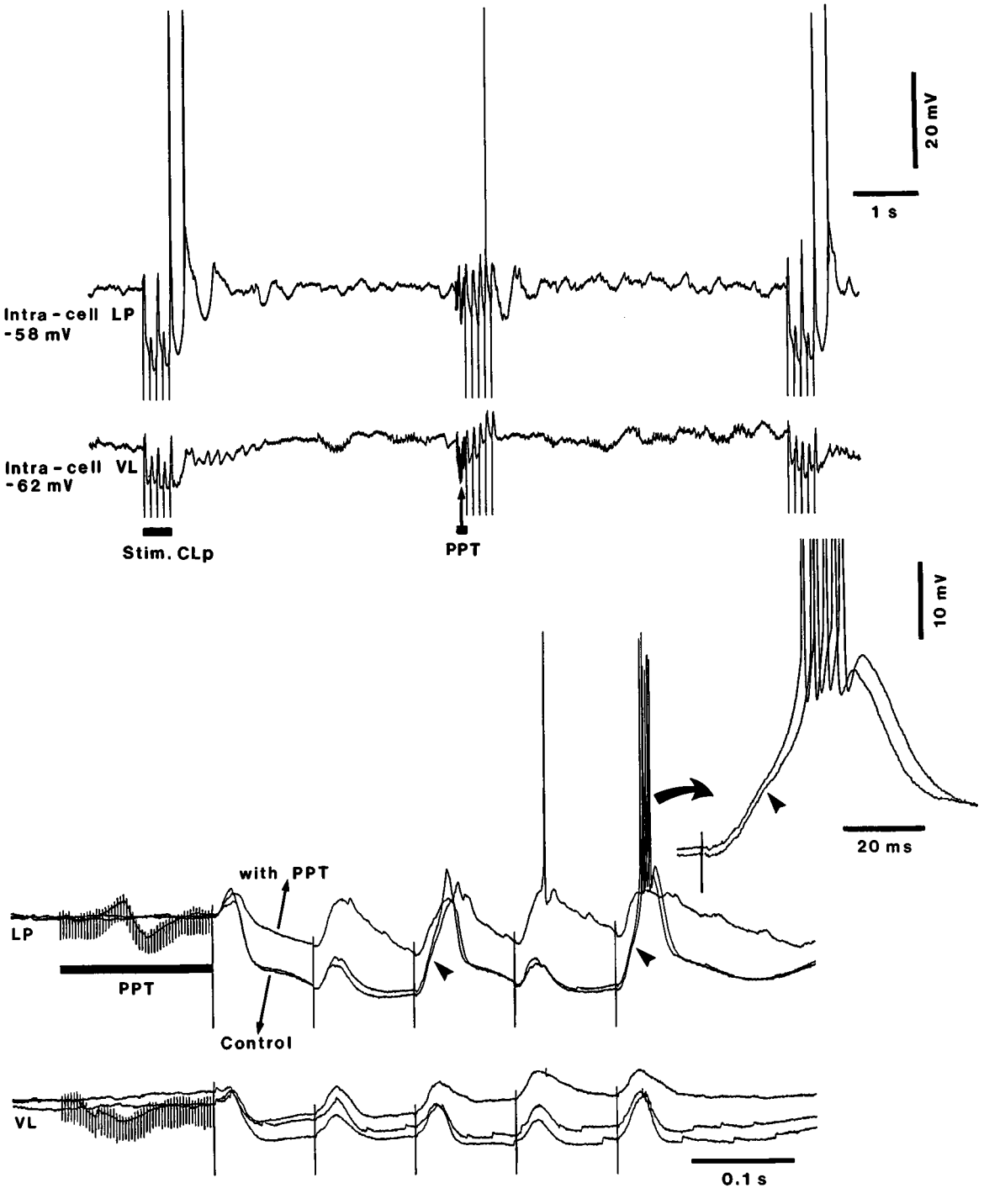
20 mV
1 s
Intra - cell LP
-58 mV
Intra - cell VL
-62 mV
Stim. CLp
PPT
10 mV
20 ms
with PPT
LP
PPT
Control
VL
0.1 s

[59] Purpura et al. (1966); Creutzfeldt et al. (1966).

[60] See neuron from area 4 in Fig. 4.28.

[61] Kawaguchi (1993; de la Peña and Geijo-Barrientos (1996).

[62] Contreras et al. (1997c).

[63] Bazhenov et al. (1998b).

4.2.2.1. Dual intracellular recordings from thalamic and cortical neurons

During thalamically evoked augmenting responses in cortical neurons, intracellular recordings revealed a selectively increased secondary depolarization, initiated at 7–16 ms and associated with diminished amplitude of the early EPSP (Fig. 4.27). In earlier studies on cortical augmenting responses [59], the increased secondary depolarization was thought to result from attenuation of hyperpolarizing potentials during repetitive stimulation. However, typical augmenting responses occur in cortical neurons even when hyperpolarizing potentials do not diminish and may even increase [60]. At least two factors may account for the increased amplitude of the secondary depolarizing component during augmentation, as follows.

(a) Dual intracellular recordings from TC and target cortical neurons show that postinhibitory spike-bursts during the LT-type augmenting responses in TC neurons (see Fig. 4.19 in section *4.2.1.1*) precede by short latencies (~3 ms) the augmented depolarization in cortical neurons (Fig. 4.28).

(b) Progressively stronger volleys from TC neurons during augmenting responses can activate local-circuit inhibitory neurons in the cortex, hyperpolarize pyramidal neurons, and deinactivate Ca^{2+}-dependent LT currents in these neurons [61], thus generating augmented waves.

During spindle oscillations too, rhythmic spike-bursts from TC neurons produce inhibitory effects on cortical pyramidal neurons, as demonstrated by the transformation of reversed IPSPs, recorded with Cl^{-}-filled micropipettes, into robust bursts resembling paroxysmal depolarizations during seizures [62]. The role of cortical inhibitory interneurons in augmenting responses was also elaborated in a computational study [63].

Fig. 4.25 (opposite) Brain activation induced by stimulation of the pedunculopontine tegmental (PPT) nucleus blocks augmenting responses in TC neurons. Decorticated cat under ketamine-xylazine anesthesia. Dual intracellular recordings from thalamic lateroposterior (LP) and ventrolateral (VL) neurons. In control conditions (before and after PPT stimulation), stimulation (five stimuli at 10 Hz) of the posterior part of the thalamic centrolateral (CLp) nucleus elicited clear-cut augmenting responses in LP neuron, developing from low-threshold (LT) rebound and followed by a self-sustained rebound cycle, whereas immediately after a pulse-train to the PPT nucleus (300 Hz, lasting for 150 ms) incremental LTSs deinactivated by membrane hyperpolarization were blocked because of the PPT-induced reduction in hyperpolarizing responses. Three epochs depicted in the top trace (control before PPT pulse-train, effects of PPT stimulation on augmenting responses, and recovery to control values after the PPT pulse-train) are superimposed and expanded (bottom). Arrowheads mark LT responses (developing from EPSPs) evoked in LP neuron by the third and fifth stimuli in the train. Full-blown spike-bursts crowning LTSs are expanded on the right. CLp stimulation evoked less obvious augmentation in the VL neuron. From Timofeev and Steriade (1998).

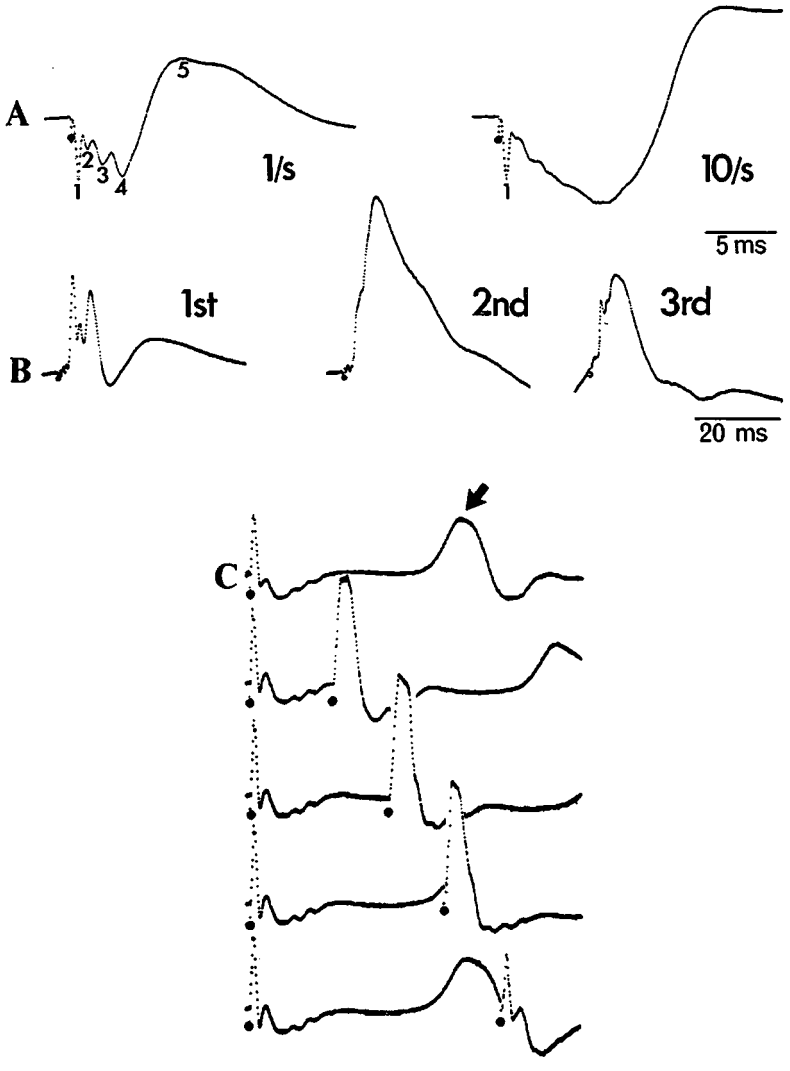

Fig. 4.26 Primary and augmented thalamocortical responses in the somatosensory system. Brainstem-transected cats (*encéphale isolé*, bulbo-spinal cut). Field potential responses in primary somatosensory cortex (S1) to 1 Hz and 10 Hz stimulation of the thalamic ventroposterior (VP) nuclear complex. Fifty averaged sweeps. Positivity down. *A*, surface recording in S1 cortex of responses to 1 Hz and 10 Hz VP stimulation. Numbers 1–5 represent presynaptic (*1*) and postsynaptic (*2*–*5*) components of thalamocortical responses (see main text and note [58]). Note unchanged presynaptic deflection with 10 Hz stimulation. *B*, another animal. Depth (0.7 mm) recording of the first, second, and third responses to a pulse-train at 10 Hz. Note, during augmentation, reduced amplitude of early postsynaptic, rapid component and prolonged duration of the slow negative wave. *C*, recording in a recording electrode descent at 0.5 mm depth. Responses to single VP stimuli (upper trace) and to paired VP stimuli separated by 60 ms, 100 ms, 140 ms, and 180 ms. Rebound component (peak latency, 150 ms) indicated by arrow. Modified from Morin and Steriade (1981).

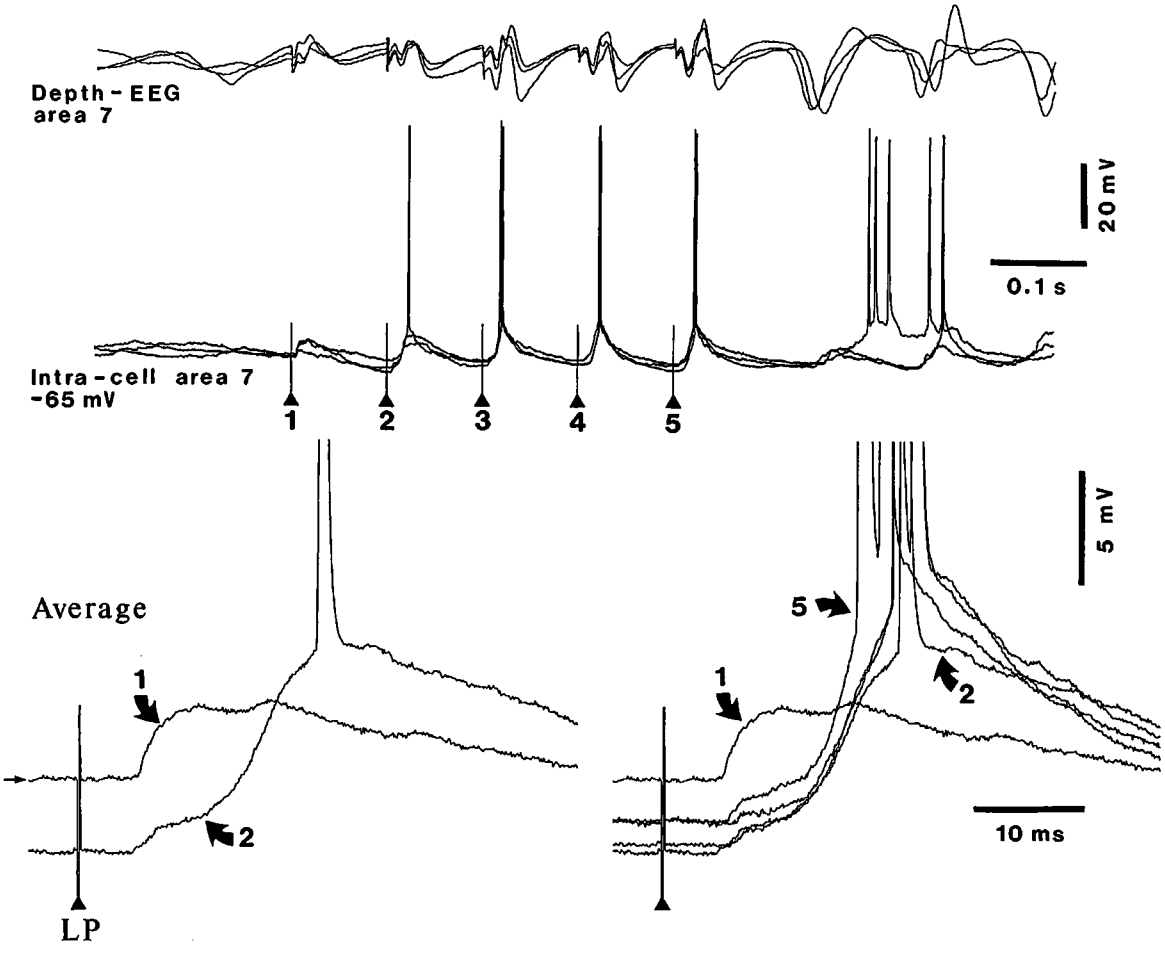

Fig. 4.27 Cortical augmenting responses to thalamic repetitive stimuli (10 Hz) develop from a late depolarization. Cat under barbiturate anesthesia. *A*, thalamic LP-evoked augmenting responses in field potentials and intracellularly recorded neuron from cortical suprasylvian area 7. Three superimposed traces. Below, average ($n = 3$) of the cellular responses to the first and second stimuli in the 10-Hz train (left) and to all five stimuli in the pulse-train (right). Note that the amplitude of the early EPSP (latency about 5 ms) diminished at the second stimulus and that a secondary depolarization (onset latency around 12 ms), leading to an action potential, appeared from the second stimulus. Modified from Steriade et al. (1998d).

[64] Steriade et al. (1998d).

[65] Grenier et al. (1998).

Simultaneous recordings of neocortical and TC neurons also demonstrate that the former display post-augmenting oscillatory activities in the frequency range of augmenting responses, whereas the latter remained hyperpolarized because of the pressure from the GABAergic RE neurons (Fig. 4.29) [64]. These data show that intracortical circuits have a major influence on the incoming inputs from TC neurons and can amplify oscillatory activity arising in the thalamus [65]. Such a view is consistent with the fact that, although spindles are generated in the thalamus, they are not passively reflected in the cortex, and cortical synaptic circuitry has a major

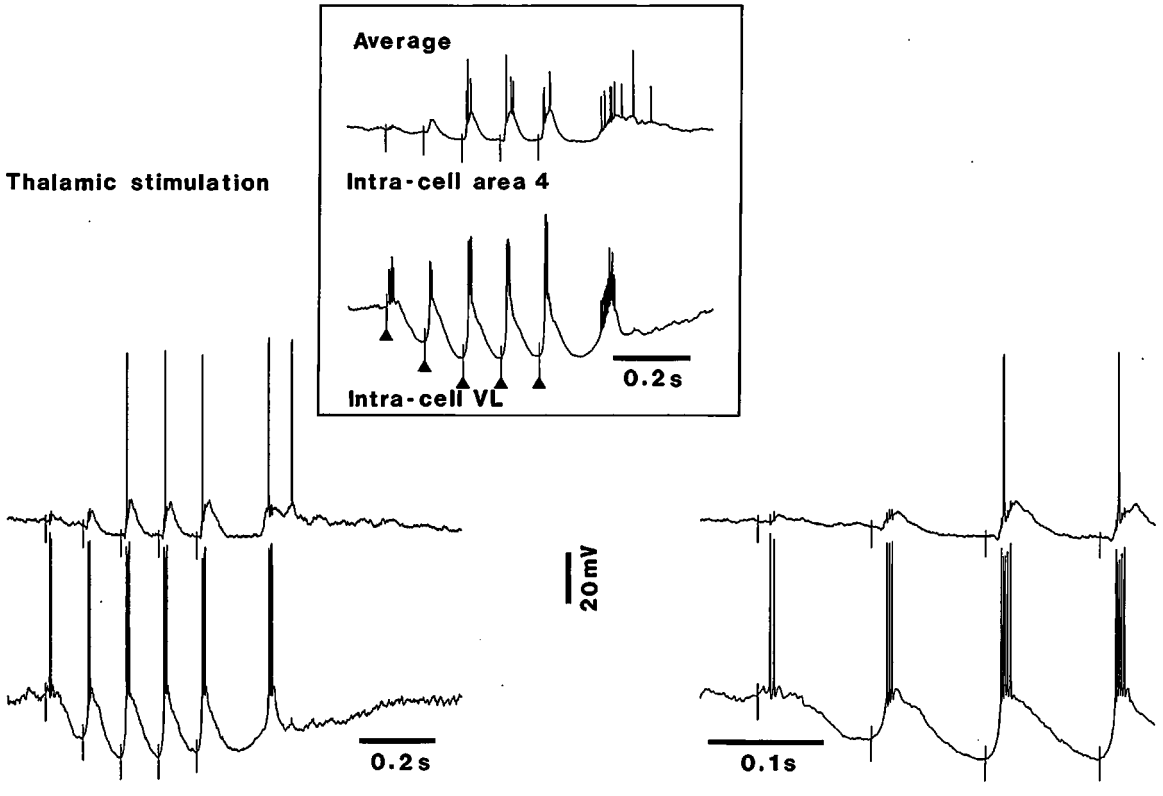

Fig. 4.28 Postinhibitory spike-bursts in TC neurons during low-threshold augmenting responses lead to secondary depolarization in cortical neurons. Dual intracellular recordings from a TC neuron in the VL nucleus and an area 4 cortical neuron. Cat under ketamine-xylazine anesthesia. Thalamically VL-evoked augmenting responses. On the right, expanded responses to the first four stimuli. Top inset shows averaged responses ($n = 5$). Small deflections in the area 4 neuron represent capacitive coupling artifacts from action potentials in the VL neuron. Modified from Steriade et al. (1998d).

[66] Kandel and Buzsáki (1997).

role in modifying and amplifying TC volleys [66]. Figure 4.30*A1–2* shows that, with single thalamic stimuli, the initial response in TC neurons led to a biphasic, $GABA_{A\text{-}B}$ IPSP, followed by a sequence of hyperpolarizations in the frequency range of spindles, which favor the occurrence of spike-bursts crowning low-threshold spikes (LTSs). The prolonged inhibition of TC neurons was probably generated by RE neurons that fired repeated spike-bursts in response to a single stimulus to the dorsal thalamus (panel *A3* in Fig. 4.30). Simultaneously, the intracellularly recorded cortical neuron displayed a depolarizing plateau giving rise to trains of action potentials that were associated with spindle-like oscillations in cortical EEG. Similarly, opposing activity patterns in TC and cortical neurons were seen with pulse-trains of five stimuli at 10 Hz (Fig. 4.30*B*). Thus, although cortical potentials were directly produced by thalamofugal volleys (see subthreshold EPSPs and full-blown action potentials in

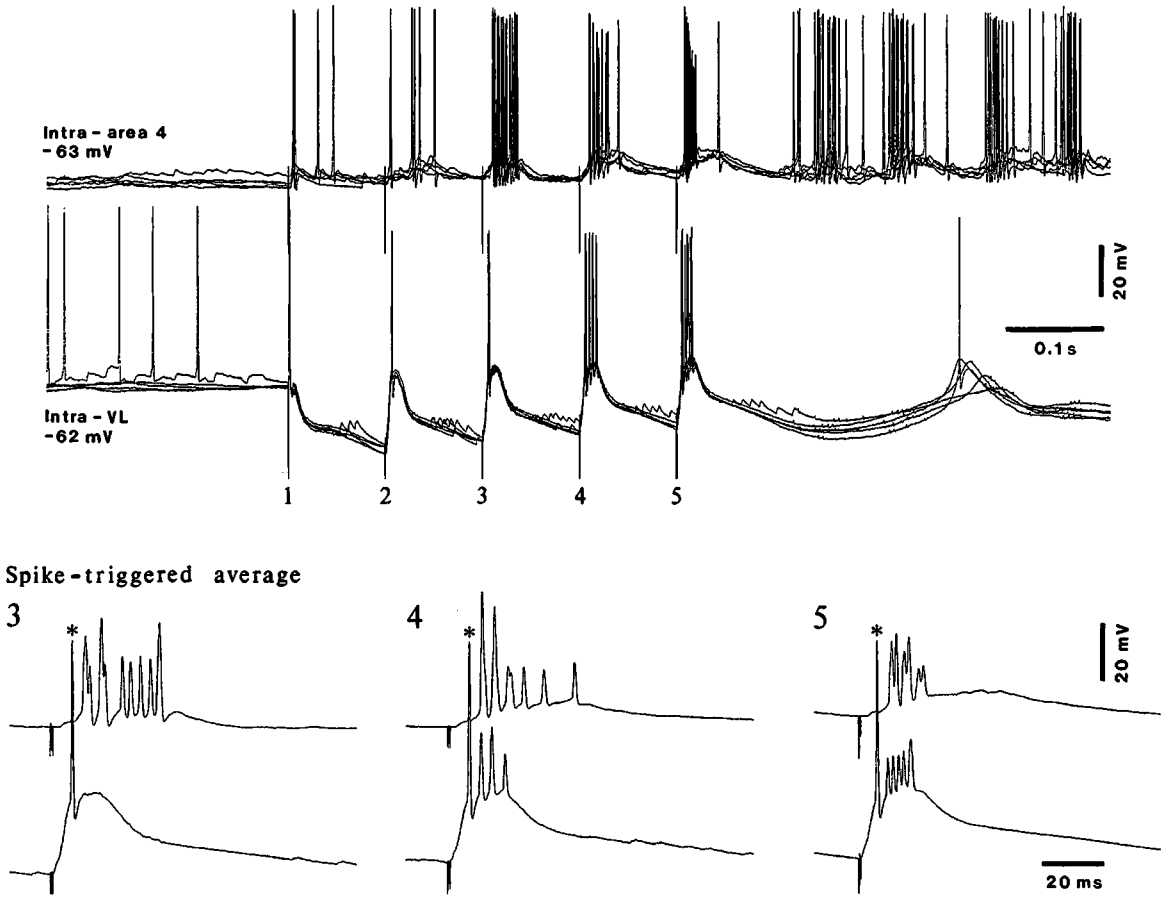

Fig. 4.29 Low-threshold augmenting responses in a thalamocortical (TC) neuron precede cortical responses but the cortical neuron displays self-sustained activity within the frequency range of augmenting responses whereas the TC neuron remains under a hyperpolarizing pressure. Dual intracellular recordings from a TC neuron in the VL nucleus and a cortical neuron from area 4 in cat under ketamine-xylazine anesthesia. Responses to five-stimulus trains at 10 Hz, applied to the VL nucleus. Spike-triggered averages of VL and cortical responses to third, fourth, and fifth stimuli in the train (the first action potentials in the spike-burst of a TC cell, marked by asterisks, triggered the average). Note self-sustained activity in the cortical neuron, following augmentation, whereas the TC neuron remained hyperpolarized because of hyperpolarizing pressure from GABAergic thalamic reticular neurons. Unpublished data by M. Steriade, I. Timofeev, and F. Grenier.

a cortical neuron, following the action potentials a in TC neuron; see panel *B3* in this figure), *the cortex used its own machinery to elaborate oscillatory responses that outlasted thalamic stimuli, despite the fact that, simultaneously, TC neurons remained under a prolonged hyperpolarization*. This activity pattern, which implicates intracortical activity that may amplify corticipetal volleys arising in the thalamus and may even be independent of thalamic activity, corroborates data on the active role of cortical circuitry in the genesis of spindles [66].

To sum up, although thalamocortical neurons have a high propensity to fire spike-bursts and trigger incremental responses

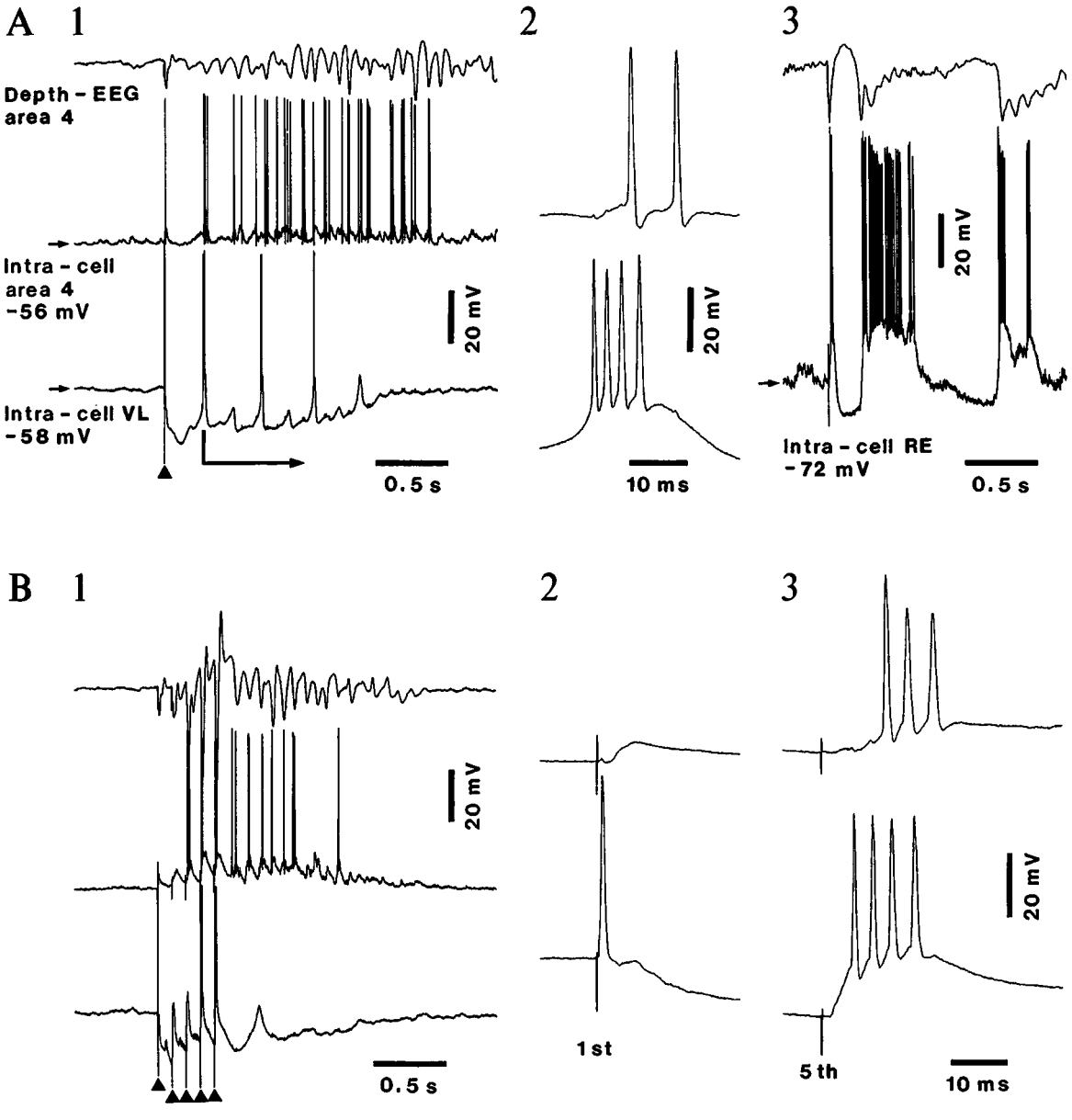

Fig. 4.30 Self-sustained oscillatory activity (~10 Hz) in a cortical neuron after augmenting responses is accompanied by sustained hyperpolarization in a simultaneously recorded TC neuron. Cat under barbiturate anesthesia. Dual intracellular recording of a cortical neuron from area 4 and a TC neuron from the ventrolateral (VL) nucleus (*A1-2* and *B*), and intracellular recording from an RE neuron in the peri-VL district (*A3*). *A1*, single stimulus (arrowhead) to the thalamic VL nucleus produces, after the initial excitation and a period of inhibition in both neurons, a series of oscillatory waves in the cortex, whereas the VL neuron remained hyperpolarized and displayed occasional LTSs and burst discharges (the first spike-burst is expanded on the right, *A2*). *A3*, same VL stimulus produced rhythmic spike-bursts in an RE neuron. *B*, pulse-train (five stimuli at 10 Hz) applied to the VL nucleus produced augmenting responses in a cortical neuron, whereas a simultaneously recorded VL neuron displayed hyperpolarization (same neurons as in *A1-2*). First and fifth responses are expanded on the right (*B2* and *B3*, respectively). Note persistent oscillatory activity at 10 Hz in the cortical neuron, after cessation of thalamic stimulation. From Steriade and Timofeev (2001).

[67] Castro-Alamancos and Connors (1996c).

in target neocortical neurons, the latter have the ability to maintain and develop self-sustained oscillations. This is an autonomous, intracortically generated activity, within the frequency range of the previous stimulus-evoked responses, since thalamocortical neurons continue to remain hyperpolarized following augmenting responses and do not fire, because of the inhibitory pressure from GABAergic thalamic reticular neurons.

The activity that develops as a consequence of augmenting responses suggests that short-term plasticity processes occur during, as well as after, these responses as well as during sleep epochs characterized by spindles that represent the natural event mimicked by augmenting potentials. This postulate is substantiated by experimental data exposed in section **4.3.**

4.2.2.2. Role played by different types of cortical neurons in augmenting responses

The augmenting phenomenon was investigated intracellularly in four types of neocortical neurons, defined electrophysiologically by their responses to depolarizing current steps: regular-spiking (RS), fast-rhythmic-bursting (FRB), intrinsically bursting (IB) and fast-spiking (FS) (see details in Chapter 2, section ***2.1.1***).

Work on slices from rat sensorimotor cortex maintained *in vitro* suggested a prevalent role of layer V IB neurons in the generation of augmenting responses [67]. This conclusion was based on data of which some follow: (*a*) the augmenting response begins in layer V neurons and appears in neurons from the upper layers during the next 5 ms; and (*b*) IB neurons have voltage-dependent conductances that serve to increase membrane excitability after hyperpolarization. That IB neurons are implicated in augmenting responses generated by rhythmic stimulation of the callosal pathway was indeed shown *in vivo* (see below, Fig. 4.33*D*), a condition under which prolonged pulse-trains at 10 Hz lead to self-sustained plasticity associated with sustained depolarization and a greatly increased number of action potentials per response, eventually leading to paroxysmal activity [43]. It is known that callosal axons reach superficial layers. However, when testing the thalamocortical pathway *in vivo*, despite the peculiar intrinsic properties of IB neurons, their augmenting responses resembled those of RS neurons recorded from the same cortical depth (Fig. 4.31). The mean latency of thalamically evoked secondary depolarization in cortical neurons (8.5 $\pm$ 0.6 ms), which characterizes augmenting responses [64], did not change from IB neurons located in layers V–VI to the less numerous IB neurons located in layers III–IV.

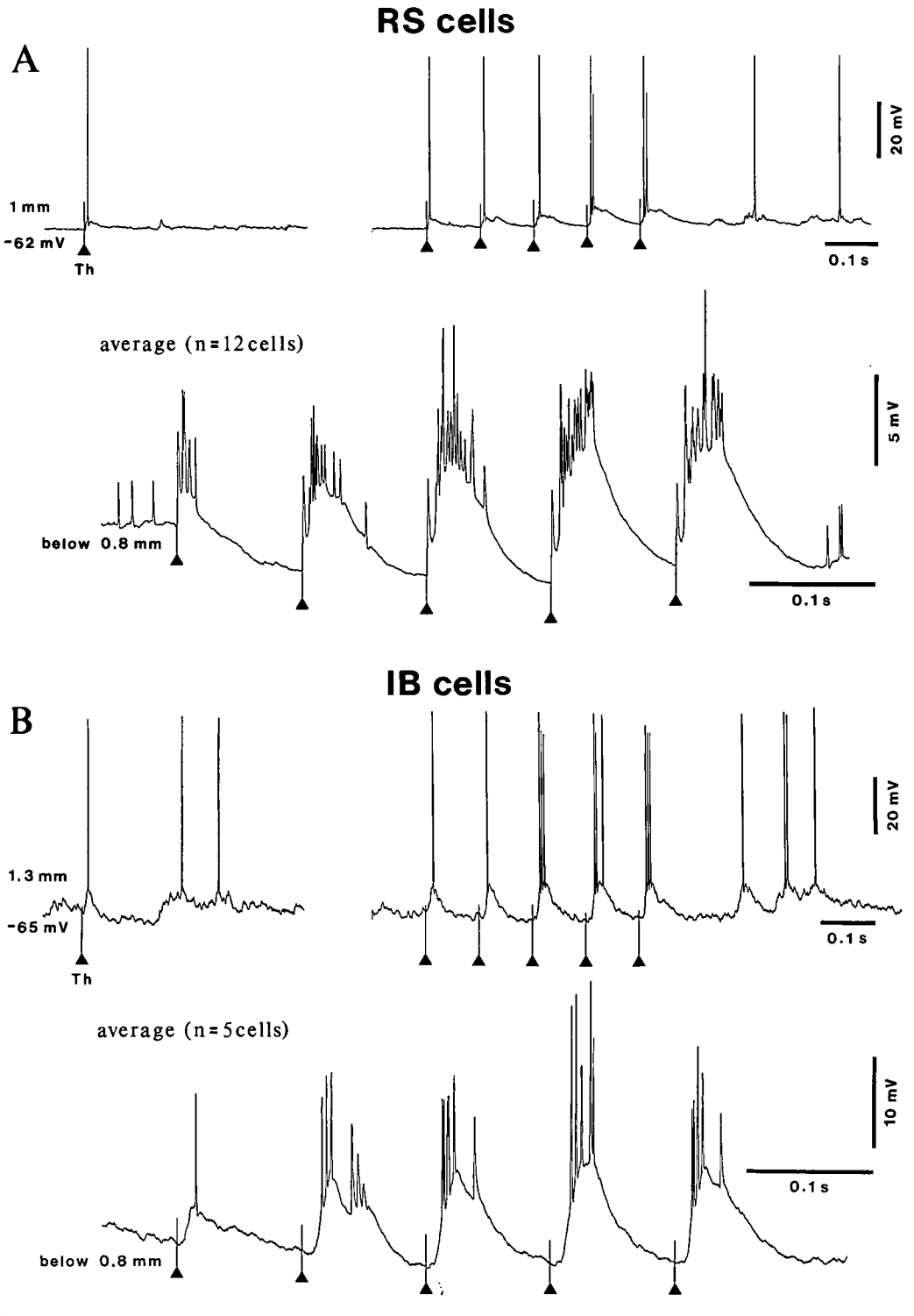

Fig. 4.31 Thalamically evoked augmenting responses in deeply lying cortical regular-spiking (RS) and intrinsically bursting (IB) neurons. Cats under barbiturate anesthesia. *A*, top trace, augmenting response in RS neuron at 1 mm in area 5, evoked by a pulse-train at 10 Hz, applied to the thalamic lateral posterior (LP) nucleus. Below, average of augmenting responses in 12 RS neurons recorded below 0.8 mm. *B*, top trace, augmenting response in IB neuron at 1.3 mm in area 7, evoked by a pulse-train at 10 Hz, applied to the thalamic intralaminar centrolateral (CL) nucleus. Below, average of augmenting responses (also evoked by stimulation of thalamic intralaminar CL nucleus) in five IB neurons recorded below 0.8 mm. From Steriade and Timofeev (2001).

In our work [68], FRB neurons recorded from deep cortical layers were found to play the major role in cortical augmentation. Figure 4.32*A–B* depicts intracellular recordings from two FRB cortical neurons, recorded at depths of 0.5 mm and 1.2 mm, and identified by their high-frequency spike-bursts (300–400 Hz) recurring rhythmically at ~35 Hz upon depolarizing current steps [69]. Augmenting potentials (panel *B*) were more pronounced in the deep FRB neuron. Averages of responses recorded from FRB neurons demonstrate that, whereas in more superficial neurons cortical augmenting responses to thalamic stimuli progressively developed from a secondary (*b*) depolarizing component, which distinctly followed the primary depolarization (*a*), the primary and secondary depolarizing components coalesced, and augmenting was associated with many more action potentials, in deeper FRB neurons.

Changing incidences of IB neurons in various experimental conditions may account for the difference in results between *in vitro* [67] and *in vivo* [68] experiments, with emphasis on IB and FRB neurons, respectively. It is now known that, whereas IB neurons may reach proportions of 40–50% in slices maintained *in vitro* [70] or in cortical slabs prepared *in vivo* [71], the incidence of this neuronal type is lower in the intact cortex and, in naturally alert animals, IB neurons represent less than 5% of sampled neurons [5].

The crucial role played by FRB neurons in widespread synchronization of augmenting responses results from thalamic projections of deeply lying cortical FRB neurons [69] and feedback projections to the cortex, even toward areas that are remote from the site where the primary corticothalamic drive originates. This was predicted in experimental and modeling investigations [63] and the morphological substrates of return pathways to distant cortical areas in corticothalamocortical loops were revealed [72].

4.2.2.3. State-dependent alterations in augmenting responses

Thalamocortical augmenting responses are of maximal amplitude during slow-wave sleep and diminish in amplitude during natural states of waking and REM sleep or as an effect of stimulating the brainstem reticular activating system in cats [73] as well as during strong arousal in rats [74]. The diminution of thalamocortical augmenting responses during brain activation processes is due to the brainstem-induced depolarization of TC neurons [55], with the consequence of abolishing the rebound spike-bursts, which trigger the secondary depolarization that characterizes cortical augmenting responses (see Fig. 4.25 in section *4.2.1.3*).

[68] Steriade and Timofeev (2001).

[69] Steriade (1997a); Steriade et al. (1998b). The fast-rhythmic-bursting (FRB) neurons, as termed in our studies, were called "chattering" neurons by Gray and McCormick (1996) who found them pyramidal-shaped and located exclusively in superficial layers. In addition to some excitatory pyramidal neurons from layers II–III with intracortical projections, many FRB neurons are also deeply located corticothalamic neurons or local-circuit inhibitory neurons, as demonstrated by their antidromic invasion from the thalamus or intracellular staining, respectively (Steriade et al., 1998b).

[70] Yang et al. (1996).

[71] Timofeev et al. (2000a). In that study, isolated cortical slabs were prepared from areas 5 and 7 of the suprasylvian gyrus. After opening a hole in the parietal bone, a small perforation was made in the dura above a part of the pia that did not contain large vessels. A homemade crescent knife was inserted along its curve into the cortex until the tip of the knife appeared about 10 mm frontally under the pia. The knife was then turned by 90° in both right and left directions. The pia was intact except at the place where the knife entered. Such slabs were about 8–10 mm long (rostro-caudal direction), 5–6 mm wide (medio-lateral direction) and 4–5 mm deep. The completeness of neuronal transections and the boundaries of the slab are illustrated in thionine-stained sections shown in Fig. 1b of that paper. Experimental recordings from small cortical slabs isolated from thalamic and cortical inputs, as well as from a larger isolated gyrus, revealed that activity was sparse and irregular in smaller slabs, but became progressively more similar to the slow oscillation observed in the intact cortical tissue as the size of the slab was increased.

[72] Kato (1990).

[73] Steriade et al. (1969); Steriade (1991).

[74] Castro-Alamancos and Connors (1996a).

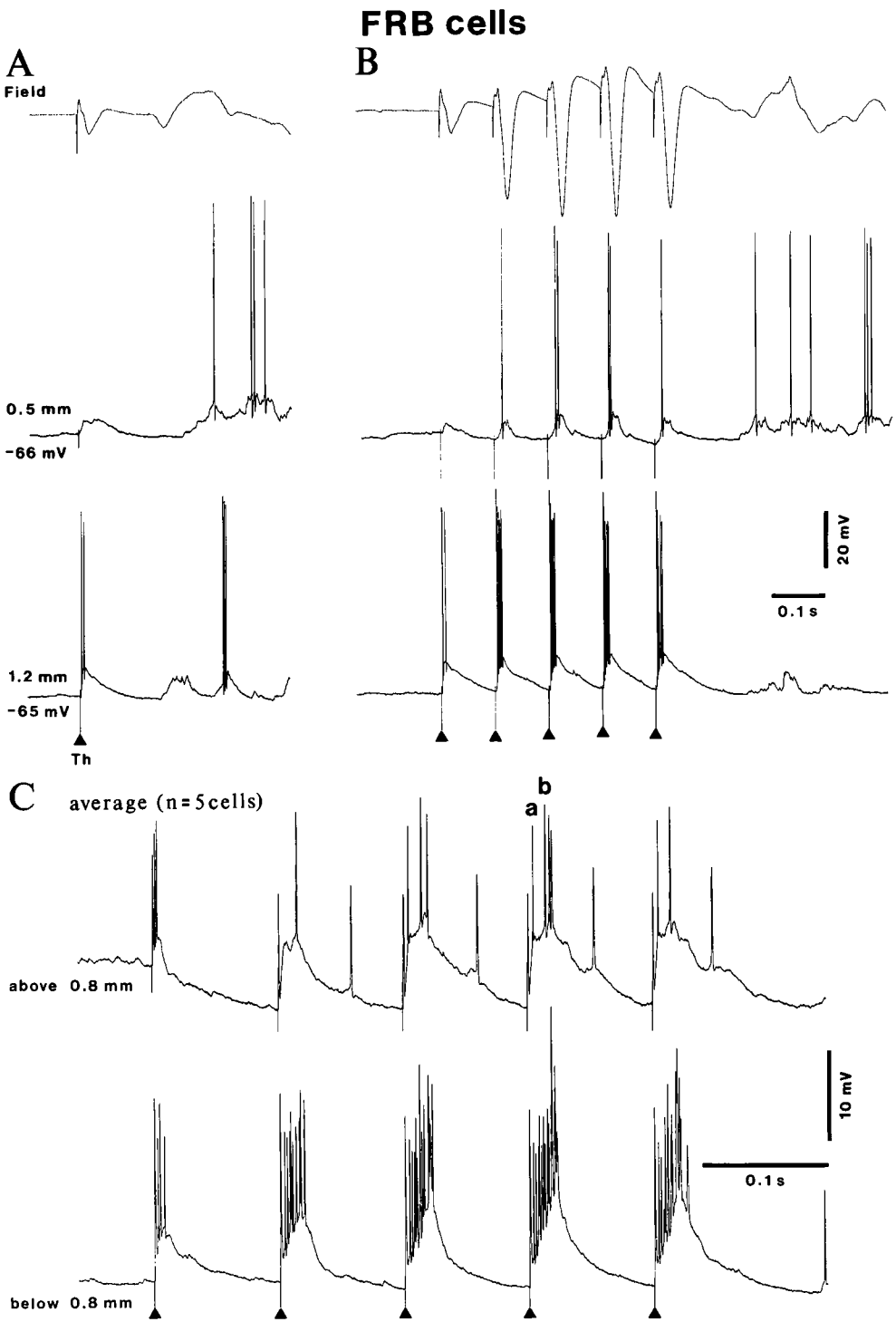

Fig. 4.32 Thalamically evoked augmenting responses in fast-rhythmic-bursting (FRB) cortical neurons recorded from suprasylvian area 7. Cats under barbiturate anesthesia. *A-B*, two FRB neurons recorded at 0.5 and 1.2 mm. In each of them, single thalamic stimulus (marked by arrowhead) was applied to the lateroposterior (LP) nucleus (*A*) and trains of five stimuli at 10 Hz were applied to the rostral intralaminar centrolateral (CL) nucleus (*B*). *C*, averages of responses from five neurons recorded above and below 0.8 mm. Responses to pulse-trains at 10 Hz. Note that cortical augmentation consisted of two components (*a-b*) in neurons recorded above 0.8 mm and that, in neurons recorded below 0.8 mm, components *a* and *b* coalesced. Positivity in field potential (EEG) recordings is upwards (as in intracellular recordings). From Steriade and Timofeev (2001).

4.2.3. Intracortical augmenting responses

4.2.3.1. Intact cortex

Compared with augmenting responses elicited in cortical neurons by thalamic stimuli, corticocortical augmenting responses are less ample and the progressively growing amplitude of successive responses is much less evident (compare panels *A–B* to panels *C–*D in Fig. 4.33). The difference is accounted for by the absence of spike-bursts arising in TC neurons when cortical stimulation is used. This could be demonstrated by using simultaneous intracellular recordings from cortical and TC neurons when testing with either thalamic or cortical repetitive volleys at 10 Hz. Figure 4.34 illustrates such an experiment in which the greater increase in amplitude of augmenting potentials evoked by thalamic stimuli is observed in both field potentials and intracellular activities recorded from thalamic and cortical cells. In particular: *(a)* with thalamic stimuli (left column in Fig. 4.34), the cortical neuron displayed augmenting responses, characterized by a secondary depolarization that followed ~3 ms after the first action potential in the rebound spike-bursts fired by the simultaneously recorded TC neuron, and rebound bursts in TC neurons were initiated with the second stimulus in the pulse-train, following the biphasic ($GABA_{A\text{-}B}$) IPSP imposed by thalamic inhibitory neurons; *(b)* in contrast, with cortical stimuli (right column in Fig. 4.34), augmenting responses in cortical neurons lacked the secondary depolarization (seen with thalamic stimuli) and developed from the early EPSP. With either thalamic or cortical stimuli, TC neurons remained under a continuous hyperpolarization, likely arising in the GABAergic RE neurons.

The amplitude and even the presence of augmenting responses of cortical neurons evoked by ipsilateral cortical stimulation depend on the distance between the stimulation and recording sites. Neurons located close to the stimulation site (<1 mm) display the build-up of strong depolarization, whereas with increasing distance between stimulation and recording sites (1–5 mm) the depolarizing shift diminishes and eventually disappears, resulting in EPSP/IPSP sequences that show negligible, if any, augmentation (Fig. 4.35). This result is similar to the distance dependency of incremental responses observed in isolated slabs *in vivo*, which are discussed below.

4.2.3.2. Isolated cortical slabs in vivo

To examine the issue of scaling the size of cortical neuronal networks that are necessary for generating slow sleep oscillations, without drastically changing the milieu of the neurons, a preparation has been developed [71] that has the advantages of both the

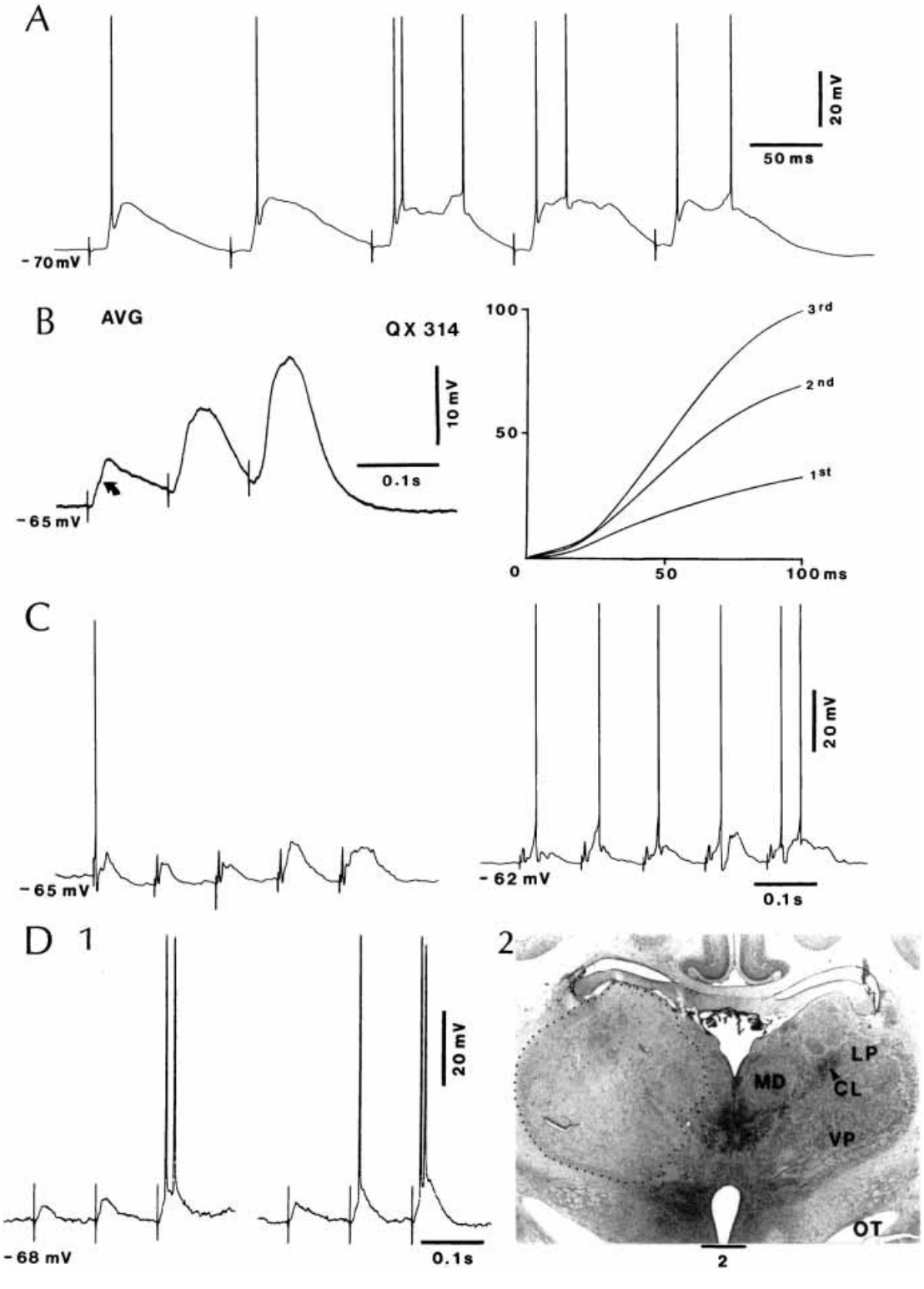
A
20 mV
50 ms
-70 mV
B
AVG
QX 314
10 mV
0.1s
-65 mV
100
50
0
50
100 ms
3rd
2nd
1st
C
-65 mV
20 mV
-62 mV
0.1s
D 1
20 mV
-68 mV
0.1s
2
LP
MD
CL
VP
OT
2

[75] Paré et al. (1998); Destexhe and Paré (1999).

in vitro and *in vivo* experimental approaches. The membrane potential of neurons in small cortical slabs (10 mm × 6 mm) was -70.4 ± 0.8 mV and the mean input resistance was 48.6 ± 4.7 MΩ (range 30–120 MΩ). These values are different from those in our database of more than 1000 neocortical neurons recorded from intact neocortical areas, which show a mean membrane potential of −62 mV and a mean input resistance of 22 MΩ. The more negative membrane potential and the large increase in input resistance of neurons recorded from isolated cortical slabs, in which the spontaneous synaptic activity is greatly reduced compared to the intact cortex, corroborate experimental and modeling studies comparing the resting properties of neocortical pyramidal neurons during periods of intense synaptic activity *in vivo* with the properties of pyramidal neurons after microperfusion with tetrodotoxin (TTX) or *in vitro* [75]. The relative percentage of neurons identified by electrophysiological criteria in the isolated slab is as follows: regular-spiking (RS) 52%, intrinsically bursting (IB) 39%, fast-rhythmic-bursting (FRB) 4%, and fast-spiking (FS) 5% [44, 71]. This is at variance with the proportions found in the intact cortex, in which IB cells constitute only ∼15%, and is especially contrasting with incidences of various cortical neuronal types during the natural state of wakefulness in chronically implanted animals in which IB neurons are less then 5%, but FS neurons reach proportions of ∼25% [5].

Some features of augmenting responses elicited in isolated cortical slabs are similar to those of corticocortical augmenting responses recorded in intact cortex, but augmenting potentials within the slab can only be evoked by using relatively high-intensity stimuli (Fig. 4.36), which suggests that they occur as a network-related phenomenon requiring a sufficient number of activated cortical neurons and axons. The aspects that are similar in slabs and intact cortex are: (*a*) the development of augmenting potentials

Fig. 4.33 (opposite) Comparison between thalamically and cortically elicited augmenting responses in cortical neurons. Cats under urethane anesthesia. *A*, augmenting responses to stimulation of the rostral intralaminar centrolateral (CL) nucleus. Regular-spiking (RS), slow-adapting neuron from area 5. The secondary depolarizing component increased and eventually triggered spikes. *B*, another cortical neuron, from area 7, with intracellular diffusion of QX-314. Averages (AVG, $n = 8$) of augmenting responses evoked by stimulation of the lateroposterior (LP) nucleus. The areas of synaptic responses are plotted on the right. Differences between the area of the first synaptic response and the areas of the following two responses were significant ($p < 0.05$) after 20 ms from the stimulus. Differences were also significant between the second and third responses after 40 ms. *C*, RS slow-adapting neuron from area 7. Repetitive (10 Hz) stimulation of the contralateral cortex elicited much slighter augmenting than depicted in *A-B* (thalamic stimulation). Note two different levels of membrane potential. *D1*, augmentation in a bursting (IB) neuron recorded at a depth of 1.5 mm in area 7, elicited by stimulation of the homotopic site in the contralateral cortex, in a thalamically lesioned cat. *D2* shows the massive kainic-acid-induced lesion of the ipsilateral thalamus (indicated by dotted line), including nuclei (CL and LP) providing major inputs to areas 5–7. Other abbreviations: MD and VP, mediodorsal and ventroposterior thalamic nuclei; OT, optic tract. Calibration in mm. From Nuñez et al. (1993).

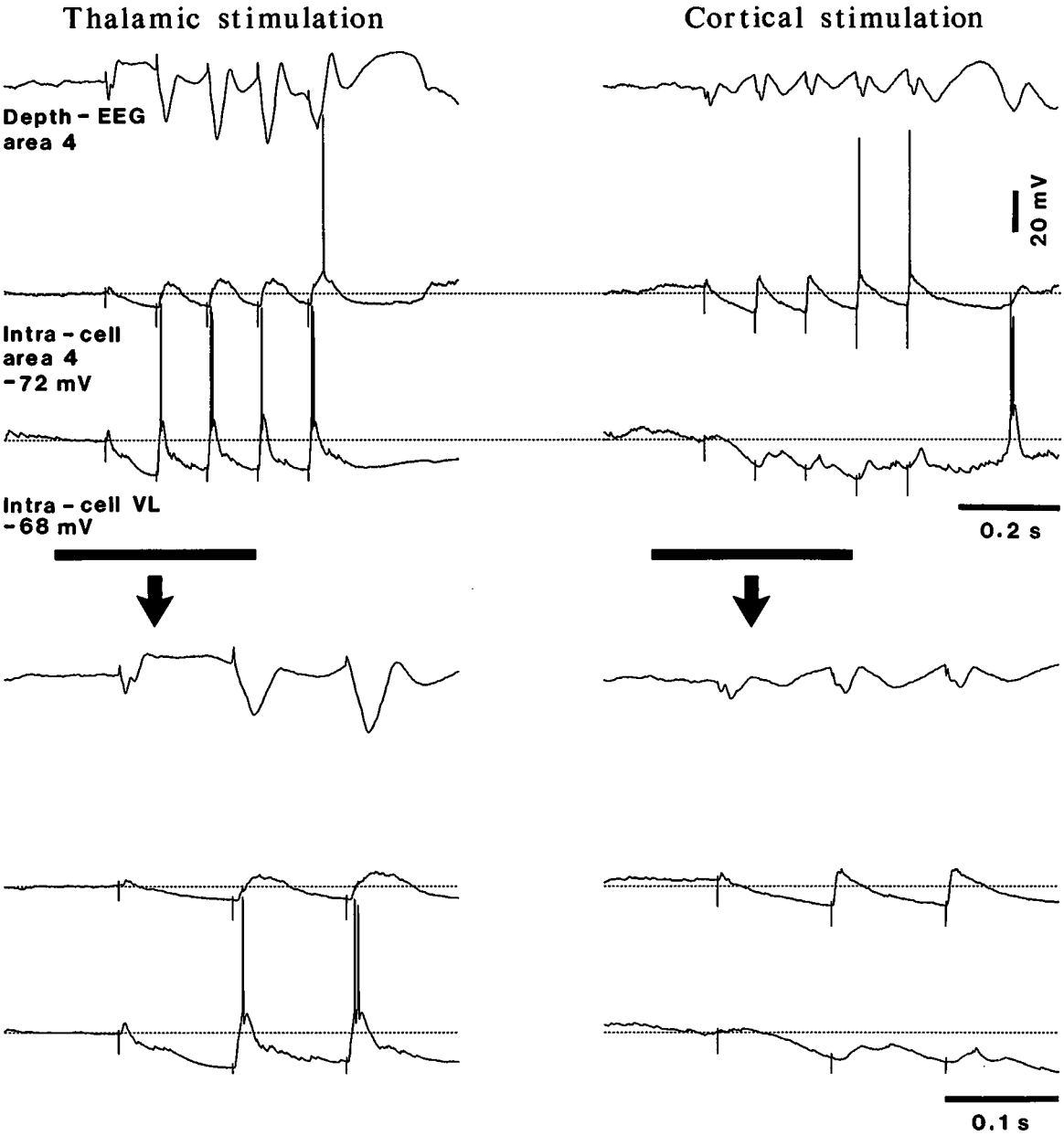

Fig. 4.34 Differences between thalamically and cortically evoked augmenting responses in the intact thalamocortico-thalamic network. Cat under barbiturate anesthesia. Dual intracellular recordings from cortical area 4 and thalamic ventrolateral (VL) nucleus, together with field potentials from the depth of area 4. Stimulation consisted of a pulse-train at 10 Hz. Left part represents responses to thalamic VL stimulation, while the right part depicts responses elicited by area 4 stimulation. First three responses are expanded below. Positivity of field (EEG) responses is up, as for intracellular recordings. Unpublished data by I. Timofeev and M. Steriade.

[76] Paré and Lang (1998).

[77] Houweling et al. (1999).

from an increased slope and amplitude of the primary EPSP (compare 0.08 mA in Fig. 4.36 with cortical stimulation in Fig. 4.34), thus lacking the secondary depolarization that characterizes thalamocortical augmenting responses (Figs. 4.27 to 4.29); this underlines the role of spike-bursts fired by TC neurons, absent in cortical slabs, in generating the secondary depolarization of augmenting responses; and (*b*) the distance dependency, that is, clear-cut augmenting responses can only be evoked at closer distances (<1 mm) between stimulating and recording electrodes, as revealed by triple intracellular recordings in the slab (Fig. 4.37). In contrast with the intact cortex, where intracortical augmenting responses occur at distances of 3–6 mm, neurons are hyperpolarized in slabs and they need high levels of excitatory inputs to reach firing threshold.

Neurons that were found to belong to different electrophysiological classes were also found to be differently involved in augmenting responses within isolated slabs. For example, FS neurons fired many more action potentials than RS neurons during the development of augmenting responses. This is illustrated in Fig. 4.38 by dual simultaneous recordings of closely located FS (cell 1) and RS (cell 2) neurons. Whereas the RS neuron had an enlarged depolarizing surface during augmenting responses but fired only single action potentials, the FS neuron increased the number of action potentials fired from one to five.

The main features of augmenting responses, such as number of spikes, amplitude of depolarization, and area of depolarization, were quantitatively analyzed in a population of neurons (3 FS, 4 IB, and 17 RS) that were recorded close to the stimulating electrode. Figure 4.39 shows that the most dramatic increase in the number of action potentials was found in FS neurons. Despite the intrinsic propensity of IB neurons to fire spike-bursts, during 10–Hz pulse-trains IB neurons fired at maximum one spike in response to the fourth and fifth stimuli. The greater increase in the amplitude of depolarization was again found in FS neurons. And, the area of depolarization from the first to the fifth stimulus increased in RS neurones by 192%, only by 120% in IB neurons, and by 520% in FS neurons.

The mechanisms that may account for augmentation in cortical slabs include, besides network operations, the intrinsic properties of neurons. Given the fact that neurons are more hyperpolarized in this experimental condition (see above) than in the intact cortex, the Ca^{2+}-dependent low-threshold current I_T could contribute to the incremental potentials. At least 15% of cortical neurons are able to generate low-threshold spike-bursts [61, 76] and modeling studies [77] also point to I_T as playing a major role in

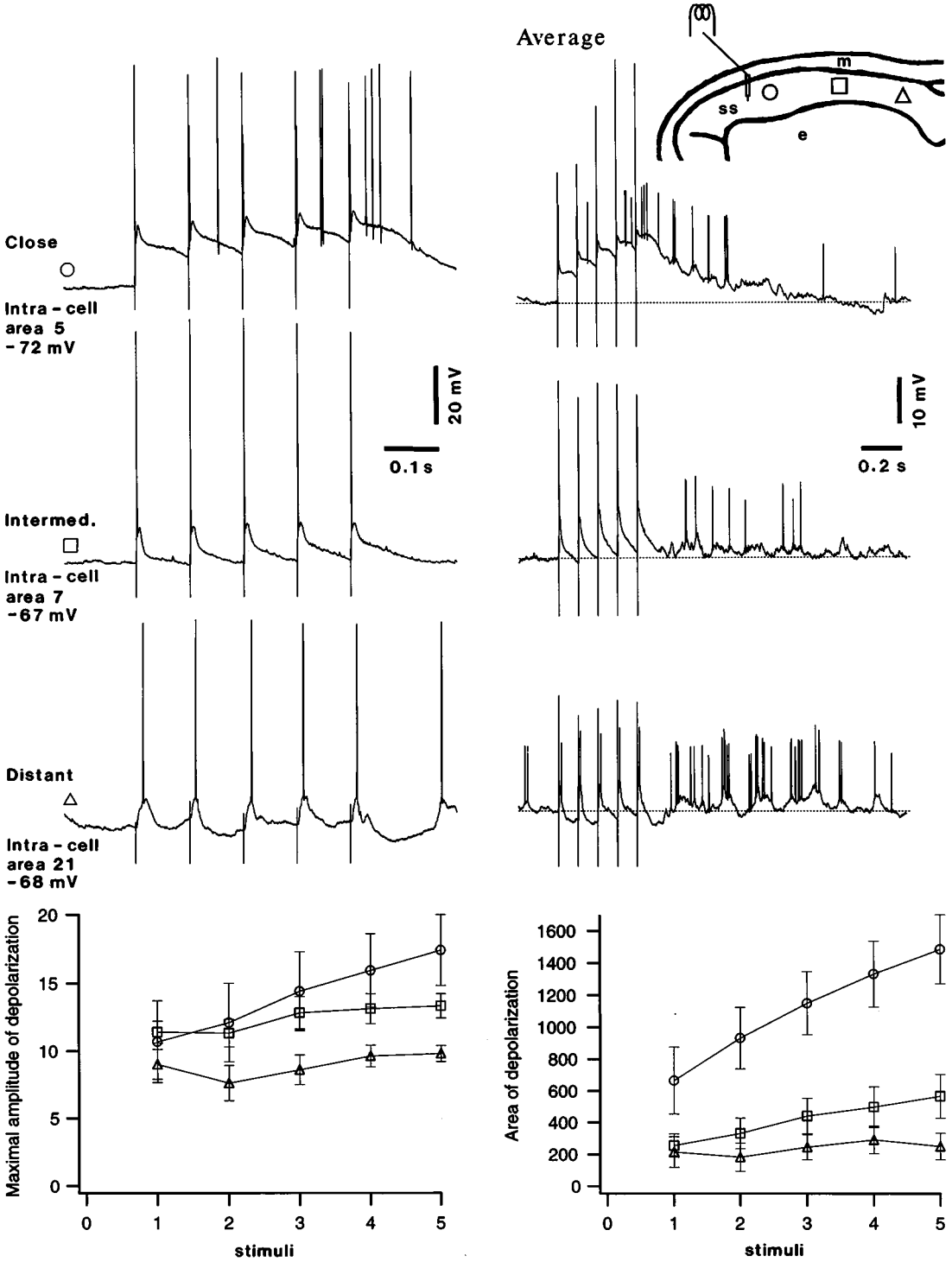
Average
m
ss
e
Close
Intra - cell
area 5
- 72 mV
20 mV
0.1 s
10 mV
0.2 s
Intermed.
Intra - cell
area 7
- 67 mV
Distant
Intra - cell
area 21
- 68 mV
Maximal amplitude of depolarization
stimuli
Area of depolarization
stimuli

intracortical augmenting. Other intrinsic currents of cortical neurons, such as $I_{Na(p)}$ and I_H, do not apparently play a role in cortically generated augmenting potentials. Realistic network models of cortical pyramidal and local-circuit inhibitory neurons [78] replicated the experimental data on augmenting responses within isolated cortical slabs obtained *in vivo* [44] and showed that the augmenting potentials in such cortical networks, associated with increased numbers of action potentials in successive responses, result from the depression of inhibitory synaptic currents.

The presence of augmenting potentials in the intact cortex [64] and, to a lesser extent, in isolated cortical slabs [44] or even in cortical slices [67; but see 79] suggests that the neocortex may be capable of producing frequency-dependent changes in synaptic responsiveness. This hypothesis and experimental data favoring it are discussed in the next section.

4.3. Plasticity of synaptic responses resulting from low-frequency oscillations

4.3.1. Generalities

Plasticity is defined as activity-dependent alteration in the strength of connections among neurons, a mechanism through which information is stored [80]. In other terms, plasticity is a short- or long-term alteration in neuronal responsiveness that depends on experience (the history of a given neuronal network), a change that may evolve from the transient strengthening of synapses to permanent formation of new connections. Such changes may occur at many different sites in the brain. Here, I will focus on experimental data in the thalamus and neocortex, placing emphasis on plasticity during sleep, when the brain is disconnected from the external world.

Firstly, a few notions and the evolution of some ideas in this field should be discussed. Perhaps the first clear hypothesis relating

[78] Houweling et al. (2002).

[79] Contreras and Llinás (2001) used high-speed optical imaging with voltage-sensitive dyes in guinea pig slices from visual and somatosensory cortices, concomitantly with intracellular recordings. In their experiments, the first and fifth responses during pulse-trains at 10 Hz produced similar optical images and depolarizing PSPs did not change in amplitude or duration with respect to the first response in cortical neurons. By contrast, spatial focusing could occur after just a few stimuli within the frequency band of gamma rhythm (40 Hz).

[80] The hypothesis that relates synaptic plasticity to different forms of memory was formulated as follows: "Activity-dependent synaptic plasticity is induced at appropriate synapses during memory formation, and is both necessary and sufficient for the information storage underlying the type of memory mediated by the brain area in which plasticity is observed" (Martin et al., 2000, p. 650). That review dealt essentially with long-term potentiation and long-term depression or depotentiation. For a review on relations between intrinsic biorhythms and plasticity during brain development, see Corner et al. (2002).

Fig. 4.35 (opposite) Cortically evoked augmenting responses display higher amplitudes in cortical neurons recorded closer to the stimulating electrode. Cat under barbiturate anesthesia. Left column illustrates responses of three neurons located in suprasylvian areas 5, 7, and 21, at close (circle), intermediate (square), and distant (triangular) sites to the stimulating electrode in area 5 (see scheme showing the location of the recorded neurons and stimulating electrode at the upper right; *m*, *ss*, and *e* are marginal, suprasylvian and ectosylvian gyri, respectively). Stimulation consisted of five pulses at 10 Hz. Right column illustrates averaged responses of five different neurons (in each of three panels), recorded at these three different sites. Of those 15 neurons, 14 were regular-spiking (RS); one neuron (that depicted in the upper part of the left column) was a fast-rhythmic-bursting (FRB) neuron. Plot at the bottom left shows the mean ± standard error (SE) of the maximal amplitude of depolarization (mV) in response to the five stimuli. Plot at the bottom right shows the mean ± SE of the depolarization area (mV × ms, above dotted line shown in the averaged responses on the left) in response to the five stimuli. The area of depolarization in response to the fifth stimulus in close and intermediate distances was calculated for 100 ms. Unpublished data by I. Timofeev and M. Steriade.

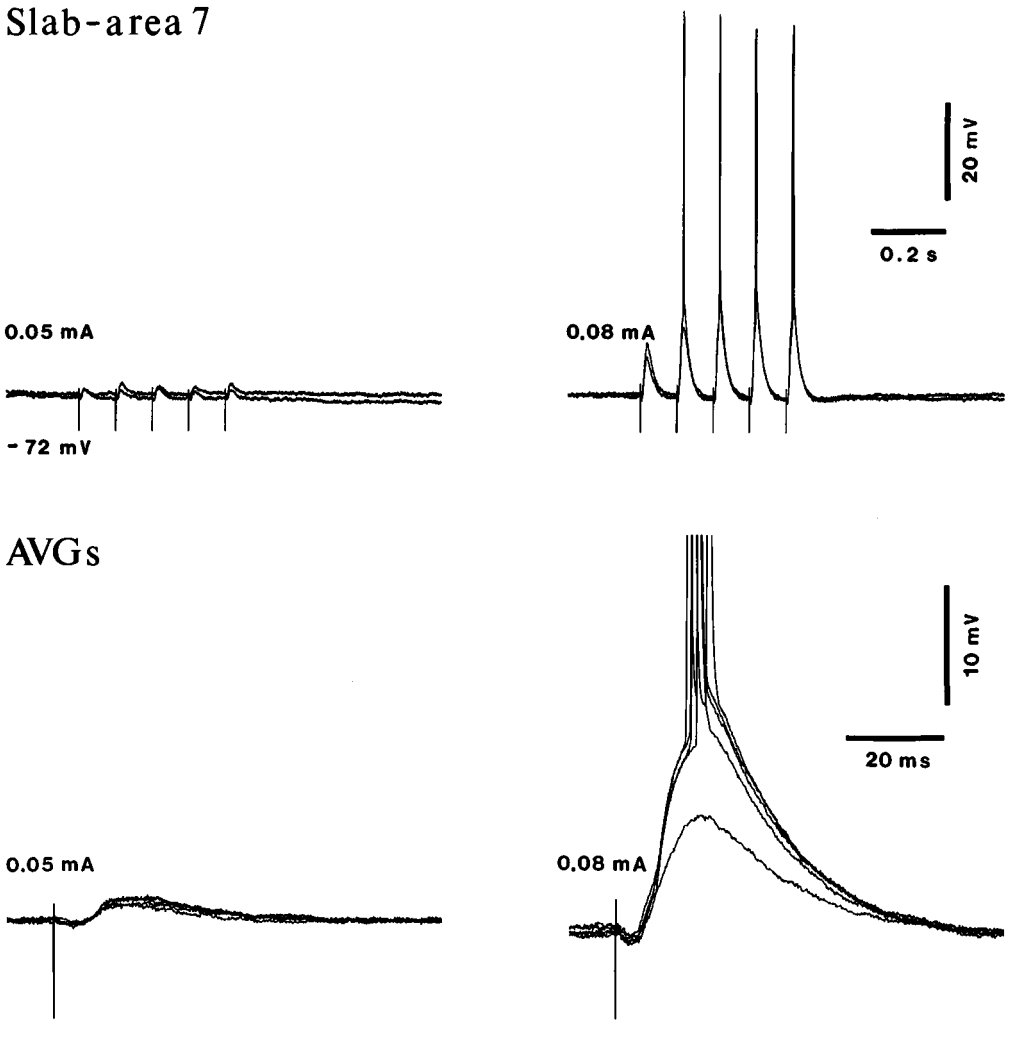

Fig. 4.36 Augmenting responses in an isolated neocortical slab from area 7 in cat under ketamine-xylazine anesthesia. Responses to two intensities (0.05 and 0.08 mA) of pulse-trains at 10 Hz are shown. Upper panel: with the lowest intensity elicited EPSPs, the responses to successive pulses had similar shapes and amplitudes; with a slight increase in stimulation intensity, there was an augmented response after the first EPSP. Bottom panel shows the superimposition of the initial part of averaged responses (AVGs). From Timofeev et al. (2002b).

Fig. 4.37 (following) Triple simultaneous intracellular recordings in isolated slab from cat area 7 (ketamine-xylazine anesthesia) demonstrate that clear-cut augmenting responses occur in foci located close to the stimulated site. Three regular-spiking neurons (cells 1, 2, and 3) were recorded together with field potentials (see scheme of recording and stimulating electrodes in the center). Augmenting responses in the vicinity of the stimulating electrode were only elicited at the maximal intensity used (0.75 mA). Upper panels show individual (left) and averaged (right) responses to pulse-trains at 10 Hz. Bottom panels (individual and averaged responses) show superimposed first and fifth responses in cells 1 to 3, from top to bottom, respectively. From Timofeev et al. (2002b).

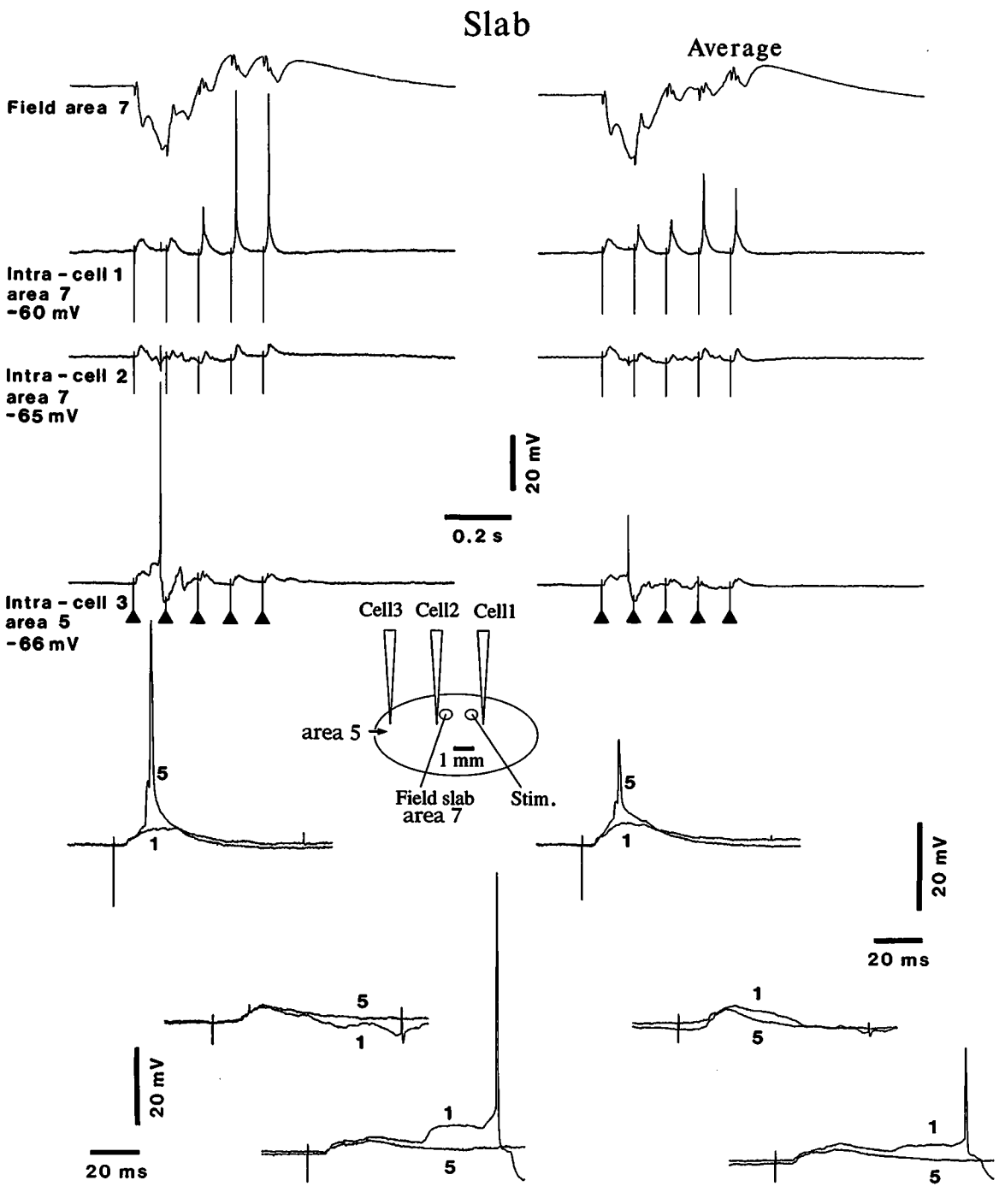
Slab
Average
Field area 7
Intra - cell 1
area 7
-60 mV
Intra - cell 2
area 7
-65 mV
20 mV
0.2 s
Intra - cell 3
area 5
-66 mV
Cell3 Cell2 Cell1
area 5
1 mm
Field slab
area 7
Stim.
5
1
20 mV
20 ms
20 mV
20 ms

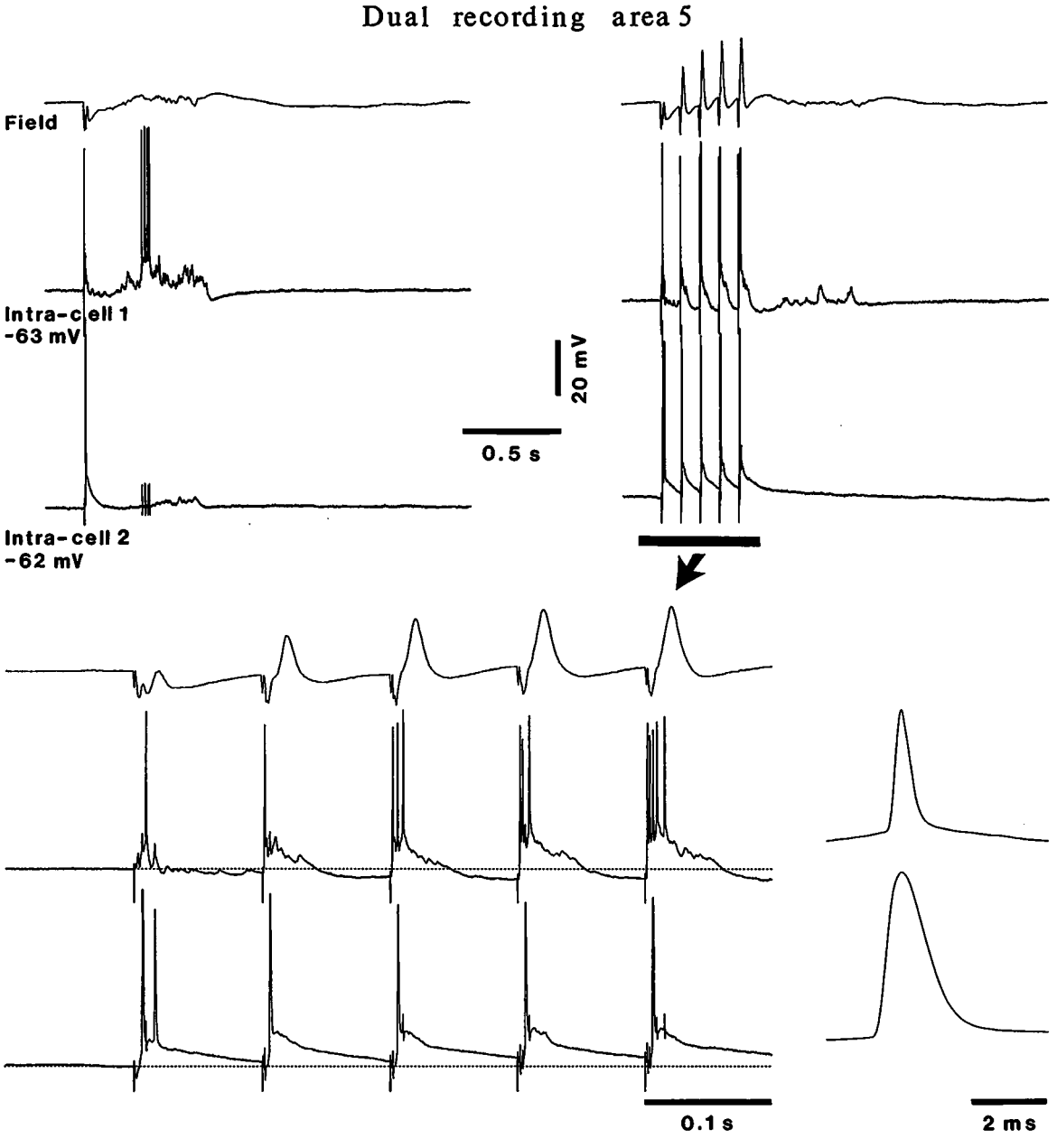

Fig. 4.38 Differential propensities to augmentation of fast-spiking (FS) and regular-spiking (RS) neocortical neurons in an isolated slab from area 5 in cat under ketamine-xylazine anesthesia. Simultaneous recording of field potentials and dual intracellular recordings from FS (cell 1) and RS (cell 2) neurons, separated by less than 0.5 mm. Upper left, responses to a single stimulus (small deflections in cell 2 are due to capacitive coupling from action potentials in cell 1). Upper right, responses evoked by a pulse-train at 10 Hz. Responses are enlarged at bottom left (arrow). Bottom right, averaged ($n = 20$) action potentials of FS (top) and RS (bottom) neurons. From Timofeev et al. (2002b).

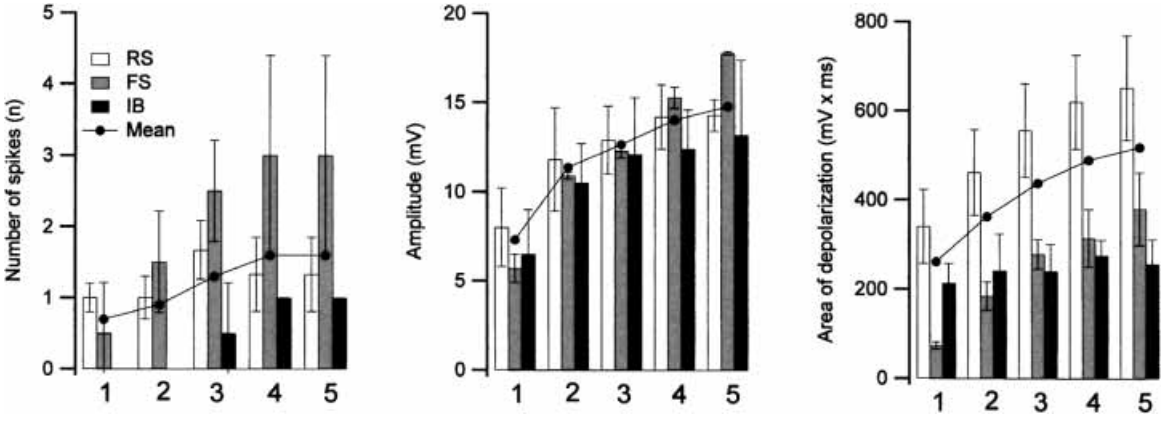

Fig. 4.39 Number of spikes, amplitude, and area of depolarization in a population ($n = 24$) of electrophysiologically identified neurons recorded from isolated slabs in areas 5 and 7 of cat under ketamine-xylazine anesthesia. Numbers at the bottom of each histogram correspond to the number of stimuli within a pulse-train at 10 Hz. Empty bars represent averaged values for RS neurons, gray bars represent FS neurons, black bars represent IB neurons, and black circles connected with a line indicate the total mean of data from all neurons. Error bars represent standard error. From Timofeev et al. (2002b).

[81] Moruzzi (1966). Different citations in the main text are from p. 353–355 and p. 375 of Moruzzi's chapter.

[82] Evarts (1964).

sleep with plastic activity in the cerebrum, and more specifically in certain types of neurons, belongs to Moruzzi [81]. This hypothesis, briefly mentioned in Chapter 3 (section *3.2.4.2*) in relation to possible functions of sleep, expressed the view that "we sleep merely (or mainly) in order to permit recovery of those synapses which are able to learn, and of those neurons which are mainly concerned with their activity". Then sleep would serve for "the recuperation of the learned synapses", since "a total arrest of the bombardment of impulses is more likely to contribute to the slow process of restoration". The entire chapter by Moruzzi is centered on the possibility that active "inhibition may be causally related to the slow processes of recovery occurring during sleep", although he recognized that data available at that time demonstrated the role of inhibitory processes in the spinal cord during the REM stage of sleep, but not in the cerebral cortex or other higher structures in the brain (see such data on inhibitory processes in neocortex during natural SWS and brain-active states, recorded extra- and intracellularly, in more recent studies discussed in section ***4.1.2***). Along this line of thinking, Moruzzi referred to Evarts' [82] hypothesis that during sleep the cortical inhibitory interneurons are depressed and suggested that "the depression of the inhibitory interneurons would ... be specifically related to the slow process of recovery from plastic activity". It is now known from intracellular recordings in naturally awake and sleeping animals that electrophysiologically identified local-circuit inhibitory (conventional fast-spiking) cortical neurons

fire even faster than pyramidal neurons during all stages of sleep [5] and that recurrent as well as feedforward inhibitory processes in pyramidal neurons are longer during slow-wave sleep than during waking (see above Figs. 4.12 and 4.14). To sum up, Moruzzi's hypothesis postulated that sleep is involved in the slow recovery of learned synapses.

There are at least two aspects related to the issue of plasticity/learning and sleep.

One of them refers to the possibility that some forms of acquiring information occur during sleep. Although some have attempted to promote the idea that learning is possible during sleep, most investigators have failed to demonstrate the transfer of information from sleep to subsequent waking and the general conclusion remains that the recall of declarative memories [83] is only possible when the acquisition of information during "sleep" took place during epochs when signals aroused the brain [84]. Indeed, the long periods of hyperpolarization associated with increased membrane conductance in TC neurons throughout slow-wave sleep [24], and especially during sequences of spindle waves [21], would prevent the transfer of incoming signals en route to the cerebral cortex, whereas brain arousal induced by setting into action generalized activating brainstem reticular systems after a learning trial succeeds in enhancing the retention of memory [85]. The molecular correlates of the impairment of memory acquisition during sleep have been studied [86] by examining some markers whose induction has been linked to memory acquisition: phosphorylated CRE-binding protein (*P-CREB*), *Arc*, and *BDNF* [87]. The results of this study [86] showed that the expression of *P-CREB*, *Arc*, and *BDNF* in the cerebral cortex of rats is high during waking and low during sleep, and the expression of these plasticity-related genes during waking depends on the norepinephrinergic systems as, after lesions of locus coeruleus, the expression of *P-CREB* during waking is reduced to reach the level seen during sleep [88]. The general conclusion of these data is that acquisition of memory is blocked during sleep, and in particular during slow-wave sleep.

The other aspect related to the issue of plasticity/learning and sleep concerns the consolidation of memory, considered as the process by which memories are resistant to amnestic factors [89] and usually defined as an avalanche of neuronal and molecular processes that culminates with enduring forms of synaptic modifications. Here, different views have been expressed as to whether slow-wave sleep (SWS) or REM sleep plays the crucial role in consolidating memory traces. Recent studies point to both these sleep stages in the sense that early SWS stages favor the retention of

[83] Declarative memory refers to information that can be brought to conscious recollection with verbal content, whereas non-declarative memory is unconscious and reflected in behavioral changes.

[84] Koukkou and Lehmann (1968).

[85] Denti et al. (1970).

[86] Cirelli and Tononi (2000). Although this study showed that the induction of the three plasticity genes mainly depends on the activity of the norepinephrinergic system (see also [88]), the role of acetylcholine in playing a similar gating role was also taken into consideration. By contrast, the role of the serotonergic system on the expression of these genes was denied (Tononi et al., 2000).

[87] Reviewed in Silva et al. (1998) and McAllister et al. (1999).

[88] Cirelli et al. (1996).

[89] Squire (1987).

declarative memories (see [83]), whereas late night sleep when episodes of REM sleep prevail, favors the retention of non-declarative memories [90]. Also a combined role of both sleep stages was invoked, with overnight improvement proportional to the amount of SWS during the early nocturnal sleep and to the amount of REM sleep in the last part of the night sleep [91].

An analysis of data on molecular changes that may be involved in the first consolidation of long-term memories led to the conclusion that some of these processes occur at higher rates during SWS than during waking and REM sleep [92]. At the neuronal level, the role of SWS in consolidation of spatial memories was shown by increases of firing, during subsequent epochs of SWS, in those hippocampal cells whose activity had increased during prior waking [93] and by increased synchronization, during SWS, of CA1 hippocampal neurons that were coactive during spatial tasks in waking [94], thus suggesting reactivation of neuronal assemblies in SWS (see also Chapter 3, section *3.2.4.2*). In the process of reactivation during SWS of traces of hippocampal neuronal activity patterns from preceding behavior, emphasis was placed on the strong excitatory drive brought about by the neuronal population generating sharp waves, associated with very high-frequency oscillations (200 Hz), called ripples [95]. Ripples are also present during the depolarizing phase of the slow sleep oscillation in neocortical neurons [96] and they lead to a form of neuronal plasticity leading to paroxysmal discharges [97]. As to the neuromodulators that control memory consolidation, experimental and clinical evidence led to the hypothesis that, while high levels of acetylcholine (ACh) are appropriate for encoding new information in the hippocampus, low levels of ACh, as during SWS, allow a stronger spread of activity within the hippocampus and from the hippocampus to the entorhinal cortex, facilitating the consolidation of memory traces [98]. Brainstem-induced arousal also induces short-term potentiation of neuronal responsiveness in thalamocortical systems (see below, [102]).

Some of the data and mechanisms that implicate SWS in consolidation of memory traces are discussed in Chapter 3 (section *3.2.4.2*). Additional information was recently reported in a study of the developing visual cortex, during the critical period in which occluding the vision of one eye produces remodeling of the visual cortex and its inputs. Experiments on cats near the peak of the critical period for ocular dominance plasticity, using microelectrode recordings and optical imaging, showed that the effects of monocular deprivation on visual cortex responses were greatly enhanced by a 6-h sleep period in the dark [99]. The enhancement of

[90] Plihal and Born (1997). Karni et al. (1994) reported dependency of visual discrimination improvement on REM sleep in humans; disruption of SWS did not affect perceptual improvement.

[91] Stickgold et al. (2000).

[92] Tononi and Cirelli (2001).

[93] Pavlides and Winson (1989).

[94] Wilson and McNaughton (1994).

[95] Buzsáki (1989); Siapas and Wilson (1998); Kudrimoti et al. (1999); Sutherland and McNaughton (2000).

[96] Grenier et al. (2001).

[97] Grenier et al. (2002); see Chapter 5.

[98] Masselmo (1999).

[99] Frank et al. (2001).

plasticity in the visual cortex depended specifically on SWS, as REM sleep amounts were negatively correlated with ocular dominance plasticity. The authors [99] ascribed one of the mechanisms underlying SWS-induced plasticity to the low-frequency brain oscillatory activity during SWS, which promotes changes in synaptic responses in corticothalamic neuronal networks [2, 100]. Indeed, if an effective way to consolidate learned information is repetition, all major types of SWS rhythms can be implicated in this process on an *a priori* ground because of prolonged, rhythmic spike-bursts and spike-trains of thalamic and neocortical neurons during these oscillations, which could produce changes in synaptic responsiveness at their targets. This topic is dealt with in the following two sections, which provide experimental data using intracellular recordings from connected neurons in thalamocorticothalamic loops.

4.3.2. Thalamus

It is conventionally thought that the cerebral cortex is mainly endowed with plastic properties, but thalamic neurons also display reorganization changes in their activities after deafferentation [101], and prolonged enhancement of synaptic responsiveness in limbic (anterior) thalamic neurons was observed as an effect of brainstem cholinergic stimulation [102], which may be related to the hypothesis that acetylcholine is involved in the consolidation of memory traces in the hippocampal-entorhinal network [98].

In this section, I focus on the role of low-frequency oscillations in thalamic plasticity. As much of the data belonging to this issue, concerning the cellular mechanisms underlying the two forms (high-threshold, HT; and low-threshold, LT) of intrathalamic augmenting responses associated with short-term plasticity, are illustrated in a previous section (*4.2.1.1*), I will only briefly summarize the plastic changes occurring *during* augmentation and mainly refer to the *self-sustained* changes that follow incremental responses within the thalamus.

Thalamic plasticity occurs during augmenting responses and consists of progressive diminution of IPSPs (see Fig. 4.17) and increased number of action potentials in HT spike-bursts elicited by thalamic volleys [41]. The depolarization area increases during successive HT-type augmenting responses. In responses elicited by pulse-trains at 10 Hz, the increase in depolarization area is about 500% from the first to the fifth response in the first train and 1270% during the same evolution from the first to the last response in the second train (see Fig. 10 in [41]).

The LT-type augmenting responses, resulting from progressive hyperpolarizations and rebound spike-bursts, are virtually

[100] Steriade (1999b).

[101] Jones (2000).

[102] Paré and Steriade (1990); Paré et al. (1990). In those experiments, conditioning electrical stimulation of the mesopontine laterodorsal tegmental (LDT) cholinergic nucleus, in reserpine-treated cats (to avoid the effects resulting from possible coactivation of monoaminergic axons), induced a ~3-fold enhancement in synaptic responsiveness of anterior thalamic neurons (tested by mammillary nucleus volleys), reaching its peak 40–50 s after the LDT pulse-train and lasting up to 4 min. The cholinergic nature of this effect was tested by application of the muscarinic blocker scopolamine that blocked the long-lasting potentiation. These data suggested that the brainstem cholinergic projections are implicated in the regulation of the information flow along the mammillo-thalamic axis, by modifying the strength of the functional relationship between the hippocampal formation and the cortical storage sites (see Squire et al., 1984).

unchanged if pulse-trains are repeated at low frequencies (~0.1–0.2 Hz), but the amplitude of hyperpolarizations decreases dramatically, and their consequences (rebound bursts) diminish, if pulse-trains are delivered at a frequency of 1 Hz or higher (Fig. 4.40). Importantly, the effects of LT augmenting responses outlast the stimulation period. Thus, control responses to single thalamic stimuli, before rhythmic pulse-trains at 10 Hz are delivered, consist of high-amplitude, biphasic ($GABA_{A-B}$) IPSPs leading to powerful rebound spike-bursts, whereas after a period of rhythmic pulse-trains at 10 Hz, the hyperpolarizations are decreased and rebound bursts are abolished or reduced up to 10 s before the recovery of control responses is observed (Fig. 4.41). These effects at the thalamic level occur even when the cerebral cortex displays self-sustained seizures, which are simultaneous with the period of decreased thalamic responsiveness. Such contrasting results in thalamus and cortex, that outlast the period of stimulation in the frequency range of sleep spindles, emphasize that the cortex is capable of generating self-sustained activity, even at a paroxysmal level, despite the decreased synaptic responsiveness at the thalamic gate (see also Chapter 5).

4.3.3. Neocortex and corticothalamic neuronal loops

Even if the above-described plastic phenomena in thalamus survive decortication [41] and are, thus, ascribable to intrathalamic events, the full development of mechanisms leading to storage of information and/or pathological processes, such as seizures, requires preserved connectivity between cortex and thalamus. Self-sustained oscillations occur in cortical neurons at the same frequency (10 Hz) as that used to evoke augmenting responses, mimicking sleep spindles, despite the fact that, simultaneously, TC neurons remain hyperpolarized because of the pressure exerted by GABAergic RE neurons (Fig. 4.42*A*). Repeated spike-bursts evoked by volleys applied to corticothalamic pathways as well as those occurring during spontaneous oscillations may lead to self-sustained activity patterns, resembling those evoked in the late stages of stimulation (Fig. 4.42*B*). Such changes are due to resonant activities in closed loops, as in "memory" processes [100].

We investigated the enhancement of neuronal responses that outlast pulse-trains at 10 Hz in neocortex [44]. Single cortical stimuli applied close to the intracellularly recorded neuron usually elicit monophasic IPSPs that rapidly decrease in amplitude during pulse-trains at 10 Hz. A repetition of pulse-trains every 1 to 3 s eventually transforms these IPSPs into depolarizing responses. In ~30% of studied neurons, we were able not only to obtain the reversal of initial IPSPs into depolarizing responses, but also to maintain

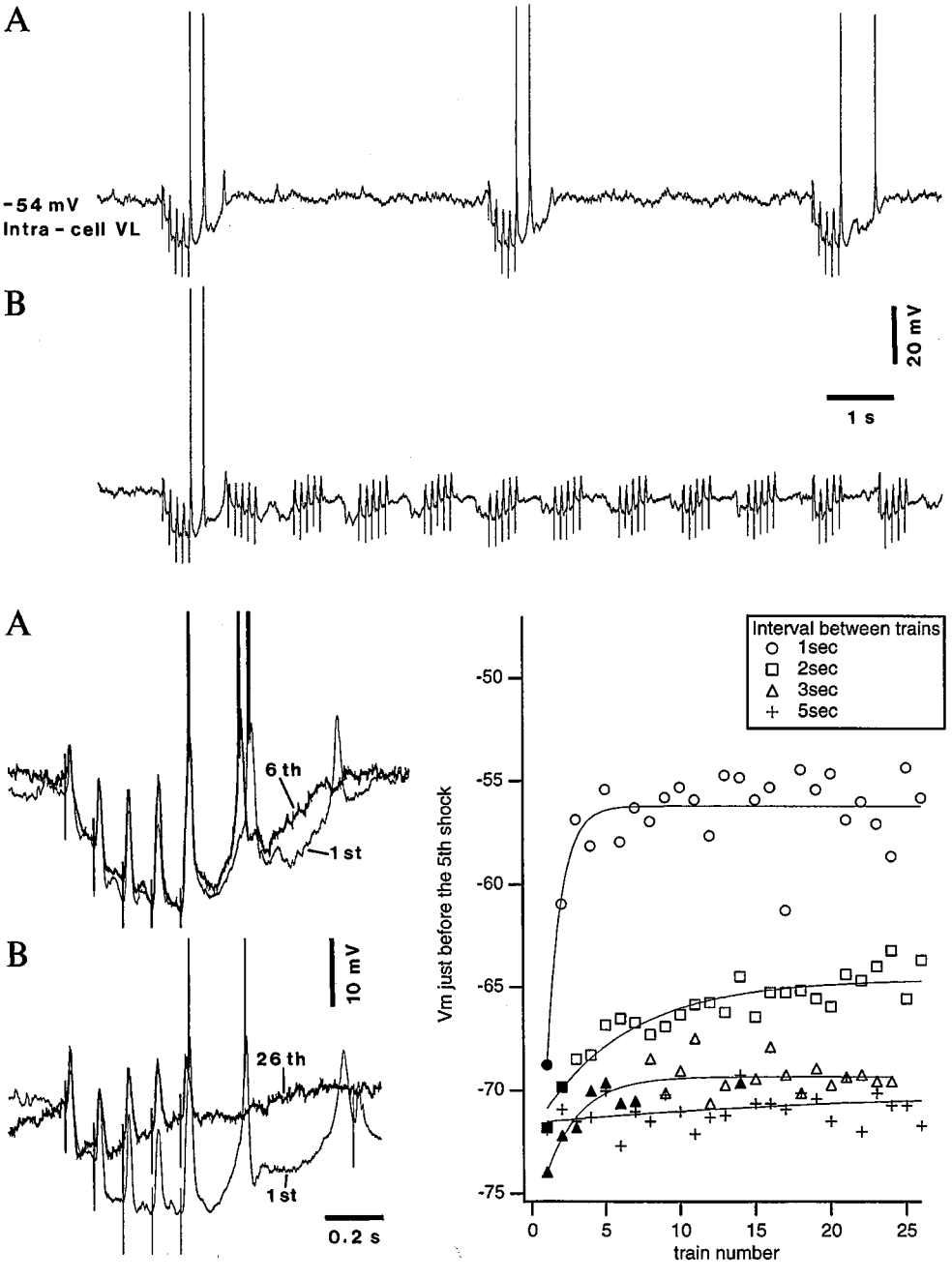

Fig. 4.40 Decreased IPSPs and, consequently, decreased low-threshold spikes (LTSs) and postinhibitory rebound spike-bursts in TC neurons during successive rhythmic pulse-trains at 10 Hz, separated by different time intervals. Intracellular recording from ventrolateral (VL) neuron in cat under barbiturate anesthesia. Top panel depicts responses to pulse-trains at 10 Hz, separated by 5 s (*A*) and 1 s (*B*). At bottom left, superimposition of responses to the first pulse-train and the pulse-train 25 s later (the sixth train in the case of a 5-s period between pulse-trains, and the 26th train in the case of a 1-s period between trains). The pulse-trains repeated with a period of 1 s clearly led to the decrease in the evoked IPSPs, which in turn led to the disappearance of rebound LTSs. This decrease in evoked IPSPs is plotted at the bottom right. The evoked hyperpolarization is represented by the value of membrane potential (V_m) 5 ms before the fifth stimulus in a train, and these values were taken from stimulations in which pulse-trains were given every 1, 2, 3, or 5 s. Filled symbols as well as + represent trains that led to a rebound LTS. From Grenier et al. (2002).

for minutes these depolarizing responses evoked by single stimuli. Figure 4.43 illustrates an example of responses displayed by a pyramidal regular-spiking neuron that fired thin spikes in which a single stimulus elicited an early IPSP. Pulse-trains at 10 Hz resulted in a diminution, up to suppression, of IPSPs (see second and third traces in the right column). Repeated 10-Hz cortical stimulation abolished the early IPSP and replaced it by an early depolarization. Thereafter, single stimuli evoked exclusively depolarizing responses. This enhancement remained unchanged for about 15 min (see bottom plot in Fig. 4.43) and suggests that electrical stimulation with a frequency range within that of spindles may induce long-lasting changes in neuronal responsiveness. Similar enhancement could be obtained after spontaneously occurring spindle sequences [44].

The increased corticocortical response seen in the last trace of the right column depicted in Fig. 4.43, following the two traces that illustrate examples of responses to pulse-trains at 10 Hz, has a paroxysmal aspect. This peculiar feature does not reflect an "epileptic" state of the neuron under investigation, as demonstrated by the response obtained before delivering pulse-trains at 10 Hz (see control response in the bottom trace). Rather, it suggests that this form of plasticity is so powerful that it reaches a level close to that underlying paroxysmal activity. Further evidence for such an enhancement is depicted in Fig. 4.44 in which the potentiation of neuronal responsiveness, which results at the end of four pulse-trains at 10 Hz, takes the pattern of a paroxysmal response. The latency and duration of the spike shunting (lasting for 20–50 ms and seen in the expanded traces at the bottom right in Fig. 4.44) is consistent with the latency and duration of the early IPSP observed in the upper right panel *A2*.

The changes in responsiveness of cortical neurons, which lead to self-sustained oscillations sometimes of the paroxysmal type, are initiated during rhythmic stimulation with pulse-trains at 10 Hz. Such changes consist of the appearance of "spontaneous" depolarizing events, occurring between pulse-trains and having the same frequency as that used in these pulse-trains (see asterisk in the expanded panel, bottom right, in Fig. 4.45).

That plastic changes in cortex are independent of thalamic events is shown not only by dual intracellular recordings demonstrating progressive depolarization, enhanced responsiveness, and self-sustained oscillations of neocortical neurons, concomitant with the hyperpolarization of TC neurons (see Figs. 4.29–4.30, 4.42, and 4.45), but also by evidence of plasticity in isolated cortical slabs *in vivo*. The repetition, every second, of pulse-trains with five stimuli

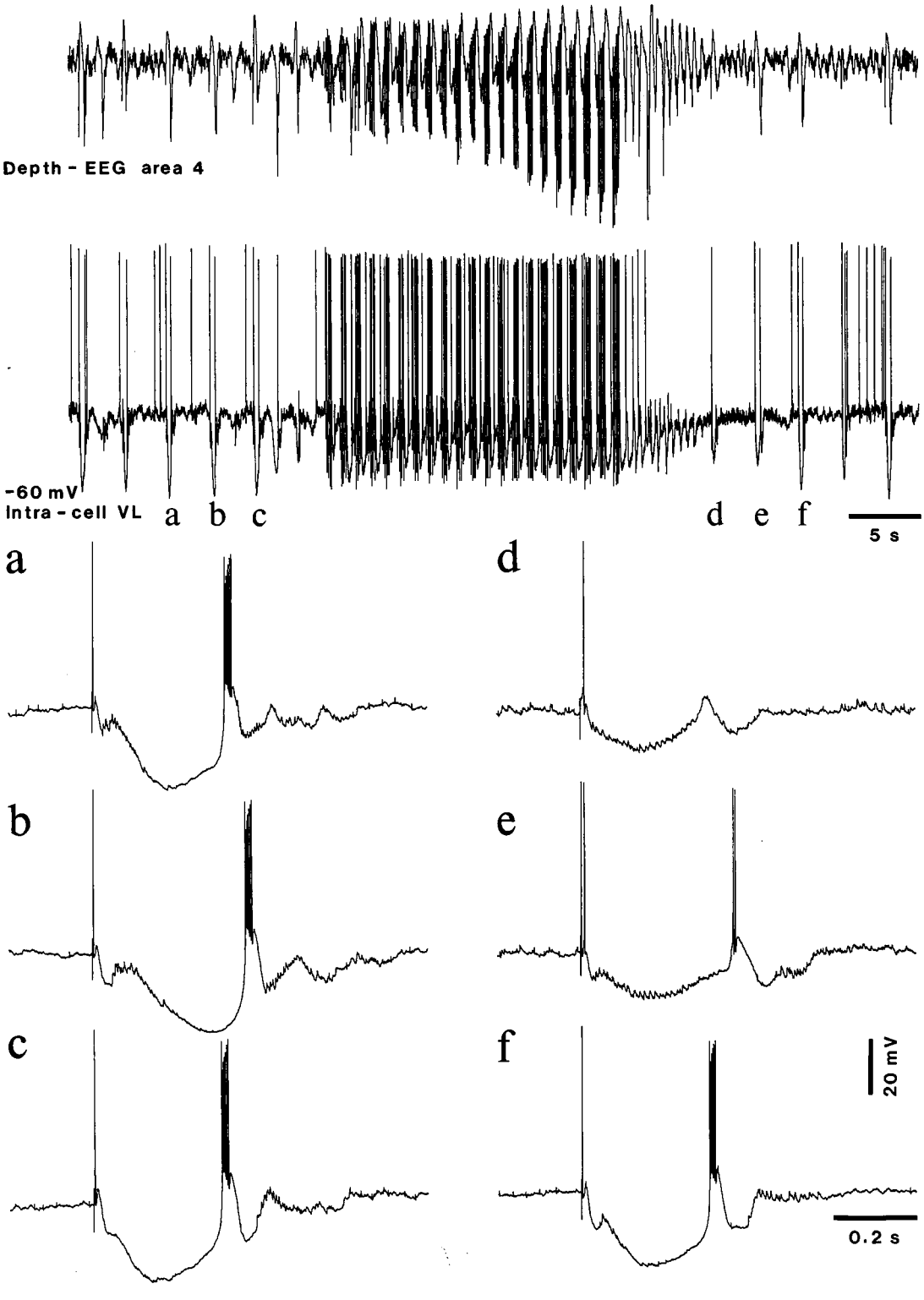
Depth - EEG area 4
-60 mV
Intra - cell VL
a b c
d e f
5 s
a
b
c
d
e
f
20 mV
0.2 s

[103] Baranyi et al. (1991).

at 10 Hz changes the response pattern within the slab. Dual intracellular recording from pairs of fast-spiking (FS, presumed local-circuit inhibitory) and regular-spiking (RS) neurons showed that, in response to the first stimulus in each pulse-train, the FS neuron dramatically increased firing (from 1 to 14 spikes), whereas the RS neuron revealed only a small increase in firing (from one to two spikes) but displayed a significant increase in the area of depolarization in response to the first stimulus in a pulse-train (Fig. 4.46). The dependency of the area of depolarization of the RS neuron on the number of action potentials in the FS neuron was exponential, which suggests that an enhancement in the depolarization surface of RS neuron was partially mediated by a change in the Cl^- reversal potential.

The plastic changes in neuronal responsiveness during augmenting responses elicited in isolated cortical slabs is mediated by synaptic [78] and intrinsic factors. To test the role of intrinsic factors in the generation of long-lasting enhancement of excitability, the paradigm of intracellular conditioning [103] or a modification of it can be used. Association between electrical stimuli within the slab that elicit subthreshold synaptic depolarizations with direct depolarizations induced by current pulses, at appropriate time intervals, can lead to suprathreshold synaptic depolarizations after a variable number of conditioning-testing stimuli (Fig. 4.47). Low-intensity, extracellular electrical stimulation within cortical slabs elicits active periods (200–300 ms) that are not associated with action potentials. In these neurons, intracellular depolarizing current pulses were applied, which lasted for the duration of stimulus-evoked active periods (200–300 ms), and elicited spikes, whose onset was delayed by 20–30 ms from the electrical stimulus applied to the slab. The association of extracellular electrical stimuli with depolarizing current steps induced, after a repetition of 20–50 such combined stimuli, a state in which extracellular stimuli, with the same intensity as when they were subthreshold, elicited active periods

Fig. 4.41 (opposite) Diminished IPSPs and rebound LTSs in TC neurons outlast rhythmic pulse-trains at 10 Hz, repeated every 1 s, whereas the cortex simultaneously displays a self-sustained seizure. Cat under barbiturate anesthesia. Intracellular recording of TC neuron activity from the VL nucleus, together with depth-EEG from cortical area 4. Top panel shows responses to a period with pulse-trains applied to the VL thalamus, delivered every second, preceded and followed by single VL stimuli delivered every 3 s. Responses to single stimuli, marked by letters (*a-c* before pulse-trains, and *d-f* after pulse-trains), are expanded below. Before pulse-trains at 10 Hz, single thalamic stimuli evoked a biphasic hyperpolarization ($GABA_{A\text{-}B}$ IPSP), sufficient to elicit a rebound spike-burst with six to seven action potentials. After the pulse-trains at 10 Hz, the evoked hyperpolarizations were smaller than the control ones, for up to 10 s, evoking smaller rebound bursts with no fast action potentials or fewer spikes than in the control period. The evoked responses recovered progressively to control values as the delay between conditioning pulse-trains and single testing stimuli increased. Unpublished experiment by F. Grenier, I. Timofeev, and M. Steriade.

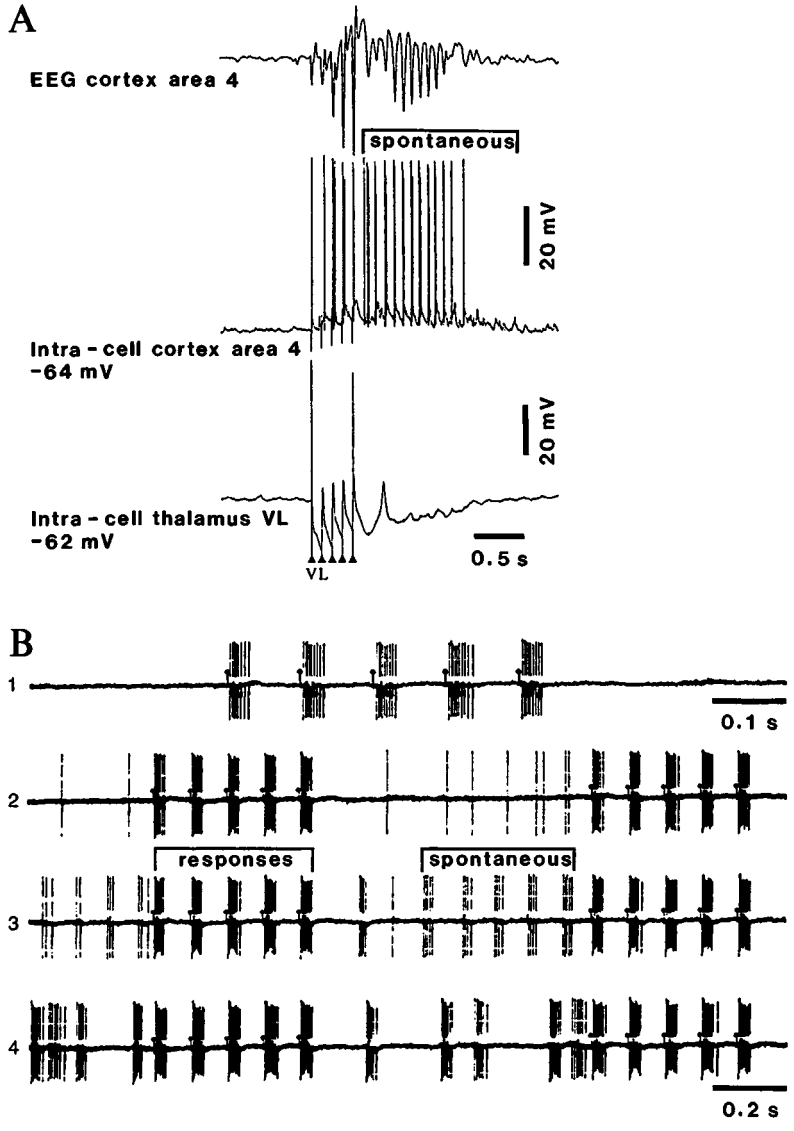

Fig. 4.42 Self-sustained oscillations in cortex and corticothalamic loops after pulse-trains at 10 Hz, mimicking sleep spindles. *A*, cat under barbiturate anesthesia. Dual intracellular recordings from a TC neuron in the ventrolateral (VL) nucleus and cortical area 4 neuron, together with depth-EEG from area 4. Stimulation (five stimuli at 10 Hz) applied to the VL nucleus. Note persistent, spindle-like (10 Hz) oscillations in cortex after 10-Hz stimulation, in spite of persistent hyperpolarization in the TC neuron, likely arising in GABAergic thalamic RE neurons. *B*, brainstem-transected cat. Cortically evoked spike-bursts in a thalamic VL neuron (*1*). Motor cortex stimulation was applied with pulse-trains at 10 Hz delivered every 1.3 s. In *1*, the pattern of cortically evoked responses at the onset of rhythmic pulse-trains (faster speed than in *2* to *4*) is shown. *2*–*4*, responses at later stages of stimulation are shown. Stimuli are marked by dots. In *2*–*4*, stimuli and evoked spike-bursts are aligned. Note the progressive appearance of spontaneous spike-bursts resembling the evoked ones, as a form of "memory" in the corticothalamic circuit. Modified from Steriade et al. (1998d, *A*) and Steriade (1991, *B*).

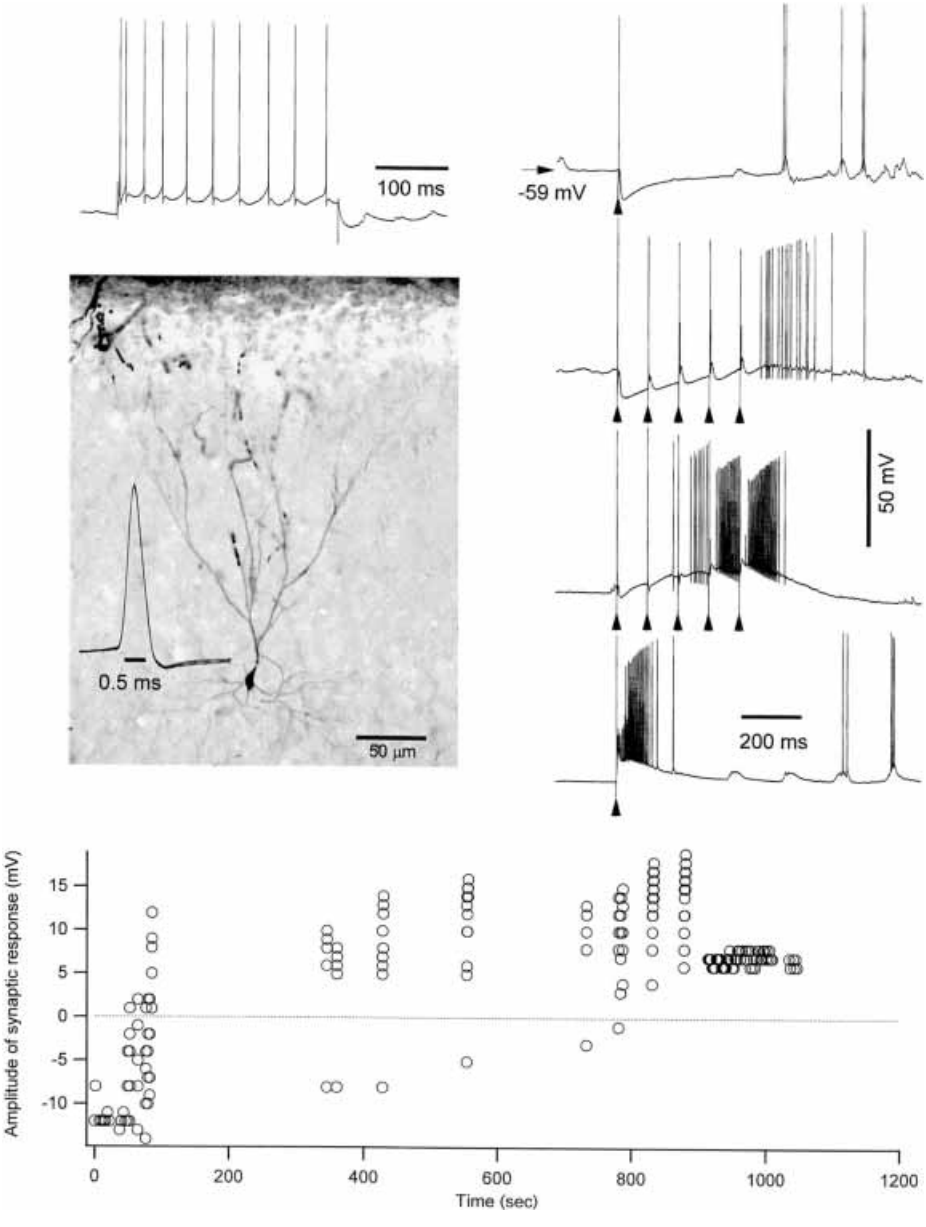

Fig. 4.43 Cortical augmenting responses lead to long-lasting enhancement of depolarizing responses in intact cortex. Cat under barbiturate anesthesia. Intracellular recording from an electrophysiologically (left upper panel) and a morphologically (left middle panel) identified area 7 pyramidal regular-spiking neuron with thin spike (see expanded action potential close to the stained neuron). Right panel shows (from top to bottom): control response to a single stimulus to the cortex, early responses to pulse-trains at 10 Hz, responses to pulse-train with the same parameters applied 12 min later, and responses to a single stimulus applied 16 min after the onset of rhythmic stimulation. Below, plot showing the amplitude of stimulus-evoked responses at 20 ms after stimulus onset. Note that initially hyperpolarizing responses became depolarizing after pulse-trains at 10 Hz. From Timofeev et al. (2002b). See Plate section for color version of this figure.

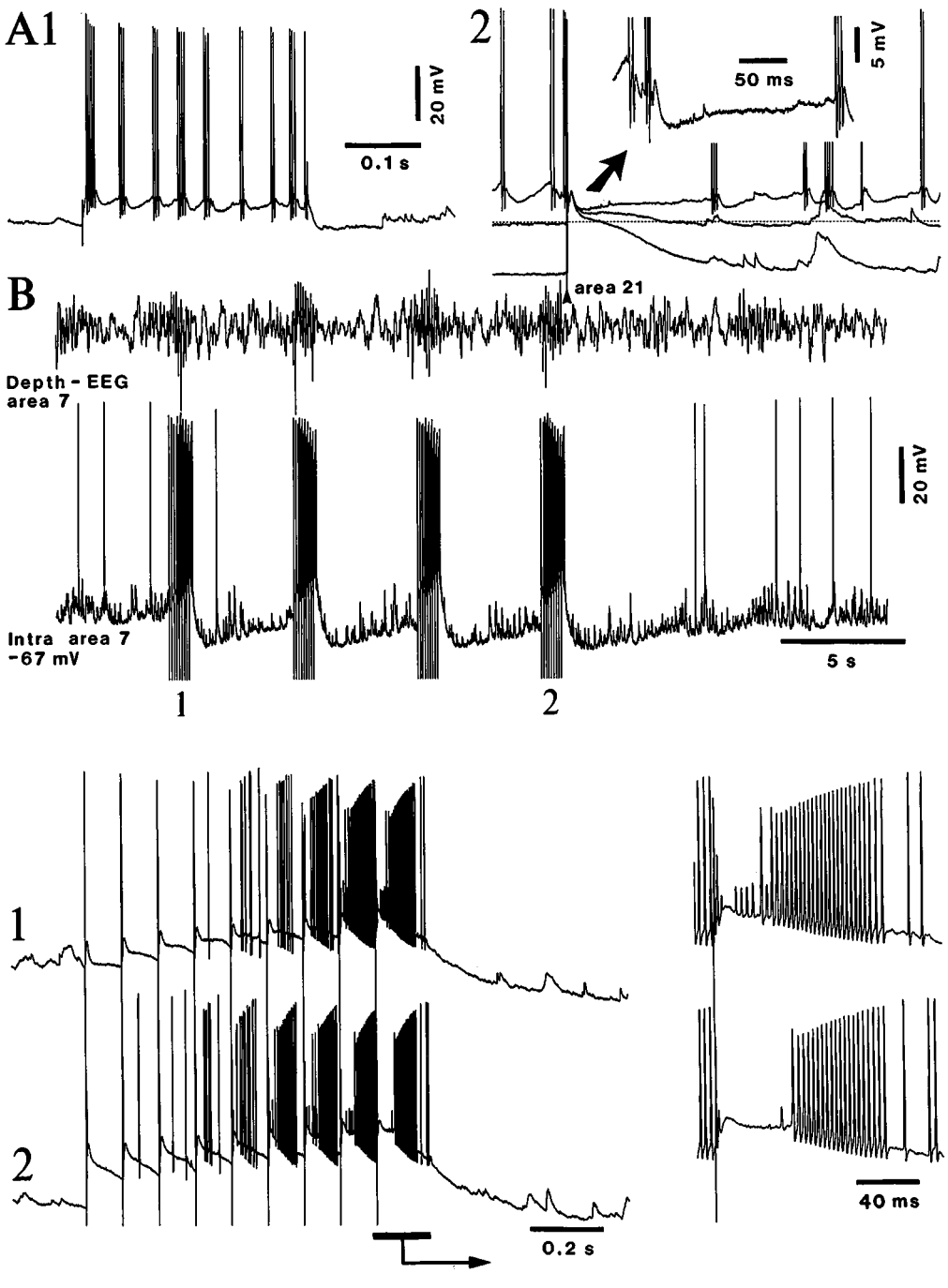

Fig. 4.44 Progressively growing depolarization during cortically evoked augmenting responses in a cortical fast-rhythmic-bursting (FRB) neuron from cat suprasylvian area 7. Barbiturate anesthesia. Close intracortical stimulation, in adjacent area 21. *A1*, identification of FRB neuron by depolarizing current step (0.5 nA). *A2*, synaptic responses of this neuron to single stimulus to area 21 are dominated by IPSPs. The three V_m levels are under +1 nA, at rest (−67 mV), and under −1 nA (some spikes truncated for clarity). *B*, responses of this FRB neuron to four pulse-trains, each consisting of nine pulses at 10 Hz applied to area 21. Responses to pulse-trains *1* and *2* (last) are expanded below, and responses to the last stimulus in these pulse-trains are further expanded on the right (arrow). The neuron was persistently depolarized during stimulation. At depolarized levels of the V_m, IPSPs evoked by area 21 stimuli (see *A2*) shunted the early occurring spikes. From Steriade and Timofeev (2002b).

Plate Section

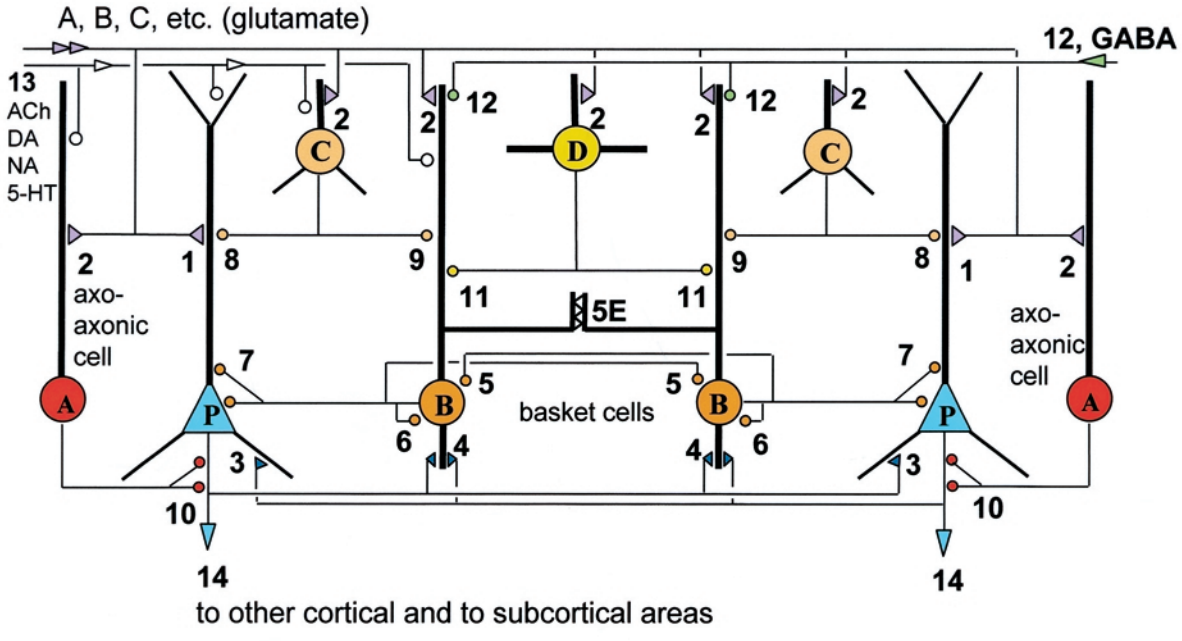

Fig. 2.8 Simplified summary of the major classes of synaptic connections in the basic cortical circuit of the cerebral cortex. Only one type of pyramidal cell (P) and a set of local-circuit GABAergic cells (filled circles) are shown. They are innervated by sets of extrinsic glutamatergic pathways (A, B, C, etc.; only one shown for clarity) making synapses with both the principal cells (1), and GABAergic interneurons (2). Ensembles of pyramidal cells are extensively interconnected (3), and also innervate some classes of GABAergic cell (4). The perisomatically terminating (7) basket cells (B) are also extensively interconnected through both chemical (5) and electrical synapses (5E), and innervate themselves through autapses (6). Several distinct classes of GABAergic cells (C, one class shown for clarity) innervate the pyramidal cells (8), and other GABAergic cells (9) in a domain-specific manner, co-aligning their termination zone with glutamatergic pathways (1, 2). The output of pyramidal cells is influenced by the GABAergic axo-axonic cells (A), which are unique to the cortex and selectively innervate (10) the axon initial segments. Some GABAergic cells (D) specialize in the innervation of other GABAergic cells (11). Extrinsic GABAergic (12) and monoaminergic (13, including acetylcholine (ACh)) afferents innervate specific interneuron classes as well as principal cells. The output of the circuit is predominantly via the pyramidal axons (14). In the isocortex, this circuit is repeated in each layer of a column, sometimes several times as multiple sets of output neurons evolved, and both tangential and columnar connections are established between the basic circuits through additional specific links, involving both the GABAeric and the glutamatergic neurons. (Modified by P. Somogyi after Somogyi et al., 1998.) Courtesy of Dr. P. Somogyi.

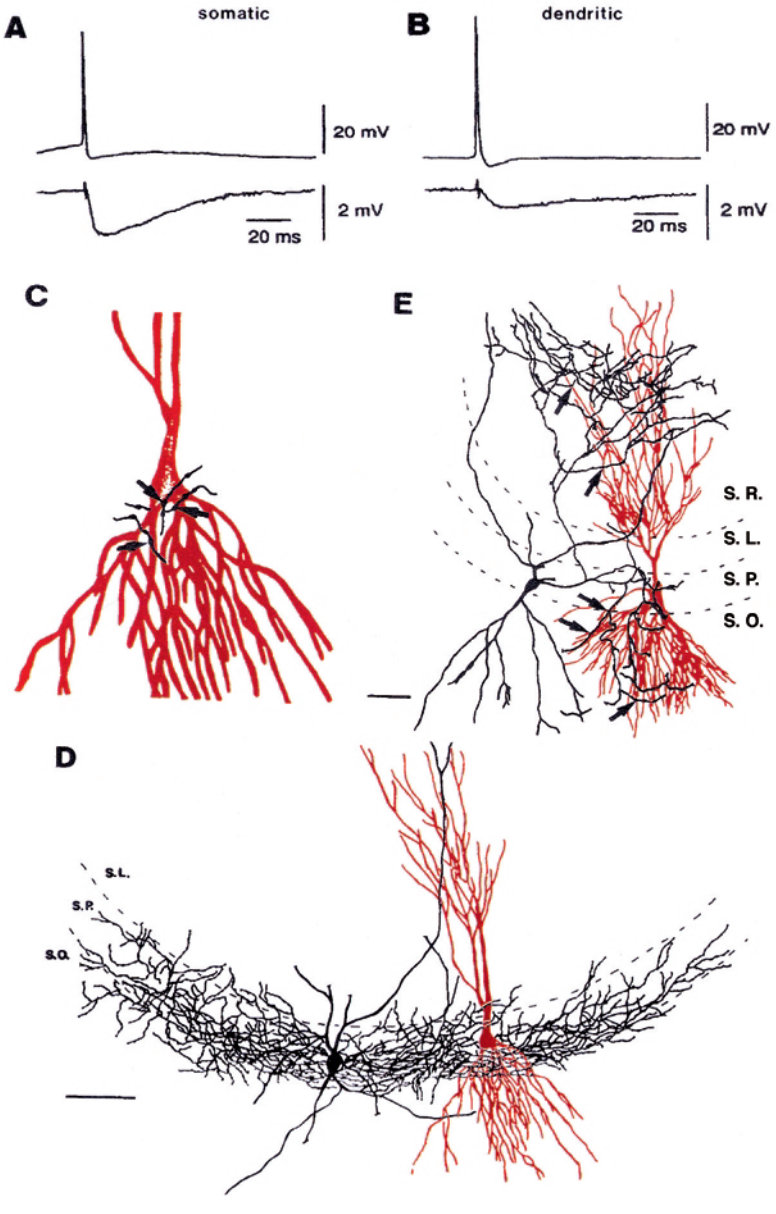

Fig. 2.17 Postsynaptic potentials evoked by inhibitory basket cells that terminate in the somatic (A) or in the dendritic region (B) of rat hippocampal pyramidal cells, as revealed by paired intracellular recordings. An action potential (upper trace) triggered by intracellular current pulse in the interneuron evoked IPSPs in the postsynaptic pyramidal cells (lower trace). The number and location of synaptic contacts were identified by light and electron microscopy, following intracellular biocytin filling. C–E, reconstructions of the cell pairs (pyramids drawn in red, interneurons in black). The basket cell in D that produced the IPSPs shown in A formed three synaptic contacts on the postsynaptic pyramidal cell, as shown by the arrows at higher magnification in C. The bistratified interneuron in E, responsible for the IPSP shown in B, arborized in strata oriens and radiatum. It formed two synapses on the apical, and three synapses on the basal, dendrites of the pyramidal cell (arrows). All contacts identified at the light microscopic level were confirmed by correlated electron microscopy. Scale bars in D–E = 50 μm. From Gulyas et al. (1993).

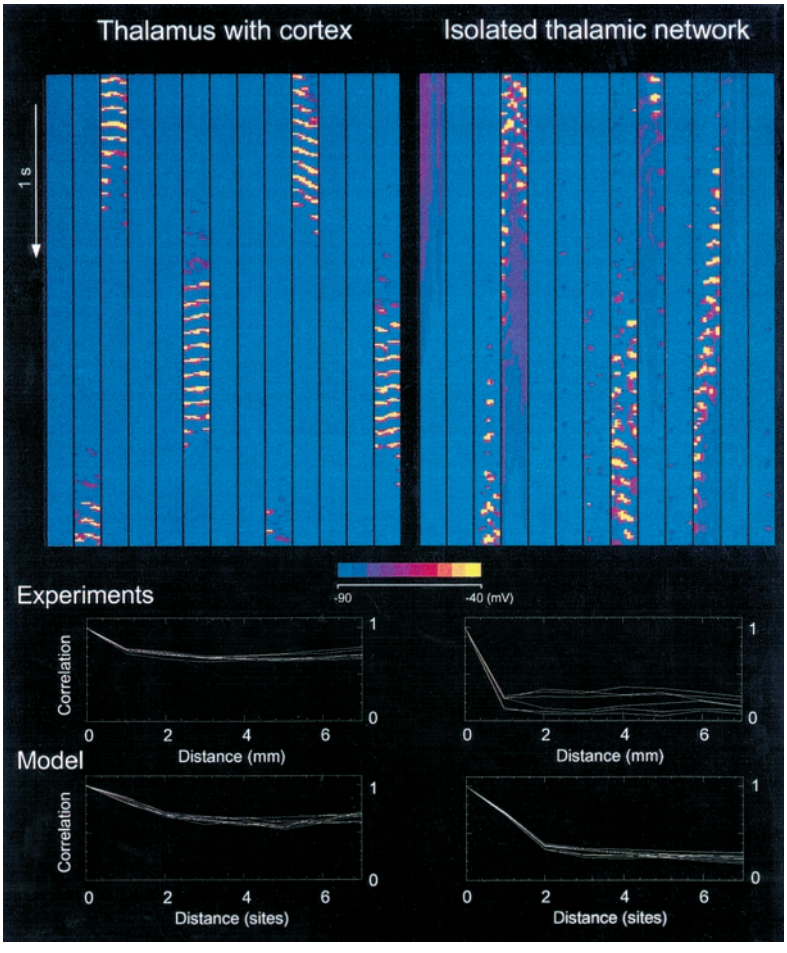

Fig. 3.12 Presence of cortical feedback determines spatiotemporal coherence of spindle oscillation in experiments and models of thalamocortical networks. *Top*: spatiotemporal maps were constructed from local thalamic averages of spontaneous spindles in the presence of cortex (left) and in an isolated thalamic network, with the same parameters (right). Each frame consisted of a horizontal stripe of 8 color spots representing the membrane potential of thalamic averages (see Fig. 5 in that paper). Frames were arranged from top to bottom in 13 columns (a total of 40 s of activity is shown). Colors ranged in 10 steps from −90 mV or below (blue) to −40 mV or above (yellow; see color scale). *Bottom*: decay of correlations with distance. Cross-correlations were computed for all possible pairs of sites and value at time zero from each correlation was represented as a function of intersite distance. Experiments: decay of correlations of thalamic local field potentials in intact (left) and decorticate (right) cats under barbiturate anesthesia. Model: decay of correlation calculated for local averaged potentials in the presence of cortex (left) and in isolated thalamic network (right). Modified from Destexhe et al. (1998).

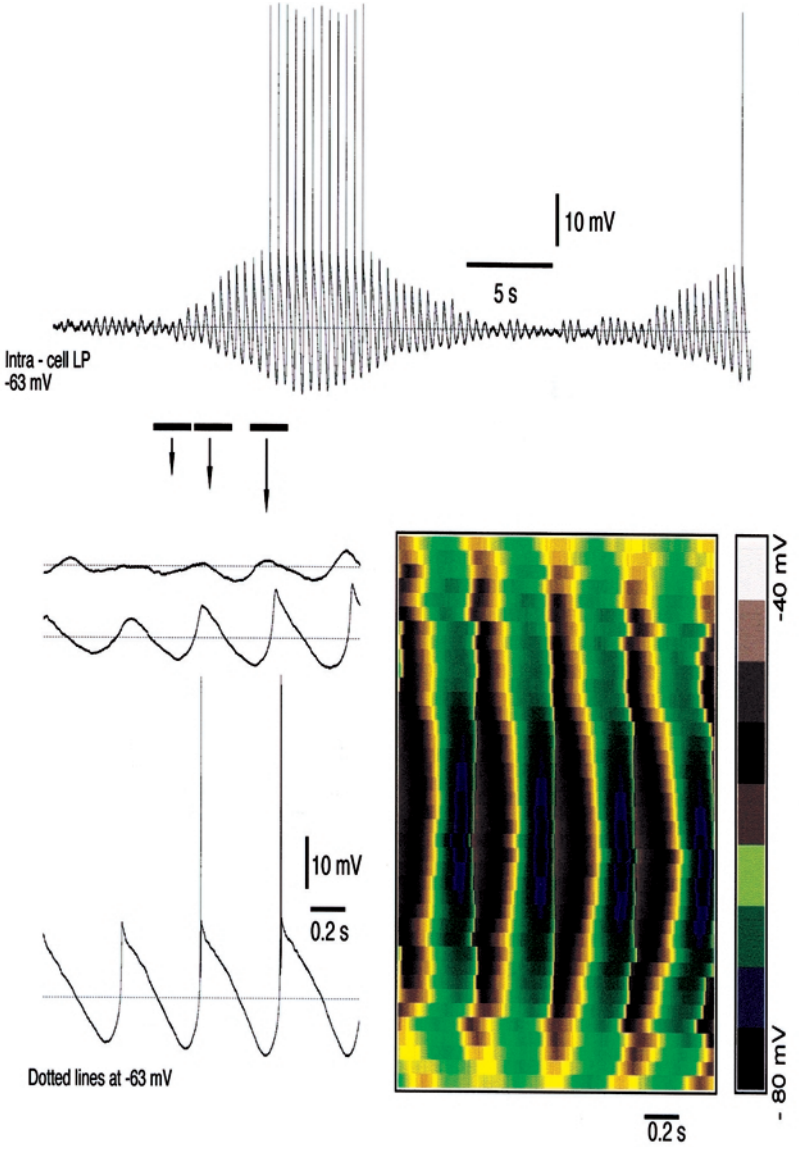

Fig. 3.22 Clock-like thalamic delta activity in decorticated cat. Ketamine-xylazine anesthesia. Intracellular recording from thalamic lateroposterior (LP) neuron. Note waxing and waning potentials. Periods of delta oscillations start from subtle fluctuations of the membrane potential. The amplitude of this activity starts and declines without changes in frequency (2.2 Hz). Periods indicated by horizontal bars are expanded below. A topographical plot of delta activity emphasizes the stable frequency of delta activity regardless of the amplitude of LTSs (right). Successive sweeps are aligned by the maximal depolarization during LTS (bottom to top); time is left to right; colors code the voltage. From Timofeev et al (2001a).

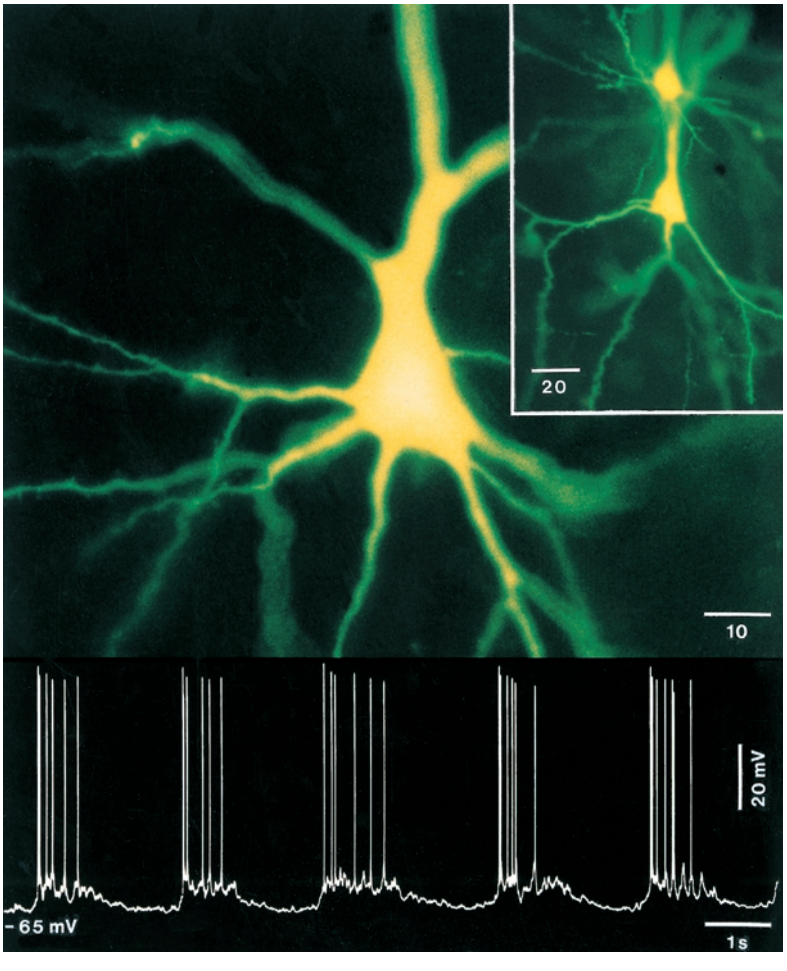

Fig. 3.24 Slow oscillation in a regular-spiking, slow-adapting pyramidal neuron, recorded at a depth of 0.7 mm in area 7. Cat under urethane anesthesia. Intracellular staining with Lucifer yellow (LY). The neuron responded with EPSPs to thalamic laterosposterior (LP) and intralaminar centrolateral (CL) nuclei. *Inset*: dye coupling following LY injection in a single cell; radially arranged neurons, at a depth of ~0.5 mm in area 5 (bars in μm). The neuron that was injected was slowly oscillating spontaneously; it displayed intrinsic bursts by depolarizing current pulses and was driven synaptically from both LP and CL thalamic nuclei. *Bottom*: intracellular recording showing the slow oscillation. Modified from Steriade et al. (1993e).

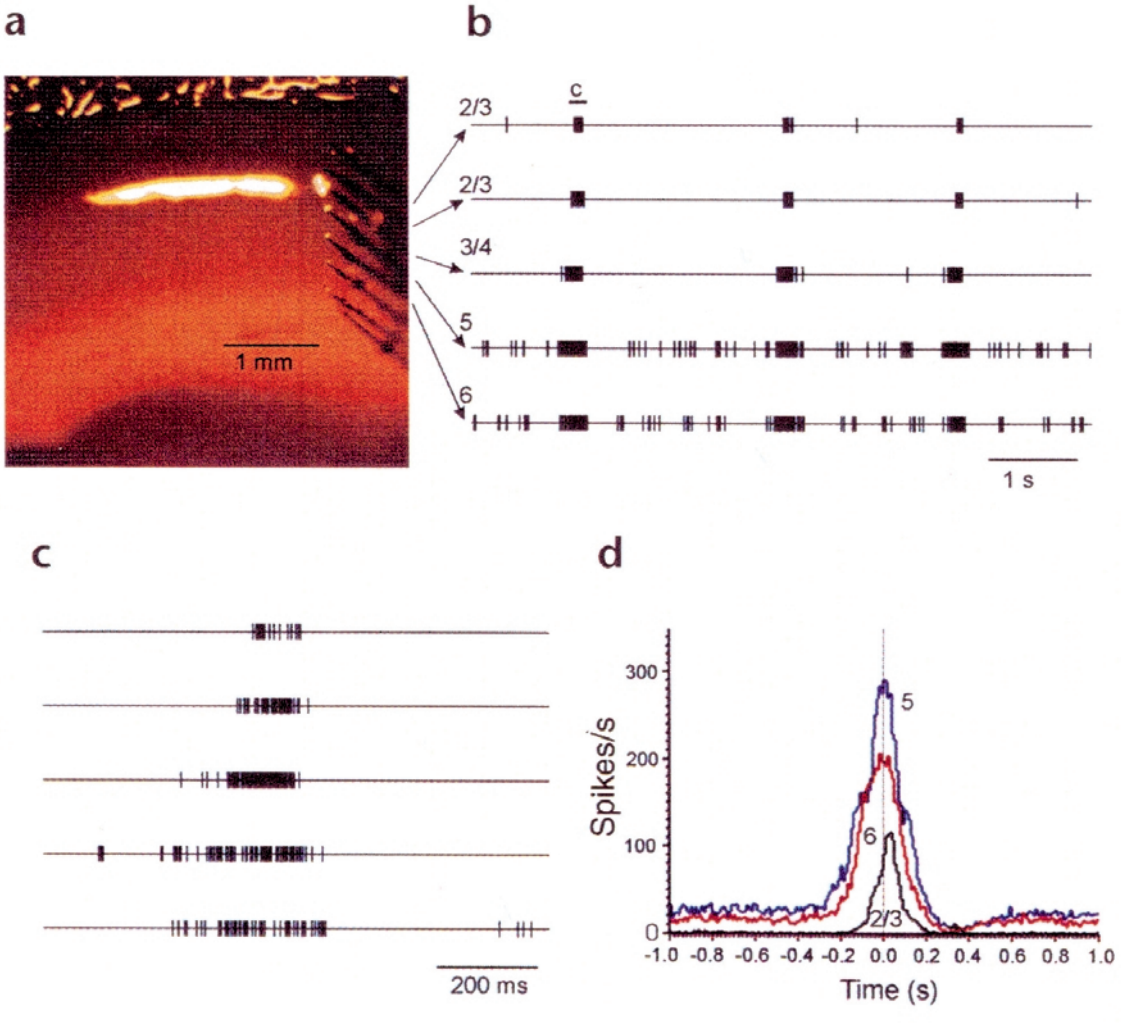

Fig. 3.46 In *in vitro* slices from ferret visual cortex, the slow oscillation is generated first around layer V and propagates vertically. (*a*), the extracellular recording microelectrode array (0.25 mm inter-electrode spacing) placed vertically in the cortical slice. (*b*), simultaneous extracellular multi-unit recording from layers II/III to VI reveal the slow oscillation to initiate around layer V, followed, on average, by activity in layers VI and II/III. The burst of activity indicated is expanded in (*c*). The third electrode was at the border between layers III and IV, whereas the fourth electrode was at the top of layer V. Each tic mark represents a detected action potential in the multi-unit recording. (*d*), unit histogram aligned to the peak of activity in layer V for each of the up-states of the slow oscillation reveals that layers V and VI generate spontaneous activity before the onset of the up-state, but that this activity decreases following the up-state. The up-state begins slightly earlier in layer V than layer VI and is more intense. See comments in note [199]. From Sanchez-Vives and McCormick (2000).

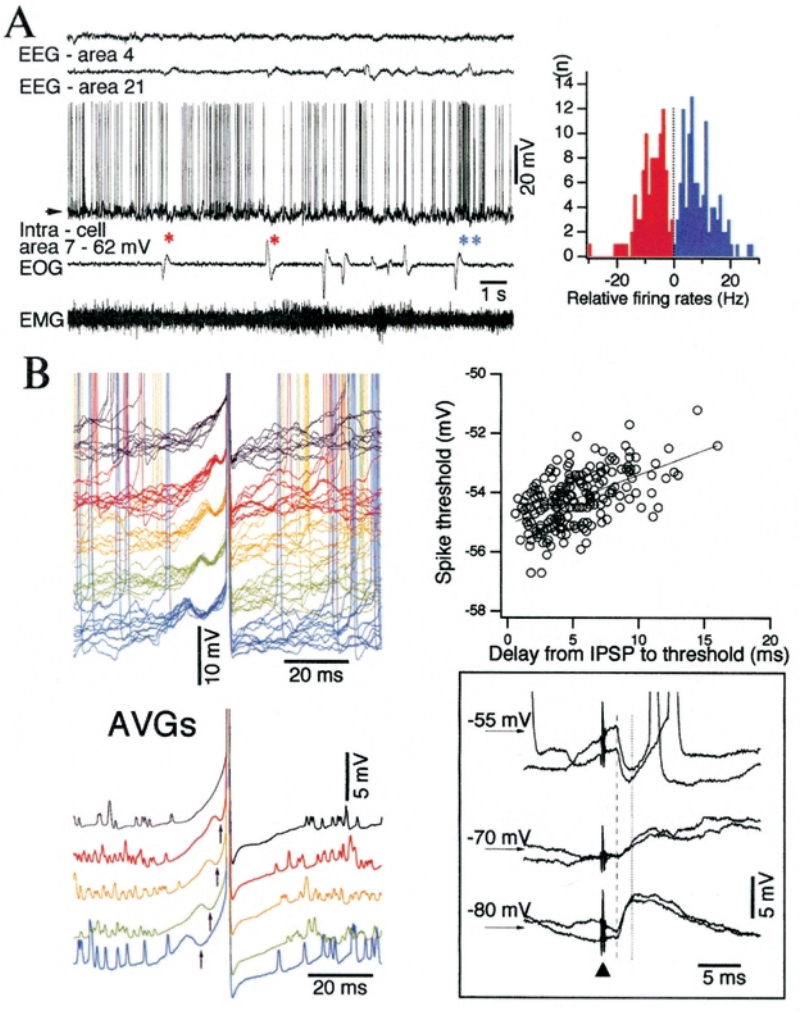

Fig. 3.59 Spontaneous IPSPs control precise firing timing of neocortical neurons in wakefulness. Intracellular recordings of cortical association neurons during natural waking in chronically implanted cats. *A*, epoch during the waking state, characterized by activated EEG, unimodal intracellular membrane potential and presence of muscular tone. Five traces depict (from top to bottom): depth-EEG from areas 4 and 21, intracellular activity of area 7 neuron, EOG, and EMG. Single asterisks (*) indicate a decrease in firing associated with eye movements, while double asterisks (**) indicate an increase in firing associated with eye movements. Histogram shows increased (blue) and decreased (red) saccade-related firing (±500 ms around saccade) for 15 neurons (>200 individual saccades), in relation to mean firing rates of the same neurons. To calculate abscissa, the firing rate during ocular sacccades was subtracted from the mean firing rate. *B*, more than one-half of the spikes during waking were associated with preceding short-lasting hyperpolarizing potentials. *Inset* (*bottom right*): another neuron from area 4, recorded in the waking state, in which short-lasting IPSPs were activated by stimulation of thalamic ventrolateral nucleus. Modified from Timofeev et al. (2001b).

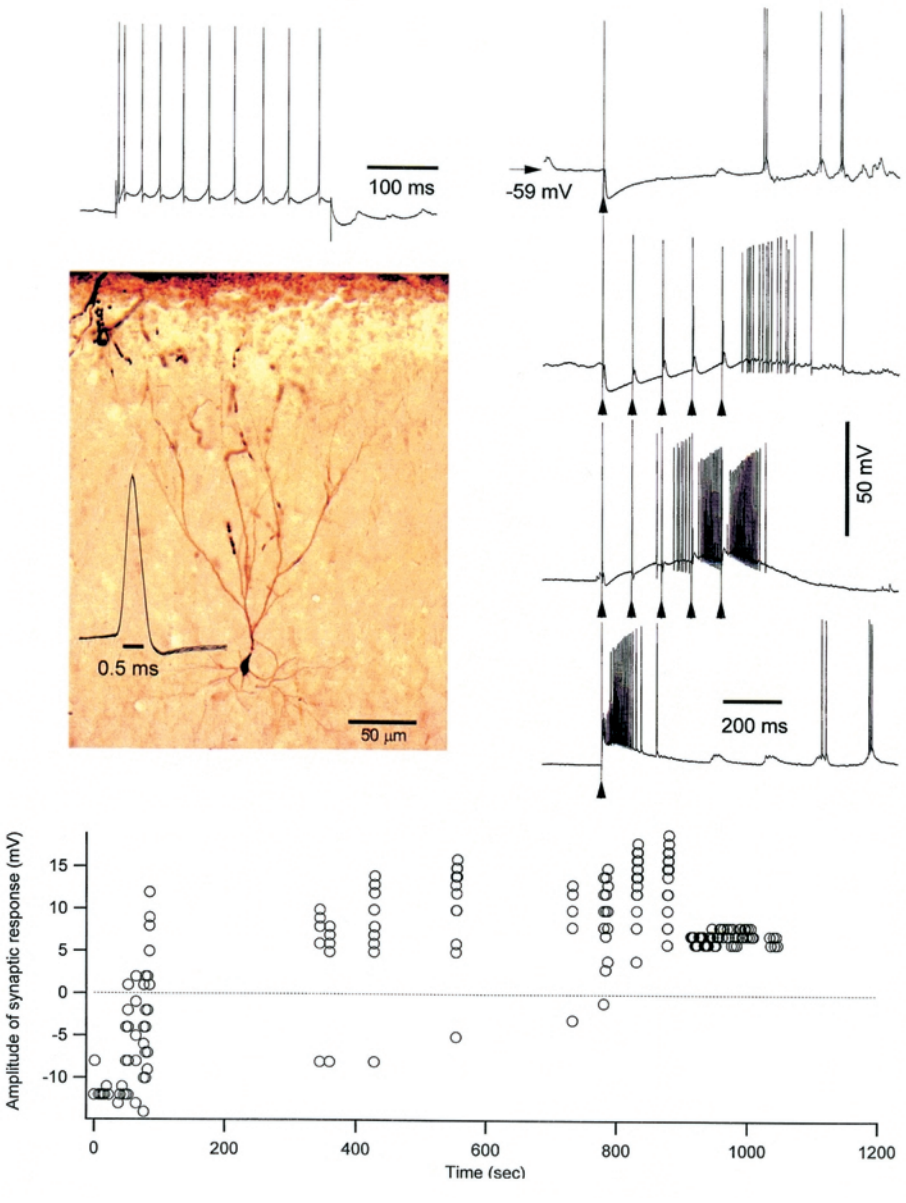

Fig. 4.43 Cortical augmenting responses lead to long-lasting enhancement of depolarizing responses in intact cortex. Cat under barbiturate anesthesia. Intracellular recording from an electrophysiologically (left upper panel) and a morphologically (left middle panel) identified area 7 pyramidal regular-spiking neuron with thin spike (see expanded action potential close to the stained neuron). Right panel shows (from top to bottom): control response to a single stimulus to the cortex, early responses to the pulse-trains at 10 Hz, responses to pulse-train with the same parameters applied 12 min later, and responses to a single stimulus applied 16 min after the onset of rhythmic stimulation. Below, plot showing the amplitude of stimulus-evoked responses at 20 ms after stimulus onset. Note that initially hyperpolarizing responses became depolarizing after pulse-trains at 10 Hz. From Timofeev et al. (2002b).

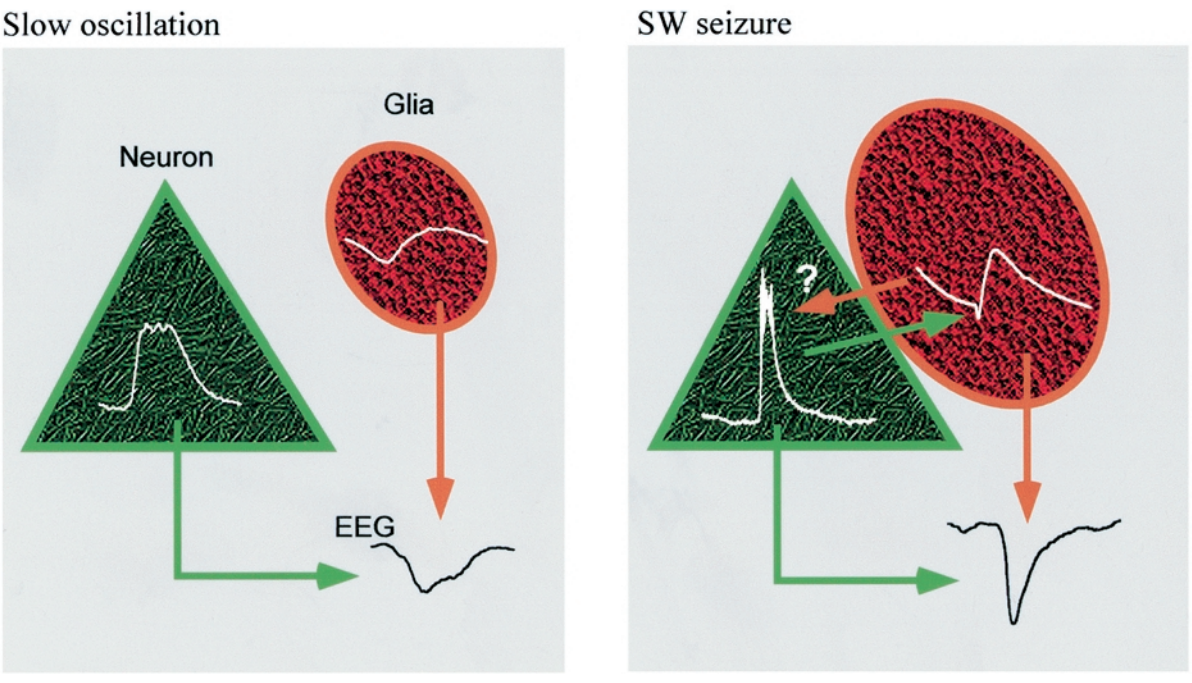

Fig. 5.19 Schematic diagram of the mechanisms generating field potentials during slow sleep oscillations (*left*) and spike-wave (SW) seizures (*right*), resulting from *in vivo* experiments on cortical and glial cells from cat under ketamine-xylazine anesthesia. An averaged cycle is drawn in each cell (*white traces*). During the slow oscillation, reversed neuronal and glial potentials contribute to the genesis of the extracellular field potential (EEG). SW seizures are accompanied by glial swelling, which may bring patches of cellular membranes into contact, allowing intraneuronal potentials to appear reversed, as field potentials,in the glial cells (arrow from neuron to glia points towards the glial negativity). The reverse pathway might also be at work. Both intraneuronal and intraglial activities contribute to the shape of the extracellular field potential. Modified from Amzica and Steriade (2000).

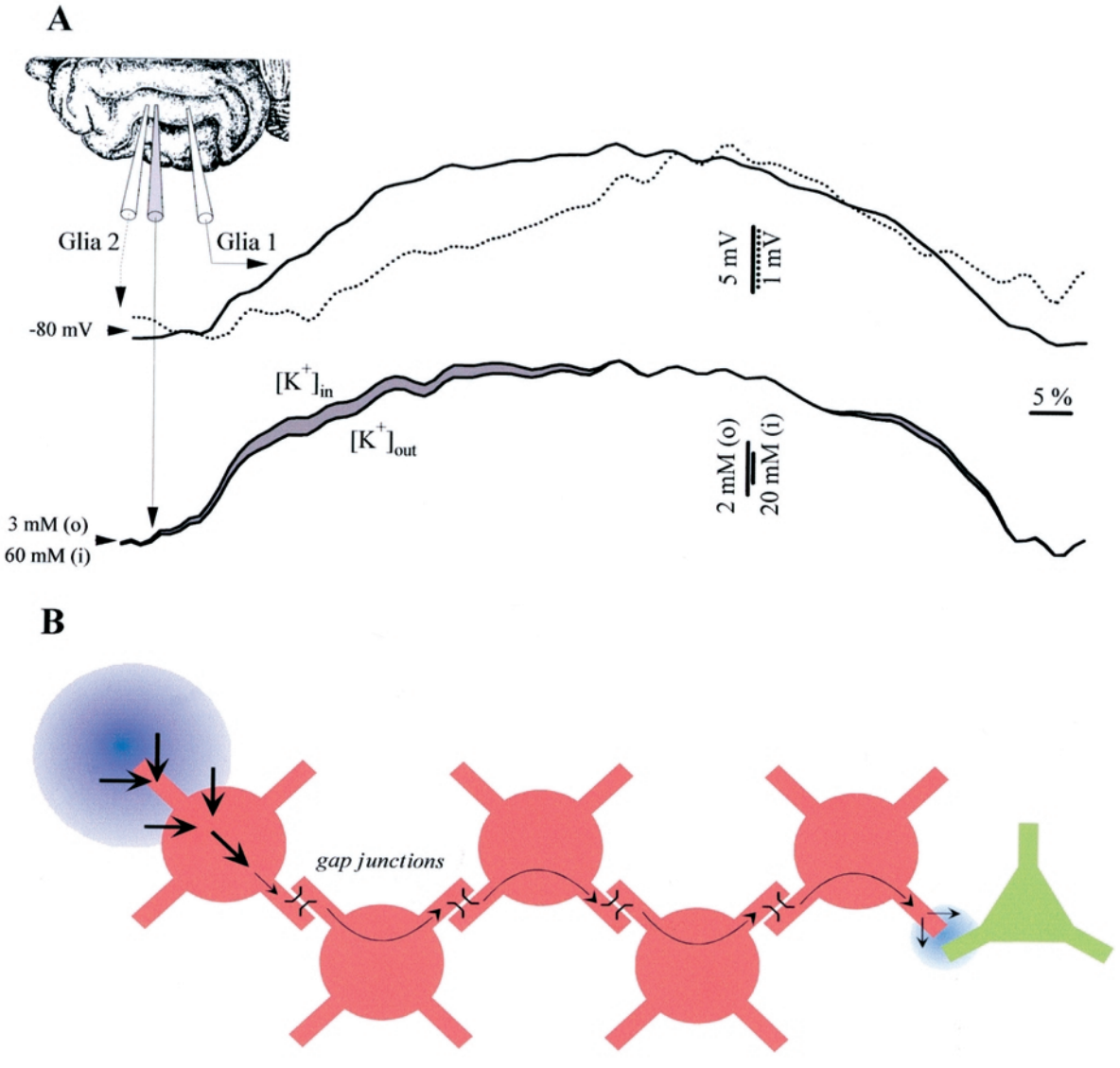

Fig. 5.76 Propagation of K^+ waves during SW seizures. Data from cats under ketamine-xylazine anesthesia. *A*, dual intraglial recording together with the extracellular K^+ concentration ($[K^+]_o$). The position of the recording electrodes in the suprasylvian gyrus is shown in the *inset*. The traces represent the average of 20 normalized seizure envelopes. The upper superimposition contains the intracellular seizures in the pair of glial cells expanded at their maximum amplitude (see different voltage calibrations – continuous line for cell 1 and dotted line for cell 2, also corresponding to the envelope traces). From the higher amplitude of the signal, it may be inferred that cell 1 is closer to a presumed seizure focus. The *lower panel* displays the intra- and extracellular K^+ concentrations superimposed and expanded at their maximum amplitude. The $[K^+]_i$ was calculated from the Nernst equilibrium potential in relation to the $[K^+]_o$ and the intracellular trace that was recorded close to the K^+ microelectrode. Toward the beginning of the seizure, the estimated $[K^+]_i$ increased faster than the $[K^+]_o$ (*gray area* between the two traces). *B*, schematic functioning of the spatial buffering during SW seizures. Red cells represent glia, green cells represent neurons. Important increases in the $[K^+]_o$ (blue circle) may not be buffered at short distances, in which case the K^+ taken up may travel through the glial syncytium and is externalized at a location with lower $[K^+]_o$ values, where it would modulate the activity of nearby neurons. Modified from Amzica et al. (2002).

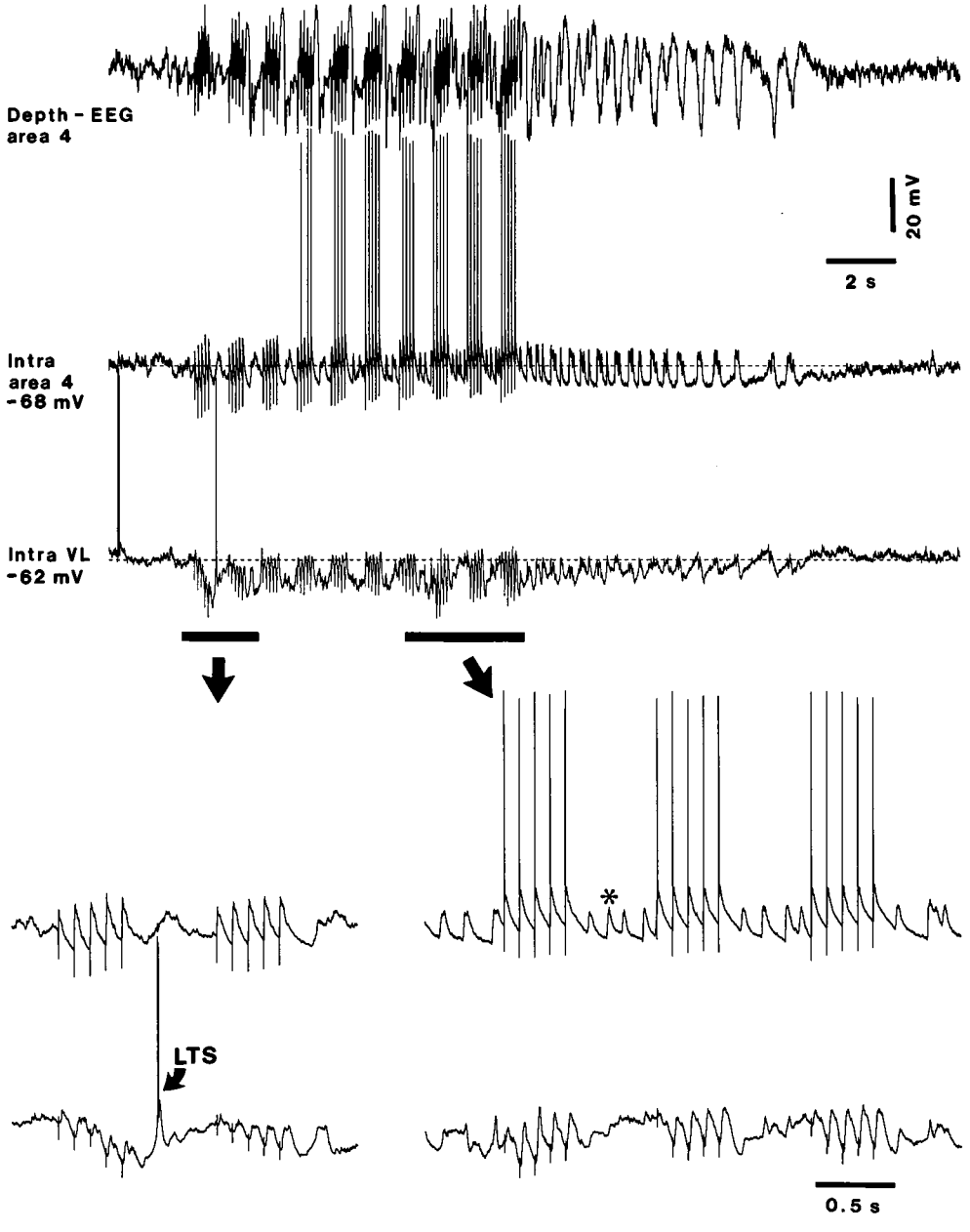

Fig. 4.45 Plastic changes in cortical responsiveness, leading to self-sustained paroxysmal oscillation, simultaneously with decreased LT-type augmenting in a TC neuron. Cat under ketamine-xylazine anesthesia. Dual intracellular recording from a TC neuron in the ventrolateral (VL) nucleus and a cortical area 4 neuron, together with depth-EEG from area 4. Stimulation applied to the cortex and consisting of pulse-trains at 10 Hz, repeated every second. Two parts, at the beginning and end of stimulation (marked by horizontal bars and arrows), are expanded below. Note that, although LT-type augmenting responses in the TC neuron diminished from the second pulse-train, cortical augmenting responses were progressively enhanced and, after finishing the stimulation period, a self-sustained oscillation at ~2 Hz ensued, lasting for ~8 s. Also note, in cortical neuronal recording, depolarizing events with a frequency similar (10 Hz) to that used in pulse-trains occurring between pulse-trains (asterisk in bottom right panel). From Steriade and Timofeev (2002b).

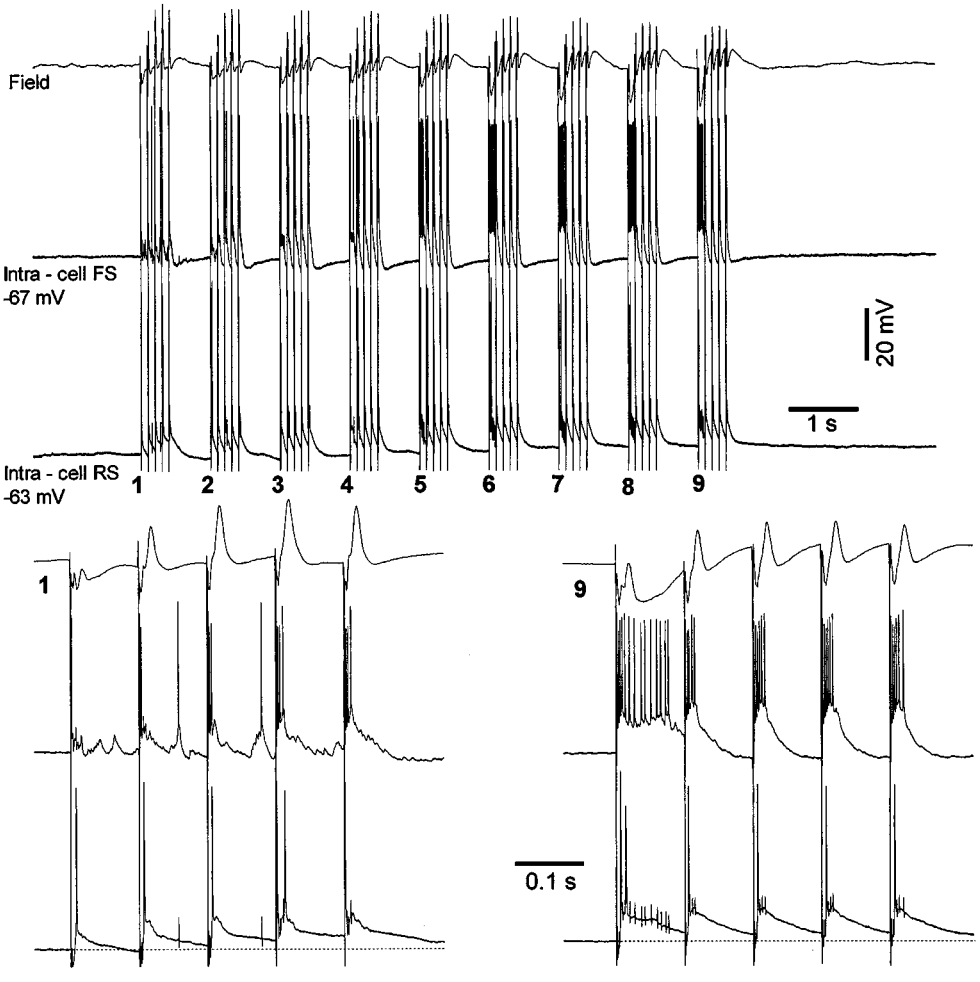

Fig. 4.46 Repeated pulse-trains at 10 Hz modify the features of augmenting responses in isolated cortical slab from area 5. Cat under ketamine-xylazine anesthesia. Upper panel shows simultaneously recorded field potentials and dual intracellular recordings from a closely located pair of fast-spiking (FS) and regular-spiking (RS) neurons. The slab was stimulated with nine pulse-trains at 10 Hz, repeated every second. Responses to the first and ninth stimuli are expanded below. Note prevalent increasing responses in the FS neuron and major increases in responses to the first stimulus in the pulse-trains as stimulation progresses. Modified from Timofeev et al. (2002b).

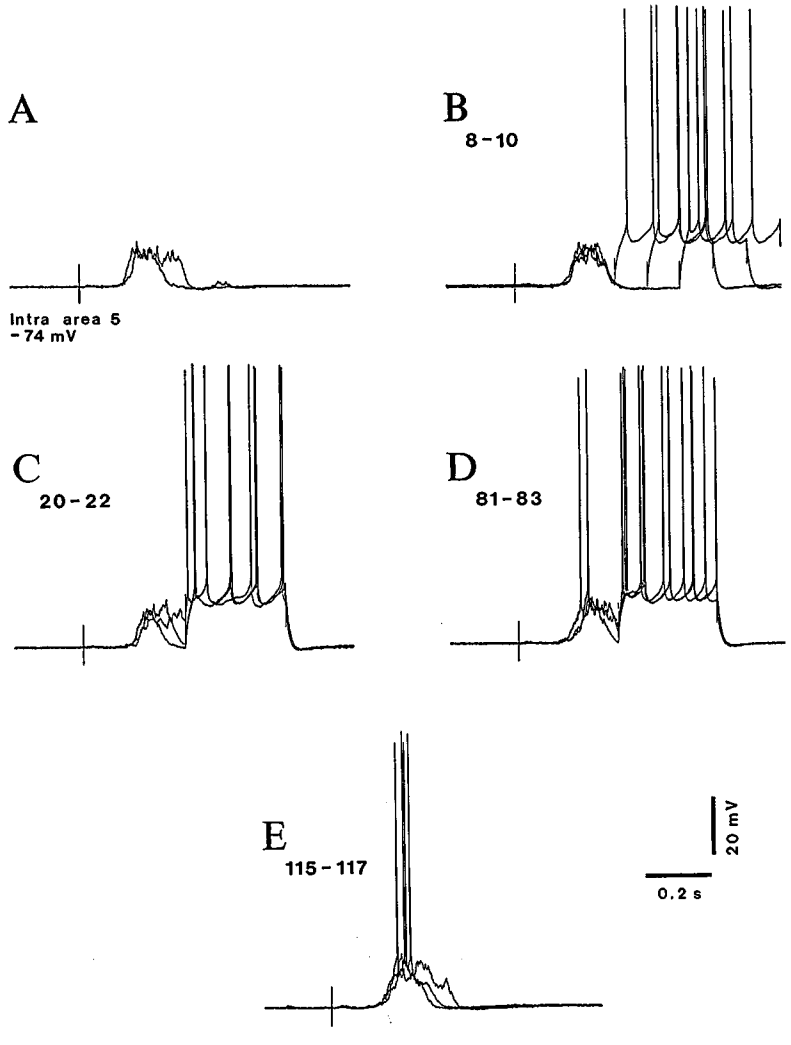

Fig. 4.47 Intracellular conditioning in a cortical slab from area 5. Cat under ketamine-xylazine anesthesia. *A*, stimulus within the slab evoked a long-latency, subthreshold depolarizing event. This was the conditioned (C) stimulus. *B*, depolarizing current pulses (unconditioned, U, stimulus) followed the C stimulus at three time intervals (trials 8–10). *C*, trials 20–22 with C immediately followed by U stimulus. *D*, beginning of development from subthreshold to suprathreshold C responses (trials 81–83). *E*, C stimulus alone elicited suprathreshold responses in all trials (115–117). The extinction procedure is not depicted here. From Steriade and Timofeev (2002b).

with action potentials (Fig. 4.48). This increased excitability could last for 3–4 min and thus indicate that synaptic responses associated with the firing of the postsynaptic response may induce a mid-term increase in the excitability of cortical neurons [104].

Finally, a repetition of 10-Hz pulse-trains in isolated cortical slabs can induce electrical seizures that are initiated with fast runs at ~10 Hz. Later phases of these seizures are composed of spike-wave (SW) or polyspike-wave (PSW) complexes at ~3 Hz (see bottom panel in Fig. 4.49). The fact that such seizures started from around 10-Hz oscillations suggests that the neuronal network in the neocortical slabs "remembers" previously induced activity and oscillates with the same frequency, as also illustrated in Fig. 4.42*B*). Neocortical slabs do not display *spontaneously* occurring seizures, thus suggesting that an initial stimulation/oscillation is essential for the induction of seizures with a given frequency.

It was postulated that the hippocampus orchestrates neocortical memory retrieval during consolidation, based on simultaneous recordings from neurons in the hippocampus and neocortex, which show that memory trace reactivation is coherent at these two levels and suggest that the initiation site of the reactivation process is area CA3 [95, 105]. Although in the intact brain the hippocampal-neocortical dialogue is obviously important in the consolidation of memory traces, the above experimental results from isolated neocortical slabs (Figs. 4.46–4.49) show that neocortical networks alone are capable of plasticity, even if at a more rudimentary level. Data from isolated cortical slabs, which display poor spontaneous activity, should be complemented with the results showing plasticity resulting from rhythmic repetition of cortical responses in the intact cortex, and even more so in intact corticothalamic loops (Figs. 4.42–4.44). In the latter preparations, the highly synchronous ongoing population activity, which takes the forms of different oscillatory types during slow-wave sleep [6, 43, 106], strongly influences the firing of individual neurons embedded in those networks and these interactions may lead to new avenues of research into internal cortical representations and sensory inputs [107]. That spontaneously occurring activity may influence cortical responses and predict their latencies further substantiates the idea that background activity may contain information and could be effective in grouping responses for further processing [108].

The mechanism(s) implicated in memory consolidation as a result of rhythmic spike-trains and spike-bursts in cortical and thalamic neurons during slow-wave sleep may be Ca^{2+} entry into these neurons [109]. The significant, long-lasting depolarization observed during cortical augmenting responses (see Fig. 4.39), with

[104] Cissé et al. (2001).

[105] Treves and Rolls (1994).

[106] Steriade et al. (1993d-f).

[107] Tsodyks et al. (1999).

[108] Fries et al. (2001). In this study, spontaneously occurring oscillations were in the gamma frequency band (40–70 Hz). The authors raised the issue of whether low-frequency brain rhythms (what is usually called the state of synchronization) or fast rhythms (termed "desynchronized" activity by these authors) are able to influence latency covariations among neurons. The fact is that fast (or gamma) activity is *not* desynchronized, but highly coherent among restricted (4–5 mm) cortical territories as well as in long-range corticothalamocortical loops (Steriade et al., 1996a-b).

[109] Steriade et al. (1993d); Berridge (2000); Sejnowski and Destexhe (2000).

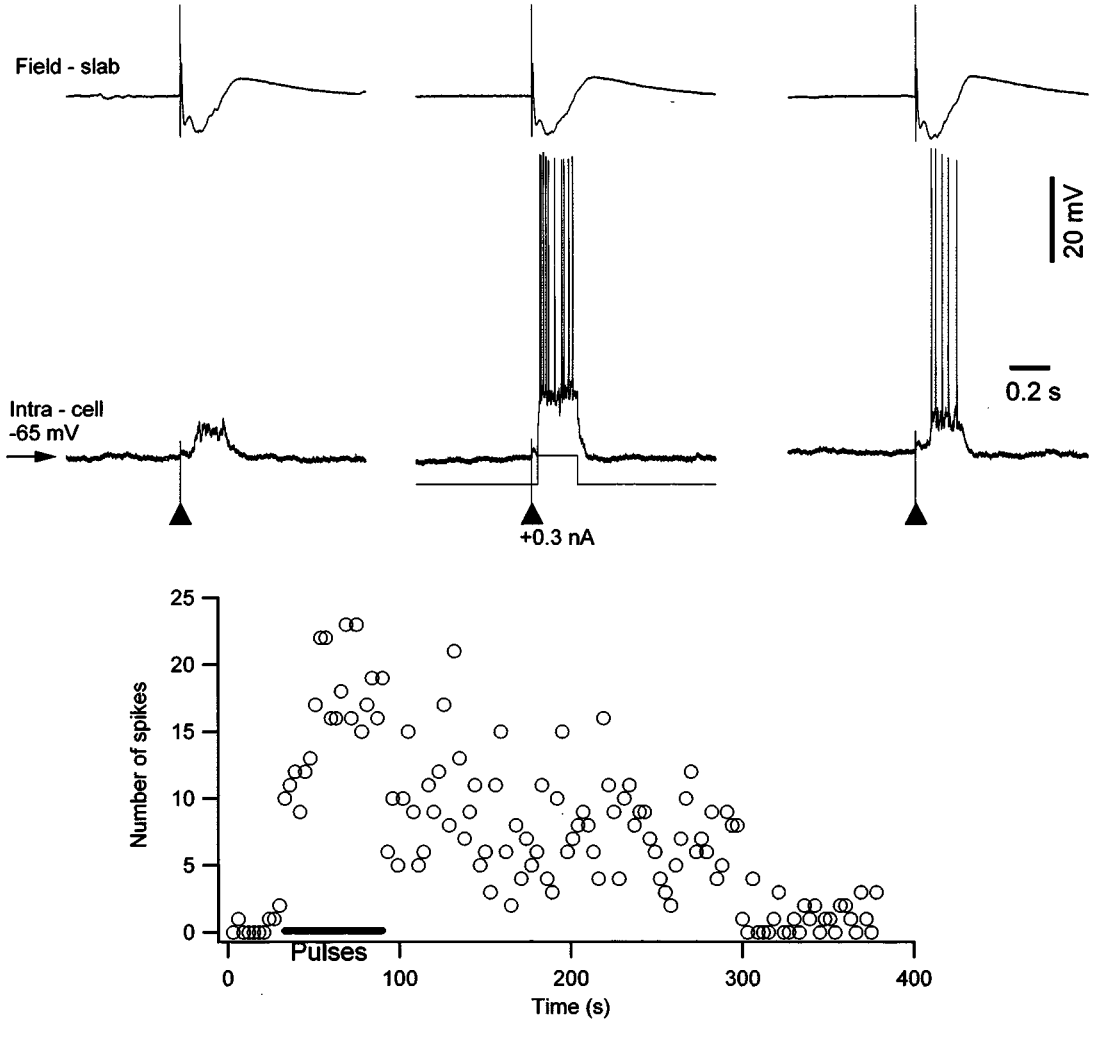

Fig. 4.48 Intracellular plasticity persists for minutes in a slab from cortical area 7. Cat under ketamine-xylazine anesthesia. Top, field potential and intracellular activities during control (left), pairing of synaptic activity with direct cellular depolarization (middle), and onset of extinction (right). In control, the slab was stimulated with low-intensity stimuli (triangles) that elicited an early EPSP followed by a sustained depolarization, lasting for 300–400 ms. An intracellular current pulse that elicited spikes and lasted for the duration of the active period (300 ms) was applied during the pairing. After 20 repetitions, current pulses were stopped. During extinction, extracellular stimuli elicited depolarizing responses accompanied by spikes. The enhancement of responses lasted for more than 200 s. Note that the field potential was identical in all responses, indicating that network excitability remained unchanged. At the bottom, there is a plot showing the number of spikes at each stimulus, produced by the neuron in chronological order, with facilitation followed by complete extinction. From Timofeev et al. (2002b).

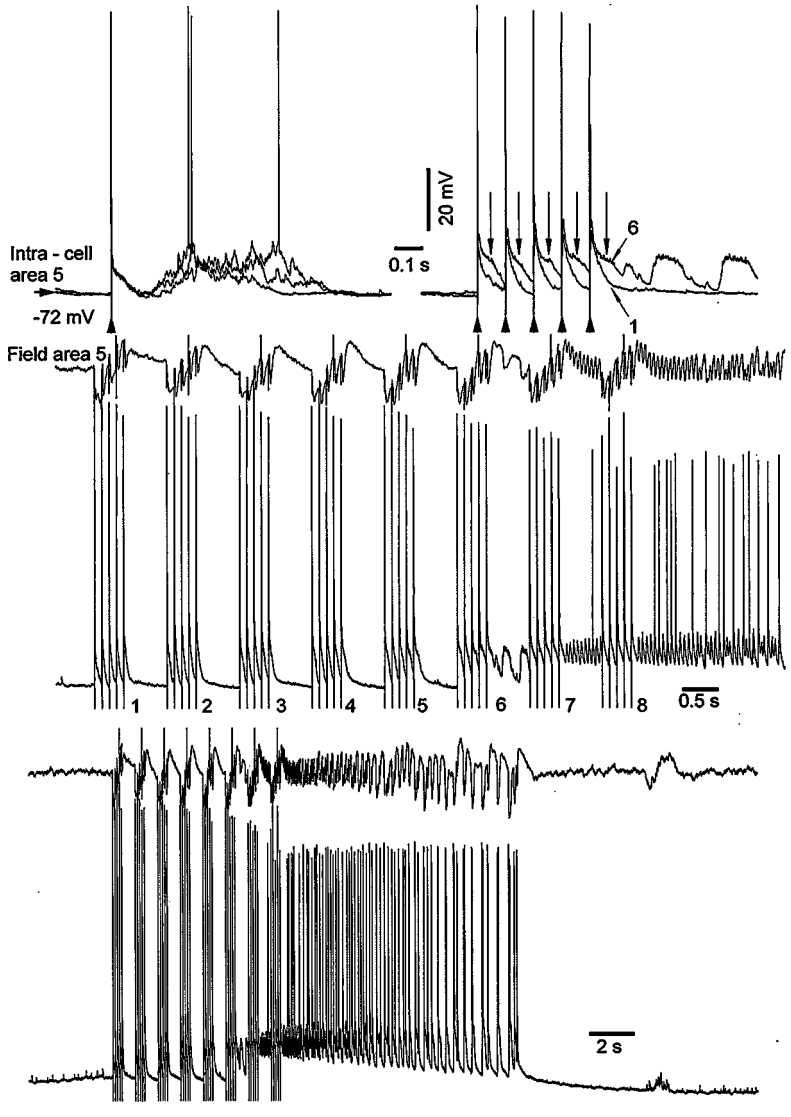

Fig. 4.49 Repeated pulse-trains at 10 Hz may lead to self-sustained paroxysm. Intracellular recordings from a neuron in an isolated slab from area 5. Cat under ketamine-xylazine anesthesia. Upper left displays responses to single stimuli within the slab. Upper right displays superimposed responses to the first and sixth trains in a series of five-stimuli pulse-trains at 10 Hz, delivered every second. Note the increased responses to the sixth train, especially in the late component of the response (marked by arrows). The whole stimulation period is shown in the middle panel. This increased responsiveness upon repeated pulse-trains at 10 Hz led to the electrical seizure shown at bottom. From Steriade and Timofeev (2002b).

[110] Traynelis and Dingledine (1988); Tasker and Dudek (1991).

[111] Abel et al. (1997).

[112] Dolmetsch et al. (2001).

large depolarization area in RS neurons, likely induces Ca^{2+} entry into neurons. There are at least two non-exclusive mechanisms that underlie increased responsiveness promoted by sleep spindles, the oscillation that we mimicked by augmenting responses. Firstly, neuronal firing during the depolarizing phases of sleep oscillations results in a local increase in the $[K^+]_o$, which increases neuronal excitability and shifts the reversal potential for $GABA_A$ IPSP to positive values [110], thus providing conditions for the amplification of responses that may remain effective for several seconds. The results obtained by association of depolarizing current pulses with synaptic activity (see Figs. 4.47–4.48), which demonstrated enhanced responsiveness for several minutes, suggest the implication of high-threshold Ca^{2+} currents accompanied by Ca^{2+} entry into the neuron. The increased $[Ca^{2+}]_i$ in association with concurrent synaptic inputs may activate protein kinase A [111] or ras/mitogen-activated protein kinase [112], which seem to be involved in memory consolidation. Thus, spontaneously occurring oscillations, accompanied by rhythmic firing in thalamic and cortical neurons, and paired with synaptic volleys, may sculpt afferent signals and promote the sensitivity of particular synapses.

4.4. Concluding remarks

(a) The responsiveness of thalamic and neocortical neurons to single volleys is higher during waking and REM sleep than in slow-wave sleep. This conclusion was drawn from analyses of antidromic and orthodromic responses in single cells as well as from field potential recordings. However, neocortical neurons behave in more diverse ways than thalamic ones, sometimes with opposite changes in two simultaneously recorded neurons; and, callosal neurons even display enhanced responsiveness in slow-wave sleep, which supports the notion that an internal dialogue is maintained during this state despite the absence of information from the external world due to thalamic inhibition of synaptic transmission. The only electrophysiological feature that may distinguish the two brain-active states of waking and REM sleep in thalamocortical systems is the diminished efficacy of inhibitory processes in REM sleep, compared to waking. The contrast between the mental content in waking and REM sleep might then be ascribed to this difference in inhibitory processes and to the virtual silence of monoamine-containing neurons during REM sleep.

(b) Responses to repetitive stimuli between 5 and 15 Hz, generally at ∼10 Hz, applied to thalamic nuclei or cortical areas evoke

augmenting (incremental) responses that represent the experimental model of naturally occurring sleep spindles (7–15 Hz). Augmenting responses as well as naturally occurring spindles lead to plastic changes in thalamic and cortical neurons, within the process of augmentation as well as outlast these responses for a given period of time (see points *g-i*). This led to the hypothesis that sleep spindles are not epiphenomena with no functional significance but electrical activities that subserve short- and medium-range plasticity.

(c) There are two types of intrathalamic augmenting potentials, in the absence of neocortex. Low-threshold responses of thalamocortical neurons to dorsal thalamic stimuli are produced by incremental responses in thalamic GABAergic reticular neurons that generate progressive hyperpolarizations with the consequence of de-inactivating I_T and leading to spike-bursts. Brainstem cholinergic systems, which depolarize thalamocortical neurons, block low-threshold augmenting responses. On the other hand, high-threshold responses of thalamocortical neurons are due to decremental responses in thalamic reticular neurons, probably due to inhibitory processes within the reticular nucleus, which would release target thalamocortical cells from inhibition, resulting in the depolarization that underlies such responses.

(d) Thalamically evoked augmenting responses in neocortical neurons reveal a selectively increased secondary depolarization, associated with diminished amplitude in the early EPSP. Two factors account for the increased amplitude of the secondary depolarizing component during augmentation: postinhibitory spike-bursts during the low-threshold-type augmenting responses in thalamocortical neurons that precede by short latencies (~3 ms) the augmented depolarization in cortical neurons; and thalamic volleys that activate local-circuit inhibitory neurons in cortex, hyperpolarize pyramidal neurons, and deinactivate Ca^{2+}-dependent low-threshold currents in these neurons. Similar phenomena occur with repetitive thalamocortical volleys during natural sleep spindles. Paired intracellular recordings of neocortical and thalamocortical neurons *in vivo* demonstrate that the former display postaugmenting oscillatory activities in the frequency range of augmenting responses, whereas the latter remained hyperpolarized because of the pressure from the thalamic GABAergic reticular neurons. These data show that intracortical circuits have a major influence on the incoming inputs and can amplify oscillatory activity arising in the thalamus. Among different cell classes in neocortex,

deeply lying fast-rhythmic-bursting neurons with antidromically identified thalamic projections play a major role in generating and widely synchronizing augmenting responses.

(e) Compared with augmenting responses elicited in neocortical neurons by thalamic stimuli, the progressively growing amplitude of intracortical augmenting responses is less evident. In isolated cortical slabs *in vivo*, augmenting responses can only be elicited by using relatively high-intensity stimuli. This suggests that augmenting responses occur as a network-generated phenomenon requiring a sufficient number of interconnected neurons.

(f) Although some promoted the idea that learning is possible during sleep, available data show that the recall of declarative memories is only possible when the acquisition of information takes place during epochs when the brain is awake. However, accumulating evidence shows that *consolidation* of memory occurs during sleep, with overnight improvement proportional to the amount of slow-wave sleep during the early nocturnal sleep and to the amount of REM sleep in the last part of the night's sleep. If an effective way to consolidate learned information is repetition, slow-wave sleep oscillations can be implicated in this process because of prolonged, rhythmic spike-bursts and spike-trains of thalamic and neocortical neurons that accompany these sleep rhythms, which could produce changes in synaptic responsiveness at their targets.

(g) The development of mechanisms leading to storage of information requires preserved connectivity within the neocortex and in corticothalamic loops. Self-sustained oscillations can occur in cortical neurons at the same frequency (10 Hz) as that used to evoke augmenting responses, despite the fact that, simultaneously, thalamocortical neurons remain hyperpolarized, due to the activity of thalamic GABAergic reticular neurons. Repeated spike-bursts evoked by volleys applied to corticothalamic pathways as well as occurring during spontaneous oscillations lead to self-sustained activity patterns, resembling those evoked in the late stages of stimulation. Such changes are due to resonant activities in closed loops, as in "memory" processes.

(h) In isolated neocortical slabs *in vivo*, protracted association of extracellular electrical stimuli with depolarizing current steps in intracellularly recorded cortical neurons induces a state in which extracellular stimuli, with the same intensity as when they were subthreshold, elicit active periods with action potentials. This increased excitability could last for 3–4 min

and thus indicates that synaptic responses associated with the firing of postsynaptic response may induce a mid-term increase in the excitability of cortical neurons.

(i) In the intact cortex, single stimuli may initially evoke IPSPs. Repetitive pulse-trains at 10 Hz, applied close to intracellularly recorded cells, progressively transform the initial IPSPs into depolarizing responses. Thereafter, single stimuli evoke exclusively depolarizing responses. This enhancement remains unchanged for about 15 min and suggests that electrical stimulation with the frequency range of spindles induces long-lasting changes in neuronal responsiveness. Similar enhancement could be obtained after spontaneously occurring spindle sequences. Eventually, such plastic changes in responsiveness may lead to self-sustained seizures.

Chapter 5 Neuronal mechanisms of seizures

This chapter is about the intrinsic neuronal properties and network operations that underlie different forms of seizures. The antagonism between concepts emphasizing the "epileptic neuron" or "epileptic networks" is obsolete as both voltage-gated properties of single neurons and synaptic articulations within different forebrain structures (neocortex, thalamus, corticothalamic loops, archicortex, and related systems) are crucial for the generation and spread of electrical paroxysms.

The knowledge of intrinsic cell properties has continuously evolved due to *in vitro* work conducted in the neocortex, thalamus, and hippocampus [1]. A series of studies pointed to various ionic currents that are implicated in potentiating the susceptibility to seizures.

The discovery of voltage-dependent Na^+ and Ca^{2+} channels in dendrites changed the model of dendrites with only passive properties and demonstrated that different intrinsic currents can amplify synaptic signals [2], which may eventually lead to abnormal cellular excitation and paroxysmal discharges [3].

The intrinsic propensity of some neocortical and hippocampal neurons to bursting is also a factor that predisposes to seizures. In fact, there is a continuum of variation in burstiness of cortical neurons. *In vivo* experiments, using intracellular recordings in acutely prepared and chronically implanted animals, have shown different incidences of intrinsically bursting (IB) neurons in different experimental conditions, depending on the degree of background firing, as well as the transformation of IB into regular-spiking (RS) neurons with enhanced synaptic activity (see ***2.1.2*** and ***2.1.3*** in Chapter 2) [4]. *In vitro*, the continuum extends from non-bursters to bursters that are induced by extrinsic depolarization as well as to spontaneously bursting neurons [5]. In CA1 hippocampal slices, this development in neuronal properties is modulated by the extracellular concentration of K^+, $[K^+]_o$. The effects of increasing $[K^+]_o$ on firing characteristics is not due to depolarization per se because depolarizing current injection does not convert RS into IB cells; rather, the increase in $[K^+]_o$ reduces the driving force of outward K^+ currents, thereby

[1] Reviewed in Llinás (1988); Gutnick and Mody (1995); Crill (1996); Huguenard (1996); Hoffman et al. (1997); Magee et al. (1998).

[2] For example, the current transmitted from dendrites to soma was measured by glutamate iontophoresis onto apical dendrites of neocortical pyramidal neurons in layer V while the soma was voltage-clamped with a second electrode (Schwindt and Crill, 1995). The results of this study showed that the persistent Na^+ current ($I_{Na(p)}$) in the dendrites can amplify synaptic signals mediated by NMDA receptors.

[3] Ward and Schmidt (1961) anticipated the recent findings on dendritic neuronal properties and their possible role in generating paroxysms by postulating that stretching dendrites may endow their arbor with epileptic properties.

[4] Much less often, neocortical neurons with regular-spiking patterns during natural slow-wave sleep develop their discharges into intrinsically bursting patterns at slightly depolarized levels during wakefulness (see Fig. 2.14 in Chapter 2).

[5] Jensen et al. (1994); Jensen and Yaari (1997).

increasing depolarizing afterpotentials (DAPs) and triggering additional spikes [5]. This transformation is probably one of the factors that explain the generation of recurring hippocampal seizures by high-K^+ solutions [6]. Perfusion with high $[K^+]_o$ has also been used in neocortical slices to increase the incidence and synchronization of bursting neurons [7]. Burst generation allows neurons to amplify signals. This led to the hypothesis that bursting neurons are pacemakers of epileptiform discharges [8]. A new class of voltage-gated K^+ channels, of the Kv3 subfamily, enables fast repolarization of action potentials, without compromising spike amplitude, and allows neurons to fire at very fast frequencies [9], which may also be a factor behind the transformation of normal into paroxysmal discharges. The frequency of spike generation may determine the extent of invasion of action potentials through the fine axonal arbors [10] in the cortex and other structures that are critical for epileptogenesis.

In a certain proportion of neocortical neurons, the hyperpolarization-activated cation current, I_H, is implicated in the repolarization of the membrane potential from the hyperpolarization associated with the "wave" component of cortically generated spike-wave complexes [11], and in the production of subsequent paroxysmal depolarizing shifts (see also section **5.6**).

Thus, a mosaic of intrinsic cell properties, changes in extracellular ion concentrations, as well as intracellular acidification [12], may play a role in the induction and/or duration of seizures.

However, the decisive role in the spread of focal or widespread synchronization of cellular discharges is played by neuronal circuitry. This view, which arises from *in vivo* investigations on brain-intact animals, was also expressed by some *in vitro* investigators who regarded epileptic properties as requiring activities in intact neuronal circuits. Thus the "need to refocus our attention on circuitry" was emphasized, and it was stated that the results from *in vitro* slices "do not argue that there are no epileptic cells per se, but do indicate that expression of epileptic properties require a minimum circuitry and/or environment" [13]. In the same vein, other investigators studying neocortical slices assumed that, although small regions of cortex may sustain synchronous activity, such limited circuits are not adequate to support spontaneous oscillations for prolonged periods of time [14].

This chapter will mainly focus on network operations underlying various forms of paroxysmal activities but will also provide data on intrinsic neuronal properties implicated in seizures. The available evidence points to the progressive build-up of seizures through synaptic operations within the cerebral cortex, the role of

[6] Zuckermann and Glaser (1968). This study was performed ***in vivo***. In hippocampal slices too, perfusion with elevated K^+ is a common procedure for eliciting paroxysmal activity (Traynelis and Dingledine, 1988; Leschinger et al., 1993), similar to that occurring in tonico-clonic seizures.

[7] Connors (1984).

[8] Schwartzkroin and Prince (1978); Gutnick et al. (1982). Bursting neurons are located prevalently, but not exclusively (Chen et al., 1996; Nishimura et al., 2001), in layer V (see Connors and Amitai, 1995). Layer V neurons that have been partially deafferented, an experimental condition that increases the propensity to seizures (see section **5.9**), have higher input resistance and longer time constants than controls (Prince and Tseng, 1993). In such neurons, the decrease in the slow Ca^{2+}-activated K^+ current ($I_{K(Ca)}$) that underlies the spike afterhyperpolarization may lead to an increased input-output function of neurons and thus contribute to the generation of seizures. Similar changes in intrinsic neuronal properties of CA1 hippocampal pyramidal cells have been reported after kainic acid lesions (Franck and Schwartzkroin, 1985) that are known as an effective tool for triggering seizures.

[9] Rudy and McBain (2001) were "unaware of any neuronal type capable of sustained or repetitive high-frequency firing that does not express at least one of the Kv3.1-Kv3.4 genes" (p. 520).

[10] Westerfield et al. (1978); Manor et al. (1991).

[11] Timofeev et al. (2002a).

[12] Xiong et al. (2000). In this study, intracellular pH (pH_i) was investigated in hippocampal slices from the dentate gyrus. During seizures induced by low-Ca^{2+}, high-K^+ perfusion, manipulation of pH_i changed the duration of large-amplitude population "spikes", with acidification resulting in the early termination of paroxysmal activity.

[13] This conclusion belongs to a chapter by Schwartzkroin (1983) in a symposium volume on neuronal hyperexcitability (p. 99–100).

[14] Chagnac-Amitai and Connors (1989).

[15] Pedley (1987).

[16] Kellaway et al. (1960).

[17] Thomas and Klass (1968); Hughes (1980).

[18] Reiher et al. (1977); White et al. (1977).

[19] Lipman and Hughes (1968).

synaptic interactions between inhibitory and projection neurons within the thalamus, the control of thalamic neurons by corticofugal projections during different types of paroxysmal activity, the short- and long-range projections linking hippocampus with related systems in seizures, and the role of cholinergic and other generalized modulatory systems in altering the susceptibility to paroxysms. All these data, presented below in different sections, justify experimental designs in intact-brain animals.

5.1. Patterns of different epileptic seizures in humans and animals

Before a classification of epileptic seizures and a description of their phenomenology, some patterns that mimic paroxysmal discharges [15] should be briefly mentioned.

Some of the EEG entities that may seem, but are not, epileptogenic include:

(a) 14- and 6-Hz positive EEG "spikes" associated with paroxysmal abdominal pain and autonomic disturbances [16].

(b) "Phantom spike-wave bursts" at ~6 Hz, with a very short duration, which do not necessarily indicate epileptic seizures but, if their amplitudes exceed ~50 μV, may predict the occurrence of seizures in more than half of subjects investigated [17].

(c) Small sharp EEG "spikes", with exceedingly short duration (<70 ms), also called benign epileptiform transients of sleep, that have little or no relation to epilepsy [18].

(d) Rhythmic mid-temporal wave-bursts at a frequency of about 5–7 Hz, which mainly occur during drowsiness and have little or no relation to psychomotor seizures within the same frequency band [19].

Despite the great diversity in the EEG patterns and clinical manifestations of epileptic syndromes, common neuronal mechanisms may underlie a series of electrical paroxysms. These mechanisms are best studied by using multi-site extra- and intracellular recordings *in vivo* and *in vitro*. Because our experimental data that aimed to reveal the intracellular mechanisms underlying brain paroxysms, which is the aim of this chapter, have mainly addressed seizures with electrographic patterns resembling those observed in absence epilepsy and Lennox–Gastaut syndrome, I shall focus in more detail on these entities (sections **5.5** and **5.6**).

Firstly (section **5.2**), I discuss the development of seizures, often without discontinuity, from various types of normal brain oscillations, particularly those that define drowsiness, somnolence or slow-wave sleep (SWS) – behavioral states during which many types

[20] Niedermeyer (1999a).

[21] Steriade and Amzica (1999).

[22] Gotman and Marciani (1985).

of seizures preferentially occur. Although it is commonly assumed that SWS rhythms are only within the relatively low frequency range (<15 Hz), fast (20–60 Hz) and very fast (80–200 Hz) rhythms also occur over the depolarizing phase of the cortically generated slow sleep oscillation (0.5–1 Hz) (see section *3.2.3.2* in Chapter 3), and both low-frequency and very fast-frequency rhythms may evolve under particular conditions into electrical paroxysms that mimic various EEG patterns of clinical seizures. As will be shown in section **5.2**, the appearance of peculiar oscillations with increased amplitudes may reliably predict the occurrence of seizures and, thus, the analysis of their underlying mechanisms may open new therapeutic avenues.

Next (section **5.3**), I deal with afterdischarges (ADs) that follow brain electrical stimulation or repetitive sensory (photic and auditory) signals. As is the case with normal oscillations developing into paroxysmal ones (section **5.2**), the patterns of ADs may faithfully reproduce, often with higher amplitudes and changing features, the shape and frequency of responses elicited by repetitive stimuli. Although epileptic seizures are defined by their "spontaneous", repetitive recurrence, the analysis of electrically and sensory evoked ADs at the intracellular level provides insights into the mechanisms of reflex epilepsy. Indeed, cerebral scars, synchronous stimuli applied to central pathways, and repetitive sensory volleys, such as stroboscopic flash-lights and repeated sounds, all acting on a hyperexcitable cortex, can trigger epileptic seizures in susceptible animals and humans.

The characteristics of EEG interictal "spikes" or "polyspikes", their difference from full-blown seizures in cortical and thalamic neurons, and the role played by intrinsic membrane properties and excitatory/inhibitory synaptic coupling in their generation are analyzed in section **5.4**. These paroxysmal events, with short duration (20–70 ms) on conventional EEG paper recordings [20] but up to ~200 ms with intracellular recordings from neocortex [21], may be isolated, interictal, postictal, and their frequency may increase after a seizure [22]. Although such unitary events are basic elements of paroxysmal activity and their rhythmic recurrence may reliably announce the onset of a fully developed seizure (see section **5.6**), not all of them reflect an epileptic condition and some are physiological waves that should be distinguished from pathological ones on the basis of morphology and especially age, as EEG "spikes" of old age do not have the same significance as in a newborn [20].

In section **5.5** I discuss the mechanisms of seizures consisting of typical spike-wave (SW) or polyspike-wave (PSW) complexes at ~3 Hz, lasting more than 3–5 s and less than 30 s, as in absence

(petit-mal) epilepsy. Although 3 Hz is the classical frequency of SW/PSW complexes, they may be faster at the onset of the seizure and slow down to 3 Hz or 2.5 Hz at the end of the paroxysmal episode [20]. The relatively faster (4–5 Hz) SW complexes with shorter duration seem to occur preferentially in subjects older than 15 years [23]. Clinically, these seizures are defined as a paroxysmal loss of consciousness only, with abrupt and sudden onset and offset, without aura or postictal state, accompanied by tonic deviation of gaze. The sudden impairment of responsiveness may also be associated with different degrees of other motor (clonic, tonic or atonic) components [24]. Absence seizures are primarily a disease of childhood and adolescence, with a peak at about age 6–7 years, but typical absence seizures, with SW complexes at 3 Hz and rolling up of the eyeballs, have been observed as early as 6 months [25]. The term *absence* is valid only for those seizures that occur during wakefulness because during natural sleep, when there is an increased incidence of such paroxysms (see section **5.5**), or in experimental animals under anesthesia, the subjects prone to these seizures are already quite absent. I would refrain from commenting on the habit of some investigators who are working on isolated brain slices and still use the term *absence seizures*. Besides, any loss of consciousness is an *absence*, making this term virtually useless when applied to generalized SW seizures [26]. The electrical patterns of these seizures will be analyzed extensively in section **5.5** because of the large numbers of experimental studies using intracellular recordings in neocortex and thalamus, both *in vivo* and *in vitro*, to elucidate the mechanisms underlying the EEG "spike" and "wave" components, as well as the origin of these seizures, usually defined as suddenly generalized and bilaterally synchronous. This definition originated with the concept of a deeply located "centrencephalic" system [27] and the fact that so-called "absence" seizures were induced in the cortex by electrical stimulation of midline thalamic nuclei at 3 Hz, at a critical level of barbiturate anesthesia [28]. In that study, only SW-like *responses* were evoked in the cortex, but no self-sustained activity. As to the existence of a "centrencephalic" system that would produce bilaterally synchronous SW complexes, it should be mentioned that there are no bilaterally projecting thalamic neurons. Brainstem core neurons with generalized projections disrupt, rather than produce, SW seizures [29]. A series of experimental studies, to be reported in section **5.5**, point to the progressive build-up of SW/PSW seizures at ~3 Hz that obey the rule of synaptic circuits, sequentially distributed through short- and long-range circuits in corticocortical and corticothalamic synaptic networks. Earlier and more recent EEG studies and toposcopic analyses

[23] Gastaut (1968).

[24] Dreifuss (1997). The classification of epileptic seizures in the chapter by this author was dictated by several factors, among them the need for an appropriate therapy. However, the author recognized, in the line of an idea expressed by John Hughlings Jackson, a pioneer of clinical neurology in the United Kingdom (see Chapter 1), that a utilitarian classification may be different from a scientific one based on morphological and physiological criteria. Jackson made the first distinction between generalized absence seizures and partial epileptic fits. For the first clinical description and origin of the term *absence*, dating back to the early 18th century, and the origin of the term *pyknolepsy* used to describe frequent daily attack, see Dreifuss (1997) and another chapter in the same textbook (Stefan and Snead, 1997).

[25] Cavazzuti et al. (1989).

[26] Porter (1993). Nonetheless, behavioral changes associated with SW seizures in the feline generalized epilepsy model indicate that, even in those animals, using instrumental conditioning procedures, the ability to respond to sensory stimuli was deeply altered during SW complexes, whereas the responsiveness between SW bursts remained unimpaired (Taylor-Courval and Gloor, 1984).

[27] Jasper and Kershman (1941); Penfield and Jasper (1954). Facing the repeated evidence that the "centrencephalic system" that is "found in the diencephalon and mesencephalon" (Penfield and Rasmussen, 1950, p. 19) cannot account for consciousness or for the generation of generalized seizures, Jasper (1990, p. 3–4) quoted a passage of Penfield in which he wrote: "It would be absurd to suppose that this central integration could take place without implication of cortical areas. . . . To suppose that centrencephalic integration is possible without utilization of the cortex would be to return to the thinking of Descartes and to enthrone again a spiritual homunculus in . . . such area as the nearby pineal gland". Also, concerning the origin of generalized seizures, Jasper mentioned the findings of Naquet and colleagues on photomyoclonic epilepsy, who failed to confirm the genesis of such seizures in the "centrencephalic system", the view of Gastaut who proposed instead the "holencephalic" hypothesis as a probable mechanism of generalized seizures, and Gloor's hypothesis on a corticoreticular system, rather than the

centrencephalic one. Gloor's view is probably the closest to the reality (see our data on seizures generated in corticothalamic systems, in the main text of section **5.5**).

[28] Jasper and Droogleever-Fortuyn (1949).

[29] Danober et al. (1995).

[30] Jasper and Hawkes (1938); Petsche (1962).

[31] Lemieux and Blume (1986). In another study, the investigation of apparently bilateral synchronous SW complexes in children with sleep-activated seizures similarly showed that the interhemispheric time differences during SW activity were 12–26 ms (Kobayashi et al., 1994).

[32] Gibbs and Gibbs (1952). Hypsarrhythmia derives form the Greek word *hypselos*, which means high and indicates the high amplitude of paroxysmal EEG waves in this epileptic syndrome.

[33] Gastaut et al. (1966); Niedermeyer (1969).

[34] Niedermeyer (1999b, p. 507).

[35] Gibbs et al. (1939).

[36] West (1841).

[37] Kellaway et al. (1979) distinguished three major groups of infantile spasms: extensor, flexor, and mixed flexor-extensor.

in humans and animals have also indicated that some SW seizures are locally generated and result from multiple, independent cortical foci [30] and topographical analyses of SW complexes in humans showed that the EEG "spike" component propagates from one hemisphere to another with time-lags as short as 15 ms [31], which cannot be estimated by visual inspection. This explains why absence seizures are less detrimental than grand-mal epilepsy, which implicates more widespread neuronal manifestations. Indeed, one of the characteristics of SW seizures is that there is little or no disruption of cognitive abilities after an ictal event. The origin of SW seizures within the thalamus or cortex was and continues to be hotly debated. However, the corticothalamic system is a reciprocally connected loop and, although some studies placed exclusive emphasis on one or another component of this unified entity, a congruent conclusion was ultimately reached; namely, that neocortical excitability represents the leading factor in controlling thalamic events during this type of seizures (see section **5.5**).

Thereafter (section **5.6**) I present data on the cellular bases of electrographic patterns in the Lennox–Gastaut syndrome, a clinical entity related to what is called *infantile spasms*, corresponding to the EEG notion of *hypsarrhythmia* [32]. The major distinction between the infantile spasms and Lennox–Gastaut syndrome [33] resides in age: the infantile spasms occurring between 4 and 30 months, whereas the Lennox–Gastaut encephalopathy usually starts between 1 and 10 years [20]. Otherwise, "no separating line is drawn between the attacks occurring in infantile spasms and Lennox–Gastaut syndrome" [34]. The Lennox–Gastaut syndrome was also called petit-mal *variant* [35] to differentiate its relatively slow (1.5–2.5 Hz) SW complexes from the classical SW complexes at 3–4 Hz occurring in absence epilepsy. The electrographic pattern of the Lennox–Gastaut syndrome is characterized by SW/PSW complexes, often associated with fast runs at 10–20 Hz, but up to 30 Hz (Fig. 5.1), and the background activity may be completely disorganized and chaotic. Clinically, infantile spasms were first described in the mid 19th century by a British physician [36] who gave his name to this epileptic condition, the West syndrome. The triad consists of different forms of spasms, such as myoclonic jerks and flexion spasms [37], EEG hypsarrhythmia, and mental retardation. This is a severe epileptic disorder and, generally, children with abnormal computed tomography do not become normal in follow-up. Although generally placed in the category of generalized seizures, focal clinical seizures are not uncommon and, indeed, our intracellular recordings of an electrographic pattern in cats, resembling that observed in clinical Lennox–Gastaut syndrome (see Fig. 5.1),

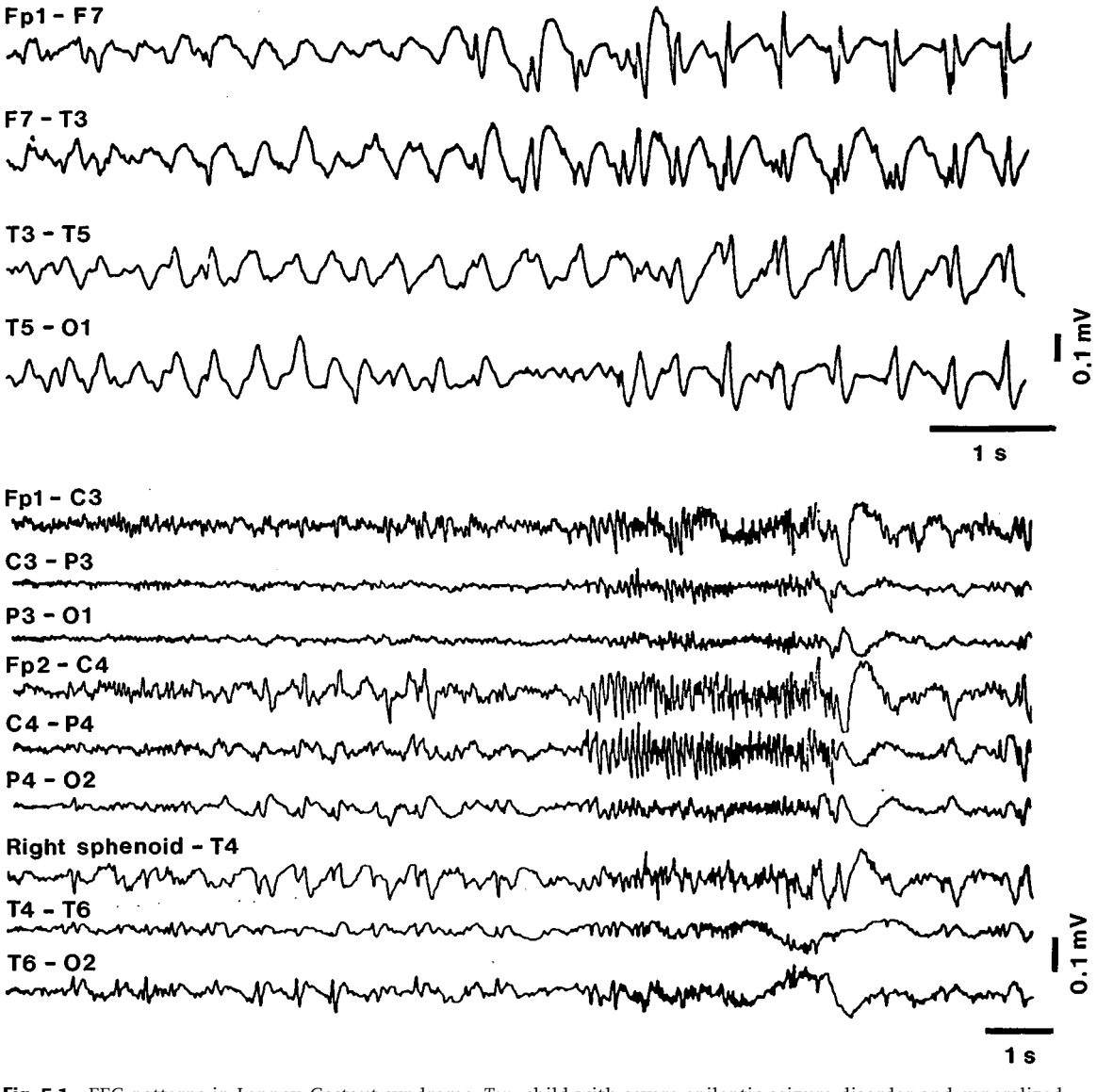

Fig. 5.1 EEG patterns in Lennox–Gastaut syndrome. *Top*, child with severe epileptic seizure disorder and generalized spike-wave (SW) complexes, mostly around 2 Hz. *Bottom*, rapid run in a 19-year-old epileptic patient, with maximum of fast waves in anterior leads. Also note a few slow SW complexes in the right temporo-occipital region. Modified from Niedermeyer (1999 a-b).

[38] This term was introduced by Gowers (1885).

[39] Zifkin and Dravet (1997).

[40] This term was introduced by Jasper et al. (1951).

[41] Gibbs et al. (1938); Lennox (1951).

[42] Feindel and Penfield (1954).

[43] Gloor et al . (1982); Gloor (1992).

[44] Gloor (1997).

demonstrate that the onset of many such spontaneously occurring seizures occurs focally in the neocortex, only to spread subsequently to thalamus (see section **5.6**).

Section **5.7** deals with grand-mal [38], tonico-clonic seizures. As such paroxysms with rich motor activity [34, 39] cannot easily be explored intracellularly in behaving animals that display convulsions, since intracellular recordings require perfect stability, I do not have personal experimental data with such seizures. In that section, I will only briefly describe the cellular and molecular processes that have been tentatively implicated in these seizures.

Mesial structures in the temporal lobe, including hippocampus and related systems (among them, parahippocampal gyrus and amygdala nuclear complex), play an important role in seizures that are included in the category of "temporal lobe epilepsy" [40]. The cellular mechanisms of seizures occurring in the hippocampus and amygdala are discussed in section **5.8**. Although some use the term temporal lobe epilepsy (TLE) as a synonym for psychic or psychomotor (complex partial) seizures [41], many patients with TLE have grand-mal seizures and some psychic seizures may arise from the fronto-orbital region [34]. Clinically, many patients with psychic seizures display déjà vu manifestations, first described by Hughlings Jackson [24], and have an emotional aura. A hallucinatory, dreaming-like experience and/or a feeling of strangeness often announce these seizures. These experiential phenomena have been intensively investigated since Jackson [24] and, more recently, by Penfield and his collaborators [27, 42] and Gloor [43, 44]. The hallucinations are mainly visual or auditory. Experiential phenomena can be affective, perceptual, and mnemonic, and they include elements from the individual's past. The most common affect is fear, from mild anxiety to terror, and arises suddenly. Fear can be elicited by stimulation of the amygdala [43]. It is known that wild monkeys are transformed into docile animals if the amygdala is lesioned and patients with bilateral lesions of the amygdala nuclear complex are unable to recognize facial expressions of fear (see ***2.2.3*** in Chapter 2). Positive emotions are less often seen in TLE and they may consist of exhilaration and erotic feelings. The mnemonic-like phenomena occurring in TLE are déjà vu illusions, which can also be elicited by electrical stimulation of the temporal lobe, and memory recall. In Gloor's data, the incidence of memory recall was higher by stimulating the amygdala than the hippocampus [44]. The mnemonic events evoked by seizures or electrical stimulation are explained by a series of parallel-distributed neuronal networks, including the direct projections from the amygdala, as well as amygdala projections mediated by perirhinal cortices, to

association neocortical areas implicated in polymodal sensory integration [45]. The onset of experiential phenomena in TLE is most often the amygdala, followed by the hippocampus [46], while scalp recordings generally fail to display significant changes in EEG. Indeed, psychomotor or complex partial seizures are more likely to occur when abnormal EEG signs are confined to the temporal lobe [47].

Brainstem seizures occur using auditory stimulation in rats with massive ablation of forebrain structures [48] and stimulating the brainstem reticular core of cats and rabbits with precollicular transection [49]. In contrast to forebrain seizures, brainstem-induced paroxysms are mainly tonic, with running/bouncing convulsions [50]. As yet, there is no intracellular analysis of brainstem-evoked seizures. There are controversial results concerning the requirement of an intact brainstem for the expression of forebrain-induced seizures [51] or the possibility of eliciting seizures in animals with precollicular transection [52]. It seems that the brainstem is not required for seizures induced by convulsant agents in a highly discrete epileptogenic site within the deep prepiriform cortex, area tempestas [53].

In section **5.9** I discuss the cellular aspects of seizures occurring after injury and deafferentation of cortical and thalamic tissues. Postlesional epilepsy accounts for more than 10% of the epilepsies with a defined cause [54]. Cortical lesions result in the development of chronic epileptogenesis [55]. The question of whether the cerebral cortex displays autonomous activity [56] or exhibits activity only when driven from other sources [57] has been the subject of hot debate. The absence of activity in earlier experiments on isolated cortical tissue [57] could have been due to cortical hypoxia, as more recent studies demonstrate that, although quite dissimilar to the activity of intact cortex, small isolated neocortical slabs display periods of spiking activity interspersed with long epochs during which miniature postsynaptic potentials (PSPs) are observed [58]. Cortical slabs isolated from human cortex at the time of surgery display paroxysmal, high-voltage activity [59]. Such epileptiform events may occur as a result of hypersensitivity by denervation, which is apparent in almost all investigated tissues, from the smooth and skeletal muscles to glands and neurons [60]. The value of this hypothesis was recently demonstrated by the higher incidence of spontaneous and electrically induced seizures in cortical slabs or undercut cortex *in vivo* [61]. One of the mechanisms underlying the appearance of stroke-induced epileptic foci could be the hyperexcitability in hypoperfused peri-ischemic areas [62]. Experimentally, pronounced hyperexcitability also occurs

[45] Amaral and Price (1984); Amaral et al. (1992).

[46] Fish et al. (1993).

[47] Gabor and Ajmone-Marsan (1968).

[48] Garcia-Cairasco et al. (1993).

[49] Kreindler et al. (1958). The results of this study, conducted in cats, were confirmed in rabbits by Bergmann et al. (1963) who circumscribed in the midbrain reticular core a low-threshold convulsive area.

[50] Browning and Nelson (1986).

[51] Velasco and Velasco (1990).

[52] Magistris et al. (1988).

[53] Browning et al. (1993).

[54] Annegers (1994).

[55] For a review of techniques used in chronically isolated cortical tissue, see Halpern (1972).

[56] Bremer (1958a).

[57] Burns (1951, 1958).

[58] Timofeev et al. (2000a).

[59] Echlin et al. (1952).

[60] Cannon and Rosenblueth (1949). The hypersensitivity by denervation may explain some unexpected results, such as the increased duration of wakefulness after chronic excitotoxic lesions of the midbrain reticular neurons. Such lesions firstly produce a loss of the waking state, but the time spent in wakefulness is increased 7–8 days after the lesion (Kitsikis and Steriade, 1981), probably due to an increased excitability of denervated structures (thalamus and basal forebrain) that are targets of midbrain reticular neurons and are also implicated in cortical activation.

[61] Topolnik et al. (2001, 2003).

[62] Pohlmann-Eden et al. (1996).

in remote brain areas after focal ischemia, as demonstrated by multi-unit recordings [63]. The mechanisms accounting for epileptogenesis in the injured and isolated brain tissue have been investigated using intracellular recordings *in vitro* and *in vivo* (see section **5.9**).

Experimental data substantiating the hypothesis of a dialogue between neurons and glia in epilepsy [64] have been obtained in studies of hippocampus and neocortex since the 1960s [65], in more recent *in vitro* studies [66], and by using dual intracellular recordings of these two cellular types *in vivo* [67]. These data are discussed in section **5.10**. The potential importance of glial cells in the synchronization and propagation of paroxysmal activity is due to the presence of receptors for different neurotransmitters (such as glutamate and GABA) on membranes of glial cells [68], the release of some transmitters by glial cells [69], and the display of intrinsic Ca^{2+} oscillations [70]. Thus, glial cells cannot be simply thought of as passively reflecting neuronal activity.

Finally, the effects of epileptic seizures on sleep cerebral states are discussed in section **5.11**.

5.2. Sleep and epilepsy: normal oscillations during non-REM sleep developing into seizures

The adage "sleep and epilepsy are common bedfellows" is supported by much clinical and experimental evidence showing that epileptic seizures of different types preferentially occur during slow-wave sleep (SWS or non-REM), whereas REM sleep is a relatively non-epileptic state [71] (see details in sections **5.5** and **5.6**).

The prevalence of paroxysmal activity during SWS is observed not only with full-blown seizures but also with interictal EEG "spiking". Most patients show maximal EEG "spiking" in SWS stages 3 and 4; because of less frequent interictal "spikes" in waking and REM sleep, recordings during these states of vigilance provide better localization of these signs for the presurgical assessment of temporal lobe epilepsy [72].

5.2.1. From low-frequency (7–15 Hz) sleep rhythms or augmenting responses to seizures

Although the clinical loss of consciousness in absence epilepsy with ~3-Hz SW complexes is only evident when such seizures occur during the waking state, the electrical correlates of these seizures preferentially appear during SWS, more often in early stages 1–2, and less often in stages 3–4, toward the end of SWS, when the

[63] Witte and Freund (1999).

[64] Orkand (1969).

[65] Grossman and Hampton (1968); Sypert and Ward (1971); Dichter et al. (1972). The density of neurons and glia in resected tissue from patients with temporal lobe epilepsy was analyzed and the authors concluded that glial density influenced the transition from interictal to ictal states, while neuronal density influenced the propagation of seizures (Spencer et al., 1999).

[66] In slices from the sclerotic CA1 area of chronic epileptic humans and pilocarpine-induced seizures in rats, Heinemann et al. (2000) found that, in areas of reduced neuronal density, there is an impairment of glial capacity for spatial K^+ buffering.

[67] Amzica and Steriade (1998b, 2000); Amzica and Neckelmann (1999); Amzica et al. (2002).

[68] Bormann and Kettenmann (1988); MacVicar et al. (1989); Steinhäuser and Gallo (1996).

[69] Levi and Gallo (1995); Araque et al. (1999).

[70] Parri et al. (2001) reported that recurrent astrocytic Ca^{2+} transients take place every 5–6 min, propagate through the glial syncytium, and trigger glutamate-dependent activity in neurons.

[71] Mahowald and Schenck (1997).

[72] Sammaritano et al. (1991).

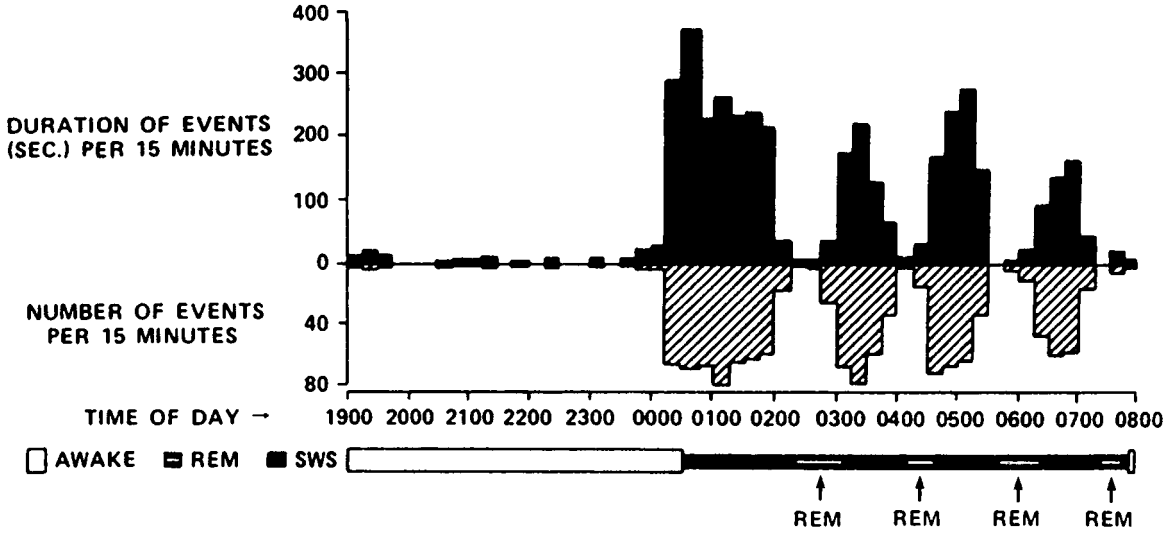

Fig. 5.2 The duration and number of SW complexes during waking, SWS, and REM sleep during the night in humans. Note the greatest incidence of SW complexes at the onset of SWS and obliteration during REM sleep. Abscissa shows the time of day and night. Modified from Kellaway and Frost (1983).

[73] Ross et al. (1966); Sato et al. (1973).

[74] Kellaway (1985). Shouse et al. (1996) discussed the possible relation between K-complexes, a major electrographic sign of light sleep, and childhood absence epilepsy. Basically similar relations between the K-complex in intracellular activities of cortical neurons and field potentials have been found during slow sleep oscillation and the paroxysmal events during complex SW seizures, the latter being just an exaggeration in amplitude and increase in frequency of the former (Steriade et al., 1998a; see sections **5.6**).

[75] Steriade (1974).

rhythmicity of SW complexes declines [73]. The appearance of seizures with pure SW and/or SW/PSW complexes at about 3 Hz during the early SWS stages is usually explained by their close relationship with sleep spindles at 7–15 Hz [74], which are a hallmark of stage 2, although experimental data show the presence of neocortical SW seizures in the absence of the thalamus and spindles (see section ***5.5.3***). Figure 5.2 shows the much higher incidence of 3-Hz SW complexes at the onset of SWS in humans, their decrement during successive SWS cycles, and their virtual absence in REM sleep.

The relation between sleep spindles and SW seizures is supported by animal experiments in which augmenting responses, the model of spindles (see section **4.2** in Chapter 4), lead progressively to self-sustained, epileptiform activity. Several forms of such transformations, from normal to paroxysmal events, have been reported. In chronically implanted, naturally drowsy or sleeping macaques, stimulation at 10 Hz (within the frequency range of spindles) applied to the motor thalamus elicits augmenting responses in precentral motor cortex, followed by typical SW complexes at ~3 Hz in the cortical depth, sometimes without reflection at the cortical surface (Fig. 5.3). The fact that the SW electrical seizure activity was only seen in the cortical depth suggested that intracortical, focal potentials generate this type of paroxysmal activity [75], which only

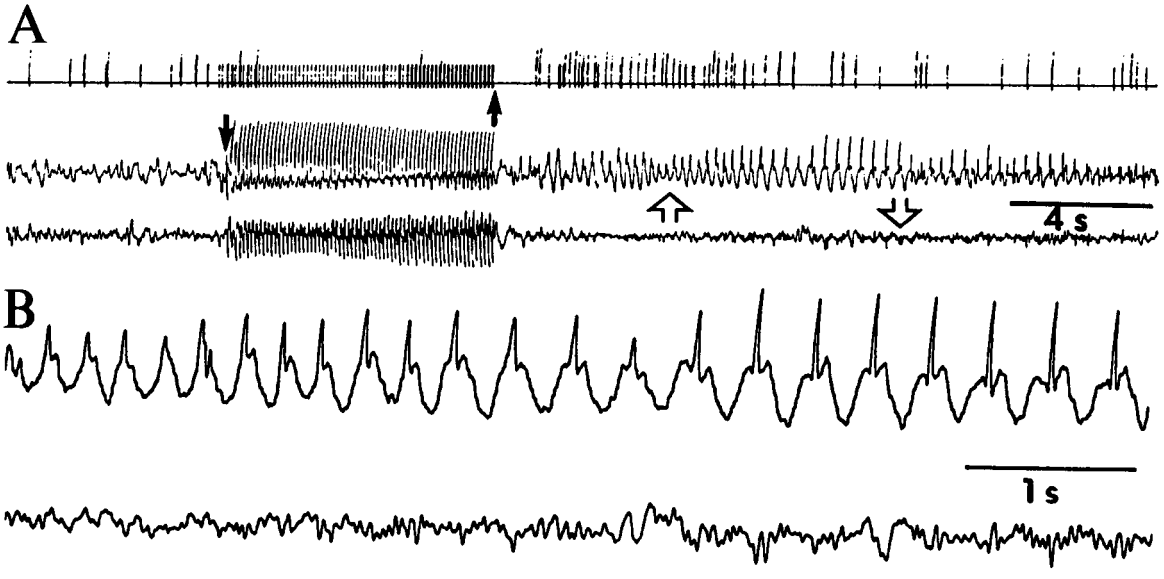

Fig. 5.3 Thalamic stimulation at 10 Hz elicits augmenting cortical responses, followed by self-sustained SW complexes at ~3 Hz. Chronically implanted monkey (*Macaca mulatta*) during a state of drowsiness. *A*, three ink-written traces show (from top to bottom): unit spikes (used to deflect the pen of the EEG machine; each deflection exceeding the lowest level represents a group of high-frequency discharges), focal slow waves (recorded by the same microelectrode as used for unit recording), and EEG surface waves. *B*, expanded portion of EEG activities depicted between arrows during self-sustained seizure in *A*. In depth- and surface-EEG recordings, positivity downwards. Modified from Steriade (1974).

[76] Golshani et al. (2001).

[77] Steriade and Contreras (1995).

subsequently spreads to other cortical areas and thalamus. Supporting evidence for the cortical generation of SW seizures is fully reported in section **5.5**.

Cortical augmenting responses are reflected in the thalamus. In particular, thalamic reticular (RE) GABAergic neurons are driven by corticofugal volleys more efficiently than thalamocortical (TC) neurons, because the numbers of some glutamate receptor subunits are much higher at corticothalamic synapses in RE neurons, compared to TC neurons [76] (see section ***2.4.3*** in Chapter 2). This accounts for the RE-mediated inhibition of the majority of TC neurons during cortically generated SW seizures (see section **5.5**). During the self-sustained seizure that follows thalamic stimulation eliciting augmenting responses at 10 Hz or during seizures developing "spontaneously" from the slow sleep oscillation, each paroxysmal depolarizing shift (PDS) in cortical neurons is faithfully followed by target RE neurons [77]. This is illustrated in Fig. 5.4, depicting a cortical seizure triggered by a pulse-train applied to the thalamic ventrolateral (VL) nucleus at a frequency (10 Hz) that is generally used to evoke augmenting responses. With a 10-Hz stimulation lasting 2 s, a 20-s electrical seizure was induced in the cortex and, without exception, every

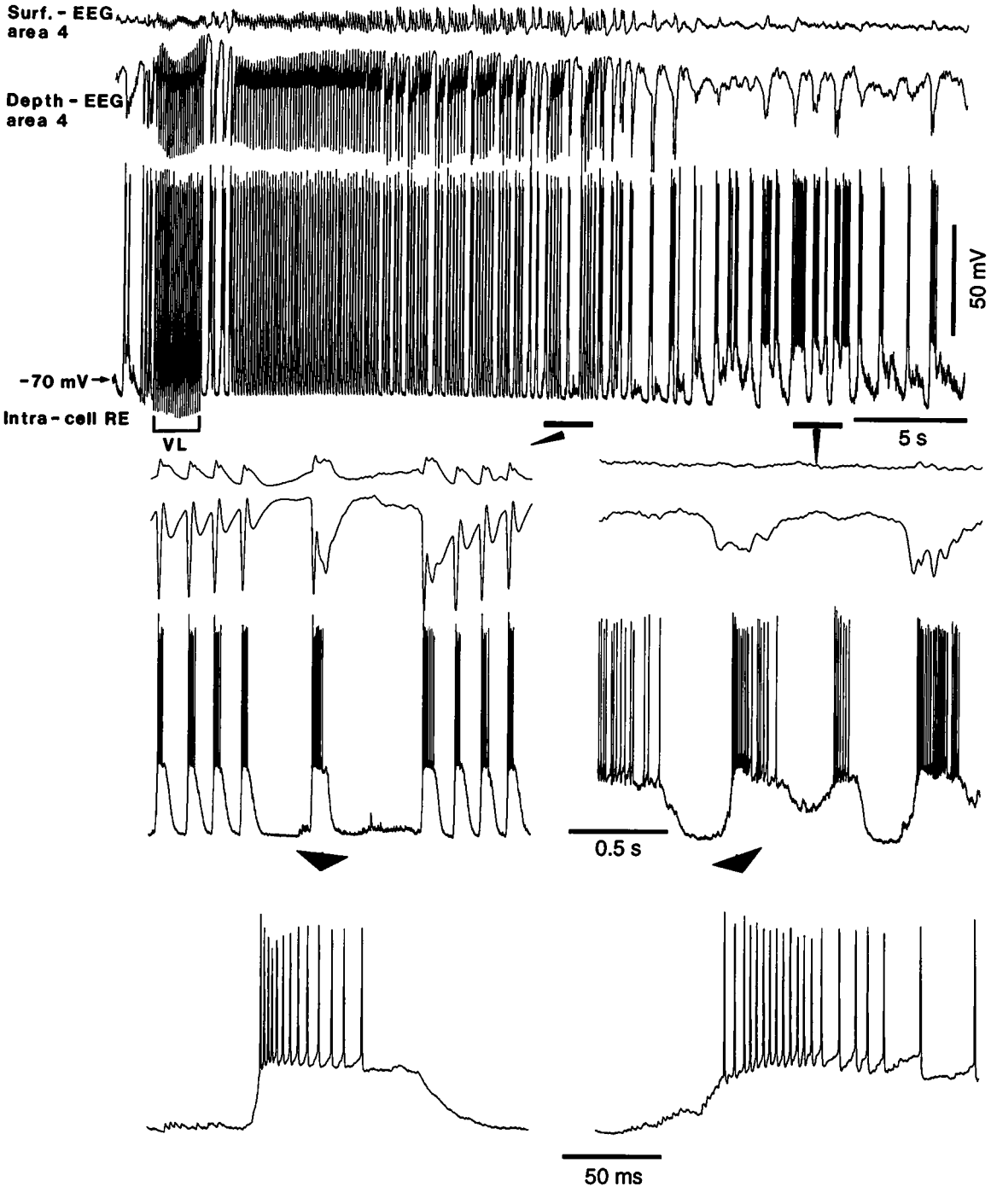

Fig. 5.4 Burst discharges in thalamic RE neurons follow normal and paroxysmal synchronous activities in neocortex. Cat under ketamine-xylazine anesthesia. Intracellular recording of RE neuron (rostral pole), together with surface- and depth-EEG from motor cortex (area 4). Stimulation at 10 Hz, lasting 2 s, was applied to thalamic VL nucleus (indicated by bar). Seizure lasted for ~20 s. Two parts marked by horizontal bars are expanded below (arrowheads). Each cortical paroxysmal depolarizing shift (PDS) was followed by a spike-burst in the RE neuron (middle panel, left). After seizure cessation, an episode of slow oscillation is seen and each depth-negative (excitatory) component in the cortical EEG is similarly followed by a spike-burst in the RE neuron (middle panel, right). One burst from each period (seizure and slow oscillation) is further expanded below. Note at bottom right, the accelerando-decelerando pattern, typical of RE neurons during sleep oscillations. From Steriade and Timofeev (2001).

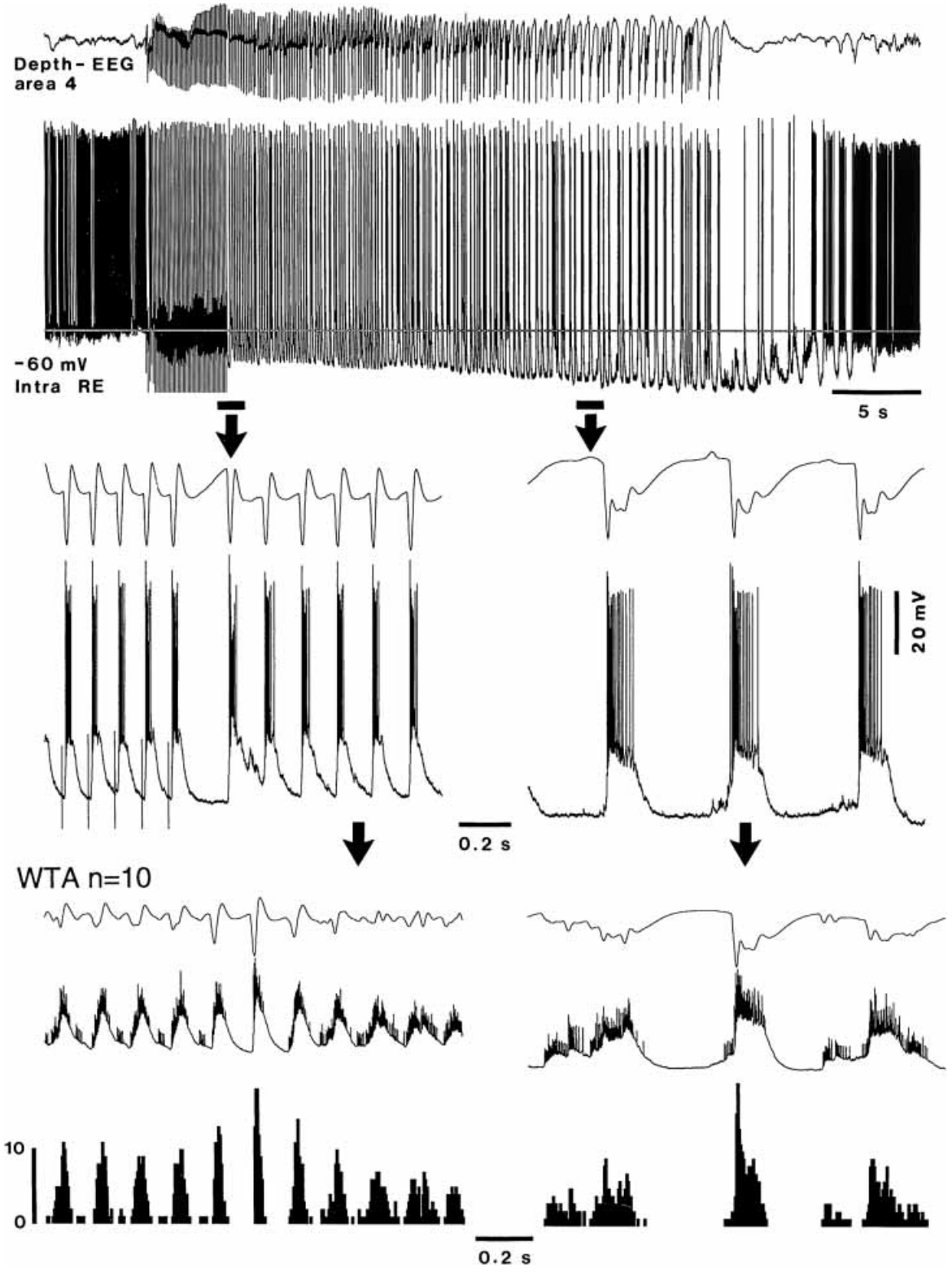
Depth - EEG
area 4
-60 mV
Intra RE
5 s
20 mV
0.2 s
WTA n=10
10
0
0.2 s

[78] Steriade et al. (1993f). Earlier data also showed that augmenting responses can be elicited in primary somatosensory cortex by 10-Hz stimulation of white matter, in animals with complete lesion of the thalamic ventrobasal complex, and that augmenting responses develop into self-sustained seizures (Steriade and Yossif, 1974).

PDS in the EEG recorded from the cortical depth was associated with a high-frequency spike-burst in the intracellularly recorded RE neuron (middle and bottom left panels). Outside the seizure epoch, when the neuron resumed its slowly rhythmic pattern, the depth-negative field potential of the slow oscillation (reflecting summated depolarizations and firing in a pool of cortical neurons) invariably triggered spike-bursts with accelerando-decelerando patterns (middle and bottom right panels), typical of RE neurons during SWS.

Stimulation of dorsal thalamic nuclei at 10 Hz elicited self-sustained activity that was initiated at the same frequency, and displayed the same pattern, as responses evoked by electrical stimulation. Thus, the cortical seizure started with runs at ~9–10 Hz and then shifted to SW and PSW complexes at ~2 Hz. The increased number of action potentials in RE cell, from single spikes or spike-doublets to high-frequency spike-bursts, probably occurred through progressive hyperpolarization of the RE cell (Fig. 5.5). The progressive hyperpolarization was associated with an increasing number of spikes per burst. Averaged activities triggered by the depth-negative cortical waves during both the initial runs at ~9 Hz and SW/PSW complexes at ~2 Hz showed the synchronous cortico-RE discharges in both components of the seizure (bottom panels in Fig. 5.5).

Other data on the progressive transformation of augmenting responses into cortical SW seizures are reported in section ***4.3.3*** of Chapter 4 (see Fig. 4.45 in intact corticothalamic systems and Fig. 4.49 in isolated neocortical slab).

The fact that cortical networks alone, in the absence of the thalamus, are able to develop both augmenting responses and self-sustained seizures was demonstrated in athalamic animals [78]. Figure 5.6 shows that repeated pulse-trains at 10 Hz, eliciting augmenting responses in callosal pathways, are associated with depolarization (7 mV) and an increased number of action potentials in spike-bursts, eventually followed by a self-sustained seizure consisting of two components: (*a*) relatively short (~50 ms) spike-bursts,

Fig. 5.5 (opposite) Self-sustained seizure in the neocortex and an RE neuron, elicited by dorsal thalamic stimulation at 10 Hz. Cat under ketamine-xylazine anesthesia. Intracellular recording of a rostral RE neuron together with depth-EEG from area 4. Stimulation consisted of pulse-trains (10 Hz, 5 s) applied to the ventrolateral (VL) nucleus. Parts indicated by horizontal bars below the intracellular trace are expanded below (arrows). The seizure started with runs at ~9 Hz, close to the frequency used during the stimulation period, and then shifted to SW and PSW complexes at ~2 Hz. Bottom panels depict wave-triggered averages (WTA) from the two epochs of fast runs (left) and SW/PSW complexes (right). Reference time was the depth-negative field potentials from area 4. Note that the RE neuron was progressively hyperpolarized during the seizure induced by electrical stimulation of the dorsal thalamus. From Timofeev et al. (1998).

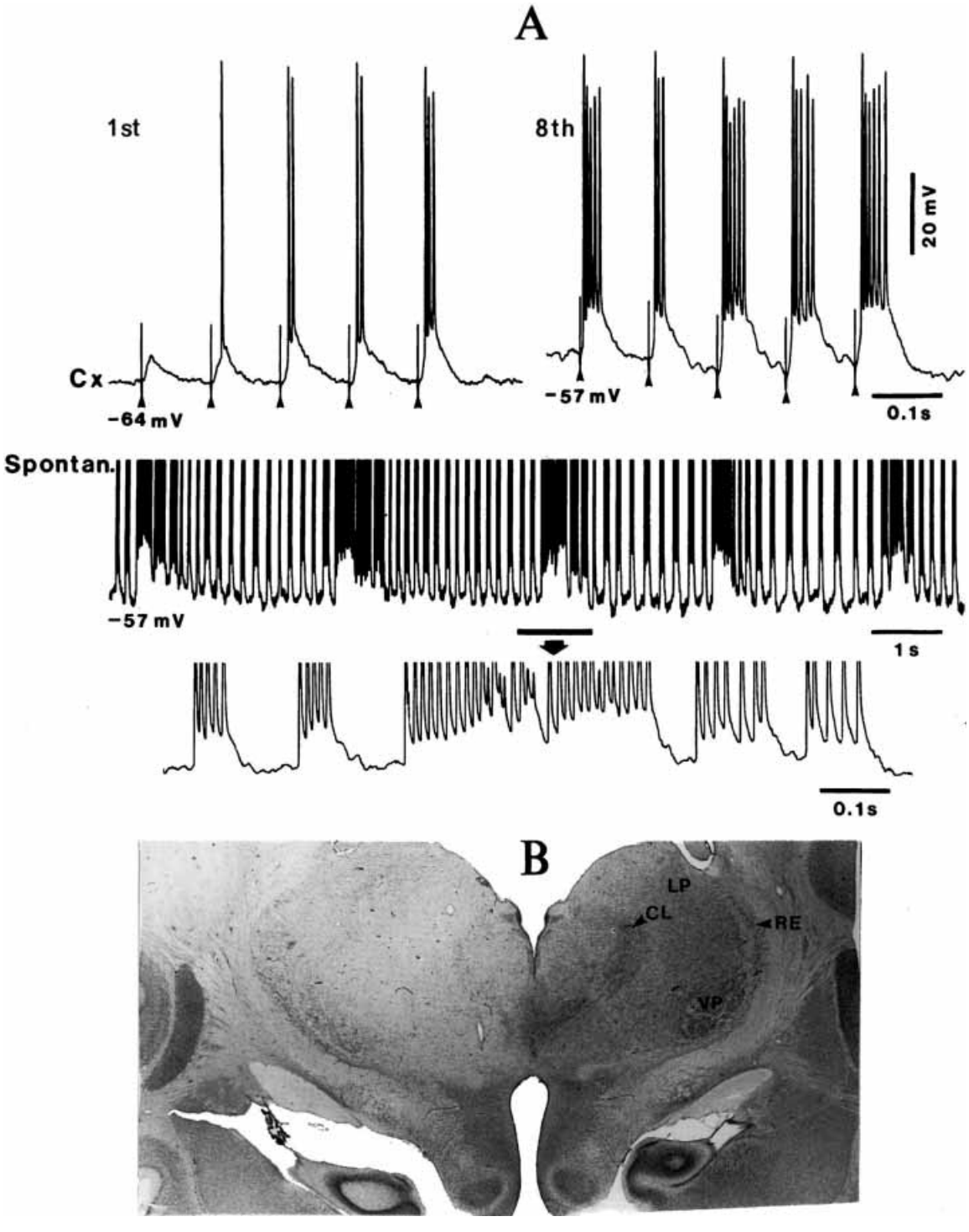

Fig. 5.6 Self-sustained seizure in a neocortical neuron after augmenting responses evoked by rhythmic callosal stimulation of the homotopic point in the contralateral hemisphere. Thalamically lesioned cat by means of kainic acid (see *B*). Urethane anesthesia. Intracellular recording of neuronal activity at a depth of 1.5 mm in area 7. *A*, responses to pulse-trains (each consisting of five stimuli at 10 Hz), repeated every 3 s, applied to contralateral area 7. The intracortical augmenting responses to the first and eighth pulse-trains are illustrated. Note depolarization by about 7 mV and increased number of action potentials within bursts after repetitive stimulation. Below, self-sustained paroxysmal discharges after augmenting responses (spikes truncated). Period marked by horizontal bar is expanded below (arrow). *B*, thalamic lesion. CL, LP and RE: central lateral, lateral posterior and reticular thalamic nuclei. Modified after Steriade et al. (1993f) and Steriade (1998).

[79] Steriade et al. (1996a-b).

[80] Grenier et al. (2001).

[81] Allen et al. (1992).

[82] Traub et al. (2001).

[83] Bragin et al. (1999a, 2000).

[84] Grenier et al. (2003).

occurring rhythmically within a frequency range close to that used in the preceding period of stimulation; and (*b*) prolonged (500–600 ms) spike-bursts, recurring within the frequency range of the slow oscillation (0.3–0.4 Hz) that dominated the background activity [78].

Thus, spontaneously occurring low-frequency oscillations (such as sleep spindles) or their experimental model (augmenting responses) may lead to self-sustained neocortical seizures, which are initiated at approximately the same frequency as that of spontaneous or evoked waves and develop into SW/PSW seizures at 2–3 Hz.

5.2.2. From very fast (80–200 Hz) rhythms during the slow sleep oscillation to seizures

During SWS, the depolarizing phase of the slow neocortical oscillation includes fast (20–60 Hz) rhythms [79] and very fast (80–200 Hz) rhythms, called ripples [80]. These activities were recorded under anesthesia as well as in chronically implanted, naturally sleeping cats (see section *3.2.3.2* and Figs. 3.40–3.42 in Chapter 3). There are several types of neocortical and hippocampal seizures with fast and very fast oscillatory components, 50–80 Hz [81], 80–130 Hz [82], and 200–500 Hz [83]. The mechanism(s) responsible for the initiation of neocortical seizures from very fast oscillations, in particular from ripples (80–200 Hz), is an important topic as it may lead to therapeutic avenues against seizures.

That ripples recorded during the slow sleep oscillation could play a role in initiating seizures is suggested by the strong correlation between neuronal excitation and the intensity of ripples [80]. To be considered as involved in seizure initiation, neocortical ripples have to be present at the transition between normal and paroxysmal activity, to show significantly increased amplitudes at the very onset of seizure, compared to epochs prior to it, and there should be fewer or no seizures in conditions that diminish neocortical ripples. Recent extra- and intracellular multi-site recordings from different neocortical areas show that, indeed, ripples are particularly strong at the onset of seizures and they decline afterwards, halothane antagonizes the occurrence of both ripples and seizures, and stimulation mimicking the pattern of ripples is a most efficient paradigm to induce seizures associated with ripple activity at the level of field potentials and individual neurons [84]. Some of these data are discussed in section **5.6**, dealing with seizures of the Lennox–Gastaut type. Here, I focus on data using electrical stimulation within the frequency range of ripples (~100 Hz).

The 100-Hz stimulation paradigm faithfully mimics the ripples crowning EEG "spikes" that occur at the onset of seizures. This

is illustrated in Fig. 5.7 by comparing spontaneous and evoked seizures during the same experiment. The 100-Hz stimulation also evokes focal seizures, within the region close to the stimulation, in non-anesthetized, chronically implanted animals [84]. When seizures are elicited using this type of stimulation, ripples appear in the EEG and/or intracellular recordings between trains of stimuli, prior to the occurrence of full-blown seizures, and neuronal activities within ripple frequencies outlast stimulation at 100 Hz, in the form of repetitive action potentials (Fig. 5.8) or subthreshold membrane potential fluctuations. The evoked ripples in paroxysmal neuronal activities are only seen in neocortical neurons, and not in simultaneously recorded thalamocortical neurons (Fig. 5.8).

The relation between ripples and seizures is more than just a temporal correlation, as data suggest that ripples are implicated in the generation of the first EEG "spike" of seizures. During repetitive seizures ripples do not appear with the same intensity *after* the first EEG "spike" is expressed as they should if they were conditional on the occurrence of the seizure. Rather, the first EEG "spike" slowly builds up with ripples present from the beginning of seizure; thereafter, successive EEG "spikes" are associated with less intense ripples (Fig. 5.9). In contrast, foci that follow the primary site display more abruptly rising successive EEG "spikes", with ripples on top of them [84]. This suggests that ripples could be dependent on neuronal depolarization during EEG "spikes" in secondary sites, but that they are involved in generating the first EEG "spike" in the primary site. Seizures in secondary sites are probably triggered by projections from the primary site.

When seizures evolve without discontinuity from the slow oscillation, strong ripples occur just before the transition between normal and paroxysmal activity. The comparison between non-paroxysmal (Fig. 5.9*A*) and the first paroxysmal (Fig. 5.9*B*) EEG-depth negativities (that reflect summated depolarizations in a pool of neurons) shows that they were similar at their onset; however, before the paroxysmal negativity reached the maximal value displayed by the non-paroxysmal one, ripples appeared over it and were present until the negativity reached its full paroxysmal peak. Thus, ripples of strong amplitude are present from the very onset of the transition between normal and paroxysmal activities.

5.3. Electrically and sensory-induced afterdischarges

The afterdischarges (ADs) elicited by electrical stimulation of various brain structures are related to seizures induced by

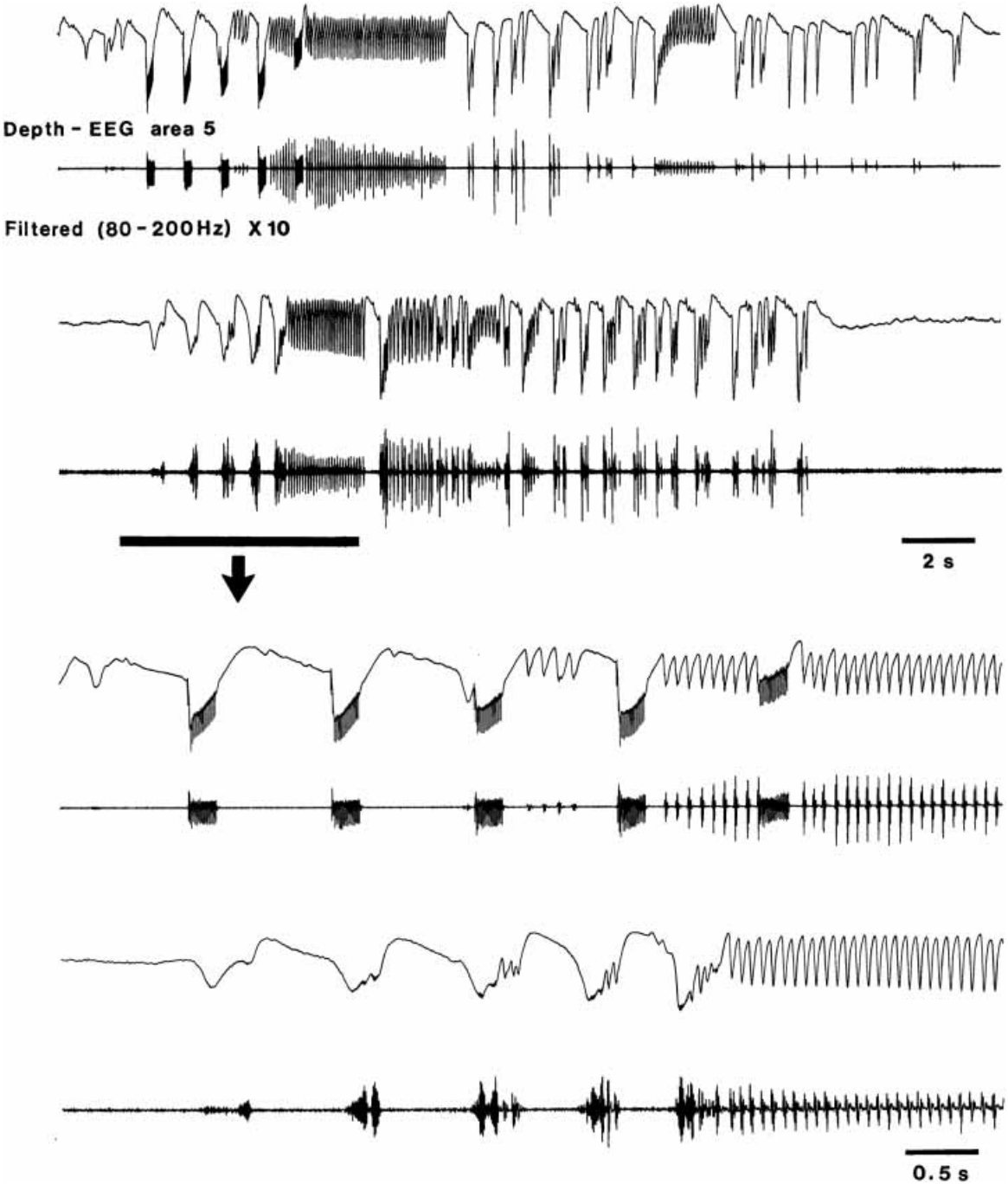

Fig. 5.7 Pulse-trains at 100 Hz mimic the onset of spontaneously occurring seizures. Cat under ketamine-xylazine anesthesia. Field potential recordings from area 7 along with the filtered trace between 80 and 200 Hz (amplified × 10). Top panels display one evoked (above) and one spontaneous (below) seizure from the same experiment. The onset of both seizures is expanded in the bottom panels to show the similarity between the stimulation paradigm (20 shocks at 100 Hz repeated every second) and the EEG "spikes" with ripples at the onset of the spontaneous seizure. From Grenier et al. (2003).

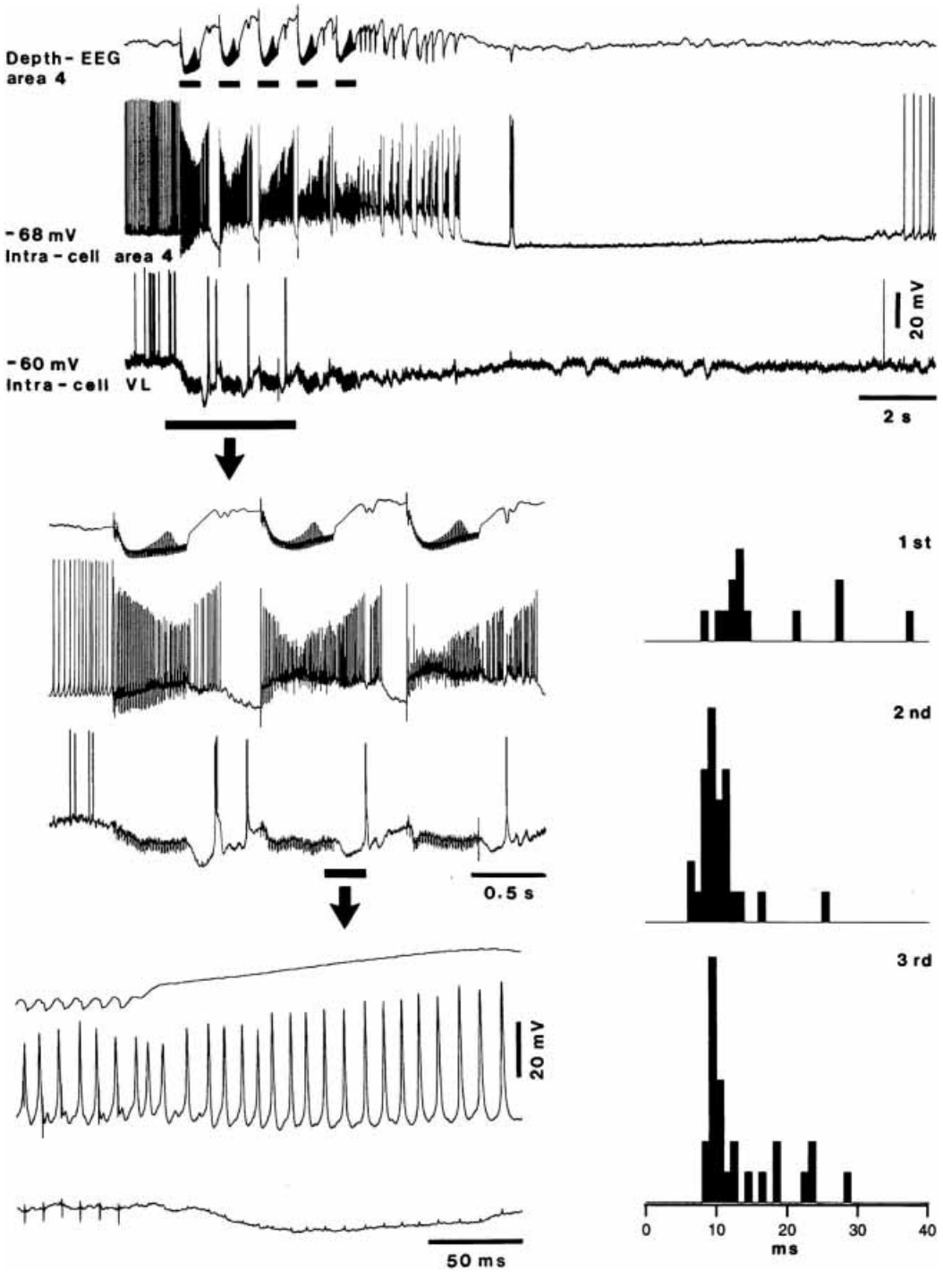

Fig. 5.8 Ripples outlast electrical stimulation at 100 Hz that leads to a self-sustained seizure in neuronal firing. Cat under ketamine-xylazine anesthesia. Dual intracellular recordings from a thalamocortical (TC) cell in the ventrolateral (VL) nucleus and an area 4 cortical cell as well as a field potential recording from area 4. Electrical stimulation of area 4 (five trains of 50 stimuli at 100 Hz, marked by horizontal bars below EEG) led to a brief seizure. The top panel displays the period of stimulation and the ensuing seizure. The first three pulse-trains of stimulation are expanded on the left, in the middle panel. The second pulse-train is further expanded at bottom left. Note the continuation of spikes in the cortical cell after the stimulation has ceased. Note also the absence of 100-Hz activity in the TC cell. On the right interspike histograms (ISIHs) are shown for the periods following the first three trains of stimulation. Note that most ISIs are clustered around values (8–11 ms) corresponding to ripple frequencies between 80 and 120 Hz. From Grenier et al. (2003).

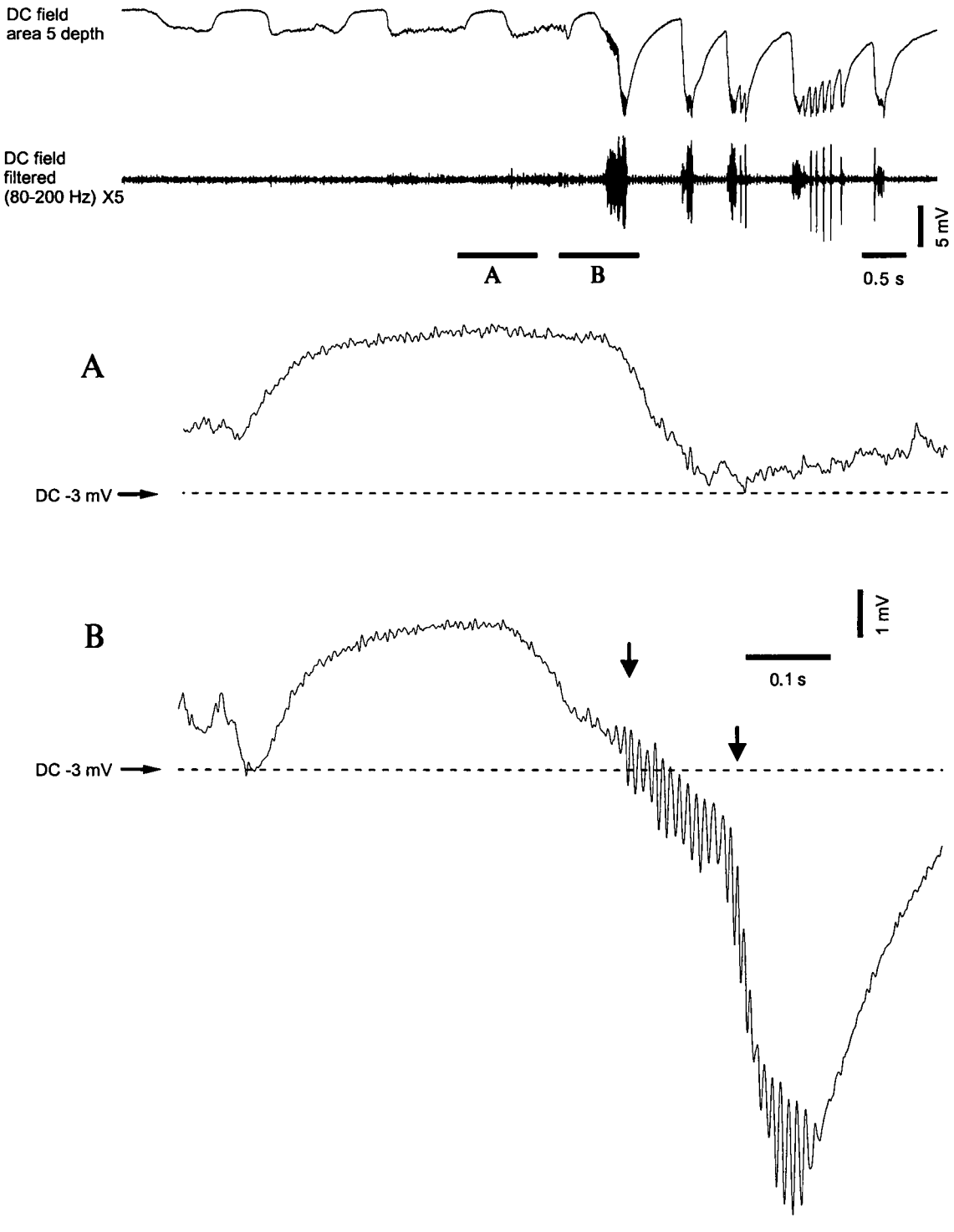

Fig. 5.9 Ripples are present at the transition between normal sleep-like activity and paroxysmal EEG "spikes", as seen with a DC field potential recording from area 5. Cat under ketamine-xylazine anesthesia. Spontaneous seizure evolving from the slow oscillation. An epoch is shown in the top panel along with the filtered trace between 80 and 200 Hz. The two underlined parts are expanded below. *A*, a depth-negative component of the slow oscillation reaching around 3 mV, with the depth-positive phase being set at 0 mV. *B*, the first field EEG "spike" of the seizure. Note that ripples appear in this case (*B*) at around the DC level reached by the non-paroxysmal (*A*) negativity, and that around 15 cycles of ripples occur before the negativity reaches values of paroxysmal EEG "spikes" (14 mV). The section between the two arrows may be considered as the transition between non-paroxysmal and paroxysmal negativities. From Grenier et al. (2003).

low-frequency and very fast rhythms, occurring spontaneously or mimicked by different stimulation paradigms (see section **5.2**).

Neocortical ADs, induced by cortical or thalamic stimulation, consist of different phases, depending on the frequency and intensity of pulse-trains. Rhythmic evoked responses are followed by a silent period and an epoch in which alternating responses appear, finally leading to self-sustained epileptiform activity [85]. Generally, trains of fast stimuli (100 Hz) applied to cortical areas induce seizures that start with fast runs (10–20 Hz) in virtually all recorded neurons. This type of faradic stimulation is used because cortical seizures often contain ripples at 100–120 Hz, both intracellularly and at the EEG level [84, 86], and such fast oscillations may have a strong impact on postsynaptic neurons. Intracellularly recorded neurons located close to the stimulation site are strongly depolarized and exhibit self-sustained oscillations at 10–20 Hz, which eventually diminish their frequencies in association with the declining plateau of depolarization [87]. With dual intracellular recordings from area 5 neurons, separated by only 0.2 mm, one neuron (cell 2 in Fig. 5.10) can be more depolarized at the onset of the seizure, immediately following the pulse-train. Accordingly, this cell is thought as having a leading role in the seizure that starts with high-frequency tonic discharges. The action potentials of cell 2 preceded those of cell 1 at the onset of the electrically induced seizure, but the reverse was observed with the declining depolarization of cell 2 (bottom right panel in Fig. 5.10). The focal nature of such seizures is demonstrated by only slight reflection of fast runs in the EEG lead from the adjacent area 7 and the complete absence of such activity in the more posterior suprasylvian area 21.

Electrically evoked ADs in neocortex do not necessarily implicate corticothalamocortical loops, as they can be induced by focal stimulation in small isolated cortical slabs [87]. Seizures consisting of two main components, SW/PSW complexes and fast runs, as in Lennox–Gastaut syndrome (see section **5.6**), could be evoked by four pulse-trains at 100 Hz. Such intracortically generated paroxysms

[85] Branch and Martin (1958); Bremer (1958b).

[86] See Figs. 8 and 14 in Steriade et al. (1998a).

[87] Timofeev et al. (1998).

Fig. 5.10 (following) Changing time-relations between two simultaneously recorded cortical neurons during a fast seizure. Cat under barbiturate anesthesia. Intracellular recordings from two neurons (0.2 mm apart) in the posterior part of area 5, together with depth-EEG from areas 7 and 21 (see brain figurine). Stimulation (100 Hz, 1 s) was applied rostral to cell 1. The elicited seizure consisted of fast runs at 10–20 Hz. Bottom left: each trace in the spike-triggered average (STA) of cell 2 was obtained by ten successive action potentials from cell 1 (top to bottom). Note progressive repolarization of cell 2 and the slowing down of fast runs' frequency (from 20 Hz to 10 Hz). The bottom right plot (same epoch as in the STA) shows that excitation in cell 2 preceded excitation in cell 1 at the beginning of seizures and that, with progressive hyperpolarization of cell 2, time-relations were reversed. Filled circles represent action potentials, and opened circles EPSPs, in cell 2. From Timofeev et al. (1998).

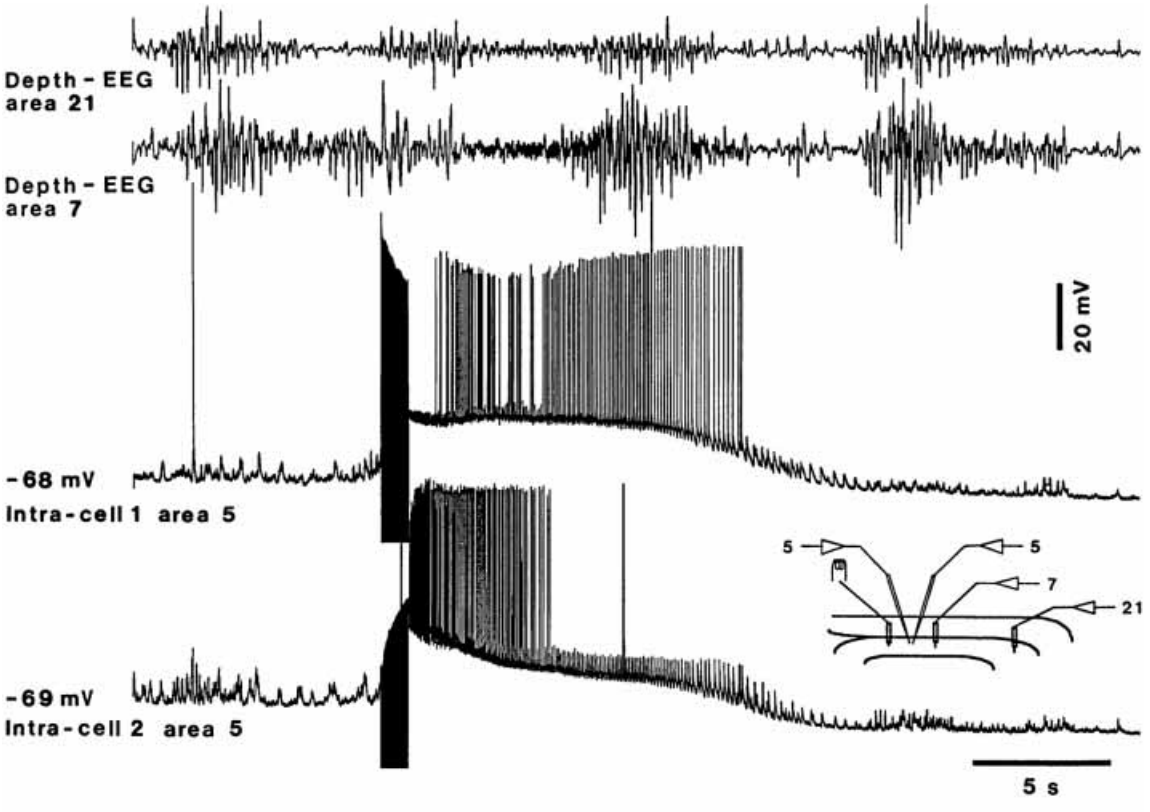
Depth - EEG
area 21
Depth - EEG
area 7
20 mV
-68 mV
Intra-cell 1 area 5
5
5
7
21
-69 mV
Intra-cell 2 area 5
5 s

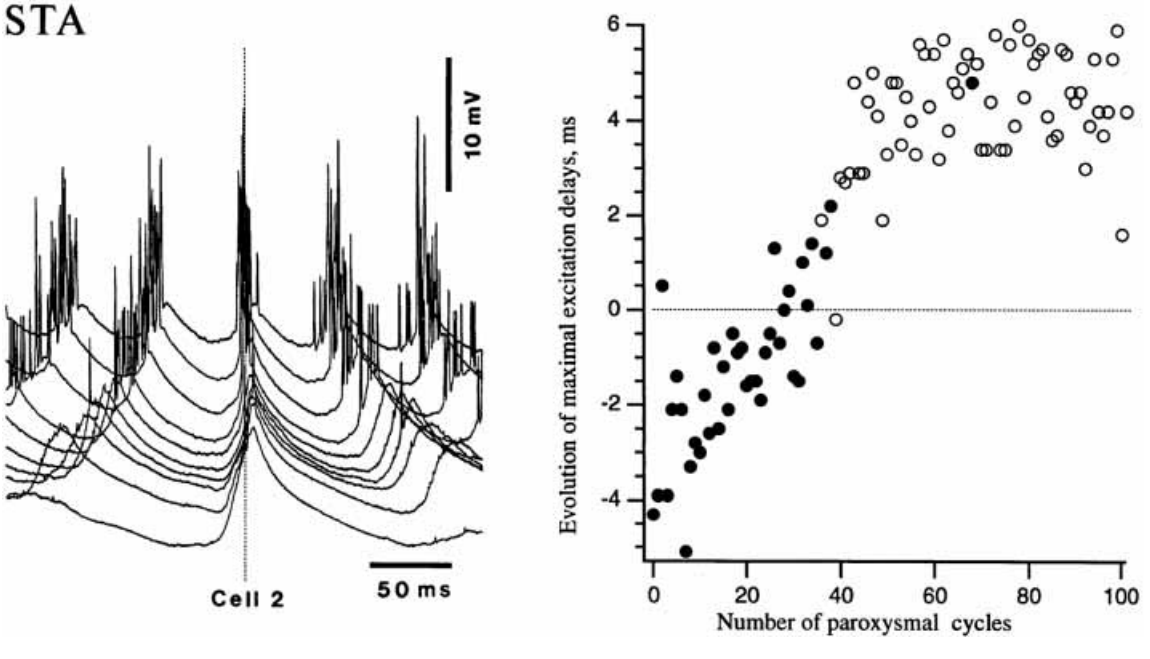
STA
10 mV
Cell 2
50 ms
Evolution of maximal excitation delays, ms
6
4
2
0
-2
-4
0
20
40
60
80
100
Number of paroxysmal cycles

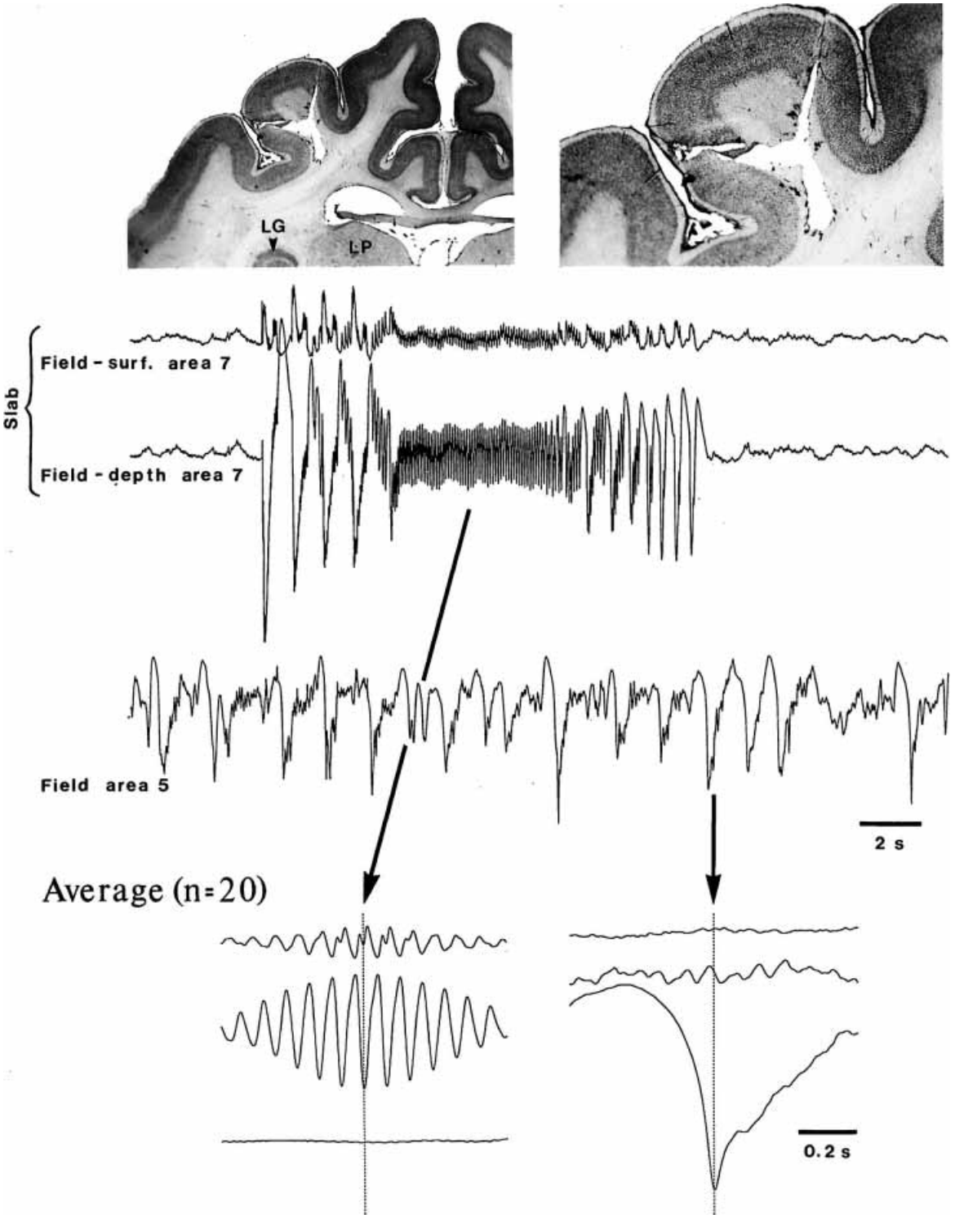
LG
LP
Slab
Field - surf. area 7
Field - depth area 7
Field area 5
2 s
Average (n=20)
0.2 s

have features very similar to those of seizures induced by electrical stimulation in the intact brain; namely, it starts with fast runs (~12 Hz) and ends with SW/PSW complexes, ~2 Hz (Fig. 5.11). The complete isolation of cortical slabs is demonstrated, besides the histological control (see top panels in Fig. 5.11), by the absence of correlated activity between the electrically induced paroxysmal fast runs in the slab and the normal activity displaying the slow oscillation (~0.7 Hz) outside the slab.

Electrical stimuli applied to the neocortex are effective in triggering paroxysmal depolarizing shifts (PDSs), which are able to follow various frequencies related to the spontaneously occurring activity [88]. Figure 5.12 shows that the spontaneous neuronal activity consisted of more or less regularly occurring PDSs, with a frequency between 0.5 and 0.8, reflected at the EEG level as "spiky" waves. The instantaneous frequencies were in a range between 0.5 and 0.8 Hz. Rhythmic cortical stimulation at a fixed frequency (1 Hz) produced faithful following by the neuron and by neighboring neuronal pools (see rhythmic EEG "spikes" at 1 Hz). The evoked PDSs had the same aspect as the spontaneous ones (bottom panel in Fig. 5.12). The stimulus-evoked PDSs occurred with an alternative pattern (inset in Fig. 5.12, with vertically expanded detail from the instantaneous frequency curve), which was the consequence of a jittering in PDSs' latencies, due to spontaneous activity that interfered with the ability of the cortical network to follow stimuli at rather fixed latencies. This generally coincides with the onset of a self-sustained activity (see last two stimuli). Indeed, spontaneous PDSs preceding the delivery of a stimulus provoked a certain disorder in the sequence of instantaneous frequencies (see right end of the inset in Fig. 5.12). In the case depicted in this figure, a few self-sustained PDSs occurred with the same frequency as used during stimulation (1 Hz) and, after a short period, PDSs resumed at control values (<0.8 Hz).

Thus, electrical stimuli to the cortex constitute hypersynchronous drives to the network and they mimic an epileptic focus because the responses are virtually identical to spontaneously

Fig. 5.11 (opposite) Electrically induced seizure in an isolated cortical slab from area 7. Cat under ketamine-xylazine anesthesia. Coronal section shows the completeness of transection producing the slab. Three traces show, from top to bottom: surface- and depth-EEG field potentials from area 7 slab, and depth-EEG from area 5, outside the slab. Four brief pulse-trains (each at 100 Hz) induced a self-sustained seizure, lasting 12 s and consisting of fast runs (~12 Hz) and SW/PSW complexes (~2 Hz). Averaged activity during paroxysmal fast runs (triggered by depth-negative EEG in the slab) shows reversal of fast activity at the surface and absence of correlation with EEG activity outside the slab. On the other hand, averaged activity triggered by the depth-negative wave of the slow oscillation (~0.7 Hz) in the intact brain shows the absence of correlation with intra-slab activity. LG, lateral geniculate; LP, lateroposterior. From Timofeev et al. (1998).

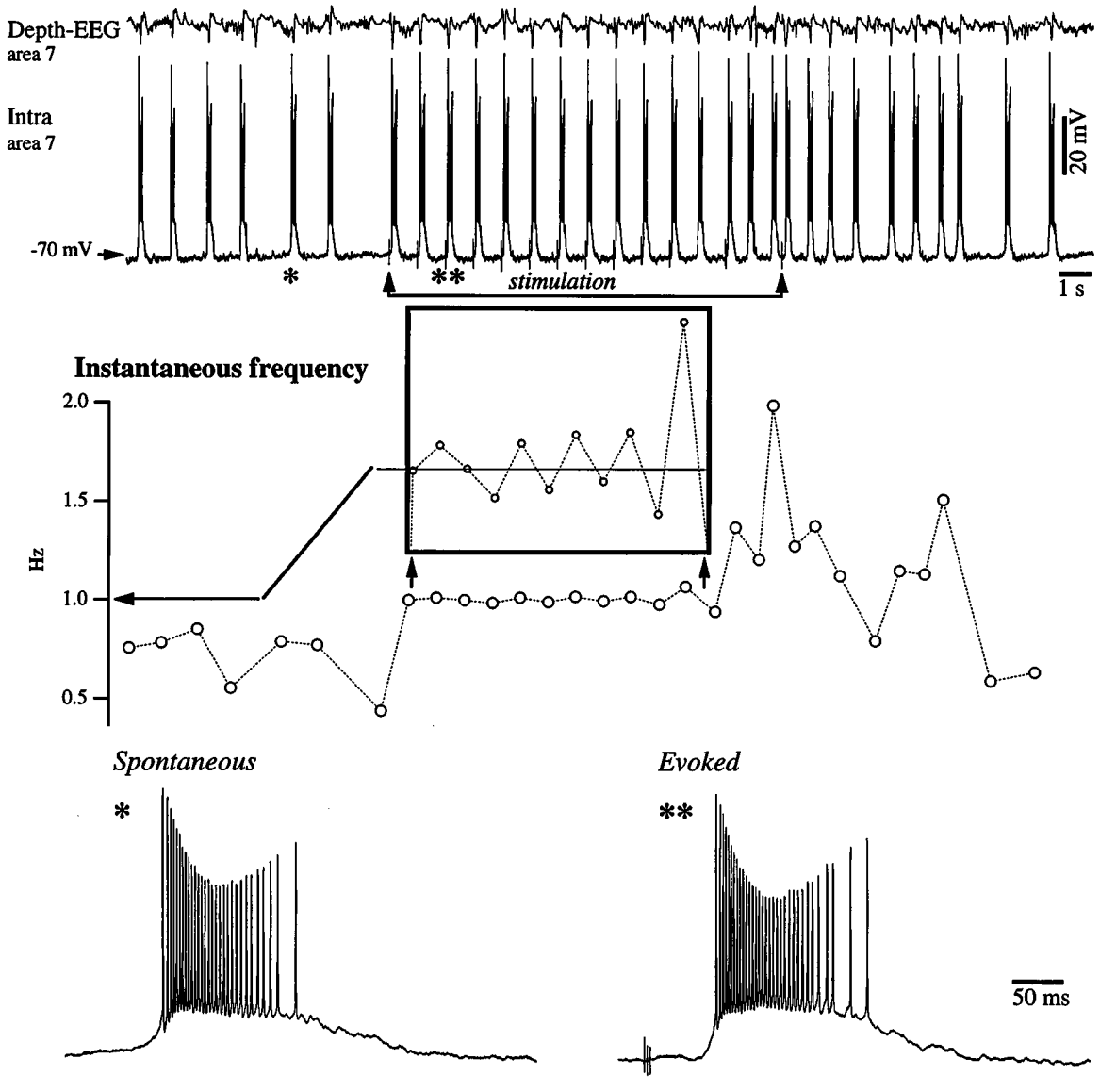

Fig. 5.12 Evolution of instantaneous frequencies during spontaneous and evoked activity. Cat under ketamine-xylazine anesthesia. Intracellular recording of area 7 neuron during rhythmic cortical stimulation in area 5. The upper panel starts with spontaneous, quasi-rhythmic paroxysmal depolarizing shifts (PDSs), then stimulation at 1 Hz is delivered to the cortex (underlined period between arrows). Two PDSs marked with one and two asterisks, respectively, are expanded at the bottom of the figure to emphasize the similarity between spontaneous (*) and triggered (**) PDSs. *Instantaneous frequencies* are the inverse of the time interval between two consecutive PDSs. The time stamps were taken at the moment of the steepest slope on the rising edge of a PDS (maximum of the first derivative). The horizontal arrow in this panel points to the stimulating frequency (1 Hz). The segment between vertical arrows is vertically expanded above to show the alternating pattern of responses around the stimulating frequency (dotted line). From Amzica and Steriade (1999).

occurring PDSs (Fig. 5.12). However, spontaneous activities interact with, and disrupt the, imposed inputs. In the great majority of cases there is an acceleration of the rhythm, eventually inducing loss of coupling, probably due to the fact that pools of neurons, other than those undergoing the stimulation, become active and attempt to drive the neuron under investigation at the time of the stimulation. It appears then probable that the relative increased entropy (less ordered behavior) of spontaneous seizures is due to distributed epileptogenic foci [88].

Ripples (80–200 Hz) can be elicited by rhythmic (10 Hz) stimuli, delivered to a cortical region close to that where two neurons were simultaneously impaled (Fig. 5.13). Both neurons faithfully followed 10-Hz stimuli but the neuron closer to the stimulation site displayed greater responses than the one situated further away, with a shorter latency, and its responses included ripples. This pattern of stimulation resulted in self-sustained seizure *only in the cortical neuron that displayed evoked ripples as well as in the EEG recorded from the same area*. The recently demonstrated role of ripples in the induction of neocortical seizures [84] is discussed in section **5.2** and, with the benefit of hindsight, can be seen in our previous papers [89].

As in the neocortex, waveforms of ADs in amygdalo-hippocampal circuits are similar to those of responses evoked during the previous period of stimulation [90]. In essence, stimulation of the basolateral amygdala with different frequencies (generally 5–6 Hz) evoked short-latency responses in the hippocampus, which progressively increased in amplitude and evolved into self-sustained potentials whose shape was virtually identical to that of responses evoked in the final stage of stimulation and generally took the pattern of paroxysmal activity (Fig. 5.14). In those experiments, AD waves were built-up from the same circuits that mediated evoked responses but, at a critical time during stimulation, they escaped from networks giving rise to normal responses and passed over those circuits to elaborate self-sustained epileptiform activity. Differential effects could be obtained by stimulating various nuclear groups of the amygdala. Whereas stimulation of the dorsally located central nucleus elicited EEG activation of cortical rhythms, and self-sustained generalized electrical seizures occurred only after cessation of stimulation, the stimulation of the ventrally located basolateral amygdala nucleus elicited the synchronization of cortical rhythms that developed into seizures [90, 91]. These results indicated that two different zones, with peculiar properties, exist within the amygdala: a dorsal activating system consisting of the central nucleus, and a ventral structure with highly synchronizing properties [92]. More recently, connectivity studies of

[88] Amzica and Steriade (1999).

[89] See ripples (~150 Hz) superimposed on the surface-positive, depth-negative EEG complexes, and EPSPs with similar frequency starting paroxysmal depolarizations, during seizures in primary somatosensory cortical area (Fig. 11*B* in Steriade and Contreras, 1995).

[90] Steriade (1964).

[91] Kreindler and Steriade (1963).

[92] Kreindler and Steriade (1964).

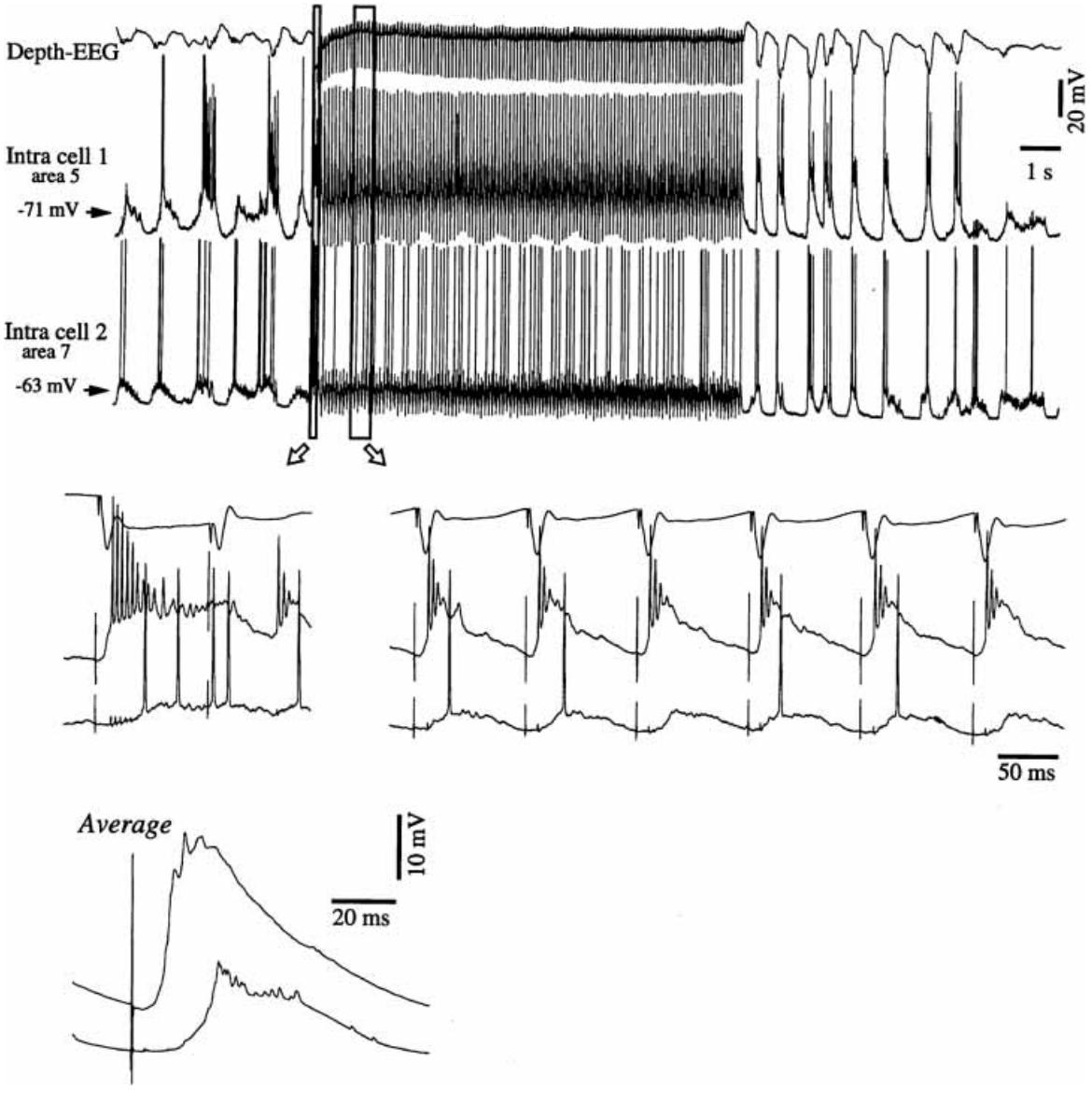

Fig. 5.13 Ripples (~200 Hz) are induced with 10-Hz cortical stimulation that leads to self-sustained electrical seizure. Cat under ketamine-xylazine anesthesia. Dual intracellular recording from cortical areas 5 and 7. Prior to stimulation, the neuron in area 5 (closer to the stimulation site) displayed paroxysmal depolarizing potentials. Two framed epochs are expanded below (arrows) to show individual responses to rhythmic stimuli. At the bottom, averaged evoked responses to 120 stimuli are shown. The latency of the area 5 neuron was 6.3 ms, while the latency of the area 7 neuron was 13 ms. Note that the evoked response in the area 5 neuron contained a group of ripples and that these very fast oscillations persisted with 10-Hz stimuli. Also note the self-sustained, short-duration electrical seizure in area 5 EEG and neuron, after cessation of stimulation. Modified from Amzica and Steriade (1999).

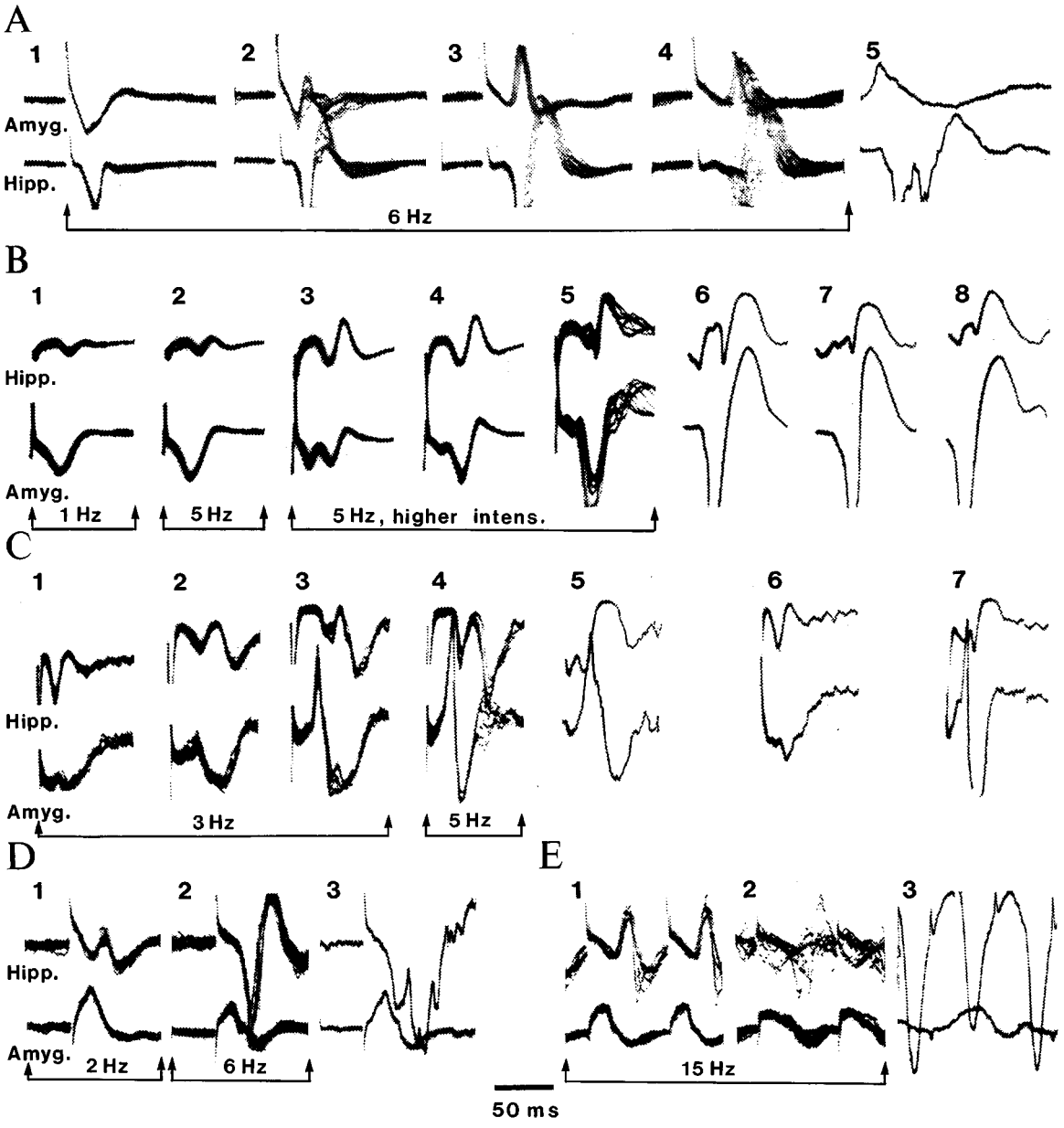

Fig. 5.14 Development of hippocampal field potential responses to amygdala stimulation into self-sustained activity. Different panels represent simultaneous recordings from amygdala (*Amyg.*), close to the stimulation site, and hippocampus (*Hipp.*). *A*, responses evoked by amygdala stimulation at 6 Hz (*1* to *4*) and self-sustained potentials immediately after cessation of rhythmic stimuli (*5*). *B*, responses evoked by amygdala stimulation at 1 Hz (*1*), 5 Hz (*2*) and 5 Hz at higher intensity (*3–5*), and self-sustained potentials immediately after stimulation (*6–8*). *C*, amygdala stimulation at 3 Hz (*1–3*) and 5 Hz (*4*) and self-sustained potentials (*5*). Potentials at extreme right (*6–7*) depict facilitation of responses by 50-Hz stimulation. *D*, amygdala stimulation at 2 Hz (*1*) and 6 Hz (*2*) and self-sustained potentials (*3*). *E*, amygdala stimulation at 15 Hz (*1–2*) and self-sustained potentials of paroxysmal type (*3*). Modified from Steriade (1964).

[93] Price and Amaral (1981); Russchen et al. (1985).

[94] Gastaut (1950); Killam et al. (1967).

[95] Servit (1959); Krushinsky (1962); Faingold and Meldrum (1990). Clonic, but not tonic, seizures of genetically audiogenic rats are controlled by GABAergic neurons of substantia nigra pars reticulata (Deransart et al., 2001).

[96] Reviewed in Naquet and Valin (1990).

[97] Cobb (1947); Gastaut et al. (1948).

[98] Shibasaki and Neshige (1987); Rubboli et al. (1999).

[99] Moody et al. (1974).

[100] Pumain et al. (1985).

[101] Merlet et al. (1996); Scherg et al. (1999).

[102] Sutherling et al. (1988); Mauguière (1992).

[103] Engel et al. (1990); Manganotti et al. (1999).

[104] Lüders et al. (1993).

[105] Barth et al. (1984).

[106] Albowitz and Kuhnt (1995); Telfeian and Connors (1998).

amygdala nuclei revealed that the central nucleus projects to the upper brainstem reticular core and basal forebrain [93], which are both implicated in cortical activation processes.

Though paroxysmal in many of the examples illustrated above, electrically evoked ADs are different from the classical cases of reflex epilepsy triggered by photic [94] or acoustic [95] stimuli, in which sensory signals trigger seizures. Visual stimulation at frequencies ~10 Hz is used to activate seizures in the photosensitive baboon *Papio papio* [96] and in humans [97], in which photic myoclonic phenomena can be induced [98]. Similarly, electrical stimulation of central brain structures or spontaneously occurring oscillations during the synchronous activity of the sleeping corticothalamic network may trigger reflex-like seizures in a hyperexcitable cortex. Cortical hyperexcitability may be due to a series of factors, such as chemical imbalance and impaired inhibition. Increased extracellular potassium concentrations are known to contribute to epileptogenesis [99] and, in photosensitive baboons, seizure onset is preceded by a three-fold increase in extracellular potassium concentration [100].

5.4. Cellular basis of EEG interictal "spikes"

Interictal EEG "spikes" (ISs) are sharp, large-amplitude (>50 μV), relatively brief (80–150 ms) potentials, sometimes followed by slow waves, which occur periodically on a background of otherwise normal activity or during short epochs that separate repetitive full-blown seizures. In human focal epilepsy, ISs are used to localize and identify different types of epileptic seizures, though the conventional scalp EEG recording is a poor tool and was recently replaced by depth-EEG recordings from cerebral cortex and subcortical structures [101], magnetoencephalography [102], and measures of cerebral tissue metabolism [103].

ISs may occur in different sites of human epileptogenic foci and multi-site subdural electrodes show that several ISs generators may fire together [104]. In humans, neuromagnetic measurements have shown that ISs may originate from a single source and distribute with an orderly field pattern and a fixed chronological sequence of discharges [105]. Experimental studies also demonstrate that the synchronicity of ISs does not necessarily imply simultaneity, as ISs propagate both vertically and tangentially across neocortical layers [106]. Using *in vivo*, multi-site recordings over an area of ~10 mm, the intracortical synchrony of EEG "spikes" (which correspond intracellularly to paroxysmal depolarizing shifts (PDSs)) was compared to that of (*a*) slow sleep oscillation in the prior background

activity and (*b*) seizures developing from successive ISs. The results showed that synchrony was greatest during seizures, followed by ISs, and then slow oscillation [107]. Figure 5.15 shows that the precursor sign of paroxysmal activity (asterisk corresponding to panel *B*) was an increased steepness and amplitude of depth-negative waves during the slow oscillation. With time, ISs grew in amplitude, started to appear rhythmically with increasing frequency, and culminated in a seizure with spike-wave (SW) and polyspike-wave (PSW) complexes at ∼2 Hz. Sequential cross-correlations showed that the intracortical synchrony was reduced with distance for all these three types of activities. *In vitro* studies have reported the characteristics and propagation of PDS in cortical slices [14, 108]. The preferred pathways and rather stereotyped propagation described in studies of ISs constitute a simpler way of propagation than in the case of complex seizures developing spontaneously from sleep patterns or elicited by small amounts of bicuculline leaked within the cortex [107].

As is the case with different types of well-developed paroxysmal activities, such as SW/PSW seizures in absence epilepsy (see section **5.5**) and seizures of the Lennox–Gastaut type (see section **5.6**), ISs predominantly appear during the stage of sleep with low-frequency, synchronized EEG patterns, in both animals [109] and humans [110].

The cellular mechanisms underlying ISs in neocortex, hippocampus, and thalamus have been investigated *in vitro* and *in vivo*. The intracellular correlate of ISs is an overt depolarization, termed PDS. Generally, the depolarization is so large that it leads to partial inactivation of Na^+ action potentials (Figs. 5.16–5.18). This can be best observed with paired intracellular recordings from the neocortex, in which the neuron closer to a hyperexcitable focus displays PDSs recurring rhythmically within the frequency range of the slow oscillation, whereas the simultaneously recorded neuron in an adjacent area fires spike-trains over the depolarizing phase of the slow oscillation, without spike inactivation (Fig. 5.16). PDSs can be generated by an imbalance between excitatory and inhibitory influences, such as impairing inhibition through application of $GABA_A$-receptor antagonists (as is the case in Fig. 5.16), by increasing the excitability of neuronal networks by raising the extracellular concentration of K^+, and by reduction of K^+ currents using application of 4-aminopyridine. Many PDSs (especially the fourth and fifth depolarizing events in Fig. 5.16) are formed by a primary spike-burst that lasts for 50–100 ms, which is followed by a secondary discharge that is probably dependent on the primary burst activating other components of the network. Studies of neocortical slices maintained

[107] Neckelmann et al. (1998). The intracortical synchrony during the slow oscillation, interictal spikes, and seizure with SW/PSW complexes, seen in multi-site recordings from cat suprasylvian areas 5 and 7 (Fig. 5.15), is due to direct connections between these areas, as demonstrated by monosynaptic EPSPs in area 5 neurons, with a latency of ∼1 ms, evoked by area 7 stimuli (Fig. 1*B1* in Neckelmann et al., 1998; see also Fig. 2 in Amzica and Steriade, 1995a, for reciprocal projections). Morphological studies corroborate these electrophysiological data by showing abundant fiber bundles connecting areas 5 and 7 in the cat suprasylvian gyrus (Grüner et al. 1974; Avendaño et al. 1988).

[108] Chervin et al. (1988); Chagnac-Amitai et al. (1990); Wadman and Gutnick (1993); Alefeld et al. (1998).

[109] Shouse (2001).

[110] Dalla Bernardina and Berghini (1976); Clemens and Majoros (1987); Terzano et al. (1991).

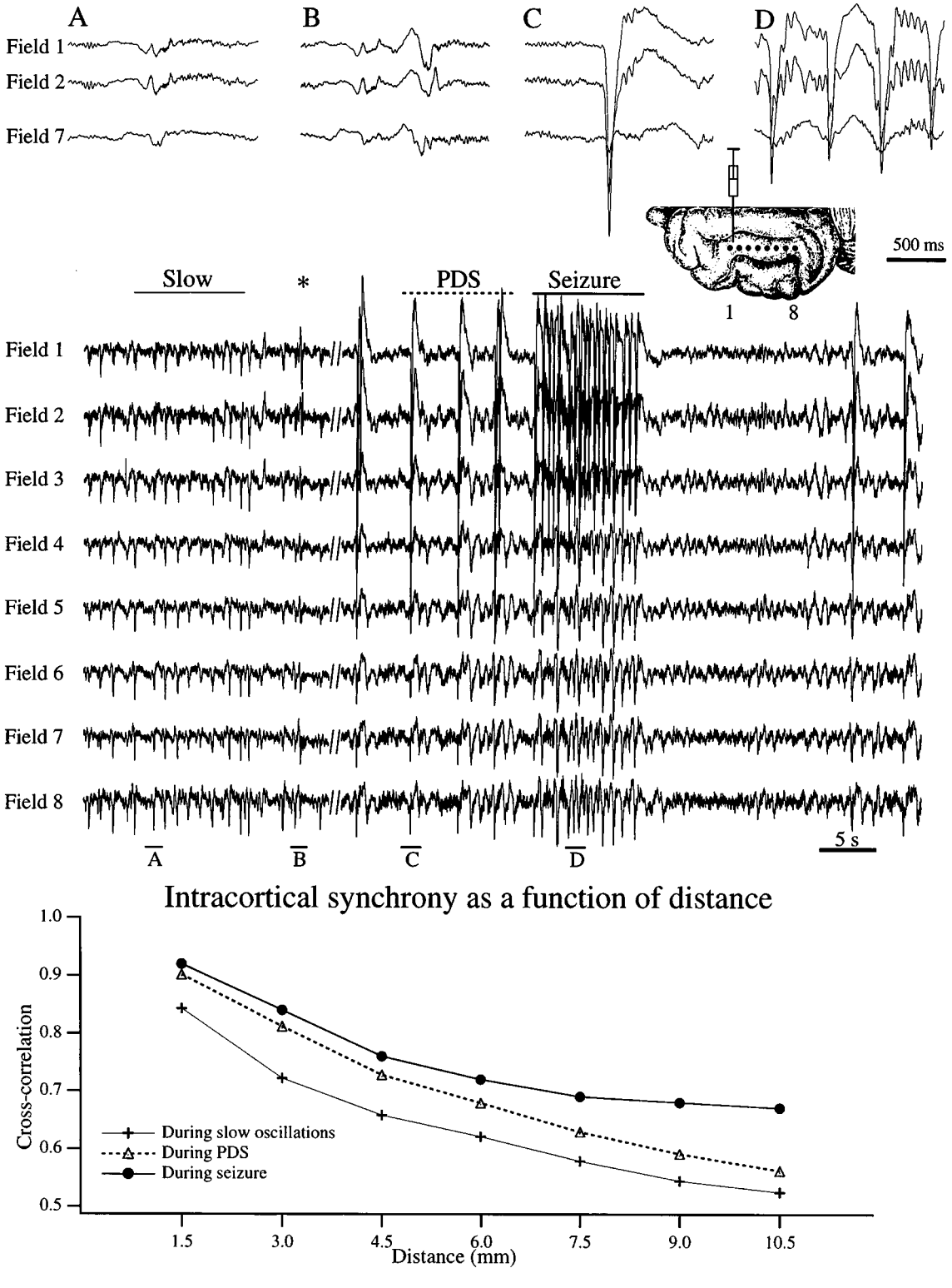
A
B
C
D
Field 1
Field 2
Field 7
500 ms
1
8
Slow
*
PDS
Seizure
Field 1
Field 2
Field 3
Field 4
Field 5
Field 6
Field 7
Field 8
A
B
C
D
5 s
Intracortical synchrony as a function of distance
Cross-correlation
1.0
0.9
0.8
0.7
0.6
0.5
During slow oscillations
During PDS
During seizure
1.5
3.0
4.5
6.0
7.5
9.0
10.5
Distance (mm)

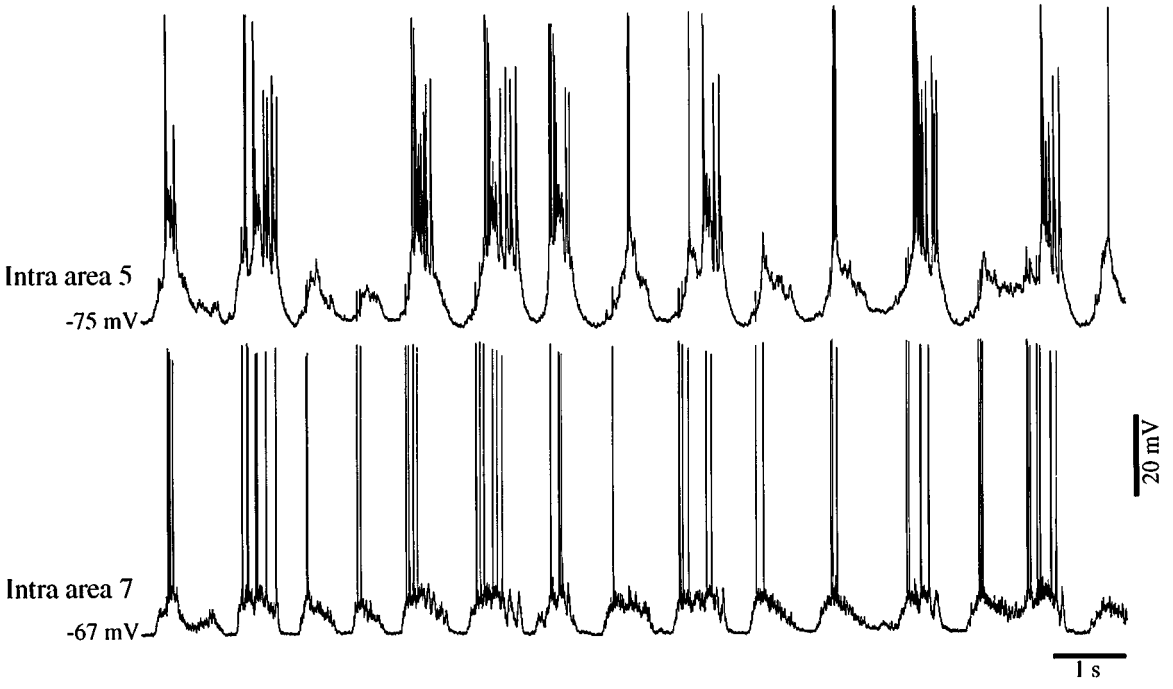

Fig. 5.16 Paroxysmal depolarizing shifts (PDSs) during the slow sleep oscillation. Cat under ketamine-xylazine anesthesia. Dual intracellular recordings from areas 5 and 7. Micropipette in area 5 was close to an epileptogenic focus created by leakage of bicuculline (a syringe filled with 10 μl of a 0.2-mM solution of bicuculline was inserted rostral to the pipette in the most anterior part of the suprasylvian gyrus; bicuculline was not injected, but very small amounts of this drug leaked into the cortex). Note rhythmic PDSs with spike inactivation in an area 5 neuron, and normal spike-trains in a neuron recorded from area 7. Modified from Neckelmann et al. (1998).

Fig. 5.15 (opposite) Intracortical synchrony of slow oscillation, bicuculline-induced EEG "spikes", and seizure with polyspike-waves (PSWs) decreases with distance. Cat under ketamine-xylazine anesthesia. Progressive changes in cortical activity and synchrony after placement of a syringe with 10 μl of 0.2 mM bicuculline in area 5. Bicuculline was not injected, but leaked into the cortex. Eight electrodes (1.5 mm apart) were inserted; the syringe was between electrodes 1 and 2 (see brain figurine). The left part shows slow oscillation (see detail *A*). A star marks the first paroxysmal EEG "spike" (*B*). Later, the field potentials became dominated by recurrent EEG "spikes" that, intracellularly, correspond to paroxysmal depolarizing shifts (PDSs, *C*), eventually leading to a seizure with a PSW pattern (*D*). *Lower panel*, sequential cross-correlation on 1-s windows between all electrode pairs. Peak amplitude of the cross-correlation function was averaged across all electrode pairs (see inter-electrode distance below the abscissa) for each of the three 10-s periods marked *Slow*, *PDS*, and *Seizure*, and plotted as a function of inter-electrode distance. From Neckelmann et al. (1998).

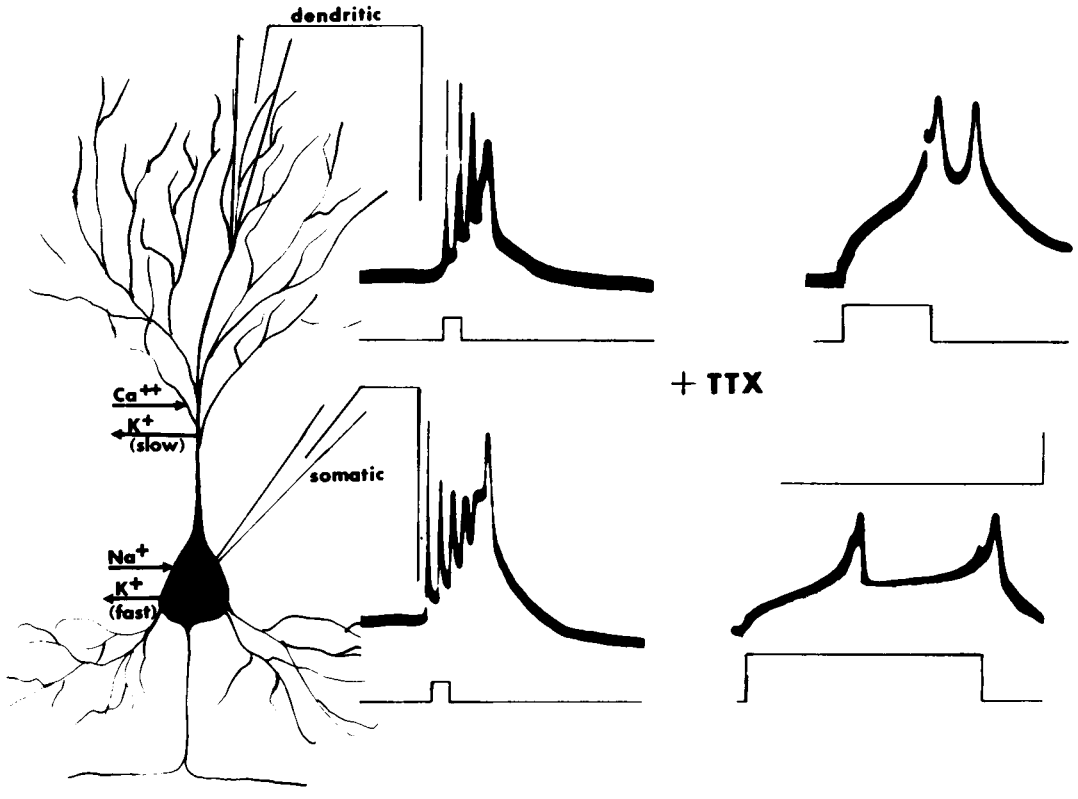

Fig. 5.17 Schematic representation of a hippocampal pyramidal neuron, showing the hypothesized conductances responsible for the generation of the spike-bursts. Na^+-K^+ fast spikes can be recorded with both somatic and dendritic impalements. Longer duration depolarization and after-hyperpolarizations are also observable with either somatic or dendritic recordings. Ca^{2+} spikes can be seen in isolation when treating the preparation with the Na^+ channel blocker tetrodotoxin (TTX). Recordings (modified from Wong et al., 1979) show intracellular voltage records and current injection. Modified from Schwartzkroin (1983).

[111] Connors (1984); Hoffman et al. (1994).

[112] Matsumoto and Ajmone-Marsan (1964); Ayala et al. (1973); Johnston and Brown (1981, 1984).

[113] Prince (1968).

[114] Schwartzkroin and Prince (1978, 1980).

in vitro placed emphasis on deeply lying intrinsically bursting (IB) cells promoting PDSs through their recurrent collaterals [111]. IB cells are also found in supragranular layers (see section ***2.1.1*** in Chapter 2), and bursting cells in any layer of neocortex, from II to VI, may promote PDSs.

Two apparently contrasting views have explained PDSs in the hippocampus and neocortex as either a sum of synchronous EPSPs generated in large groups of neurons in which increased excitation and depressed inhibition take place [112] or, alternatively, resulting from intrinsic neuronal properties [113]. However, these hypotheses are not mutually exclusive as both factors contribute to the slow envelope of the PDS [114] (see also introduction to this chapter).

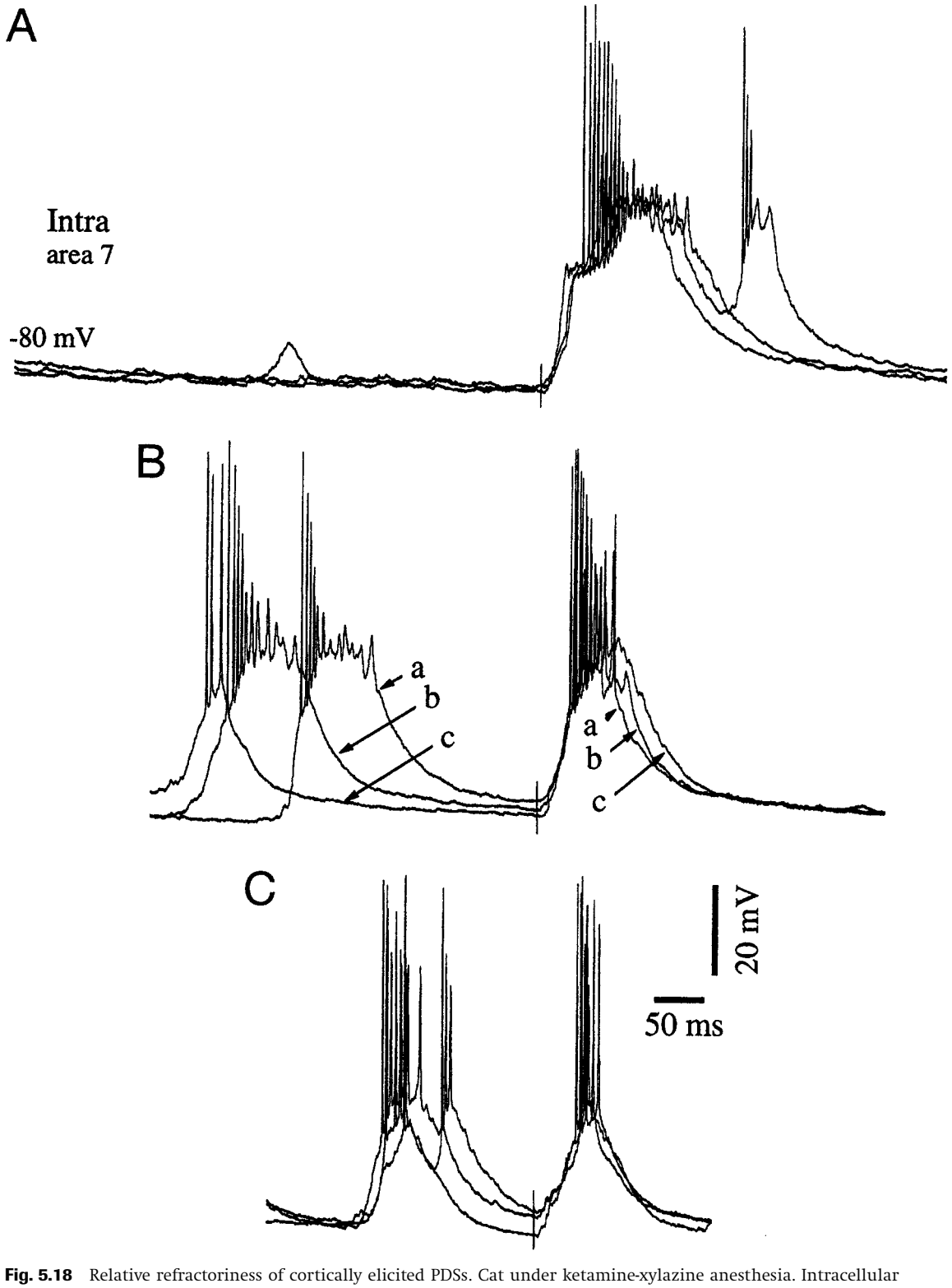

Fig. 5.18 Relative refractoriness of cortically elicited PDSs. Cat under ketamine-xylazine anesthesia. Intracellular recording of an area 7 neuron. Three PDSs elicited by cortical stimuli to area 5 were superimposed and aligned; see stimuli artifacts in *A* to *C*. The amplitude and duration of cortically evoked PDS depended on their "time-distance" from the preceding (spontaneously occurring) PDSs (compare *A* to *B* and *C*). From Steriade and Amzica (1999).

[115] Reviewed in Prince (1983).

[116] Goldring et al. (1999); Johnston et al. (2000).

[117] McCormick (1989).

Thus, hippocampal CA3 pyramidal neurons possess special properties in both soma and dendrites, which endow them with the capability of generating spike-bursts even during normal spontaneous activity, and more so in seizure-prone states. At the soma, Na^+ and K^+ channels predominate and generate fast action potentials, while at the dendrites Ca^+ and slow K^+channels predominate, generating long-duration depolarizations and after-hyperpolarizations (Fig. 5.17). The propensity of CA3 hippocampal pyramidal cells to generate paroxysmal discharges is very high and earlier studies qualified them as pacemakers of epileptogenic activity in hippocampus, since the generation of PDSs in area CA1 seemed to follow PDSs in CA3, and epileptiform activity was much less evident or even absent in the dentate gyrus [115]. More recent studies have demonstrated that CA1 pyramidal neurons also generate intrinsic bursts in response to prolonged depolarizing current steps through the activation of dendritic Ca^{2+} spikes [116].

In the neocortex, neurons exhibit some differences compared to hippocampal pyramidal cells, which make them less susceptible to generating PDSs. These differences consist of a lower propensity to generate slow depolarizations and spike-bursts, less prominent Ca^{2+} conductances, and inward rectification mediated predominantly by Na^+, whereas both Na^+ and Ca^{2+} mediate the inward rectification during depolarization of hippocampal pyramidal cells [115]. These differences explain why synaptic conductances play a more important role in generating PDSs in neocortex than in hippocampus. Cortical PDSs are followed by a prolonged after-hyperpolarization that is generated by the activation of various K^+ currents [112, 117]. The long-lasting hyperpolarization may explain, at least partially, the refractory period of PDSs. The largest PDSs can be triggered at more than 500 ms from previous PDSs (Fig. 5.18*A*). When spontaneously occurring PDSs end at time-intervals of ~100 ms before the tested PDSs, they produce a shortening of about 50–70% in the evoked PDSs (Fig. 5.18*B*). Further reduction in the evoked PDSs is observed when they are preceded at shorter time-intervals by spontaneously occurring paroxysmal events (Fig. 5.18*C*).

Although neocortical cells are less prone to epileptiform discharges than hippocampal pyramidal neurons, some neuronal types in the neocortex can generate high-frequency burst discharges through incompletely elucidated conductances. These neocortical neurons are intrinsically bursting (IB) and fast-rhythmic-bursting (FRB) neurons (see section ***2.1.1*** in Chapter 2).

IB pyramidal cells have been proposed to promote PDS generation [7, 14] and FRB cells from either deep or supragranular layers are predominantly implicated in generating repetitive PDSs during the fast runs of Lennox–Gastaut-type seizures [118]. For other intrinsic conductances of neocortical and hippocampal neurons, implicated in the generation of PDSs, see a recent review [119].

The network operations that underlie PDSs in hippocampus and neocortex are, basically, local recurrent excitation among pyramidal cells that generate summated EPSPs and impaired inhibition that is produced experimentally by $GABA_A$-receptor antagonists. The view that the depolarization underlying the PDS is a large synaptic potential is supported by small, repetitive EPSPs that build up at the onset of PDSs during seizures (see Fig. 5.18, especially panel *C*). Then, PDSs can be initiated by gradual summation of EPSPs [120]. The late component of PDSs is mediated by activation of glutamate receptors of the AMPA and NMDA types [121]. In addition to EPSPs, PDSs also contain an important inhibitory component. Recordings with Cl^--filled pipettes revealed depolarizing shifts by 10–30 mV during the EEG "spike" component, and conventional fast-spiking inhibitory interneurons (some of them intracellularly stained and showing aspiny dendrites and locally arborizing axons) discharged at very high rates (500–600 Hz) during the EEG "spike" component [122] (see also section **5.5**). The synchronization of pyramidal neurons may result from rebound responses due to hyperpolarization induced by the activation of local GABAergic interneurons [123]. Another factor accounting for neuronal synchronization, especially in area CA1 of the hippocampus, is ephaptic interaction [124] that influences the timing of action potential generation in coupled cells and brings them to synchrony. During paroxysmal bursting, swelling of neurons and glia [125] reduces the extracellular space (Fig. 5.19) and increases field interactions [126]. Shrinkage of the extracellular space is one of the factors that contribute to an enhanced concentration of $[K^+]_0$ [127], which, in turn, enhances neuronal excitability and promotes seizures.

In thalamic reticular (RE) neurons, different patterns characterize interictal PDSs, compared to the rhythmic paroxysmal potentials during a full-blown seizure [128]. The duration of active periods in RE neurons during interictal PDSs is two to three times longer than during seizures (Fig. 5.20). Simultaneous recordings from cortical and RE neurons during seizures and interictal PDS showed that, during seizures, RE neurons fired low-threshold spike-bursts, whereas during interictal spikes RE neurons fired trains

[118] Fig. 7 in Steriade et al. (1998a).

[119] De Curtis and Avanzini (2001, p. 543–545).

[120] Chamberlin et al. (1990); Hoffman and Haberly (1991).

[121] Swann et al. (1993).

[122] Steriade et al. (1998c); Steriade and Timofeev (2001); Timofeev et al. (2002c).

[123] Cobb et al. (1995).

[124] Jefferys and Haas (1982); Dudek et al. (1986); Jefferys (1995).

[125] McBain et al. (1990); Andrew and MacVicar (1994); Amzica and Neckelmann (1999).

[126] Amzica and Steriade (2000).

[127] Jensen et al. (1996).

[128] Steriade and Timofeev (2001).

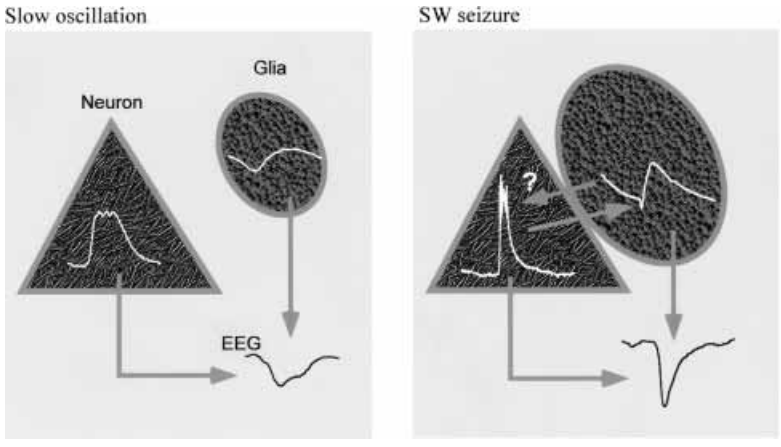

Fig. 5.19 Schematic diagram of the mechanisms generating field potentials during slow sleep oscillations (*left*) and spike-wave (SW) seizures (*right*), resulting from *in vivo* experiments on cortical and glial cells from cat under ketamine-xylazine anesthesia. An averaged cycle is drawn in each cell (*white traces*). During the slow oscillation, reversed neuronal and glial potentials contribute to the genesis of the extracellular field potential (EEG). SW seizures are accompanied by glial swelling, which may bring patches of cellular membranes into contact, allowing intraneuronal potentials to appear reversed, as field potentials, in the glial cells (arrow from neuron to glia points towards the glial negativity). The reverse pathway might also be at work. Both intraneuronal and intraglial activities contribute to the shape of the extracellular field potential. Modified from Amzica and Steriade (2000). See Plate section for color version of this figure.

of single action potentials preceded by tonic firing (Fig. 5.20), which suggests a previous, progressive depolarization. In both cases (seizure and interictal PDSs), paroxysmal potentials in cortical neurons triggered, without failure, spike-bursts or spike-trains, respectively, in RE neurons. The powerful drive from the cortex to RE neurons explains a series of phenomena that are discussed in the following section.

5.5. Seizures with spike–wave complexes at ~3 Hz

Seizures with spike-wave (SW) or polyspike-wave (PSW) complexes at ~3 Hz occur in petit-mal or *absence* epilepsy. The clinical aspect

Fig. 5.20 (following) Different activity patterns of cortical and thalamic reticular (RE) neurons during a full-blown seizure and during isolated EEG "spikes" (PDSs). Cat under ketamine-xylazine anesthesia. Simultaneous recordings of EEG field potential from the depth of cortical area 4, intracellular activity from the same area, and extracellular activity of an RE neuron from the peri-ventrolateral sector of the nucleus. Upper panel shows a fragment of the electrically elicited seizure, with SW complexes at 3 Hz, followed by isolated interictal spikes. Parts indicated by horizontal bars and arrowheads are expanded below. At the bottom, wave-triggered averages (WTA) of field potential, an intracellular trace of cortical neuronal activity, and peri-wave histograms of RE cell activity are shown. The maximum of the depth-positive ("wave") component was taken as time 0 to generate averages. Note the tonic firing of the RE neuron during interictal spikes that preceded high-frequency spike-trains associated with PDSs. Also, note that the maximal depolarization reached by the cortical neuron during interictal PDSs is 10 mV lower than that in active periods during PDSs associated with seizures. Modified from Steriade and Timofeev (2001).

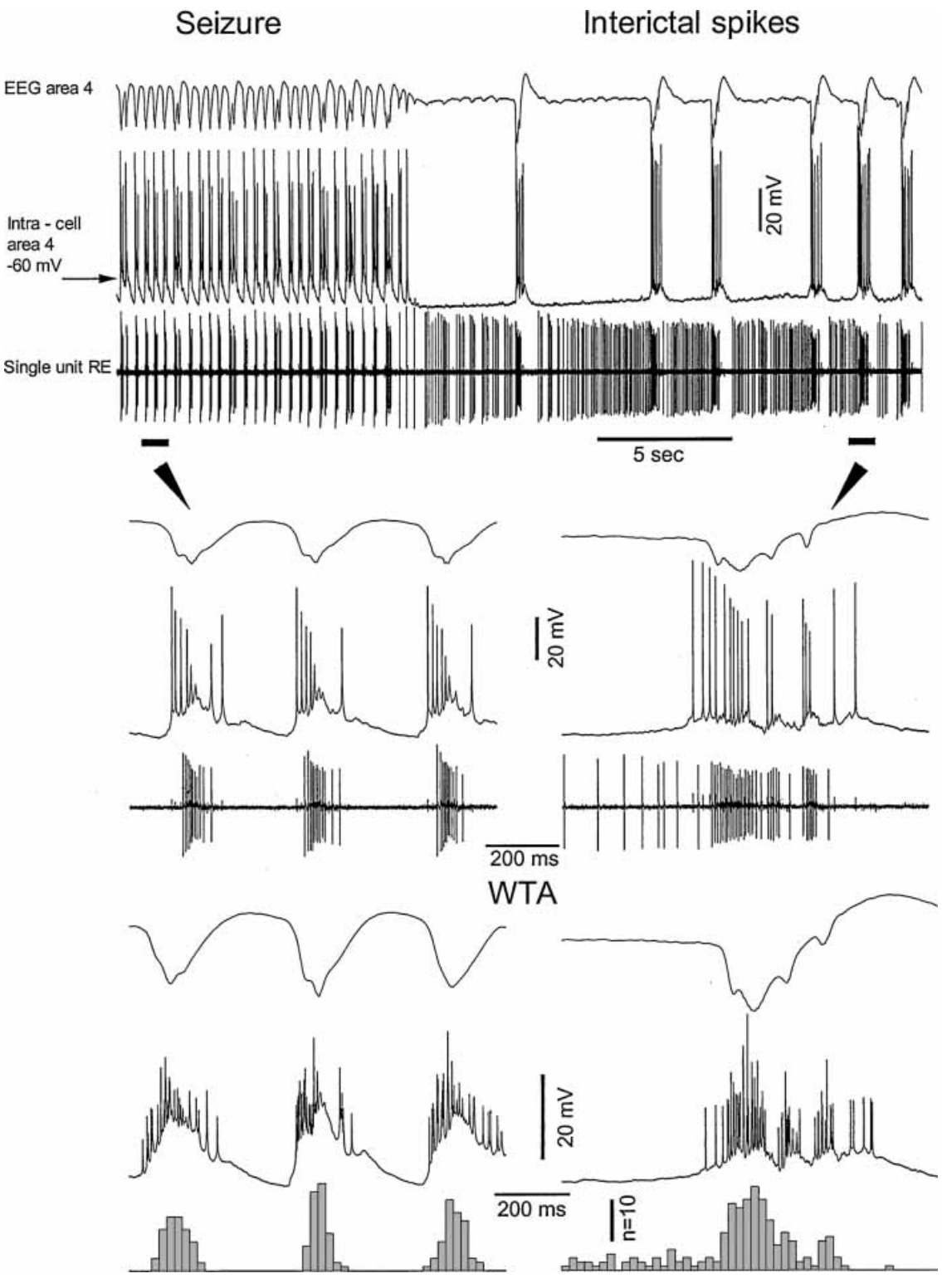
Seizure
Interictal spikes
EEG area 4
Intra - cell
area 4
-60 mV
Single unit RE
20 mV
5 sec
20 mV
200 ms
WTA
20 mV
200 ms
n=10

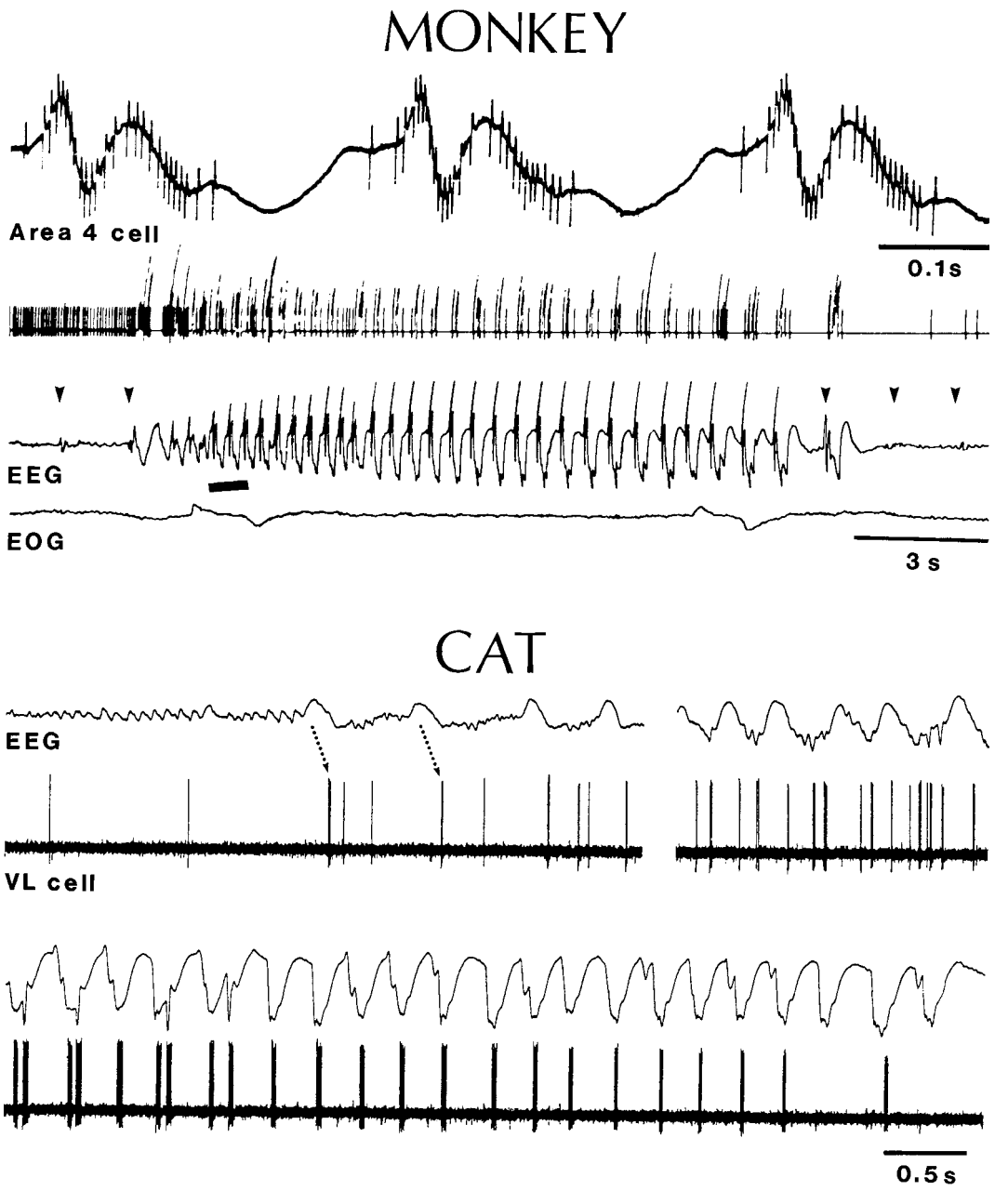

Fig. 5.21 Spike-wave (SW) seizures in monkey and cat. *Top panel*, neuronal activity during a seizure with SW complexes at 3 Hz during drowsiness in the behaving monkey. Chronically implanted *Macaca mulatta*. Single neuron recorded from the arm area in the precentral gyrus (area 4). The top oscilloscopic trace indicates the corresponding part (marked by horizontal bar) in the depicted ink-written record below (the three traces represent: unit spikes used to deflect a pen of the EEG machine; each deflection exceeding the common level representing a group of high-frequency spikes; focal slow EEG waves, simultaneously recorded by the same microelectrode; and eye movements, EOG). Arrowheads indicate stimuli applied to the appropriate thalamic nucleus for neuronal identification. When the experimenter observed an increased

of absence seizures, their prevalent appearance in childhood and adolescence, and some notions concerning their apparently sudden generalization, are briefly discussed in section **5.1**. Several types of absence seizures, without and with various motor components, have been described [129].

The SW complexes should not be equated with absence epilepsy as they also occur in other types of epilepsies [20]. Needless to say, a disease entity is not just an electrographic pattern. This distinction prevents me using the term *epilepsy* when describing the neuronal mechanisms of electrical seizures in animals. What neurophysiologists usually do is find the aspect that is closest to the clinical case and search for its neuronal substrates in terms of both intrinsic and network neuronal properties. SW complexes are so stereotyped at the single-neuron and field-potential levels that what is described in animal experiments performed *in vivo* is probably similar to the mechanisms underlying this electrographic correlate of absence epilepsy in humans. Also, although I restrict the term *absence epilepsy* to clinical studies in which the state of consciousness during wakefulness is clearly obliterated during such seizures, experimental studies on behaving monkeys [75] showed that paroxysms consisting of typical SW complexes at ~3 Hz were accompanied by tonic eye movements at the onset and end of seizures, as in clinical absence epilepsy (Fig. 5.21, *MONKEY*). The eyelid movements during childhood petit-mal seizures were first described in the 18th century by the French physician Tissot [130].

In this section, I first elaborate on these points and discuss the dependency of SW/PSW seizures on the behavioral state of vigilance. Next, I present cellular and molecular data related to the cortical generation of these seizures and their reflection in two major types of thalamic neurons.

[129] Loiseau (1992) distinguished among absence seizures (ASs), simple absences with only impairment of consciousness, ASs with mild clonic components (restricted to the eyelids), ASs with tonic components, ASs with atonic components, ASs with automatisms, and ASs with autonomic components.

[130] See Snead (1995).

Fig. 5.21 Caption for Fig. 5.21 (*cont.*) amplitude of the evoked field potential (second stimulus), stimuli were interrupted and the seizure developed in the absence of any stimulus. Note spike-bursts over the depth-negative (upward in this case) field potential of the SW complexes (the EEG "spike") and silent firing during the late part of the depth-positive "wave" component of SW complexes. *Also note tonic eye movements at the onset and end of the SW seizure. Bottom panel*, cat under ketamine-xylazine anesthesia. Simultaneous recordings of EEG field potentials from cortical area 4 and extracellular activity of a neuron from the thalamic ventrolateral nucleus. Paroxysm developing progressively, with increasing amplitudes of slow oscillation in area 4 and leading to SW complexes at 3–4 Hz (see arrows). Despite the fact that the VL neuron apparently displayed brisk firing associated with the depth-negative component of cortical SW complexes, this activity did not reflect spike-bursts as, intracellularly, it was evident that these were spike-trains at a depolarized level, triggered by depolarizing cortico-VL projections (see Fig. 7*B1* in Steriade and Contreras, 1995). Modified from Steriade (1974) and Steriade and Contreras (1995).

[131] O'Brien et al. (1959).

[132] Watson and Bowker (1960).

[133] Steriade et al. (1998a).

5.5.1. Generalized and focal spike-wave seizures

Clinical and experimental studies have pointed out that, instead of being suddenly generalized and bilaterally synchronous as conventionally defined and envisaged according to the "centrencephalic" hypothesis, some SW seizures are progressively built up within corticocortical and corticothalamic networks (see section **5.1**). EEG studies in humans show that a significant percentage of patients with absence seizures associated with SW complexes at ~3 Hz may present focal or multi-focal clinical and EEG abnormalities. Multiple, independent cortical foci and "focal larval petit mal" discharges have been described since the 1930s [30, 32]. Focal abnormalities have been described in 35% of cases [131] and asymmetrical flash-evoked PSW responses have been described in investigated patients [132]. Then, some SW/PSW seizures display focal paroxysmal activity, confined to one cortical area or to a few contiguous cortical fields. This is in line with the concept that SW/PSW complexes originate in the neocortex and are disseminated through mono-, oligo- and multi-synaptic intracortical circuits, before they spread to the thalamus and exhibit generalized features. This idea was based on SW seizures elicited by augmenting potentials and occurring in the depth of the neocortex, without any reflection at the cortical surface (see Fig. 5.3), and by a series of experimental data exposed below.

In our experiments on chronically implanted, naturally awake and sleeping cats [133], the majority (~65%) of spontaneous cortical SW seizures occurred during the behavioral state of resting sleep, while the remaining paroxysms occurred during wakefulness; none of them occurred during rapid-eye-movement (REM) sleep. When they appeared during wakefulness, phasic eye movements and increases in muscular tone were no longer observed throughout the seizures (Fig. 5.22). The occurrence of *spontaneous* cortical SW seizures in chronically implanted animals, which was shown in behaving monkeys [75] and also documented in cats [133], is probably due to the great number of coaxial macroelectrodes and microelectrodes in various cortical areas and thalamic nuclei that may have produced small lesions and gliosis, combined with the fact that electrical stimuli are often applied to identify the input-output organization of cortical and thalamic neurons. It may also be possible that many spontaneous electrographic seizures in "normal" subjects are unrecognized, and that those sleeping individuals pass in and out of seizures during their slow sleep oscillation, as shown experimentally [133]. In acute preparations, spontaneous SW/PSW seizures occur under ketamine-xylazine anesthesia in a

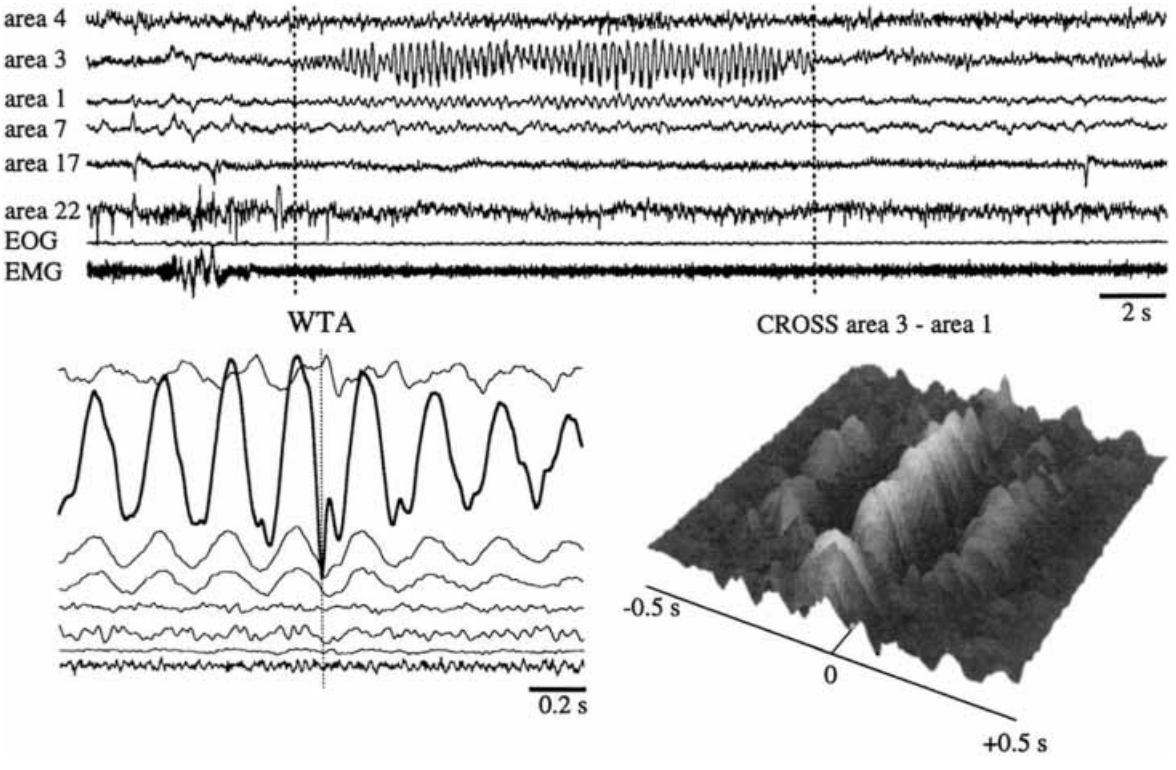

Fig. 5.22 Spontaneously occurring, focal cortical SW seizure, and its synchronization with adjacent, but not with distant, cortical areas. Chronically implanted cat. Eight traces in the top panel depict: field potentials from the depths of areas 4, 3, 1, 7, 17, and 22; electrooculogram (EOG), and electromyogram (EMG). The duration of the seizure was ~15 s. *Bottom left panel* illustrates the wave-triggered average (WTA) from the seizure period between the dotted lines in the panel above; reference time is represented by peak negativities (dotted line) in area 3 where SW complexes at 4 Hz were prominent. Note that SW complexes in area 3 were reflected by lower-amplitude, clear-cut waves at the same frequencies in areas 1 and 7, but not in areas 4, 17, and 22. The WTA were calculated as follows: negative peaks for each EEG spike in area 3 were detected, and equal windows around that point (1 s before and 1 s after) were extracted from all channels. All sweeps belonging to a given channel were finally averaged. *Bottom right panel* depicts a perspective view of a three-dimensional sequence of cross-correlations (CROSS) between activities in the primary focus of SW seizure (area 3) and the adjacent area 1. The same windows as for WTA also served to generate sequential field correlations (see method in Amzica and Steriade 1995a). Briefly, the three-dimensional surface was derived as follows: each couple of sweeps from two EEG leads (e.g., area 3 and area 1) corresponding to a given EEG spike was cross-correlated, thus producing a correlation trace. Then, all correlation traces were sequentially aligned in order to produce a three-dimensional surface in which the abscissa (−0.5 s to +0.5 s) corresponds to the time-lags; each point of the ordinate is a time mark for an EEG spike; and the *z*-axis represents the strength of the correlation. The shadows on the three-dimensional surface attribute white to high positive correlations, and black to high but negative correlation. Downward deflections of field potentials indicate negativity (as in intracellular recordings). From Steriade et al. (1998a).

[134] Marescaux et al. (1992 a-b); Jandó et al. (1995).

[135] Noebels (1984); Kostopoulos (1992); Silva-Barrat et al. (1994).

[136] Rosen and Andrew (1990).

[137] Gomez and Westmoreland (1987).

[138] McKeown and McNamara (2001).

[139] Litt et al. (2001, p. 61).

relatively high proportion (20–30%) of animals, possibly because of the high level of synchronization in corticothalamic networks, as demonstrated by the coalescence of cortically generated slow oscillation and thalamically generated spindle and delta rhythms (see section *3.2.3.2* in Chapter 3). Other factors, which remained uncontrolled in our studies, may consist of genetic and sex differences between experimental animals [134], imbalance between norepinephrinergic and other neuromodulatory systems [135], or hyposmolarity increasing seizures [136].

That SW seizures can be localized within relatively circumscribed neocortical territories was shown by wave-triggered averages (WTA) and sequential cross-correlations of focal field potentials from multiple sites (Fig. 5.22). At visual inspection, the 4-Hz SW seizure depicted in this figure was only visible in somatosensory area 3, but WTA and cross-correlations indicated related activities at ~4 Hz in adjacent area 1 as well as in association area 7. However, the motor (area 4), primary visual (area 17), and auditory (area 22) leads did not exhibit signs of paroxysmal activity. Figure 5.23 illustrates a typical, brief SW seizure at 3 Hz, occurring in two adjacent sites within the cortical suprasylvian area 5. The two extracellularly recorded neurons invariably discharged spike-trains or spike-bursts during the depth-negative "spike" EEG component and were silent during the depth-positive wave component of SW complexes.

The idea that some SW seizures may occur focally is supported by clinical data on absence epilepsies showing that interictal abnormalities may occur within restricted cortical regions, most commonly over the frontal lobe [137], as well as by experimental data showing a progressive development of the duration of seizures, starting with embryonic seizures that, if not followed by more developed paroxysms, would not have been detected as precursor of full-blown SW seizures [77]. Such a case is shown in Fig. 5.24 that depicts a series of SW seizures, starting with one that would barely be recognized on the EEG (panel *A*) if not analyzed within the whole sequence of paroxysms, which were associated with progressively increased amplitudes of hyperpolarizations in the simultaneously recorded thalamocortical (TC) neuron (see details on this behavior of TC neurons in section *5.5.3.2*).

Clinical results related to the above issue raised the question: "when do epileptic seizures *really* begin"? The data referred to in the commentary that asked the question [138] were computerized analyses of EEGs recorded from patients with mesial temporal lobe epilepsy during evaluation for surgery [139]. The authors reported

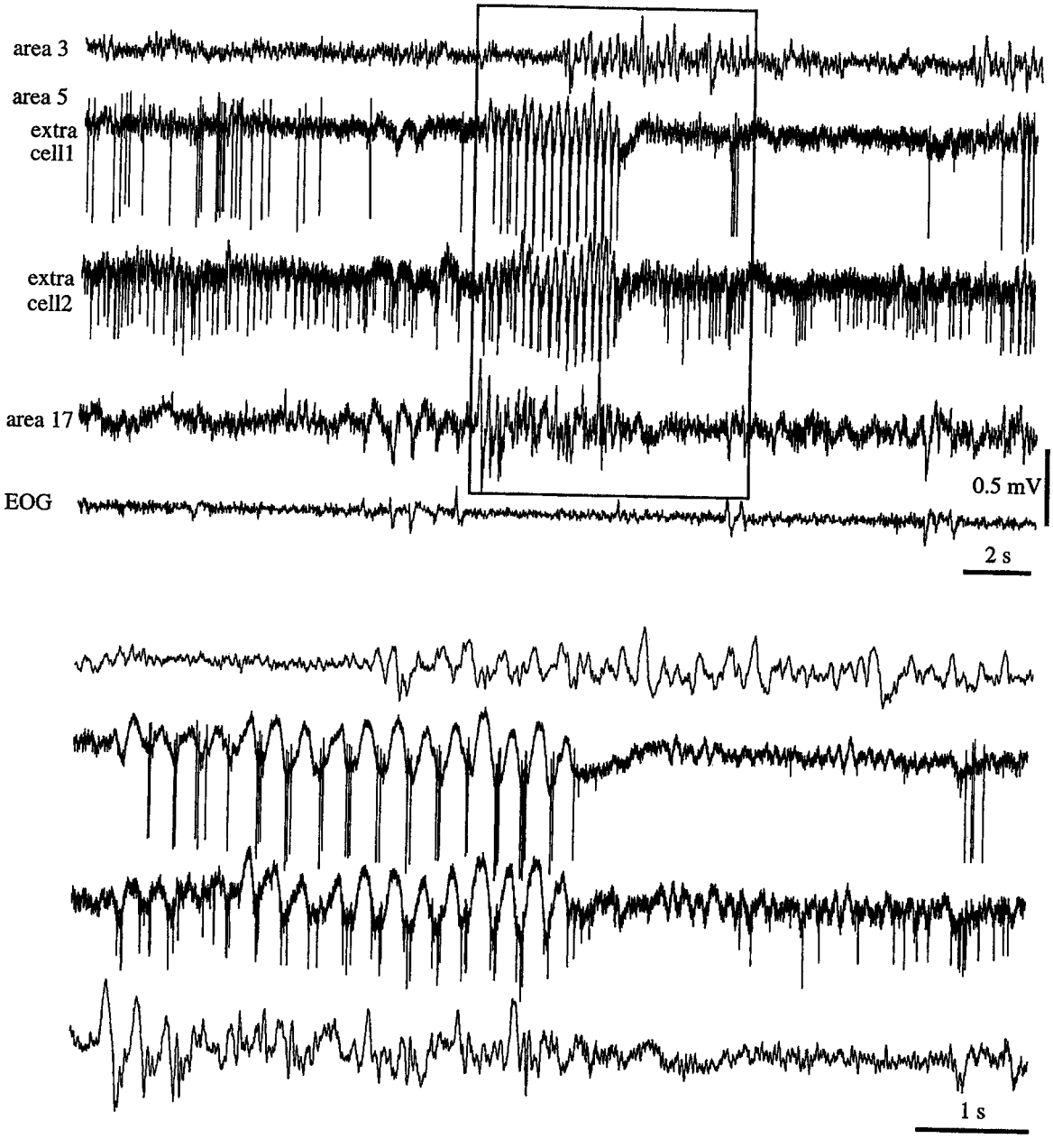

Fig. 5.23 Spontaneously occurring cortical SW seizure in chronically implanted cat. Five traces depict (from top to bottom): field potentials from the depth of somatosensory area 3; extracellular unit activities of two cells from association suprasylvian area 5 (1 and 2), each recorded simultaneously with focal slow waves through the same microelectrode; field potentials from the depth of visual area 17; and electrooculogram (EOG). The seizure, consisting of SW complexes at 3 Hz, occurred within two sites in area 5. The part framed in the top panel is expanded below. Note close time-relations between spike-trains or spike-bursts of cortical neurons and focal negative waves. From Steriade et al. (1998a).

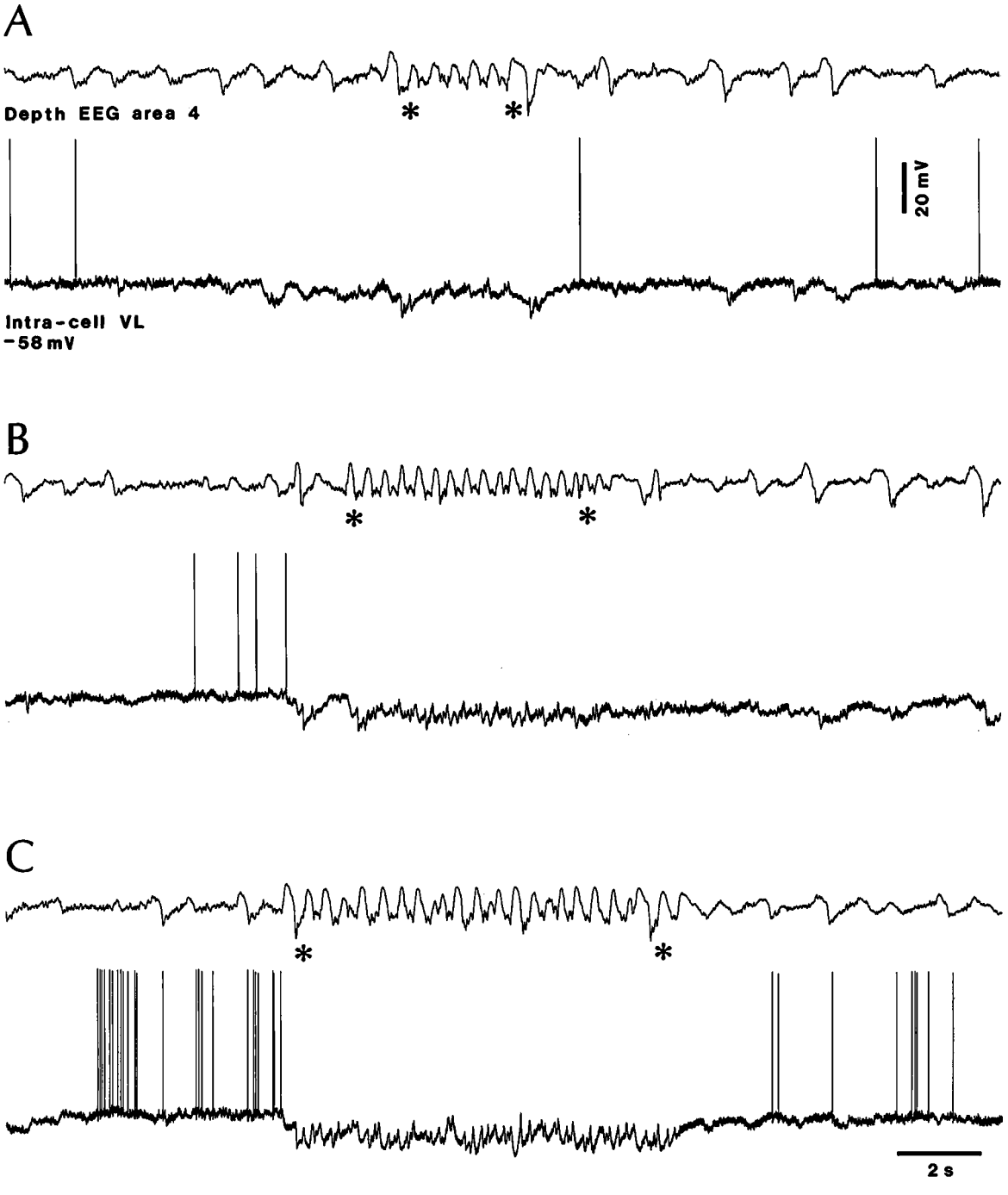

Fig. 5.24 Development from embryonic SW activity to longer-lasting SW seizures. Cat under ketamine-xylazine anesthesia. Depth-EEG recording from cortical area 4 together with intracellular recording from thalamocortical neuron in the ventrolateral (VL) nucleus. Note progressive development of SW seizures (between asterisks) from *A* to *C*, associated with progressive hyperpolarization and phasic IPSPs in a thalamic VL neuron. From Steriade and Contreras (1995).

[140] Schiff et al. (1999). The authors based their assumption, besides the commonality of some electrographic data, on the fact that inhibitory mechanisms are prominently implicated in both temporal lobe epilepsy and absence seizures (Fromm, 1986; Engel, 1995) and some thalamic nuclei (parts of pulvinar and of the rostral intralaminar complex) are connected with the temporal lobe (Yeterian and Pandya, 1989), thus providing a substrate for a partial overlap of temporal lobe and SW seizures. See also Sadler and Blume (1989) for synchronous SW complexes in patients with unilateral and bilateral focal EEG "spikes" in temporal lobes.

[141] Jones (1985); Steriade et al. (1997).

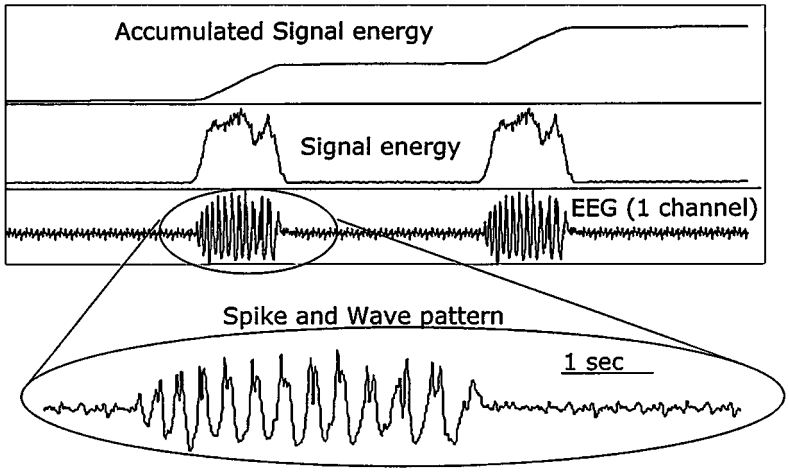

Fig. 5.25 Schematic representation of an EEG trace and the quantities computed from it. The recording from an EEG channel is shown (bottom trace) with a enlargement around a spike- and wave burst (enlarged area). The computed signal energy associated with the EEG channel is also shown (middle trace). Note the large increases in signal energy at the time of the spike and wave bursts. The accumulated signal energy increases during each successive increase in signal energy (top trace). From McKeown and McNamara (2001) See also the target article (Litt et al., 2001) of this commentary.

that *accumulated energy* (see Fig. 5.25) increases in the 50 min before seizure onset, and suggested that "changes in cellular and network function that lead to epileptic seizures likely develop over hours" [139]. Although apparently far from the electrographic aspect of absence seizures, non-linear autoregressive analysis of EEG traces revealed common dynamics between absence seizures and temporal lobe seizures, leading to the conclusion that, in some patients, the temporal lobe paroxysms share common circuit mechanisms with those underlying 3-Hz SW complexes [140].

The focal initiation of SW seizures in cortex and their subsequent spread through corticocortical and corticothalamic pathways was studied using multi-site field potentials recordings. In more than 1500 recorded seizures, the paroxysmal activity first appeared focally in the cortex [107]. Field potentials were recorded from three reciprocally interconnected regions: cortical areas 5 and 7, and the thalamic centrolateral (CL) nucleus of the rostral intralaminar complex. The CL nucleus was chosen as a preferred site for recording because of its widespread connections with cortex [141] that may be implicated in the synchronization of seizures. A spontaneous SW seizure in these cortical and thalamic structures is shown in the upper panel of Fig. 5.26. The paroxysmal activity first appeared in area 7, then spread to the adjacent area 5, and finally reached

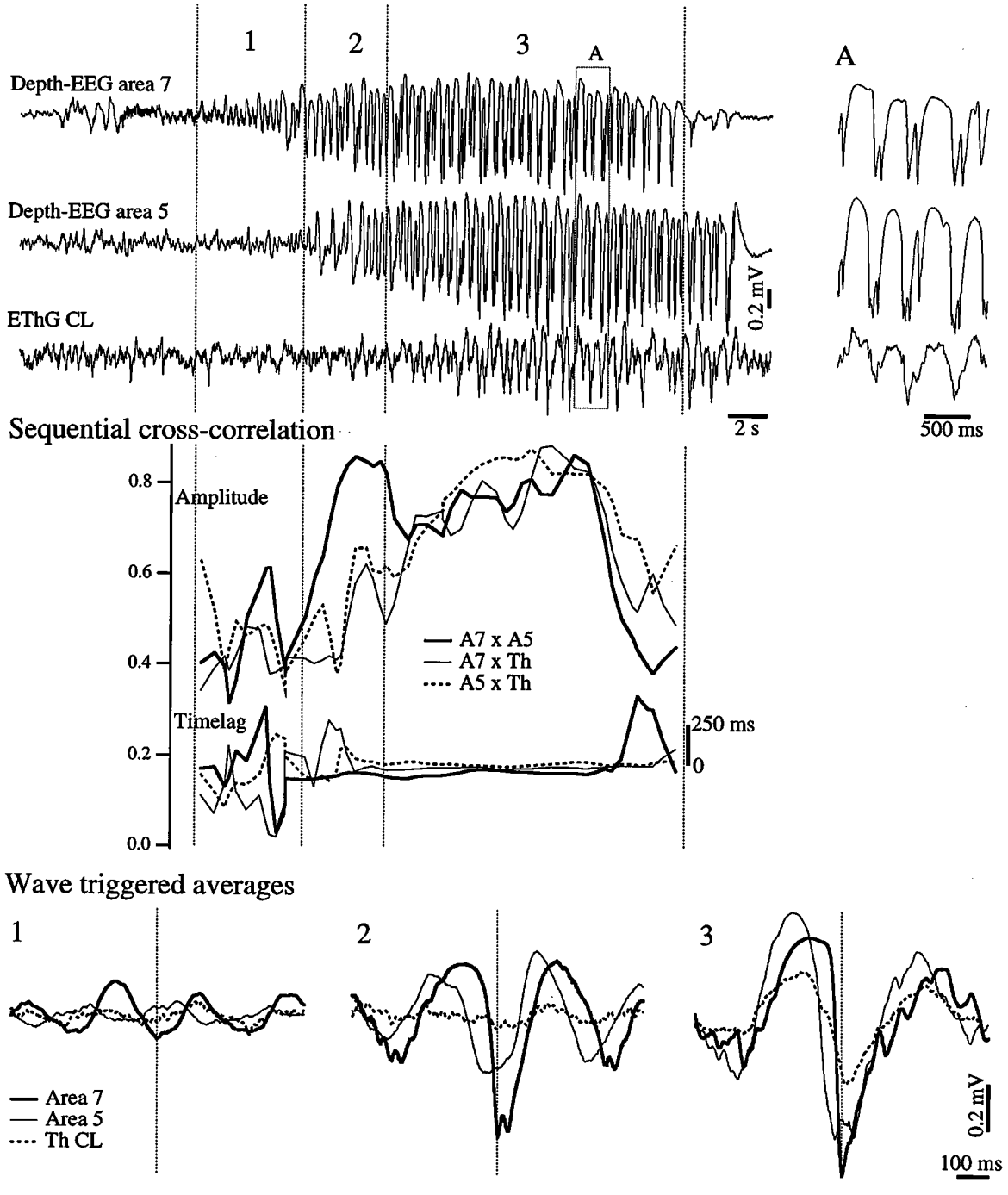

Fig. 5.26 Spontaneous SW seizures appear focally in some neocortical areas, and spread intracortically before related thalamic nuclei are entrained. Cat under ketamine-xylazine anesthesia. Depth-EEGs from areas 7 and 5, and electrothalamogram (EThG) from the intralaminar CL nucleus during a spontaneously occurring seizure (*upper panel*). *A*, expanded detail of the period marked A in the left panel. *Middle panel:* sequential cross-correlation of 500-ms windows from periods marked 1 to 3; peak amplitude on left ordinate; displacement of this peak from time zero of the cross-correlation function (right ordinate; see calibration bar from 0 to 250 ms). Thick lines represent the cross-correlation of area 7 with area 5 (*A7* × *A5*), thin line area 7 with thalamus (*A7* × *Th*), and dotted line area 5 with thalamus (*A5* × *Th*). The wave-triggered averages ($n = 12$) were taken from the period marked 1, 2 and 3, respectively (*lower three panels*). The spiky negativity of SW complexes, immediately following a wave in area 7, was used as reference time. From Neckelmann et al. (1998).

[142] Feucht et al. (1998).

[143] Steriade and Amzica (1994).

[144] Gökyigit and Caliscan (1995).

[145] Gibbs and Gibbs (1947); Niedermeyer (1965); Penry et al. (1971); Kellaway et al. (1980); Kellaway and Frost (1983); Shouse (2001).

[146] Cadilhac et al. (1965); Frank (1969).

[147] Glenn and Steriade (1982).

the thalamus. Sequential cross-correlations between cortical and thalamic activities showed a stabilization of intracortical time-lags and a concurrent increase in peak amplitude of the intracortical synchrony before the thalamus was entrained in the seizure. The amplitude of cross-correlation functions remained high until the paroxysmal activity ended, first in area 7, where it initially started. The increased intracortical synchrony during a seizure, established well before related thalamic nuclei were entrained, was a general finding in such analyses.

A non-linear modeling approach of EEG data recorded during SW seizures in children [142], in which the occurrence of "spikes" amplitudes in some frontal sites was reminiscent of earlier data showing the intracortical spread of SW complexes [31], supported the idea, arising from experiments using multi-site cellular and field potential recordings [143], that SW paroxysms are generated progressively by synaptic build up and are sequentially distributed through intracortical synaptic linkages (see section ***5.5.3***). That SW complexes in clinical absence seizures may *not* occur as a suddenly generalized paroxysm, that they are announced by precursor EEG events with increased amplitudes, and that they do not end suddenly on all cortical leads can be seen even by visual inspection of some EEG records (Fig. 5.27*A*). The same holds true for the SW seizures in feline penicillin epilepsy (Fig. 5.27*B*).

The focal occurrence of some SW seizures within restricted neocortical areas, at least at their onset, may explain the less detrimental effect of these paroxysms on cognitive abilities, compared to grand-mal or other types of seizures. Even more diffuse SW seizures may not be associated with behavioral change or intellectual decline [144].

5.5.2. Dependency of spike-wave seizures on behavioral state of vigilance

Although clinical absences can only be detected in the waking state, the electrographic correlates of these seizures, i.e., SW complexes at ~3 Hz, preferentially occur during the early or late stages of slow-wave sleep (SWS) [73]. Since the 1940s [74, 145], the relation between SW seizures and the EEG correlates of SWS has been demonstrated by several groups of investigators. By contrast, SW seizures are decreased or totally absent during REM sleep [73, 146].

In humans, epochs with sleep spindles are associated with a strikingly increased incidence of SW paroxysms (see above, Fig. 5.2). Starting from experimental data in naturally sleeping cats in which rostral intralaminar thalamocortical neurons fired spike-bursts within the frequency range of spindles [147], Kellaway and

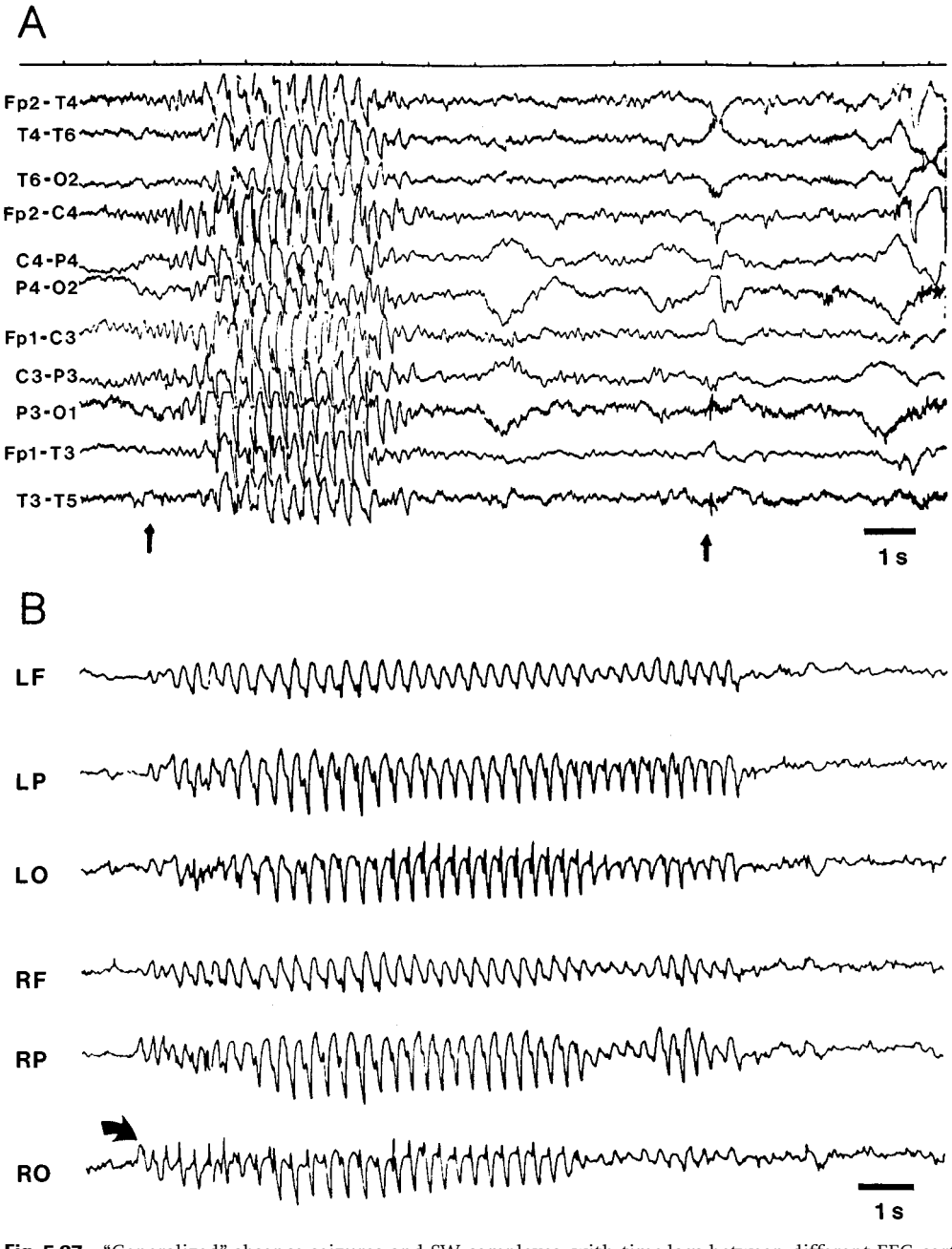

Fig. 5.27 "Generalized" absence seizures and SW complexes, with time-lags between different EEG cortical leads. *A*, absence of 12 s duration during the first year of life. Female child with normal development. The onset and termination of the behavioral seizure are shown by arrows. Note precursor EEG signs, preceding the full-blown SW seizure. *B*, SW seizure in cat after intramuscular administration of penicillin. LF, LP, and LO, left frontal, parietal, and occipital leads. RF, RP, and RO, corresponding right leads. Note that activity in the RO lead preceded that in LF, LP, LO, and RF leads by ~0.5 s. Modified from Cavazzuti et al. (1989, *A*) and Guberman et al. (1975, *B*).

[148] Kellaway et al. (1990).

[149] Gloor et al. (1990). The first description of spike-wave discharges elicited by parenteral injection of penicillin belongs to Prince and Farrell (1963).

[150] Patry (1931); Noachtar (2001).

[151] Arduini and Arduini (1954).

[152] See Fig. 4 in Prince and Shanzer (1966).

[153] Avoli et al. (1983).

[154] Szymusiak et al. (1996).

[155] Curró Dossi et al. (1991).

[156] Hirsch et al. (1983).

[157] Jung (1962).

[158] Danober et al. (1993).

colleagues [148] investigated the time-ordered relationship between spindles and 3-Hz SW complexes and found a non-random, positive relation between these two, sleep and paroxysmal, oscillations. In those few cases in which the concentration of SW complexes was low and the concentration of spindles was high, or vice-versa, it was assumed that this reciprocal relation is the result of an interference of SW complexes with spindle occurrence. This is the case in an experimental model of SW seizures, the feline generalized penicillin epilepsy (FGPE) [149], in which spindles are totally replaced by sequences of SW discharges. At variance, both spindles and SW complexes are present during the natural SWS in humans [148]. These relations between spindles and SW seizures are valid in intact-brain animals, in which the minority of thalamocortical neurons may fire low-threshold spike-bursts during SW seizures [77], but the minimal substrate for the generation of these seizures is the neocortex as they occur in thalamectomized preparations in which spindles are absent (see section ***5.5.3***).

The occurrence of SW seizures is facilitated during transitional states, especially between waking and SWS, during the state of drowsiness. This was observed in behaving primates [75] and in humans [150]. Under some experimental conditions, the opposite transition, from SWS to arousal, may also be accompanied by the occurrence of SW seizures. In pentobarbital-treated cats, the EEG response to high-frequency stimulation of the brainstem reticular core, which is usually blocked by this anesthetic [151], is occasionally an activity resembling that of SW complexes [152]. Moreover, in chronically implanted cats treated with systemically administered penicillin, a substance that promotes the appearance of SW complexes [149, 153], brainstem reticular stimulation during SWS elicits thalamic responses with interburst intervals similar to those seen in SW complexes, whereas no such responses are evoked during waking and REM sleep [154]. The rhythmic, SW-like thalamic responses to brainstem reticular stimulation may seem paradoxical in view of data showing that high-frequency reticular stimulation depolarizes thalamic relay neurons [155]. However, in those experiments [154], the effect was selectively elicited during SWS when the membrane potential of thalamocortical neurons is hyperpolarized [156] and single-pulse stimuli reaching thalamic cells could evoke a few low-threshold spike-bursts at the frequency of SW complexes.

In general, SW seizures are dramatically reduced or abolished with transition from SWS to spontaneous or sensory-elicited arousal [157] as well as during repetitive brainstem reticular formation stimulation [29], and they are increased after administration of low doses of a cholinergic receptor antagonist [158]. The results

obtained with lesions of nucleus basalis [159] are difficult to interpret because, in addition to their cortical projections, basalis neurons project to thalamic reticular nucleus [160] and, while the cholinergic projection to the cortex is facilitatory, the projection (both cholinergic and GABAergic) to thalamic reticular neurons is inhibitory.

5.5.3. Origin(s) and cellular mechanisms of spike-wave seizures

The fallacy of the earlier concept proposing a "centrencephalic" system that generates SW seizures, based on experiments using midline thalamic stimulation, was briefly exposed in section **5.1**. This hypothesis envisaged a system responsible for the so-called "suddenly generalized, bilaterally synchronous" paroxysmal discharges. Neither the morphological substrate, thought to be located "in the diencephalons and mesencephalon" [161], nor the physiological evidence could support the existence of such a deeply located structure that would lead to the strictly simultaneous occurrence of SW complexes over widespread cortical territories. As absence seizures, characterized by SW complexes at ~3 Hz, are accompanied by loss of consciousness, it is worth remembering that a century before the appearance of the "centrencephalic" hypothesis, William Carpenter also located consciousness in the deep, brainstem and thalamic, *automatic* apparatus, endowed with "the guidance of reason", but only if activated from cortex [162].

Despite the lack of experimental evidence supporting the "centrencephalic" concept, recent hypotheses and electrophysiological studies continue to elaborate on the origin of SW seizures in deep brain structures, particularly in the thalamus. The usually cited studies, which seemingly favor this idea, are the earliest experiments in this direction that did *not* demonstrate self-sustained SW seizures following midline thalamic stimulation [28], an EEG study using simultaneous recordings from thalamus and cortex in children with absence attacks accompanied by 3-Hz SW complexes in both structures but unable to distinguish where these paroxysms were initiated [163], and a more recent paper using positron emission tomography, which also showed thalamic activation but, again, could not detect the origin of activation [164]. Other data, taken to support the role played by the thalamus in promoting SW seizures, come from studies in slices maintained *in vitro* (see section *5.5.3.2*) that can provide, at best, analyses of cellular events which mimic the configuration of SW complexes after the administration of GABA receptor antagonists (sometimes called "*absence* seizures"!) but, in the absence of cortex, cannot distinguish the complexity of *in vivo* circuitry [165].

[159] Danober et al. (1994); Silveira et al. (2000).

[160] Steriade et al. (1987b); Parent et al. (1988).

[161] Penfield and Rasmussen (1950, p. 19).

[162] See Walshe (1957).

[163] Williams (1953).

[164] Prevett et al. (1995).

[165] Snead (1995) reproduced a remark of the late Gerhardt Fromm at the 1993 meeting of the American Epilepsy Society: "On going from behavioral observations in awake animals to recording single neuron activity *in vivo* and to recording more and more isolated neurons *in vitro* and eventually studying subcellular fragments, there is a progressive increase in the precision of the measurements, but at the same time also a progressive decrease in the neuron's connections to the rest of the nervous system". And Snead to continue: "Since circuitry is everything in generalized absence seizures, this admonition is particularly à propos to any discussion of future experimental approaches to this disorder" (p. 155).

The reader already understands the message here; namely, that the neocortex initiates and synchronizes SW seizures, before these paroxysms reach the thalamus. Before the more recent *in vivo*, and especially *in vitro*, studies that pointed to the thalamus as the crucial structure implicated in the genesis of SW seizures, I proposed that thalamic reticular (RE) GABAergic neurons are not only pacemakers of sleep spindles but are also crucially involved in SW seizures [166]. This idea stemmed from the evolution of spindles into SW seizures [74, 148, 149] and from data showing that ethosuximide, a drug that is effective in clinical and experimental SW epilepsy [167], markedly reduces spike-barrages of RE neurons, shifting the activity of these cells into tonic firing [168]. Ethosuximide and dimethadione, another anti-absence drug, reversibly reduce, in a dose-dependent manner, the low-threshold spike (LTS) of thalamocortical neurons *in vitro* [169]. However, depressing actions of ethosuximide on inhibitory processes in cultured cortical neurons have also been reported [170]. This is why we hypothesized, in view of the persistence of SW seizures in athalamic animals [171], that the action of ethosuximide in absence epilepsy may be envisaged as an effect at the cortical level. At the present time, I still think that RE neurons are implicated in a major cellular phenomenon of SW seizures, while, considering recent experimental evidence, this role is not in promoting these paroxysms but rather in inhibiting the great majority of thalamocortical (TC) neurons during cortically generated SW paroxysmal activity [77]. These data are discussed below (section *5.5.3.2*), after presenting the evidence for a cortical role in initiating SW seizures.

5.5.3.1. Evidence for a cortical role in initiation of spike-wave seizures

Several studies have reported the loss of SW seizures after thalamic lesions or functional inactivation, and concluded that the development of SW seizures requires the presence of both a functional cortex and a functional thalamus [172]. Other studies, focused on the role played by thalamic RE neurons, injected Cd^{2+} intrathalamically, a substance that blocks the low-threshold Ca^{2+} current (that gives rise to spike-bursts in RE neurons), which led to a significant decrement in ipsilateral SW paroxysmal activity [173], thus supporting the hypothesis concerning the role played by these GABAergic cells in SW seizures [166].

However, penicillin-induced SW complexes with frequencies lower than the classical 3 Hz have been found in the cortex devoid of thalamic inputs [174]. More importantly, SW seizures occur in athalamic cats and monkeys, both acutely prepared and chronically implanted, after cortical freezing or bilateral applications

[166] Steriade (1990): "... the idea can be advanced that any pharmacological manipulation that would decrease or abolish the inhibitory efficacy of RE spindle pacemaker upon thalamocortical neurons, thus diminishing the probability of high-frequency rebound bursts being transferred to the cerebral cortex, would also decrease the incidence of epileptic discharges" (p. 165).

[167] Guberman et al. (1975); Sato et al. (1982).

[168] Pellegrini et al. (1989).

[169] Coulter et al. (1989). More recent studies on rat and cat thalamocortical (TC) neurons *in vitro* (Leresche et al. 1998) questioned, however, the reduction or blockage of the low-threshold T-current by ethosuximide (ETX). Leresche and her colleagues showed that ETX decreased a non-inactivating Na^+ current, $I_{Na(p)}$, but had no effect on the I_T. These results warrant caution on the "ETX-Ca^{2+}" hypothesis. This study also discusssed the requirement of intracellular recordings to support the concept of low-threshhold spike-bursts fired by TC neurons in various models of genetic "absence epilepsy" as, with some exceptions, such studies were conducted with extracellular recordings (see also main text related to this issue). The exceptions are those that used intracellular recordings from rats with genetic SW seizures and found that the overwhelming majority of TC neurons do *not* fire low-threshold spike-bursts during SW seizures (Pinault et al., 1998; Slaght et al., 2000, 2002), thus corroborating our data (Steriade and Contreras, 1995). See the comprehensive review on channels and neuronal networks in absence epilepsy by Crunelli and Leresche (2002).

[170] Barnes and Dichter (1984).

[171] Steriade and Contreras (1998). It was assumed that SW seizures in athalamic animals display SW complexes with "a different morphology from the typical thalamocortical spike-and-wave pattern and ... (are) also slower in frequency" (Destexhe et al., 1999c). However, the expanded part in Fig. 5.28, from such an experiment with hemithalamectomy, shows that SW complexes are quite classic in morphology and their frequency is 3 Hz at the onset of the long-lasting seizure, slowing down to 2 Hz toward its end, as usually happens in SW seizures recorded from intact-brain animals. As to the argument in the paper by

Destexhe et al. (1999c) concerning negative findings (namely, results indicating the absence of SW in athalamic animals; Vergnes and Marescaux, 1992), I submit that positive findings (presence of such seizures after thalamectomy) would prevail since removal of the thalamus is a heroic procedure that may have drastic influences on the ability of the neocortex to sustain SW seizures. Recent studies on a genetic model of absence epilepsy firmly support the cortical origin of such seizures (Meeren et al., 2002).

[172] Avoli and Gloor (1981); Gloor and Fariello (1988); Vergnes and Marescaux (1992).

[173] Avanzini et al. (1992).

[174] Pellegrini et al. (1979).

[175] Marcus and Watson (1966, p. 606); Marcus et al. (1968a).

[176] Marcus et al. (1968b, p. 371).

of strychnine, pentylenetetrazol or conjugated estrogen [175, 176]. In some of these animals, "bilateral synchronous discharges were accompanied by ... transient suspension or imperfect continuation of a repetitive act followed by resumption of the action as the abnormal cortical discharge terminated" [175]. Also, cortical SW seizures in athalamic monkeys were associated with "apparent impairment of awareness during the (SW) burst (absence or reduction of responses to visual, tactile or painful stimuli)" [176]. These data convincingly demonstrate that seizures with SW complexes at ~3 Hz, accompanied by behavioral signs that are similar to those occurring in human petit mal epilepsy, may be generated in the absence of the thalamus.

The thalamus can certainly play a role in the maintenance and widespread synchronization of SW discharges. The presence of an intact thalamus, in particular the rostral intralaminar and ventromedial nuclei with widespread cortical projections [141], may reinforce the coherence of paroxysmal activity arising in various neocortical areas.

The issue is: *what is the minimal substrate that initiates and sustains SW seizures?* In our hands, all available data demonstrate that such seizures are initiated in the cortex, without thalamic participation at their very onset. These findings are as follows.

(a) Total hemithalamectomy did not prevent the occurrence of SW seizures elicited by local injection of bicuculline in the cortex [171]. The ipsilateral cortical EEG had little spontaneous activity and showed no spindling, but bicuculline induced long sequences (from 1–2 min up to 6–7 min) of continuous SW activity at 2–4 Hz, with a spectacular synchronization across all cortical leads (Fig. 5.28). Simultaneously, the contralateral cortex exhibited the normal sequences of spindle waves. Of course, we simply use the term *electrical SW seizure* and do not consider it as necessarily homologous to different forms of clinical absence epilepsy because these experiments were conducted under barbiturate anesthesia and seizures were induced by bicuculline. Nonetheless, other experimental evidence, from spontaneously occurring SW seizures (see below), also point to a prevalent role of neocortex in generating SW seizures.

(b) Another approach in determining the relative contributions of cortical and thalamic networks in the generation of seizures after blockade of inhibition consisted of systemically injecting the $GABA_A$ antagonist bicuculline in animals in which the cortex of the left hemisphere was completely removed while the

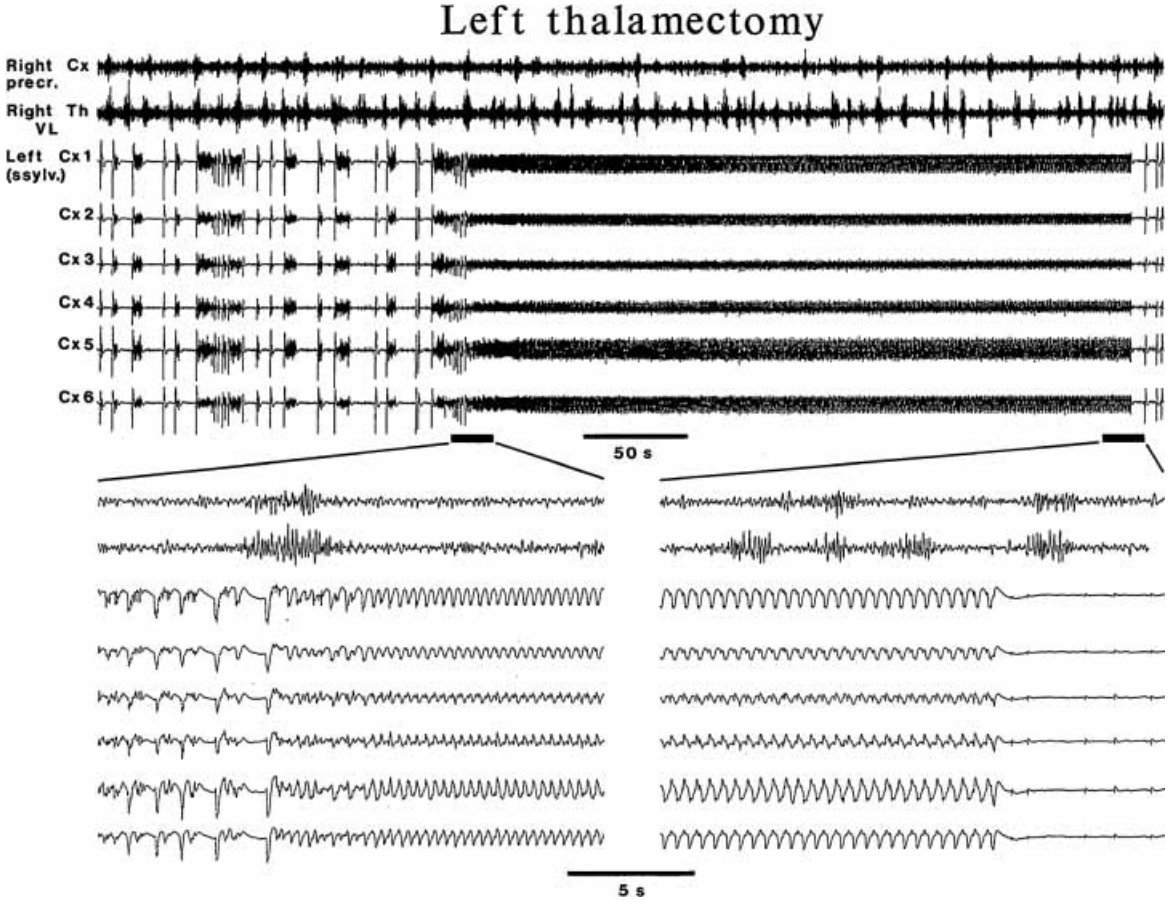

Fig. 5.28 Prolonged SW seizure appears in the cortex after ipsilateral thalamectomy. Cat under barbiturate anesthesia. Removal of the left thalamus was done either acutely by suction (entering through the right hemisphere and midline) or by kainic acid injection 2 days before the experiment (see histological aspects of kainic-induced thalamic lesions in Steriade et al., 1993f). In this figure, seizure patterns were induced by local injection of bicuculline in the left suprasylvian cortex after unilateral (left) thalamectomy. Note the appearance of extremely long runs (~5 min duration) of cortical SW complexes at 2–4 Hz. The EEG from the contralateral (right) precruciate cortex and thalamic ventrolateral (VL) nucleus showed spontaneous spindling. From Steriade and Contreras (1998).

[177] Contreras et al. (1996a); Timofeev and Steriade (1996).

cortex of the right hemisphere was left intact and multi-unit recordings were made from the left thalamus of the decorticated hemisphere (Fig. 5.29). Despite the absence of cortex on the left, a condition that diminishes the spatio-temporal coherence of thalamic spindles and tends to disorganize them (see section *3.2.1.2* in Chapter 3), thalamic spindle sequences occurred synchronously because of the proximity of recording sites [177]. Systemic injection of bicuculline led to the appearance of high-amplitude, isolated spikes in the right cortical EEG (Fig. 5.29*A*) and, subsequently, within 1–3 min, a

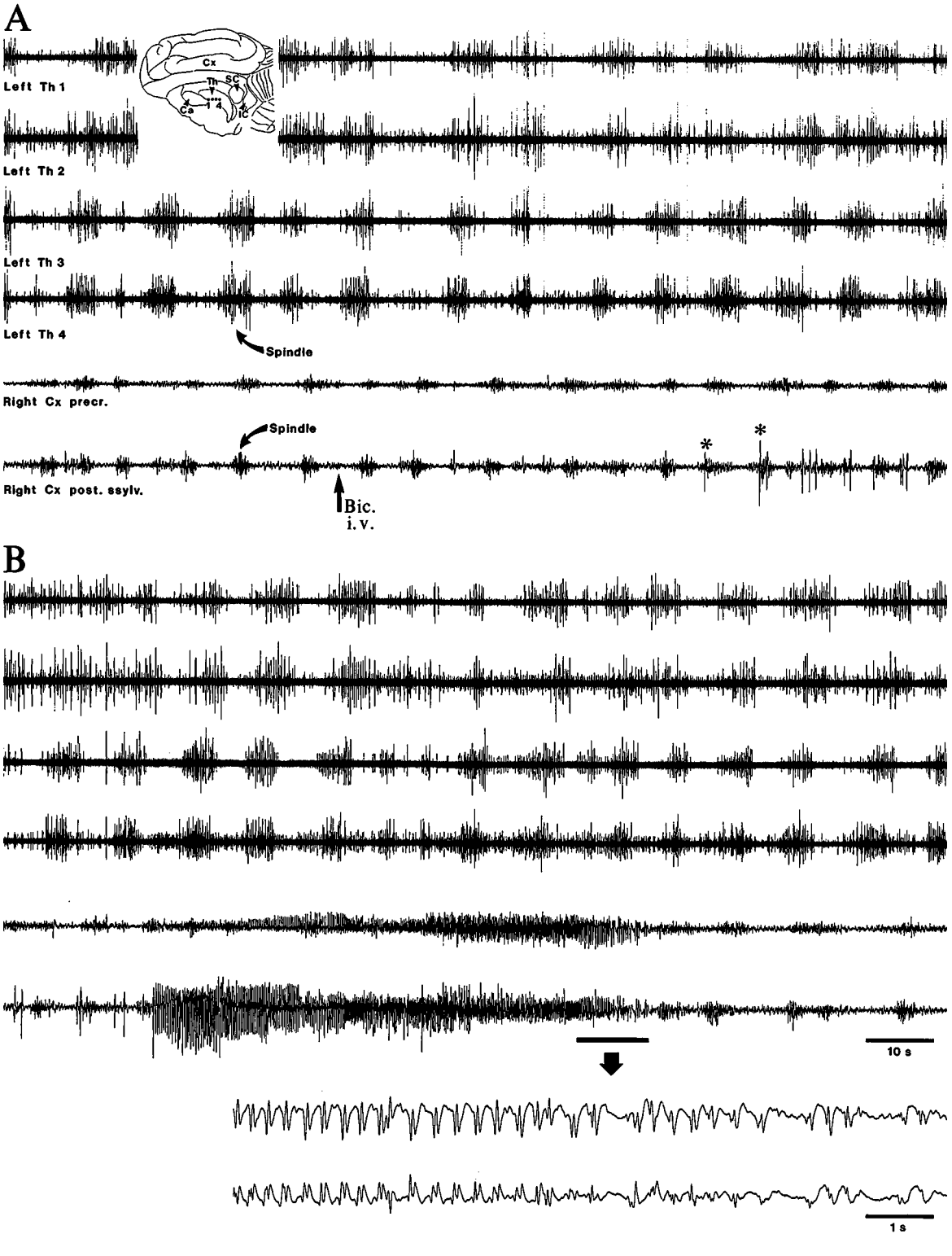
A
Cx
Th
SC
Ce
IC
Left Th 1
Left Th 2
Left Th 3
Left Th 4
Spindle
Right Cx precr.
Spindle
Right Cx post. ssylv.
Bic.
i.v.
B
10 s
1 s

[178] Bal et al. (1995a).

[179] Castro-Alamancos (1999).

full-blown seizure with SW complexes at ~3 Hz appeared in both right cortical foci (Fig. 5.29*B*). In contrast, thalamic activity in the decorticated hemisphere was largely unaffected, although some additional spike activity could occasionally be observed on the background of ongoing spindling.

(c) Finally, in these experiments using extracellular recordings, bicuculline was injected into restricted thalamic territories in order to determine the possible co-participation of the thalamus in SW seizures. About 20 min after an injection of bicuculline, the number of action potentials per spike-burst during spindles increased, the repetition rate of spike-bursts decreased from that of spindling (~10 Hz) to ~4 Hz, the synchrony of spike-bursts between cells increased, and cortical EEG also showed a slowed frequency and increased amplitude of spindles, but no paroxysmal pattern compared to the *bona fide* SW seizures depicted in Figs. 5.28–5.29. This result [171] is similar to the slowed spindles reported in thalamic slices from ferrets [178] and to observations of rats, in which thalamic injections of bicuculline gave rise to hypersynchronous and slow spindles, but not to SW seizures [179]. *In conclusion, thalamic injection of bicuculline induces a pattern of highly synchronous slowed spindling, but not SW seizures.*

Experiments using multi-site, field potential, extracellular, and intracellular recordings of spontaneously occurring seizures under ketamine-xylazine anesthesia (see section ***5.5.1*** for some factors explaining the relative high percentage, 20–30%, of spontaneous SW seizures in such preparations) further demonstrated the intracortical synchronization of SW paroxysms [143]. During the self-sustained activity that followed repetitive photic stimulation or rhythmic pulse-trains applied to diffusely projecting thalamic nuclei, spike-trains of cortical neurons were superimposed over the depth-negative field component or "spike" (depolarizing phase) of SW complexes, and neuronal silence occurred during the depth-positive field component or "wave" (hyperpolarizing phase) of

Fig. 5.29 (opposite) Intact-cortex hemisphere has a lower threshold for seizure initiation, induced by systemic injection of bicuculline, than the decorticated one. Cat under barbiturate anesthesia. *A–B*, four multi-unit thalamic recordings from left decorticated hemisphere (*Left Th 1 to 4*; interelectrode distance was 0.4 mm) showing spike-bursts corresponding to spindle sequences. Two lower traces are bipolar EEG traces from precruciate cortex (*Right Cx precr.*) and posterior suprasylvian gyrus (*Right Cx post. ssylv.*) in the right (intact) hemisphere showing spontaneous spindle oscillations. After the injection of bicuculline i.v. (*arrow, Bic. i.v.*), paroxysmal spikes preferentially appeared on the EEG (*asterisks*) until a full-blown cortical seizure dominated the EEG, displaying SW complexes at about 3 Hz (arrow in panel *B* indicates expanded trace with SW complexes). Thalamic leads showed virtually no alteration of normal spontaneous spindling activity. From Steriade and Contreras (1998).

these complexes. The degree of synchrony among simultaneously recorded neurons increased progressively from the pre-seizure (sleep-like) period to the early stage of SW seizure and, further, to the late stage of the seizure (Fig. 5.30). These data showed that, although the conventional definition of SW seizures as "suddenly generalized" paroxysms might be valid at the EEG level (however, even at this macroscopic level, some cortical leads may be seen to precede other sites by times up to ~0.5 s; see Fig. 5.27), cortical neurons display time-lags as short as 3–10 ms up to 50 ms or even longer intervals that cannot be detected by visually inspecting the EEG. Then, the build up of SW seizures obeys the rule of synaptic circuits, sequentially distributed through short-, medium-, and long-scale synaptic linkages [143].

Dual intracellular recordings during spontaneous SW seizures reinforced the notion of intracortical synchronization of SW seizures [107]. The delays between corresponding events in simultaneously recorded cortical neurons were reduced during spontaneously occurring seizures, as compared to the preceding epochs of slow sleep-like oscillation. The range of values observed during seizures had decreased variability, as well as a central tendency closer to zero. This was most pronounced for the 3-Hz SW complexes (Fig. 5.31). In this figure, the area 5 neuron preceded the area 7 neuron in >95% of the depolarizing phases, corresponding to the EEG "spike" component. Compared to the time-lags measured during the slow oscillation, prior to seizure, the time-lags between the two simultaneously recorded areas 5 and 7 neurons were significantly smaller during both slower SW complexes (1–2 Hz; $p < 0.01$) and faster SW complexes (3 Hz; $p < 0.00001$).

Basically similar findings were obtained by recording intracellularly from two cortical neurons while small amounts of bicuculline leaked into the cortex. The following parameters were quantified: the individual time-lag (between a pair of corresponding events); the sign (+ or −) of the individual time-lag (indicating which site comes first); and the dynamic evolution of these two parameters. In 80% of seizures, the sign of the individual time-lags alternated throughout the seizure. The example in Fig. 5.32 shows a simultaneous dual intracellular recording from areas 5 and 7, in conjunction with a depth-EEG from the same areas. Below, the relations between times of maximal slope (highest $\Delta V_m/\Delta t$) at the onset of depolarization in the two recorded neurons are plotted. This demonstrates that the time relations between those two neurons changed continuously, so that they alternated in preceding each other (panels *A* and *B*). Figure 5.32 also illustrates that even though the paroxysmal activity was induced by a bicuculline-filled

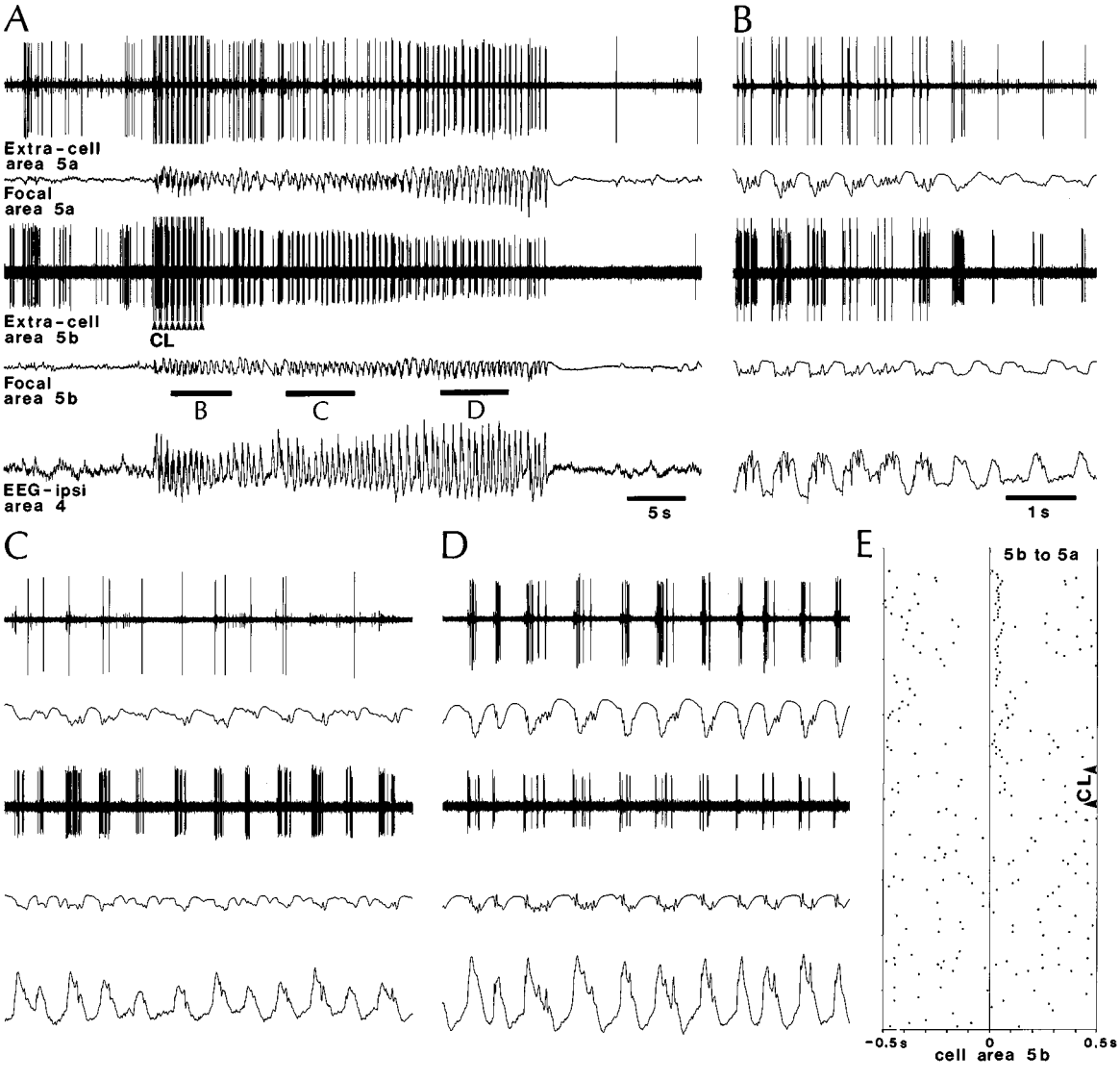

Fig. 5.30 Self-sustained spike-wave (SW) seizure at 2–3 Hz following thalamic centrolateral (CL) stimulation. Cat under ketamine-xylazine anesthesia. *A*, simultaneous recordings of unit discharges and focal waves (field potentials) in cortical association areas 5a and 5b as well as ipsilateral EEG from motor area 4. CL stimulation (arrowheads) consisted of pulse-trains (three stimuli at 10 Hz, repeated every 0.5 s). After nine pulse-trains, self-sustained SW activity lasted for 30 s. *B–D*, traces marked by horizontal bars in *A*, are expanded below (without the EEG from area 4) to show the relation between cell firing and various components of SW complexes in field potentials. Time calibration is the same from *B* to *D*. Note that the two neurons recorded from area 5 (*a* and *b* in *B*) became synchronous only toward the end of SW activity, in *D*. In *E*, first-spike analysis (see figure source paper for the method for such analysis), to be read from bottom to top, of relations between the neuron with a large spike (*a*) in area 5a and the neuron in area 5b, before and during CL stimulation as well as during the subsequent SW seizure. Time is indicated on the abscissa (from 0 to 0.5 s). The polarity of extracellularly recorded action potentials and focal waves is the same as for intracellular recordings (positivity up). From Steriade and Amzica (1994).

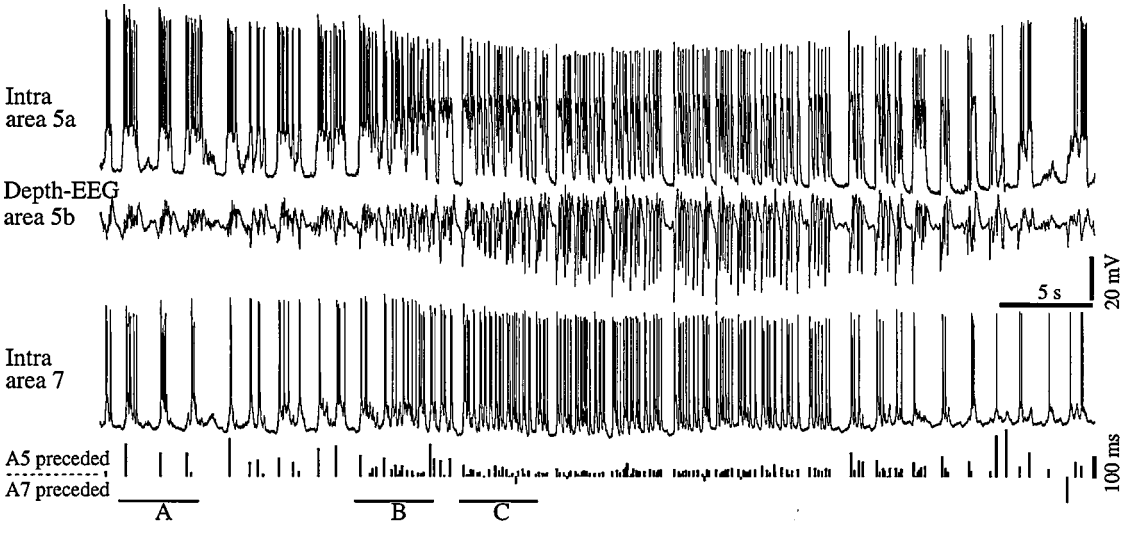

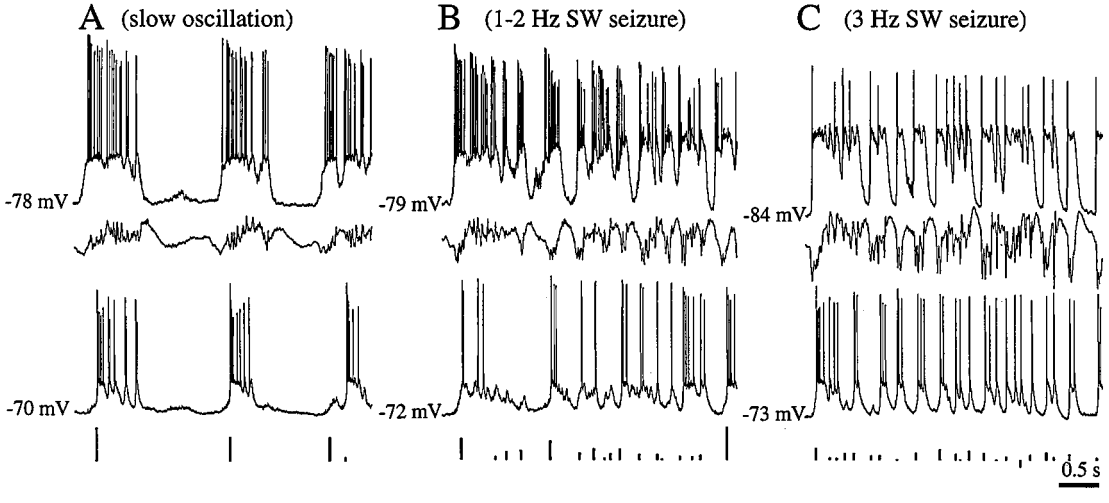

Time relation histograms between cells

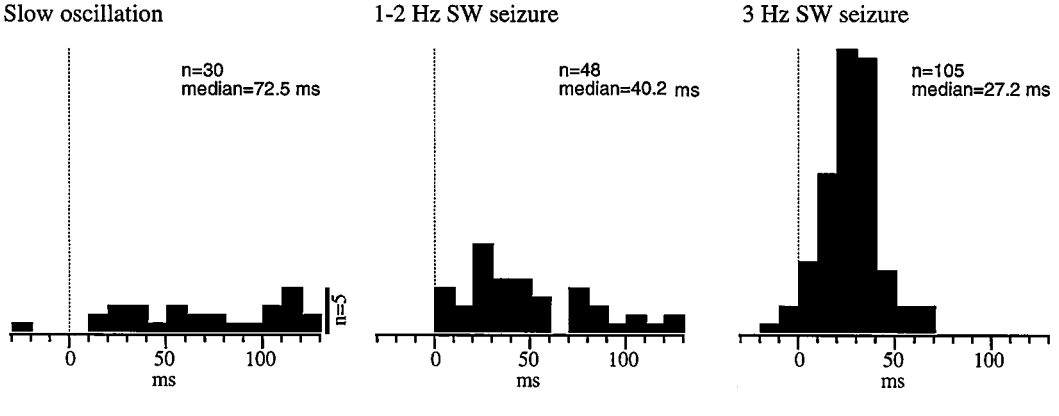

syringe inserted rostrally to the area 5 neuron, the cell in the distant area 7 actually preceded the cell in area 5 for most of the seizure. In most seizures the activity far away from the focal bicuculline diffusion in the rostral part of the suprasylvian gyrus was observed to precede the activity closer to the infusion, at least intermittently.

To study the effect of disconnecting intracortical pathways on the synchronization of SW paroxysmal activities and the possible role of the thalamus in the partial or total recovery of the synchronization, complete coronal transections of the suprasylvian gyrus were performed. Before the transection, the wave-triggered averages performed with reference to the sharp depth-negativities in area 7 showed a high intracortical synchrony of bicuculline-induced seizures (Fig. 5.33). Using averages triggered by the focal negativities in the thalamic centrolateral (CL) nucleus, the thalamus was only weakly synchronized with the activity in area 7, but it was better synchronized with the activity in area 5. After transection between areas 5 and 7, the average triggered by area 7 activity demonstrated impaired intracortical synchrony. The negativity in area 5, which was evident before transection, was no longer observed. By contrast, with averages triggered by thalamic CL activity, synchronous paroxysmal spikes were seen both in areas 5 and 7, thus suggesting that the synchrony may be achieved for brief periods through corticothalamocortical pathways. Thus, SW seizures are generated and synchronized within intracortical networks and, after disconnection of these synaptic linkages, corticothalamocortical loops may partially and intermittently recover the synchrony.

Fig. 5.31 (opposite) Time-lags between activities in simultaneously impaled neurons from areas 5 and 7 decrease in amplitude and variability during the development from slow oscillation to spontaneously occurring SW seizure. Cat under ketamine-xylazine anesthesia. Between intracellular traces, field potential recording from a more posterior site in area 5. For each cell and each depolarization complex we selected the time-point of the steepest slope of the membrane potential (highest $\Delta V_m/\Delta t$). The time-point of the area 5 cell was subtracted from the corresponding time-point of the area 7 cell, and the resulting time-lag plotted along the ordinate as a line starting from zero (see calibration from 0 to 100 ms at the extreme right, below the intracellular trace from area 7). Vertical lines appear at the time-point of the area 7 neuron. The *lower three panels* show the distribution of these intercellular time-lags during slow oscillation (*left*), the initial part of the seizure when slow (1–2 Hz) SW complexes were present (*middle*), and the latter part of the seizure with SW complexes at 3 Hz (*right*). During the period analyzed, the area 5 cell preceded the area 7 cell in 178 of the 182 analyzed depolarizations. The following bins were used to display the time-lags between the firing of the two neurons in different (sleep-like and seizure) epochs. The three bins to the left of zero contain time-lags of −200 to −100 ms, −100 to −30 ms, and −30 to 0 ms, respectively. Between 0 and 100 ms, the bin width is 10 ms. The three bins above 100 ms contain time-lags of 100–150 ms, 150–200 ms, and 200–300 ms, respectively. The time-lags between the two cells differed from the slow oscillation to the 1- to 2-Hz seizure epoch ($p < 0.01$) and 3-Hz seizure epoch ($p < 0.00001$). Within the seizure, time-lags were significantly shorter during the 3-Hz part compared to the 1–2 Hz part ($p < 0.0001$; all comparisons performed with the Mann-Whitney *U*-test). From Neckelmann et al. (1998).

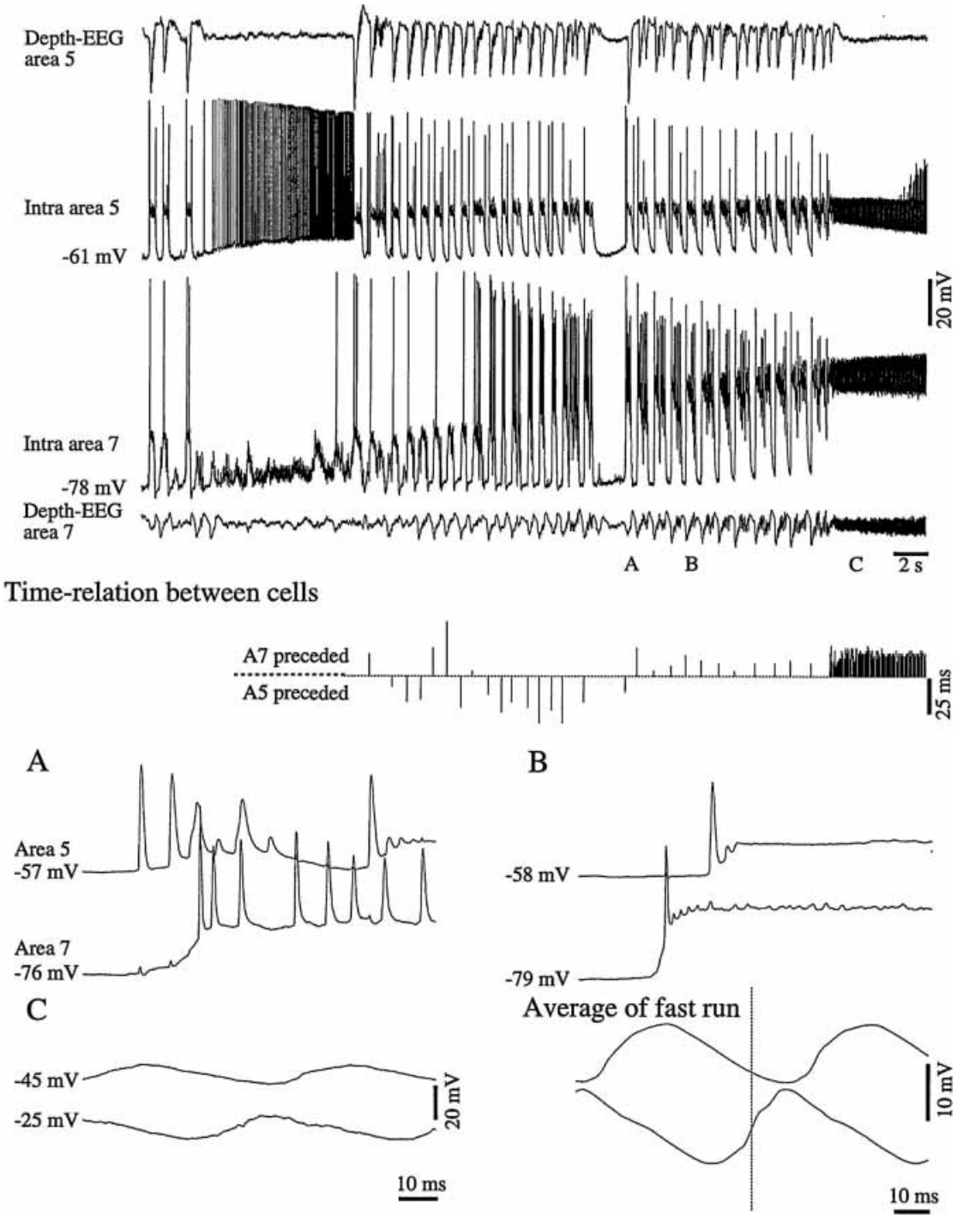

Fig. 5.32 Time-relations between intracellularly recorded neurons vary during the course of a bicuculline-induced seizure. Cat under ketamine-xylazine anesthesia. Seizure in an animal with a syringe with 10 μl of 0.2 mM bicuculline in area 5. The bicuculline was not injected but only leaked. *Upper panel*, simultaneous dual intracellular recording together with depth-EEG from areas 5 and 7. For each cell and each depolarization complex, the time-point of the steepest slope of the membrane potential (highest $\Delta V_m/\Delta t$) was selected. The time-point of the area 7 cell was subtracted from the corresponding time-point of the area 5 cell, and the resulting time-lags were plotted along the ordinate as vertical lines from zero, with the time-point of the area 5 cell along the abscissa (see time calibration, 25 ms, at the extreme right). Period *A*: the neuron in area 5 clearly preceded the neuron in area 7. This order was reversed in periods *B* and *C*. *Bottom right panel*: event-related average ($n = 100$) of the two cells triggered by the time-point of the area 7 neuron (dotted line) to estimate the relationship between the two neurons during the fast runs. From Neckelmann et al. (1998).

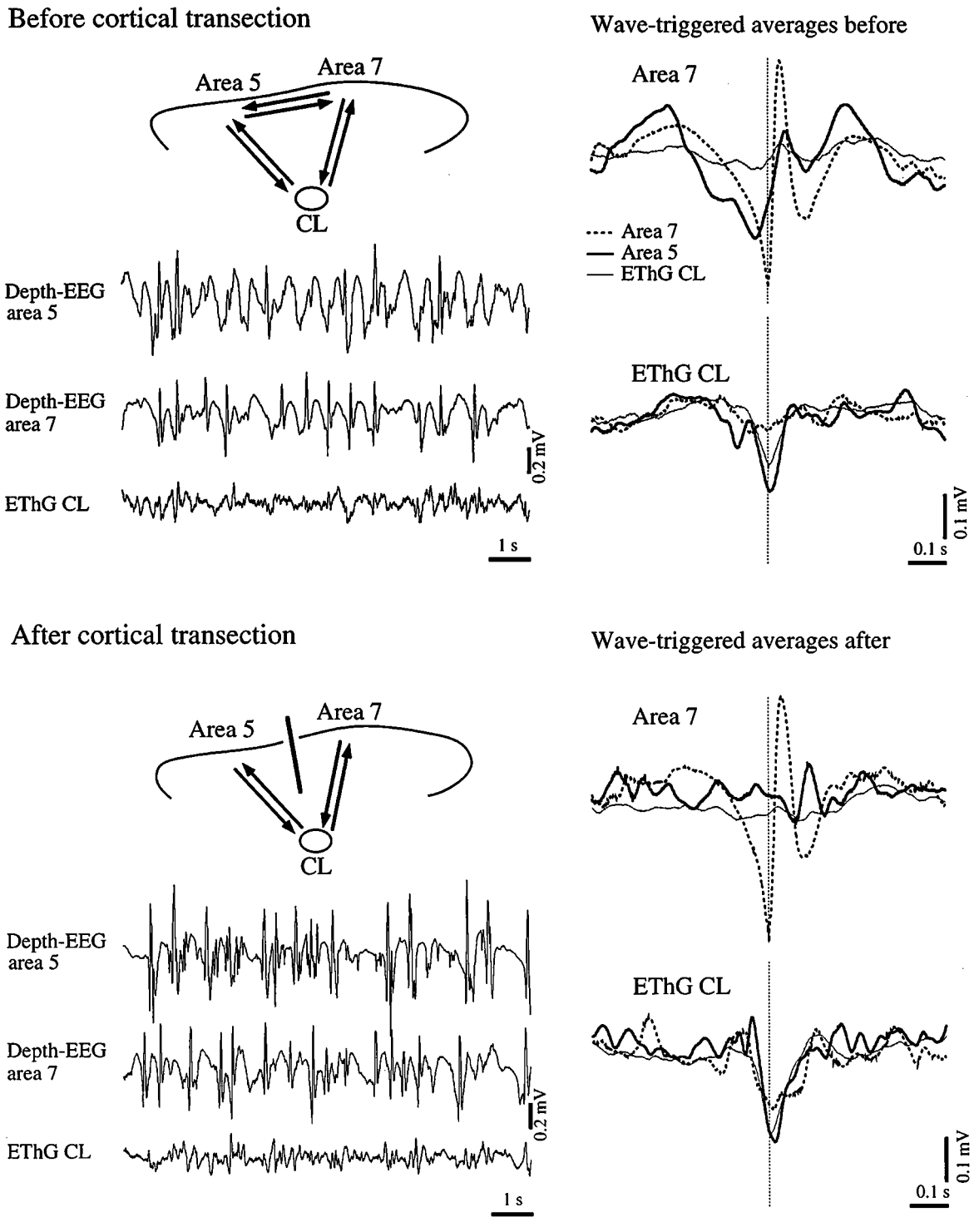

Fig. 5.33 Transection of intracortical pathways impaired intracortical synchronization of bicuculline-induced paroxysmal activity; however, intracortical synchrony could be restored intermittently by corticothalamocortical pathways. Cat under ketamine-xylazine anesthesia. *Upper panels*: schematic drawing illustrates the reciprocal intracortical and corticothalamic connections in the brain-intact animal. *Below*, depth-EEG recordings from cortical area 5 and 7 and electrothalamogram (EThG) from the thalamic centrolateral (CL) nucleus after the animal had received 2 mg/kg bicuculline i.v. Wave-triggered averages ($n = 50$), with reference time taken on depth-negativity in area 7, demonstrate intracortical synchrony. *Lower panels*: same animal, after complete transection of the suprasylvian gyrus leading to disconnection of intracortical pathways; see intermittent recovery through corticothalamocortical loops. From Neckelmann et al. (1998).

[180] Contreras et al. (1997a).

[181] McKeown et al. (1999); Rodin (1999). See also [30].

The synchronization of cortically generated SW seizures, which is impaired after transections between areas 5 and 7 [107], stands in contrast with the cortical coherence of the thalamically generated spindle oscillation, which survives deep cuts in the middle of the suprasylvian gyrus [180]. The quasi-simultaneity of sleep spindles is due to divergent corticothalamic and intrathalamic connectivity [180]. Although thalamic neuronal activities are apparently not essential for the development of seizures with SW/PSW complexes at 2–3 Hz, as they occur in athalamic animals [171, 175, 176] and even in small cortical slabs [87], the thalamus may effectively assist intracortical synchronization processes of SW seizures through cellular processes discussed in the following section.

The absence of SW seizures in cortical slices is probably because there are no long-range, intrahemispheric and callosal, connections to synchronize this paroxysmal activity.

To sum up, cortical SW seizures are *not* generated simultaneously over widespread territories. On the contrary, they arise in some areas, in which unknown (metabolic and/or neuronal circuit) factors render neurons more excitable, and propagate with short or long delays to other cortical fields before reaching the thalamus. EEG recordings from humans with absence epilepsy have also questioned the absolute bilateral synchrony of paroxysmal discharges and presented evidence for different, independent sources of SW complexes [181].

5.5.3.2. Thalamic reticular and thalamocortical neurons in spike-wave seizures

During cortically generated SW seizures, two major types of thalamic neurons, reticular (RE) and thalamocortical (TC), undergo opposite influences: the former faithfully follow each PDS of SW complexes, whereas the majority of the latter are steadily hyperpolarized and display phasic IPSPs that do not succeed in de-inactivating Ca^{2+}-dependent low-threshold spikes (LTSs), and thus do *not* transfer spike-bursts to the cortex. This is due to the much greater synaptic power of the excitatory cortical projection to RE neurons than to TC neurons (see section ***2.4.3*** and Fig. 2.39 in Chapter 2). Consequently, driving RE neurons ultimately leads to inhibition of TC neurons.

The behavior of the third type of thalamic neurons, GABAergic local interneurons located in different dorsal thalamic nuclei of cats and primates, has not yet been systematically investigated but, in view of the general aspect of SW seizures, it is expected that these local-circuit cells play an ancillary role in SW seizures.

[182] Domich et al. (1986); Steriade et al. (1986); Avanzini et al. (1989); Huguenard and Prince (1992); Bal et al. (1995b).

[183] Tsakiridou et al. (1995); Avanzini et al. (1999). See also the role of RE neurons in experiments on genetically determined absence seizures recorded *in vivo* (Slaght et al., 2002).

[184] Steriade and Timofeev (2001).

Firstly, I report data from electrophysiological studies of RE neurons during SW seizures. Next, I present data on the inhibition of TC neurons during these seizures. Finally, I discuss the hypothesized role of GABAergic processes in the induction of SW paroxysms.

Simultaneous recordings of cortical EEG and RE neurons revealed that spontaneous cortical seizures with SW/PSW complexes at 2–4 Hz, developing without discontinuity from sleep-like patterns, are associated with spike-bursts in RE neurons, which follow each paroxysmal "spike" in cortical EEG (Fig. 5.34). Note that the usual spike-bursts (duration ∼40 ms) of the RE neuron during sleep-like patterns, prior to the paroxysmal episode (first nine traces in panel *C*), developed into longer-duration spike-bursts (∼200 ms) during the initial part of the seizure with SW complexes at ∼1.5–2 Hz (next 11 traces), and that the reduced duration of the RE cell's spike-bursts (40–100 ms) occurred during the cortical SW complexes at ∼4 Hz (next 30 traces). The spike-bursts fired by RE neurons have a much longer duration (generally up to ∼50 ms) than those fired by TC neurons (5–15 ms) [182]. Such low-threshold spike-bursts may reach 200 ms during SW seizures.

During cortical seizures with SW complexes at ∼3 Hz, simultaneous recordings of cortical EEG activity, RE cell's unit discharges, and the intracellular activity of a TC neuron from the ventrolateral (VL) nucleus, a target of RE cells, showed the same faithful following of each cortical EEG "spike" by the RE cell and, in contrast, IPSPs in the TC cell at the same frequency as that displayed by cortical EEG "spikes" and RE cells' spike-bursts (Fig. 5.35). RE neurons faithfully follow, with prolonged spike-bursts, each cortical paroxysmal discharge during SW seizures, as was also demonstrated intracellularly (see the end of the seizure depicted in Fig. 5.5, section ***5.2.1***). Acutely dissociated RE cells demonstrate a selective increase in the amplitude of Ca^{2+}-dependent T-current in a genetic model of absence epilepsy [183].

In summary, then, *GABAergic RE neurons participate actively during cortically generated SW seizures*. This conclusion is drawn from cellular data showing the increased propensity of RE cells to bursting during SW seizures [77, 184], an increase in the ionic current underlying the spike-bursts of RE cells in these seizures [183], and a decrease in ipsilateral SW activity following Cd^{2+}-induced blockage of RE cells' spike-bursts [173].

The opposite was shown to occur in TC cells. Before presenting cellular data demonstrating that the majority of TC cells are inhibited during cortically generated SW seizures, we should discuss previous concepts favoring the contrary; namely, the active role

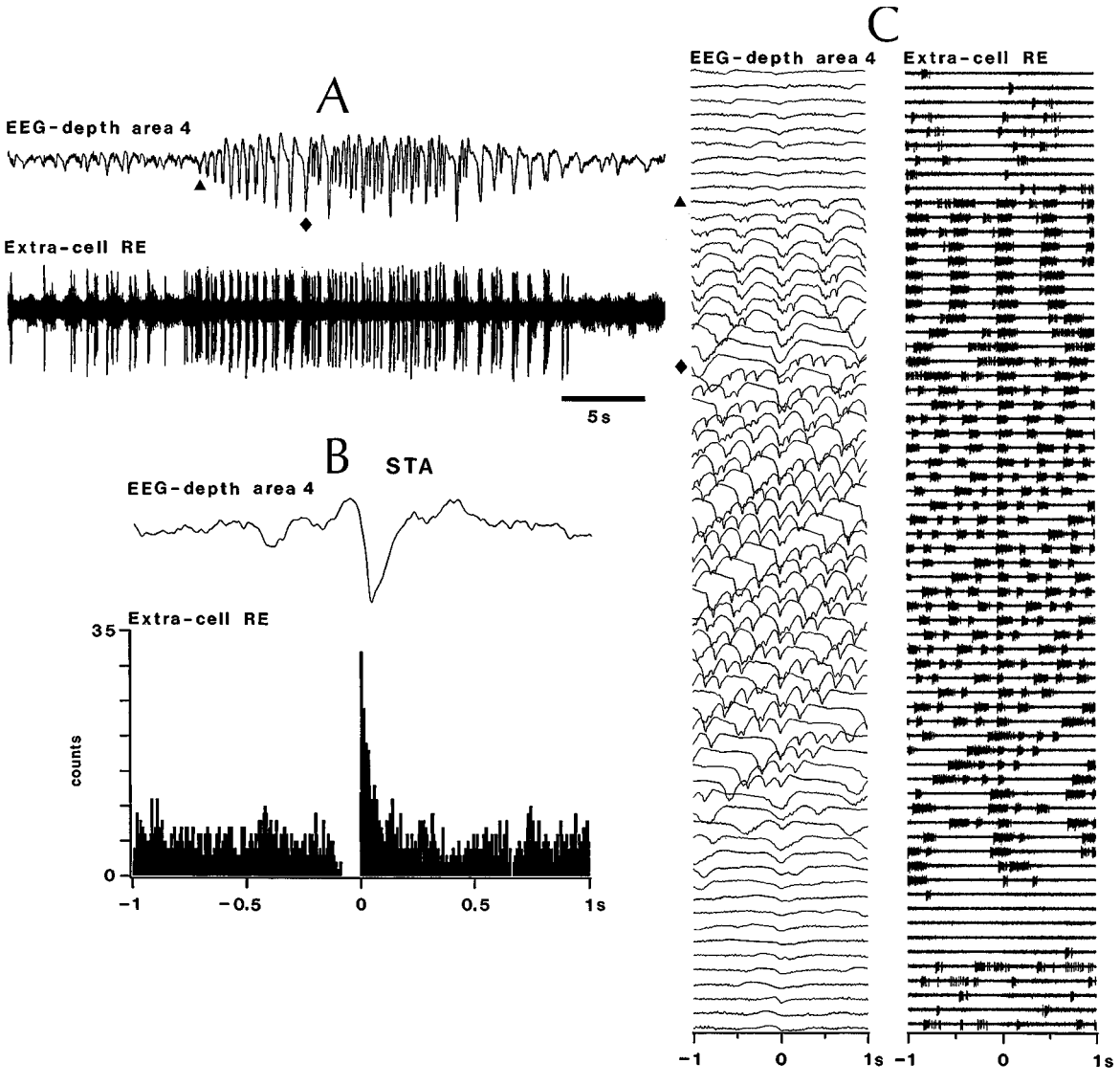

Fig. 5.34 Resonant activities in the neocortex and a thalamic reticular (RE) neuron. Cat under ketamine-xylazine anesthesia. *A*, spontaneously occurring paroxysmal episode, with SW/PSW complexes at 2–4 Hz, recorded from the depth of cortical area 4 and from a rostral RE neuron. *B*, spike-triggered average (STA). RE cell's spike-bursts were aligned at time zero and were used to trigger depth-EEG waves. Note correspondence between pre-burst silenced firing and depth-positive (upward) EEG waves of the slow oscillation, and between RE cell's excitation and depth-negative spiky EEG negative deflection. *C*, sequential analysis of cortical EEG activity and related discharges of an RE neuron, triggered by the peak negativity of field potentials in the depth of cortical area 4 (time zero) over a window of 1 s (to be read from top to bottom). ▲ and ♦ in *C* correspond to the same symbols in *A*. From Steriade and Contreras (1995).

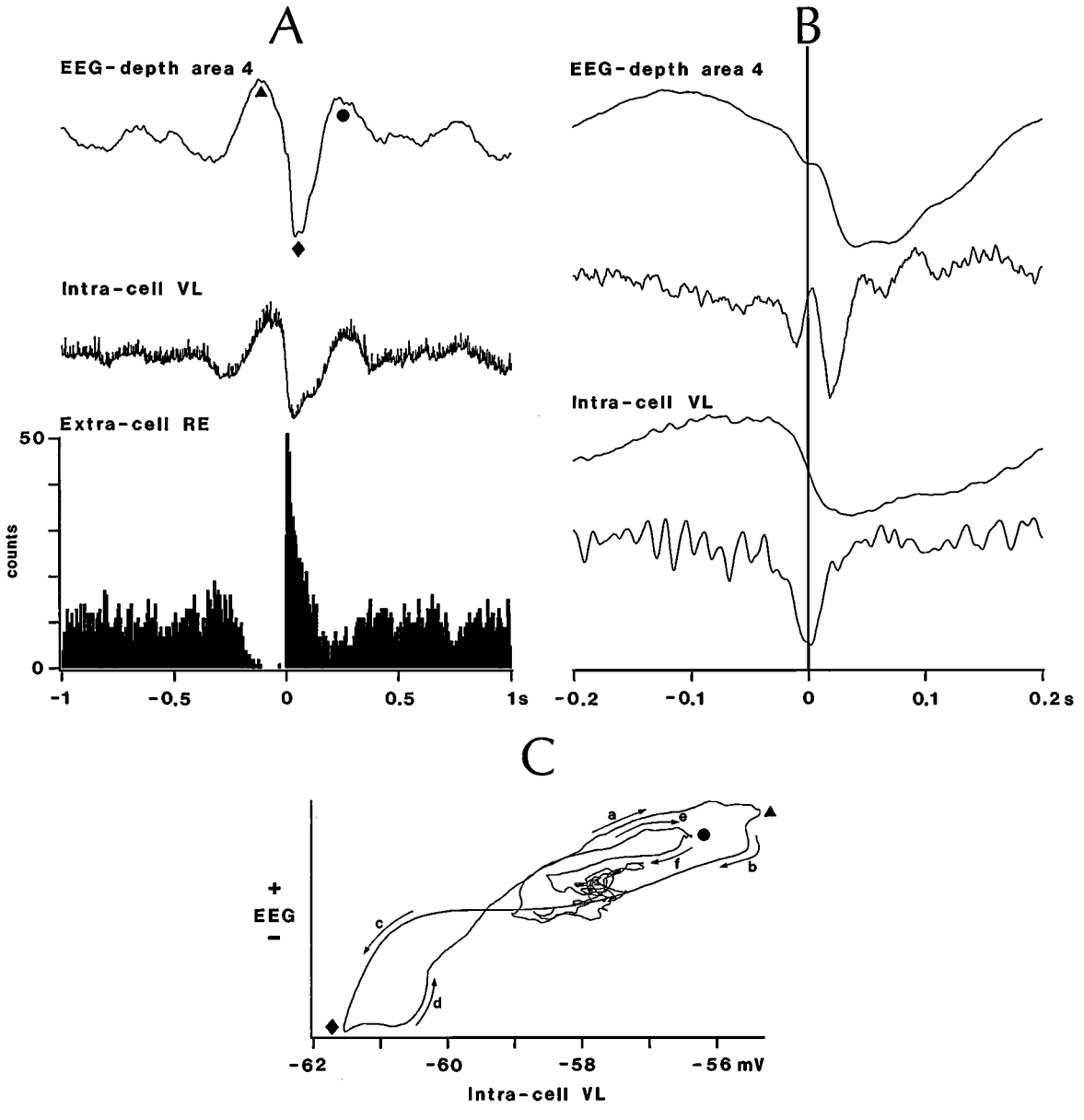

Fig. 5.35 Temporal sequence of events in motor cortical EEG and as well as thalamic neurons from the rostrolateral RE sector and ventrolateral (VL) nucleus during a SW paroxysm at 3 Hz. Cat under ketamine-xylazine anesthesia. *A*, spike-triggered averages (RE cell spike-bursts at time zero) of depth-EEG in area 4 and intracellularly recorded VL neuron. Symbols on the EEG trace correspond to those in *C*. *B*, relation between the peak of IPSP in VL neuron (time zero) and EEG events. In both EEG and VL activities, the bottom trace is the first derivative. *C*, Lissajous figure illustrating the evolution of VL intracellular activity (abscissa) against the positivity and negativity of SW phases in cortical paroxysmal activity. The trace should be followed along the arrows from *a* to *f*. Symbols ▲, ♦, and ● correspond to the same symbols in *A*. From Steriade and Contreras (1995).

played by TC cells in promoting such seizures. These ideas, derived from a series of data obtained in experiments performed *in vivo* and *in vitro*, are discussed below.

The concept of Gloor and his colleagues proposed that SW seizures develop from spindles in cats after cortical application or systemic injections of penicillin [149, 185]. However, in contrast to the "centrencephalic" hypothesis, Gloor proposed that sleep spindles develop into SW seizures because of an enhanced excitability of neocortical neurons. This view was found to be closer to reality, as the major role in the induction of SW seizures was not ascribed to a deeply located brain structure, but to the increased excitability of cortical neurons. Although SW seizures may occur in thalamectomized animals, in which spindles are absent [171], in the intact brain spindles might lead to SW seizures. One likely possibility is that sleep spindles are prevalently linked with the occurrence of SW seizures in humans [74, 148], whereas the slow sleep oscillation distinctly leads to patterns resembling Lennox–Gastaut syndrome or hypsarrhythmia (see below, section **5.6**).

An important finding in experiments on feline generalized penicillin epilepsy was that while SW complexes were induced by systemic administration or cortical application, as also obtained with bicuculline [171], but penicillin injection into the thalamus did not produce SW seizures [149, 185]. Instead, spindles with slowed frequencies were obtained, as was also the case with bicuculline injections into the thalamus, both *in vivo* [171] and *in vitro* [179, 186]. The transformation from ~8-Hz spindles to ~3-Hz spindles with increased amplitudes after thalamic injections of penicillin, but not to SW seizures, can also be found in earlier EEG recordings (Fig. 5.36) [187]. Another finding, pointing to the requirement of the cortex in the generation of SW seizures, was the fact that the thalamus of a decorticated cat exhibited *no* SW discharge in response to an intramuscular dose of penicillin [149]. This explains why the so-called "absence seizures" occurring in thalamic slices after bath applications of a disinhibitory substance [186] are not SW paroxysms, but just spindles with increased synchrony and decreased frequencies. Although Gloor thought that both the cortex and the thalamus are required for generalized SW seizures, his experiments did "not in themselves invalidate the . . . hypothesis that *only a change in cortical excitability is needed for SWs to appear*" (see p. 202 in [149]; italics mine).

More recent developments related to the concept of thalamic- and/or spindle-induced SW discharges arose from experiments on animal models with inherited absence epilepsy, as the genetic absence epilepsy in rats from Strasbourg (GAERS) [188], WAG/Rij

[185] Kostopoulos (2000).

[186] Von Krosigk et al. (1993). Commonly, bicuculline methiodide was used to block $GABA_A$ receptors in thalamic neurons. However, it was shown that bicuculline methiodide, methobromide and methochloride essentially block the LTS-burst afterhyperpolarization and small-conductance channels (Debarbieux et al., 1998). Thus, bicuculline-free bases should be used to assess GABAergic network interactions.

[187] Ralston and Ajmone-Marsan (1956).

[188] Reviewed in Danober et al. (1998).

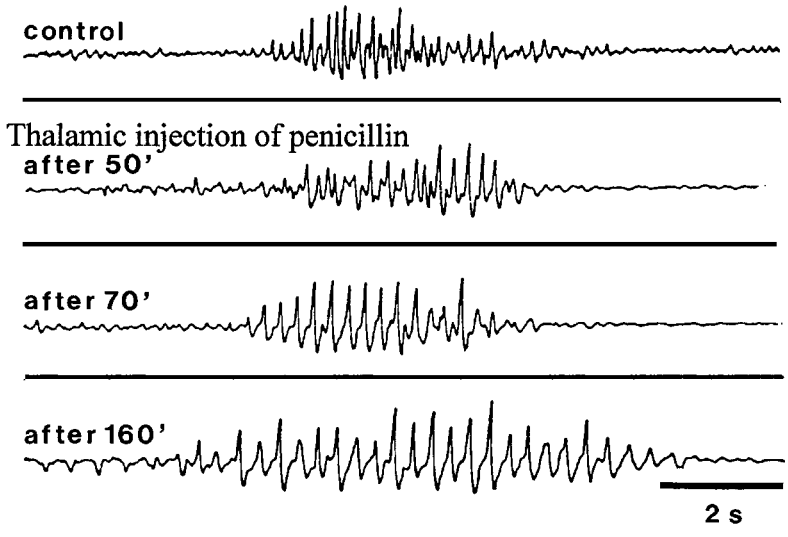

Fig. 5.36 Modification of spindles into slowed spindles after thalamic injection of penicillin. Cat under barbiturate anesthesia. Note progressive slowing of normal spindle frequency (*control*) after thalamic injection of penicillin. Modified from Ralston and Ajmone-Marsan (1956).

rats [189], and other models [190]. The seizures investigated in the GAERS model of genetic absence epilepsy are different in some ways from other types of SW seizures: *(a)* their frequency is at least twice as high (6–9 Hz) than in conventional SW seizures; *(b)* while SW seizures appearing during natural sleep in humans [74] or after systemic administration of penicillin in cats [149, 153] both occur as a consequence of spindle oscillations (7–15 Hz), paroxysmal oscillations in GAERS develop from a different oscillatory type (5–9 Hz) that is seemingly not related to spindles or hippocampal theta activity, but is generated by neuroleptanalgesia [191]. The cellular mechanisms of this rhythm (5–9 Hz) remain unknown; the participation of thalamic neuronal networks was suggested on the basis of extracellular recordings, though oscillations in this frequency range (i.e., theta) usually arise in rat hippocampus and related subsystems. Despite the uncertainty of the mechanisms underlying this oscillation, it gave rise to SW complexes at about the same frequencies (5–9 Hz), and it was concluded that the synchronization of thalamic neurons during "absence seizures" of rats is generated by corticothalamic inputs [191], as previously demonstrated by intracellular recordings *in vivo* [77, 107].

The idea of a corticothalamic drive was also reached in experiments on slices maintained *in vitro*, showing that corticothalamic stimulation induces bursting at 3 Hz in thalamic neurons; however,

[189] Van Luijtelaar and Coenen (1986).

[190] See Buzsáki (1990) for the model of "high-voltage spike-and-wave spindles" (HVS) in rodents, which was thought to meet the criteria of a phenomenon mimicking SW seizures as being "spontaneous, episodic, recurrent and paroxysmal", according to the definition by Ward et al. (1969). HVSs may be triggered by cortical stimulation during periods of immobility (Buzsáki et al., 1988b).

[191] Pinault et al. (2001). Although this study was performed with extracellular recordings of thalamic (RE and TC) neurons, and the mechanisms of spike-bursts (or spike-trains?) remain largely unknown with this method (see main text and note [169]), thalamic neurons were stained using juxtacellular labeling (Pinault, 1996) and, at least, the location of recorded neurons was firmly demonstrated.

following the removal of the cortex, such bursts can no longer be evoked in the thalamus [192]. In mouse corticothalamic slices, prolonged paroxysmal depolarizing potentials elicited by $GABA_A$-receptor antagonists were present in cortex isolated from the thalamus, but not in thalamus isolated from the cortex [193]. Finally, the idea that corticofugal volleys are decisive in the induction of paroxysmal thalamic activity at 3–4 Hz [77, 107], first advanced on the basis of experiments using extracellular recordings of thalamic SW seizures induced by corticothalamic rhythmic stimuli [194] (Fig. 5.37), is now confirmed in work conducted on corticothalamic slices maintained *in vitro* [195] (Fig. 5.38). This idea stands in contrast to the previous hypothesis from work on thalamic slices [186]; namely, that thalamic networks are alone implicated in the genesis of SW seizures.

What is the behavior of TC neurons during cortically generated SW seizures? Firstly, a methodological issue should be stated: only intracellular recordings can answer this question as, with extracellular recordings, the so-called "spike-bursts" reported in some studies on SW seizures may just represent brisk firing due to prevalent excitation of TC neurons by corticofugal inputs during the depth-negative component of SW complexes. Such activity does not reflect low-threshold bursts de-inactivated by the hyperpolarization of TC neurons as, intracellularly, it was evident that these were trains of single action potentials at a depolarized level, triggered by depolarizing corticothalamic projections (see Fig. 7*B1* in [77]; see also below, Fig. 5.42). Then, this firing pattern reflects excitation of TC neurons from the cortex, rather than postinhibitory rebound spike-bursts. Recently, extracellular recordings from thalamic intralaminar neurons in a genetic model of absence epilepsy allowed a similar conclusion to be reached, on the basis of the dampening effect exerted by ionotopic and metabotropic glutamate receptors on the SW-related firing of thalamic neurons [196]. The origin of these glutamatergic effects is the tempestuous activity during seizures in the cerebral cortex. Therefore, the assumptions that low-threshold spike-bursts in TC neurons are the leading factors in the genesis of SW seizures are not substantiated by data from *in vivo* experiments.

Dual simultaneous intracellular recordings from the cortex and thalamus, *in vivo*, show that, during cortically generated seizures consisting of SW/PSW complexes at 2–3 Hz, most (60%) TC neurons display a steady hyperpolarization as well as phasic IPSPs, closely related to the "spike" component of cortical SW/PSW

[192] Kao and Coulter (1997).

[193] Golshani and Jones (1999).

[194] Steriade et al. (1976).

[195] Bal et al. (2000); Blumenfeld and McCormick (2000). The demonstration of a leading role of cortex in absence seizures *in vivo* (Meeren et al., 2002) also confirmed previous data [77, 194].

[196] Seidenbecher and Pape (2001). This study on thalamic intralaminar neurons also reported an usually high discharge frequency of these neurons, compared to TC neurons, during SW seizures, and concluded that "burst activity in intralaminar neurons relies on a set of membrane processes different from the low-threshold burst of relay cells in specific thalamic nuclei" (p. 1542). This conclusion corroborates intracellular data from cat intralaminar neurons that reported unusually high intraburst discharges (800–1000 Hz) in rhythmic bursts (Steriade et al., 1993c). Data in the recent paper by Seidenbecher and Pape (2001) and in a previous study by the same group (Seidenbecher et al., 1998) support the idea that corticothalamic projections control the synchrony and frequency of paroxysmal oscillations in the thalamus, and that the synchronization of electrical activity in a pattern indicative of SW discharges is seen in the cortex first (see also Fig. 5.26).

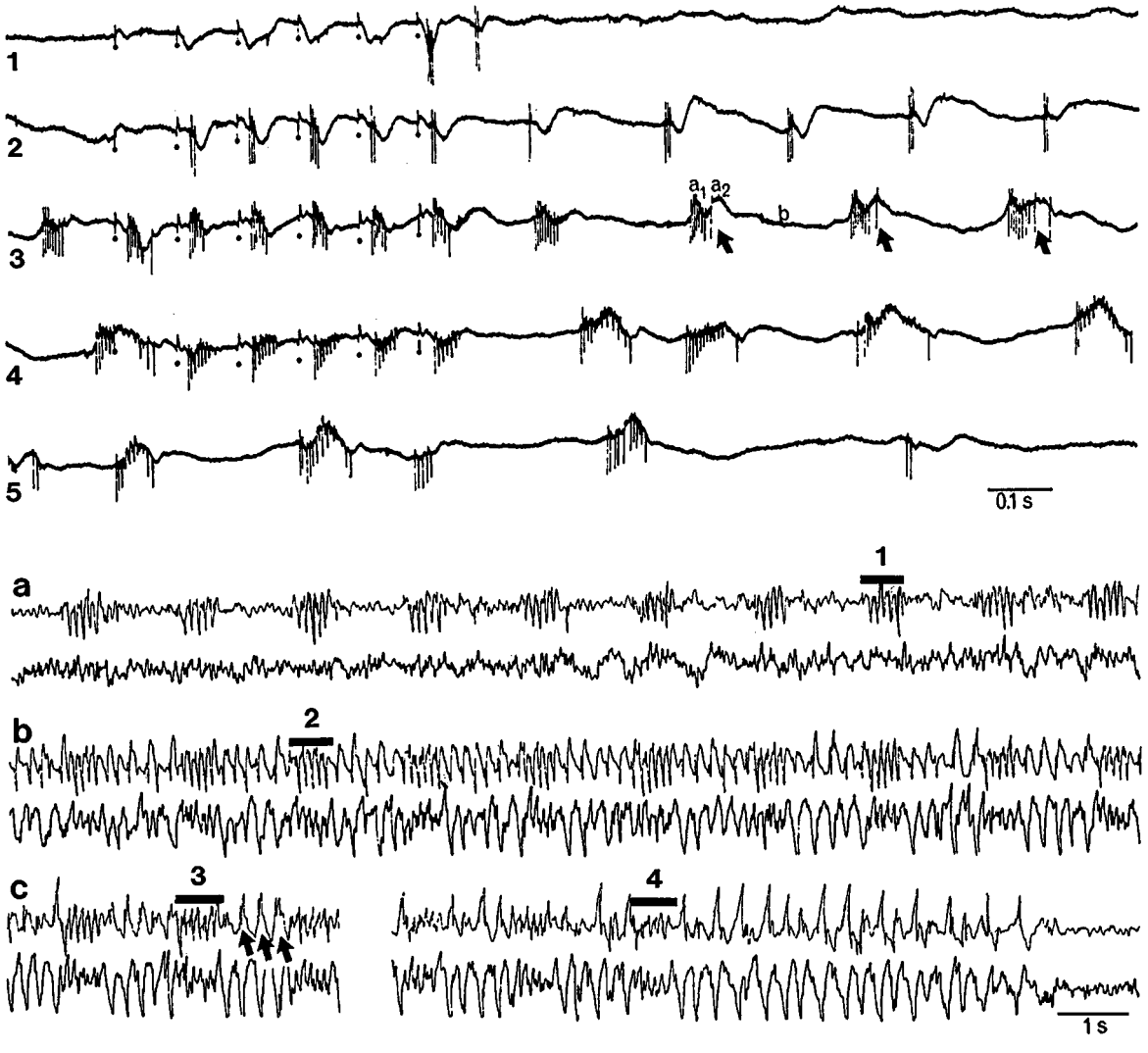

Fig. 5.37 Cortically elicited spike-wave (SW) afterdischarges in thalamic neurons. Brainstem-transected cat (bulbo-spinal cut, *encéphale isolé* preparation). Development of responses elicited in the lateroposterior (LP) thalamic neuron by pulse-trains (six stimuli at 10 Hz) applied to cortical area 7. Below the five oscilloscopic traces (*1–5*), three (*a–c*) ink-written samples depict adequately amplified focal slow waves recorded from the LP nucleus by the same microelectrode as used for extracellular unit recording (upper trace) and surface EEG rhythms from the contralateral cortical area 7 (bottom trace). Numbers (*1–4*) on the upper traces correspond to periods of stimulation indicated by the same numbers on oscilloscopic traces and represent the 8th (*1*), the 16th (*2*), the 28th (*3*) and the last, 35th (*4*) cortical pulse-train. Non-depicted periods of 5 s separate EEG traces *a–b*, *b–c*, and the two parts of trace *c*. The three SW complexes indicated by arrows in the oscilloscopic trace *3* correspond to those indicated by arrows in the ink-written trace *c*. From Steriade et al. (1976).

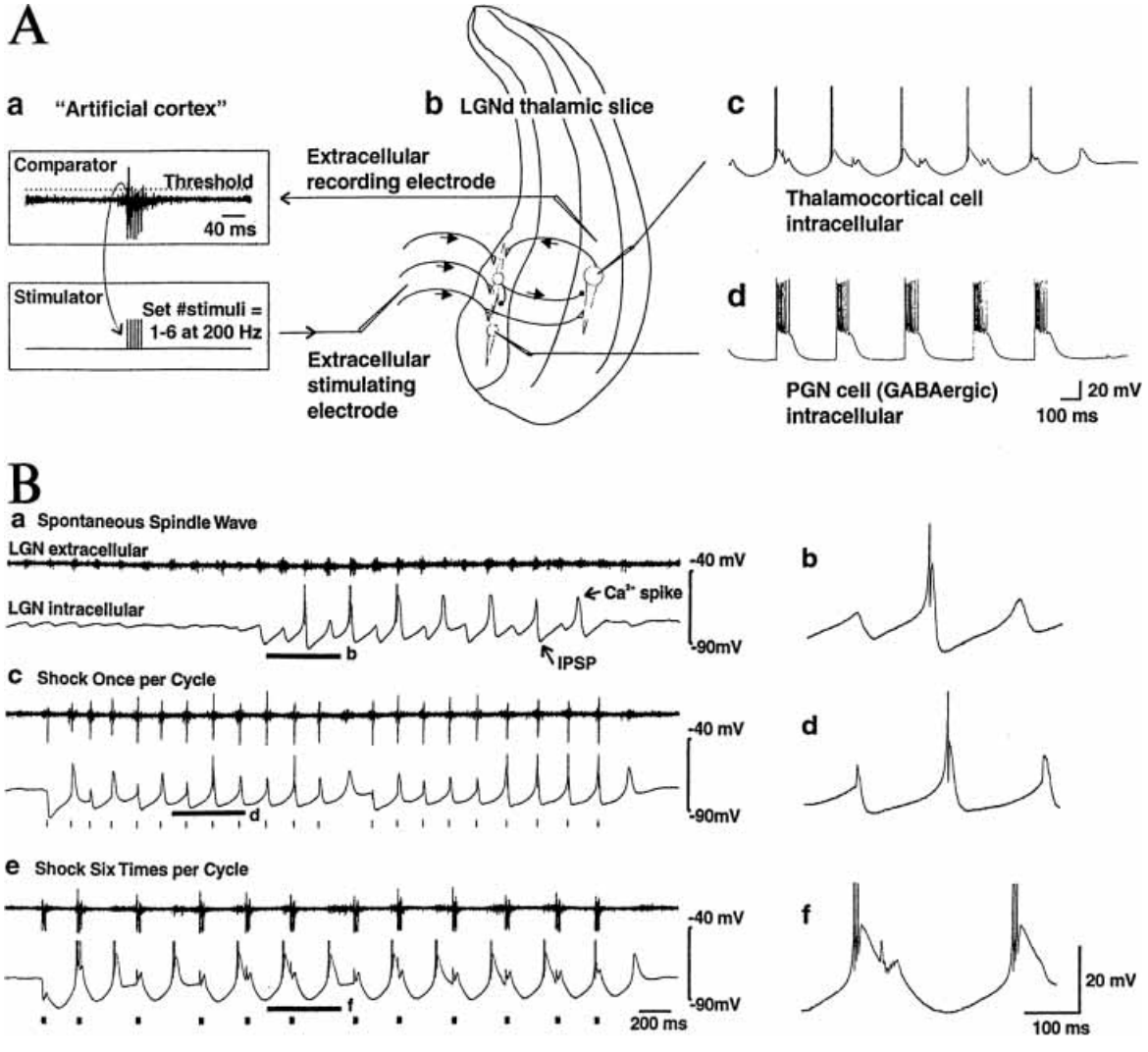

Fig. 5.38 Increased firing of neocortical neurons may cause increased firing of GABAergic thalamic reticular neurons, ultimately triggering SW complexes at 3–4 Hz. Corticothalamic slice of ferret. *A*, artificial cortex circuit. a, the artificial cortex consisted of a threshold comparator and a stimulator. The threshold of the comparator was adjusted to be triggered by multi-unit activity in the A laminae of the thalamic lateral geniculate nucleus (LGN). The stimulator was adjusted such that this stimulation unit was usually only activated by bursts of activity in the LGN and was set to deliver either single stimuli or brief 200-Hz bursts of six stimuli to the optic radiation. b, a drawing of the placement of recording and stimulating electrodes. c–d, intracellular recordings from thalamocortical and perigeniculate (PGN, reticular) GABAergic neurons. Recordings shown are with the stimulator set to deliver six corticothalamic stimuli per thalamic burst, producing sustained PGN firing, slow IPSPs, and postinhibitory rebounds in a thalamocortical neuron. *B*, spontaneous spindles (a); in b, single corticothalamic stimuli elicit spindle waves (6–10 Hz); in c, high-frequency bursts of six stimuli elicit 3–4 Hz stimulation. On the right, b, d, and f are expanded portions of the left traces. Modified from Blumenfeld and McCormick (2000).

[197] Lytton et al. (1997).

[198] Pinault et al. (1998); Slaght et al. (2000).

complexes (Fig. 5.39*A*). At the end of the cortical seizure, TC neurons fire at high rates, as if they were released from the inhibition that occurred during the seizure. A similar aspect is illustrated in Fig. 5.40, which shows that, following repetitive IPSPs related to cortical paroxysmal discharges, during a short period of quiescence of cortical activity occurring within the SW seizure, the TC neuron resumed its activity consisting of IPSPs and instead fired single potentials (middle part in panel 2). The source of inhibition of TC cells should be searched for in GABAergic RE neurons that fire spike-bursts during each PDS of cortical neurons (see Figs 5.5, 5.34, and 5.35). Modeling studies [197] based on data shown in Fig. 5.40 showed that increasing the strength of TC neuron inhibition by GABAergic RE neurons favors the quiescent mode in the former.

The phase relations between cortical and thalamic neurons during the pre-seizure epoch of sleep-like patterns are preserved during the SW/PSW seizure, but the amplitude of membrane excursions is accentuated (Fig. 5.39*B*). The similar relations between field potential and intracellular activities during slow-wave sleep and SW/PSW seizures are due to similar mechanisms that account for the depolarizing/hyperpolarizing components of the slow sleep oscillation, on one hand, and the EEG "spike" and "wave" components of SW complexes, on the other [133] (see section **5.6**). Although all these data point to cortically initiated SW seizures and to the steady hyperpolarization in a majority of thalamocortical neurons during such seizures, the remaining TC neurons are capable of firing rebound spike-bursts during a cortical SW seizure [77] and, thus, may potentiate and disseminate cortical seizures.

Subsequent research by other teams [198], using intracellular recordings from TC neurons during spontaneous SW discharges in the genetic model of "absence epilepsy" (GAERS), similarly demonstrated that the main events which characterize the activity of the overwhelming majority (>90%) of TC neurons are a tonic hyperpolarization, present throughout the SW seizure, and rhythmic IPSPs (Fig. 5.41). These data corroborate our findings [77].

Then, at the resting membrane potential (V_m) of TC neurons (generally −55 to −60 mV), these cells are steadily hyperpolarized and display phasic IPSPs during cortical SW seizures. Low-threshold spike-bursts can only be elicited in TC cells by artificially hyperpolarizing them below the level at which I_T is de-inactivated (Fig. 5.42). At levels more negative than −75 mV, TC neurons display continuously low threshold spikes, occasionally crowned by Na^+ action potentials, in close time-relation with the depth-negative (surface-positive) EEG "spike" component of cortical SW complexes

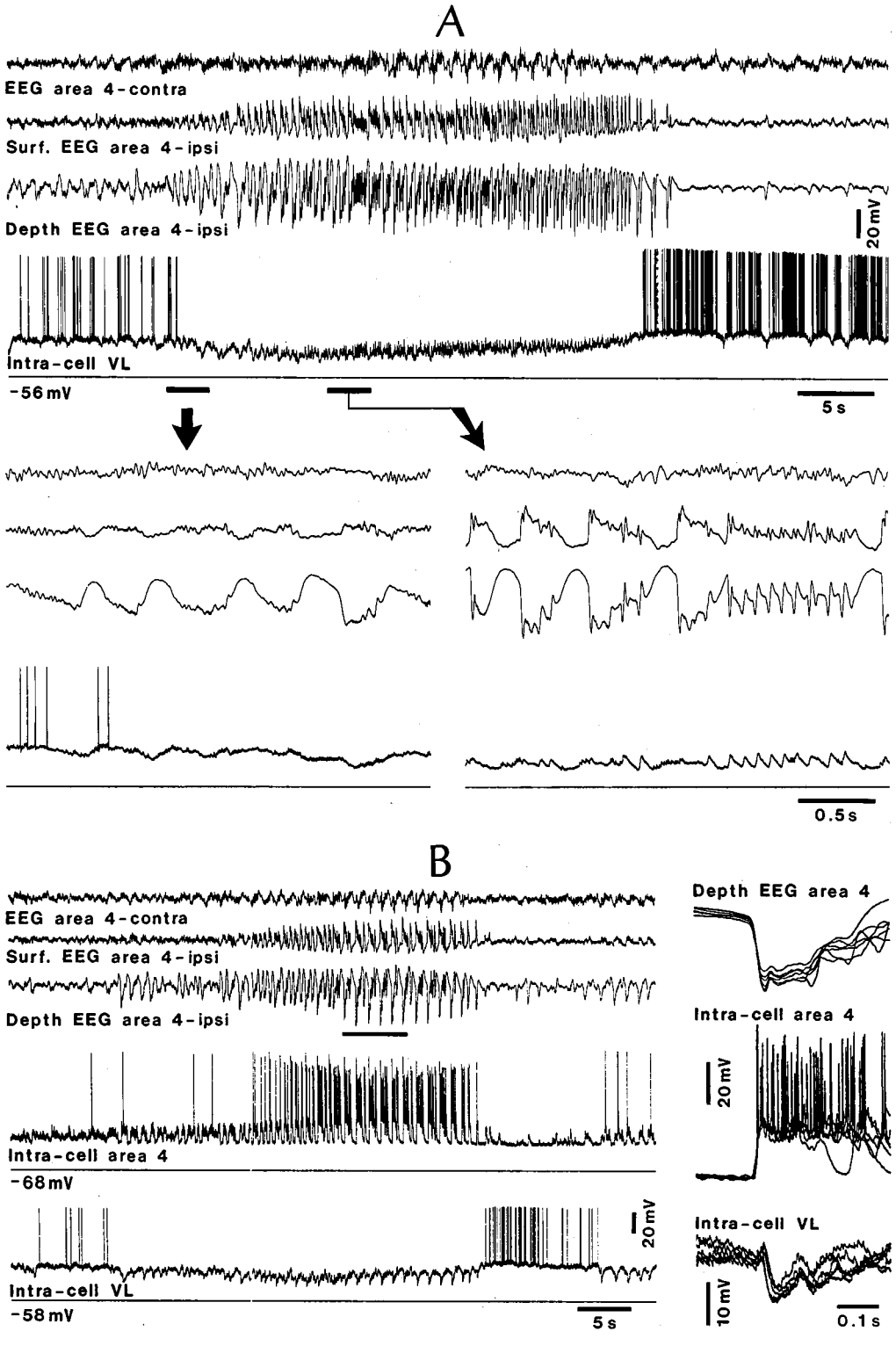
A
EEG area 4-contra
Surf. EEG area 4-ipsi
Depth EEG area 4-ipsi
20 mV
Intra-cell VL
-56 mV
5 s
0.5 s
B
EEG area 4-contra
Surf. EEG area 4-ipsi
Depth EEG area 4-ipsi
Intra-cell area 4
-68 mV
20 mV
Intra-cell VL
-58 mV
5 s
Depth EEG area 4
Intra-cell area 4
20 mV
Intra-cell VL
10 mV
0.1 s

[199] Bazhenov et al. (1999).

[200] Jasper (1969, p.435).

[201] Pollen (1964).

[202] Giaretta et al. (1987).

(Fig. 5.43). Similar manipulations of the V_m used during penicillin-induced recurrent seizures of the SW type were used to analyze cortical seizures and the associated behavior of TC neurons during different epochs, without current (−66 mV), with depolarizing current steps bringing the membrane potential to −62 mV or slightly more positive, and with hyperpolarizing current steps bringing the membrane potential to −78 mV [184]. At the resting membrane potential or slightly depolarized levels, no spike-bursts were elicited, but the TC neuron fired trains of single action potentials under direct depolarization. Powerful spike-bursts were triggered only when the membrane potential was artificially hyperpolarized (Fig. 5.44). At voltages negative to −75 mV, the reversed IPSPs were crowned by LTSs and spike-bursts (see bottom right panel in Fig. 5.44). This suggests that, similar to RE neurons [199], reversed IPSPs in TC neurons may directly trigger LTSs and spike-bursts. However, such negative V_ms are rarely seen in TC neurons during natural states of vigilance.

I shall now discuss the present state of knowledge of GABA's involvement in RE and TC, as well as neocortical, neurons. Since Jasper's time [200], SW seizures have been regarded as a type of paroxysm in which "inhibitory rather than excitatory mechanisms play a leading role". Jasper specifically pointed to the inhibitory nature of the "wave" component of SW complexes. This view is in line with earlier [201] and more recent [202] data claiming that the EEG "wave" is due to a Cl^--dependent IPSP. As shown below, more recent experiments conducted *in vivo* and *in vitro* showed that, during the EEG "wave" component of SW complexes, cortical neurons

Fig. 5.39 (opposite) Dual intracellular recordings from neocortical (area 4) and thalamocortical (ventrolateral, VL) neurons demonstrating hyperpolarization of the VL neuron during spike-wave (SW) seizure depolarization and spike-bursts in an area 4 neuron. Cats under ketamine-xylazine anesthesia. *A*, four traces depict EEG from the skull over the right area 4, surface and depth EEG from left area 4, and intracellular activity of a thalamocortical neuron from the left VL nucleus (bottom line shows the current monitor). Two parts are expanded below (arrows). The cortical paroxysm was initiated by progressively increased amplitudes of depth-positive EEG waves in left area 4 (see expanded trace on the left) and was characterized by ∼2.5-Hz SW/PSW complexes, alternating with activity at 10 Hz. The VL cell was hyperpolarized throughout the seizure and disinhibited at the cessation of cortical paroxysm. *B*, five traces depict simultaneous recordings of EEG from the skull over the right cortical area 4, surface- and depth-EEGs from the left area 4, as well as intracellular activities of a left area 4 cortical neuron and thalamic VL neuron (below each intracellular trace, current monitor). The seizure was initiated by a series of EEG waves at 0.9 Hz in the depth of left area 4, and continued with SW/PSW discharges at ∼2 Hz. These periods were faithfully reflected in the intracellular activity of the cortical neuron, whereas the thalamic VL neuron displayed a tonic hyperpolarization throughout the seizure, with phasic sequences of IPSPs related to the large cortical paroxysmal depolarizations and spike-bursts occurring at the end of the seizure. Note disinhibition of the VL neuron after cessation of cortical seizure. Inset on the right shows superimposition of spiky depth-negative EEG deflections associated with depolarization of cortical neurons and rhythmic IPSPs of the thalamic VL neuron. Modified from Steriade and Contreras (1995).

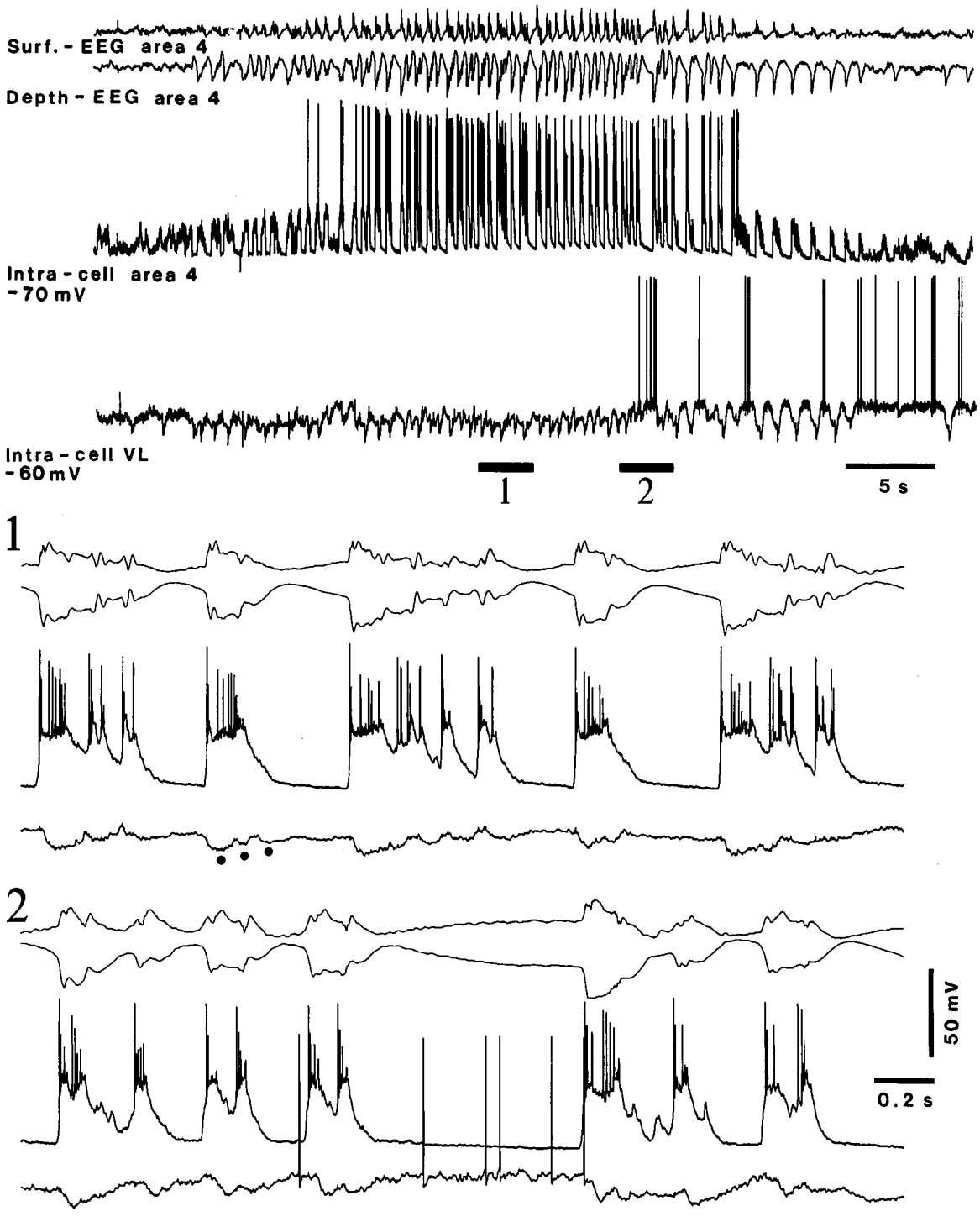

Fig. 5.40 Thalamocortical (TC) neurons display phasic IPSPs, but not spike-bursts, during a cortically generated SW seizure. Cat under ketamine-xylazine anesthesia. Dual intracellular recordings from an area 4 cortical neuron and a TC neuron from the ventrolateral (VL) nucleus, together with surface- and depth-EEG from cortical area 4. The SW seizure developed, without discontinuity, from sleep-like EEG patterns. Parts marked by *1* and *2* are expanded below. Note progressive depolarization and paroxysmal depolarizing shifts (PDSs) in the cortical neuron, and phasic IPSPs, related to cortical PDSs in VL neuron. Also note that, during a brief period of quiescence in cortical seizure (in *2*), the hyperpolarization of the TC neuron was removed and the neuron fired single action potentials. Dots in panel *1* indicate IPSPs in thalamocortical VL cell. Unpublished data by M. Steriade and D. Contreras.

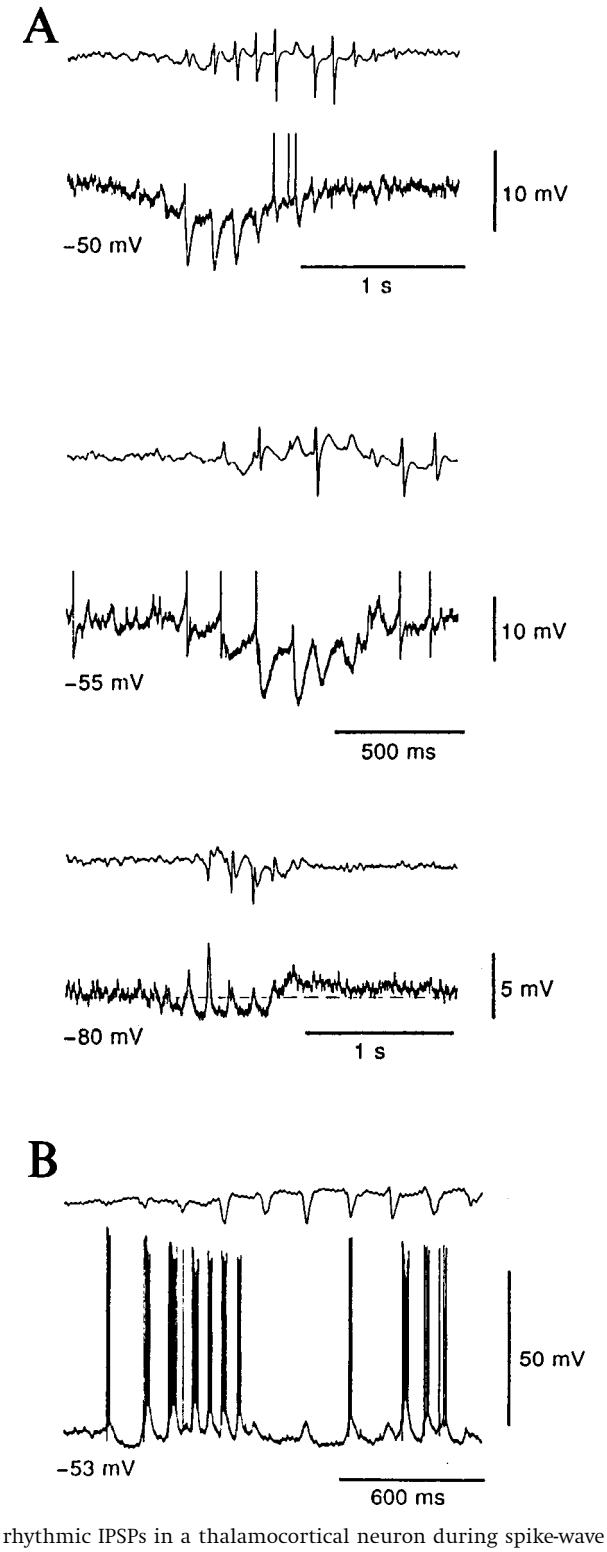

Fig. 5.41 Tonic hyperpolarization and rhythmic IPSPs in a thalamocortical neuron during spike-wave (SW) seizures from a genetic model of absence epilepsy in rats from Strasbourg (GAERS). *A*, *top*, intracellular voltage records show the tonic hyperpolarization present during spontaneous SW discharges (upper record is cortical EEG); *middle* and *bottom records* are from the same neuron. At −80 mV, the tonic hyperpolarization and the tonic depolarization present at the end of SW discharges are clearly visible. Spikes were truncated for clarity. *B*, intracellular activity recorded with a KCl-filled electrode shows the lack of any rhythmic hyperpolarizing potentials at −53 mV, and the presence of a hyperpolarization starting well before the first large "spike" in the EEG. Modified from Pinault et al. (1998).

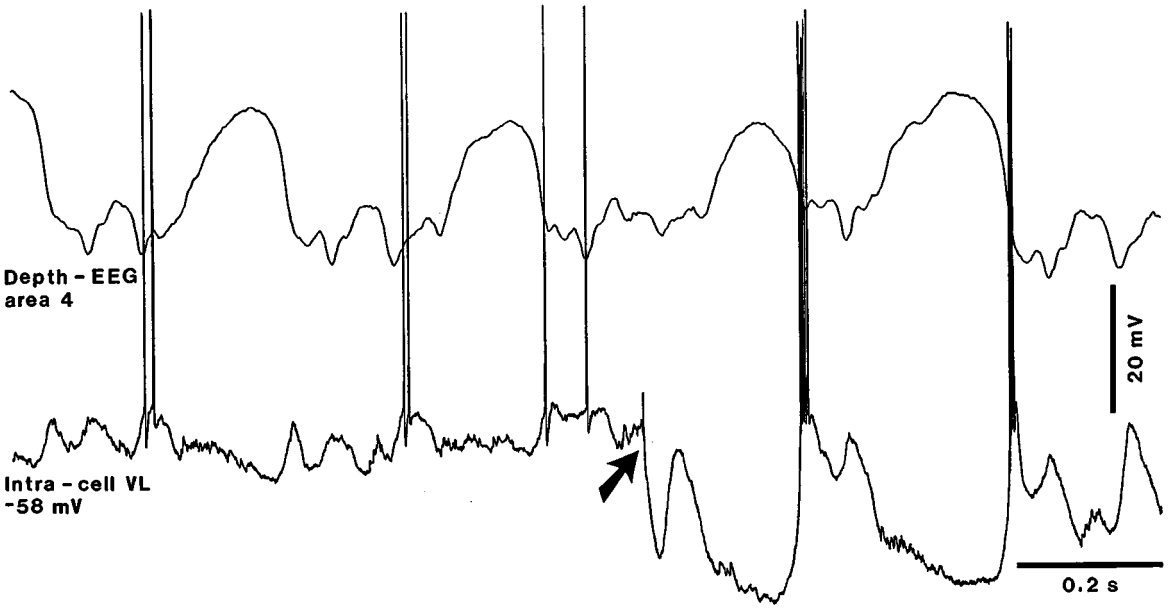

Fig. 5.42 Thalamic neuronal activity during a cortical spike-wave (SW) seizure. Cat under ketamine-xylazine anesthesia. Intracellular recording from a thalamic ventrolateral (VL) relay neuron together with depth-EEG field potentials from cortical area 4. The period illustrated represents part of a seizure with cortical SW complexes at 2.5–3 Hz. At the resting membrane potential (V_m), −58 mV, the VL neuron fired single action potentials or spike-doublets in relation with cortical field negativities (EEG "spike" component; downward deflections), but not spike-bursts. Only after direct hyperpolarization (−0.8 nA), bringing the V_m to −76 mV (arrow), did the neuron fire low-threshold spike-bursts after the prolonged hyperpolarization related to the cortical EEG "wave" component. Unpublished data by M. Steriade and D. Contreras.

[203] Bernusconi et al. (1992); Hosford et al. (1992, 1997); Liu et al. (1992); Marescaux et al. (1992a-b); Snead (1995); Smith and Fisher (1996); Huguenard (1999); Kostopoulos (2000).

[204] Bernusconi et al. (1999); Lingenhoehl et al. (1999).

[205] Snead et al. (1999, 2000).

display an increased input resistance, which is incompatible with the idea of a Cl^--dependent, $GABA_A$-receptor-mediated IPSP.

During the 1990s, the attention has shifted to $GABA_B$-mediated processes, as they induce longer-lasting IPSPs that can de-inactivate LTSs, which seemed to be critical in the generation of SW discharges in cortical and thalamic neurons, whereas $GABA_B$ receptor antagonists were regarded as potential anti-absence drugs [203]. Gamma-hydroxybutyric acid (GHB) is a metabolite of GABA and some evidence indicates that GHB may be a weak $GABA_B$ receptor agonist [204], which led to the use of this substance to promote seizures with SW complexes [205].

Work on thalamic slices investigated the cellular mechanisms of GABAergic actions on TC and RE neurons, related to various phenomena mimicking SW discharges. In TC cells, bicuculline-induced blockade of $GABA_A$ receptors left more molecules of GABA available to act on $GABA_B$ receptors, which induced slowed spindles [186] but, as shown *in vivo* [171], those oscillations are *not* paroxysmal discharges. In RE neurons, clonazepam, a drug used for its

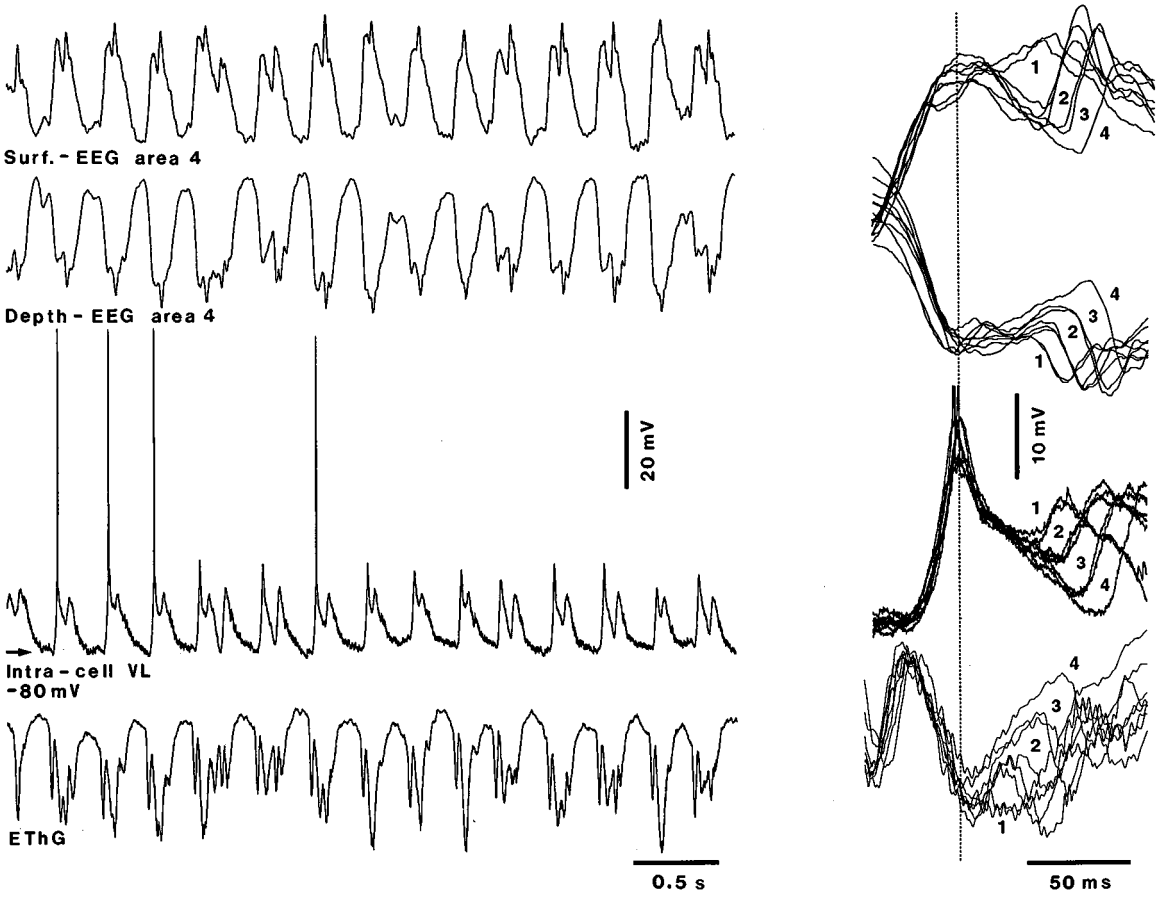

Fig. 5.43 Cortical SW seizures at 3 Hz and low-threshold spikes (LTSs) in simultaneously recorded thalamocortical (TC) neuron. Cat under ketamine-xylazine anesthesia. EEG recordings from surface and depth of area 4, intracellular recording of a TC neuron in the VL nucleus, and electrothalamogram (EThG) from the VL nucleus. Membrane potential of TC neuron, −80 mV (under 0.8 nA steady hyperpolarizing current). Numbers (*1–4*) in superimpositions of EEG recordings correspond to those in intracellular VL activity and EThG. Unpublished data by M. Steriade and D. Contreras.

[206] Huguenard and Prince (1994a); Gibbs et al. (1996). While clonazepam increases the decay time of inhibitory postsynaptic currents (IPSCs) in RE neurons, it has no such effects on TC cells recorded from the ventroposterior nucleus (Browne et al., 2001).

[207] Huntsman et al. (1999). Computational models were used to examine this type of inhibitory interaction among RE neurons (Sohal et al., 2000).

anti-absence action, reinforces $GABA_A$ receptors, increasing the inhibitory interactions among these cells and thus reducing the output of the RE nucleus, eventually reducing $GABA_B$-mediated IPSPs in target TC neurons (Fig. 5.45) [206]. Mice lacking the β_3 subunit of the $GABA_A$ receptor display a reduced strength and duration of $GABA_A$ synapses among RE neurons, without affecting those from RE to TC neurons, which may lead to an increase in oscillations evoked by internal capsule stimulation [207].

The use of genetic absence epilepsy in two different strains of rats permitted a re-analysis of the contribution of $GABA_A$ and $GABA_B$ receptors to the generation of SW seizures at the thalamic level. One of these studies used *in vivo* intracellular recordings

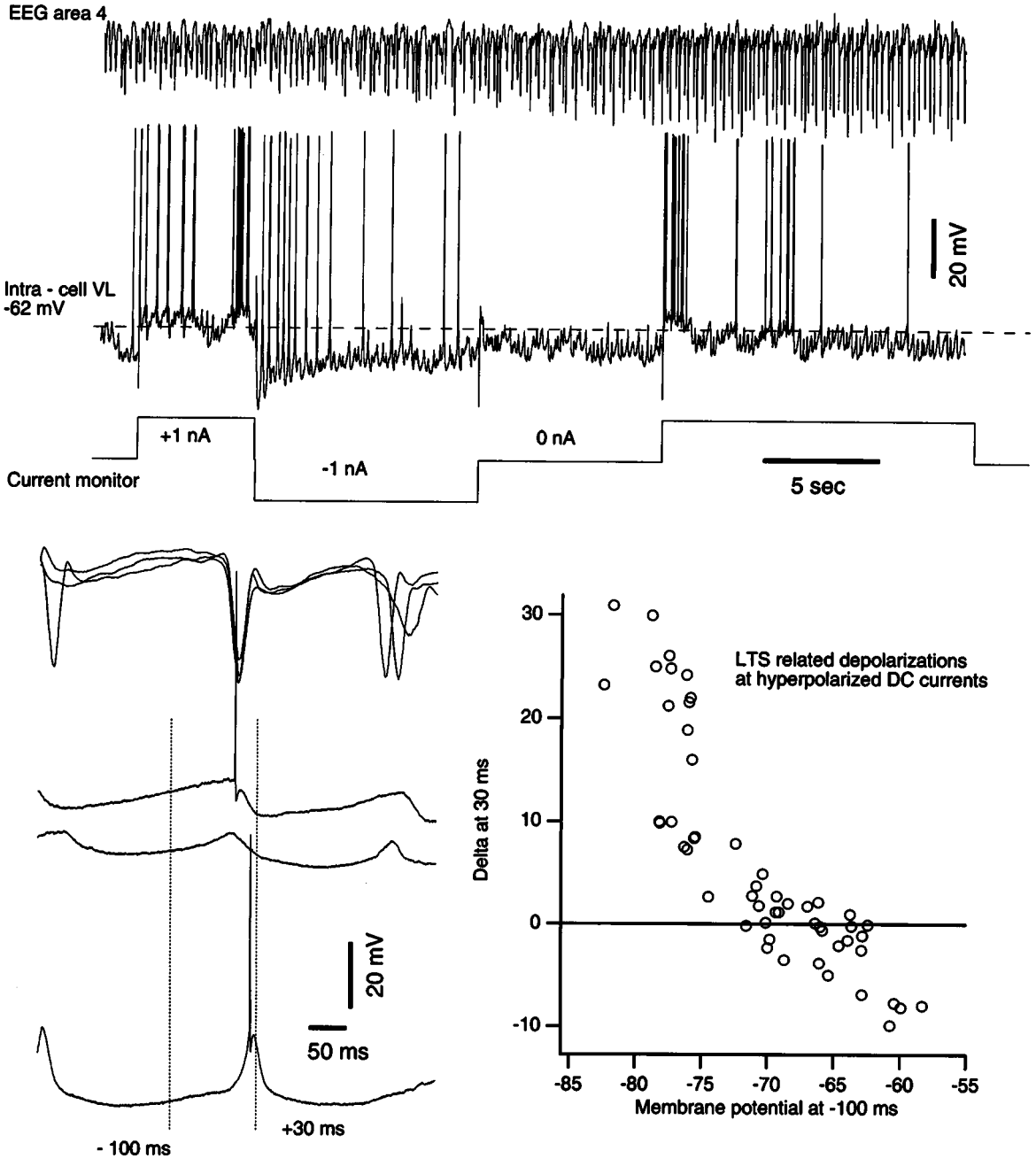

Fig. 5.44 During a cortical seizure, a thalamocortical (TC) neuron fires single action potentials or low-threshold spike-bursts at different levels of membrane potential. Cat under ketamine-xylazine anesthesia. Subintrant seizures were induced by systemic administration of penicillin (300 000 i.u./kg., i.m.). *Top panel* depicts a very long seizure in cortical EEG and the behavior of a TC neuron from the VL nucleus at different levels of membrane potential (without current, with +1 nA and with −1 nA). *Bottom right panel* shows estimated reversal potential of IPSPs (during seizure, IPSPs reversed between −65 and −70 mV) and LTS-related depolarizations under hyperpolarized DC currents. Voltage values were taken at the times indicated in the bottom left panel. To estimate the reversal potential for IPSPs in TC neurons, which accompany cortical seizures, we chose points that corresponded to a maximal hyperpolarization in intracellular recordings that occurred after the cortical EEG "spike" during intracellular injections of depolarizing currents (see, in bottom left panel, the right dotted line lying, in the top intracellular trace, just below the EEG trace). As a reference point, we chose a point in the intracellular trace that occurred 100 ms before the peak of EEG depth-negative wave ("spike"), namely, during the EEG depth-positive wave ("wave" component), indicated by the left dotted line labelled 100 ms. To calculate the reversal potential for IPSPs, we took differences between these two points, indicated as delta in the bottom right panel. At voltages below –75 mV, the reversed IPSPs were crowned by LTSs and spike-bursts. From Steriade and Timofeev (2001).

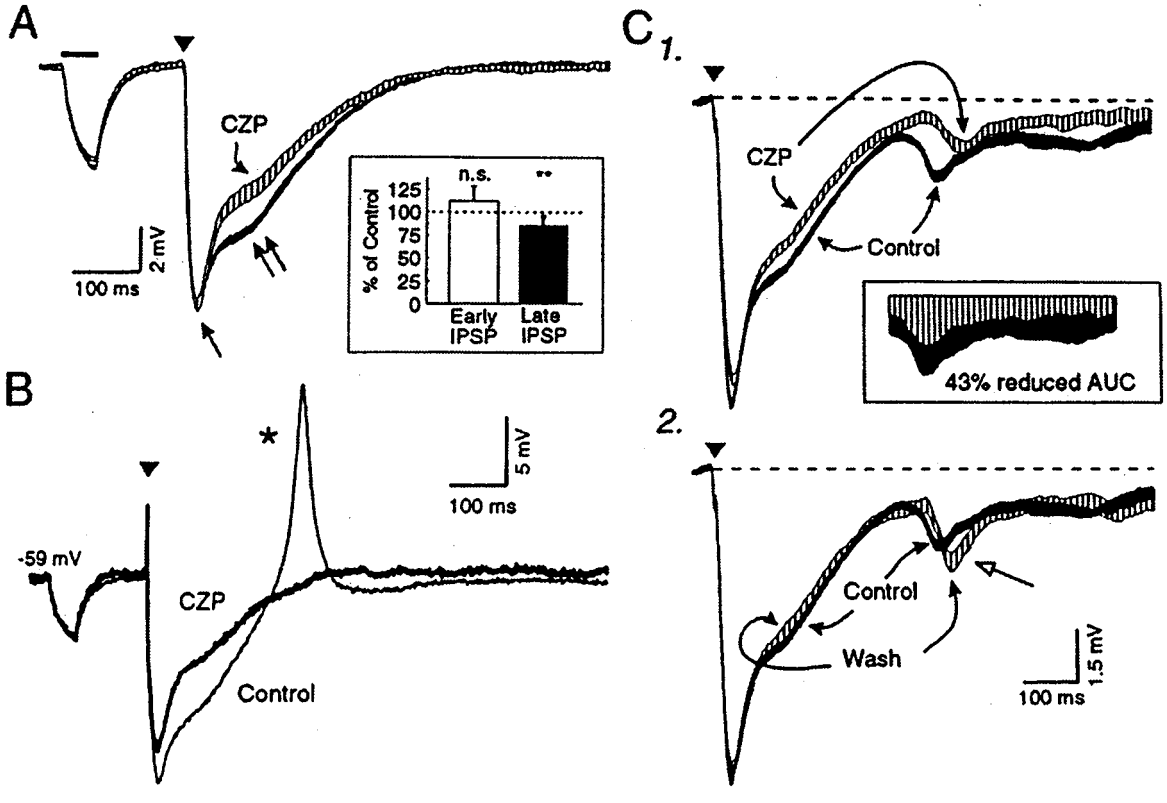

Fig. 5.45 The anti-absence drug clonazepam acts by reducing $GABA_B$ IPSPs in TC cells. Thalamic slice maintained *in vitro*. Bath application of clonazepam reduces IPSPs in ventrobasal (VB) thalamic relay neurons of rats. *A*, biphasic IPSP evoked by stimulation of the thalamic reticular (RE) nucleus (triangle) consists of an initial $GABA_A$ component and a late $GABA_B$ component (double arrow). Only the $GABA_B$-mediated component was reduced by bath application of clonazepam (see inset). *B*, similar protocol in another cell. The biphasic IPSP evoked a rebound burst (control). Application of clonazepam resulted in the depression of both $GABA_A{}^-$ and $GABA_B$-mediated components of the IPSP and abolished the rebound burst response. *C*, secondary "feedback" IPSPs (open arrow in *C* 2) occur at a latency of ~350 ms and are reduced by clonazepam in a reversible fashion. Larger reduction of secondary IPSPs than in the $GABA_A$ and $GABA_B$ IPSPs (43% compared to 7% and 15%, respectively). From Huguenard and Prince (1994a).

[208] Charpier et al. (1999). Even earlier studies that tested the hypothesis of $GABA_B$ergic processes in absence epilepsy denied such an implication (Knight and Bowery, 1992). These authors used the techique of autoradiography to study the binding of [^{3}H]-GABA to $GABA_A$ and $GABA_B$ receptors in a variety of brain structures of rats predisposed to absence seizures (among them neocortex and thalamus) but found no statistical difference compared to control animals.

[209] Staak and Pape (2001).

of cortical and TC cells from the GAERS model [208]. The other study investigated *in vivo* the $GABA_{A-B}$ processes in TC cells from the WAG/Rij strain of rats [209]. Both these studies refuted the idea that $GABA_B$-mediated IPSPs in TC neurons play a role in SW seizures, as previously suggested in experiments conducted on thalamic slices [186, 210] and in computational models [211]. In the GAERS model of absence epilepsy, there were no rhythmic $GABA_B$ IPSPs and no LTSs crowned by spike-bursts in TC neurons during SW discharges [208], as was also reported in other studies on SW seizures in such rats [198] showing that the IPSPs are mediated by $GABA_A$ receptors (reversed at −68 mV) and that SW seizures are

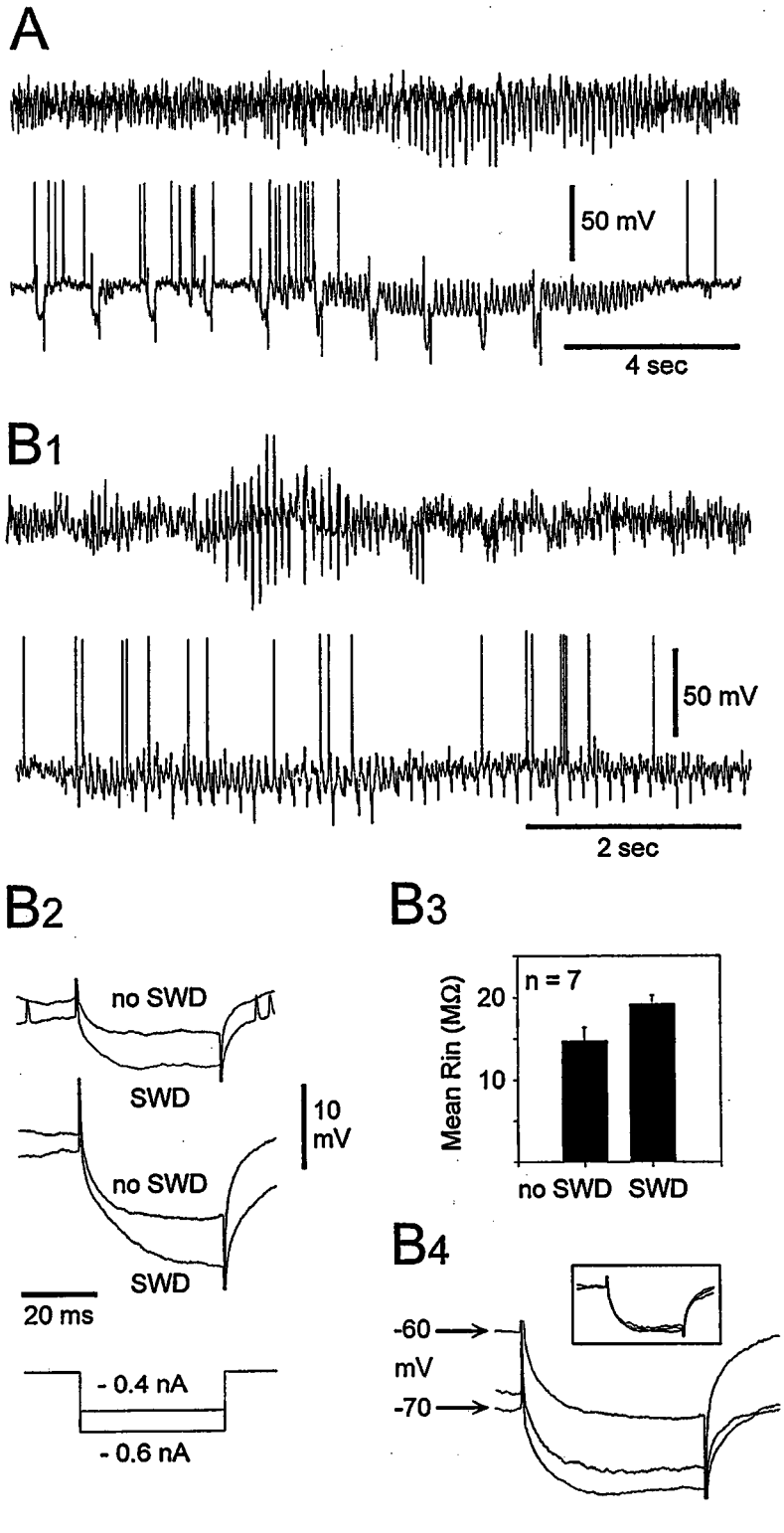
A
50 mV
4 sec
B1
50 mV
2 sec
B2
no SWD
SWD
10 mV
no SWD
SWD
20 ms
- 0.4 nA
- 0.6 nA
B3
n = 7
Mean Rin (MΩ)
20
10
no SWD
SWD
B4
-60
mV
-70

[210] Kim et al. (1997).

[211] Destexhe (1998).

[212] Neckelmann et al. (2000).

accompanied by a steady hyperpolarization in the overwhelming majority of TC neurons. More recent studies, using the WAG/Rij genetic model of SW seizures in rats, support the view that $GABA_A$-receptor-mediated events are recruited with each SW complex in thalamocortical neurons and that the SW-related activity can be evoked with no significant contribution of $GABA_B$ receptors [209].

In neocortical neurons, the "wave" component of SW complexes was previously viewed as reflecting summated IPSPs that were ascribed to GABAergic processes triggered in pyramidal neurons by local-circuit inhibitory cells [201, 202]. In more recent computational models, the "wave" was similarly regarded as produced by active inhibitory processes, more precisely, $GABA_B$-mediated IPSPs [211]. If "wave" components were GABAergic IPSPs, measurements of input resistance during SW seizures should find an increased membrane conductance during the "wave" components. Instead, the opposite was found *in vivo*, during SW seizures from the genetic model GAERS [208] and spontaneous SW seizures in cats [212]. Figure 5.46 shows that neocortical neurons display an increase in the apparent input resistance during SW seizures compared to inter-SW epochs, leading to the conclusion that the overall change detected in pyramidal neurons is that of a decrease in membrane conductance, an effect that was ascribed to a disfacilitation process during SW seizures [208]. In our experiments [212], the input resistance was measured in neocortical neurons during both the slow oscillation and the SW seizures that may develop without discontinuity from sleep-like patterns [77]. Figure 5.47 shows that three distinct phases in the EEG could be discerned during the slow

Fig. 5.46 (opposite) An increase in the apparent input resistance of cortical neurons accompanies the expression of spontaneous SW discharge (SWD). Intracellular recordings from the neocortex of the GAERS strain of rats, initially anesthetized with pentobarbital and maintained under neurolept analgesia with fentanyl and haloperidol. *A*, during SWD (top trace) the size of the voltage response to a 160-ms hyperpolarizing current pulse of constant amplitude (0.8 nA) is larger during the SWD than in the preceding period, indicating an increase in the apparent input resistance of the neuron. The voltage–current relationship of this neuron in the voltage region where these measurements were made was linear. *B1*, intracellular (bottom trace) and EEG (top trace) records from a different cortical neuron on which a more detailed analysis of the increase in input resistance during SWD was carried out. *B2*, averaged ($n > 8$) voltage traces show the increase in resistance during SWD. Measurements were made at −60 mV (resting membrane potential) using two current pulses of different amplitude (shown in the bottom traces). *B3*, histogram showing the statistically significant ($p < 0.05$) increase in the apparent input resistance (R_{in}) during seven consecutive SWDs versus the corresponding inter-SWDs periods. *B4*, three superimposed and averaged ($n > 8$) voltage responses to current injection (0.6 nA, 40 ms) were generated during inter-SWDs periods at the indicated membrane potentials (achieved by DC injection). They show the lack of rectification in the voltage region (−60 to −80 mV) spanned by the waveform of the SWDs. In the inset, the same three records are graphically superimposed by matching the membrane potential before the start of the pulse. All records in this figure were obtained with K^+-acetate-filled electrodes. Modified from Charpier et al. (1999).

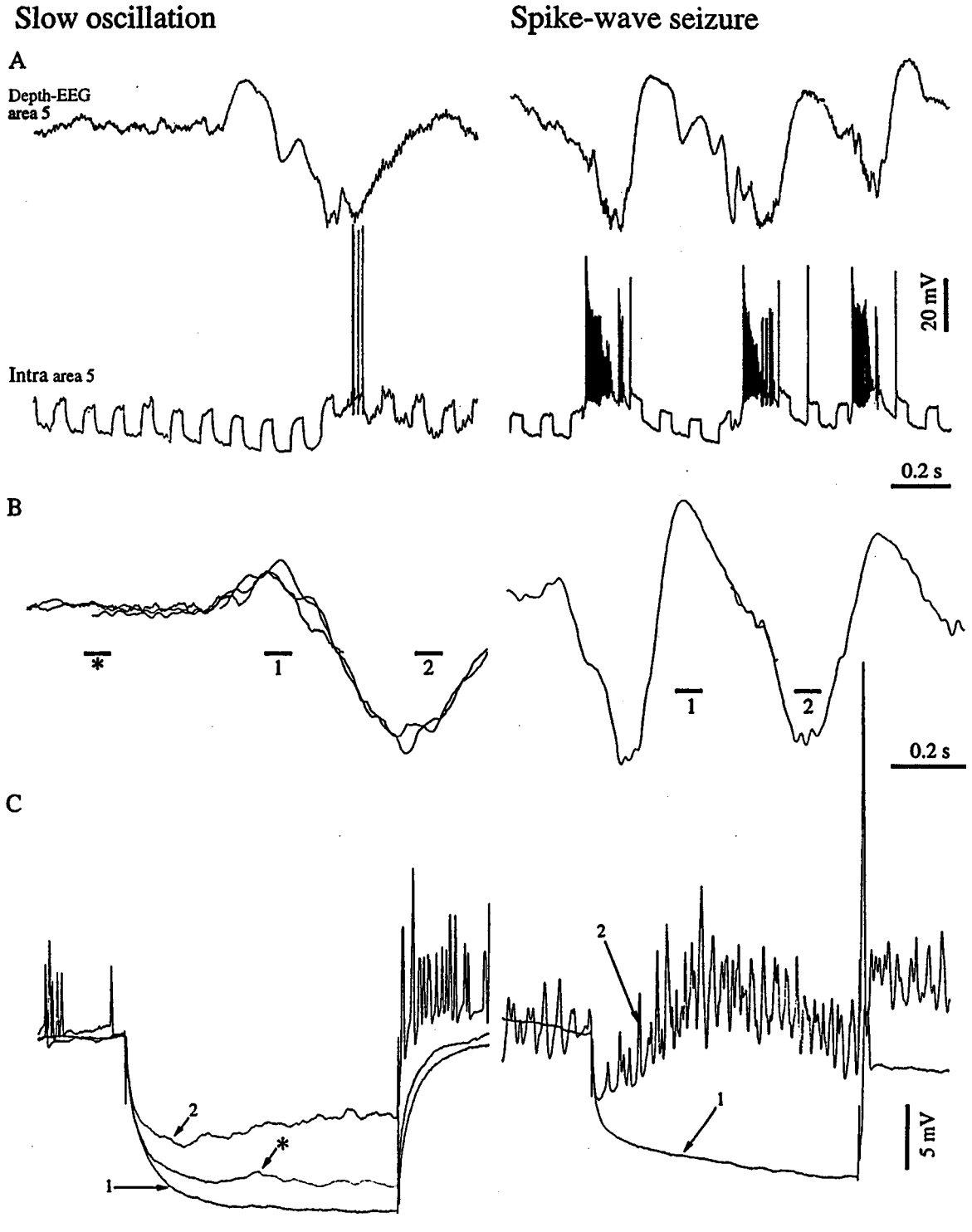
Slow oscillation
Spike-wave seizure
A
Depth-EEG
area 5
Intra area 5
20 mV
0.2 s
B
*
1
2
1
2
0.2 s
C
2
*
1
2
1
5 mV

[213] Contreras et al. (1996b).

[214] Steriade et al. (1998c); Timofeev et al. (2002c).

sleep oscillation: the depth-positive EEG wave (*1*), the depth-negative EEG wave (*2*), and a phase of varying duration (marked by an asterisk in panel *B*), with low-amplitude, fast-frequency activity, preceding the next depth-positive EEG wave. Similar to the results from a previous study [213], the conductance was found to be smallest during the depth-positive wave of the slow oscillation (range, 19–74 nS), maximal during the depth-negative wave (range, 36–120 nS), and intermediate during the period preceding the depth-positive wave. The SW seizure depicted in the right column of Fig. 5.47 occurred spontaneously in the same neuron. During the depth-positive EEG "wave" component of SW complexes (reflecting summated hyperpolarizations in a pool of neurons), the conductance of this neuron was 45 nS (range, 41–140 nS), whereas it increased to 144 nS during the depth-negative EEG "spike" (range, 90 to greater than 400 nS).

The above data show either an increase in the apparent input resistance of cortical neurons during SW seizures in the GAERS model of absence epilepsy [208] or a very slight decrease in input resistance but only compared with the largely increased input resistance during the hyperpolarizing phase of the slow sleep oscillation [212] (see panel *C* in Fig. 5.47). In any case, neither of these two studies [208, 212] demonstrated a significant *decrease* in input resistance, as expected if the "wave" components of SW complexes were due to GABAergic processes.

In parallel studies on cortically generated SW seizures, we also demonstrated that recordings with KCl-filled pipettes did not significantly affect the "wave"-related hyperpolarized phase of SW seizures [214]. As to the possibility that $GABA_B$-mediated IPSPs underlie the "wave" component of SW seizures [211], including QX-314 (60 mM) in the recording pipette to block the G-protein-coupled

Fig. 5.47 (opposite) Neuronal conductance during the sleep-like slow oscillation and SW seizures. Cat under ketamine-xylazine anesthesia. Intracellular recording from an area 5 neuron together with a depth-EEG from the vicinity in area 5. *A*, square current pulses of 0.5 nA amplitude and 60 ms duration were injected through the recording pipette every 100 ms during slow oscillation (*left*) and during a spontaneous SW seizure, 6 min later (*right*). *B*, superimposition of averaged fragments of the EEG, extracted around the times when the pulses were applied during slow oscillation (*left*), and SW seizure (*right*). The fragments were positioned to create averaged oscillation cycles. *C*, left column: 20 pulses were averaged from each of the three phases of the slow oscillation (*1*: the EEG depth-positive phase associated with the cell's hyperpolarization; *2*: the EEG depth-negative phase associated with cellular depolarization; and ∗: the relatively stable period, intermediate level, that separated each positive-negative cycle). *C*, right column: 20 pulses were averaged (*1*: the "wave" associated with cellular hyperpolarization; and *2*: the "spike" associated with cellular depolarization during the SW seizure). Compared to the slow oscillation, the conductance was greatly increased during the depolarizing ("spike") component of SW seizures and slightly increased during the hyperpolarizing ("wave") component of SW seizures. From Neckelmann et al. (2000).

[215] Jensen et al. (1993); Deisz et al. (1997).

[216] Halliwell (1986); Schwindt et al. (1988a).

[217] Llinás (1964).

[218] Cowan and Wilson (1994).

[219] Kim et al. (2001) generated a mutation of a subunit (α_{1G}) of the T-type Ca^{2+} channels and reported that mice in which this subunit was absent lacked the burst mode firing related to SW seizures.

$GABA_B$-evoked K^+ current [215] did not significantly affect the hyperpolarization in our experiments. Together, these data suggest that GABA-mediated currents are not important for the hyperpolarization during these cortically generated seizures. Another factor relates to different K^+ currents [216]. Recordings with Cs^+-filled pipettes to non-selectively block K^+ currents showed that, during the "wave" component of SW seizures, pyramidal neurons displayed depolarizing potentials [214]. Thus, at least some role is played by K^+ currents, most probably $I_{K(Ca)}$ because in recordings with pipettes filled with BAPTA (100 mM) the "wave"-related hyperpolarizations were reduced and the apparent input resistance increased [214]. Concerning another factor that may be responsible for the "wave"-related hyperpolarization, *disfacilitation seems to be the most important mechanism underlying the hyperpolarization during cortically generated SW seizures*. This conclusion resulted from studies conducted *in vivo* on two types of spontaneous SW seizures [208, 212]. Hyperpolarization due to disfacilitation has been described to occur in spinal cord [217] and corticostriatal [218] neurons. The fact that the apparent input resistance decreased very slightly during the "wave"-related hyperpolarization of SW seizures, as compared to the hyperpolarizing phase of the slow sleep oscillation (see trace *1* in panel *C* of Fig. 5.47), indicates that the hyperpolarizations during SW seizure are due to the combined effect of disfacilitation, which would increase the input resistance, and some K^+ currents, mainly $I_{K(Ca)}$, which would decrease it.

To sum up the relations between paroxysms consisting of SW complexes at 2–4 Hz and thalamic circuits that generate sleep spindles, we should first point to the multiple forms of SW seizures. Both apparently "suddenly generalized" and focal SW seizures exist, but the generalized seizures emerge from synaptic interactions among initially focal seizures, with short time-lags between various cortical recording leads, which are demonstrated using cellular recordings but cannot be appreciated by visually inspecting the EEG. It is likely that the neuronal substrates of SW complexes are similar in different forms of this paroxysmal type. In essence, *during cortically generated SW seizures, RE neurons follow each paroxysmal discharge of neocortical neurons, whereas the majority of TC neurons are hyperpolarized and display short IPSPs*. However, the remaining TC cells may fire spike-bursts if the membrane potential is more negative, either naturally or by direct hyperpolarizing current (see Figs. 5.42–5.44), and thus may reinforce the cortical SW seizures [219].

[220] Halasz (1991); Niedermeyer (1999a-b).

[221] Dulac and N'Guyen (1993); Yaqub (1993).

[222] Burnstine et al. (1991); Kotagal (1995).

[223] Miyauchi et al. (1988); Reutens et al. (1993).

5.6. Patterns of Lennox–Gastaut syndrome

In humans, this syndrome is characterized by intractable seizures and mental retardation, associated with a complex EEG pattern, consisting of SW/PSW complexes at 2.5–3 Hz or lower frequencies (1.5–2.5 Hz) and fast runs at ~10–20 Hz (see Fig. 5.1). The clinical paroxysms are myoclonic, generalized tonico-clonic, or atypical absence seizures. The close relation between such seizures and slow-wave sleep has repeatedly been mentioned [220]. Although these seizures are described as generalized [221], multifocal independent EEG "spikes" and SW patterns have also been described in this sleep-activated syndrome [222]. Most investigators pointed to intracortical neuronal networks as generators of these seizures because of focal disturbances of cortical metabolism and a favorable outcome for overall seizure frequency after callosotomy or focal corticectomy [223]. As will be shown in this section, the occurrence of this syndrome during patterns of natural slow-wave sleep or during sleep-like patterns under ketamine-xylazine anesthesia, as well as the generation of such seizures within the neocortex are corroborated by our cellular studies.

Needless to mention, the experimental studies presented in this section cannot shed light on the mechanisms of generation of Lennox–Gastaut seizures in humans. Nonetheless, data show that the patterns of field potentials and intracellular recordings bear striking resemblances to EEG records in clinical seizures. Thus, the electrophysiological aspects of these cortically generated paroxysms, revealed in our studies performed *in vivo*, are probably similar to those occurring in humans. Data discussed below resulted from a series of experimental manipulations, sometimes using focal leakage of bicuculline into the neocortex, but more often investigating *spontaneously developing seizures* from sleep-like slow oscillations under ketamine-xylazine anesthesia (see section ***5.5.1*** for possible factors determining the spontaneous occurrence of these paroxysms and of seizures with pure SW/PSW complexes).

Data on the cellular mechanisms of Lennox–Gastaut seizures will be presented in the following order. Firstly, seizures resulting from topical leakage of bicuculline into the cortex will be illustrated. Secondly, basically similar seizures, which developed spontaneously from the slow oscillation, will be analyzed with emphasis on the nature of both SW/PSW complexes and fast runs. Similar relations between field potentials and intracellular activities are demonstrated to exist during the cortically generated sleep-like slow oscillation and during Lennox–Gastaut seizures. Next, the

crucial role played by very fast oscillations (80–200 Hz), called ripples, in the initiation of these seizures, and the role of cortical fast-rhythmic-bursting cells in such paroxysms will be documented. Finally, the reflection of cortical seizures in thalamic neurons will be discussed.

5.6.1. Bicuculline-induced cortical seizures

Microsyringes filled with bicuculline were inserted into the most rostral part of the suprasylvian gyrus (area 5a) and very small amounts of bicuculline (~0.02–0.05 μl of a 0.2 mM solution) leaked into the cortex. Seizures predictably appeared after about half an hour in the adjacent area 5b (Fig. 5.48). The seizure patterns were similar to those occurring spontaneously or after electrical stimulation of the cortex and thalamus (see following sections); namely, they consisted of SW/PSW complexes at 2–2.5 Hz, alternating with fast runs at ~10 Hz, but lasted 3–4 min, compared to the ~20–50 s in the case of spontaneous seizures. Also similar to spontaneous seizures (see below, Fig. 5.49), neurons were tonically depolarized and fired rhythmic spike-bursts during the fast runs whereas they displayed long-lasting hyperpolarizations during the EEG "wave" component of SW/PSW complexes. The depth-profile of field potentials, recorded in conjunction with the intracellular recording (Fig. 5.48), was also similar to that observed during spontaneous seizures, showing reversal of surface-recorded SW/PSW complexes and fast runs below ~0.4–0.5 mm.

5.6.2. Spontaneous seizures developing from the slow sleep oscillation

The general characteristics of the slow sleep oscillation in animals and humans (0.5–1 Hz during natural sleep or under ketamine-xylazine anesthesia), the mechanisms underlying its depolarizing and hyperpolarizing phases ("up" and "down" states), and the grouping of other low-frequency as well as fast-frequency rhythms by the slow oscillation are dealt with in Chapter 3. Figure 5.49 shows a typical seizure of the Lennox–Gastaut type developing spontaneously and without discontinuity from the sleep-like slow oscillation. At the EEG level, the slow oscillation consisted of long-lasting depth-positive waves followed by prolonged depth-negative waves, repeated at a frequency of ~0.8 Hz. During the depth-positive EEG waves cortical neurons were hyperpolarized, whereas during the depth-negative wave neurons were depolarized. The recorded neuron was identified by depolarizing current pulses as a fast-rhythmic-bursting (FRB) neuron (see details on this cortical cell type in section ***2.1.1***, Chapter 2) and displayed pronounced changes in its

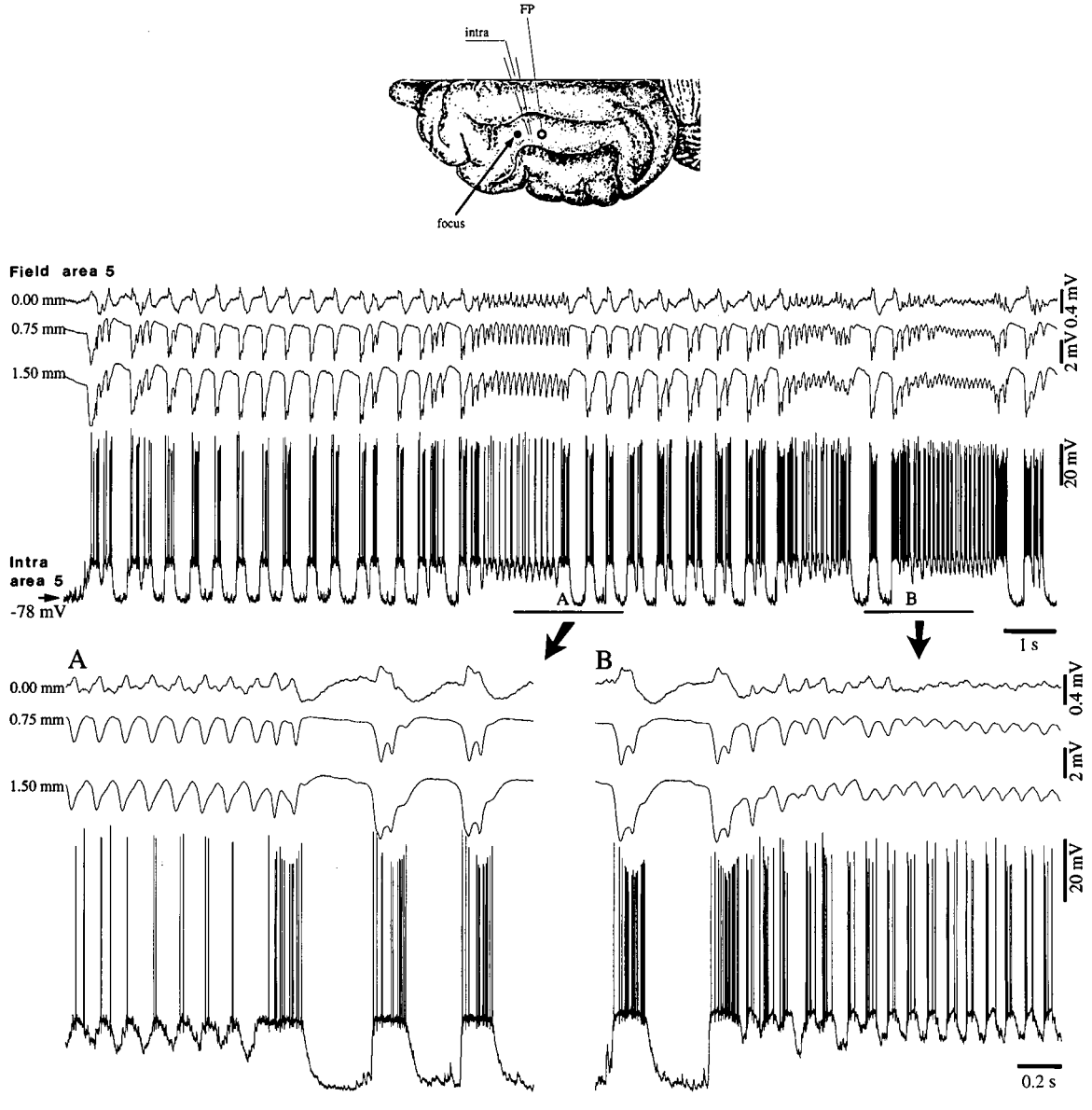

Fig. 5.48 Patterns of bicuculline-induced cortical seizure, consisting of SW/PSW complexes at ~2–2.5 Hz and fast runs at ~9–10 Hz. Cat under ketamine-xylazine anesthesia. These patterns are similar to those occurring spontaneously (see following figures). A microsyringe with bicuculline was inserted into the anterior part of area 5 (*focus* in the top brain figurine), while intracellular and field potential (FP) recordings were performed from a more posterior site in the same area (see figurine). Bicuculline was not injected but diffused from the syringe (see text). A full-blown seizure is depicted in the top panel, with fast runs and PSW complexes in *A*, and PSW complexes and fast runs in *B* (expanded below). From Steriade et al. (1998a).

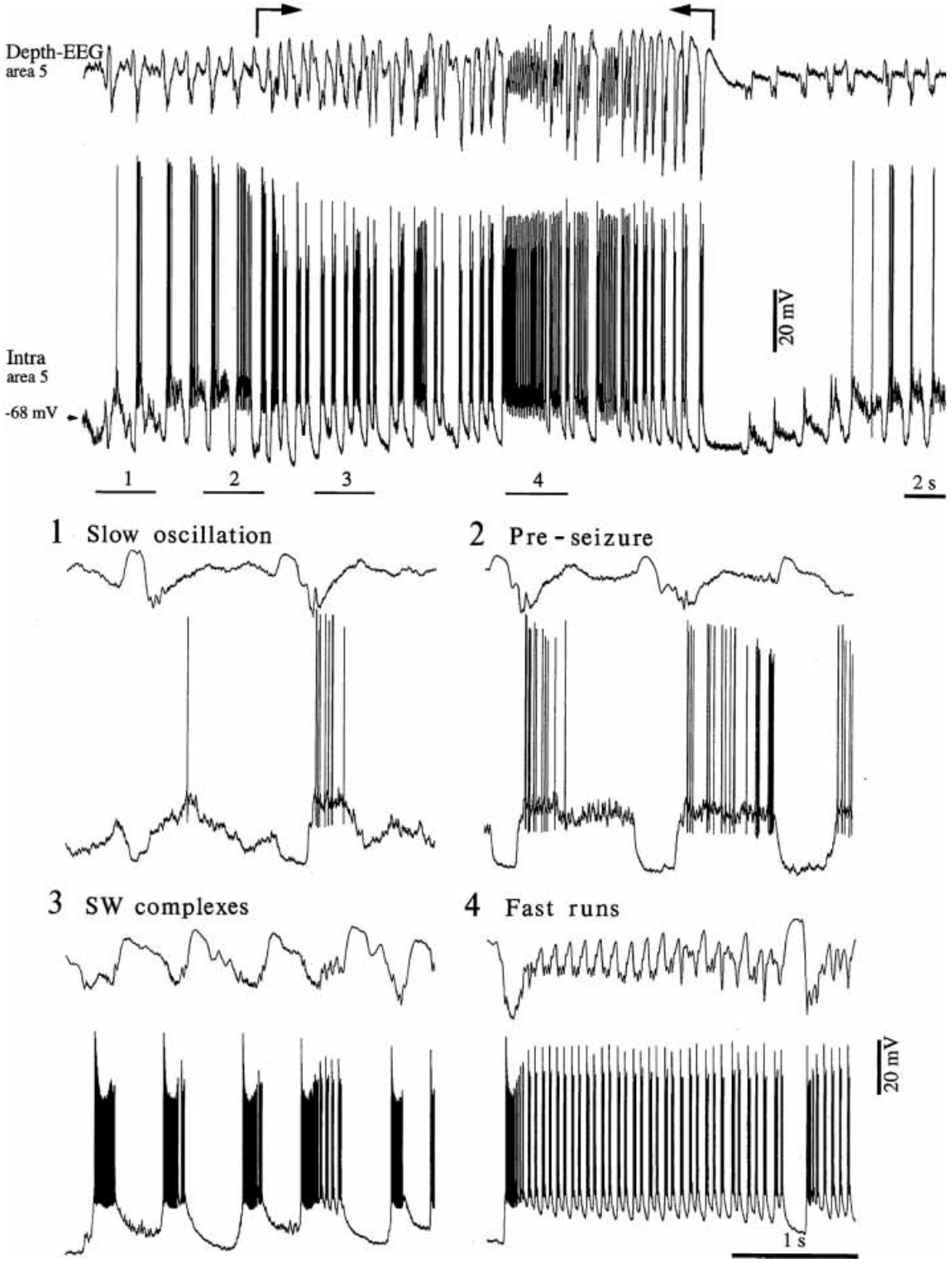
Depth-EEG
area 5
Intra
area 5
-68 mV
20 mV
1
2
3
4
2 s
1 Slow oscillation
2 Pre-seizure
3 SW complexes
4 Fast runs
20 mV
1 s

activity pattern before a seizure was apparent in the depth-EEG recorded close to the cell (*pre-seizure* panel in Fig. 5.49). The cardinal role played by FRB neurons in the generation of SW/PSW seizures has been proposed [133] and is documented below (section *5.6.2.4*). Comparing the cellular pattern of the slow oscillation to that during the pre-seizure epoch revealed that the slope as well as the amplitude of the shift in the membrane potential from hyperpolarized to depolarized levels increased. The shift from the depolarized to the hyperpolarized membrane potential was also steeper. During the pre-seizure stage, the shape of the action potentials and the fast after-hyperpolarization (AHP) remained unchanged. At variance, during the initial part of the seizure characterized by SW/PSW complexes, the action potentials were partially inactivated and the AHP disappeared. The following period, with fast runs, was characterized by EEG "spikes" at 10–20 Hz and, at the neuronal level, a tonically depolarized membrane potential, with smaller depolarizations superimposed. The end of the seizure was associated with a short period of hyperpolarization, followed by resumption of the sleep-like slow oscillation. This was the general aspect of spontaneous seizures of the Lennox–Gastaut type.

These seizures were distinguished by episodes with fast runs (10–20 Hz) intermingled with SW/PSW complexes (2–3 Hz). Most (80%) of cortical fast components had frequencies similar to those of polyspikes that build up PSW complexes in Lennox–Gastaut seizures [133].

5.6.2.1. Asynchrony of fast runs recorded from different cortical foci

Multi-site recordings showed that the fast runs did *not* occur simultaneously in all neocortical areas, had slightly different frequencies in various cortical foci, and the same neuron exhibited frequency variations as well as differences in time relations with field potentials during various fast oscillatory epochs [87]. A typical example of these variations among different epochs of the same spontaneously occurring seizure, consisting of both SW complexes and fast runs, is illustrated in Fig. 5.50, showing simultaneous

Fig. 5.49 (opposite) Spontaneously occurring seizure developing without discontinuity from the slow sleep-like oscillation. Cat under ketamine-xylazine anesthesia. Intracellular recording from an area 5 fast-rhythmic-bursting (FRB) neuron together with depth-EEG from the vicinity in area 5. The seizure occurred during the period indicated by arrows. Detail *1* shows typical activity during slow oscillation. During *2* there are pre-seizure changes in the activity of the cell, whereas the depth-EEG is not significantly altered. Detail *3* shows typical SW/PSW complexes at around 2 Hz in the depth-EEG. The cell displayed high-frequency spike-bursts, with an intra-burst frequency of 300–600 Hz. The fourth depth-negativity in the EEG had a PSW pattern, similar to the start of the fast run, depicted in *4*; the cell displayed high-frequency spike-bursts also during the fast runs and remained tonically depolarized in this period. The membrane potential is indicated by an arrow. From Neckelmann et al. (2000).

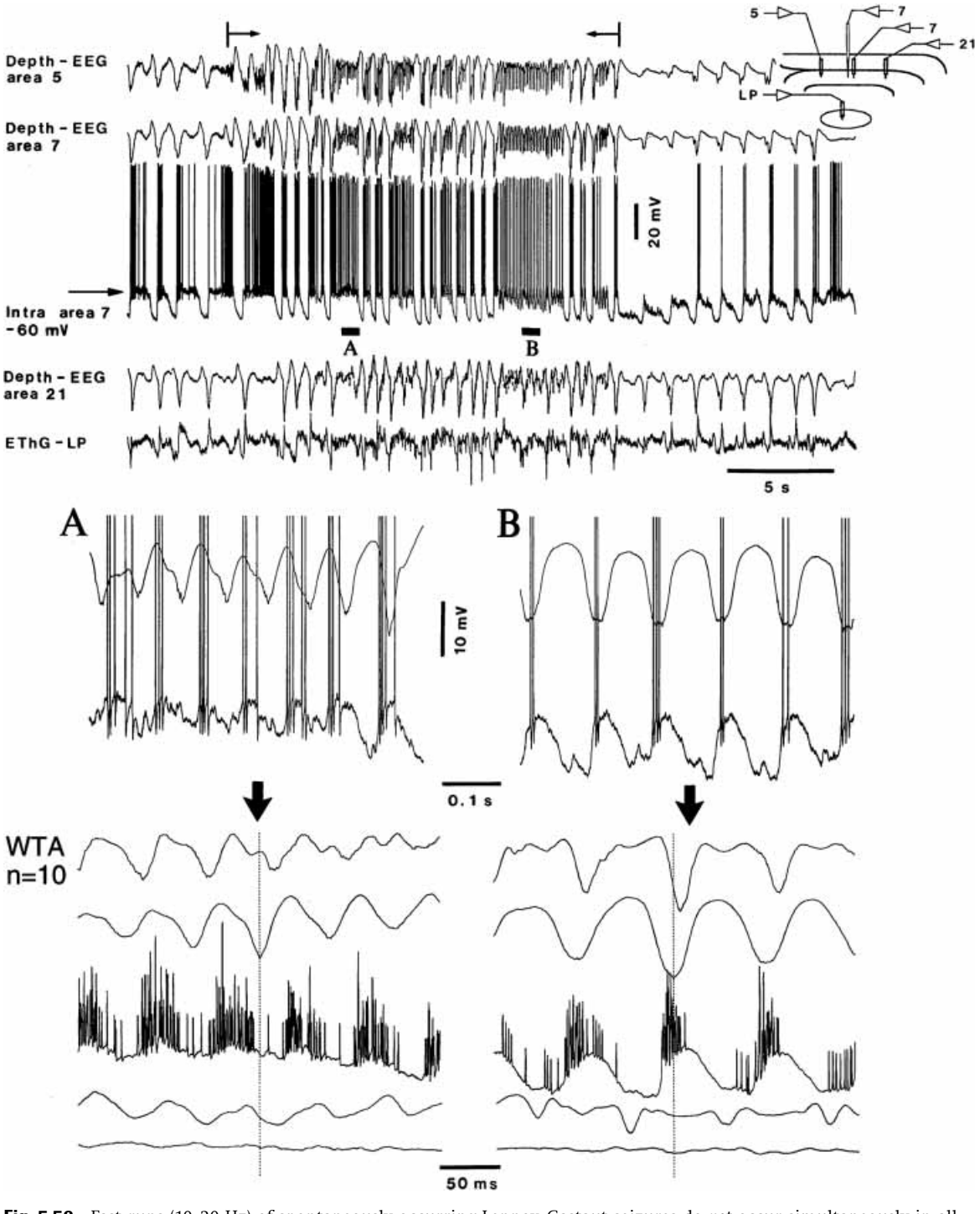

Fig. 5.50 Fast runs (10–20 Hz) of spontaneously occurring Lennox–Gastaut seizures do *not* occur simultaneously in all recorded neocortical areas. Cat under ketamine-xylazine anesthesia. Intracellular recording of a fast-rhythmic-bursting (FRB) neuron from area 7, together with field potential recordings from the depth of cortical areas 5, 7, and 21, and from the thalamic LP nucleus (see top right diagram). Two epochs with fast runs indicated in *A* and *B* are expanded below (the two traces represent intracellular and field potential recordings from area 7). Wave-triggered averages (WTA) from the same epochs are depicted below (arrows) with all five recording sites (peaks of depth-negative field potentials from area 7 are taken as reference time). From Timofeev et al. (1998).

intracellular and field potential recordings from different cortical sites. The area 7 neuron, an FRB cell similar to that depicted in the previous Fig. 5.49, was intracellularly recorded together with field potentials from the depth of adjacent suprasylvian areas 5 and 21 as well as the electrothalamogram (EThG) from the appropriate thalamic lateroposterior (LP) nucleus that provides inputs to these association cortical areas. During epoch *A*, the area 7 neuron discharged high-frequency spike-bursts at ~14 Hz that were *not* fired as expected, during the peak of depth-negative field potentials recorded from the same area, but during the descending depth-positive phase. Distinctly, during epoch *B*, the same neuron discharged lower-frequency (~11 Hz) spike-bursts that were closely related to the depth-negative cortical field potential, thus indicating synchrony between the single neuron and the neuronal pool giving rise to the field potential. During the same epoch *B*, wave-triggered averages showed that field potentials from area 21 were not in phase with those from areas 5 and 7. The time-lag between areas 7 and 21 was ~40 ms, and that between areas 5 and 21 was ~50 ms, which may explain the absence of oscillation in the thalamic LP nucleus. The frequency differences in fast runs during epochs *A* and *B* in Fig. 5.50 were likely due to slight differences in the membrane potential that was relatively depolarized (−60 mV) in *A*, with faster frequency, as compared to *B* (−67 mV), with lower frequency.

The above data demonstrate changes in frequencies of fast runs during different epochs of the same seizure and the absence of perfect synchrony between cortical neuronal pools during different epochs of cortical seizures with fast runs, which may explain why corticothalamic inputs do not elicit synchronous fast oscillations in the thalamus during this type of seizure. In keeping with the idea of cortical asynchrony during fast runs, macroelectrodes recorded fast runs arising from different pools of neurons oscillating at a similar frequency, but not synchronously. Such fast oscillations (~10 Hz) were not in phase in some epochs (see depth-EEG in panel *A* of Fig. 5.51) but could coalesce after a few seconds, thus resulting in fast EEG runs with higher amplitudes (panel *B* in the same figure). Correlatively, the amplitudes of EEG waves increased fivefold during those seizure epochs when the previously quasi-independent fast oscillators coalesced their rhythms.

5.6.2.2. I_H *and LTSs are implicated in the initiation of cortical paroxysmal cycles*

Figure 5.52 shows that the long-lasting hyperpolarizations associated with the EEG "wave" components of SW/PSW complexes

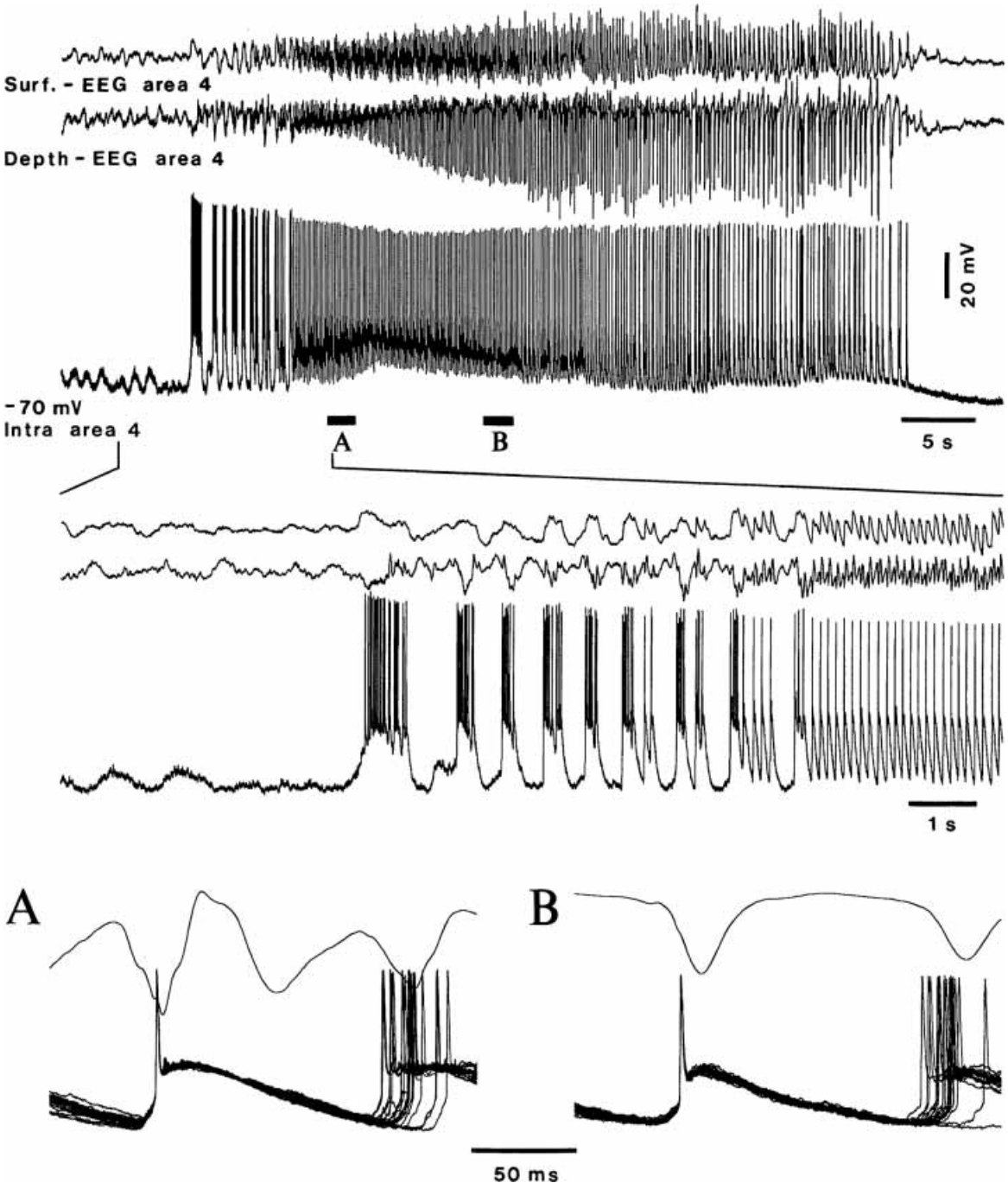

Fig. 5.51 Coalescence of two fast cortical oscillators into a single one with the progression of seizure. Cat under ketamine-xylazine anesthesia. Intracellular recording from area 4 together with surface- and depth-EEG from the same area. The area 4 neuron fired high-frequency spike-bursts at the onset of spontaneously occurring seizures, with SW/PSW complexes, and single action potentials during fast runs. The onset of seizure is expanded below the top panel. Further below, two panels (*A* and *B*), as indicated below the intracellular trace in the top panel, illustrate spike-triggered averages (STA, $n = 20$) showing that the intracellularly recorded neuron participated in one of the two oscillating patterns. Note that, at cortical depth, field potentials display two oscillations with a frequency of 9–10 Hz (*A*) and that, later on, they coalesce into a single oscillatory pattern (*B*). *The amplitude of field potentials in A is amplified by 5.* From Timofeev et al. (1998).

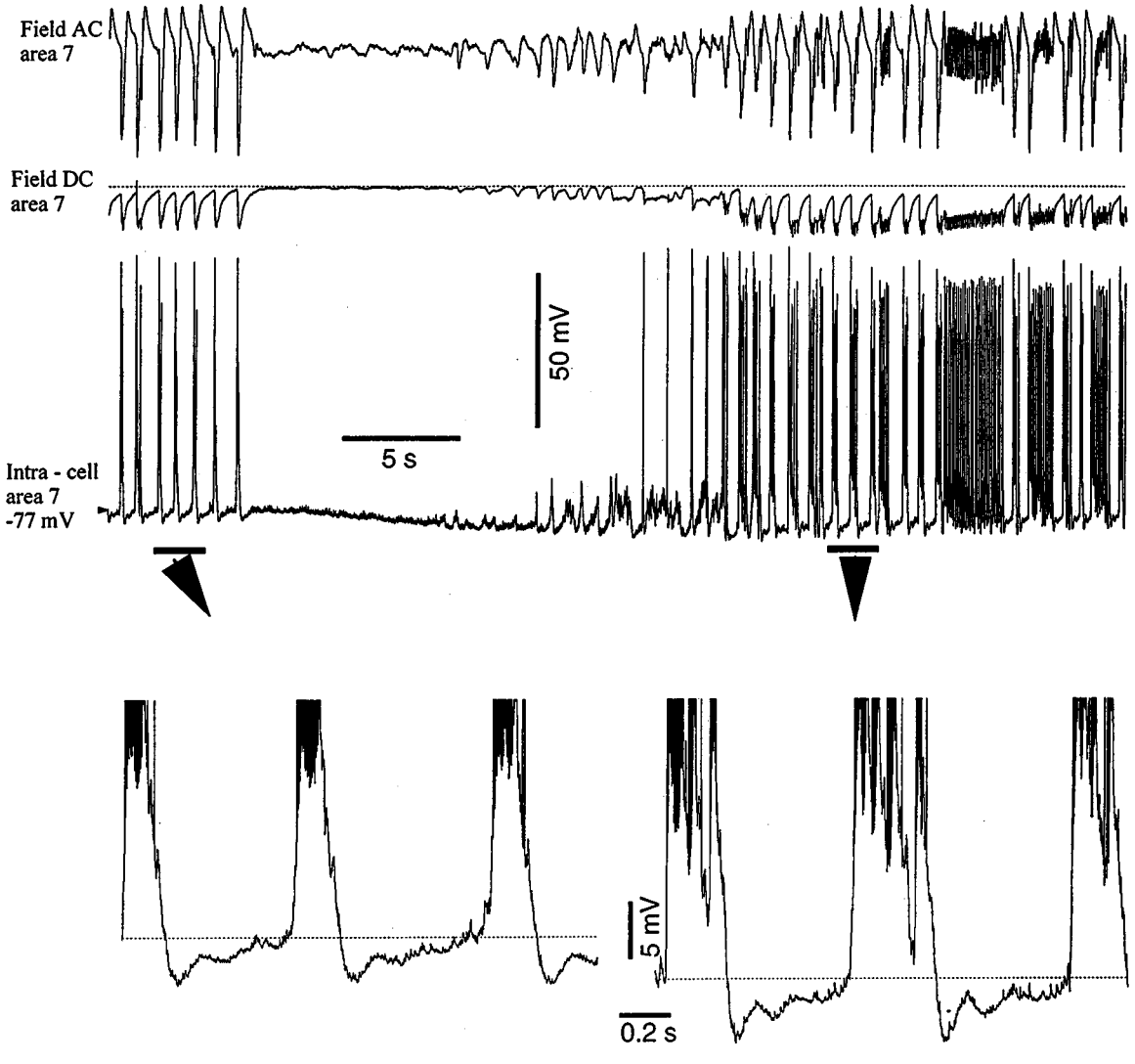

Fig. 5.52 Slowly repolarizing potentials in cortical neurons during the EEG "wave" component of SW/PSW complexes. Cat under ketamine-xylazine anesthesia. AC and DC field potentials and intracellular activity from area 7. Seizures were induced by infusion of bicuculline into distantly located area 4. Immediately after the first paroxysmal episode, the neuron was hyperpolarized and a new episode with SW/PSW complexes started. Note in both episodes (arrows) that hyperpolarizations during the EEG "wave" components of SW/PSW complexes ended with depolarizing sags. See also text. From Timofeev et al. (2002a).

[224] Destexhe et al. (2001).

[225] de la Peña and Geijo-Barrientos (1996).

terminate with depolarizing sags, and that the ensuing paroxysmal cycles started with high-frequency spike-bursts. About 20% of neocortical neurons recorded *in vivo* possess a hyperpolarization-activated cation current, I_H [11], which gives rise to a depolarizing sag, eventually leading to low-threshold spikes (LTSs) crowned by Na^+ action potentials [224], which can initiate new paroxysmal cycles of the SW/PSW type. *In vitro* studies estimated that only a relatively low, while significant, proportion of cortical neurons possess the Ca^{2+}-dependent I_T that generates LTSs [225]. Then, cortical neurons fire trains of single action potentials during depolarizing current pulses and generate spike-bursts at the break of hyperpolarizing current pulses, both *in vivo* and *in vitro* (Fig. 5.53). Modeling studies showed that no oscillatory behavior could be obtained if cortical neurons (up to 20%) had LTSs similar to those illustrated in Fig. 5.53. However, when $GABA_A$-receptor-mediated inhibitory processes were suppressed, the disinhibited cortex generated SW/PSW complexes and all cortical cells in the simulated network produced paroxysmal discharge patterns [224], which were similar to the experimental data demonstrating SW seizures in athalamic animals [171]. The presence of Ca^{2+}-dependent spike-bursts in cortical neurons and their role in the induction of SW seizures, in conjunction with some difficulties met by the idea of I_T blockade by ethosuximide [169], may corroborate our hypothesis that this anti-absence drug may (also) act at the cortical level (see section *5.5.3.1*).

5.6.2.3. Similar field-cellular relations in sleep and seizure patterns

The major components of Lennox–Gastaut seizures in intracellularly recorded cortical regular-spiking neurons, which constitute the majority of cortical neurons, are illustrated in Fig. 5.54. The seizure evolved without apparent discontinuity from the slow sleep-like oscillation at 0.9 Hz (left part in panel *A*), which was characterized by its alternating depolarizing and hyperpolarizing components. The first part of the seizure, lasting ~16 s, was formed by SW complexes at 2 Hz; it was followed by a period of ~2 s with fast runs at ~15 Hz; thereafter, SW complexes appeared again and decreased their frequency; and the seizure ended with a postictal depression of ~6 s. The seizure was associated with a progressive depolarization, associated with partial spike inactivation, which reached a maximum during the fast runs. Such seizures progressively evolved from sleep patterns, and the relations between field potentials and intracellular activity were similar during the pre-seizure epoch dominated by sleep patterns to those recorded during the seizure. These facts were demonstrated by analyses using wave-triggered averages (WTAs) of intracellular and field potential

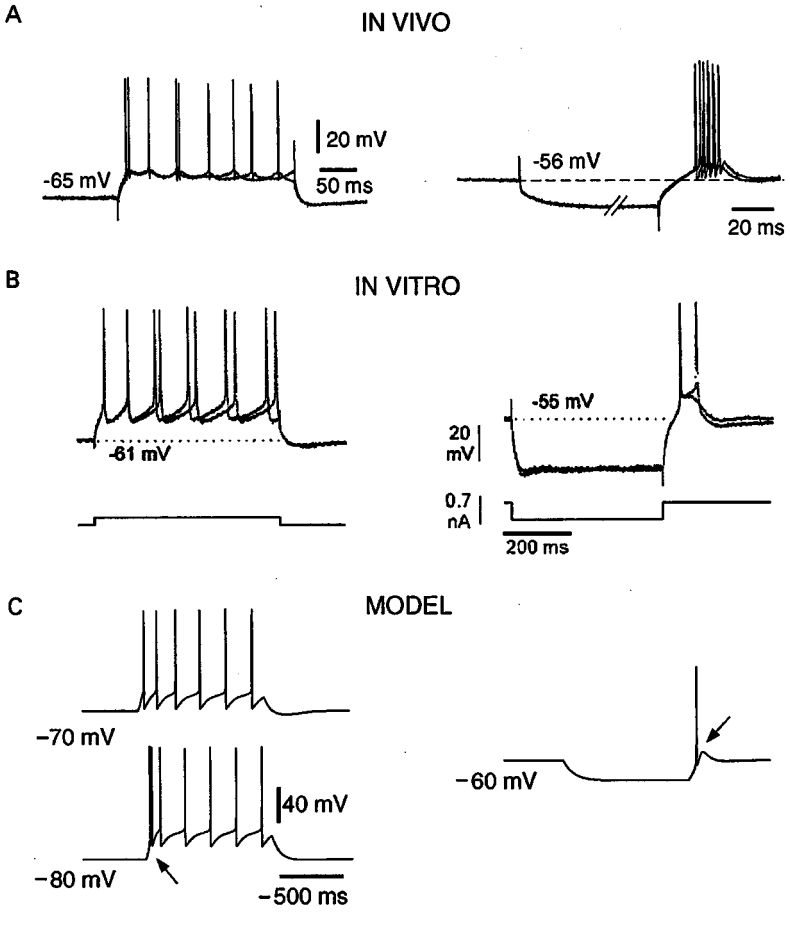

Fig. 5.53 Rebound bursting properties of cortical pyramidal cells. *A*, rebound bursting cell from cat cerebral cortex (barbiturate anesthesia). The hyperpolarizing pulse was 0.2 s and was truncated for clarity. *B*, rebound bursting cell from guinea pig frontal cortex *in vitro* (adapted from de la Peña and Geijo-Barrientos, 1996). *C*, model pyramidal cell comprising I_{Na}, I_K, I_M, and I_T currents. *Left*, repetitive firing with adaptation following the injection of depolarizing current (0.1 nA). *Right*, rebound burst response at the offset of a hyperpolarizing current pulse (−0.1 nA). Arrows indicate rebound responses due to I_T. From Destexhe et al. (2001).

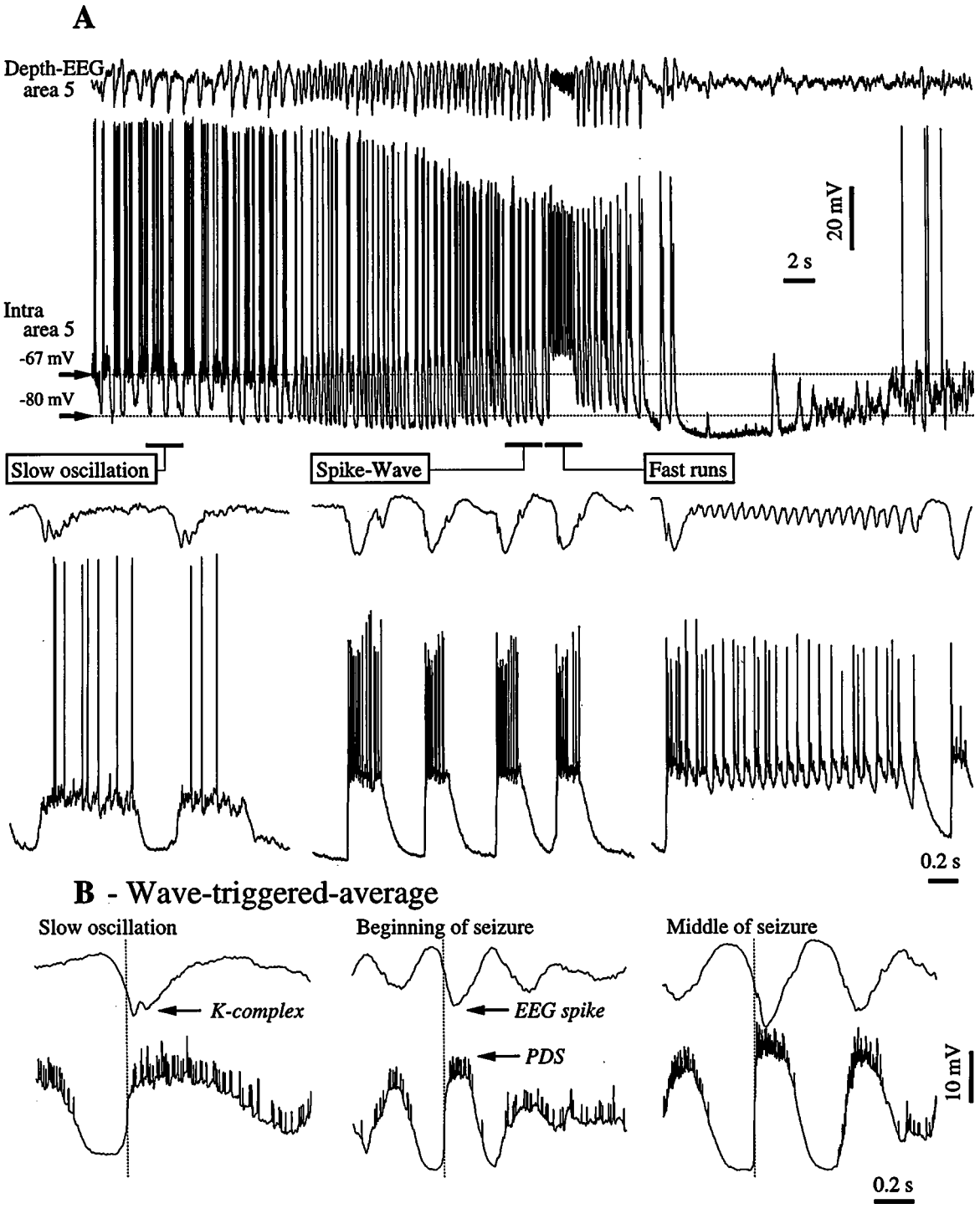
A
Depth-EEG
area 5
Intra
area 5
-67 mV
-80 mV
20 mV
2 s
Slow oscillation
Spike-Wave
Fast runs
0.2 s
B - Wave-triggered-average
Slow oscillation
Beginning of seizure
Middle of seizure
K-complex
EEG spike
PDS
10 mV
0.2 s

[226] See Fig. 5 in Steriade and Amzica (1994).

activities, triggered by the steepest slope of the depolarizing onset in the area 5 neuron. These analyses show (*a*) the close time-relation between the depolarizing component of the slow sleep-like oscillation and the depth-negative cortical field potential, representing the K-complex at the EEG level; and (*b*) the increased amplitude of the depolarizing component of the slow oscillation, reaching the level of paroxysmal depolarizing shifts (PDSs) during the seizure, as well as the increased frequencies of these paroxysmal events to become SW complexes at ∼2–3 Hz.

Thus, the patterns of SW complexes during Lennox–Gastaut seizures are an exaggeration of depolarizing and hyperpolarizing components of sleep patterns, while keeping similar relations between intracellular activities and EEG components. Additional aspects during the seizure are as follows. The depolarizing envelope during the seizure evolves simultaneously with increased hyperpolarization; note, in Fig. 5.54, the evolution of the membrane potential, above and below dotted lines at −67 mV and −80 mV, respectively. By contrast, such events do not occur during the sleep-like slow oscillation. Also, a sudden arrest, with a postictal depression, was found to be associated with a long-lasting hyperpolarization.

The progressive depolarizing envelope during the seizure depicted in Fig. 5.54 eventually led to a plateau, with a "clamped" membrane, during which action potentials were partially or totally inactivated. Only IPSPs can be elicited by thalamocortical volleys during large depolarizing envelopes [226]. Nonetheless, many neurons remain capable of firing action potentials during the depolarizing plateau, which explains why the excitatory circuits are maintained. The fact that the progressive depolarization and the plateau with spike inactivation are more pronounced in some instances (Fig. 5.54) than in others (see below, Figs. 5.58–5.59) is explained by the closer vicinity of the primary focus in the former case. The depolarizing envelope throughout the seizure is ascribed to the

Fig. 5.54 (opposite) Spontaneously occurring seizure of Lennox–Gastaut type, developing without discontinuity from a slow sleep-like oscillation: similar field-cellular relations during sleep and different components of seizure. Cat under ketamine-xylazine anesthesia. Intracellular recording from a regular-spiking area 5 neuron together with depth-EEG from the vicinity in area 5. *A*, smooth transition from slow oscillation to complex seizure consisting of SW complexes at ∼2 Hz and fast runs at ∼15 Hz. The seizure lasted for ∼25 s. Epochs of slow oscillation preceding the seizure, SW complexes, and fast runs are indicated and expanded below. Note postictal depression (hyperpolarization) in the intracellularly recorded neuron (∼6 s), associated with suppression of EEG slow oscillation (compare to left part of trace). *B*, Wave-triggered average during the slow oscillation, at the beginning of the seizure, and during the middle part of the seizure. Averaged activity was triggered by the steepest part of the depolarizing component in cortical neuron (dotted lines), during the three epochs. The depth-negative field component of the slow oscillation (associated with cell depolarization) is termed K-complex. During the seizure, the depolarizing component reaches the level of a paroxysmal depolarizing shift (PDS), associated with an EEG "spike". From Steriade et al. (1998a).

[227] Fisher et al. (1992).

progressive entrainment of excitatory circuits through sequentially distributed synaptic linkages [143]. The propagation across the neocortex is mediated by short- and long-scale linkages, with particular types of neurons playing a prevalent role in driving their targets and entraining them into the seizure. Among these neuronal types, the fast-rhythmic-bursting cells play a leading role, which is discussed below.

5.6.2.4. Role of ripples and fast-rhythmic-bursting cells in promoting seizures

Very fast oscillations (80–200 Hz), termed ripples, are associated in neocortical neurons with the depolarizing phase of the slow sleep oscillation (see section *3.2.3.2* in Chapter 3). The slow oscillation may evolve into seizures with Lennox–Gastaut patterns and ripples proved to have a leading role in the initiation of such neocortical paroxysms, as they are present at the transition between normal and paroxysmal activity, they show significantly increased amplitudes at the very onset of seizure compared to epochs prior to it, and conditions that diminish neocortical ripples also reduce or abolish the propensity to seizures [84]. Very fast oscillations have also been described in other types of paroxysmal activity [81–83, 227]. Data on seizures elicited by using paradigms of electrical stimulation within the frequency range of ripples are discussed above (section ***5.2.2***). Here, I elaborate on the temporal relationships between the occurrence of ripples and the initiation of neocortical seizures using multi-site recordings, and the neuronal substrates of these very fast oscillations during paroxysmal activity.

Ripples display their highest amplitude at the onset of seizures. This was determined by measuring the mean ripple amplitude (MRA) in filtered traces (80–200 Hz) of field potential (EEG) recordings. Epochs with the highest MRA are found at the onset of isolated seizures evolving from the slow oscillation or at the onset of recurrent paroxysms (Fig. 5.55). The analysis of the relative amplitude for different frequency bands (from 0 to 250 Hz) revealed that the only oscillations that displayed the pattern of strongest amplitude at the onset of seizures were within the ripple frequency. Could neocortical ripples simply be a consequence of strong neuronal depolarization during seizures and have nothing to do with initiating these paroxysms? With multi-site field potential recordings from the neocortex during recurring seizures, ripples were present from seizure onset *within the site where paroxysmal activity started*. The site where the first EEG "spike" occurred changed from seizure to seizure, and the time of appearance of ripples at seizure

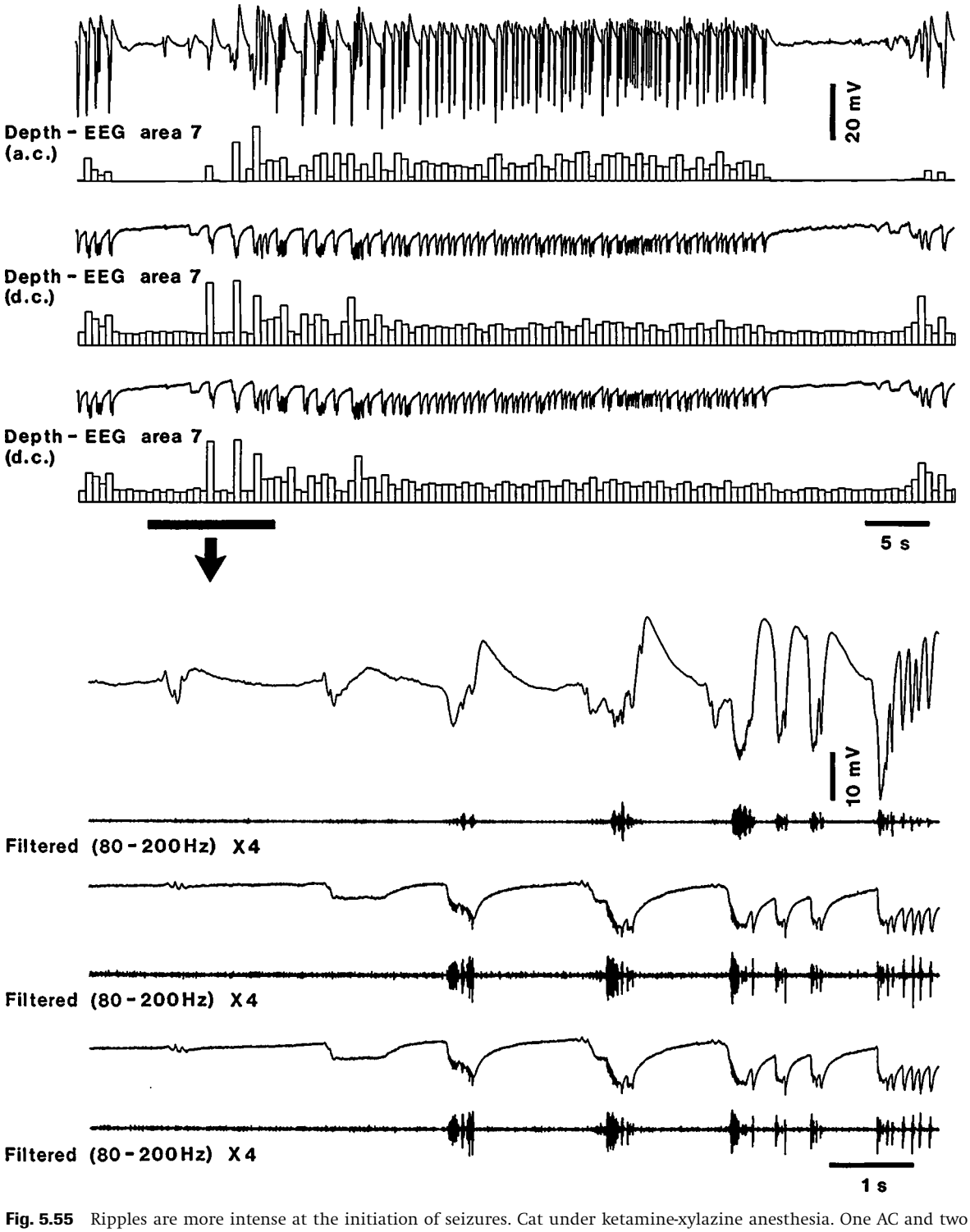

Fig. 5.55 Ripples are more intense at the initiation of seizures. Cat under ketamine-xylazine anesthesia. One AC and two DC field potentials from area 7 during spontaneous seizures. The top panel displays one of these spontaneous seizures. The mean amplitude of ripples (from the filtered traces × 200) was calculated for 0.5-s intervals for each trace. Ripples had a greater amplitude at the start of the seizure. The onset of the seizure is expanded below with the filtered traces (80–200 Hz). Ripples were stronger during the first few EEG "spikes" in the AC trace, and they were maximal at the start of the seizure in the two DC traces. This indicates that while ripples show a progressive increase during the first two to three paroxysmal events in some cortical sites, they are maximal at the onset of seizure in other sites. From Grenier et al. (2003).

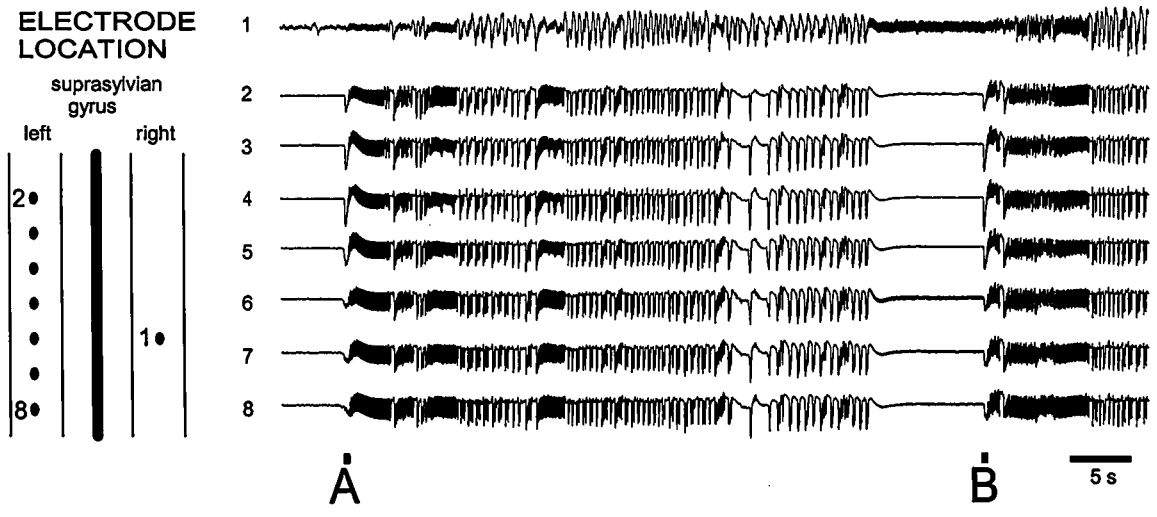

ONSET OF: (–) FIRST EEG SPIKE IN SEIZURES AND (--) RIPPLES

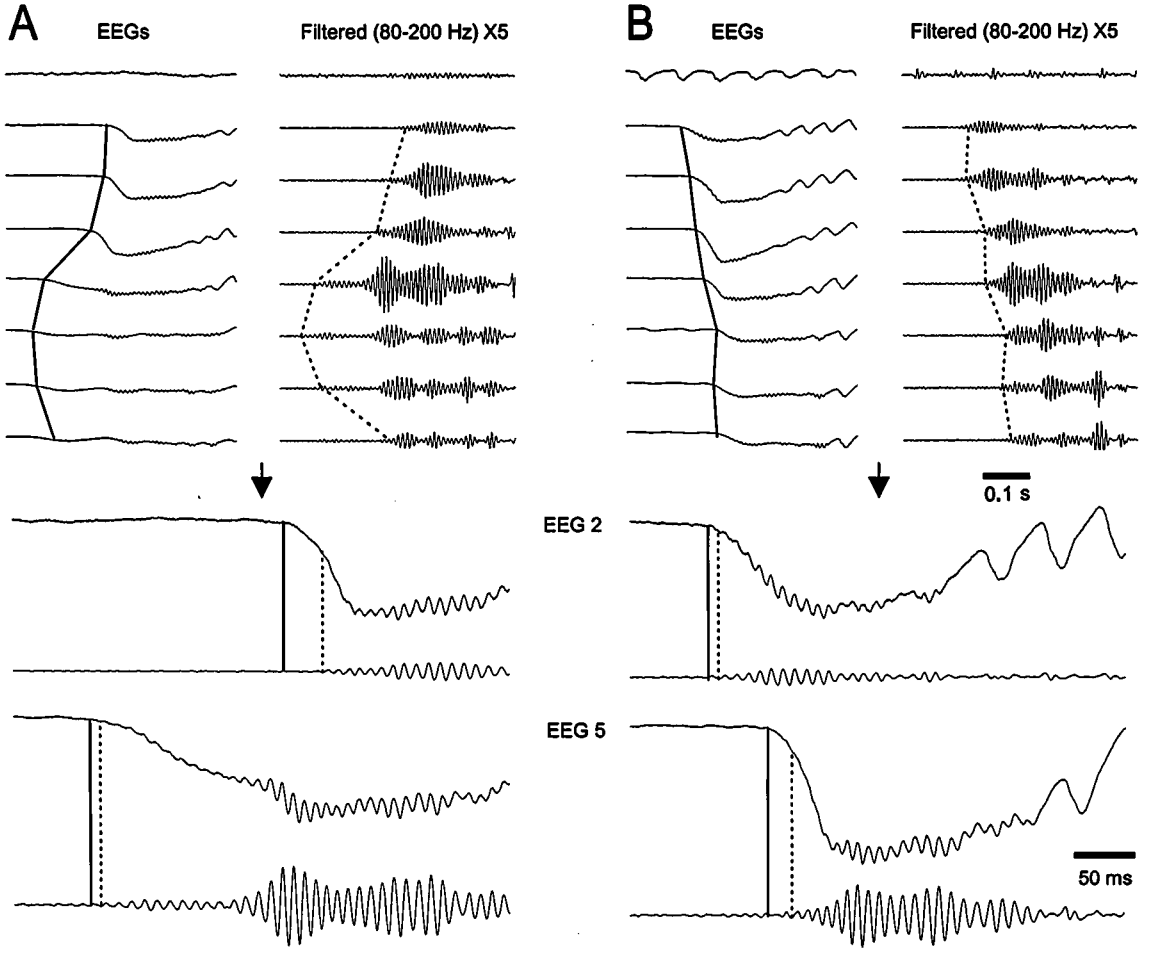

onset (dotted lines, middle and bottom panels, Fig. 5.56) closely followed the onset of the first EEG "spike" in different sites (continuous lines, middle and bottom panels in this figure). Ripples were present from the onset of the first (precursor) EEG "spike", whereas they appeared with some delay over the abruptly rising follower EEG "spikes". This suggests that ripples are involved in the generation of the EEG "spike" itself in sites from which seizures originate, while the paroxysmal activity in secondary sites could be triggered by projections from the primary site. These data also suggest that ripples are involved in the generation of the first one or few EEG paroxysmal "spikes" in the site from which the seizure is initiated and, from then on, the seizure has other mechanisms for sustaining itself, since it can continue without ripples. This hypothesis would explain the recordings in which ripples are not present at the very onset of seizures or are completely absent at that time. These recordings would correspond to secondary sites.

If ripples had a role in initiating seizures, manipulations that would block ripples would also have an obliterating effect on such seizures. Indeed, halothane, a substance that blocks gap junctions, decreases the intensity of ripples and blocks the occurrence of seizures within a minute of its administration (Fig. 5.57) [228]. After the termination of halothane administration, there was a progressive return of ripples, and seizures restarted at about the time when ripples reached the level they had displayed between recurrent seizures before halothane administration. The hypothesis that gap junctions could be implicated, via their role in very fast oscillations, in the initiation of neocortical seizures was also advanced on the basis of the presence of fast oscillations at the start of seizures in human EEG recordings, blockade of fast oscillations in hippocampal slices by gap junction blockers, and modeling studies showing that axo-axonic gap junctions between principal cells could explain the presence of these fast oscillations [82].

[228] Gap junctions between fast-spiking neurons may play an important role in generating neocortical ripples occurring during non-pathological conditions, such as slow-wave sleep [80]. This suggestion is based on the demonstration that gap junctions exist between these inhibitory neurons and may result in tight synchrony in their firing (Galarreta and Hestrin, 1999; Gibson et al., 1999). FS cells firing is phase-locked with ripples and $GABA_A$-mediated IPSPs are important in the patterning of ripples occurring during the slow sleep oscillation [80]. Gap junctions are also present in glial cells (Dermietzel and Spray, 1993). That gap junction blockers abolish very fast oscillations has also been shown by Ylinen et al. (1995), Draguhn et al. (1998) and Jones et al. (2000). Gap junction blockers have also been shown to disturb paroxysmal network activities (Amzica and Massimini, 2000; Perez-Velazquez and Carlen, 2000).

Fig. 5.56 (opposite) EEG paroxysmal "spikes" start from ripples in sites where seizures are initiated. Cat under ketamine-xylazine anesthesia. Depth field potential recordings from an array of seven electrodes separated by 1.5 mm each along the antero-posterior axis of the left suprasylvian gyrus, plus one electrode in the contralateral gyrus (see scheme at top left). Seizures occurred spontaneously. Recordings during two seizures are shown at the top right. The onsets of both seizures are expanded in middle panels, *A* (first seizure) and *B* (second seizure), along with the filtered trace (80–200 Hz). The onset of the first EEG "spike" is tentatively indicated by a continuous line in panels with EEG traces, and the onset of ripples in panels with filtered traces is indicated by a dashed line. This shows that ripples appear first in sites in which EEG "spikes" appear first. EEG and filtered traces from two sites (2 and 5) are further expanded in the bottom panels, revealing that the EEG "spikes" started with ripples in early sites (possibly the seizure focus), while in other sites (possibly receiving excitation from the seizure focus) ripples appeared when the EEG "spike" had already started. From Grenier et al. (2003).

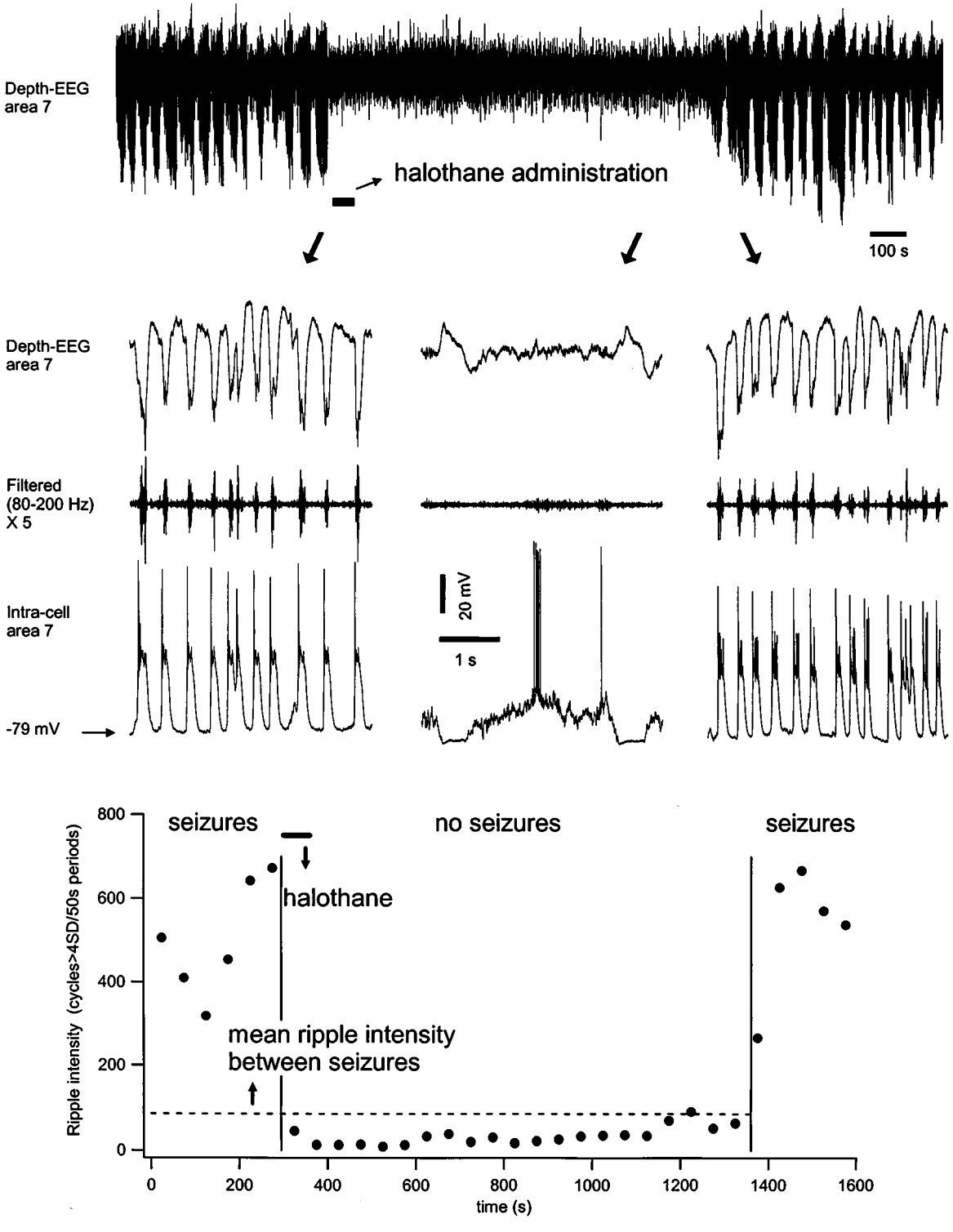
Depth-EEG
area 7
halothane administration
100 s
Depth-EEG
area 7
Filtered
(80-200 Hz)
X 5
Intra-cell
area 7
-79 mV
20 mV
1 s
seizures
no seizures
seizures
halothane
mean ripple intensity
between seizures
Ripple intensity (cycles>4SD/50s periods)
800
600
400
200
0
0
200
400
600
800
1000
1200
1400
1600
time (s)

The neuronal substrates of ripples during complex seizures of the Lennox–Gastaut type have been investigated in major neuronal classes recorded from neocortical areas, *in vivo*. As such seizures are characterized by epochs with fast runs (10–20 Hz), special emphasis was placed on relations between field potentials and intracellular activities during these activities [133]. Whereas regular-spiking (RS) neurons discharged single action potentials or spike-doublets during either depth-negative fast EEG runs or polyspikes of PSW complexes, fast-rhythmic-bursting (FRB) neurons discharged spike-bursts consisting of up to six to seven action potentials during the depolarizing component of fast runs as well as during each of the multiple EEG "spikes" composing the PSW complexes (Fig. 5.58). Ripples appeared superimposed on the depth-negative EEG envelope of the slow oscillation, they were significantly enhanced during seizures with PSWs complexes, and FRB cell firing was enhanced during, and correlated with, ripples during paroxysmal activity (bottom panel in Fig. 5.59).

The dynamics of FRB cells' intrinsic excitability during the transition from the sleep slow oscillation to Lennox–Gastaut seizures (Fig. 5.60) corroborates data from field potential recordings, showing most prominent ripples at seizure onset (see Figs. 5.55–5.56). Typical high-frequency (300–600 Hz), rhythmic (20–40 Hz) spike-bursts of FRB cells, which were elicited by depolarizing current steps, occurred during the initial few seconds of seizures with SW/PSW complexes, evolving insidiously from the slow oscillation (panel *A* in Fig. 5.60), but deteriorated during the full-blown seizure (panel *B* in the same figure).

Because of the high-frequency, fast repetitive spike-bursts that characterize FRB neurons (see above, Fig. 5.58*B*), we hypothesized that, if rhythmically stimulated, their impact on local networks could be sufficient to initiate seizures focally and, possibly, in related structures. Protracted series of repetitive (10 Hz) depolarizing

Fig. 5.57 (opposite) Halothane diminishes ripples and stops seizures. Cat under ketamine-xylazine anesthesia. Field potential and intracellular recordings from area 7. *Top panel* depicts the depth-EEG during an epoch with spontaneous seizures that stopped after halothane administration (60 s, bar in top panel). Spontaneous seizures reappeared ~17 min after the end of halothane administration. Periods with original and filtered (80–200 Hz, amplified × 5) field potentials and intracellular recordings of a regular-spiking neuron are expanded in the middle panel for three different conditions: left, during seizures before halothane; middle, after halothane administration, during the seizure-free period; and right, after halothane when seizures were present again. Ripple intensity was calculated for 50-s periods by taking the standard deviation of the filtered trace immediately after halothane administration, and counting the number of ripple cycles that exceeded four times this value (plot at bottom). Ripples were much less numerous or virtually absent during periods without seizures. Ripple intensity was also calculated for short periods in between seizures (dotted line). Ripples during the seizure-free period progressively increased toward that value, and seizures re-occurred shortly after ripples were back to about those values. From Grenier et al. (2003).

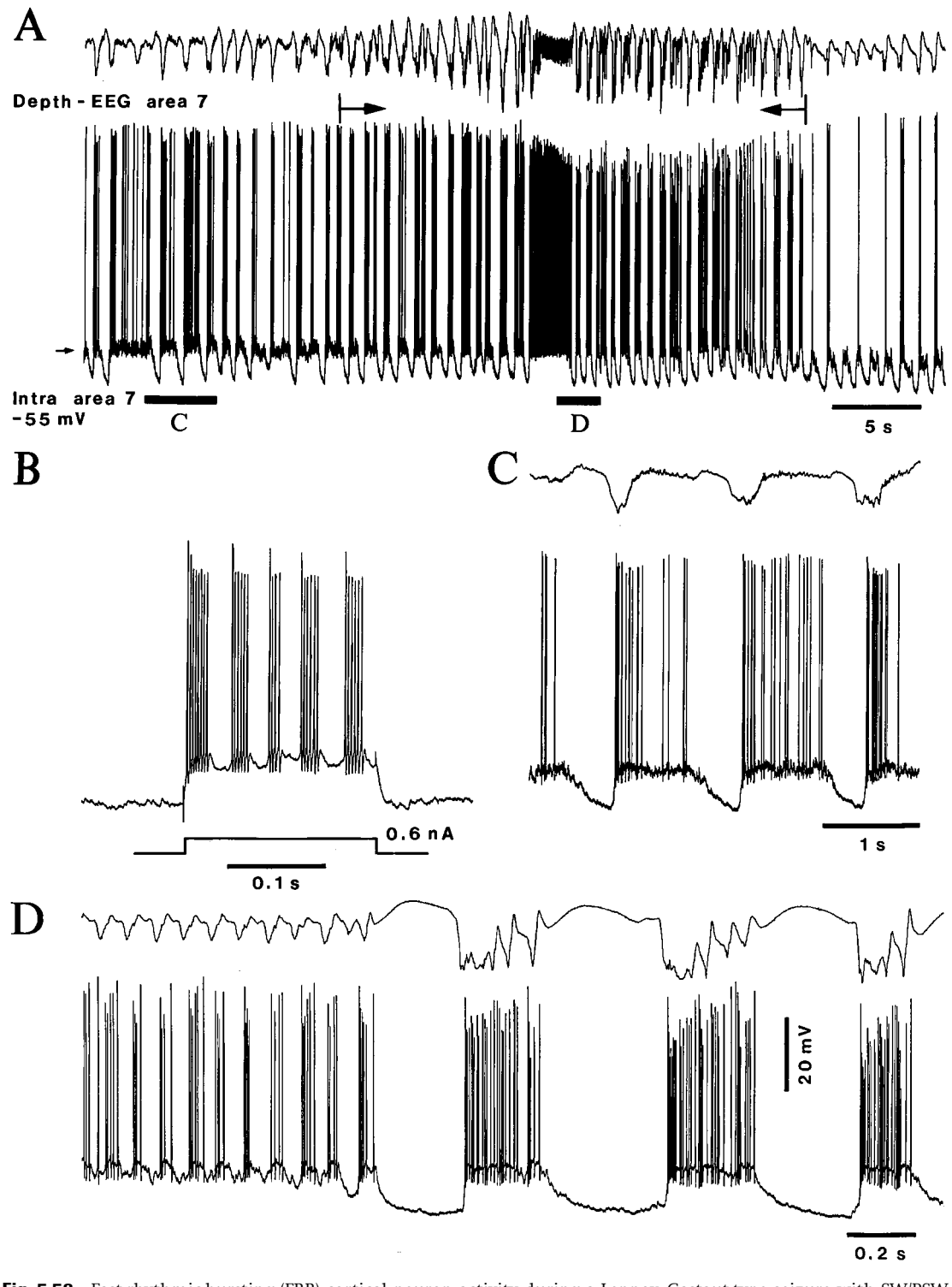

Fig. 5.58 Fast-rhythmic-bursting (FRB) cortical neuron activity during a Lennox–Gastaut-type seizure with SW/PSW complexes and fast runs, developing spontaneously from slow sleep oscillation. Cat under ketamine-xylazine anesthesia. Top panel (*A*) illustrates intracellular and depth-EEG recordings from area 7. The seizure is indicated by arrows (below the EEG trace) and lasted for ~26 s. *B*, electrophysiological identification of an FRB neuron by a depolarizing current pulse (0.2 s). Epochs *C* and *D* in the top panel are expanded below. Panel *C* depicts the slow oscillation before the seizure. Panel *D* shows both fast runs (~12 Hz) and PSW complexes (~2 Hz). Note high-frequency spike-bursts in neuron activity during each depth-negativity of fast EEG runs (compare with single action potentials in the regular-spiking cell in Fig. 6 of that article and with single spikes or spike-doublets in the present Fig. 5.54). From Steriade et al. (1998a).

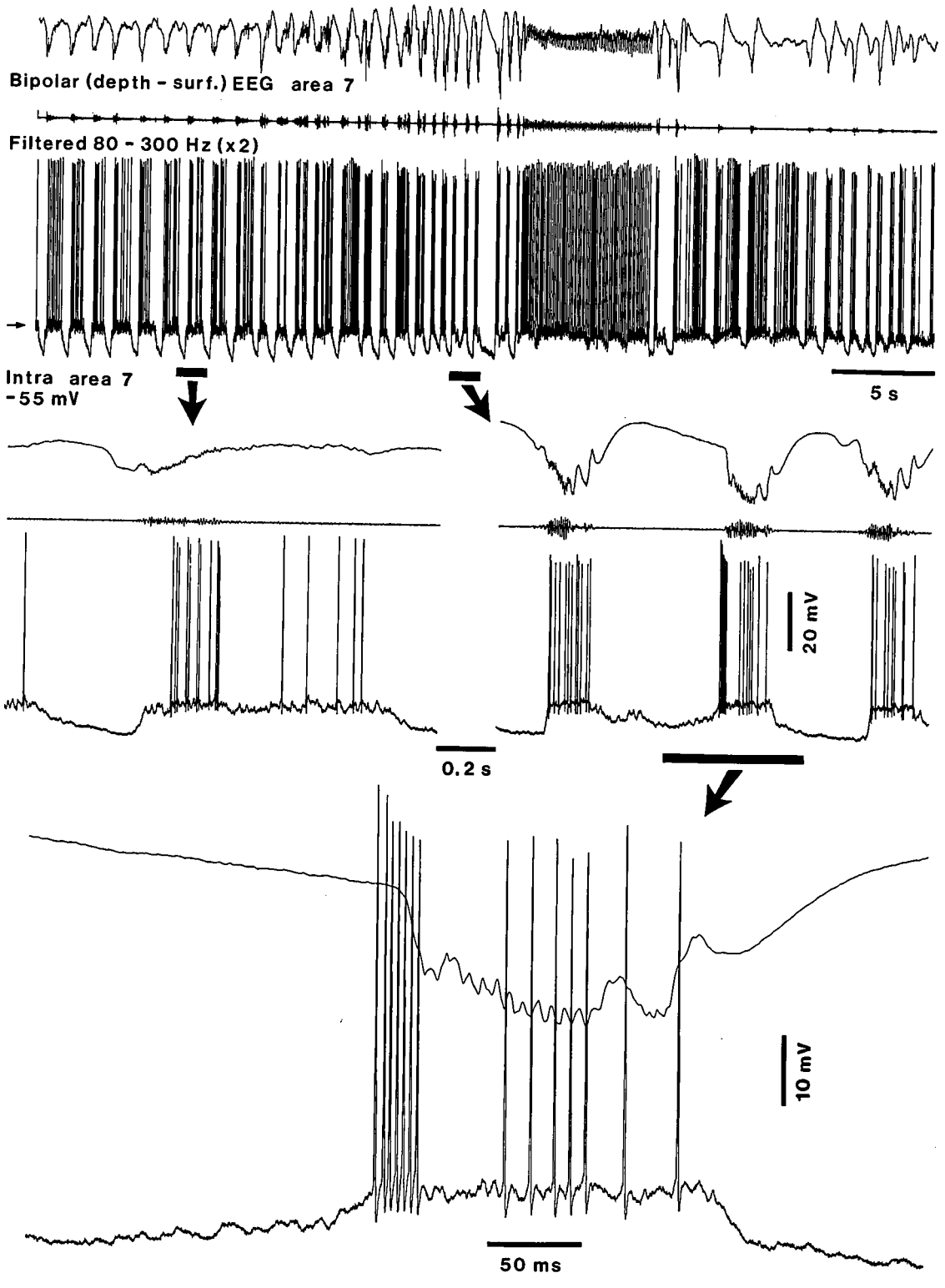

Fig. 5.59 Ripples (~120 Hz) during a spontaneous cortical seizure of the Lennox–Gastaut type, developing from a slow oscillation. Cat under ketamine-xylazine anesthesia. Intracellular and EEG recording from area 4. FRB neuron (identified as in Fig. 5.58*B*). The 2nd trace in the top panel is EEG filtered for fast events (80–300 Hz) and amplified. Two horizontal bars (below the intracellular trace) indicate the slow sleep oscillation (left) and the seizure (right), and are expanded below (arrows). One PSW complex of seizure is further expanded below (arrow). Note close time-relation between action potentials and EEG ripples. From Steriade et al. (1998a).

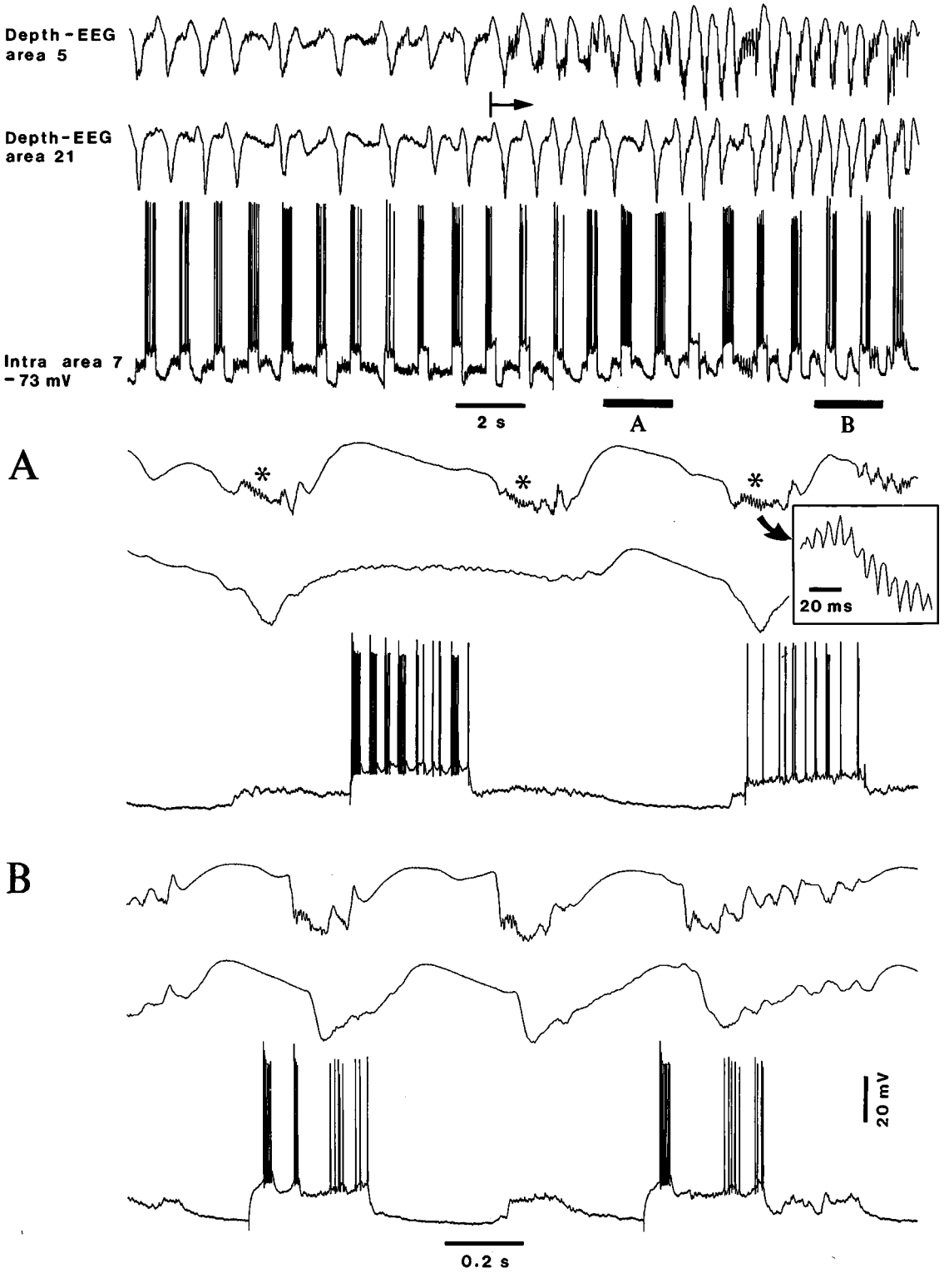
Depth-EEG area 5
Depth-EEG area 21
Intra area 7 -73 mV
2 s
A
B
A
20 ms
B
20 mV
0.2 s

[229] Data by M. Steriade and F. Amzica (see Steriade, 2001a).

current pulses in FRB neurons resulted in Lennox–Gastaut type seizures, which appeared not only in the stimulated neuron but also in the focal EEG recorded from the same area as well as in related cortical areas and appropriate thalamic nuclei (see Fig. 15 in [133]). In those cases, the seizures were the first to appear during the course of experiments and were not observed when depolarizing current pulses were delivered, with the same parameters, to RS cells.

While ripples were reflected in RS neurons, which fired within the frequency range of ripples in close correlation to the negative peaks of ripples in field potential recordings (Fig. 5.61), the peri-event histograms in intrinsically bursting (IB) cells displayed less clear-cut correlations with individual ripples because of the higher frequency of spike-bursts fired by those neurons (Fig. 5.62). However, histograms revealed that the action potentials of IB cells did not occur completely independently from the ripples, as one of the action potentials of the spike-burst tended to occur in phase with the depth-negative peak of ripples.

5.6.2.5. Hyperpolarizing seizures associated with a decrease in input resistance

An interesting similarity between TC and some neocortical neurons should be mentioned. Neocortical neurons generally display a tonic depolarization during Lennox–Gastaut seizures (see Fig. 5.54), whereas most TC neurons are tonically hyperpolarized during these paroxysms, due to summated IPSPs from RE neurons [87, 133]. However, we also observed seizures associated with an exclusively hyperpolarizing envelope in neocortical neurons, which lasted throughout the seizure and was initiated from the very onset of the paroxysm [229]. The hyperpolarization associated with such seizures started with the first sharp depth-negative EEG "spike"

Fig. 5.60 (opposite) Dynamic changes in excitability of a fast-rhythmic-bursting (FRB) cortical neuron during slow oscillation and a Lennox–Gastaut seizure. The paroxysm was initiated with SW/PSW complexes at 2 Hz (as illustrated in the top panel) and evolved with epochs characterized by fast runs (not depicted here). Cat under ketamine-xylazine anesthesia. Intracellular recording of fast-rhythmic-bursting neuron activity from area 7, together with depth-EEG from areas 5 and 21. The onset of the seizure is indicated by arrow (below the top EEG trace). Depolarizing current pulses (0.5 nA, 0.3 s) were applied at a rate of 1 Hz. Before seizure, during the slow oscillation, the neuron discharged high-frequency (400 Hz) spike-bursts recurring rhythmically at ~25 Hz. This pattern also occurred at the beginning of the PSW seizure (see the first depolarizing current pulse in *A*, ~4 s after seizure onset). Later on, however, the responses to depolarizing current pulses degenerated to single-spikes or a spike-doublet (second depolarizing current pulse in *A*) and to a single spike-burst followed by single-spikes or spike-doublets (*B*). Asterisks in *A* point to fast ripples (~120–140 Hz) during the depth-negativity of PSW complexes; one of these epochs is expanded on the right. Note that depth-EEG from areas 5 and 21 showed greater synchrony during the full-blown PSW seizure at 2 Hz (with area 5 preceding, in *B*) than what was observed during the early period of seizure (*A*). From Steriade et al. (1998a).

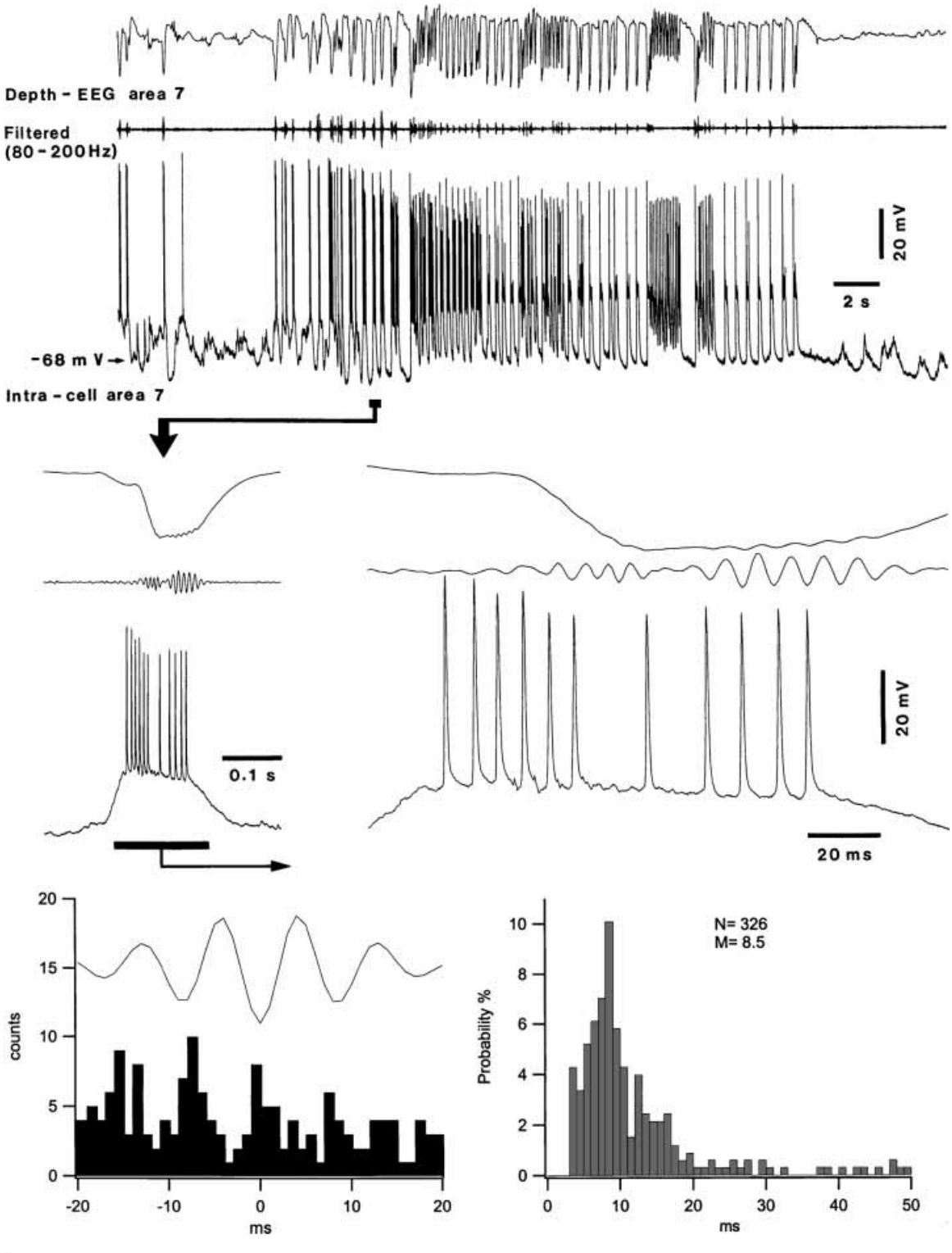

Fig. 5.61 Regular-spiking neuron fires in relation to ripples during seizures. Cat under ketamine-xylazine anesthesia. Intracellular and field potential recordings from area 7. A spontaneous seizure is displayed in the top panel, also showing the EEG trace filtered between 80 and 200 Hz. The underlined paroxysmal depolarizing shift is expanded in the middle left panel, and further expanded on the right to show the relation between action potentials and ripples. A peri-event histogram (PEH) reveals that neuronal firing was related to the depth-negative peaks of ripples. The fact that the neuron fired in relation to ripples is also shown by an interspike interval histogram showing that the main interval (8.5 ms) was very similar to the mean period of ripples during the seizure (8 ms). From Grenier et al. (2003).

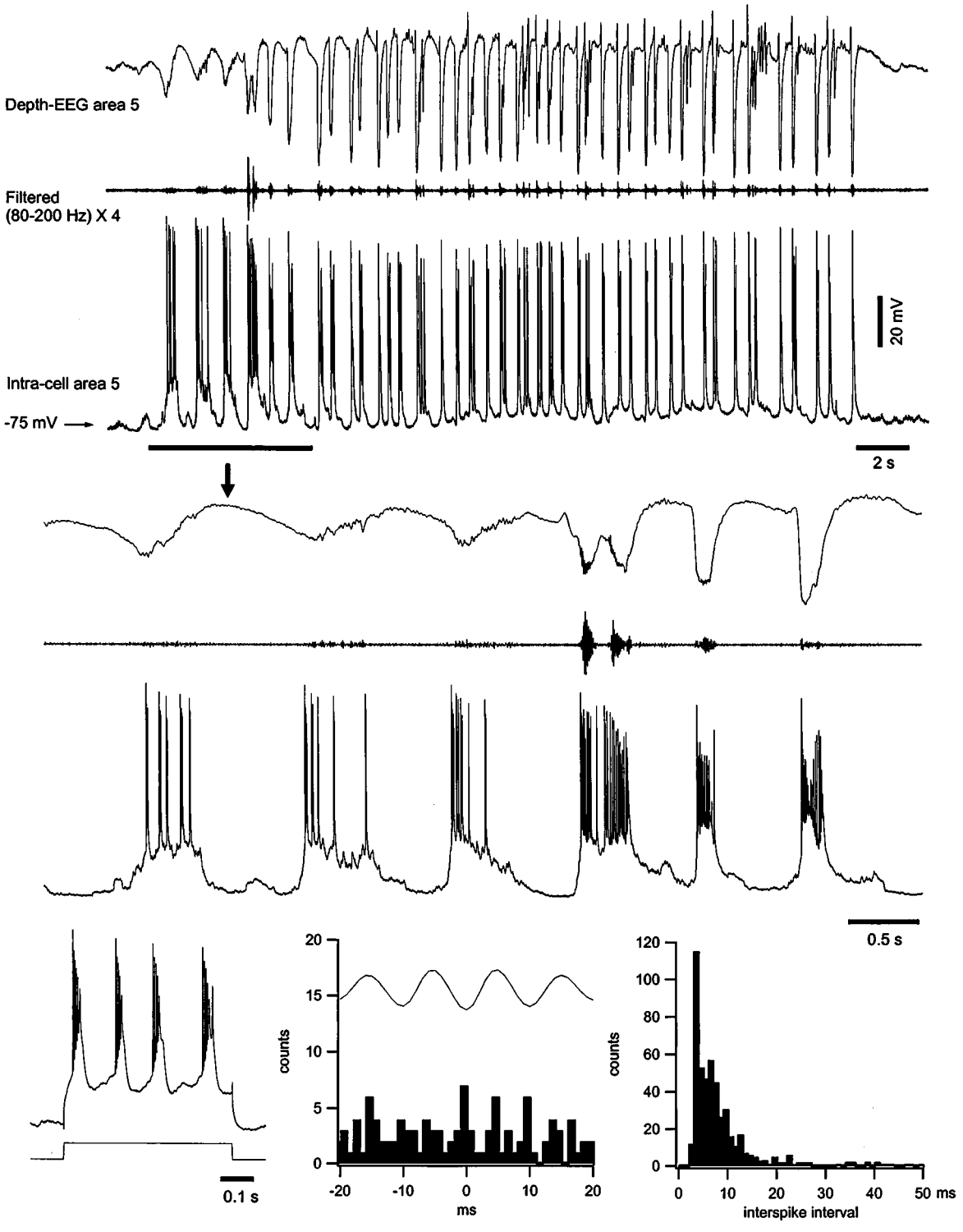

Fig. 5.62 Intrinsically bursting (IB) cortical neuron fires with ripples during seizures. Cat under ketamine-xylazine anesthesia. Intracellular and field potential recordings from area 5. The *top panel* depicts an epoch comprising an entire seizure along with the EEG trace filtered between 80 and 200 Hz. The neuron was an IB cell as revealed by its response to a depolarizing current pulse (bottom left). The beginning of the seizure is expanded in the middle panel. The neuron fired in phase with ripples, but its tendency to spike-bursts at higher frequencies than ripples accounts for action potentials occurring also out of phase (bottom center), and for the interspike-interval histogram showing a peak at 3.5 ms (bottom right). From Grenier et al. (2003).

[230] The unusually long latency of antidromic response (12.5 ms) in the neuron illustrated in Fig. 5.64*A* is attributable to the low-intensity stimulation of a thin axonal collateral.

that reflected summated PDSs in cortical neurons and gave rise to seizures consisting of fast runs (10–20 Hz), followed by SW/PSW complexes at 2 Hz (Fig. 5.63). During this prolonged hyperpolarization, cortical neurons exhibited voltage excursions that were synchronous with the SW/PSW field activity at 2 Hz, but that only rarely reached the firing threshold. The input resistance was dramatically decreased during the hyperpolarizing periods associated with SW/PSW seizures (Fig. 5.63*B*). This suggests that such cortical neurons, displaying an exclusive and prolonged hyperpolarization during SW/PSW seizures, are the prevalent targets of local inhibitory neurons. The hyperpolarization of some RS neocortical cells during seizures is homologous to that of TC neurons that are targets of GABAergic RE neurons, themselves driven by corticothalamic neurons during SW/PSW seizures [77] (see above, section *5.5.3.2.*).

5.6.2.6. Excitability of cortical neurons during Lennox–Gastaut-type seizures

The synaptic responses tested intracellularly during control (pre- and post-seizure) and seizures of Lennox–Gastaut type show a progressively decreased latency, increased amplitude, and faster slope at the EPSP onset during the transition from the slow oscillation to paroxysms that are initated by SW/PSW complexes at ∼2 Hz [21]. Contrasting results were obtained during the two main components of SW/PSW paroxysms; namely (*a*) during the hyperpolarization following each PDS and related to the EEG "wave" component of SW complexes, cortical stimuli reliably elicited PDSs that started at ∼3 ms, similar to the EPSP latency prior to seizure; (*b*) however, when falling during the PDSs associated with the "spike" component of SW complexes, the same stimuli were completely ineffective in eliciting an overt response (see Fig. 2 in [21]).

The comparison between antidromic and orthodromic responses in the same cortical neuron provided evidence for the dependency of both responses on the membrane potential and network activity (Fig. 5.64).

(a) The antidromic response was elicited during the EEG "wave" component of SW complexes only upon steady depolarization, bringing the membrane potential to −65 mV (panel *B*1 in Fig. 5.64), but failed at the hyperpolarized level of the resting membrane potential (−80 mV) [230]. During the EEG "spike" component, antidromic action potentials were only elicited during the declining, repolarizing phase of PDSs, but were absent if stimuli fell during the middle of PDSs (panel *C1*).

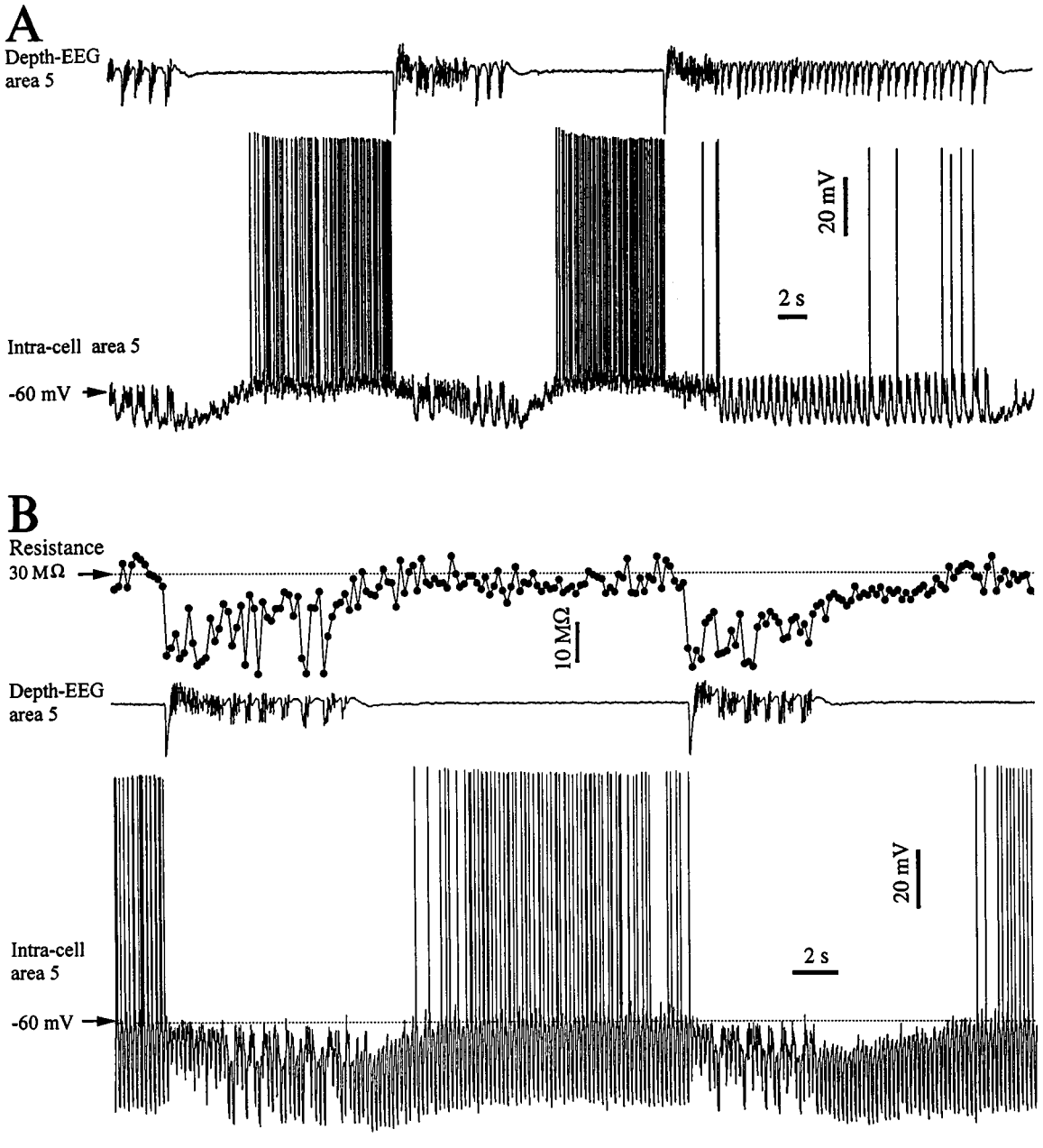

Fig. 5.63 Hyperpolarization throughout cortical SW/PSW seizures, associated with decreased input resistance. Intracellular recordings of two RS neurons (*A* and *B*) from area 5, together with field potentials from area 5, in cats under ketamine-xylazine anesthesia. *A*, the end of a seizure and two other seizures. The last, prolonged (~25 s) seizure consisted of a short period with fast runs (20 Hz) followed by PSW complexes at 2 Hz. *B*, decreased input resistance (measured by hyperpolarizing current pulses; duration: 70 ms) during the hyperpolarization associated with cortical seizures. Data by M. Steriade and F. Amzica (see Steriade, 2001a).

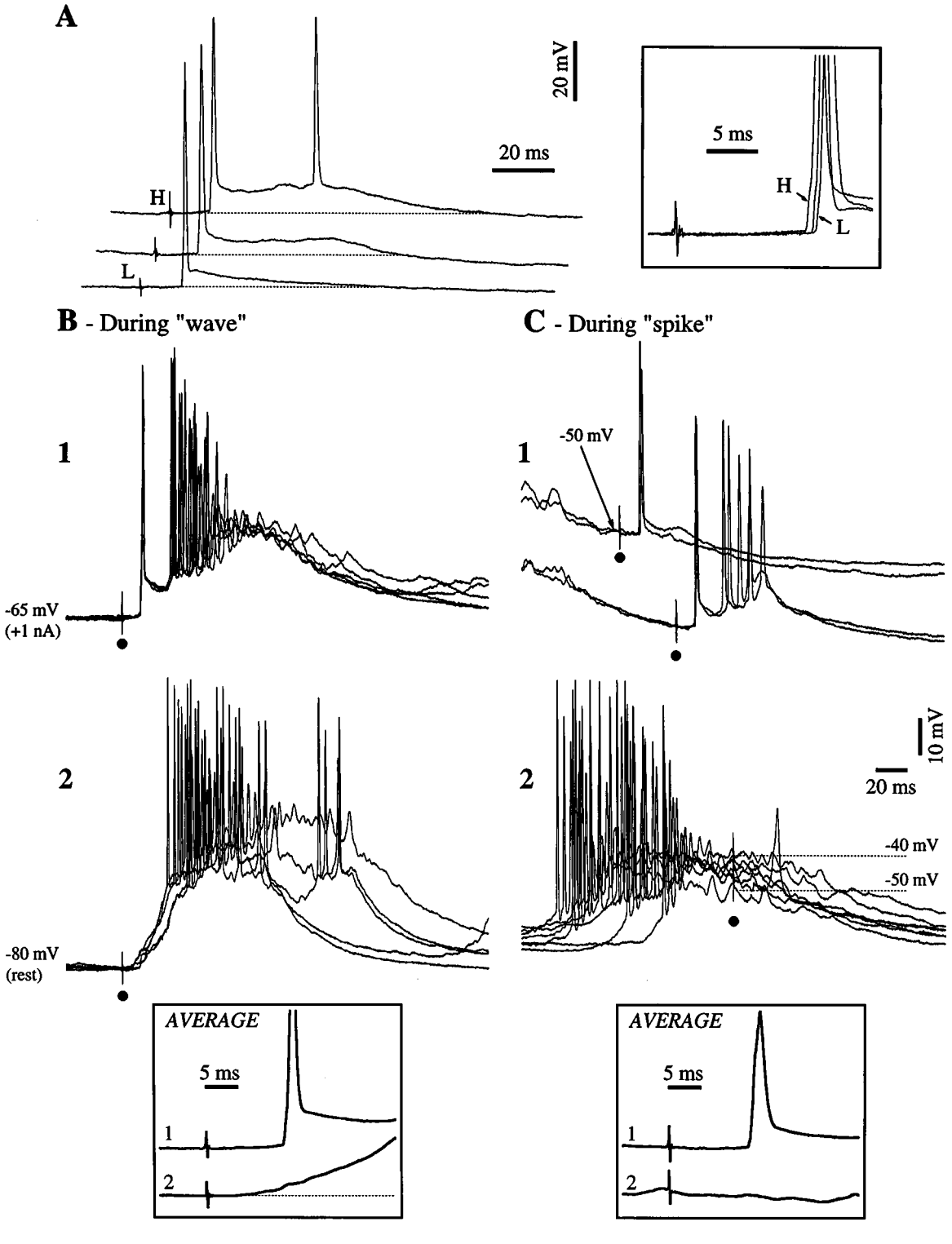
A
20 mV
20 ms
H
L
5 ms
H
L
B - During "wave"
1
-65 mV
(+1 nA)
2
-80 mV
(rest)
C - During "spike"
1
-50 mV
2
10 mV
20 ms
-40 mV
-50 mV
AVERAGE
5 ms
1
2
AVERAGE
5 ms
1
2

Collision with orthodromic spikes is precluded because stimuli were delivered during an epoch with no spontaneous discharges (panel *C2*).

(b) Synaptically elicited PDSs were present during the EEG "wave", after the antidromic spike (panel *B1*) or in isolation, at a more hyperpolarized membrane potential. At the hyperpolarized level (−80 mV), when the antidromic response failed, the onset of PDSs constantly revealed small-amplitude EPSPs that, by summation, gave rise to the giant synaptic potential crowned by high-frequency spike-bursts (panel *B2*). During the fast runs (10–20 Hz) of Lennox–Gastaut seizures, the responsiveness to centrally applied stimuli is as low as during the EEG "spike" (see above) because the membrane conductance is very high during both the PDSs of SW/PSW complexes (median, 252 nS) and the fast runs (median, 230 nS), compared to the EEG "wave" component (median, 71 nS) [212].

The decreased excitability of neocortical neurons during the EEG "spike" component related to SW/PSW complexes in Lennox–Gastaut type seizures (Fig. 5.64) is mainly because PDSs during these complexes contain an important inhibitory component due to the firing at high frequencies of fast-spiking (FS) neurons, whose discharges precede and last throughout this component [214]. Since the activity of FS neurons dominates RS neuron activity during PDSs, and the relative role of FS neurons significantly decreases during fast runs, the temporal relations of FS cell firing was studied in paired cellular recordings from FS and RS neurons (Fig. 5.65). In such cell couples, recorded with a lateral gap of less than 0.2 mm between them, the first spike of the FS neuron preceded the first spike of the RS neuron during the PDSs of SW/PSW complexes by 2–10 ms. The opposite was found during epochs with fast runs

Fig. 5.64 (opposite) Comparison between antidromic and orthodromic responses during the EEG "spike" and "wave" components of a spontaneously occurring seizure with SW/PSW complexes and fast runs. Cat under ketamine-xylazine anesthesia. Intracellular recording of area 7 neuron activated antidromically and orthodromically from the posterior part of area 5. *A*, antidromic response to low (L), intermediate, and higher (H) intensities. To obtain antidromic responses, the neuron was steadily depolarized by injecting 1 nA through the recording pipette. The long-latency (12.5 ms) of the antidromic spike was probably due to the low-intensity stimulation of a thin axonal collateral. Note take off from the baseline. Note also the depolarizing plateau potential whose amplitude and duration were a function of stimulus strength; at H intensity, single action potentials were occasionally triggered at a latency of 30–40 ms. *B*, during the "wave" of SW seizure, cortical stimulus (intensity H) elicited an antidromic spike followed, after 30–40 ms, by a PDS when the V_m was depolarized (−65 mV). The same stimulus elicited only a PDS at the resting V_m (−80 mV). *C*, During the EEG "spike", the antidromic response survived, but only toward the end of PDSs, when the V_m tended to hyperpolarize. *Averages* ($n = 5$) of cortically evoked early responses during "wave", under steady depolarization (*1*) and at rest (*2*), are depicted at the bottom left. *Averages* at different periods of the "spike" component (full depolarization, *2*; and declining period, *1*) are depicted at the bottom right. Modified from Steriade and Amzica (1999).

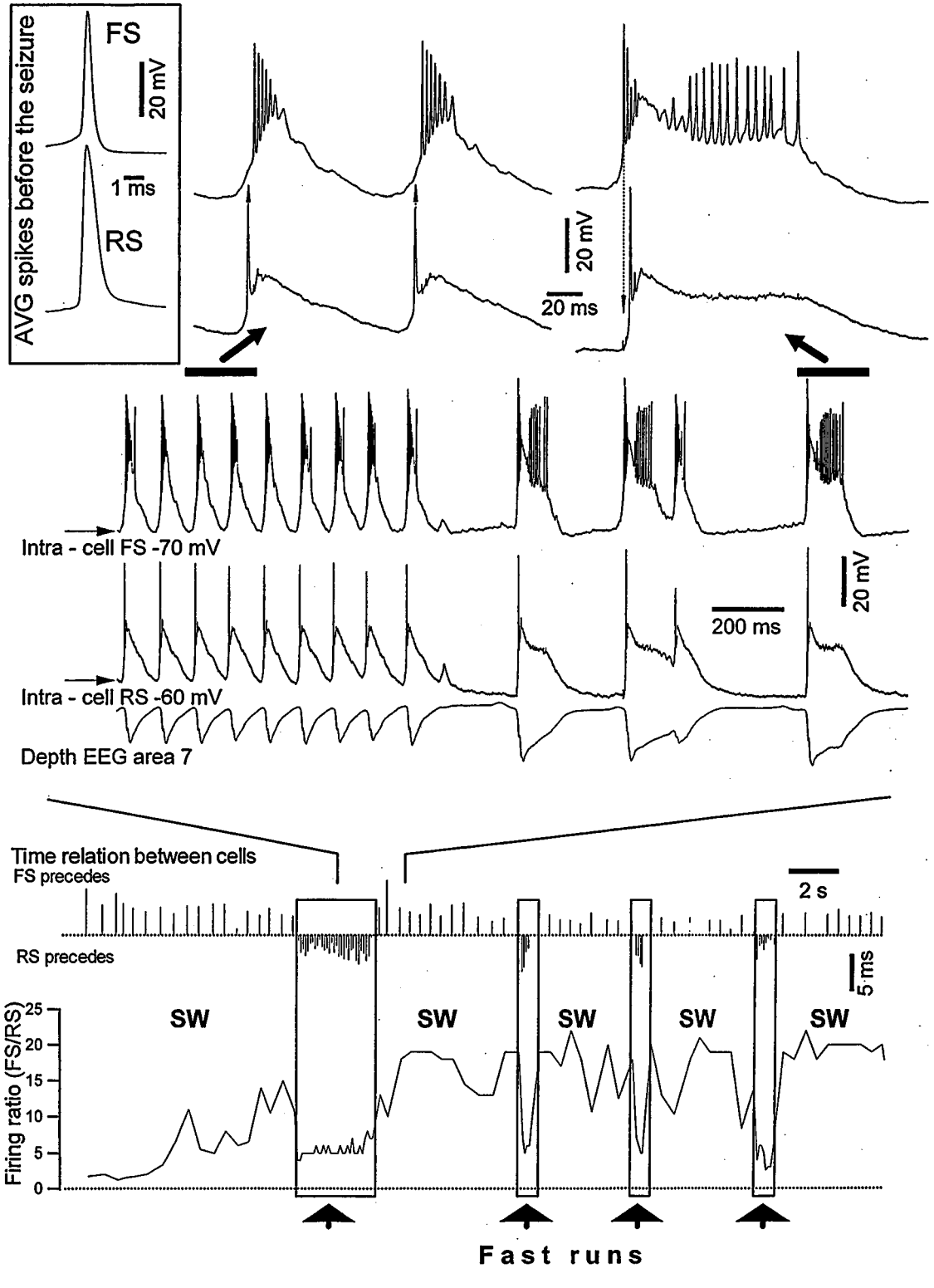
AVG spikes before the seizure
FS
20 mV
1 ms
RS
20 mV
20 ms
Intra - cell FS -70 mV
200 ms
20 mV
Intra - cell RS -60 mV
Depth EEG area 7
Time relation between cells
FS precedes
2 s
RS precedes
5 ms
SW
SW
SW
SW
SW
Firing ratio (FS/RS)
25
20
15
10
5
0
Fast runs

[231] Thompson and Gähwiler (1989).

[232] Contreras et al. (1997c-d).

[233] Mulle et al. (1986); Contreras et al. (1992).

(Fig. 5.65) during which FS neurons decreased their firing rates (Fig. 5.66).

Does the depolarizing action of GABAergic FS neurons excite or inhibit the postsynaptic neurons? Both scenarios are valid. During Lennox–Gastaut seizures, the reversal potential of IPSPs is shifted to depolarized values, which results in the depolarization of target neurons [214]. Repetitive firing of FS inhibitory neurons during PDSs results in prolonged opening of Cl^- channels and $[Cl^-]_i$ easily reaches the levels of $[Cl^-]_o$. This may decrease the amplitude and even change the polarity of IPSPs in hippocampus [231]. Similarly, intracellular recordings from RS neocortical neurons, using Cl^--filled pipettes, showed that these neurons produce depolarizing IPSPs that are covered with Na^+ spikes [232]. These factors seem to be sufficient to mediate Cl^--dependent postsynaptic depolarizations during seizures. On the other hand, the high $GABA_A$-dependent Cl^- conductance prevents postsynaptic neurons from firing and the role of these potentials would be to control the level of depolarization of postsynaptic neurons. Overall, our data suggest that massive activity of inhibitory networks *in vivo* leads to paradoxical excitation in postsynaptic networks [214].

5.6.3. Thalamic neurons during cortically generated seizures

The behavior of thalamic neurons during the SW/PSW complexes associated with Lennox–Gastaut seizures is similar to that undergone during cortically generated seizures with pure SW/PSW complexes, namely spike-bursts in GABAergic RE cells following each cortical PDS and steady hyperpolarization with phasic IPSPs in target TC neurons (see section *5.5.3.2*).

During epochs with fast runs (10–20 Hz), single spikes or spike-doublets of extracellularly recorded RE neurons were time-locked with the cortical field potentials (Fig. 5.67). As demonstrated by intracellular studies of RE neurons showing that their high-frequency spike-bursts occur at a hyperpolarized membrane potential, whereas single-spike firing appears at a more depolarized level [233], the extracellular data depicted in Fig. 5.67 suggest two distinct levels of membrane potential in RE neurons during the

Fig. 5.65 (opposite) Leading role of fast-spiking (FS) cortical neurons during PDSs of SW/PSW complexes and the leading role of regular-spiking (RS) neurons during fast runs. Cat under ketamine-xylazine anesthesia. Middle panel shows a fragment of a Lennox–Gastaut-type seizure with simultaneous EEG and dual intracellular recordings from FS and RS neurons. Fragments of fast runs and SW complexes are indicated by horizontal bars and arrows are expanded in top panel. Top left inset shows a comparison of action potentials fired by the two neurons before the seizure onset. At the bottom, plots show the time-relation of firing between neurons and the firing ratio during the seizure. Fragments marked by upward arrows indicate the fragments of seizure that are expanded in the middle panel. From Timofeev et al. (2002c).

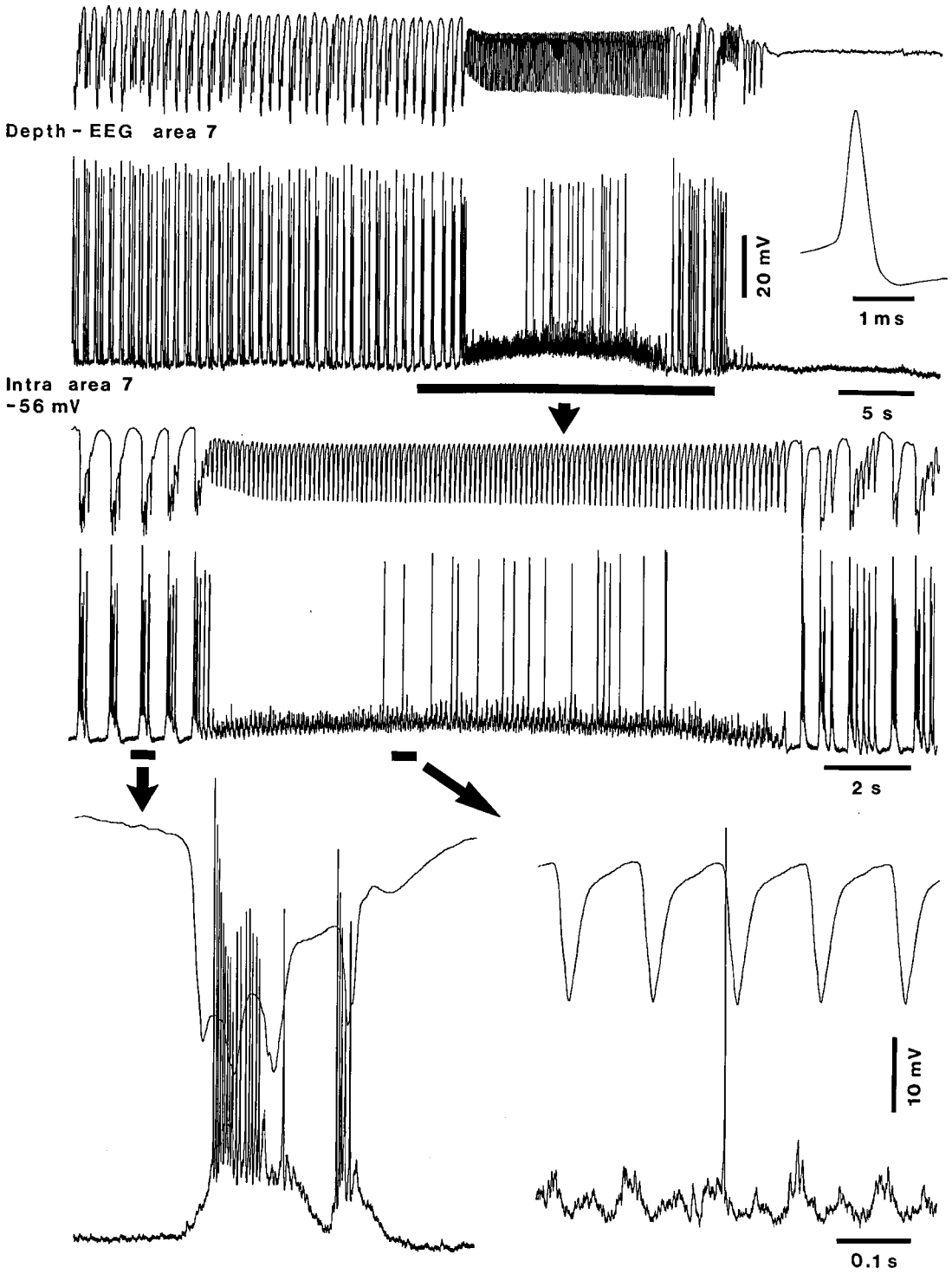

Fig. 5.66 Conventional fast-spiking (FS, presumably local inhibitory) cortical neuron decreases its firing rate during fast runs of polyspike-wave (PSW) seizures. Intracellular recording of area 7 cortical neuron together with depth-EEG from the same area in cat under ketamine-xylazine anesthesia. The neuron responded with fast tonic firing without frequency adaptation to depolarizing current pulses (not shown); an action potential (0.35 ms at half amplitude) is expanded at top right. Part marked by horizontal bar in the top panel is expanded below (arrow). Two parts in the middle panel are further expanded below (arrows). Note the presence of numerous action potentials during the "spikes" of PSW complexes and the reduction in firing rates during the fast runs when the neuron received multiple asynchronous synaptic potentials. From Timofeev et al. (2002c).

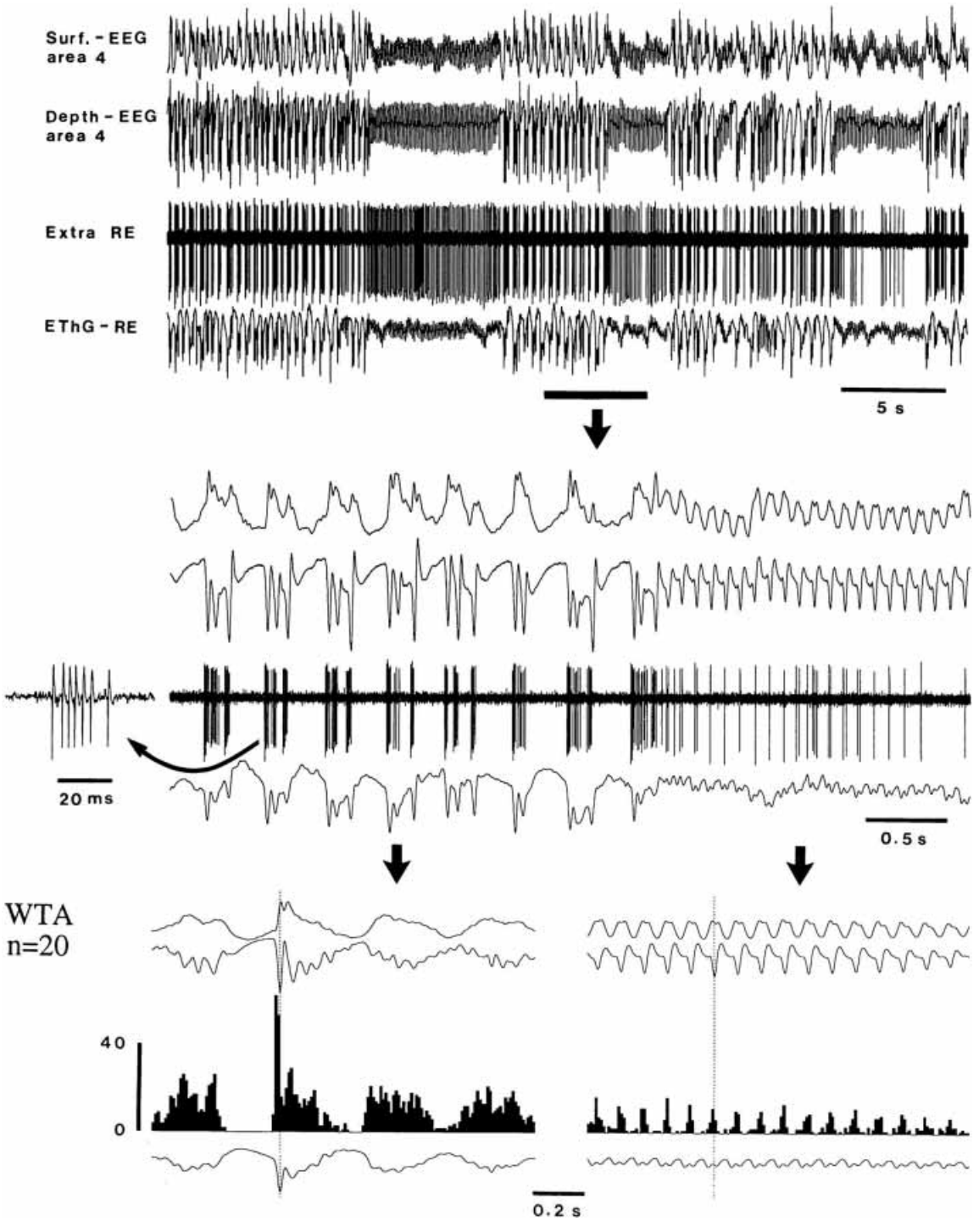

Fig. 5.67 Two types of firing patterns in extracellularly recorded RE cells during SW/PSW complexes at ~2.5 Hz and fast runs at ~10 Hz suggest different membrane polarization. Cat under ketamine-xylazine anesthesia. Extracellular recording of rostral RE neuron activity together with focal field potentials picked up by the same microelectrode in the RE nucleus and surface- and depth-EEG from cortical area 4. Spontaneously occurring seizure consisting of SW/PSW complexes and fast runs. Part marked by horizontal bar in the top panel is expanded below. Note high-frequency spike-bursts (~300 Hz) during virtually each polyspike of PSW complexes (left; typical accelerando-decelerando burst is expanded on the left, arrow) and single action potentials during fast runs (right). This suggests that the RE cell is more depolarized during fast runs (see following Fig. 5.68). Below, wave-triggered average (WTA) triggered by the peak of depth-negative EEG waves (dotted line) during both SW/PSW complexes and fast runs. From Timofeev et al. (1998).

[234] Evidence for the dendritic origin of such events, marked by asterisk in Fig. 5.68, was shown *in vivo* (Contreras et al. 1993; Destexhe et al. 1996).

[235] Gastaut and Broughton (1972).

[236] Samoriski and Applegate (1997).

[237] Traub et al. (1993).

two major components of Lennox–Gastaut seizures, SW/PSW complexes and fast runs. This assumption was confirmed by intracellular recordings (Fig. 5.68) showing that the difference between the trough of hyperpolarizations during SW/PSW complexes and epochs with fast runs was 8 mV (−85 mV and −77 mV, respectively). In contrast with prolonged, high-frequency spike-bursts during SW/PSW complexes, fast runs were associated with single action potentials, spike-doublets or triplets followed by an afterdepolarization hump on which presumed dendritic spikes were superimposed (see bottom panel in Fig. 5.68 [234]).

The membrane potential of TC neurons was more depolarized during fast runs than during SW/PSW complexes (Fig. 5.69), probably because they received fewer hyperpolarizing inputs from GABAergic RE neurons that fired less numerous action potentials than during SW/PSW complexes.

5.7. Grand-mal, tonico-clonic seizures

The generalized tonico-clonic seizures are expressed at the EEG level by an initial period of fast runs at ∼10–15 Hz, associated with tonic motor manifestations, followed by rhythmic SW/PSW complexes at ∼3 Hz, associated with clonic manifestations (Fig. 5.70) [235]. In this figure the recording was obtained with partial muscle relaxation and is less contaminated by muscle artifacts. In animal experiments, it was assumed that clonic manifestations require the integrity of forebrain structures, whereas the brainstem is sufficient for the expression of tonic and running/bouncing events [49, 50, 236]. It is obvious that such motoric events prevent intracellular analyses *in vivo*. However, the striking resemblance between the fast runs and SW/PSW complexes in this type of seizure and in Lennox–Gastaut paroxysms may suggest similar cellular mechanisms underlying EEG components in these otherwise different epileptic entities. The mechanisms of seizures resembling the electrographic aspects of grand-mal epilepsy have been investigated in hippocampal slices maintained *in vitro* (after reduction of $GABA_A$ inhibition, increases in $[K^+]_o$, and repetitive stimulation) and *in computo* (Fig. 5.71). Briefly, it was suggested that seizures in networks of CA3 pyramidal neurons are elicited by activation of NMDA receptors that induce a prolonged depolarization in the dendritic domain, resulting in dendritic spikes, which eventually succeed in driving spike-bursts in the soma [237]. During burst discharges, $[K^+]_o$ increases from ∼3 mM to ∼10–12 mM, which results in an increase of epileptogenesis through enhancement of depolarizing

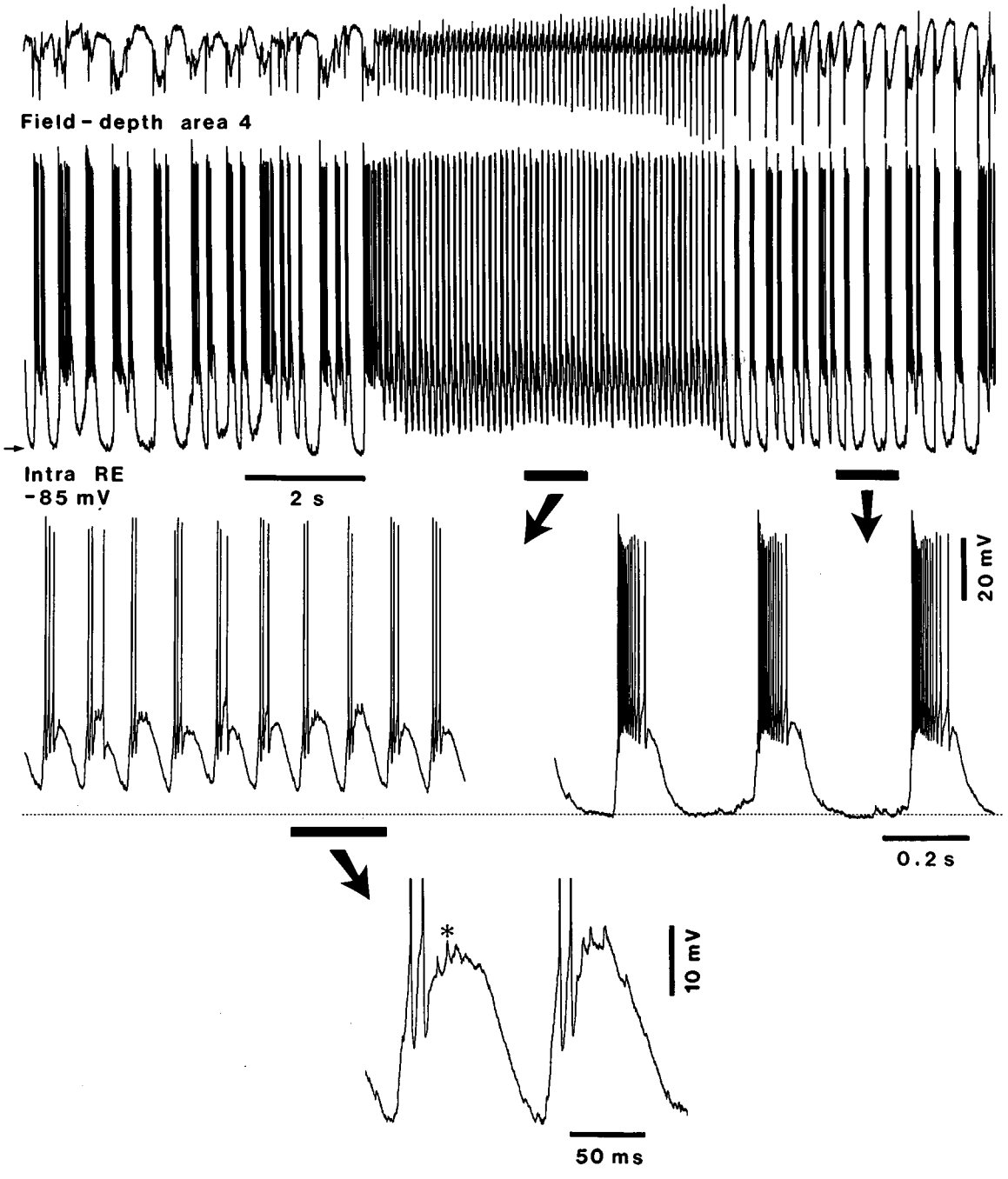

Fig. 5.68 The membrane potential of RE neurons is more depolarized during fast runs than during SW/PSW complexes. Cat under ketamine-xylazine anesthesia. Intracellular recording of rostral RE neuron activity together with depth-EEG from area 4. The spontaneous seizure consisted of SW/PSW complexes at 2–3 Hz (left and right part) and fast runs at 10–11 Hz. Parts marked by horizontal lines during fast runs and SW complexes are expanded below (arrows). Two cycles of fast runs are further expanded below to depict presumed dendritic spikes (asterisk). From Timofeev et al. (1998).

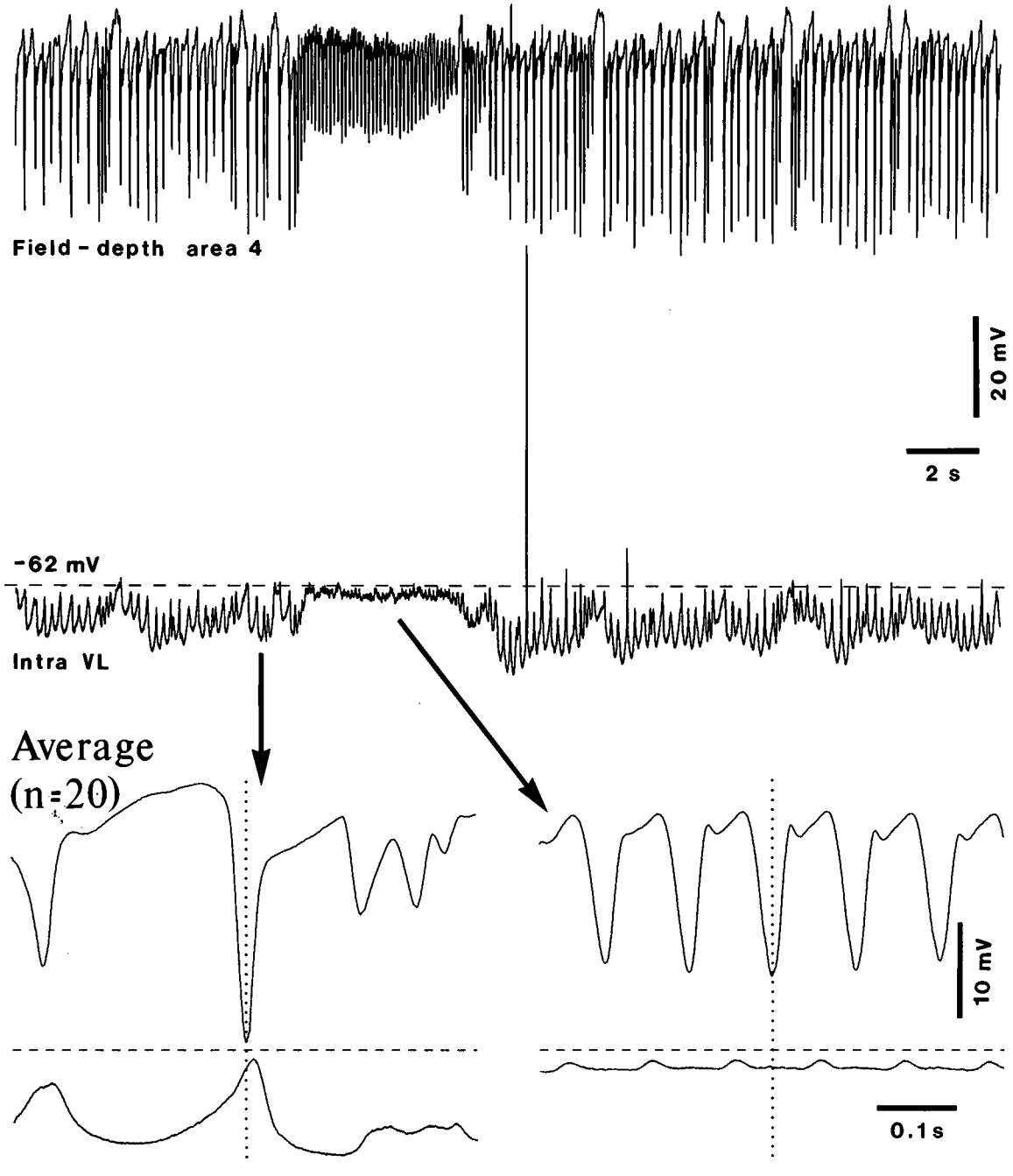

Fig. 5.69 During fast runs of spontaneously occurring Lennox–Gastaut seizures, TC neurons are relatively depolarized, compared to epochs with SW/PSW complexes. Cat under ketamine-xylazine anesthesia. Intracellular recording of VL neuron activity together with focal waves (EThG) from the VL nucleus and depth-EEG from area 4. The seizure lasted for 80 s. An epoch of ~30 s is shown in the top panel. During SW/PSW complexes at ~3–4 Hz, the neuron was steadily hyperpolarized by ~8 mV and displayed IPSPs in close time-relation with cortical SW complexes, whereas during the fast runs the neuron almost completely recovered its resting membrane potential (−62 mV) and displayed EPSPs. Averages triggered by a sharp depth-negative EEG wave in area 4 show temporal relations between cortical and thalamic events during both SW complexes (left) and fast runs (right). From Timofeev et al. (1998).

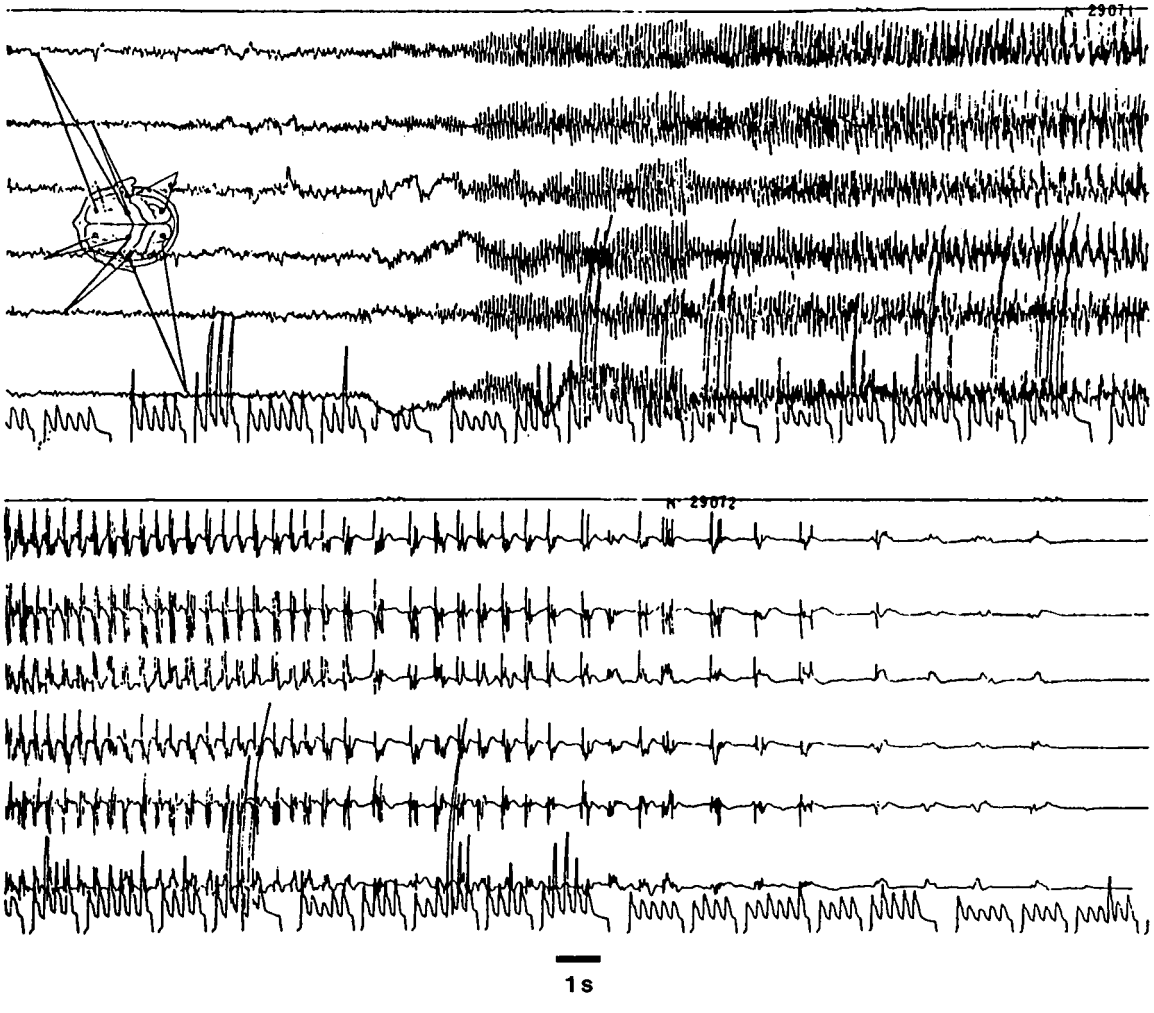

Fig. 5.70 EEG patterns of human grand-mal, tonico-clonic seizure. The first 10 s of EEG was recorded prior to the clinical seizure. The seventh channel (bottom) is the output of a Grey Walter frequency analyzer. The subsequent 10 s corresponds to the tonic phase, with prominent 9–10 Hz rhythmic activity throughout. Note the increased amplitude of EEG waves with transition to the clonic phase, which is fully developed in the lower fragment showing rhythmic 3-Hz SW/PSW complexes that slow progressively and are followed by a period of relative flattening. Modified from Gastaut and Broughton (1972).

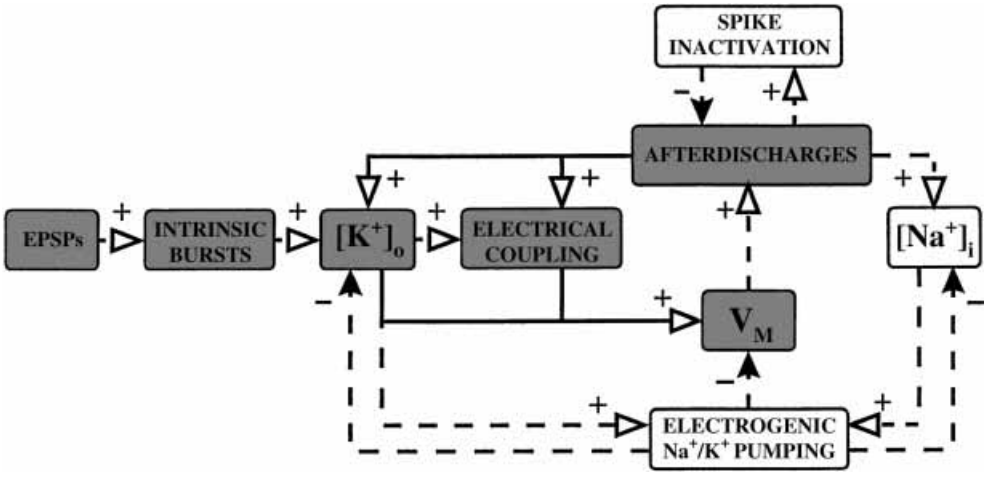

Fig. 5.71 Proposed scheme for the initiation, build-up, and termination of K^+-induced ictal episodes in CA1. The scheme illustrates the essential mechanisms, as suggested by experimental data, that mediate positive feedback (shaded boxes connected with uninterrupted lines) and negative feedback (white boxes connected with dashed lines) between CA1 intrinsically burst firing pyramidal cells (PCs). A seizure episode is initiated by an excitatory synaptic input, which is amplified locally by the recruitment of PCs. Further amplification in space and time is provided by K^+ accumulation and electrical coupling, which depolarize the neurons ($+V_m$), leading to the expansion of the discharge zone and to the generation of afterdischarge. The increased $[K^+]_o$ also enhances electrical coupling via the associated decrease in extracellular space. All these interactions are mutually reinforcing. With some delay, the $[K^+]_o$ elevation and the associated increase in $[Na^+]_i$ stimulate electrogenic Na^+/K^+ pumping, which opposes the activity-induced ionic perturbations and repolarizes the neurons ($+V_m$). This process in conjunction with spike inactivation ultimately arrests the seizure process. From Jensen and Yaari (1997).

[238] Traynelis and Dingledine (1988).

[239] The low seizure threshold of hippocampus (Green, 1969) explains that most complex partial seizures in human temporal lobe epilepsy are generated and/or elaborated in this structure (Spencer et al., 1987). Recently, morphological studies and patch-clamp recordings of monkey's hippocampal neurons *in utero* showed the sequential development of GABAergic and glutamatergic synapses, the synchronization of low-frequency network oscillations, and the possibility of evoking epileptiform discharges by blockade of $GABA_A$-mediated inhibition, thus leading to the conclusion that the primate hippocampus is already capable of generating paroxysmal activity *in utero* (Khazipov et al., 2001).

[240] In addition to hippocampus, entorhinal cortex, and amygdala, complex partial seizures also arise in cingulate fields and orbito-frontal cortex.

actions, decreases the hyperpolarizing influence of K^+ currents, and increases ephaptic interactions [238].

5.8. Temporal lobe epilepsy

The sensory and affective, "experiential" phenomena that are associated with temporal lobe epilepsy (TLE) are briefly summarized in section **5.1**. It is commonly recognized that TLE accounts for ~40% of the total incidence of epilepsy and is a multi-factorial syndrome that primarily involves the hippocampus [239], the entorhinal cortex, amygdala nuclear complex, but also some neocortical areas [240]. The *complex partial* seizures that characterize TLE are termed this way because such paroxysms arise in specific structures of the forebrain, while the term *complex* would indicate that consciousness is altered or lost. TLE patients display a typical pattern of brain damage, hippocampal atrophy and sclerosis, usually known as mesial temporal sclerosis [44]. Data indicating pathological changes associated with TLE in structures adjacent to the

hippocampus (entorhinal cortex and amygdala), or even in the thalamus, have also been reported [241]. The long debate about whether lesions in the hippocampus and related systems generate seizures or are the results of seizures started with the contradictory findings of Sommer and Pfleger, more than a century ago [242].

As in other fields of epilepsy research, the cellular and biophysical mechanisms of TLE have been investigated in numerous chronic and acute animal models, *in vivo* and *in vitro*, among them kindling [243], injections with kainic acid [244], slices from rodent and human hippocampus treated with pilocarpine or 4-aminopyridine [245], and intrahippocampal injection of tetanus toxin [246]. Generally, such studies reported the presence of high-frequency spike-bursts during various epochs of paroxysmal activity [247] (see details below). However, cross-correlation analyses of neuronal activities from depth-recordings in humans with complex partial seizures showed that, at least in the interictal state, *synchronous* burst discharges are *not* distinguishing features of epileptogenic regions in those patients, and that synchrony resulted from relations between single action potentials [248]. This result led the authors to conclude that existing models of TLE "may not accurately represent the interictal state in human partial seizure disorders" and "may not appropriately reproduce the transition from the interictal to the ictal state" [248].

Nevertheless, the only way to understand the cellular and biophysical mechanisms of TLE is intracellular work in different experimental models. I will discuss the neuronal substrates of seizures resembling the features of TLE in hippocampus, entorhinal cortex, and amygdala.

5.8.1. Hippocampus and entorhinal cortex

Epileptiform spike-bursts in hippocampal neurons can be induced by the intra-ventricular injection of kainate, which leads to this discharge pattern over several weeks. This phenomenon involves loss of CA3 pyramidal cells and synaptic reorganization resulting in the hyperexcitability of postsynaptic CA1 cells [249].

The spike-burst is produced by a synaptically evoked slow depolarization due to the unmasking of an NMDA-receptor-mediated component that follows an AMPA-receptor-mediated fast EPSP [114, 250]. The synchronized output of CA1 is not merely dependent on excitatory synaptic events mediated by recurrent axonal collaterals of pyramidal cells, as these are coupled with intrinsic neuronal properties, operations in inhibitory circuits, and gap-junctional communication [251]. Dendrites of CA1 pyramidal neurons possess

[241] Margerison et al. (1966); Hudson et al. (1993).

[242] See Wasterlain et al. (1999).

[243] Reviewed in Lothman et al. (1991).

[244] Ben-Ari (1985); Chronin and Dudek (1988); Davenport et al. (1990); Bragin et al. (1999b).

[245] Perreault and Avoli (1992); Avoli et al. (1996); Nagao et al. (1996).

[246] Finnerty and Jefferys (2000).

[247] Single spike-bursts have been extracellularly recorded in humans, with an intraburst frequency of 200–300 Hz, similar to that of PDSs recorded intracellularly in animals (see Fig. 3 in Babb, 1999).

[248] Colder et al. (1996, p. 2496 and 2506). Other investigators also emphasized differences between the results obtained in hippocampal slices and the reality of an intact brain that generates epileptic seizures: "...slices may not display the full range of epileptic activity that is encountered in the intact brain. Accordingly, relying solely on *in vitro* work may confound our appreciation of factors in the functional anatomy of epilepsy and seizures" (Lothman et al., 1991, p. 9).

[249] Wheal et al. (1998).

[250] Turner and Wheal (1991); Hirsch et al. (1996); Williamson and Wheal (1992). Neuronal recordings in the hippocampus of epileptic patients showed that, during sleep, there is a significantly higher rate of bursting than in non-epileptic hippocampal neurons (Staba et al., 2002).

[251] Synchronization of GABAergic interneurons in epileptiform activity in the CA1 area was shown by Perez-Velazquez and Carlen (1999). For mechanisms of electric coupling in epileptogenesis in the CA1 area, see Perez-Velazquez et al. (1994) and reviews by Carlen et al. (1996) and Perez-Velazquez and Carlen (2000).

[252] Wong and Stewart (1992); Johnston et al. (1996); Miles et al. (1996).

[253] Hess and Gustafsson (1990).

[254] Lehman et al. (2000).

[255] Jensen and Yaari (1997).

[256] Finnerty and Jefferys (2000).

[257] Tauck and Nadler (1985); Sutula et al. (1988); Ben-Ari and Represa (1990); Houser et al. (1990).

[258] Ribak and Peterson (1991); Sloviter (1992); Okazaki et al. (1995).

[259] Wuarin and Dudek (1996). In those experiments, membrane excitability was also increased with 6 mM $[K^+]_o$.

voltage-gated Na^+ and Ca^{2+} channels than can reinforce the depolarization to initiate action potentials, while $GABA_A$ IPSPs can block the somatic output [252]. Perfusion with $GABA_A$-receptor antagonists produces a potentiation of development from EPSPs to population spikes [253]. In human TLE and pilocarpine-treated rats, one of the factors accounting for the enhanced recurrent excitation is the increased activity in axon collaterals of CA1 pyramidal neurons, projecting via aberrant collaterals to strata pyramidale and radiatum in field CA1 [254]. In the elevated K^+ model of hippocampal epilepsy [6], intrinsic bursters in field CA1 are active before or at the very onset of the first paroxysmal depolarization, and they recruit other bursters as well as non-bursters via synaptic, electrical, and K^+-mediated excitatory interactions [255] (Fig. 5.71).

The synchrony of population spike firing in right and left CA1 fields, which form the major output of hippocampi, is associated with an oscillation at ~10–15 Hz of field potentials, which was thought to play a role in the secondary generalization of focal seizures induced by unilateral injection of tetanus toxin [256]. The seizure generalization to the neocortex may be regarded in view of similar rhythms (10–15 Hz) recorded during complex seizures consisting of SW/PSW complexes and fast runs at 10–15 Hz [133, 171] (see section **5.6**). However, the fast runs are generated within the neocortex as they have been recorded in isolated cortical slabs [87]. The various degrees of propensity to epileptiform seizures in the dentate gyrus and fields CA1/CA3, as resulting from work in hippocampal slices, are discussed elsewhere [243].

The hyperexcitability of the hippocampus may be based on some morphological alterations, such as "mossy fiber sprouting" (MFS) of dentate granule cells and spine loss. MFS was found in animal models of TLE and humans with hippocampal epilepsy [257]. Sprouted mossy fiber axons of granule cells form synapses that contribute to functional recurrent excitation between dentate granule cells, but may also promote the inhibition of these neurons through a bisynaptic pathway involving prior activation of basket cells [258]. The isolation of the excitatory circuits from inhibitory effects may lead to spontaneously occurring or antidromically evoked seizures in a majority of hippocampal slices with MFS, but not in control slices [259]. These data pointed to increased susceptibility of the dentate gyrus with MFS to seizure and the fact that synaptic inhibition may oppose this enhanced hyperexcitability. As to spine loss, decreased spine density, and dendritic varicose swellings of pyramidal neurons and inhibitory interneurons, which has been observed in human and animal neocortical and

hippocampal epileptic tissue [260], these alterations were generally regarded to be the consequence of seizure-induced neuronal injury, probably a result of the excessive release of glutamate during paroxysmal activity [261]. Other studies, however, reported the presence of severe seizures in infant rats without massive neuronal loss [262].

Seizures elicited by stimulation of the entorhinal cortex in an isolated whole-brain preparation originate in the entorhinal/hippocampus complex, spread to amygdala nuclei, and display the typical pattern of tonico-clonic seizures, consisting of initial fast runs followed by rhythmic paroxysmal discharges at ~1.5–2 Hz (Fig. 5.72) [263]. While $GABA_A$-mediated inhibition limits the spread of the entorhinal-induced seizure, $GABA_B$-mediated inhibition plays no role in this paroxysmal activity. In other models of epileptiform discharges, GABAergic function is preserved and, using 4-aminopyridine application in hippocampal slices, long-lasting depolarizations contributed by a synchronous $GABA_A$-receptor-mediated inward conductance may even initiate ictal discharges driven from the entorhinal cortex [264].

Limbic seizures are not only associated with functional and morphological changes in the hippocampus and entorhinal cortex, but are also accompanied by neuronal loss in the mediodorsal (MD) thalamic nucleus [265]. On the other hand, the MD nucleus may play a critical role in the generation of limbic seizures elicited focally from the piriform cortex [266].

5.8.2. Amygdala

The active role played by the in TLE was shown by neurosurgeons who electrically stimulated this nuclear complex in awake, locally anesthetized epileptic patients, and evoked the automatisms of TLE [42]. The bias in favor of the hippocampus being a main generator of TLE was explained by its laminated structure, which creates open electrical fields that can be detected at some distance, partly by volume conduction, whereas the closed fields in the amygdala may be missed for biophysical reasons [267]. Several data have been invoked to state that the amygdala may play at least an equally important role in epileptogenesis compared to the hippocampus, if not a more important role. Thus, a more favorable clinical outcome of temporal lobectomy was reported when the amygdala was removed and the hippocampus spared or minimally resected, while removal of the hippocampus added little advantage to the surgical treatment of TLE [268]. Experimentally, the amygdala kindles faster

[260] Purpura et al. (1982); Al-Noori and Swann (2000).

[261] Scheibel et al. (1974); Isokawa and Levesque (1991); Swann et al. (2000).

[262] Nitecka et al. (1984) showed that, after systemic administration of kainic acid in immature rats (less than 18 days), there was no sign of damage even after prolonged tonico-clonic convulsions, but progressive increases in the severity of neuronal damage was reached between 18 and 25 days after birth. See also Jensen et al. (1992).

[263] Federico and MacVicar (1996). The idea that the hyperexcitability of entorhinal cortex neurons may serve as a primary focus for seizures to spread to hippocampus (see also Scharfman et al., 1998) is corroborated by EEG data in humans suggesting that, in patients with TLE, the entorhinal cortex may be the site of seizure initiation (Spencer and Spencer, 1994).

[264] Avoli et al. (1996); Lopantsev and Avoli (1998).

[265] Bertram and Scott (2000).

[266] Cassidi and Gale (1998).

[267] Gloor (1987).

[268] Feindel and Rasmussen (1991).

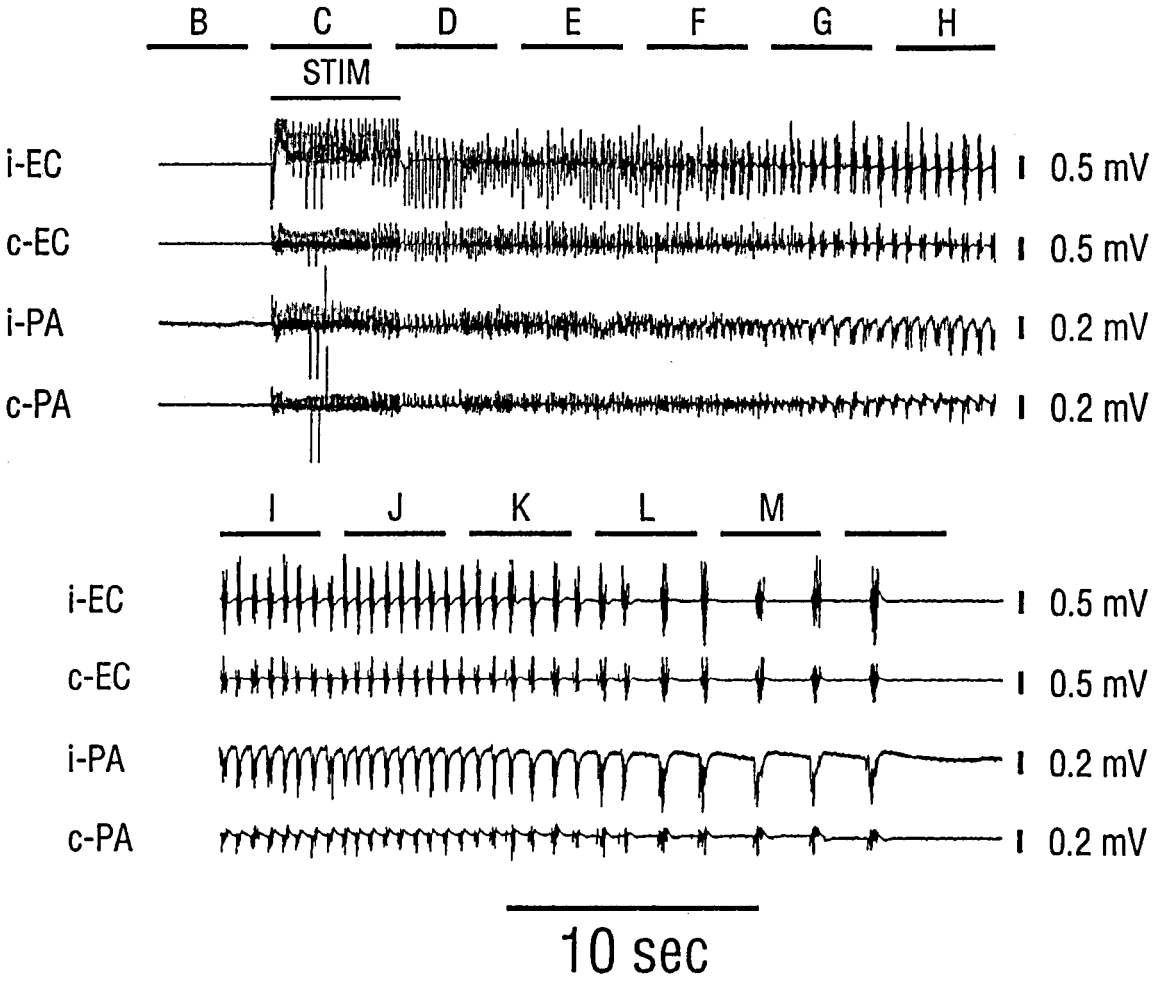

Fig. 5.72 Extracellular recordings of seizure activity evoked by unilateral stimulation of the lateral entorhinal cortex in the isolated whole-brain preparation of guinea pig. Recording electrodes were placed bilaterally in the entorhinal cortex and posteromedial cortical amygdaloid nucleus. Stimulation of the lateral entorhinal cortex (5 Hz, 5 s, 10 V) evoked tonic-clonic seizure activity bilaterally in the entorhinal cortex and posteromedial cortical amygdaloid nucleus. Bars and letters over traces indicate the time during which optical recordings were made (see Fig. 7 in that paper). From Federico and MacVicar (1996).

than the hippocampus [269]. Also, the relatively small degree of histologically verified amygdala damage found in patients undergoing surgery for drug-resistant TLE [270], which could be explained by partial involvement of only some amygdaloid nuclei, has been challenged by an experimental study showing severe neuronal damage in some, but not all, amygdala regions [271].

Despite the above clinical, morphological, and macrophysiological evidence for amygdala involvement, there are very few

[269] Morimoto et al. (1986); Racine et al. (1986).

[270] Miller et al. (1994).

[271] Tuunanen et al. (1999).

intracellular studies of amygdala neurons during experimental models of limbic epilepsy. Kindling reduces GABAergic inhibitory neurotransmission and enhances both NMDA- and non-NMDA-receptor-mediated glutamatergic neurotransmission in the basolateral amygdala [272]. In a chronic model of seizures, afferent stimulation of epileptic pyramidal neurons from the basal nucleus of the amygdala elicited prolonged depolarizations, leading to multiple action potentials, but inhibitory potentials were absent, which contrasted with their presence in a third of control basal amygdala neurons [273].

Limbic epilepsy is under the control of cholinergic neurotransmission. Some investigators reported that physostigmine increases the sensitivity to kindling stimulation in limbic forebrain structures [274] and that muscarinic antagonists retard the development of amygdala kindling [275]. Contrasting effects were obtained by using the method of selective loss of basal forebrain cholinergic neurons [276], which accelerated hippocampal kindling and promoted the late stages of amygdala kindling, with the conclusion that cholinergic systems suppress kindling epileptogenesis [277], similar to the suppressing effects exerted by brainstem cholinergic systems on genetic models of absence seizures [158, 159].

5.8.3. The disinhibition hypothesis in the generation of limbic seizures

Although a reduction of GABAergic synaptic inhibition has long been thought to produce paroxysmal discharges in the hippocampus [114, 278], several issues remain controversial; namely, whether this reduction in synaptic inhibition is a necessary requisite for the hyperexcitability of pyramidal neurons, whether there is global loss of inhibitory processes or selective impairment of various classes of inhibitory interneurons, whether inhibition is impaired over the whole soma-dendritic membrane or is domain-specific, and even whether inhibition is affected at all in these types of seizures resembling TLE. Moreover, some experimental studies concluded that inhibitory processes are increased, possibly due to postsynaptic up-regulation of $GABA_A$ receptors and/or increased transmitter release [279]. Conclusions about preserved or even enhanced inhibition, similar to those from investigations using kindling, were also drawn from data on human TLE [280]. However, in a rat model of progressive epilepsy, the distinction has been made between the CA1 hippocampal field and the dentate gyrus, with loss of inhibition in the former and enhanced of GABAergic inhibitory processes in the latter [281]. Also, in a model of experimental TLE, GABAergic

[272] Gean et al. (1989); Rainnie et al. (1992). Inhibition of synaptic transmission in the basolateral nucleus of amygdala is mediated by two pharmacologically distinct presynaptic metabotropic glutamate receptors (Neugebauer et al., 1997).

[273] Mangan et al. (2000).

[274] Girgis (1980).

[275] Westerberg and Corcoran (1987).

[276] Selective lesion of basal forebrain cholinergic neurons can be obtained by intracerebral administration of the immunotoxin 192 IgG-saporin (see Torres et al., 1994).

[277] Ferencz et al. (1997, 2000).

[278] Miles and Wong (1983, 1987).

[279] Kamphuis et al. (1990). Otis et al. (1994) reported an increase in $GABA_A$ postsynaptic receptors on granule cells in the dentate gyrus following kindling. However, the kindled $GABA_A$ channels became Zn^{2+}-sensitive, a state they did not display before plasticity induced by kindling (Buhl et al., 1996) and Zn^{2+} is known to inhibit certain types of $GABA_A$ receptors (Smart et al., 1994; Gibbs et al., 1997). Indeed, in granule cells from dentate gyrus Zn^{2+} produces a marked decrease in miniature inhibitory postsynaptic currents (Buhl et al., 1996; see also Mody, 1998). For the hypothesis of Zn^{2+}-sensitive GABA receptors, see also Coulter's (1999) review.

[280] GABAergic inhibition may be reduced but also slightly enhanced in dentate granule cells from humans with temporal lobe sclerosis (Williamson et al., 1995) and an increased proportion of glutamic-acid-decarboxylase-positive neurons has been found in the hippocampus of humans with TLE (Babb et al., 1989).

[281] Lopes da Silva et al. (1995).

inhibition was increased in the soma of CA1 pyramidal cells but the frequency of IPSCs was significantly lower in the distal dendrites of these cells, and the balance between excitation and inhibition was shifted toward excitation in dendrites [282].

A correlated issue is: to what extent are inhibitory interneurons impaired in TLE? Although a series of experimental and clinical studies have reported different degrees of reduction in local-circuit GABAergic neurons in different animal models of limbic seizures [283] and human TLE [284], the surviving interneurons are not dormant, they discharge spike-bursts in response to afferent volleys, and their activity is synchronized to that of other interneurons as well as to pyramidal neurons [285]. The hypothesis of selective loss of distinct subpopulations of *presumed* inhibitory interneurons in human TLE, such as neuropeptide-Y-, somatostatin- or parvalbumin-immunoreactive [286] cells, might be correlated with data showing selective alterations in $GABA_A$ receptors in human TLE [287].

These complex changes in inhibitory processes, all related to the disinhibition hypothesis, are challenged by a recent study of the dentate gyrus that showed, using intracellular and field potential recordings *in vivo*, (*a*) similar IPSP conductances and reversal potentials in seizure-resistant and seizure-sensitive animals; (*b*) no evidence of disinhibition at the onset of spontaneous seizures; and (*c*) similar densities of GABA-immunoreactive somata in the dentate gyrus [288]. The conclusion was that, at least for this species (gerbils) and model of naturally epileptic animals, seizures do not involve an imbalance of GABAergic cell numbers or the loss of GABAergic inhibition of granule cells in the dorsal hippocampus. In tissue from the dentate gyrus of human epileptic patients, a strong reduction was found in the numbers of some parvalbumin-positive neurons, which provide inhibitory inputs to somata and initial segment axons of granule cells, but other inhibitory neurons, which form vertical clusters as do axo-axonic cells, were even more numerous than in control patients [289]. The general conclusion of this study is that, in human TLE, the perisomatic inhibitory input to granule cells is preserved.

5.9. Seizures after injury and deafferentation of neocortex

Severe head injury may be followed by seizure activity [290] that is produced by a series of factors, such as contusional hemorrhage, edema caused by mechanical disruption of blood vessels, and cellular loss with replacement gliosis [291]. Recent clinical treatises acknowledge that the mechanisms of posttraumatic seizures are unknown and hypothesize that loss of inhibitory interneurons and/or

[282] Cossart et al. (2001). The enhancement of GABAergic tonic inhibition in the soma of principal cells was also reported to occur in febrile seizures (Chen et al., 1999) and other forms of epileptogenesis (Otis et al., 1994; Prince and Jacobs, 1998). The depolarizing action of GABA at the dendritic level (Andersen et al., 1980a; Staley et al., 1995) is present from early postnatal life (Cherubini et al., 1991).

[283] Sloviter (1987); Houser and Esclapez (1996); Morin et al. (1998).

[284] DeLanerolle et al. (1989); Mathern et al. (1995).

[285] Esclapez et al. (1997); Rempe et al. (1997); Bernard et al. (2000).

[286] Bernard et al. (1999) remarked that it remains to be demonstrated that these cellular types are also GABAergic. The hypothesis of a selective loss of neuropeptide-Y-and somatostatin-synthesizing neurons in fascia dentata of humans with TLE was tested and led to the conclusion that, while neuropeptide-Y-mRNA- and somatostatin mRNA-positive neurons are reduced in some patients with TLE compared with others, the selective loss of these neurons with respect to overall hilar cell loss seemed unlikely (Sundstrom et al., 2001).

[287] Loup et al. (2000) analyzed three $GABA_A$ receptor subunits in surgical specimens from TLE patients and found a layer-specific loss of α1-subunit-immunoreactive interneurons in hippocampus and altered dendritic morphology in surviving interneurons immunopositive for the α1-subunit.

[288] Buckmaster et al. (2000) obtained these results in gerbils, selectively bred for or against epilepsy in their colony.

[289] Wittner et al. (2001).

[290] Reviewed in Dinner (1993).

[291] Willmore (1999).

synaptic reorganization increasing recurrent excitation in different cortical areas may favor epileptogenesis (see also section **5.1**).

Electrophysiological studies of different experimental models *in vitro* and *in vivo* have approached the mechanisms of seizures after transient ischemia, after trauma caused by dropping a mass on slices maintainted *in vitro*, or after injury leading to deafferentation [292]. Thus, following axotomy of corticospinal neurons, by sectioning the cervical spinal cord, there is an increased input resistance in these pyramidal neurons, reduced afterhyperpolarizing potentials, and a reduction in the number of neurons in which IPSPs could be elicited [293]. Although these changes reflect an increased excitability of corticospinal cells, there was no evidence of epileptogenesis in field potentials, probably because axotomy did not produce new connections and these neurons represent a minority of neuronal ensembles in the motor cortex [294]. To produce paroxysmal discharges, it is sufficient to undercut cortical areas, leaving the blood supply intact [295]. In rodents, the model of chronic epileptogenesis induces paroxysmal discharges in layer V after 10 days but sometimes much later [296]. A computational model of posttraumatic epileptogenesis in partially isolated cortical islands concluded that paroxysmal discharges are due to changes in intrinsic properties of pyramidal cells and enhanced NMDA synaptic conductances, without altered or even increased inhibition [297]. At variance, experimental data from rat somatosensory slices divided into a superficial part (~0.45 mm from the pia) and a deep segment showed that the dendrotomized deep segment displayed abnormally increased excitability, partially due to disinhibition produced by the removal of inhibition-rich superficial layers [298].

The epileptogenic property of neocortical areas was investigated in acute experiments performed *in vivo*, following partial deafferentation leading to disfacilitation and changes in intrinsic neuronal properties [61]. Hyperpolarizations during periods of disfacilitation, lasting for a few hundred milliseconds, can activate a cation current, I_H (see Chapter 3, section *3.2.2.1*), which leads to a depolarizing sag and overexcitation of neurons at the end of the disfacilitation epoch, thus triggering a paroxysmal cycle [11]. Also, cortical areas partially deprived of synaptic activity display a strikingly increased proportion of intrinsically bursting (IB) neurons, up to 40–60%, as seen in slices and in isolated small cortical slabs *in vivo* (see Chapter 2, section ***2.1.2***) and single-axon presynaptic spike-bursts have stronger postsynaptic effects compared to single action potentials. After cortical injury, the level of $[K^+]_o$ increases and can change the pattern of regular-spiking cells into that of

[292] Epilepsy occurs in up to 25% of stroke patients (Kotila and Waltimo, 1992). In experimental conditions, following photothrombotic cortical ischemia, there is a hyperexcitability of cortical neurons in the perilesional areas, with markedly increased unit discharges and decreased inhibition that underlies this neuronal activity; the hyperexcitability was regarded as a response to deafferentation (see Witte and Freund, 1999). Transient cerebral ischemia in rat cortical slices also led to the conclusion that neuronal hyperexcitability is produced, at least partly, by a functional reduction in the efficacy of the intracortical GABAergic system (Luhmann et al., 1999). In traumatic injury of CA1 hippocampal slices, gap junctions increase the cellular propensity to seizures (Frantseva et al., 2002).

[293] Tseng and Prince (1996). These results are similar to those obtained following axotomy of spinal cord motoneurons, which results in increased input resistance and prominent regenerative dendritic responses (Eccles et al., 1958; Sernagor et al., 1986).

[294] Huguenard et al. (1996) reported that the axotomy of thalamocortical neurons results in their retrograde degeneration, that the low-threshold Ca^{2+} current (I_T) is transiently increased up to 170% of the control values, and there is a slightly reduced sensitivity to some anti-epileptic substances (see Chung et al., 1993).

[295] Prince and Tseng (1993). Hoffman et al. (1994) used transcortical or white matter transections; following transcortical transections, epileptogenesis (with interictal and ictal events) developed after a period of 1–2 weeks, but the region of abnormal excitability did not extend beyond ~2 mm from the lesioned area.

[296] The intrinsic membrane properties, synaptic connectivity, and long-term reorganization cortical circuitry in postlesional, chronic models of epileptogenesis are discussed in Gutnick et al. (1992) and Jacobs et al. (2000).

[297] Bush et al. (1999).

[298] Yang and Benardo (1997).

[299] Amzica et al. (2002).

[300] Drake et al. (1994).

[301] Malow et al. (1997).

bursting neurons [5, 7]. All these factors may promote development to seizures. Indeed, after undercutting the white matter below the suprasylvian gyrus, which produced partial disconnection from neocortical inputs and from thalamocortical afferents, the sleep-like slow oscillation was replaced by seizure activity that occurred two to four hours after the undercut was made and was generally initiated at the border between the intact and undercut cortex (Fig. 5.73). The highest synchrony among field potential recordings during seizures that followed partial deafferentation was associated with the strongest depolarization in intracellularly recorded neurons (Fig. 5.74).

5.10. Dialogue between neurons and glial cells in neocortical seizures

Glial cells are endowed with receptors for, and release, some neurotransmitters. The evidence for an active role of glia in some neuronal operations, deriving from work on cultures or on slices maintained *in vitro*, and the possible implication of glial cells in epilepsy are briefly mentioned in section **5.1**. Dual intracellular recordings from neocortical neurons and glial cells, or from two glial cells, were recently performed during sleep and seizures *in vivo* [67]. These studies led to the following conclusions. (*a*) The membrane potential of glial cells displays negative events related to the onset of paroxysmal depolarizing shifts in cortical neurons and maximal glial depolarization is reached after the end of the neuronal depolarization (Fig. 5.75). This may control the pace of paroxysmal oscillations. (*b*) The propagation of paroxysmal activity in the neocortex can use spatial buffering through the glial syncytium rather than simple diffusion through the extracellular space (Fig. 5.76) [299]. This mechanism may complement that of progressively increased inter-neuronal synchrony with the development of the slow sleep oscillation to seizures [107, 133].

5.11. Effects of epileptic seizures on sleep states

Among sleep disorders in epileptic patients, the most common are excessive daytime sleepiness, with intermittent tiredness and feelings of depression and irritability [300], difficulty in initiating and maintaining sleep, and obstructive sleep apnea syndrome (OSAS). In a study of epileptic patients referred for polysomnography, OSAS was diagnosed in ~70% of those with sleep disorders [301] and some authors reported improvement in seizure frequency following

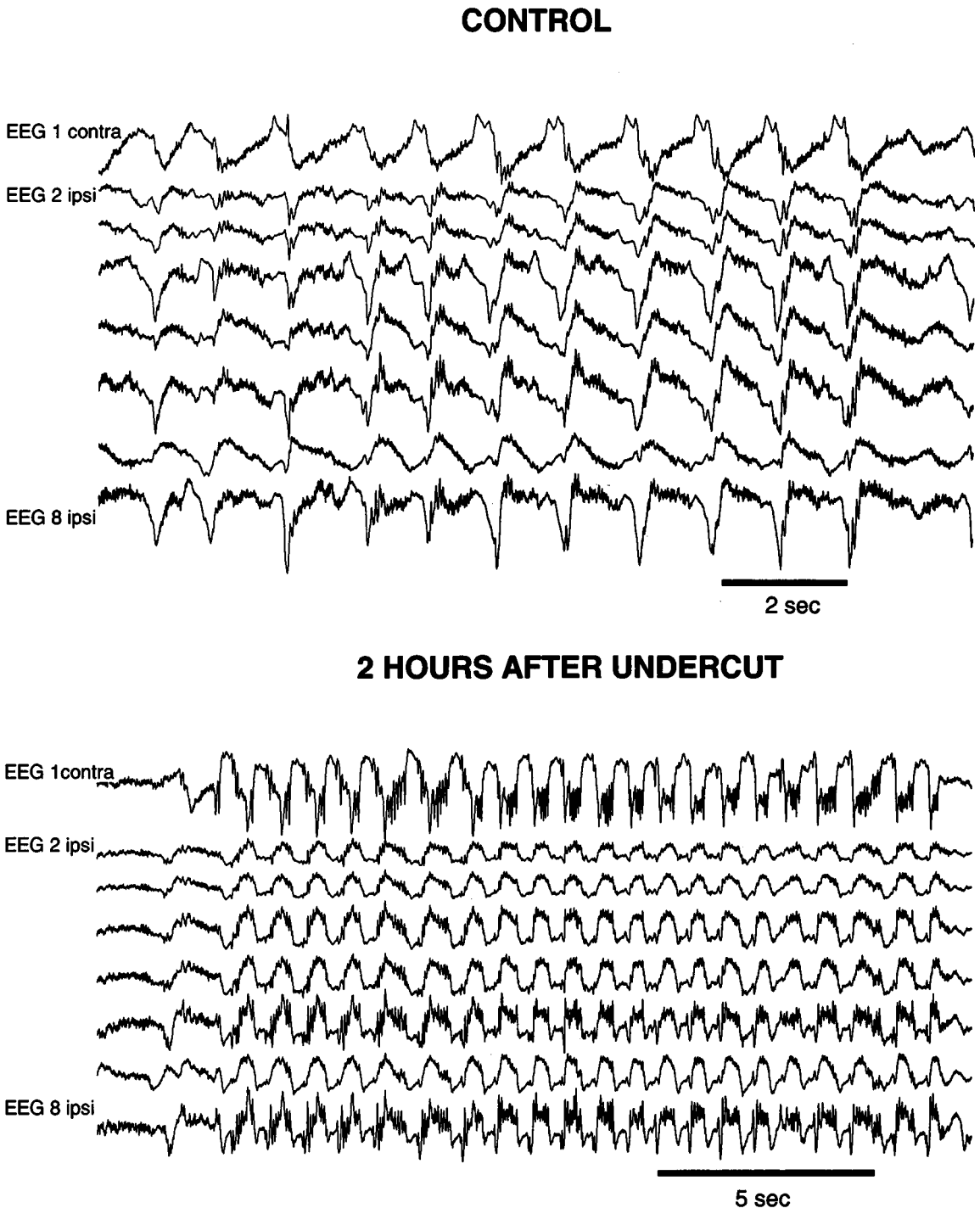

Fig. 5.73 Spontaneous seizure after an undercut is made throughout the white matter underlying suprasylvian areas 7 and 5. Cat under ketamine-xylazine anesthesia. The cut was performed in a posterior-to-anterior direction. Field potential recordings: electrode 1 was placed on the contralateral (right) suprasylvian cortex; electrodes 2 to 8 were placed from posterior (2) to anterior (8) sites in the left suprasylvian cortex. Note slow oscillation before the undercut and paroxysmal activity 2 h after the cut. From Topolnik et al. (2003).

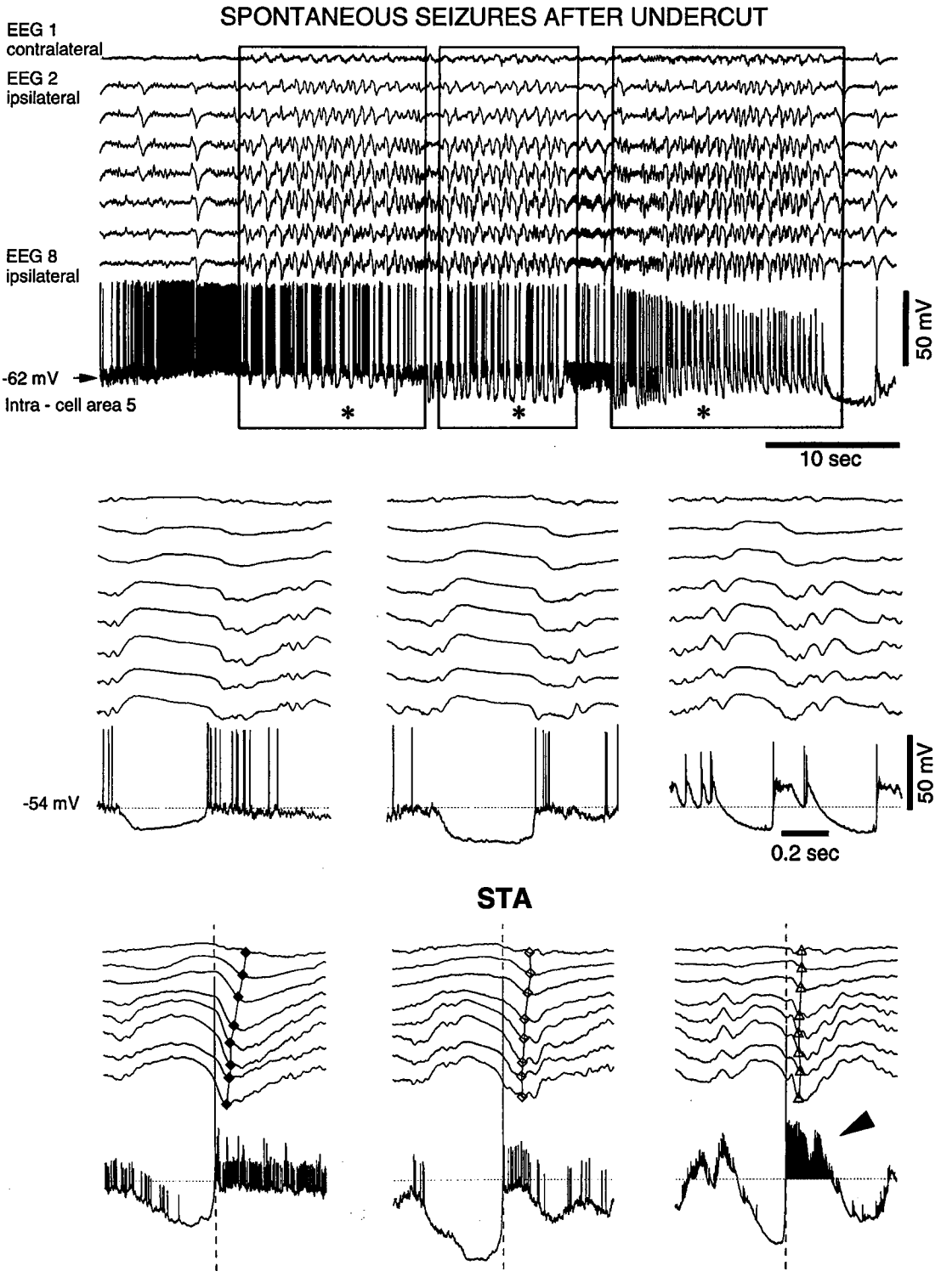

Fig. 5.74 Spontaneous seizures occurring 2 h after undercut. Cat under ketamine-xylazine anesthesia. Same procedure as in Fig. 5.73. Multi-site field potential recordings (same arrangement as in Fig. 5.73) together with intracellular recordings from an area 5 neuron. The three parts of the seizures are framed (marked with asterisks) and expanded below. *Bottom panel* illustrates spike-triggered averages (STA) using the first action potential after hyperpolarization as time zero. Lines with symbols show the propagation of the excitation. Note that the highest synchrony among field potential recordings was associated with strongest depolarization in the intracellularly recorded neuron (gray area and arrow). From Topolnik et al. (2003).

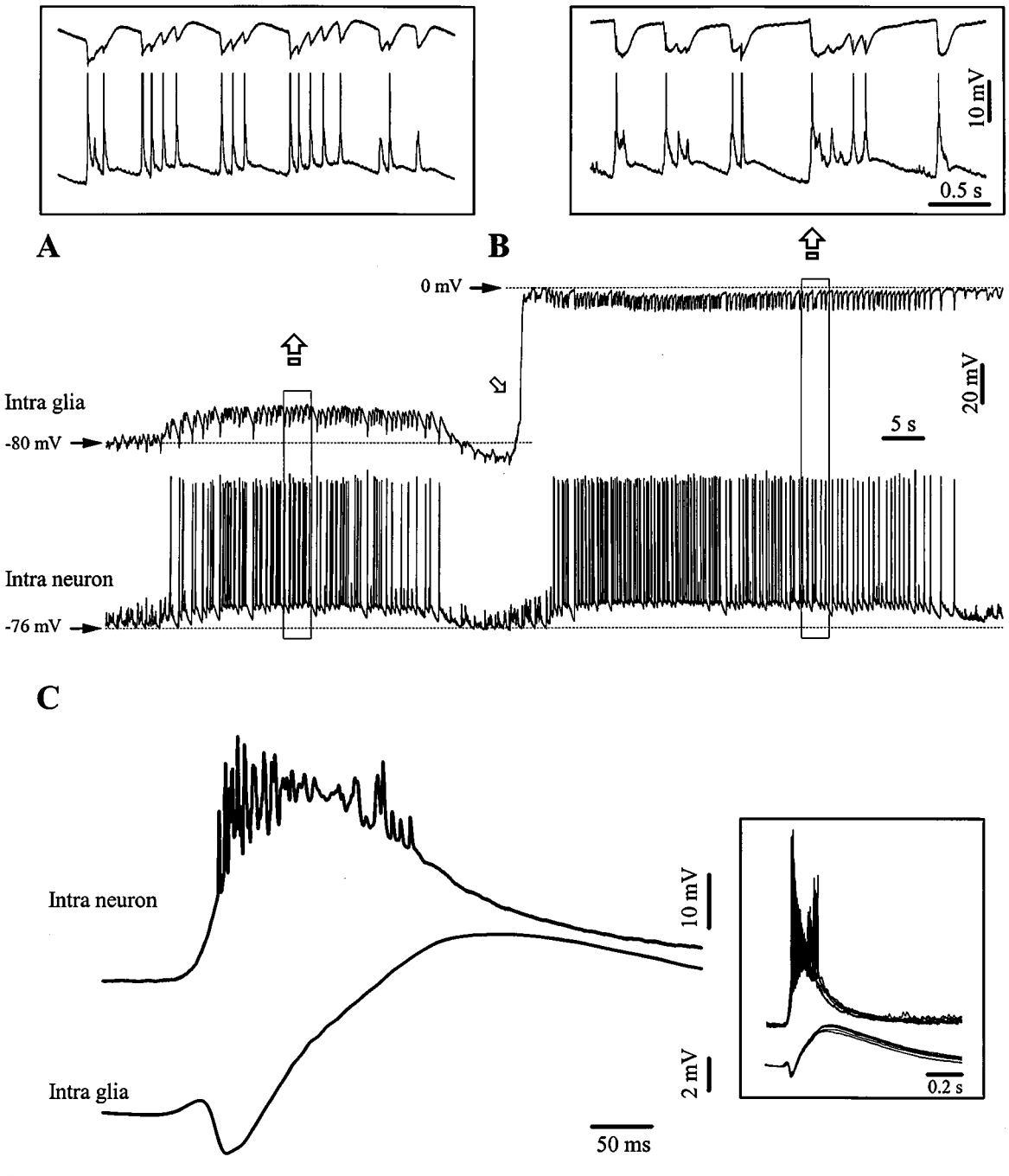

Fig. 5.75 Simultaneous intracellular recordings from cortical neurons and glial cells show that, during seizures, glial transient negativities reflect neuronal depolarization and that glial depolarization outlasts that of neurons. Cats under ketamine-xylazine anesthesia. *A–B*, continuous recording with a double neuron-glia impalement (in *A*, pipettes separated by less than 1 mm) followed by neuronal field recording (*B*). The transition from *A* to *B* is marked by withdrawal of the pipette from the glia (oblique open arrowhead). Epochs within the squares are expanded above. Note the recurrent sharp negative intraglial deflections associated with neuronal depolarizing potentials (*A*). *C*, average ($n = 50$) of simultaneously recorded neuronal and glial activity during cortical seizures (several original traces are superimposed in the inset). Note the negative glial potential associated with neuronal depolarization and the glial depolarization outlasting the neuronal one (see text). Modified from Amzica and Steriade (2000).

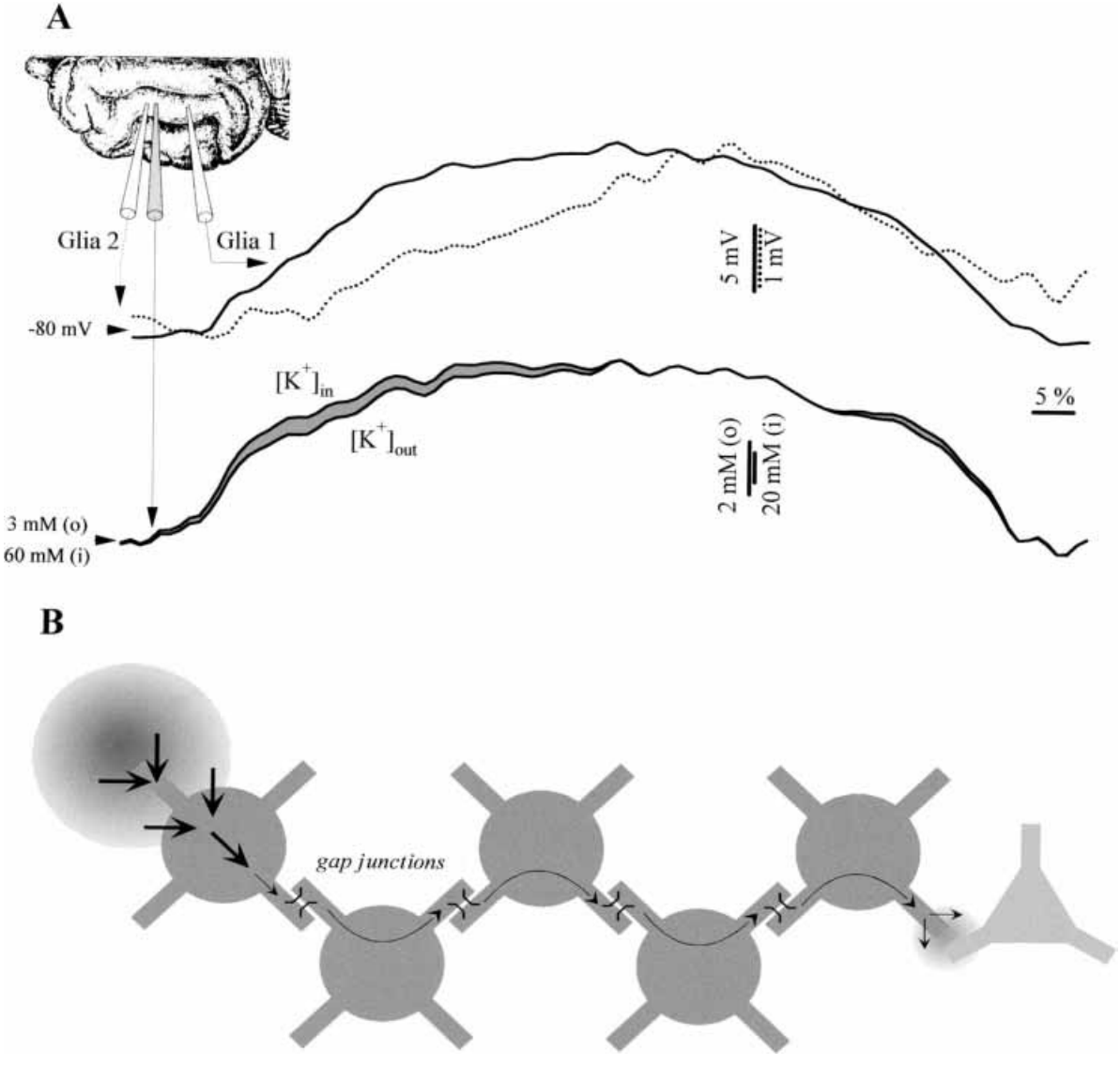

Fig. 5.76 Propagation of K^+ waves during SW seizures. Data from cats under ketamine-xylazine anesthesia. *A*, dual intraglial recording together with the extracellular K^+ concentration ($[K^+]_{out}$). The position of the recording electrodes in the suprasylvian gyrus is shown in the *inset*. The traces represent the average of 20 normalized seizure envelopes. The upper superimposition contains the intracellular seizures in the pair of glial cells expanded at their maximum amplitude (see different voltage calibrations – continuous line for cell 1 and dotted line for cell 2, also corresponding to the envelope traces). From the higher amplitude of the signal, it may be inferred that cell 1 is closer to a presumed seizure focus. The *lower panel* displays the intra- and extracellular K^+ concentrations superimposed and expanded at their maximum amplitude. The $[K^+]_{in}$ was calculated from the Nernst equilibrium potential in relation to the $[K^+]_{out}$ and the intracellular trace that was recorded close to the K^+ microelectrode. Toward the beginning of the seizure, the estimated $[K^+]_{in}$ increased faster than the $[K^+]_{out}$ (*gray area* between the two traces). *B*, schematic functioning of the spatial buffering during SW seizures. Red cells represent glia, green cells represent neurons. Important increases in the $[K^+]_{out}$ (blue circle) may not be buffered at short distances, in which case the K^+ taken up may travel through the glial syncytium and is externalized at a location with lower $[K^+]_{out}$ values, where it would modulate the activity of nearby neurons. Modified from Amzica et al. (2002). See Plate section for color version of this figure.

[302] Devinsky et al. (1994).

[303] Reviewed in Foldvary (2001).

OSAS treatment [302]. Antiepileptic drugs produce a variety of alterations in sleep architecture [303].

5.12. Concluding remarks

(a) Both intrinsic neuronal properties and synaptic articulations in complex forebrain networks are crucial for understanding the mechanisms underlying the generation of seizures. The decisive role in the spread of focal or widespread synchronization of cellular discharges is played by neuronal circuitry. Those studying slices maintained *in vitro* emphasized the need to refocus our attention on circuitry and stated that the expression of epileptic properties requires a minimum circuitry and/or environment.

(b) The adage "sleep and epilepsy are common bedfellows" is supported by clinical and experimental evidence showing that epileptic seizures preferentially occur during a drowsy state and slow-wave sleep, whereas REM sleep is a non-epileptic state. Thus, spontaneously occurring sleep spindles (7–15 Hz) or their experimental model, augmenting responses (~10 Hz), may lead to self-sustained neocortical seizures, which may develop into spike-wave (SW) and/or polyspike-wave (PSW) seizures at 2–3 Hz. Also, very fast oscillations, called ripples (80–200 Hz), which appear over the depolarizing phase of the slow sleep oscillation, are one of the best experimental paradigms for eliciting cortical seizures. When seizures evolve without discontinuity from the slow oscillation, strong ripples occur just before the transition between normal and paroxysmal activity. Thus, ripples of strong amplitude announce the imminent occurrence of seizures.

(c) The intracellular correlate of interictal spikes (ISs) is an overt depolarization, termed paroxysmal depolarizing shift (PDS), which can be generated by an imbalance between excitatory and inhibitory influences, such as impairing inhibition through the application of $GABA_A$ antagonists, or by increasing the excitability of neuronal networks via an increased extracellular concentration of K^+. The hypotheses explaining the PDS as a sum of synchronous EPSPs or, alternatively, resulting from intrinsic neuronal properties are not mutually exclusive as both factors contribute to the slow envelope of the PDS. PDSs also contain an important inhibitory component. Recordings with Cl^--filled pipettes reveal depolarizing shifts by 10–30 mV during EEG "spikes", and conventional fast-spiking inhibitory interneurons discharge at very high rates (500–600 Hz) during

PDSs. *In vivo* comparison between the intracortical synchrony of PDSs, that of the slow sleep oscillation in the prior background activity, and that of seizures developing from successive ISs shows highest synchrony during seizures, followed by ISs, and finally slow oscillation. With time, ISs grow in amplitude, start to appear rhythmically with increasing frequency, and culminate into SW/PSW seizures.

(d) Clinical and experimental studies point out that, instead of being "suddenly generalized and bilaterally synchronous", as conventionally regarded according to the "centrencephalic" hypothesis, many SW seizures (some of them characterizing typical absence epilepsy) are progressively built up within corticocortical and corticothalamic networks. Multiple, independent cortical foci and asymmetrical SW/PSW complexes have been described in patients and also found in animal experiments. Thus, some SW/PSW seizures display focal paroxysmal activity, confined to one cortical area or to a few contiguous cortical fields. This is in line with the concept that SW/PSW complexes originate in the neocortex and are disseminated through mono-, oligo-, and multi-synaptic intracortical circuits, before they spread to the thalamus and exhibit generalized features.

(e) In experiments on acutely prepared or chronically implanted animals, seizures with SW/PSW complexes at ~2–3 Hz originate in the neocortex (even in athalamic preparations) and, in intact-brain preparations, such seizures spread to the thalamus after their cortical initiation. Experiments using multisite, field potential, extracellular, and intracellular recordings of spontaneously occurring seizures demonstrate the intracortical synchronization of SW/PSW paroxysms. The degree of synchrony among simultaneously recorded cortical neurons increases progressively from the pre-seizure (sleep-like) period to the early stage of SW/PSW seizure and, further, to the late stage of the seizure. Then, the build up of SW seizures obeys the rule of synaptic circuits, sequentially distributed through synaptic linkages. Dual intracellular recordings during spontaneous SW/PSW seizures reinforce the notion of intracortical synchronization of SW seizures. The absence of SW seizures in cortical slices is probably due to the absence of long-range connections that synchronize paroxysmal activity.

(f) During cortically generated SW seizures, two types of thalamic neurons, reticular GABAergic and thalamocortical cells, undergo opposite influences: the former follow each PDS of SW complexes, whereas the majority of the latter (~60–90%

in different experiments) are steadily hyperpolarized and display phasic IPSPs that do not de-inactivate the Ca^{2+}-dependent low-threshold spikes, and thus do not transfer spike-bursts to the cortex. This is due to the greater power of the excitatory cortical projections to reticular neurons compared to thalamic relay neurons. However, the remaining thalamic relay cells may reinforce the coherence of seizure activity arising in neocortical areas.

(g) While the EEG "spike" component of SW/PSW complexes contains an important inhibitory component (see point *c*), the hyperpolarization associated with the EEG "wave" component of these complexes is *not* due to GABAergic IPSPs. If the EEG "wave" components were GABAergic IPSPs, one should find a decreased input resistance during these components. Instead, the opposite was found *in vivo*, during spontaneous SW/PSW seizures in cats as well as in similar seizures in a genetic model of absence epilepsy in rats. Data showed that the apparent input resistance is higher during the EEG "wave" component of SW/PSW complexes, reflecting summated hyperpolarizations in a pool of neurons, compared to the depth-negative EEG "spike" component.

(h) Spontaneously occurring seizures consisting of SW/PSW complexes at ∼1.5–2.5 Hz, interspersed with fast runs at 10–20 Hz, resemble the EEG patterns in Lennox–Gastaut syndrome. Multi-site extracellular and intracellular recordings from the neocortex and thalamus were used to investigate the neuronal substrates of these seizures. The polyspike events have similar frequencies to those of fast runs. Such seizures occur preferentially during patterns of slow-wave sleep. Similar relations between field potentials and intracellular activities were detected during slow-wave sleep and Lennox–Gastaut-type seizures; that is, an increased amplitude of the depolarizing component of slow sleep oscillation reached the level of PDSs during seizures, and the depolarizing phases of the slow sleep oscillation increased their frequencies to become paroxysmal SW complexes at ∼2–3 Hz.

(i) The neuronal bases of neocortical and thalamic events implicated in SW/PSW complexes during Lennox–Gastaut syndrome are similar to those exposed above for pure SW/PSW seizures at ∼3 Hz (see *e*–*g*). As to the fast runs at 10–20 Hz, they demonstrate changes in frequencies during different epochs of the same seizure and the absence of perfect synchrony between cortical neuronal pools, which explains why corticothalamic inputs do not elicit synchronous fast oscillations in the

thalamus during this type of seizures. Compared to other types of neocortical neurons, fast-rhythmic-bursting cells fire more action potentials during each depolarizing component of fast runs.

(j) Very fast neocortical oscillations (ripples, see *b*) display their highest amplitudes at the onset of Lennox–Gastaut-type seizures and pharmacological manipulations that block ripples also obliterate these seizures.

(k) Seizures are accompanied by an increased extracellular K^+ concentration ($[K^+]_o$), which may convert regular-spiking neurons into bursters by increasing depolarizing afterpotentials (DAPs). In fast-rhythmic-bursting neurons, which are among the best candidates for promoting neocortical seizures, the increased number of action potentials within a burst stems from DAPs. During seizures, the activation of intrinsic depolarizing currents involves the persistent Na^+ current, which leads to a progressive depolarization of neocortical neurons up to the level of spike inactivation. The increased synaptic activity during paroxysmal episodes is an important factor for triggering a cascade of extracellular and intrinsic neuronal processes resulting in the tonic depolarization that underlies fast runs at 10–20 Hz, which are associated with SW/PSW complexes in seizures of the Lennox–Gastaut type.

(l) In experimental models of temporal lobe epilepsy, the spike-bursts of hippocampal pyramidal cells are produced by a synaptically evoked slow depolarization that follows a fast EPSP. Besides synaptic events, the synchronized output of area CA1 is also dependent on intrinsic neuronal properties, excitatory feedback through recurrent axonal collaterals of pyramidal cells, and gap-junctional communication. Although a global reduction in GABAergic inhibition has long been assumed to account for paroxysmal discharges in the hippocampus, several recent data challenged this hypothesis on several grounds: loss of inhibition in field CA1, but increased GABAergic inhibition in the dentate gyrus; increased GABAergic inhibition in the soma of CA1 pyramidal cells, but a lower frequency of inhibitory postsynaptic currents in the distal dendrites of these cells; and, even similar IPSP conductances and reversal potentials in seizure-resistant and seizure-sensitive animals, with no evidence of disinhibition at the onset of spontaneous seizures.

References

Abel, T., Nguyen, P.V., Barad, M., Deuel, T.A., Kandel, E.R. and Bourtchouladze, R. (1997) Genetic demonstration of a role for PKA in the late phase of LTP and in hippocampus-based long-term memory. *Cell* **88**: 615–626.

Abramson, B.P. and Chalupa, L.M. (1985) The laminar distribution of cortical connections with the tecto- and cortico-recipient zones in the cat's lateral posterior nucleus. *Neuroscience* **15**: 81–95.

Achermann, P. and Borbély, A. (1997) Low-frequency (<1 Hz) oscillations in the human sleep EEG. *Neuroscience* **81**: 213–222.

Achermann, P. and Borbély, A. (1998a) Coherence analysis of the human sleep electroencephalogram. *Neuroscience* **85**: 1195–1208.

Achermann, P. and Borbély, A. (1998b) Temporal evolution of coherence and power in the human sleep electroencephalogram. *Journal of Sleep Research* **7** (Suppl. 1): 36–41.

Adey, W.R. (1967) Hippocampal states and functional relations with corticosubcortical systems in attention and learning. *Progress in Brain Research* **27**: 228–245.

Adolphs, R., Tranel, D., Damasio, H. and Damasio, A. (1994) Impaired recognition of emotion in facial expression following bilateral damage to the human amygdala. *Nature* **372**: 669–672.

Adrian, E.D. and Matthews, B.H.C. (1934) The Berger rhythm: potential changes from the occipital lobes in man. *Brain* **57**: 355–384.

Agmon, A. and Connors, B.W. (1991) Thalamocortical responses of mouse somatosensory (barrel) cortex *in vitro*. *Neuroscience* **41**: 365–379.

Ajmone-Marsan, C. (1975) Focal electrical stimulation. In *Experimental Models of Epilepsy*, ed. D.P. Purpura, J.K. Penry, D.B. Tower, D.M. Woodbury and R.D. Walter, pp. 147–172, New York: Raven Press.

Aladjalova, N.A. (1964) *Slow Electrical Processes in the Brain. Progress in Brain Research* (vol. 7). Amsterdam: Elsevier.

Albe-Fessard, D. and Buser, P. (1955) Activités intracellulaires recueillies dans le cortex sigmoïde du chat: participation des neurones pyramidaux au "potential évoqué" somesthésique. *Journal de Physiologie (Paris)* **47**: 67–69.

Albowitz, B. and Kuhnt, U. (1993) The contribution of intracortical connections to horizontal spread of activity in the neocortex as revealed by voltage sensitive dyes and a fast optical recording method. *European Journal of Neuroscience* **5**: 1349–1359.

Albowitz, B. and Kuhnt, U. (1995) Epileptiform activity in the guinea-pig neocortical slice spreads preferentially along supragranular layers – recordings with voltage-sensitive dyes. *European Journal of Neuroscience* **7**: 1273–1284.

Albrecht, D., Royl, G. and Kaneoke, Y. (1998) Very slow oscillatory activities in lateral geniculate neurons of freely moving and anesthetized rats. *Neuroscience Research* **32**: 209–220.

Alefeld, M., Sutor, B. and Luhmann, H.J. (1998) Pattern and pharmacology of propagating epileptiform activity in mouse cerebral cortex. *Experimental Neurology* **153**: 113–122.

Alger, B.E. and Nicoll, R.A. (1982) Feed-forward dendritic inhibition in rat hippocampal pyramidal cells studied *in vitro*. *Journal of Physiology (London)* **328**: 105–123.

Allen, P.J., Fish, D.R. and Smith, S.J. (1992) Very high-frequency rhythmic activity during SEEG suppression in frontal lobe epilepsy. *Electroencephalography and Clinical Neurophysiology* **82**: 155–159.

Al-Noori, S. and Swann, J. (2000) A role for sodium and chloride in kainic acid-induced beading of inhibitory interneuron dendrites. *Neuroscience* **101**: 337–348.

Alonso, A. and Klink, R. (1993) Differential electroresponsiveness of stellate and pyramidal-like cells of medial entorhinal cortex layer II. *Journal of Neurophysiology* **70**: 128–143.

Alonso, A. and Köhler, C. (1984) A study of the reciprocal connection between the septum and the entorhinal area using anterograde and retrograde axonal transport methods in the rat brain. *Journal of Comparative Neurology* **225**: 327–343.

Alonso, A. and Llinás, R. (1989) Subthreshold Na^+-dependent theta-like rhythmicity in stellate cells of entorhinal cortex layer II. *Nature* **342**: 175–177.

Alonso, A., De Curtis, M. and Llinás, R. (1990) Postsynaptic Hebbian and non-Hebbian long-term potentiation of synaptic efficacy in the entorhinal cortex in slices and in isolated adult guinea pig brain. *Proceedings of the National Academy of Sciences of the USA* **87**: 9280–9284.

Altman, J. and Bayer, S.A. (1979) Development of the diencephalons in the rat. V. Thymidine-radiographic observations on internuclear and intranuclear gradients in the thalamus. *Journal of Comparative Neurology* **188**: 473–500.

Alvarez-Maubecin, V., Garcia-Hernandez, F., Williams, J.T. and van Bockstaele, E.J. (2000) Functional coupling between neurons and glia. *Journal of Neuroscience* **20**: 4091–4098.

Amadeo, M. and Shagass, C. (1973) Brief latency click-evoked potentials during waking and sleep in man. *Psychophysiology* **10**: 244–250.

Amaral, D.G. and Price, J.L. (1984) Amygdalo-cortical projections in the monkey (*Macaca fascicularis*). *Journal of Comparative Neurology* **230**: 465–496.

Amaral, D.G. and Witter, M.P. (1989) The three-dimensional organization of the hippocampal formation: a review of anatomical data. *Neuroscience* **31**: 571–591.

Amaral, D.G., Price, J.L., Pitkänen, A. and Carmichael, S.T. (1992) Anatomical organization of the primate amygdaloid complex. In *The Amygdala*, ed. J.P. Aggleton, pp. 1–66, New York: Wiley-Liss.

Amzica, F. and Massimini, M. (2000) Modulation of glia and neuronal activities by halothane. *Society for Neuroscience Abstracts* **26**: 734.

Amzica, F. and Massimini, M. (2002) Glia and neuronal interactions during slow wave and paroxysmal activities in the neocortex. *Cerebral Cortex* **12**: 1101–1113.

Amzica, F. and Neckelmann, D. (1999) Membrane capacitance of cortical neurons and glia during sleep oscillations and spike-wave seizures. *Journal of Neurophysiology* **82**: 2731–2746.

Amzica, F. and Steriade, M. (1995a) Disconnection of intracortical synaptic linkages disrupts synchronization of a slow oscillation. *Journal of Neuroscience* **15**: 4658–4677.

Amzica, F. and Steriade, M. (1995b) Short- and long-range neuronal synchronization of the slow (<1 Hz) cortical oscillation. *Journal of Neurophysiology* **75**: 20–38.

Amzica, F. and Steriade, M. (1996) Progressive cortical synchronization of ponto-geniculo-occipital potentials during rapid eye movement sleep. *Neuroscience* **72**: 309–314.

Amzica, F. and Steriade, M. (1997) The K-complex: its slow (<1 Hz) rhythmicity and relation to delta waves. *Neurology* **49**: 952–959.

Amzica, F. and Steriade, M. (1998a) Cellular substrates and laminar profile of sleep K-complex. *Neuroscience* **82**: 671–686.

Amzica, F. and Steriade, M. (1998b) Electrophysiological correlates of sleep delta waves. *Electroencephalography and Clinical Neurophysiology* **107**: 69–83.

Amzica, F. and Steriade, M. (1999) Spontaneous and artificial activation of neocortical seizures. *Journal of Neurophysiology* **82**: 3123–3138.

Amzica, F. and Steriade, M. (2000) Neuronal and glial membrane potentials during sleep and paroxysmal oscillations in the cortex. *Journal of Neuroscience* **20**: 6646–6665.

Amzica, F. and Steriade, M. (2002) The functional significance of K-complexes. *Sleep Medicine Reviews* **6**: 139–149.

Amzica, F., Nuñez, A. and Steriade, M. (1992) Delta-frequency (1–4 Hz) oscillations of perigeniculate thalamic neurons and their modulation by light. *Neuroscience* **51**: 285–294.

Amzica, F., Neckelmann, D. and Steriade, M. (1997) Instrumental conditioning of fast (20- to 50-Hz) oscillations in corticothalamic networks. *Proceedings of the National Academy of Sciences of the USA* **94**: 1985–1989.

Amzica, F., Massimini, M. and Manfridi, A. (2002) Spatial buffering during slow and paroxysmal oscillations in cortical networks of glial cells *in vivo*. *Journal of Neuroscience* **22**: 1042–1053.

Anderer, P., Klösch, G., Gruber, G., Trenker, E., Pascual-Marqui, R.D., Zeitlhofer, J., Barbanoj, M.J., Rappelsberger, P. and Saletu, B. (2001) Low-resolution brain electromagnetic tomography revealed simultaneously active frontal and parietal sleep spindle sources in the human cortex. *Neuroscience* **103**: 581–592.

Andersen, P. and Andersson, S.A. (1968) *Physiological Basis of the Alpha Rhythm*. New York: Appleton-Century-Crofts.

Andersen, P. and Sears, T.A. (1964) The role of inhibition in the phasing of spontaneous thalamocortical discharge. *Journal of Physiology (London)* **173**: 459–480.

Andersen, P., Eccles, J.C. and Løyning, Y. (1964) Location of postsynaptic inhibitory synapses on hippocampal pyramids. *Journal of Neurophysiology* **27**: 592–607.

Andersen, P., Blackstad, T.W. and Lømo, T. (1966) Location and identification of excitatory synapses on hippocampal pyramidal cells. *Experimental Brain Research* **1**: 236–248.

Andersen, P., Gross, G.N., Lømo, T. and Sveen, O. (1969) Participation of inhibitory and excitatory interneurons in the control of hippocampal cortical output. In *The Interneuron*, ed. M. Brazier, pp. 415–465, Los Angeles: University of California Press.

Andersen, P., Dingledine, R., Gjerstad, L., Langmoen, I.A. and Laursen, A.M. (1980a) Two different responses of hippocampal pyramidal cells to application of gamma-aminobutyric acid. *Journal of Physiology (London)* **305**: 279–296.

Andersen, P., Silfvenius, H., Sundberg, S.H. and Sveen, O. (1980b) A comparison of distal and proximal dendritic synapses on CA1 pyramids in hippocampal slices in vitro. *Journal of Physiology (London)* **307**: 273–299.

Andre, P. and Arrighi, P. (2001) Modulation of Purkinje cell response to glutamate during the sleep-waking cycle. *Neuroscience* **105**: 731–746.

Andreasen, M. and Hablitz, J.J. (1993) Local anesthetics block transient outward potassium currents in rat neocortical neurons. *Journal of Neurophysiology* **69**: 1966–1975.

Andrew, R.D. and Mac Vicar, B.A. (1994) Imaging cell volume changes and neuronal excitation in the hippocampal slice. *Neuroscience* **62**: 371–383.

Annegers, J.W. (1994) The natural course of epilepsy: an epidemiologic perspective. In *The Surgical Management of Epilepsy*, ed. A.R. Wyler and B.P. Hermann, pp. 3–7, Boston: Butterworth-Heinemann.

Araque, A., Sanzgiri, R.P., Parpura, V. and Haydon, P.G. (1998) Calcium elevation in astrocytes causes an NMDA receptor-dependent increase in the frequency of miniature synaptic currents in cultured hippocampal neurons. *Journal of Neuroscience* **18**: 6822–6829.

Araque, A., Parpura, V., Sanzgiri, R.P. and Haydon, P.G. (1999) Tripartite synapses: glia, the unacknowledged partner. *Trends in Neurosciences* **22**: 208–215.

Arduini, A. and Arduini, M. (1954) Effect of drugs and metabolic alterations on brainstem arousal mechanism. *Journal of Pharmacology and Experimental Therapy* **110**: 76–85.

Asanuma, C. (1989) Axonal arborizations of a magnocellular basal nucleus input, and their relation to the neurons in the thalamic reticular nucleus of rats. *Proceedings of the National Academy of Sciences of the USA* **86**: 4746–4750.

Asanuma, C. (1997) Distribution of neuromodulatory inputs in the reticular and dorsal thalamic nuclei. In *Thalamus*, vol. 2 (*Experimental and Clinical Aspects*), ed. M. Steriade, E.G. Jones and D.A. McCormick, pp. 93–153, Oxford: Elsevier.

Asanuma, C. and Porter, L.L. (1990) Light and electron microscopic evidence for a GABAergic projection from the caudal basal forebrain to the thalamic reticular nucleus in rats. *Journal of Comparative Neurology* **302**: 159–172.

Aserinsky, E. and Kleitman, N. (1953) Regularly occurring periods of eye motility and concomitant phenomena during sleep. *Science* **118**: 273–274.

Aserinsky, E. and Kleitman, N. (1955) Two types of ocular motility occurring in sleep. *Journal of Applied Physiology* **8**: 11–18.

Aston-Jones, G. and Bloom, F.E. (1981) Activity of norepinephrine-containing locus coeruleus neurons in behaving rats anticipates fluctuations in the sleep-waking cycle. *Journal of Neuroscience* **1**: 876–886.

Avanzini, G., De Curtis, M., Panzica, F. and Spreafico, R. (1989) Intrinsic properties of nucleus reticularis thalami neurones of the rat studied *in vitro*. *Journal of Physiology (London)* **416**: 111–122.

Avanzini, G., De Curtis, M., Marescaux, C., Panzica, F., Spreafico, R. and Vergnes, M. (1992) Role of thalamic reticular nucleus in the generation of rhythmic thalamo-cortical activities subserving spike and waves. *Journal of Neural Transmission* **35** (Suppl.): 85–95.

Avanzini, G., De Curtis, M., Pape, H.C. and Spreafico, R. (1999) Intrinsic properties of reticular thalamic neurons relevant to genetically determined spike-wave generation. In *Jasper's Basic Mechanisms of the Epilepsies* (3rd edn.), ed. A.V. Delgado-Escucta, W.A. Wilson, R.W. Olsen and R.J. Porter, pp. 297–309, Philadelphia: Lippincott – Williams & Wilkins.

Avendaño, C., Rausell, E. and Reinoso-Suárez, F. (1985) Thalamic projections to areas 5a and 5b of the parietal cortex in the cat: a retrograde horseradish peroxidase study. *Journal of Neuroscience* **5**: 1446–1470.

Avendaño, C., Rausell, E., Perez-Aguilar, D. and Isorna, S. (1988) Organization of the association cortical afferent connections of area 5: a retrograde tracer study in the cat. *Journal of Comparative Neurology* **278**: 1–33.

Avoli, M. and Gloor, P. (1981) The effects of transient functional depression of the thalamus on spindles and on bilateral synchronous epileptic discharges of feline generalized penicillin epilepsy. *Epilepsia* **22**: 443–452.

Avoli, M., Gloor, P., Kostopoulos, G. and Gotman, J. (1983) An analysis of penicillin-induced generalized spike and wave discharges using simultaneous recordings of cortical and thalamic single neurons. *Journal of Neurophysiology* **50**: 819–837.

Avoli, M., Barbarosie, M., Lücke, A., Nagao, T., Lopantsev, V. and Köhling, R. (1996) Synchronous GABA-mediated potentials and epileptiform discharges in the rat limbic system *in vitro*. *Journal of Neuroscience* **16**: 3912–3924.

Ayala, G.F., Dichter, M., Gumnit, R.J., Matsumoto, H. and Spencer, W.A. (1973) Genesis of epileptic spikes: new knowledge of cortical feedback systems suggests a neurophysiological explanation of brief paroxysms. *Brain Research* **52**: 1–17.

Babb, T.L. (1999) Hippocampal neurophysiology in humans. In *The Epilepsies – Etiologies and Prevention*, ed. P. Kotagal and H.O. Lüders, pp. 167–170, San Diego: Academic Press.

Babb, T.L., Pretorius, J.K., Kupfer, W.R. and Crandall, P.H. (1989) Glutamate decarboxylase-immunoreactive neurons are preserved in human epileptic hippocampus. *Journal of Neuroscience* **9**: 2562–2574.

Bal, T. and McCormick, D.A. (1993) Mechanisms of oscillatory activity in guinea-pig nucleus reticularis thalami *in vitro*: a mammalian pacemaker. *Journal of Physiology (London)* **466**: 669–691.

Bal, T. and McCormick, D.A. (1996) What stops synchronized thalamocortical oscillations? *Neuron* **17**: 297–308.

Bal, T., von Krosigk, M. and McCormick, D.A. (1995a) Synaptic and membrane mechanisms underlying synchronized oscillations in the ferret lateral geniculate nucleus *in vitro*. *Journal of Physiology (London)* **483**: 641–663.

Bal, T., von Krosigk, M. and McCormick, D.A. (1995b) Role of the ferret perigeniculate nucleus in the generation of synchronized oscillations *in vitro*. *Journal of Physiology (London)* **483**: 665–685.

Bal, T., Debay, D. and Destexhe A. (2000) Cortical feedback controls the frequency and synchrony of oscillations in the visual thalamus. *Journal of Neuroscience* **20**: 7478–7488.

Baranyi, A., Szente, M.B. and Woody, C.D. (1991) Properties of associative long-lasting potentiation induced by cellular conditioning in the motor cortex of conscious cats. *Neuroscience* **42**: 321–334.

Barnes, D.M. and Dichter, M.A. (1984) Effects of ethosuximide and tetramethylsuccinimide on cultured cortical neurons. *Neurology* **34**: 620–625.

Barth, D.S., Sutherling, W., Engle, J. Jr. and Beatty, J. (1984) Neuromagnetic evidence of spatially distributed sources underlying epileptiform spikes in the human brain. *Science* **223**: 293–296.

Bassetti, C., Mathis, J., Gugger, M., Lövblad, K.O. and Hess, C.W. (1996) Hypersomnia following paramedian thalamic stroke: a report of 12 patients. *Annals of Neurology* **39**: 471–480.

Bazhenov, M., Timofeev, I., Steriade, M. and Sejnowski, T.J. (1998a) Cellular and network models for intrathalamic augmenting responses during 10-Hz stimulation. *Journal of Neurophysiology* **79**: 2730–2748.

Bazhenov, M., Timofeev, I., Steriade, M. and Sejnowski, T.J. (1998b) Computational models of thalamocortical augmenting responses. *Journal of Neuroscience* **18**: 6444–6465.

Bazhenov, M., Timofeev, I., Steriade, M. and Sejnowski, T.J. (1999) Self-sustained rhythmic activity in the thalamic reticular nucleus mediated by depolarizing $GABA_A$ receptor potentials. *Nature Neuroscience* **2**: 168–174.

Bazhenov, M., Timofeev, I., Steriade, M. and Sejnowski, T. (2000) Spiking-bursting activity in the thalamic reticular nucleus initiates sequences of spindle oscillations in thalamic networks. *Journal of Neurophysiology* **84**: 1076–1087.

Bazhenov, M., Timofeev, I., Steriade, M. and Sejnowski, T.J. (2002) Model of thalamocortical slow-wave sleep oscillations and transitions to activated states. *Journal of Neuroscience* **22**: 8691–8704.

Beevor, C.E. and Horsley, V. (1890) A record of the results obtained by electrical excitation of the so-called motor cortex and internal capsule in an orang-outan (*Simia satyrus*). *Philosophical Transactions of the Royal Society of London (B)* **181**: 129–158.

Bekisz, M. and Wróbel, A. (1993) 20 Hz rhythm of activity in visual system of perceiving cat. *Acta Neurobiologiae Experimentalis (Warszaw)* **53**: 175–182.

Ben-Ari, Y. (1985) Limbic seizures and brain damage produced by kainic acid: mechanisms and relevance to human temporal lobe epilepsy. *Neuroscience* **14**: 375–403.

Ben-Ari, Y. and Represa, A. (1990) Brief seizure episodes induce long-term potentiation and mossy fibre sprouting in the hippocampus. *Trends in Neurosciences* **8**: 312–318.

Ben-Ari, Y., Le Gal La Salle, G. and Champagnat, J. (1974) Lateral amygdala unit activity. I. Relationship between spontaneous and evoked activity. *Electroencephalography and Clinical Neurophysiology* **37**: 449–461.

Ben-Ari, Y., Krnjeviæ, K., Reiffenstein, R.J. and Reinhardt, W. (1981) Inhibitory conductance changes and action of γ-aminobutyrate in rat hippocampus. *Neuroscience* **6**: 2445–2463.

Benazzouz, A. and Hallett, M. (2000) Mechanism of action of deep brain stimulation. *Neurology* **55** (Suppl. 6): S13–S16.

Benington, J.H. and Heller, H.C. (1995) Restoration of brain energy metabolism as the function of sleep. *Progress of Neurobiology* **45**: 347–360.

Benson, D.L., Isackson, P.J., Hendry, S.H.C. and Jones, E.G. (1991) Differential gene expression for glutamic acid decarboxylase and type II calcium-calmodulin-dependent protein kinase in basal ganglia, thalamus and hypothalamus of the monkey. *Journal of Neuroscience* **11**: 1540–1564.

Beranek, L., Obál, F. Jr., Taishi, P., Bodosi, B., Laczi, F. and Krueger, J.M. (1997) Changes in rat sleep after single and repeated injections of the long-acting somatostatin analog octreotide. *American Journal of Physiology* **273**: R1484–1491.

Berger, H. (1929) Uber das Elektroencephalogramm des Menschen. *Archive für Psychiatrie und Nervenkrankheiten* **87**: 527–570.

Berger, H. (1937) Uber das Elektroencephalogramm des Menschen. Dreizehnte Mitteilung. *Archive für Psychiatrie und Nervenkrankheiten* **106**: 577–584.

Bergmann, F., Costin, A. and Gutman, J. (1963) A low-threshold convulsive area in the rabbit's mesencephalon. *Electroencephalography and Clinical Neurophysiology* **15**: 683–690.

Bernard, C., Hirsch, J.C. and Ben-Ari, Y. (1999) Excitation and inhibition in temporal lobe epilepsy: a close encounter. In *Jasper's Basic Mechanisms of the Epilepsies* (3rd edn.), ed. A.V. Delgado-Escueta, W.A. Wilson, R.W. Olsen and R.J. Porter, pp. 821–828, Philadelphia: Lippincott – Williams & Wilkins.

Bernard, C., Cossart, R., Hirsch, J.C., Esclapez, M. and Ben-Ari, Y. (2000) What is GABAergic inhibition? How is it modified in epilepsy? *Epilepsia* **41** (Suppl. 6): S90–S95.

Bernusconi, R., Lauber, J., Marescaux, C., Vergnes, M., Martin, P., Rubio, V., Leonhardt, T., Reymann, N. and Bitiiger, H. (1992) Experimental absence seizures: potential role of gamma-hydroxybutyric acid and $GABA_B$ receptors. *Journal of Neural Transmission* **35** (Suppl.): 155–177.

Bernusconi, R., Mathivet, P., Bischoff, S. and Marescaux, C. (1999) γ-Hydroxybutyric acid: an endogenous neuromodulator with abuse potential? *Trends in Pharmacological Sciences* **20**: 135–141.

Berridge, M.J. (1998) Neuronal calcium signaling. *Neuron* **21**: 13–26.

Berridge, M.J. (2000) Calcium signaling systems in neurons: synaptic plasticity and sleep. In *The Regulation of Sleep*, ed. A.A. Borbély, O. Hayaishi, T.J. Sejnowski and J.S. Altman, pp. 65–75, Strasbourg: Human Frontier Science Program.

Bertram, E.H. and Scott, C. (2000) The pathological substrate of limbic epilepsy: neuronal loss in the medial dorsal thalamus nucleus as the consistent change. *Epilepsia* **41** (Suppl. 6): S3–S8.

Beurrier, C., Bioulac, B., Audin, J. and Hammond, C. (2001) High-frequency stimulation produces a transient blockade of voltage-gated currents in subthalamic neurons. *Journal of Neurophysiology* **85**: 1351–1356.

Bezzi, P. and Volterra, A. (2001) A neuron-glia signaling network in the active brain. *Current Opinion in Neurobiology* **11**: 387–394.

Bignall, K.E., Imbert, M. and Buser, P. (1966) Optic projections to non visual cortex in the cat. *Journal of Neurophysiology* **29**: 396–409.

Bishop, P.O., Burke, W. and Hayhow, W.R. (1959) Repetitive stimulation of optic nerve and lateral geniculate synapses. *Experimental Neurology* **1**: 534–555.

Bland, B.H. and Colom, L.V. (1993) Extrinsic and intrinsic properties underlying oscillation and synchrony in limbic cortex. *Progress in Neurobiology* **41**: 157–208.

Blumenfeld, H. and McCormick, D.A. (2000) Corticothalamic inputs control the pattern of activity generated in thalamocortical networks. *Journal of Neuroscience* **20**: 5153–5162.

Borbély, A.A. (1982) A two process model of sleep regulation. *Human Neurobiology* **1**: 195–204.

Borbély, A.A. (1984) *Das Geheimnis der Schlafs*. Stuttgart: Deutsche Verlags-Anstalt.

Borbély, A.A. and Tobler, I. (1989) Endogenous sleep-promoting substances and sleep regulation. *Physiological Reviews* **69**: 605–670.

Bormann, J. and Kettenmann, H. (1988) Patch clamp study of GABA receptor Cl^- channels in cultured astrocytes. *Proceedings of the National Academy of Sciences of the USA* **85**: 8336–8340.

Borst, J.G. and Sakmann, B. (1999) Depletion of calcium in the synaptic cleft of a calyx-type synapse in the rat brainstem. *Journal of Physiology (London)* **521**: 123–133.

Bougousslavsky, J., Miklossy, J., Deruz, J.P., Regli, F. and Assai, G. (1986) Unilateral left paramedian infarction of the thalamus and midbrain: a clinico-pathological study. *Journal of Neurology, Neurosurgery and Psychiatry* **49**: 686–694.

Bourassa, J., Pinault, D. and Deschênes, M. (1995) Corticothalamic projections from the cortical barrel field to the somatosensory thalamus in rats: a single-fiber study using biocytin as an anterograde tracer. *European Journal of Neuroscience* **7**: 19–30.

Bouyer, J.J., Montaron, M.F., Vahnée, J.M., Albert, M.P. and Rougeul, A. (1987) Anatomical localization of cortical beta rhythm in cat. *Neuroscience* **22**: 863–869.

Bragin, A., Engel, J. Jr., Wilson, C.L., Fried, I. and Mathern, G.W. (1999a) Hippocampal and entorhinal cortex high-frequency oscillations (100–500 Hz) in human epileptic brain and in kainic acid-treated rats with chronic seizures. *Epilepsia* **40**: 127–137.

Bragin, A., Engel, J. Jr., Wilson, C.L., Vizentin, E. and Mathern, G.W. (1999b) Electrophysiologic analysis of a chronic seizure model after unilateral hippocampal KA injection. *Epilepsia* **40**: 1210–1221.

Bragin, A., Wilson, C.L. and Engel, J. Jr. (2000) Chronic epileptogenesis requires development of a network of pathologically interconnected neuron clusters: a hypothesis. *Epilepsia* **41** (Suppl. 6): S144–S152.

Branch, C.L. and Martin, A.R. (1958) Inhibition of Betz cell activity by thalamic and cortical stimulation. *Journal of Neurophysiology* **21**: 380–390.

Bratz, E. (1899) Ammonshornbefunde bei Epileptischen. *Archives für Psychiatrie und Nervenkrankheiten* **31**: 820–835.

Braun, A.R., Balkin, T.J., Wesensten, N.J., Carson, R.E., Varga, M., Baldwin, P., Selbie, S., Belenky, G. and Herscovitch, P. (1997) Regional cerebral blood flow throughout the sleep-wake cycle. *Brain* **120**: 1173–1197.

Brazier, M.A.B. (1961) *A History of the Electrical Activity of the Brain.* London: Pitman.

Bremer, F. (1935) Cerveau "isolé" et physiologie du sommeil. *Comptes Rendus de la Société de Biologie (Paris)* **118**: 1235–1241.

Bremer, F. (1937) L'activité cérébrale au cours du sommeil et de la narcose. Contribution à l'étude du mécanisme du sommeil. *Bulletin de l'Académie Royale de Médecine de Belgique* **4**: 68–86.

Bremer, F. (1949) Considérations sur l'origine et la nature des "ondes" cérébrales. *Electroencephalography and Clinical Neurophysiology* **1**: 177–193.

Bremer, F. (1958a) Cerebral and cerebellar potentials. *Physiological Reviews* **38**: 357–388.

Bremer, F. (1958b) Le processus d'excitation et d'inhibition dans les phénomènes épileptiques. In *Bases Physiologiques et Aspects Cliniques de l'Épilepsie*, ed. T. Alajouanine, pp. 1–35, Paris: Masson.

Bremer, F. (1973) Preoptic hypnogenic area and reticular activating system. *Archives Italiennes de Biologie* **111**: 85–111.

Bremer, F. (1975) The isolated brain and its aftermath. In *The Neurosciences: Paths of Discovery*, ed. F.G. Worden, J.P. Swazey and G.A. Adelman, pp. 267–274. Cambridge, MA: The MIT Press.

Bremer, F., Stoupel, N. and Van Reeth, P.C. (1960) Nouvelles recherches sur la facilitation et l'inhibition des potentiels évoqués corticaux dans l'éveil réticulaire. *Archives Italiennes de Biologie* **98**: 229–247.

Bringuier, V., Frégnac, Y., Baranyi, A., Debanne, D. and Shulz, D.E. (1997) Synaptic origin and stimulus dependency of neuronal oscillatory activity in the primary visual cortex of the cat. *Journal of Physiology (London)* **500**: 751–774.

Brown, A.M., Schwindt, P.C. and Crill, W.E. (1993) Voltage dependence and activation kinetics of pharmacologically defined components of high-threshold calcium current in rat neocortical neurons. *Journal of Neurophysiology* **70**: 1530–1543.

Brown, R.E., Sergeeva, O.A., Eriksson, K.S. and Haas, H.L. (2002) Convergent excitation of dorsal raphe serotonin neurons by multiple arousal systems (orexin/hypocretin, histamine and noradrenaline). *Journal of Neuroscience* **22**: 8850–8859.

Browne, S.H., Kang, J., Akk, G., Chiang, L.W., Schulman, H., Huguenard, J.R. and Prince, D.A. (2001) Kinetic and pharmacological properties of $GABA_A$ receptors in single thalamic neurons and $GABA_A$ subunit expression. *Journal of Neurophysiology* **86**: 2312–2322.

Browning, R.A. and Nelson, D.K. (1986) Modification of electroshock and pentylenetetrazol seizure patterns in rats after precollicular transections. *Experimental Neurology* **93**: 546–556.

Browning, R., Maggio, R., Sahibzada, N. and Gale, K. (1993) Role of brainstem structures in seizures initiated from the deep prepiriform cortex of rats. *Epilepsia* **34**: 393–407.

Brumberg, J.C., Nowak, L.G. and McCormick, D.A. (2000) Ionic mechanisms underlying repetitive high-frequency burst firing in supragranular cortical neurons. *Journal of Neuroscience* **20**: 4829–4943.

Buchhalter, J.R. (1993) Animal models of inherited epilepsy. *Epilepsia* **34** (Suppl. 3): S31–S41.

Buckmaster, P.S., Jongen-Rêlo, A.L., Davari, S.B. and Wong, E.H. (2000) Testing the disinhibition hypothesis of epileptogenesis *in vivo* and during spontaneous seizures. *Journal of Neuroscience* **20**: 6232–6240.

Budde, T., Mager, R. and Pape, H.C. (1992) Different types of potassium outward current in relay neurons acutely isolated from the lateral geniculate nucleus. *European Journal of Neuroscience* **4**: 708–722.

Buhl, E.H., Otis, T.S. and Mody, I. (1996) Zinc-induced collapse of augmented inhibition by GABA in a temporal lobe epilepsy model. *Science* **271**: 369–373.

Bullock, T.H. (1997) Signals and signs in the nervous system: the dynamic anatomy of electrical activity is probably information-rich. *Proceedings of the National Academy of Sciences of the USA* **94**: 1–6.

Burns, B.D. (1951) Some properties of isolated cerebral cortex in the unanaesthetised cat. *Journal of Physiology (London)* **112**: 156–175.

Burns, B.D. (1958) *The Mammalian Cortex*. London: Monographs of the Physiological Society.

Burnstine, T.H., Vining, E.P., Uematsu, S. and Lesser, R.P. (1991) Multifocal independent epileptiform discharges in children: ictal correlates and surgical therapy. *Neurology* **41**: 1223–1228.

Bush, P.C., Prince, D.A. and Miller, K.D. (1999) Increased pyramidal excitability and NMDA conductance can explain posttraumatic epileptogenesis without disinhibition: a model. *Journal of Neurophysiology* **82**: 1748–1758.

Buzsáki, G. (1989) Two-stage model of memory trace formation: a role for "noisy" brain states. *Neuroscience* **31**: 551–570.

Buzsáki, G. (1990) Petit-mal epilepsy and parkinsonian tremor: hypothesis of a common pacemaker. *Neuroscience* **36**: 1–14.

Buzsáki, G. (1998) Memory consolidation during sleep: a neurophysiological perspective. *Journal of Sleep Research* **7** (Suppl. 1): 17–23.

Buzsáki, G. (2002) Theta oscillations in the hippocampus. *Neuron*, **33**: 325–340.

Buzsáki, G. and Chrobak, J.J. (1995) Temporal structure in spatially organized neuronal ensembles: a role for interneuron networks. *Current Opinion in Neurobiology* **5**: 504–510.

Buzsáki, G., Grastyan, E., Tveritskaya, I. and Czopf, J. (1979) Hippocampal evoked potentials and EEG changes during classical conditioning in the rat. *Electroencephalography and Clinical Neurophysiology* **47**: 64–74.

Buzsáki, G., Leung, L. and Vanderwolf, C.H. (1983) Cellular bases of hippocampal EEG in the behaving rat. *Brain Research Reviews* **6**: 139–171.

Buzsáki, G., Bickford, R.G., Armstrong, D.M., Ponomareff, G., Chen, K.S., Ruiz, R., Thal, L.G. and Gage, F.H. (1988a) Electrical activity in the neocortex of freely moving young and aged rats. *Neuroscience* **26**: 735–744.

Buzsáki, G., Bickford, R.G., Ponomareff, G., Thal, L.J., Mandel, R. and Gage, F.H. (1988b) Nucleus basalis and thalamic control of neocortical activity in the freely moving rat. *Journal of Neuroscience* **8**: 4007–4026.

Buzsáki, G., Kennedy, B., Solt, V.B. and Ziegler, M. (1991) Noradrenergic control of thalamic oscillations: the role of α-2 receptors. *European Journal of Neuroscience* **3**: 222–229.

Buzsáki, G., Penttonen, M., Nádasdy, Z. and Bragin, A. (1996) Pattern and inhibition-dependent invasion of pyramidal cell dendrites by fast spikes in the hippocampus *in vivo*. *Proceedings of the National Academy of Sciences of the USA* **93**: 9921–9925.

Cadilhac, J., Vlahovitch, B. and Delange, M. (1965) Considerations on the changes in epileptic discharges during the phase of eye movements. *Electroencephalography and Clinical Neurophysiology* **18**: 96.

Calvet, J., Calvet, M.C. and Scherrer, J. (1964) Etude stratigraphique corticale de l'activité EEG spontanée. *Electroencephalography and Clinical Neurophysiology* **17**: 109–125.

Cannon, W.B. and Rosenblueth, A. (1949) *The Supersensitivity of Denervated Structures: A Law of Denervation.* New York: Macmillan.

Canu, M.H. and Rougeul, A. (1992) Nucleus reticularis thalami participates in sleep spindles, not in beta rhythms concomitant with attention in cat. *Comptes Rendus de l'Académie des Sciences (Paris)* **315**: 513–520.

Cape, E.G. and Jones, B.E. (1998) Differential modulation of high-frequency γ-electroencephalogram activity and sleep-wake state by noradrenaline and serotonin microinjections into the region of cholinergic basalis neurons. *Journal of Neuroscience* **18**: 2653–2666.

Cape, E.G. and Jones, B.E. (2000) Effects of glutamate versus procaine microinjections into the basal forebrain cholinergic cell area upon gamma and theta EEG activity and sleep-wake state. *European Journal of Neuroscience* **12**: 2166–2184.

Carlen, P., Perez-Velazquez, J.L., Valiante, T.A., Jahromi, S.S. and Bardakjian, B.L. (1996) Electric coupling in epileptogenesis. In *Gap Junctions in the Nervous System*, ed. D.C. Spray and R. Dermietzel, pp. 289–299, Austin, TX: Landes Company.

Carli, G., Diete-Spiff, K. and Pompeiano, O. (1967) Presynaptic and postsynaptic inhibition of transmission of somatic afferent volleys through the cuneate nucleus during sleep. *Archives Italiennes de Biologie* **105**: 52–82.

Carskadon, M.A. and Dement, W.C. (2000) Normal human sleep: an overview. In *Principles and Practice of Sleep Medicine*, ed. M.H. Kryger, T. Roth and W.C. Dement, pp. 15–25, Philadelphia: W.B. Saunders.

Cassidi, R.M. and Gale, K. (1998) Mediodorsal thalamus plays a critical role in the development of limbic motor seizures. *Journal of Neuroscience* **18**: 9002–9009.

Castaigne, P., Buge, A., Escourolle, R. and Mason, M. (1962) Ramollissement pédonculaire médian, tegmentothalamique avec ophtalmoplégie et hypersomnie. *Revue Neurologique (Paris)* **106**: 357–367.

Castro-Alamancos, M. (1999) Neocortical synchronized oscillations induced by thalamic disinhibition *in vivo*. *Journal of Neuroscience* (online) **19**: RC27.

Castro-Alamancos, M. (2002a) Different temporal processing of sensory inputs in the rat thalamus during quiescent and information processing states *in vivo*. *Journal of Physiology (London)* **539**: 567–578.

Castro-Alamancos, M. (2002b) Properties of primary sensory (lemniscal) synapses in the ventrobasal thalamus and the relay of high-frequency sensory inputs. *Journal of Neurophysiology* **87**: 946–953.

Castro-Alamancos, M. and Calcagnotto, M.E. (2001) High-pass filtering of corticothalamic activity by neuromodulators released in the thalamus during arousal: *in vitro* and *in vivo*. *Journal of Neurophysiology* **85**: 1489–1497.

Castro-Alamancos, M.A. and Connors, B.W. (1996a) Short-term plasticity of a thalamocortical pathway dynamically modulated by behavioral state. *Science* **272**: 274–277.

Castro-Alamancos, M.A. and Connors, B.W. (1996b) Spatiotemporal properties of short-term plasticity in sensorimotor thalamocortical pathways of the rat. *Journal of Neuroscience* **16**: 2767–2779.

Castro-Alamancos, M.A. and Connors, B.W. (1996c) Cellular mechanisms of the augmenting response: short-term plasticity in a thalamocortical pathway. *Journal of Neuroscience* **16**: 7742–7756.

Caton, R. (1875) The electric currents of the brain. *British Medical Journal* **2**: 278.

Caton, R. (1887) Interim report on investigations of the electric currents of the brain. *British Medical Journal* (Suppl. 1): 62.

Cauli, B., Audinat, E., Lambolez, B., Angulo, M.C., Ropert, N., Tauzuki, K., Hestrin, S. and Rossier, J. (1997) Molecular and physiological diversity of cortical nonpyramidal cells. *Journal of Neuroscience* **17**: 3894–3906.

Cauller, L.J. and Connors, B.W. (1994) Synaptic physiology of horizontal afferents in layer I in slices of rat SI neocortex. *Journal of Neuroscience* **14**: 751–762.

Cavazzuti, G.B., Ferrari, F., Galli, V. and Benatti, A. (1989) Epilepsy with typical absence seizures with onset during the first year of life. *Epilepsia* **30**: 802–806.

Celio, M.R. (1986) Parvalbumin in most gamma-aminobutyric acid-containing neurons of rat cerebral cortex. *Science* **231**: 995–997.

Cespuglio, R., Gomez, M.E., Walker, E. and Jouvet, M. (1979) Effets du refroidissement et de la stimulation des noyaux du système du raphé sur les états de vigilance chez le chat. *Electroencephalography and Clinical Neurophysiology* **47**: 289–308.

Cespuglio, R., Faradji, H., Hahn, Z. and Jouvet, M. (1984) Voltammetric detection of brain 5-hydroxyindolamines by means of electrochemically treated carbon fibre electrodes: chronic recordings for up to one month with movable cerebral electrodes in the sleeping or waking rat. In *Measurement of Neurotransmitter Release in Vivo* (IBRO Handbook Series, vol. 6), ed. C.A. Marsden, pp. 173–191, New York: Wiley.

Chagnac-Amitai, Y. and Connors, B.W. (1989) Synchronized excitation and inhibition driven by bursting neurons in neocortex. *Journal of Neurophysiology* **62**: 1149–1162.

Chagnac-Amitai, Y., Luhmann, H.J. and Prince, D.A. (1990) Burst generating and regular spiking layer 5 pyramidal neurons of rat neocortex have different morphological features. *Journal of Comparative Neurology* **296**: 598–613.

Chamberlin, N.L., Traub, R.D. and Dingledine, R. (1990) Role of EPSPs in initiation of spontaneous synchronized burst firing in rat hippocampal neurons bathed in high potassium. *Journal of Neurophysiology* **64**: 1000–1008.

Chandler, S.H., Chase, M.H. and Nakamura, Y. (1980) Intracellular analysis of synaptic mechanisms controlling trigeminal motoneurons activity during sleep and wakefulness. *Journal of Neurophysiology* **44**: 359–371.

Chang, H.T. (1950) The repetitive discharges of corticothalamic reverberating circuit. *Journal of Neurophysiology* **13**: 235–257.

Charnay, Y., Bouras, C., Vallet, P.G., Golaz, J., Guntern, R. and Constantinidis, J. (1989) Immunohistochemical colocalization of delta-sleep-inducing peptide and luteinizing hormone-releasing hormone in rabbit brain neurons. *Neuroscience* **31**: 495–505.

Charpier, S., Leresche, N., Deniau, J.M., Mahon, S., Hughes, S.W. and Crunelli, V. (1999) On the putative contribution of $GABA_B$ receptors to the electrical events occurring during spontaneous spike and wave discharges. *Neuropharmacology* **38**: 1699–1706.

Chase, M.H. and Morales, F.R. (1983) Subthreshold excitatory activity and motoneuron discharge during REM periods of active sleep. *Science* **221**: 1195–1198.

Chase, M.H., Chandler, S.H. and Nakamura, Y. (1980) Intracellular determination of membrane potential of trigeminal motoneurons during sleep and wakefulness. *Journal of Neurophysiology* **44**: 349–358.

Chen, K., Baram, T.Z. and Soltesz, I. (1999) Febrile seizures in the developing brain result in persistent modifications of neuronal excitability in limbic circuits. *Nature Medicine* **5**: 888–894.

Chen, W., Zhang, J.J., Hu, G.Y. and Wu, C.P. (1996) Electrophysiological and morphological properties of pyramidal and non-pyramidal neurons in the cat motor cortex *in vitro*. *Neuroscience* **73**: 39–55.

Cherubini, E., Gaiarsa, J.L. and Ben-Ari, Y. (1991) GABA: an excitatory transmitter in early postnatal life. *Trends in Neurosciences* **14**: 515–519.

Chervin, R.D., Pierce, P.A. and Connors, B.W. (1988) Periodicity and directionality in the propagation of epileptiform discharges across neocortex. *Journal of Neurophysiology* **60**: 1695–1713.

Chou, T.C., Bjorkum, A.A., Gaus, S.E., Lu, J., Scammel, T.E. and Saper, C.B. (2002) Afferents to the ventrolateral preoptic nucleus. *Journal of Neuroscience* **22**: 977–990.

Chow, A., Erisir, A., Farb, C., Nadal, M.S., Ozaita, A., Lau, D., Welker, E. and Rudy, B. (1999) K^+ channel expression distinguishes subpopulations of parvalbumin- and somatostatin-containing neocortical interneurons. *Journal of Neuroscience* **19**: 9332–9345.

Chrobak, J.J. and Buzsáki, G. (1996) High-frequency oscillations in the output networks of the hippocampal-entorhinal axis of the freely behaving rat. *Journal of Neuroscience* **16**: 3056–3066.

Chronin, E.P. and Dudek, F.E. (1988) Chronic seizures and collateral sprouting of dentate mossy fibers after kainic acid treatment in rats. *Brain Research* **474**: 181–184.

Chung, J.M., Huguenard, J.R. and Prince, D.A. (1993) Transient enhancement of low-threshold calcium current in thalamic relay neurons after corticectomy. *Journal of Neurophysiology* **70**: 1–7.

Cirelli, C. and Tononi, G. (2000) Differential expression of plasticity-related genes in waking and sleep and their regulation by the noradrenergic system. *Journal of Neuroscience* **20**: 9187–9194.

Cirelli, C., Pompeiano, M. and Tononi, G. (1996) Neuronal gene expression in the waking state: a role for locus coeruleus. *Science* **274**: 1211–1215.

Cissé, Y., Timofeev, I., Grenier, F. and Steriade, M. (2001) Intracellular pairing with synaptic activation leads to neocortical plasticity. *Society for Neuroscience Abstracts* **27**: 366.

Cissé, Y., Grenier, F., Timofeev, I. and Steriade, M. (2003) Electrophysiological properties and input-output organization of callosal neurons in cat association cortex. *Journal of Neurophysiology*, in press.

Claes, E. (1939) Contribution à l'étude physiologique de la fonction visuelle. I. Analyse oscillographique de l'activité spontanée et sensorielle de l'aire visuelle corticale chez le chat non anesthésié. *Archives Internationales de Physiologie* **48**: 1181–1237.

Claparède, E. (1905) Esquisse d'une théorie biologique du sommeil. *Archives de Psychologie* **4**: 246–349.

Clemens, B. and Majoros, E. (1987) Sleep studies in benign epilepsy of childhood with rolandic spikes. II. Analysis of discharge frequency and its relation to sleep dynamics. *Epilepsia* **28**: 24–27.

Clements, J.R. and Grant, S. (1990) Glutamate-like immunoreactivity in neurons of the laterodorsal tegmental and pedunculopontine nuclei in the rat. *Neuroscience Letters* **120**: 70–73.

Cobb, S. (1947) Photic driving as a cause of clinical seizures in epileptic patients. *Archives of Neurology and Psychiatry (Chicago)* **58**: 70–71.

Cobb, S.R., Buhl, E.H., Halasy, K., Paulsen, O. and Somogyi, P. (1995) Synchronization of neuronal activity in hippocampus by individual GABAergic interneurons. *Nature* **378**: 811–817.

Coenen, A.M.L. and Vendrik, A.J.H. (1972) Determination of the transfer ratio of cat's geniculate neurons through quasi-intracellular recordings and the relation with the level of alertness. *Experimental Brain Research* **14**: 227–242.

Colder, B.W., Wilson, C.L., Frysinger, R.C., Chao, L.C., Harper, R.M. and Engel, J. Jr. (1996) Neuronal synchrony in relation to burst discharge in epileptic human temporal lobes. *Journal of Neurophysiology* **75**: 2496–2508.

Collins, D.R., Lang, E.J. and Paré, D. (1999) Spontaneous activity of the perirhinal cortex in behaving cats. *Neuroscience* **89**: 1025–1039.

Collins, D.R., Pelletier, J.G. and Paré, D. (2001) Slow and fast (gamma) neuronal oscillations in the perirhinal cortex and lateral amygdala. *Journal of Neurophysiology* **85**: 1661–1672.

Collins, R.L. (1975) Audiogenic seizures. In *Experimental Models of Epilepsy*, ed. D.P. Purpura, J.K. Penry, D.B. Tower, D.M. Woodbury and R.D. Walter, pp. 347–372, New York: Raven Press.

Colonnier, M. (1966) The structural design of the neocortex. In *Brain and Conscious Experience*, ed. J.C. Eccles, pp. 1–23, New York: Springer.

Colonnier, M. (1968) Synaptic patterns on different cell types in the different laminae of the visual cortex. An electron microscope study. *Brain Research* **9**: 268–287.

Coombs, S.J., Eccles, J.C. and Fatt, P. (1955) The electrical properties of the motoneurone membrane. *Journal of Physiology (London)* **130**: 291–325.

Connors, B.W. (1984) Initiation of synchronized neuronal bursting in neocortex. *Nature* **310**: 685–687.

Connors, B.W. and Amitai, Y. (1995) Functions of local circuits in neocortex: synchrony and laminae. In *The Cortical Neuron*, ed. M.J. Gutnick and I. Mody, pp. 123–140, New York: Oxford University Press.

Connors, B.W. and Gutnick, M.J. (1990) Intrinsic firing patterns of diverse neocortical neurons. *Trends in Neurosciences* **13**: 99–104.

Connors, B.W. and Prince, D.A. (1982) Effects of local anesthetic QX-314 on the membrane properties of hippocampal pyramidal neurons. *Journal of Pharmacology and Experimental Therapy* **220**: 476–481.

Connors, B.W., Gutnick, M.J. and Prince, D.A. (1982) Electrophysiological properties of neocortical neurons *in vitro*. *Journal of Neurophysiology* **48**: 1302–1320.

Connors, B.W., Malenka, R. and Silva, L.R. (1988) Two inhibitory postsynaptic potentials, and $GABA_A$ and $GABA_B$ receptor-mediated responses in neocortex of rat and cat. *Journal of Physiology (London)* **406**: 443–468.

Consolazione, A., Priestley, J.V. and Cuello, A.C. (1984) Serotonin-containing projections to the thalamus in the rat revealed by a horseradish peroxidase and peroxidase antiperoxidase double-staining technique. *Brain Research* **322**: 233–243.

Contreras, D. and Llinás, R. (2001) Voltage-sensitive dye imaging of neocortical spatio-temporal dynamics to afferent activation frequency. *Journal of Neuroscience* **21**: 9403–9413.

Contreras, D. and Steriade, M. (1995) Cellular basis of EEG slow rhythms: a study of dynamic corticothalamic relationships. *Journal of Neuroscience* **15**: 604–622.

Contreras, D. and Steriade, M. (1996) Spindle oscillation: the role of corticothalamic feedback in a thalamically generated rhythm. *Journal of Physiology (London)* **490**: 159–179.

Contreras, D., Curró Dossi, R. and Steriade, M. (1992) Bursting and tonic discharges in two classes of reticular thalamic neurons *in vivo*. *Journal of Neurophysiology* **68**: 973–977.

Contreras, D., Curró Dossi, R. and Steriade, M. (1993) Electrophysiological properties of cat reticular neurones *in vivo*. *Journal of Physiology (London)* **470**: 273–294.

Contreras, D., Destexhe, A., Sejnowski, T.J. and Steriade, M. (1996a) Control of spatiotemporal coherence of a thalamic oscillation by corticothalamic feedback. *Science* **274**: 771–774.

Contreras, D., Timofeev, I. and Steriade, M. (1996b) Mechanisms of long-lasting hyperpolarizations underlying slow sleep oscillations in cat corticothalamic networks. *Journal of Physiology (London)* **494**: 251–264.

Contreras, D., Destexhe, A., Sejnowski, T.J. and Steriade, M. (1997a) Spatiotemporal patterns of spindle oscillations in cortex and thalamus. *Journal of Neuroscience* **17**: 1179–1196.

Contreras, D., Destexhe, A. and Steriade, M. (1997b) Spindle oscillations during cortical spreading depression in naturally sleeping cats. *Neuroscience* **77**: 933–996.

Contreras, D., Destexhe, A. and Steriade, M. (1997c) Intracellular and computational characterization of the intracortical inhibitory control of synchronized thalamic inputs in vivo. *Journal of Neurophysiology* **78**: 335–350.

Contreras, D., Dürmüller, N. and Steriade, M. (1997d) Absence of a prevalent laminar distribution of IPSPs in association cortical neurons of cat. *Journal of Neurophysiology* **78**: 2742–2753.

Corner, M.A., van Pelt, J., Wolters, P.S., Baker, R.E. and Nuytinck, R.H. (2002) Physiological effects of sustained blockade of excitatory synaptic transmission on spontaneously active developing neuronal networks – an inquiry into the reciprocal linkage between intrinsic biorhythms and neuroplasticity in early ontogeny. *Neuroscience and Behavioral Reviews* **26**: 127–185.

Cossart, R., Dinocourt, C., Hirsch, J., Merchan-Perez, A., De Felipe, J., Ben-Ari, Y., Esclapez, M. and Bernard, C. (2001) Dendritic but not somatic GABAergic inhibition is decreased in experimental epilepsy. *Nature Neuroscience* **4**: 52–62.

Coulter, D.A. (1999) Chronic epileptogenic cellular alterations in the limbic system after status epilepticus. *Epilepsia* **40** (Suppl. 1): S23–S33.

Coulter, D.A., Huguenard, J.R. and Prince, D.A. (1989) Characterization of ethosuximide reduction of low-threshold calcium current in thalamic neurons. *Annals of Neurology* **25**: 582–593.

Cowan, R.L. and Wilson, C.J. (1994) Spontaneous firing patterns and axonal projections of single corticostriatal neurons in the rat medial agranular cortex. *Journal of Neurophysiology* **71**: 17–32.

Cragg, B.G. (1975) The development of synapses in the visual system of the cat. *Journal of Comparative Neurology* **160**: 147–166.

Creutzfeldt, O.D., Watanabe, S. and Lux, H.D. (1966) Relations between EEG phenomena and potentials of single cortical cells. I. Evoked responses after thalamic and epicortical stimulation. *Electroencephalography and Clinical Neurophysiology* **20**: 1–18.

Crill, W.E. (1996) Persistent sodium current in mammalian central neurons. *Annual Reviews of Physiology* **58**: 349–362.

Crochet, S. and Sakai, K. (1999) Effects of microdialysis application of monoamines on the EEG and behavioural states in the cat mesopontine tegmentum. *European Journal of Neuroscience* **11**: 3738–3752.

Crowne, D.P. and Radcliffe, D.D. (1975) Some characteristics and functional relations of the electrical activity of the primate hippocampus and hypotheses of hippocampal function. In *The Hippocampus*, ed. R.L. Isaacson and J.H. Pribram, pp. 185–203, New York: Plenum.

Crunelli, V. and Leresche, N. (1991) A role for $GABA_B$ receptors in excitation and inhibition of thalamocortical neurons. *Trends in Neuroscience* **14**: 16–21.

Crunelli, V. and Leresche, N. (2002) Childhood absence epilepsy: genes, channels, neurons and networks. *Nature Reviews Neuroscience* **3**: 371–382.

Crunelli, V., Kelly, J.S., Leresche, N. and Pirchio, M. (1987) The ventral and dorsal lateral geniculate nucleus of the rat: intracellular recordings *in vitro*. *Journal of Physiology (London)* **384**: 587–601.

Crunelli, V., Haby, M., Jassik-Gerschenfeld, D., Leresche, N. and Pirchio, M. (1988) Cl^- and K^+-dependent inhibitory postsynaptic potentials evoked by interneurons of the rat lateral geniculate nucleus. *Journal of Physiology (London)* **399**: 153–176.

Csicsvari, J., Hirase, H., Czurkó, A. and Buzsáki, G. (1998) Reliability and state dependence of pyramidal cell – interneuron synapses in the hippocampus: an ensemble approach in the behaving rat. *Neuron* **21**: 179–189.

Csicsvari, J., Hirase, H., Czurkó, A., Mamiya, A. and Buzsáki, G. (1999) Fast network oscillations in the hippocampal CA1 region of the behaving rat. *Journal of Neuroscience* **19**: RC20 (1–4), 1999.

Cunningham, E.T. and LeVay, S. (1986) Laminar and synaptic organization of the projection from the thalamic nucleus centralis to primary visual cortex in the cat. *Journal of Comparative Neurology* **254**: 65–77.

Curró Dossi, R., Paré, D. and Steriade, M. (1991) Short-lasting nicotinic and long-lasting muscarinic depolarizing responses of thalamocortical neurons to stimulation of mesopontine cholinergic nuclei. *Journal of Neurophysiology* **65**: 393–406.

Curró Dossi, R., Nuñez, A. and Steriade, M. (1992a) Electrophysiology of a slow (0.5–4 Hz) intrinsic oscillation of cat thalamocortical neurones *in vivo*. *Journal of Physiology (London)* **447**: 215–234.

Curró Dossi, R., Paré, D. and Steriade, M. (1992b) Various types of inhibitory postsynaptic potentials in anterior thalamic cells are differentially altered by stimulation of laterodorsal tegmental cholinergic nucleus. *Neuroscience* **47**: 279–289.

Curtis, D.R. and Eccles, J.C. (1960) Synaptic action during and after repetitive stimulation. *Journal of Physiology (London)* **150**: 374–398.

Daikoku, S., Kawano, H., Noguchi, M., Nakanishi, J., Tokuzen, M., Chihara, K. and Nagatsu, I. (1986) GRF neurons in the rat hypothalamus. *Brain Research* **399**: 250–261.

Dalla Bernardina, B. and Berghini, G. (1976) Rolandic spikes in children with or without epilepsy (20 subjects polygraphically studied during sleep). *Epilepsia* **17**: 161–167.

Danober, L. and Pape, H.C. (1998) Strychnine-sensitive glycine responses in neurons of the lateral amygdala: an electrophysiological and immunocytochemical characterization. *Neuroscience* **85**: 427–441.

Danober, L., Depaulis, A., Marescaux, C. and Vergnes, M. (1993) Effects of cholinergic drugs on genetic absence seizures in rats. *European Journal of Pharmacology* **234**: 263–268.

Danober, L., Vergnes, M., Depaulis, A. and Marescaux, C. (1994) Nucleus basalis lesions suppress spike and wave discharges in rats with spontaneous absence epilepsy. *Neuroscience* **59**: 531–539.

Danober, L., Depaulis, A., Vergnes, M. and Marescaux, C. (1995) Mesopontine cholinergic control over generalized non-convulsive seizures in a genetic model of absence epilepsy in the rat. *Neuroscience* **69**: 1183–1193.

Danober, L., Deransart, C., Depaulis, A., Vergnes, M. and Marescaux, C. (1998) Pathophysiological mechanisms of genetic absence epilepsy in the rat. *Progress in Neurobiology* **55**: 27–57.

Datta, S., Curró Dossi, R., Paré, D., Oakson, G. and Steriade, M. (1991) Substantia nigra reticulata neurons during sleep-waking states: relation with ponto-geniculo-occipital waves. *Brain Research* **566**: 344–347.

Davenport, C.J., Brown, W.J. and Babb, T.L. (1990) Sprouting of GABAergic and mossy fibers axons in the dentate gyrus following intrahippocampal kainate in the rats. *Experimental Neurology* **109**: 180–190.

Dawson, T.M., Bredt, D.S., Fotuhi, M., Hwang, P.M. and Snyder, S.H. (1991) Nitric oxide synthase and neuronal NADPH diaphorase are identical in brain and peripheral tissues. *Proceedings of the National Academy of Sciences of the USA* **88**: 7797–7801.

Deans, M.R., Gibson, J.R., Sellitto, C., Connors, B.W. and Paul, D.L. (2001) Synchronous activity of inhibitory networks in neocortex requires electrical synapses containing connexin36. *Neuron* **31**: 477–485.

Debarbieux, F., Brunton, J. and Charpak, S. (1998) Effect of bicuculline in thalamic activity: a direct blockade of I_{AHP} in reticularis neurons. *Journal of Neurophysiology* **79**: 2911–2918.

De Curtis, M. and Avanzini, G. (2001) Interictal spikes in focal epileptogenesis. *Progress in Neurobiology* **63**: 541–567.

DeFelipe, J. (1993) Neocortical neuronal diversity: chemical heterogeneity revealed by co-localization studies of classic transmitters, neuropeptides, calcium-binding proteins and cell surface molecules. *Cerebral Cortex* **3**: 273–289.

DeFelipe, J. (1999) Chandelier cells and epilepsy. *Brain* **122**: 1807–1822.

DeFelipe, J. and Farinas, I. (1992) The pyramidal neuron of the cerebral cortex: morphological and chemical characteristics of the synaptic inputs. *Progress in Neurobiology* **39**: 563–607.

Dégenètais, E., Thierry, A.M., Glowinski, J. and Gioanni, Y. (2002) Electrophysiological properties of pyramidal neurons in the rat prefrontal cortex: an *in vivo* intracellular recording study. *Cerebral Cortex* **12**: 1–16.

De Gennaro, L., Ferrara, M. and Bertini, M. (2001) The boundary between wakefulness and sleep: quantitative electroencephalographic changes during the sleep onset period. *Neuroscience* **107**: 1–11.

Deiber, M.P., Ibanez, V., Bastuji, H., Fischer, C. and Mauguière, F. (1988) Changes of middle latency auditory evoked potentials during natural sleep in humans. *Neurology* **39**: 806–813.

Deisz, R.A., Billard, J.M. and Zieglgänsberger, W. (1997) Presynaptic and postsynaptic GABAB receptors of neocortical neurons of the rat *in vitro*: differences in pharmacology and ionic mechanisms. *Synapse* **25**: 62–72.

DeLanerolle, N., Kim, J., Robbins, R. and Spencer, D. (1989) Hippocampal interneuron loss and plasticity in human temporal lobe epilepsy. *Brain Research* **495**: 387–395.

Dell, P. and Padel, Y. (1965) Rapid falling asleep provoked by selective stimulation of vagal afferents in the cat. *Electroencephalography and Clinical Neurophysiology* **18**: 725.

Delphs, J.R. and Dichter, M.A. (1983) Effects of somatostatin on mammalian cortical neurons in culture: physiological actions and unusual dose response characteristics. *Journal of Neuroscience* **3**: 1176–1188.

Dement, W.C. (2001) Remembering Nathaniel Kleitman. *Archives Italiennes de Biologie* **139**: 11–17.

Dement, W.C. and Kleitman, N. (1957) Cyclic variations in EEG during sleep and their relation to eye movements, body motility, and dreaming. *Electroencephalography and Clinical Neurophysiology* **9**: 673–690.

Dement, W.C., Hendricksen, S., Jacobs, B.L. and Mitler, M.M. (1973) Biogenic amines, phasic events, and behavior. In *Pharmacology and the Future of Man*, ed. F.E. Bloom and G.H. Acheson, pp. 74–89, New York: Karger.

Dempsey, E.W. and Morison, R.S. (1942) The production of rhythmically recurrent cortical potentials after localized thalamic stimulation. *American Journal of Physiology* **135**: 293–300.

Denti, A., McGaugh, J.L., Landfield, P.W. and Shinkman, P.G. (1970) Effects of posttrial electrical stimulation of the mesencephalic reticular formation on avoidance learning in rats. *Physiology and Behavior* **5**: 659–662.

Deransart, C., Lé-Pham, B.T., Hirsch, E., Marescaux, C. and Depaulis, A. (2001) Inhibition of the substantia nigra suppresses absences and clonic seizures in audiogenic rats, but not tonic seizures: evidence for seizure specificity of the nigral control. *Neuroscience* **105**: 203–211.

Dermietzel, R. and Spray, D.C. (1993) Gap junctions in the brain: where, what type, how many and why? *Trends in Neurosciences* **16**: 186–192.

Descarries, L., Gisiger, V. and Steriade, M. (1997) Diffuse transmission by acetylcholine in the CNS. *Progress in Neurobiology* **53**: 603–625.

Deschênes, M. and Hu, B. (1990) Electrophysiology and pharmacology of the corticothalamic input to lateral thalamic nuclei: an intracellular study in the cat. *European Journal of Neuroscience* **2**: 140–152.

Deschênes, M., Paradis, M., Roy, J.P. and Steriade, M. (1984) Electrophysiology of neurons of lateral thalamic nuclei in cat: resting properties and burst discharges. *Journal of Neurophysiology* **51**: 1196–1219.

Deschênes, M., Madariaga-Domich, A. and Steriade, M. (1985) Dendrodendritic synapses in cat reticularis thalami nucleus, a structural basis for thalamic spindle synchronization. *Brain Research* **334**: 169–171.

Desmedt, J.E. (1981) Scalp-recorded cerebral event-related potentials in man as point of entry into the analysis of cognitive processing. In *The Organization of the Cerebral Cortex*, ed. F.O. Schmitt, F.G. Worden, G. Adelman and S.G. Dennis, pp. 441–473, Cambridge, MA: The MIT Press.

Desmedt, J.E. and Tomberg, C. (1994) Transient phase-locking of 40 Hz electrical oscillations in prefrontal and parietal human cortex reflects the process of conscious somatic perception. *Neuroscience Letters* **168**: 126–129.

Destexhe, A. (1998) Spike-and-wave oscillations based on the properties of $GABA_B$ receptors. *Journal of Neuroscience* **18**: 9099–9111.

Destexhe, A. and Paré, D. (1999) Impact of network activity on the integrative properties of neocortical pyramidal neurons *in vivo*. *Journal of Neurophysiology* **81**: 1531–1547.

Destexhe, A. and Sejnowski, T.J. (2001) *Thalamocortical Assembly.* Oxford: Oxford University Press.

Destexhe, A., Contreras, D., Sejnowski, T.J. and Steriade, M. (1994a) A model of spindle rhythmicity in the isolated thalamic reticular nucleus. *Journal of Neurophysiology* **72**: 803–818.

Destexhe, A., Contreras, D., Sejnowski, T.J. and Steriade, M. (1994b) Modeling the control of reticular thalamic oscillations by neuromodulators. *NeuroReport* **5**: 2217–2220.

Destexhe, A., Contreras, D. Steriade, M., Sejnowski, T.J. and Huguenard, J.R. (1996) *In vivo*, *in vitro* and computational analysis of dendritic calcium currents in thalamic reticular neurons. *Journal of Neuroscience* **16**: 169–185.

Destexhe, A., Contreras, D., and Steriade, M. (1998) Mechanisms underlying the synchronizing action of corticothalamic feedback through inhibition of thalamic relay cells. *Journal of Neurophysiology* **79**: 999–1016.

Destexhe, A., Contreras, D. and Steriade, M. (1999a) Neocortical excitability controls the coherence of thalamic-generated oscillations through corticothalamic feedback. *Neuroscience* **92**: 427–443.

Destexhe, A., Contreras, D. and Steriade, M. (1999b) Spatiotemporal analysis of local field potentials and unit discharges in cat cerebral cortex during natural wake and sleep states. *Journal of Neuroscience* **19**: 4595–4608.

Destexhe, A., McCormick, D.A. and Sejnowski, T.J. (1999c) Thalamic and thalamocortical mechanisms underlying 3 Hz spike-and-wave discharges. *Progress in Brain Research* **121**: 289–307.

Destexhe, A., Contreras, D. and Steriade, M. (2001) LTS cells in cerebral cortex and their role in generating spike-and-wave oscillations. *Neurocomputing* **38–40**: 555–563.

Détári, L. and Vanderwolf, C.H. (1987) Activity of identified cortically projecting neurones during large slow waves and cortical activation in anaesthetized rats. *Brain Research* **437**: 1–8.

Détári, L., Juhasz, G. and Kukorelli, T. (1984) Firing properties of cat basal forebrain neurones during sleep-wakefulness cycle. *Electroencephalography and Clinical Neurophysiology* **58**: 362–368.

Détári, L., Rasmusson, D.D. and Semba, K. (1997) Phasic relationship between the activity of basal forebrain neurons and cortical EEG in urethane-anesthetized rat. *Brain Research* **759**: 112–121.

Devinsky, O., Ehremberg, B., Barthlen, G.M., Abramson, H.S. and Luciano, D. (1994) Epilepsy and sleep apnea syndrome. *Neurology* **44**: 2060–2064.

Dichter, M.A. and Spencer, W.A. (1969a) Penicillin-induced interictal discharges from the cat hippocampus. I. Characteristics and topographical features. *Journal of Neurophysiology* **32**: 649–662.

Dichter, M.A. and Spencer, W.A. (1969b) Penicllin-induced interictal discharges from the cat hippocampus. II. Mechanisms underlying origin and restriction. *Journal of Neurophysiology* **32**: 663–687.

Dichter, M.A., Herman, C.J. and Selzer, M. (1972) Silent cells during interictal discharges and seizures in hippocampal penicillin foci. Evidence for the role of extracellular K^+ in the transition from the interictal state to seizures. *Brain Research* **48**: 173–183.

Dickson, C.T. and Alonso, A. (1997) Muscarinic induction of synchronous population activity in the entorhinal cortex. *Journal of Neuroscience* **17**: 6729–6744.

Dickson, C.T., Kirk, I.J., Oddie, S.D. and Bland, B.H. (1995) Classification of theta-related cells in the entorhinal cortex: cell discharges are controlled by the ascending brainstem synchronizing pathway in parallel with hippocampal theta-related cells. *Hippocampus* **5**: 306–319.

Dickson, C.T., Mena, A.R. and Alonso, A. (1997) Electroresponsiveness of medial entorhinal cortex layer III neurons *in vitro*. *Neuroscience* **81**: 937–950.

Dijk, D.J. and Czeisler, C.A. (1995) Contribution of the circadian pacemaker and sleep homeostat to sleep propensity, sleep structure, electroencephalographic slow waves, and sleep spindle activity. *Journal of Neuroscience* **15**: 3526–3538.

Dijk, D.J., Hayes, B. and Czeisler, C.A. (1993) Dynamics of electroencephalographic sleep spindles and slow wave activity in men: effect of sleep deprivation. *Brain Research* **626**: 190–199.

Dinner, D.S. (1993) Posttraumatic epilepsy. In *The Treatment of Epilepsy: Principles*, ed. E. Wyllie, pp. 654–658, Philadelphia: Lea & Fibinger.

Do, K.Q., Binns, K.E. and Salt, T.E. (1994) Release of the nitric oxide precursor, arginine, from the thalamus upon sensory afferent stimulation, and its effect on thalamic neurons *in vivo*. *Neuroscience* **60**: 581–586.

Dolmetsch, R.E., Pajvani, U., Fife, K., Spotts, J.M. and Greenberg, M.E. (2001) Signaling to the nucleus by an L-type calcium channel-calmodulin complex through the MPA kinase pathway. *Science* **294**: 333–339.

Domich, L., Oakson, G. and Steriade, M. (1986) Thalamic burst patterns in the naturally sleeping cat: a comparison between cortically projecting and reticularis neurones. *Journal of Physiology (London)* **379**: 429–449.

Domich, L., Oakson, G. and Steriade, M. (1987) Thalamic and cortical spindles during early ontogenesis in kittens. *Developmental Brain Research* **31**: 140–142.

Douglas, R. and Martin, K. (1991) A functional microcircuit for cat visual cortex. *Journal of Physiology (London)* **440**: 735–769.

Draguhn, A., Traub, R.D., Schmitz, D. and Jefferys, J.G. (1998) Electrical coupling underlies high-frequency oscillations in the hippocampus in vitro. *Nature* **394**: 189–192.

Drake, M.E., Weate, S.J., Newell, S.A., Padamadan, H. and Pakalnis, A. (1994) Multiple sleep latency tests in epilepsy. *Clinical Electroencephalography* **25**: 59–62.

Dreifuss, F.E. (1997) Classification of epileptic seizures. In *Epilepsy: A Comprehensive Textbook*, ed. J. Engel Jr. and T.A. Pedley, pp. 517–524, Philadelphia: Lippincott-Raven.

Dudek, F.E., Snow, R.S. and Taylor, C.P. (1986) Role of electrical interactions in synchronization of epileptiform bursts. *Advances in Neurology* **44**: 593–617.

Dulac, O. and N'Guyen, T. (1993) The Lennox-Gastaut syndrome. *Epilepsia* **34** (Suppl. 7): S7–S17.

Dunwiddie, T.V. (1985) The physiological role of adenosine in the central nervous system. *International Review of Neurobiology* **27**: 63–139.

Dusser de Barenne, J.G. and McCulloch, W.S. (1938) The direct functional interrelation of sensory cortex and optic thalamus. *Journal of Neurophysiology* **1**: 176–186.

Dzubay, J.A. and Jahr, C.E. (1999) The concentration of synaptically released glutamate outside of the climbing fiber – Purkinje cell synaptic cleft. *Journal of Neuroscience* **19**: 5265–5274.

Eccles, J.C. (1961) Chairman's opening remarks. In *The Nature of Sleep*, ed. G.E.W. Wolstenholme and M. O'Connor, pp. 1–3, London: Churchill.

Eccles, J.C., Libet, B. and Young, R.R. (1958) The behavior of chromatolysed motoneurones studied by intracellular recording. *Journal of Physiology (London)* **143**: 11–40.

Eccles, J.C., Ito, M. and Szentágothai, J. (1967) *The Cerebellum as a Neuronal Machine.* New York: Springer.

Echlin, F.A., Arnett, V. and Zoll, J. (1952) Paroxysmal high voltage discharges from isolated and partially isolated cerebral cortex as a mechanism in focal cortical epilepsy. *Electroencephalography and Clinical Neurophysiology* **4**: 147–164.

Eckhorn, R., Bauer, R., Jordan, W., Brosch, M., Kruse, W., Munk, M. and Reitboeck, H.J. (1988) Coherent oscillations: a mechanism of feature linking in the visual cortex? *Biological Cybernetics* **60**: 121–130.

Economo, C. von (1918) *Die Encephalitis Lethargica.* Vienna: Deuticke.

Economo, C. von (1929) Schlaftheorie. *Ergebnisse der Physiologie* **28**: 312–339.

Egan, T.M. and North, R.A. (1985) Acetylcholine acts on m_2-muscarinic receptors to excite rat locus coeruleus neurones. *British Journal of Pharmacology* **85**: 733–735.

Eisenman, J.S. (1982) Electrophysiology of the anterior hypothalamus: thermoregulation and fever. In *Pyretics and Antipyretics*, ed. G. Milton, pp. 187–217, Berlin: Springer.

Elton, M., Winter, O., Heslenfeld, D., Loewy, D., Campbell, K. and Kok, A. (1997) Event-related potentials to tones in the absence and presence of sleep spindles. *Journal of Sleep Research* **6**: 78–83.

Engel, A., König, P., Kreiter, A. and Singer, W. (1991) Interhemispheric synchronization of oscillatory neuronal responses in cat visual cortex. *Science* **252**: 1177–1179.

Engel, J. (1995) Inhibitory mechanisms of epileptic seizure generation. *Advances in Neurology* **67**: 157–171.

Engel, J. Jr., Henry, T.R., Risinger, M.W., Mazziotta, J.C., Sutherling, W.W., Levesque, M.F. and Phelps, M.E. (1990) Presurgical evaluation for partial epilepsy: relative contributions of chronic depth electrode recordings versus FDG-PET and scalp-sphenoidal ictal EEG. *Electroencephalography and Clinical Neurophysiology* **40**: 1670–1677.

Esclapez, M., Hirsch, J., Khazipov, R., Ben-Ari, Y. and Bernard, C. (1997) Operative GABAergic inhibition in hippocampal CA1 pyramidal neurons in experimental epilepsy. *Proceedings of the National Academy of Sciences of the USA* **94**: 12151–12156.

Evarts, E.V. (1964) Temporal patterns of discharge of pyramidal tract neurons during sleep and waking. *Journal of Neurophysiology* **27**: 152–171.

Everson, C.A., Smith, C.B. and Sokoloff, L. (1994) Effects of prolonged sleep deprivation on local rates of cerebral energy metabolism in freely moving rats. *Journal of Neuroscience* **14**: 6769–6778.

Facon, E., Steriade, M. and Wertheimer, N. (1958) Hypersomnie prolongée engendrée par des lésions bilatérales du système activateur médial: le syndrome thrombotique de la bifurcation du tronc basilaire. *Revue Neurologique (Paris)* **98**: 117–133.

Faingold, C.L. and Meldrum, B.S. (1990) Excitant amino acids in epilepsy. In *Generalized Epilepsy*, ed. M. Avoli, P. Gloor, G. Kostopoulos and R. Naquet, pp. 102–117, Boston: Birkhäuser.

Farid, H. and Adelson, E.H. (2001) Synchrony does not promote grouping in temporally structured displays. *Nature Neuroscience* **4**: 875–876.

Farmer, S.F. (1998) Rhythmicity, synchronization and binding in human and primate motor cortex. *Journal of Physiology (London)* **509**: 3–14.

Federico, P. and MacVicar, B.A. (1996) Imaging the induction and spread of seizure activity in the isolated brain of guinea pig: the roles of GABA and glutamate receptors. *Journal of Neurophysiology* **76**: 3471–3492.

Feinberg, I. and Campbell, I.G. (1993) Ketamine administration during waking increases delta EEG intensity in rat sleep. *Neuropharmacology* **9**: 41–48.

Feindel, W. and Penfield, W. (1954) Localization of discharge in temporal lobe automatism. *Archives of Neurology and Psychiatry (Chicago)* **72**: 605–630.

Feindel, W. and Rasmussen, T. (1991) Temporal lobectomy with amygdalectomy and minimal hippocampal resection: review of 100 cases. *Canadian Journal of Neurological Sciences* **18**: 603–605.

Feldberg, L.A. and Sherwood, P.D. (1954) Injections of drugs into the lateral ventricle of the cat. *Journal of Physiology (London)* **123**: 148–167.

Fencl, V., Koski, G. and Pappenheimer, J.R. (1971) Factors in cerebrospinal fluid from goats that affect sleep and activity in rats. *Journal of Physiology (London)* **216**: 565–589.

Ferencz, I., Kokaia, M., Keep, M., Elmér, E., Metsis, M., Kokaia, Z. and Lindvall, O. (1997) Effects of cholinergic denervation on seizure development and neurotrophin messenger RNA regulation in rapid hippocampal kindling. *Neuroscience* **80**: 389–399.

Ferencz, I., Leanza, G., Nanobashvili, A., Kokaia, M. and Lindvall, O. (2000) Basal forebrain neurons suppress amygdala kindling via cortical but not hippocampal cholinergic projections in rats. *European Journal of Neuroscience* **12**: 2107–2116.

Ferrara, M., De Gennaro, L., Curcio, G., Cristiani, R., Corvasce, C. and Bertino, M. (2002) Regional differences of the human sleep electroencephalogram in response to selective slow-wave sleep deprivation. *Cerebral Cortex* **12**: 737–748.

Ferrier, D. (1876) *The Functions of the Brain*. London: Smith, Elder & Co.

Ferster, D. and Lindström, S. (1985) Augmenting responses evoked in area 17 of the cat by intracortical axonal collaterals of cortico-geniculate cells. *Journal of Physiology (London)* **367**: 217–232.

Fetz, E.E., Chen, D., Murphy, V.N. and Matsumara, M. (2000) Synaptic interactions mediating synchrony and oscillations in primate sensorimotor cortex. *Journal de Physiologie (Paris)* **94**: 323–331.

Feucht, M., Möller, U., Witte, H., Schmidt, K., Arnold, M., Benninger, F., Steinberger, K. and Friedrich, M.H. (1998) Nonlinear dynamics of 3 Hz spike-and-wave discharges recorded during typical absence seizures in children. *Cerebral Cortex* **8**: 524–533.

Finnerty, G.T. and Jefferys, J.G.R. (2000) 9–16 Hz oscillation precedes secondary generalization of seizures in the rat tetanus toxin model of epilepsy. *Journal of Neurophysiology* **83**: 2217–2226.

Fischer-Perroudon, C., Mouret, J. and Jouvet, M. (1974) Sur un cas d'agrypnie (4 mois sans sommeil) au cours d'une maladie de Morvan: effet favorable du 5–hydroxytryptophane. *Electroencephalography and Clinical Neurophysiology* **36**: 1–18.

Fiset, P., Paus, T., Daloze, T., Plourde, G., Meuret, P., Bonhomme, V., Hajj-Ali, N., Backman, S.B. and Evans, A.C. (1999) Brain mechanisms of propofol-induced loss of consciousness in humans: a positron emission tomography study. *Journal of Neuroscience* **19**: 5506–5513.

Fish, D.R., Gloor, P., Quesney, L.F. and Olivier, A.O. (1993) Clinical responses to electrical brain stimulation of the temporal and frontal lobes in patients with epilepsy. *Brain* **116**: 397–414.

Fisher, R.S. and Prince, D.A. (1977) Spike-wave rhythms in cat cortex induced by parenteral penicillin. I. Electroencephalographic patterns. *Electroencephalography and Clinical Neurophysiology* **42**: 608–624.

Fisher, R.S., Buchwald, N.A., Hull, C.D. and Levine, M.S. (1988) GABAergic basal forebrain neurons project to the neocortex: the localization of glutamic acid decarboxylase and choline acetyltransferase in feline corticopetal neurons. *Journal of Comparative Neurology* **272**: 489–502.

Fisher, R.S., Webber, W.R., Lesser, R.P., Arroyo, S. and Uematsu, S. (1992) High-frequency EEG activity at the start of seizures. *Journal of Clinical Neurophysiology* **9**: 441–448.

Fleidervish, I.A. and Gutnick, M.J. (1996) Kinetics of slow inactivation of persistent sodium current in layer V neurons of mouse neocortical slices. *Journal of Neurophysiology* **76**: 2125–2130.

Foehring, R.C., Schwindt, P.C. and Crill, W.E. (1989) Norepinephrine selectively reduces slow Ca^{2+}- and Na^{+}-mediated currents in cat neocortical neurons. *Journal of Neurophysiology* **61**: 245–256.

Foldvary, N. (2001) Sleep disorders in epilepsy. In *Epilepsy and Sleep*, ed. D.S. Dinner and H.O. Lüders, pp. 191–201, San Diego: Academic Press.

Ford, B., Holmes, C.J., Mainville, L. and Jones, B.E. (1995) GABAergic neurons in the rat pontomesencephalic tegmentum: codistribution with cholinergic and other tegmental neurons projecting to the posterior lateral hypothalamus. *Journal of Comparative Neurology* **363**: 177–196.

Foulkes, D. (1967) Nonrapid eye movement mentation. *Experimental Neurology* **19**: 28–38.

Franck, J.E. and Schwartzkroin, P.A. (1985) Do kainite-lesioned hippocampi become epileptogenic? *Brain Research* **329**: 309–313.

Frank, G. (1969) A study of the inter-relations of spike discharge density and sleep stages in epileptic patients. *Electroencephalography and Clinical Neurophysiology* **26**: 238.

Frank, M.G., Issa, N.P. and Stryker, M.P. (2001) Sleep enhances plasticity in the developing visual cortex. *Neuron* **30**: 275–287.

Frantseva, M.V., Kokarovtseva, L., Naus, C.G., Carlen, P.L., MacFabe, D. and Perez Velazquez, J.L. (2002) Specific gap junctions enhance the neuronal vulnerability to brain traumatic injury. *Journal of Neuroscience* **22**: 644–653.

Freeman, W.J. (1975) *Mass Action in the Nervous System.* New York: Academic Press.

Freeman, W.J. and Van Dijk, B.W. (1988) Spatial patterns of visual cortical fast EEG during conditioned reflex in a rhesus monkey. *Brain Research* **422**: 267–276.

French, C.R., Sah, P., Buckett, K.J. and Gage, P.W. (1990) A voltage-dependent persistent sodium current in mammalian hippocampal neurons. *Journal of General Physiology* **95**: 1139–1157.

Freund, T.F. (1993) Anterograde PHAL-tracing combined with pre- and postembedding immunocytochemistry. In *Immunohistochemistry*, ed. A.C. Cuello, pp. 329–348, New York: Wiley.

Freund, T.F. and Buzsáki, G. (1988) Alterations in excitatory and GABAergic inhibitory connections in hippocampal transplants. *Neuroscience* **27**: 373–385.

Freund, T.F. and Buzsáki, G. (1996) Interneurons of the hippocampus. *Hippocampus* **6**: 347–470.

Fries, P., Neuenschwander, S., Engel, A.K., Goebel, R. and Singer, W. (2001a) Rapid feature selective neuronal synchronization through correlated latency shifting. *Nature Neuroscience* **4**: 194–200.

Fries, P., Reynolds, J.H., Rorie, A.E. and Desimone, R. (2001b) Modulation of oscillatory neuronal synchronization by selective visual attention. *Science* **291**: 1560–1563.

Fritsch, G. and Hitzig, E. (1870) Uber die elektrische Erregbarkeit des Grosshirns. *Archive für Anatomie, Physiologie und wissenschaftliche Medizin* **37**: 300–332.

Fromm, G.H. (1986) Role of inhibitory mechanisms in staring spells. *Journal of Clinical Neurophysiology* **3**: 297–311.

Futamachi, K.J., Mutani, R. and Prince, D.A. (1974) Potassium activity in rabbit cortex. *Brain Research* **75**: 5–25.

Gabor, A.J. and Ajmone-Marsan, C. (1968) Coexistence of focal bilateral diffuse paroxysmal discharges in epileptics. *Epilepsia* **10**: 453–472.

Gais, S., Plihal, W., Wagner, U. and Born, J. (2000) Early sleep triggers memory for early visual discrimination skills. *Nature Neuroscience* **3**: 1335–1339.

Gais, S., Mölle, M., Helms, K. and Born, J. (2002) Learning-dependent increases in sleep density. *Journal of Neuroscience* **22**: 6830–6834.

Galarreta, M. and Hestrin, S. (1998) Frequency-dependent synaptic depression and the balance of excitation and inhibition in the neocortex. *Nature Neuroscience* **1**: 587–594.

Galarreta, M. and Hestrin, S. (1999) A network of fast-spiking cells in the neocortex connected by electrical synapses. *Nature* **402**: 72–75.

Gallopin, T., Fort, P., Eggerman, E., Cauli, B., Luppi, P.H., Rossier, J., Audinat, E., Mühlethaler, and Serafin, M. (2000) Identification of sleep-promoting neurons *in vitro*. *Nature* **404**: 992–995.

Garcia-Cairasco, N., Terra, V.C. and Doretto, M.C. (1993) Midbrain substrates of audiogenic seizures in rats. *Behavioral and Brain Research* **58**: 57–67.

Garcia-Rill, E., Skinner, R.D., Miyazato, H. and Homma, Y. (2001) Pedunculopontine stimulation induces prolonged activation of pontine reticular neurons. *Neuroscience* **104**: 455–465.

Gastaut, H. (1950) Combined photic and metrazol activation of the brain. *Electroencephalography and Clinical Neurophysiology* **2**: 263–275.

Gastaut, H. (1968) Clinical and electroencephalographic correlates of generalized spike and wave bursts occurring spontaneously in man. *Epilepsia* **9**: 179–184.

Gastaut, H. and Broughton, R. (1972) *Epileptic Seizures. Clinical and Electrographic Features, Diagnosis and Treatment*. Springfield, ILL: Charles C. Thomas.

Gastaut, H., Roger, J. and Gastaut, Y. (1948) Les formes expérimentales de l'épilepsie humaine. I. L'épilepsie induite par la stimulation lumineuse intermittente rythmée, ou épilepsie photogénique. *Revue Neurologique (Paris)* **80**: 161–183.

Gastaut, H., Roger, J., Soulayrol, R., Tassinari, C.T., Régis, H., Dravet, C., Bernard, R., Pinsard, N. and Saint-Jean, M. (1966) Childhood epileptic encephalopathy with diffuse slow spike-waves (otherwise known as "petit mal variant") or Lennox syndrome. *Epilepsia* **7**: 139–179.

Gaudin-Chazal, G., Portalier, P., Barrit, M.C. and Puizillout, J.J. (1982) Serotonin-like immunoreactivity in paraffin-sections of the nodose ganglia of the cat. *Neuroscience Letters* **33**: 169–172.

Gean, P.W., Shinnick-Gallagher, P. and Anderson, C. (1989) Spontaneous epileptiform activity and alterations of GABA- and NMDA-mediated neurotransmission in amygdala neurons kindled *in vivo*. *Brain Research* **494**: 177–181.

Gevins, A., Smith, E.M., McEvoy, L. and Yu, D. (1997) High-resolution EEG mapping of cortical activation related to working memory: effects of task difficulty, type of processing, and practice. *Cerebral Cortex* **7**: 374–385.

Giaretta, D., Avoli, M. and Gloor, P. (1987) Intracellular recordings in precruciate neurons during spike and wave discharges of feline generalized penicillin epilepsy. *Brain Research* **405**: 68–79.

Gibbs, E.L. and Gibbs, F.A. (1947) Diagnostic and localizing value of electroencephalographic studies in sleep. *Research Publications of the Association for the Research of Nervous and Mental Diseases* **26**: 366–376.

Gibbs, F.A. and Gibbs, E.L. (1952) *Atlas of Electroencephalography*, 2nd edn. Cambridge, MA: Addison-Wesley.

Gibbs, F.A., Gibbs, E.L. and Lennox, W.G. (1937) Epilepsy: a paroxysmal cerebral dysrhythmia. *Brain* **60**: 377–388.

Gibbs, F.A., Gibbs, E.L. and Lennox, W.G. (1938) Cerebral dysrhythmias of epilepsy: measures for their control. *Archives of Neurology and Psychiatry (Chicago)* **39**: 298.

Gibbs, F.A., Gibbs, E.L. and Lennox, W.G. (1939) The influence of the blood sugar level on the wave and spike formation in petit mal epilepsy. *Archives of Neurology and Psychiatry (Chicago)* **47**: 1111–1116.

Gibbs, J.W., Berkow-Schroeder, G. and Coulter, D.A. (1996) $GABA_A$ receptor function in developing rat thalamic reticular neurons: whole cell recordings of GABA-mediated currents and modulation by clonazepam. *Journal of Neurophysiology* **76**: 2568–2579.

Gibbs, J.W., Shumate, M.D. and Coulter, D.A. (1997) Differential epilepsy-associated alterations in postsynaptic $GABA_A$ receptor function in dentate granule cells and CA1 neurons. *Journal of Neurophysiology* **77**: 1924–1938.

Gibson, J.R., Beierlein, M. and Connors, B.W. (1999) Two networks of electrically coupled inhibitory neurons in neocortex. *Nature* **402**: 75–79.

Gilbert, C.D. (1992) Horizontal integration and cortical dynamics. *Neuron* **9**: 1–13.

Gilbert, C.D. and Wiesel, T.N. (1983) Clustered intrinsic connections in cat visual cortex. *Journal of Neuroscience* **3**: 1116–1133.

Gilliland, M.A., Bergmann, B.M. and Rechtschaffen, A. (1989) Sleep deprivation in the rat. VIII. High EEG amplitude sleep deprivation. *Sleep* **12**: 53–59.

Girgis, M. (1980) Participation of muscarinic cholinergic receptors may be an important requirement of the kindling process. *Experimental Neurology* **70**: 458–461.

Glenn, L.L. and Dement, W.C. (1981) Membrane potential, synaptic activity and excitability of hindlimb motoneurons during wakefulness and sleep. *Journal of Neurophysiology* **46**: 839–854.

Glenn, L.L. and Steriade, M. (1982) Discharge rate and excitability of cortically projecting intralaminar thalamic neurons during waking and sleep states. *Journal of Neuroscience* **2**: 1287–1404.

Glenn, L.L., Hada, J., Roy, J.P., Deschênes, M. and Steriade, M. (1982) Anterograde tracer and field potential analysis of the neocortical layer I projection from the nucleus ventralis medialis of the thalamus in cat. *Neuroscience* **7**: 1861–1877.

Gloor, P. (1969) *Hans Berger on the Electroencephalogram of Man*. Amsterdam: Elsevier (Suppl. no. 28 of *Electroencephalography and Clinical Neurophysiology*).

Gloor, P. (1976) Generalized and widespread bilateral paroxysmal abnormalities. In *Handbook of Electroencephalography and Clinical Neurophysiology*, vol. 11/B, ed. A. Rémond, pp. 11B52–11B87, Amsterdam: Elsevier.

Gloor, P. (1987) Volume conductor principles: their application to the surface and depth electroencephalogram. In *Presurgical Evaluation of Epileptics*, ed. H.G. Wieser and C.E. Elger, pp. 59–68, Berlin: Springer.

Gloor, P. (1991) Mesial temporal sclerosis: historical background and an overview from a modern perspective. In *Epilepsy Surgery*, ed. H. Lüders, pp. 689–703, New York: Raven Press.

Gloor, P. (1992) Role of the amygdala in temporal lobe epilepsy. In *The Amygdala: Neurobiological Aspects of Emotion, Memory, and Mental Dysfunction*, ed. J.P. Aggleton, pp. 505–538, New York: Wiley-Liss.

Gloor, P. (1997) *The Temporal Lobe and Limbic System.* New York: Oxford University Press.

Gloor, P. and Fariello, R.G. (1988) Generalized epilepsy: some of its cellular mechanisms differ from those of focal epilepsy. *Trends in Neuroscience* **11**: 63–68.

Gloor, P., Ball, G. and Schaul, N. (1977) Brain lesions that produce delta waves. *Neurology* **27**: 326–333.

Gloor, P., Olivier, A., Quesney, L.F., Anderman, F. and Horowitz, S. (1982) The role of the limbic system in experiential phenomena of temporal lobe epilepsy. *Annals of Neurology* **12**: 129–144.

Gloor, P., Avoli, M. and Kostopoulos, G. (1990) Thalamocortical relationships in generalized epilepsy with bilaterally synchronous spike-and-wave discharges. In *Generalized Epilepsies*, ed. M. Avoli, P. Gloor, G. Kostopoulos and R. Naquet, pp. 190–212, Boston: Birkhäuser.

Goff, W.R., Allison, T., Shapiro, A. and Rosner, B.S. (1966) Cerebral somatosensory responses evoked during sleep in man. *Electroencephalography and Clinical Neurophysiology* **21**: 1–9.

Gökyigit, A. and Caliskan, A. (1995) Diffuse spike-wave seizures of 9–year duration without behavioral change or intellectual decline. *Epilepsia* **36**: 210–213.

Goldensohn, E.S. and Purpura, D.P. (1963) Intracellular potentials of cortical neurons during focal epileptogenic discharges. *Science* **139**: 840–842.

Goldman-Rakic, P.S. (1987) Circuitry of the prefrontal cortex and the regulation of behavior by representational memory. In *Handbook of*

Physiology (vol. V, *The Nervous System*), ed. F. Plum and V.B. Mountcastle, pp. 373–417, Bethesda: American Physiological Society.

Goldman-Rakic, P.S. (1988) Changing concepts of cortical connectivity: parallel distributed cortical networks. In *Neurobiology of Neocortex*, ed. P. Kakic and W. Singer, pp. 177–202, New York: Wiley.

Goldring, N.L., Jung, H.Y., Mickus, T. and Spruston, N. (1999) Dendritic calcium spikes initiation and repolarization are controlled by distinct potassium channel subtypes in CA1 pyramidal neurons. *Journal of Neuroscience* **19**: 8789–8798.

Goldring, S., Edwards, I., Harding, G.W. and Bernardo, K.L. (1992) Results of anterior temporal lobectomy that spares the amygdala in patients with complex partial seizures. *Journal of Neurosurgery* **77**: 185–193.

Golomb, D., Wang, X.J. and Rinzel, J. (1994) Synchronization properties of spindle oscillations in a thalamic reticular nucleus model. *Journal of Neurophysiology* **72**: 1109–1126.

Golshani, P. and Jones, E.G. (1999) Synchronized paroxysmal activity in the developing thalamocortical network mediated by corticothalamic projections and "silent" synapses. *Journal of Neuroscience* **19**: 2865–2875.

Golshani, P., Liu, X.B. and Jones, E.G. (2001) Differences in quantal amplitude reflect GluR4–subunit number at corticothalamic synapses on two populations of thalamic neurons. *Proceedings of the National Academy of Sciences of the USA* **98**: 4172–4177.

Gomez, M.R. and Westmoreland, B.F. (1987) Absence seizures. In *Clinical Medicine and the Nervous System: Epilepsy – Electroclinical Syndromes*, ed. H. Lüders and R.P. Lesser, pp. 105–129, New York: Springer.

Gonchar, Y. and Burkhalter, A. (1997) Three distinct families of GABAergic neurons in rat visual cortex. *Cerebral Cortex* **7**: 347–358.

Gotman, J. and Marciani, M.G. (1985) Electroencephalographic spiking activity, drug levels and seizure occurrence in epileptic patients. *Annals of Neurology* **17**: 597–603.

Gottselig, J.M., Bassetti, C.L. and Achermann, P. (2002) Power and coherence of sleep spindle frequency activity following hemispheric strokes. *Brain* **125**: 373–383.

Gowers, W.R. (1885) *Epilepsy and Other Chronic Convulsive Disorders.* New York: William Wood.

Grace, A.A. and Bunney, B.S. (1979) Paradoxical GABA excitation of nigral dopaminergic cells: indirect mediation through reticulata inhibitory neurons. *European Journal of Pharmacology* **59**: 211–218.

Grace, A.A. and Bunney, B.S. (1985) Opposing effects of striatonigral feedback pathways on midbrain dopamine cell activity. *Brain Research* **333**: 271–284.

Gray, C.M. and McCormick, D.A. (1996) Chattering cells: superficial pyramidal neurons contributing to the generation of synchronous oscillations in the visual cortex. *Science* **274**: 109–113.

Gray, C.M., König, P., Engel, A.K. and Singer, W. (1989) Stimulus-specific neuronal oscillations in cat visual cortex exhibit inter-columnar

synchronization which reflects global stimulus properties. *Nature* **338**: 334–337.

Gray, C.M., Engel, A.K., König, P. and Singer, W. (1990) Stimulus-dependent neuronal oscillations in cat visual cortex: receptive field properties and feature dependence. *European Journal of Neuroscience* **2**: 607–619.

Gray, E.G. (1959) Axo-somatic and axo-dendritic synapses of the cerebral cortex: an electron microscope study. *Journal of Anatomy* **93**: 420–433.

Graybiel, A.M. and Elde, R.P. (1983) Somatostatin-like immunoreactivity characterizes neurons of the nucleus reticularis thalami in the cat and monkey. *Journal of Neuroscience* **3**: 1303–1321.

Graybiel, A.M. and Ragsdale, C.W. (1979) Fiber connections of the basal ganglia. In *Development and Chemical Specificity of Neurons*, ed. M. Cuénod, G.W. Kreutzberg and F.E. Bloom, pp. 239–283, Amsterdam: Elsevier.

Green, J.D. (1969) The hippocampus. *Physiological Reviews* **44**: 561–608.

Greene, R.W., Haas, H.L. and McCarley, R.W. (1986) A low-threshold calcium spike mediates firing pattern alterations in pontine reticular neurons. *Science* **234**: 738–740.

Grenier, F., Timofeev, I. and Steriade, M. (1998) Leading role of thalamic over cortical neurons during postinhibitory rebound excitation. *Proceedings of National Academy of Sciences of the USA* **95**: 13929–13934.

Grenier, F., Timofeev, I. and Steriade, M. (2001) Focal synchronization of ripples (80–200 Hz) in neocortex and their neuronal correlates. *Journal of Neurophysiology* **86**: 1884–1898.

Grenier, F., Timofeev, I. and Steriade, M. (2002) Thalamic short-term plasticity and its impact on the neocortex. *Thalamus and Related Systems* **1**: 331–340.

Grenier, F., Timofeev, I. and Steriade, M. (2003) Neocortical ripples (80–200 Hz) and their role in initiation of electrical seizures. *Journal of Neurophysiology*, in press.

Grill, W.M. and McIntyre, C.C. (2001) Extracellular excitation of central neurons: implications for the mechanisms of deep brain stimulation. *Thalamus and Related Systems* **1**: 269–277.

Gritti, I., Mainville, L. and Jones, B.E. (1994) Projections of GABAergic and cholinergic basal forebrain and GABAergic preoptic-anterior hypothalamic neurons to the posterior lateral hypothalamus of the rat. *Journal of Comparative Neurology* **339**: 251–268.

Grossman, R.G. and Hampton, T. (1968) Depolarization of cortical glial cells during electrical activity. *Brain Research* **11**: 316–324.

Grüner, J.E., Hirsch, J.C. and Sotelo, C. (1974) Ultrastructural features of the isolated suprasylvian gyrus in the cat. *Journal of Comparative Neurology* **154**: 1–28.

Guberman, A., Gloor, P. and Sherwin, A.L. (1975) Response of generalized epilepsy in the cat to ethosuximide and diphenylhydantoin. *Neurology* **25**: 758–764.

Gulyas, A.I., Miles, R., Sok, A., Toth, K., Tamamaki, N. and Freund, T.F. (1993) Hippocampal pyramidal cells excite inhibitory neurons through a single release site. *Nature* **366**: 683–687.

Gupta, A., Wang, Y. and Markram, H. (2000) Organizing principles for a diversity of GABAergic interneurons and synapses in the neocortex. *Science* **287**: 273–278.

Gutfreund, Y., Yarom, Y. and Segev, I. (1995) Subthreshold oscillations and resonant frequency in guinea-pig cortical neurons: physiology and modelling. *Journal of Physiology (London)* **483**: 621–640.

Gutnick, M.J. and Mody, I. (eds.) (1995) *The Cortical Neuron*. Oxford: Oxford University Press.

Gutnick, M.J., Heinemann, U. and Prince, D.A. (1979) Stimulus induced and seizure related changes in extracellular potassium concentration in cat thalamus (VPL). *Electroencephalography and Clinical Neurophysiology* **47**: 329–344.

Gutnick, M.J., Connors, B.W. and Prince, D.A. (1982) Mechanisms of neocortical epileptogenesis in vitro. *Journal of Neurophysiology* **48**: 1321–1335.

Gutnick, M.J., Amitai, Y. and Barkai, E. (1992) Chronic models of cortical epilepsy: experimental manipulations leading to long-term reorganization of local neocortical circuitry. In *Molecular Neurobiology of Epilepsy*, ed. J. Engel Jr., C. Wasterlain, E.A. Cavalheiro, U. Heinemann and G. Avanzini, pp. 221–229, Amsterdam: Elsevier.

Haas, H.L. and Greene, R.W. (1986) Effects of histamine on hippocampal pyramidal cells of the rat *in vitro*. *Experimental Brain Research* **62**: 123–130.

Halasz, P. (1991) Runs of rapid spikes in sleep: a characteristic EEG expression of generalized malignant epileptic encephalopathies. A conceptual review with new pharmacological data. *Epilepsy Research* (*Suppl.*) **2**: 49–71.

Halgren, E., Smith, M.E. and Stapleton, J.M. (1985) Hippocampal field potentials evoked by repeated vs nonrepeated words. In *Electrical Activity of the Archicortex*, ed. G. Buzsáki and C.H. Vanderwolf, pp. 67–81, Budapest: Akademiai Kiadó.

Hallanger, A.E. and Wainer, B.H. (1988) Ultrastructure of ChAT-immunoreactive synaptic terminals in the thalamic reticular nucleus of the rat. *Journal of Comparative Neurology* **278**: 486–497.

Hallanger, A.E., Levey, A.I., Lee, H.J., Rye, D.B. and Wainer, B.H. (1987) The origins of cholinergic and other subcortical afferents to the thalamus in the rat. *Journal of Comparative Neurology* **262**: 105–124.

Halliwell, J.V. (1986) M-current in human neocortical neurones. *Neuroscience Letters* **67**: 1–6.

Halpern, L.M. (1972) Chronically isolated aggregates of mammalian cerebral cortical neurons studied *in situ*. In *Experimental Models of Epilepsy*, ed. D.P. Purpura, J.F. Penry, D.B. Tower, D.M. Woodbury and R.D. Walter, pp. 197–221, New York: Raven.

Han, Z.S., Buhl, E.H., Lorinczi, Z. and Somogyi, P. (1993) A high degree of spatial selectivity in the axonal and dendritic domains of physiologically identified local-circuit neurons in the dentate gyrus of the rat hippocampus. *European Journal of Neuroscience* **5**: 395–410.

Hansen, J.C. and Hillyard, S. (1980) Endogenous brain potentials associated with auditory selective attention. *Electroencephalography and Clinical Neurophysiology* **49**: 277–290.

Harding, B.N. and Powell, T.P.S. (1972) An electron microscopic study of afferent fibre connexions to the monkey thalamus from motor cortex and basal ganglia. *Journal of Anatomy* **111**: 503–504.

Haulica, I., Ababei, L., Branisteanu, D. and Topoliceanu, F. (1973) Preliminary data on the possible hypnogenic role of adenosine. *Journal of Neurochemistry* **21**: 1019–1020.

Hayaishi, O. (1988) Sleep-wake regulation by prostaglandin D2 and E2. *Journal of Biological Chemistry* **263**: 14593–14596.

Heath, R. (1954) *Studies in Schizophrenia: A Multidisciplinary Approach to Mind-Brain Relationships*. Cambridge, MA: Harvard University Press.

Heilman, K.M., Bowers, D., Coslett, H.B., Whelan, H. and Watson, R.T. (1985) Direction hypokinesia: prolonged reaction times for leftward movements in patients with right hemisphere lesions and neglect. *Neurology* **35**: 855–860.

Heinemann, U. and Pumain, R. (1981) Effects of tetrodotoxin on changes in extracellular free calcium induced by repetitive electrical stimulation and iontophoretic application of excitatory amino acids in the sensorimotor cortex of cats. *Neuroscience Letters* **21**: 87–91.

Heinemann, U., Gabriel, S., Jauch, R., Schulze, K., Kivi, A., Eilers, A., Kovacs, R. and Lehmann, T.N. (2000) Alterations of glial cell function in temporal lobe epilepsy. *Epilepsia* **41**: S185–S189.

Heller, H.C., Glotzbach, S., Grahn, D. and Radeke, C. (1988) Sleep-dependent changes in the thermoregulatory system. In *Clinical Physiology of Sleep*, ed. R. Lydic and J.F. Biebuyck, pp. 145–169, Bethesda: American Physiological Society.

Hennevin, E., Hars, B., Maho, C. and Bloch, V. (1995) Processing of learned information in paradoxical sleep: relevance for memory. *Behavioral and Brain Research* **69**: 125–135.

Herculano-Houzel, S., Munk, M.H.J., Neuenschwander, S. and Singer, W. (1999) Precisely synchronized oscillatory firing patterns require electroencephalographic activation. *Journal of Neuroscience* **19**: 3992–4010.

Herkenham, M. (1987) Mismatches between neurotransmitter and receptor localization in brain: observations and implications. *Neuroscience* **23**: 1–38.

Hernández-Cruz, A. and Pape, H.C. (1989) Identification of two calcium currents in acutely dissociated neurons from the rat lateral geniculate nucleus. *Journal of Neurophysiology* **61**: 1270–1283.

Hess, G. and Gustafsson, B. (1990) Changes in field excitatory postsynaptic potential shape induced by tetanization in the CA1 region of the guinea-pig hippocampal slice. *Neuroscience* **37**: 61–69.

Hess, W.R. (1944) Das Schlafsyndrom als Folge dienzephaler Reizung. *Helvetica Physiologica et Pharmacologica Acta* **2**: 305–344.

Hestrin, S. and Armstrong, W.E. (1996) Morphology and physiology of cortical neurons in layer I. *Journal of Neuroscience* **16**: 5290–5300.

Hikosaka, O. and Wurtz, R.H. (1983) Visual and oculomotor function of monkey substantia nigra pars reticulata. IV: relation of substantia nigra to superior colliculus. *Journal of Neurophysiology* **49**: 1285–1301.

Hille, B. (1992) *Ionic Channels of Excitable Membranes*. Sunderland, MA: Sinauer.

Hirsch, J.C. and Burnod, Y. (1987) A synaptically evoked late hyperpolarization in the rat dorsolateral geniculate neurons *in vitro*. *Neuroscience* **23**: 457–468.

Hirsch, J.C., Fourment, A. and Marc, M.E. (1983) Sleep-related variations of membrane potential in the lateral geniculate body relay neurons of the cat. *Brain Research* **259**: 308–312.

Hirsch, J.C., Quesada, O., Esclapez, M., Gozlan, H., Ben-Ari, Y. and Bernard, C.L. (1996) Enhanced NMDAR-dependent epileptiform activity is controlled by oxidizing agents in a chronic model of temporal lobe epilepsy. *Journal of Neurophysiology* **76**: 4185–4189.

Hobson, J.A. and Pace-Schott, E.F. (2002) The cognitive neuroscience of sleep: neuronal systems, consciousness and learning. *Nature Reviews Neuroscience* **3**: 679–693.

Hobson, J.A., McCarley, R.W. and Wyzinski, P.W. (1975) Sleep cycle oscillation: reciprocal discharge by two brain stem neuronal groups. *Science* **189**: 55–58.

Hobson, J.A., Pace-Schott, E. and Stickgold, R. (2000) Dreaming and the brain: toward a cognitive neuroscience of conscious states. *Brain and Behavioral Sciences* **23**: 793–842.

Hoffman, D.A., Magee, J.C., Colbert, C.M. and Johnston, D. (1997) K^+ channel regulation of signal propagation in dendrites of hippocampal pyramidal neurons. *Nature* **387**: 869–875.

Hoffman, S.N., Salin, P.A. and Prince, D.A. (1994) Chronic neocortical epileptogenesis *in vitro*. *Journal of Neurophysiology* **71**: 1762–1772.

Hoffman, W.H. and Haberly, L.B. (1991) Bursting induced epileptiform EPSPs in slices of piriform cortex are generated by deep cells. *Journal of Neuroscience* **11**: 2021–2031.

Hofle, N., Paus, T., Reutens, D., Fiset, P., Gotman, J., Evans, A.C. and Jones, B.E. (1997) Regional cerebral blood flow changes as a function of delta and spindle activity during slow wave sleep in humans. *Journal of Neuroscience* **17**: 4800–4808.

Homma, Y., Skinner, R.D. and Garcia-Rill, E. (2002) Effects of pedunculopontine nucleus (PPN) stimulation on caudal pontine reticular formation (PnC) neurons in vitro. *Journal of Neurophysiology* **87**: 3033–3047.

Honda, T. and Semba, K. (1995) An ultrastructural study of cholinergic and non-cholinergic neurons in the laterodorsal and pedunculopontine tegmental nuclei in the rat. *Neuroscience* **68**: 837–853.

Hoogland, P.V., Wouterlood, F.G., Welker, E. and Van der Loos, H. (1991) Ultrastructure of giant and small thalamic terminals of cortical origin: a study of the projections from the barrel cortex in mice using *Phaseolus vulgaris*-leucoagglutinin (PHA-L). *Experimental Brain Research* **87**: 159–172.

Horne, J. (1988) *Why We Sleep*. Oxford: Oxford University Press.

Hosford, D.A., Clark, S., Cao, Z., Wilson, W.A. Jr., Lin, F.H., Morrisett, R.A. and Huin, A. (1992) The role of $GABA_B$ receptor activation in absence seizures of lethargic (lh/lh) mice. *Science* **257**: 398–401.

Hosford, D.A., Caddick, S.J. and Lin, F.H. (1997) Generalized epilepsies: emerging insights into cellular and genetic mechanisms. *Current Opinion in Neurology* **10**: 115–120.

Houser, C.R. and Esclapez, M. (1996) Vulnerability and plasticity of the GABA system in the pilocarpine model of spontaneous recurrent seizures. *Epilepsy Research* **26**: 207–218.

Houser, C.R., Vaughan, J.E., Barber, R.P. and Roberts, E. (1980) GABA neurons are the major cell type of the nucleus reticularis thalami. *Brain Research* **200**: 341–354.

Houser, C.R., Miyashiro, J.E., Swartz, B.E., Walsh, G.O., Rich, J.R. and Delgado-Escueta, A.V. (1990) Altered patterns of dynorphin immunoreactivity suggest mossy fiber reorganization in human hippocampal epilepsy. *Journal of Neuroscience* **10**: 267–282.

Houweling, A., Bazhenov, M., Timofeev, I., Steriade, M. and Sejnowski, T.J. (1999) Cortical and thalamic components of augmenting responses: a modelling study. *Neurocomputing* **26–27**: 735–742.

Houweling, A.R., Bazhenov, M., Timofeev, I., Grenier, F., Steriade, M. and Sejnowski, T.J. (2002) Frequency-selective augmenting responses by short-term synaptic depression in cat neocortex. *Journal of Physiology (London)* **542**: 599–617.

Hu, B., Bouhassira, D., Steriade, M. and Deschênes, M. (1988) The blockage of ponto-geniculo-occipital waves in the cat lateral geniculate nucleus by nicotinic antagonists. *Brain Research* **473**: 394–397.

Hu, B., Steriade, M. and Deschênes, M. (1989a) The effects of peribrachial stimulation on reticular thalamic neurons: the blockage of spindle waves. *Neuroscience* **31**: 1–12.

Hu, B., Steriade, M. and Deschênes, M. (1989b) The effects of brainstem peribrachial stimulation on neurons of the lateral geniculate nucleus. *Neuroscience* **31**: 13–24.

Hu, B., Steriade, M. and Deschênes, M. (1989c) The cellular mechanism of thalamic ponto-geniculo-occipital waves. *Neuroscience* **31**: 25–35.

Hubel, D.H. (1960) Single unit activity in lateral geniculate body and optic tract of unrestrained cats. *Journal of Physiology (London)* **150**: 91–104.

Hudson, L.P., Munoz, D.G., Miller, L., McLahlan, R.S., Girvin, J.P. and Blume, W.T. (1993) Amygdaloid sclerosis in temporal lobe epilepsy. *Annals of Neurology* **33**: 622–631.

Hughes, J.R. (1980) Two forms of the 6/sec spike and wave complex. *Electroencephalography and Clinical Neurophysiology* **48**: 535–550.

Huguenard, J.R. (1996) Low-threshold calcium currents in central nervous system neurons. *Annual Review of Physiology* **58**: 329–348.

Huguenard, J.R. (1999) Neuronal circuitry of thalamocortical epilepsy and mechanisms of antiabsence drug action. *Advances in Neurology* **79**: 991–999.

Huguenard, J.R. and Prince, D.A. (1992) A novel T-type current underlies prolonged Ca^{2+}-dependent burst firing in GABAergic neurons of rat thalamic reticular nucleus. *Journal of Neuroscience* **12**: 3804–3817.

Huguenard, J.R. and Prince, D.A. (1994a) Clonazepam suppresses $GABA_B$-mediated inhibition in thalamic relay neurons through effects in nucleus reticularis. *Journal of Neurophysiology* **71**: 2576–2581.

Huguenard, J.R. and Prince, D.A. (1994b) Intrathalamic rhythmicity studied in vitro: nominal T current modulation causes robust antioscillatory effects. *Journal of Neuroscience* **14**: 5485–5502.

Huguenard, J.R., Chung, J.M. and Prince, D.A. (1996) Excitability changes in thalamic and neocortical neurons after injury. In *Progressive Nature of Epileptogenesis (Epilepsy Research*, Suppl. 12), ed. U. Heinemann, pp. 129–135, Amsterdam: Elsevier.

Huntsman, M.M. and Huguenard, J.R. (2000) Nucleus-specific differences in $GABA_A$ receptor mediated inhibition are enhanced during thalamic development. *Journal of Neurophysiology* **83**: 350–358.

Huntsman, M.M., Porcello, D.M., Homanics, G.E., DeLorey, T.M. and Huguenard, J.R. (1999) Reciprocal inhibitory connections and network synchrony in the mammalian thalamus. *Science* **283**: 541–543.

IFSECN (1974) A glossary of terms most commonly used by clinical electroencephalographers. *Electroencephalography and Clinical Neurophysiology* **37**: 538–548.

Imig, T.J. and Reale, R.A. (1981) Ipsilateral corticocortical projections related to binaural columns in cat primary auditory cortex. *Journal of Comparative Neurology* **203**: 1–14.

Immon, H., Ito, K., Dauphin, L. and McCarley, R.W. (1996) Electrical stimulation of the cholinergic laterodorsal tegmental nucleus elicits scopolamine-sensitive excitatory postsynaptic potentials in medial pontine reticular formation neurons. *Neuroscience* **74**: 393–401.

Inglis, W.L. and Semba, K. (1996) Colocalization of ionotropic glutamate receptor subunits with NADPH-diaphorase-containing neurons in the rat mesopontine tegmentum. *Journal of Comparative Neurology* **368**: 17–32.

Ingvar, D.H., Sjölund, B. and Ardo, A. (1976) Correlation between ECG frequency, cerebral oxygen uptake and blood flow. *Electroencephalography and Clinical Neurophysiology* **41**: 268–276.

Innocenti, B., Parpura, V. and Haydon, P.G. (2000) Imaging extracellular waves of glutamate during calcium signaling in cultured astrocytes. *Journal of Neuroscience* **20**: 1800–1808.

Isokawa, M. and Levesque, M.F. (1991) Increased NMDA responses and dendritic degeneration in human epileptic hippocampal neurons in slices. *Neuroscience Letters* **132**: 212–216.

Ito, H., Halldin, C. and Farde, L. (1999) Localization of $5\text{-}HT_{1A}$ receptors in the living human brain using [carbonyl-11C]WAY-100635: PET with anatomic standardization technique. *Journal of Nuclear Medicine* **40**: 102–109.

Ito, K. and McCarley, R.W. (1984) Alterations in membrane potential and excitability of cat medial pontine reticular formation neurons during changes in naturally occurring sleep-wake states. *Brain Research* **292**: 169–175.

Ito, K., Yanagihara, M., Imon, L., Dauphin, L. and McCarley, R.W. (2002) Intracellular recordings of pontine medial gigantocellular tegmental field neurons in the naturally sleeping cat: behavioral state-related activity and soma size difference in order of recruitment. *Neuroscience*, **114**: 23–37.

Iyer, K.S. and McCann, S.M. (1987) Delta sleep inducing peptide (DSIP) stimulates growth hormone (GH) release in the rat by hypothalamic and pituitary actions. *Peptides* **8**: 45–48.

Jackson, J.H. (1864) Illustrations of diseases of the nervous system: clinical lectures and reports by the medical staff of the London hospital. *London Hospital Reports* **1**: 337–387.

Jackson, J.H. (1931) *Selected Writings of John Hughlings Jackson* (vol. 1, *On Epilepsy and Epileptiform Convulsions*), ed. J. Taylor, London: Hodder and Stroughton.

Jacobs, K.M., Graber, K.D., Kharazia, V.N., Parada, I. and Prince, D.A. (2000) Postlesional epilepsy: the ultimate brain plasticity. *Epilepsia* **41** (Suppl. 6): S153–S161.

Jacobsen, R.B., Uhlrich, D. and Huguenard, J.R. (2001) $GABA_B$ and NMDA receptors contribute to spindle-like oscillations in rat thalamus *in vitro*. *Journal of Neurophysiology* **86**: 1365–1375.

Jahnsen, H. and Llinás, R. (1984a) Electrophysiological properties of guinea-pig thalamic neurones: an *in vitro* study. *Journal of Physiology (London)* **349**: 205–226.

Jahnsen, H. and Llinás, R. (1984b) Ionic basis for electroresponsiveness and oscillatory properties of guinea-pig thalamic neurones *in vitro*. *Journal of Physiology (London)* **349**: 227–247.

Jandó, G., Carpi, D., Kandel, A., Urioste, R., Horvath, Z., Pierre, E., Vati, D., Vadasz, C. and Buzsáki, G. (1995) Spike-and-wave epilepsy in rats: sex differences and inheritance of physiological traits. *Neuroscience* **64**: 301–317.

Jasper, H.H. (1949) Diffuse projection systems: the integrative action of the thalamic reticular system. *Electroencephalography and Clinical Neurophysiology* **1**: 405–420.

Jasper, H.H. (1969) Mechanism of propagation. In *Brain Mechanisms of the Epilepsies*, ed. H.H. Jasper, A.A. Ward and A. Pope, pp. 421–438, Boston: Little, Brown.

Jasper, H.H. (1975) Application of experimental models to human epilepsy. In *Experimental Models of Epilepsy*, ed. D.P. Purpura, J.K. Penry, D.B. Tower, D.M. Woodbury and R.D. Walter, pp. 585–601, New York: Raven Press.

Jasper, H.H. (1981) Problems relating cellular or modular specificity to cognitive functions: importance of state-dependent reactions. In *The Organization of the Cerebral Cortex*, ed. F.O. Schmitt, F.G. Worden, G. Adelman and S.G. Dennis, pp. 375–393, Cambridge, MA: The MIT Press.

Jasper, H.H. (1990) Historical introduction. In *Generalized Epilepsies*, ed. M. Avoli, P. Gloor, G. Kostopoulos and R. Naquet, pp. 1–15, Boston: Birkhäuser.

Jasper, H.H. and Droogleever-Fortuyn, J. (1949) Experimental studies on the functional anatomy of petit-mal epilepsy. *Research Publications of the Association of Nervous and Mental Diseases* **26**: 272–298.

Jasper, H.H. and Hawkes, W.A. (1938) Electroencephalography. IV. Localization of seizure waves in epilepsy. *Archives of Neurology (Chicago)* **39**: 885–901.

Jasper, H.H. and Kershman, J. (1941) Electroencephalographic classification of the epilepsies. *Archives of Neurology and Psychiatry* **45**: 903–943.

Jasper, H.H. and Shagass, C. (1941) Conscious time judgments related to conditioned time intervals and voluntary control of the alpha rhythm. *Journal of Experimental Psychology* **28**: 503–508.

Jasper, H.H. and Tessier, J. (1971) Acetylcholine liberation from cerebral cortex during paradoxical (REM) sleep. *Science* **172**: 601–602.

Jasper, H.H., Pertuiset, B. and Flaniginn H. (1951) EEG and cortical electrogram in patients with temporal lobe epilepsy. *Archives of Neurology and Psychiatry (Chicago)* **65**: 272–290.

Jasper, H.H., Ward, A.A. Jr. and Pope, A. (eds) (1969) *Basic Mechanisms of the Epilepsies*. Boston: Little, Brown.

Jeanmonod, D., Magnin, M., Morel, A., Siegemund, M., Cancro, A., Lanz, M., Llinás, R., Ribary, U., Kronberg, E., Schulman, J. and Zonenshayn, M. (2001) Thalamocortical dysrhythmia. II. Clinical and surgical aspects. *Thalamus and Related Systems* **1**: 245–254.

Jefferson, G. (1958) Reticular formation and clinical neurology. In *Reticular Formation of the Brain*, ed. H.H. Jasper, L.D. Proctor, R.S. Knighton, W.C. Noshay and R.T. Costello, pp. 729–738, Boston: Little, Brown.

Jefferys, J.G.R. (1995) Nonsynaptic modulation of neuronal activity in the brain: electric currents and extracellular ions. *Physiological Reviews* **75**: 689–723.

Jefferys, J.G.R. and Haas, H.L. (1982) Synchronized bursting of CA1 pyramidal cells in absence of synaptic transmission. *Nature* **300**: 448–450.

Jensen, F.E., Holmes, G.L., Lombroso, C.T., Blume, H.K. and Firkusny, I.R. (1992) Age-dependent changes in long-term seizures susceptibility and behavior after hypoxia in rats. *Epilepsia* **33**: 971–980.

Jensen, M.S. and Yaari, Y. (1997) Role of intrinsic burst firing, potassium accumulation, and electrical coupling in the elevated postassium model of hippocampal epilepsy. *Journal of Neurophysiology* **77**: 1224–1233.

Jensen, M.S., Cherubini, E. and Yaari, Y. (1993) Opponent effects of potassium on $GABA_A$-mediated postsynaptic inhibition in the rat hippocampus. *Journal of Neurophysiology* **69**: 764–771.

Jensen, M.S., Azouz, R. and Yaari, Y. (1994) Variant firing patterns in rat hippocampal pyramidal cells modulated by extracellular potassium. *Journal of Neurophysiology* **71**: 831–839.

Jensen, M.S., Azouz, R. and Yaari, Y. (1996) Spike afterdepolarization and burst generation in adult rat hippocampal CA1 pyramidal cells. *Journal of Physiology (London)* **492**: 199–210.

Jobert, M., Poiseau, E., Jähnig, P., Schulz, H. and Kubicki, S. (1992) Topographical analysis of sleep spindle activity. *Neuropsychobiology* **26**: 210–217.

Johnston, D. and Brown, T.H. (1981) Giant spike potential hypothesis for epileptiform activity. *Science* **211**: 294–297.

Johnston, D. and Brown, T.H. (1984) The synaptic nature of the paroxysmal depolarizing shift in hippocampal neurons. *Annals of Neurology* **16** (Suppl.): S65–S75.

Johnston, D., Magee, J.C., Colbert, C.M. and Cristie, B.R. (1996) Active properties of neuronal dendrites. *Annual Reviews of Neuroscience* **19**: 165–186.

Johnston, D., Hoffman, D.A., Magee, J.C., Poolos, N.P., Watanabe, S., Colbert, C.M. and Migliore, M. (2000) Dendritic potassium channels in hippocampal pyramidal neurons. *Journal of Physiology (London)* **525**: 75–81.

Jones, B.E. (1995) Reticular formation: cytoarchitecture, transmitters, and projections. In *The Rat Nervous System*, 2nd edn., ed. G. Paxinos, pp. 155–171, New York: Academic.

Jones, B.E. (2000) Basic mechanisms of sleep-wake states. In *Principles and Practice of Sleep Medicine*, ed. M.H. Kryger, T. Toth and W.C. Dement, pp. 134–154, Philadelphia: Saunders.

Jones, E.G. (1975) Varieties and distribution of non-pyramidal cells in the somatic sensory cortex of the squirrel monkey. *Journal of Comparative Neurology* **160**: 205–268.

Jones, E.G. (1985) *The Thalamus*. New York: Plenum.

Jones, E.G. (1995) Overview: basic elements of the cortical network. In *The Cortical Neuron*, ed. M.J. Gutnick and I. Mody, pp. 111–122, New York: Oxford University Press.

Jones, E.G. (1998) What are local circuits? In *Neurobiology of Neocortex*, ed. P. Rakic and W. Singer, pp. 137–152, New York: Wiley.

Jones, E.G. (2000) Cortical and subcortical contributions to activity-dependent plasticity in primate somatosensory cortex. *Annual Reviews of Neuroscience* **23**: 1–37.

Jones, E.G. (2001) The thalamic matrix and thalamocortical synchrony. *Trends in Neurosciences* **24**: 595–601.

Jones, E.G. and Powell, T.P.S. (1969) An electron microscopic study of the mode of transmission of cortico-thalamic fibres within the sensory relay nuclei of the thalamus. *Proceedings of the Royal Society of London (Series B)* **172**: 173–185.

Jones, E.G., Coulter, J.D. and Hendry, S.H.C. (1978) Intracortical connectivity of architectonic fields in somatic sensory, motor and parietal cortex of monkeys. *Journal of Comparative Neurology* **181**: 291–348.

Jones, M.S. and Barth, D.S. (1999) Spatiotemporal organization of fast (>200 Hz) electrical oscillations in rat vibrissa/barrel cortex. *Journal of Neurophysiology* **82**: 1599–1609.

Jones, M.S., MacDonald, K.D., Choi, B., Dudek, F.E. and Barth, D.S. (2000) Intracellular correlates of fast (>200 Hz) electrical oscillations in rat somatosensory cortex. *Journal of Neurophysiology* **84**: 1505–1518.

Jones, R.S. and Heinemann, V. (1988) Synaptic and intrinsic responses of medial entorhinal cortical cells in normal and magnesium-free medium *in vitro*. *Journal of Neurophysiology* **59**: 1476–1496.

Jouvet, M. (1962) Recherches sur les structures nerveuses et les mécanismes responsables des différentes phases du sommeil physiologique. *Archives Italiennes de Biologie* **100**: 125–206.

Jouvet, M. (1965) Paradoxical sleep – a study of its nature and mechanisms. *Progress in Brain Research* **18**: 20–57.

Jouvet, M. (1972) The role of monoamines and acetylcholine-containing neurons in the regulation of the sleep-waking cycle. *Ergebnisse der Physiologie* **64**: 166–307.

Jouvet, M. (1986) Programmation génétique itérative et sommeil paradoxal. *Confrontations Psychiatriques* **27**: 153–181.

Jouvet, M. (1988) The regulation of paradoxical sleep by the hypothalamo-hypophysis. *Archives Italiennes de Biologie* **126**: 259–274.

Jouvet, M. (1992) *Le Château des Songes*. Paris: Odile Jacob.

Jouvet, M. (1999) *The Paradox of Sleep*. Cambridge, MA: The MIT Press.

Jouvet, M. and Michel, F. (1959) Corrélations électromyographiques du sommeil chez le chat décortiqué et mésencéphalique chronique. *Comptes Rendus de la Société de Biologie (Paris)* **153**: 422–425.

Jouvet, M., Michel, F. and Courjon, J. (1959) Sur un stade d'activité électrique cérébrale rapide au cours du sommeil physiologique. *Comptes Rendus de la Société de Biologie (Paris)* **153**: 1024–1028.

Jouvet-Mounier, D., Astic, L. and Lacote, D. (1970) Ontogenesis of the states of sleep in rat, cat, and guinea-pig during the first postnatal month. *Developmental Psychobiology* **2**: 216–239.

Jung, R. (1962) Blocking of petit-mal attacks by sensory arousal and inhibition of attacks by an active change in attention during the epileptic aura. *Epilepsia* **3**: 435–437.

Kammermeier, P.J. and Jones, S.W. (1997) High-voltage-activated calcium currents in neurons acutely isolated from the ventrobasal nucleus of the rat thalamus. *Journal of Neurophysiology* **77**: 465–475.

Kamondi, A., Williams, J.A., Hutcheon, B. and Reiner, P.B. (1992) Membrane properties of mesopontine cholinergic neurons studied with the whole-cell patch-clamp technique: implications for behavioral state control. *Journal of Neurophysiology* **68**: 1359–1372.

Kamondi, A., Acsády, L. and Buzsáki, G. (1998) Dendritic spikes are enhanced by cooperative network activity in the intact hippocampus. *Journal of Neuroscience* **18**: 3919–3928.

Kamphuis, W., Huisman, E., Dreijer, A.M., Ghijsen, W.E., Verhage, M. and Lopes da Silva, F.H. (1990) Kindling increases the K^+-evoked Ca^{2+}-dependent release of endogenous GABA in area CA1 of rat hippocampus. *Brain Research* **511**: 63–70.

Kandel, A. and Buzsáki, G. (1997) Cellular-synaptic generation of sleep spindles, spike-and-wave discharges, and evoked thalamocortical responses in the neocortex of rat. *Journal of Neuroscience* **17**: 6783–6797.

Kandel, E.R. and Spencer, W.A. (1961) Electrophysiology of hippocampal neurons. II. After-potentials and repetitive firing. *Journal of Neurophysiology* **24**: 243–259.

Kandel, E.R., Spencer, W.A. and Brinley, F.J. Jr. (1961) Electrophysiology of hippocampal neurons. I. Sequential invasion and synaptic organization. *Journal of Neurophysiology* **24**: 225–242.

Kang, J., Jiang, L., Goldman, S.A. and Nedergaard, M. (1998) Astrocyte-mediated potentiation of inhibitory synaptic transmission. *Nature Neuroscience* **1**: 683–692.

Kang, Y. and Kayano, F. (1994) Electrophysiological and morphological characteristics of layer VI pyramidal cells in the cat motor cortex. *Journal of Neurophysiology* **72**: 578–591.

Kang, Y. and Kitai, S.T. (1990) Electrophysiological properties of pedunculopontine neurons and their postsynaptic responses following stimulation of substantia nigra reticulata. *Brain Research* **535**: 79–95.

Kao, C.Q. and Coulter, D.A. (1997) Physiology and pharmacology of corticothalamic stimulation-evoked responses in rat somatosensory thalamic neurons *in vitro*. *Journal of Neurophysiology* **77**: 2661–2676.

Kapas, L., Obal, F. Jr. and Krueger, J.M. (1993) Humoral regulation of sleep. *International Reviews of Neurobiology* **35**: 131–160.

Karni, A., Tanne, D., Rubenstein, B.S., Askenasy, J.J.M. and Sagi, D. (1994) Dependence on REM sleep of overnight improvement of a perceptual skill. *Science* **265**: 679–682.

Kato, N. (1990) Cortico-thalamo-cortical projection between visual cortices. *Brain Research* **509**: 150–152.

Kawaguchi, Y. (1993) Groupings of nonpyramidal and pyramidal cells with specific physiological and morphological characteristics in rat frontal cortex. *Journal of Neurophysiology* **69**: 416–431.

Kawaguchi, Y. (1995) Physiological subgroups of nonpyramidal cells with specific morphological characteristics in layers II/III of rat frontal cortex. *Journal of Neuroscience* **15**: 2638–2655.

Kawaguchi, Y. and Kubota, Y. (1993) Correlation of physiological subgroups of nonpyramidal cells with parvalbumin- and calbindin$_{D28k}$-immunoreactive neurons in layer V of rat frontal cortex. *Journal of Neurophysiology* **70**: 387–396.

Kawaguchi, Y. and Kubota, Y. (1996) Physiological and morphological identification of somatostatin- or vasoactive intestinal polypeptide-containing cells among GABAergic cell subtypes in rat frontal cortex. *Journal of Neuroscience* **16**: 2701–2715.

Kawaguchi, Y. and Kubota, Y. (1997) GABAergic cell subtypes and their synaptic connections in rat frontal cortex. *Cerebral Cortex* **7**: 476–486.

Kayama, Y., Sugitani, M. and Iwama, K. (1982) Effects of locus coeruleus stimulation on neuronal activities of dorsal lateral geniculate nucleus and perigeniculate reticular nucleus of the rat. *Neuroscience* **7**: 655–666.

Keifer, J.C., Baghdoyan, H.A., Becker, L. and Lydic, R. (1994) Halothane decreases pontine acetylcholine release and increases spindles. *NeuroReport* **5**: 577–580.

Kellaway, P. (1985) Sleep and epilepsy. *Epilepsia* **26** (Suppl. 1): 15–30.

Kellaway, P. and Frost, J.D. Jr. (1983) Biorhythmic modulation of epileptic events. In *Recent Advances in Epilepsy* (vol. 1), ed. T.A. Pedley and B.S. Meldrum, pp. 139–154, London: Churchill-Livingstone.

Kellaway, P., Crawley, J.W. and Kagawa, N. (1960) Paroxysmal pain and autonomic disturbances of cerebral origin: a specific electroclinical syndrome. *Epilepsia* **1**: 466–483.

Kellaway, P., Hrachovy, R.A., Frost, J.D. Jr. and Zion, T. (1979) Precise characterization and quantification of infantile spasms. *Annals of Neurology* **6**: 214–218.

Kellaway, P., Frost, J.D. Jr. and Crawley, J.W. (1980) Time modulation of spike-and-wave activity in generalized epilepsy. *Annals of Neurology* **8**: 491–500.

Kellaway, P., Frost, J.D. Jr. and Crawley, J.W. (1990) The relations between sleep spindles and spike-and-wave bursts in human epilepsy. In *Generalized Epilepsy*, ed. M. Avoli, P. Gloor, G. Kostopoulos and R. Naquet, pp. 36–48, Boston: Birkhäuser.

Keller, A. (1993) Intrinsic synaptic organization of the motor cortex. *Cerebral Cortex* **3**: 43–51.

Kennedy, C., Gillin, J.C., Mendelson, W., Suda, S., Miyaoka, M., Ito, M., Nakamura, R.K., Storch, F.I., Pettigrew, K., Mishkin, M. and Sokoloff, L. (1982) Local cerebral glucose utilization in non-rapid eye movement sleep. *Nature* **297**: 325–327.

Kettenmann, H. and Schachner, M. (1985) Pharmacological properties of γ-aminobutyric acid-, glutamate-, and aspartate-induced depolarizations in cultured astrocytes. *Journal of Neuroscience* **5**: 3295–3301.

Khateb, A., Serafin, M. and Mühlethaler, M. (1989) Midbrain reticular neurones *in vitro* are sensitive to amines and opiates. *Society of Neuroscience Abstracts* **15**: 451.

Khateb, A., Serafin, M., Jones, B.E., Alonso, A. and Mühlethaler, M. (1991) Pharmacological study of basal forebrain neurons in guinea pig brain slices. *Society for Neuroscience Abstracts* **17**: 881.

Khateb, A., Fort, P., Alonso, A., Jones, B.E. and Mühlethaler, M. (1993) Pharmacological and immunohistochemical evidence for serotonergic modulation of cholinergic nucleus basalis neurons. *European Journal of Neuroscience* **5**: 541–547.

Khazipov, R., Esclapez, M., Caillard, O., Bernard, C., Khalikov, I., Tyzio, R., Hirsch, J., Dzhala, V., Berger, B. and Ben-Ari, Y. (2001) Early development of neuronal activity in the primate hippocampus *in utero*. *Journal of Neuroscience* **21**: 9770–9781.

Kia, H.K., Miquel, M.C., Brisorgeuil, M.J., Daval, G., Riad, M., Mestikawy, S., Hamon, M. and Verge, D. (1996) Immunocytochemical localization of serotonin 1A receptors in the rat central nervous system. *Journal of Comparative Neurology* **365**: 289–305.

Killam, K.F., Killam, E.K. and Naquet, R. (1967) An animal model of light sensitive epilepsy. *Electroencephalography and Clinical Neurophysiology* **22**: 497–513.

Kim, D., Song, I., Keum, S., Lee, T., Jeong, M.J., Kim, S.S., McEnery, M.W. and Shin, H.S. (2001) Lack of the burst firing of thalamocortical relay neurons and resistance to absence seizures in mice lacking α_{1G} T-type Ca^{2+} channels. *Neuron* **31**: 35–45.

Kim, U. and McCormick, D.A. (1998) Functional and ionic properties of a slow afterhyperpolarization in ferret perigeniculate neurons *in vitro*. *Journal of Neurophysiology* **80**: 1222–1235.

Kim, U., Bal, T. and McCormick, D.A. (1995) Spindle waves are propagating synchronized oscillations in the ferret LGNd *in vitro*. *Journal of Neurophysiology* **74**: 1301–1323.

Kim, U., Sanchez-Vives, M.V. and McCormick, D.A. (1997) Functional dynamics of GABAergic inhibition in the thalamus. *Science* **278**: 130–134.

Kinomura, S., Larsson, J., Gulyás, B. and Roland, P. (1996) Activation by attention of the human reticular formation and thalamic intralaminar nuclei. *Science* **271**: 512–515.

Kita, Y. and Kitai, S.T. (1990) Electrophysiological properties of pedunculopontine neurons and their postsynaptic responses following stimulation of substantia nigra pars reticulata. *Brain Research* **535**: 79–95.

Kitsikis, A. and Steriade, M. (1981) Immediate behavioral effects of kainic acid injections into the midbrain reticular core. *Behavioral Brain Research* **3**: 361–380.

Kleitman, N. (1963) *Sleep and Wakefulness.* Chicago: University of Chicago Press.

Kleitman, N. (1993) Basic rest-activity cycle. In *Encyclopedia of Sleep and Dreaming*, ed. M.A. Carskadon, pp. 65–66, New York: Macmillan.

Klink, R. and Alonso, A. (1997a) Muscarinic modulation of the oscillatory and repetitive firing properties of entorhinal cortex layer II neurons. *Journal of Neurophysiology* **77**: 1813–1828.

Klink, R. and Alonso, A. (1997b) Ionic mechanisms of muscarinic depolarization in entorhinal cortex layer II neurons. *Journal of Neurophysiology* **77**: 1829–1843.

Klüver, H. and Bucy, P.C. (1937) An analysis of certain effects of bilateral lobectomy in the rhesus monkey, with special reference to "psychic blindness". *Journal of Psychology* **5**: 33–54.

Knight, A.R. and Bowery, N.G. (1992) GABA receptors in rats with spontaneous generalized nonconvulsive epilepsy. *Journal of Neural Transmission* **35** (Suppl.): 189–196.

Knowles, W.D. and Schwartzkroin, P.A. (1981) Local circuit synaptic interactions in hippocampal brain slices. *Journal of Neuroscience* **1**: 318–322.

Kobayashi, K., Nishibayashi, N., Ohtsuka, Y., Oka, E. and Ohtahara, S. (1994) Epilepsy with electrical status epilepticus during slow sleep and secondary bilateral synchrony. *Epilepsia* **35**: 1097–1103.

Konorski, J. (1967) *Integrative Activity of the Brain*. Chicago: University of Chicago Press.

Kosaka, T., Kosaka, K., Hataguchi, Y., Nagatsu, I., Wu, J.Y., Ottersen, O.P., Storm-Mathisen, J. and Hama, K. (1987) Catecholaminergic neurons containing GABA-like and/or glutamic acid decarboxylase-like immunoreactivities in various brain regions of the rat. *Experimental Brain Research* **66**: 191–201.

Kostopoulos, G. (1992) The tottering mouse: a critical review of its usefulness in the study of neuronal mechanisms underlying epilepsy. *Journal of Neural Transmission* **35** (Suppl.): 21–36.

Kostopoulos, G. (2000) Spike-and-wave discharges of absence seizures as a transformation of sleep spindles: the continuing development of a hypothesis. *Clinical Neurophysiology* **111** (Suppl. 2): S27–S38.

Kotagal, P. (1995) Multifocal independent spike syndrome: relationship to hypsarrhthymia and the slow spike-wave (Lennox-Gastaut) syndrome. *Clinical Electroencephalography* **26**: 23–29.

Kotila, M. and Waltimo, O. (1992) Epilepsy after stroke. *Epilepsia* **33**: 495–498.

Koukkou, M. and Lehmann, D. (1968) EEG and memory storage in sleep experiments with humans. *Electroencephalography and Clinical Neurophysiology* **25**: 455–462.

Kreindler, A. (1965) *Experimental Epilepsy. Progress in Brain Research* (vol. 19), Amsterdam: Elsevier.

Kreindler, A. and Steriade, M. (1963) Functional differentiation within the amygdaloid complex inferred from peculiarities of afterdischarges. *Electroencephalography and Clinical Neurophysiology* **15**: 811–826.

Kreindler, A. and Steriade, M. (1964) EEG patterns of arousal and sleep induced by stimulating various amygdaloid levels in the cat. *Archives Italiennes de Biologie* **102**: 576–586.

Kreindler, A., Zuckermann, E., Steriade, M. and Chimion, D. (1958) Electroclinical features of the convulsive fit induced experimentally through stimulation of the brain stem. *Journal of Neurophysiology* **21**: 430–436.

Krnjević, K., Pumain, R. and Renaud, L. (1971) The mechanisms of excitation by acetylcholine in the cerebral cortex. *Journal of Physiology (London)* **215**: 247–268.

Krueger, J.M. and Toth, L.A. (1994) Cytokines as regulators of sleep. *Annals of New York Academy of Sciences* **739**: 299–310.

Krueger, J.M., Pappenheimer, J.R. and Karnovsky, M.L. (1982) Sleep-promoting effects of muramyl peptides. *Proceedings of the National Academy of Sciences of the USA* **79**: 6102–6106.

Krueger, J.M., Walter, J., Karnovsky, M.L., Chedid, L., Choay, J.P., Lefrancier, P. and Lederer, E. (1984) Muramyl peptides. Variation of somnogenic activity with structure. *Journal of Experimental Medicine* **159**: 68–76.

Krueger, J.M., Obal, F. Jr. and Fang, J. (1999) Humoral regulation of physiological sleep: cytokines and GHRH. *Journal of Sleep Research* **8** (Suppl. 1): 53–59.

Krushinsky, L.V. (1962) Study of pathophysiological mechanism of cerebral haemorrhages provoked by reflex epileptic seizures in rats. *Epilepsia* **3**: 363–380.

Kudrimoti, H.S., Barnes, C.A. and McNaughton, B.L. (1999) Reactivation of hippocampal cell assemblies: effects of behavioral state, experience, and EEG dynamics. *Journal of Neuroscience* **19**: 4090–4101.

Lacaille, J.C. and Schwartzkroin, P.A. (1988a) Stratum lacunosum-moleculare interneurons of hippocampal CA1 region. I. Intracellular response characteristics, synaptic responses and morphology. *Neuroscience* **8**: 1400–1410.

Lacaille, J.C. and Schwartzkroin, P.A. (1988b) Stratum lacunosum-moleculare interneurons of hippocampal CA1 region. II. Intrasomatic and intradendritic recordings of local circuit synaptic interactions. *Neuroscience* **8**: 1411–1424.

Lai, Y.Y., Clements, J.R. and Siegel, J.M. (1993) Glutamatergic and cholinergic projections to the pontine inhibitory area identified with horseradish peroxidase retrograde transport and immunohistochemistry. *Journal of Comparative Neurology* **336**: 321–330.

Lampl, I., Reichova, I. and Ferster, D. (1999) Synchronous membrane potential fluctuations in neurons of the cat visual cortex. *Neuron* **22**: 361–374.

Lancel, M., van Riezen, H. and Glatt, A. (1992) The time course of σ activity and slow-wave activity during NREMS in cortical and thalamic EEG of the cat during baseline and after 12 hours of wakefulness. *Brain Research* **596**: 285–295.

Landisman, C.E., Long, M.A., Beierlein, M., Deans, M.R., Paul, D.L. and Connors, B.W. (2002) Electrical synapses in the thalamic reticular nucleus. *Journal of Neuroscienc* **22**: 1002–1009.

Lang, E.J. and Paré, D. (1997) Synaptic and synaptically activated intrinsic conductances underlie inhibitory potentials in cat lateral amygdaloid projection neurons *in vivo*. *Journal of Neurophysiology* **77**: 353–363.

Lang, E.J. and Paré, D. (1998) Synaptic responses of interneurons of the cat lateral amygdaloid nucleus. *Neuroscience* **83**: 877–889.

Laureys, S., Peigneux, P., Phillips, C., Fuchs, S., Degueldre, C., Aerts, J., Del Fiore, G., Petiau, C., Luxen, A., Van der Linden, M., Cleeremans, A., Smith, C. and Maquet, P. (2001) Experience-dependent changes in cerebral functional connectivity during human rapid eye movement sleep. *Neuroscience* **105**: 521–525.

Lavoie, B. and Parent, A. (1994) Pedunculopontine nucleus in the squirrel monkey: distribution of cholinergic and monoaminergic neurons in the mesopontine tegmentum with evidence for the presence of glutamate in cholinergic neurons. *Journal of Comparative Neurology* **344**: 190–209.

LeDoux, J.E. (1996) *The Emotional Brain*. New York: Simon and Schuster.

LeDoux, J.E., Cicchetti, P., Xagoraris, A. and Romanski, L.M. (1990) The lateral amygdaloid nucleus: sensory interface of the amygdala in fear conditioning. *Journal of Neuroscience* **10**: 1062–1069.

Lee, K. and McCormick, D.A. (1996) Abolition of spindle oscillations by serotonin and norepinephrine in the ferret lateral geniculate and perigeniculate nuclei *in vitro*. *Neuron* **17**: 309–321.

Lehmann, T.N., Gabriel, S., Kovacs, R., Eilers, A., Kivi, A., Schulze, K., Lanksch, W.R., Meencke, H.J. and Heinemann, U. (2000) Alterations in neuronal connectivity in area CA1 of hippocampal slices from temporal lobe epilepsy patients and pilocarpine-treated epileptic rats. *Epilepsia* **41** (Suppl. 6): S190–S194.

Lemieux, J.F. and Blume, W.T. (1986) Topographical evolution of spike-wave complexes. *Brain Research* **373**: 275–287.

Lennox, W.G. (1951) Phenomena and correlates of the psychomotor triad. *Archives of Neurology* **1**: 357–371.

Lennox, W.G. and Lennox, M.A. (1960) *Epilepsy and Related Disorders.* London: Churchill.

Leonard, C.S. and Llinás, R.R. (1990) Electrophysiology of mammalian pedunculopontine and laterodorsal tegmental neurons *in vitro*: implications for the control of REM sleep. In *Brain Cholinergic Systems*, ed. M. Steriade and D. Biesold, pp. 205–223, Oxford: Oxford University Press.

Leonard, C.S. and Llinás, R.R. (1994) Serotonergic and cholinergic inhibition of mesopontine cholinergic neurons controlling REM sleep: an *in vitro* electrophysiological study. *Neuroscience* **59**: 309–330.

Leonard, C.S., Rao, S. and Sanchez, R.M. (1995) Patterns of neuromodulation and the nitric oxide signaling pathway in mesopontine cholinergic neurons. *Seminars in the Neurosciences*, ed. M. Steriade, **7**: 319–328.

Leonard, C.S., Michaelis, E.K. and Mitchell, K.M. (2001) Activity-dependent nitric oxide concentration dynamics in the laterodorsal tegmental nucleus *in vitro*. *Journal of Neurophysiology* **86**: 2159–2172.

Leresche, N., Jassik-Gerschenfeld, D., Haby, M., Soltesz, I. and Crunelli, V. (1990) Pacemaker-like and other types of spontaneous membrane potential oscillations of thalamocortical cells. *Neuroscience Letters* **113**: 72–77.

Leresche, N., Lightowler, S., Soltesz, I., Jassik-Gerschenfeld, D. and Crunelli, V. (1991) Low-frequency oscillatory activities intrinsic to rat and cat thalamocortical cells. *Journal of Physiology (London)* **441**: 155–174.

Leresche, N., Parri, H.R., Erdemli, G., Guyon, A., Turner, J.P., Williams, S.R., Asprodini, E. and Crunelli, V. (1998) On the action of the anti-absence drug ethosuximide in the rat and cat thalamus. *Journal of Neuroscience* **18**: 4842–4853.

Leresche, N., Asprodini, E., Emri, Z., Cope, D.W. and Crunelli, V. (2000) Somatostatin inhibits GABAergic transmission in the sensory thalamus via presynaptic receptors. *Neuroscience* **98**: 513–522.

Leschinger, A., Stabel, J., Igelmund, P. and Heinemann, U. (1993) Pharmacological and electrographic properties of epileptiform activity induced by elevated K^+ and lowered Ca^{2+} and Mg^{2+} concentration in rat hippocampal slices. *Experimental Brain Research* **96**: 230–240.

Letinic, K. and Rakic, P. (2001) Telencephalic origin of human thalamic GABAergic neurons. *Nature Neuroscience* **4**: 931–936.

Lévesque, M., Charara, A., Gagnon, S., Parent, A. and Deschênes, M. (1996) Corticostriatal projections from layer V cells in rat are collaterals of long-range corticofugal axons. *Brain Research* **709**: 311–315.

Levi, G. and Gallo, V. (1995) Release of neuroactive amino acids from glia. In *Neuroglia*, ed. H. Kettenmann and B.R. Ransom, pp. 815–826, New York: Oxford University Press.

Li, C.L. and McIlwain, H. (1957) Maintenance of resting membrane potentials in slices of mammalian cerebral cortex and other tissues *in vitro*. *Journal of Physiology (London)* **139**: 178–190.

Li, X.G., Somogyi, P., Ylinen, A. and Buzsáki, G. (1994) The hippocampal CA3 network: an *in vivo* intracellular labeling study. *Journal of Comparative Neurology* **339**: 181–208.

Lin, J.S., Sakai, K. and Jouvet, M. (1988) Evidence for histaminergic arousal mechanisms in the hypothalamus of cats. *Neuropharmacology* **27**: 111–122.

Lin, J.S., Sakai, K., Vanni-Mercier, G. and Jouvet, M. (1989) A critical role of the posterior hypothalamus in the mechanisms of wakefulness determined by microinjections of muscimol in freely moving cats. *Brain Research* **479**: 225–240.

Lingenhoehl, K., Brom, R., Heid, J., Beck, P., Froestl, W., Kaupmann, K., Bettler, B. and Mosbacher, J. (1999) γ-hydroxybutyrate is a weak agonist at recombinant $GABA_B$ receptors. *Neuropharmacology* **38**: 1667–1674.

Lipman, I.J. and Hughes, J.R. (1968) Rhythmic mid-temporal discharges. *Electroencephalography and Clinical Neurophysiology* **27**: 43–47.

Lisman, J.E. (1997) Bursts as a unit of neural information: making unreliable synapses reliable. *Trends in Neurosciences* **20**: 38–43.

Litt, B., Esteller, R., Echauz, J., D'Alessandro, M., Shor, R., Henry, T., Pennell, P., Epstein, C., Bakay, R., Dichter, M. and Vachtsevanos, G. (2001) Epileptic seizures may begin hours in advance of clinical onset: a report of five patients. *Neuron* **30**: 51–64.

Liu, X.B. and Jones, E.G. (1999) Predominance of corticothalamic synaptic inputs to thalamic reticular nucleus neurons in the rat. *Journal of Comparative Neurology* **414**: 67–79.

Liu, X.B., Warren, R.A. and Jones, E.G. (1995) Synaptic distribution of afferents from reticular nucleus in ventroposterior nucleus of cat thalamus. *Journal of Comparative Neurology* **352**: 187–202.

Liu, X.B., Bolea, S., Golshani, P. and Jones, E.G. (2001) Differentiation of corticothalamic and collateral thalamocortical synapses on mouse reticular nucleus by EPSC amplitude and AMPA receptor subunit composition. *Thalamus and Related Systems* **1**: 15–29.

Liu, Z., Vergnes, M., Depaulis, A. and Marescaux, C. (1992) Involvement of intrathalamic $GABA_B$ neurotransmission in the control of absence seizures in the rat. *Neuroscience* **48**: 87–93.

Livingstone, M.S. and Hubel, D.H. (1981) Effects of sleep and arousal on the processing of visual information in the cat. *Nature* **291**: 554–561.

Llinás, R.R. (1964) Mechanisms of supraspinal action upon spinal cord activities. Differences between reticular and cerebellar inhibitory action upon alpha extensor motorneurones. *Journal of Neurophysiology* **27**: 1117–1126.

Llinás, R.R. (1985) Electrotonic transmission in the mammalian central nervous system. In *Gap Junctions*, ed. M.V.L. Bennett, pp. 337–353, New York: Cold Harbor Spring.

Llinás, R.R. (1988) The intrinsic electrophysiological properties of mammalian neurons: insights into central nervous system function. *Science* **242**: 1654–1664.

Llinás, R.R. and Paré, D. (1991) Of dreaming and wakefulness. *Neuroscience* **44**: 521–535.

Llinás, R.R. and Ribary, U. (1993) Coherent 40-Hz oscillation characterizes dream state in humans. *Proceedings of the National Academy of Sciences of the USA* **90**: 2078–2081.

Llinás, R.R. and Terzuolo, C.A. (1964) Mechanisms of supraspinal actions upon spinal cord activities. Reticular inhibitory mechanisms on alpha-extensor motoneurons. *Journal of Neurophysiology* **27**: 579–591.

Llinás, R., Grace, A.A. and Yarom, Y. (1991) *In vitro* neurons in mammalian cortical layer 4 exhibit intrinsic oscillatory activity in the 10- to 50-Hz frequency range. *Proceedings of the National Academy of Sciences of the USA* **88**: 897–901.

Llinás, R., Ribary, U., Jeanmonod, D., Kronberg, E. and Mitra, P.P. (1999) Thalamocortical dysrhythmia: a neurological and neuropsychiatric syndrome characterized by magneto-encephalography. *Proceedings of the National Academy of Sciences of the USA* **96**: 15222–15227.

Llinás, R., Ribary, U., Jenamonod, D., Cancro, R., Kronberg, E., Schulman, J., Zonenshayn, M., Magnin, M., Morel, A. and Siegemund, M. (2001) Thalamocortical dysrhythmia. I. Functional and imaging aspects. *Thalamus and Related Systems* **1**: 237–244.

Loiseau, P. (1992) Human absence epilepsies. *Journal of Neural Transmission* **35** (Suppl.): 1–6.

Loomis, A.L., Harvey, N. and Hobart, G.A. (1938) Distribution of disturbance patterns in the human electroencephalogram, with special reference to sleep. *Journal of Neurophysiology* **1**: 413–430.

Lopantsev, V. and Avoli, M. (1998) Participation of $GABA_A$-mediated inhibition in ictal-like discharges in the rat entorhinal cortex. *Journal of Neurophysiology* **79**: 352–360.

Lopes da Silva, F.H., van Rotterdam, A., Storm van Leeuwen, W. and Tielen, A.M. (1970) Dynamic characteristics of visual evoked potentials in the dog. II. Beta frequency selectivity in evoked potentials and background activity. *Electroencephalography and Clinical Neurophysiology* **29**: 260–268.

Lopes da Silva, F.H., Witter, M.P., Boeijinga, P.H. and Lohman, A.H.M. (1990) Anatomic organization and physiology of the limbic system. *Physiological Reviews* **70**: 453–511.

Lopes da Silva, F.H., Kamphuis, W., Titulaer, M., Vreugdenhil, M. and Wadman, W.J. (1995) An experimental model of progressive epilepsy: the development of kindling of the hippocampus of the rat. *Italian Journal of Neurological Sciences* **16**: 45–57.

LoPiccolo, M.A. (1977) *Behavioral and Neuronal Effects of EEG Synchronizing Stimuli in the Cat.* Ph.D. Thesis, McMaster University, Hamilton (Ontario).

Lorente de Nó, R. (1933) Studies on the structure of the cerebral cortex. I. The area entorhinalis. *Journal of Psychology and Neurology* **45**: 381–438.

Loszádi, D.A. (1995) Organization of connections between the thalamic reticular and the anterior thalamic nuclei in the rat. *Journal of Comparative Neurology* **358**: 233–246.

Lothman, E.W., Bertram, E.H. and Stringer, J.L. (1991) Functional anatomy of hippocampal seizures. *Progress in Neurobiology* **37**: 1–82.

Loup, F., Wieser, H.G., Yonekawa, Y., Aguzzi, A. and Fritschy, J.M. (2000) Selective alterations in $GABA_A$ receptor subtypes in human temporal lobe epilepsy. *Journal of Neuroscience* **20**: 5401–5419.

Lübke, J.I., Greene, R.W., Semba, K., Kamondi, A., McCarley, R.W. and Reiner, P.B. (1992) Serotonin hyperpolarizes cholinergic low-threshold burst neurons in the rat laterodorsal tegmental nucleus *in vitro*. *Proceedings of the National Academy of Sciences of the USA* **89**: 743–747.

Luciani, L. (1911) *Fisiologia dell'uomo.* Milano: Societa Editrice Libraria.

Lucretius, T.C. (1988) *On the Nature of the Universe* (translated by R.E. Latham). London: Penguin Books.

Lüders, H.O., Engel, J. Jr. and Munari, C. (1993) General principles. In *Surgical Treatment of the Epilepsies*, ed. J. Engel Jr., pp. 137–153, New York: Raven.

Luhmann, H.J., Mittmann, T., Schmidt-Kastner, R., Eysel, U.T., Mudrick-Donnon, L.A. and Heinemann, U. (1999) Hyperexcitability after focal lesions and transient ischemia in rat neocortex. In *Progressive Nature of Epileptogenesis* (*Epilepsy Research*, Suppl. 12), ed. U. Heinemann, pp. 119–128, Amsterdam: Elsevier.

Lüthi, A. and McCormick, D.A. (1998) Periodicity of thalamic synchronized oscillations: the role of Ca^{2+}-mediated upregulation of I_h. *Neuron* **20**: 553–63.

Lux, H.D. and Neher, E. (1973) The equilibrium time course of $[K^+]_o$ in cat cortex. *Experimental Brain Research* **17**: 190–205.

Lydic, R., McCarley, R.W. and Hobson, J.A. (1987) Serotonin neurons and sleep. II. Time course of dorsal raphe discharge frequency, PGO waves, and behavioral states. *Archives Italiennes de Biologie* **126**: 1–28.

Lytton, W.W. and Sejnowski, T.J. (1991) Simulation of cortical pyramidal neurons synchronized by inhibitory interneurons. *Journal of Neurophysiology* **66**: 1059–1079.

Lytton, W.W., Contreras, D., Destexhe, A. and Steriade, M. (1997) Dynamic interactions determine partial thalamic quiescence in a computer network model of spike-and-wave seizures. *Journal of Neurophysiology* **77**: 1679–1696.

MacDonald, K.D., Fifkova, E., Jones, M.S. and Barth, D.S. (1998) Focal stimulation of the thalamic reticular nucleus induces focal gamma waves in cortex. *Journal of Neurophysiology* **79**: 474–477.

Macnish, R. (1830) *The Philosophy of Sleep.* Glasgow: M'Phun.

MacVicar, B.A. (1985) Depolarizing prepotentials are Na^+-dependent in CA1 pyramidal neurons. *Brain Research* **333**: 378–381.

MacVicar, B.A. and Dudek, F.E. (1981) Electrotonic coupling between pyramidal cells: a direct demonstration in rat hippocampal slices. *Science* **213**: 782–785.

MacVicar, B.A. and Dudek, F.E. (1982) Electrotonic coupling between granule cells of rat dentate gyrus. Physiological and anatomical evidence. *Journal of Neurophysiology* **47**: 579–592.

MacVicar, B.A., Tse, F.W., Crichton, S.A. and Kettenmann, H. (1989) GABA-activated Cl^- channels in astrocytes of hippocampal slices. *Journal of Neuroscience* **9**: 3577–3583.

Maffei, L., Moruzzi, G. and Rizzolatti, G. (1965) Influence of sleep and wakefulness on the response of lateral geniculate units to sinewave photic stimulation. *Archives Italiennes de Biologie* **103**: 596–608.

Magee, J., Hoffman, D., Colbert, C. and Johnston, D. (1998) Electrical and calcium signaling in dendrites of hippocampal pyramidal neurons. *Annual Reviews of Physiology* **60**: 327–346.

Magill, P.J., Bolam, P. and Bevan, M.D. (2000) Relationship of activity in the subthalamic nucleus – globus pallidus network to cortical EEG. *Journal of Neuroscience* **20**: 820–833.

Magill, P.J., Bolam, J.P. and Bevan, M.D. (2001) Dopamine regulates the impact of the cerebral cortex on the subthalamic nucleus-globus pallidus network. *Neuroscience* **106**: 313–330.

Magistris, M.R., Mouradian, M.S. and Gloor, P. (1988) Generalized convulsions induced by pentylenetetrazol in the cat: participation of forebrain, brainstem, and spinal cord. *Epilepsia* **29**: 379–388.

Mahon, S., Deniau, J.M. and Charpier, S. (2001) Relationship between EEG potentials and intracellular activity of striatal and cortico-striatal neurons: an *in vivo* study under different anesthetics. *Cerebral Cortex* **11**: 360–373.

Mahowald, M.K. and Schenck, C.H. (1997) Sleep disorders. In *Epilepsy: A Comprehensive Textbook*, ed. J. Engel Jr. and T.A. Pedley, pp. 2705–2715, Philadelphia: Lippincot-Raven.

Malow, B.A., Fromes, G.A. and Aldrich, M.S. (1997) Usefulness of polysomnography in epilepsy patients. *Neurology* **48**: 1389–1394.

Manaye, K.F., Zweig, R., Wu, D., Hersh, L.B., De Lacalle, S., Saper, C.B. and German, D.C. (1999) Quantification of cholinergic and select non-cholinergic mesopontine neuronal populations in the human brain. *Neuroscience* **89**: 759–770.

Mangan, P.S., Scott, C.A., Williamson, J.M. and Bertram, E.H. III (2000) Aberrant neuronal physiology in the basal nucleus of the amygdala in a model of chronic limbic epilepsy. *Neuroscience* **101**: 377–391.

Manganotti, P., Zanette, G., Beltramello, A., Puppini, G., Miniussi, C., Maravita, A., Santorum, E., Marzi, C.A., Fiaschi, A. and Dalla Bernardina, B. (1999) Spike topography and fMRI in benign rolandic epilepsy with spikes evoked by tapping stimulation. *Electroencephalography and Clinical Neurophysiology* **107**: 88–92.

Manor, Y., Koch, C. and Segev, I. (1991) Effect of geometrical irregularities on propagation delay in axonal trees. *Biophysical Journal* **60**: 1424–1437.

Mao, B.Q., Hamzei-Sichani, F., Aronov, D., Froemke, R.C. and Yuste, R. (2001) Dynamics of spontaneous activity in neocortical slices. *Neuron* **32**: 883–898.

Maquet, P. (2000) Functional neuroimaging of normal human sleep by positron emission tomography. *Journal of Sleep Research* **9**: 207–231.

Maquet, P. and Phillips, C. (1998) Functional imaging of human sleep. *Journal of Sleep Research* **7** (Suppl. 1): 42–47.

Maquet, P., Dive, D., Salmon, E., Sadzot, B., Franco, G., Poirrier, R. and Franck, G. (1992) Cerebral glucose utilization during stage 2 sleep in man. *Brain Research* **571**: 149–153.

Maquet, P., Péters, J.M., Aerts, J., Delfiore, G., Degueldre, C., Luxen, A. and Franck, G. (1996) Functional neuro-anatomy of human rapid-eye-movement sleep and dreaming. *Nature* **383**: 163–166.

Maquet, P., Degueldre, C., Delfiore, G., Aerts, J., Péters, J.P., Luxen, A. and Franck, G. (1997) Functional neuroanatomy of human slow wave sleep. *Journal of Neuroscience* **17**: 2807–2812.

Maquet, P., Laureys, S., Peigneux, P., Fuchs, S., Petiau, C., Phillips, C., Aerts, J., Del Fiore, G., Degueldre, C., Meulemans, T., Luxen, A., Franck, G., Van der Linden, M., Smith, C. and Cleeremans, A. (2000) Experience-dependent changes in cerebral activation during human REM sleep.

Marco, P. and DeFelipe, J. (1997) Altered synaptic circuitry in the human temporal neocortex removed from epileptic patients. *Experimental Brain Research* **114**: 1–10.

Marcus, E.M. and Watson, C.W. (1966) Bilateral synchronous spike-wave electrographic patterns in the cat. *Archives of Neurology (Chicago)* **14**: 601–610.

Marcus, E.M., Watson, C.W. and Simon, S.A. (1968a) An experimental model of some varieties of petit mal epilepsy. Electrical-behavioral correlations of acute bilateral epileptogenic foci in cerebral cortex. *Epilepsia* **9**: 233–248.

Marcus, E.M., Watson, C.W. and Simon, S.A. (1968b) Behavioral correlates of acute bilateral symmetrical epileptogenic foci in monkey cerebral cortex. *Brain Research* **9**: 370–373.

Marescaux, C., Vergnes, M. and Bernusconi, R. (1992a) $GABA_B$ receptor antagonists: potential new anti-absence drugs. *Journal of Neural Transmission* **35** (Suppl.): 179–188.

Marescaux, C., Vergnes, M. and Depaulis, A. (1992b) Genetic absence epilepsy in rats from Strasbourg – a review. *Journal of Neural Transmission* **35** (Suppl.): 37–69.

Margerison, J.H. and Corsellis, J.A.N. (1966) Epilepsy and the temporal lobe: a clinical, electroencephalographic and neuropathological study of the brain in epilepsy, with particular reference to the temporal lobes. *Brain* **89**: 499–530.

Marini, G., Macchi, G. and Mancia, M. (1992) Potentiation of electroencephalographic spindles by ibotenate microinjections into nucleus reticularis thalami of cats. *Neuroscience* **51**: 759–762.

Mariño, J., Canedo, A. and Aguilar, J. (2000) Sensorimotor cortical influences on cuneate nucleus rhythmic activity in the anesthetized cat. *Neuroscience* **95**: 657–673.

Markram, H. (1997) A network of tufted layer 5 pyramidal neurons. *Cerebral Cortex* **7**: 523–533.

Markram, H. and Sakmann, B. (1994) Calcium transients in dendrites of neocortical neurons evoked by single subthreshold excitatory postsynaptic potentials via low-voltage-activated calcium channels. *Proceedings of the National Academy of Sciences of the USA* **91**: 5207–5211.

Markram, H., Lübke, J., Frötscher, M., Roth, A. and Sakmann, B. (1997a) Physiology and anatomy of synaptic connections between thick tufted pyramidal neurones in the developing rat neocortex. *Journal of Physiology (London)* **500**: 409–440.

Markram, H., Lübke, J., Frötscher, M. and Sakmann, B. (1997b) Regulation of synaptic efficacy by coincidence of postsynaptic APs and EPSPs. *Science* **275**: 213–215.

Markram, H., Wang, M. and Tsodycs, M. (1998) Differential signaling via the same axon of neocortical pyramidal neurons. *Proceedings of the National Academy of Sciences of the USA* **95**: 5323–5328.

Marshall, L.H. (1987) An annotated interview with Giuseppe Moruzzi, 1910–1986. *Experimental Neurology* **97**: 225–242.

Marshall, L.H. and Magoun, H.W. (1998) *Discoveries in the Human Brain – Neuroscience Prehistory, Brain Structure, and Function.* Totowa, NJ: Humana Press.

Marshall, L., Mölle, M., Fehm, H.L. and Born, J. (1998) Scalp recorded direct current brain potentials during human sleep. *European Journal of Neuroscience* **10**: 1167–1178.

Martin, J.H. (1991) Autoradiographic estimation of the extent of reversible inactivation produced by microinjections of lidocaine and muscimol in the rat. *Neuroscience Letters* **127**: 160–164.

Martin, J.H. and Ghez, C. (1988) Red nucleus and motor cortex: parallel motor systems for the initiation and control of skilled movement. *Behavioral Brain Research* **28**: 217–223.

Martin, S.J., Grimwood, P.D. and Morris, R.G.M. (2000) Synaptic plasticity and memory: an evaluation of the hypothesis. *Annual Reviews of Neuroscience* **23**: 649–711.

Martina, M., Royer, S. and Paré, D. (1999) Physiological properties of central medial and central lateral amygdala neurons. *Journal of Neurophysiology* **82**: 1843–1854.

Martina, M., Vida, I. and Jonas, P. (2000) Distal initiation and active propagation of action potentials in interneuron dendrites. *Science* **287**: 295–300.

Mason, A. and Larkman, A. (1990) Correlations between morphology and electrophysiology of pyramidal neurons in slices of rat visual cortex. II. Electrophysiology. *Journal of Neuroscience* **10**: 1415–1428.

Masselmo, M.E. (1999) Neuromodulation: acetylcholine and memory consolidation. *Trends in Cognitive Sciences* **3**: 351–359.

Massimini, M. and Amzica, F. (2001) Extracellular calcium fluctuations and intracellular potentials in the cortex during the slow sleep oscillation. *Journal of Neurophysiology* **85**: 1346–1350.

Mathern, G.W., Babb, T.L., Pretorius, J.K. and Leite, J.P. (1995) Reactive synaptogenesis and neuron densities for neuropeptide Y, somatostatin, and glutamate decarboxylase immunoreactivity in the epileptogenic human fascia dentate. *Journal of Neuroscience* **15**: 3990–4004.

Matsumoto, H. and Ajmone-Marsan, C. (1964) Cortical cellular phenomena in experimental epilepsy. *Experimental Neurology* **9**: 286–304.

Matsumoto, H., Ayala, G.F. and Gumnit, R.J. (1969) Neuronal behavior and triggering mechanism in cortical epileptic focus. *Journal of Neurophysiology* **32**: 688–703.

Mauguière, P. (1992) A consensus statement on relative merits of EEG and MEG. *Electroencephalography and Clinical Neurophysiology* **82**: 317–319.

McAllister, A.K., Katz, L.C. and Lo, D.C. (1999) Neurotrophins and synaptic plasticity. *Annual Reviews of Neuroscience* **22**: 295–318.

McCarley, R.W. and Hobson, J.A. (1975) Neuronal excitability modulation over the sleep cycle: a structural and mathematical model. *Science* **189**: 58–60.

McCarley, R.W. and Massequoi, S.G. (1986) A limit cycle mathematical model of the REM sleep oscillator system. *American Journal of Physiology* **251**: R1033–R1036.

McCarley, R.W., Benoit, O. and Barrionuevo, G. (1983) Lateral geniculate nucleus unitary discharge in sleep and waking: state- and rate-specific aspects. *Journal of Neurophysiology* **50**: 798–818.

McCormick, D.A. (1989) GABA as an inhibitory neurotransmitter in the human cerebral cortex. *Journal of Neurophysiology* **62**: 1018–1027.

McCormick, D.A. (1991) Functional properties of a slowly inactivating potassium current I_{As} in guinea pig dorsal lateral geniculate relay neurons. *Journal of Neurophysiology* **66**: 1176–1189.

McCormick, D.A. (1992) Neurotransmitter actions in the thalamus and cerebral cortex and their role in neuromodulation of thalamocortical activity. *Progress in Neurobiology* **39**: 337–388.

McCormick, D.A. and Contreras, D. (2001) On the cellular and network bases of epileptic seizures. *Annual Reviews of Physiology* **63**: 815–846.

McCormick, D.A. and Von Krosigk, M. (1992) Corticothalamic activation modulates thalamic firing through glutamate metabotropic receptors. *Proceedings of the National Academy of Sciences of the USA* **89**: 2774–2778.

McCormick, D.A. and Pape, H.C. (1988) Acetylcholine inhibits identified interneurons in the cat lateral geniculate nucleus. *Nature* **334**: 246–248.

McCormick, D.A. and Pape, H.C. (1990a) Properties of a hyperpolarization-activated cation current and its role in rhythmic oscillation in thalamic relay neurones. *Journal of Physiology (London)* **431**: 291–318.

McCormick, D.A. and Pape, H.C. (1990b) Noradrenergic and serotonergic modulation of a hyperpolarization-activated cation current in thalamic relay cells. *Journal of Physiology (London)* **431**: 319–342.

McCormick, D.A. and Prince, D.A. (1986) Acetylcholine induces burst firing in thalamic reticular neurones by activating a K^+ conductance. *Nature* **319**: 147–165.

McCormick, D.A. and Prince, D.A. (1987) Actions of acetylcholine in the guinea pig and cat medial and lateral geniculate nuclei, *in vitro*. *Journal of Physiology (London)* **392**: 147–165.

McCormick, D.A. and Prince, D.A. (1988) Noradrenergic modulation of firing pattern in guinea pig and cat thalamic neurones, *in vitro*. *Journal of Neurophysiology* **59**: 978–996.

McCormick, D.A. and Wang, Z. (1991) Serotonin and noradrenaline excite GABAergic neurones of the guinea-pig and cat nucleus reticularis thalami. *Journal of Physiology (London)* **442**: 235–255.

McCormick, D.A. and Williamson, A. (1991) Modulation of neuronal firing mode in cat and guinea-pig LGNd by histamine: possible cellular mechanisms of histaminergic control of arousal. *Journal of Neuroscience* **11**: 3188–3199.

McCormick, D.A., Connors, B.W., Lighthall, J.W. and Prince, D.A. (1985) Comparative electrophysiology of pyramidal and sparsely spiny stellate neurons of the neocortex. *Journal of Neurophysiology* **54**: 782–806.

McDonald, A.J. (1994) Calretinin immunoreactive neurons in the basolateral amygdala of the rat and monkey. *Brain Research* **667**: 238–242.

McDonald, A.J. and Augustine, J.R. (1993) Localization of GABA-like immunoreactivity in the monkey amygdala. *Neuroscience* **52**: 281–294.

McGinty, D.J. and Harper, R.M. (1976) Dorsal raphe neurons: depression of firing during sleep in cats. *Brain Research* **101**: 569–575.

McGinty, D.J. and Sterman, M.B. (1968) Sleep suppression after basal forebrain lesions in the cat. *Science* **160**: 1253–1255.

McKeown, M.J. and McNamara, J.O. (2001) When do epileptic seizures *really* begin? *Neuron* **30**: 1–3.

McKeown, M.J., Humphries, C., Iragui, V. and Sejnowski, T.J. (1999) Spatially fixed patterns account for the spike and wave features in absence seizures. *Brain Tomography* **12**: 107–116.

McNaughton, B.L., Barnes, C.A. and Andersen, P. (1981) Synaptic efficacy and EPSP summation in granule cells of rat fascia dentata studied *in vitro*. *Journal of Neurophysiology* **46**: 952–966.

Meeren, H.K.M., Pijn, J.P.M., van Luijtelaar, E.J.L.M., Coenen, A.M.L. and Lopes da Silva, F.H. (2002) Cortical focus drives widespread corticothalamic networks during spontaneous absence seizures in rats. *Journal of Neuroscience* **22**: 1480–1495.

Meis, S., Munsch, T. and Pape, H.C. (2002) Antioscillatory effects of nociceptin/orphanin FQ in synaptic networks of the rat thalamus. *Journal of Neuroscience* **22**: 718–727.

Merica, H., Blois, R., Fortune, R.D. and Gaillard, J.M. (1997) Evolution of delta activity within the nonREM sleep episode: a biphasic hypothesis. *Physiology and Behavior* **62**: 213–219.

Merlet, I., Garcia-Larrea, L., Grégoire, M.C., Lavenne, F. and Mauguière, F. (1996) Source propagation of interictal spikes in temporal lobe epilepsy. *Brain* **119**: 377–392.

Metherate, R., Cox, C.L. and Ashe, J.H. (1992) Cellular bases of neocortical activation: modulation of neural oscillations by the nucleus basalis and endogenous acetylcholine. *Journal of Neuroscience* **12**: 4701–4711.

Miles, R. and Wong, R.K.S. (1983) Single neurones can initiate synchronized population discharges in the hippocampus. *Nature* **306**: 371–373.

Miles, R. and Wong, R.K.S. (1987) Latent synaptic pathways revealed after titanic stimulation in the hippocampus. *Nature* **329**: 724–726.

Miles, R., Toth, K., Gulyas, A.I., Hajos, N. and Freund, T.F. (1996) Differences between somatic and dendritic inhibition in the hippocampus. *Neuron* **16**: 815–823.

Miller, L.A., McLachlan, R.S., Bouwer, M.S., Hudson, L.P. and Munoz, M.G. (1994) Amygdalar sclerosis: preoperative indicators and outcome after temporal lobe lobectomy. *Journal of Neurology, Neurosurgery and Psychiatry* **57**: 1099–1105.

Minamimoto, T. and Kimura, M. (2002) Participation of the thalamic CM-Pf complex in attentional orienting. *Journal of Neurophysiology* **87**: 3090–3101.

Mineff, E.M. and Weinberg, R.J. (2000) Differential synaptic distribution of AMPA receptor subunits in the ventral posterior and reticular thalamic nuclei of the rat. *Neuroscience* **101**: 969–982.

Mitchell, S.J. and Ranck, J.B.J. (1980) Generation of theta rhythm in medial entorhinal cortex of freely moving rats. *Brain Research* **189**: 49–66.

Miyauchi, T., Nomura, Y., Ohno, S., Kishimoto, H. and Matsushita, M. (1988) Positron emission tomography in three cases of Lennox-Gastaut syndrome. *Japanese Journal of Psychiatry Neurology* **42**: 795–804.

Mody, I. (1998) Ion channels in epilepsy. *International Review of Neurobiology* **42**: 199–226.

Mogilner, A.I., Benabid, A.L. and Rezai, A. (2001) Brain stimulation: current applications and future prospects. *Thalamus and Related Systems* **1**: 255–267.

Mölle, M., Marshall, L., Gais, S. and Born, J. (2003) Grouping of spindle activity during slow oscillations in human non-REM sleep. *Journal of Neuroscience* **22**: 10941–10947.

Monckton, J.E. and McCormick, D.A. (2002) The neuromodulatory role of serotonin in the ferret thalamus. *Journal of Neurophysiology*, in press.

Montero, V.M. (1987) Ultrastructural identification of synaptic terminals from the axon of type 3 interneurons in the cat lateral geniculate nucleus. *Journal of Comparative Neurology* **264**: 268–283.

Montero, V.M. (1991) A quantitative study of synaptic contacts on interneurons and relay cells of the cat lateral geniculate nucleus. *Experimental Brain Research* **86**: 257–270.

Montero, V.M. and Singer, W. (1985) Ultrastructural identification of somata and neural processes immunoreactive to antibodies against glutamic acid decarboxylase (GAD) in the dorsal lateral geniculate nucleus of the cat. *Experimental Brain Research* **59**: 151–165.

Moody, W.J. Jr., Futamachi, K.J. and Prince, D.A. (1974) Extracellular potassium activity during epileptogenesis. *Experimental Neurology* **42**: 248–263.

Morales, F.R. and Chase, M.H. (1978) Intracellular recording of lumbar motoneuron membrane potential during sleep and wakefulness. *Experimental Neurology* **62**: 821–827.

Morimoto, K., Dragunow, M. and Goddard, G.V. (1986) Deep prepyriform cortex kindling and its relation to amygdala kindling in the rat. *Experimental Neurology* **94**: 637–648.

Morin, D. and Steriade, M. (1981) Development from primary to augmenting responses in the somatosensory system. *Brain Research* **205**: 49–66.

Morin, F., Beaulieu, C. and Lacaille, J.C. (1998) Selective loss of GABA neurons in area CA1 of the rat hippocampus after intraventricular kainate. *Epilepsy Research* **32**: 363–369.

Morison, R.S. and Bassett, D.L. (1945) Electrical activity of the thalamus and basal ganglia in decorticated cats. *Journal of Neurophysiology* **8**: 309–314.

Morison, R.S. and Dempsey, E.W. (1942) Mechanism of thalamocortical augmentation and repetition. *American Journal of Physiology* **138**: 297–308.

Morrell, F. (1960) Secondary epileptogenic lesions. *Epilepsia* **1**: 538–560.

Morrison, J.H. and Foote, SL. (1986) Noradrenergic and serotoninergic innervation of cortical, thalamic and tectal visual structures in old and new world monkeys. *Journal of Comparative Neurology* **243**: 117–138.

Moruzzi, G. (1964) The historical development of the deafferentation hypothesis of sleep. *Proceedings of the American Philosophical Society* **108**: 19–28.

Moruzzi, G. (1966) The functional significance of sleep with particular regard to the brain mechanisms underlying consciousness. In *Brain and Conscious Experience*, ed. J.C. Eccles, pp. 345–379, New York: Springer.

Moruzzi, G. (1969) Sleep and instinctive behavior. *Archives Italiennes de Biologie* **107**: 175–216.

Moruzzi, G. (1972) The sleep-waking cycle. *Ergebnisse der Physiologie* **64**: 1–165.

Moruzzi, G. and Magoun, H.W. (1949) Brain stem reticular formation and activation of the EEG. *Electroencephalography and Clinical Neurophysiology* **1**: 455–473.

Mountcastle, V.B. (1997) The columnar organization of the neocortex. *Brain* **120**: 701–722.

Mountcastle, V.B. (1998) *Perceptual Neuroscience – The Cerebral Cortex*. Cambridge, MA: Harvard University Press.

Mouret, J. and Coindet, J. (1980) Polygraphic evidence against a critical role of the raphe nuclei in sleep in the rat. *Brain Research* **186**: 273–287.

Mulle, C., Steriade, M. and Deschênes, M. (1985) Absence of spindle oscillations in the cat anterior thalamic nuclei. *Brain Research* **334**: 169–171.

Mulle, C., Madariaga, A. and Deschênes, M. (1986) Morphology and electrophysiological properties of reticularis thalami neurons in cat: *in vivo* study of a thalamic pacemaker. *Journal of Neuroscience* **6**: 2134–2145.

Munk, M.H.J., Roelfsema, P.R., König, P., Engel, A.K. and Singer, W. (1996) Role of reticular activation in the modulation of intracortical synchronization. *Science* **272**: 271–274.

Murthy, V.N. and Fetz, E.E. (1992) Coherent 25- to 35-Hz oscillations in the sensorimotor cortex of awake behaving monkeys. *Proceedings of National Academy of Sciences of the USA* **89**: 5670–5674.

Murthy, V.N. and Fetz, E.E. (1997a) Oscillatory activity in sensorimotor cortex of awake monkeys: synchronization of local field potentials and relation to behavior. *Journal of Neurophysiology* **76**: 3949–3967.

Murthy, V.N. and Fetz, E.E. (1997b) Synchronization of neurons during local field potential oscillations in sensorimotor cortex of awake monkeys. *Journal of Neurophysiology* **76**: 3968–3982.

Nadler, J.V., Perry, B.W. and Cotman, C.W. (1978) Preferential vulnerability of hippocampus to intraventricular kainic acid. In *Kainic Acid as a Tool in Neurobiology*, ed. E.G. McGeer, J.W. Olney and P.L. McGeer, pp. 219–237, New York: Raven Press.

Nagao, T., Alonso, A. and Avoli, M. (1996) Epileptiform activity induced by pilocarpine in the rat hippocampal-entorhinal slice preparation. *Neuroscience* **72**: 399–408.

Nagy, J.I., Yamamoto, T., Shiosaka, S., Dewar, K.M., Whittaker, M.E. and Hertzberg, E.L. (1988) Immunohistochemical localization of gap junction protein in rat CNS: a preliminary account. In *Gap Junctions*, ed. E.L. Hertzberg and R.G. Johnson, pp. 375–389, New York: A.R. Liss.

Nakabayashi, T., Uchida, S., Maehara, T., Hirai, N., Nakamura, M., Arakaki, H., Shimisu, H. and Okubo, Y. (2001) Absence of sleep spindles in human medial and basal temporal lobes. *Psychiatry and Clinical Neuroscience* **55**: 57–65.

Nakamura, A., Nakashima, M., Sugao, T., Kanemoto, H., Fukumura, Y. and Shiomi, H. (1988) Potent antinociceptive effect of centrally administered delta-sleep-inducing peptide (DSIP). *European Journal of Pharmacology* **155**: 247–253.

Nakamura, A., Nakashima, M., Sakai, K., Niwa, M., Nozaki, M. and Shiomi. H. (1989) Delta-sleep-inducing peptide (DSIP) stimulates the release of immunoreactive Met-enkephalin from rat lower brainstem slices in vitro. *Brain Research* **481**: 165–168.

Naquet, R. and Meldrum, B.S. (1975) In *Experimental Models of Epilepsy*, ed. D.P. Purpura, J.K. Penry, D.B. Tower, D.M. Woodbury and R.D. Walter, pp. 373–406, New York: Raven Press.

Naquet, R. and Valin, A. (1990) Focal discharges in photosensitive generalized epilepsy. In *Generalized Epilepsy*, ed. M. Avoli, P. Gloor, G. Kostopoulos and R. Naquet, pp. 273–285, Boston: Birkhäuser.

Nathan, T., Jensen, M.S. and Lambert, J.D. (1990) The slow inhibitory postsynaptic potential in rat hippocampal CA1 neurones is blocked by intracellular injection of QX-314. *Neuroscience Letters* **110**: 309–313.

Nauta, W.J.H. (1946) Hypothalamic regulation of sleep in rats. Experimental study. *Journal of Neurophysiology* **9**: 285–316.

Neckelmann, D., Amzica, F. and Steriade, M. (1998) Spike-wave complexes and fast components of cortically generated seizures. III. Synchronizing mechanisms. *Journal of Neurophysiology* **80**: 1480–1494.

Neckelmann, D., Amzica, F. and Steriade, M. (2000) Changes in neuronal conductance during different components of cortically generated spike-wave seizures. *Neuroscience* **96**: 475–485.

Nelson, J.P., McCarley, R.W. and Hobson J.A. (1983) REM sleep burst neurons, PGO waves, and eye movement information. *Journal of Neurophysiology* **50**: 784–797.

Neugebauer, V., Keele, N.B. and Shinnick-Gallagher, P. (1997) Epileptogenesis *in vivo* enhances the sensitivity of inhibitory presynaptic metabotropic glutamate receptors in basolateral amygdala neurons *in vitro*. *Journal of Neuroscience* **17**: 983–995.

Nicholson, C. (1980) Modulation of extracellular calcium and its functional implications. *Federation Proceedings* **39**: 1519–1523.

Nicoll, R.A., Malenka, R.C. and Kauer, J.A. (1990) Functional comparison of neurotransmitter receptor subtypes in mammalian central nervous system. *Physiological Reviews* **70**: 513–565.

Niedermeyer, E. (1965) Sleep electroencephalograms in petit mal. *Archives of Neurology* **12**: 625–630.

Niedermeyer, E. (1969) The Lennox-Gastaut syndrome: a severe type of childhood epilepsy. *Deutsche Zeitschrift für Nervenheilkrankheiten* **195**: 263–282.

Niedermeyer, E. (1993) Historical aspects. In *Electroencephalography: Basic Principles, Clinical Applications and Related Field*, 3rd edn., ed. E. Niedermeyer and F. Lopes da Silva, pp. 1–14, Baltimore: Williams & Wilkins.

Niedermeyer, E. (1999a) Abnormal EEG patterns (epileptic and paroxysmal). In *Electroencephalography: Basic Principles, Clinical Applications and Related Fields*, 4th edn., ed. E. Niedermeyer and F. Lopes da Silva, pp. 235–260, Baltimore: Williams & Wilkins.

Niedermeyer, E. (1999b) Epileptic seizure disorders. In *Electroencephalography: Basic Principles, Clinical Applications and Related Fields*, 4th edn., ed. E. Niedermeyer and F. Lopes da Silva, pp. 476–585, Baltimore: Williams & Wilkins.

Nielsen, T. (2000) Cognition in REM and NREM sleep. *Brain and Behavioral Sciences* **23**: 851–866.

Nishimura, Y., Kitagawa, H., Saitoh, K., Asahi, M., Itoh, K., Yoshioka, K., Asahara, T., Tanaka, T. and Yamamoto, T. (1996) The burst firing in the layer III and V pyramidal neurons of the cat sensorimotor cortex in vitro. *Brain Research* **727**: 212–216.

Nishimura, Y., Asahi, M., Saitoh, K., Kitagawa, H., Kumazawa, Y., Itoh, K., Lin, M., Akamine, T., Shibuyam, H., Asahara, T. and Yamamoto, T. (2001) Ionic mechanisms underlying burst firing of layer III sensorimotor cortical neurons of the cat: and *in vitro* slice study. *Journal of Neurophysiology* **86**: 771–781.

Nitecka, L., Tremblay, E., Charton, G., Bouillot, J.P., Berger, M.L. and Ben-Ari, Y. (1984) Maturation of kainic acid seizure-brain damage syndrome in the rat. II. Histopathological sequelae. *Neuroscience* **13**: 1073–1094.

Nitz, D. and Siegel, J.M. (1997a) GABA release in the dorsal raphe nucleus: role in the control of REM sleep. *American Journal of Physiology* **273**: R451–455.

Nitz, D. and Siegel, J.M. (1997b) GABA release in the locus coeruleus as a function of sleep/wake state. *Neuroscience* **78**: 795–801.

Noachtar, S. (2001) Generalized epilepsy and sleep. In *Epilepsy and Sleep*, ed. D.S. Dinner and H.O. Lüders, pp. 75–83, San Diego: Academic Press.

Noebels, J.L. (1984) A single error of noradrenergic axon growth synchronizes central neurons. *Nature* **310**: 409–411.

Noebels, J.L. (1999) Single-gene models of epilepsy. *Advances in Neurology* **79**: 227–238.

Nosjean, A., Arluison, M. and Laguzzi, R.F. (1987) Increase in paradoxical sleep after destruction of serotoninergic innervation in the nucleus tractus solitarius of the rat. *Neuroscience* **23**: 469–481.

Nuñez, A. (1996) Unit activity of rat basal forebrain neurons: relationship to cortical activity. *Neuroscience* **72**: 757–766.

Nuñez, A., Amzica, F. and Steriade, M. (1992a) Intrinsic and synaptically generated delta (1–4 Hz) rhythms in dorsal lateral geniculate neurons and their modulation by light-induced fast (30–70 Hz) events. *Neuroscience* **51**: 269–284.

Nuñez, A., Amzica, F. and Steriade, M. (1992b) Intracellular evidence for incompatibility between spindle and delta oscillations in thalamocortical neurons of cat. *Neuroscience* **48**: 75–85.

Nuñez, A., Amzica, F. and Steriade, M. (1992c) Voltage-dependent fast (20–40 Hz) oscillations in long-axoned neocortical neurons. *Neuroscience* **51**: 7–10.

Nuñez, A., Amzica, F. and Steriade, M. (1993) Electrophysiology of cat association cortical neurons *in vivo*: intrinsic properties and synaptic responses. *Journal of Neurophysiology* **70**: 418–430.

Obál, F. Jr., Alfoldi, P., Cady, A.B., Johannsen, L., Sary, G. and Krueger, J.M. (1988) Growth hormone-releasing factor enhances sleep in rats and rabbits. *American Journal of Physiology* **255**: R310–316.

Obál, F. Jr., Payne, L., Kapas, L., Opp, M. and Krueger, J.M. (1991) Inhibition of growth hormone-releasing factor suppresses both sleep and growth hormone secretion in the rat. *Brain Research* **557**: 149–153.

O'Brien, J.L., Goldensohn, E.S. and Hoefer, R.T. (1959) Electroencephalographic abnormalities in addition to bilaterally synchronous 3 cycle per second spike and wave activity in petit mal. *Electroencephalography and Clinical Neurophysiology* **13**: 747–761.

Oertel, W.H., Graybiel, A.M., Mugnaini, E., Elde, R.P., Schmechel, D.E. and Kopin, I.J. (1983) Coexistence of glutamic acid decarboxylase and somatostatin-like immunoreactivity in neurons of the feline nucleus reticularis thalami. *Journal of Neuroscience* **3**: 1322–1332.

Ogawa, J. (1963) Midbrain reticular influences upon single neurons in lateral geniculate nucleus. *Science* **139**: 343–344.

Ohara, P.T. and Lieberman, A.R. (1985) The thalamic reticular nucleus of the adult rat: experimental anatomical studies. *Journal of Neurocytology* **14**: 365–411.

Ojima, H. (1994) Terminal morphology and distribution of corticothalamic fibers originating from layers 5 and 6 of cat primary auditory cortex. *Cerebral Cortex* **4**: 646–663.

Okasaki, M.M., Evenson, D.A. and Nadler, J.V. (1995) Hippocampal mossy fiber sprouting and synapse formation after status epilepticus in rats: visualization after retrograde transport of biocytin. *Journal of Comparative Neurology* **352**: 515–534.

O'Leary, J.L. and Goldring, S. (1976) *Science and Epilepsy*. New York: Raven Press.

Orkand, R.K. (1969) Neuroglial-neuronal interactions. In *Basic Mechanisms of the Epilepsies*, ed. H.H. Jasper, A.A. Ward Jr. and A. Pope, pp. 737–746, Boston: Little, Brown.

Otis, T.S., De Koninck, Y. and Mody, I. (1994) Lasting potentiation of inhibition is associated with an increased number of γ-aminobutyric acid type A receptors activated during miniature inhibitory postsynaptic currents. *Proceedings of the National Academy of Sciences of the USA* **91**: 7698–7702.

Pabst, M.J., Beranova-Giorgianni, S. and Krueger, J.M. (1999) Effects of muramyl peptides on macrophages, monokines and sleep. *Neuroimmunomodulation* **6**: 261–283.

Pape, H.C. (1995) Nitric oxide: an adequate modulatory link between biological oscillators and control systems in the mammalian brain. *Seminars in the Neurosciences* **7**: 329–340.

Pape, H.C. (1996) Queer current and pacemaker: the hyperpolarization-activated cation current in neurons. *Annual Reviews of Physiology* **58**: 299–327.

Pape, H.C. and Eysel, U.T. (1987) Modulatory actions of the reticular transmitters norepinephrine and 5–hydroxytryptamine (serotonin) in the cat's visual thalamus. *Society for Neuroscience Abstracts* **13**: 86.

Pape, H.C. and Mager R. (1992) Nitric oxide controls oscillatory activity in thalamocortical neurons. *Neuron* **9**: 441–448.

Pape, H.C. and McCormick, D.A. (1989) Noradrenaline and serotonin selectively modulate thalamic burst firing by enhancing a hyperpolarization-activated cation current. *Nature* **340**: 715–718.

Pape, H.C. and McCormick, D.A. (1995) Electrophysiological and pharmacological properties of interneurons in the cat dorsal lateral geniculate nucleus. *Neuroscience* **68**: 1105–1125.

Pape, H.C., Budde, T., Mager, R. and Kisvrday, Z.F. (1994) Prevention of Ca^{2+}-mediated action potentials in GABAergic local circuit neurones of rat thalamus by a transient K^+ current. *Journal of Physiology (London)*. **478**: 403–422.

Pappenheimer, J.R., Miller, T.B. and Goodrich, C.A. (1967) Sleep-promoting effects of cerebrospinal fluid from sleep-deprived goats. *Proceedings of the National Academy of Sciences of the USA* **58**: 513–517.

Paré, D. and Gaudreau, H. (1996) Projection cells and interneurons of the lateral and basolateral amygdala: distinct firing patterns and differential relation to theta and delta rhythms in conscious cats. *Journal of Neuroscience* **16**: 3334–3350.

Paré, D. and Lang, E.J. (1998) Calcium electrogenesis in neocortical pyramidal neurons *in vivo*. *European Journal of Neuroscience* **10**: 3164–3170.

Paré, D. and Llinás, R. (1995) Conscious and pre-conscious processes as seen from the standpoint of sleep-waking cycle neurophysiology. *Neuropsychologia* **33**: 1155–1168.

Paré, D. and Smith, Y. (1993) Distribution of GABA immunoreactivity in the amygdaloid complex of the cat. *Neuroscience* **57**: 1061–1076.

Paré, D. and Smith, Y. (1994) GABAergic projection from the intercalated cell masses of the amygdala to the basal forebrain in cats. *Journal of Comparative Neurology* **344**: 33–49.

Paré, D. and Smith, Y. (1996) Thalamic collaterals of corticostriatal axons: their termination field and synaptic targets in cats. *Journal of Comparative Neurology* **372**: 551–567.

Paré, D. and Steriade, M. (1990) Control of mamillothalamic axis by brainstem cholinergic laterodorsal tegmental afferents: possible involvement in mnemonic processes. In *Brain Cholinergic Systems*, ed. M. Steriade and D. Biesold, pp. 337–354, Oxford: Oxford University Press.

Paré, D., Steriade, M., Deschênes, M. and Oakson, G. (1987) Physiological properties of anterior thalamic nuclei, a group devoid of inputs from the reticular thalamic nucleus. *Journal of Neurophysiology* **57**: 1669–1685.

Paré, D., Smith, Y., Parent, A. and Steriade, M. (1988) Projections of upper brainstem cholinergic and non-cholinergic neurons of cat to intralaminar and reticular thalamic nuclei. *Neuroscience* **25**: 69–88.

Paré, D., Steriade, M., Deschênes, M. and Bouhassira, D. (1990) Prolonged enhancement of anterior thalamic synaptic responsiveness by stimulation of a brainstem cholinergic group. *Journal of Neuroscience* **10**: 20–33.

Paré, D., Curró Dossi, R. and Steriade, M. (1991) Three types of inhibitory postsynaptic potentials generated by interneurons in the anterior thalamic complex of cat. *Journal of Neurophysiology* **66**: 1190–1204.

Paré, D., Smith, Y. and Paré, J.F. (1995) Intra-amygdaloid projections of the basolateral and basomedial nuclei in the cat: *Phaseolus vulgaris*-leucoagglutinin anterograde tracing at the light electron microscopic level. *Neuroscience* **69**: 567–583.

Paré, D., Shink, E., Gaudreau, H., Destexhe, A. and Lang, E.J. (1998) Impact of spontaneous synaptic activity on the resting properties of cat neocortical pyramidal neurons *in vivo*. *Journal of Neurophysiology* **79**: 1450–1460.

Paré, D., Collins, D.R. and Pelletier, J.G. (2002) Amygdala oscillations and the consolidation of emotional memories. *Trends in Cognitive Sciences* **6**: 306–314.

Parent, A. and Steriade, M. (1984) Midbrain tegmental projections of nucleus reticularis thalami of cat and monkey: a retrograde transport and antidromic identification study. *Journal of Comparative Neurology* **229**: 548–558.

Parent, A., Paré, D., Smith, Y. and Steriade, M. (1988) Basal forebrain cholinergic and non-cholinergic projections to the thalamus and brainstem in cats and monkeys. *Journal of Comparative Neurology* **277**: 281–301.

Parmeggiani, P.L. (1988) Thermoregulation during sleep from the view point of homeostasis. In *Clinical Physiology of Sleep*, ed. R. Lydic and J.F. Biebuyck, pp. 159–179, Bethesda: American Physiological Society.

Parmeggiani, P.L., Azzaroni, A., Cevolani, D. and Ferrari, G. (1986) Polygraphic study of anterior hypothalamic-preoptic neuron thermosensitivity during sleep. *Electroencephalography and Clinical Neurophysiology* **63**: 289–295.

Parmentier, R., Ohtsu, H., Djebarra-Hannas, Z., Valatx, J.L., Watanabe, T. and Lin, J.S. (2002) Anatomical, physiological, and pharmacological characteristics of histidine decarboxylase knock-out mice: evidence for the role of brain histamine in behavioral and sleep-wake control. *Journal of Neuroscience* **22**: 7695–7711.

Parpura, V., Basarsky, T.A., Liu, F., Jeftinija, K. and Haydon, P.G. (1994) Glutamate-mediated astrocyte-neuron signaling. *Nature* **369**: 744–747.

Parri, H.R. and Crunelli, V. (1998) Sodium current in rat and cat thalamocortical neurons: role of a non-inactivating component in tonic and burst firing. *Journal of Neuroscience* **18**: 854–867.

Parri, H.R., Gould, T.M. and Crunelli, V. (2001) Spontaneous astrocytic Ca^{2+} oscillations *in situ* drive NMDAR-mediated neuronal excitation. *Nature Neuroscience* **4**: 803–812.

Passouant, P. (1984) Historical aspects of sleep and epilepsy. In *Epilepsy and Sleep Deprivation*, ed. R. Degen and E. Niedermeyer, pp. 67–73, Amsterdam: Elsevier.

Patry, F.L. (1931) The relation of time of day, sleep and other factors to the incidence of epileptic seizures. *American Journal of Psychiatry* **10**: 789–813.

Pavlides, C. and Winson, J. (1989) Influences of hippocampal place cell firing in awake state on the activity of these cells during subsequent sleep episodes. *Journal of Neuroscience* **9**: 2907–2918.

Pavlov, I.P. (1923) "Innere Hemmung" der bedingten Reflexe und der Schlaf – ein und derselbe Prozess. *Skandinavische Archive für Physiologie* **44**: 42–58.

Pedley, R.A. (1987) Epilepsy. In *A Textbook of Clinical Neurology*, ed. A.M. Halliday, S.R. Butler and R. Paul, pp. 231–268, New York: Wiley.

Pedroarena, C. and Llinás, R. (1997) Dendritic calcium conductances generate high-frequency oscillation in thalamocortical neurons. *Proceedings of the National Academy of Sciences of the USA* **94**: 24–28.

Pedroarena, C. and Llinás, R. (2001) Interactions of synaptic and intrinsic electroresponsiveness determine corticothalamic activation dynamics. *Thalamus and Related Systems* **1**: 3–14.

Pellegrini, A., Musgrave, J. and Gloor, P. (1979) Role of afferent input of subcortical origin in the genesis of bilaterally synchronous epileptic discharges of feline generalized penicillin epilepsy. *Experimental Neurology* **64**: 155–173.

Pellegrini, A., Curró Dossi, R., Dal Pos, F., Ermani, M., Zanotto, I. and Testa, F. (1989) Ethosuximide alters intrathalamic and thalamocortical synchronizing mechanisms: a possible explanation of its antiabsence effect. *Brain Research* **497**: 344–360.

Peña, E. de la and Geijo-Barrientos, E. (1996) Laminar localization, morphology, and physiological properties of pyramidal neurons that have low-threshold calcium current in the guinea-pig medial frontal cortex. *Journal of Neuroscience* **16**: 5301–5311.

Penfield, W. and Jasper, H.H. (1954) *Epilepsy and the Functional Anatomy of the Human Brain*. Boston: Little, Brown.

Penfield, W. and Rasmussen, T. (1950) *The Cerebral Cortex of Man. A Clinical Study of Localization of Function*. New York: Macmillan Co.

Penry, J.K., Porter, R.J. and Dreifuss, F.E. (1971) Patterns of paroxysmal abnormal discharges in twelve-hour telemetered EEGs of untreated children with absence (petit mal) seizures. *Neurology* **21**: 392.

Perez-Velazquez, J.L. and Carlen, P.L. (1999) Synchronization of GABAergic interneuronal networks during seizure-like activity in the rat horizontal hippocampal slice. *European Journal of Neuroscience* **1111**: 4110–4118.

Perez-Velazquez, J.L. and Carlen, P.L. (2000) Gap junctions, synchrony and seizures. *Trends in Neurosciences* **23**: 68–74.

Perez-Velazquez, J.L., Valiante, T.A. and Carlen, P.L. (1994) Modulation of gap junctional mechanisms during calcium-free induced field burst activity: a possible role for electrotonic coupling in epileptogenesis. *Journal of Neuroscience* **14**: 4308–4317.

Perkins, K.L. and Wong, R.K.S. (1995) Intracellular QX-314 blocks the hyperpolarization-activated inward current I_q in hippocampal CA1 pyramidal cells. *Journal of Neurophysiology* **73**: 911–915.

Perreault, M.C., Qin, Y., Heggelund, P. and Zhu, J.J. (2003) Postsynaptic development of GABAergic signaling in the rat lateral geniculate nucleus: presynaptic dendritic mechanisms. *Journal of Physiology (London)* **546**: 137–148.

Perreault, P. and Avoli, M. (1992) 4-Aminopyridine-induced epileptiform activity and a GABA-mediated long-lasting depolarization in the rat hippocampus. *Journal of Neuroscience* **12**: 104–115.

Perrin, F., Garcia-Larrea, L., Mauguière, F. and Bastuji, H. (1999) A differential brain response to the subject's own name persists during sleep. *Clinical Neurophysiology* **110**: 2153–2164.

Petsche, H. (1962) Pathophysiologie und Klinik des Petit-Mal. *Wiener Zeitschrift für Nervenheilkrankheiten* **19**: 345–442.

Petsche, H., Pockberger, H. and Rappelsberger, P. (1984) On the search for the sources of the electroencephalogram. *Neuroscience* **11**: 1–27.

Piéron, H. (1913) *Le Problème Physiologique du Sommeil*. Paris: Masson.

Pinault, D. (1996) A novel single-cell staining procedure performed *in vivo* under electrophysiological control: morpho-functional features of juxtacellularly labelled thalamic cells and other central neurons with biocytin or Neurobiotin. *Journal of Neuroscience Methods* **65**: 113–136.

Pinault, D. and Deschênes, M. (1992a) Voltage-dependent 40-Hz oscillations in rat reticular thalamic neurons *in vivo*. *Neuroscience* **51**: 245–258.

Pinault, D. and Deschênes, M. (1992b) Control of 40-Hz firing of reticular thalamic cells by neurotransmitters. *Neuroscience* **51**: 259–268.

Pinault, D., Smith, Y. and Deschênes, M. (1997) Dendrodendritic and axoaxonic synapses in the thalamic reticular nucleus of the adult rat. *Journal of Neuroscience* **17**: 3215–3233.

Pinault, D., Leresche, N., Charpier, S., Deniau, J.M., Marescaux, C., Vergnes, M. and Crunelli, V. (1998) Intracellular recordings in thalamic neurones during spontaneous spike and wave discharges in rats with absence epilepsy. *Journal of Physiology (London)* **509**: 449–456.

Pinault, D., Vergnes, M. and Marescaux, C. (2001) Medium-voltage 5–9 Hz oscillations give rise to spike-and-wave discharges in a genetic model of absence epilepsy: *in vivo* dual extracellular recordings of thalamic relay and reticular neurons. *Neuroscience* **105**: 181–201.

Pirchio, M., Turner, J.P., Williams, S.R., Asprodini, E. and Crunelli, V. (1997) Postnatal development of membrane properties and δ oscillations in thalamocortical neurons of the cat dorsal lateral geniculate nucleus. *Journal of Neuroscience* **17**: 5428–5444.

Plihal, W. and Born, J. (1997) Effects of early and late nocturnal sleep on declarative and procedural memory. *Journal of Cognitive Neuroscience* **9**: 534–547.

Plum, F. (1991) Coma and related global disturbances of the human conscious state. In *Cerebral Cortex* (vol. 9, *Normal and Altered States of Function*), ed. A. Peters and E.G. Jones, pp. 359–425, New York: Plenum.

Pohlmann-Eden, B., Hoch, D.B., Cochius, J.I. and Chiappa, K.H. (1996) Periodic lateralized epileptiform discharges – a critical review. *Journal of Clinical Neurophysiology* **13**: 519–530.

Pollen, D.A. (1964) Intracellular studies of cortical neurons during thalamic induced wave and spike. *Electroencephalography and Clinical Neurophysiology* **17**: 398–404.

Pollen, D. and Lux, H. (1966) Conductance changes during inhibitory postsynaptic potentials in normal and strychninized cortical neurons. *Journal of Neurophysiology* **29**: 367–381.

Pompeiano, O. (1967a) The neurophysiological mechanisms of the postural and motor events during desynchronized sleep. *Proceedings of the Association for the Research of Nervous and Mental Diseases* **45**: 351–423.

Pompeiano, O. (1967b) Sensory inhibition during motor activity in sleep. In *Neurophysiological Basis of Normal and Abnormal Motor Activities*, ed. M.D. Yahr and D.P. Purpura, pp. 323–375, New York: Raven Press.

Pool, J.L. (1954) Psychosurgery in older people. *Journal of American Geriatric Society* **2**: 456–465.

Porkka-Heiskanen, T., Strecker, R.E., Thakkar, M., Bjorkum, A.A., Greene, R.W. and McCarley, R.W. (1997) Adenosine: a mediator of the sleep-inducing effects of prolonged wakefulness. *Science* **276**: 1265–1268.

Portas, C.M., Thakkar, M., Rainnie, D.G., Greene, R.W. and McCarley, R.W. (1997) Role of adenosine in behavioral state modulation: a microdialysis study in the freely moving cat. *Neuroscience* **79**: 225–235.

Portas, C.M., Krakow, K., Allen, P., Josephs, O., Armony, J.L. and Frith, C.D. (2000) Auditory processing across the sleep-wake cycle: simultaneous EEG and fMRI monitoring in humans. *Neuron* **28**: 991–999.

Porter, R.J. (1993) The absence epilepsies. *Epilepsia* **34** (Suppl. 3): S42–S48.

Preuss, T.M. and Goldman-Rakic, P.S. (1987) Crossed corticothalamic and thalamocortical connections of macaque prefrontal cortex. *Journal of Comparative Neurology* **257**: 269–281.

Prevett, M.C., Duncan, J.S., Jones, T., Fish, D.R. and Brooks, D.J. (1995) Demonstration of thalamic activation during typical absence seizures during $H_2^{15}O$ and PET. *Neurology* **45**: 1396–1402.

Price, J.L. and Amaral, D. (1981) An autoradiographic study of the projections of the central nucleus of the monkey amygdala. *Journal of Neuroscience* **1**: 1242–1259.

Prince, D.A. (1968) Inhibition in "epileptic" neurons. *Experimental Neurology* **21**: 467–485.

Prince, D.A. (1975) Topical convulsants drugs and metabolic antagonists. In *Experimental Models of Epilepsy*, ed. D.P. Purpura, J.K. Penry, D.B. Tower, D.M. Woodbury and R.D. Walter, pp. 51–83, New York: Raven Press.

Prince, D.A. (1983) Ionic mechanisms in cortical and hippocampal epileptogenesis. In *Basic Mechanisms of Neuronal Hyperexcitability*, ed. H.H. Jasper and N.M. van Gelder, pp. 217–238, New York: Alan R. Liss.

Prince, D.A. and Farrell, D. (1963) "Centrencephalic" spike-wave discharges following parenteral injection of penicillin in the cat. *Neurology* **19**: 309–310.

Prince, D.A. and Jacobs, K. (1998) Inhibitory function in two models of chronic epileptogenesis. *Epilepsy Research* **32**: 83–92.

Prince, D.A. and Shanzer, S. (1966) Effects of anesthetics upon the EEG response to reticular stimulation of slow synchrony. *Electroencephalography and Clinical Neurophysiology* **21**: 578–588.

Prince, D.A. and Tseng, G.F. (1993) Epileptogenesis in chronically injured cortex: *in vitro* studies. *Journal of Neurophysiology* **69**: 1276–1291.

Puizillout, J.J. and Ternaux, J. (1974) Endormement vago-aortique après section sagittale médiane du tronc cérébral et après administration de *p*-chlophenylalanine or destruction des noyaux du raphé. *Brain Research* **70**: 9–42.

Puizillout, J.J., Gaudin-Chazal, G., Daszuta, A., Seyfritz, N. and Ternaux, J.P. (1979) Release of endogenous serotonin from *encéphale isolé* cats. II. Correlations with raphe neuronal activity and sleep and wakefulness. *Journal de Physiologie (Paris)* **75**: 531–537.

Puizillout, J.J., Gaudin-Chazal, G. and Bras, H. (1984) Vagal mechanisms in sleep regulation. In *Sleep Mechanisms*, ed. A. Borbély and J.L. Valatx, pp. 19–38 (Suppl. 8 of *Experimental Brain Research*), Berlin: Springer.

Pumain, R., Menini, C., Heinemann, U., Louvel, J. and Silva-Barrat, C. (1985) Chemical synaptic transmission is not necessary for epileptic seizures to persist in the baboon *Papio papio*. *Experimental Neurology* **89**: 250–258.

Purpura, D.P. (1970) Operations and processes in thalamic and synaptically related neural subsystems. In *The Neuroscience: Second Study Program*, ed. F.O. Schmitt, pp. 458–470, New York: Rockefeller University Press.

Purpura, D.P. and Cohen, B. (1962) Intracellular recording from thalamic neurons during recruiting responses. *Journal of Neurophysiology* **25**: 621–635.

Purpura, D.P. and Shofer, R.J. (1963) Intracellular recording from thalamic neurons during reticulocortical activation. *Journal of Neurophysiology* **26**: 494–505.

Purpura, D.P., McMurtry, J.G. and Maekawa, K. (1966) Synaptic events in ventrolateral thalamic neurons during suppression of recruiting responses by brain stem reticular stimulation. *Brain Research* **1**: 63–76.

Purpura, D.P., Bodick, N., Suzuki, K., Rapin, I. and Wurtzelmann, S. (1982) Microtubule disarray in cortical dendrites and neurobehavioral failure. I. Golgi and electron microscope studies. *Brain Research* **281**: 287–297.

Qin, Y.L., McNaughton, B.L., Skaggs, W.E. and Barnes, C.A. (1997) Memory reprocessing in corticocortical and hippocampocortical neurons ensembles. *Philosophical Transactions of the Royal Society (London, Series B)* **352**: 1525–1533.

Quirk, G.J., Muller, R.U., Kubie, J.L. and Ranck, J.B. Jr. (1992) The positional firing properties of medial entorhinal neurons: description and comparison with hippocampal place cells. *Journal of Neuroscience* **12**: 1945–1963.

Racine, R.J., Burnham, W.M., Gilbert, M. and Kairiss, E.W. (1986) Kindling mechanisms. I. Electrophysiological studies. In *Kindling 3*, ed. J.A. Wada, pp. 263–282, New York: Raven.

Raczkowski, D. and Fitzpatrick, D. (1989) Organization of cholinergic synapses in the cat's dorsal lateral geniculate and perigeniculate nuclei. *Journal of Comparative Neurology* **288**: 231–254.

Radulovacki, M. (1985) Role of adenosine in sleep in rats. *Review of Clinical and Basic Pharmacology* **5**: 327–339.

Raichle, M.E. (1998) Behind the scenes of functional brain imaging: a historical and physiological perspective. *Proceedings of the National Academy of Sciences of the USA* **95**: 765–772.

Rainey, W.T. and Jones, E.G. (1983) Spatial distribution of individual medial lemniscal axons in the thalamic ventrobasal complex of the cat. *Experimental Brain Research* **49**: 229–246.

Rainnie, D.G., Holmes, K.H. and Shinnick-Gallagher, P. (1992) Kindling-induced long-lasting changes in synaptic transmission in the basolateral amygdala. *Journal of Neurophysiology* **67**: 443–454.

Rainnie, D.G., Grünze, H.C.R., McCarley, R.W. and Greene, R.W. (1994) Adenosine inhibition of mesopontine cholinergic neurons: implications for EEG arousal. *Science* **263**: 689–692.

Ralston, B. and Ajmone-Marsan, C. (1956) Thalamic control of certain normal and abnormal cortical rhythms. *Electroencephalography and Clinical Neurophysiology* **8**: 559–582.

Ramm, P. and Frost, B.J. (1983) Regional metabolic activity in the rat brain during sleep-like activity. *Sleep* **6**: 196–216.

Rámon y Cajal, S. (1911) *Histologie du Système Nerveux de l'Homme et des Vertébrés* (2 vol.), translated by L. Azoulay. Paris: Maloine. Also the 1952 edition, Madrid: Consejo Superior de Investigaciones Scientificas, Instituto Rámon y Cajal.

Rasmusson, D.D., Clow, K. and Szerb, J.C. (1994) Modification of neocortical acetylcholine release and electroencephalogram desynchronization due to brainstem stimulation by drugs applied to the basal forebrain. *Neuroscience* **60**: 665–677.

Rasmusson, D.D., Szerb, J.C. and Jordan, J.L. (1996) Differential effects of α-amino-3-hydroxy-5-methyl-4-isoxazole propionic acid and *N*-methyl-D-aspartate receptor antagonists applied to the basal forebrain on cortical acetylcholine release and EEG desynchronization. *Neuroscience* **72**: 419–427.

Rechtschaffen, A. (1998) Current perspectives on the function of sleep. *Perspectives in Biology and Medicine* **41**: 359–390.

Rechtschaffen, A., Lovell, R.A., Freedman, D., Whitehead, W.E. and Aldrich, M. (1973) The effect of parachlorophenylalanine on sleep in the rat: some implications for the serotonin sleep hypothesis. In *Serotonin and Behavior*, ed. J. Barchas and E. Usdin, pp. 401–418, New York: Academic.

Rechtschaffen, A., Bergmann, B.M., Everson, C.A., Kushida, C.A. and Gilliland, M.A. (1989a) Sleep deprivation in the rat. I. Conceptual issues. *Sleep* **12**: 1–4.

Rechtschaffen, A., Bergmann, B.M., Everson, C.A., Kushida, C.A. and Gilliland, M.A. (1989b) Sleep deprivation in the rat. X. Integration and discussion of the findings. *Sleep* **12**: 68–87.

Reiher, J., Lebel, M. and Klass, D.W. (1977) Small sharp spikes (SSS): reassessment of electroencephalographic characteristics and clinical significance. *Electroencephalography and Clinical Neurophysiology* **43**: 775.

Rempe, D.A., Bertram, E.H., Williamson, J.M. and Lothman, E.W. (1997) Interneurons in area CA1, stratum radiatum and stratum oriens remain functionally connected to excitatory synaptic input in chronically epileptic animals. *Journal of Neurophysiology* **78**: 1504–1515.

Renaud, L., Kelly, J. and Provini, L. (1974) Synaptic inhibition in pyramidal tract neurons: membrane potential and conductance changes evoked by pyramidal tract and cortical surface stimulation. *Journal of Neurophysiology* **37**: 1144–1155.

Reutens, D.C., Bye, A.M., Hopkins, I.J., Danks, A., Somerville, E., Walsh, J., Bleasel, A., Ouvrier, R., McKenzie, R.A. and Manson, J.I. (1993) Corpus callosotomy for intractable epilepsy: seizure outcome and prognostic factors. *Epilepsia* **34**: 904–909.

Ribak, C.E. and Peterson, G.M. (1991) Intragranular mossy fibers in rats and gerbils form synapses with the somata and proximal dendrites of basket cells in the dentate gyrus. *Hippocampus* **1**: 355–364.

Riou, F., Cespuglio, R. and Jouvet, M. (1982) Endogenous peptides and sleep in the rat. III. The hypnogenic properties of vasoactive intestinal peptide. *Neuropeptides* **2**: 265–277.

Rodin, E. (1999) Decomposition and mapping of generalized spike-wave complexes. *Clinical Neurophysiology* **110**: 1868–1875.

Roffwarg, H.P., Muzio, J.N. and Dement, W.C. (1966) Ontogenetic development of the human sleep-dream cycle. *Science* **152**: 604–619.

Roger, A., Rossi, G.F. and Zirondoli, A. (1956) Le rôle des afférences des nerfs craniens dans le maintien de l'etat vigile de la preparation "encéphale isolé". *Electroencephalography and Clinical Neurophysiology* **8**: 1–13.

Romanski, L.M. and LeDoux, J.E. (1992) Equipotentiality of thalamo-amygdala and thalamo-cortico-amygdala circuits in auditory fear conditioning. *Journal of Neuroscience* **12**: 4501–4509.

Rosen, A.S. and Andrew, R.D. (1990) Osmotic effects upon excitability in rat neocortical slices. *Neuroscience* **38**: 579–590.

Ross, J.J., Johnson, L.C. and Walter, R.D. (1966) Spike and wave discharges during stages of sleep. *Annals of Neurology* **14**: 399–407.

Roth, M., Shaw, J. and Green, J. (1956) The form, voltage distribution and physiological significance of the K-complex. *Electroencephalography and Clinical Neurophysiology* **8**: 385–402.

Rougeul-Buser, A., Bouyer, J.J., Montaron, M.F. and Buser, P. (1983) Patterns of activities in the ventrobasal thalamus and somatic cortex SI during behavioural immobility in the awake cat: focal waking rhythms. *Experimental Brain Research* **7** (Suppl.): 69–87.

Roy, J.P., Clercq, M., Steriade, M. and Deschênes, M. (1984) Electrophysiology of neurons of the lateral thalamic nuclei in cat: mechanisms of long-lasting hyperpolarizations. *Journal of Neurophysiology* **51**: 1220–1235.

Roy, S.A., Dear, S.P. and Alloway, K.D. (2001) Long-range cortical synchronization without concomitant oscillations in the somatosensory system of anesthetized cats. *Journal of Neuroscience* **21**: 1795–1808.

Royer, S., Martina, M. and Paré, D. (1999) An inhibitory interface gates impulse traffic between the input and output stations of the amygdala. *Journal of Neuroscience* **19**: 10575–10583.

Royer, S., Martina, M. and Paré, D. (2000a) Polarized synaptic interactions between intercalated neurons of the amygdala. *Journal of Neurophysiology* **83**: 3509–3518.

Royer, S., Martina, M. and Paré, D. (2000b) Bistable behavior of inhibitory neurons controlling impulse traffic through amygdala: role

of a slowly deinactivating K^+ current. *Journal of Neuroscience* **20**: 9034–9039.

Rubboli, G., Meletti, S., Gardella, E., Zaniboni, A., D'Orsi, G., Dravet, C. and Tassinari, C.A. (1999) Photic reflex myoclonus: a neuropphysiological study in progressive myoclonus epilepsies. *Epilepsia* **40** (Suppl. 4): 50–58.

Ruch-Monachon, M.A., Jaffre, M. and Haefely, W. (1976) Drugs and PGO waves in the lateral geniculate body of the curarized cat. IV. The effects of acetylcholine, GABA and benzodiazepines on PGO wave activity. *Archives Internationales de Pharmacodynamie et Thérapie* **219**: 308–325.

Rudy, B. and McBain, C.J. (2001) Kv3 channels: voltage-gated K^+ channels designed for high-frequency repetitive firing. *Trends in Neurosciences* **24**: 517–526.

Russchen, F.T., Amaral, D.G. and Price, J.L. (1985) The afferent connections of the substantia innominata in the monkey, *Macaca fascicularis*. *Journal of Comparative Neurology* **242**: 1–27.

Sadler, R.M. and Blume, W.T. (1989) Significance of bisynchronous spike-wave in patients with temporal lobe spikes. *Epilepsia* **30**: 143–146.

Sakai, K. and Crochet, S. (2000) Serotonergic dorsal raphe neurons cease firing by disfacilitation during paradoxical sleep. *NeuroReport* **11**: 3237–3241.

Sakai, K. and Crochet, S. (2001a) Differentiation of presumed serotonergic dorsal raphe neurons in relation to behavior and wake-sleep states. *Neuroscience* **104**: 1141–1155.

Sakai, K. and Crochet, S. (2001b) Role of dorsal raphe neurons in paradoxical sleep generation in the cat: no evidence for a serotonergic mechanisms. *European Journal of Neuroscience* **13**: 103–112.

Sakai, K. and Jouvet, M. (1980) Brain stem PGO-on cells projecting directly to the cat dorsal lateral geniculate nucleus. *Brain Research* **194**: 500–505.

Sakai, K., El Mansari, M. and Jouvet, M. (1990) Inhibition by carbachol microinjections of presumptive cholinergic PGO-on neurons in freely moving cats. *Brain Research* **527**: 213–223.

Sakai, K., Crochet, S. and Onoe, H. (2001) Pontine structures and mechanisms involved in the generation of paradoxical (REM) sleep. *Archives Italiennes de Biologie* **139**: 93–107.

Sakakura, H. (1968) Spontaneous and evoked unitary activities of cat lateral geniculate neurons in sleep and wakefulness. *Japanese Journal of Physiology* **18**: 23–42.

Sallanon, M., Sakai, K., Buda, C., Puymartin, M. and Jouvet, M. (1986) Augmentation du sommeil paradoxal, induite par l'injection d'acide iboténique dans l'hypothalamus ventrolatéral postérieur, chez le chat. *Comptes Rendus de l'Académie de Sciences (Paris)* **303**: 175–179.

Sallanon, M., Denoyer, M., Kitahama, K., Aubert, C., Gay, N. and Jouvet, M. (1989) Long-lasting insomnia induced by preoptic lesions and its transient reversal by muscimol injection into the posterior hypothalamus in the cat. *Neuroscience* **32**: 669–683.

Sammaritano, M., Gigli, G.L. and Gotman, J. (1991) Interictal spiking during wakefulness and sleep and the localization of foci in temporal lobe epilepsy. *Neurology* **41**: 290–297.

Samoriski, G.M. and Applegate, C.D. (1997) Repeated generalized seizures induce time-dependent changes in the behavioral seizure response independent of continued seizure induction. *Journal of Neuroscience* **17**: 5581–5590.

Sanchez, R. and Leonard, C.S. (1996) NMDA-receptor-mediated synaptic currents in guinea pig laterodorsal tegmental neurons in vitro. *Journal of Neurophysiology* **76**: 1101–1111.

Sanchez-Vives, M.V. and McCormick, D.A. (1997a) Functional properties of perigeniculate inhibition of dorsal lateral geniculate nucleus thalamocortical neurons *in vitro*. *Journal of Neuroscience* **17**: 8880–8893.

Sanchez-Vives, M.V. and McCormick, D.A. (1997b) Inhibitory interactions between perigeniculate GABAergic neurons. *Journal of Neuroscience* **17**: 8894–8908.

Sanchez-Vives, M.V. and McCormick, D.A. (2000) Cellular and network mechanisms of rhythmic recurrent activity in neocortex. *Nature Neuroscience* **3**: 1027–1034.

Sanchez-Vives, M.V., Bal, T. and McCormick, D.A. (1997) Inhibitory interactions between perigeniculate GABAergic neurons. *Journal of Neuroscience* **17**: 8894–8908.

Saper, C.B., Chou, T.C. and Scammell, T.E. (2001) The sleep switch: hypothalamic control of sleep and wakefulness. *Trends in Neurosciences* **24**: 726–731.

Sato, S., Dreifuss, F.E. and Penry, J.K. (1973) The effects of sleep on spike-wave discharges in absence seizures. *Neurology* **23**: 1335–1345.

Sato, S., White, B.G., Penry, J.K., Dreifuss, F.E., Sackellares, J.C. and Kupferberg, H.J. (1982) Valproic acid versus ethosuximide in the treatment of absence seizures. *Neurology* **32**: 157–163.

Saunders, M.G. and Westmoreland, B.F. (1979) The EEG in evaluation of disorders affecting the brain diffusely. In *Current Practice of Clinical Electroencephalography*, ed. D.W. Klass and D.D. Daly, pp. 343–379, New York: Raven Press.

Sawyer, S.F., Tepper, J.M. and Groves, P.M. (1994) Cerebellar-responsive neurons in the thalamic ventroanterior-ventrolateral complex of rats: light and electron microscopy. *Neuroscience* **63**: 725–745.

Scharfman, H.E., Goodman, J.H., Du, F. and Schwarcz, R. (1998) Chronic changes in synaptic responses of entorhinal and hippocampal neurons after amino-oxyacetic acid (AOAA)-induced entorhinal cortical neuron loss. *Journal of Neurophysiology* **80**: 3031–3046.

Scheibel, M.E., Crandall, P.H. and Scheibel, A.B. (1974) The hippocampal-dentate complex in temporal lobe epilepsy. *Epilepsia* **15**: 55–80.

Scherg, M., Bast, T. and Berg, P. (1999) Multiple source analysis of interictal spikes: goals, requirements and clinical value. *Journal of Clinical Neurophysiology* **16**: 214–224.

Schiff, N.D., Labar, D.R. and Victor, J.D. (1999) Common dynamics in temporal lobe seizures and absence seizures. *Neuroscience* **91**: 417–428.

Schwartzkroin, P.A. (1975) Characteristics of CA1 neurons recorded intracellularly in the hippocampal *in vitro* slice preparation. *Brain Research* **85**: 423–432.

Schwartzkroin, P.A. (1977) Further characteristics of hippocampal CA1 cells *in vitro*. *Brain Research* **128**: 53–68.

Schwartzkroin, P.A. (1983) Local circuit considerations and intrinsic neuronal properties involved in hyperexcitability and cell synchronization. In *Basic Mechanisms of Neuronal Hyperexcitability*, ed. H.H. Jasper and N.M. van Gelder, pp. 75–105, New York: Alan R. Liss.

Schwartzkroin, P.A. and Mueller, A.L. (1987) Electrophysiology of hippocampal neurons. In *Cerebral Cortex* (vol. 6, *Further Aspects of Cortical Function, Including Hippocampus*), ed. E.G. Jones and A. Peters, pp. 295–343, New York: Plenum.

Schwartzkroin, P.A. and Prince, D.A. (1978) Cellular and field potential properties of epileptogenic hippocampal slices. *Brain Research* **147**: 117–130.

Schwartzkroin, P.A. and Prince, D.A. (1980) Changes in excitatory and inhibitory synaptic potentials leading to epileptogenic activity. *Brain Research* **183**: 61–73.

Schwindt, P.C. and Crill, W.E. (1995) Amplification of synaptic currents by persistent sodium conductance in apical dendrite of neocortical neurons. *Journal of Neurophysiology* **74**: 2220–2224.

Schwindt, P.C., Spain, W.J., Foehring, R.C., Stafstrom, C.E., Chubb, M.C. and Crill, W.E. (1988a) Multiple potassium conductances and their functions in neurons from cat sensorimotor cortex *in vitro*. *Journal of Neurophysiology* **59**: 424–449.

Schwindt, P.C., Spain, W.J., Foehring, R.C., Chubb, M.C. and Crill, W.E. (1988b) Slow conductances in neurons from cat sensorimotor cortex *in vitro* and their role in slow excitability changes. *Journal of Neurophysiology* **59**: 450–467.

Schwindt, P.C., Spain, W.J. and Crill, W.E. (1989) Long-lasting reduction of excitability by a sodium-dependent potassium current in cat neocortical neurons. *Journal of Neurophysiology* **61**: 233–244.

Scott, D.E. (1993) *The History of Epileptic Therapy: Account of How Medication was Discovered*. Pearl River, NY: The Parthenon Publishing Group.

Seidenbecher, T. and Pape, H.C. (2001) Contribution of intralaminar thalamic nuclei to spike-and-wave-discharges during spontaneous seizures in a genetic model of absence epilepsy. *European Journal of Neuroscience* **13**: 1537–1546.

Seidenbecher, T., Staak, R. and Pape, H.T. (1998) Relations between cortical and thalamic cellular activities during absence seizures in rats. *European Journal of Neuroscience* **10**: 1103–1112.

Sejnowski, T.J. and Destexhe, A. (2000) Why do we sleep? *Brain Research* **886**: 208–223.

Semba, K. and Fibiger, H. (1992) Afferent connections of the laterodorsal and the pedunculopontine tegmental nuclei in the rat: a retro- and anterograde transport and immunohistochemical study. *Journal of Comparative Neurology* **323**: 387–410.

Semba, K., Reiner, P.B., McGeer, E.G. and Fibiger, H. (1989) Brainstem projecting neurons in the rat basal forebrain: neurochemical, topographical, and physiological distinctions from cortically projecting cholinergic neurons. *Brain Research Bulletin* **22**: 501–509.

Señaris, R.M., Humphrey, P.P.A. and Emson, P.C. (1994) Distribution of somatostatin receptors 1, 2 and 3 mRNA in rat brain and pituitary. *European Journal of Neuroscience* **6**: 1883–1896.

Sernagor, E., Yarom, Y. and Werman, R. (1986) Sodium-dependent regenerative responses in dendrites of axotomized motoneurons in the cat. *Proceedings of the National Academy of Sciences of the USA* **83**: 7966–7970.

Servit, Z. (1959) Audiogenic epilepsy in rats as a model of reflex mechanisms in the pathogenesis of epileptic seizures. *Journal of Experimental Medical Sciences* **3**: 37–44.

Seyfried, T.N. and Todorova, M. (1999) Experimental models of epilepsy. In *The Epilepsies*, ed. P. Kotagal and H.O. Lüders, pp. 527–542, San Diego: Academic Press.

Shadlen, M.N. and Movshon, J.A. (1999) Synchrony unbound: a critical evaluation of the temporal binding hypothesis. *Neuron* **24**: 67–77.

Shatz, C.J. (1983) The prenatal development of the cat's retinogeniculate pathway. *Journal of Neuroscience* **3**: 482–499.

Shatz, C.J. and Rakic, P. (1981) The genesis of efferent connections from the visual cortex of fetal rhesus monkey. *Journal of Comparative Neurology* **196**: 287–308.

Sheer, D. (1984) Focused arousal, 40 Hz, and dysfunction. In *Selfregulation of the Brain and Behavior*, ed. T. Ebert, pp. 64–84, Berlin: Springer.

Sherin, J.E., Shiromani, P.J., McCarley, R.W. and Saper, C.B. (1996) Activation of preoptic neurons during sleep. *Science* **271**: 216–219.

Sherrington, C.S. (1955) *Man on his Nature*. New York: Doubleday.

Shibasaki, H. and Neshige, R. (1987) Photic cortical reflex myoclonus. *Annals of Neurology* **22**: 252–257.

Shibata, M., Blatteis, C.M., Krueger, J.M., Obál, F. Jr. and Opp, M. (1989) Pyrogenic, inflammatory and somnogenic responses to cytokines: differential modes of action. In *Thermoregulation Research and Clinical Applications*, ed. P. Lomax and E. Schanbaun, pp. 69–73, Basel: Karger.

Shima, K., Nakahama, H. and Yamamoto, M. (1986) Firing properties of two types of nucleus raphe dorsalis neurons during the sleep-waking cycle and their responses to sensory stimuli. *Brain Research* **399**: 317–326.

Shoham, S. and Krueger, J.M. (1988) Muramyl dipeptide-induced sleep and fever: effects of ambient temperature and time of injections. *American Journal of Physiology* **255**: R157–165.

Shoham, S., Davenne, D., Cady, A.B., Dinarello, C.A. and Krueger, J.M. (1987) Recombinant tumor necrosis factor and interleukin 1 enhance slow-wave sleep. *American Journal of Physiology* **253**: R142–149.

Shouse, M.N. (2001) Physiology underlying relationship of epilepsy and sleep. In *Epilepsy and Sleep*, ed. D.S. Dinner and H.O. Lüders, pp. 43–62, San Diego: Academic Press.

Shouse, M.N., Martins da Silva, A. and Sammaritano, M. (1996) Circadian rhythm, sleep, and epilepsy. *Journal of Clinical Neurophysiology* **13**: 32–50.

Siapas, A.G. and Wilson, M.A. (1998) Coordinated interactions between hippocampal ripples and cortical spindles during slow-wave sleep. *Neuron* **21**: 1123–1128.

Sik, A., Penttonen, M., Ylinen, A. and Buzsáki, G. (1995) Hippocampal CA1 interneurons: an *in vivo* intracellular study. *Journal of Neuroscience* **15**: 6651–6665.

Silva, A.J., Kogan, J.H., Frankland, P.W. and Kida, S. (1998) CREB and memory. *Annual Reviews of Neuroscience* **21**: 127–148.

Silva-Barrat, C., Champagnat, J., Leiva, J. and Pavlik, V. (1994) Noradrenaline mediates paradoxical effects on rat neocortical neurons after GABA withdrawal. *Journal of Neurophysiology* **71**: 1139–1150.

Silveira, D.C., Holmes, G.L., Schachter, S.C., Geula, C. and Schomer, D.L. (2000) Increased susceptibility to generalized seizures after immunolesions of the basal forebrain cholinergic neurons in rats. *Brain Research* **878**: 223–227.

Simon, N.R., Lopes da Silva, F.H. and Manshanden, I. (1999) Preliminary results from a whole-head MEG study of sleep. In *Recent Advances in Biomagnetism*, ed. T. Yoshimoto, pp. 373–376, Sendai: Tohoku University Press.

Simon, N.R., Mandshanden, I. and Lopes da Silva, F.H. (2000) A MEG study of sleep. *Brain Research* **860**: 64–76.

Singer, W. (1977) Control of thalamic transmission by corticofugal and ascending pathways in the visual system. *Physiological Reviews* **57**: 386–420.

Singer, W. (1990a) Search for coherence: a basic principle of cortical self-organization. *Concepts in Neuroscience* **1**: 1–26.

Singer, W. (1990b) Role of acetylcholine in use-dependent plasticity of the visual cortex. In *Brain Cholinergic Systems*, ed. M. Steriade and D. Biesold, pp. 314–336, Oxford: Oxford University Press.

Slaght, S., Charpier, S., Deniau, J.M., Leresche, N. and Crunelli, V. (2000) *In vivo* intracellular recordings in neurones of the nucleus reticularis thalami during spike and wave discharges in the GAERS genetic model of absence epilepsy. *Society of Neuroscience Abstracts* **26**: 735.

Slaght, S.J., Leresche, N., Deniau, J.M., Crunelli, V. and Charpier, S. (2002) Activity of thalamic reticular neurons during spontaneous genetically determined spike and wave discharges. *Journal of Neuroscience* **22**: 2323–2334.

Sloviter, R.S. (1987) Decreased hippocampal inhibition and a selective loss of interneurons in experimental epilepsy. *Science* **235**: 73–76.

Sloviter, R.S. (1992) Possible functional consequences of synaptic reorganization in the dentate gyrus of kainite-treated rats. *Neuroscience Letters* **137**: 91–96.

Smart, T.G., Xie, X. and Krishek, B.J. (1994) Modulation of inhibitory and excitatory amino acid receptor ion channels by zinc. *Progress in Neurobiology* **42**: 393–441.

Smith, K.A. and Fisher, R.S. (1996) The selective $GABA_B$ antagonist CGP-35348 blocks spike-wave bursts in the cholesterol synthesis rat absence epilepsy model. *Brain Research* **729**: 147–150.

Smith, T.G. and Purpura, D.P. (1960) Electrophysiological studies on epileptogenic lesions of cat cortex. *Electroencephalography and Clinical Neurophysiology* **12**: 59–82.

Smith, Y., Paré, D., Deschênes, M., Parent, A. and Steriade, M. (1988) Cholinergic and non-cholinergic projections from the upper brainstem to the visual thalamus in the cat. *Experimental Brain Research* **70**: 166–180.

Snead, O.C. (1995) Basic mechanisms of generalized absence seizures. *Annals of Neurology* **37**: 146–157.

Snead, O.C., Depaulis, A., Vergnes, M. and Marescaux, C. (1999) Absence epilepsy: advances in experimental animal models. In *Jasper's Basic Mechanisms of the Epilepsies*, ed. A.V. Delgado-Escueta, W. Wilson, R.W. Olsen and R.J. Porter, 253–278, New York: Raven.

Snead, O.C., Banerjee, P.K., Burnham, M. and Hampson, D. (2000) Modulation of absence seizures by the $GABA_A$receptor: a critical role for metabotropic glutamate receptor (mGluR4). *Journal of Neuroscience* **20**: 6218–6224.

Snyder, S.H. and Bredt, D.A. (1991) Nitric oxide as a neuronal messenger. *Trends in Pharmacological Sciences* **12**: 125–128.

Soderling, T.R. and Derkach, V.A. (2000) Postsynaptic protein phosphorylation and LTP. *Trends in Neurosciences* **23**: 75–80.

Sohal, V.S., Huntsman, M.M. and Huguenard, J.R. (2000) Reciprocal inhibitory connections regulate the spatiotemporal properties of intrathalamic oscillations. *Journal of Neuroscience* **20**: 1735–1745.

Solomon, J.S., Doyle, J.F., Burkhalter, H. and Nerbonne, J.M. (1993) Differential expression of hyperpolarization-activated currents reveals distinct classes of visual cortical projection neurons. *Journal of Neuroscience* **13**: 5082–5091.

Soltesz, I. and Crunelli, V. (1992) $GABA_A$ and pre- and post-synaptic $GABA_B$ receptor-mediated responses in the lateral geniculate nucleus. In *Progress in Brain Research* (vol. 90), ed. R.R. Mize, R.E. Marc and A.M. Sillito, pp. 151–169, Amsterdam: Elsevier.

Soltesz, I., Lightowler, S., Leresche, N., Jassik-Gerschenfeld, D. and Crunelli, V. (1991) Two inward currents and the transformation of low-frequency oscillations of rat and cat thalamocortical cells. *Journal of Physiology (London)* **441**: 175–197.

Somogyi, P. (1977) A specific "axo-axonal" interneuron in the visual cortex of the rat. *Brain Research* **136**: 345–350.

Somogyi, P. (1989) Synaptic organisation of GABAergic neurons and $GABA_A$ receptors in the lateral geniculate nucleus and visual cortex. In *Retina Research Foundation Symposium*, vol. 2, *Neural mechanisms of visual perception*, ed. D.K.T. Lam and C.D. Gilbert, pp. 35–62, Woodlands, TX: Portfolio.

Somogyi, P. and Cowey, A. (1981) Combined Golgi and electron microscopic study on the synapses formed by double bouquet cells in the visual cortex of the cat and monkey. *Journal of Comparative Neurology* **195**: 547–566.

Somogyi, P. and Freund, T.F. (1989) Immunocytochemistry and synaptic relationships of physiologically characterized, HRP-filled neurons. In *Neuroanatomical Tract-Tracing Methods* (vol. 2), ed. L. Heimer and L. Zaborsky, pp. 239–264, New York: Plenum.

Somogyi, P. and Soltesz, I. (1986) Immunogold demonstration of GABA synaptic terminals of intracellularly recorded, horseradish peroxidase-filled basket cells and clutch cells in the cat's visual cortex. *Neuroscience* **19**: 1051–1065.

Somogyi, P., Hajdu, F. and Tömböl, T. (1978) Ultrastructure of the anterior ventral and anterior medial nuclei of the cat thalamus. *Experimental Brain Research* **31**: 417–431.

Somogyi, P., Smith, A.D., Nunzi, M.G., Gorio, A., Takagi, H. and Wu, J.Y. (1983) Glutamate decarboxylase immunoreactivity in the hippocampus of the cat: distribution of immunoreactive synaptic terminals with special reference to the axon initial segment of pyramidal neurons. *Journal of Neuroscience* **3**: 1450–1468.

Somogyi, P., Freund, T.F., Hodgson, A.J., Somogyi, J., Beroukas, D. and Chubb, I.W. (1985) Identified axo-axonic cells are immunoreactive for GABA in the hippocampus and visual cortex of cats. *Brain Research* **332**: 143–149.

Somogyi, P., Tamás, G., Lujan, R. and Buhl, E.H. (1998) Salient features of synaptic organisation in the cerebral cortex. *Brain Research Reviews* **26**: 113–135.

Sontheimer, H., Kettenmann, H., Backus, K.H. and Schachner, M. (1988) Glutamate opens Na^+/K^+ channels in cultured astrocytes. *Glia* **1**: 328–336.

Spencer, S.S. and Spencer, D.D. (1994) Entorhinal-hippocampal interactions in medial temporal lobe epilepsy. *Epilepsia* **35**: 721–727.

Spencer, S.S., Williamson, P.D., Spencer, D.D. and Mattson, R.H. (1987) Human hippocampal seizure spread studied by depth and subdural recording: the hippocampal commissure. *Epilepsia* **28**: 479–489.

Spencer, S.S., Kim, J., DeLanerolle, N. and Spencer, D.D. (1999) Differential neuronal and glia relations with parameters of ictal discharge in mesial temporal lobe epilepsy. *Epilepsia* **40**: 708–712.

Spencer, W.A. and Brookhart, J.M. (1961) Electrical patterns of augmenting and recruiting waves in the depths of the sensorimotor cortex of cat. *Journal of Neurophysiology* **24**: 26–49.

Spencer, W.A. and Kandel, E.R. (1961) Electrophysiology of hippocampal neurons. IV. Fast pre-potentials. *Journal of Neurophysiology* **24**: 272–285.

Spreafico, R., De Curtis, M., Frassoni, C. and Avanzini, G. (1988) Electrophysiological characteristics of morphologically identified reticular thalamic neurons from rat slices. *Neuroscience* **27**: 629–638.

Spreafico, R., Frassoni, C., Regondi, M.C., Arcelli, P. and De Biasi, S. (1993) Interneurons in the mammalian thalamus, a marker of species? In *Thalamic Networks for Relay and Modulation*, ed. D. Minciacchi, M. Molinari, G. Macchi and E.G. Jones, pp. 17–28, New York: Pergamon Press.

Squire, L.R. (1987) *Memory and Brain.* New York: Oxford University Press.

Squire, L.R., Cohen, N.J. and Nadel, L. (1984) The medial temporal region and memory consolidation: a new hypthesis. In *Memory Consolidation*, ed. H. Weingartner and E. Parker, pp. 185–201, Hillsdale: Erlbaum.

Staak, R. and Pape, H.C. (2001) Contribution of $GABA_A$ and $GABA_B$ receptors to thalamic neuronal activity during spontaneous absence seizures in rats. *Journal of Neuroscience* **21**: 1378–1384.

Staba, R.J., Wilson, C.L., Bragin, A., Fried, I. and Engel Jr., J. (2002) Sleep states differentiate single neuron activity recorded from human epileptic hippocampus, entorhinal cortex, and subiculum. *Journal of Neuroscience* **22**: 5694–5704.

Stafstrom, C.E., Schwindt, P.C., Chubb, M.C. and Crill, W.E. (1985) Properties of persistent sodium conductance and calcium conductance of layer V neurons from cat sensorimotor cortex *in vitro*. *Journal of Neurophysiology* **53**: 153–170.

Staley, K.J., Soldo, B.L. and Proctor, W.R. (1995) Ionic mechanisms of neuronal excitation by inhibitory $GABA_A$ receptors. *Science* **269**: 977–981.

Stefan, H. and Snead, O.C. Jr. (1997) Absence seizures. In *Epilepsy: A Comprehensive Textbook*, ed. J. Engel Jr. and T.A. Pedley, pp. 579–590, Philadelphia: Lippincot-Raven.

Steinhäuser, C. and Gallo, V. (1996) News on glutamate receptors on glial cells. *Trends in Neurosciences* **19**: 339–345.

Steininger, T.L., Rye, D.B. and Wainer, B.H. (1992) Afferent projections to the cholinergic pedunculopontine tegmental nucleus and adjacent midbrain extrapyramidal area in the albino rat. *Journal of Comparative Neurology* **321**: 515–543.

Steininger, T.L., Gong, H., McGinty, D. and Szymusiak, R. (2001) Subregional organization of preoptic/anterior hypothalamic projections to arousal-related monoaminergic cell groups. *Journal of Comparative Neurology* **429**: 638–653.

Steriade, M. (1960) Mechanisms of facilitation and inhibition in focal cortical epilepsy induced by penicillin. *Studies and Research in Neurology* **5**: 463–471 (in Romanian).

Steriade, M. (1964) Development of evoked responses into self-sustained activity within amygdalo-hippocampal circuits. *Electroencephalography and Clinical Neurophysiology* **16**: 221–236.

Steriade, M. (1970) Ascending control of thalamic and cortical responsiveness. *International Review of Neurobiology* **12**: 87–144.

Steriade, M. (1974) Interneuronal epileptic discharges related to spike-and-wave cortical seizures in behaving monkeys. *Electroencephalography and Clinical Neurophysiology* **37**: 247–263.

Steriade, M. (1976) Cortical inhibition during sleep and waking. In *Mechanisms in Transmission of Signal for Conscious Behavior*, ed. T. Desiraju, pp. 209–248, Amsterdam: Elsevier.

Steriade, M. (1978) Cortical long-axoned cells and putative interneurons during the sleep-waking cycle. *Behavioral and Brain Sciences* **3**: 465–514.

Steriade, M. (1981) Mechanisms underlying cortical activation: neuronal organization and properties of the midbrain reticular core and intralaminar thalamic nuclei. In *Brain Mechanisms of Perceptual Awareness and Purposeful Behavior*, ed. O. Pompeiano and C. Ajmone-Marsan, pp. 327–377, New York: Raven Press.

Steriade, M. (1984) The excitatory-inhibitory sequence in thalamic and neocortical cells: state-related changes and regulatory systems. In *Dynamic Aspects of Neocortical Function*, ed. G.M. Edelman, W.E. Gall and W.M. Cowan, pp. 107–157, New York: Wiley.

Steriade, M. (1990) Spindling, incremental thalamocortical responses, and spike-wave epilepsy. In *Generalized Epilepsy*, ed. M. Avoli, P. Gloor, G. Kostopoulos and R. Naquet, pp. 161–180, Boston: Birkäuser.

Steriade, M. (1991) Alertness, quiet sleep, dreaming. In *Cerebral Cortex* (vol. 9, *Normal and Altered States of Function*), ed. A. Peters and E.G. Jones, pp. 279–357, New York: Plenum.

Steriade, M. (1995) Two channels in the cerebellothalamocortical system. *Journal of Comparative Neurology* **354**: 57–70.

Steriade, M. (1997a) Synchronized activities of coupled oscillators in the cerebral cortex and thalamus at different levels of vigilance. *Cerebral Cortex* **7**: 583–604.

Steriade, M. (1997b) Thalamic substrates of disturbances in states of vigilance and consciousness in humans. In *Thalamus* (vol. 2, *Experimental and Clinical aspects*), ed. M. Steriade, E.G. Jones and D.A. McCormick, pp. 721–742, Oxford: Elsevier.

Steriade, M. (1998) Corticothalamic networks, oscillations, and plasticity. In *Consciousness: At the Frontiers of Neuroscience* (vol. 77, *Advances in Neurology*), ed. H.H. Jasper, L. Descarries, V.F. Castellucci and S. Rossignol, pp. 105–134, Philadelphia: Lippincott-Raven.

Steriade, M. (1999a) Cellular substrates of brain rhythms. In *Electroencephalography: Basic Principles, Clinical Applications, and Related Fields*, 4th edn., ed. E. Niedermeyer and F. Lopes Da Silva, pp. 28–75, Baltimore: Williams & Wilkins.

Steriade, M. (1999b) Coherent oscillations and short-term plasticity in corticothalamic networks. *Trends in Neurosciences* **22**: 337–345.

Steriade, M. (2000) Corticothalamic resonance, states of vigilance, and mentation. *Neuroscience* **101**: 243–276.

Steriade, M. (2001a) Impact of network activities on neuronal properties in corticothalamic systems. *Journal of Neurophysiology* **86**: 1–39.

Steriade, M. (2001b) *The Intact and Sliced Brain*. Cambridge, MA: The MIT Press.

Steriade, M. (2001c) The GABAergic reticular nucleus: a preferential target of corticothalamic projections. *Proceedings of the National Academy of Sciences of the USA* **98**: 3625–3627.

Steriade, M. (2003) Presynaptic dendrites of thalamic local-circuit neurons and sculpting inhibition during activated states. *Journal of Physiology (London)* **546**: 1.

Steriade, M. and Amzica, F. (1994) Dynamic coupling among neocortical neurons during evoked and spontaneous spike-wave seizure activity. *Journal of Neurophysiology* **72**: 2051–2069.

Steriade, M. and Amzica F. (1996) Intracortical and corticothalamic coherency of fast spontaneous oscillations. *Proceedings of National Academy of Sciences of the USA* **93**: 2533–2538.

Steriade, M. and Amzica, F. (1998) Coalescence of sleep rhythms and their chronology in corticothalamic networks. *Sleep Research Online* **1**: 1–10.

Steriade, M. and Amzica, F. (1999) Intracellular study of excitability in the seizure-prone neocortex *in vivo*. *Journal of Neurophysiology* **82**: 3108–3122.

Steriade, M. and Buzsáki, G. (1990) Parallel activation of thalamic and cortical neurons by brainstem and basal forebrain cholinergic systems. In *Brain Cholinergic Systems*, ed. M. Steriade and D. Biesold, pp. 3–63, Oxford: Oxford University Press.

Steriade, M. and Contreras, D. (1995) Relations between cortical and thalamic cellular events during transition from sleep pattern to paroxysmal activity. *Journal of Neuroscience* **15**: 623–642.

Steriade, M. and Contreras, D. (1998) Spike-wave complexes and fast runs of cortically generated seizures. I. Role of neocortex and thalamus. *Journal of Neurophysiology* **80**: 1439–1455.

Steriade, M. and Demetrescu, M. (1960) Unspecific systems of inhibition and facilitation of potentials evoked by intermittent light. *Journal of Neurophysiology* **23**: 602–617.

Steriade, M. and Deschênes, M. (1974) Inhibitory processes and interneuronal apparatus in motor cortex during sleep and waking. II. Recurrent and afferent inhibition of pyramidal tract neurons. *Journal of Neurophysiology* **37**: 1093–1113.

Steriade, M. and Deschênes, M. (1984) The thalamus as a neuronal oscillator. *Brain Research Reviews* **8**: 1–63.

Steriade, M. and Deschênes, M. (1987) Inhibitory processes in the thalamus. *Journal of Mind and Behavior* **8**: 559–572.

Steriade, M. and Deschênes, M. (1988) Intrathalamic and brainstem-thalamic networks involved in resting and alert states. In *Cellular Thalamic Mechanisms*, ed. M. Bentivoglio and R. Spreafico, pp. 37–62, Amsterdam: Elsevier.

Steriade, M. and Glenn, L.L. (1982) Neocortical and caudate projections of intralaminar thalamic neurons and their synaptic excitation from the midbrain reticular core. *Journal of Neurophysiology* **48**: 352–371.

Steriade, M. and Llinás, R.R. (1988) The functional states of the thalamus and the associated neuronal interplay. *Physiological Reviews* **68**: 649–742.

Steriade, M. and McCarley, R.W. (1990) *Brainstem Control of Wakefulness and Sleep*. New York: Plenum.

Steriade, M. and Morin, D. (1981) Reticular influences on primary and augmenting responses in the somatosensory cortex. *Brain Research* **205**: 67–80.

Steriade, M. and Timofeev, I. (1997) Short-term plasticity during intrathalamic augmenting responses in decorticated cats. *Journal of Neuroscience* **17**: 3778–3795.

Steriade, M. and Timofeev, I. (2001) Corticothalamic operations through prevalent inhibition of thalamocortical neurons. *Thalamus and Related Systems* **1**: 225–236.

Steriade, M. and Timofeev, I. (2002a) Generators of ictal and interictal electroencephalograms associated with infantile spasms: intracellular studies of cortical and thalamic neurons. *International Review of Neurobiology* **49**: 77–98.

Steriade, M. and Timofeev, I. (2002b) Neuronal plasticity during sleep oscillations in corticothalamic systems. In *Sleep and Brain Plasticity*, ed. P. Maquet, R. Stickgold and C.S. Smith, in press, Oxford: Oxford University Press.

Steriade, M. and Wyzinski, P. (1972) Cortically elicited activities in thalamic reticularis neurons. *Brain Research* **42**: 514–520.

Steriade, M. and Yossif, G. (1974) Spike-and-wave afterdischarges in cortical somatosensory neurons of cat. *Electroencephalography and Clinical Neurophysiology* **37**: 633–648.

Steriade, M., Iosif, G. and Apostol, V. (1969) Responsiveness of thalamic and cortical motor relays during arousal and various stages of sleep. *Journal of Neurophysiology* **32**: 251–265.

Steriade, M., Apostol, V. and Oakson, G. (1971) Control of unitary activities in cerebellothalamic pathway during wakefulness and synchronized sleep. *Journal of Neurophysiology* **34**: 389–413.

Steriade, M., Wyzinski, P. and Apostol, V. (1972) Corticofugal projections governing rhythmic thalamic activity. In *Corticothalamic Projections and Sensorimotor Activities*, ed. T.L. Frigyesi, E. Rinvik and M.D. Yahr, pp. 221–272. New York: Raven Press.

Steriade, M., Deschênes, M. and Oakson, G. (1974a) Inhibitory processes and interneuronal apparatus in motor cortex during sleep and waking. I. Background firing and synaptic responsiveness of pyramidal tract neurons and interneurons. *Journal of Neurophysiology* **37**: 1065–1092.

Steriade, M., Deschênes, M., Wyzinski, P. and Hallé, J.P. (1974b) Input-output organization of the motor cortex during sleep and waking. In *Basic Sleep Mechanisms*, ed. O. Petre-Quadens and J. Schlag, pp. 144–200, New York: Academic Press.

Steriade, M., Oakson, G. and Diallo, A. (1976) Cortically elicited spike-wave afterdischarges in thalamic neurons. *Electroencephalography and Clinical Neurophysiology* **41**: 641–644.

Steriade, M., Diallo, A., Oakson, G. and White-Guay, B. (1977a) Some synaptic inputs and ascending projections of lateral posterior thalamic neurons. *Brain Research* **131**: 39–53.

Steriade, M., Oakson, G. and Diallo, A. (1977b) Reticular influences on lateralis posterior thalamic neurons. *Brain Research* **131**: 55–71.

Steriade, M., Kitsikis, A. and Oakson, G. (1979a) Excitatory-inhibitory processes in parietal association neurons during reticular activation and sleep-waking cycle. *Sleep* **1**: 339–355.

Steriade, M., Kitsikis, A. and Oakson, G. (1979b) Selectively REM-related increased firing rates in association interneurons during sleep: possible implications for learning. In *Brain Mechanisms in Memory and Learning*, ed. M.A. Brazier, pp. 47–52, New York: Raven Press.

Steriade, M., Parent, A. and Hada, J. (1984) Thalamic projections of nucleus reticularis thalami: a study using retrograde transport of horseradish peroxidase and double fluorescent tracers. *Journal of Comparative Neurology* **229**: 531–547.

Steriade, M., Deschênes, M., Domich, L. and Mulle, C. (1985) Abolition of spindle oscillations in thalamic neurons disconnected from nucleus reticularis thalami. *Journal of Neurophysiology* **54**: 1473–1497.

Steriade, M., Domich, L. and Oakson, G. (1986) Reticularis thalami neurons revisited: activity changes during shifts in states of vigilance. *Journal of Neuroscience* **6**: 68–81.

Steriade, M., Domich, L., Oakson, G. and Deschênes, M. (1987a) The deafferented reticularis thalami nucleus generates spindle rhythmicity. *Journal of Neurophysiology* **57**: 260–273.

Steriade, M., Parent, A., Paré, D. and Smith, Y. (1987b) Cholinergic and non-cholinergic neurons of cat basal forebrain project to reticular and mediodorsal thalamic nuclei. *Brain Research* **408**: 372–376.

Steriade, M., Paré, D., Parent, A. and Smith, Y. (1988) Projections of cholinergic and non-cholinergic neurons of the brainstem core to relay and associational thalamic nuclei in the cat and macaque monkey. *Neuroscience* **25**: 47–67.

Steriade, M., Datta, S., Paré, D., Oakson, G. and Curró Dossi, R. (1990a) Neuronal activities in brainstem cholinergic nuclei related to tonic activation processes in thalamocortical systems. *Journal of Neuroscience* **10**: 2541–2559.

Steriade, M., Jones, E.G. and Llinás, R.R. (1990b) *Thalamic Oscillations and Signaling.* New York: Wiley-Interscience.

Steriade, M., Paré, D., Datta, S., Oakson, G. and Curró Dossi, R. (1990c) Different cellular types in mesopontine cholinergic nuclei related to ponto-geniculo-occipital waves. *Journal of Neuroscience* **10**: 2560–2579.

Steriade, M., Gloor, P., Llinás, R.R., Lopes da Silva, F.H. and Mesulam, M.M. (1990d) Basic mechanisms of cerebral rhythmic activities. *Electroencephalography and Clinical Neurophysiology* **76**: 481–508.

Steriade, M., Curró Dossi, R. and Nuñez, A. (1991a) Network modulation of a slow intrinsic oscillation of cat thalamocortical neurons implicated in sleep delta waves: cortical potentiation and brainstem cholinergic suppression. *Journal of Neuroscience* **11**: 3200–3217.

Steriade, M., Curró Dossi, R., Paré, D. and Oakson, G. (1991b) Fast oscillations (20–40 Hz) in thalamocortical systems and their potentiation by mesopontine cholinergic nuclei in the cat. *Proceedings of the National Academy of Sciences of the USA* **88**: 4396–4400.

Steriade, M., Amzica, F. and Nuñez, A. (1993a) Cholinergic and noradrenergic modulation of the slow (∼0.3 Hz) oscillation in neocortical cells. *Journal of Neurophysiology* 70: 1384–1400.

Steriade, M., Contreras, D., Curró Dossi, R. and Nuñez, A. (1993b) The slow (<1 Hz) oscillation in reticular thalamic and thalamocortical neurons: scenario of sleep rhythm generation in interacting thalamic and neocortical networks. *Journal of Neuroscience* **13**: 3284–3299.

Steriade, M., Curró Dossi, R. and Contreras, D. (1993c) Electrophysiological properties of intralaminar thalamocortical cells discharging rhythmic (∼40 Hz) spike-bursts at ∼1000 Hz during waking and rapid eye movement sleep. *Neuroscience* **56**: 1–9.

Steriade, M., McCormick, D.A. and Sejnowski, T.J. (1993d) Thalamocortical oscillation in the sleeping and aroused brain. *Science* **262**: 679–685.

Steriade, M., Nuñez, A. and Amzica, F. (1993e) A novel slow (<1 Hz) oscillation of neocortical neurons *in vivo*: depolarizing and hyperpolarizing components. *Journal of Neuroscience* **13**: 3252–3265.

Steriade, M., Nuñez, A. and Amzica, F. (1993f) Intracellular analysis of relations between the slow (<1 Hz) neocortical oscillation and other sleep rhythms. *Journal of Neuroscience* **13**: 3266–3283.

Steriade, M., Amzica, F. and Contreras, D. (1994a) Cortical and thalamic cellular correlates of electroencephalographic burst-suppression. *Electroencephalography and Clinical Neurophysiology* **90**: 1–16.

Steriade, M., Contreras, D. and Amzica, F. (1994b) Synchronized sleep oscillations and their paroxysmal developments. *Trends in Neuroscience* **17**: 199–208.

Steriade, M., Amzica, F. and Contreras, D. (1996a) Synchronization of fast (30–40 Hz) spontaneous cortical rhythms during brain activation. *Journal of Neuroscience* **16**: 392–417.

Steriade, M., Contreras, D., Amzica, F. and Timofeev, I. (1996b) Synchronization of fast (30–40 Hz) spontaneous oscillations in intrathalamic and thalamocortical networks. *Journal of Neuroscience* **16**: 2788–2808.

Steriade, M., Jones, E.G. and McCormick, D.A. (1997) *Thalamus* (vol. 1, *Organisation and Function*). Oxford: Elsevier.

Steriade, M., Amzica, F., Neckelmann, D. and Timofeev, I. (1998a) Spike-wave complexes and fast runs of cortically generated seizures. II. Extra- and intracellular patterns. *Journal of Neurophysiology* **80**: 1456–1479.

Steriade, M., Timofeev, I., Dürmüller, N. and Grenier, F. (1998b) Dynamic properties of corticothalamic neurons and local cortical interneurons generating fast rhythmic (30–40 Hz) spike bursts. *Journal of Neurophysiology* **79**: 483–490.

Steriade, M., Timofeev, I. and Grenier, F. (1998c) Inhibitory components of cortical spike-wave seizures *in vivo*. *Society for Neuroscience Abstracts* **24**: 2143.

Steriade, M., Timofeev, I., Grenier, F. and Dürmüller, N. (1998d) Role of thalamic and cortical neurons in augmenting responses: dual intracellular recordings *in vivo*. *Journal of Neuroscience* **18**: 6425–6443.

Steriade, M., Timofeev, I. and Grenier, F. (2001a) Natural waking and sleep states: a view from inside neocortical neurons. *Journal of Neurophysiology* **85**: 1969–1985.

Steriade, M., Timofeev, I. and Grenier, F. (2001b) Intrinsic, antidromic and synaptic excitability of cortical neurons during natural waking-sleep cycle. *Society for Neuroscience Abstracts* **27**: 240.

Sterman, M.B. and Clemente, C.D. (1962a) Forebrain inhibitory mechanisms: cortical synchronization induced by basal forebrain stimulation. *Experimental Neurology* **6**: 91–102.

Sterman, M.B. and Clemente, C.D. (1962b) Forebrain inhibitory mechanisms: sleep patterns induced by basal forebrain stimulation in the behaving cat. *Experimental Neurology* **6**: 103–117.

Stevens, D.R., Greene, R.W. and McCarley, R.W. (1992) Serotonin 1 and serotonin 2 receptors hyperpolarize and depolarize separate populations of medial pontine reticular formation neurons in vitro. *Neuroscience* **47**: 545–553.

Stewart, M. and Fox, S.E. (1991) Hippocampal theta activity in monkeys. *Brain Research* **538**: 59–63.

Stickgold, R., Whitbee, D., Schirmer, B., Patel, V. and Hobson, J.A. (2000) Visual discrimination improvement. A multi-step process occurring during sleep. *Journal of Cognitive Neuroscience* **12**: 246–254.

Stuart, G. and Sakmann, B. (1995) Amplification of EPSPs by axosomatic sodium channels in neocortical pyramidal neurons. *Neuron* **15**: 1065–1076.

Sugita, S., Tanaka, E. and North, R.A. (1993) Membrane properties and synaptic potentials of three types of neurone in rat lateral amygdala. *Journal of Physiology (London)* **460**: 705–718.

Sundstrom, L.E., Brana, C., Gatherer, M., Mepham, J. and Rougier, A. (2001) Somatostatin- and neuropeptide Y-synthesizing neurones in the fascia dentate of humans with temporal lobe epilepsy. *Brain* **124**: 688–697.

Sutherland, G.R. and McNaughton, B. (2000) Memory traces reactivation in hippocampal and neocortical neuronal ensembles. *Current Opinion in Neurobiology* **10**: 180–186.

Sutherling, W.W., Crandall, P.H., Cahan, L.D. and Barth, D.S. (1988) The magnetic field of epileptic spikes agrees with intracranial localizations in complex partial epilepsy. *Neurology* **38**: 778–786.

Sutula, T., He, X.X., Cavazos, J. and Scott, G. (1988) Synaptic reorganization in the hippocampus induced by abnormal functional activity. *Science* **239**: 1147–1150.

Suzuki, W.A. (1996) The anatomy, physiology and functions of the perirhinal cortex. *Current Opinion in Neurobiology* **6**: 179–186.

Svensson, T.H., Bunney, B.S. and Aghajanian, G.K. (1975) Inhibition of both noradrenergic and serotonergic neurons in brain by the alpha-adrenergic agonist clonidine. *Brain Research* **92**: 291–306.

Swann, J.W., Smith, K.L. and Brady, R.J. (1993) Localized excitatory synaptic interactions mediate the sustained depolarization of

electrographic seizure in developing hippocampus. *Journal of Neuroscience* **13**: 4680–4689.

Swann, J.W., Al-Noori, S., Jiang, M. and Lee, C.L. (2000) Spine loss and other dendritic abnormalities in epilepsy. *Hippocampus* **10**: 617–625.

Sypert, G.W. and Ward, A.A. Jr. (1971) Unidentified neuroglia potentials during propagated seizures in neocortex. *Experimental Neurology* **33**: 239–255.

Szentágothai, J. (1978) The neuron network of the cerebral cortex: a functional interpretation. The Ferrier Lecture. *Proceedings of the Royal Society (London, Series B)* **201**: 219–248.

Szentágothai, J. and Arbib, M.A. (1974) Conceptual models of neural organization. *Neuroscience Research Program Bulletin* **12**: 307–510.

Szymusiak, R. and McGinty, D. (1986) Sleep-related neuronal discharge in the basal forebrain of cats. *Brain Research* **370**: 82–92.

Szymusiak, R. and McGinty, D. (1989) Sleep-waking discharge of basal forebrain projection neurons in cats. *Brain Research Bulletin* **22**: 423–430.

Szymusiak, R., Shouse, M.N. and McGinty, D. (1966) Brainstem stimulation during sleep evokes abnormal rhythmic activity in thalamic neurons in feline penicillin epilepsy. *Brain Research* **713**: 253–260.

Szymusiak, R., Steininger, T., Alam, N. and McGinty, D. (2001) Preoptic area sleep-regulating mechanisms. *Archives Italiennes de Biologie* **139**: 77–92.

Tamás, G., Buhl, E.H. and Somogyi, P. (1997) Fast IPSPs elicited via multiple synaptic release sites by distinct types of GABAergic neurone in the cat visual cortex. *Journal of Physiology (London)* **500**: 715–738.

Tancredi, V., Biagini, G., D'Antuono, M., Louvel, J., Pumain, R. and Avoli, M. (2000) Spindle-like thalamocortical synchronization in a rat brain slice preparation. *Journal of Neurophysiology* **84**: 1093–1097.

Tasker, G.J. and Dudek, F.E. (1991) Electrophysiology of GABA-mediated synaptic transmission and possible roles in epilepsy. *Neurochemical Research* **16**: 251–262.

Tauck, D.L. and Nadler, J.V. (1985) Evidence of functional mossy fiber sprouting in hippocampal formation of kainic acid-treated rats. *Journal of Neuroscience* **5**: 1016–1022.

Taylor-Courval, D. and Gloor, P. (1984) Behavioral alterations associated with generalized spike and wave discharges in the EEG of the cat. *Experimental Neurology* **83**: 167–186.

Telfeian, A.E. and Connors, B.W. (1998) Layer-specific pathways for the horizontal propagation of epileptiform discharges in neocortex. *Epilepsia* **39**: 700–708.

Temkin, O. (1971) *The Falling Sickness.* Baltimore: Johns Hopkins University Press.

Terman, D., Bose, A. and Kopell, N. (1996) Functional reorganization in thalamocortical networks: transition between spindling and delta sleep rhythms. *Proceedings of the National Academy of Sciences of the USA* **93**: 15417–15422.

Terzano, M.G., Parrino, L. and Spaggiari, M.C. (1988) The cyclic alternating pattern sequences in the dynamic organization of sleep. *Electroencephalography and Clinical Neurophysiology* **69**: 437–447.

Terzano, M.G., Parrino, L., Spaggiari, M.C., Barusi, R. and Simeoni, S. (1991) Discriminatory effect of cyclic alternating pattern in focal lesioned and benign rolandic interictal spikes during sleep. *Epilepsia* **32**: 616–628.

Thomas, J.E. and Klass, D.W. (1968) Six-per-second spike and wave pattern in the electroencephalogram. *Neurology* **18**: 587–593.

Thompson, S.M. and Gähwiler, B.H. (1989) Activity-dependent disinhibition. I. Repetitive stimulation reduces IPSP driving force and conductance in the hippocampus *in vitro*. *Journal of Neurophysiology* **61**: 501–511.

Thomson, A.M. (1988a) Inhibitory postsynaptic potentials evoked in thalamic neurons by stimulation of the reticularis nucleus evoke slow spikes in isolated rat brain slices. *Neuroscience* **25**: 491–502.

Thomson, A.M. (1988b) Biphasic responses of thalamic neurons to GABA in isolated rat brain slices. *Neuroscience* **25**: 503–512.

Thomson, A.M. (1997) Activity-dependent properties of synaptic transmission at two classes of connections made by rat neocortical pyramidal axons *in vitro*. *Journal of Physiology (London)* **502**: 131–147.

Thomson, A.M. and Deuchars, J. (1997) Synaptic interactions in neocortical local circuits: dual intracellular recordings *in vitro*. *Cerebral Cortex* **7**: 510–522.

Thomson, A.M. and West, D.C. (1993) Fluctuations in pyramid-pyramid excitatory postsynaptic potentials modified by presynaptic firing pattern and postsynaptic membrane potential using paired intracellular recordings in rat neocortex. *Neuroscience* **54**: 329–346.

Thomson, A.M., Girldestone, D. and West, D.C. (1988) Voltage-dependent currents prolong single-axon postsynaptic potentials in layer III pyramidal neurons in rat neocortical slices. *Journal of Neurophysiology* **60**: 1896–1907.

Thomson, A.M., Deuchars, J. and West D.C. (1993a) Large, deep layer pyramid-pyramid single axon EPSPs in slices of rat motor cortex display paired pulse and frequency-dependent depression, mediated presynaptically and self-facilitation, mediated postsynaptically. *Journal of Neurophysiology* **70**: 2354–2369.

Thomson, A.M., Deuchars, J. and West, D.C. (1993b) Single axon excitatory postsynaptic potentials in neocortical interneurons exhibit pronounced paired pulse facilitation. *Neuroscience* **54**: 347–360.

Thomson, A.M., West, D.C. and Deuchars, J. (1995) Properties of single axon excitatory postsynaptic potentials elicited in spiny interneurons by action potentials in pyramidal neurons in slices of rat neocortex. *Neuroscience* **69**: 727–738.

Thomson, A.M., West, D.C., Hahn, J. and Deuchars, J. (1996) Single axon IPSPs elicited in pyramidal cells by three classes of interneurons in slices of rat neocortex. *Journal of Physiology (London)* **496**: 81–102.

Timofeev, I. and Steriade, M. (1996) Low-frequency rhythms in the thalamus of intact-cortex and decorticated cats. *Journal of Neurophysiology* **76**: 4152–4168.

Timofeev, I. and Steriade, M. (1997) Fast (mainly 30–100 Hz) oscillations in the cat cerebellothalamic pathway and their synchronization with cortical potentials. *Journal of Physiology (London)* **504**: 153–168.

Timofeev, I. and Steriade, M. (1998) Cellular mechanisms underlying intrathalamic augmenting responses of reticular and relay neurons. *Journal of Neurophysiology* **79**: 2716–2729.

Timofeev, I., Contreras, D. and Steriade, M. (1996) Synaptic responsiveness of cortical and thalamic neurons during various phases of slow oscillation in cat. *Journal of Physiology (London)* **494**: 265–278.

Timofeev, I., Grenier, F. and Steriade, M. (1998) Spike-wave complexes and fast runs of cortically generated seizures. IV. Paroxysmal fast runs in cortical and thalamic neurons. *Journal of Neurophysiology* **80**: 1495–1513.

Timofeev, I., Grenier, F., Bazhenov, M., Sejnowski, T.J. and Steriade, M. (2000a) Origin of slow oscillations in deafferented cortical slabs. *Cerebral Cortex* **10**: 1185–1199.

Timofeev, I., Grenier, F., Bazhenov, M., Sejnowski, T.J. and Steriade, M. (2000b) Impact of intrinsic properties and synaptic factors on the activity of neocortical networks *in vivo*. *Journal of Physiology (Paris)* **94**: 343–355.

Timofeev, I., Bazhenov, M., Sejnowski, T.J. and Steriade M. (2001a) Contribution of intrinsic and synaptic factors in the desynchronization of thalamic oscillatory activity. *Thalamus and Related Systems* **1**: 53–69.

Timofeev, I., Grenier, F. and Steriade, M. (2001b) Disfacilitation and active inhibition in the neocortex during the natural sleep-wake cycle: an intracellular study. *Proceedings of the National Academy of Sciences of the USA* **98**: 1924–1929.

Timofeev, I., Bazhenov, M., Sejnowski, T.J. and Steriade, M. (2002a) Cortical I_H takes part in the generation of paroxysmal activities. *Proceedings of the National Academy of Sciences of the USA* **99**: 9533–9537.

Timofeev, I., Grenier, F., Bazhenov, M., Houweling, A., Sejnowski, T.J. and Steriade, M. (2002b) Short- and medium-term plasticity associated with augmenting responses in cortical slabs and spindles in intact cortex of cats *in vivo*. *Journal of Physiology (London)* **542**: 583–598.

Timofeev, I., Grenier, F. and Steriade, M. (2002c) The role of chloride-dependent inhibition and the activity of fast-spiking neurons during cortical spike-wave seizures. *Neuroscience* **114**: 1115–1132.

Tononi, G. and Cirelli, C. (2001) Some considerations on sleep and neural plasticity. *Archives Italiennes de Biologie* **139**: 221–241.

Tononi, G., Cirelli, C. and Shaw, P.J. (2000) The molecular correlates of sleep, waking and sleep deprivation. In *The Regulation of Human (Human Frontier Workshop VIII)*, ed. A. Borbély, O. Hayaishi, T.J. Sejnowski and J.S. Altman, pp. 155–167, Strasbourg: Human Frontier Science Program.

Topolnik, L., Steriade, M. and Timofeev, I. (2001) Neocortical deafferentation potentiates development of paroxysmal activities. *Society for Neuroscience Abstracts* **27**: 288.

Topolnik, L., Steriade, M. and Timofeev, I. (2003) Partial cortical deafferentation promotes development of paroxysmal activity. Submitted.

Torres, E.M., Perry, T.A., Blockland, A., Wilkinson, L.S., Wiley, R.G., Lappi, D.A. and Dunnet, S.B. (1994) Behavioural, histochemical and biochemical consequences of selective immunolesion in discrete regions of the basal forebrain cholinergic system. *Neuroscience* **63**: 95–122.

Traub, R.D. and Llinás, R. (1979) Hippocampal pyramidal cells: significance of dendritic ionic conductances for neuronal function and epileptogenesis. *Journal of Neurophysiology* **42**: 476–496.

Traub, R.D. and Wong, R.K.S. (1981) Penicillin-induced epileptiform activity in the hippocampal slice: a model of synchronization of CA3 pyramidal cell bursting. *Neuroscience* **6**: 223–230.

Traub, R.D., Miles, R. and Jefferys, J.G.R. (1993) Synaptic and intrinsic conductances shape picrotoxin-induced synchronized after-discharges in the guinea-pig hippocampal slices. *Journal of Physiology (London)* **461**: 525–547.

Traub, R.D., Whittington, M.A., Stanford, I.M. and Jefferys, J.G.R. (1996) A mechanism for generation of long-range synchronous fast oscillations in the cortex. *Nature* **383**: 621–624.

Traub, R.D., Jefferys, J.G.R. and Whittington, M.A. (1999a) *Fast Oscillations in Cortical Circuits*. Cambridge, MA: The MIT Press.

Traub, R.D., Schmitz, D., Jefferys, J.G.R. and Draguhn A. (1999b) High-frequency population oscillations are predicted to occur in hippocampal pyramidal neuronal networks interconnected by axoaxonal gap junctions. *Neuroscience* **92**: 407–426.

Traub, R.D., Whittington, M.A., Bühl, E.H., LeBeau, F.N., Bibbig, A., Boyd, S., Cross, H. and Baldeweg, T.A. (2001) A possible role for gap junctions in generation of very fast EEG oscillations preceding the onset of, and perhaps initiating, seizures. *Epilepsia* **42**: 153–170.

Traub, R.D., Buhl, E.H., Gloveli, T. and Whittington, M.A. (2003) A model of a layer 2/3 neocortical pyramidal neuron demonstrating multiple compartment-specific firing patterns, including fast rhythmic bursting. *Journal of Neurophysiology*, in press.

Traynelis, S.F. and Dingledine, R. (1988) Potassium-induced spontaneous electrographic seizures in the rat hippocampal slice. *Journal of Neurophysiology* **59**: 259–276.

Treitman, L.J. and Treitman, D.M. (1999) Genetic epilepsy – generalized. In *The Epilepsies*, ed. P. Kotagal and H.O. Lüders, pp. 543–549, San Diego: Academic Press.

Treves, A. and Rolls, E.T. (1994) A computational analysis of the role of the hippocampus in memory. *Hippocampus* **4**: 374–391.

Trulson, M.E. and Jacobs, B.L. (1979) Raphe unit activity in freely moving cats: correlation with level of behavioral arousal. *Brain Research* **163**: 135–150.

Trulson, M.E., Crisp, T. and Trulson, V.M. (1984) Activity of serotonin-containing nucleus centralis superior (raphe medianus) neurons in freely moving cats. *Experimental Brain Research* **54**: 33–44.

Tsakiridou, E., Bertollini, L., De Curtis M., Avanzini, G. and Pape, H.C. (1995) T-type calcium conductance in the reticular thalamic nucleus: a contribution to absence epilepsy. *Journal of Neuroscience* **15**: 3110–3117.

Tseng, G.F. and Prince, D.A. (1996) Structural and functional alterations in rat corticospinal neurons following axotomy. *Journal of Neurophysiology* **75**: 248–267.

Tseng, K.Y., Kasanetz, F., Kargieman, L., Riquelne, L.A. and Murer, M.G. (2001) Cortical slow oscillatory activity is reflected in the membrane potential and spike trains of striatal neurons in rats with chronic nigrostriatal lesions. *Journal of Neuroscience* **21**: 6430–6439.

Tsodyks, M., Kenet, T., Grinvald, A. and Arieli, A. (1999) Linking spontaneous activity of single cortical neurons and the underlying functional architecture. *Science* **286**: 1943–1946.

Turner, D.A. and Wheal, H.V. (1991) Excitatory synaptic potentials in kainic acid-denervated rat CA1 pyramidal neurons. *Journal of Neuroscience* **11**: 2786–2794.

Turrini, P., Casu, M.A., Wong, T.P., De Koninck, Y., Ribeiro-da-Silva, A. and Cuello, A.C. (2001) Cholinergic nerve terminals establish classical synapses in the rat cerebral cortex: synaptic pattern and age-related atrophy. *Neuroscience* **105**: 277–285.

Tuunanen, J., Lukasiuk, K., Halonen, T. and Pitkänen, A. (1999) Status epilepticus-induced neuronal damage in the rat amygdaloid complex: distribution, time-course and mechanisms. *Neuroscience* **94**: 473–495.

Uchida, S., Maloney, T., March, J.D., Azari, R. and Feinberg, I. (1991) Sigma (12–15 Hz) and delta (0.3–3.0 Hz) EEG oscillate reciprocally within NREM sleep. *Brain Research Bulletin* **27**: 93–96.

Ueno, R., Honda, K., Inoue, S. and Hayaishi, O. (1983) Prostaglandin D_2, a cerebral sleep-inducing substance in rats. *Proceedings of the National Academy of Sciences of the USA* **80**: 1735–1737.

Uhl, G.R., Tran, V., Snyder, S.H. and Martin, J.B. (1985) Somatostatin receptors: distribution in rat central nervous system and human frontal cortex. *Journal of Comparative Neurology* **240**: 266–304.

Uhlrich, D. and Huguenard, J.R. (1996) $GABA_B$ receptor-mediated responses in GABAergic projection neurones of rat nucleus reticularis thalami *in vitro*. *Journal of Physiology (London)* **493**: 845–854.

Uhlrich, D. and Huguenard J.R. (1997) $GABA_A$-receptor-mediated rebound burst firing and burst shunting in thalamus. *Journal of Neurophysiology* **78**: 1748–1751.

Uhlrich, D.J., Manning, K.A. and Xue, J.T. (2002) Effects of activation of the histaminergic tuberomammillary nucleus on visual responses of neurons in the dorsal lateral geniculate nucleus. *Journal of Neuroscience* **22**: 1098–1107.

Umbriaco, D., Watkins, K.C., Descarries, L., Cozzari, C. and Hartman, B.K. (1994) Ultrastructural and morphometric features of the acetylcholine

innervation in adult rat parietal cortex. An electron microscopic study in serial sections. *Journal of Comparative Neurology* **348**: 351–373.

Urbano, F.J., Leznik, E. and Llinás, R.R. (2001) Cortical activation patterns evoked by afferent axons stimuli at different frequencies: an *in vitro* voltage sensitive dye imaging study. *Thalamus and Related Systems* **1**: 371–378.

Van Brederode, J. and Spain, W. (1995) Differences in inhibitory synaptic input between layer II–III and layer V neurons of the cat neocortex. *Journal of Neurophysiology* **74**: 1149–1166.

Vanderwolf, C.H. (1969) Hippocampal electrical activity and voluntary movement in the rat. *Electroencephalography and Clinical Neurophysiology* **26**: 407–418.

Vanderwolf, C.H. (1988) Cerebral activity and behavior: control by central cholinergic and serotonergic systems. *International Reviews of Neurobiology* **30**: 225–340.

Van Hoesen, G.W., Hyman, B.T. and Damasio, A.R. (1991) Entorhinal cortex pathology in Alzheimer's disease. *Hippocampus* **1**: 1–8.

Van Luijtelaar, E.L. and Coenen, A.M. (1986) Two types of electrocortical paroxysms in an inbred strain of rats. *Neuroscience Letters* **70**: 393–397.

Vanni-Mercier, G., Sakai, K. and Jouvet, M. (1984) Neurones spécifiques de l'éveil dans l'hypothalamus postérieur du chat. *Comptes Rendus de l'Académie des Sciences (Paris)* **298**: 195–200.

Velasco, F. and Velasco, M. (1990) Mesencephalic structures and tonic-clonic generalized seizures. In *Generalized Epilepsy: Cellular, Molecular and Pharmacological Approach*, ed. M. Avoli, P. Gloor, G. Kostopoulos and R. Naquet, pp. 368–384, Boston: Birkhäuser.

Velasco, F., Velasco, M., Cepeda, C. and Munoz, H. (1980) Wakefulness-sleep modulation of cortical and subcortical somatic evoked potentials in man. *Electroencephalography and Clinical Neurophysiology* **48**: 64–72.

Velasco, F., Velasco, M., Velasco, A.L., Jiménez, F., Márquez, I. and Rise, M. (1995) Electrical stimulation of the centromedian thalamic nucleus in the control of intractable seizures: long-term studies. *Epilepsia* **36**: 63–71.

Velasco, F., Velasco, M., Jiménez, F., Velasco, A.L., Rojas, B. and Perez, M.L. (2001) Centromedian nucleus stimulation for epilepsy: clinical, electroencephalographic, and behavioral observations. *Thalamus and Related Systems* **1**: 387–398.

Velayos, J.L., Jimenez-Castellanos, J. Jr. and Reinoso-Suárez, F. (1989) Topographical organization of the projections from the reticular thalamic nucleus to the intralaminar and medial thalamic nuclei in the cat. *Journal of Comparative Neurology* **279**: 457–469.

Vergnes, M. and Marescaux, C. (1992) Cortical and thalamic lesions in rats with genetic absence epilepsy. *Journal of Neural Transmission* **35** (Suppl.): 71–83.

Vertes, R.P. and Kocsis, B. (1997) Brainstem-diencephalo-septohippocampal systems controlling the theta rhythm of the hippocampus. *Neuroscience* **81**: 893–926.

Villablanca, J. (1974) Role of the thalamus in sleep control: sleep-wakefulness studies of chronic cats without the thalamus: the "athalamic cat". In *Basic Sleep Mechanisms*, ed. O. Petre-Quadens and J. Schlag, pp. 51–81, New York: Academic.

Villablanca, J.R., De Andrés, I. and Olmstead, C.E. (2001) Sleep-waking states develop independently in the isolated forebrain and brain stem following early postnatal midbrain transection in cats. *Neuroscience* **106**: 717–731.

Von Krosigk, M., Bal, T. and McCormick, D.A. (1993) Cellular mechanisms of a synchronized oscillation in the thalamus. *Science* **261**: 361–364.

Wada, J.A. and Terao, A. (1970) Effect of parachlorophenylalanine on basal forebrain stimulation. *Experimental Neurology* **28**: 501–506.

Wadman, W.J. and Gutnick, M.J. (1993) Non-uniform propagation of epileptiform discharge in brain slices of rat neocortex. *Neuroscience* **53**: 899–904.

Walshe, F.M.R. (1957) The brain-stem conceived as the "highest level" of function in the nervous system: with particular reference to the "automatic apparatus" of Carpenter (1850) and to the "centrencephalic integrating system" of Penfield. *Brain* **80**: 510–539.

Walter, G. (1936) The location of cerebral tumors by electroencephalography. *Lancet* **8**: 305–308.

Wang, X.J. and Rinzel, J. (1993) Spindle rhythmicity in the reticularis thalami nucleus: synchronization among mutually inhibitory neurons. *Neuroscience* **53**: 899–904.

Wang, Z. and McCormick, D.A. (1993) Control of firing mode of corticotectal and corticopontine layer V burst-generating neurons by norepinephrine, acetylcholine and 1*S*, 3*R*-ACPD. *Journal of Neuroscience* **13**: 2199–2216.

Ward, A.A. (1975) Topical convulsants metals. In *Experimental Models of Epilepsy*, ed. D.P. Purpura, J.K. Penry, D.B. Tower, D.M. Woodbury and R.D. Walter, pp. 13–35, New York: Raven Press.

Ward, A.A. and Schmidt, R.P. (1961) Some properties of single epileptic neurons. *Archives of Neurology* **5**: 308–313.

Ward, A.A., Jasper, H.H. and Pope, A. (1969) Clinical and experimental challenges of the epilepsies. In *Basic Mechanisms of the Epilepsies*, ed. H.H. Jasper, A.A. Ward and A. Pope, pp. 1–12, Boston: Little, Brown.

Watson, C.W. and Bowker, R. (1960) On the significance of circumscribed electroencephalographic abnormalities in genetic light sensitive states including cases of genetic epilepsy with "centrencephalic" epilepsy. *Electroencephalography and Clinical Neurophysiology* **12**: 551.

Weber, A.J., Kalil, R.E. and Behan, M. (1989) Synaptic connections between corticogeniculate axons and interneurons in the dorsal lateral geniculate nucleus of the cat. *Journal of Comparative Neurology* **289**: 156–164.

Werth, E., Achermann, P., Dijk, D.J. and Borbély, A. (1997) Spindle frequency activity in the sleep EEG: individual differences and topographical distribution. *Electroencephalography and Clinical Neurophysiology* **103**: 535–542.

West, W.J. (1841) On a particular form of infantile convulsions. *Lancet* **1**: 724–725.

Westerberg, V. and Corcoran, M.E. (1987) Antagonism of central but not peripheral cholinergic receptors retards amygdala kindling in rats. *Experimental Neurology* **95**: 194–206.

Westerfield, M., Joyner, R.W. and Moore, J.W. (1978) Temperature-sensitive conduction failure at axon branch points. *Journal of Neurophysiology* **41**: 1–8.

Westgaard, J.H., Bonato, P. and Holte, K.A. (2002) Low-frequency oscillations (<0.3 Hz) in the electromyographic (EMG) activity of the human trapezius muscle during sleep. *Journal of Neurophysiology* **88**: 1177–1184.

Wheal, H.V., Bernard, C., Chad, J.E. and Cannon, R.C. (1998) Pro-epileptic changes in synaptic function can be accompanied by pro-epileptic changes in neuronal excitability. *Trends in Neurosciences* **21**: 167–174.

White, J.C. (1940) Autonomic discharge from stimulation of the hypothalamus. In *The Hypothalamus and Central Levels of Autonomic Function*, ed. J.F. Fulton, S.W. Ranson and A.M. Frantz, pp. 854–863, Baltimore: Williams and Wilkins.

White, J.C., Langston, J.W. and Pedley, T.A. (1977) Benign epileptiform transients of sleep: clarification of the small sharp spike controversy. *Neurology* **27**: 1061–1068.

Wilcox, K.S., Gutnick, M.J. and Cristoph, G.R. (1988) Electrophysiological properties of neurons in the lateral habenular nucleus: an *in vitro* study. *Journal of Neurophysiology* **59**: 212–225.

Wilcox, K.S., Grant , S.J., Burkhart, B.A. and Cristoph, G.R. (1989) *In vivo* electrophysiology of neurons in the lateral dorsal tegmental nucleus. *Brain Research Bulletin* **22**: 557–560.

Wilder, B.J. and Morrell, F. (1967) Cellular behavior in secondary epileptic lesions. *Neurology* **17**: 1193–1204.

Williams, D. (1953) A study of thalamic and cortical rhythms in Petit Mal. *Brain* **76**: 50–69.

Williams, J.A. and Reiner, P.B. (1993) Noradrenaline hyperpolarizes identified rat mesopontine cholinergic neurons *in vitro*. *Journal of Neuroscience* **13**: 3878–3883.

Williams, J.A., Comisarow, J., Day, J., Fibiger, H.C. and Reiner, P.B. (1994) State-dependent release of acetylcholine in rat thalamus measured by *in vivo* microdialysis. *Journal of Neuroscience* **14**: 5236–5242.

Williamson, A.M., Ohara, P.T. and Ralston, H.J. (1993) Electron microscopic evidence that cortical terminals make direct contacts onto cells of the thalamic reticular nucleus in the monkey. *Brain Research* **631**: 175–179.

Williamson, A., Telfeian, A.E. and Spencer, D.D. (1995) Prolonged GABA responses in dentate granule cells in slices isolated from patients with temporal lobe sclerosis. *Journal of Neurophysiology* **74**: 378–387.

Williamson, R. and Wheal, H.V. (1992) The contribution of AMPA and NMDA receptors to graded bursting activity in the hippocampal CA1 region in an acute *in vitro* model of epilepsy. *Epilepsy Research* **12**: 179–188.

Willmore, L.J. (1999) How does trauma cause epilepsy? In *The Epilepsies – Etiologies and Prevention*, ed. P. Kotagal and H.O. Lüders, pp. 289–291, San Diego: Academic Press.

Wilson, C.J. (1993) The generation of natural firing patterns in neostriatal neurons. *Progress in Brain Research* **99**: 277–297.

Wilson, C.J. and Kawaguchi, Y. (1996) The origin of two-state spontaneous membrane potential fluctuations of neostriatal spiny neurons. *Journal of Neuroscience* **16**: 2397–2410.

Wilson, M.A. and McNaughton, B.L. (1994) Reactivation of hippocampal ensemble memories during sleep. *Science* **265**: 676–679.

Wilson, S., Kinnier, A. and Bruce, A. (1955) *Neurology*. Baltimore: Williams & Wilkins.

Winson, J. and Abzug, C. (1978) Neuronal transmission through hippocampal pathways dependent on behavior. *Journal of Neurophysiology* **41**: 716–732.

Winter, O., Kok, A., Kenemans, J.L. and Elton, M. (1995) Auditory event-related potentials (AEPs) to deviant stimuli during drowsiness and sleep. *Electroencephalography and Clinical Neurophysiology* **96**: 398–412.

Wise, S.P., Fleshman, J.W. Jr. and Jones, E.G. (1979) Maturation of pyramidal cell form in relation to developing afferent and efferent connections of rat somatic sensory cortex. *Neuroscience* **4**: 1275–1297.

Witte, O.W. and Freund, H.J. (1999) Neuronal dysfunction, epilepsy, and postlesional brain plasticity. *Advances in Neurology* **81**: 25–36.

Wittner, L., Maglóczky, Z., Borhegyi, S., Halász, P., Tóth, S., Eröss, L., Szabó, Z. and Freund, T.F. (2001) Preservation of perisomatic inhibitory input of granule cells in the epileptic human dentate gyrus. *Neuroscience* **108**: 587–600.

Wolpert, S. (1982) *A New History of India.* New York: Oxford University Press.

Wong, R.K.S. and Stewart, M. (1992) Different firing patterns generated in dendrites and somata of CA1 pyramidal neurones in guinea-pig hippocampus. *Journal of Physiology (London)* **457**: 675–687.

Wong, R.K.S., Prince, D.A. and Basbaum, A.I. (1979) Intradendritic recordings from hippocampal neurons. *Proceedings of the National Academy of Sciences of the USA* **76**: 986–990.

Woody, C.D., Gruen, E. and Wang, X.F. (2003) Electrical properties affecting discharge of units of the mid and posterolateral thalamus of conscious cats. *Neuroscience*, in press.

Wuarin, J.P. and Dudek, F.E. (1996) Electrographic seizures and new recurrent excitatory circuits in the dentate gyrus of hippocampal slices from kainate-treated epileptic rats. *Journal of Neuroscience* **16**: 4438–4448.

Xiong, Z.Q., Saggau, P. and Stringer, J.L. (2000) Activity-dependent intracellular acidification correlates with the duration of seizure activity. *Journal of Neuroscience* **20**: 1290–1296.

Yamada, T., Kameyama, S., Fuchigami, Z., Nakazumi, Y., Dickins, Q.S. and Kimura, J. (1988) Changes of short latency somatosensory evoked

potential in sleep. *Electroencephalography and Clinical Neurophysiology* **70**: 126–136.

Yamamoto, C. and McIlwain, H. (1966) Electrical activities in thin sections from the mammalian brain maintained in chemically defined media *in vitro*. *Journal of Neurochemistry* **13**: 1333–1343.

Yamashita, A., Watanabe, Y. and Hayaishi, O. (1983) Autoradiographic localization of a binding protein(s) specific for prostaglandin D_2 in rat brain. *Proceedings of the National Academy of Sciences of the USA* **80**: 6114–6118.

Yang, C.R., Seamans, J.K. and Gorelova, N. (1996) Electrophysiological and morphological properties of layers V–VI principal pyramidal cells in rat prefrontal cortex *in vitro*. *Journal of Neuroscience* **16**: 1904–1921.

Yang, L. and Benardo, L.S. (1997) Epileptogenesis following neocortical trauma from two sources of disinhibition. *Journal of Neurophysiology* **78**: 2804–2810.

Yaqub, B.A. (1993) Electroclinical seizures in Lennox-Gastaut syndrome. *Epilepsia* **34**: 120–127.

Yen, C.T., Conley, M., Hendry, S.H.C. and Jones, E.G. (1985) The morphology of physiologically identified GABAergic neurons in the somatic sensory part of the thalamic reticular nucleus in the cat. *Journal of Neuroscience* **5**: 2254–2268.

Yeterian, E.H. and Pandya, D.N. (1989) Thalamic connections of the superior temporal sulcus in the rhesus monkey. *Journal of Comparative Neurology* **282**: 80–97.

Ylinen, A., Bragin, A., Nádasdy, Z., Jandó, G., Szabó, I., Sik, A. and Buzsáki, G. (1995) Sharp wave-associated high-frequency oscillation (200 Hz) in the intact hippocampus: network and intracellular mechanisms. *Journal of Neuroscience* **15**: 30–46.

Yoshida, M., Sasa, M. and Takaori, S. (1984) Serotonin-mediated inhibition from dorsal raphe nucleus of neurons in dorsal geniculate and thalamic reticular nuclei. *Brain Research* **290**: 95–105.

Young, M.P., Tanaka, K. and Yamane, S. (1992) On oscillating neuronal responses in the visual cortex of the monkey. *Journal of Neurophysiology* **67**: 1464–1474.

Yue, B.W. and Huguenard, J.R. (2001) The role of H-current in regulating strength and frequency of thalamic network oscillations. *Thalamus and Related Systems* **1**: 95–103.

Yuste, R. and Tank, D.W. (1996) Dendritic integration in mammalian neurons, a century after Cajal. *Neuron* **16**: 701–716.

Zhang, S.J., Huguenard, J.R. and Prince, D.A. (1997) $GABA_A$ receptor-mediated Cl^- currents in rat thalamic reticular and relay neurons. *Journal of Neurophysiology* **78**: 2280–2286.

Zhang, Y., Perez-Velazquez, J.L., Tian, G.F., Wu, C.P., Skinner, F.K., Carlen, P.L. and Zhang, L. (1998). Slow oscillations ($\leq$1 Hz) mediated by GABAergic interneuronal networks in rat hippocampus. *Journal of Neuroscience* **18**: 9256–9268.

Zhu, J.J. and Lo, F.S. (1999) Three GABA receptor-mediated postsynaptic potentials in interneurons in the rat lateral geniculate nucleus. *Journal of Neuroscience* **19**: 5721–5730.

Zhu, J.J. and Uhlrich, D.J. (1998) Cellular mechanisms underlying two muscarinic receptor-mediated depolarizing responses in relay cells of the rat lateral geniculate nucleus. *Neuroscience* **87**: 767–781.

Zhu, J.J., Lytton, W.W., Xue, J.T. and Uhlrich, D.J. (1999a) An intrinsic oscillation in interneurons of the rat lateral geniculate nucleus. *Journal of Neurophysiology* **81**: 702–711.

Zhu, J.J., Uhlrich, D.J. and Lytton, W.W. (1999b) Burst firing in identified rat geniculate interneurons. *Neuroscience* **91**: 1445–1460.

Zifkin, B.G. and Dravet, C. (1997) Generalized convulsive seizures. In *Epilepsy: A Comprehensive Textbook*, ed. J. Engel Jr. and T.A. Pedley, pp. 567–577, Philadelphia: Lippincott-Raven.

Zola-Morgan, S. and Squire, L.R. (1993) Neuroanatomy of memory. *Annual Reviews of Neuroscience* **16**: 547–563.

Zuckermann, E.C. and Glaser, G.H. (1968) Hippocampal epileptic activity induced by localized ventricular perfusion with high-potassium cerebrospinal fluid. *Experimental Neurology* **20**: 87–110.

Zygierewicz, J., Blinowska, K.J., Durka, P.J., Szelenberger, W., Niemcewicz, S. and Androsiuk, W. (1999) High resolution study of sleep spindles. *Clinical Neurophysiology* **110**: 2136–2147.

Index

References to entry words in notes are indicated thus: 289[n24] – note 24 on page 289